Phosphate Tether-mediated Strategies for the Synthesis of Complex Polyols, Natural Products, and Analogs

By

Gihan C. Dissanayake

Submitted to the graduate degree program in the Department of Chemistry and the graduate faculty of the University of Kansas in partial fulfillment of the requirements of the degree of Doctor of Philosophy.

_____
Paul R. Hanson, Chair

_____
Jon A.Tunge

_____
Helena C. Malinakova

_____
Michael Rubin

_____
Zarko Boskovic

03/31/2022
Date Defended

The Dissertation Committee for Gihan C. Dissanayake certifies that this is the approved version of the following dissertation:

Phosphate Tether-mediated Strategies for the Synthesis of Complex Polyols, Natural Products, and Analogs

Paul R. Hanson, Chair

Jon A.Tunge

Helena C. Malinakova

Michael Rubin

Zarko Boskovic

04/01/2022
Date Approved

Abstract

Gihan C Dissanayake

Department of Chemistry

The University of Kansas

Naturally occurring and synthetic macrocycles are considered as useful scaffolds as therapeutics and probes in both medicine and chemical biology. Due to the pre-organized nature and unique architecture, macrocycles have emerged as an important entity for chemical probe discovery in medicinal chemistry and chemical biology. Moreover, naturally derived macrocyclic secondary metabolites have demonstrated profound pharmacological properties.

Chapter 1 discusses synthetic strategies to 14-membered macrolides possessing various chemotypes. In this regard, the family of 14-membered macrolides were divided into six categories based on structural characteristics, namely macrolides containing (i) lactone rings, (ii) α,β-unsaturated macrolactones, (iii) THP rings (iv) pyran hemiketal rings, (v) fused ring systems, and (vi) amides and enamide macrolides. The synthesis of aforementioned chemotypes were discussed briefly in a retrosynthetic fashion to provide a global understanding on distinct synthetic strategies.

Chapter 2 focuses on a modular synthetic strategy employing a phosphate-tether mediated-one-pot sequential approach for the formal synthesis of (2*S*)-epimer of sanctolide A, and the total synthesis of sanctolide A. Sanctolide A is a polyketide nonribosomal peptide (PK-NRP) macrolide, which comprises a 14-membered enamide macrolactone core. A phosphate-tether mediated double diastereotopic group differentiation protocol was employed as the key step for the formal synthesis of the (2*S*)-epimer of sanctolide A. Concurrently, a phosphate-tether mediated one-pot sequential RCM/CM/substrate-controlled "H_2" /tether removal approach was utilized with improved atom- and step-economy to accomplish the total synthesis of the natural product sanctolide A. In order to deconvolute complex characterization issues due to

C2 epimerization of the C2-methyl bearing stereocenter, as well as amide rotamers and E/Z isomers, comprehensive and detailed ^{1}H and ^{13}C NMR analysis was carried out, which enabled identification of the source of epimerization and allowed for new conditions to circumvent the issue. Collectively, a strategy for simpler and more stable analogs was developed and reported in Chapter 3.

Chapter 3 provides the details of the synthesis of a small library of macrocyclic analogs of aforementioned natural product, sanctolide A that was carried out by adopting a build-couple-couple-pair (BCCP) strategy coupled with phosphate tether one-pot sequential protocols. The synthetic strategy was focused on generating simplified, *des*-methyl sanctolide analogs containing an α,β-unsaturated lactone moiety to simplify the synthesis and importantly, to improve the stability of the analogs. In this regard, a total of 5 α,β-unsaturated macrolides, and 2 enamide macrolides with variable substituents and sidechains were generated. In addition, a one-pot CM/RCM/H_2/LAH protocol was developed in the "build phase" for the synthesis of the C1–C10 1,3-*anti*-diol-containing subunit (sanctolide numbering).

Chapter 4 outlines a pot-economical approach for the streamlined synthesis of advanced polyol subunits. The key reactions involved are iterative use of a phosphate tether-mediated one-pot sequential RCM/CM/H_2 with subsequent utilization of either a regio-/diasteroselective cuprate addition or a Pd-catalyzed allylic transposition. This method highlights the asymmetric synthesis of 12 complex polyol subunits in 4–6 one-pot sequential operations with a total of 12–14 reactions, with minimal workup and purification procedures.

Chapter 5 provides experimental details and spectroscopic data of new compounds, as well as full spectrum ^{1}H, ^{13}C, ^{31}P, ^{19}F, DEPT, ^{1}H ^{1}H COSY, ^{1}H ^{13}C HSQC, ^{1}H ^{13}C HMBC, and nOe. In addition, X-ray data, IR and mass spectral data are provided, as well as a general experimental section detailing instruments used throughout this thesis.

Dedication

To my Parents and Family

Acknowledgments

First and foremost, I would like to thank my parents for their love, prayers, sacrifices, and encouragement for educating me and shaping me into the person I am now. I would like to express my thanks to my dear sister, brother, sister in law and brother in law for their love and support. Also, I would like to extend my gratitude to all my teachers who provided me with all the knowledge and guided me to success.

I would like to express my sincere gratitude to my supervisor Prof. Paul Hanson for the continuous support of my Ph.D. and invaluable guidance throughout my research. It was a great privilege and honor to work and study under your guidance. Also, I would like to thank you for being a friendly, kind, and understanding mentor. I would like to extend my gratitude to Yumi for all the kind words, bits of advice, and suggestions you gave us and for the lovely dinners you prepared for us. And thank you for your acceptance and patience during the lengthy discussion I had with Paul when preparing manuscripts and my thesis.

Besides my supervisor, I would like to thank the rest of my thesis committee: Prof. Jon Tunge, Prof. Helena Malinakova, Prof. Michael Rubin, and Prof. Zarko Boskovic, for the guidance and suggestions during my Ph.D. research and the kind recommendation letters you provided for my job applications.

I would like to extend my gratitude to Dr. Benson for kind recommendation letters and for all the guidance and support you gave me during my work as a lecture TA.

I would like to express my gratitude to all of my past and present lab members:

Salim, thank you for being a great mentor. You taught me everything in organic synthesis, from setting up reactions, and purifications to all the tricks and tips needed in synthesis.

Arghya, thank you for being a great friend and labmate. I will remember all the sleepless nights we spent in the lab working hard and all the stimulating discussions we had.

Jana, we did not get a chance to spend much time together in the lab since you graduated soon after I joined the lab. However, even during those short encounters, the advice you gave me helped me immensely in my Ph.D., so thank you for those valuable suggestions.

Cornelius, thank you for being a great friend and labmate. I will remember all the stimulating and encouraging discussions we had during our projects, especially in the sanctolide A synthesis. It would not be possible to complete the synthesis without your guidance and help.

Viena, you were an awesome friend and a colleague from the first day we joined the Hanson lab. Thank you for sharing all the fun and the sleepless nights we had, working hard, and meeting deadlines. You always lent a helping hand when I needed it most. Thank you for everything you have done for Dimuthu and me.

Gaurav and James, I cannot thank you enough for all the help you have given me by reading my thesis chapters and providing valuable suggestions. I will remember all the stimulating discussions we had in the lab. I wish you all the very best!

I would like to extend my gratitude to Sarah and Justin for maintaining an excellent NMR facility. I would like to thank Justin for teaching the NMR spectroscopy course, where I learned all the NMR techniques that were very useful for my research. Also, I would like to pay my gratitude to Sarah for helping me with running my samples and accepting my constant requests on short notice without hesitation. It would be impossible for me to complete my research without your help. Also, I would like to thank Larry for maintaining an excellent mass spectrometer facility and Victor for running my X-ray samples on short notice.

I would like to thank all the other group members from Tunge lab, Clift lab, Rubin Lab, Jackson Lab, Barybin Lab, Blakemore lab, Bowman-James, Altmann lab, Boskovic lab, and Bloom lab for lending me chemicals and other equipment when needed. It would not be possible to conduct my research without your help and support.

I would like to express my gratitude to the great staff members of the Department of Chemistry.

Ruben, you were my graduate student coordinator when I joined the graduate program. You helped me during the graduate application process, and even after that, you were there for me with all my countless questions and helped me with a smiling face. Liz, thank you for all the help and support you have given me throughout my Ph.D., with kind words and countless room reservations for my practice talks. All the current and past front office and stock room members: Susan, Beth, Betsy, Donnie, Dan, Megan, Avery, Laurie, Emily, it would be impossible to achieve my goals without all of your assistance and support. I'm deeply grateful for all the time and effort you put into helping all the graduate students in the chemistry department. Also, I would like to extend my gratitude to all the building maintenance crew members who made our move from Malott to ISB much easier.

I would like to express my gratitude to all the Sri Lankans who live in Lawrence who made it so much easier to live far away from home by bringing all of us closer as one Sri Lankan Family. I'm so grateful and proud to be a part of the Lawrence Sri Lankan community.

Last but not least, I would like to thank my loving and caring wife, Dimuthu, for all your endless support and encouragement. Thank you for all the endless nights you spend with me practicing my talks, studying together for exams and for sharing my happiness and sorrow. It would not have been possible to achieve this goal without your love and support.

Phosphate Tether-mediated Strategies for the Synthesis of Complex Polyols, Natural Products, and Analogs

CONTENTS Page #

Abbreviations

AAC	Azide Alkyne Cycloadditions
aq	aqueous
Bn	benzyl
BnBr	benzyl bromide
brsm	based on recovered starting material
9-BBN	9-Borabicyclo[3.3.1]nonane
BCCP	build-couple-couple-pair
t-BuOH	*t*-Butanol
CBS	Corey–Bakshi–Shibata
cat.	catalytic
COSY	correlation spectroscopy
C	carbon
Cl	chlorine
CM	cross metathesis
DAST	Diethylaminosulfur trifluoride
DBU	1,8-diazabicycloundec-7-ene
DCM (CH_2Cl_2)	dichloromethane
DCE	1,2-Dichloroethane
DCC	*N*,*N*'-Dicyclohexylcarbodiimide
DHP	dihydropyran
DIAD	diisopropyl azodicarboxylate
DIPEA/Hünig's base	*N*,*N*'-Diisopropylethylamine
DMAP	4-(dimethylamino)pyridine
DMP	Dess-Martin periodinane
DOS	diversity oriented synthesis
Et	ethyl
Et_2O	diethyl ether

EtOAc	ethyl acetate
EDC (EDCI)	1-ethyl-3-(3-dimethylaminopropyl)carbodiimide
G-I	Grubbs' first generation catalyst
G-II	Grubbs second-generation catalyst
GC	gas chromatography
HATU	1-hydroxy-7-azabenzotruiazole
HG-II	Hoveyda-Grubbs second generation catalyst
HRMS	high resolution mass spectrometry
h	hours
HWE	Horner–Wadsworth–Emmons
Hz	hertz
IR	infrared radiation
i-Bu	isobutyl
i-Pr	isopropyl
LCMS	Liquid chromatography–mass spectrometry
M	molarity
Me	methyl
MeOH	methanol
MeI	methyl iodide
Mmol	millimole(s)
MOM	methoxymethyl-
NMO	*N*-methylmorpholine-*N*-oxide
NMR	nuclear magnetic resonance
NIH	National Institutes of Health
nBuLi	n-butyllithium
OMe	methoxy
o-NBSH	*o*-nitrobenzene sulfonyl hydrazine
PMB	*para*-methoxybenzyl
ppm	parts per million

Ph	phenyl
PCy_3	tricyclohexylphosphine
PTSA	*p*-toluenesulfonic Acid
RCM	ring closing metathesis
RCEM	ring closing enyne metathesis
ROCM	ring-opening cross metathesis
rt	room temperature
sat.	saturated
SAE	Sharpless asymmetric epoxidation
NaO*t*Bu	sodium *tert*-Butoxide
NaHMDS	sodium hexamethyldisilazide
NaOH	sodium hydroxide
NOESY	Nuclear Overhauser Effect
SAR	structure activity relationship
TASF	tris(dimethylamino)sulfonium difluorotrimethylsilicate
TBACl	tetrabutyl ammonium chloride
TBAF	tetrabutyl ammonium fluoride
TIPS	triisopropylsilyl-
$TiCl_4$	titanium tetrachloride
TBS	*tert*-butyl(dimethyl)silyl-
TFA	trifluoroacetic acid
THF	tetrahydrofuran
THP	Tetrahydropyran
TEMPO	2,2,6,6-Tetramethylpiperidin-1-yl)oxyl
PPh_3	triphenylphosphine
TLC	thin layer chromatography
t-Bu	*tert*-butyl
Et_3N	triethylamine
2,2-DMP	dimethoxypropane

PPTS	pyridinium p-toluenesulfonate
LLS	longest linear sequence
LAH	lithium aluminum hydride
TSC	total step count
Me_3Al	trimethylaluminum

Chapter 1

Strategies to synthesize 14-membered macrolactones and analogs

1.1 Introduction

Macrocycles are considered as an important class of scaffolds which have had a tremendous impact in both medicine and chemical biology. Macrocycles represent a rich source of diversity in terms of both structure and function and have a wide range of medicinal properties.[1] A number of diverse macrocycles are naturally occurring and occupy a wide range of chemical space that are not usually covered by small molecules. There are over hundred drugs approved or in clinical stages which incorporate macrocyclic scaffolds as the active substance (Figure 1.1).[2] Some interesting aspects of this intriguing class of molecules include diverse functionality and stereochemical complexity, which many times occupy a conformationally pre-organized ring structure due to restricted rotation within the molecule.[3] This intriguing class of privileged structures displays unique features, such as conformational pre-organization, flexibility, selectivity, and potential higher affinity with protein targets,[4] and are thus promising molecules for the modulation of challenging processes.[5] Moreover, macrocycles are not completely rigid, and thus can retain the required flexibility to potentially form optimal interactions, which ultimately can lower the entropic cost of binding to an active site of a biomolecule.[2a,d]

Macrocycles are also many times generally considered as outliers of "Lipinski's rule of five" due to exceedingly high molecular weights that they possess.[6] In spite of this property, macrocycles have proven utility as useful therapeutics owing due to drug-like physicochemical and pharmacokinetic properties, such as good solubility, lipophilicity, resistance to metabolic degradation, and bioavailability.[2a,7] Moreover, macrocycles have

been extensively utilized as chemical probes in chemical biology to aid in further our understanding of protein-protein interactions (PPI).[8]

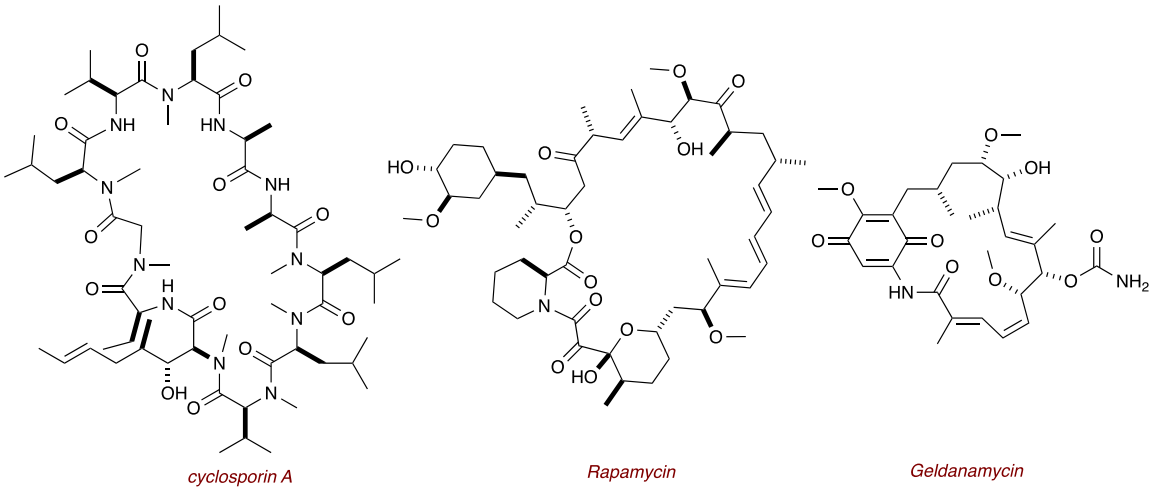

Figure 1.1 *Representative macrocyclic drugs.*

1.2 Therapeutic and biologically active macrocyclic lactones

Macrocyclic lactones can be classified into different classes based on the size of the carbon skeleton which typically include a 12- or higher membered ring architecture. Despite structural complexity and associated synthetic challenges, a number of macrocycles have been identified as therapeutic targets and compounds with unrivalled biological activities.[9] Representative structures of select macrocyclic therapeutics and biologically active macrocycles of various ring structures are shown in Figure 1.2. The macrolide antibiotic erythromycin, bearing a 14-membered macrocyclic lactone, is one of the most studied antibiotics, and was isolated from the fungus *Saccharopolyspora erythraea* and used against bacterial infections.[10] Azithromycin, a 15-membered aza-macrolide with extended ring derived from erythromycin is another effective antibacterial therapeutic that belongs to this macrocyclic lactone family.[11] Ivermectin is a highly

effective antiparasitic and anthelmintic agent bearing a 16-membered macrocyclic lactone ring, and is on the World Health Organizations (WHO) essential medicine list due to its medicinal properties.[12] (–)-laulimalide is a highly potent 20-membered macrocyclic lactone isolated from marine sponges, which shows a similar mode of action to Taxol,® and activity against multidrug-resistant cancer cell lines.[13]

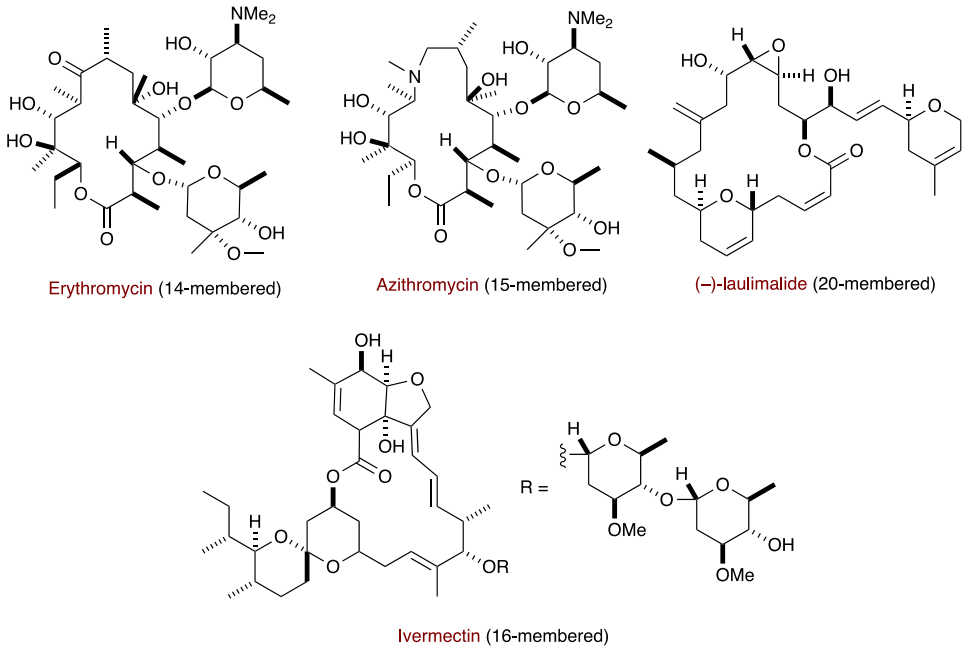

Figure 1.2: *Therapeutics/ biologically active macrocycles with different ring sizes.*

Taken collectively, naturally occurring, and synthetic macrocycles are thus considered as useful scaffolds as therapeutics and probes in both medicine and chemical biology. This chapter focuses mainly on targeted-oriented synthetic (TOS) methods that have been utilized in the syntheses of naturally derived 14-membered macrolactones, and related macrolides and analogs. The advent of new macrocyclization methods, such as RCM,[14,15] has undoubtedly changed synthetic strategies. Moreover, the emergence of

diversity-oriented synthesis (DOS),[16] has also populated macromolecular space, and will undoubtedly impact the field for years to come.

While extensive reviews exist in the literature outlining physical properties and syntheses of macrocyclic drugs and biologically active macrocyclic natural products,[17] reviews organized encompassing structural feature subtypes (chemotypes) within a given ring-size are not apparent. In this regard, 14-membered macrocyclic lactones have attracted much attention in the synthetic, medicinal and chemical biology communities due to their complex ring architectures and unique biological activities. Synthetic efforts carried out by many groups toward the synthesis of 14-membered lactone macrolides and their analogs stand as a testament for the importance of these macrocyclic structures.[17] This chapter will report a comparative mini-review highlighting the synthesis and applications of various 14-membered macrocyclic lactone/lactam systems, organized around chemotypes possessed within.

1.3 14-Membered macrolactones

The 14-membered macrocyclic core is frequently seen in several naturally derived secondary metabolites with diverse and unique architectures. For this chapter, the 14-membered macrolide natural products are categorized into the following chemotypes, namely (Figure 1.3).

1.3.1 14-Membered macrolactones.
1.3.1.1 α,β-Unsaturated 14-membered macrolactones.
1.3.2 Pyran/tetrahydropyran/dihydropyran subunit-containing macrolactones.
1.3.3 Pyran hemiketal subunit-containing macrolactones.
1.3.4 Fused core-containing macrolactones.
1.3.5 14-Membered macrolactams and macrocyclic enamides.

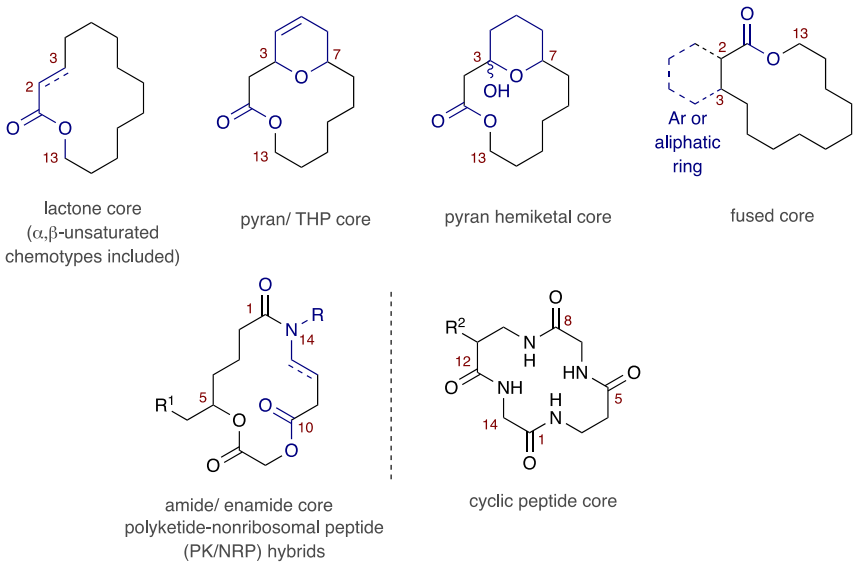

Figure 1.3: *Representative chemotypes of 14-membered macrolides*.

1.3.1 Lactone core containing 14-membered macrolides

The synthesis of polyketide macrolides has notably inspired the development of synthetic methods within organic chemistry over a significant period of time. After the first total synthesis of the polyketide 14-membered macrolide erythromycin A in 1981 by Woodward and coworkers,[18] several state-of-the-art developments have been made over the past 40 years in the organic synthesis. Since this seminal synthesis, a number of elegant total syntheses were reported over the next few decades for macrocyclic scaffolds possessing similar architecture such as oleandomycin,[19] erythromycins A[18] and B,[20] erythronolides A[21] and B,[22] (9*S*)-dihydroerythronolide A,[23] and 6-deoxyerythronolide B.[24]

Historically, methods for macrocyclization to deliver the macrolactone core of above antibiotic macrolides were largely carried out via macrolactonization of the stereochemically-defined *seco*-acids (Figure 1.4).[25] A number of acid activation strategies have been utilized in the macrocyclization step and are summarized in Figure 1.4. The

Corey-Nicolaou method employing 2-pyridinethiol ester activation method[26] was readily utilized to construct the macrolide core of erythromycin A, erythronolide A and B. Moreover, the Yamaguchi method,[27] which uses 2,4,6-trichlorobenzoyl mixed anhydride as the carboxy acid activation group has been even more frequently applied in the macrolactonization step. In 1986, Stork utilized modified Steglich esterification conditions,[28] employing DCC and DMAP for the macrolactonization step of (9*S*)-dihydroerythronolide A.[23b] In 1990, Tatsuta utilized an intramolecular Horner Wadsworth Emmons (HWE)[29] cyclization in their synthesis of oleandomycin (Figure 1.4).[19a]

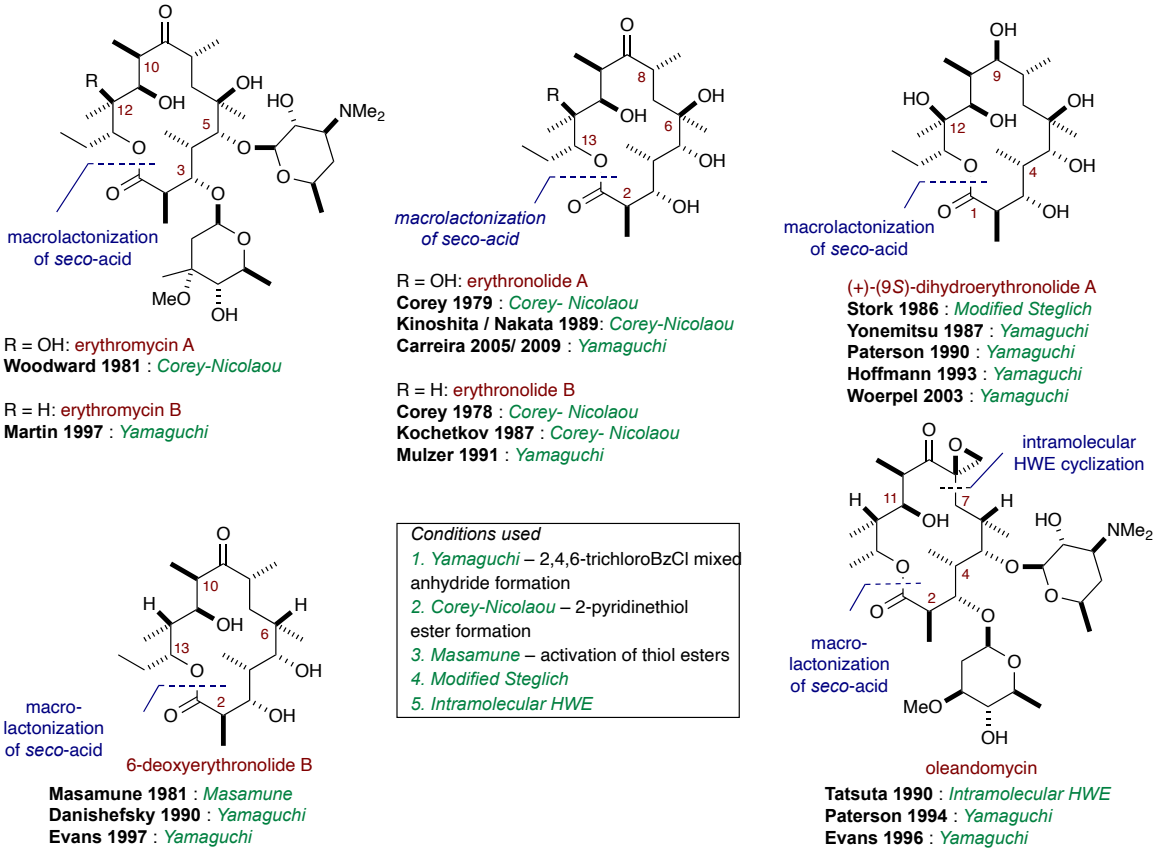

Figure 1.4 *Acid activation strategies in the macrocyclization to erythronolide A, B and oleandomycin.*

In 2009, White and coworkers reported a novel approach for the macrocyclization of 6-deoxyerythronolide B (6-deb) core using a late-stage C-H oxidative macrolactonization method.[24d,30] In this work, the Pd-catalyzed oxidative macrolactonization reaction proceeded with high regio-, chemo- and diastereoselectivity to generate the required macrolide core from the advanced linear precursor under chelate-controlled conditions (Scheme 1.1). Synthesis of the acyclic alkenoic acid was carried out via using a diastereoselective Meyer's alkylation[31] to install the C11 carbinol center, while two highly selective Evans *syn*-aldol reactions,[32] followed by Meyers alkylation were used to install the C10, C8 and C6 stereocenters, respectively. Generation of the C5, C4 and C3 centers were carried out via a *syn*-aldol, followed by a chelation-controlled reduction.

In this work, a Pd-catalyzed oxidative macrolactonization under chelate-controlled conditions was employed to afford the macrolactone with required configuration at the C13 center. It is worthy to note that the authors were also able to carry out the synthesis of the 13-epi-6-deb diastereomer using nonchelation-controlled conditions, which also however, removed the element of stereocontrol during the late-stage macrolactonization event.

In 2013, Krische and coworkers achieved the synthesis of the macrolactone core of 6-deoxyerythronolide B, using a ring-closing enyne metathesis reaction (RCEM) as the macrocyclization step (Scheme 1.1).[24e] In this work, the authors used an enyne precursor for the RCEM reaction. The main enyne-containing fragment was generated from a Yamaguchi esterification of two advanced subunits, which in turn were generated via use of the authors signature Ru-catalyzed *syn*-crotylation[33] and Ir-catalyzed double *anti*-crotylation[34] methods, respectively.

Scheme 1.1 *Synthetic strategies to 6-deoxyerthronolide B.*

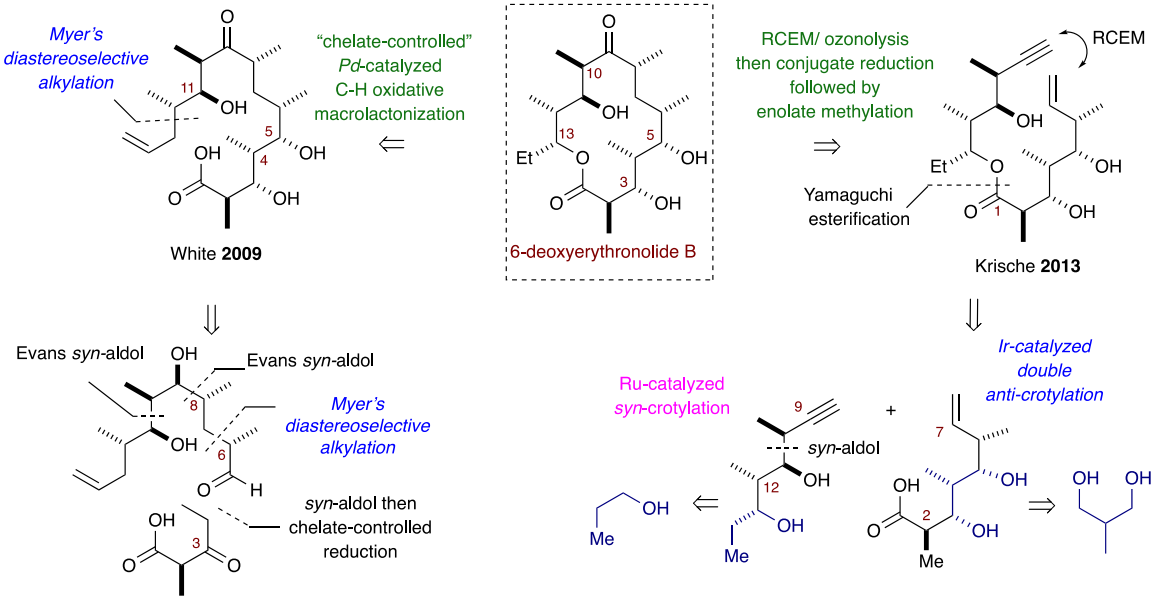

1.3.1.1 α,β-Unsaturated 14-membered macrolactones.

Macrolactone cores comprising α,β-unsaturated chemotypes are commonly seen in many polyketide-derived natural products.[17e] A number of 14-membered macrolides have been isolated and respective syntheses have been carried out over the past few decades. ripostatin B,[35] narbonolide,[36] pikromycin,[37] SCH-725674[38] and gliomasolide A-D[39] are representative examples for the aforementioned class of compounds (Figure 1.5).

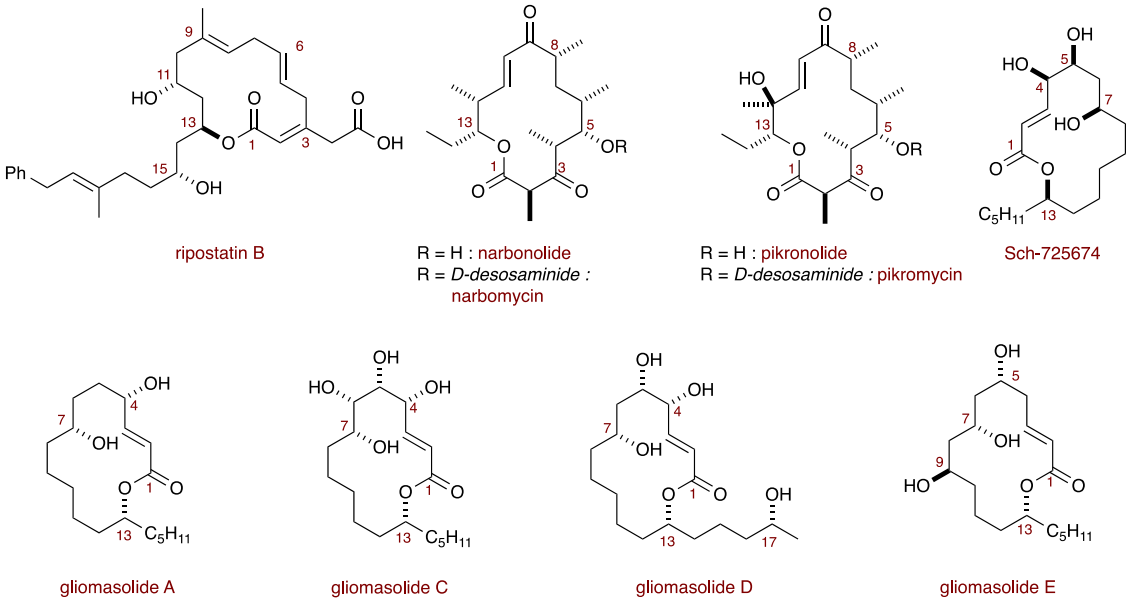

Figure 1.5 *Macrolactone cores comprising α,β-unsaturated chemotypes.*

In 2012, the first three syntheses of ripostatin B were reported independently by Altmann, [40] Christmann[41] and Prusov[42] (Scheme 1.2). All three syntheses utilize a late-stage Ru-catalyzed RCM macrocyclization event using either Grubbs I or II catalysts **G-I**, $[(PCy_3)_2(Cl)_2Ru{=}CHPh]$[43] **G-II**, $[(ImesH_2)(PCy_3)(Cl)_2Ru{=}CHPh]$.[44] In the Altmann synthesis, the final macrocyclization was carried out using the Grubbs **G-I** catalyst. The diene precursor was synthesized utilizing a Yamaguchi esterification, followed by a Stille coupling[45] with $Bu_3SnCH_2CH{=}CH_2$. Installation of the triol was carried out via a diastereoselective aldol reaction (Paterson conditions)[46] and Evans–Tishchenko *anti* 1,3-reduction.[47] While the end game of the Christmann synthesis is similar to the Altmann synthesis, the installation of the triol was carried out via a linchpin coupling and diastereoselective reduction of ketone using Evans–Tishchenko conditions.[47] In the Prusov synthesis of ripostatin B, the final macrocyclization was carried out using the Grubbs

G-II catalyst. The diene precursor was installed via a Yamaguchi esterification, followed by a double Stille cross-coupling reaction. Installation of the stereotriad was accomplished by utilizing a Paterson aldol reaction,[46] followed by a diastereoselective *anti* 1,3-reduction[47] of the post-aldol ketone moiety.

Scheme 1.2 *Three syntheses of ripostatin B.*

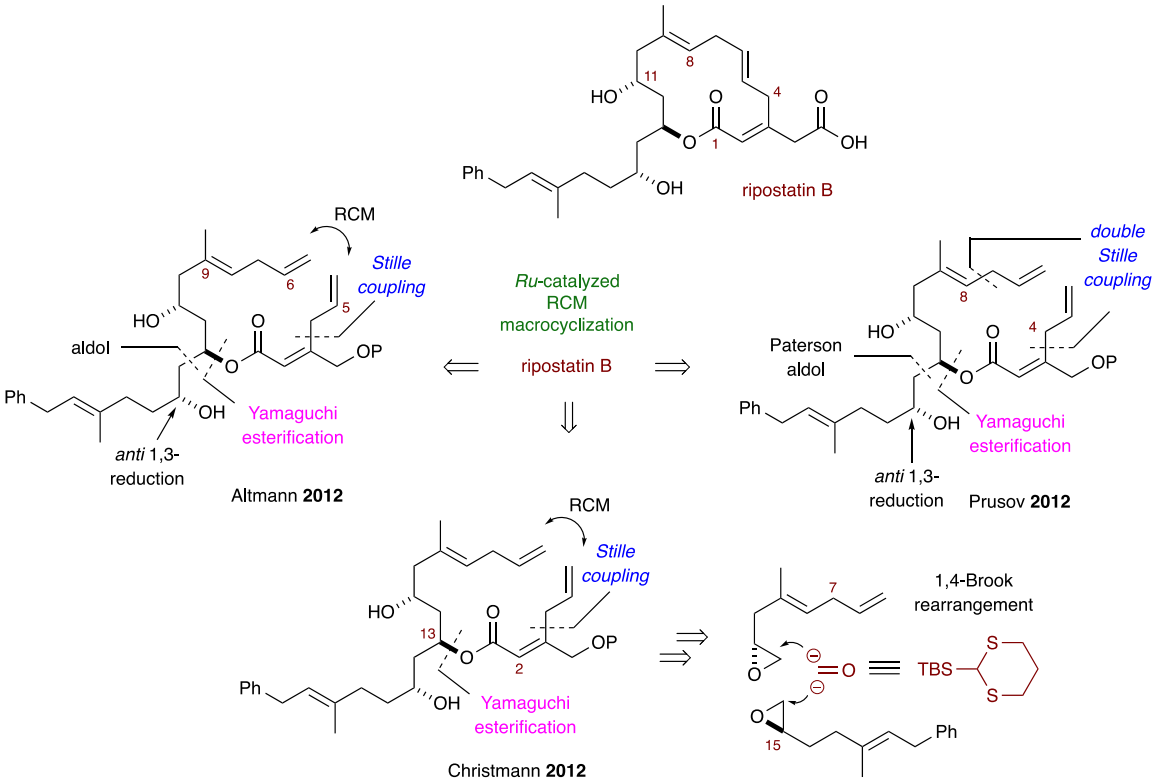

Narbomycin and pikromycin are polyketide-derived 14-membered natural products belonging to the pikromycin macrolide family (Figure 1.5). Narbonolide is the aglycon of narbomycin. The first total synthesis of Narbonolide was reported in 1982 by Masamune and coworkers (Scheme 1.3).[48] The final macrolactonization of the *seco*-acid was carried out via activation of the carboxylic acid using a phosphoric acid mixed anhydride. Installation of the α,β-unsaturated ketone was accomplished via utilization of a Peterson

olefination reaction.[46] The linear C1–C9 precursor was synthesized according to their previous synthesis of 6-deoxyerythronolide B.[24a]

In 2006, Fecik and coworkers carried out the total synthesis of narbonolide and biotransformed the aglycon into pikromycin using *pikAI* deletion mutant of *Streptomyces venezuelae* (see Figure 1.5 for structures).[49] The α,β-unsaturated macrolide aglycon was furnished with an intramolecular Nozaki-Hiyama-Kishi coupling[50] followed by Dess-Martin oxidation.[51] Synthesis of the linear chain was carried out via transformation comprising Evans *syn* aldol[32] and protecting group manipulations.

In 2008, Kang and coworkers reported their efforts towards the synthesis of the aglycon narbonolide utilizing an RCM macrocyclization as the final step.[52] The diene precursor for the RCM reaction was generated via a Yamaguchi esterification of the fragment generated via consecutive use of asymmetric *syn*-aldol reactions.[32]

Scheme 1.3 *Syntheses of narbomycin.*

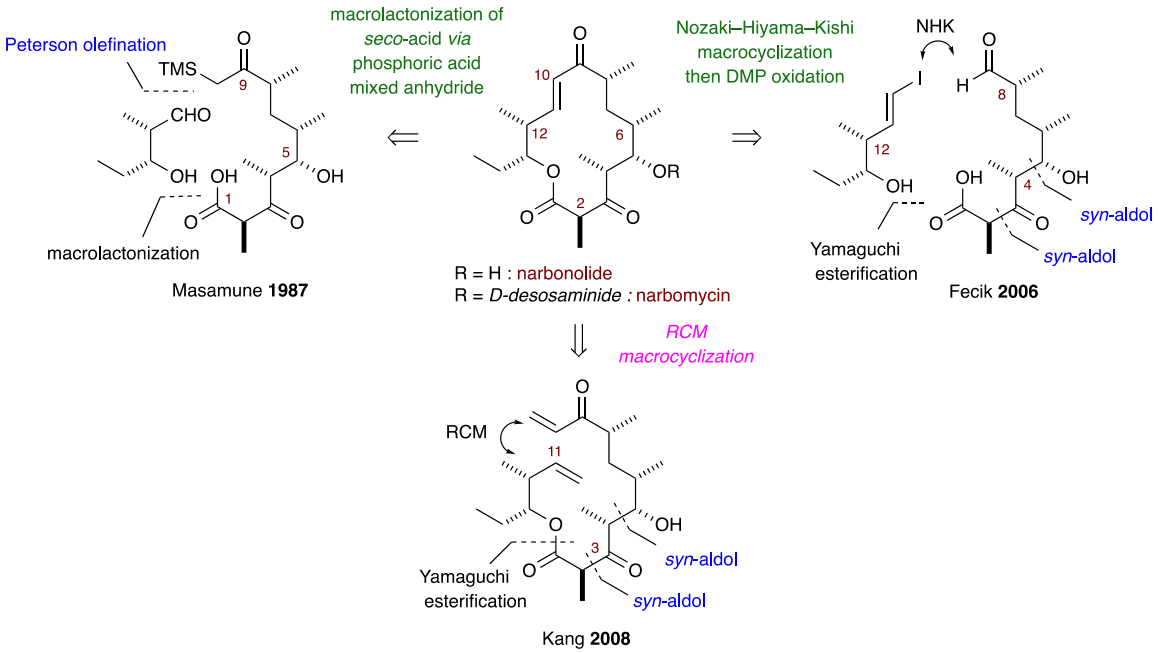

In 1987, Yonemitsu and coworkers reported the first synthesis of the aglycon of pikromycin where the final macrocyclization was furnished via an intramolecular HWE reaction.[53] The linear precursor was generated via Yamaguchi esterification of C1–C10 and C11-C13 subunits. The key stereocenters were installed using an *erythro*-selective Cram addition of crotyl-tri-*n*-butyltin[54] to the Prelog-Djerassi lactone[55] equivalent compound bearing four stereogenic centers present in pikromycin core (Scheme 1.4).

In 2012, Kang and coworkers reported the synthesis of the macrolide antibiotic pikromycin using an RCM reaction for the final macrocyclization of the aglycon (Scheme 1.4).[56] In this work, the synthesis of the aglycon was carried out in a similar fashion to their previous narbonolide synthesis in 2008.[52] The aglycon was coupled with the trichloroacetimidate derivative of D-desosamine under Lewis acidic conditions,[57] to afford pikromycin.

Scheme 1.4 *Syntheses of pikromycin and aglycon pikronolide.*

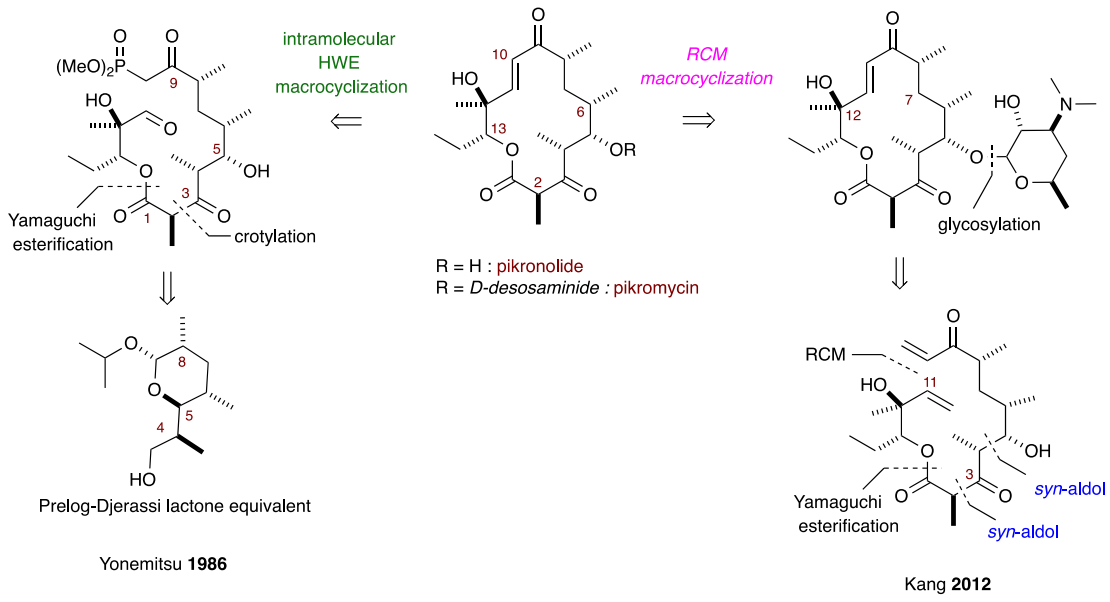

Sch-725674 is another prominent 14-membered macrolide that contains an *E*-configured α,β-unsaturated chemotype and four stereogenic centers including a 1,3-*anti*-diol subunit. Sch-725674 was isolated from the culture of *Aspergillus sp.* by Yang and coworkers in 2005. (Figure 1.5).[38]

In 2012, Curran and coworkers carried out the first total synthesis of macrocyclic lactone natural product Sch-725674 and complete library of stereoisomers, using an elegant and efficient fluorous tagging technique developed in their laboratory (Scheme 1.5).[58] In this work, an encoded method was used that employed four mixtures of four fluorous-tagged quasiisomers that were synthesized, de-mixed, and de-tagged to generate 16 stereoisomers of the Sch725674. The authors developed a new bare-minimum tagging pattern which needed only two tags, one fluorous and one non-fluorous, to encode four stereoisomers. Using this method the authors were able to assign the absolute structure of

Scheme 1.5 *Currans fluorous-tagging strategy to all stereoisomers of Sch-725674.*

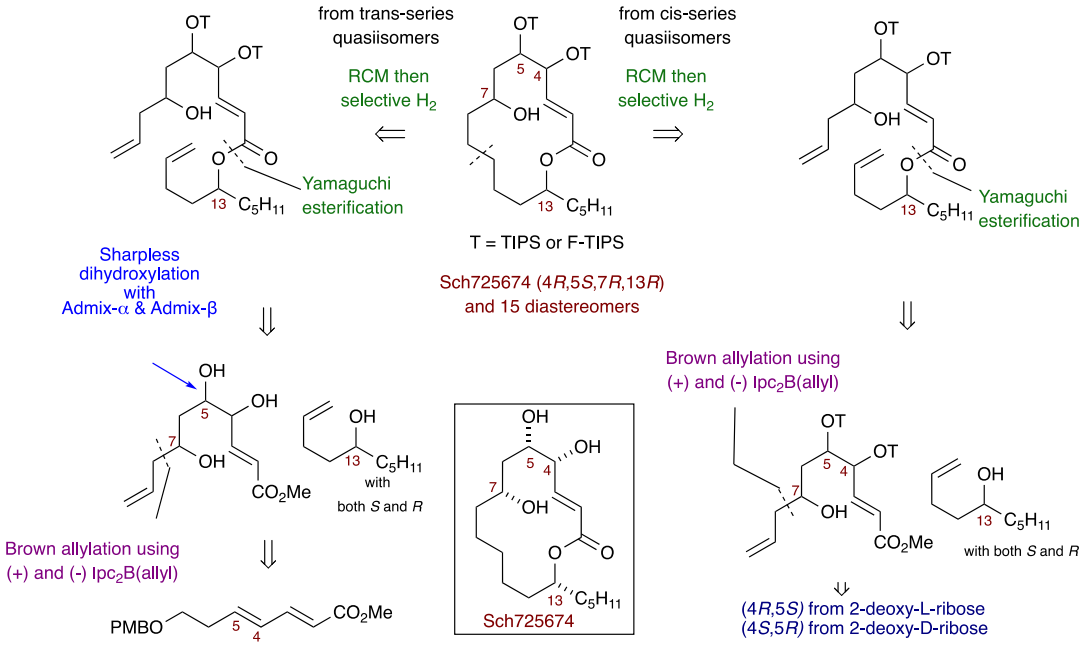

Sch725674 as (5R,6S,8R,14R,*E*)-5,6,8-trihydroxy-14-pentyloxacyclotetradec-3-en-2-one. In addition, the authors provided structural insights as to when/why related compounds have the same or different spectra. This latter feature of the work was made possible via comparisons of the spectra of 32 lactones (16 with tags, 16 without) and 16 ester precursors (8 with tags, 8 without) (Scheme 1.5).

In 2014, Prasad and coworkers carried out an enantioselective total synthesis of Sch-725674 (Scheme 1.6), whereby final macrocyclization was furnished via an intramolecular RCM reaction.[59] The C3–C13 linear precursor containing the four requisite stereogenic centers was generated via key reactions involving Ley's dithiaketalization[60] of an alkynone derived from *bis*-Weinreb amide of tartaric acid and an Evans *anti*-reduction.[61]

Scheme 1.6 *Synthetic strategies to Sch-725674.*

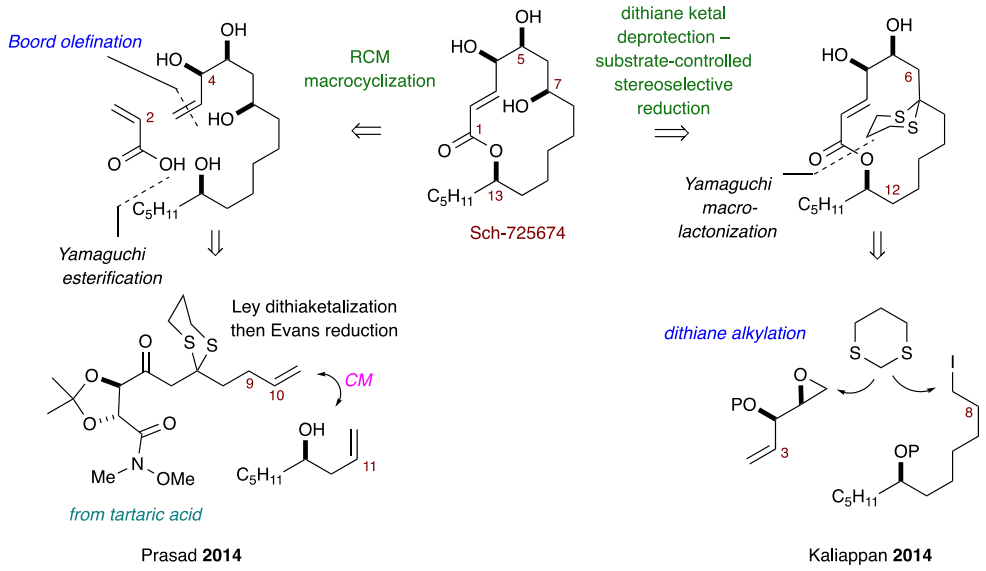

In 2015, Kaliappan and coworkers reported a 13-step synthesis of Sch-725674.[62] Synthesis of the macrolactone core was furnished via a Yamaguchi

macrolactonization. Assembly of the *seco*-acid precursor was carried out utilizing a dithiane alkylation,[63] followed by a cross metathesis with methyl acrylate (Scheme 1.6).

In 2016, Hanson and coworkers reported a pot-economical total synthesis of Sch-725674, taking the advantage of one-pot, sequential transformations coupled to phosphate tether-mediated protocols developed in their lab (Figure 1.7).[64,65,66] Final macrolactone core of the macrolide was furnished via an intramolecular RCM reaction. Phosphate tether-mediated RCM/CM chemoselective hydrogenation,[67] tether removal followed by a Sharpless asymmetric epoxidation (SAE)[68] and a one-pot, Finkelstein reaction/Boord olefination[69]/acetonide deprotection sequence was utilized to generate the diene precursor possessing the requisite stereotetrad. In addition, the authors published related efforts to a modular synthesis of novel electrophilic macrocycles bearing α,β-unsaturated 14-membered chemotypes through a series of one-pot, sequential protocols (Scheme 1.7).[65d]

Scheme 1.7 *Synthetic strategies to Sch-725674 and related analogs.*

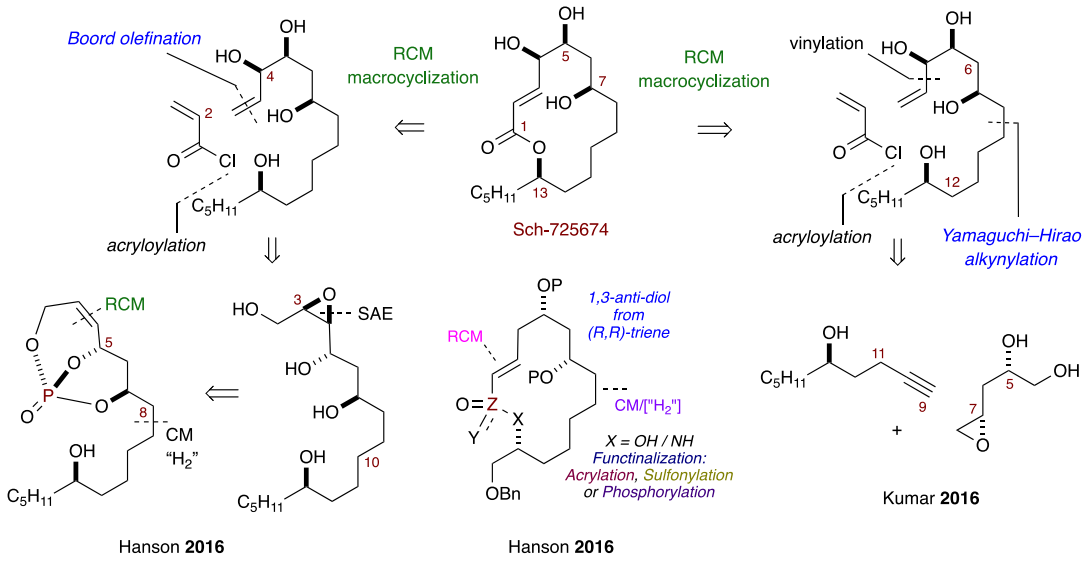

In 2016, Kumar and coworkers reported the total synthesis of Sch-725674 utilizing an RCM macrocyclization strategy to generate the macrolide core (Scheme 1.7).[70] The diene precursor with the required four sterogenic centers was assembled via Yamaguchi-Hirao alkynylation,[71] followed by substrate controlled-diastereoselective vinyl Grignard addition, and subsequent acryloylation.

In 2016, Reddy and coworkers reported a short synthesis of Sch-725674. Generation of the 14-membered macrolide core was carried out via a Yamaguchi macrolactonization (Scheme 1.8).[72] Cross metathesis, followed by Wacker-type oxidation,[73] delivered the acyclic *seco*-acid precursor. Subsequent Yamaguchi macrolactonization and transannular diastereoselective reduction of ketone, delivered the natural product.

In 2016, Sabitha and coworkers completed their synthesis of Sch-725674 by utilizing a Yamaguchi macrolactonization to deliver the macrolide core (Scheme 1.8).[74] The linear precursor of the *seco*-acid was generated via HWE[29] olefination and a diastereoselective CBS reduction.[75]

In 2016, Aggarwal and coworkers carried out a nine-step concise total synthesis of Sch-725674 involving use of a novel desymmetrizing enantioselective diboration of divinyl carbinol to generate the C3–C13 subunit (Scheme 1.8).[76] After the initial diboration reaction to establish the C4 and C5 stereocenters, two consecutive lithiation borylation oxidation (L-B-O)[77] reactions were carried out to install the required C7 and C13 stereocenters. Subsequent cross metathesis, followed by Yamaguchi macrolactonization, furnished the macrolactone core in a highly efficient manner.

Scheme 1.8 *Synthetic strategies to Sch-725674.*

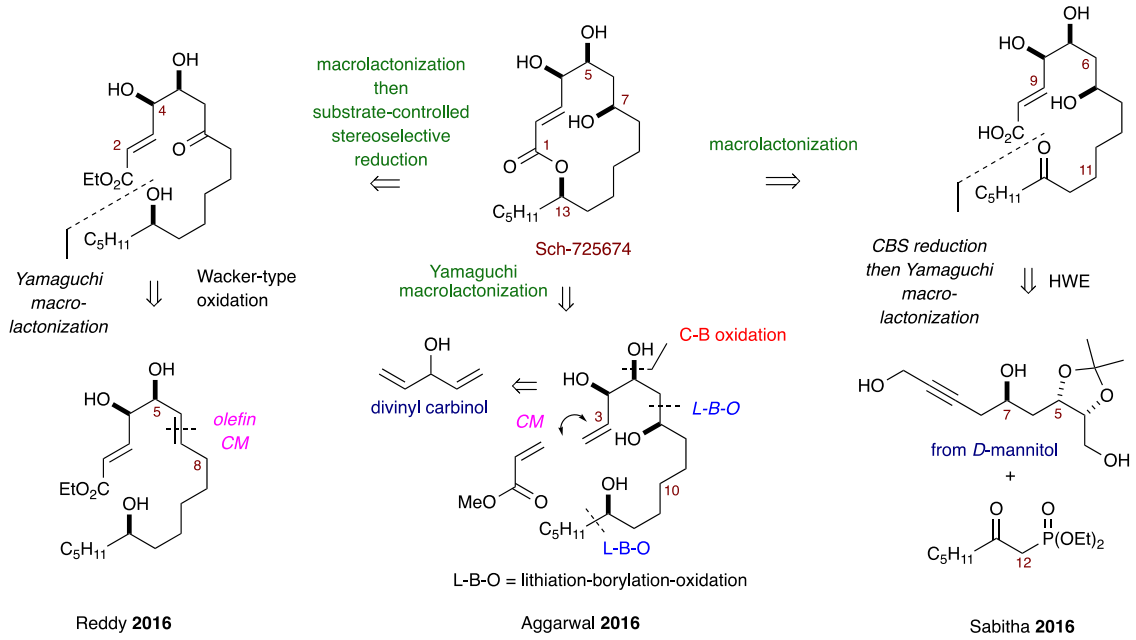

The 14-membered macrolides gliomasolide A–E were isolated from the sponge-derived fungus *Gliomastix* sp. ZSDS1-F7-2 by the Liu and Xu groups in 2015 (for structures, see Figure 1.5 and Scheme 1.9).[39] During the isolation, the authors were able to confirm the structure and stereochemical configuration of gliomasolide A and gliomasolide B via 2D NMR analysis, followed by single-crystal X-ray analysis. The structure of the gliomasolide C was also determined by 2D NMR analysis, and was further confirmed by Reddy and coworkers during their synthesis in 2016, *vide infra*.[78] Furthermore, during the initial report by Liu and Xu groups, the absolute configuration of C17 in gliomasolide D was not established due to the limited supply of the isolated natural products.

In 2016, Reddy and coworkers generated the 14-membered macrolide core of gliomasolide D using an intramolecular RCM macrocyclization (Scheme 1.9).[78] Cross

metathesis, followed by substrate-controlled dihydroxylation, and subsequent acryloylation delivered the linear diene precursor. Spectral data for the synthesized macrolactone were identical to the reported data, which further confirmed the structure and stereochemical configuration of gliomasolide C established by the Liu and Xu groups in 2015.[39]

In 2017, Reddy and coworkers focused their efforts toward determining the absolute configurations within gliomasolide D by synthesizing both C17 epimers of the natural product (Scheme 1.9).[79] The synthesis of gliomasolide D resembled the key features of their Sch-725674 synthesis, wherein the 14-membered macrolide core was delivered via a Yamaguchi macrolactonization, and subsequent substrate-controlled ketone reduction.[72] Cross metathesis, followed by a regioselective Wacker-type oxidation of the C7 olefinic carbon, generated the *seco*-acid. After careful analysis of the ^{13}C NMR data and specific

Scheme 1.9 *Synthetic strategies to gliomasolide C and D.*

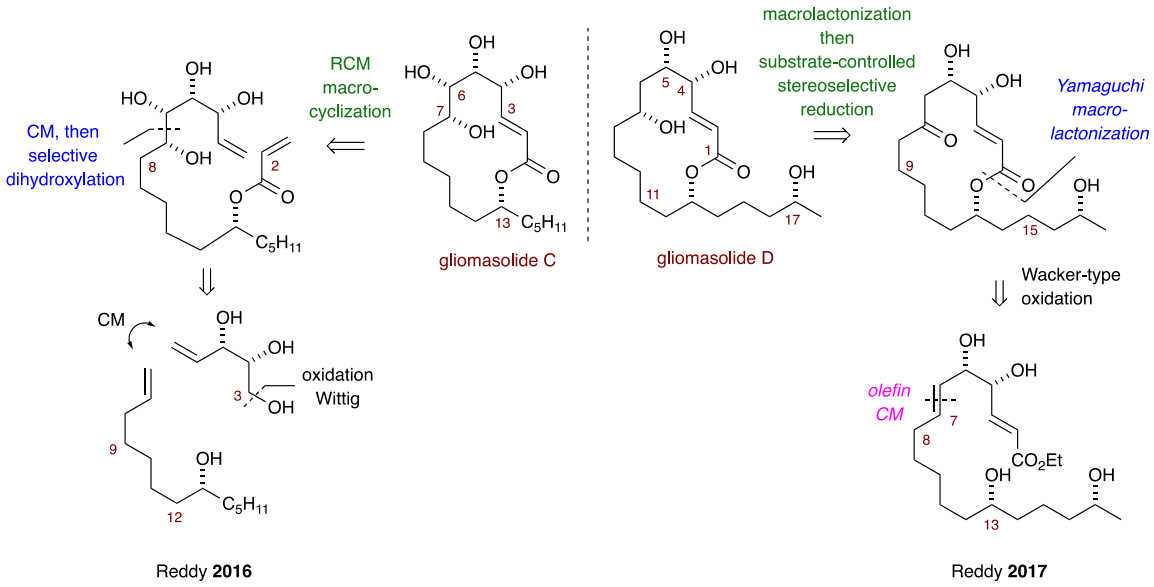

rotation data of the two epimers, the authors were able to conclude that the absolute configuration at the C17 carbinol center is 17-*R*. It is worth noting, that the C9 carbinol center of gliomasolide E was not established during the initial report.

In 2017, Mahopatra and coworkers used total synthesis to establish the absolute configuration of the C9 carbinol within of gliomasolide E (Scheme 1.10).[80] The 14-membered macrolactone core was furnished utilizing an intramolecular HWE macrocyclization. The linear precursor was accessed from a Yamaguchi-Hirao alkynylation[71] of the requiste epoxide. The authors carried out the synthesis of both C9 epimers of the natural product. Based on the spectral and specific rotation data, determination was made of absolute C9-*R* carbinol configuration of gliomasolide E.

Scheme 1.10 *Synthetic strategies to gliomasolide A and E*

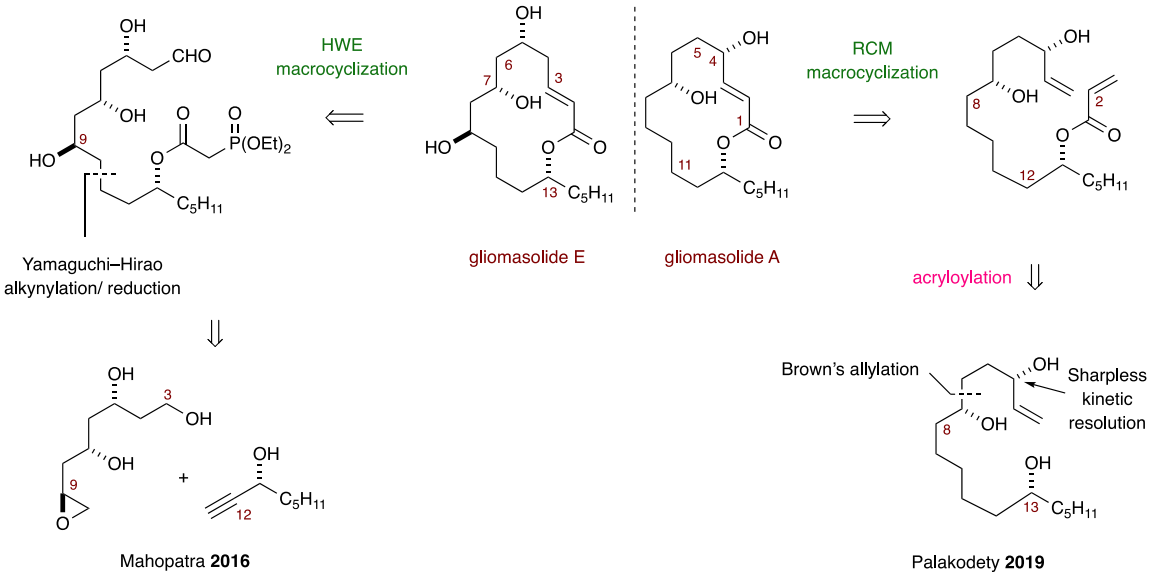

In 2019, Palakodety and coworkers reported the first total synthesis of gliomasolide A.[81] The final macrolactone core was furnished via an intramolecular RCM reaction of the corresponding diene. The diene precursor was generated utilizing a Brown asymmetric allylation,[82] a Sharpless kinetic resolution[83] and subsequent acryloylation.

1.3.2 Pyran/tetrahydropyran/dihydropyran subunit-containing macrolactones.

Tetrahydropyran (THP) and dihydropyran (DHP) motifs are another unique structural feature embedded within some 14-membered macrolide natural products. To the best of our knowledge, there are only a few THP/DHP-containing 14-membered macrocyclic lactones reported in the literature,[17] namely aspergillide A–C,[84] neopeltolide[85] and paecilomycin B.[86] Due to their promising biological activities and intriguing chemical architecture, numerous successful synthetic efforts have been carried out for the synthesis of these natural products over the past few decades.

The 14-membered macrolides aspergillide A, B and C were isolated in 2008 by Kusumi and coworkers from marine fungus *Aspergillus ostianus* strain 01F313 (Figure 1.6).[84] These secondary metabolites were shown to exhibit significant toxicity against mouse lymphocytic leukemia cells with IC_{50} values of 2.1, 70, and 2.0 μg/mL, respectively. The originally proposed structures for aspergillides A and B were revised[87] by X-ray crystallography studies by the same authors and the structure of aspergillide C was confirmed via synthesis in 2009 by Kuwahara and coworkers (Figure 1.6), *vide infra*.[88] Their unique biological profile and challenging chemical architectures have attracted

considerable attention over the past few decades, which has led to a number of successful syntheses (more than 20) for all three natural products aspergillide A–C.

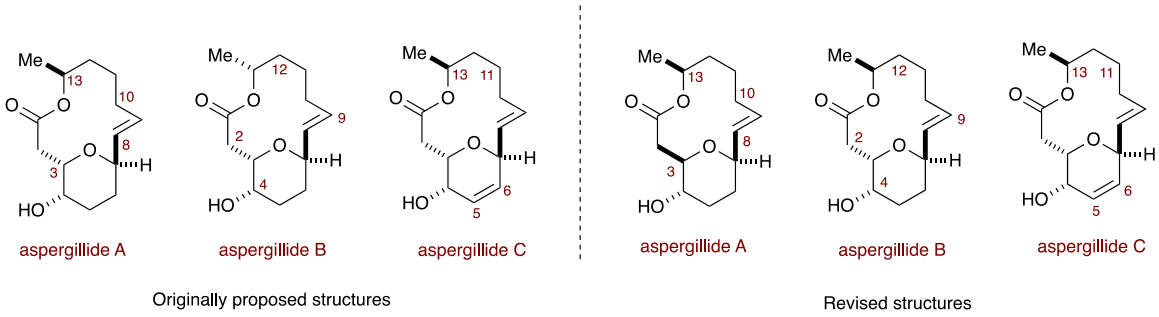

Figure 1.6 – *Aspergillide family of THP/DHP-containing 14-membered macrolactones.*

The first total synthesis of aspergillide A was attempted by Uenishi and coworkers in 2009.[89] However, the spectral data of the synthetic aspergillide A was non-identical with aspergillide A, but did match with naturally occurring aspergillide B. This discrepancy led to a structural revision of the two natural products and Kusumi and coworkers unequivocally determined the correct structure for aspergillide A and B via X-ray crystallography.[87] After the structural revision, more than seven syntheses have been reported for aspergillide B,[90] including Kuwahara (2009),[90a] Marco (2009),[90b] She (2009),[90c] Jennings (2010),[90d] Trost (2012),[90e] Srihari (2013)[90f] and Yadav (2018).[90g] More than ten syntheses have been reported for aspergillide A[91], including Kuwahara (2010),[91a] Marco (2010),[91b] Fuwa (2010),[91c] Yadav (2010),[91d] Takahashi (2011),[91e] Shishido (2011),[91f] Kuwahara (2011),[91g] Marco (2011),[91h] Gomez and Fall (2011, formal synthesis).[91i] More recently Fuwa (2013),[91j], Commu (2015, formal synthesis),[91k] and Loh

(2015)[91l] have carried out syntheses.[i] For aspergillide C, five total syntheses have been reported,[92] Kuwahara (2009),[92a] Waters-(2009),[92b] Shishido (2011),[92c,d] and Srihari (2011).[92e] For the purpose of this chapter review, selected applications with unique synthetic strategies for each natural product will be discussed.

In 2012, Trost[90e] and coworkers reported a highly efficient total synthesis of aspergillide B utilizing a Zn-ProPhenol-catalyzed asymmetric alkyne addition[93] in conjunction with a Ru-catalyzed *trans*-hydrosilylation (Scheme 1.11).[94] Final macrolide core synthesis was achieved via a macrolactonization using Yamaguchi-conditions. The C3/C7 *trans*-substituted pyran ring was generated via an intramolecular oxy-Michael addition of the corresponding α, β-unsaturated ester moiety.

Scheme 1.11 *Synthetic strategies to aspergillide B.*

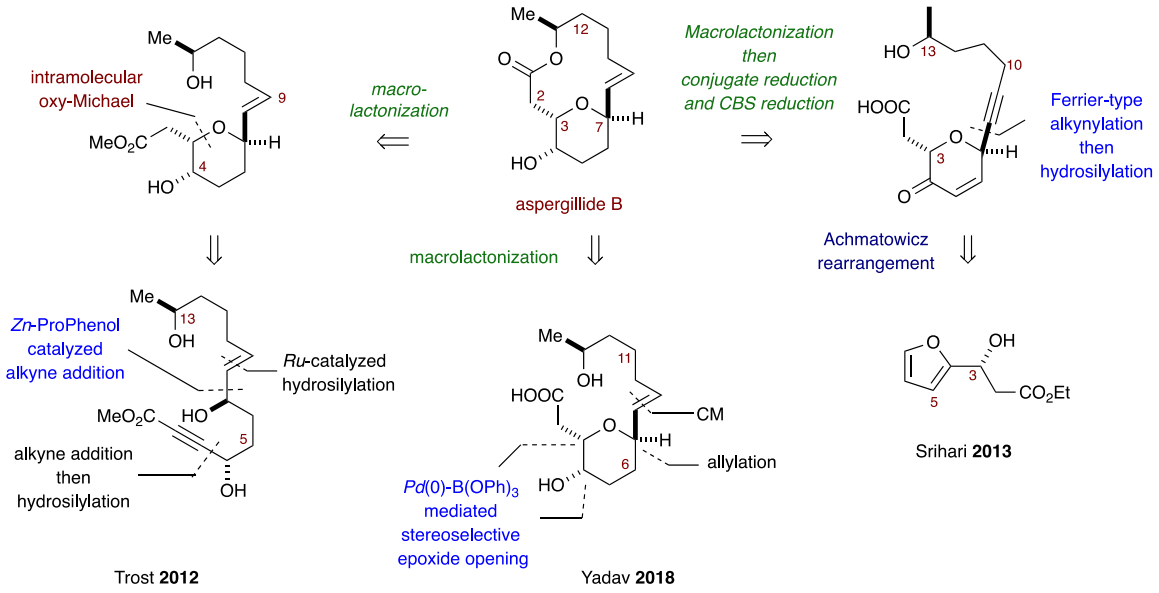

[i] Note: references 91c, 91f, 91h and 91k describe the formal and total syntheses of both natural products aspergillide A and B].

In 2013, Srihari carried out the total synthesis of aspergillide B and 7-*epi*-aspergillide A (Scheme 1.11).[90f] The synthesis of the key acetal intermediate was generated via an Achmatowicz rearrangement.[95] Subsequent Ferrier-type alkynylation,[96] followed by hydrosilylation—similar to the approach Trost and coworkers[94] used in the above protocol, delivered the *seco*-acid for the macrolactonization. Final CBS-reduction[75] completed the synthesis.

In 2018, Yadav and coworkers carried out the total synthesis of aspergillide B utilizing a highly diastereoselective Pd(0)-$B(OPh)_3$ mediated *syn*-*vic*-diol formation from an epoxide[97] to generate the C3/C4 carbinol centers (Scheme 1.11).[90g] Synthesis of the C3/C7 *trans*-substituted pyran ring was achieved via an iodine-catalyzed allylation strategy developed by their group.[98] Cross metathesis and subsequent macrolactonization delivered the final macrolide.

In 2010, Kuwahara and coworkers reported the first total synthesis of aspergillide A (Scheme 1.12).[91a] In this work, the cyclic acetal with 3,7-*trans* substitution was achieved by Ferrier-type reaction.[96] Epimerization of the C3 position for the synthesis of aspergillide A was carried out utilizing the Massi–Dondoni protocol[99] employing proline as the epimerization catalyst. Julia–Kocienski olefination[100] and Yamaguchi macrolactonization completed the synthesis.

In 2010, Fuwa and coworkers completed the total synthesis of both aspergillide A and B macrolides by accessing a common intermediate (Scheme 1.12).[91c] The pyran ring with required *cis*-stereochemistry was furnished via an intramolecular oxy-Michael

reaction. Utilization of Suzuki-Miyaura coupling,[101] followed by Yamaguchi macrolactonization, completed the synthesis.

In 2015, Loh and coworkers demonstrated the synthesis of aspergillide A macrolide core, whereby all the carbon atoms of the molecule originated from biomass derived platform chemicals such as ethanol, levulinic acid and 5-hydroxymethylfurfural (Scheme 1.12).[91l] The synthesis of the key pyran ring was carried out by an Achmatowicz rearrangement.[95] Subsequent Negishi coupling,[102] and a macrolactonization, completed the synthesis.

Scheme 1.12 *Synthetic strategies to aspergillide A.*

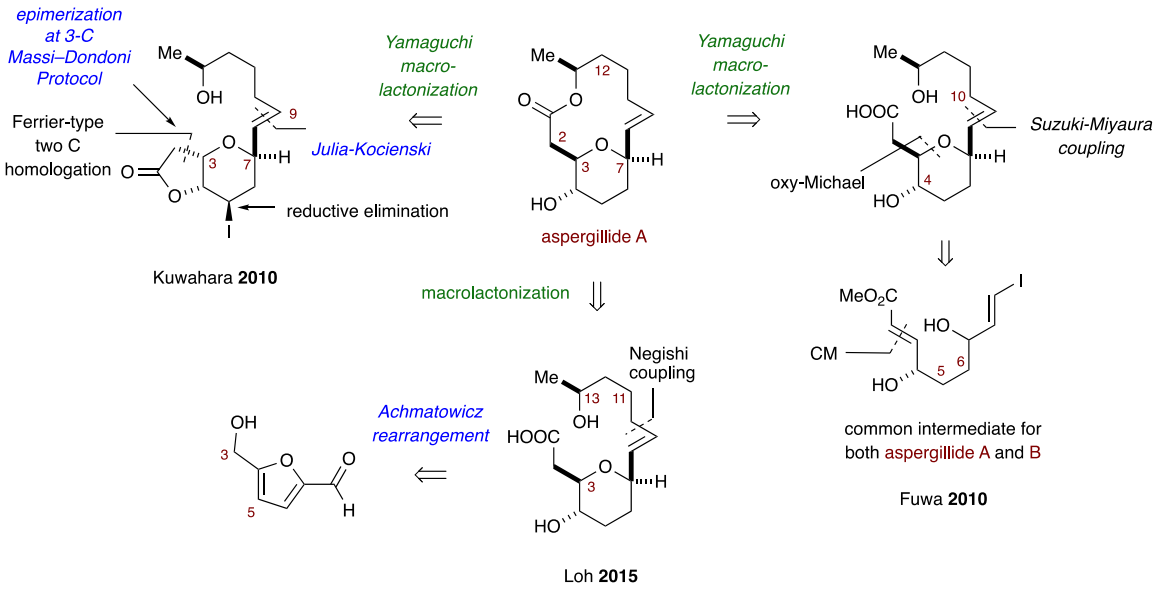

In 2009, Waters and coworkers completed the synthesis of aspergillide C.[92b] Installation of the C3/C7 *trans*-substituted dihydropyran ring was achieved by a Ferrier-type addition,[96] followed by a Pd-catalyzed oxidative lactonization.[103] An *E*-selective Julia-Kocienski[100] olefination, and a subsequent macrolactonization, were utilized to complete the synthesis (Scheme 1.13).

In 2011, Shishido and coworkers utilized a transannular oxy-Michael reaction to install the C3/C7 *trans*-substituted tetrahydropyran ring in their synthesis of aspergillide C.[92d] Synthesis of the *seco*-acid precursor was carried out with a CM reaction, followed by HWE Wittig[29] olefination. After the macrolactonization event, a transannular oxy-Michael reaction was performed to generate aspergillide C (Scheme 1.13).

Scheme 1.13 *Synthetic strategies to aspergillide C.*

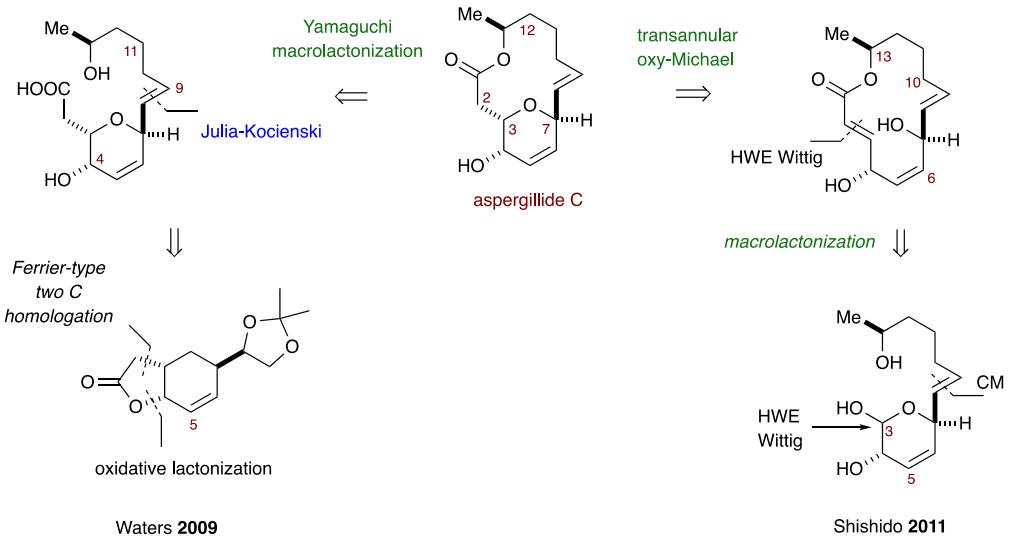

Neopeltolide is a THP-containing macrolide isolated in 2007 by Wright and coworkers from the deep–water sponge family Neopeltidae.[85] The first proposed structure of neopeltolide was revised by Panek and coworkers after their first total synthesis in 2007 (Figure 1.7).[104] Along with its intriguing chemical architecture, neopeltolide has a unique pharmaceutical profile, demonstrating extremely potent anti-proliferative activity against cancer cell lines, including P388 murine leukemia (IC_{50} = 0.56 nM), A-549 human lung

adenocarcinoma (IC_{50} = 1.2 nM), and NCI-ADR-RES human ovarian sarcoma (IC50 = 5.1 nM). Additionally, it has shown significant cytostatic inhibitory effects in PANC-1 pancreatic and DLD-1 colorectal cell lines. Neopeltolide also exhibits potent antifungal activity against pathogenic yeast *Candida albicans*.[105] Neopeltolide has attracted much attention within the synthetic community due to its potent biological activity, as well as the challenging chemical structure, thus inspiring a number of total[106] and formal syntheses.[107]

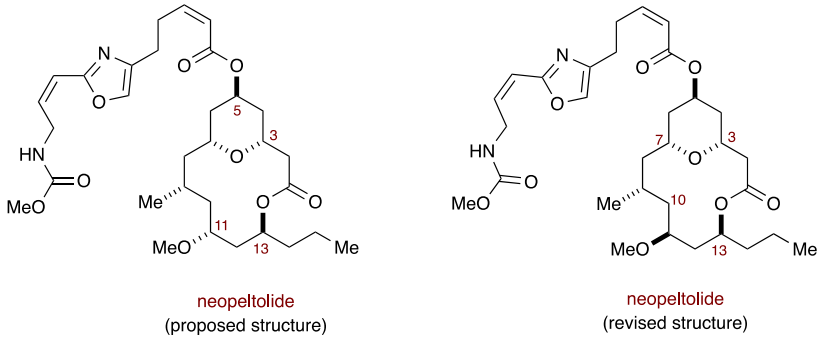

Figure 1.7 *Neopeltolide and revised structure*.

In 2015, Dai and coworkers provided the field with an excellent comprehensive review of all total syntheses in chronological fashion, mainly focusing on the construction of the *cis*-tetrahydropyran-containing macrolactone core (Figure 1.14).[108] In 2016, Fuwa also summarized total and formal syntheses of neopeltolide as well as analog syntheses.[109] For the purpose of this Chapter, two notable bodies of work— contained in the Dai review, are highlighted below (Dai in 2014, and Hoveyda in 2015), along with one total synthesis by Kadota in 2019. It is also worth noting that one additional formal synthesis was reported by Boddy in 2016,[107i] and one analog synthesis of fluorescence-labeled neopeltolide derivatives was reported by Fuwa in 2019.[107j]

In 2014, Dai and coworkers applied their Pd-catalyzed alkoxycarbonylative macrolactonization method to synthesize 9-demethylneopeltolide, a simplified analog of neopeltolide with similar biological activity (Scheme 1.14).[106n] The linear precursor was synthesized utilizing a similar approach reported in the synthesis of neopeltolide by Fuwa in 2008.[106f] Subsequent Pd-catalyzed alkoxycarbonylative macrolactonization conditions[110] delivered the C3/C7 *cis*-substituted pyran ring, while final ketal removal and substrate-controlled reduction delivered the macrolactone.

In 2015, Hoveyda and coworkers reported an elegant synthesis of neopeltolide where they utilized catalyst controlled stereoselective olefin metathesis[111] throughout, including enantioselective ring-opening cross metathesis (ROCM) for synthesizing the THP ring, as well as Z-selective CM as key steps (Scheme 1.14).[106o] The installation of the

Scheme 1.14 *Recent representative synthetic strategies to neopeltolide.*

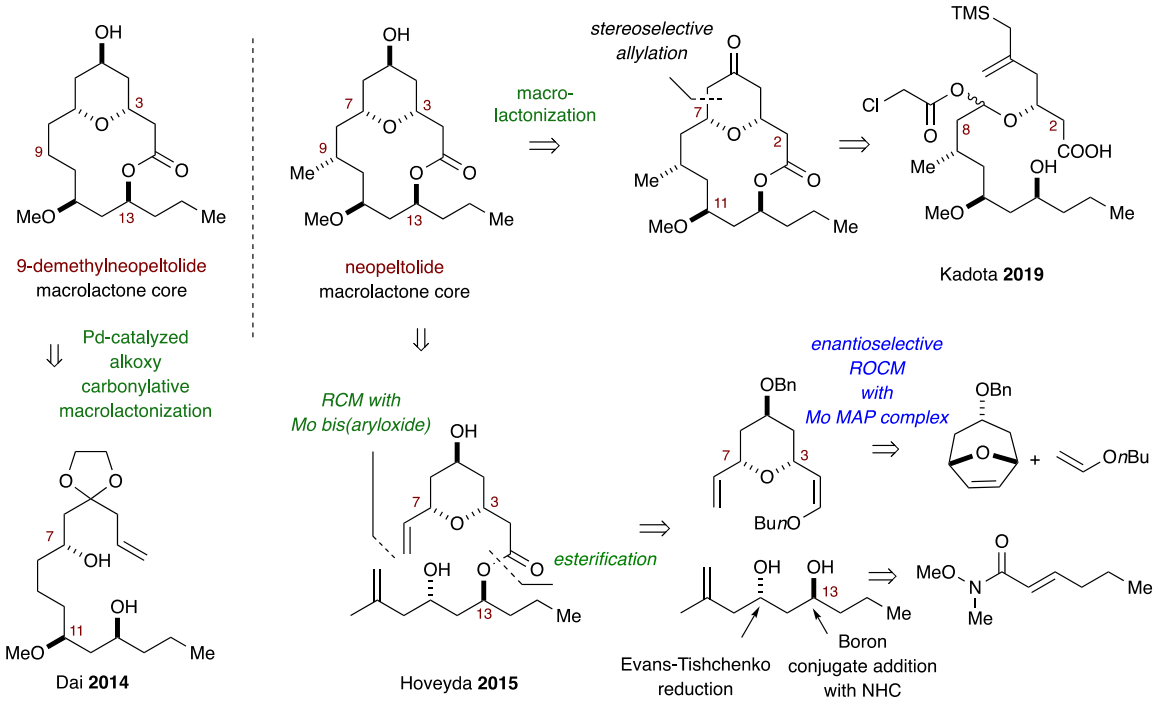

1,3-*anti*-diol subunit was carried out via enantioselective boron conjugate addition with a chiral NHC catalyst,[112] followed Evans-Tishchenko reduction.[47] Final macrolactone synthesis was carried out via a macrocyclic RCM using the Hoveyda-Schrock bis(aryloxide) Mo-catalyst.[113]

In 2019, Kadota and coworkers reported a stereoselective synthesis of the macrolactone core of the neopeltolide (Scheme 1.14).[106p] The *cis*-THP ring was generated via a key intramolecular allylation of an α-acetoxy ether, and final macrolactonization was used to deliver the macrolide core.

Paecilomycin B is another 14-membered macrolide isolated by Chen and Wei in 2010 from mycelial solid cultures of *Paecilomyces* sp (Figure 1.8).[86] SC0924 along with other secondary metabolites paecilomycin A, C–F.[86] Paecilomycins showed high to moderate antiplasmodial activities. Later, paecilomycins G–I[114] and Paecilomycins J–M[115] were isolated and characterized. Interestingly, only paecilomycin B contains a characteristic THP ring. The remainder of the 14-membered paecilomycins, namely paecilomycins A, E, F, G, and I are benzofused (benzannulated) macrolides, while paecilomycins J, L, K and M possess a tetrahydrofuran (THF) moiety. A more detailed discussion of the retrosynthesis of additional macrolactones within the family of fused 14-membered paecilomycins, will be highlighted later on in this chapter.

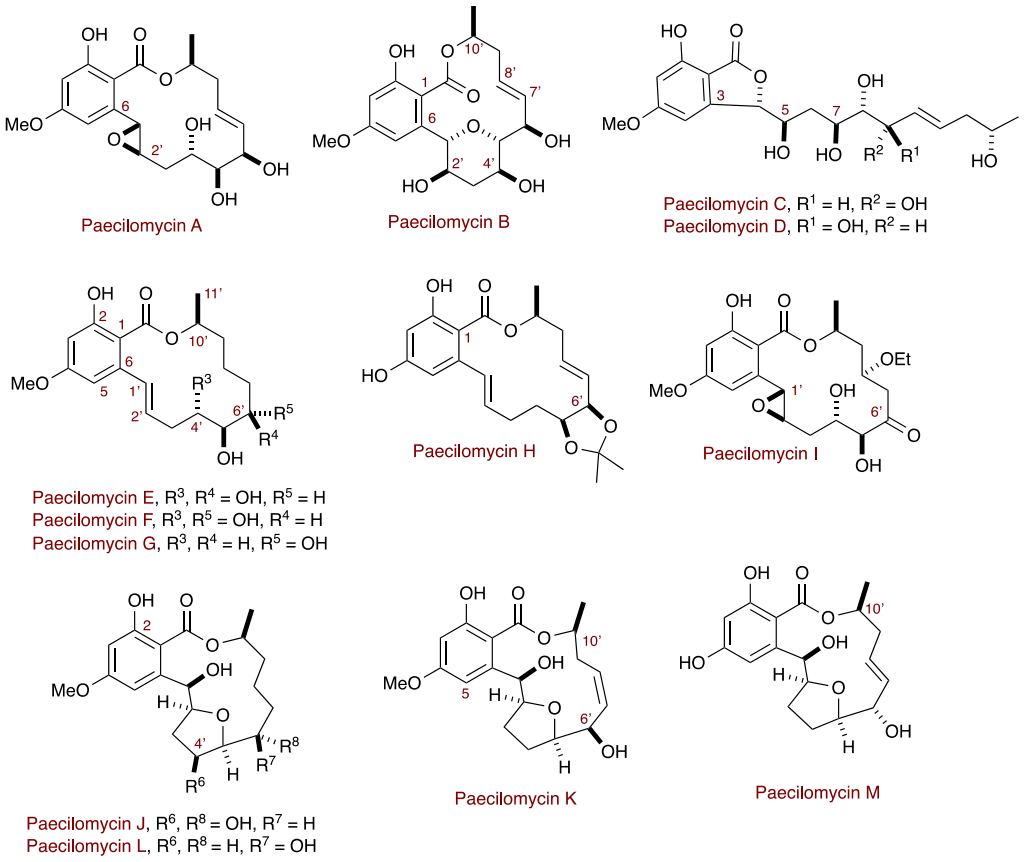

Figure 1.8 *Paecilomycin family of fused-aromatic/-THF 14-membered macrolactones*.

In 2015, Nakata and coworkers reported the first of two total syntheses of the macrolide paecilomycin B, containing a fused benzene ring and a *cis*-tetrahydropyran (THP) moiety as the key structural features (Schemes 1.15).[116] The synthesis of the macrolactone core was achieved via a key RCM macrocyclization reaction. The diene precursor was derived from a spiroketal, which was generated via a Barbier-type coupling reaction[117] of the δ-lactone and aryl bromide, as well as a Mitsunobu esterification reaction.[118]

In 2018, Nakata and coworkers[119] explored two different macrocyclization strategies utilizing (i) an intramolecular Nozaki–Hiyama–Kishi (NHK)[50] coupling reaction onto an alpha-THP-substituted aldehyde and (ii) an intramolecular nucleophilic addition reaction of an aryl iodide to establish the *cis*-fused THP ring. By employing these two methods, the authors were able to achieve the synthesis of paecilomycin B and 6′-epi-paecilomycin B (Scheme 1.15).

Scheme 1.15 *Synthetic strategies to paecilomycin B*.

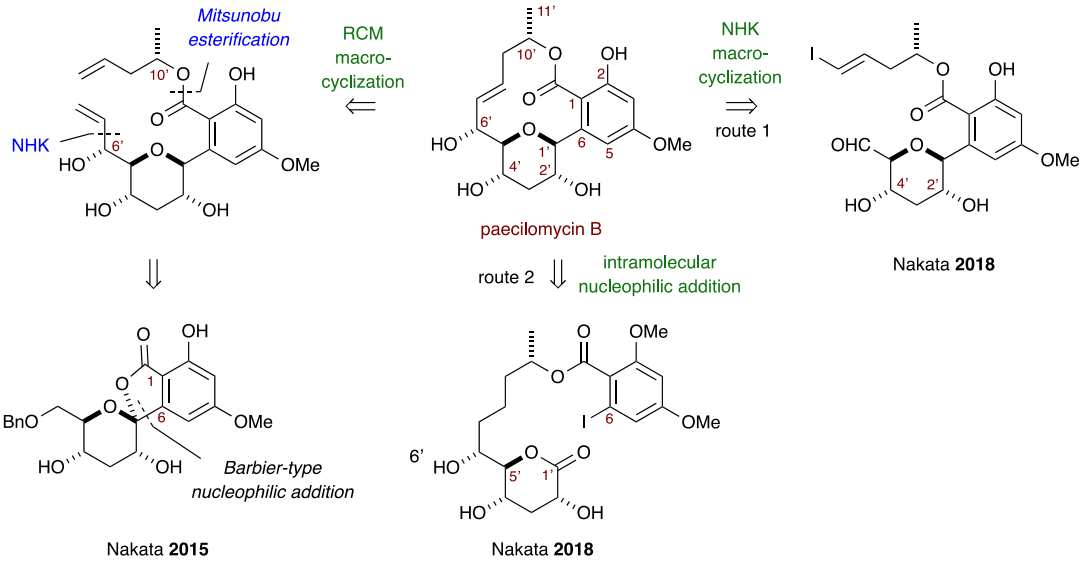

1.3.3 Pyran hemiketal subunit-containing macrolactones.

14-membered macrolides containing a pyran hemiketal subunit are a diverse subfamily of macrolides with a wide range of pharmaceutical profiles, particularly anti-cancer activity. Macrolides (–)-lyngbouilloside,[120] (–)-lyngbyaloside B[121], auriside[122] and callipeltoside A belong to this subfamily of macrolides with similar structural features and interesting biological activities. A number of total and formal syntheses have been reported for the above natural products and will be briefly discussed in this section.

(–)-Lyngbouilloside and (–)-lyngbyaloside B are two related cytotoxic 14-membered macrolides that were isolated in 2002 by Hoffmann and coworkers from two different marine cyanobacteria of the genus *lyngbya bouillonii* (*Oscillatoriaceae*).[123] Biological studies carried out by the Gerwick[120] and Moore[121] groups discovered, lyngbouilloside exhibited moderate cytotoxic activity towards neuroblastoma cells (IC_{50} = 17 μM),[120] while lyngbyaloside B was weakly cytotoxic against KB cell lines (IC_{50} = 4.3 μM) (Figure 1.9).[121]

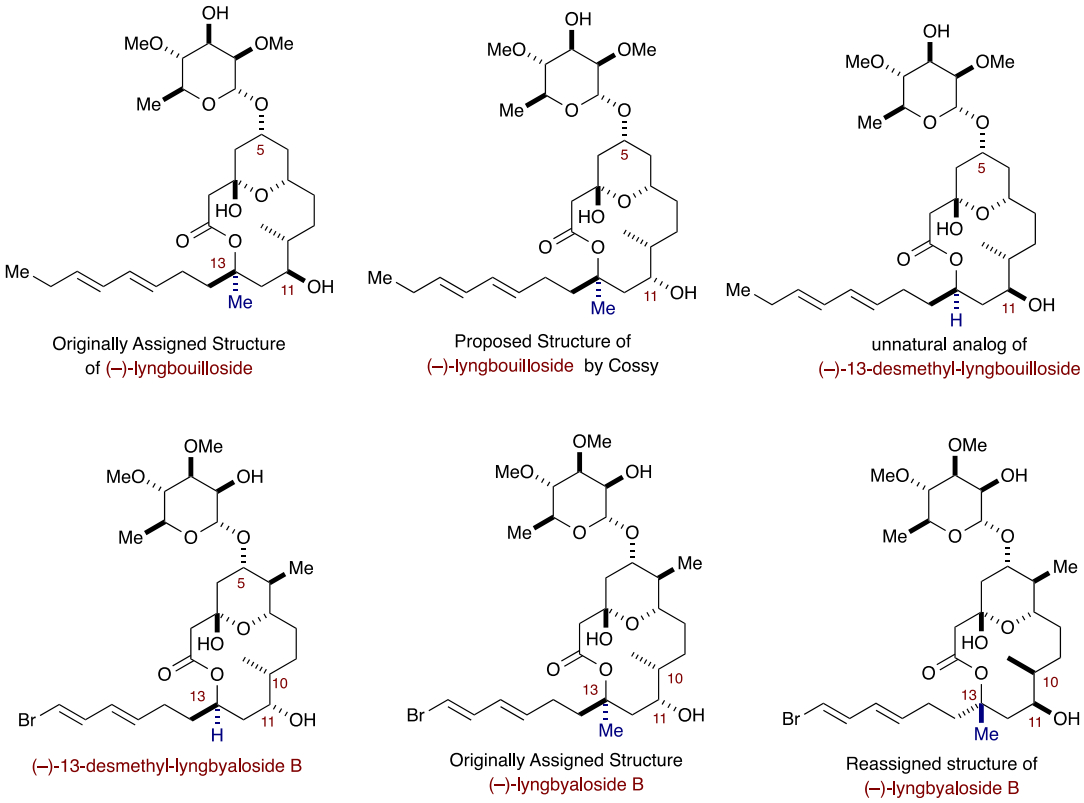

Figure 1.9 *(–)-Lyngbouilloside and (–)-lyngbyaloside B and 13-desmethyl variants.*

The original structure of lyngbouilloside was determined after exhaustive 1D and 2D NMR analysis, HR-FABMS, IR, and UV absorption experiments, which revealed the presence of a glycosylated 14-membered macrolactone, three secondary carbinol stereogenic centers at C5, C7, and C11, as well as a tertiary carbinol stereogenic center at C13 (Figure 1.9). The original structural analysis also revealed the relative configuration of the stereogenic centers in the aglycon portion of the natural product, a methyl-bearing stereogenic center at C10 of the macrolactone with *anti*-C10/11 stereochemistry, and an embedded C3/C7-*cis*-disubstituted pyran possessing a pyranyl hemiketal at C3. The macrolactone also possesses a pendant *E*,*E*-configured octyldienyl side chain, and an L-rhamnose-derived glycoside conjugated at the C5 carbinol center.[120]

In 2012, Cossy and coworkers proposed a change of stereochemistry at the C11 carbinol center and revised the structure of (–)-lyngbouilloside through synthetic studies, *vide infra*.[124] The nature of the sugar, was assigned by correlations in the ^{1}H-^{1}H COSY and HMBC spectral data and comparison with the sugar unit present in auriside A. In concurrent total synthetic work on lyngbyaloside B, Fuwa in 2016 would reassign C10, C11 and C13 and shed light on a potential similar issue within lyngbouilloside, *vide infra*.[125]

Due to stereochemical ambiguities, biological activity and natural scarcity, these analogs have attracted several synthetic efforts, most recently reviewed by Cossy and coworkers in 2013.[126] The first three retrosynthetic approaches by Ley, Cossy and Fuwa en route to nominal (–)-lyngbouilloside and (–)-13-desmethyllyngbyaloside B are outlined in Scheme 1.16. In 2008, Cossy and coworkers, reported the first stereoselective synthesis

of the carbon backbone of nominal (–)-lyngbouilloside using a key cross-metathesis (CM) between the C1–C8 and C9–C13 fragments.[127] In 2009, Ley and coworkers reported a synthesis of the lyngbouilloside macrolactone core using an aldol disconnection at the C2/C3 bonds and a late-stage ring-closing metathesis (RCM)/hydrogenation sequence for macrocyclization.[128] In the Ley work, the authors used spectroscopic analysis and DFT chemical shift calculations to reveal stereochemical issues regarding this natural product.

In 2012, Cossy and coworkers completed the first total synthesis of the (–)-lyngbouilloside aglycon using a pivotal acylketene macrolactonization of the C13 tertiary methyl carbinol and verified the stereochemical issues previously reported by Ley (Scheme 1.16).[124] In this work, the Boeckman acylketene macrocyclization[129,130] allowed Cossy to circumvent fundamental issues associated with macrolactonization events of sterically encumbered alcohols. It is worthy to note, efforts by Hoye and coworkers in 2008 who reported a dual macrolactonization/pyran–hemiketal formation event using acylketenes with applications to the synthesis of (−)-callipeltoside A and a lyngbyaloside B model systems.[131]

In their synthesis of (–)-lyngbouilloside, Cossy proposed the aforementioned revised structure of lyngbouilloside with stereochemical reassignment of the C11 stereogenic center as the C11-epimer, and thus a potential C10/C11 *syn* relationship that the authors would later revisit in a 2016 report, *vide infra*.[132] In 2012, Taylor and coworkers reported a stereoselective synthesis of the C9–C19 fragment of related lyngbyaloside B and C, highlighted by an extension of their ether transfer method, which enables the formation of tertiary ethers.[133]

In 2013, Fuwa and co-workers initially reported the total synthesis of (–)-13-desmethyl lyngbyaloside B, bearing a secondary carbinol at C13 using a Yamaguchi esterification/RCM strategy for the efficient cyclization to the macrocycle (Scheme 1.16).[134] In this work, the authors also reported reliable methods for the introduction of the conjugated diene side chain and the L-rhamnose residue onto the macrocyclic framework.

Scheme 1.16 *Synthetic strategies to originally/nominally assigned structure of (–)-lyngbouilloside, lyngbyaloside B/C, and (–)-13-desmethyl lyngbyaloside B.*

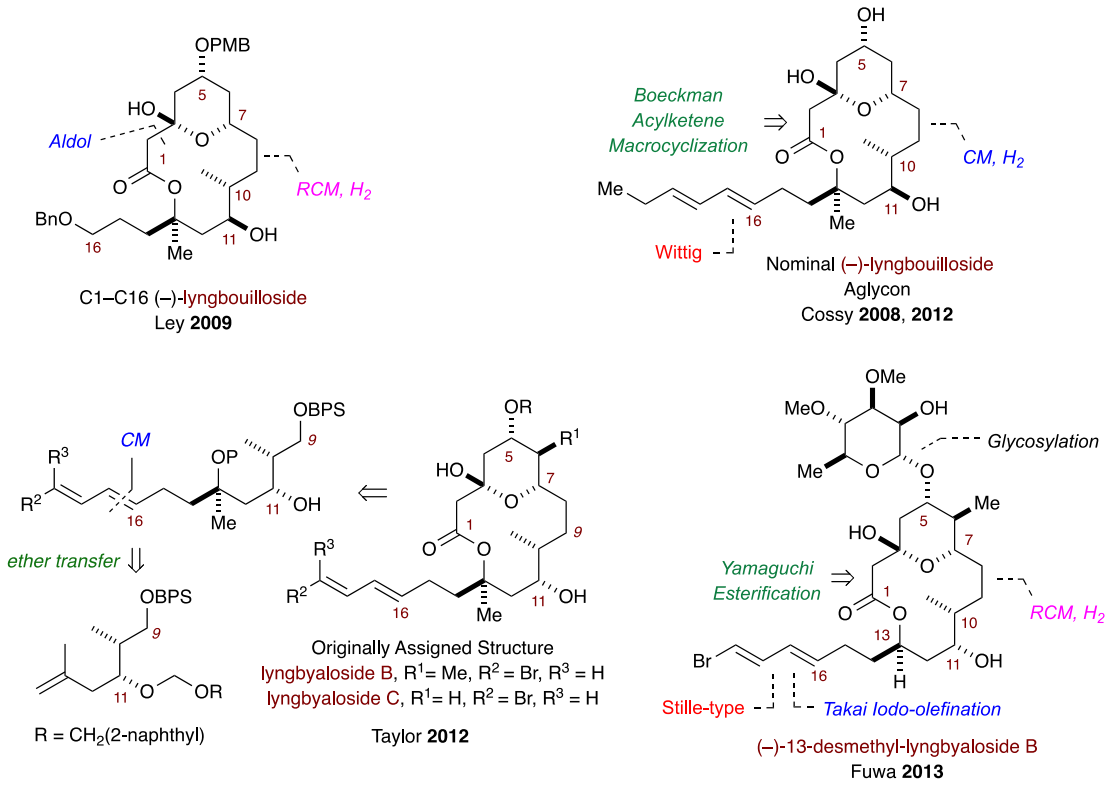

In 2013, Yadav and coworkers,[135] reported a highly stereoselective synthesis of the C1–C16 macrolactone core segment of the cytotoxic macrolide lyngbyaloside B. A crucial intermolecular acylketene trapping (Boeckman esterification) by the tertiary C13 carbinol, and a subsequent RCM served to unite the northern and southern hemisphere subunits to

construct the macrolactone core (Scheme 1.17). In 2014, Yadav reported the synthesis of C1–C8 and C9–C16 fragments of the revised structure of (–)-lyngbouilloside starting from geraniol and D-malic acid.[136]

In 2015[137] and 2016,[125] Fuwa and coworkers reported an elegant total synthesis of (–)-lyngbyaloside B (**2b**), where they employed an innovative use of an Abiko–Masamune *anti*-aldol and a vinylogous Mukaiyama to install the requisite stereochemistry in the starting building blocks and used the Boeckman acyl ketene method for macrocyclization (Scheme 1.17). Fuwa and coworkers made stereochemical reassignment of (–)-lyngbyaloside B having epimeric stereogenic centers at C10/C11 and C13 as shown for the reassigned lyngbyaloside B (Figure 1.9 and Scheme 1.17) when compared with the original assigned structure of lyngbyaloside B. Synthetic, spectroscopic and molecular modeling studies collectively provided unequivocal proof. The authors also surmised that the structures of (–)-lyngbouilloside and the natural congeners of (–)-lyngbyaloside B be reconsidered accordingly, which Cossy and coworkers corroborated in their 2016 report, *vide infra*.

Scheme 1.17 *Synthetic strategies to lyngbyaloside B.*

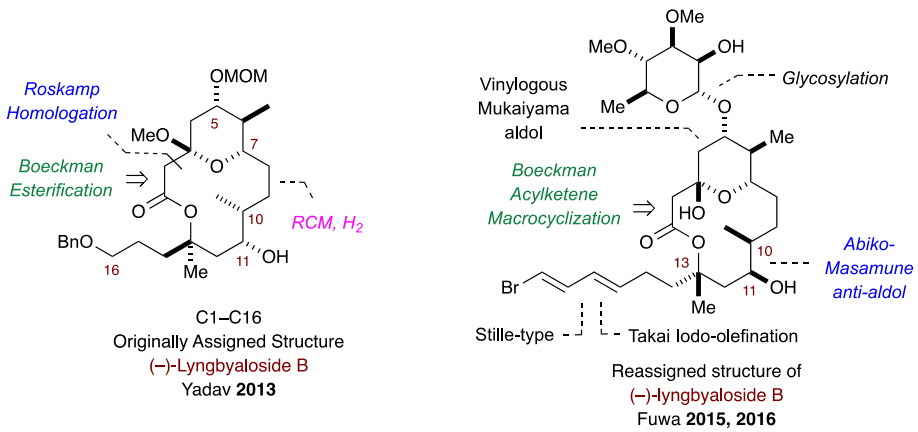

In 2015, Hanson and coworkers reported the synthesis of the originally assigned structure of lyngbouilloside macrolactone (Scheme 1.18). The core macrocycle was synthesized via a phosphate tether-mediated, one-pot, sequential RCM/CM/ chemoselective hydrogenation reaction, Roskamp homologation,[138] and a high yielding Boeckman acylketene cyclization.[139]

In 2016, Cossy and coworkers,[132] reported an elegant total synthetic effort to the putative 11-epi-lyngbouilloside aglycon featuring a Boeckman esterification, RCM strategy to form the 14-membered ring macrolactone, Wittig olefination for late-stage sidechain introduction, and a glycosylation for installation of rhamnose (Scheme 1.18). In this work, the authors provided careful and detailed analysis of the spectroscopic data of their synthetic product with the original data reported for lyngbouilloside, and noted that discrepancies still remained. Taken collectively, their work on the C11-epimer substantiate the aforementioned total synthetic and reassignment efforts within C10, C11 and C13 stereotriad of lyngbyaloside B reported by Fuwa and coworkers,[125,137] and set the stage for similar work on lyngbouilloside.

Scheme 1.18 *Synthetic strategies to the original assignment of lyngbouilloside and 11-epi-lyngbouilloside.*

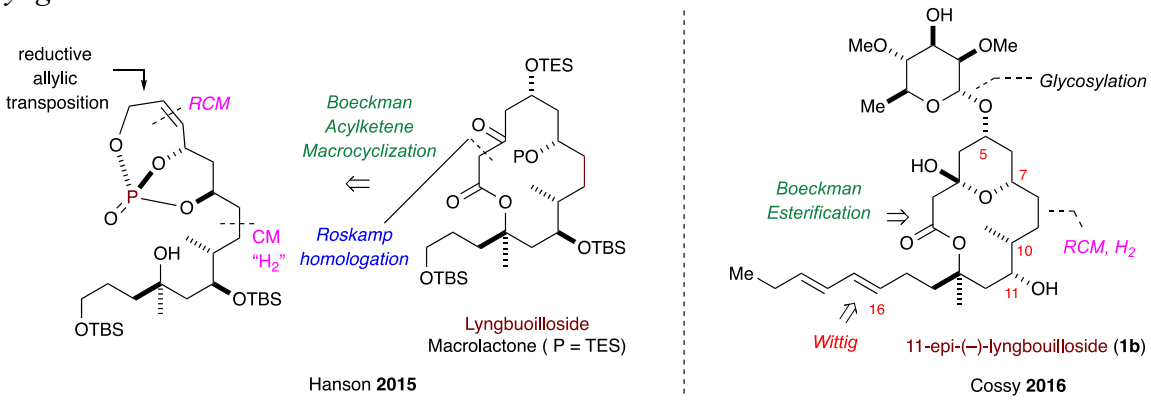

In 2021, Hanson group reported application of an iterative use of a one-pot, sequential RCM/CM/chemoselective hydrogenation protocol for the synthesis of the C1–C16 polyol-containing macrolactone of 13-desmethyl lyngbouilloside, bearing the originally assigned macrolactone core at the C10/C11 and C13 stereocenters (Scheme 1.19).[66] Linear precursor for the key pyran mixed-ketal formation step was generated via an iterative phosphate tether mediated RCM/ CM/ chemoselective hydrogenation protocol, where the C10 methyl stereocenter was installed by a regio- and diastereoselective anti-S_N2' displacement of the allylic phosphate within the bicyclo[4.3.1]phosphate. Reductive allylic transposition of bicyclic phosphate intermediate followed by modified Johnson-Lemieux protocol[140] and subsequent Roskamp homologation[138] afforded β-keto ester which set the stage for the key pyran mixed-ketal formation. Acid-catalyzed pyran mixed-ketal formation and subsequent Yamaguchi macrolactonization delivered the mixed-ketal, macrolactone aglycone core of (–)-13-desmethyl-lyngbouilloside, albeit in low yield (~25 %, bsrm).

Scheme 1.19 *Synthetic strategy to 13-desmethyl lyngbouilloside.*

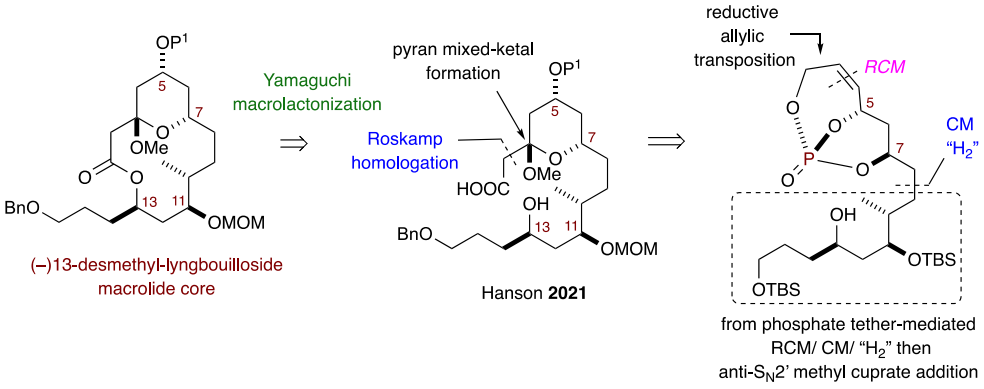

Callipeltoside A, B and C are structurally similar 14-membered macrolides which contain a pyran hemiketal moiety (Figure 1.10). Callipeltoside A, B and C were isolated by Minale and coworkers in 1996 from the shallow water lithistida marine sponge *Callipelta* sp.[141] Interestingly, the callipeltosides have a common macrolide core with a tetra-substituted tetrahydropyran (THP) hemiketal motif embedded into the 14-membered macrolactone, and only differ at the attached sugar unit, which plays an important role in moderating cytotoxic activity against human bronchopulmonary NSCLC-N6 (IC_{50} values are shown in Figure 1.10).

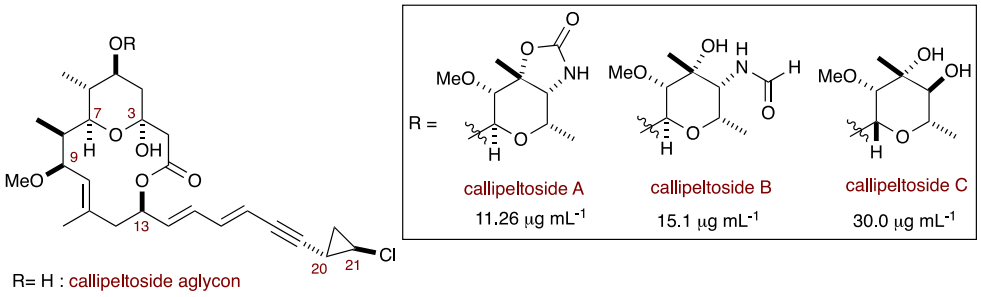

Figure 1.10 *Callipeltoside A, B and C possessing THP-hemiketal subunit.*

The callipeltoside family has attracted significant attention due to their potent biological activities and challenging chemical architecture. A number of synthetic efforts for the total synthesis of this natural product have been reported during the past two decades. The absolute and relative configurations of stereocenters C13, C20 and C21 remained unresolved after initial isolation. The relative configuration of C13 was first established by Paterson in 2001, during their initial efforts towards the synthesis of callipeltoside A aglycon.[142] In 2002, Trost and coworkers carried out the first total synthesis of (–)-callipeltoside A while reporting the unambiguous assignment of the

absolute and relative configuration of the natural product.[143] Next , the Evans (2002),[144] Panek (2004)[145] and Hoye (2008)[146, 131b] groups successfully carried out the total synthesis of callipeltoside A.

In 2008, MacMillan group completed the first total synthesis of callipeltoside C, reassigning the stereochemistry of the sugar molecule form *D*- to *L*-configured.[147] In 2012 Ley and coworkers completed the callipeltoside series by synthesizing callipeltoside B.[148] Synthetic strategies towards callipeltosides have been reviewed extensively. In 2005, Paterson and coworkers summarized the contributions of Paterson, Trost, Evans and Panek groups toward the synthesis of callipeltoside A.[149] In 2013, Hussain and coworkers reported a broad review of all the total syntheses, formal syntheses, fragment syntheses and carbohydrate derivative syntheses.[150] Very recently, Ley and coworkers published a book chapter entitled "The Callipeltoside Story".[151] In this regard, only the total synthetic approaches toward callipeltosides will be discussed.

In 2001, Paterson and coworkers reported the first synthesis of callipeltoside aglycon, followed by the total synthesis of callipeltoside A in 2003 adapting the same reaction sequence (Scheme 1.20).[142,152] In this work, generation of the acyclic precursor for the hemiketal formation and subsequent macrolactonization was carried out via a sequence of aldol reactions. A Yamamoto vinylogous aldol reaction[153] was employed to install the racemic 13-carbinol center. A boron-mediated *anti*-aldol reaction[154] was employed for the installation of the 9-carbinol center, and an Evans-Tishchenko reduction[47] was used to set the 1,3-*anti*-diol subunit after β-keto ester formation, which was carried out via a Mukaiyama aldol reaction[155] Acid-catalyzed hemiketal formation,

followed by Yamaguchi macrolactonization, delivered the aglycon. The total synthesis of callipeltoside A was achieved via late-stage Sonogashira coupling and Schmidt-type glycosylation.[156]

In 2002, Trost and coworkers performed the first total synthesis of callipeltoside A detailing the absolute and relative stereochemistry of the molecule (Scheme 1.20).[143] The synthesis of the aglycon was achieved via a key ruthenium-catalyzed Alder-ene-type reaction[157] to install the trisubstituted alkene, and a stereoselective Pd-catalyzed allylic alkylation[158] was employed to install the C13 carbinol stereogenic center. The authors used a Cram-type addition to install the C6/C7-stereodiad and a Mukaiyama aldol reaction to

Scheme 1.20

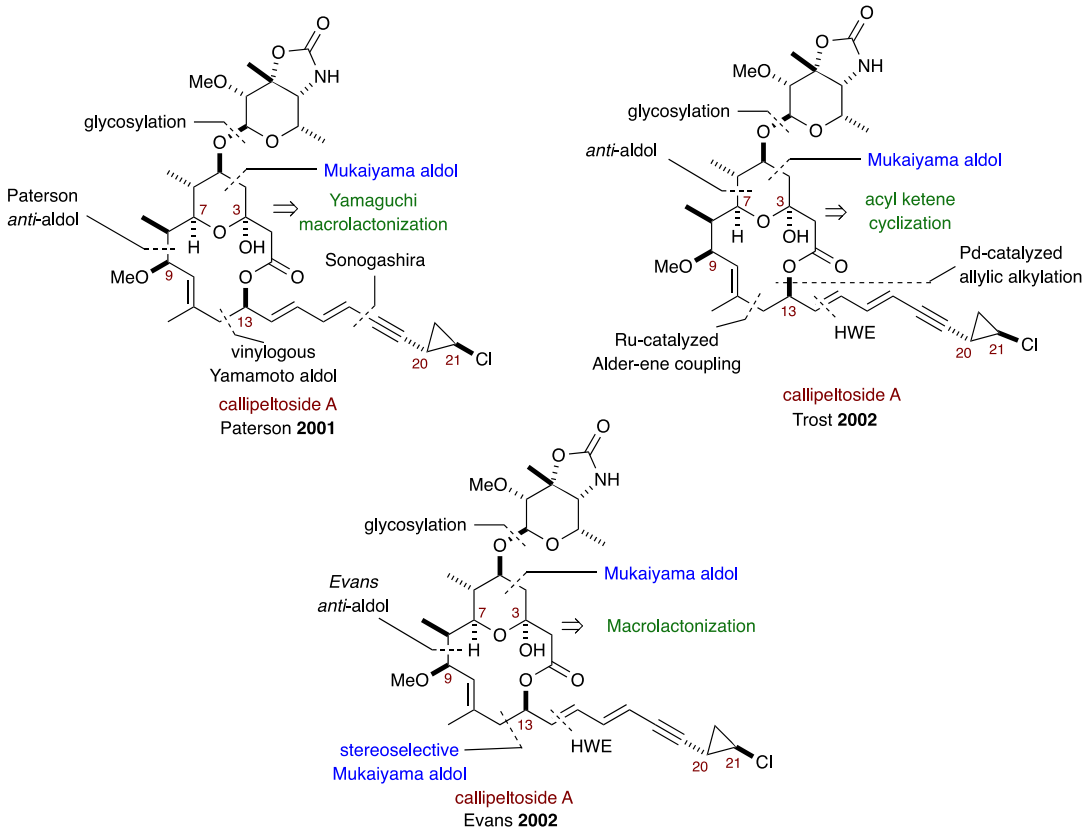

generate the acyclic dioxolanone precursor. Macrolactonization was carried out via the Boeckman method[129] of acylketene trapping with the C13 carbinol and concomitant hemiketal formation. The authors used both a HWE olefination and olefin cross metathesis to connect the side chain to the aglycone, with final glycosylation completing the synthesis.

In 2002, Evans and coworkers employed a sequence of aldol reactions to generate the acyclic precursor for the macrolactonization (Scheme 1.20).[144] This synthetic approach with three aldol disconnections was similar to the Paterson synthesis where the C13 stereocenter was installed via a vinylogous Mukaiyama aldol.[142] However, for the crucial C8–C9 anti-aldol reaction, they utilized an Evans oxazolidinone based strategy.[159] A late-stage HWE olefination to connect the side chain, and subsequent glycosylation reaction completed the synthesis.

In 2004, Panek and coworkers completed the synthesis of the aglycone of callipeltoside A by employing a Julia-Kocienski olefination[100] to install the key (*E*)-configured trisubstituted olefin (Scheme 1.21).[145] The substituted tetrahydropyran hemiketal was synthesized using an allylsilane [4+2]-annulation method developed in their group.[160] Yamaguchi macrolactonization, followed by HWE olefination, and Stille-cross-coupling furnished the aglycone with the requisite chlorocyclopropane side-chain. The synthesis was completed using a glycosylation reaction with an activated sugar moiety.

In 2008, MacMillan and coworkers reported the first total synthesis of callipeltoside C using methods develop in their lab as the key transformations (Scheme 1.21).[147] The THP moiety was synthesized utilizing an organocatalytic double diastereo-differentiating aldol reaction,[161] in combination with the Semmelhack alkoxycarbonylation.[162]

Construction of the C13 carbinol stereocenter was achieved via use of an organocatalytic formyl α-oxyamination, and subsequent reductive N–O bond cleavage.[163] Construction of the aglycone was carried out via a chelation-controlled diastereoselective alkylation with a vinyl Grignard to establish the C9 stereogenic center, followed by macrolactonization. Subsequent HWE Wittig reaction to install the C14–C21 cyclopropyl sidechain, and glycosylation of the aglycone delivered callipeltoside C.

Scheme 1.21 *Synthetic strategies to callipeltoside C.*

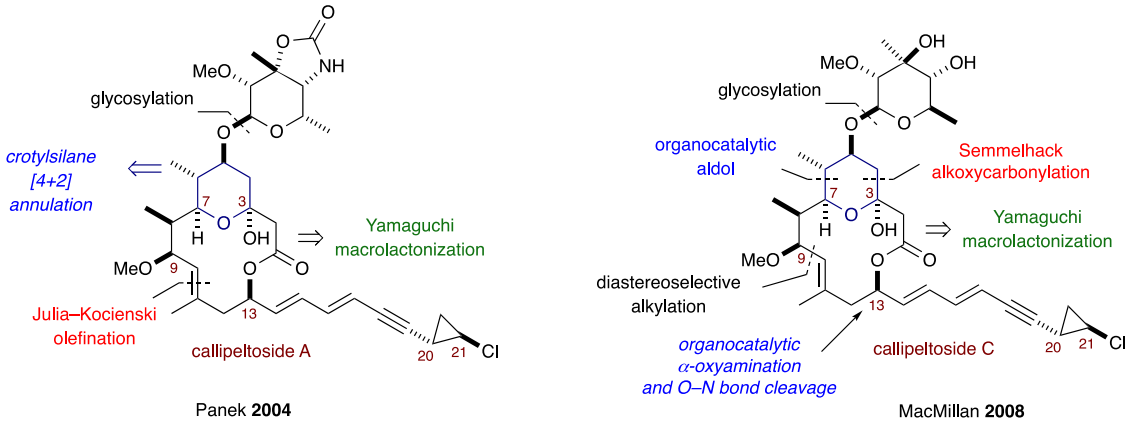

In 2010, Hoye and coworkers completed the synthesis of callipeltoside A utilizing a dual macrolactonization/pyran hemiketal formation sequence and implementation of a relay ring closing metathesis (RRCM) protocol as the key steps to furnish the macrolide core (Scheme 1.22).[148] In this work, the authors established a highly efficient acylketene mediated dual macrolactonization/pyran-hemiketal formation reaction, converting the linear precursor directly to the bridged bicyclic macrolactone, thus completing the synthesis of callipeltoside A.

In 2012, Ley and coworkers demonstrated a highly convergent approach synthesis of all three callipeltosides A, B and C (Scheme 1.22). The macrolactone core was

synthesized using a diastereoselective alkenyl metal addition to an aldehyde-containing pyran moiety to install the C9 stereocenter and complete macrolactonization. Synthesis of the *cis*-pyran was carried out via a catalytic $AuCl_3$-induced cyclization protocol developed in the Ley group.[164] The sugar moiety was installed via a glycosylation reaction where the sugars were activated as thioglycosides.

Scheme 1.22 *Synthetic strategies to callipeltoside A and B.*

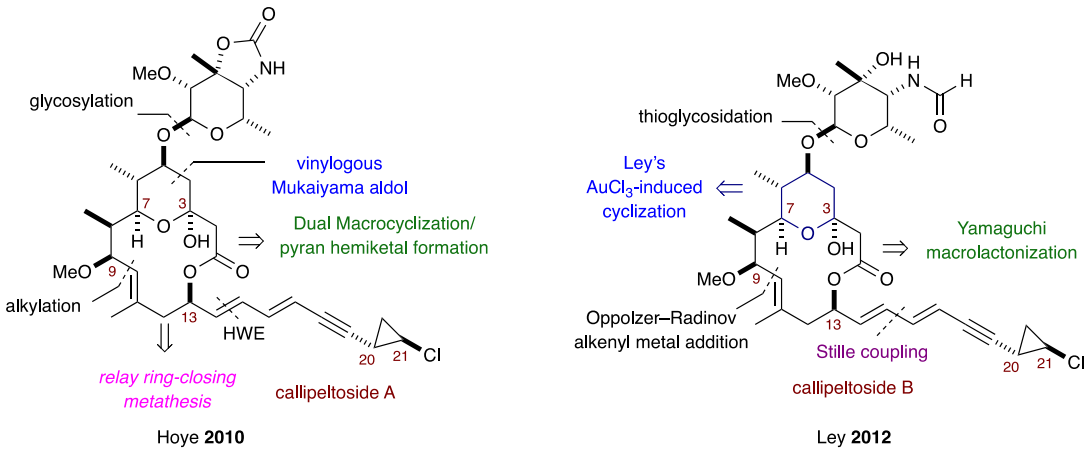

1.3.4 Fused core-containing macrolactones.

A number of families of interesting 14-membered macrolides have a variety of fused ring subunits appended to them, including: (i) fused spirotetronic acids, (ii) fused substituted decalins, (iii) fused substituted cyclohexanes, and (iv) fused phenolic rings to name a few. This interesting subclass has attracted significant attention due to their complex and diverse chemical structures, as well as potent biological activities. Isolation and total syntheses of a number within this subclass have been reported, namely (–)-chlorothricin,[165] pyrrolosporin A,[166] cytochalasin A and B (Figure 1.11),[167] paecilomycin

A, E, F,G, and I[86,114,115] (previously mentioned in Section 1.3.3), and cochliomycin A, B and C (Figure 1.12).[168]

Chlorothricin (isolated in 1972),[165] and pyrrolosporin A (1996)[166] belong to family of natural products possessing both fused spirotetronic acid and fused substituted decalin moieties. Extensive studies toward the total syntheses of chlorothricolide, the aglycon of chlorothricin, have been carried out and reviewed.[169,170] Cytochalasin A, B and F (isolated in 1967)[167] are highly potent 14-membered macrolactones with fused ring systems and a number of elegant syntheses have been reported for this family and reviewed recently.[171, 172] Furthermore, the synthesis and biological importance of resorcylic acid lactones such as paecilomycins and cochliomycins, and related macrolide, were subjected to a review by Nanda and Jana in 2018.[173] For the purpose of this Chapter, the more recently isolated paecilomycins and cochliomycins, as well as the related resorcylic acid lactones—and their total syntheses, will be discussed.

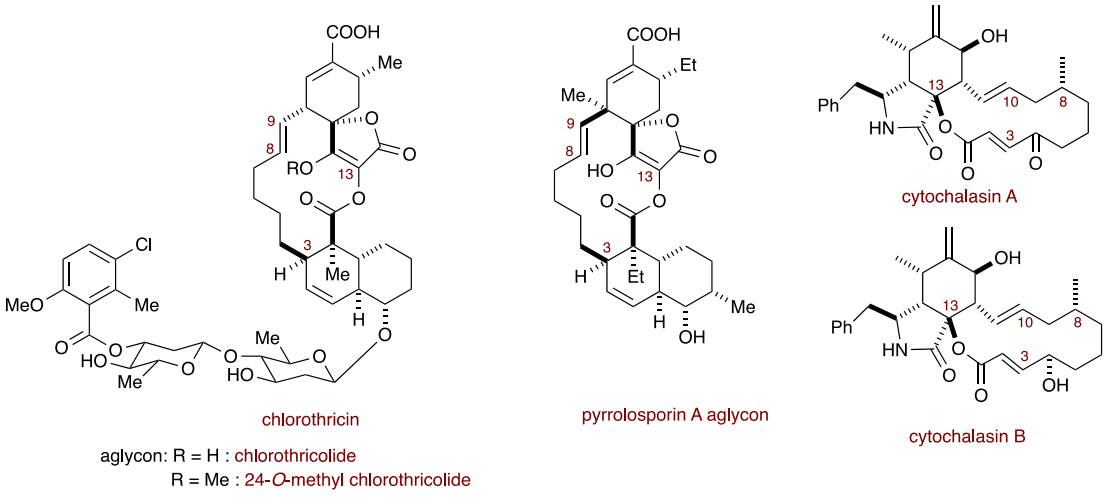

Figure 1.11 *(–)-Chlorothricin, pyrrolosporin A aglycon and cytochalasin A and B.*

Paecilomycins A, E, F and G are 14-membered macrolides that were isolated by Chen and Wei in 2010 from mycelial solid cultures of *Paecilomyces* sp. SC0924, along with other secondary metabolites, paecilomycin B, C and D (Figure 1.12).[86,114,115] The paecilomycins show high to moderate antiplasmodial activities. Paecilomycin A, E, F and G have an interesting chemical architecture where the 14-membered macrolactone has a fused phenolic ring.

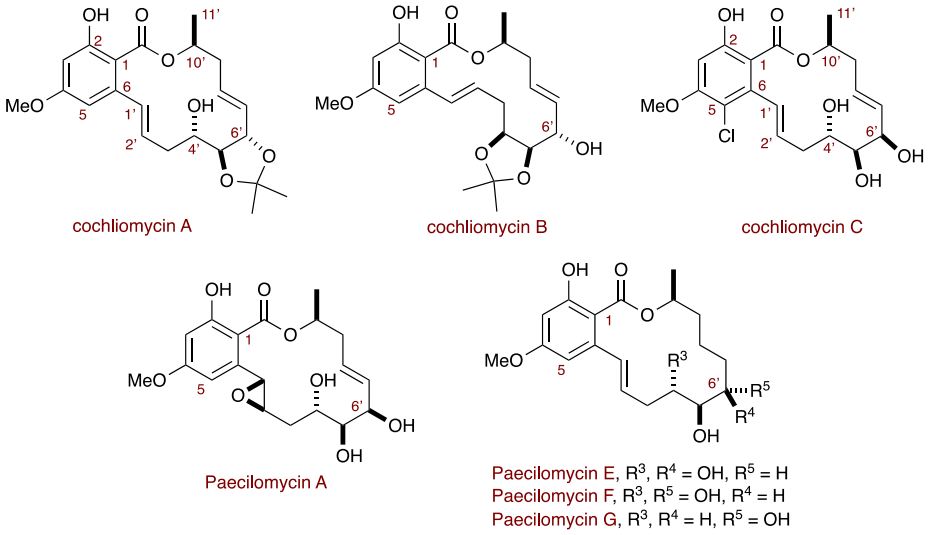

Figure 1.12. *Cochliomycin A, B and C and paecilomycins A, E, F and G.*

Total syntheses of paecilomycin E have been carried out by number of synthetic groups in recent years.[174] In 2012, Srihari and coworkers employed a Mitsunobu esterification,[118] and subsequent RCM macrocyclization to furnish the macrolide paecilomycin E (Scheme 1.23).[174b] Synthesis of the alkenol fragment was generated from L(+)-diethyl tartrate (DET) via an epoxide opening reaction, and Zn-mediated allylation. The aromatic fragment was synthesized via regioselective methylation and Stille coupling.[45]

In 2014, Nanda and coworkers generated the macrolide paecilomycin E via a Julia–Kocienski olefination[100] and a subsequent Yamaguchi macrolactonization (Scheme 1.23).[174c] The linear aliphatic precursor was synthesized via a *Z*-selective Julia–Kocienski olefination or Wittig olefination, followed by substrate controlled -diastereoselective dihydroxylation.

In 2019, Reddy and coworkers utilized a similar approach to Srihari, where the macrolide synthesis was achieved via use of Mitsunobu esterification,[118] followed by RCM macrocyclization.[174f] The acyclic enol fragment was generated via cross metathesis of two polyol fragments derived from D-ribose (Scheme 1.23). The aromatic acid was synthesized from diene and alkyne ester subunits via an Alders-Rickert reaction.[175] Collectively, the syntheses of paecilomycin E, F and two congeners cochliomycin C and 6-epi-cochliomycin C are readily seen in literature due to their structural similarities.

Scheme 1.23 *Synthetic strategies to paecilomycin E and F.*

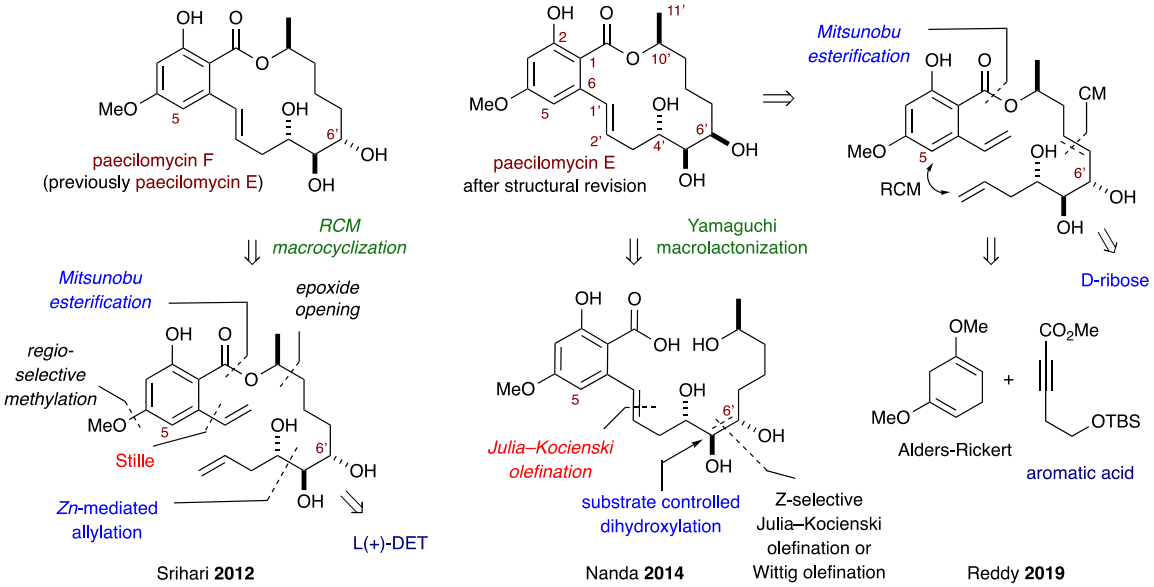

In 2015, Srihari and coworkers reported efforts toward the first total synthesis of cochliomycin C and 6-epi-cochliomycin C, along with synthesis of paecilomycin E and F (Scheme 1.24).[174d] Synthesis of the acylic alkenol fragment C3'–C10' was furnished via alkynyl epoxide opening reaction as the key reaction. The C4'–C6' alkyne subunit with stereotriad was generated from use of the known Ohira-Bestmann protocol of protected D-lyxose.[176] Esterification with conditions developed by De Brabander and coworkers,[177] followed by RCM macrocylization delivered the macrolides. After the synthesis of paecilomycin E and F, the synthesis of the related congeners, cochliomycin C and 6-epi-cochliomycin C , was carried out by installing the C5-chloro moiety via a chlorination reaction with sulfuryl chloride.

Scheme 1.24 – *Synthetic Strategies to paecilomycin E, F, cochliomycin C and 6'-epi- cochliomycin C*

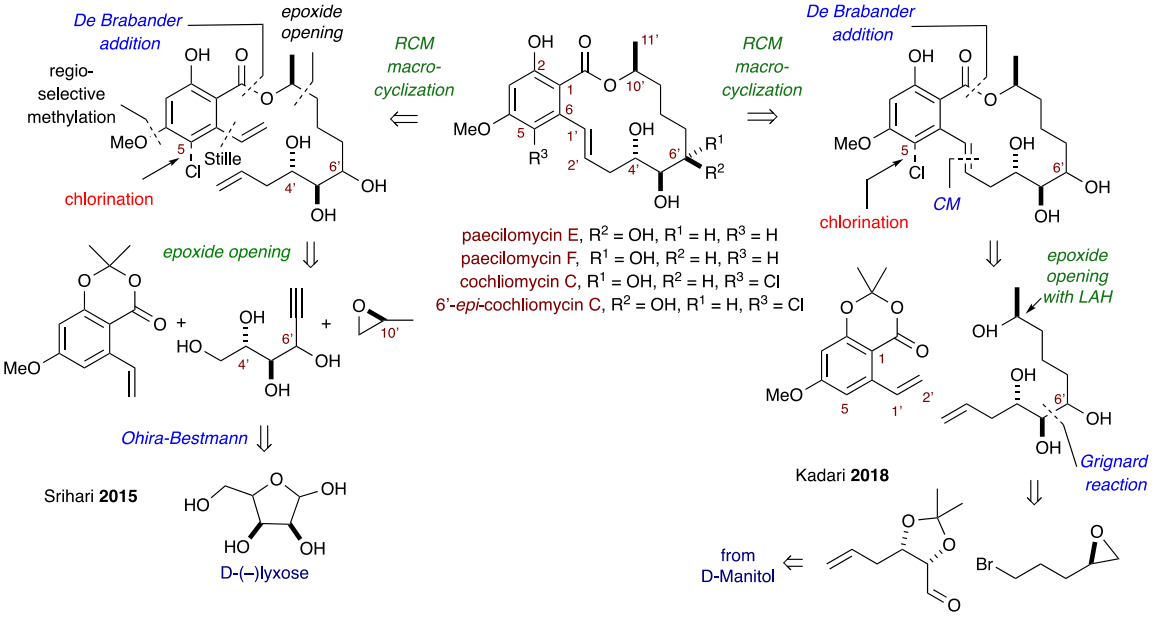

In 2018, Kadari and coworkers demonstrated the synthesis of the four macrolactones paecilomycin E, F and two congeners cochliomycin C and 6-epi-cochliomycin C utilizing olefine metathesis and base promoted De Brabander-type macrolactonization (Scheme 1.24).[174e] Key acyclic alkenol was synthesized from D-mannitol utilizing LAH promoted epoxide-opening and Grignard addition. Late-stage chlorination, with sulfuryl chloride, delivered cochliomycin C and 6-epi-cochliomycin C.

1.3.5 14-Membered macrolactams and macrocyclic enamides.

14-Membered macrolactams and macrocyclic enamides belong to a rare subclass of macrolides. Macrolides with amide and enamide functional groups are commonly derived from cyclic peptides and polyketide/non-ribosomal peptides (PK/NRP), respectively.[178] While there are several larger ringed lactam- and enamide-containing macrolides and some 12-membered, there are relatively few 14-membered macrolides reported for these two classes of macrolides namely, cyclic peptides cyclocinamide A and cyclocinamide B, as well as the PK/NRP macrolide, sanctolide A (Figure 1.13).

The cyclic peptide cyclocinamide A was first isolated in 1997 by Crews and coworkers form marine sponge *Psammocinia* sp.[179] Crew and coworkers reported a$\beta^2\alpha\beta^2\alpha$ 14-membered macrolide without chiral centers as the structure of cyclocinamide A. In their initial report, the two stereogenic centers at C4 and C11 were not defined, both the C7 and C14 stereogenic were assigned as *S*-configured. In order to identify the stereogenic at C4 and C11, all four diastereomers were synthesized, and neither the C4-(*R*)/C11-(*R*) diastereomer nor the C4-(*S*)/C11-(*S*) diastereomer were identical to the natural product.[180]

In addition, the two remaining C4-(*S*)/C11-(*R*) and C4-(*S*)/C11-(*S*) diastereomers failed to cyclize at the C1–amide bond.[181] In 2008, Crew and coworkers carried out a second isolation of the natural product and reassessed the absolute configuration of cyclocinamide A, where they ultimately surmised that all stereocenters were *S*-configured.[182] In 2007, Cyclocinamide B was isolated by Ireland and coworkers and the structural characteristics were identical to cyclocinamide A, yet stereochemically different at the C4-(*S*), C7-(*R*), C11-(*S*), and C14-(*R*) stereogenic centers.[183]

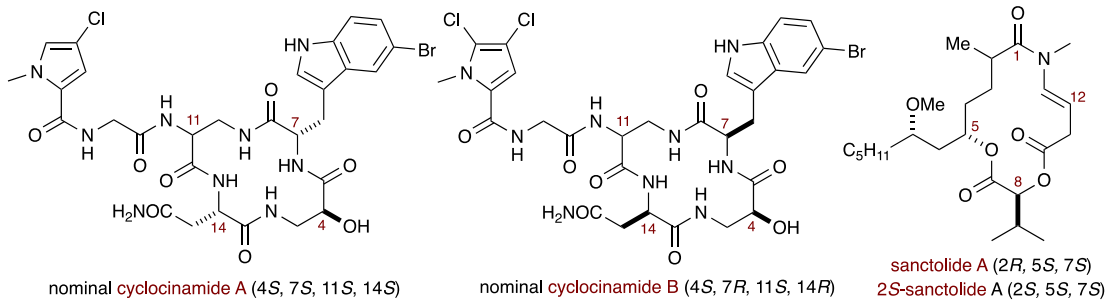

Figure 1.13 *Cyclocinamide A, cyclocinamide B, and sanctolide A.*

In 2012, Konopelski and coworkers carried out the first total synthesis of the nominally termed C11-(*S*)- and C11-(*R*) epimers of cyclocinamide A (Scheme 1.25).[184] The synthesis of macrolactam core was achieved via an amide coupling of acyclic precursor in the presence of the Shiori reagent [diphenylphosphoryl azide (DPPA)].[185] The two key diastereomers of the linear fragment were synthesized with two protected amide coupling partners via an EDCI-mediated coupling reaction. The two coupling partners were easily accessed from an oxazolidinone and (cyclo)Asn subunits using previously developed protocols by their lab.[186] The authors compared their analytical data with the reported data for the natural product. To their surprise, none of the two synthetic macrolactams matched

with the reported data of the isolated natural product, which suggested that a revision of stereochemical information for this molecule is needed.

In 2015, Konopelski and coworkers attempted the first total synthesis of the nominally termed cyclocinamide B with C4-(*S*), C7-(*R*), C11-(*S*), and C14-(*R*) configuration (Scheme 1.25).[187] A sequence of amide coupling reactions and protecting group manipulations were used to synthesize the linear precursor needed for the final macrocyclization. Macrocyclization was achieved via a [3-(diethoxyphosphoryloxy)-1,2,3-benzotriazin-4(3H)-one] DEPBT-mediated lactam formation reaction. However, the final spectral data were not in accordance with the reported data for the natural product

Scheme 1.25 *Synthetic strategies to cyclocinamide A and B.*

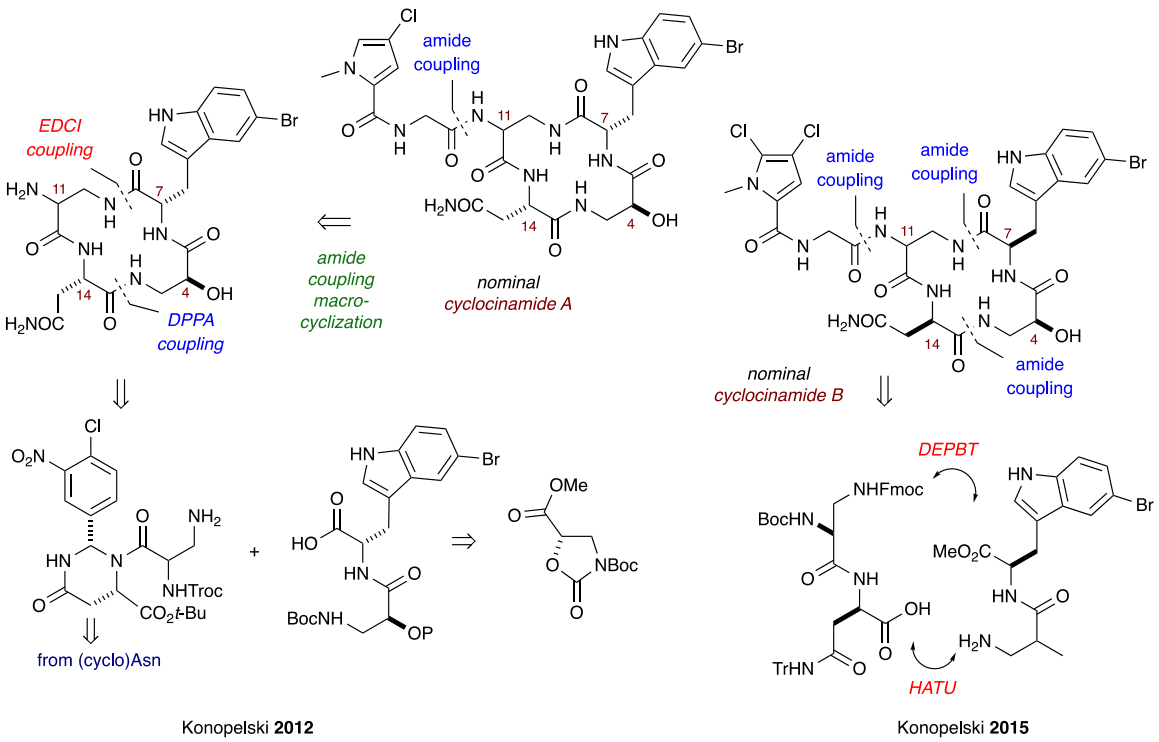

cyclocinamide B, which suggested that a revision of stereo-assignment is needed for cyclocinamide B as well. In conclusion, the synthesis of both cyclic amides has not been successful so far, and more studies are needed to be carried out to determine the absolute stereochemistry of these intriguing peptide-derived macrolactams.

The polyketide/nonribosomal peptide (PK-NRP) hybrid is a rare and small class of cyclic enamide/amides containing natural products. Sanctolide A is a 14-membered PK-NRP hybrid which was isolated from the cultured cyanobacterium *Oscillatoria sancta* (SAG 74.79) by Orjala and coworkers in 2012 (Figure 1.13).[188] To-date, two total syntheses of this natural product have been reported, and will be discussed briefly in this section before providing for a more detailed synthesis in chapter two of this thesis.

In 2014, Brimble and coworkers reported the first total synthesis of 2*S*-sanctolide A (Scheme 1.26).[189] Completion of the 2*S*-sanctolide A was achieved via an RCM macrocyclization, followed by late-stage Ru-catalyzed deconjugative isomerization of an allyl amide group, to install the requisite and unique *N*-methyl enamide moiety. A transamination reaction mediated by trimethyl aluminum (Me_3Al) was utilized to open the lactone methyl ether and deliver the requisite amide intermediate. The corresponding lactone methyl ether was synthesized from the 1,3-*anti*-diol olefin subunit via esterification, and RCM, followed by substrate controlled stereoselective hydrogenation of the intermediate dihydropyranone. The 1,3-*anti*-diol subunit was generated using a double asymmetric allylation strategy.[190]

In 2015, Yadav and coworkers carried out the total synthesis of sanctolide A utilizing an acid catalyzed intramolecular dehydrative enamide condensation as the final

macrocyclization step (Scheme 1.26).[191] The acyclic amide precursor was generated via a Yamaguchi esterification reaction. The 1,3-*anti*-diol-containing alcohol subunit was generated via a chiral allylation,[192] followed by diastereoselective metalated alkyne addition to a β-methoxy-aldehyde.

Scheme 1.26 *Synthetic strategies to sanctolide A*.

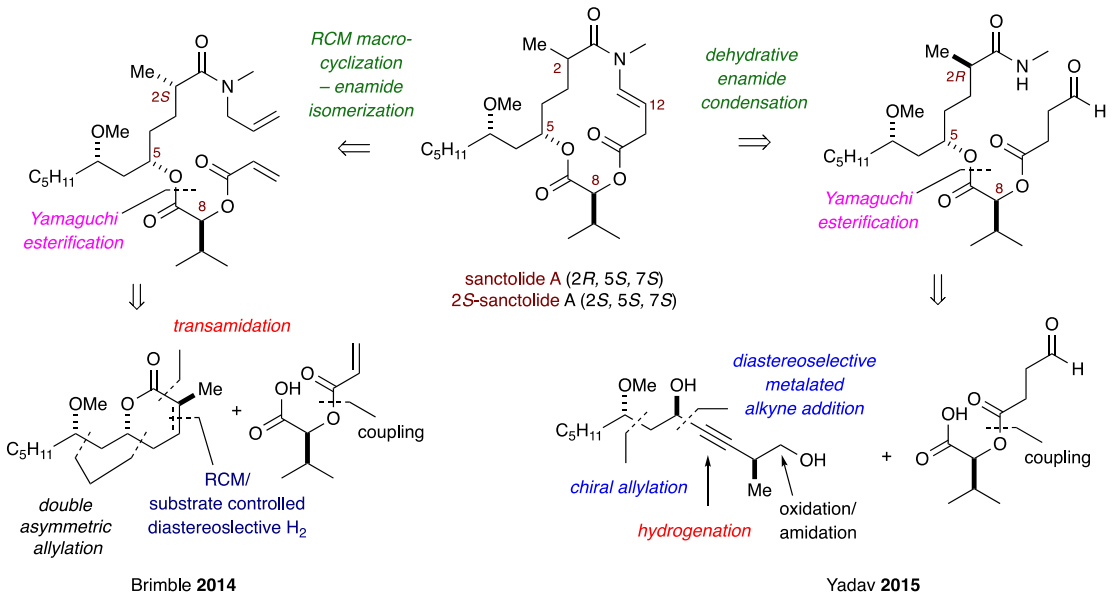

1.4 Conclusion

In summary, the synthetic strategies to 14-membered macrolides possessing various chemotypes has been summarized in a retrosynthetic manner. In this regard, the family of 14-membered macrolides were divided into six categories based on structural features, namely macrolides containing (i) lactone rings, (ii) α,β-unsaturated macrolactones, (iii) THP rings (iv) pyran hemiketal rings, (v) fused ring systems, and (vi) amides and enamide macrolides. Collectively, the synthesis of aforementioned chemotypes were discussed

briefly in a retrosynthetic fashion to provide a global understanding on distinct synthetic strategies.

1.5 References cited

[1] (a) Takamatsu, S.; Kim, Y. P.; Hayashi, M.; Hiraoka, H.; Natori, M.; Komiyama, K.; Omura, S. Macrosphelide, a novel inhibitor of cell-cell adhesion molecule. II. Physiochemical properties and structural elucidation. *J. Antibiot. (Tokyo)* **1996**, *49*, 95–98. (b) Zhang, H.; Tomoda, H.; Tabata, N.; Miura, H.; Namikoshi, M.; Yamaguchi, Y.; Masuma, R.; Omura, S. Cladospolide D, a new 12-membered macrolide antibiotic produced by Cladosporium sp. FT-0012. *J. Antibiot. (Tokyo)* **2001**, *54*, 635–641. (c) Njardarson, J. T.; Gaul, C.; Shan, D.; Huang, X. -Y.; Danishefsky, S. J. Discovery of potent cell migration inhibitors through total synthesis: lessons from structure-activity studies of (+)-migrastatin. *J. Am. Chem. Soc*. **2004**, *126*, 1038–1040. (d) Gallagher, B. M.; Fang, Jr., F. G.; Johannes, C. W.; Pesant, M.; Tremblay, M. R.; Zhao, H.; Akasaka, K.; Li, X.; Liu, J.; Littlefield, B. A. Synthesis and biological evaluation of (-)-laulimalide analogues. *Bioorg. Med. Chem. Lett.* **2004**, *14*, 575–579 and references therein. (e) Yang, S. W.; Chan, T. M.; Terracciano, J.; Loebenberg, D.; Patel, M.; Chu, M.; Structure elucidation of Sch 725674 from Aspergillus Sp. *J. Antibiot*. *(Tokyo)* **2005**, *58*, 535–538. (f) Nakae, K.; Nishimura, Y.; Ohba, S.; Akamatsu, Y. Migrastatin acts as a muscarinic acetylcholine receptor antagonist. *J. Antibiot. (Tokyo)* **2006**, *59*, 685–692. (g) Keller, S.; Nicholson, G.; Drahl, C.; Sorensen, E.; Fiedler, H. -P.; Süssmuth, R. D. Abyssomicins G and H and atrop-abyssomicin C from the marine Verrucosispora strain AB-18-032. *J. Antibiot.* **2007**, *60*, 391–394. (h) Jung, W. -H.; Harrison, C.; Shin, Y.; Fournier, J. -H.; Balachandran, R.; Raccor, B. S.; Sikorski, R. P.; Vogt, A.; Curran, D. P.; Day, B. W. Total synthesis and biological evaluation of C16 analogs of (-)-dictyostatin. *J. Med. Chem.* **2007**, *50*, 2951–2966 and references therein. (i) Xing, Y.; O'Doherty, G. A. De novo asymmetric synthesis of cladospolide B-D: structural reassignment of cladospolide D via the synthesis of its enantiomer. *Org. Lett.* **2009**, *11*, 1107–1110. (j) Freundlich, J. S.; Lalgondar, M.; Wei, J.-R.; Swanson, S.; Sorensen, E. J.; Rubin, E. J.; Sacchettini, J. C. The

abyssomicin C family as in vitro inhibitors of Mycobacterium tuberculosis. *Tuberculosis* **2010,** *90*, 298–300. (k) Low, W. K.; Li, J.; Zhu, M.; Kommaraju, S. S.; Shah-Mittal, J.; Hull, K.; Liu, J. O.; Romo, D. Second-generation derivatives of the eukaryotic translation initiation inhibitor pateamine A targeting eIF4A as potential anticancer agents. *Bioorg. Med. Chem.* **2014**, *22*, 116–125. (l) Zhang, J.; Lin, X. -P.; Li, L. -C.; Zhong, B. -L.; Liao, X. -J.; Liu, Y. -H.; Xu, S. -H. Gliomasolides A–E, unusual macrolides from a sponge-derived fungus *Gliomastix* Sp. ZSDS1-F7-2. *RSC Adv.* **2015**, *5*, 54645–54648.

[2] (a) Wessjohann, L.A., Ruijter, E., Garcia-Rivera, D. & Brandt, W. What can a chemist learn from nature's macrocycles?—a brief, conceptual view. *Mol. Divers.* **2005**, *9*, 171–186. (b) Driggers, E. M.; Hale, S. P.; Lee, J.; Terrett, N. K. The Exploration of Macrocycles for Drug Discovery - an Underexploited Structural Class. *Nat. Rev. Drug Discov.* **2008**, *7*, 608–624. (c) Swinney, D. C.; Anthony, J. How Were New Medicines Discovered? *Nat. Rev. Drug Discov.* **2011**, *10*, 507–519. (d) Madsen, C. M.; Clausen, M. H. Biologically Active Macrocyclic Compounds - From Natural Products to Diversity-Oriented Synthesis. *Eur. J. Org. Chem.* **2011**, 3107–3115. (e) Mallinson, J.; Collins, I. Macrocycles in new drug discovery. *Future Med. Chem.* **2012**, *4*, 1409–1438. (f) Giordanetto, F.; Kihlberg, J. Macrocyclic Drugs and Clinical Candidates: What Can Medicinal Chemists Learn from Their Properties? *J. Med. Chem.* **2014**, *57*, 278–295. (g) Rodrigues, T.; Reker, D.; Schneider, P.; Schneider, G. Counting on natural products for drug design. *Nat. Chem.* **2016**, *8*, 531–541.

[3] (a) Schreiber, S. L. Organic synthesis toward small-molecule probes and drugs. *Proc Natl Acad Sci.* **2011**, *108*, 6699–6702.

[4] (a) Udugamasooriya, D. G.; Spaller, M. R. Conformational constraint in protein ligand design and the inconsistency of binding entropy. *Biopolymers* **2008**, *89*, 653–667. (b) Wessjohann, L. A.; Ruijter, E.; Garcia-Rivera, D.; Brandt, W. What

can a chemist learn from nature's macrocycles? - A brief, conceptual view. *Mol. Divers.* **2005**, *9*, 171–186. (c) Giordanetto, F.; Kihlberg, J. Macrocyclic Drugs and Clinical Candidates: What Can Medicinal Chemists Learn from Their Properties? *J. Med. Chem.* **2014**, *57***,** 278–295. (d) Yudin, A. K. Macrocycles: lessons from the distant past, recent developments, and future directions. *Chem. Sci.* **2015**, *6*, 30–49.

[5] (a) Driggers, E. M.; Hale, S. P.; Lee, J.; Terrett, N. K. The exploration of macrocycles for drug discovery--an underexploited structural class. *Nat. Rev. Drug Discov.* **2008**, *7*, 608–624. (b) Bauer, R. A.; Wurst, J. M.; Tan, D. S. Expanding the range of 'druggable' targets with natural product-based libraries: an academic perspective. *Curr. Opin. Chem. Biol.* **2010**, *14*, 308–314. (c) Doak, B. C.; Zheng, J.; Dobritzsch, D.; Kihlberg, J. How Beyond Rule of 5 Drugs and Clinical Candidates Bind to Their Targets. *J. Med. Chem.* **2015**, 59, 2312–2327. (d) Beckmann, H. S. G.; Nie, F. L.; Hagerman, C. E.; Johansson, H.; Tan, Y. S.; Wilcke, D.; D. R. A strategy for the diversity-oriented synthesis of macrocyclic scaffolds using multidimensional coupling. *Nat. Chem.* **2013**, *5*, 861–867. (e) Grossmann, A.; Bartlett, S.; Janecek, M.; Hodgkinson, J. T.; Spring, D. R. Diversity-Oriented Synthesis of Drug-Like Macrocyclic Scaffolds Using an Orthogonal Organo- and Metal Catalysis Strategy. *Angew. Chem. Int. Edit.* **2014**, *53*, 13093–13097. (f) Nie, F.; Kunciw, D. L.; Wilcke, D.; Stokes, J. E.; Galloway, W. R. J. D.; Bartlett, S.; Sore, H. F.; Spring, D. R. A Multidimensional Diversity-Oriented Synthesis Strategy for Structurally Diverse and Complex Macrocycles. *Angew. Chem. Int. Ed.* **2016**, *55, 11139–11143*. (g) Kitsiou, C.; Hindes, J. J.; I'Anson, P.; Jackson, P.; Wilson, T. C.; Daly, E. K.; Felstead, H. R.; Hearnshaw, P.; Unsworth, W. P. The Synthesis of Structurally Diverse Macrocycles By Successive Ring Expansion. *Angew. Chem. Int. Edit.* **2015**, *54*, 15794–15798. (h) Kopp, F.; Stratton, C. F.; Akella, L. B.; Tan, D. S. A diversity-oriented synthesis approach to macrocycles via oxidative ring expansion. *Nat. Chem. Biol.* **2012**, *8*, 358–365. (i) Marcaurelle, L. A.; Comer, E.; Dandapani, S.; Duvall, J. R.; Gerard, B.; Kesavan, S.; Lee, M. D.; Liu, H. B.; Lowe, J. T.; Marie,

J. C.; Mulrooney, C. A.; Pandya, B. A.; Rowley, A.; Ryba, T. D.; Suh, B. C.; Wei, J. Q.; Young, D. W.; Akella, L. B.; Ross, N. T.; Zhang, Y. L.; Fass, D. M.; Reis, S. A.; Zhao, W. N.; Haggarty, S. J.; Palmer, M.; Foley, M. A. An Aldol-Based Build/Couple/Pair Strategy for the Synthesis of Medium- and Large-Sized Rings: Discovery of Macrocyclic Histone Deacetylase Inhibitors. *J. Am. Chem. Soc.* **2010**, *132*, 16962–16976.

[6] (a) Lipinski, C.A. Drug-like properties and the causes of poor solubility and poor permeability. *J. Pharmacol. Toxicol. Methods* **2000**, *44*, 235–249. (b) Vistoli, G., Pedretti, A.; Testa, B. Assessing drug-likeness—what are we missing? *Drug Discov. Today* **2008**, *13*, 285–294.

[7] (a) Marsault, E.; Peterson, M.L. Macrocycles are great cycles: applications, opportunities, and challenges of synthetic macrocycles in drug discovery. *J. Med. Chem.* **2011**, *54*, 1961–2004. (b) Mallinson, J. & Collins, I. Macrocycles in new drug discovery. *Future Med. Chem.* **2012**, *4*, 1409–1438. (c) Giordanetto, F. & Kihlberg, J. Macrocyclic drugs and clinical candidates: what can medicinal chemists learn from their properties? *J. Med. Chem.* **2014**, *57*, 278–295.

[8] (a) Villar, E. A.; Beglov, D.; Chennamadhavuni, S.; Porco, J. A.; Kozakov, D.; Vajda, S.; Whitty, A. How proteins bind macrocycles. *Nat. Chem. Biol.* **2014**, *10*, 723–731. (b) Drahl, C.; Cravatt, B. F.; Sorensen, E. J. Protein-reactive natural products. *Angew. Chem. Int. Ed.* **2005**, *44*, 5788–5809.

[9] (a) Driggers, E.M.; Hale, S.P.; Lee, J.; Terrett, N.K. The exploration of macrocycles for drug discovery—An underexploited structural class. *Nat. Rev. Drug Discov*. **2008**, *7*, 608–624. (b) Shen, B. A new golden age of natural products drug discovery. *Cell* **2015**, *163*, 1297–1300.

[10] (a) McDaniel, R.; Welch, M.; Hutchinson, C.R. Genetic Approaches to Polyketide Antibiotics. 1. *Chem. Rev.* **2005**, *105*, 543–558. (b) Ma, X.; Ma, S. Significant

breakthroughs in search for anti-infectious agents derived from erythromycin A. *Curr. Med. Chem.* **2011**, *18*, 1993–2015.

[11] (a) Alvarez-Elcoro, S.; Enzler, M.J. The Macrolides: Erythromycin, Clarithromycin, and Azithromycin. *Mayo Clin. Proc*. **1999**, *74*, 613–634. (b) Zuckerman, J.M.; Qamar, F.; Bono, B.R. Review of Macrolides (Azithromycin, Clarithromycin),Ketolids (Telithromycin) and Glycylcyclines (Tigecycline). *Med. Clin. N. Am.* **2011**, *95*, 761–791.

[12] (a) Campbell, W.C.; Fisher, M.H.; Stapley, E.O.; Albers-Sch nberg, G.; Jacob, T.A. Ivermectin: A potent new antiparasitic agent. *Science* **1983,** *221*, 823–828. (b) Campbell, W. Ivermectin: an update. *Parasitol. today* **1985**, *1*, 10–16. (c) Geary, T. G. Ivermectin 20 years on: maturation of a wonder drug. *Trends Parasitol.* **2005**, *21*, 530–532. (d) Omura, S. Ivermectin: 25 years and still going strong. *Int. J. Antimicrob. Agents* **2008**, *31*, 91–98. (e) Ashour, D. S. Ivermectin: From theory to clinical application. *Int. J. Antimicrob. Agents* **2019**, *54*, 134–142. (f) Tang, M.; Hu, X.; Wang, Y.; Yao, X.; Zhang, W.; Yu, C.; Cheng, F.; Li, J.; Fang, Q. Ivermectin, a potential anticancer drug derived from an antiparasitic drug. *Pharmacol. Res.* **2021**, *163*, 105207–105217

[13] (a) Ghosh, A. K.; Wang, Y. Total synthesis of (−)-laulimalide. *J. Am. Chem. Soc.* **2000**, *122*, 11027–11028. (b) Ghosh, A. K.; Wang, Y.; Kim, J. T. Total Synthesis of Microtubule-Stabilizing Agent (−)-Laulimalide1. *J. Org. Chem.* **2001**, *66*, 8973–8982. (c) Mulzer, J.; Öhler, E. An intramolecular case of Sharpless kinetic resolution: total synthesis of laulimalide. *Angew. Chem. Int. Ed.* **2001**, *40*, 3842–3846. (d) Pryor, D. E.; O'Brate, A.; Bilcer, G.; Díaz, J. F.; Wang, Y.; Wang, Y.; Kabaki, M.; Jung, M. K.; Andreu, J. M.; Ghosh, A. K. The microtubule stabilizing agent laulimalide does not bind in the taxoid site, kills cells resistant to paclitaxel and epothilones, and may not require its epoxide moiety for activity. *Biochemistry* **2002**, *41*, 9109–9115. (e) Gaitanos, T. N.; Buey, R. M.; Díaz, J. F.; Northcote, P.

T.; Teesdale-Spittle, P.; Andreu, J. M.; Miller, J. H. Peloruside A does not bind to the taxoid site on β-tubulin and retains its activity in multidrug-resistant cell lines. *Cancer research* **2004**, *64*, 5063–5067. (f) Gapud, E. J.; Bai, R.; Ghosh, A. K.; Hamel, E. Laulimalide and paclitaxel: a comparison of their effects on tubulin assembly and their synergistic action when present simultaneously. *Mol. Pharmacol.* **2004**, *66*, 113–121. (g) Uenishi, J. i.; Ohmi, M. Total Synthesis of (−)-Laulimalide: Pd-Catalyzed Stereospecific Ring Construction of the Substituted 3, 6-Dihydro [2H] pyran Units. *Angew. Chem.* **2005**, *117*, 2816–2820. (h) Hamel, E.; Day, B. W.; Miller, J. H.; Jung, M. K.; Northcote, P. T.; Ghosh, A. K.; Curran, D. P.; Cushman, M.; Nicolaou, K.; Paterson, I. Synergistic effects of peloruside A and laulimalide with taxoid site drugs, but not with each other, on tubulin assembly. *Mol. Pharmacol.* **2006**, *70*, 1555–1564. (i) Gollner, A.; Altmann, K.-H.; Gertsch, J.; Mulzer, J. Synthesis and biological evaluation of a des-dihydropyran laulimalide analog. *Tetrahedron Lett.* **2009**, *50*, 5790–5792.

[14] (a) O'Leary, D. J.; Grubbs, R. H., Handbook of Metathesis, Volume 2: Applications in Organic Synthesis. Grubbs, R. H.; Wenzel, A. G.; O'Leary, D. J.; Khosravi, E., Eds.; Wiley-VCH: Weinheim, 2015.(b) Hanson, P. R.; Maitra, S.; Chegondi, R.; Markley, J. L. General Ring-Closing Metathesis. In Handbook of Metathesis: Application in Organic Synthesis, 2nd ed.; Grubbs, R. H.; Wenzel, A. G.; O'Leary, D. J.; Khosravi, E., Eds.; Wiley-VCH: Weinheim, 2015; Vol. 2, Chapter 1, pp 1–170. (c) O'Leary, D. J.; O'Neil, G. W. Cross-Metathesis. In Handbook of Metathesis, 2nd ed.; Grubbs, R. H.; Wenzel, A. G.; O'Leary, D. J.; Khosravi, E., Eds.; Wiley-VCH: Weinheim, 2015; Vol. 2, Chapter 2, pp 171– 294. (d) Metathesis in Natural Product Synthesis: Synthesis: Strategies, Substrates and Catalysts, ed. J. Cossy, S. Arseniyadis and C. Meyer, Wiley-VCH, Weinheim, Germany, 2010.

[15] (a) Deiters, A.; Martin, S. F. Synthesis of Oxygen- and Nitrogen-Containing Heterocycles by Ring-Closing Metathesis. *Chem. Rev*. **2004**, *104*, 2199–2238. (b) Fuerstner, A.; Langemann, K. Macrocycles by ring-closing metathesis.

Synthesis **1997**, 792–803. (c) Fürstner, A. Metathesis in total synthesis. *Chem. Commun.* **2011**, *47*, 6505–6511. (d) Ogbaa, O. M.; Warnera, N. C.; O'Leary, D. J.; Grubbs, R. H. Recent advances in ruthenium-based olefin metathesis. *Chem. Soc. Rev*. **2018**, *47*, 4510–4544. (e) Lecourt, C.; Dhambri, S.; Allievi, L.; Sanogo, Y.; Zeghbib, N.; Othman, R. B.; Lannou, M.-I.; Sorin, G.; Ardisson, J. Natural products and ring-closing metathesis: synthesis of sterically congested olefins. *Nat. Prod. Rep.* **2018**, *35*, 105–124.

[16] (a) Isidro-Llobet, A.; Georgiou, K. H.; Galloway, W.; Giacomini, E.; Hansen, M. R.; Mendez-Abt, G.; Tan, Y. S.; Carro, L.; Sore, H. F.; Spring, D. R., A diversity-oriented synthesis strategy enabling the combinatorial-type variation of macrocyclic peptidomimetic scaffolds. *Org. Biomol. Chem.* **2015**, *13*, 4570–4580. (b) Beckmann, H. S. G.; Nie, F. L.; Hagerman, C. E.; Johansson, H.; Tan, Y. S.; Wilcke, D.; Spring, D. R., A strategy for the diversity-oriented synthesis of macrocyclic scaffolds using multidimensional coupling. *Nat. Chem.* **2013**, *5*, 861–867. (c) Galloway, W.; Isidro-Llobet, A.; Spring, D. R., Diversity-oriented synthesis as a tool for the discovery of novel biologically active small molecules. *Nat. Commun.* **2010**, 1–13. (d) Sauer, W. H. B.; Schwarz, M. K., Molecular shape diversity of combinatorial libraries: A prerequisite for broad bioactivity. *J. Chemical Inf. Comput. Sci.* **2003**, *43*, 987–1003. (e) Schreiber, S. L. Target-oriented and diversity-oriented organic synthesis in drug discovery. *Science* **2000**, *287*, 1964–1969. (f) Dow, M.; Fisher, M.; James, T.; Marchetti, F.; Nelson, A. Towards the systematic exploration of chemical space. *Org. Biomol. Chem.* **2012**, *10*, 17–28. (g) Lenci, E.; Guarna, A.; Trabocchi, A., Diversity-Oriented Synthesis as a Tool for Chemical Genetics. *Molecules* **2014**, *19*, 16506–16528. (h) Tan, D. S., Diversity-oriented synthesis: exploring the intersections between chemistry and biology. *Nat. Chem. Biol.* **2005,** *1*, 74–84.

[17] (a) Tatsuta, K.; Hosokawa, S. Total syntheses of polyketide-derived bioactive natural products. *The Chemical Record* **2006**, *6*, 217–-233. (b)Tatsuta, K. Total

synthesis and development of bioactive natural products. *Proceedings of the Japan Academy, Series B* **2008**, *84*, 87–106.(c) Tatsuta, K. Total synthesis of the big four antibiotics and related antibiotics. *J. Antibiot.* **2013**, *66*, 107–129. (d) Yu, X.; Sun, D. Macrocyclic drugs and synthetic methodologies toward macrocycles. *Molecules* **2013**, *18*, 6230–6268. (e) Martí-Centelles, V.; Pandey, M. D.; Burguete, M. I.; Luis, S. V. Macrocyclization Reactions: The Importance of Conformational, Configurational, and Template-Induced Preorganization. *Chem. Rev.* **2015**, *115*, 8736–8834. (f) Alihodžić, S.; Bukvić, M.; Elenkov, I. J.; Hutinec, A.; Koštrun, S.; Pešić, D.; Saxty, G.; Tomašković, L.; Žiher, D. Current trends in macrocyclic drug discovery and beyond-Ro5. *Prog Med Chem* **2018**, *57*, 113–233. (g) Ha, M. W.; Song, B. R.; Chung, H. J.; Paek, S.-M. Design and synthesis of anti-cancer chimera molecules based on marine natural products. *Marine drugs* **2019**, *17*, 500. (h) Zheng, K.; Hong, R. Stereoconfining macrocyclizations in the total synthesis of natural products. *Nat. Prod. Rep.* **2019**, *36*, 1546–1575. (i) Stockdale, T. P.; Lam, N. Y.; Anketell, M. J.; Paterson, I. The Stereocontrolled Total Synthesis of Polyketide Natural Products: A Thirty-Year Journey. *Bull. Chem. Soc. Jpn.* **2021**, *94*, 713–731.

[18] (a) Woodward, R.; Logusch, E.; Nambiar, K.; Sakan, K.; Ward, D.; Au-Yeung, B.; Balaram, P.; Browne, L.; Card, P.; Chen, C. Asymmetric total synthesis of erythromcin. 1. Synthesis of an erythronolide A secoacid derivative via asymmetric induction. *J. Am. Chem. Soc.* **1981**, *103*, 3210-3213. (b) Woodward, R.; Au-Yeung, B.; Balaram, P.; Browne, L.; Ward, D.; Au-Yeung, B.; Balaram, P.; Browne, L.; Card, P.; Chen, C. Asymmetric total synthesis of erythromycin. 2. Synthesis of an erythronolide A lactone system. *J. Am. Chem. Soc.* **1981**, *103*, 3213–3215. (c) Woodward, R.; Logusch, E.; Nambiar, K.; Sakan, K.; Ward, D.; Au-Yeung, B.; Balaram, P.; Browne, L.; Card, P.; Chen, C. Asymmetric total synthesis of erythromycin. 3. Total synthesis of erythromycin. *J. Am. Chem. Soc.* **1981**, *103*, 3215–3217.

[19] (a) Tatsuta, K.; Ishiyama, T.; Tajima, S.; Koguchi, Y.; Gunji, H. The total synthesis of oleandomycin. *Tetrahedron Lett.* **1990**, *31*, 709–712. (b) Paterson, I.; Ward, R. A.; Romea, P.; Norcross, R. D. Substrate-Controlled Aldol Reactions of Chiral Ethyl Ketones: Application to the Total Synthesis of Oleandomycin. *J. Am. Chem. Soc.* **1994**, *116*, 3623–3624. (c) Evans, D. A.; Kim, A. S. Enantioselective Synthesis of the Macrolide Antibiotic Oleandomycin Aglycon. *J. Am. Chem. Soc.* **1996**, *118*, 11323–11324.

[20] Martin, S. F.; Hida, T.; Kym, P. R.; Loft, M.; Hodgson, A. The asymmetric synthesis of erythromycin B. *J. Am. Chem. Soc.* **1997**, *119*, 3193–3194.

[21] (a) Corey, E.; Hopkins, P. B.; Kim, S.; Yoo, S.-E.; Nambiar, K. P.; Falck, J. Total synthesis of erythromycins. 5. Total synthesis of erythronolide A. *J. Am. Chem. Soc.* **1979**, *101*, 7131–7134. (b) Nakata, M.; Arai, M.; Tomooka, K.; Ohsawa, N.; Kinoshita, M. Total synthesis of erythronolide A. *Bull. Chem. Soc. Jpn.* **1989**, *62*, 2618–2635. (c) Muri, D.; Lohse-Fraefel, N.; Carreira, E. M. Total synthesis of erythronolide a by MgII-mediated cycloadditions of nitrile oxides. *Angew. Chem.* **2005**, *117*, 4104-4106. (d) Muri, D.; Carreira, E. M. Stereoselective synthesis of erythronolide A via nitrile oxide cycloadditions and related studies. *The Journal of organic chemistry* **2009**, *74*, 8695–8712.

[22] (a) Corey, E.; Kim, S.; Yoo, S.-E.; Nicolaou, K.; Melvin Jr, L. S.; Brunelle, D. J.; Falck, J.; Trybulski, E. J.; Lett, R.; Sheldrake, P. W. Total synthesis of erythromycins. 4. Total synthesis of erythronolide B. *J. Am. Chem. Soc.* **1978**, *100*, 46204622. (b) Sviridov, A.; Ermolenko, M.; Yashunsky, D.; Borodkin, V.; Kochetkov, N. Total synthesis of erythronolide B. 2. Skeleton assembly in (C5–C9)+(C3–C4)+(C1–C2)+(C11–C13) sequence. *Tetrahedron Lett.* **1987**, *28*, 3839–3842. (c) Mulzer, J.; Kirstein, H. M.; Buschmann, J.; Lehmann, C.; Luger, P. Total synthesis of 9-dihydroerythronolide B derivatives and of erythronolide B. *J. Am. Chem. Soc.* **1991**, *113*, 910–923.

[23] (a) Tone, H.; Nishi, T.; Oikawa, Y.; Hikota, M.; Yonemitsu, O. A stereoselective total synthesis of (9S)-9-dihydroerythronolide A from D-glucose. *Tetrahedron Lett.* **1987**, *28*, 4569–4572. (b) Stork, G.; Rychnovsky, S. D. Concise total synthesis of (+)-(9S)-dihydroerythronolide A. *J. Am. Chem. Soc*. **1987**, *109*, 1565–1567. (c) Paterson, I.; Rawson, D. J. Studies in macrolide synthesis: a highly stereoselective synthesis of (+)-(9S)-dihydroerythronolide A using macrocyclic stereocontrol. *Tetrahedron Lett.* **1989**, *30*, 7463–7466. (d) Stürmer, R.; Ritter, K.; Hoffmann, R. W. A Short, Linear Synthesis of (9S)-Dihydroerythronolide A. *Angewandte Chemie International Edition in English* **1993**, *32*, 101–103. (e) Peng, Z.-H.; Woerpel, K. [3+ 2] Annulation of Allylic Silanes in Acyclic Stereocontrol: Total Synthesis of (9 S)-Dihydroerythronolide A. *J. Am. Chem. Soc.* **2003**, *125*, 6018–6019.

[24] (a) Masamune, S.; Hirama, M.; Mori, S.; Ali, S. A.; Garvey, D. S. Total synthesis of 6-deoxyerythronolide B. *J. Am. Chem. Soc.* **1981**, *103*, 1568-1571. (b) Myles, D. C.; Danishefsky, S. J.; Schulte, G. Development of a fully synthetic stereoselective route to 6-deoxyerythronolide B by reiterative applications of the Lewis acid catalyzed diene aldehyde cyclocondensation reaction: a remarkable instance of diastereofacial selectivity. *J. Org. Chem.* **1990**, *55*, 1636–1648.(c) Evans, D. A.; Kim, A. S. Synthesis of 6-deoxyerythronolide B. Implementation of a general strategy for the synthesis of macrolide antibiotics. *Tetrahedron Lett.* **1997**, *38*, 53–56. (d) Stang, E. M.; White, M. C. Total synthesis and study of 6-deoxyerythronolide B by late-stage C–H oxidation. *Nature chemistry* **2009**, *1*, 547–551. (e) Gao, X.; Woo, S. K.; Krische, M. J. Total synthesis of 6-deoxyerythronolide B via C–C bond-forming transfer hydrogenation. *J. Am. Chem. Soc.* **2013**, *135*, 4223–4226.

[25] (a) Wu, X.; Neumann, H.; Beller, M. Update 1 of: macrolactonizations in the total synthesis of natural products. *Chem. Rev.* **2013**, *113*, 1–35. (b) Yakovleva, M.;

Denisova, K.; Vydrina, V.; Tolstikov, A.; Ishmuratov, G. Y. Methods for Macrolactonization of Seco Acids in the Synthesis of Natural and Biologically Active Compounds. *Russ. J. Org. Chem.* **2021**, *57*, 679–729. (c) Majhi, S. Applications of Yamaguchi Method to Esterification and Macrolactonization in Total Synthesis of Bioactive Natural Products. *Chemistry Select* **2021**, *6*, 4178–4206. (d) Parenty, A.; Moreau, X.; Niel, G.; Campagne, J.-M. Macrolactonizations in the Total Synthesis of Natural Products. *Chem. Rev.* **2013**, *113*, PR1–PR40.

[26] Corey, E.; Nicolaou, K. C. Efficient and mild lactonization method for the synthesis of macrolides. *J. Am. Chem. Soc.* **1974**, *96*, 5614–5616.

[27] Inanaga, J.; Hirata, K.; Saeki, H.; Katsuki, T.; Yamaguchi, M. A rapid esterification by means of mixed anhydride and its application to large-ring lactonization. *Bull. Chem. Soc. Jpn.* **1979**, *52*, 1989–1993.

[28] Boden, E. P.; Keck, G. E. Proton-transfer steps in Steglich esterification: a very practical new method for macrolactonization. *J. Org. Chem.* **1985**, *50*, 2394–2395.

[29] Wadsworth Jr, W. S. Synthetic Applications of Phosphoryl-Stabilized Anions. *Org. React.* **2004**, *25*, 73–253.

[30] Stang, E. M.; White, M. C. On the macrocyclization of the erythromycin core: Preorganization is not required. *Angew. Chem. Int. Ed.* **2011**, *50*, 2094–2097.

[31] Myers, A. G.; Yang, B. H.; Chen, H.; McKinstry, L.; Kopecky, D. J.; Gleason, J. L. Pseudoephedrine as a practical chiral auxiliary for the synthesis of highly enantiomerically enriched carboxylic acids, alcohols, aldehydes, and ketones. *J. Am. Chem. Soc.* **1997**, *119*, 6496–6511.

[32] Evans, D. A.; Bartroli, J.; Shih, T. Enantioselective aldol condensations. 2. Erythro-selective chiral aldol condensations via boron enolates. *J. Am. Chem. Soc.* **1981**, *103*, 2127–2129.

[33] (a) Shibahara, F.; Bower, J. F.; Krische, M. J. Ruthenium-catalyzed C−C bond forming transfer hydrogenation: Carbonyl allylation from the alcohol or aldehyde oxidation level employing acyclic 1, 3-dienes as surrogates to preformed allyl metal reagents. *J. Am. Chem. Soc.* **2008**, *130*, 6338–6339. (b) Zbieg, J. R.; Yamaguchi, E.; McInturff, E. L.; Krische, M. J. Enantioselective CH crotylation of primary alcohols via hydrohydroxyalkylation of butadiene. *Science* **2012**, *336*, 324-327. (c) McInturff, E. L.; Yamaguchi, E.; Krische, M. J. Chiral-anion-dependent inversion of diastereo-and enantioselectivity in carbonyl crotylation via ruthenium-catalyzed butadiene hydrohydroxyalkylation. *J. Am. Chem. Soc.* **2012**, *134*, 20628–20631.

[34] (a) Kim, I. S.; Han, S. B.; Krische, M. J. anti-Diastereo-and enantioselective carbonyl crotylation from the alcohol or aldehyde oxidation level employing a cyclometallated iridium catalyst: α-Methyl allyl acetate as a surrogate to preformed crotylmetal reagents. *J. Am. Chem. Soc.* **2009**, *131*, 2514–2520. (b) Gao, X.; Han, H.; Krische, M. J. Direct generation of acyclic polypropionate stereopolyads via double diastereo-and enantioselective iridium-catalyzed crotylation of 1, 3-diols: Beyond stepwise carbonyl addition in polyketide construction. *J. Am. Chem. Soc.* **2011**, *133*, 12795–12800.

[35] Augustiniak, H.; Höfle, G.; Irschik, H.; Reichenbach, H. Antibiotics from Gliding Bacteria, LXXVIII. Ripostatin A, B, and C: Isolation and Structure and Structure Elucidation of Novel Metabolites from Sorangium cellulosum. *Liebigs Annalen* **1996**, *1996*, 1657–1663.

[36] Maezawa, I.; Kinumaki, A.; Suzuki, M. Isolation and Identification of Picronolide, Methynolide and Neomethynolide Produced by Streptomyces Venezuelae. *J. Antibiot.* **1974**, *27*, 84–85.

[37] (a) Corbaz, R.; Ettlinger, L.; Gaumann, E.; Keller-Schierlein, W.; Neipp, L.; Prelog, V. P. Reusser u. H. ZÄ Hner: Stoffwechselprodukte von Actinomyceten.

Angolamycin. *Helv. Chim. Acta* **1955**, *38*, 1202–1209. (b) Maezawa, I.; Hori, T.; Kinumaki, A.; Suzuki, M. Biological conversion of narbonolide to picromycin. *J. Antibiot.* **1973**, *26*, 771–775.

[38] Yang, S.-W.; Chan, T.-M.; Terracciano, J.; Loebenberg, D.; Patel, M.; Chu, M. Structure elucidation of Sch 725674 from Aspergillus sp. *J. Antibiot.* **2005**, *58*, 535–538.

[39] Zhang, J.; Lin, X.-P.; Li, L.-C.; Zhong, B.-L.; Liao, X.-J.; Liu, Y.-H.; Xu, S.-H. Gliomasolides A–E, unusual macrolides from a sponge-derived fungus Gliomastix sp. ZSDS1-F7-2. *RSC Advances* **2015**, *5*, 54645–54648.

[40] Glaus, F.; Altmann, K. H. Total synthesis of the bacterial RNA polymerase inhibitor ripostatin B. *Angew. Chem. Int. Ed.* **2012**, *51*, 3405–3409.

[41] Winter, P.; Hiller, W.; Christmann, M. Access to Skipped Polyene Macrolides through Ring-Closing Metathesis: Total Synthesis of the RNA Polymerase Inhibitor Ripostatin B. *Angew. Chem. Int. Ed.* **2012**, *51*, 3396–3400.

[42] Tang, W.; Prusov, E. V. Total Synthesis of RNA-Polymerase Inhibitor Ripostatin B and 15-Deoxyripostatin A. *Angew. Chem. Int. Ed.* **2012**, *51*, 3401–3404.

[43] (a) Schwab, P.; France, M. B.; Ziller, J. W.; Grubbs, R. H. A Series of Well-Defined Metathesis Catalysts–Synthesis of [RuCl2(CHR′)(PR3)2] and Its Reactions. *Angew. Chem. Int. Ed. Engl.* **1995**, *34*, 2039–2041. (b) Wu, Z.; Nguyen, S. T.; Grubbs, R. H.; Ziller, J. W. Reactions of ruthenium carbenes of the type $(PPh_3)_2$ (X)2Ru:CH-CH:CPh_2 (X= Cl and CF_3COO) with strained acyclic olefins and functionalized olefins. *J. Am. Chem. Soc.* **1995**, *117*, 5503–5511. (c) Schwab, P.; Grubbs, R. H.; Ziller, J. W. Synthesis and Applications of $RuCl_2(CHR')(PR_3)_2$: The Influence of the Alkylidene Moiety on Metathesis Activity. *J. Am. Chem. Soc.* **1996**, *118*, 100–110.

[44] (a) Scholl, M.; Ding, S.; Lee, C. W.; Grubbs, R. H. Synthesis and activity of a new generation of ruthenium-based olefin metathesis catalysts coordinated with 1,3-dimesityl-4,5-dihydroimidazol-2-yli-dene ligands. *Org. Lett.* **1999**, *1*, 953−956. (b) Nam, Y. H.; Snapper, M. L. Ruthenium-Catalyzed Tandem Metathesis/Non-Metathesis Processes. In Handbook of Metathesis, 2nd ed.; Grubbs, R. H.; Wenzel, A. G.; O'Leary, D. J.; Khosravi, E., Eds.; Wiley-VCH: Weinheim, 2015; pp 311−380. (c) Ogba, O.; Warner, N.; O'Leary, D.; Grubbs, R. Recent advances in ruthenium-based olefin metathesis. *Chem. Soc. Rev.* **2018**, *47*, 4510–4544. (d) Cheng-Sánchez, I.; Sarabia, F. Recent Advances in Total Synthesis via Metathesis Reactions. *Synthesis* **2018**, *50*, 3749–3786.

[45] Stille, J. K. The palladium-catalyzed cross-coupling reactions of organotin reagents with organic electrophiles [new synthetic methods (58)]. *Angew. Chem. Int. Ed* **1986**, *25*, 508–524.

[46] Paterson, I.; Goodman, J. M. Aldol reactions of methylketones using chiral boron reagents: A reversal in aldehyde enantioface selectivity. *Tetrahedron Lett.* **1989**, *30*, 997–1000.

[47] Evans, D. A.; Hoveyda, A. H. Samarium-catalyzed intramolecular Tishchenko reduction of. beta.-hydroxy ketones. A stereoselective approach to the synthesis of differentiated anti 1, 3-diol monoesters. *J. Am. Chem. Soc.* **1990**, *112*, 6447–6449.

[48] Kaiho, T.; Masamune, S.; Toyoda, T. Macrolide synthesis: narbonolide. *J. Org. Chem.* **1982**, *47*, 1612–1614.

[49] Venkatraman, L.; Salomon, C. E.; Sherman, D. H.; Fecik, R. A. Total synthesis of narbonolide and biotransformation to pikromycin. *J. Org. Chem.* **2006**, *71*, 9853–9856.

[50] Okude, Y.; Hirano, S.; Hiyama, T.; Nozaki, H. Grignard-type carbonyl addition of allyl halides by means of chromous salt. A chemospecific synthesis of homoallyl alcohols. *J. Am. Chem. Soc.* **1977**, *99*, 3179–3181.

[51] Ireland, R. E.; Liu, L. An improved procedure for the preparation of the Dess-Martin periodinane. *J. Org. Chem.* **1993**, *58*, 2899–2899.

[52] Xuan, R.; Oh, H.-S.; Lee, Y.; Kang, H.-Y. Total synthesis of 10-deoxymethynolide and narbonolide. *The Journal of organic chemistry* **2008**, *73*, 1456-1461.

[53] Nakajima, N.; Tanaka, T.; Hamada, T.; Oikawa, Y.; Yonemitsu, O. Highly Stereoselective Total Synthesis of Pikronolide, the Aglycon of the First Macrolide Antibiotic Pikromycin. Crucial Role of Benzyl-Type Protecting Groups Removable by 2, 4-Dichloro-5, 6-dicyanobenzoquinone Oxidation. *Chem. Pharm. Bull.* **1987**, *35*, 2228–2237.

[54] (a) Yamamoto, Y.; Yatagai, H.; Naruta, Y.; Maruyama, K. Erythro-selective addition of crotyltrialkyltins to aldehydes regardless of the geometry of the crotyl unit. Stereoselection independent of the stereochemistry of precursors. *J. Am. Chem. Soc.* **1980**, *102*, 7107–7109. (b) Yamamoto, Y.; Yatagai, H.; Ishihara, Y.; Maeda, N.; Maruyama, K. Stereo-and regiocontrol of acyclic systems via the lewis acid mediated reaction of allylic stannanes with aldehydes. *Tetrahedron* **1984**, *40*, 2239–2246.

[55] Oikawa, Y.; Tanaka, T.; Horita, K.; Noda, I.; Nakajima, N.; Kakusawa, N.; Hamada, T.; Yonemitsu, O. Highly Stereoselective Total Synthesis of Methynolide, the Aglycon of the 12-Membered Macrolide Antibiotic Methymycin. I. Synthesis of a Prelog-Djerassi Lactone-Type Chiral Intermediate from D-Glucose. *Chem. Pharm. Bull.* **1987**, *35*, 2184–2195.

[56] Oh, H.-S.; Kang, H.-Y. Total synthesis of pikromycin. *J. Org. Chem.* **2012**, *77*, 1125–1130.

[57] Schmidt, R. R.; Jung, K.-H. Oligosaccharide Synthesis with Trichloroacetimidates. In Preparative Carbohydrate Chemistry; Hanessian, S., Ed.; Marcel Dekker: New York, 1997; p 283.

[58] Moretti, J. D.; Wang, X.; Curran, D. P. Minimal fluorous tagging strategy that enables the synthesis of the complete stereoisomer library of SCH725674 macrolactones. *J. Am. Chem. Soc.* **2012**, *134*, 7963–7970.

[59] Bali, A. K.; Sunnam, S. K.; Prasad, K. R. Enantiospecific total synthesis of macrolactone Sch 725674. *Org. Lett.* **2014**, *16*, 4001–4003.

[60] Sneddon, H. F.; van den Heuvel, A.; Hirsch, A. K.; Booth, R. A.; Shaw, D. M.; Gaunt, M. J.; Ley, S. V. Double conjugate addition of dithiols to propargylic carbonyl systems to generate protected 1, 3-dicarbonyl compounds. *J. Org. Chem.* **2006**, *71*, 2715–2725.

[61] Evans, D.; Chapman, K.; Carreira, E. Directed reduction of. beta.-hydroxy ketones employing tetramethylammonium triacetoxyborohydride. *J. Am. Chem. Soc.* **1988**, *110*, 3560–3578.

[62] Ramakrishna, K.; Kaliappan, K. P. An enantioselective total synthesis of Sch-725674. *Org. Biomol. Chem* **2015**, *13*, 234–240.

[63] Smith, A. B.; Adams, C. M. Evolution of dithiane-based strategies for the construction of architecturally complex natural products. *Acc. Chem. Res.* **2004**, *37*, 365–377.

[64] Bodugam, M.; Javed, S.; Ganguly, A.; Torres, J.; Hanson, P. R. A Pot-Economical Approach to the Total Synthesis of Sch-725674. *Org. Lett.* **2016**, *18*, 516–519.

[65] (a) Whitehead, A.; McReynolds, M. D.; Moore, J. D.; Hanson, P. R. Multivalent Activation in Phosphate Tethers: A New Tether for Small Molecule Synthesis. *Org. Lett.* **2005**, *7,* 3375–3378. (b) Hanson, P. R.; Jayasinghe, S.; Maitra, S; Markley, J. L. (authors with equal contribution) Phosphate Tethers in Natural Product Synthesis. In Phosphorus Chemistry II: Synthetic Methods; Montchamp, J.-L., Ed.; Topics in Current Chemistry 361; Springer-Verlag Berlin Heidelberg, **2015**; pp 253–271. (c) Maitra, S.; Bodugam, M.; Javed, S.; Hanson, P. R. Synthesis of the C9-C25 Subunit of Spirastrellolide B. *Org. Lett.* **2016**, *18*, 3094–3097. (d) Javed, S.; Bodugam, M.; Torres, J.; Ganguly, A.; Hanson, P. R. Modular Synthesis of Novel Macrocycles Bearing α,β-Unsaturated Chemotypes through a Series of One-Pot, Sequential Protocols. *Chem. Eur. J.* **2016**, *22*, 6755–6758.

[66] Ganguly, A.; Javed, S.; Bodugam, M.; Dissanayake, G. C.; Chegondi, R.; Hanson, P. R. Synthesis of the C1− C16 Polyol-containing Macrolactone of 13-desmethyl Lyngbouilloside, an Unnatural Analog of the Originally Assigned Structure of (−)-Lyngbouilloside. *Isr. J. Chem.* **2021**, *61*, 401–408.

[67] (a) Waetzig, J. D.; Hanson, P. R. Temporary Phosphate Tethers: A Metathesis Strategy to Differentiated Polyol Subunits. *Org. Lett.* **2006**, *8*, 1673–1676. (b) Venukadasula, P. K. M.; Chegondi, R.; Suryn, G. M.; Hanson, P. R. A Phosphate Tether-Mediated, One-Pot, Sequential Ring-Closing Metathesis/Cross-Metathesis/Chemoselective Hydrogenation Protocol. *Org. Lett.* **2012**, *14*, 2634–2637 and references cited therein. (c)

[68] Katsuki, T.; Sharpless, K. B. The first practical method for asymmetric epoxidation. *J. Am. Chem. Soc.* **1980**, *102*, 5974–5976.

[69] Swallen, L. C.; Boord, C. E. The Synthesis of Beta-Bromo-Alkyl Ethers and Their Use in Further Syntheses1, 2. *J. Am. Chem. Soc.* **1930**, *52*, 651–660.

[70] Sharma, B. M.; Gontala, A.; Kumar, P. Enantioselective Modular Total Synthesis of Macrolides Sch725674 and C-4-epi-Sch725674. *Eur. J. Org. Chem.* **2016**, *2016*, 1215–1226.

[71] Yamaguchi, M.; Hirao, I. An efficient method for the alkynylation of oxiranes using alkynyl boranes. *Tetrahedron Lett.* **1983**, *24*, 391–394.

[72] Seetharamsingh, B.; Khairnar, P. V.; Reddy, D. S. First Total Synthesis of Gliomasolide C and Formal Total Synthesis of Sch-725674. *J. Org. Chem.* **2016**, *81*, 290–296.

[73] Narute, S. B.; Kiran, N. C.; Ramana, C. V. A [Pd]-mediated ω-alkynone cycloisomerization approach for the central tetrahydropyran unit and the synthesis of C (31)–C (48) fragment of aflastatin A. *Org. Biomol. Chem.* **2011**, *9*, 5469–5475.

[74] Reddy, Y.; Sabitha, G. Total Synthesis of Antifungal Macrolide Sch 725674. *ChemistrySelect* **2016**, *1*, 2156–2158.

[75] Corey, E.; Bakshi, R. K.; Shibata, S.; Chen, C. P.; Singh, V. K. A stable and easily prepared catalyst for the enantioselective reduction of ketones. Applications to multistep syntheses. *J. Am. Chem. Soc.* **1987**, *109*, 7925–7926.

[76] Fawcett, A.; Nitsch, D.; Ali, M.; Bateman, J. M.; Myers, E. L.; Aggarwal, V. K. Regio-and Stereoselective Homologation of 1, 2-Bis (Boronic Esters): Stereocontrolled Synthesis of 1, 3-Diols and Sch 725674. *Angew. Chem.* **2016**, *128*, 14883–14887.

[77] (a) Toribatake, K.; Nishiyama, H. Asymmetric Diboration of Terminal Alkenes with a Rhodium Catalyst and Subsequent Oxidation: Enantioselective Synthesis of Optically Active 1, 2-Diols. *Angew. Chem.* **2013**, *125*, 11217–11221. (b) Coombs, J. R.; Haeffner, F.; Kliman, L. T.; Morken, J. P. Scope and mechanism of the Pt-catalyzed enantioselective diboration of monosubstituted alkenes. *J. Am. Chem. Soc.* **2013**,*135*, 11222–11231. (c) Toribatake, K.; Miyata, S.; Naganawa, Y.; Nishiyama, H. Asymmetric synthesis of optically active 3-amino-1, 2-diols from N-acyl-protected allylamines via catalytic diboration with Rh [bis (oxazolinyl) phenyl] catalysts. *Tetrahedron* **2015**, *71*, 3203–3208.

[78] Seetharamsingh, B.; Khairnar, P. V.; Reddy, D. S. First Total Synthesis of Gliomasolide C and Formal Total Synthesis of Sch-725674. *J. Org. Chem.* **2016**, *81*, 290–296.

[79] Seetharamsingh, B.; Ganesh, R.; Reddy, D. S. Determination of the absolute configuration of gliomasolide D through total syntheses of the C-17 epimers. *J. Nat. Prod.* **2017**, *80*, 560–564.

[80] Reddy, R. G.; Venkateshwarlu, R.; Ramakrishna, K. V.; Yadav, J. S.; Mohapatra, D. K. Asymmetric Total Syntheses of Two Possible Diastereomers of Gliomasolide E and Its Structural Elucidation. *J. Org. Chem.* **2017**, *82*, 1053–1063.

[81] Kare, N.; Kundoor, G. R.; Palakodety, R. K. Studies towards the stereoselective total synthesis of Gliomasolide A. *Tetrahedron Lett.* **2019**, *60*, 151169–151171.

[82] Ramachandran, P. V.; Chen, G.-M.; Brown, H. C. Efficient synthesis of enantiomerically pure C2-symmetric diols via the allylboration of appropriate dialdehydes. *Tetrahedron Lett.* **1997**, *38*, 2417–2420.

[83] Sharpless, K. B.; Behrens, C. H.; Katsuki, T.; Lee, A. W.; Martin, V. S.; Takatani, M.; Viti, S. M.; Walker, F. J.; Woodard, S. S. Stereo and regioselective openings

of chiral 2, 3-epoxy alcohols. Versatile routes to optically pure natural products and drugs. Unusual kinetic resolutions. *Pure Appl. Chem*. **1983**, *55*, 589–604.

[84] Kito, K.; Ookura, R.; Yoshida, S.; Namikoshi, M.; Ooi, T.; Kusumi, T. New cytotoxic 14-membered macrolides from marine-derived fungus Aspergillus ostianus. *Org. Lett.* **2008**, *10*, 225–228.

[85] Wright, A. E.; Botelho, J. C.; Guzmán, E.; Harmody, D.; Linley, P.; McCarthy, P. J.; Pitts, T. P.; Pomponi, S. A.; Reed, J. K. Neopeltolide, a macrolide from a lithistid sponge of the family Neopeltidae. *J. Nat. Prod.* **2007**, *70*, 412–416.

[86] Xu, L.; He, Z.; Xue, J.; Chen, X.; Wei, X. β-Resorcylic acid lactones from a Paecilomyces fungus. *J. Nat. Prod.* **2010**, *73*, 885–889.

[87] Ookura, R.; Kito, K.; Saito, Y.; Kusumi, T.; Ooi, T. Structure revision of aspergillides A and B, cytotoxic 14-membered macrolides from Aspergillus ostianus, by X-ray crystallography. *Chem. Lett.* **2009**, *38*, 384–384.

[88] Nagasawa, T.; Kuwahara, S. Enantioselective total synthesis of aspergillide C. *Org. Lett.* **2009**, *11*, 761–764.

[89] Hande, S. M.; Uenishi, J. i. Total synthesis of aspergillide B and structural discrepancy of aspergillide A. *Tetrahedron Lett.* **2009**, *50*, 189–192.

[90] Aspergillide B: (a) Nagasawa, T.; Kuwahara, S. Enantioselective synthesis of aspergillide B. *Bioscience, biotechnology, and biochemistry* **2009**, *73*, 1893–1894. (b) Díaz-Oltra, S.; Angulo-Pachón, C. A.; Kneeteman, M. N.; Murga, J.; Carda, M.; Marco, J. A. Stereoselective synthesis of the cytotoxic macrolide aspergillide B. *Tetrahedron Lett.* **2009**, *50*, 3783-3785. (c) Liu, J.; Xu, K.; He, J.; Zhang, L.; Pan, X.; She, X. Concise total synthesis of (+)-aspergillide B. *J. O. Chem.* **2009**, *74*, 5063–5066. (d) Hendrix, A. J. M.; Jennings, M. P. Convergent synthesis of (+)-aspergillide B via a highly diastereoselective oxocarbenium allylation. *Tetrahedron*

Lett. **2010**, *51*, 4260–4262. (e) Trost, B. M.; Bartlett, M. J. Transition-metal-catalyzed synthesis of aspergillide B: An alkyne addition strategy. *Org. Lett.* **2012**, *14*, 1322–1325. (f) Sridhar, Y.; Srihari, P. Stereodivergent total synthesis of (+)-Aspergillide B and (+)-7-epi-Aspergillide A. *Eur. J. Org. Chem.* **2013**, *2013*, 578–587. (g) Bhavani, K.; GyanChander, E.; Das, S.; Yadav, J. S. Studies towards the Total Synthesis of Aspergillide-B. *ChemistrySelect* **2018**, *3*, 3391–3393.

[91] Aspergillide A: (a) Nagasawa, T.; Kuwahara, S. Synthesis of aspergillide A from a synthetic intermediate of aspergillide B. *Tetrahedron Lett.* **2010**, *51*, 875–877. (b) Diaz-Oltra, S.; Angulo-Pachón, C. A.; Murga, J.; Carda, M.; Marco, J. A. Stereoselective synthesis of the cytotoxic 14-membered macrolide aspergillide A. *The Journal of organic chemistry* **2010**, *75*, 1775–1778. (c) Fuwa, H.; Yamaguchi, H.; Sasaki, M. A unified total synthesis of aspergillides A and B. *Org. Lett.* **2010**, *12*, 1848–1851. (d) Sabitha, G.; Reddy, D. V.; Rao, A. S.; Yadav, J. Stereoselective formal synthesis of aspergillide A. *Tetrahedron Lett.* **2010**, *51*, 4195–4198. (e) Izuchi, Y.; Kanomata, N.; Koshino, H.; Hongo, Y.; Nakata, T.; Takahashi, S. Formal total synthesis of aspergillide A. *Tetrahedron: Asymmetry* **2011**, *22*, 246–251. (f) Kanematsu, M.; Yoshida, M.; Shishido, K. Total Synthesis of Aspergillide A and B Based on the Transannular Oxy-Michael Reaction. *Angew. Chem.* **2011**, *123*, 2666–2668. (g) Nagasawa, T.; Nukada, T.; Kuwahara, S. Synthesis of aspergillide A via proline-catalyzed trans-to-cis isomerization of a substituted tetrahydropyran. *Tetrahedron* **2011**, *67*, 2882-2888. (h) Díaz-Oltra, S.; Angulo-Pachón, C. A.; Murga, J.; Falomir, E.; Carda, M.; Marco, J. A. Synthesis and Biological Properties of the Cytotoxic 14-Membered Macrolides Aspergillide A and B. *Chem. Eur. J.* **2011**, *17*, 675–688. (i) Zúñiga, A.; Pérez, M.; González, M.; Gómez, G.; Fall, Y. Formal Synthesis of Aspergillide A from Tri-O-acetyl-D-glucal. *Synthesis* **2011**, *2011*, 3301–3306. (j) Fuwa, H.; Noto, K.; Kawakami, M.; Sasaki, M. Synthesis and biological evaluation of aspergillide A/neopeltolide chimeras. *Chem. Lett.* **2013**, *42*, 1020–1022. (k) Kammari, B. R.; Bejjanki, N. K.; Kommu, N. Total synthesis of decytospolides A, B and a formal synthesis of

aspergillide A starting from d-mannitol via tandem/domino reactions by Grubb's catalysts. *Tetrahedron: Asymmetry* **2015**, *26*, 296–303. (l) Koh, P.-F.; Loh, T.-P. Synthesis of biologically active natural products, aspergillides A and B, entirely from biomass derived platform chemicals. *Green Chemistry* **2015**, *17*, 3746–3750.

[92] Aspergillide C: (a) Nagasawa, T.; Kuwahara, S. Enantioselective total synthesis of aspergillide C. *Org. Lett.* **2009**, *11*, 761–764. (b) Panarese, J. D.; Waters, S. P. Enantioselective formal total synthesis of (+)-aspergillide C. *Org. Lett.* **2009**, *11*, 5086-5088. (c) Kanematsu, M.; Yoshida, M.; Shishido, K. Total synthesis of (+)-aspergillide C. *Tetrahedron Lett.* **2011**, *52*, 1372–1374. (d) Kobayashi, H.; Kanematsu, M.; Yoshida, M.; Shishido, K. Efficient access to a dihydropyran-containing macrolide via a transannular oxy-Michael reaction: total synthesis of (+)-aspergillide C. *Chem. Commun.* **2011**, *47*, 7440–7442. (e) Srihari, P.; Sridhar, Y., Total synthesis of both enantiomers of macrocyclic lactone Aspergillide C. *Eur. J. Org. Chem.* **2011**, 6690–6697.

[93] Trost, B. M.; Weiss, A. H.; Jacobi von Wangelin, A. Dinuclear Zn-catalyzed asymmetric alkynylation of unsaturated aldehydes. *J. Am. Chem. Soc.* **2006**, *128*, 8–9.

[94] Trost, B. M.; Ball, Z. T. Alkyne hydrosilylation catalyzed by a cationic ruthenium complex: efficient and general trans addition. *J. Am. Chem. Soc.* **2005**, *127*, 17644–17655.

[95] Achmatowicz Jr, O.; Bielski, R. Stereoselective total synthesis of methyl α-D-and α-L-glucopyranosides. *Carbohydr. Res.* **1977**, *55*, 165–176.

[96] (a) Isobe, M.; Nishizawa, R.; Hosokawa, S.; Nishikawa, T. Stereocontrolled synthesis and reactivity of sugar acetylenes. *Chem. Commun.* **1998**, 2665–2676. (b) Saeeng, R.; Sirion, U.; Sahakitpichan, P.; Isobe, M. Iodine catalyzes C-

glycosidation of D-glucal with silylacetylene. *Tetrahedron Lett.* **2003**, *44*, 6211–6215.

[97] Yu, X. Q.; Yoshimura, F.; Ito, F.; Sasaki, M.; Hirai, A.; Tanino, K.; Miyashita, M. Palladium-Catalyzed Stereospecific Substitution of α, β-Unsaturated γ, δ-Epoxy Esters by Alcohols with Double Inversion of Configuration: Synthesis of 4-Alkoxy-5-hydroxy-2-pentenoates. *Angew. Chem. Int. Ed.* **2008**, *47*, 750–754.

[98] Yadav, J. S.; Gyanchander, E.; Mishra, A. K.; Adithya, P.; Das, S. Novel iodine catalyzed diastereoselective synthesis of trans-2, 6-disubstituted tetrahydro-2H-pyrans: synthesis of C1–C13 fragment of bistramide-A. *Tetrahedron Lett.* **2013**, *54*, 5879–5882.

[99] Massi, A.; Nuzzi, A.; Dondoni, A. Microwave-assisted organocatalytic anomerization of α-C-glycosylmethyl aldehydes and ketones. *J. Org. Chem*. **2007**, *72*, 10279–10282.

[100] (a) Julia, M.; Paris, J.-M. Syntheses a l'aide de sulfones v (+)-methode de synthese generale de doubles liaisons. *Tetrahedron Lett.* **1973**, *14*, 4833–4836. (b) Kocienski, P. J.; Lythgoe, B.; Ruston, S. Scope and stereochemistry of an olefin synthesis from β-hydroxysulphones. *J. Chem. Soc., Perkin Trans. 1* **1978**, 829–834. (c) Chatterjee, B.; Bera, S.; Mondal, D. Julia–Kocienski olefination: a key reaction for the synthesis of macrolides. *Tetrahedron: Asymmetry* **2014**, *25*, 1–55.

[101] Miyaura, N.; Yamada, K.; Suzuki, A. A new stereospecific cross-coupling by the palladium-catalyzed reaction of 1-alkenylboranes with 1-alkenyl or 1-alkynyl halides. *Tetrahedron Lett.* **1979**, *20*, 3437–3440.

[102] King, A. O.; Okukado, N.; Negishi, E.-i. Highly general stereo-, regio-, and chemo-selective synthesis of terminal and internal conjugated enynes by the Pd-catalysed

reaction of alkynylzinc reagents with alkenyl halides. *J. Chem. Soc., Chem. Commun.* **1977**, 683–684.

[103] Larock, R. C.; Hightower, T. R. Synthesis of unsaturated lactones via palladium-catalyzed cyclization of alkenoic acids. *J. Org. Chem*. **1993**, *58*, 5298–5300.

[104] Youngsaye, W.; Lowe, J. T.; Pohlki, F.; Ralifo, P.; Panek, J. S. Total synthesis and stereochemical reassignment of (+)-neopeltolide. *Angew. Chem.* **2007**, *119*, 9371–9374.

[105] (a) Gallon, J.; Reymond, S.; Cossy, J. Neopeltolide, a new promising antitumoral agent. *Comptes Rendus Chimie* **2008**, *11*, 1463–1476. (b) Kinghorn, A. D.; Chin, Y.-W.; Swanson, S. M. Discovery of natural product anticancer agents from biodiverse organisms. *Curr Opin Drug Discov Devel.* **2009**, *12*, 189–196. (c) Zhu, X.-L.; Zhang, R.; Wu, Q.-Y.; Song, Y.-J.; Wang, Y.-X.; Yang, J.-F.; Yang, G.-F. Natural product neopeltolide as a cytochrome bc_1 complex inhibitor: mechanism of action and structural modification. *J. Agric. Food. Chem.* **2019**, *67*, 2774–2781.

[106] Total syntheses: (a) Custar, D. W.; Zabawa, T. P.; Scheidt, K. A. Total synthesis and structural revision of the marine macrolide neopeltolide. *J. Am. Chem. Soc.* **2008**, *130*, 804–805. (b) Custar, D. W.; Zabawa, T. P.; Hines, J.; Crews, C. M.; Scheidt, K. A. Total synthesis and structure− activity investigation of the marine natural product neopeltolide. *J. Am. Chem. Soc.* **2009**, *131*, 12406-12414. (c) Vintonyak, V. V.; Kunze, B.; Sasse, F.; Maier, M. E. Total synthesis and biological activity of neopeltolide and analogues. *Chem. Euro. J.* **2008**, *14*, 11132–11140. (d) Woo, S. K.; Kwon, M. S.; Lee, E. Total synthesis of (+)-neopeltolide by a Prins macrocyclization. *Angew. Chem. Int. Ed.* **2008**, *47*, 3242–3244. (e) Ulanovskaya, O. A.; Janjic, J.; Suzuki, M.; Sabharwal, S. S.; Schumacker, P. T.; Kron, S. J.; Kozmin, S. A. Synthesis enables identification of the cellular target of leucascandrolide A and neopeltolide. *Nat. Chem. Biol.* **2008**, *4*, 418-424. (f) Fuwa, H.; Naito, S.; Goto, T.; Sasaki, M. Total synthesis of (+)-neopeltolide. *Angew.*

Chem. **2008**, *120*, 4815–4817. (g) Paterson, I.; Miller, N. A. Total synthesis of the marine macrolide (+)-neopeltolide. *Chem. Commun.* **2008**, 4708–4710. (h) Guinchard, X.; Roulland, E. Total synthesis of the antiproliferative macrolide (+)-neopeltolide. *Org. Lett.* **2009**, *11*, 4700–4703. (i) Tu, W.; Floreancig, P. E. Oxidative carbocation formation in macrocycles: Synthesis of the neopeltolide macrocycle. *Angew. Chem. Int. Ed.* **2009**, *48*, 4567–4571. (j) Cui, Y.; Tu, W.; Floreancig, P. E. Total synthesis of neopeltolide and analogs. *Tetrahedron* **2010**, *66*, 4867–4873. (k) Cui, Y.; Balachandran, R.; Day, B. W.; Floreancig, P. E. Synthesis and biological evaluation of neopeltolide and analogs. *J. Org. Chem.* **2012**, *77*, 2225–2235. (l) Martinez-Solorio, D.; Jennings, M. P. Formal synthesis of (−)-neopeltolide featuring a highly stereoselective oxocarbenium formation/reduction sequence. *J. Org. Chem.* **2010**, *75*, 4095–4104. (m) Ghosh, A. K.; Shurrush, K. A.; Dawson, Z. L. Enantioselective total synthesis of macrolide (+)-neopeltolide. *Org. Biomol. Chem.* **2013**, *11*, 7768–7777. (n) Bai, Y.; Davis, D. C.; Dai, M. Synthesis of Tetrahydropyran/Tetrahydrofuran-Containing Macrolides by Palladium-Catalyzed Alkoxycarbonylative Macrolactonizations. *Angew. Chem. Int. Ed.* **2014**, *53*, 6519–6522. (o) Yu, M.; Schrock, R. R.; Hoveyda, A. H. Catalyst-Controlled Stereoselective Olefin Metathesis as a Principal Strategy in Multistep Synthesis Design: A Concise Route to (+)-Neopeltolide. *Angew. Chem. Int. Ed.* **2015**, *54*, 215–220. (p) Meissner, A.; Tanaka, N.; Takamura, H.; Kadota, I. Stereocontrolled synthesis of the macrolactone core of neopeltolide. *Tetrahedron Lett.* **2019**, *60*, 432–434.

[107] Formal syntheses (a) Vintonyak, V. V.; Maier, M. E. Formal total synthesis of neopeltolide. *Org. Lett.* **2008**, *10*, 1239–1242. (b) Kartika, R.; Gruffi, T. R.; Taylor, R. E. Concise enantioselective total synthesis of neopeltolide macrolactone highlighted by ether transfer. *Org. Lett.* **2008**, *10*, 5047–5050. (c) Kim, H.; Park, Y.; Hong, J. Stereoselective Synthesis of 2, 6-cis-Tetrahydropyrans through a Tandem Allylic Oxidation/Oxa-Michael Reaction Promoted by the gem-Disubstituent Effect: Synthesis of (+)-Neopeltolide Macrolactone. *Angew. Chem.*

Int. Ed. **2009**, *48*, 7577–7581. (d) Yadav, J. S.; Krishana, G. G.; Kumar, S. N. A concise stereoselective formal total synthesis of the cytotoxic macrolide (+)-Neopeltolide via Prins cyclization. *Tetrahedron* **2010**, *66*, 480–487. (e) Yang, Z.; Zhang, B.; Zhao, G.; Yang, J.; Xie, X.; She, X. Concise formal synthesis of (+)-neopeltolide. *Org. Lett.* **2011**, *13*, 5916–5919. (f) Sharma, G. V.; Reddy, S. V.; Ramakrishna, K. V. Synthesis of the macrolactone core of (+)-neopeltolide by transannular cyclization. *Org. Biomol. Chem.* **2012**, *10*, 3689–3695. (g) Raghavan, S.; Samanta, P. K. Stereoselective synthesis of the macrolactone core of (+)-neopeltolide. *Org. Lett.* **2012**, *14*, 2346–2349. (h) Athe, S.; Chandrasekhar, B.; Roy, S.; Pradhan, T. K.; Ghosh, S. Formal total synthesis of (+)-neopeltolide. *The Journal of organic chemistry* **2012**, *77*, 9840-9845. (i) Hari, T. P.; Wilke, B. I.; Davey, J. A.; Boddy, C. N. Diastereoseletive Transannular Oxa-Conjugate Addition Generates the 2, 6-cis-Disubstituted Tetrahydropyran of Neopeltolide. *The J. Org. Chem.* **2016**, *81*, 415–423. (j) Yanagi, S.; Sugai, T.; Noguchi, T.; Kawakami, M.; Sasaki, M.; Niwa, S.; Sugimoto, A.; Fuwa, H. Fluorescence-labeled neopeltolide derivatives for subcellular localization imaging. *Org. Biomol.Chem.* **2019**, *17*, 6771–6776.

[108] Bai, Y.; Dai, M. Strategies and methods for the synthesis of anticancer natural product neopeltolide and its analogs. *Curr. Org. Chem.* **2015**, *19*, 871–885.

[109] Fuwa, H. Contemporary strategies for the synthesis of tetrahydropyran derivatives: Application to total synthesis of neopeltolide, a marine macrolide natural product. *Marine drugs* **2016**, *14*, 65–105.

[110] (a) Cernak, T. A.; Lambert, T. H. Multicatalytic synthesis of α-pyrrolidinyl ketones via a tandem palladium (II)/indium (III)-catalyzed aminochlorocarbonylation/Friedel− Crafts acylation reaction. *J. Am. Chem. Soc.* **2009**, *131*, 3124–3125. (b) Ambrosini, L. M.; Cernak, T. A.; Lambert, T. H.

Development of oxidative formylation and ketonylation reactions. *Synthesis* **2010**, *2010*, 870–881.

[111] (a) Hoveyda, A. H. Evolution of Catalytic Stereoselective Olefin Metathesis: from Ancillary Transformation to Purveyor of Stereochemical Identity. *J. Org. Chem.* **2014**, *79*, 4763−4792. (b) Hoveyda, A. H.; Kahn, R. K. M.; Torker, S.; Malcolmson, S. J. Catalyst-Controlled Stereoselective Olefin Metathesis. In Handbook of Metathesis, 2nd ed.; Grubbs, R. H.; Wenzel, A. G.; O'Leary, D. J.; Khosravi, E., Eds.; Wiley-VCH: Weinheim, Germany 2015; Vol. 2, Chapter 7, pp 503–559.

[112] Hirsch-Weil, D.; Abboud, K. A.; Hong, S. Isoquinoline-based chiral monodentate N-heterocyclic carbenes. *Chem. Commun.* **2010**, *46*, 7525–7527.

[113] Jiang, A. J.; Zhao, Y.; Schrock, R. R.; Hoveyda, A. H. Highly Z-selective metathesis homocoupling of terminal olefins. *J. Am. Chem. Soc.* **2009**, *131*, 16630–16631.

[114] Xu, L.; Xue, J.; Zou, Y.; He, S.; Wei, X. Three New β-Resorcylic Acid Lactones from Paecilomyces sp. SC0924. *Chin. J. Chem* . **2012**, *30*, 1273–1277.

[115] (a) Xu, L.-X.; Wu, P.; Wei, H.-H.; Xue, J.-H.; Hu, X.-P.; Wei, X.-Y. Paecilomycins J–M, four new β-resorcylic acid lactones from Paecilomyces sp. SC0924. *Tetrahedron Lett.* **2013**, *54*, 2648–2650. (b) Xu, L. X.; Xue, J. H.; Wu, P.; You, X. Y.; Wei, X. Y. Absolute Configurations of Four Resorcylic Acid Lactones, Paecilomycins J− M, by CD/TDDFT Calculations. *Chirality* **2014**, *26*, 44–50.

[116] Ohba, K.; Nakata, M. Total synthesis of Paecilomycin B. *Org. Lett.* **2015**, *17*, 2890–2893.

[117] Ohba, K.; Koga, Y.; Nomura, S.; Nakata, M. Functionalized aryl-β-C-glycoside synthesis by Barbier-type reaction using 2, 4, 6-triisopropylphenyllithium. *Tetrahedron Lett.* **2015**, *56*, 1007–1010.

[118] (a) Mitsunobu, O.; Yamada, M.; Mukaiyama, T. Preparation of esters of phosphoric acid by the reaction of trivalent phosphorus compounds with diethyl azodicarboxylate in the presence of alcohols. *Bull. Chem. Soc. Jpn.* **1967**, *40*, 935–939. (b) Swamy, K. C. K.; Kumar, N. N. B.; Balaraman, E.; Kumar, K. V. P. P. Mitsunobu and Related Reactions: Advances and Applications. *Chem. Rev.* **2009**, *109*, 2551–2651.(c) Fletcher, S. The Mitsunobu reaction in the 21 st century. *Org. Chem. Front.* **2015**, *2*, 739–752. (d) Heravi, M. M.; Ghalavand, N.; Ghanbarian, M.; Mohammadkhani, L. Applications of Mitsunobu Reaction in total synthesis of natural products. *Appl. Organomet. Chem.* **2018**, *32*, e4464.

[119] Ohba, K.; Nakata, M. Convergent Total Synthesis of Paecilomycin B and 6′-epi-Paecilomycin B by a Barbier-Type Reaction Using 2, 4, 6-Triisopropylphenyllithium. *J. Org. Chem.* **2018**, *83*, 7019–7032.

[120] Tan, L. T.; Márquez, B. L.; Gerwick, W. H. Lyngbouilloside, a Novel Glycosidic Macrolide from the Marine Cyanobacterium Lyngbya bouillonii. *J. Nat. Prod.* **2002**, *65*, 925–928.

[121] Luesch, H.; Yoshida, W. Y.; Harrigan, G. G.; Doom, J. P.; Moore, R. E.; Paul, V. J. Lyngbyaloside B, a new glycoside macrolide from a Palauan marine cyanobacterium, Lyngbya sp. *J. Nat. Prod.* **2002**, *65*, 1945–1948.

[122] Sone, H.; Kigoshi, H.; Yamada, K. Aurisides A and B, cytotoxic macrolide glycosides from the Japanese sea hare Dolabella auricularia. *J. Org. Chem*. **1996**, *61*, 8956–8960.

[123] Hoffmann, L.; Demoulin, V. marine cyanophyceae of papua-new-guinea. 2. Lyngbya-bouillonii sp-nov a remarkable tropical reef-inhabiting blue-green-alga. *Belg. J. Bot.* **1991**, *124*, 82–88.

[124] EIMarrouni, A.; Lebeuf, R.; Gebauer, J.; Heras, M.; Arseniyadis, S.; Cossy, J. Total Synthesis of the Nominal Lyngbouilloside Aglycon. *Org. Lett.* **2012**, *14*, 314–317.

[125] Fuwa, H.; Yamagata, N.; Okuaki, Y.; Ogata, Y.; Saito, A.; Sasaki, M. Total Synthesis and Complete Stereostructure of a Marine Macrolide Glycoside (–)-Lyngbyaloside B. *Chem. Eur. J.* **2016**, *22*, 6815–6829.

[126] For an excellent review, see: ElMarrouni, A.; Kolleth, A.; Lebeuf, R.; Gebauer, J.; Prevost, S.; Heras, M.; Arseniyadis, S.; Cossy, J., Lyngbouilloside and related macrolides from marine cyanobacteria. *Nat. Prod. Commun.* **2013**, *8*, 965–72 and references cited therein.

[127] Gebauer, J.; Arseniyadis, S.; Cossy, J. Facile Synthesis of the C1-C13 Fragment of Lyngbouilloside. *Synlett* **2008**, 712–714.

[128] Webb, D.; van den Heuvel, A.; Kögl, M.; Ley, S. V. Enantioselective synthesis of the lyngbouilloside macrolactone core. *Synlett* **2009**, 2320–2324.

[129] (a) Boeckman, R. K.; Pruitt, J. R. A new, highly efficient, selective methodology for formation of medium-ring and macrocyclic lactones via intramolecular ketene trapping: an application to a convergent synthesis of (-)-kromycin. *J. Am. Chem. Soc.* **1989**, *111*, 8286–8288. (b) Mottet, C.; Hamelin, O.; Garavel, G.; Deprés, J. -P., Greene, A. E. A Simple and Efficient Preparation of Propargylic β-Keto Esters through Transesterification. *J. Org. Chem.* **1999**, *64*, 1380–1382. (c) Marshall, J. A.; Eidam, P. M. A Formal Synthesis of the Callipeltoside Aglycone. *Org. Lett.* **2008**, *10*, 93–96.

[130] For an excellent review on intermolecular and intramolecular trappings of acylketenes with application to natural product synthesis, see: Reber, K. P.; Tilley, S. D.; Sorensen, E. Bond formations by intermolecular and intramolecular trappings of acylketenes and their applications in natural product synthesis. *Chem. Soc. Rev.* **2009**, *38*, 3022–3034.

[131] (a) Hoye, T. R.; Danielson, M. E.; May, A. E.; Zhao, H. Dual macrolactonization/pyran–hemiketal formation via acylketenes: applications to the synthesis of (−)-callipeltoside A and a lyngbyaloside B model system. *Angew. Chem. Int. Ed.* **2008**, *47*, 9743–9746. (b) Hoye, T. R.; Danielson, M. E.; May, A. E.; Zhao, H. Total Synthesis of (−)-Callipeltoside A. *J. Org. Chem.* **2010**, *75*, 7052–7060. (c) Williams, D. R.; Myers, B. J.; Mi, L.; Binder, R. J. Studies for the Total Synthesis of Amphidinolide P. *J. Org. Chem.* **2013**, *78*, 4762–4778.

[132] Kolleth, A.; Gebauer, J.; ElMarrouni, A.; Lebeuf, R.; Arseniyadis, S.; Cossy, J.; Prevost, C.; Brohan, E., Total Synthesis of Putative 11-epi-Lyngbouilloside Aglycon. *Front. Chem.* **2016**, *4*, 34.

[133] Stefan, E.; Taylor, R. E. Stereoselective Synthesis of the C9–C19 Fragment of Lyngbyaloside B and C via Ether Transfer. *Org. Lett.* **2012**, *14*, 3490–3493.

[134] Fuwa, H.; Yamagata, N.; Saito, A.; Sasaki, M. Total Synthesis of 13-Demethyllyngbyaloside B. *Org. Lett.* **2013**, *15*, 1630–1633.

(135) (a) Yadav, J. S.; Haldar, A.; Maity, T. Towards the Synthesis of Lyngbyaloside B: Stereoselective Synthesis of the C1–C16 Macrolactone Core Segment. *Eur. J. Org. Chem.* **2013**, 3076–3085. (b) Sabitha, G.; Reddy, T. R.; Yadav, J. S.; Sirisha, K. Stereoselective synthesis of the C1–C8 and C9–C16 fragments of revised structure of (−)-lyngbouilloside. *RSC Adv.* **2014**, *4*, 3149–3152.

(136) Sabitha, G.; Reddy, T. R.; Yadav, J. S.; Sirisha, K. Stereoselective synthesis of the C1–C8 and C9–C16 fragments of revised structure of (−)-lyngbouilloside. *RSC Adv.* **2014**, *4*, 3149–3152.

[137] Fuwa, H.; Okuaki, Y.; Yamagata, N.; Sasaki, N. Total Synthesis, Stereochemical Reassignment, and Biological Evaluation of (–)-Lyngbyaloside B. *Angew. Chem. Int. Ed.* **2015**, *54*, 868–873.

[138] Holmquist, C. R.; Roskamp, E. J. A selective method for the direct conversion of aldehydes in to β-keto esters with ethyl diazoacetate catalyzed by Tin(II) chloride. *J. Org. Chem.* **1989**, *54*, 3258–3260.

[139] Chegondi, R.; Hanson, P. R. Synthetic Studies to Lyngbouilloside: A Phosphate Tether-Mediated Synthesis of the Macrolactone Core. *Tetrahedron Lett.* **2015**, *56*, 3330–3333.

[140] Yu, W.; Mei, Y.; Kang, Y.; Hua, Z.; Jin, Z. Improved Procedure for the Oxidative Cleavage of Olefins by OsO_4−$NaIO_4$. *Org. Lett.* **2004**, *6*, 3217–3219.

[141] a) Zampella, A.; D'Auria, M. V.; Minale, L.; Debitus, C.; Roussakis, C. Callipeltoside A: a cytotoxic aminodeoxy sugar-containing macrolide of a new type from the marine Lithistida sponge Callipelta sp. *J. Am. Chem. Soc.* **1996**, *118*, 11085–11088. b) Zampella, A.; D'Auria, M. V.; Minale, L.; Debitus, C. Callipeltosides B and C, two novel cytotoxic glycoside macrolides from a marine lithistida sponge Callipelta sp. *Tetrahedron* **1997**, *53*, 3243–3248.

[142] Paterson, I.; Davies, R. D.; Marquez, R. Total synthesis of the callipeltoside aglycon. *Angew. Chem.* **2001**, *113*, 623–627.

[143] Trost, B. M.; Gunzner, J. L.; Dirat, O.; Rhee, Y. H. Callipeltoside A: total synthesis, assignment of the absolute and relative configuration, and evaluation of synthetic analogues. *J. Am. Chem. Soc.* **2002**, *124*, 10396–10415.

[144] Evans, D. A.; Hu, E.; Burch, J. D.; Jaeschke, G. Enantioselective total synthesis of callipeltoside A. *J. Am. Chem. Soc.* **2002**, *124*, 5654–5655

[145] Huang, H.; Panek, J. S. Total synthesis of callipeltoside A. *Org. Lett.* **2004**, *6*, 4383–4385.

[146] Hoye, T. R.; Danielson, M. E.; May, A. E.; Zhao, H. Dual Macrolactonization/Pyran–Hemiketal Formation via Acylketenes: Applications to the Synthesis of (−)-Callipeltoside A and a Lyngbyaloside B Model System. *Angew. Chem.* **2008**, *120*, 9889–9892.

[147] Carpenter, J.; Northrup, A. B.; Chung, d.; Wiener, J. J.; Kim, S. G.; MacMillan, D. W. Total synthesis and structural revision of callipeltoside C. *Angew. Chem.* **2008**, *120*, 3624–3628.

[148] Frost, J. R.; Pearson, C. M.; Snaddon, T. N.; Booth, R. A.; Ley, S. V. Convergent total syntheses of callipeltosides A, B, and C. *Angew. Chem. Int. Ed.* **2012**, *51*, 9366–9371.

[149] Yeung, K.-S.; Paterson, I. Advances in the total synthesis of biologically important marine macrolides. *Chem. Rev.* **2005**, *105*, 4237–4313.

[150] Hussain, H.; Green, I. R.; Krohn, K.; Ahmed, I. Advances in the total synthesis of biologically important callipeltosides: a review. *Nat. Prod. Rep.* **2013**, *30*, 640–693.

[151] Frost J.R., Ley S.V. (2020) The Callipeltoside Story. In: Kiyota H. (eds) Marine Natural Products. Topics in Heterocyclic Chemistry, vol *58*. Springer.

[152] Paterson, I.; Davies, R. D.; Heimann, A. C.; Marquez, R.; Meyer, A. Stereocontrolled total synthesis of (−)-callipeltoside A. *Org. Lett.* **2003**, *5*, 4477–4480.

[153] Saito, S.; Shiozawa, M.; Ito, M.; Yamamoto, H. Conceptually new directed aldol condensation using aluminum tris (2, 6-diphenylphenoxide). *J. Am. Chem. Soc.* **1998**, *120*, 813–814.

[154] Paterson, I.; Perkins, M. V. Studies in polypropionate synthesis: stereoselective synthesis of (−)-denticulatins A and B. *Tetrahedron Lett.* **1992**, *33*, 801–804.

[155] Brownbridge, P.; Chan, T.; Brook, M.; Kang, G. Chemistry of enol silyl ethers. A general synthesis of 3-hydroxyhomophthalates and a biomimetic synthesis of sclerin. *Can. J. Chem.* **1983**, *61*, 688–693.

[156] Schmidt, R. R.; Michel, J. Facile synthesis of α-and β-O-glycosyl imidates; preparation of glycosides and disaccharides. *Angew. Chem. Int. Ed.* **1980**, *19*, 731–732.

[157] Trost, B. M.; Toste, F. D.; Pinkerton, A. B. Non-metathesis ruthenium-catalyzed C− C bond formation. *Chem. Rev.* **2001**, *101*, 2067–2096.

[158] Trost, B.; Toste, F. Regio-and enantioselective allylic alkylation of an unsymmetrical substrate: a working model. *J. Am. Chem. Soc.* **1999**, *121*, 4545–4554.

[159] Evans, D. A.; Ng, H. P.; Clark, J. S.; Rieger, D. L. Diastereoselective Anti Aldol Reactions of Chiral Ethyl Ketones. Enantioselective Processes for the Synthesis of Polypropionate Natural Products. *Tetrahedron* **1992**, *48*, 2127–2142.

[160] Huang, H.; Panek, J. S. Stereoselective synthesis of functonalized dihydropyrans via a formal [4+ 2]-annulation of chiral crotylsilanes. *J. Am. Chem. Soc.* **2000**, *122*, 9836-9837.

[161] Northrup, A. B.; MacMillan, D. W. The first direct and enantioselective cross-aldol reaction of aldehydes. *J. Am. Chem. Soc.* **2002**, *124*, 6798–6799.

[162] Semmelhack, M.; Kim, C.; Zhang, N.; Bodurow, C.; Sanner, M.; Dobler, W.; Meier, M. Intramolecular alkoxy-carbonylation of hydroxy alkenes promoted by Pd (II). *Pure Appl. Chem.* **1990**, *62*, 2035–2040.

[163] Brown, S. P.; Brochu, M. P.; Sinz, C. J.; MacMillan, D. W. The direct and enantioselective organocatalytic α-oxidation of aldehydes. *J. Am. Chem. Soc.* **2003**, *125*, 10808–10809.

[164] Dieguez-Vazquez, A.; Tzschucke, C. C.; Crecente-Campo, J.; Mcgrath, S.; Ley, S. V. AuCl3-Catalyzed Hydroalkoxylation of Conjugated Alkynoates: Synthesis of Five-and Six-Membered Cyclic Acetals. *Euro. J. Org. Chem.* **2009**, 1698–1706.

[165] (a) Keller-Schierlein, W.; Muntwyler, R.; Pache, W.; Zähner, H. Stoffwechselprodukte von Mikroorganismen 73. Mitteilung [1] Chlorothricin und Des-chlorothoricin. *Helv. Chim. Acta* **1969**, *52*, 127–142. (b) Brufani, M.; Cerrini, S.; Fedeli, W.; Mazza, F.; Muntwyler, R. Stoffwechselprodukte von Mikroorganismen. 108. Mitteilung. Kristallstrukturanalyse des Chlorothricolid-methylesters. *Helv. Chim. Acta* **1972**, *55*, 2094–2102.

[166] Schroeder, D. R.; Colson, K. L.; Klohr, S. E.; Lee, M. S.; Matson, J. A.; Brinen, L. S.; Clardy, J. Pyrrolosporin A, a New Antitumor Antibiotic from Micromonospora sp. C39217-R109-7. *J. Antibiot.* **1996**, *49*, 865-872. (b)

[167] Aldridge, D.; Armstrong, J.; Speake, R.; Turner, W. The cytochalasins, a new class of biologically active mould metabolites. *ChemComm.* **1967**, 26–27.

[168] Shao, C.-L.; Wu, H.-X.; Wang, C.-Y.; Liu, Q.-A.; Xu, Y.; Wei, M.-Y.; Qian, P.-Y.; Gu, Y.-C.; Zheng, C.-J.; She, Z.-G. Potent antifouling resorcylic acid lactones from the gorgonian-derived fungus Cochliobolus lunatus. *J. Nat. Prod.* **2011**, *74*, 629–633.

[169] (a) Ireland, R. E.; Thompson, W. J. An approach to the total synthesis of chlorothricolide: the synthesis of the top half. *J. Org. Chem.* **1979**, *44*, 3041–3052. (b) Ireland, R. E.; Thompson, W. J.; Srouji, G. H.; Etter, R. Approach to the total synthesis of chlorothricolide: synthesis of" 7-epi-bottom half" and its union with" top half" systems. *J. Org. Chem.***1981**, *46*, 4863–4873. (c) Hall, S. E.; Roush, W. R. Synthesis of the bottom half of chlorothricolide. *J. Org. Chem.* **1982**, *47*, 4611–4621. (d) Snider, B. B.; Burbaum, B. W. Intramolecular Diels-Alder reactions of alkenylallenes. A model study for the bottom half of chlorothricolide. *J. Org. Chem.* **1983**, *48*, 4370–4374. (e) Schmidt, R. R.; Hirsenkorn, R. Investigations for synthesizing chlorothricolide. *Tetrahedron Lett.* **1984**, *25*, 4357–4360. (f) Marshall, J. A.; Audia, J. E.; Grote, J. Intramolecular Diels-Alder cyclization of conjugated aldehydes. Synthesis of a chlorothricolide intermediate. *J. Org. Chem.* **1984**, *49*, 5277–5279. (g) Roush, W. R.; Kageyama, M. Enantioselective synthesis of the bottom-half of chlorothricolide. *Tetrahedron Lett.* **1985**, *26*, 4327–4330. (h) Ireland, R. E.; Varney, M. D. Approach to the total synthesis of chlorothricolide: synthesis of (.+-.)-19, 20-dihydro-24-O-methylchlorothricolide methyl ester ethyl carbonate. *J. Org. Chem.* **1986**, *51*, 635–648. (i). Roush, W. R.; Riva, R. Enantioselective synthesis of the bottom half of chlorothricolide. 2. A comparative study of substituent effects on the stereoselectivity of the key intramolecular Diels-Alder reaction. *J. Org. Chem.* **1988**, *53*, 710–712. (j) Okumura, K.; Okazaki, K.; Takeda, K.; Yoshii, E. Methyl α-acyloxy-γ-methylene-β-tetronate. Preparation and

use as a building block for the synthesis of the spirotetronic acid structure of chlorothricolide. *Tetrahedron Lett.* **1989**, *30*, 2233–2236. (k) Roush, W. R.; Sciotti, R. J. Enantioselective total synthesis of (−)-chlorothricolide via the tandem inter- and intramolecular Diels−Alder reaction of a hexaenoate intermediate. *J. Am. Chem. Soc.* **1998**, *120*, 7411–7419.

[170] For reviews see: (a) Takao, K.-i.; Munakata, R.; Tadano, K.-i. Recent advances in natural product synthesis by using intramolecular Diels− Alder reactions. *Chem. Rev.* **2005**, *105*, 4779–4807. (b) Zografos, A. L.; Georgiadis, D. Synthetic strategies towards naturally occurring tetronic acids. *Synthesis* **2006**, 3157–3188. (c) Princiotto, S.; Jayasinghe, L.; Dallavalle, S. Recent advances in the synthesis of naturally occurring tetronic acids. *Bioorg. Chem.* **2021**, 105552–105584.

[171] (a) Masamune, S.; Hayase, Y.; Schilling, W.; Chan, W. K.; Bates, G. S. Activation of thiol esters. Partial synthesis of cytochalasins A and B. *J. Am. Chem. Soc.* **1977**, *99*, 6756–6758. (b) Stork, G.; Nakahara, Y.; Nakahara, Y.; Greenlee, W. Total synthesis of cytochalasin B. *J. Am. Chem. Soc.* **1978**, *100*, 7775–7777. (c) Kim, M. Y.; Starrett Jr, J. E.; Weinreb, S. M. Synthetic approach to cytochalasins. *J. Org. Chem.* **1981**, *46*, 5383–5389. (d) Stork, G.; Nakamura, E. A simplified total synthesis of cytochalasins via an intramolecular Diels-Alder reaction. *J. Am. Chem. Soc.* **1983**, *105*, 5510–5512. (e) Haidle, A. M.; Myers, A. G. An enantioselective, modular, and general route to the cytochalasins: Synthesis of L-696,474 and cytochalasin B. *Proc. Nat. Acad. Sci.* **2004**, *101*, 12048–12053.

[172] For a review on the syntheses of cytochalasins, see: Scherlach, K.; Boettger, D.; Remme, N.; Hertweck, C. The chemistry and biology of cytochalasans. *Natural product reports* **2010**, *27*, 869–886.

[173] Jana, N.; Nanda, S. Resorcylic acid lactones (RALs) and their structural congeners: recent advances in their biosynthesis, chemical synthesis and biology. *New J. Chem.* **2018**, *42*, 17803–17873.

[174] (a) Srihari, P.; Mahankali, B.; Rajendraprasad, K. Stereoselective total synthesis of paecilomycin E. *Tetrahedron Lett.* **2012**, *53*, 56–58. (b) Jana, N.; Nanda, S. Asymmetric total synthesis of 5′-epi-paecilomycin-F. *Tetrahedron: Asymmetry* **2012**, *23*, 802–808. (c) Pal, P.; Jana, N.; Nanda, S. Asymmetric total synthesis of paecilomycin E, 10′-epi-paecilomycin E and 6′-epi-cochliomycin C. *Org. Biomol. Chem.* **2014**, *12*, 8257–8274. (d) Mahankali, B.; Srihari, P. A Carbohydrate Approach for the First Total Synthesis of Cochliomycin C: Stereoselective Total Synthesis of Paecilomycin E, Paecilomycin F and 6′-epi-Cochliomycin C. *Eur. J. Org. Chem.* **2015**, *2015*, 3983–3993. (e) Kadari, S.; Yerrabelly, H.; Yerrabelly, J. R.; Gogula, T.; Goud, Y.; Thalari, G.; Doda, S. R. Stereoselective total synthesis of paecilomycin E and F and its two congeners Cochliomycin C and 6-epi-Cochliomycin C. *Synth. Commun.* **2018**, *48*, 1867–1875. (f) Reddy, A. S.; Bhavani, G.; Jonnala, S.; Bantu, R.; Reddy, B. S. A Concise and Stereoselective Total Synthesis of Paecilomycin E. *Nat. Prod. Commun.* **2019**, *14*, 131–133.

[175] (a) Patterson, J. W. The Alder-Rickert Reaction in a Synthesis of *m*-Chlorophenols and 4-Chloromycophenolic Acid. *J. Org. Chem.* **1995**, *60*, 560–563.

[176] Müller, S.; Liepold, B.; Roth, G. J.; Bestmann, H. J. An improved one-pot procedure for the synthesis of alkynes from aldehydes. *Synlett* **1996**, *1996*, 521–522.

[177] Bhattacharjee, A.; De Brabander, J. K. Synthesis of side chain truncated apicularen A. *Tetrahedron Lett.* **2000**, *41*, 8069–8073.

[178] (a) Meutermans, W. D.; Bourne, G. T.; Golding, S. W.; Horton, D. A.; Campitelli, M. R.; Craik, D.; Scanlon, M.; Smythe, M. L. Difficult macrocyclizations: new strategies for synthesizing highly strained cyclic tetrapeptides. *Org. Lett.* **2003**, *5*, 2711–2714. (b) Blunt, J. W.; Copp, B. R.; Keyzers, R. A.; Munro, M. H.; Prinsep, M. R. Marine natural products. *Nat. Prod. Rep.* **2014**, *31*, 160–258. (c) Wakimoto,

T.; Tan, K. C.; Tajima, H.; Abe, I., Cytotoxic cyclic peptides from the marine sponges. In *Handbook of anticancer drugs from marine origin*, Springer **2015**; pp 113–144. (d) Fischbach, M. A.; Walsh, C. T. Assembly-line enzymology for polyketide and nonribosomal peptide antibiotics: logic, machinery, and mechanisms. *Chem. Rev.* **2006**, *106*, 3468–3496. (e) Han, S.-Y.; Kim, Y.-A. Recent development of peptide coupling reagents in organic synthesis. *Tetrahedron* **2004**, *60*, 2447–2467.

[179] Clark, W. D.; Corbett, T.; Valeriote, F.; Crews, P. Cyclocinamide A. An Unusual Cytotoxic Halogenated Hexapeptide from the Marine Sponge Psammocinia. *J. Am. Chem. Soc.* **1997**, *119*, 9285–9286.

[180] Grieco, P. A.; Reilly, M. Studies related to the absolute configuration of cyclocinamide A: total synthesis of 4 (R), 11 (R)-cyclocinamide A. *Tetrahedron Lett.* **1998**, *39*, 8925–8928.

[181] Liu, L., *I.* Synthesis of differentially linked beta-C-disaccharides. II. Synthetic studies towards the cyclic peptide cyclocinamide A. Ph.D Thesis, Wayne State University, Detroit, MI, **2002**.

[182] Rubio, B. K.; Robinson, S. J.; Avalos, C. E.; Valeriote, F. A.; de Voogd, N. J.; Crews, P. Revisiting the sponge sources, stereostructure, and biological activity of cyclocinamide A. *J. Nat. Prod.* **2008**, *71*, 1475–1478.

[183] Laird, D. W.; LaBarbera, D. V.; Feng, X.; Bugni, T. S.; Harper, M. K.; Ireland, C. M. Halogenated cyclic peptides isolated from the sponge Corticium sp. *J. Nat. Prod.* **2007**, *70*, 741–746.

[184] Garcia, J. M.; Curzon, S. S.; Watts, K. R.; Konopelski, J. P. Total Synthesis of Nominal (11 S)-and (11 R)-Cyclocinamide A. *Org. Lett.* **2012**, *14*, 2054–2057.

[185] Shioiri, T.; Ninomiya, K.; Yamada, S. Diphenylphosphoryl azide. New convenient reagent for a modified Curtius reaction and for peptide synthesis. *J. Am. Chem. Soc.* **1972**, *94*, 6203–6205.

[186] Hopkins, S. A.; Ritsema, T. A.; Konopelski, J. P. Enantiomerically Pure Tetrahydropyrimidinones in Asymmetric Synthesis: Preparation of a Protected α-Methylasparagine Derivative and Corresponding Dipeptides. *J. Org. Chem.* **1999**, *64*, 7885–7889.

[187] Curzon, S. S.; Garcia, J. M.; Konopelski, J. P. Total synthesis of nominal cyclocinamide B and investigation into the identity of the cyclocinamides. *Tetrahedron Lett.* **2015**, *56*, 2991–2994.

[188] Kang, H. S; Krunic, A.; Orjala, J. Sanctolide A, a 14-Membered PK-NRP Hybrid Macrolide from the Cultured Cyanobacterium *Oscillatoria sancta* (SAG 74.79). *Tetrahedron Lett.* **2012**, *53*, 3563–3567.

[189] Wadsworth, A. D.; Furkert, D. P.; Brimble, M. A. Total Synthesis of the Macrocyclic *N*-Methyl Enamides Palmyrolide A and 2*S*-Sanctolide A. *J. Org. Chem.* **2014**, *79*, 11179–11193.

[190] Marco, J. A.; García-Pla, J.; Carda, M.; Murga, J.; Falomir, E.; Trigili, C.; Notararigo, S.; Díaz, J. F.; Barasoain, I. Design and synthesis of pironetin analogues with simplified structure and study of their interactions with microtubules. *Euro. J. of Med. Chem.* **2011**, *46*, 1630–1637.

[191] Yadav, J. S.; Surresh, B.; Srihari, P. Stereoselective Total Synthesis of the Marine Macrolide Sanctolide A. *Eur. J. Org. Chem.* **2015**, *26*, 5856–5863.

[192] Hanawa, H.; Hashimoto, T.; Maruoka, K. Bis (((S)-binaphthoxy)(isopropoxy) titanium) oxide as a μ-oxo-type chiral Lewis acid: application to catalytic asymmetric allylation of aldehydes. *J. Am. Chem. Soc.* **2003**, *125*, 1708–1709.

Chapter 2

Total Synthesis of Sanctolide A and Formal Synthesis of (2S)-Sanctolide A

2.1 Introduction

Polyketides (PK) and nonribosomal peptides (NRP) represent two important classes of natural products.[1] The biosyntheses of these natural products are accomplished by polyketide synthases (PKSs) and nonribosomal peptide synthetases (NRPSs) in a modular fashion that occupy either an "assembly-line" or an iterative synthesis.[2] The PKS and NRPS modules work together to generate PK-NRP hybrids.[3] The PK-NRP hybrid family of cyclic enamide/amide-containing natural products is rare and relatively small, comprised namely of the 14-membered cyclic enamide sanctolide A (**2.1-A**),[4] (+)-*ent*-palmyrolide A,[5] madangolide,[6,7] laingolides,[6a,7] tricholides,[8] unnarmicin D,[8] and the nemamides.[1]

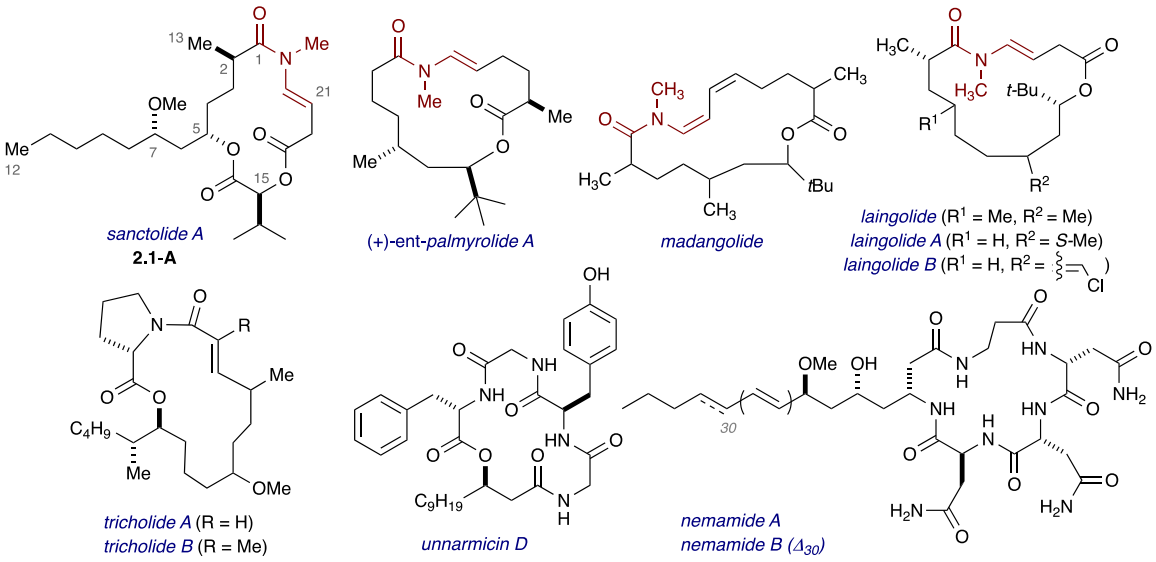

Figure 2.1 *Sanctolide A and other* PK-NRP *hybrid natural products.*

2.1.1 Sanctolide A: Isolation and background

The 14-membered PK–NRP hybrid macrolide, sanctolide A (**2.1A**) was isolated from the cyanobacterium *Oscillatoria sancta* (SAG 74.79) by Orjala and coworkers in

2012 (Figure 2.1).[9] Sanctolide A belongs to a new class of cyanobacterial natural products where the two amino acid precursors, Gly and Val, are integrated into a polyketide chain to form a 14-membered macrolide. This hybrid macrolide possesses a 1,3-*anti*-diol subunit, a lipophilic pentyl side-chain, and a macrocyclic portion with a diester linkage and *N*-methyl trans enamide moiety. Interest in the synthesis and characterization of biologically active natural products and corresponding analogs has inspired work in the total synthesis of sanctolide A and analogs, which is reported in Chapters 2 and 3.

The biosynthesis of sanctolide A involves the formation of a hexaketide chain (C1–C12) utilizing six PKS modules.[9] The branched C13 methyl is proposed to be originated from a *S*-adenosyl-*L*-methionine (SAM)-dependent methyl transferase (MT) domain.[10] Further expansion of the polyketide chain is carried out by a cooperative NRPS module, which adds glycine with a ketide extension.[5] Reduction at the β-carbonyl, subsequent dehydration, followed by double bond isomerization from the C20−C21 olefin forms the C21–C22 enamide. Methylation of the enamide is predicted via a SAM-dependent MT domain.[10,11] The removal of the amino group by transamination of Val to generate alpha-ketoisovalerate, followed by reduction, generates the hydroxyisovaleric acid component connected to the C5 hydroxyl group. Completion of the biosynthesis of sanctolide A is proposed via a final esterification event between the C15 carbinol and the C19 carboxyl group.

The initial biological evaluation of sanctolide A demonstrated moderate toxicity in brine shrimp toxicity assays with a LD_{50} value of 23.5 μM.[12] Though the pharmacological profile of secondary cyclic enamides are well-known in the literature, and include greater

than 200 cyclopeptide alkaloids,[13] the biological potential of cyclic tertiary enamide—in particular, the *N*-methyl enamide—is under explored except for the natural product, palmyrolide A.[14] Therefore, synthesis of natural product belonging to the cyclic tertiary enamide family is interesting, and investigation of a modular synthetic approach is warranted. Of particular importance are syntheses of analogous compounds which allow for library generation and subsequent biological screening. In this regard, we herein report our synthetic efforts toward the modular synthesis of sanctolide A (**2.1**) and the formal synthesis of its C2-epimer, 2*S*-sanctolide A (2*S*-**2.1A**).

2.1.2 Synthesis of (*2S*)-Sanctolide A by Brimble and coworkers.

In 2014, Brimble and coworkers reported the total synthesis of (2*S*)-sanctolide A [(2*S*)-**2.1-A**] utilizing an RCM/olefin isomerization strategy as the key macrocyclization step (Figure 2.2).[15] The motivation associated with the synthesis of 2*S*-epimer in their synthesis was to resolve the ambiguity associated with the absolute stereochemistry at the C2 methyl center of the natural product.[9]

Retrosynthetic analysis of 2*S*-sanctolide A [(2*S*)-**2.1-A**] involves application of an RCM/olefin isomerization strategy for the macrocyclization to install the *N*-methyl enamide moiety (Figure 2.2). Ester **2.2.4** could be generated via an esterification of the carboxylic acid **2.2.3** and the amide-alcohol subunit **2.2.2**, which is the ring-opened product of the 2*S*-lactone methyl ether (2*S*)-**2.1.6**. Lactone methyl ether (2*S*)-**2.1.6** could be formed from the 1,3-*anti*-diol containing olefinic subunit **2.1.4** via esterification, subsequent RCM,

followed by substrate-controlled stereoselective hydrogenation of the intermediate dihydropyranone.

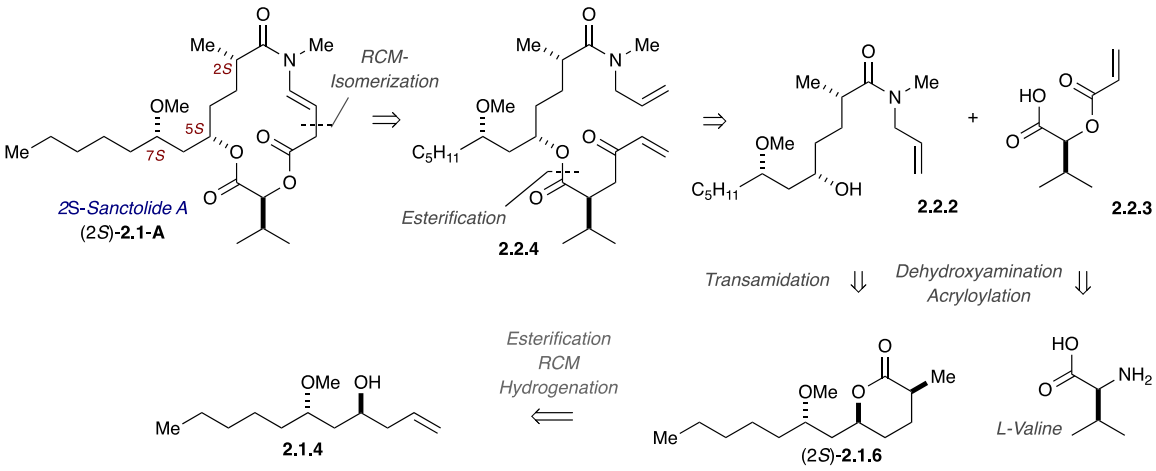

Figure 2.2 *Retrosynthetic analysis of 2*S*-sanctolide A by Brimble and coworkers.*

The forward synthesis commenced with the generation of the 1,3-*anti*-diol containing olefinic subunit **2.1.4** by utilizing an iterative sequence of epoxidation, hydrolytic kinetic resolution (HKR), and vinyl-Grignard addition (Scheme 2.1). Epoxidation of hept-1-ene with *m*-CPBA provided the racemic epoxide (not shown). Chiral epoxide formation accomplished with Jacobsen's (*S,S*)-salenCo^{III}-OAc catalyst,[16] to furnish epoxide **2.1.1** in 86% yield. Vinyl-magnesium bromide addition to epoxide **2.1.1** using catalytic copper (I) iodide, generated the homo-allylic alcohol, which was subsequently methylated with sodium hydride and methyl iodide to provide **2.1.2** in excellent overall yield. Next, the olefin was epoxidized with *m*-CPBA to deliver epoxide methyl ether in 95% yield as 1:1 mixture of diastereomers. Subsequent chiral epoxide formation with (*R,R*)-salenCo^{III}-OAc, and epoxide opening with vinyl-MgBr/CuI (cat.), afforded the 1,3-*anti*-diol product **2.1.4** in 93% yield as a single diastereomer.

Methacryloylation with methacryloyl chloride, followed by RCM with 10 mol% of the second-generation Grubbs catalyst[17] [**G-II**, $(ImesH_2)(PCy_3)(Cl)_2Ru{=}CHPh$], furnished the dihydropyranone **2.1.5** in good yields. Installation of the 2*S*-configured methyl center was carried out by a substrate-controlled diastereoselective hydrogenation with H_2 (30 bar) and Pd/C (10 mol%), to generate the lactone (2*S*)-**2.1.6** in quantitative yields.

Scheme 2.1 *Synthesis of lactone (2*S*)-**2.1.6**.*

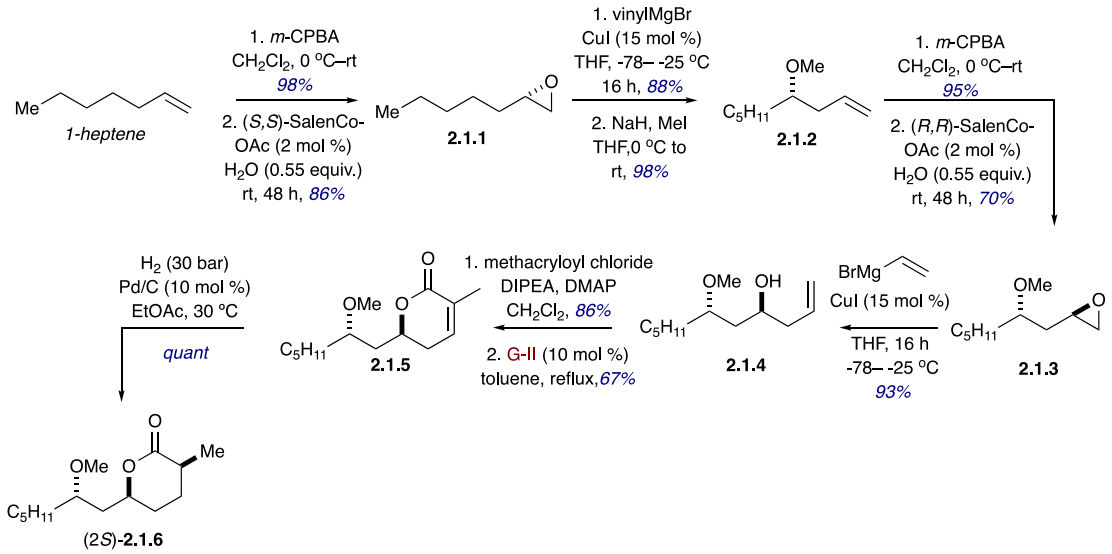

Subsequent lactone ring-opening of (2*S*)-**2.1.6** with *in-situ*-generated dimethylaluminum amine **2.2.1** furnished the amide **2.2.2** in 63% yield (Scheme 2.2). The Yamaguchi esterification[18] of the amide **2.2.2** with *in-situ*-generated 2,4,6-trichlorobenzoyl mixed anhydride of the acid **2.2.3** provided the diene precursor **2.2.4** in 92% yield. The acid **2.2.3** was generated via 2-hydroxyisovaleric acid (commercially available or 1 step from L-valine)[19] with acryloyl chloride in the presence of triethylamine. Subsequent RCM reaction with 30 mol% of the Grubbs **G-II** catalyst, in chloroform at refluxing conditions, delivered macrocyclic tertiary amide **2.2.5** in 50% yield, as a 1:1 mixture of *E*- and *Z*-

isomers. Completion of the *E*-configured *N*-methyl-enamide 2*S*-sanctolide A [(2*S*)-**2.1**-**A**)] was accomplished via a Ru-hydride-mediated olefin isomerization employing $(PPh_3)_3RuH(CO)Cl$[20] in 50% yield. The analysis of ^1H NMR data and optical rotation data provided useful information about the stereochemical configuration of the product, where the authors concluded that the final product was the C2-epimer of the desired natural product sanctolide A (**2.1**-**A**).

Scheme 2.2 *RCM/isomerization endgame strategy to 2*S*-sanctolide A by Brimble (2014).*

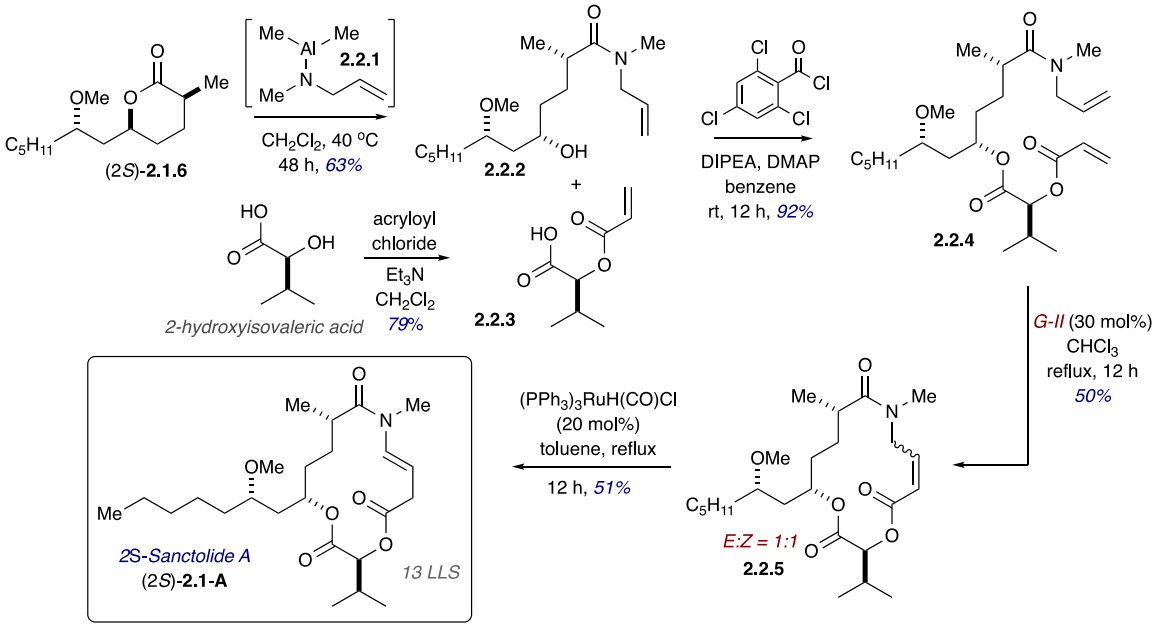

The aforementioned synthetic strategy employing an RCM/olefin isomerization sequence by Brimble and coworkers to generate the *N*-methylenamide moiety, was utilized by Dai and Ye in the syntheses of related natural products, namely, the laingolides A/B,[7] and (–)-palmyrolide A.[21] Moreover, we incorporated this late-stage strategy in our studies of Sanctolide A and analogs described in this Chapter, *vide infra*.

In 2018, Dai and coworkers utilized the Brimble RCM/olefin isomerization protocol to furnish the natural product (+)-laingolide B (**2.3-A**, Figure 2.3).[7] The diene precursor **2.3-C** was generated as a single diastereomer and a 1:1 mixture of amide rotamers (as evident by ^{1}H and ^{13}C NMR—but this is not mentioned by the authors), via an EDCI coupling of the carboxylic acid moiety (not shown) with *N*-allylmethylamine. The carboxylic acid was generated from an acid hydrolysis of Myers alkylation product comprising the (2*R*)-methyl center.

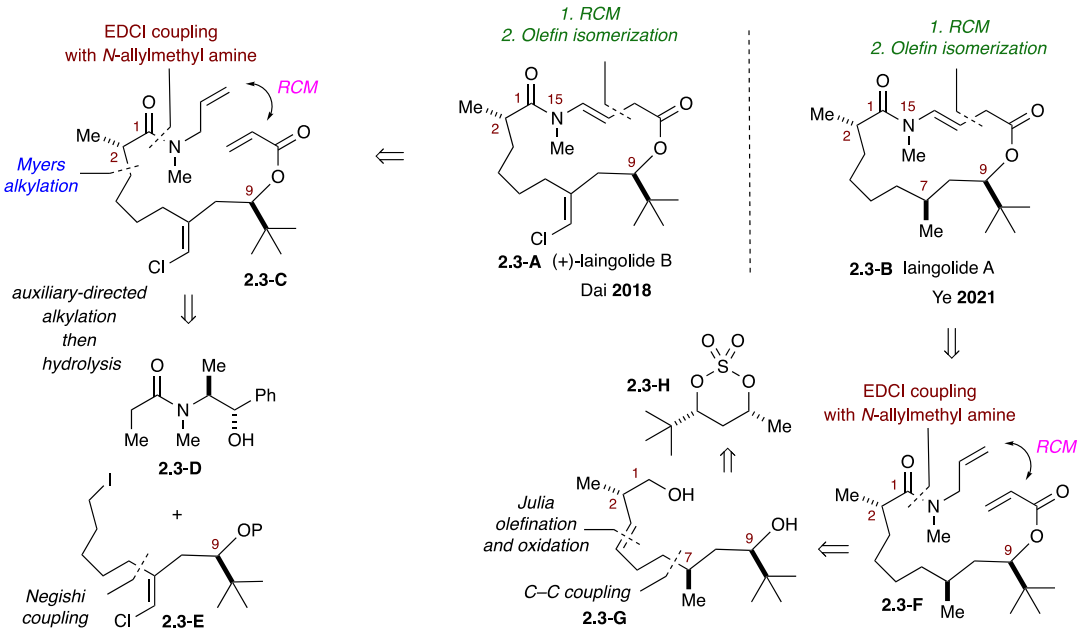

Figure 2.3 *Retrosynthetic analysis of 15-membered enamide macrolides laingolide B and laingolide A by Dai (2018) and Ye (2021), respectively.*

In 2021, Ye and coworkers reported the synthesis and stereochemical reassignment of laingolide A (**2.3-B**) by also utilizing the Brimble RCM/olefin isomerization protocol as the endgame (Figure 2.3).[7] The diene **2.3-F** was furnished via an EDCI coupling of the carboxylic acid moiety, which was generated by an oxidation of **2.3-G**. The linear

precursor **2.3-G** was delivered via a Julia-Kocienski olefination, where the C7-methyl center was installed via a Cu-catalyzed Kumada coupling reaction on the corresponding 1,3-*anti*-diol containing cyclic sulfate **2.3-H**. In this elegant work the authors made all four stereoisomers with variations at the C2 and C7 stereogenic centers.

2.1.3 Total Synthesis of Sanctolide A by Yadav and coworkers

In 2015, Yadav and coworkers published the total synthesis of sanctolide A (**2.1-A**).[22] The retrosynthetic analysis involved an intramolecular dehydrative enamide condensation of the *N*-methyl amide with aldehyde **2.1-B** as the key final step to deliver the natural product (Figure 2.4). The amide **2.1-B** could be generated via a late-stage deprotection-oxidation event from the protected alcohol subunit **2.4.4**, which was derived in 3 steps from diester **2.4.2**. The diester **2.4.2** could be generated by coupling the acid

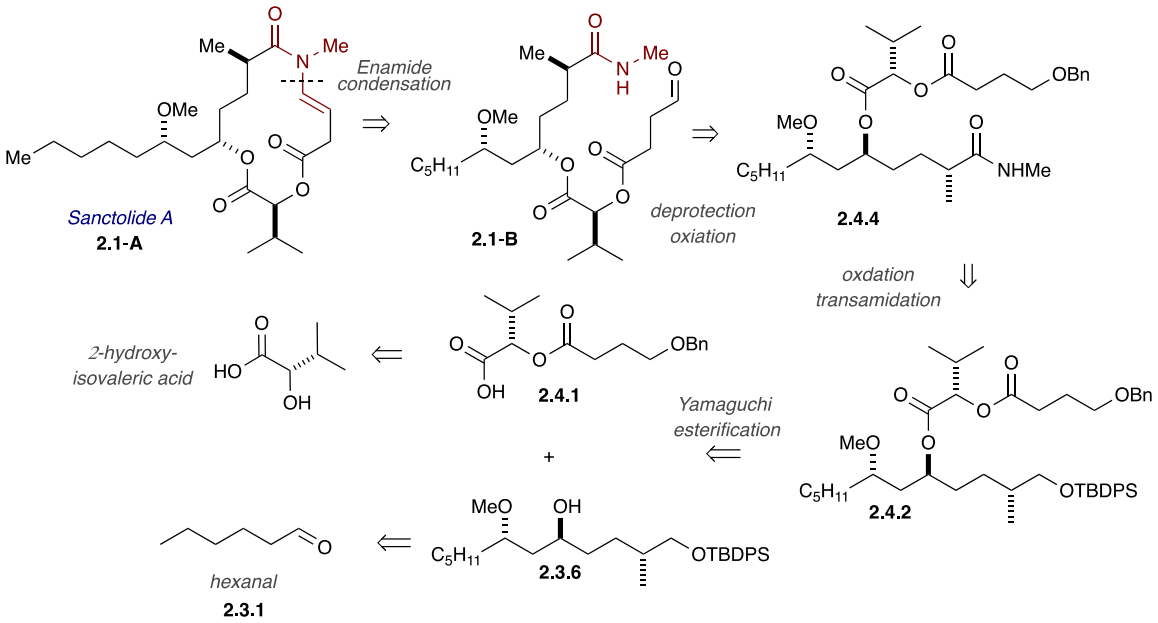

Figure 2.4 *Retrosynthetic analysis to sanctolide A by Yadav and coworkers.*

2.4.1, derived from 2-hydroxyisovaleric acid,[19] and the 1,3-*anti*-diol-containing subunit **2.3.6**. The 1,3-*anti*-diol-containing subunit **2.3.6** was generated from hexanal (**2.3.1**) in five steps.

The forward synthesis commenced with generation of homoallylic alcohol methyl ether **2.1.2** from commercially available hexanal (**2.3.1**), using an asymmetric allylation developed by Maruoka[23] and coworkers (Scheme 2.3). In this regard, the allyl alcohol (not shown) was furnished in 85% yield and 99% enantiomeric excess by employing asymmetric allylation with allyltributyltin and bis-(*R*)-Ti(IV) oxide catalyst, using the protocol developed by Maruoka and coworkers, where the subsequent methylation afforded the corresponding homoallylic alcohol methyl ether **2.1.2** in good yields. Subsequent use of the Upjohn dihydroxylation,[24] with oxidative cleavage of the diol using $NaIO_4$, delivered the terminal aldehyde, which was coupled with lithiated alkyne **2.3.2** to generate a diastereomeric mixture of propargyl 1,3-skipped diol product in 90% yield, albeit with modest selectivity (*dr* = 60:40, *syn*:*anti*). The undesired *syn*-diastereomer **2.3.3**

Scheme 2.3 *Stereoselective synthesis of* ***2.3.6****.*

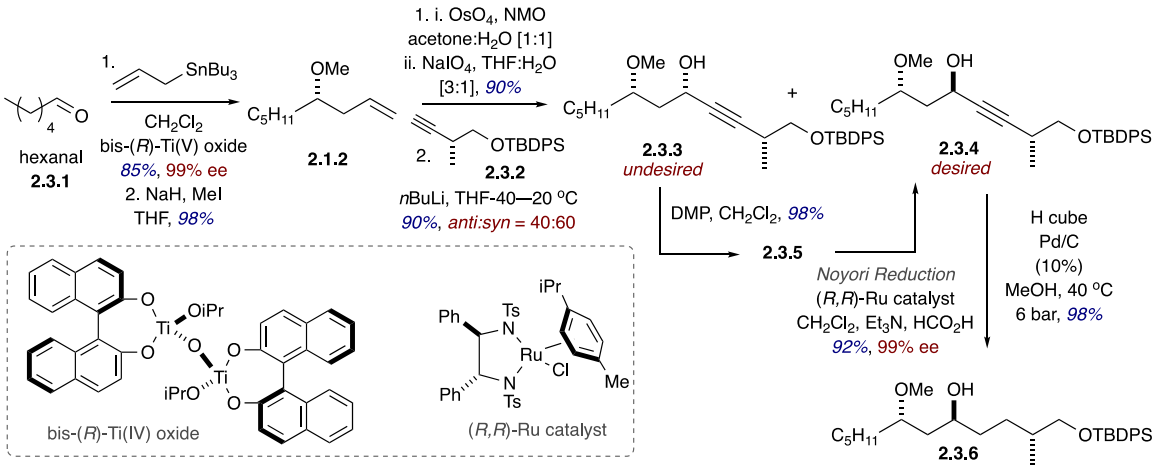

was further recycled via sequential oxidation with Dess-Martin periodinane (DMP),[25] followed by diastereoselective Noyori reduction[26] of the resultant ketone, to furnish the desired alcohol *anti*-**2.3.4** in excellent overall yield and selectivity. Alkyne reduction of **2.3.4** with an H-cube hydrogenation instrument, employing a Pd/C (10%) cartridge under pressure (3 bar), delivered the secondary alcohol **2.3.6** in 98% yield.

The hydroxy acid coupling partner **2.4.1** was synthesized from commercially available 2-hydroxyisovaleric acid in three steps. Coupling of the acid and the secondary alcohol **2.3.6** was carried out under Yamaguchi conditions (2,4,6-trichlorobenzoylchloride, DIPEA, DMAP),[18] at room temperature to deliver the diester **2.4.2** in 90% yield. Silyl-deprotection with TBAF, followed by DMP oxidation, and Pinnick oxidation,[27] furnished

Scheme 2.4 *Endgame of Yadav's synthesis of sanctolide A.*

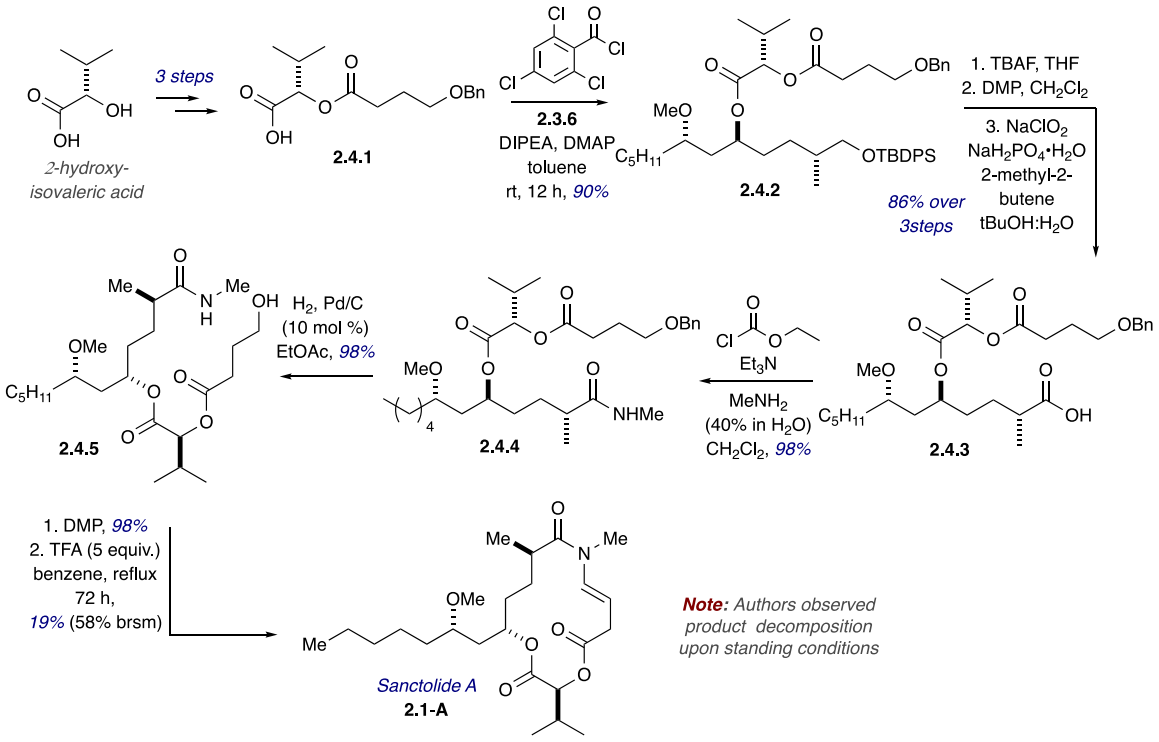

the corresponding acid **2.4.3** in good yields over 3 steps. The conversion of the acid into the mixed anhydride, and subsequent amidation with aqueous methyl amine, afforded **2.4.4** in 98% yield.

The removal of the benzyl protecting group with Pd/C (10 mol%) mediated catalyzed generated the primary alcohol **2.4.5** in near quantitative yields. Subsequent DMP oxidation of the primary alcohol in refluxing benzene, followed by treatment with five equivalents of trifluoroacetic acid (TFA) over 3 days, afforded the natural product sanctolide A (**2.1-A**), albeit in low yield (19%, 58% based on recovered starting material). The analytical data obtained was in good agreement with the reported natural product,[4] and thus confirmed the absolute configuration of the natural product as 2*R*-sanctolide A. It is worthy to note, that the authors reported an unexpected degradation of the synthesized product in standing conditions even at lower temperatures, *vide infra*.

2.2 Results and discussion

2.2.1 Formal synthesis of (2*S*)-sanctolide A

Toward the initial development of a modular synthetic approach for the synthesis of 2*S*-sanctolide, we envisioned utilization of a double diastereotopic group differentiation strategy as the key transformation to install the critical 2*S*-stereocenter of the molecule. Our retrosynthetic analysis involved the formation of the C2-epimer of sanctolide A [(2*S*)-**2.1-A**] using a Yamaguchi esterification, and subsequent late-stage RCM/olefin isomerization of the diene precursor **2.2.4**, which would intersect the synthetic efforts of Brimble and coworkers at the stage of the Brimble lactone (2*S*)-**2.1.6** in the synthesis of 2*S*-sanctolide A (Figure 2.5), and thus be a formal synthesis.[15]

In this regard, the secondary alcohol containing amide **2.2.2** would be accessed by the same $AlMe_3$-mediated lactone opening of the lactone methyl ether (2*S*)-**2.1.6** used by Brimble and coworkers. To access the lactone methyl ether (2*S*)-**2.1.6**, we envisioned a five-step sequence from the phosphate triene, **2.6.2** utilizing a phosphate tether-mediated, one-pot sequential CM/ per-hydrogenation/ tether removal strategy,[28] coupled with oxidative lactone formation. The diester coupling partner **2.2.3** could be derived from 2-hydroxyisovaleric acid in one step.

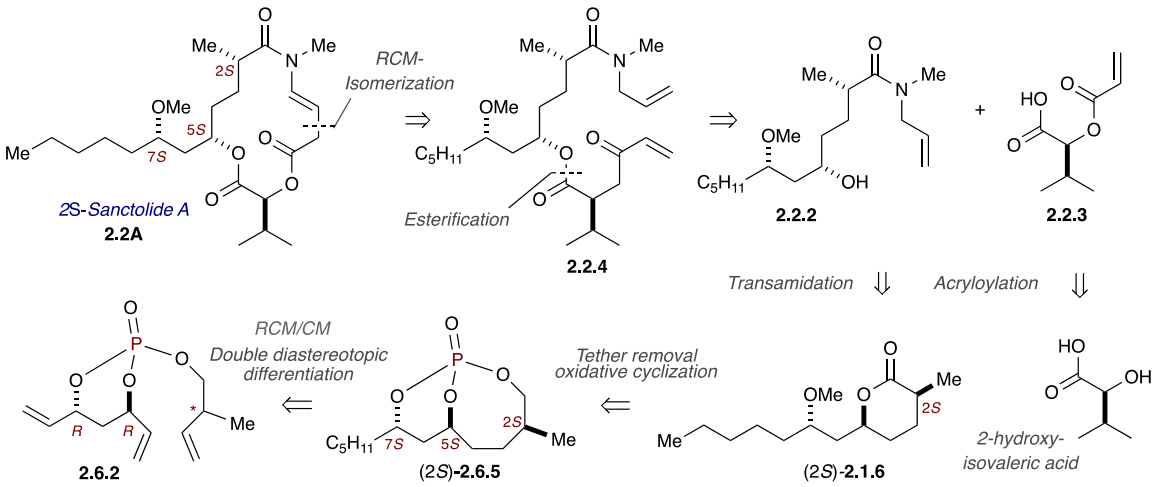

Figure 2.5 *Retrosynthetic analysis of 2S-sanctolide A.*

In 2013, our group reported a phosphate tether-mediated double diastereotopic group differentiation of a phosphate triene **2.5.3** in generating bicyclo[5.3.1]phosphate **2.5.4** (Scheme 2.5A).[29,30] During this synthesis, racemic 2-methyl homoallylic alcohol **2.5.1** was coupled to monochlorophosphate (*S*,*S*)-**2.5.2** to generate a 1:1 epimeric mixture at the methyl bearing stereogenic center within phosphate triene **2.5.3** bearing a non-stereogenic phosphorus atom. Subsequent group selective RCM reaction with 3 mol% of the Grubbs **G-II** catalyst [$(ImesH_2)(PCy_3)(Cl)_2Ru{=}CHPh$],[17] in refluxing CH_2Cl_2,

delivered bicyclo[5.3.1]phosphate **2.5.4** as a single *P*-stereogenic diastereomer in 39% yield, where the unreacted diastereo-enriched triene **2.5.5** was recovered in 27% yield. The absolute stereochemistry of the bicyclo[5.3.1]phosphate **2.5.4** was determined using X-ray crystallographic analysis. The mechanistic rationale for obtaining a single diastereomer was explained by the 1,2-steric interactions introduced between the methyl substituent and the metallocyclobutane at the transition state (**2.5.6** and **2.5.7**).[29,30]

An energetically disfavored steric interaction is predicted between the allyl methyl substituent at the *exo*-face of the bicyclophosphate and the Ru-metallocyclobutane which is also formed in the *exo*-face of the bicyclic phosphate (*exo*-*exo*-***2.5.6***) due to its concave nature. When the allyl methyl substituent is directed at the *endo*- face to the bicyclophosphate, the olefin metathesis will undergo via an energetically favorable TS (*exo*-*endo*-**2.5.7**), hence delivering bicyclo[5.3.1]phosphate **2.5.4** as a single diastereomer.

Inspired by this model, we proposed a similar double diastereotopic RCM group differentiation, which after phosphate tether removal, would generate the C1–C12, 1,3-*anti* diol-containing subunit (2*S*)-**2.6.6** bearing the requisite stereogenic centers for 2*S*-sanctolide A [(2*S*)-**2.1**-**A**] (Scheme 2.5B). Thus, coupling of chiral, racemic 2-methyl homoallylic alcohol **2.5.1** with the monochlorophosphate (*R*,*R*)-**2.5.2** will generate the phosphate triene **2.6.2**. The ring-closing metathesis of the phosphate triene **2.6.2**, with subsequent cross metathesis, followed by global hydrogenation would furnish the required bicyclo[5.3.1]phosphate [(2*S*)-**2.6.5**] with 2*S*-configured methyl center having all the required stereocenters for the synthesis of 2*S*-sanctolide A [(2*S*)-**2.1**-**A**]. Final tether

removal would generate the key triol (2*S*)-**2.6.6** *en route* to the Brimble lactone methyl ether (2*S*)-**2.1.6.**

Scheme 2.5 *Double diastereotopic differentiation and mechanistic rationale.*

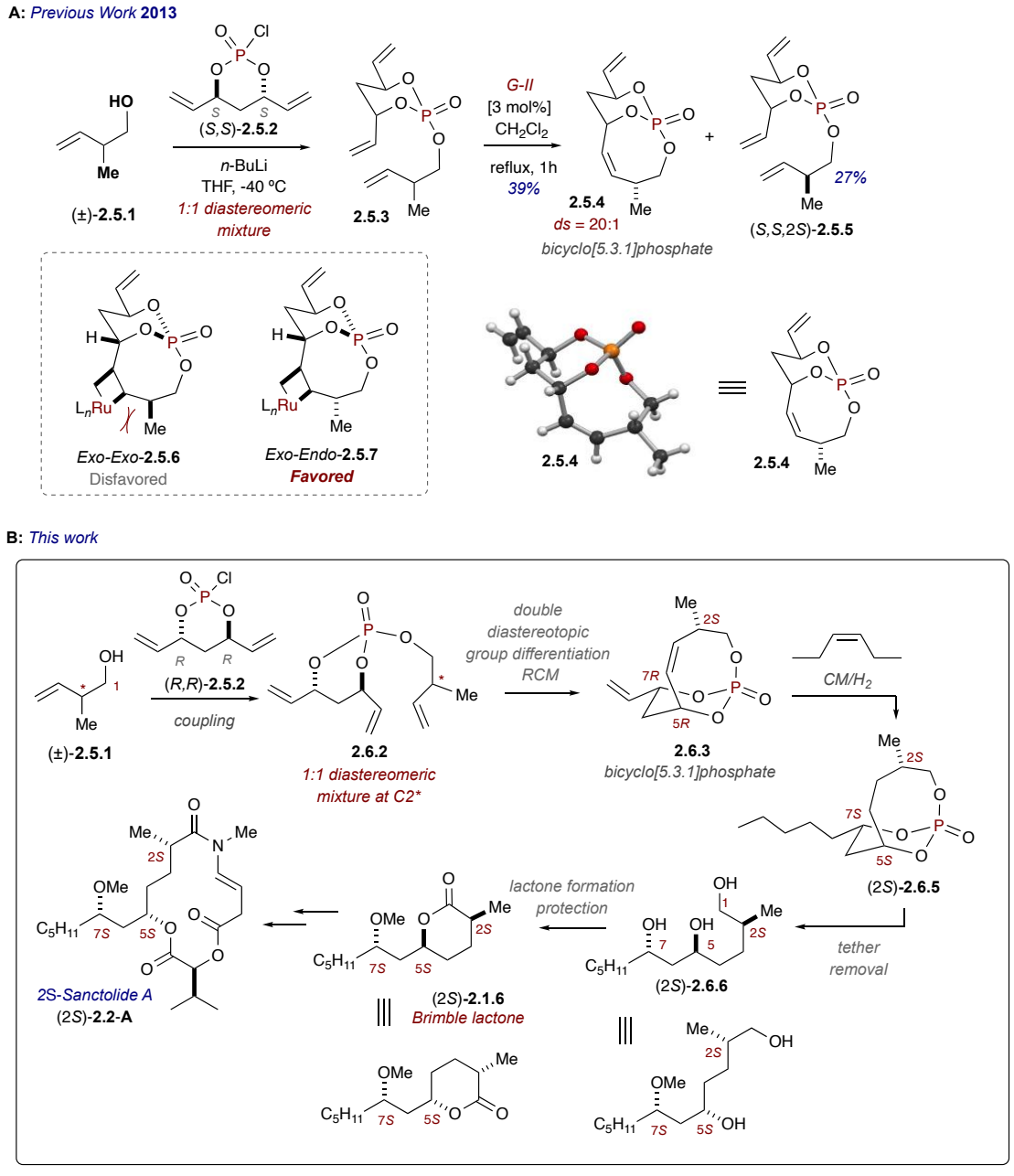

The synthesis commenced with coupling of the lithiated chiral, racemic homoallylic alcohol **2.5.1** to the monochloro phosphate (*R*,*R*)-**2.5.2** (Scheme 2.5) derived from the C_2-symmetric diene-diol (*R*,*R*)-**2.6.1**, in THF to provide the pseudo-C_2-symmetric triene phosphate **2.6.2** in 80% yield (Scheme 2.6). Subsequent double diastereotopic differentiation of the phosphate triene **2.6.2** with 1.5 mol% of the Grubbs **G-II** catalyst[17] [$(ImesH_2)(PCy_3)(Cl)_2Ru{=}CHPh$], in refluxing CH_2Cl_2, delivered the bicyclo[5.3.1]-phosphate **2.6.3** as a single *P*-stereogenic diastereomer in 38% yield along with 42% of unreacted triene. The absolute stereochemistry of the methyl-bearing center of the bicyclo[5.3.1]phosphate **2.6.3** was confirmed via X-ray crystallography analysis as 2*S* (sanctolide numbering).

Scheme 2.6 *Phosphate tether-mediated one-pot sequential protocol to (2S)-2.1.6*

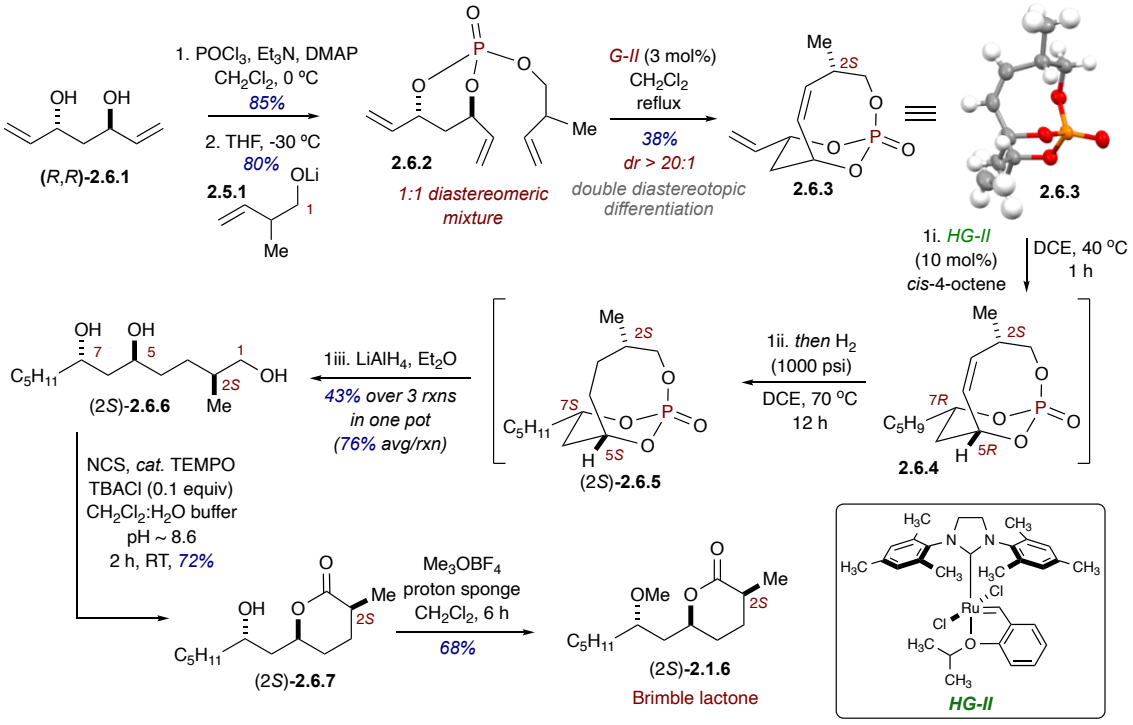

Next, a one-pot sequential cross metathesis was carried out with *cis*-4-octene in the presence of 10 mol% of the Hoveyda-Grubbs second-generation catalyst[31] (**HG-II**) in DCE to generate the unsaturated bicyclophosphate (2*S*)-**2.6.5**. Succeeding "same-pot" global hydrogenation with residual **HG-II**,[32] and tether removal with LAH in Et_2O, afforded the triol (2*S*)-**2.6.6** bearing the requisite C2, C5, and C7 stereogenic centers in 43% overall yield over the 3 reaction, one-pot protocol.[i]

With triol (2*S*)-**2.6.6** in hand, we set out to generate the C1–C12 Brimble lactone methyl ether (2*S*)-**2.1.6.** In this regard, regioselective oxidative lactone formation on triol (2*S*)-**2.6.6,** mediated by catalytic TEMPO in the presence of the *N*-chlorosuccinimide (NCS) as the secondary oxidant and phase-transfer catalyst tetrabutylammonium chloride (TBACl), furnished lactone (2*S*)-**2.6.7** in 72% yield. Subsequent selective methylation of the C7-carbinol with trimethyloxonium tetrafluroborate (Me_3OBF_4) as the methylating reagent and proton sponge, afforded the C1–C12 Brimble lactone methyl ether (2*S*)-**2.1.6**. With the successful synthesis of the (2*S*)-**2.1.6** in hand, the formal synthesis of the 2*S*-sanctolide A was completed in a total of eight reactions and six "pots", starting from (*R*,*R*)-**2.6.1** utilizing phosphate tether-mediated one pot sequential protocols.

[i] [It should be noted, that after hydrogenation, IUPAC priority of the C5/C7 stereogenic centers switches from C5-*R*/C7-*R* to C5-*S*/C7-*S*].

2.2.2 Total synthesis of Sanctolide A

The double diastereotopic group differentiation method coupled with a pot economical approach in the synthesis of the 2*S*-epimer of sanctolide A demonstrated the multifaceted nature and the one-pot amenability of the use of phosphate tether-mediated protocols. While this method allowed for the synthesis of the Brimble lactone methyl ether (2*S*)-**2.1.6** in six steps from the diene diol (*R*,*R*)-**2.6.1**, from an atom economical prospective,[33] the double diastereotopic group differentiation method has a drawback in that the theoretical yield can only be 50% (we report ~38%) with recovery of the unreacted C2 epimer (Sanctolide numbering). Therefore, our synthetic efforts were redirected towards the development of an alternative modular, atom and step[34] economical approach to address these limitations.

In our reworked proposed route, the synthesis of the bicyclo[5.3.1]phosphate **2.7.5** bearing a trisubstituted olefin was envisioned to start from the readily prepared homologated (*S*,*S*)-homoallylic diene-diol **2.7.3** (Figure 2.6), whereby hydrogenation from the convex face would afford the saturated bicyclo[5.3.1]phosphate (2*S*)-**2.6.5** with expected requisite stereochemistry. Generation of phosphate triene **2.7.4** would occur via the coupling of pseudo-C_2-symmetric monochlorophosphate (*S*,*S*)-**2.5-A** and lithiated β-methallyl alcohol. Subsequent RCM would deliver the bicyclo[5.3.1]phosphate **2.7.5**. During the RuH-mediated hydrogenation, the delivery of the hydrogen was initially envisioned to occur from the sterically less crowded convex face of the unsaturated bicyclo[5.3.1]phosphate **2.7.5**, to furnish the *S*-configured methyl center at the C2 position (sanctolide numbering).

Overall, this protocol would introduce a modular synthetic route to the existing synthesis with improved atom economy, where a complete conversion of the triene was expected after the RCM/CM/H_2 sequence. Moreover, step economy could be further improved by employing the Krische Ir-catalyzed transfer hydrogenation allylation method for the generation of the starting homologated (*S*,*S*)-homoallylic diene-diol **2.7.3**.[35] In addition, if LAH-mediated tether removal could be linked into the one-pot sequential protocol, we could carry out four reactions in one pot, e.g. RCM/CM/H_2/LAH.

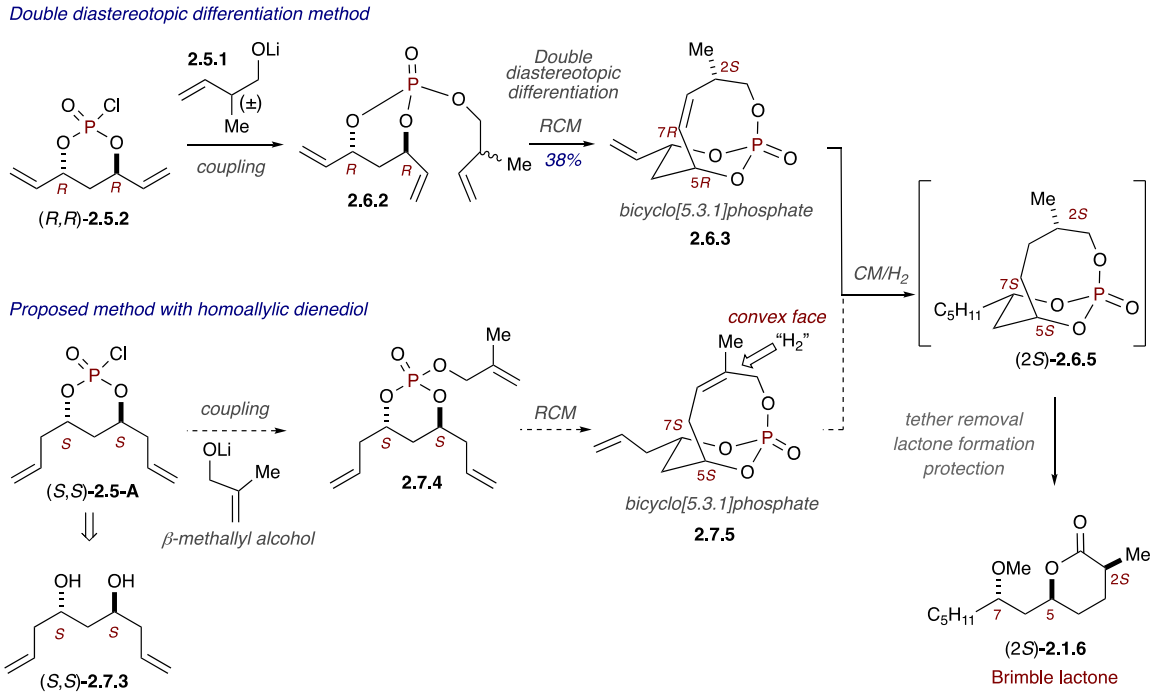

Figure 2.6 *Proposed route with (S,S)-homoallylic diene-diol **2.7.3**.*

The forward synthesis was commenced with the generation of the phosphate triene **2.7.4** from homologated diene diol **2.7.3**. Two distinct synthetic approaches were utilized in the synthesis of the (*S*,*S*)-homoallylic diene-diol **2.7.3** (Scheme 2.7). The addition of the vinyl Grignard to the (*R*,*R*)-diepoxide **2.7.1**, in the presence of catalytic CuCN, delivered

the (*S*,*S*)-homoallylic diene-diol (*S*,*S*)-**2.7.3** in 70% yield.[36] In addition, the same homoallylic diene-diol (*S*,*S*)-**2.7.3** was generated in a more direct atom and step economical fashion from commercially available propane 1,3-diol (**2.7.2**), by utilizing the Krische Ir-catalyzed transfer hydrogenation allylation method.[35] With the (*S*,*S*)-homoallylic diene-diol in hand, tripodal coupling with $POCl_3$ and lithiated β-methallyl alcohol was carried out to deliver the pseudo-C_2-symmetric phosphate triene **2.7.4** in good yields. Exposure of **2.7.4** to the Hoveyda-Grubbs second-generation catalyst[31] (**HG-II**) in

Scheme 2.7

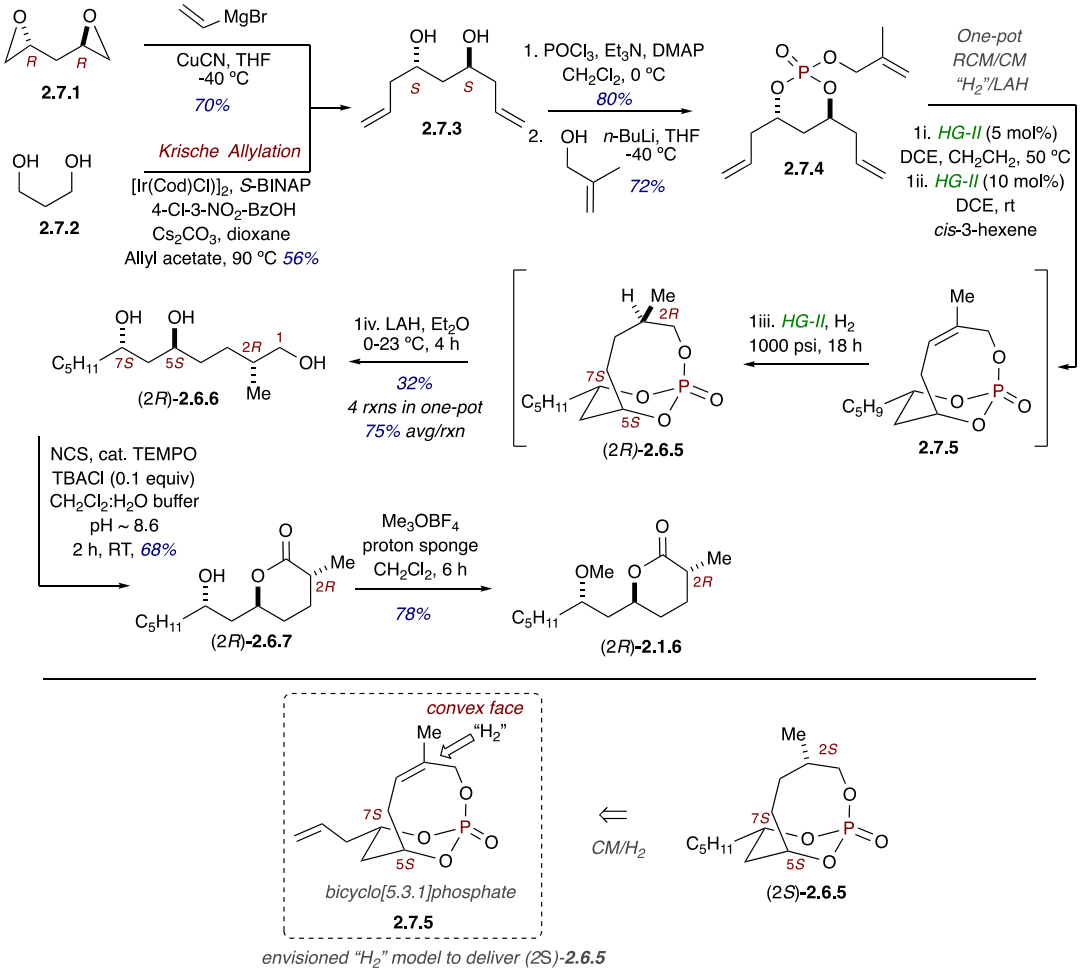

*envisioned "H_2" model to deliver (2S)-**2.6.5***

DCE, in the presence of ethylene gas,[37] cleanly generated the bicyclo[5.3.1]phosphate **2.7.5** in good yields. Subsequent CM with *cis*-3-hexene, followed by global hydrogenation of the unpurified CM product with residual Ru catalyst,[32] in the presence of H_2 at 1000 psi, furnished the saturated bicyclophosphate intermediate **2.6.5**.

A convex face approach of the RuH was expected to deliver bicyclo[5.3.1]phosphate (2*S*)-**2.6.5** with 2*S*-methyl center during the hydrogenation, as described in (Figure 2.6 and Scheme 2.7). However, comparison of the initial normal phase TLC analysis of bicyclo[5.3.1]phosphate (2*S*)-**2.6.5** generated from the double diastereotopic differentiation method and the bicyclo[5.3.1]phosphate **2.6.5** from the diastereoselective hydrogenation method showed a significant R_f difference in the TLC with EtOAc as the eluent, indicating a possible generation of a diastereomer (2*R*)-**2.6.5** at this stage (Scheme 2.7), *vide infra*. Subsequent tether removal of the unpurified bicyclo[5.3.1]phosphate intermediate (2*R*)-**2.6.5** with LAH delivered the advanced polyol intermediate (2*R*)-**2.6.6** in 49% average yield over 4 reactions. In order to shed light on the origins of potential C2 epimers revealed by the discrepancies in TLC R_f values between the two triol samples of triol **2.6.6**—which were generated from the two different pathways, detailed NMR and molecular modeling studies and were carried out.

A comparison of Δδ ppm values of ^{13}C NMR data for selected carbon centers within the two potential C2 epimers of **2.6.6** was compiled and is shown in Figure 2.7.[ii] As seen, a substantial Δδ ppm difference |Δδ ~1.7 ppm| was observed at the C2 methyl-bearing

[ii] A complete data table is enclosed in the experimental section

centers of the two triols in question. In addition, 0.4, 0.4, and 0.3 Δδ ppm differences were observed at the C5 and C7 carbinol centers, and at the C13 methyl center, respectively. The data confirmed the presence of two different diastereomers of the two triol intermediates. Thus, the triol that was formed via the substrate-controlled diastereoselective hydrogenation (Scheme 2.7) was deemed that of 2*R*-configuration [(2*R*)-**2.6.6**].

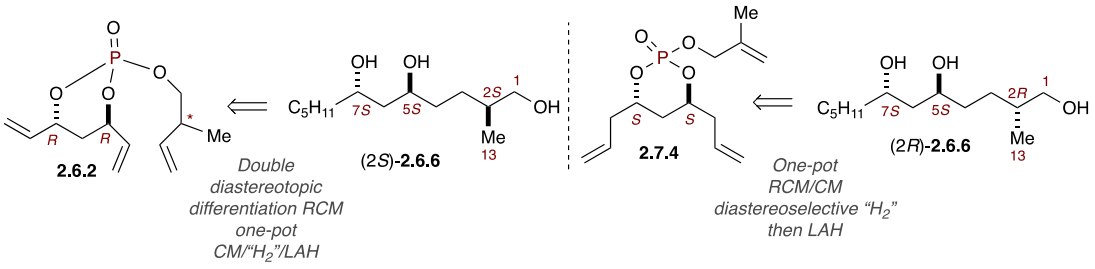

C #	(2*S*)-**2.6.6** ppm	(2*R*)-**2.6.6** ppm	Δδ ppm
1	67.9	68.0	0.1
2	34.3	36.0	1.7
3	29.2	29.3	0.1
4	25.5	25.6	0.1
5	69.5	69.9	0.4
6	37.4	37.5	0.1
7	69.2	69.6	0.4
13	16.6	16.9	0.3

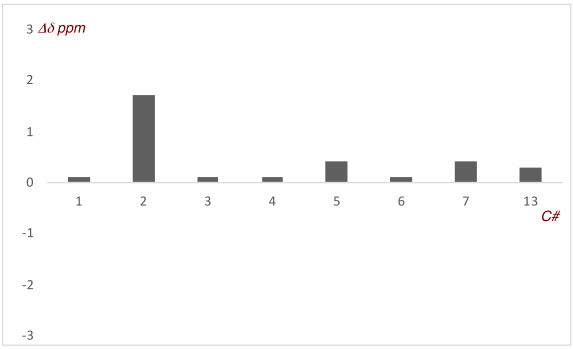

Figure 2.7

With this result in hand, we had confirmed that our original hypothesis for facial selectivity in the hydrogenation event was in error—in which we had reasoned hydrogenation would produce the 2*S*-saturated bicyclophosphate (2*S*)-**2.6.5** from hydrogenation of the convex face within **2.7.5**. In order to shed light on this issue, we tried to use X-ray crystallographic analysis. Unfortunately, efforts aimed at obtaining a viable X-ray crystallographic structure for the bicyclo[5.3.1]phosphate intermediate, or its derivatives, have thus far been unsuccessful. It is worthy to note that we had previously

assigned the absolute stereochemistry of the methyl-bearing center of the bicyclo[5.3.1]phosphate **2.6.3** as 2*S,* which was confirmed via X-ray crystallography analysis (sanctolide numbering) [see previous Scheme 2.6 and Figure 2.8 below).

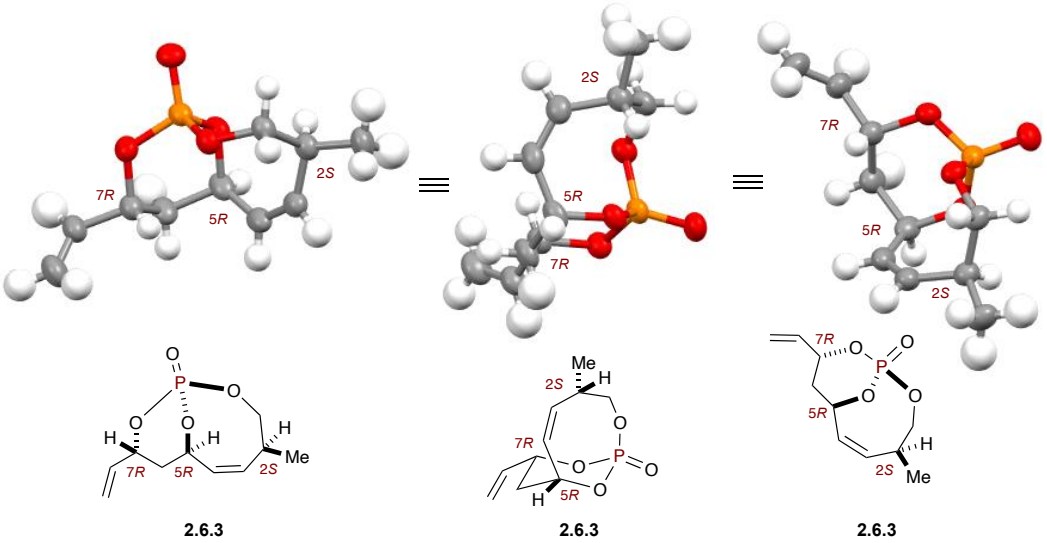

Figure 2.8 *Different orientations of the X-ray for the bicyclo[5.3.1]phosphate* ***2.6.3****.*

We next turned to molecular modeling to shed light on this discrepancy and carried out an energy minimized calculation utilizing ChemAxon Marvin calculator plugins[38] and PyMOL[39] as the molecular graphic system (Figure 2.9). In the molecular model, an unexpected "bend" was observed at the methyl center of the tri-substituted internal olefin, which changes the overall shape of the bicyclo[5.3.1]phosphate **2.7.5** significantly. This "bend" presents a new convex face at the bridging centers of the bicyclo[5.3.1]phosphate architecture, which in turn increases the transannular steric interactions between the phosphate center and the methyl center, and thus **2.7.5** presents a new concave face that we had not anticipated. On account of the steric interactions at the concave face, the approach

of the RuH from the more accessible convex face is envisioned to deliver the 2*R*-configured saturated bicyclo[5.3.1]phosphate (2*R*)-**2.6.5** during the hydrogenation event.

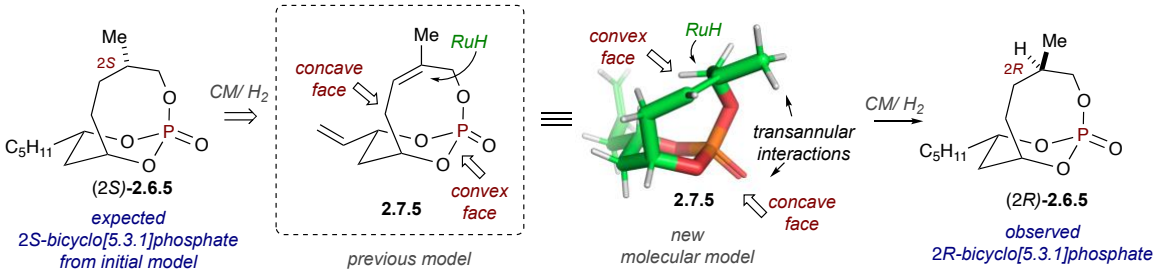

Figure 2.9 *molecular model studies for the bicyclo[5.3.1]phosphate* ***2.7.5***

Next, the triol fragment (2*R*)-**2.6.6** was subjected to a catalytic TEMPO-mediated oxidative lactone formation with NCS secondary oxidant and TBACl phase-transfer catalyst, to deliver the lactone carbinol (2*R*)-**2.6.7** in good yields (Scheme 2.7). Selective methylation of the C7(*S*) carbinol was carried out with Me_3OBF_4 and proton sponge, to afford the (2*R*)-configured lactone methyl ether (2*R*)-**2.2.E** in good yield [(C2-epimer of the Brimble 2*S*-lactone methyl ether]. With these products in hand, we focused our efforts on addition detailed NMR studies to map out trends in both the lactone carbinol (2*S/2R*)-**2.6.7** and lactone methyl ether (2*S/2R*)-**2.1.6** as shown in Figures 2.10 and 2.11.

A comparison of ^{13}C NMR chemical shifts Δδ ppm values (2*S* δ ppm - 2*R* δ ppm) for both the lactone carbinol and lactone methyl ether was next carried out to further confirm the diastereomers at each stage of the synthesis, and to rule out epimerization at any stage up to the Brimble lactone. The ^{13}C NMR Δδ ppm chemical shift values for the two 2*S*/2*R* epimeric lactone carbinols are depicted in Figure 2.10.[iii] The two lactone

[iii] Complete data tables are enclosed in the experimental section.

carbinols displayed significant deviations at multiple carbons of > ±2 Δδ ppm at carbons C1–C5. These deviations observed at the ppm level for the diastereomers can be reasoned by the chair conformational differences in the ground state. These data confirmed the presence of two diastereomeric lactone carbinols at this stage of the synthesis, namely, (2*S*)-**2.6.7** and 2*R*)-**2.6.7**.

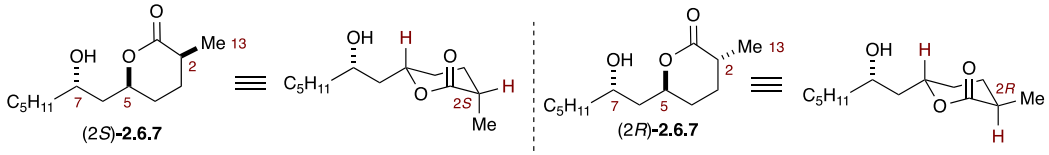

C#	(2*S*)-**2.6.7** ppm	(2*R*)-**2.6.7** ppm	Δδ ppm
1	176.6	174.4	-2.2
2	33.3	36.3	3.0
3	25.8	28.8	3.0
4	27.4	30.0	2.6
5	75.0	78.8	3.8
6	42.9	43.9	1.0
7	67.7	67.6	-0.1
13	16.2	17.6	1.4

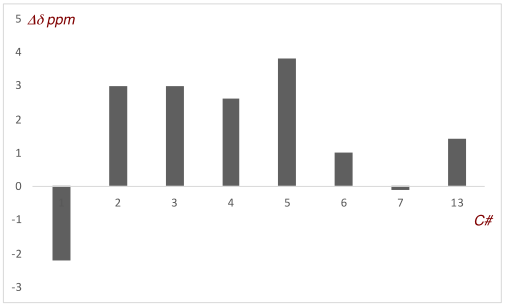

Figure 2.10

Next, a comparison of ^{13}C NMR chemical shifts was carried out |Δδ ppm values| for the two (2*S*)-lactone methyl ethers (2*S*)-**2.1.6** derived from double diastereotopic differentiation synthesis and the original Brimble synthesis[15] (Figure 2.11a). Infinitesimal deviations of the two lactone methyl ethers at the ppm level were observed, which confirmed that the lactone methyl ether that was generated from our double diastereotopic differentiation method is identical to the lactone methyl ether furnished from the Brimble synthesis, and thus of (2*S*)-configuration. Concurrently, a Δδ ppm data comparison was carried out for the two lactone methyl ethers generated from our two routes, namely the

double diastereotopic group differentiation and diastereoselective hydrogenation, (2*S*)-**2.1.6** and (2*R*)-**2.1.6**, respectively (Figure 2.11b). As expected, significant ppm Δδ ppm differences were observed at several carbons for the two C2-epimeric lactone methyl ethers. Notably, the differences at the ppm levels were consistent with the values obtained for the lactone carbinols in Figure 2.10. Taken collectively, the significant deviations of the Δδ ppm values strongly suggest that the lactone methyl ether derived from diastereoselective hydrogenation method, (2*R*)-**2.1.6**, has 2*R*-configuration.[iv]

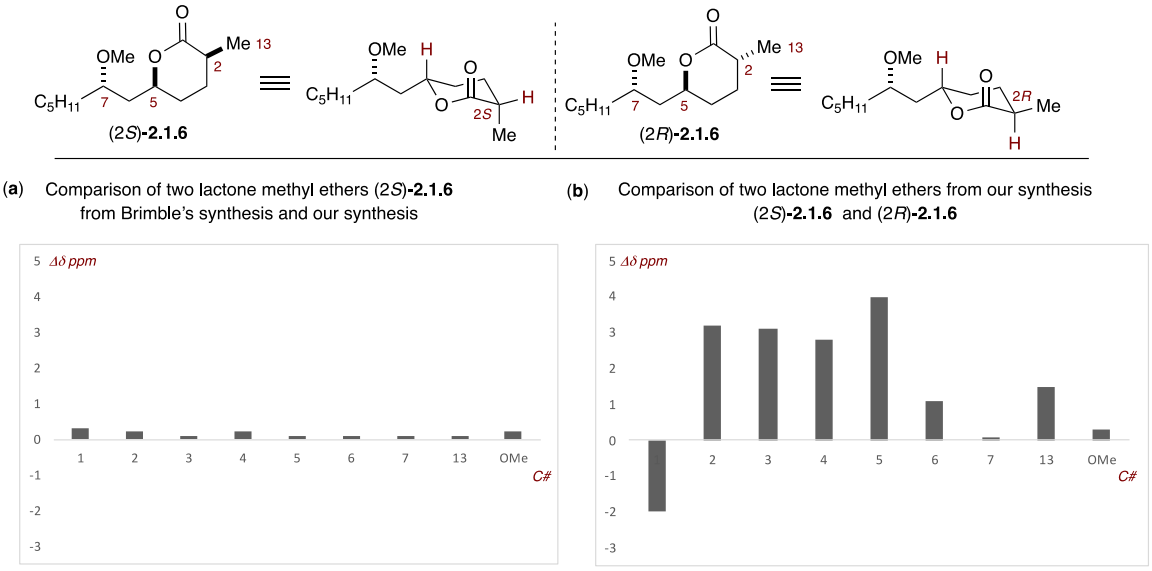

Figure 2.10

It is also worthy to note that when taken collectively, the aforementioned data suggest that no epimerization had taken place in transforming the respective triols, (2*S*)-**2.6.6** and (2*R*)-**2.6.6**, to the corresponding lactone carbinols (2*S*)-**2.6.7** and (2*R*)-**2.6.7**, and

[iv] Complete data tables are enclosed in the experimental section.

lactone methyl ethers, (2*S*)-**2.1.6** and (2*R*)-**2.1.6**, during the corresponding TEMPO/NCS-oxidation protocol and $(Me_3O)BF_4$/proton sponge-methylation event.

To further investigate the spatial correlations of proximal protons of the two lactone carbinols, (2*R*)- and (2*S*)-**2.6.7**, and lactone methyl ethers, (2*R*)- and (2*S*)-**2.1.6**, Nuclear Overhauser Effect correlation (NOESY) experiments were carried out (Figure 2.12).[40] A strong through-space correlations were observed for the two H_{ax} and H_{eq} protons (1,4-*syn*) of both the 2*S*-lactone carbinol (2*S*)-**2.6.5** and 2*S*-lactone methyl ether (2*S*)-**2.1.6** (Figure 2.12A and 2.12B). As expected, such correlations were not observed for the 2*R*-configured lactone carbinol, (2*R*)-**2.6.7** and lactone methyl ether (2*R*)-**2.1.6**, due to the 1,4-*anti* relationship between the two H_{ax} protons (Figures 2.12C and 2.12D).

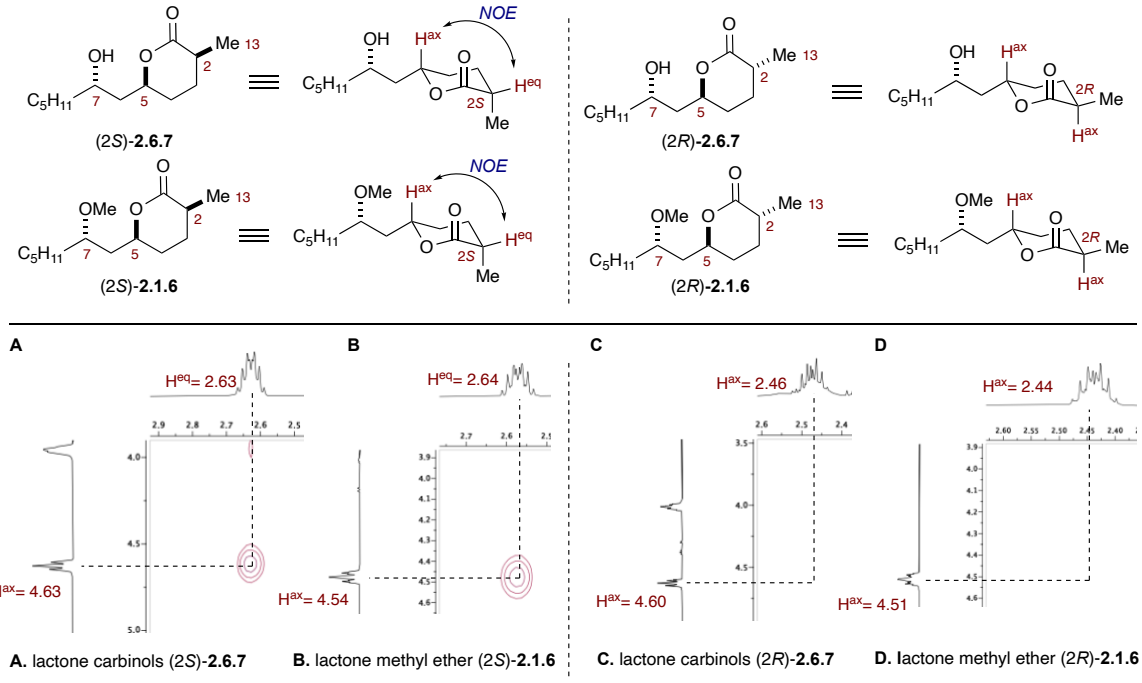

Figure 2.12 *NOESY correlations A/B and lack of correlations C/D.*

With these experimental results in hand, we next focused our efforts to complete the synthesis of the natural product, 2*R* sanctolide A (Scheme 2.8). Lactone methyl ether (2*R*)-**2.1.6** was initially subjected to a Me_3Al-mediated lactone opening reaction using conditions developed by Weinreb (*N*-allylmethylamine, Me_3Al in CH_2Cl_2)[41] to furnish the allylamide-alcohol **2.2.2** in 50% yield as a mixture of two C2-methyl diastereomers [*dr* = 1:1, 2*R*:2*S*) and 1:1 amide rotamers (Scheme 2.8, Reaction (A)].[v] As highlighted in Figures 2.13 and 2.14, the diastereomers were identified using extensive ^1H and ^{13}C NMR analysis (see experimental section for full analysis), whereby the ^{13}C NMR peaks for the product appeared as four singlets instead of two singlets (as one would expect for only a mixture of amide rotamers).[vi]

Scheme 2.8 *$AlMe_3$-mediated lactone opening of (2*S*)-**2.1.6** and (2*R*)-**2.1.6**.*

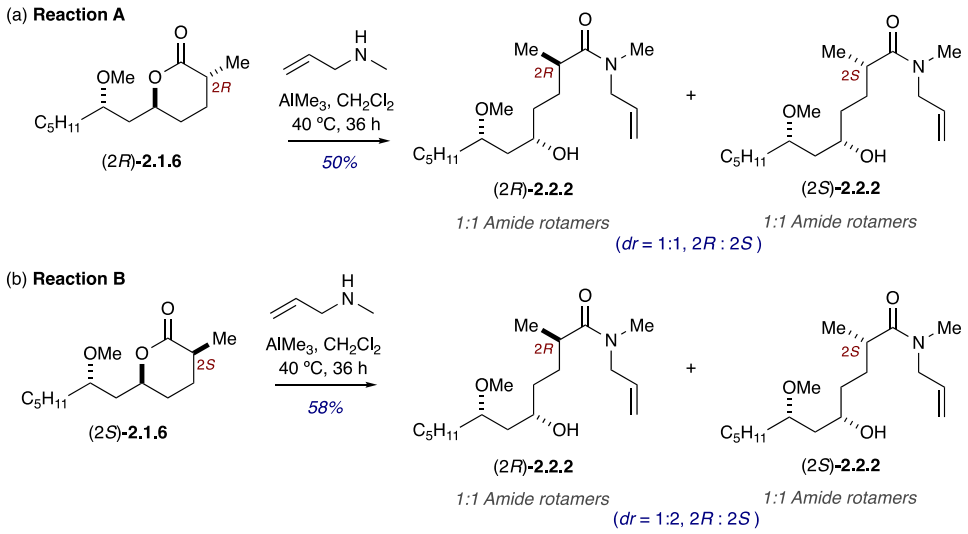

[v] This result was contradictory and unexpected compared to the observations made by Brimble and coworkers who only reported amide rotamers, but not C2 epimers, which are apparent in their spectra based on our observation.
[vi] A detailed analysis of spectral data can be found in Table 5.4 in the experimental section.

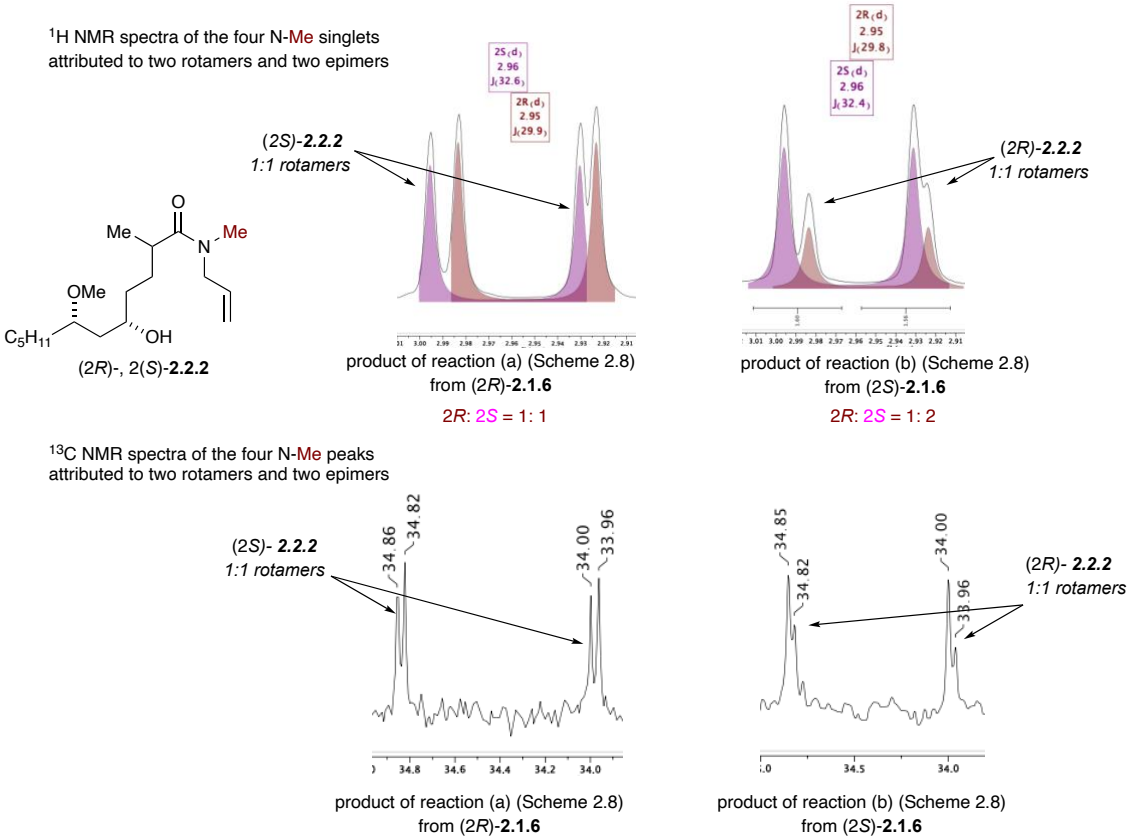

Figure 2.13

To further investigate the epimerization of the 2C-methyl center, the lactone methyl ether (2*S*)**-2.1.6**—which was generated via the double diastereotopic differentiation method, was also subjected to the lactone opening reaction using the same $AlMe_3$ conditions [Scheme 2.8, Reaction (B)]. In this experiment, the *N*-allylamide alcohol subunit **2.2.2** was also delivered as a mixture of two inseparable diastereomers (*dr* = 1:2, 2*R*:2*S*), as well as the 1:1 mixture of amide rotamers (Figure 2.13). Notably, the ^{1}H and ^{13}C NMR spectra, which were obtained for the product [Scheme 2.8, reaction (b)] also showed four ^{13}C NMR peaks appearing as four singlets for several carbons and matched the NMR of the product as seen in Reaction (A) of Scheme 2.8. In addition, the ^{1}H NMR spectra of the N-Me peak of the acyclic amide-alcohol showed 4 distinct singlet peaks attributed to

the 2 amide rotamers and 2 epimers (2*S* and 2*R*) (Figure 2.13).[vii] The 2*S* and 2*R* epimers were identified by comparing to the pure 2*R*-epimer, which was generated in the latter part of this synthesis, *vide infra* (for a comparison table, see Table 5.5 in experimental section). In addition, extensive ^{13}C spectral data analysis was also carried out for each carbon center of the molecule to confirm the epimeric amide rotamers in both Reactions (A) and (B) of Scheme 2.8, whereby a selected set of ^{13}C NMR data are depicted in Figure 2.14 [the ^{13}C NMR expansion for the C1, C13, C20, and C21 carbons (sanctolide numbering) are depicted in Figure 2.14]. A similar comparison for ^{1}H NMR data were difficult due to peak overlaps in several ppm ranges having complex splitting patterns (overlapping multiplets).

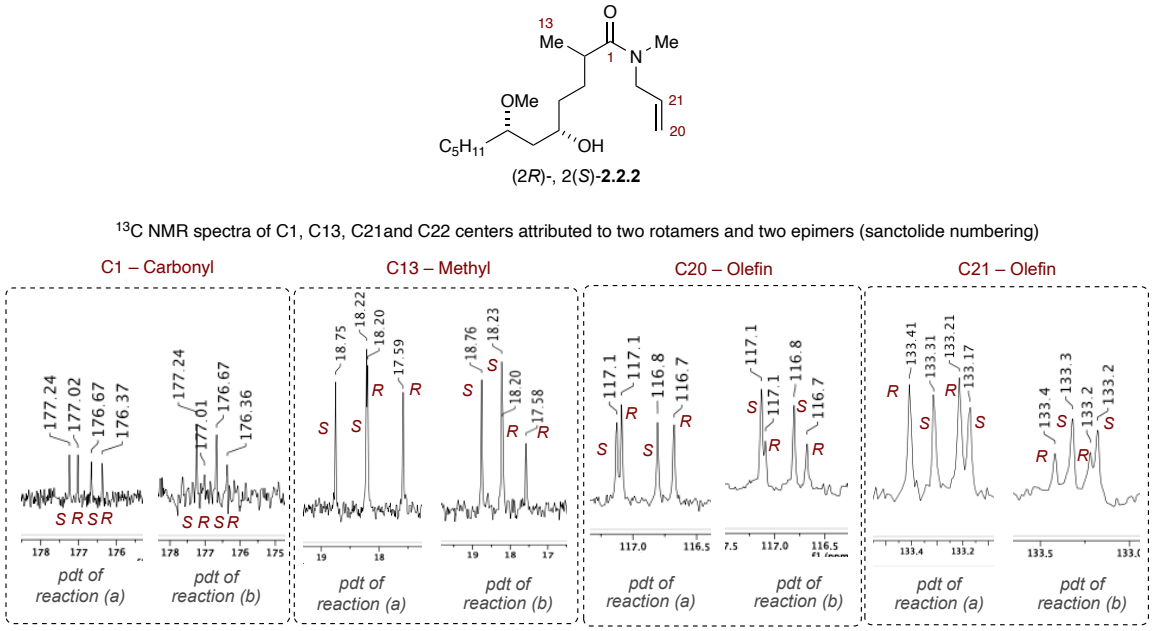

Figure 2.14. *The ^{13}C NMR expansion for the C1, C13, C20, and C21 carbons.*

[vii] We have ruled out homoallylic coupling as the source of the four singlets, as homoallyic coupling is typically $^{5}J = 0–8$ Hz, since the two peaks were separated by $J =$ 32 and 30 Hz for 2*S* and 2*R* epimers (Figure 2.12). In addition, as noted, the ^{13}C NMR showed several carbons split into four singlets.

A comparison of the ^{13}C Δδ ppm values (error ± 0.1 ppm) was also carried out to confirm the presence of epimeric amide rotamer product mixtures of the two Reactions (A) and (B) (Scheme 2.8). Full comparison tables are enclosed in the experimental section, and a graphical depiction is shown in Figure 2.15. The ^{13}C ppm values for the two product mixtures—importantly, in which all resonances existed as four singlets, were nearly identical for the majority of the carbon centers at ± 0.1 ppm level (17-of-18 resonances, Figure 2.15.). Only the C6 carbon of the 2*R*-epimer showed an infinitesimal Δδ ppm difference 0.1ppm at (± 0.1) and 0.04 ppm at (± 0.01) levels. Importantly, all the critical C2-, C5- and C7-stereocenters had identical ^{13}C singlets, which strongly suggested the generation of amide rotamers of both epimers, 2*S* and 2*R*.

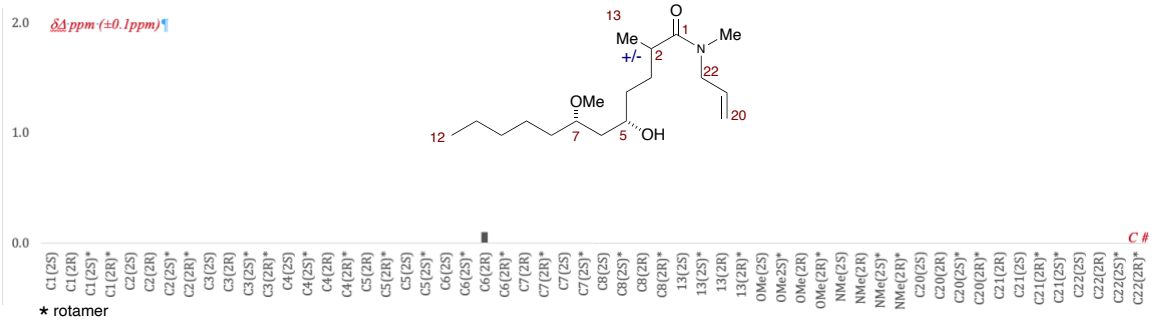

Figure 2.15 *Δδ ppm comparison for the products of two reactions in Scheme 2.8.*

Remarkably, the two lactone methyl ethers (2*S*)-**2.1.6** and (2*R*)-**2.1.6** have different epimerization rates during the lactone opening event, as evident by the diastereomeric ratios obtained for the two reactions, namely Reactions (A) and (B) in Scheme 2.8. To-date, the reason for this discrepancy of differential epimerization rates, which leads to

partial epimerization, is not entirely clear. However, our interests are currently aligned to further elucidate the origins of this unprecedented epimerization event, and corresponding studies will be reported in due course. In the meantime, we forged ahead to complete the synthesis with the diastereomeric mixture in hand, and then reinvestigated the lactone opening reaction in hopes of circumventing epimerization at C2, *vide infra*.

We next completed the synthesis of the enamide macrolide with the mixture of the C2 epimers (Scheme 2.9). Thus, Yamaguchi esterification of amide-alcohol **2.2.2** with *in-situ*-generated 2,4,6-trichlorobenzoyl mixed anhydride of the acid **2.2.3**, provided the diene **2.2.4** in good yields also in an inseparable mixture of diastereomers (*dr* = 1:2, 2*R*:2*S*). Subsequent RCM with the Grubbs **G-II** catalyst in refluxing $CHCl_3$, delivered a complex mixture of 2*R*, 2*S* and *E*, *Z* diastereomers (2*R, E,Z*)-, (2*S*, *E,Z*)-**2.2.5** that were fully characterized. Subsequent olefin isomerization of the α,β-unsaturated lactone amide, using

Scheme 2.9

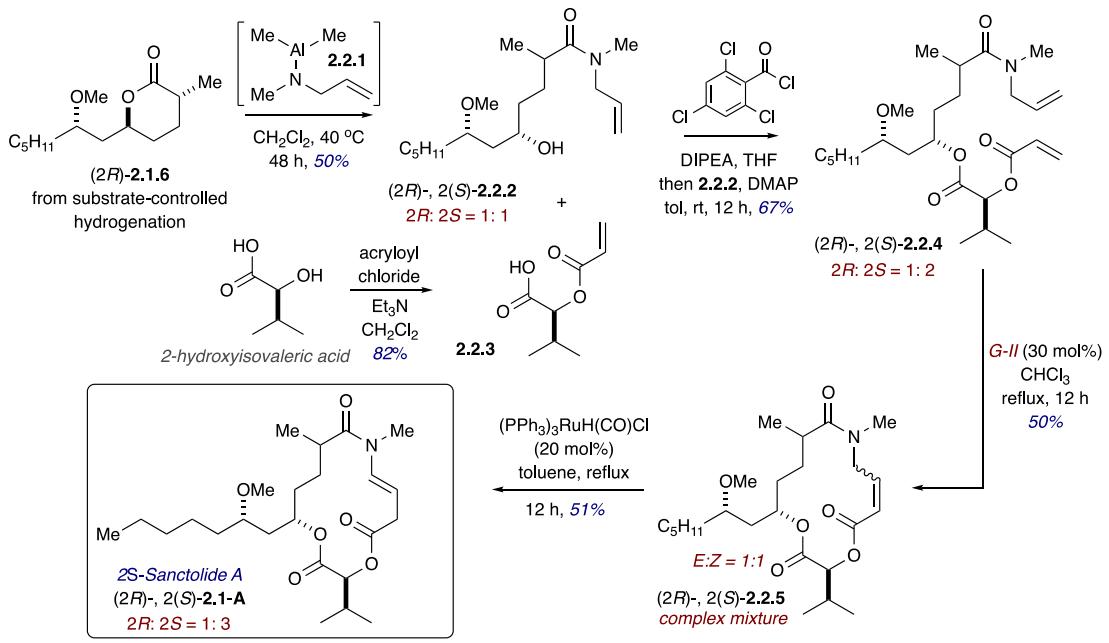

$(PPh_3)_3RuH(CO)Cl$[7,15,21,20] in refluxing toluene, generated the final mixture of inseparable enamide diastereomer products (2*S*)-, (2*R*)-**2.1**-**A**. in 45% yield in a diastereomeric ratio of *dr* = 1:3, 2*R*:2*S*, as evident by the signature doublets in the respective 1H NMR spectra occurring at 7.17 ppm for the 2*S* epimer as noted by Brimble,[15] and the 6.73 ppm for the 2*R* epimer as noted by Yadav.[22]

With these results in hand, we next explored additional methods toward the lactone opening reactions without utilizing a Lewis acid activator, as $AlMe_3$ was strongly believed to be the cause of C2 epimerization. Numerous attempts at adding the secondary allyl methyl amine without a Lewis acid activator were unsuccessful. Next, the addition of primary amines to the lactone was explored, whereby if successful, subsequent *N*-allylation at the secondary methyl-amide would deliver the requisite *N*-methylallylated product **2.2.4** without epimerization. In this regard, the addition of methylamine to the lactone methyl ether (2*R*)-**2.1.6** was preformed successfully with methylamine hydrochloride in neat Et_3N at 90 ºC, to deliver the amide alcohol as a single diastereomer and 10:1 mixture of amide rotamers. Gratifyingly, no epimerization at the 2C center was observed, as seen in both ^1H and ^{13}C NMR data [Reaction (c), Figure 2.16].

The ^1H NMR peak for the N-Me moiety of the lactone opened product **2.10.1** appeared as a doublet with a coupling constant of ^3J = 4.8 Hz (NHMe). Importantly, no epimeric doublets were observed in the ^1H NMR for **2.10.1** when compared to the 4 singlets previously observed for the corresponding amide-alcohol (2*R*)-, (2*S*)-**2.2.2** (Figure 2.16). Also, ^{13}C data confirmed the presence of a major epimer, which we tentatively assigned as 2*R*-**2.10.1**, existing as two amide rotamers (Major: Minor, 10:1), with direct comparison

after TBS-silyl protection of the C5-carbinol, *N*-allylation and desilylatioin being made in the subsequent study, *vide infra* (Scheme 2.10 and Figure 2.17).

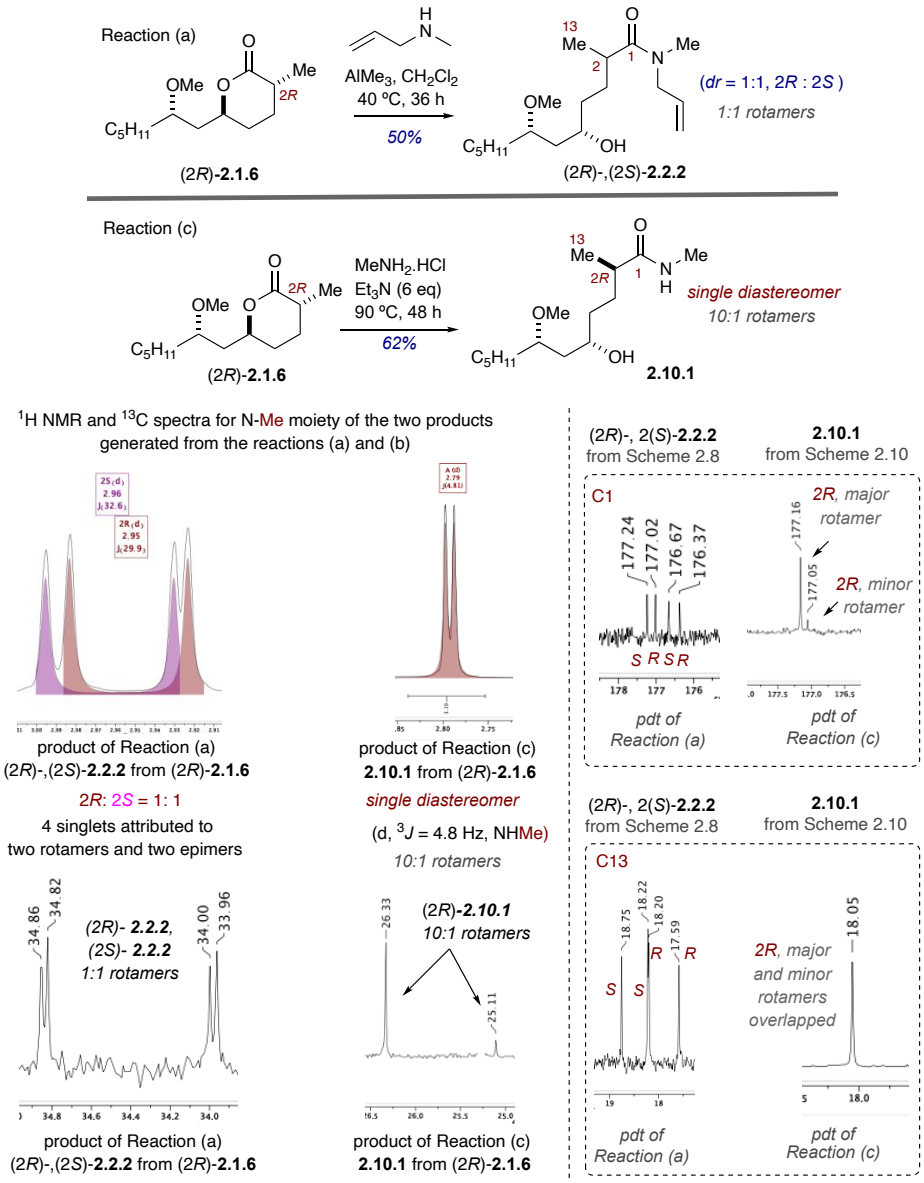

Figure 2.16 *^{1}H and ^{13}C NMR analysis of selected resonances for Rxns (a) and (c).*

After successful lactone opening reaction to obtain amide-alcohol **2.10.1** as a single diastereomer (10:1 mixture of amide rotamers), investigations began of the *N*-allylation

event at the secondary *N*-methyl amide. In this regard, the secondary carbinol center of the amide-alcohol **2.10.1** was protected with a TBS-protection to deliver **2.10.2**. Alkylation of the secondary methyl-amide **2.10.2** was carried out with allyl bromide and tetrabutyl ammonium iodide (TBAI) in the presence of 3 equivalents of NaH as the base at 40 ºC using *N*-alkylation conditions developed by Spring and coworkers.[42] It is worthy of noting that, the reaction did not go to completion even at prolonged stirring (up to 48 h) and the product **2.10.3** was furnished as a single diastereomer. Subsequent, deprotection of the TBS-alcohol with TBAF in THF generated the amide-alcohol (2*R*)-**2.2.2** as a single diastereomer in 1:1 amide rotamer mixture. Gratifyingly, no epimerization was observed at the 2C methyl center, during the alkylation event and was strongly enforced by the ^{1}H and ^{13}C NMR data (Figure 2.17, and supplementary information).

With the pure (2*R*)-epimer in hand, next Yamaguchi esterification was carried out with the acid partner **2.2.3** to deliver diene (2*R*)-**2.2.4** in moderate yields (Scheme 2.10). Subsequent RCM macrocyclization of the diene (2*R*)-**2.2.4** furnished the macrolide core (2*R*)-2.2.5 as a 1:1 inseparable mixture of *E* and *Z* diastereomers. Ensuing olefin isomerization of the *N*-allylamide moiety into the corresponding enamide using $(PPh_3)_3RuH(CO)Cl$[7,15,21,20] catalyst, afforded the natural product sanctolide A (**2.1**-**A**) in 51% yield. The spectral data for the synthesized macrolide was in a good agreement with the spectral data of reported natural product and the macrolide synthesized by Yadav and coworkers (Tables 2.1 and 2.2).[4,22] Interestingly, a similar decomposition of the final enamide macrolide upon standing conditions over several days was observed as reported by Yadav and coworkers.[22]

Scheme 2.10

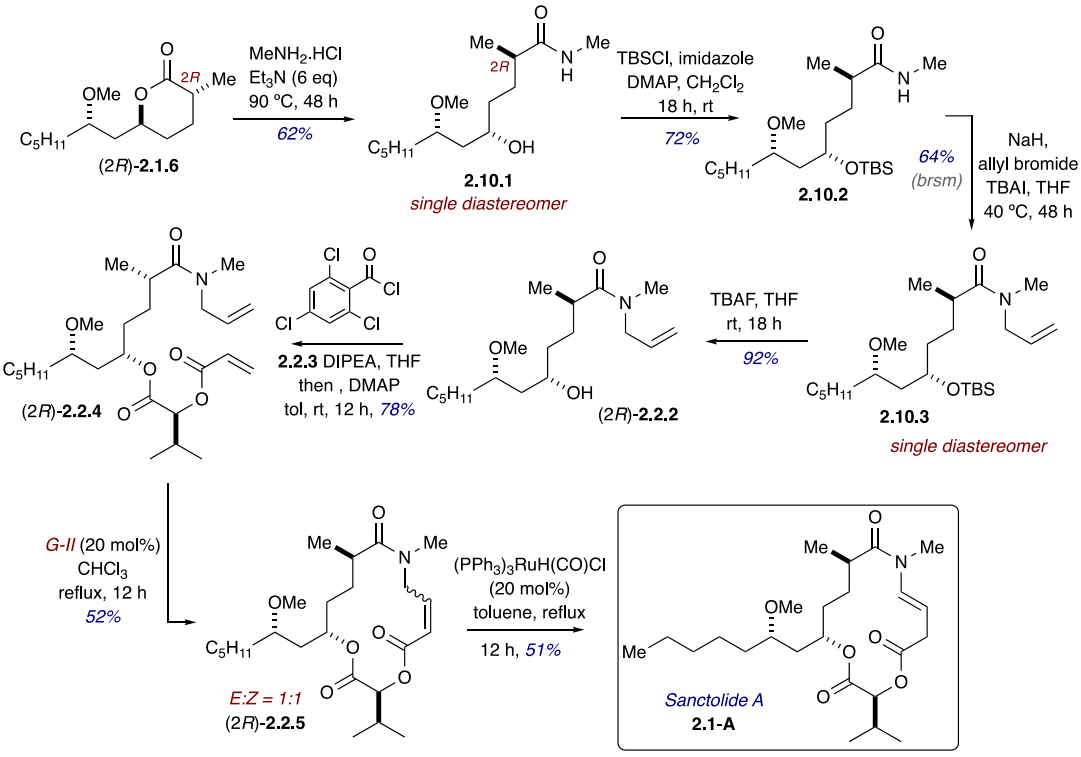

We next compared the two products that we obtained from the $Al(Me)_3$-mediated lactone opening reaction with *N*-allylmethyl amine, namely, (2*R*)- and (2*S*)-**2.2.2**, with that of the method involving lactone opening with methylamine—followed by *N*-allylation (Figure 2.17). ^{1}H NMR spectra of the N-Me moiety of **2.2.2** generated from *N*-allylation of the methyl-amide gave only two singlets, which was attributed to the two amide rotamers of a single diastereomer. Since we did not observe an epimerization at the NaH-promoted *N*-allylation step (as evident by crude NMR), we reasoned that the epimer that stayed obtained at this stage is the (2*R*)-**2.2.2**. Notably, the ^{13}C spectral data was also in a good agreement, whereas only two ^{13}C resonance peaks were observed in the ^{13}C NMR spectra for each carbon center of the molecule, compared to the quadruplet peaks that were

observed for the epimeric amide rotamer mixtures (2*R*)-, (2*S*)-**2.2.2** delivered from the $AlMe_3$-mediated method (see the selected spectral data shown in Figure 2.17).

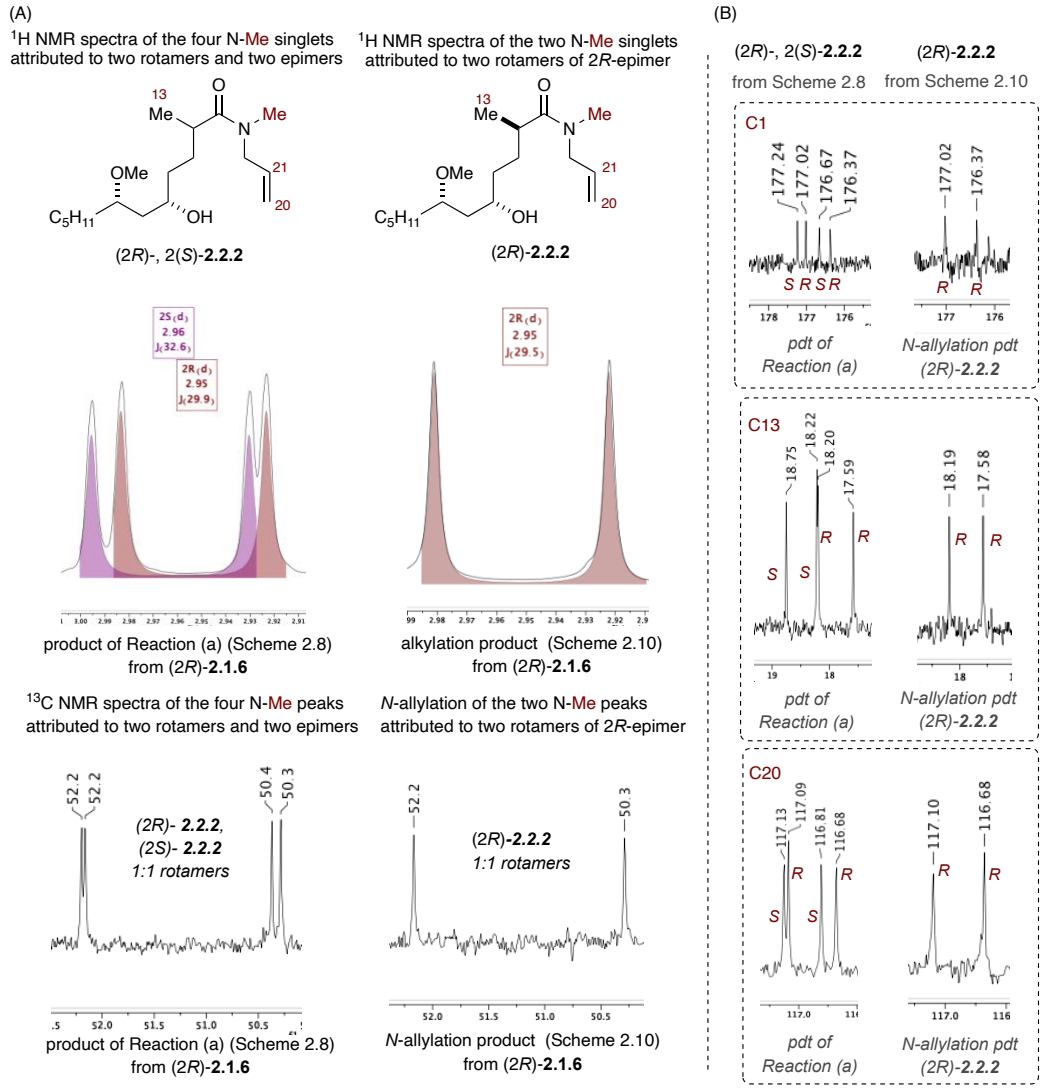

Figure 2.17 *^{1}H and ^{13}C NMR analysis of two methods to amide **2.2.2**.*

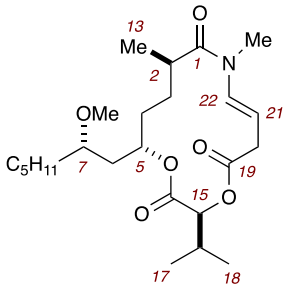

Table 2.1 *[1]H NMR chemical shifts comparison of original NMR (from isolation paper) and our final NMR (sanctolide numbering)*

C#	Original ^{1}H NMR sanctolide A in $CDCl_3$ ($CHCl_3$ reference of 7.24 ppm)[9]	Final ^{1}H NMR of sanctolide A (2*R*)-**2.1**-**A** in $CDCl_3$ ($CHCl_3$ reference of 7.24 ppm)	δΔ ppm	Final ^{1}H NMR of sanctolide A (2*R*)-**2.1**-**A** in $CDCl_3$ ($CHCl_3$ reference of 7.26 ppm)
2	2.56	2.56	0.00	2.58
5	5.00	5.00	0.00	5.02
7	3.12	3.12	0.00	3.14
13	1.13	1.13	0.00	1.15
15	5.11	5.11	0.00	5.13
17	0.94	0.95	0.01	0.97
18	0.90	0.90	0.00	0.92
20a	3.15	3.15	0.00	3.17
20b	3.20	3.19	0.01	3.21
21	5.12	5.12	0.00	5.14
22	6.70	6.71	0.01	6.73
OMe	3.28	3.28	0.00	3.30
NMe	3.06	3.07	0.01	3.09

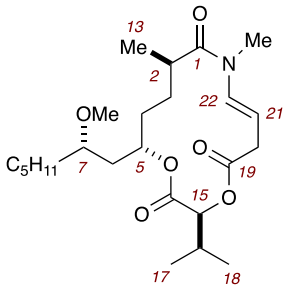

Table 2.2 ^{1}H NMR chemical shifts comparison of Yadav NMR of sanctolide A, and the final NMR of the product from the RCM/isomerization of diene (2*R*)-**2.2.4** *(sanctolide numbering)*.

C#	Yadav ^{1}H NMR of sanctolide A in $CDCl_3$ ($CHCl_3$ reference of 7.24 ppm)	Final ^{1}H NMR of sanctolide A (2*R*)-**2.1-A** in $CDCl_3$ ($CHCl_3$ reference of 7.24 ppm)	δΔ ppm	Final ^{1}H NMR of sanctolide A (2*R*)-**2.1-A** in $CDCl_3$ ($CHCl_3$ reference of 7.26 ppm)
2	2.60–2.52	2.61–2.53	-	2.63–2.55
5	5.03–4.97	5.03–4.97	-	5.05–4.99
7	3.14–3.08	3.13–3.19	-	3.15–3.21
13	1.12	1.13	0.01	1.15
15	5.10	5.11	0.01	5.13
17	0.94	0.95	0.01	0.97
18	0.89	0.90	0.01	0.92
20a	3.15	3.15	0	3.17
20b	3.19	3.19	0	3.21
21	5.15–5.08	5.15–5.08	-	5.17–5.10
22	6.70	6.71	0.01	6.73
OMe	3.27	3.28	0.01	3.30
NMe	3.06	3.07	0.01	3.09

2.3 Conclusion

In conclusion, a phosphate-tether mediated one-pot sequential approach for the formal synthesis of the (2*S*) epimer of sanctolide A [(2*S*)-**2.1**-**A**], and the total synthesis of sanctolide A, (2*R*)-**2.1**-**A**, is reported. A phosphate-tether-mediated double diastereotopic group differentiation protocol of the pseudo-C_2-symmetric (*R*,*R*)-phosphate triene **2.6.2** was utilized to generate the requisite stereocenters of the key C1–C12 subunit, we have termed the Brimble lactone methyl ether (2*S*)-**2.1.6**. Concurrently, a phosphate-tether-mediated one-pot sequential RCM/CM/substrate-controlled "H_2" /tether removal approach utilizing a homologated pseudo-C_2-symmetric (*S*,*S*)-phosphate triene **2.7.4** was utilized to improve the atom- and step-economy of the synthesis. Interestingly, this new route directed us to investigate on an unexpected hydrogenation event of the trisubstituted olefin within the unsaturated bicyclo[5.3.1]phosphate **2.7.5**., and to the synthesis of the 2*R*-epimer of the Brimble lactone methyl ether (2*R*)-**2.1.6**. Extensive ^{1}H and ^{13}C NMR data were utilized to identify the C2 epimers, and corresponding amide rotamers. at each stage of the synthesis. In addition, an unprecedented epimerization at the C2-methyl center was observed during the Me_3Al-mediated lactone opening reaction of both (2*S*)- and (2*R*)-lactone methyl ethers, which was further supported by extensive spectral analysis. A new route, circumventing the C2-epimerization event, was worked out and employed the use of methylamine for lactone opening, followed by a NaH-promoted *N*-allylation reaction, to deliver the critical amide-alcohol (2*R*)-**2.2.2**. Subsequent coupling of (2*R*)-**2.2.2** with acid subunit **2.2.3** afforded diene subunit (2*R*)-**2.2.4**, followed by RCM and final olefin isomerization completed the total synthesis of the natural product sanctolide A, (2*R*)-**2.1**-**A**. Interestingly,

the synthesized enamide macrolide was unstable at standing conditions as previously reported. The unusual stability of this natural product attracted our attention and underscores the need for making analogs that are more stable and has thus directed our efforts to generate simplified sanctolide analogs with improved stability and reactivity. In this regard, we detail the development of a library amenable, modular phosphate-tether-mediated approach to simplified sanctolide A analogs, which will be discussed in the next chapter (Chapter 3).

2.4 References Cited

[1] Shou, Q.; Feng, L.; Long, Y.; Han, J.; Nunnery, J. K.; Powell, D. H.; Butcher, R. A. A hybrid polyketide–nonribosomal peptide in nematodes that promotes larval survival. *Nat. Chem. Biol.* **2016**, *12*, 770–772.

[2] Fischbach, M. A.; Walsh, C. T. Assembly-line enzymology for polyketide and nonribosomal peptide antibiotics: logic, machinery, and mechanisms. *Chem. Rev.* **2006**, *106*, 3468–3496.

[3] Nivina, A.; Yuet, K. P.; Hsu, J.; Khosla, C. Evolution and Diversity of Assembly-Line Polyketide Synthases. *Chem. Rev.* **2019**, *119*, 12524–12547.

[4] Kang, H. S; Krunic, A.; Orjala, J. Sanctolide A, a 14-Membered PK-NRP Hybrid Macrolide from the Cultured Cyanobacterium *Oscillatoria sancta* (SAG 74.79). *Tetrahedron Lett.* **2012**, *53*, 3563–3567.

[5] (a) Pereira, A. R.; Cao, Z.; Engene, N.; Soria-Mercado, I. E.; Murray, T. F.; Gerwick, W. H. Palmyrolide A, an Unusually Stabilized Neuroactive Macrolide from Palmyra Atoll Cyanobacteria. *Org. Lett.* **2010**, *12*, 4490–4493 (b) Tello-Aburto, R.; Johnson, E. M.; Valdez, K. C.; Maio, W. A. Asymmetric Total Synthesis and Absolute Stereochemistry of the Neuroactive Marine Macrolide Palmyrolide A. *Org. Lett.* **2012**, *14*, 2150–2153.

[6] (a) Klein, D.; Braekman, J. C.; Daloze, D.; Hoffmann, L.; Castillo, G.; Demoulin, V. Madangolide and Laingolide A, Two Novel Macrolides from *Lyngbya bouillonii* (Cyanobacteria). *J. Nat. Prod*. **1999**, *62*, 934−936; (b) Klein, D.; Braekman, J.-C.; Daloze, D. Laingolide, a Novel 15-Membered Macrolide from *Lyngbya bouillonii* (cyanophyceae). *Tetrahedron Lett.* **1996**, *37*, 7519−7520; (c) Matthew, S.; Salvador, L. A.; Schupp, P. J.; Paul, V. J.; Luesch, H. Cytotoxic Halogenated Macrolides and Modified Peptides from the Apratoxin-Producing Cyanobacterium *Lyngbya bouillonii* from Guam. *J. Nat. Prod*. **2010**, *73*, 1544−1552.

[7] (a) Cui, C.; Dai, W.-M. Total synthesis of laingolide B stereoisomers and assignment of absolute configuration. *Org. Lett.* **2018**, *20*, 3358–3361. (b) Wu, F.; Zhang, T.; Yu, J.; Guo, Y.; Ye, T. Total Synthesis and Structural Reassignment of Laingolide A. *Mar. Drugs* **2021**, *19*, 247–245.

[8] Bertin, M. J.; Roduit, A. F.; Sun, J.; Alves, G. E.; Via, C. W.; Gonzalez, M. A.; Zimba, P. V.; Moeller, P. D. Tricholides A and B and unnarmicin D: new hybrid PKS-NRPS macrocycles isolated from an environmental collection of Trichodesmium thiebautii. *Marine drugs* **2017**, *15*, 206–217.

[9] Kang, H. S; Krunic, A.; Orjala, J. Sanctolide A, a 14-Membered PK-NRP Hybrid Macrolide from the Cultured Cyanobacterium *Oscillatoria sancta* (SAG 74.79). *Tetrahedron Lett.* **2012**, *53*, 3563–3567.

[10] Jones, A. C.; Monroe, E. A.; Eisman, E. B.; Gerwick, L.; Sherman, D. H.; Gerwick, W. H. The unique mechanistic transformations involved in the biosynthesis of modular natural products from marine cyanobacteria. *Nat. Prod. Rep.* **2010**, *27*, 1048–1065.

[11] Grindberg, R. V.; Ishoey, T.; Brinza, D.; Esquenazi, E.; Coates, R. C.; Liu, W.-t.; Gerwick, L.; Dorrestein, P. C.; Pevzner, P.; Lasken, R. Single cell genome amplification accelerates identification of the apratoxin biosynthetic pathway from a complex microbial assemblage. *PloS one* **2011**, *6*, e18565.

[12] Harwig, J.; Scott, P. Brine shrimp (Artemia salina L.) larvae as a screening system for fungal toxins. *Applied microbiology* **1971**, *21*, 1011–1016.

[13] (a) Kuranaga, T.; Sesoko, Y.; Inoue, M. Cu-mediated Enamide Formation in the Total Synthesis of Complex Peptide Natural Products. *Nat. Prod. Rep.* **2014**, *31*, 514–532, and references cited therein; (b) El-Seedi, H. R.; Zahra, M. H.; Goransson, U.; Verpoorte, R. Cyclopeptide Alkaloids. *Phytochem. Rev.* **2007**, *6*, 143–165.

[14] (a) Costa, M.; Costa-Rodrigues, J.; Fernandes, M. H.; Barros, P.; Vasconcelos, V.; Martins, R. Marine cyanobacteria compounds with anticancer properties: a review on the implication of apoptosis. *Mar. Drugs* **2012**, *10*, 2181–2207. (b) Mehrotra, S.; Duggan, B. M.; Tello-Aburto, R.; Newar, T. D.; Gerwick, W. H.; Murray, T. F.; Maio, W. A. Detailed Analysis of (−)-Palmyrolide A and Some Synthetic Derivatives as Voltage-Gated Sodium Channel Antagonists. *J. Nat. Prod.* **2014**, *77*, 2553–2560. (c) Wang, M.; Zhang, J.; He, S.; Yan, X. A review study on macrolides isolated from cyanobacteria. *Mar. Drugs* **2017**, *15*, 126–135.

[15] Wadsworth, A. D.; Furkert, D. P.; Brimble, M. A. Total Synthesis of the Macrocyclic *N*-Methyl Enamides Palmyrolide A and 2*S*-Sanctolide A. *J. Org. Chem.* **2014**, *79*, 11179–11193.

[16] Tokunaga, M.; Larrow, J. F.; Kakiuchi, F.; Jacobsen, E. N. Asymmetric Catalysis with Water: Efficient Kinetic Resolution of Terminal Epoxides by Means of Catalytic Hydrolysis. *Science* **1997***, 277*, 936–938.

[17] (a) Scholl, M.; Ding, S.; Lee, C. W.; Grubbs, R. H. Synthesis and Activity of a New Generation of Ruthenium-Based Olefin Metathesis Catalysts Coordinated with 1,3-Dimesityl-4,5-dihydroimidazol-2-ylidene Ligands. *Org. Lett.* **1999**, *1*, 953–956. (b) Chatterjee, A. K.; Choi, T.-L.; Sanders, D. P.; Grubbs, R. H. A General Model for Selectivity in Olefin Cross Metathesis. *J. Am. Chem. Soc.* **2003**, *125*, 11360–11370. (c) Ogbaa, O. M.; Warnera, N. C.; O'Leary, D. J.; Grubbs, R. H. Recent advances in ruthenium-based olefin metathesis. *Chem. Soc. Rev*. **2018**, *47*, 4510–4544.

[18] (a) Inanga, J.; Hirata, K.; Saeki, H.; Katsuki, T.; Yamaguchi, M. A Rapid Esterification by Means of Mixed Anhydride and Its Application to Large-ring Lactonization. *Bull. Chem. Soc. Jpn.* **1979**, *52*, 1989–1993;

[19] Müller, J.; Feifel, S. C.; Schmiederer, T.; Zocher, R.; Süssmuth, R. D. In vitro Synthesis of New Cyclodepsipeptides of the PF1022-Type: Probing the α-D-Hydroxy Acid Tolerance of PF1022 Synthetase. *Chem. Bio. Chem.* **2009**, *10*, 323−328.

[20] (a) Vaska, L. Hydridocarbonyl Complexes of Osmium by Reaction with Alcohols. *J. Am. Chem. Soc.* **1964**, *86*, 1943–1950 and reference there in. (b) Hiraki, K.; Matsunaga, T.; Kawano, H. Reactions of $RuClH(CO)(PPh_3)_3$ with Allylic Amines: Insertions and an Unusual Carbon-Nitrogen Bond Cleavage of Allylic Amines. *Organometallics* **1994**, *13*, 1878–1885. (c) Wakamatsu, H.; Nishida, M.; Adachi, N.; Mori, M. Isomerization Reaction of Olefin Using $RuClH(CO)(PPh_3)_3$. *The J. Org. Chem.* **2000**, *65*, 3966–3970. (d) Yue, C. J.; Liu, Y.; He, R. Olefins isomerization by hydride-complexes of ruthenium. *J. Mol. Catal. A: Chem.* **2006**, *259*, 17–23. (e) Larionov, E.; Li, H.; Mazet, C. Well-defined transition metal hydrides in catalytic isomerizations. *Chem. Commun.* **2014**, *50*, 9816–9826.

[21] Lai, Y.; Dai, W. M. Modular Total Synthesis of (–)-Palmyrolide A and (+)-(5 S, 7 S)-Palmyrolide A via Ring-Closing Metathesis and Alkene Isomerization. *Chin. J. Chem* . **2021**, *39*, 69–74.

[22] Yadav, J. S.; Surresh, B.; Srihari, P. Stereoselective Total Synthesis of the Marine Macrolide Sanctolide A. *Eur. J. Org. Chem.* **2015**, *26*, 5856–5863.

[23] (a) Hanawa, H.; Hashimoto, T.; Maruoka, K. Bis (((S)-binaphthoxy)(isopropoxy) titanium) oxide as a μ-oxo-type chiral Lewis acid: application to catalytic asymmetric allylation of aldehydes. *J. Am. Chem. Soc.* **2003**, *125*, 1708–1709. (b) Li, Y.; Chen, J.; Cao, X.-P. A stereoselective synthesis of (4E, 7S)-(-)-7-methoxydodec-4-enoic acid. *Synthesis* **2006**, *2006*, 320–324.

[24] Van Rheenen, V; Kelly, R. C.; Cha, D. Y. An Improved Catalytic OsO_4 Oxidation of Olefins to *cis*-1,2-Glycols Using Tertiary Amine Oxides as the Oxidant. *Tetrahedron Lett.* **1976**, *17,* 1973–1976.

[25] (a) Dess, D. B.; Martin, J. A useful 12-I-5 triacetoxyperiodinane (the Dess-Martin periodinane) for the selective oxidation of primary or secondary alcohols and a variety of related 12-I-5 species. *J. Am. Chem. Soc.* **1991**, *113*, 7277–7287. (b) Paterson, I.; Anderson, E. A.; Dalby, S. M.; Lim, J. H.; Genovino, J.; Maltas, P.; Moessner, C. Total Synthesis of SpirastrellolideA Methyl Ester—Part1: Synthesis

of an Advanced C17–C40 Bis-spiroacetal Subunit. *Angew. Chem. Int. Ed.* **2008**, *47*, 3021–3025.

[26] (a) Uematsu, N.; Fujii, A.; Hashiguchi, S.; Ikariya, T.; Noyori, R. Asymmetric Transfer Hydrogenation of Imines. *J. Am. Chem. Soc*. **1996**, *118*, 4916–4917; (b) Denmark, S. E.; Yang, S.-M. Total Synthesis of (+)-Brasilenyne. Application of an Intramolecular Silicon-Assisted Cross-Coupling Reaction. *J. Am. Chem. Soc.* **2004**, *126*, 12432–12440; (c) Raghavan, S.; Kumar, V. V. A Stereoselective Synthesis of the C9–C19 Subunit of (+)-Peloruside A. *Org. Biomol. Chem*. **2013**, *11*, 2847–2858; (d) Arai, N.; Satosh, H.; Utsumi, N.; Murata, K.; Tsutsumi, K.; Ohkuma, T. Asymmetric Reduction of Diynones and the Total Synthesis of (S)-Panaxjapyne A. *Org. Lett*. **2013**, *15*, 3030–3033.

[27] (a) Lindgren, B. O.; Nilsson, T. Preparation of Carboxylic Acids from Aldehydes (Including Hydroxylated Benzaldehydes) by Oxidation with Chlorite. *Acta Chem. Scand.* **1973**, *27*, 888–890; (b) Bal, B. S.; Childers, W. E.; Pinnick, H. W. Oxidation of α,β-Unsaturated Aldehydes. *Tetrahedron* **1981**, *37*, 2091–2096.

[28] (a) Venukadasula, P. K. M.; Chegondi, R.; Suryn, G.; Hanson, P. R. A Phosphate Tether-Mediated, One-pot, Sequential Ring-Closing Metathesis/Cross-Metathesis/Chemoselective Hydrogenation Protocol. *Org. Lett.* **2012**, *14*, 2634–2637; (b) Jayasinghe, S.; Venukadasula, P. K. M.; Hanson, P. R. An Efficient, Modular Approach for the Synthesis of (+)-Strictifolione and a Related Natural Product. *Org. Lett.* **2014**, *16*, 122–125; (c) Bodugam, M.; Javed, S.; Ganguly, A.; Torres, J.; Hanson, P. R. A Pot-Economical Approach to the Total Synthesis of Sch-725674. *Org. Lett.* **2016**, *18*, 516–519; (d) Hanson, P. R.; Jayasinghe, S.; Maitra, S.; Ndi, C. N.; Chegondi, R. A Modular Phosphate Tether-mediated Divergent Strategy to Complex Polyols. *Beilstein J. Org. Chem.* **2014**, *10*, 2332–2337; (e) Javed, S.; Bodugam, M.; Torres, J.; Ganguly, A.; Hanson, P. R. Modular Synthesis of Novel Macrocycles Bearing α,β-Unsaturated Chemotypes via a Series of One-Pot, Sequential Protocols. *Chem. Eur. J.* **2016**, *22*, 6755–6758.

[29] (a) Chegondi, R.; Maitra, S.; Markley, J. L.; Hanson, P. R. Phosphate-Tether-Mediated Ring-Closing Metathesis for the Preparation of Complex 1,3-anti-Diol-Containing Subunits. *Chem. Eur. J.* **2013**, *19*, 8088–8093. For related papers, see: (b) Maitra, S.; Markley, J. L.; Chegondi, R.; Hanson, P. R. Phosphate tether-mediated ring-closing metathesis for the generation of medium to large, *P*-stereogenic bicyclo[n.3.1]phosphates, *Tetrahedron* **2015**, *71*, 5734–5740. (c) Markley, J. L.; Maitra, S.; Hanson, P. R. Phosphate Tether-Mediated Ring-Closing Metathesis for the Generation of P-Stereogenic, Z-Configured Bicyclo[7.3.1]- and Bicyclo[8.3.1]phosphates. *J. Org. Chem.* **2016**, *81* (3), 899–911.

[30] (a) Maitra, S. Phosphate Tether-Mediated Metathesis Studies and Application Towards Natural Product Synthesis. Ph.D. Thesis, University of Kansas, Lawrence, KS, June 2016. (b) Markley, J. L. *P*-Stereogenic, Bicyclic Phosphorus Heterocycles and Temporary Tether Strategies for the Synthesis of Complex Polyols**.** Ph.D. Thesis, University of Kansas, Lawrence, KS,

[31] (a) Kingsbury, J. S.; Harrity, J. P. A.; Bonitatebus, P. J., Jr.; Hoveyda, A. H. A Recyclable Ru-Based Metathesis Catalyst. *J. Am. Chem. Soc*. **1999**, *121*, 791−799; (b) Garber, S. B.; Kingsbury, J. S.; Gray, B. L.; Hoveyda, A. H. Efficient and Recyclable Monomeric and Dendritic Ru-Based Metathesis Catalysts. *J. Am. Chem. Soc*. **2000**, *122*, 8168−8179.

[32] Louie, J.; Bielawski, C. W.; Grubbs, R. H. Tandem Catalysis: The Sequential Mediation of Olefin Metathesis, Hydrogenation, and Hydrogen Transfer with Single-Component Ru Complexes. *J. Am. Chem. Soc.*, **2001**, *123*, 11312–11313.

[33] (a) Trost, B. M. The atom economy: a search for synthetic efficiency. *Science* **1991**, *254*, 1471–1477. (b) Trost, B. M. Atom economy - a challenge for organic synthesis: homogeneous catalysis leads the way. *Angew. Chem. Int. Ed.* **1995**, *34*, 259–281. (c) Newhouse, T.; Baran, P. S.; Hoffmann, R. W. The economies of synthesis. *Chem. Soc. Rev.* **2009**, *38*, 3010–3021.

[34] (a) Wender, P. A.; Verma, V. A.; Paxton, T. J.; Pillow, T. H. Function-Oriented Synthesis, Step Economy, and Drug Design. *Acc. Chem. Res.* **2008**, *41*, 40–49. (b) Young, I. S.; Baran, P. S. Protecting-group-free synthesis as an opportunity for invention. *Nat. Chem.* **2009**, *1*, 193–205. (c) Hoffmann, R. W. Protecting-group-free synthesis. *Synthesis* **2006**, 3531–3541. (d) Wender, P. A. Toward the ideal synthesis and molecular function through synthesis-informed design. *Nat. Prdt. Rep.* **2014**, *31*, 433–440.

[35] (a) Hassan, A.; Lu, Y.; Krische, M. J. Elongation of 1,3-Polyols via Iterative Catalyst-Directed Carbonyl Allylation from the Alcohol Oxidation Level. *Org. Lett.* **2009**, *11*, 3112–3115. (b) Han, S. B.; Hassan, A.; Kim, I. S.; Krische, M. J. Total synthesis of (+)-roxaticin via C− C bond forming transfer hydrogenation: A departure from stoichiometric chiral reagents, auxiliaries, and premetalated nucleophiles in polyketide construction. *J. Am. Chem. Soc.* **2010**, *132*, 15559–15561. (c) Perez, F.; Waldeck, A. R.; Krische, M. J. Total Synthesis of Cryptocaryol A by Enantioselective Iridium-Catalyzed Alcohol C− H Allylation. *Angew. Chem.* **2016**, *128*, 5133–5136.

[36] (a) Marino, J. P.; Fernandez de la Pradilla, R.; Laborde, E. Regio-and stereoselectivity of the reaction between cyanocuprates and cyclopentene epoxides. Application to the total synthesis of prostaglandins. *J. Org. Chem.* **1987**, *52*, 4898–4913. (b) Mori, S.; Nakamura, E.; Morokuma, K. Mechanism of SN2 alkylation reactions of lithium organocuprate clusters with alkyl halides and epoxides. Solvent Effects, BF3 effects, and trans-diaxial epoxide opening. *J. Am. Chem. Soc.* **2000**, *122*, 7294–7307. (c) The Chemistry of Organocopper Compounds: Part 1 and Part 2; Rappoport, Z.; Marek, I., Eds.; Wiley: Chichester, **2009**.

[37] (a) Mori, M.; Sakakibara, N.; Kinoshita, A. Remarkable effect of ethylene gas in the intramolecular enyne metathesis of terminal alkynes. *J. Org. Chem.* **1998**, *63*, 6082–6083. (b) McReynolds, M. D.; Dougherty, J. M.; Hanson, P. R. Synthesis of Phosphorus and Sulfur Heterocycles via Ring-Closing Olefin Metathesis. *Chem. Rev.* **2004**, *104*, 2239–2258. (c) Conrad, J. C.; Fogg, D. E. Ruthenium-catalyzed

ring-closing metathesis: recent advances, limitations and opportunities. *Curr. Org. Chem.* **2006**, *10*, 185–202.

[38] Marvin Calculator Plugins were used for structure property prediction and calculation, Marvin 21.4.0, 2021, ChemAxon (http://www.chemaxon.com)

[39] The PyMOL Molecular Graphics System, Version 2.0 Schrödinger, LLC.

[40] (a) Schirmer, R. E.; Noggle, J. H.; Davis, J. P.; Hart, P. A. Determination of molecular geometry by quantitative application of the nuclear Overhauser effect. *J. Am. Chem. Soc.* **1970**, *92*, 3266–3273. (b) Kumar, A.; Ernst, R.; Wüthrich, K. A 2D NOE experiment for the elucidation of complete proton-proton cross-relaxation networks in biological macromolecules. *Biochem. Biophys. Res. Commun* **1980**, *95*, 1–6. (c) A. & RANI GRACE, R. C. 2017. Nuclear Overhauser Effect A2 - Lindon, John C. In: TRANTER, G. E. & KOPPENAAL, D. W. (eds.) Encyclopedia of Spectroscopy and Spectrometry (Third Edition). Oxford: Academic Press.

[41] Basha, A.; Lipton, M.; Weinreb, S. M. A mild, general method for conversion of esters to amides. *Tetrahedron Lett.* **1977**, *18*, 4171–4172.

[42] Spandl, R. J.; Rudyk, H.; Spring, D. R. Exploiting domino enyne metathesis mechanisms for skeletal diversity generation. *Chem. Commun.* **2008**, *26*, 3001–3003.

Chapter 3

A Build-Couple-Couple-Pair (BCCP) Approach for the Synthesis of 2-desmethyl Sanctolide A and Simplified Analogs

3.1 Introduction

3.1.1 Natural product analog libraries

Historically, natural products have continued to influence the design of new therapeutics as well as aiding in the identification of biologically active targets.[1] Natural products can also act as a starting point for derivatization and reprogramming of the existing structures. These modifications can potentially enhance the chemical space of the starting small molecule and thus serve to deliver lead-like compounds (hit-to-lead strategies) and chemical probes.[2] According to an analysis done by Newman and coworkers in 2014, out of 175 small molecules approved for cancer therapeutics in the period of 1940–2014, 85 (48.6%) were either natural products or directly derived from natural products.[1b,3] Moreover, natural products and their core-derivatives are considered as privileged structures, since they have already interacted with the biological entities such as enzymes and proteins during their biosynthesis, and gain an advantage over unnatural molecules to occupy a chemical space, which is already well-suited to interact with proteins.[4,5]

In this regard, there has been a growing interest in the synthetic community to deliver natural product-inspired small molecular libraries to understand biological processes.[6,23b] Towards this goal, a number of (bio)synthetic groups have taken the initiative to modify skeletons of active natural products as novel lead compounds, which has prompted extensive reviews.[4,7] In these reviews, topics such as Diversity-Oriented Synthesis (DOS), Diverted Total Synthesis (DTS), Function-Oriented Synthesis (FOS), Biology-Oriented Synthesis (BIOS), as well as high-throughput and combinatorial strategies coupled with both solid- and solution-phase syntheses are discussed.

Additionally, in 2018, Alihodžic and coworkers nicely summarized the importance, synthetic approaches, and challenges related to synthesis of natural product-inspired macrocyclic analogs.[8]

The next two sub-sections (3.1.2 and 3.1.3) discuss two interesting reports of natural product-inspired macrocyclic analog syntheses from recent literature.

3.1.2 Natural product inspired hybrid macrocyclic analogs

In 2018, Gade and coworkers reported a novel approach for designing hybrid natural product analogs by combining "critical structural features" (topology) of three different classes of natural products.[9] In this work, the authors coined a new term, they called topology-directed synthesis (TDS), which is based on the concept of exploring common "critical structural features" that are present in a class of natural products and combine those features to attain new hybrid cyclic scaffolds. During the design of the hybrid molecules, the authors incorporated three-dimensional chiral backbones from three distinct natural product families, amphidinolide T,[10] migrastatin[11] and rhizoxin[12] to deliver complex, hybrid macrocycles. The selection of these three natural product families for the analog synthesis was based on their profound anti-cancer activity.

The amphidinolide T family is comprised of five compounds (T1–T5) which exhibit moderate cytotoxicity (IC_{50} = 7–18 μg/mL) against KB human epidermoid carcinoma cells.[13] In terms of "critical structural features" of this family, all five compounds contain a characteristic tri-substituted tetrahydrofuran (THF) moiety in the macrocyclic core **3.1-A** (Figure 3.1). Therefore, fragment **3.1.3** was selected as the critical structural unit for incorporation into hybrid macrocycles. Similarly, migrastatin and related

molecules in the migrastatin family exhibit various biological activities such as inhibition of cell migration and anchorage-independent growth of cancer cells.[14] Notably, the secondary metabolites migrastatin (**3.1-B)** and isomigrastatin (**3.1-C)** of this family carry a common stereo-enriched 2-methyl-1,3,4-triol fragments **3.1.6** in their macrocyclic core, and therefore this fragment was selected to include in the hybrid macrocyclic scaffolds (Figure 3.1B). In addition, rhizoxin D (**3.1-E**) and related analogs of the rhizoxin family carry a substituted δ-lactone moiety **3.1.9** in their macrocyclic cores (Figure 3.1C). Importantly, rhizoxins have shown potent antitumor activity through binding to β-tubulin.

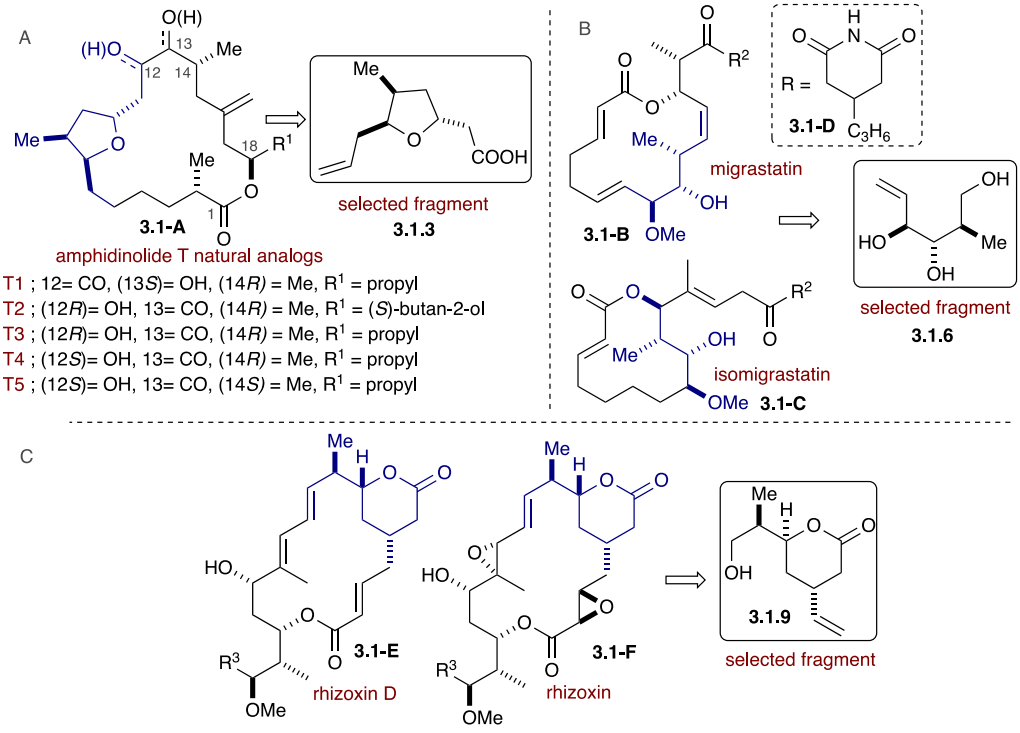

Figure 3.1 *Amphidinolide T, migrastatin and rhizoxin natural product families*

By considering the common topological features within each family of natural products and their anti-cancer activity, two macrocyclic hybrid analogs were designed with

the aim of possessing unique biological properties as well as to act as a probe to study cancer cell migration and mortality.[9]

Retrosynthetic approaches for the synthesis of two hybrid analogs **3.2.3** and **3.2.4** are depicted in Figure 3.2. Both 14-membered macrocycle **3.2.3** and 15-membered macrocycle **3.2.4** comprising six stereogenic centers would be synthesized using a BCP strategy. The authors planned to generate advanced intermediates **3.1.3**, **3.1.6**, and **3.1.9** from stereo-divergent intermediates **3.1.1**, **3.1.4**, and **3.1.7** at the build-phase of the synthesis. Intermolecular esterification (coupling phase) followed by RCM (pairing phase) would furnish the desired hybrid macrolactone cores. The 14-membered macrolactone analog amphidinolide T-isomigrastatin would be delivered after hydrogenation.[9]

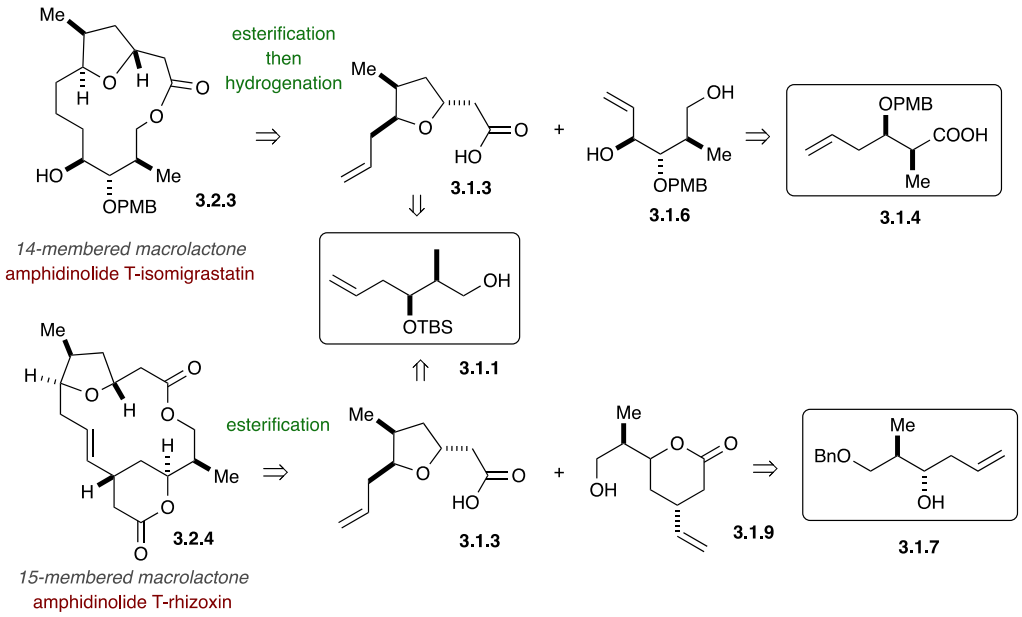

Figure 3.2 *Retrosynthetic analysis of hybrid analogs*

The characteristic tetrahydrofuran moiety of amphidinolide T family **3.1.3** was synthesized from alcohol **3.1.1** utilizing a known procedure published by the same authors in 2010 (Scheme 3.1).[15] Alcohol **3.1.1** was subjected to Dess-Martin periodinane oxidation, followed by Wittig homologation and hydrolysis, to deliver aldehyde **3.1.2**. Next, Wittig olefination with carbethoxymethylenetriphenylphosphorane afforded the corresponding α,β-unsaturated ester. Silyl deprotection and subsequent intramolecular oxy-Michael reaction constructed the key THF ring. Subsequent transesterification, followed by saponification, delivered the required amphidinolide T fragment **3.1.3** as an inseparable (desired: undesired 4:1) mixture of diastereomers. Moreover, the migrastatin polyol fragment **3.1.6** was generated from acid **3.1.4** using the reported protocol. The protected acid was subjected to White oxidation to form lactone **3.1.5** in 65% yield with good diastereoselectivity (*dr* = 9:1).[16] Subsequent DIBAL-H reduction furnished the migrastatin polyol fragment **3.1.6**.

Scheme 3.1 *The Synthesis of characteristic THF, polyol and δ-lactone moieties*

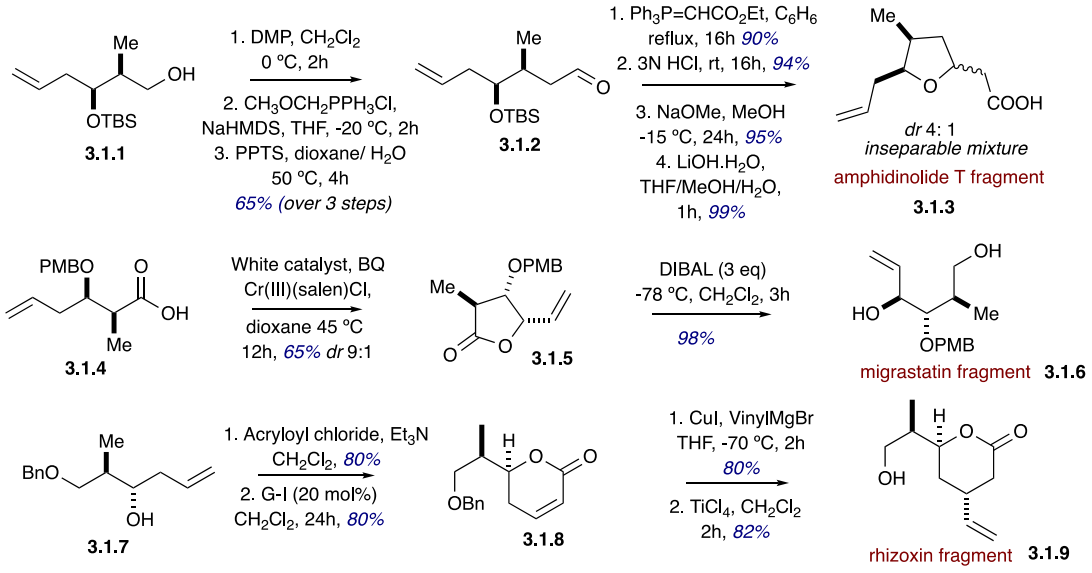

The rhizoxin δ-lactone was generated employing a known method.[17] Thus, acryloylation in methylene chloride, followed by RCM with the Grubbs **G-I** catalyst, generated the enone moiety **3.1.8** in good yields. Stereoselective 1,4-addition of vinyl magnesium bromide with catalytic copper, and subsequent debenzylation by $TiCl_4$, afforded the desired rhizoxin δ-lactone **3.1.9**.

With all the "build" components in hand, Gade and coworkers focused their efforts on the completion of the synthesis of the two hybrid analogs (Scheme 3.2).[9] The diastereomeric mixture (4:1) of substituted THF-containing acid **3.1.3** was coupled with the polyol fragment of migrastatin **3.1.6** utilizing the Steglich esterification conditions (couple-phase) to generate a diene with the same mixture of the starting two diastereomers (4:1). Subsequent RCM with the Grubbs **G-II** catalyst, in methylene chloride (pair-phase), delivered the undesired scaffold **3.2.1** as a single diastereomer and the desired scaffold **3.2.2** as a mixture of *E* and *Z* isomers. Finally, Pd/C-mediated hydrogenation of **3.2.2** furnished the desired hybrid macrolactone in excellent yield. Similarly, the diastereomeric mixture of acid **3.1.3** was then coupled with rhizoxin fragment **3.1.9** by Steglich esterification. Final RCM of the diene afforded the macrocycle as an inseparable mixture of diastereomers. However, the authors were able to purify the desired hybrid analog **3.2.4** by recrystallization.

In summary, the authors successfully synthesized hybrid macrolactone scaffolds by incorporating the critical structural features of biologically active natural products belonging to three distinct families.

Scheme 3.2 *The synthesis of hybrid analogs* ***3.2.3*** *and* ***3.2.4***

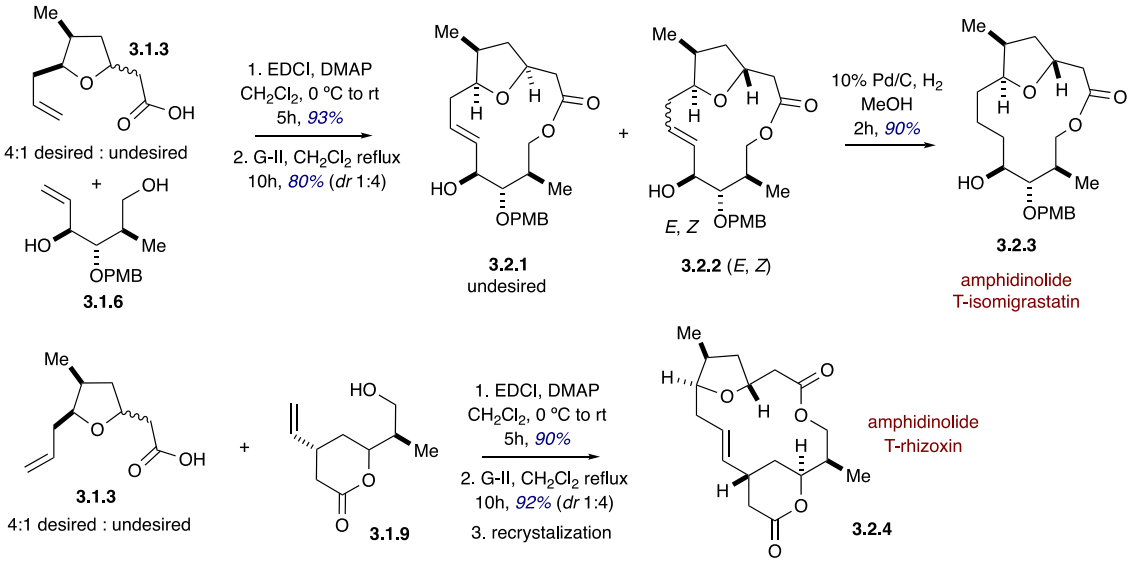

3.1.3 Design and synthesis of potent leupyrrin analogs: leupylogs

In 2020, Menche and coworkers reported the synthesis of highly active and simplified analogs of leupyrrin natural products, they termed leupylogs.[18] Leupyrrins belong to a complex macrolide family, which contain an 18-membered macrocyclic core with an unusually substituted γ-butyrolactone, along with a pyrrole and oxazoline in combination with a substituted dihydrofuran sidechain (Figure 3.3). Leupyrrins exhibit potent antifungal activity and anti-HIV properties.[19] However, exploration of the SAR and other biochemical relationships has been limited due to the low availability and synthetic challenges associated with the complex structural features of the molecule. Moreover, the diene moiety substituted to the dihydrofuran in the side chain is prone to double bond migration, hence making the synthesis more challenging.[18] Therefore, the authors envisioned a modular strategy to synthesize analogs that vary in the side chain, to include,

the furan, the oxazoline, the pyrrole and the diacid fragments (Figure 3.3). These simplifications not only reduced the number of synthetic steps, but also introduced stability to the molecular structure, a strategy that guided our efforts for sanctolide A analogs described later in this chapter, *vide infra*.

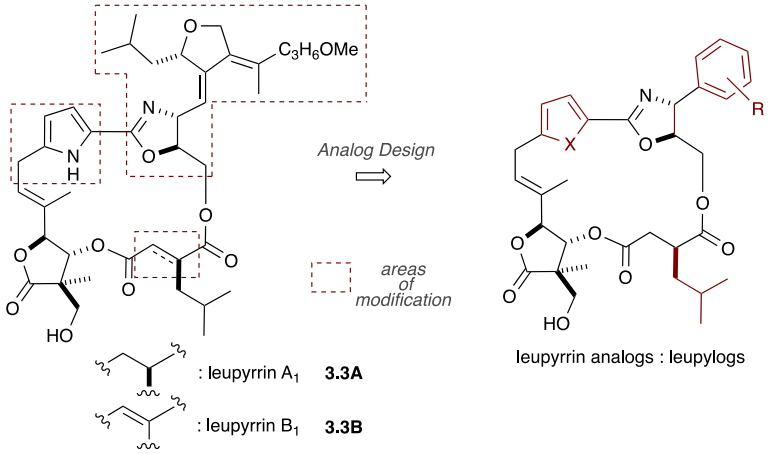

Figure 3.3 *A modular strategy to synthesize leupyrrin analogs*

The authors envisioned that the labile furan ring and its substituted alkylidene units could be replaced by an aromatic system that would not only simplify the synthesis, but also provide stability. These efforts led to the synthesis of two analogs **3.3.14** and **3.3.15** as shown in Scheme 3.3. The synthesis commenced with the generation of eastern fragments of **3.3.8**, **3.3.9** from known epoxy alcohols **3.3.1**, **3.3.2** and diacid **3.3.3** (Scheme 3.3). In this regard, Shiina esterification,[20] followed by regio- and diastereoselective epoxide opening with sodium azide, and subsequent azide reduction delivered the eastern fragments **3.3.6** and **3.3.7** in good yields.

Scheme 3.3 *Synthesis of leupylog analogs* ***3.3.14*** *and* ***3.3.15***

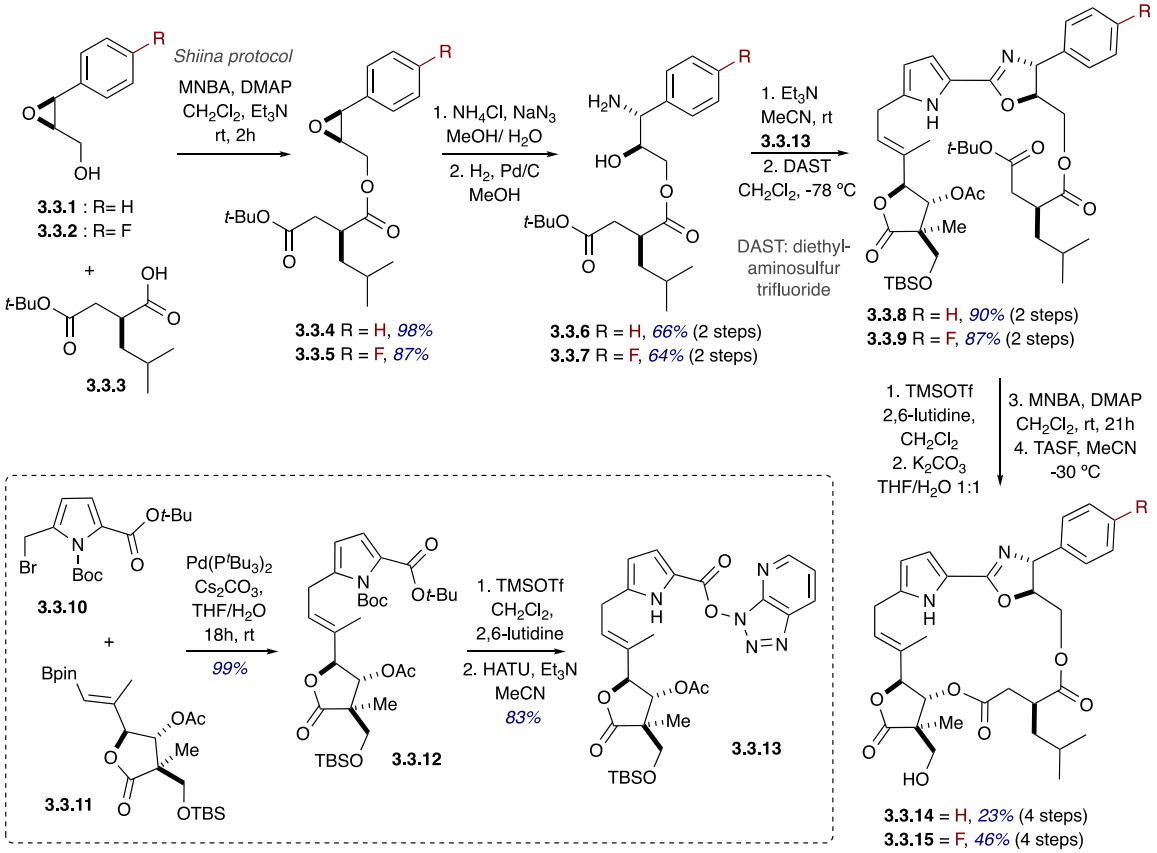

Next, the synthesis of the azabenzotriazole **3.3.13** commenced using a previously reported Pd-catalyzed sp^2-sp^3 cross-coupling reaction between **3.3.10** and **3.3.11**.[21] Subsequent Boc-deprotection and *tert*-butyl ester cleavage, followed by coupling of 1-hydroxy-7-azabenzotruiazole (HATU) with the free acid, delivered the western fragment in good yields.[22] Amide formation under basic conditions, followed by cyclodehydration with DAST, generated the oxazolines **3.3.8** and **3.3.9**. *Tert*-butyl ester cleavage, and selective acetate saponification with K_2CO_3, furnished the *seco* acids in good yields. Finally, Shiina macrocyclization, followed by TASF-mediated TBS-deprotection, delivered the required macrolactone analogs **3.3.14** and **3.3.15**. Since the two analogs

containing simplified side chains demonstrated biological activity, the authors opted for further modifications within the pyrrole moiety as shown in Scheme 3.4.

Scheme 3.4 *Synthesis of leupylog analogs **3.4.9** and **3.4.10***

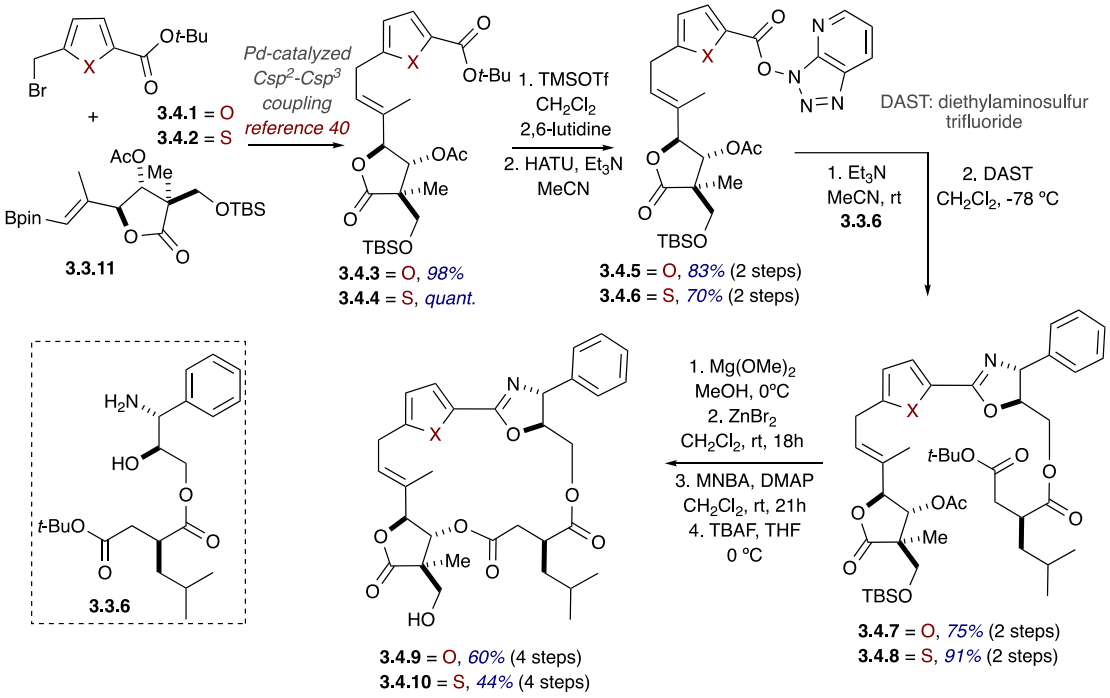

The pyrrole moiety was replaced with furan and thiophene to generate analogs **3.4.9** and **3.4.10** (Scheme 3.4). Synthesis of the northwestern fragment commenced with a Pd-catalyzed cross-coupling reaction between furan **3.4.1** or thiophene **3.4.2**, with **3.3.11**, to deliver **3.4.3** and **3.4.4**, respectively. Next, the two azabenzotriazoles **3.4.5**, **3.4.6**, and oxazolines (**3.4.7**, **3.4.8**) were generated following the same protocol shown in Scheme 3.4. Selective cleavage of the acetate occurred via transesterification with magnesium methoxide, and subsequent *tert*-butyl ester cleavage was promoted by zinc bromide in methylene chloride with water quench. Shiina macrocyclization, followed by deprotection

of the silyl protecting group, delivered the two analogs **3.4.9** and **3.4.10** with substituted furan and thiophene moieties, respectively.

Scheme 3.5 *The synthesis of leupylog analog **3.5.6***

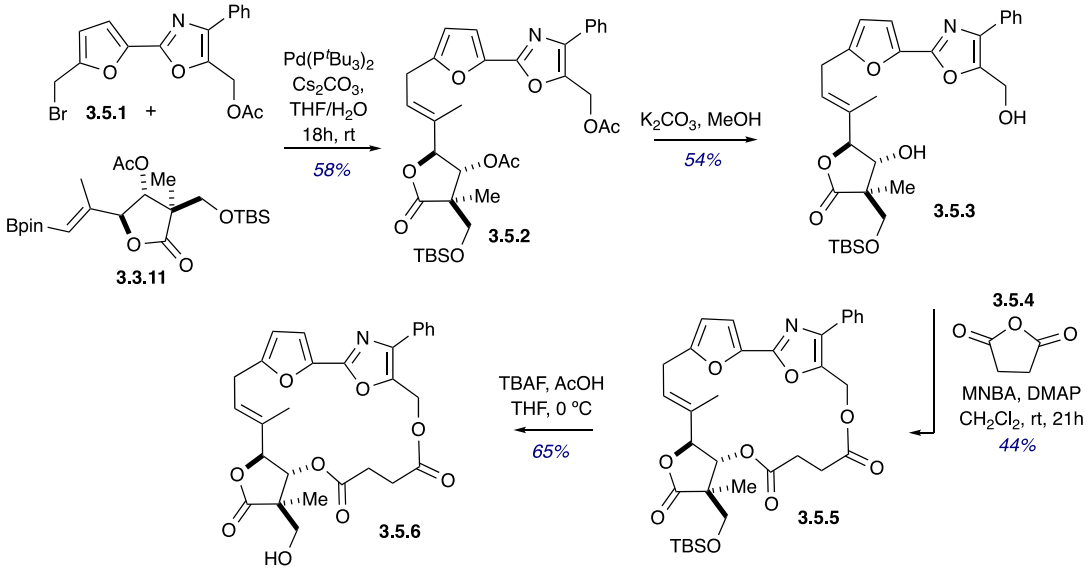

Next, the authors targeted the synthesis of a more truncated leupylog analog containing an oxazole, instead of oxazoline, and simplified diacid building block (Scheme 3.5). The key western fragment was synthesized utilizing Pd-catalyzed cross-coupling reaction of alkyl bromide **3.5.1** with vinyl boronate **3.3.11**.[21] Subsequent saponification of the acetate, followed by one-pot macrolactonization with succinic anhydride in the presence of MNBA and DMAP (Shiina protocol), delivered the macrolactone **3.5.5**. Final TBS-deprotection with TBAF yielded the required truncated leupylog **3.5.6**.

Furthermore, the authors carried out the biological evaluation of the synthesized analogs. Leupylogs **3.3.14** and **3.3.15**, displayed antifungal activity against *R. glutinis*, similar to the natural products leupyrrins. However, furan leupylog **3.4.9** was less active and thiophene leupylog **3.4.10** was essentially inactive, which demonstrated the necessity

of the pyrrole moiety for the activity of the molecule. Moreover, the truncated analog **3.5.6** containing the furan-oxazole moiety led to complete loss of activity. In addition, analogs **3.3.14**, **3.3.15**, and **3.5.6** demonstrated antiproliferative activity towards murine fibroblast cell line L929 similar to leupyrrin. These biological data revealed the importance of the macrocyclic core, flexibility of the diacid fragment, and the stability of the side chain. The study collectively demonstrated that the overall structure can be simplified without diminishing its biological activity significantly and, most importantly, analogs can be accessed with fewer synthetic steps making them more accessible than their parent natural products.

In summary for this introductory material, the synthesis of natural product analogs with diverse structural and functional features can be useful for enhancing biological activity as well as identifying new targets with broad pharmaceutical profiles. Macrocyclic natural products are relatively less explored compared to other small molecules due to the synthetic challenges associated with them. Development of modular synthetic strategies to generate simpler macrocyclic libraries are frequently coupled with diversity-oriented synthesis (DOS). In this regard, we herein report in Chapter 3, an account of the application of a build/couple/couple/pair (BCCP) strategy for the synthesis of simplified, *des*-methyl macrocyclic analogs of the natural product sanctolide A.

3.1.4 DOS and Build/Couple/Pair (B/C/P)

Diversity-oriented synthesis (DOS) provides strategies that have the potential to generate libraries of small molecules with unique biological and physico-chemical

properties which can be utilized in establishing structure-activity relationship (SAR) studies,[23] activity-based protein profiling (ABPP) studies,[24] and the discovery of new therapeutics.[25] Over the past two decades, the application of DOS for target identification[26] has gained significant attention, and presented challenges with increasing scaffold diversity.[27,28] This in turn has prompted the development of enabling strategies to address this need. Among many strategies are build/couple/pair (B/C/P),[29] oxidative ring expansion,[30] fragment-based domain shuffling,[31] two-directional synthesis,[32] and multi-dimensional coupling.[33]

Taken collectively, these unique strategies have been utilized in the synthesis of small-molecule libraries and in drug discovery processes.[34] In particular, the synthesis of small molecules with macrocyclic ring systems has proved challenging, even though the macrocycles can provide diverse stereochemical substituents with complex architecture, which potentially can have enhanced interactions with biological macromolecules.[35] A number of macrocyclization strategies have been utilized to date in DOS library synthesis such as the use of macrocyclic (i) ring-closing metathesis (RCM),[36] (ii) Azide-Alkyne Cycloadditions (AAC),[37,38] (iii) Diels-Alder reaction[39], and (iv) transition metal-catalyzed cross-coupling reactions.[40] Application of the aforementioned macrocyclization methods in diversity oriented synthesis (DOS) was recently highlighted by Spring and coworkers.[41]

The remainder of Chapter 3 will provide the details of the synthesis of a small library of macrocyclic analogs of aforementioned natural product, sanctolide A that was carried out by adopting a build-couple-couple-pair (BCCP) strategy coupled with phosphate tether one-pot sequential protocols. The synthetic strategy was focused on

generating simplified, *des*-methyl sanctolide analogs containing an α, β-unsaturated lactone moiety to simplify the synthesis and importantly, to improve the stability of the analogs. In this regard, a total of five, α, β -unsaturated macrolides, and two enamide macrolides with variable substituents and sidechains were generated. In addition, a one-pot CM/RCM/H_2/LAH protocol was developed in the "build phase" for the synthesis of the C1–C10 1,3-*anti*-diol-containing subunit (sanctolide numbering).

3.2 Results and discussion

Sanctolide A is a polyketide- nonribosomal peptide (PK-NRP) hybrid macrolide and was first isolated in 2012 by Orjala and coworkers from the cultured cyanobacterium *Oscillatoria sancta* (SAG 74.79).[42] Sanctolide A showed moderate toxicity in the brine shrimp toxicity assays with a LD_{50} value of 23.5 μL (l M) . Total synthesis of the assigned structure of sanctolide A and its 2*S*-sanctolide epimer were carried out by Yadav,[43] and Brimble,[44] respectively, as noted in Chapter 2. Recently, we utilized a phosphate tether mediated approach for the formal synthesis of the 2*S*-epimer and total synthesis of the natural product sanctolide A (see Chapter 2 of this thesis).

Biological evaluation of sanctolide A has not been done extensively. Compared to other enamide natural products belonging to the PK/NRP family, (e.g. palmerolide A), sanctolide A displays a relatively lower biological activity. This lower biological activity has been suspected to contribute to the instability of the molecule within biological systems. Orjala and coworkers, in their initial isolation report, observed an unusual hydrolysis of the enamide group to its corresponding aldehyde when exposed to water.[42]

In addition, Yadav reported a decomposition of their synthesized natural product even at low temperatures.[43] We also observed a rapid decomposition of the synthesized natural product with prolonged storage even at low temperatures (Chapter 2). Due to the scarcity of the natural product, as well as the unusual instability of the synthetic macrolide, the biological evaluation of sanctolide A has been a challenge and inspired us to design and synthesize a library of analogs with enhanced stability and modulated reactivity for biological screening.

Towards the aforementioned goal, we envisioned the synthesis of a small library of macrocyclic analogs library by adopting a build-couple-couple-pair (BCCP) strategy. This strategy would be amenable for library construction, and would employ the phosphate tether-mediated one-pot sequential protocol developed in our lab (Figure 3.4). Our synthetic strategy focused on generating simplified, *des*-methyl sanctolide analogs containing an α,β-unsaturated lactone moiety. Removal of the 2-methyl center of the macrocyclic analog would simplify the synthesis and importantly, solve the epimerization problem that we experienced during the Me_3Al-mediated lactone opening reaction in the sanctolide A natural product synthesis (see chapter 2 of this thesis). In addition, forgoing the olefin isomerization after RCM, would produce an amide/α,β-unsaturated lactone functionality—instead of enamide/lactone functionality, and thus increase the stability of the macrocyclic analogs. This will potentially modulate the reactivity of the parent compound, sanctolide A. The synthetic plan employing a DOS strategy is depicted in Figure 3.4.

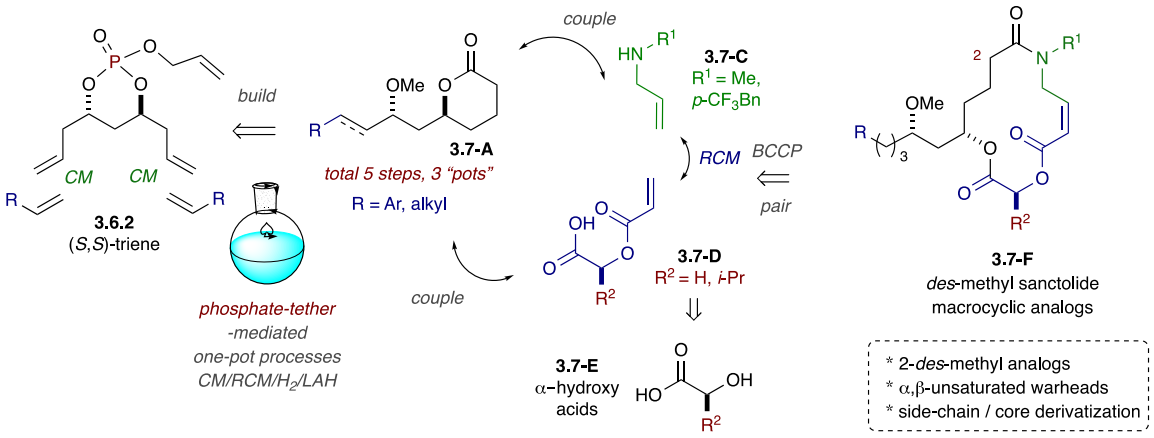

Figure 3.4 *The synthetic plan employing a DOS strategy*

In this regard, we envisioned a BCCP strategy that would couple lactone methyl ethers **3.7-A**, synthesized from (*S*,*S*)-triene **3.6.2** using a phosphate tether-mediated one-pot CM/RCM/H_2/LAH protocol for the synthesis of the C1–C10 1,3-*anti*-diol-containing subunit (sanctolide numbering) in the build phase. Coupling would then proceed via a Lewis acid-mediated lactone ring opening with different amines **3.7-C** using the Weinreb conditions,[45] followed by Yamaguchi esterification with acid subunits **3.7-E** (coupling), to deliver the diene precursors. The final pairing-phase with an RCM macrocyclization would afford the macrocyclic lactone analogs **3.7-F**. Subsequent olefin isomerization using the Brimble conditions would then deliver the enamide analogs.

Synthesis of the lactone intermediates commenced by coupling the readily-prepared (*S*,*S*)-1,3 *anti*-diol homoallylic diene-diol **3.6.1** with $POCl_3$, followed by lithiated-allyl alcohol, to deliver the (*S*,*S*)-phosphate triene **3.6.2** in good yields. With the (*S*,*S*)-phosphate triene in hand, we then examined the RCM reaction with the Grubbs **G-II** catalyst (**G-II**, [$(ImesH_2)(PCy_3)(Cl)_2Ru$=CHPh]) in refluxing methylene chloride. To our surprise, the RCM reaction proceeded with significantly lower yields compared to the

yields that were obtained for bicyclo[5.3.1]phosphate **3.6.3** with the 2-methyl center (see previous chapter) (Table 3.1). From careful NMR and TLC experiments, we identified that the lower yield resulted from a RuH-mediated isomerization and dimerization.

Scheme 3.6 *The Synthesis of bicyclo[5.3.1]phosphate*

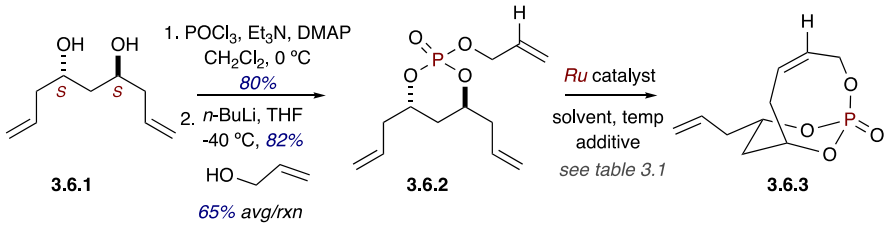

Reaction optimizations were carried out with both Grubbs **G-II** and Hoveyda-Grubbs **HG-II** catalysts using different reaction conditions, namely (i) variable concentrations to minimize dimerization, (ii) use of *para*-benzoquinone (PBQ) to re-oxidize RuH-species, and (iii) use of ethylene gas[46] to regenerate the active Ru catalyst from unproductive Ru-metallocyclobutane intermediates at the distal olefins (Table 3.1). Unfortunately, none of the above optimization conditions generated the bicylo[5.3.1]phosphate intermediate in good yields to continue the build-phase of the synthesis in a sufficiently larger scale.

Next, we focused our efforts to investigate the addition sequence, switching to an CM/RCM protocol where the phosphate triene would first undergo cross metathesis at high concentration with the CM partner in the presence of **HG-II** at room temperature, followed by RCM in the same "pot" to close the ring in a diastereoselective group differentiation step at refluxing DCE temperature (89ºC), similar to the study published by Bressy and coworkers in 2017 (Table 3.2).[47]

Table 3.1 *–Reaction optimizations for RCM reaction (Scheme 3.6)*[i].

Entry	catalyst	Solvent	Temp/ ºC	Additive	Yield
1	G-II	CH_2Cl_2	40 ºC	-	<35%
2	G-II	1,2-DCE	90 ºC	-	<30%
3	G-II	toluene	110 ºC	-	<10%
4	HG-II	CH_2Cl_2	40 ºC	-	<20%
5	HG-II	1,2-DCE	90 ºC	-	<20%
6	G-II	CH_2Cl_2	40 ºC	CH_2CH_2	42%
7	G-II	CH_2Cl_2	40 ºC	PBQ	45%
8	G-II	1,2-DCE	90 ºC	PBQ	47%
9	HG-II	CH_2Cl_2	40 ºC	PBQ	32%
10	G-II	CH_2Cl_2	40 ºC	CuI[48]	38%

Initial studies were carried out with styrene as the cross partner. Gratifyingly, we observed a significant improvement of yields for the combined CM/RCM step with styrene in the presence of HG-II catalyst and PBQ as an additive (Table 3.2, entries 3 and 4) in 1,2-dichloroethane (DCE, 0.1M for CM, 0.001M for RCM). The initial CM reaction was carried out at room temperature until all the starting material was consumed (TLC monitoring), and subsequently, the concentration was adjusted accordingly, and the RCM proceeded under refluxing condition for 18h until the reaction was complete. Furthermore,

[i] Relatively lower yields were observed for reactions carried out at more concentrated 0.01M concentration. The yields are reported in the table are for reactions carried out at 0.005M concentration.

the same CM/RCM reaction sequence was applied successfully with *cis*-3-hexene cross partner to deliver corresponding bicyclophosphate intermediate **3.7.2** in good yields (entry 6).

Table 3.2 *One-pot CM-RCM approach for C1–C10 1,3-anti-diol-containing subunit.*

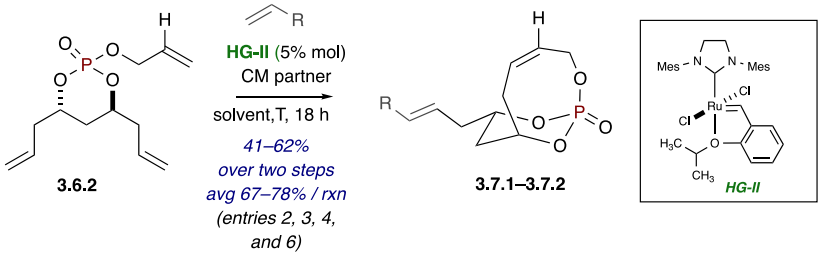

Entry	CM partner	Conditions.[b]	Additives	Y% [av./rxn%]
1	Styrene (10 Equiv.)	CH_2Cl_2 at 40 ºC, [0.01 M][a]	N/A	32%[c]
2	Styrene (5 Equiv.)	1,2-DCE at 90 ºC, [0.005 M][b]	N/A	45% (67%)
3	Styrene (5 Equiv.)	Conditions **B**	PBQ	62% (79%)
4	Styrene (2.5 Equiv.)	Conditions **B**	PBQ	63% (79%)
5	Styrene (1 Equiv.)	Conditions **B**	PBQ	<20%
6	cis-3-hexene	Conditions **B**	PBQ	60% (78%)

[a] Conditions **A**. CH_2Cl_2 at 40 ºC, [0.01 M]
[b] Conditions **B**. 1,2-DCE at 90ºC, [0.005 M].
[c] Rxn incomplete.

Next, crude bicyclo[5.3.1]phosphate intermediates **3.7.1** and **3.7.2** were subjected to a one-pot *per*-hydrogenation reaction in the presence of residual Ru catalyst using the

Louie/Grubbs conditions[49] that we have previously used in the group (Scheme 3.7).[50] Subsequent tether removal with LAH delivered the triol intermediates **3.7.3** and **3.7.4** in 75% and 74% average yields, over three steps for pentane sidechain and phenyl sidechain, respectively.

With triol fragments **3.7.3** and **3.7.4** in hand, the catalytic TEMPO-mediated oxidative cyclization was carried out in the presence of diacetoxyiodobenzene (DAIB) as the secondary oxidant. Subsequent, methylation of the C7 carbinol center was carried out with trimethyloxonium tetrafluroborate (Me_3OBF_4) and proton-sponge® to afford protected lactone methyl ethers **3.7.9** and **3.7.10** in good yields over a total of five steps.

Scheme 3.7 *Synthesis of protected lactone methyl ethers **3.7.9** and **3.7.10***

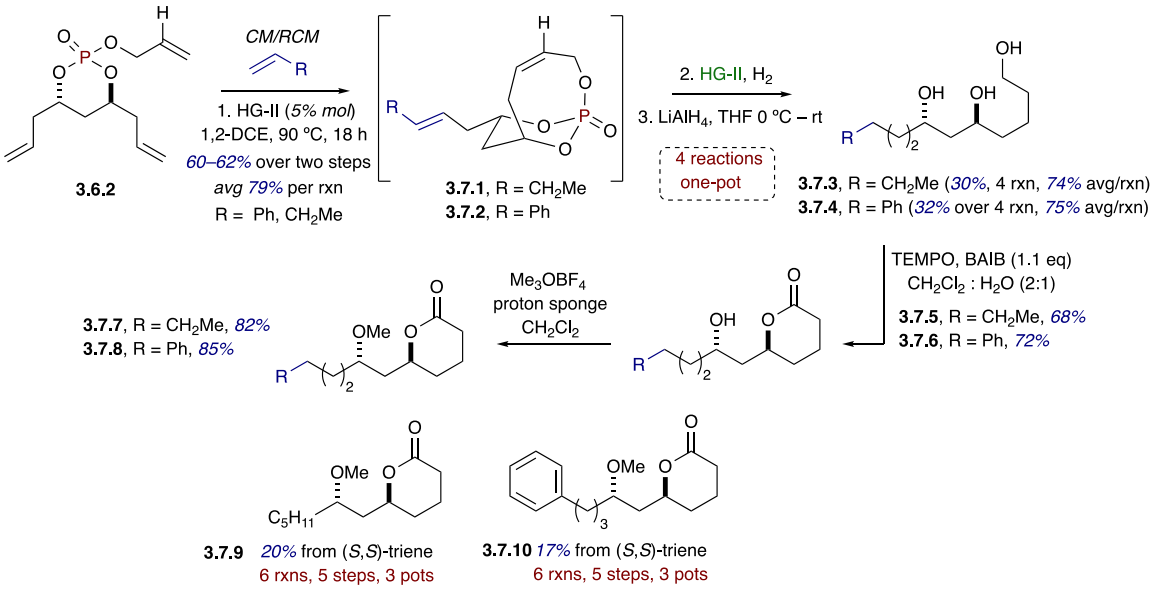

Next, the lactone methyl ether **3.7.9** was subjected to an $AlMe_3$-mediated lactone opening reaction (coupling-phase) with *N*-allylmethylamine to generate the allyl amide alcohol **3.8.1** in 46% yield as a mixture of amide 1:1 rotamers (Scheme 3.8 and Figure 3.5). A similar lactone opening reaction was carried out with *N*-(4-

(trifluoromethyl)benzyl)allylamine for the lactone methyl ether **3.7.9** to deliver the corresponding amide as a 2:1 mixture of rotamers in moderate yields (Figure 3.5).

Scheme 3.8 *Synthesis of dienes **3.8.4**, **3.8.5** and **3.8.8***

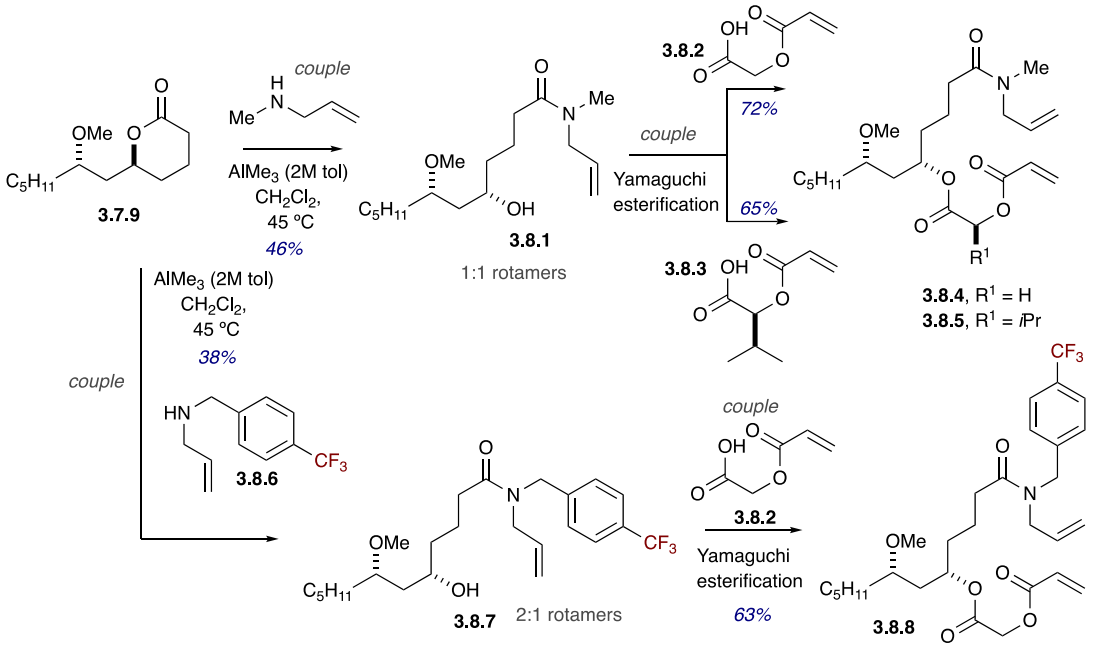

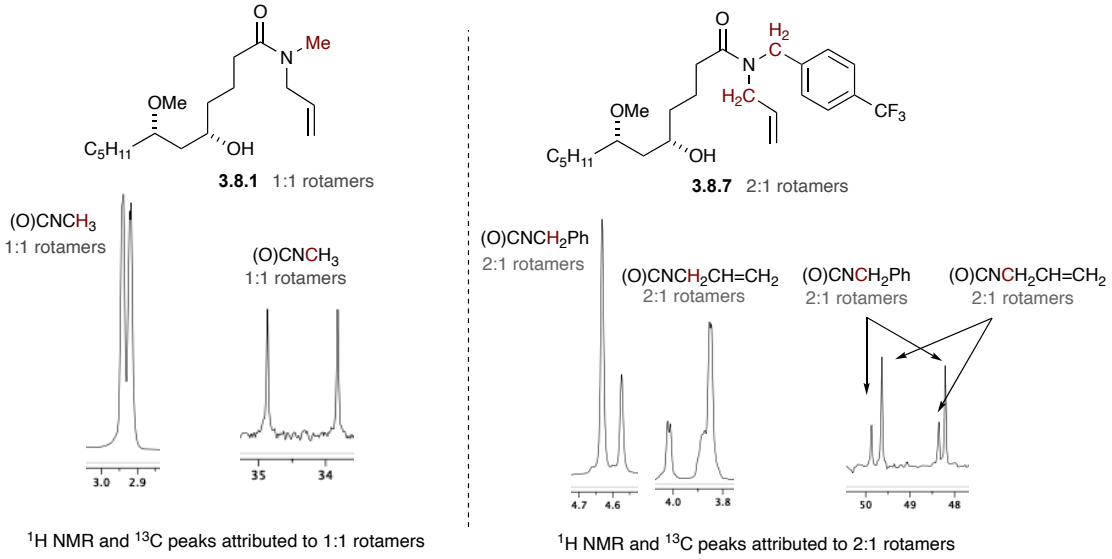

Figure 3.5 *^{1}H NMR resonances for rotamers*

After the key lactone opening reaction, the amide alcohol **3.8.1** was subjected to a Yamaguchi esterification reaction with two α,β-unsaturated alkenoic acids (coupling-phase), **3.8.2** and **3.8.3**, which were generated via an acryloylation reaction in one step, from commercially available 2-hydroxy-isovaleric acid and glycolic acid, respectively following the method reported by Brimble.[44] Esterification of the alkenoic acid derivatives and the secondary alcohol was performed smoothly in good to moderate yields via 2,4,6-trichlorobenzoyl mixed anhydride intermediates.[43,51]Following the same reaction conditions, the amide alcohol with *N*-(4-(trifluoromethyl)benzyl) moiety was coupled with **3.8.2** to generate the diene precursor **3.8.8**.

Scheme 3.9 *Synthesis of dienes **3.9.2** and **3.9.3***

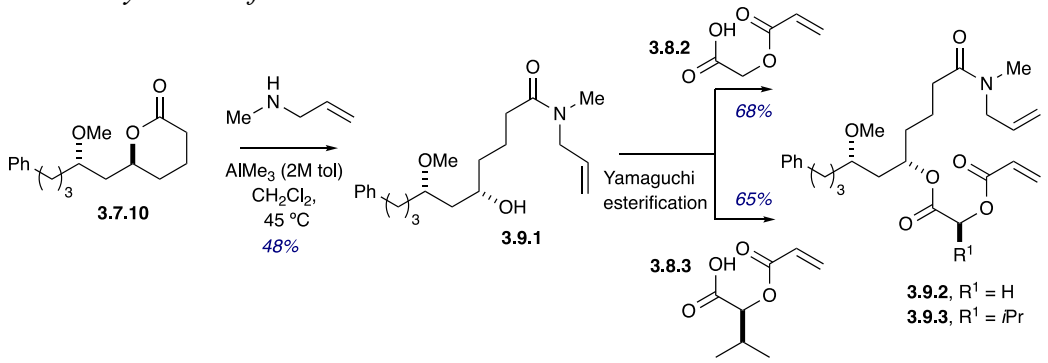

Next, the lactone methyl ether containing aromatic sidechain **3.7.10** was subjected to Lewis acid-mediated lactone opening with *N*-allylmethylamine to deliver the amide alcohol **3.9.1** in good yields (Scheme 3.9). Subsequent Yamaguchi esterification with two alkenoic acids **3.8.2** and **3.8.3** furnished the two diene precursors **3.9.2** and **3.9.3** in moderate yields. Collectively, five diene precursors **3.8.4**, **3.8.5**, **3.8.8**, **3.9.2**, and **3.9.3** were generated.

With these dienes in hand, the pairing step was carried out using an RCM macrocyclization, with the Grubbs **G-II** catalyst in refluxing $CHCl_3$ for 18 hours, to afford the final natural product-like α,β-unsaturated macrolide analogs with exclusive Z-configured olefins (Scheme 3.10). Remarkably, selective *Z*-olefination was observed for the generated 2-*des*-methyl macrocyclic analogs of sanctolide A, contrary to the *E/Z* mixtures observed for the actual natural product with a 2-methyl center.

Scheme 3.10 *Synthesis of macrocyclic lactones (pairing phase)*

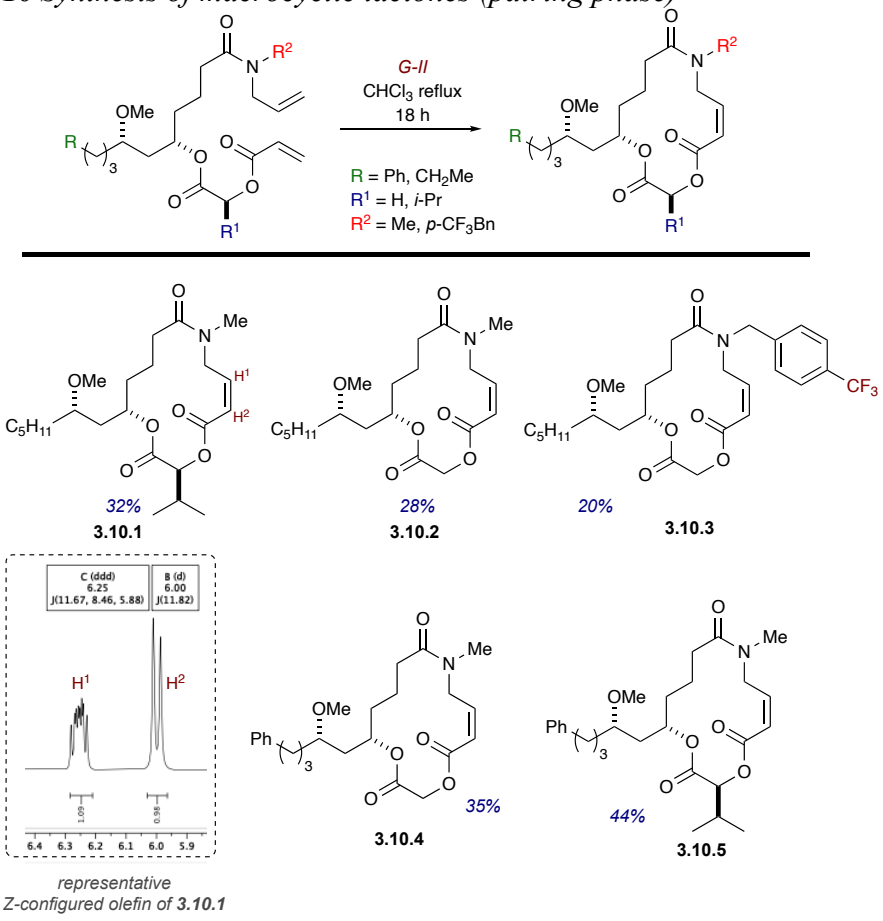

Finally, olefin isomerization with $(PPh_3)_3RuH(CO)Cl$[52] was carried out for compounds **3.10.2** and **3.10.1** to generate enamide macrolides using the conditions reported

by Brimble and coworkers (Scheme 3.11).[44] Even though the isomerization proceeded smoothly, rapid decomposition was observed during purification on silica. Crude NMR and mass spectrometry data were used to confirm the identity of the compound. Full characterization and NMR assignments were difficult due to insufficient material of enamide macrolides.

Scheme 3.11 *Olefin isomerization of **3.10.2** and **3.10.1***

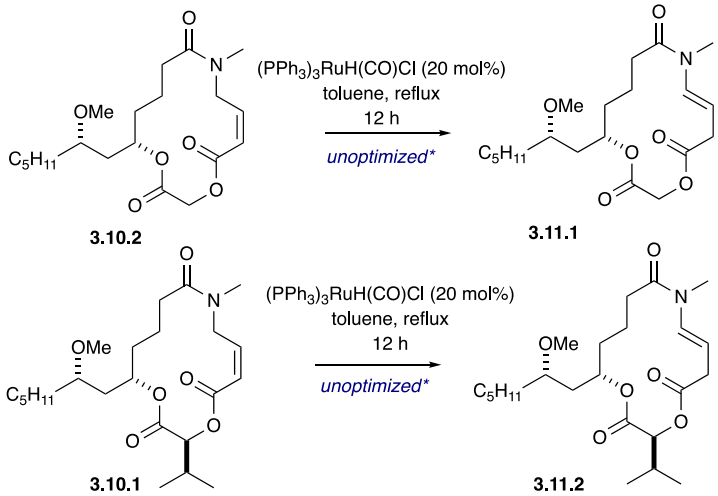

* Full reaction conversion (TLC)
However, full characterization was difficult due to decompostion of material
Mass and crude ^{1}HNMR data are available.

3.3 Conclusion and future directions

In conclusion, a BCCP-DOS strategy coupled with phosphate tether-mediated one-pot sequential protocols are reported for the synthesis of simplified, *des*-methyl sanctolide A natural product analogs. A one-pot, RCM/CM/hydrogenation/tether-removal protocol was utilized as key steps during the build-phase. Subsequent coupling steps and the final RCM pairing step delivered five stable macrocyclic analogs. Attempts towards the conversion of enamide macrolides were unsuccessful due to low stability. Biological

evaluation and ^{19}F-NMR assisted *in vitro* reactivity profiling studies of synthesized macrocyclic analogs will be carried out and reported in due course.

3.4 References cited

[1] (a)Newman, D.; Cragg, G. Natural Products, Derivatives and Mimics as Antitumour Agents. *Spec. Publ. - R. Soc. Chem.* **2011**, *320*, 3–36. (b) Lomenick, B.; Olsen, R. W.; Huang, J. Identification of direct protein targets of small molecules. *ACS chemical biology* **2011**, *6*, 34-46. (c) Newman, D. J.; Cragg, G. M. Natural Products as Sources of New Drugs from 1981 to 2014. *J. Nat. Prod.* **2016**, *79*, 629–661. (d) Fernandes, P.; Martens, E.; Pereira, D. Nature nurtures the design of new semi-synthetic macrolide antibiotics. *The Journal of antibiotics* **2017**, *70*, 527–533.

[2] Solinski, A. E.; Koval, A. B.; Brzozowski, R. S.; Morrison, K. R.; Fraboni, A. J.; Carson, C. E.; Eshraghi, A. R.; Zhou, G.; Quivey, R. G.; Voelz, V. A.; Buttaro, B. A.; Wuest, W. M. Diverted Total Synthesis of Carolacton-Inspired Analogs Yields Three Distinct Phenotypes in Streptococcus mutans Biofilms. *J. Am. Chem. Soc.* **2017**, *139*, 7188–7191.

[3] Newman, D. J.; Cragg, G. M. Natural Products As Sources of New Drugs over the 30 Years from 1981 to 2010. *J. Nat. Prod.* **2012**, *75*, 311–335.

[4] (a) Nandy, J. P.; Prakesch, M.; Khadem, S.; Reddy, P. T.; Sharma, U.; Arya, P. Advances in solution-and solid-phase synthesis toward the generation of natural product-like libraries. *Chem. Rev.* **2009**, *109*, 1999–2060. (b) Maier, M. E. Design and synthesis of analogues of natural products. *Org. Biomol. Chem.***2015**, *13*, 5302–5343

[5] Saldívar-González, F.I.; Pilón-Jiménez, B.A.; Medina-Franco, J.L. Chemical space of naturally occurring compounds. *Phys. Sci. Rev*. **2018**, 1–14.

[6] (a) Gehrtz, P.; London, N. Electrophilic Natural Products as Drug Discovery Tools. *Trends Pharmacol. Sci.* **2021**, *42*, 434–447. (b) Huang, M.; Lu, J.-J.; Ding, J. Natural products in cancer therapy: Past, present and future. *Nat. prod* **2021**, 1–9. (

[7] (a) Szychowski, J.; Truchon, J.-F.; Bennani, Y. L. Natural products in medicine: transformational outcome of synthetic chemistry. *J. Med. Chem.* **2014**, *57*, 9292–9308. (b) Nicolaou, K. The chemistry-biology-medicine continuum and the drug discovery and development process in academia. *Chem. Biol.* **2014**, *21*, 1039–1045. (c) Bathula, S. R.; Akondi, S. M.; Mainkar, P. S.; Chandrasekhar, S. "Pruning of biomolecules and natural products (PBNP)": an innovative paradigm in drug discovery. *Org. Biomol. Chem.* **2015**, *13*, 6432–6448. (d) Thaker, M. N.; Wright, G. D. Opportunities for synthetic biology in antibiotics: expanding glycopeptide chemical diversity. *ACS Synth. Biol.* **2015**, *4*, 195–206. (e) Stockdale, T. P.; Williams, C. M. Pharmaceuticals that contain polycyclic hydrocarbon scaffolds. *Chem. Soc. Rev.* **2015**, *44*, 7737–7763. (f) Yoganathan, S.; Miller, S. J. Structure diversification of vancomycin through peptide-catalyzed, site-selective lipidation: a catalysis-based approach to combat glycopeptide-resistant pathogens. *J. Med. Chem.* **2015**, *58*, 2367–2377. (g) Toneto Novaes, L. F.; Martins Avila, C.; Pelizzaro-Rocha, K. J.; Vendramini-Costa, D. B.; Pereira Dias, M.; Barbosa Trivella, D. B.; Ernesto de Carvalho, J.; Ferreira-Halder, C. V.; Pilli, R. A. (−)-Tarchonanthuslactone: Design of New Analogues, Evaluation of their Antiproliferative Activity on Cancer Cell Lines, and Preliminary Mechanistic Studies. *ChemMedChem* **2015**, *10*, 1687–1699. (h) Oguri, H. Biomimetic Assembly Lines Producing Natural Product Analogs: Strategies from a Versatile Manifold to Skeletally Diverse Scaffolds. *Chem. Rec.* **2016**, *16*, 652–666. (i) Barnes, E. C.; Kumar, R.; Davis, R. A. The use of isolated natural products as scaffolds for the generation of chemically diverse screening libraries for drug discovery. *Nat. Prod. Rep.* **2016**, *33*, 372-381. (j) Brzozowski, R. S.; Wuest, W. M. Twelve-membered macrolactones: privileged scaffolds for the development of new therapeutics. *Chem. Biol. Drug Disc.* **2017**, *89*, 169–191. (k) Itoh, H.; Inoue, M. Comprehensive Structure–Activity Relationship Studies of Macrocyclic Natural Products Enabled by Their Total Syntheses. *Chem. Rev.* **2019**, *119*, 10002–10031. (l) Majhi, S.; Das, D. Chemical derivatization of natural products: semisynthesis

and pharmacological aspects-A decade update. *Tetrahedron* **2020**, 131801–131822 (m) Verma, S.; Pathak, R. K., Chapter 16 - Discovery and optimization of lead molecules in drug designing. In *Bioinformatics*, Singh, D. B.; Pathak, R. K., Eds. Academic Press, **2022**; pp 253–267.

[8] Alihodžić, S.; Bukvić, M.; Elenkov, I. J.; Hutinec, A.; Koštrun, S.; Pešić, D.; Saxty, G.; Tomašković, L.; Žiher, D. Current trends in macrocyclic drug discovery and beyond-Ro5. *Prog. Med. Chem.* **2018**, *57*, 113–233.

[9] Gade, N. R.; Iqbal, J. Natural Product Inspired Topology Directed Synthesis of Hybrid Macrocyclic Compounds: A Simple Approach to Natural Product Analogues. *ChemistrySelect* **2018**, *3*, 6262–6266.

[10] (a)Tsuda, M.; Endo, T.; Kobayashi, J. i. Amphidinolide T, novel 19-membered macrolide from marine dinoflagellate Amphidinium sp. *J. Org. Chem.* **2000**, *65*, 1349–1352. (b) Kubota, T.; Endo, T.; Tsuda, M.; Shiro, M.; Kobayashi, J. i. Amphidinolide T5, a new 19-membered macrolide from a dinoflagellate and X-ray structure of amphidinolide T1. *Tetrahedron* **2001**, *57*, 6175–6179. (c) Kobayashi, J. i.; Kubota, T.; Endo, T.; Tsuda, M. Amphidinolides T2, T3, and T4, new 19-membered macrolides from the dinoflagellate Amphidinium sp. and the biosynthesis of amphidinolide T1. *J. Org. Chem.* **2001**, *66*, 134–142. (d) Kobayashi, J. i.; Kubota, T.; Endo, T.; Tsuda, M. Amphidinolides T2, T3, and T4, new 19-membered macrolides from the dinoflagellate Amphidinium sp. and the biosynthesis of amphidinolide T1. *J. Org. Chem.* **2001**, *66*, 134–142.

[11] Nakae, K.; Yoshimoto, Y.; Sawa, T.; Homma, Y.; Hamada, M.; TAKEUCH, T.; Imoto, M. Migrastatin, a new inhibitor of tumor cell migration from Streptomyces sp. MK929-43F1 taxonomy, fermentation, isolation and biological activities. *J. Antibiot.* **2000**, *53*, 1130–1136. (b) Nakae, K.; Yoshimoto, Y.; Ueda, M.; Sawa, T.; Takahashi, Y.; Naganawa, H.; Takeuchi, T.; Imoto, M. Migrastatin, a novel 14-membered lactone from Streptomyces sp. MK929-43F1. *J. Antibiot.* **2000**, *53*, 1228–1230. (c) Takemoto, Y.; Nakae, K.; Kawatani, M.; Takahashi, Y.; Naganawa,

H.; Imoto, M. Migrastatin, a novel 14-membered ring macrolide, inhibits anchorage-independent growth of human small cell lung carcinoma Ms-1 cells. *J. Antibiot.* **2001**, *54*, 1104–1107.

[12] (a) Iwasaki, S.; Kobayashi, H.; Furukawa, J.; Namikoshi, M.; Okuda, S.; Sato, Z.; Matsuda, I.; Noda, T. Studies on Macrocyclic Lactone Antibiotics. Vii Structure of aPhytotoxin. *J. Antibiot.* **1984**, *37*, 354–362. (b) Iwasaki, S.; Namikoshi, M.; Kobayashi, H.; Furukawa, J.; Okuda, S.; Itai, A.; Kasuya, A.; Iitaka, Y.; Sato, Z. Studies on Macrocyclic Lactone Antibiotics Viii. Absolute Structures of Rhizoxin And A Related Compound. *J. Antibiot.* **1986**, *39*, 424–429. (c) Iwasaki, S.; Namikoshi, M.; Kobayashi, H.; Furukawa, J.; Okuda, S. Studies on macrocyclic lactone antibiotics. IX: Novel macrolides from the fungus Rhizopus chinensis: Precursors of rhizoxin. *Chem. Pharm. Bull.* **1986**, *34*, 1387–1390.

[13] Kobayashi, J. i.; Kubota, T.; Endo, T.; Tsuda, M. Amphidinolides T2, T3, and T4, new 19-membered macrolides from the dinoflagellate Amphidinium sp. and the biosynthesis of amphidinolide T1. *J. Org. Chem.* **2001**, *66*, 134–142.

[14] Nakae, K.; Nishimura, Y.; Ohba, S.; Akamatsu, Y. Migrastatin acts as a muscarinic acetylcholine receptor antagonist. *The Journal of antibiotics* **2006**, *59*, 685–692.

[15] Sasmal, P. K.; Abbineni, C.; Iqbal, J.; Mukkanti, K. Stereoselective synthesis of an advanced seco ester intermediate as a precursor toward the synthesis of amphidinolides T1, T3, and T4. *Tetrahedron* **2010**, *66*, 5000–5007.

[16] Gade, N. R.; Iqbal, J. A Common Synthetic Protocol for the Cyclic and Acyclic Core of Migrastatin, Isomigrastatin, and Dorrigocin via a Chiral β-Hydroxy-γ-butyrolactone Intermediate. *Eur. J. Org. Chem.* **2014**, *2014*, 6558–6564.

[17] Padakanti, S.; Pal, M.; Mukkanti, K.; Iqbal, J. Stereoselective synthesis of the C1–C10 fragment of rhizoxin D. *Tetrahedron Lett.* **2006**, *47*, 5969–5971.

[18] Wosniok, P. R.; Knopf, C.; Dreisigacker, S.; Orozco-Rodriguez, J. M.; Hinkelmann, B.; Mueller, P. P.; Brönstrup, M.; Menche, D. SAR Studies of the

Leupyrrins: Design and Total Synthesis of Highly Potent Simplified Leupylogs. *Chem. Eur. J.* **2020**, *26*, 15074–15078.

[19] (b) Bode, H. B.; Irschik, H.; Wenzel, S. C.; Reichenbach, H.; Müller, R.; Höfle, G. The Leupyrrins: A Structurally Unique Family of Secondary Metabolites from the Myxobacterium Sorangium c ellulosum[#]. *J. Nat. Prod.* **2003**, *66*, 1203–1206. (b) Martinez, J. P.; Hinkelmann, B.; Fleta-Soriano, E.; Steinmetz, H.; Jansen, R.; Diez, J.; Frank, R.; Sasse, F.; Meyerhans, A. Identification of myxobacteria-derived HIV inhibitors by a high-throughput two-step infectivity assay. *Microb. Cell Fact.* **2013**, *12*, 1–9.

[20] Shiina, I.; Kubota, M.; Oshiumi, H.; Hashizume, M. An effective use of benzoic anhydride and its derivatives for the synthesis of carboxylic esters and lactones: A powerful and convenient mixed anhydride method promoted by basic catalysts. *J. Org. Chem.* **2004**, *69*, 1822–1830.

[21] Herkommer, D.; Thiede, S.; Wosniok, P. R.; Dreisigacker, S.; Tian, M.; Debnar, T.; Irschik, H.; Menche, D. Stereochemical Determination of the Leupyrrins and Total Synthesis of Leupyrrin A1. *J. Am. Chem. Soc.* **2015**, *137*, 4086–4089.

[22] Abdelmoty, I.; Albericio, F.; Carpino, L. A.; Foxman, B. M.; Kates, S. A. Structural studies of reagents for peptide bond formation: crystal and molecular structures of HBTU and HATU. *Lett. Pept. Sci.* **1994**, *1*, 57–67.

[23] (a) Kidd, S. L.; Osberger, T. J.; Mateu, N.; Sore, H. F.; Spring, D. R. Recent applications of diversity-oriented synthesis toward novel, 3-dimensional fragment collections. *Front. Chem.* **2018**, *6*, 460–468. (b) Truax, N. J.; Romo, D. Bridging the gap between natural product synthesis and drug discovery. *Nat. Prod. Rep.* **2020**, *37*, 1436–1453. (c) Temml, V.; Kutil, Z. Structure-based molecular modeling in SAR analysis and lead optimization. *Comput. Struct. Biotechnol. J.* **2021**, *19*, 1431–1444.

[24] (a) Cravatt, B. F.; Wright, A. T.; Kozarich, J. W. Activity-based protein profiling: from enzyme chemistry to proteomic chemistry. *Annu. Rev. Biochem.* **2008**, *77*,

383–414. (b) Speers, A. E.; Cravatt, B. F. Activity-based protein profiling (ABPP) and click chemistry (CC)–ABPP by MudPIT mass spectrometry. *Curr. protoc. chem. biol.* **2009**, *1*, 29–41. (c) Krysiak, J.; Breinbauer, R. Activity-based protein profiling for natural product target discovery. *Activity-Based Protein Profiling* **2011**, 43–84. (d) Lee, J. S.; Lee, J. W.; Kang, N.; Ha, H. H.; Chang, Y. T. Diversity-Oriented Approach for Chemical Biology. *Chem. Rec.* **2015**, *15*, 495–510. (e) Deng, H.; Lei, Q.; Wu, Y.; He, Y.; Li, W. Activity-based protein profiling: Recent advances in medicinal chemistry. *Eur. J. Med. Chem.* **2020**, *191*, 112151–112171.

[25] (a) Galloway, W. R.; Isidro-Llobet, A.; Spring, D. R. Diversity-oriented synthesis as a tool for the discovery of novel biologically active small molecules. *Nature communications* **2010**, *1*, 1–13. (b) Schreiber, S. L.; Kotz, J. D.; Li, M.; Aubé, J.; Austin, C. P.; Reed, J. C.; Rosen, H.; White, E. L.; Sklar, L. A.; Lindsley, C. W. Advancing biological understanding and therapeutics discovery with small-molecule probes. *Cell* **2015**, *161*, 1252–1265. (c) Gerry, C. J.; Schreiber, S. L. Recent achievements and current trajectories of diversity-oriented synthesis. *Curr. Opin. Chem. Biol.* **2020**, *56*, 1–9.

[26] Collins, S.; Bartlett, S.; Nie, F.; Sore, H. F.; Spring, D. R. Diversity-oriented synthesis of macrocycle libraries for drug discovery and chemical biology. *Synthesis* **2016**, *48*, 1457–1473.

[27] (a) Thomas, G. L.; Spandl, R. J.; Glansdorp, F. G.; Welch, M.; Bender, A.; Cockfield, J.; Lindsay, J. A.; Bryant, C.; Brown, D. F.; Loiseleur, O. Anti-MRSA agent discovery using diversity-oriented synthesis. *Angew. Chem. Int. Ed.* **2008**, *47*, 2808-2812. (b) Heidebrecht Jr, R. W.; Mulrooney, C.; Austin, C. P.; Barker Jr, R. H.; Beaudoin, J. A.; Cheng, K. C.-C.; Comer, E.; Dandapani, S.; Dick, J.; Duvall, J. R. Diversity-oriented synthesis yields a novel lead for the treatment of malaria. *ACS medicinal chemistry letters* **2012**, *3*, 112–117. (c) Ibbeson, B. M.; Laraia, L.; Alza, E.; O'Connor, C. J.; Tan, Y. S.; Davies, H. M.; McKenzie, G.; Venkitaraman, A. R.; Spring, D. R. Diversity-oriented synthesis as a tool for identifying new modulators of mitosis. *Nat. Commun.* **2014**, *5*, 1–8. (d) Mateu, N.; Kidd, S. L.;

Osberger, T. J.; Stewart, H. L.; Bartlett, S.; Galloway, W. R. J. D.; North, A. J. P.; Sore, H. F.; Spring, D. R., Chapter 2 The Application of Diversity-oriented Synthesis in Chemical Biology. In *Chemical and Biological Synthesis: Enabling Approaches for Understanding Biology*, The Royal Society of Chemistry**2018**; pp 8–44.

[28] For recent reviews on the value of chemical libraries, see: (a) Laraia, L.; Robke, L.; Waldmann, H. Bioactive compound collections: From design to target identification. *Chem* **2018**, *4*, 705–730. (b) Karageorgis, G.; Foley, D. J.; Laraia, L.; Waldmann, H. Principle and design of pseudo-natural products. *Nature chemistry* **2020**, *12*, 227-235. (c) Whitmarsh-Everiss, T.; Laraia, L. Small molecule probes for targeting autophagy. *Nat. Chem. Biol* **2021**, *17*, 653–664.

[29] (a) Nielsen, T. E.; Schreiber, S. L. Towards the optimal screening collection: a synthesis strategy. *Angew. Chem. Int. Ed.* **2008**, *47*, 48–56. (b) Uchida, T.; Rodriquez, M.; Schreiber, S. L. Skeletally diverse small molecules using a build/couple/pair strategy. *Org. Lett.* **2009**, *11*, 1559–1562. (c) Marcaurelle, L. A.; Comer, E.; Dandapani, S.; Duvall, J. R.; Gerard, B.; Kesavan, S.; Lee IV, M. D.; Liu, H.; Lowe, J. T.; Marie, J.-C. An aldol-based build/couple/pair strategy for the synthesis of medium-and large-sized rings: discovery of macrocyclic histone deacetylase inhibitors. *J. Am. Chem. Soc.* **2010**, *132*, 16962–16976. (c) Fitzgerald, M. E.; Mulrooney, C. A.; Duvall, J. R.; Wei, J.; Suh, B.-C.; Akella, L. B.; Vrcic, A.; Marcaurelle, L. A. Build/couple/pair strategy for the synthesis of stereochemically diverse macrolactams via head-to-tail cyclization. *Image result for ACS combinatorial science abbreviation ACS Comb. Sci.* **2012**, *14*, 89–96. (d) Srinivasulu, V.; Sieburth, S. M.; El-Awady, R.; Kariem, N. M.; Tarazi, H.; O'Connor, M. J.; Al-Tel, T. H. Post-Ugi cascade transformations for accessing diverse chromenopyrrole collections. *Org. Lett.* **2018**, *20*, 836–839.

[30] (a) Kopp, F.; Stratton, C. F.; Akella, L. B.; Tan, D. S. A diversity-oriented synthesis approach to macrocycles via oxidative ring expansion. *Nat. Chem. Biol* **2012**, *8*, 358–365. (b) Bauer, R. A.; Wenderski, T. A.; Tan, D. S. Biomimetic diversity-

oriented synthesis of benzannulated medium rings via ring expansion. *Nat. Chem. Biol* **2013**, *9*, 21–29. (c) Guney, T.; Wenderski, T. A.; Boudreau, M. W.; Tan, D. S. Synthesis of Benzannulated Medium-ring Lactams via a Tandem Oxidative Dearomatization-Ring Expansion Reaction. *Chemistry* **2018**, *24*, 13150–13157. (d) Stephens, T. C.; Lawer, A.; Thomas French, D.; Unsworth, W. P. Iterative assembly of macrocyclic lactones using successive ring expansion reactions. *Chemistry* **2018**, *24*, 13947–13953.

[31] (a) Comer, E.; Liu, H.; Joliton, A.; Clabaut, A.; Johnson, C.; Akella, L. B.; Marcaurelle, L. A. Fragment-based domain shuffling approach for the synthesis of pyran-based macrocycles. *Proc. Nat. Acad. Sci.* **2011**, *108*, 6751–6756.

[32] (a) O'Connell, K. M.; Beckmann, H. S.; Laraia, L.; Horsley, H. T.; Bender, A.; Venkitaraman, A. R.; Spring, D. R. A two-directional strategy for the diversity-oriented synthesis of macrocyclic scaffolds. *Org. Biomol.* **2012**, *10*, 7545–7551. (b) O'Connell, K. M.; Díaz-Gavilán, M.; Galloway, W. R.; Spring, D. R. Two-directional synthesis as a tool for diversity-oriented synthesis: Synthesis of alkaloid scaffolds. *Beilstein J. Org. Chem.* **2012**, *8*, 850–860.

[33] (a) Beckmann, H. S.; Nie, F.; Hagerman, C. E.; Johansson, H.; Tan, Y. S.; Wilcke, D.; Spring, D. R. A strategy for the diversity-oriented synthesis of macrocyclic scaffolds using multidimensional coupling. *Nat. Chem* **2013**, *5*, 861–867. (b) Nie, F.; Kunciw, D. L.; Wilcke, D.; Stokes, J. E.; Galloway, W. R.; Bartlett, S.; Sore, H. F.; Spring, D. R. A multidimensional diversity-oriented synthesis strategy for structurally diverse and complex macrocycles. *Angew. Chem. Int. Ed.* **2016**, *55*, 11139–11143.

[34] (a) O'Connor, C. J.; Beckmann, H. S.; Spring, D. R. Diversity-oriented synthesis: producing chemical tools for dissecting biology. *Chem. Soc. Rev.* **2012**, *41*, 4444–4456. (b) Gerry, C. J.; Schreiber, S. L. Chemical probes and drug leads from advances in synthetic planning and methodology. *Nat. Rev. Drug Discov.* **2018**, *17*, 333–352. (c) Kharchenko, S. H.; Iampolska, A. D.; Radchenko, D. S.; Vashchenko,

B. V.; Voitenko, Z. V.; Grygorenko, O. O. A diversity-oriented approach to large libraries of artificial macrocycles. *Eur. J. Org. Chem.* **2021**, *2021*, 2313–2330. (d) Clarke, A. K.; Unsworth, W. P. A happy medium: the synthesis of medicinally important medium-sized rings via ring expansion. *Chem. Sci.* **2020**, *11*, 2876–2881.

[35] Schreiber, S. L. Target-oriented and diversity-oriented organic synthesis in drug discovery. *Science* **2000**, *287*, 1964–1969.

[36] (a) Grimwood, M. E.; Hansen, H. C. Synthesis of Macrocyclic Scaffolds Suitable for Diversity-Oriented Synthesis of Macrolides. *Tetrahedron* **2009**, *65*, 8132−8138. (b) Heckrodt, T. J.; Singh, R. General Route for the Preparation of Diverse 17-Membered Macrocycles Based on RCM and Examination of the E/Z Selectivity. *Synth. Commun*. **2012**, *42*, 2854−2865. (c) Grossmann, A.; Bartlett, S.; Janecek, M.; Hodgkinson, J. T.; Spring, D. R. Diversity-Oriented Synthesis of Drug-Like Macrocyclic Scaffolds Using an Orthogonal Organo- and Metal Catalysis Strategy. *Angew. Chem., Int. Ed*. **2014**, *53*, 13093−13097. (d) Kotha, S.; Meshram, M.; Dommaraju, Y. Design and Synthesis of Polycycles, Heterocycles, and Macrocycles via Strategic Utilization of Ring-Closing Metathesis. *Chem. Rec.* **2018**, *18*, 1613–1632. (e) Mandal, T.; Dash, J. Ring closing metathesis for the construction of carbazole and indole-fused natural products. *Org. Biomol. Chem* **2021**, *19*, 9797–9808.

[37] Bahulayan, D.; Arun, S. An Easy Two Step Synthesis of Macrocyclic Peptidotriazoles via a Four-Component Reaction and Copper Catalyzed Intramolecular Azide-Alkyne [3 + 2] Click Cycloaddition. *Tetrahedron Lett.* **2012**, *53*, 2850−2855. (b) Raj, P. J.; Bahulayan, D. An efficient click-multicomponent strategy for the diversity oriented synthesis of 15–18 membered macrocyclic peptidomimetic fluorophores. *Tetrahedron Lett.* **2015**, *56*, 2451–2455.

[38] For reviews, see : (a) Thirumurugan, P.; Matosiuk, D.; Jozwiak, K. Click chemistry for drug development and diverse chemical–biology applications. *Chem. Rev.* **2013**, *113*, 4905–4979. (b) Singh, M. S.; Chowdhury, S.; Koley, S. Advances of

azide-alkyne cycloaddition-click chemistry over the recent decade. *Tetrahedron* **2016**, *72*, 5257–5283.

[39] (a) Dong, X.; Wang, Q.; Zhang, Q.; Xu, S.; Wang, Z. Construction of Dihydropyran-Bridged Macrocycles by Inverse-Electron-Demand Diels-Alder Reaction. *Tetrahedron* **2013**, *69*, 11144−11154. (b) Krieger, J.-P.; Ricci, G.; Lesuisse, D.; Meyer, C.; Cossy, J. Efficient and Modular Synthesis of New Structurally Diverse Functionalized [n]Paracyclophanes by a Ring-Distortion Strategy. *Angew. Chem.,Int. Ed*. **2014**, *53*, 8705−8708. (c)

[40] (a) Zapf, C. W.; Bloom, J. D.; McBean, J. L.; Dushin, R. G.; Nittoli, T.; Ingalls, C.; Sutherland, A. G.; Sonye, J. P.; Eid, C. N.; Golas, J.; et al.Design and SAR of Macrocyclic Hsp90 Inhibitors with Increased Metabolic Stability and Potent Cell-Proliferation Activity. Bioorg. Med.Chem. Lett. 2011, 21, 2278−2282. (b) Zapf, C. W.; Bloom, J. D.; McBean, J. L.; Dushin, R. G.; Nittoli, T.; Otteng, M.; Ingalls, C.; Golas, J. M.; Liu, H.; Lucas, J.; et al. Macrocyclic Lactams as Potent Hsp90 Inhibitors with Excellent Tumor Exposure and Extended Biomarker Activity. Bioorg. Med. Chem. Lett. 2011, 21, 3411−3416. (c) Zapf, C. W.; Bloom, J. D.; McBean, J. L.; Dushin, R. G.; Golas, J. M.; Liu, H.; Lucas, J.; Boschelli, F.; Vogan, E.; Levin, J. I. Discovery of a Macrocyclic O-Aminobenzamide Hsp90 Inhibitor with Heterocyclic Tether That Shows Extended Biomarker Activity and in Vivo Efficacy in a Mouse Xenograft Model. Bioorg. Med. Chem. Lett. 2011, 21, 3627−3631. (c) Zapf, C. W.; Bloom, J. D.; Li, Z.; Dushin, R. G.; Nittoli, T.; Otteng, M.; Nikitenko, A.; Golas, J. M.; Liu, H.; Lucas, J.; et al. Discovery of a Stable Macrocyclic O-Aminobenzamide Hsp90 Inhibitor Which Significantly Decreases Tumor Volume in a Mouse Xenograft Model. Bioorg. Med. Chem. Lett. 2011, 21, 4602−4607.

[41] Mortensen, K. T.; Osberger, T. J.; King, T. A.; Sore, H. F.; Spring, D. R. Strategies for the diversity-oriented synthesis of macrocycles. *Chem. Rev.* **2019**, *119*, 10288–10317.

[42] Kang, H. S; Krunic, A.; Orjala, J. Sanctolide A, a 14-Membered PK-NRP Hybrid Macrolide from the Cultured Cyanobacterium *Oscillatoria sancta* (SAG 74.79). *Tetrahedron Lett.* **2012**, *53*, 3563–3567.

[43] Yadav, J. S.; Suresh, B.; Srihari, P. Stereoselective total synthesis of the marine macrolide sanctolide A. *Eur. J. Org. Chem.* **2015**, *2015*, 5856–5863.

[44] Wadsworth, A. D.; Furkert, D. P.; Brimble, M. A. Total Synthesis of the Macrocyclic N-Methyl Enamides Palmyrolide A and 2 S-Sanctolide A. *J. Org. Chem.* **2014**, *79*, 11179–11193.

[45] Basha, A.; Lipton, M.; Weinreb, S. M. A mild, general method for conversion of esters to amides. *Tetrahedron Lett.* **1977**, *18*, 4171–4172.

[46] (a) Mori, M.; Sakakibara, N.; Kinoshita, A. Remarkable effect of ethylene gas in the intramolecular enyne metathesis of terminal alkynes. *J. Org. Chem.* **1998**, *63*, 6082–6083. (b) McReynolds, M. D.; Dougherty, J. M.; Hanson, P. R. Synthesis of Phosphorus and Sulfur Heterocycles via Ring-Closing Olefin Metathesis. *Chem. Rev.* **2004**, *104*, 2239–2258. (c) Conrad, J. C.; Fogg, D. E. Ruthenium-catalyzed ring-closing metathesis: recent advances, limitations and opportunities. *Curr. Org. Chem.* **2006**, *10*, 185–202.

[47] Merad, J.; Borkar, P.; Caijo, F.; Pons, J.-M.; Parrain, J.-L.; Chuzel, O.; Bressy, C. Double Catalytic Kinetic Resolution (DoCKR) of Acyclic anti-1,3-Diols: The Additive Horeau Amplification. *Angew. Chem., Int. Ed.* **2017**, *56*, 16052–16056.

[48] K. Voigtritter, S. Ghorai, and B. H. Lipshutz, "Rate enhanced olefin cross-metathesis reactions: the copper iodide effect," *J. Org. Chem.* **2011**, *76*, 4697–4702.

[49] Louie, J.; Bielawski, C. W.; Grubbs, R. H. Tandem Catalysis: The Sequential Mediation of Olefin Metathesis, Hydrogenation, and Hydrogen Transfer with Single-Component Ru Complexes. *J. Am. Chem. Soc.*, **2001**, *123*, pp 11312–11313.

[50] (a) Whitehead, A.; McReynolds, M. D.; Moore, J. D.; Hanson, P. R. Multivalent Activation in Phosphate Tethers: A New Tether for Small Molecule Synthesis. *Org. Lett.* **2005**, *7*, 3375–3378. (b) Markley, J. L. *P*-Stereogenic, Bicyclic Phosphorus Heterocycles and Temporary Tether Strategies for the Synthesis of Complex Polyols**.** Ph.D. Thesis, University of Kansas, Lawrence, KS,

[51] Müller, J.; Feifel, S. C.; Schmiederer, T.; Zocher, R.; Süssmuth, R. D. In vitro Synthesis of New Cyclodepsipeptides of the PF1022-Type: Probing the α-D-Hydroxy Acid Tolerance of PF1022 Synthetase. *Chem. Bio. Chem.* **2009**, *10*, 323−328.

[52] (a) Vaska, L. Hydridocarbonyl Complexes of Osmium by Reaction with Alcohols. *J. Am. Chem. Soc.* **1964**, *86*, 1943–1950 and reference therein. (b) Hiraki, K.; Matsunaga, T.; Kawano, H. Reactions of $RuClH(CO)(PPh_3)_3$ with Allylic Amines: Insertions and an Unusual Carbon-Nitrogen Bond Cleavage of Allylic Amines. *Organometallics* **1994**, *13*, 1878–1885. (c) Wakamatsu, H.; Nishida, M.; Adachi, N.; Mori, M. Isomerization Reaction of Olefin Using $RuClH(CO)(PPh_3)_3$. *The J. Org. Chem.* **2000**, *65*, 3966–3970. (d) Yue, C. J.; Liu, Y.; He, R. Olefins isomerization by hydride-complexes of ruthenium. *J. Mol. Catal. A: Chem.* **2006**, *259*, 17–23. (e) Larionov, E.; Li, H.; Mazet, C. Well-defined transition metal hydrides in catalytic isomerizations. *Chem. Commun.* **2014**, *50*, 9816–9826.

Chapter 4

An Iterative Phosphate Tether-mediated Approach for the

Synthesis of Complex Polyols Subunits

4.1 Introduction

The development of atom-,[1] step-,[2,3,] redox-,[4] and pot-economical[5,6,7] methods to generate important subunits common to a variety of biologically relevant natural products is an important component of modern-day synthesis and drug discovery. Among many synthetic approaches that aspire towards these goals are domino/cascade/multi-component reactions, [8] one-pot telescoped strategies,[9,10] and iterative methods,[11,12,13] to name a few. Many times, this subset of strategies utilizes bi- or multi-functional reagents to enable the method.[14,15,16] The modern fields of oligopeptide, oligonucleotide, and oligosaccharide syntheses have exploited the simple concept of bifunctional reagents that can be utilized in repetitive coupling, manipulation, and deprotection cycles,[17] providing opportunities in automation and flow processes.[18,19] Polyketide natural products are also constructed in nature in an iterative/modular manner using the power of enzymatic assembly with simple building blocks.[20,21] This in turn has inspired the development of synthetic methods to access complex polyols, which have enabled the synthesis of polyketides, analogs, and other natural products, allowing SAR studies and biological evaluation.[11-13,22,23,24] Towards this goal, we herein report, an iterative, pot efficient process for the synthesis of complex polyols. More specifically, this iterative method employs enantiomeric multi-faceted phosphate trienes, namely, (*S,S*)-**1** and (*R,R*)-**1**, to access the embedded polyol subunits bearing 1,3 and 7,9 *anti*-diol subunits with variability at the C4 and C10 positions. These fragment and analog subunits are contained within the 14-membered macrolides, lyngbouilloside[25] and neopeltolide,[2d,26] the 36-membered caylobolides A/B, [27] as well as the 28-membered macrolides AB-023A/B[28] and takanawaenes A–C[29] (Figure 4.1).

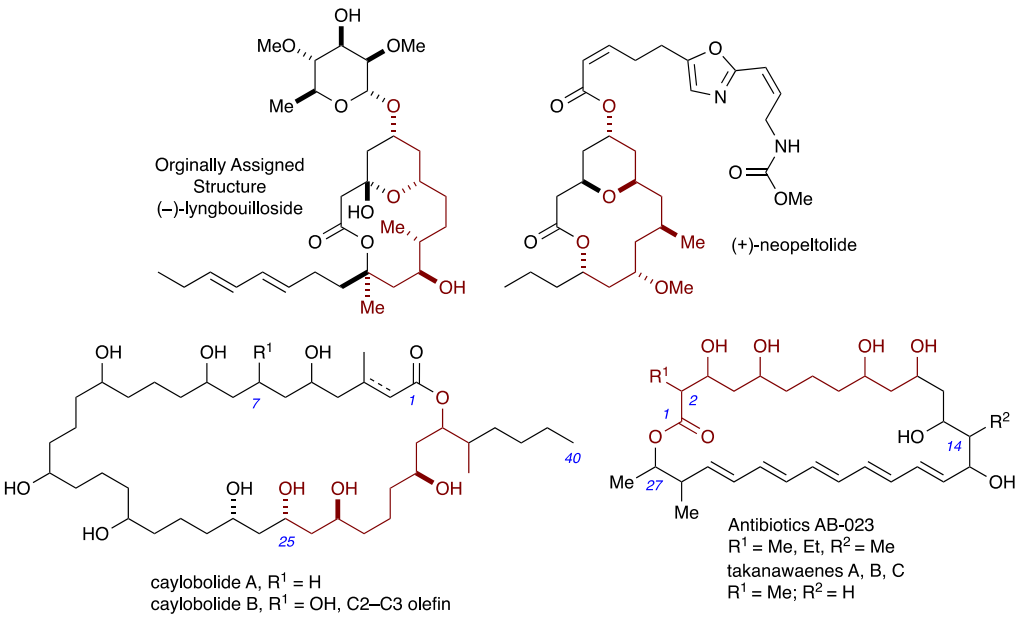

Figure 4.1 *Examples of polyketide natural products*

Recent reviews have highlighted a number of elegant examples that are testament to the concepts of iterative/bifunctional reagents.[11-13] In 1995, Rychnovsky and Patterson reported two reviews on the synthesis of oxo polyene macrolide antibiotics and bioactive marine macrolides.[24] The use of iterative methods in total syntheses of polyketides was reviewed by Zeng, Xie and Hong in 2015.[11] In 2018, Burke and coworkers provided the field with a comprehensive review towards the generalized iterative synthesis of small molecules using a building block approach.[12] In 2020, Friestad reviewed developments in 1,5-polyol synthesis, several methods which were iterative and that were dedicated to remote stereocontrol.[13] Collectively, the authors in these reviews highlight a number of elegant iterative methods employing bifunctional reagents, representative examples with application to polyketides are shown in Scheme 4.1 and include: (a) iterative cyclopropanation-fragmentation for the installation of 1,3-dimethyl groups using simple

bifunctional allylic alcohols developed by Ghosh and coworkers,[30] (b) iridium-catalyzed transfer-hydrogenative carbonyl allylation for complex polyketide fragments using simple bifunctional diols pioneered by Krische and coworkers,[23c,d,31] (c) iterative Suzuki couplings using bifunctional iodopolyenyl MIDA boronates that exploit reversible protection with *N*-methyliminodiacetic acid (MIDA) championed by Burke;[32] (d) an iterative configuration-encoded strategy developed by Friestad and coworkers that exploits Julia−Kocienski couplings of enantiopure bifunctional α-silyloxy-γ-sulfononitrile building blocks for iterative 1,5-polyol synthesis,[13,23b,33] (e) the synthesis of complex 1,3-polyols using supersilyl-directed aldol reactions developed by Yamamoto and coworkers,[23g] and (f) copper(I)-catalyzed asymmetric iterative/domino cross-aldol reactions spearheaded by Kanai and coworkers.[23h]

Scheme 4.1

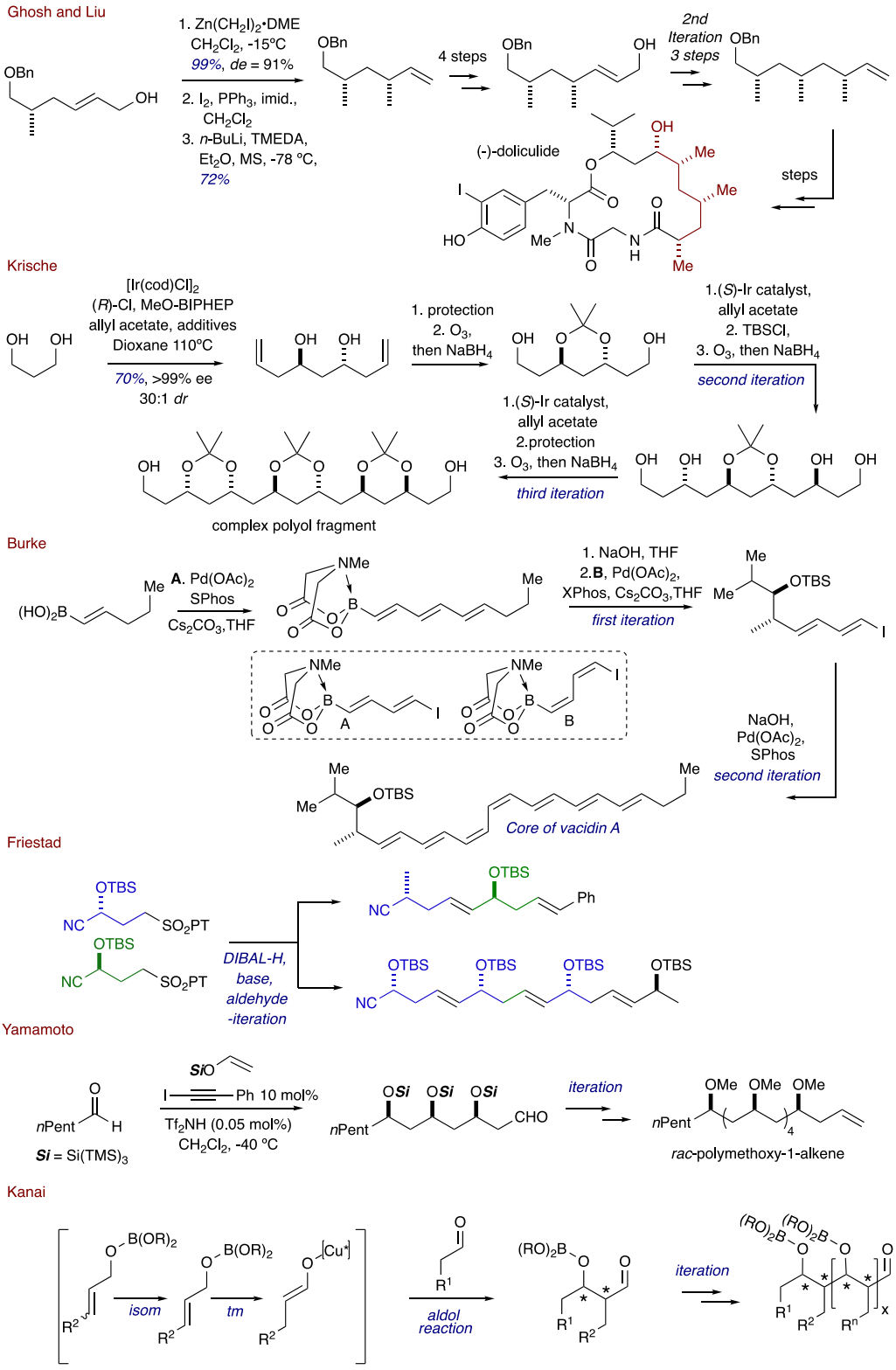
Ghosh and Liu
1. Zn(CH2I)2•DME
CH2Cl2, -15°C
99%, de = 91%
2. I2, PPh3, imid., CH2Cl2
3. n-BuLi, TMEDA, Et2O, MS, -78 °C, 72%
4 steps
2nd Iteration 3 steps
(-)-doliculide
steps
Krische
[Ir(cod)Cl]2
(R)-Cl, MeO-BIPHEP
allyl acetate, additives
Dioxane 110°C
70%, >99% ee
30:1 dr
1. protection
2. O3, then NaBH4
1.(S)-Ir catalyst,
allyl acetate
2. TBSCl,
3. O3, then NaBH4
second iteration
1.(S)-Ir catalyst,
allyl acetate
2.protection
3. O3, then NaBH4
third iteration
complex polyol fragment
Burke
A. Pd(OAc)2
SPhos
Cs2CO3, THF
1. NaOH, THF
2.B, Pd(OAc)2,
XPhos, Cs2CO3,THF
first iteration
NaOH,
Pd(OAc)2,
SPhos
second iteration
Core of vacidin A
Friestad
DIBAL-H,
base,
aldehyde
-iteration
Yamamoto
Si = Si(TMS)3
Ph 10 mol%
Tf2NH (0.05 mol%)
CH2Cl2, -40 °C
iteration
rac-polymethoxy-1-alkene
Kanai
isom
tm
aldol reaction
iteration

4.2 Results and discussion

Our interest in the development of phosphate-tethered methods to complex polyol formation and bioactive natural products and analogs,[34,35] leads us to report a pot-economical approach for the streamlined synthesis of advanced polyol subunits bearing 1,3 and 7,9 *anti*-diol subunits with variability at positions C4 and C10. The key reactions involved in the synthesis of these advanced polyols fragments are iterative use of a telescoped phosphate tether-mediated one-pot sequential RCM/CM/chemoselective diimide reduction,34-36 and either of two methods for installing variability at the C4, and or C10 positions, namely (i) a diastereoselective cuprate addition (cuprate formed from commercially available zincates such as Et_2Zn, and catalyzed with CuCN•2LiCl)34a,36,37 or (ii) a Tsuji-Trost type Pd-catalyzed reductive allylic transposition using $Pd(OAc)_2$ catalyst.[38,39]

The study commenced with the aforementioned previously reported one-pot sequential RCM/CM/chemoselective diimide reduction protocol[40] starting with triene phosphate (*S*,*S*)-**4.2.1** and CM partners **4.2.4** and **4.2.5**[41] catalyzed by the Hoveyda-Grubbs II catalyst (Scheme 4.2).[42] This method exploits type-III olefin character (as originally defined by Chatterjee and Grubbs)[43] in the intermediate bicyclo[4.3.1]phosphate. Subsequent chemoselective hydrogenation of the exocyclic olefin was carried out with *o*-NBSH.[44] Overall, this one-pot sequential protocol provided the desired bicyclic phosphates **4.2.2** and **4.2.3** in good yields.

Scheme 4.2

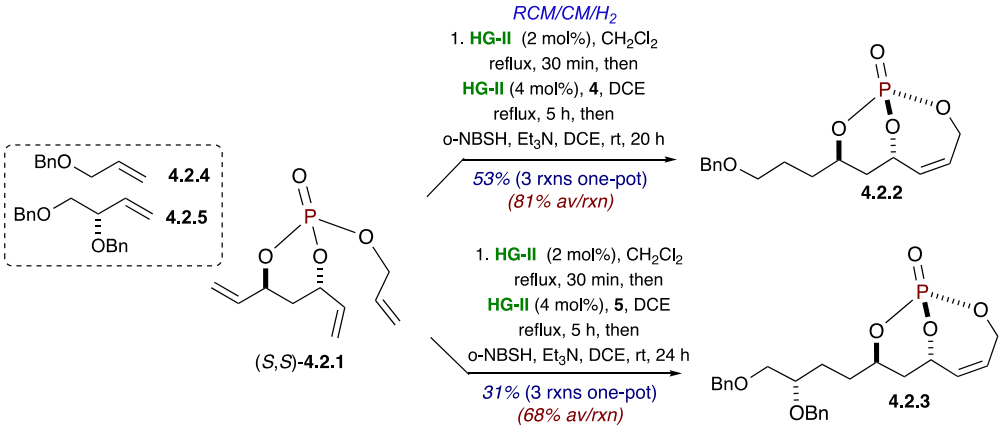

Next, our studies were focused on exploring the scope of the allylic transposition reactions on bicyclic intermediate **4.2.2** using alkyl cuprates- or hydride nucleophiles (Scheme 4.3). Previously, we reported regio- and diastereoselective anti-S_N2' displacement (Corey-Boaz)[45] of the allylic phosphate within the bicyclo[4.3.1]phosphate of **4.2.2** using Me_2Zn/CuCN•2LiCl. Following a similar protocol, an allylic transposition reaction with dimethyl cuprate was carried out, where the cuprate was generated *in situ* from the combination of dimethyl zinc, copper(I) chloride, and lithium chloride at -30 ºC in dry THF. The resulting phosphoric acid was reacted with Red-Al® to remove the phosphate moiety to generate diol **4.3.1** as a single diastereomer. Overall, this two-step process yielded the 1,3-*anti*-diol-containing stereotriad within **4.3.1** in a 65% yield (80.5% average per reaction) and with high diastereoselectivity over the two-pot protocol from **4.2.2**.

A similar method was followed for the nucleophilic diethyl cuprate addition to afford diol **4.3.2** in 62% yield over the two-pot protocol from **4.2.2** (79% average per reaction). Dihexyl cuprate was also successfully utilized as a nucleophilic source by generating the reactive dihexylcuprate from the corresponding lithium reagent and

generating **4.3.3** in 54% over the two-pot protocol from **4.2.2** (74% average per reaction). It is worth noting that nucleophilic addition reactions carried out with branched alkyl or phenyl cuprates have thus far been unsuccessful.

Scheme 4.3

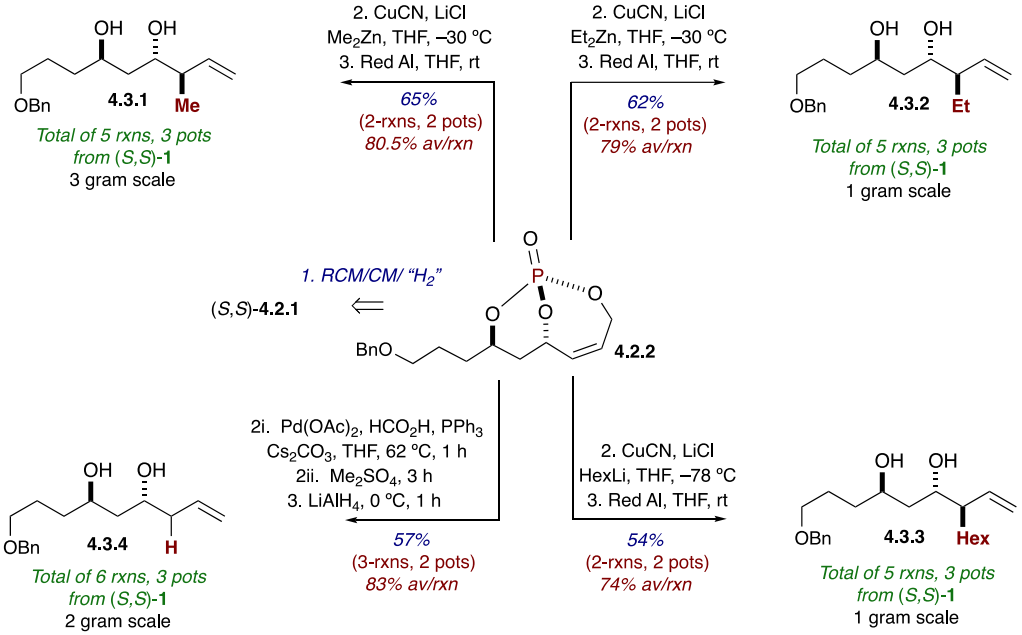

Efforts were next directed at using a hydride nucleophile in the allylic transposition reaction on phosphate **4.2.2**. Thus, a Tsuji-Trost type Pd-catalyzed reductive allylic transposition using $Pd(OAc)_2$ catalyst was performed in THF [$Pd(OAc)_2$, PPh_3, HCO_2H/Cs_2CO_3], in which hydride was generated *in situ* from the combination of formic acid and cesium carbonate. The resulting phosphoric acid was methylated in the same pot via dropwise addition of dimethyl sulfate, and subsequent filtration of the catalyst and reductive tether removal on the crude material in a second pot with $LiAlH_4$ in THF furnished diol **4.3.4** in 57% yield over the two-pot, 3-reaction sequence (83% average per

reaction). Collectively, the Bn-protected triols **4.3.1**–**4.3.4** were all generated on gram-to-multigram scale in a total of 5–6 reactions and three-pots from (*S,S*)-**4.2.1**.

Similarly, the synthesis of tetrols **4.4.1** and **4.4.2** were accomplished utilizing bicyclo[4.3.1]phosphate **4.2.3**. (Scheme 4.4) Thus, nucleophilic cuprate addition reaction with $Me_2Zn/CuCN•2LiCl$ as well as Pd-catalyzed allylic transposition reactions under the aforementioned conditions [$Pd(OAc)_2$, PPh_3, HCO_2H/Cs_2CO_3], followed by reductive tether removal, afforded the tetrol fragments **4.4.1** and **4.4.2**, respectively, in good yields over the two reaction, two-pot protocols (77% and 82% average per reaction).

Scheme 4.4

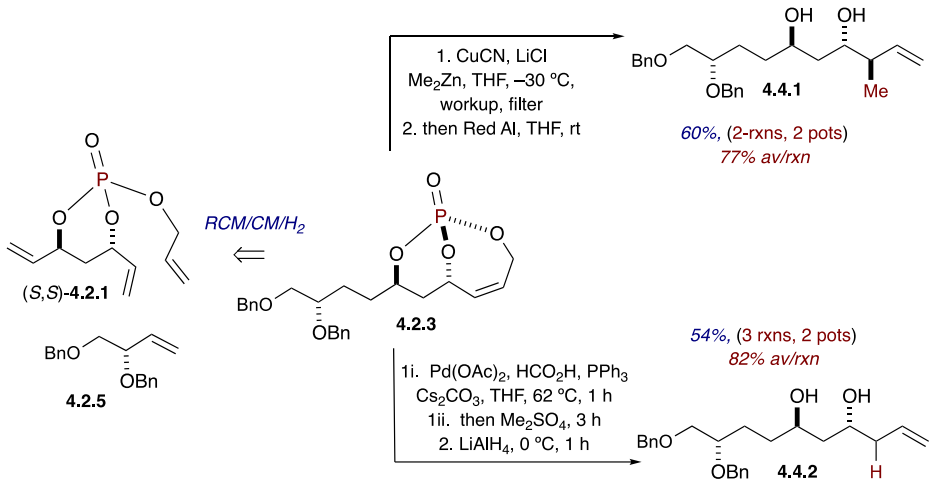

The triol homoallyl alcohol cross partners **4.3.1** and **4.3.4** were next differentially protected (Scheme 4.5) before carrying out an additional one-pot sequential iterative RCM/CM/chemoselective diimide reduction process, followed by the nucleophilic allylic transposition/tether removal protocol (Scheme 4.6). Thus, mono-TIPS protection **4.3.1** using the Hatakeyama protocol[46] generated **4.5.1** in good yield, while selective TIPS and

subsequent MOM protection derived **4.5.2**. Finally, di-MOM-protection under standard conditions produced **4.5.3**.

Scheme 4.5

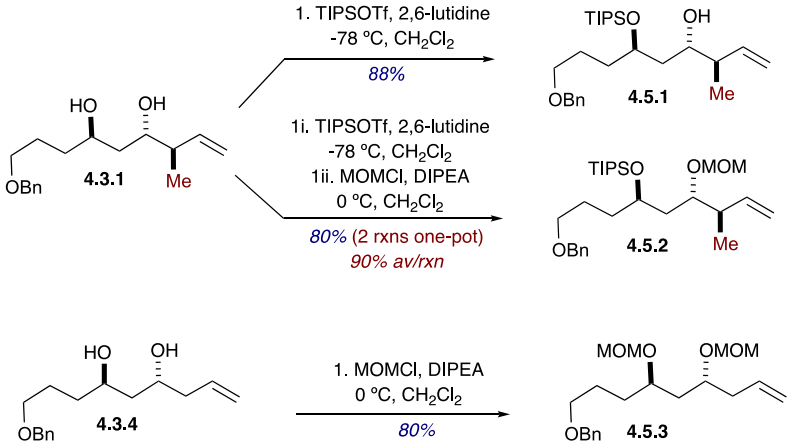

With the differentially protected diol cross-partners **4.5.1**–**4.5.3** in hand, studies were aimed at generating the advanced polyols **4.6.2** and **4.6.3** thru an iterative process (Scheme 4.6). Thus, the mono-TIPS protected diol cross-partner **4.5.1** was subjected to an iterative RCM/CM/chemoselective diimide reduction sequence with phosphate triene (*R*,*R*)-**4.2.1** to deliver bicyclo[4.3.1]phosphate **4.6.1** in moderate overall yields. Subsequent, diastereoselective nucleophilic allylic transposition, using the aforementioned dimethyl cuprate addition or Pd-catalyzed hydride conditions, followed by the previously described tether removal protocols, and hydrolysis with HCl, afforded two advanced polyol fragments **4.6.2** and **4.6.3** in moderate yields over the three-pot processes (Scheme 4.6). Collectively, while the second RCM/CM/H_2 sequences were relatively less yielding, and the hydrogenation steps were much slower–compared to the first set of reactions, the overall process produced **4.6.2** and **4.6.3** in a total of 7 and 6 reactions, respectively, and

four pots from **4.5.2**. Moreover, **4.6.2** and **4.6.3** were generated in a total of 13 and 12 reactions, respectively, and eight pots from the readily prepared phosphate triene SM, (*S,*S)-**4.2.1**.

Scheme 4.6

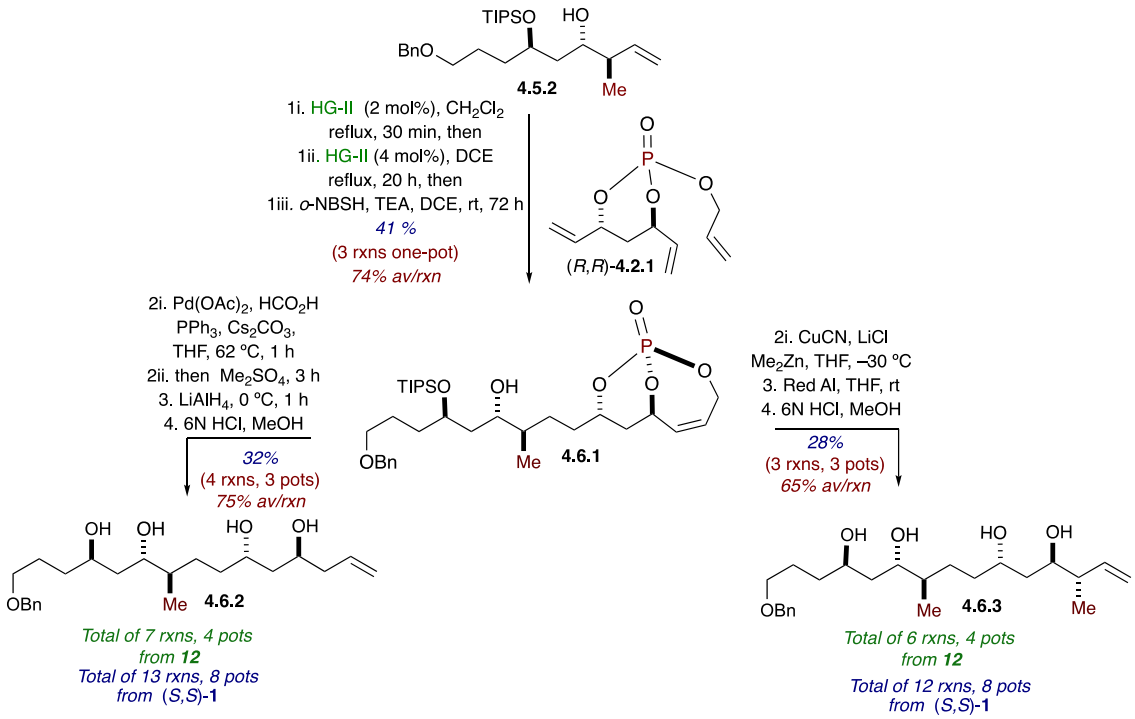

A similar approach was carried out with both TIPS, MOM protected, and di-MOM protected diol compounds **4.5.2** and **4.5.3** (Scheme 4.7). Thus, the differentially-protected TIPS and MOM triols **4.5.2** and **4.5.3** were first subjected to the RCM/CM/chemoselective diimide reduction protocol to deliver the advanced bicyclo[4.3.1]phosphate intermediates **4.7.1** and **4.7.2**. Advanced intermediate with TIPS and MOM-protected ethers were then subjected to the Pd-catalyzed allylic transposition reactions and nucleophilic cuprate addition reactions, followed by reductive tether removal with LAH to afford the respective pentol subunits. Subsequent deprotection of both TIPS and MOM groups with HCl

delivered the pentol **4.6.2** and **4.6.3** in 30 and 40% yields, respectively, over the four reaction three-pot processes. Similar efforts towards the addition of a hexyl group in the allylic transposition reaction yielded an unexpected debenzylation product **4.7.3** in moderate yields (43%) over two reactions in two pots. Next, a Pd-catalyzed allylic transposition reaction was carried out with the bis-MOM protected bicyclo[4.3.1]phosphate **4.7.2** utilizing a hydride nucleophile.

Scheme 4.7

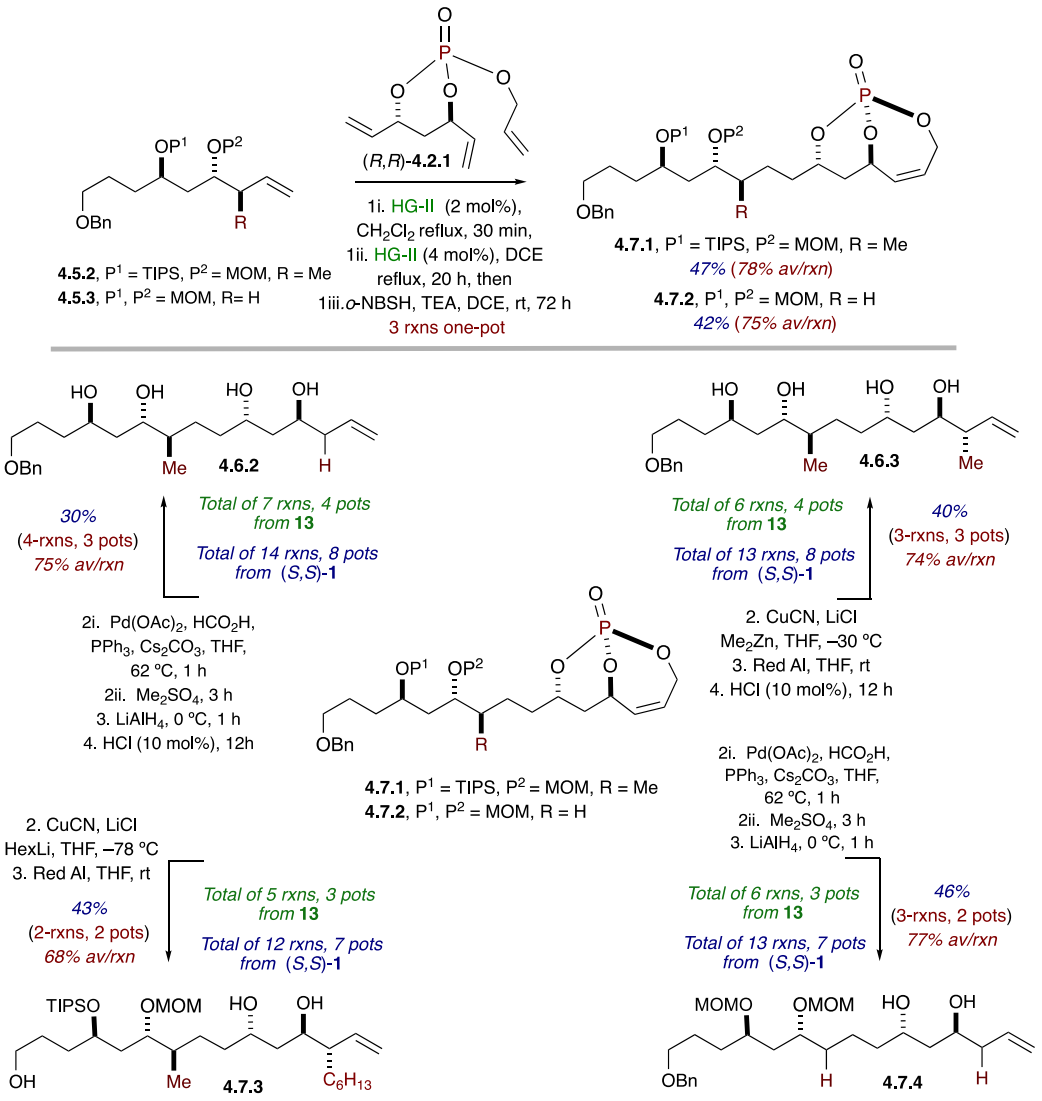

Subsequent tether removal and deprotection of protecting groups yielded **4.7.4** in 46% yield, with an average yield of 77% over the 3 reaction, two-pot process.

Finally, the bis-benzyl protected tetrol **4.8.1**[47] was subjected to the RCM/CM/chemoselective diimide reduction protocol with the phosphate triene (*R*,*R*)-**4.2.1** as the CM partner, followed by chemoselective hydrogenation to afford advanced bicyclo phosphate intermediate **4.8.2** in 47% yield, with an average yield of 78% over the three reaction, one-pot process (Scheme 4.8). Advanced intermediate **4.8.2** was subjected to the iterative cuprate reaction, followed by tether removal on the crude intermediate with RedAl® to obtain polyol fragment **4.8.3** in a 56% yield, with an average yield of 75% over the two reaction, two-pot process.

Scheme 4.8

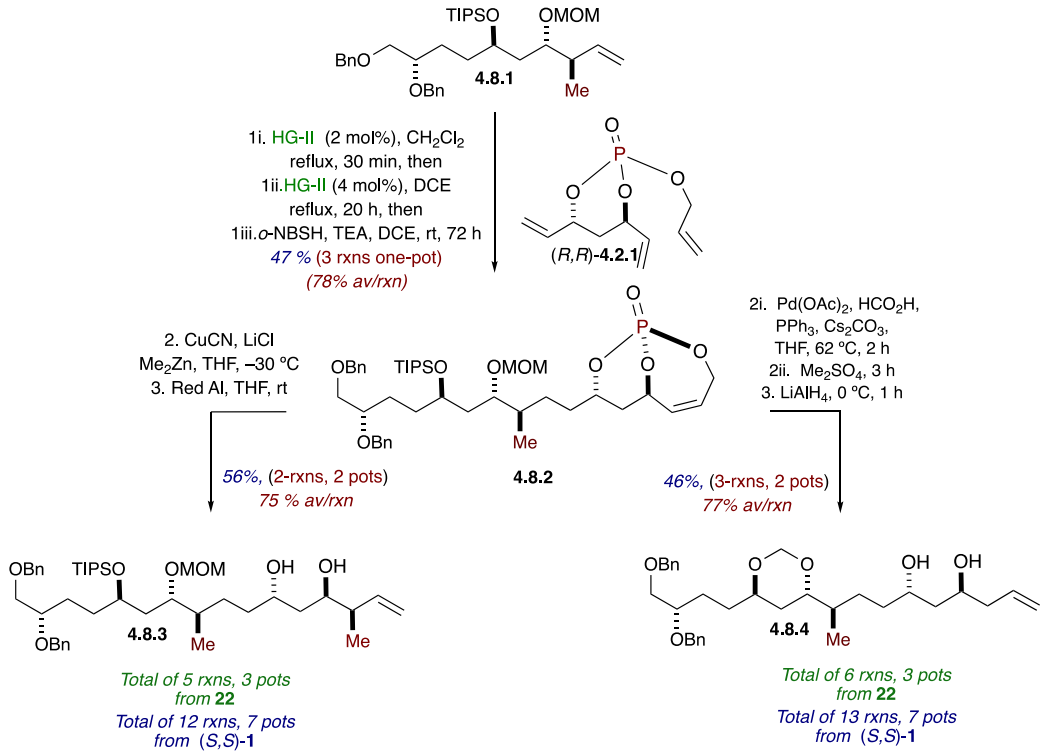

It should be noted that efforts towards addition of a hydride nucleophile in a reductive allylic transposition reaction afforded an unclassical product **4.8.4** as the sole product with a methylene protection of 1,3 *anti*-diol. The formation of **4.8.4** is believed to be due to catalytic removal of the OMe group and subsequent nucleophilic attack from a nearby unprotected alcohol as precedented by Zhou and coworkers.[48]

4.3 Conclusion

In conclusion, an iterative method for the asymmetric synthesis of complex polyols that relies on the uses of telescoped phosphate-tether-mediate protocols has been reported. This method has enabled the asymmetric synthesis of 12 complex polyol subunits in 4–6 one-pot sequential operations, with a total of 12–14 reactions, including 6 catalytic reactions. Collectively, the multi-faceted phosphate tether mediates a number of transformations, including (i) the desymmetrization of a starting C_2-symmetric diene diol, (ii) the RCM/CM/chemoselective diimide reduction protocol that can be exploited in an iterative manner, and (iii) chemo- and regioselective functionalization of the complex polyol fragment. It is our hope that the emergence of these iterative protocols can aid in enabling the rapid synthesis of polyketide macrolides and their analogs, allowing more SAR studies and biological evaluation of these interesting classes of natural products. Additional studies aimed at expanding this method, total synthetic efforts, and analog production are in order and will be reported in due course.

4.4 References cited

[1] (a) Trost, B. M. The atom economy: a search for synthetic efficiency. *Science* **1991**, *254*, 1471–1477. (b) Trost, B. M. Atom economy - a challenge for organic synthesis: homogeneous catalysis leads the way. *Angew. Chem. Int. Ed.* **1995**, *34*, 259–281. (c) Newhouse, T.; Baran, P. S.; Hoffmann, R. W. The economies of synthesis. *Chem. Soc. Rev.* **2009**, *38*, 3010–3021.

[2] (a) Wender, P. A.; Verma, V. A.; Paxton, T. J.; Pillow, T. H. Function-Oriented Synthesis, Step Economy, and Drug Design. *Acc. Chem. Res.* **2008**, *41*, 40–49. (b) Young, I. S.; Baran, P. S. Protecting-group-free synthesis as an opportunity for invention. *Nat. Chem.* **2009**, *1*, 193–205. (c) Hoffmann, R. W. Protecting-group-free synthesis. *Synthesis* **2006**, 3531–3541. (d) Wender, P. A. Toward the ideal synthesis and molecular function through synthesis-informed design. *Nat. Prdt. Rep.* **2014**, *31*, 433–440.

[3] Peters, D. S.; Pitts, C. R.; McClymont, K. S.; Stratton, T. P.; Bi, C.; Baran, P. S. Ideality in Context: Motivations for Total Synthesis. *Acc. Chem. Res.* **2021**, *54*, 605–617.

[4] Burns, N. Z; Baran, P. S.; Hoffmann, R. W. Redox-economy in organic synthesis. *Angew. Chem. Int. Ed.* **2009**, *48*, 2854–2867. (b) Meyer, C. C.; Ortiz, E.; Krische, M. J. Catalytic reductive aldol and mannich reactions of enone, acrylate, and vinyl heteroaromatic pronucleophiles. *Chem. Rev.* **2020**, *120*, 3721–3748.

[5] (a) Vaxelaire, C.; Winter, P.; Christmann, M. One-Pot Reactions Accelerate the Synthesis of Active Pharmaceutical Ingredients. *Angew. Chem. Int. Ed.* **2011**, *50*, 3605–3607. (b) Albrecht, L.; Jiang, H.; Jorgensen, K. A. A Simple Recipe for Sophisticated Cocktails: Organocatalytic One-Pot Reactions-Concept, Nomenclature, and Future Perspectives. *Angew. Chem. Int. Ed.* **2011**, *50*, 8492–8509. (c) Hong, B. C.; Raja, A.; Sheth, V. M. Asymmetric Synthesis of Natural Products and Medicinal Drugs through One-Pot-Reaction Strategies. *Synthesis* **2015**, *47*, 3257–3285.

[6] Hayashi, Y. Pot economy and one-pot synthesis. *Chem. Sci.* **2016**, *7*, 866–880. (b) Hayashi, Y.; Tomikawa, M.; Mori, N. Three-Pot Synthesis of Chiral Anti-1,3-diols through Asymmetric Organocatalytic Aldol and Wittig Reactions Followed by Epoxidation and Reductive Opening of the Epoxide. *Org. Lett.* **2021**, *23*, 5896–5900. (c) Hayashi, Y. Time and Pot Economy in Total Synthesis. *Acc. Chem. Res.* **2021**, *54*, 1385–1398. (d) Hayashi, Y. Time and Pot Economy in Total Synthesis. *Acc. Chem. Res.* **2021**, *54*, 1385–1398.

[7] For pot economical Ru-catalyzed protocols employing multiple transformations, see: Seigal, B. A.; Fajardo, C.; Snapper, M. L. Tandem catalysis: generating multiple contiguous carbon− carbon bonds through a ruthenium-catalyzed ring-closing metathesis/Kharasch addition. *J. Am. Chem. Soc.* **2005**, *127*, 16329–16332. (b) Scholte, A. A.; An, M. H.; Snapper, M. L. Ruthenium-catalyzed tandem olefin metathesis− oxidations. *Org. Lett.* **2006**, *8*, 4759–4762. (c) Murelli, R. P.; Snapper, M. L. Ruthenium-catalyzed tandem cross-metathesis/Wittig olefination: Generation of conjugated dienoic esters from terminal olefins. *Org. Lett.* **2007**, *9*, 1749–1752. (d) Murelli, R. P.; Catalan, S.; Gannon, M. P.; Snapper, M. L. Ruthenium-catalyzed tandem enyne-cross metathesis–cyclopropanation: Three-component access to vinyl cyclopropanes. *Tetrahedron Lett.* **2008**, *49*, 5714–5717. (e) Alcaide, B.; Almendros, P.; Luna, A. Grubbs' Ruthenium-Carbenes Beyond the Metathesis Reaction: Less Conventional Non-Metathetic Utility. *Chem. Rev.* **2009,** *109*, 3817–3858 (f) Nam, Y. H.; Snapper, M. L. Ruthenium-Catalyzed Tandem Metathesis/Non-Metathesis Processes. In Handbook of Metathesis, 2nd ed.; Grubbs, R. H.; Wenzel, A. G.; O'Leary, D. J.; Khosravi, E., Eds.; Wiley-VCH: Weinheim, 2015; pp 311−380.

[8] (a) Teitze, L. F. Domino Reactions in Organic Synthesis. *Chem. Rev.* **1996**, *96*, 115−136. (b) Nicolaou, K.; Edmonds, D. J.; Bulger, P. G. Cascade reactions in total synthesis. *Angew. Chem. Int. Ed.* **2006**, *45*, 7134–7186. (c) Nicolaou, K. C.; Chen, J. S. The art of total synthesis through cascade reactions. *Chem. Soc. Rev*. **2009***, 38*, 2993–3009. (d) Grondal, C.; Jeanty, M.; Enders, D. Organocatalytic cascade

reactions as a new tool in total synthesis. *Nat. Chem.* **2010**, *2*, 167–178. (e) Ruijter, E.; Scheffelaar, R.; Orru, R. V. Multicomponent reaction design in the quest for molecular complexity and diversity. *Angew. Chem. Int. Ed*. **2011**, *50*, 6234–6246. (f) Zarganes-Tzitzikas, T.; Chandgude, A. L.; Dömling, A. Multicomponent reactions, union of MCRs and beyond. *Chem. Rec.* **2015**, *15*, 981–99X. (g) Chanda, T.; Zhao, J. C. G. Recent progress in organocatalytic asymmetric domino transformations. *Adv. Synth. Catal.* **2018**, *360*, 2–79. (h) Evans, C. S.; Davis, L. O. Recent advances in organocatalyzed domino C–C bond-forming reactions. *Molecules* **2018**, *23*, 33–46. (i) Pellissier, H. Stereocontrolled domino reactions. *Chem. Rev.* **2013**, *113*, 442–524.

[9] (a) Albrecht, Ł.; Jiang, H.; Jørgensen, K. A. A Simple Recipe for Sophisticated Cocktails: Organocatalytic One-Pot Reactions—Concept, Nomenclature, and Future Perspectives. *Angew. Chem. Int. Ed.* **2011**, *50*, 8492–8509. (b) Desai, A. A.; Molitor, E. J.; Anderson, J. E. Process intensification via reaction telescoping and a preliminary cost model to rapidly establish value. *Org. Process Res. Dev.* **2012**, *16*, 160–165. (c). Vaxelaire, C.; Winter, P.; Christmann, M. One-Pot Reactions Accelerate the Synthesis of Active Pharmaceutical Ingredients. *Angew. Chem. Int. Ed.* **2011**, *50*, 3605–3607. (d) Cioc, R. C.; Ruijter, E.; Orru, R. V. Multicomponent reactions: advanced tools for sustainable organic synthesis. *Green Chem.* **2014**, *16*, 2958–2975. (e) Zhao, W.; Chen, F.-E. One-pot synthesis and its practical application in pharmaceutical industry. *Curr. Org. Synth.* **2012**, *9*, 873–897. (h) Sydnes, M. O. One-pot reactions: a step towards greener chemistry. *Curr. Green Chem.* **2014**, *1*, 216-226. (f) Crawford, D. E.; Miskimmin, C. K.; Cahir, J.; James, S. Continuous multi-step synthesis by extrusion–telescoping solvent-free reactions for greater efficiency. *Chem. Commun.* **2017**, *53*, 13067–13070.

[10] (a) Britton, J.; Raston, C. L. Multi-step continuous-flow synthesis. *Chem. Soc. Rev*. **2017**, *46* (5), 1250–1271. (b) Gérardy, R.; Monbaliu, J.-C. M., Multistep Continuous-Flow Processes for the Preparation of Heterocyclic Active

Pharmaceutical Ingredients. In *Flow Chemistry for the Synthesis of Heterocycles*, Springer 2018; pp 1–102.

[11] Zeng, K.; Xie, C.; Hong, R. Bioinspired iterative synthesis of polyketides. *Front. Chem.* **2015**, *3*, 32.

[12] Lehmann, J. W.; Blair, D. J.; Burke, M. D. Towards the generalized iterative synthesis of small molecules. *Nature Rev. Chem.* **2018**, *2*, 1–20.

[13] Friedrich, R. M.; Friestad, G. K. Inspirations from tetrafibricin and related polyketides: new methods and strategies for 1,5-polyol synthesis. *Nat. Prod. Rep.* **2020**, *37*, 1229–1261.

[14] For representative examples of bi- or multi-functional reagents, see: (a) Trost, B. M. 3+2 Cycloaddition Approaches To 5-Membered Rings Via Trimethylenemethane and Its Equivalents. *Angew. Chem. Int. Ed. Engl.* **1986**, *25*, 1–20. (b) Piers, E.; Karunaratne, V. Bifunctional Reagents In Organic Synthesis: Total Syntheses Of The Sesquiterpenoids Pentalenene And 9-Epi-Petalenene. *Can. J. Chem.* **1989**, *67*, 160–164. (c) Wang, X.; Meng, Q.; Nation, A. J.; Leighton, J. L., Strained Silacycles in Organic Synthesis: The Tandem Aldol−Allylation Reaction. *J. Am. Chem. Soc.* **2002**, *124*, 10672–10673. (c) Trost, B. M.; Shin, S.; Sclafani, J. A. Direct Asymmetric Zn−Aldol Reaction of Methyl Vinyl Ketone and Its Synthetic Applications. *J. Am. Chem. Soc.* **2005**, *127*, 8602–8603. (d) Gillis, E. P; Burke, M. D., A Simple and Modular Strategy for Small Molecule Synthesis: Iterative Suzuki−Miyaura Coupling of b -Protected Haloboronic Acid Building Blocks. *J. Am. Chem. Soc*. **2007**, *129,* 6716–6717. (e) Lee, S. J.; Anderson, T. M.; Burke, M. D.*,* A Simple and General Platform for Generating Stereochemically Complex Polyene Frameworks by Iterative Cross-Coupling. *Angew. Chem. Int. Ed.* **2010**, *49*, 8860–8863. (f) Tang, S.; Xie, X.; Wang, X.; He, L.; Xu, K.; She, X., Concise Total Syntheses of (+)-Strictifolione and (6R)-6-[(4R,6R)-4,6-Dihydroxy-10-phenyldec-1-enyl]-5,6-dihydro-2H-pyran-2-one. *J. Org. Chem.* **2010**, *75*, 8234–8240. (g) Li, J.; Burke, M. D., Pinene-Derived Iminodiacetic Acid (PIDA): A Powerful Ligand for Stereoselective Synthesis and Iterative Cross-Coupling of

C(sp3) Boronate Building Blocks. *J. Am. Chem. Soc.* **2011***, 133,* 13774–13777. (h) He, Z.; Yudin, A. K. Amphoteric α-Boryl Aldehydes. *J. Am. Chem. Soc.* **2011***, 133,* 13770–13773.

[15] (a) Harrison, T. J.; Rabbat, P. M.; Leighton, J. L. An "aprotic" Tamao oxidation/syn-selective tautomerization reaction for the efficient synthesis of the C (1)–C (9) fragment of fludelone. *Org. Lett.* **2012**, *14*, 4890–4893. (b) Reznik, S. K.; Marcus, B. S.; Leighton, J. L. Complex Fragment Coupling by Crotylation: A Powerful Tool for Polyketide Natural Product Synthesis. *Chem. Sci.* **2012**, *3*, 3326–3330. (c) Chalifoux, W. A.; Reznik, S. K.; Leighton, J. L. Direct and highly regioselective and enantioselective allylation of b–diketones. *Nature* **2012**, *487*, 86–89. (d) Chen, M.; Roush, W. R. Enantioselective Synthesis of (*Z*)- and (*E*)-2-Methyl-1,5-*anti*-Pentenediols via an Allene Hydroboration–Double-Allylboration Reaction Sequence *J. Am. Chem. Soc.* **2013***, 135,* 9512–9517. (e) Shin, I.; Wang, G.; Krische, M. J. Catalyst-Directed Diastereo- and Site-Selectivity in Successive Nucleophilic and Electrophilic Allylations of Chiral 1,3-Diols: Protecting Group-Free Synthesis of substituted Pyrans. *Chem. Eur. J.* **2014**, *20*, 13382–13389. (f) Shin, I.; Hong, S.; Krische, M. Total Synthesis of Swinholide A: An Exposition in Hydrogen Mediated C–C bond Formation. *J. Am. Chem. Soc.* **2016***, 138,* 14246–14249.

[16] Huang, H.-M.; Bellotti, P.; Ma, J.; Dalton, T.; Glorius, F. Bifunctional reagents in organic synthesis. *Nature Rev. Chem.* **2021**, *5*, 301–321.

[17] (a) Feuerbacher, N.; Vögtle, F. Iterative synthesis in organic chemistry. *Dendrimers* **1998**, 1–18. (b) Wen, L.; Edmunds, G.; Gibbons, C.; Zhang, J.; Gadi, M. R.; Zhu, H.; Fang, J.; Liu, X.; Kong, Y.; Wang, P. G. Toward automated enzymatic synthesis of oligosaccharides. *Chem. Rev.* **2018**, *118*, 8151–8187. (c) Weishaupt, M.; Eller, S.; Seeberger, P. H. Solid phase synthesis of oligosaccharides. *Methods Enzymol.* **2010**, *478*, 463–484. (d) Seeberger, P. H. Automated oligosaccharide synthesis. *Chem. Soc. Rev.* **2008**, *37*, 19–28. (e) Molina, A. G.; Sanghvi, Y. S. Liquid-Phase Oligonucleotide Synthesis: Past, Present, and Future Predictions. *Curr. Protoc.*

Nucleic Acid Chem. **2019**, *77*, e82. (f) Dhanawat, M.; Shrivastava, S. K. Solid-phase synthesis of oligosaccharide drugs: a review. *Mini Rev. Med. Chem.* **2009**, *9*, 169–185.

[18] (a) Hartrampf, N.; Saebi, A.; Poskus, M.; Gates, Z. P.; Callahan, A. J.; Cowfer, A. E.; Hanna, S.; Antilla, S.; Schissel, C. K.; Quartararo, A. J.; Ye, X.; Mijalis, A. J.; Simon, M. D.; Loas, A.; Liu, S.; Jessen, C.; Nielsen, T.E.; Pentelute, B.L. Synthesis of proteins by automated flow chemistry. *Science* **2020**, *368*, 980–987. (b) Li, C.; Callahan, A. J.; Simon, M. D.; Totaro, K. A.; Mijalis, A. J.; Phadke, K.-S.; Zhang, G.; Hartrampf, N.; Schissel, C. K.; Zhou, M. Zong, H.; Hanson, G. J.;Loas, A.; Pohl, N. L. B.; Verhoeven, D. E.; Pentelute, B. L. Fully automated fast-flow synthesis of antisense phosphorodiamidate morpholino oligomers. *Nat. Commun.* **2021**, *12*, 1–8.

[19] (a) Plutschack, M. B.; Pieber, B.; Gilmore, K.; Seeberger, P. H. The Hitchhiker's Guide to Flow Chemistry. *Chem. Rev.* **2017**, *117*, 11796–11893. (b) Guberman, M. N.; Seeberger, P. H. Automated glycan assembly: A perspective. *J. Am. Chem. Soc.* **2019**, *141*, 5581–5592 (c) Zhu, Y.; Delbianco, M.; Seeberger, P. H. Automated Assembly of Starch and Glycogen Polysaccharides. *J. Am. Chem. Soc.* **2021**, *143*, 9758–9768.

[20] (a) Walsh, C. T. Polyketide and non-ribosomal peptide antibiotics: modularity and versatility. *Science,* **2004**, *303*, 1805–1810. (b) Fischbach, M. A.; Walsh, C. T. Assembly-line enzymology for polyketide and non-ribosomal peptide antibiotics: logic, machinery, and mechanisms. *Chem. Rev.* **2006**, *106*, 3468–3496.

[21] (a) Rohr, J. A New Role for Polyketides. *Angew. Chem. Int. Ed. Engl.* **2000**, *39*, 2847–2849. (b) Staunton, J.; Weissman, K. J. Polyketide biosynthesis: a millennium review. *Nat. Prod. Rep.* **2001**, *18*, 380–416.

[22] For representative examples of step-economical syntheses to PK, see: (a) Han, S.-B.; Hassan, A.; Kim, I.-S.; Krische, M. J. Total Synthesis of (+)-Roxaticin via C−C Bond Forming Transfer Hydrogenation: A Departure from Stoichiometric Chiral

Reagents, Auxiliaries, and Premetalated Nucleophiles in Polyketide Construction. *J. Am. Chem. Soc.* **2010**, *132*, 15559–15561. (b) Ho, S.; Bucher, C.; Leighton, J. L. A Highly Step-Economical Synthesis of Dictyostatin. *Angew. Chem.* **2013**, *125*, 6889–6893. (c) Yu, M.; Schrock, R. R.; Hoveyda, A. H. Catalyst-Controlled Stereoselective Olefin Metathesis as a Principal Strategy in Multistep Synthesis Design: A Concise Route to (+)-Neopeltolide. *Angew. Chem. Int. Ed.* **2015**, *54*, 215–220. (d) Grisin, A.; Evans, P. A. A highly convergent synthesis of the C1–C31 polyol domain of amphidinol 3 featuring a TST-RCM reaction: confirmation of the revised relative stereochemistry. *Chem. Sci.* **2015**, *6*, 6407–6412. (e) Trost, B. M.; Wang, Y.; Buckl, A. K.; Huang, Z.; Nguyen, M. H.; Kuzmina, O. Total synthesis of bryostatin 3. *Science* **2020**, *368*, 1007–1011. (f) Balieu, S.; Hallett, G. E.; Burns, M.; Bootwicha, T.; Studley, J.; Aggarwal, V. K. Toward Ideality: The Synthesis of (+)-Kalkitoxin and (+)-Hydroxyphthioceranic Acid by Assembly-Line Synthesis. *J. Am. Chem. Soc.* **2015**, *137*, 4398–4403. (g) He, C.; Chu, H.; Stratton, T. P.; Kossler, D.; Eberle, K. J.; Flood, D. T.; Baran, P. S. Total Synthesis of Tagetitoxin. *J. Am. Chem. Soc.* **2020**, *142*, 13683–13688.

[23] (a) Binder, J. T.; Kirsch, S. F. Iterative approach to polyketide-type structures: stereoselective synthesis of 1,3-polyols utilizing the catalytic asymmetric Overman esterification. *Chem. Commun.* **2007**, *40***,** 4164–4166. (b) Friestad, G. K.; Sreenilayam, G. Versatile Configuration-Encoded Strategy for Rapid Synthesis of 1,5-Polyol Stereoisomers. *Org. Lett.* **2010**, *12*, 5016–5019. (c) Hassan, A.; Lu, Y.; Krische, M. J. Elongation of 1,3-Polyols via Iterative Catalyst-Directed Carbonyl Allylation from the Alcohol Oxidation Level. *Org. Lett.* **2009**, *11*, 3112–3115. (d) Lu, Y.; Kim, I. S.; Hassan, A.; Del Valle, D. J.; Krische, M. J. 1,n-Glycols as Dialdehyde Equivalents in Iridium-Catalyzed Enantioselective Carbonyl Allylation and Iterative Two-Directional Assembly of 1,3-Polyols. *Angew. Chem. Int. Ed.* **2009**, *48*, 5018–5021. (e) Kondekar, N. B.; Kumar, P. Iterative Approach to Enantiopure syn/anti-1,3-Polyols via Proline-Catalyzed Sequential alpha-Aminoxylation and Horner-Wadsworth-Emmons Olefination of Aldehydes. *Org.*

Lett. **2009**, *11*, 2611–2614. (f) Smith, A. B.; Xian, M. Anion relay chemistry: an effective tactic for diversity oriented synthesis. *J. Am. Chem. Soc.* **2006**, *128*, 66–67. (g) Albert, B. J.; Yamaoka, Y.; Yamamoto, H. Rapid total syntheses utilizing "supersilyl" chemistry. *Angew. Chem.* **2011**, *123*, 2658–2660. (h) Lin, L. Q.; Yamamoto, K.; Mitsunuma, H.; Kanzaki, Y.; Matsunaga, S.; Kanai, M. Catalytic Asymmetric Iterative/Domino Aldehyde Cross-Ale Reactions for the Rapid and Flexible Synthesis of 1,3-Polyols. *J. Am. Chem. Soc.* **2015**, *137*, 15418–15421. (i) Bootwicha, T.; Feilner, J. M.; Myers, E. L.; Aggarwal, V. K. Iterative assembly line synthesis of polypropionates with full stereocontrol. *Nat. Chem.* **2017**, *9*, 896–902. (j) Che, W.; Li, Y.-Z.; Liu, J.-C.; Zhu, S.-F.; Xie, J.-H.; Zhou, Q.-L. Stereodiverse iterative synthesis of 1, 3-polyol arrays through asymmetric catalytic hydrogenation. formal total synthesis of (−)-cyanolide A. *Org. Lett.* **2019**, *21*, 2369–2373. (k) Barrett, A. G. M.; Hamprecht, D.; White, A. J. P.; Williams, D. J. Iterative Cyclopropanation: A Concise Strategy for the Total Synthesis of the Hexacyclopropane Cholesteryl Ester Transfer Protein Inhibitor U-106305. *J. Am. Chem. Soc.* **1997**, *119*, 8608–8615.

[24] (a) Oishi, T.; Nakata, T. New aspects of stereoselective synthesis of 1,3-polyols. *Synthesis* **1990**, 635–645. (b) Rychnovsky, S. D. Oxo polyene macrolide antibiotics. *Chem. Rev.* **1995**, *95*, 2021–2040. (c) Norcross, R. D.; Paterson, I. Total Synthesis of Bioactive Marine Macrolides. *Chem. Rev.* **1995**, *95*, 2041–2114.

[25] (a) Luesch, H.; Yoshida, W. Y.; Harrigan, G. G.; Doom, J. P.; Moore, R. E.; Paul, V. J. Lyngbyaloside B, a new glycoside macrolide from a Palauan marine cyanobacterium, Lyngbya sp. *J. Nat. Prod.* **2002**, *65*, 1945–1948. (b) MacMillan, J. B.; Molinski, T. F. Caylobolide A, a Unique 36-Membered Macrolactone from a Bahamian Lyngbya m ajuscula. *Org. Lett.* **2002**, *4*, 1535–1538. (c) Gebauer, J.; Arseniyadis, S.; Cossy, J. Facile synthesis of the C1-C13 fragment of lyngbouilloside. *Synlett.* **2008**, 712–714. (d) ElMarrouni, A.; Kolleth, A.; Lebeuf, R.; Gebauer, J.; Prevost, S.; Heras, M.; Arseniyadis, S.; Cossy, J. Lyngbouilloside and related macrolides from marine cyanobacteria. *Nat. Prod. Comm.* **2013**, *8*,

1934578X1300800723. (e) Sabitha, G.; Yadav, J. S.; Sirisha, K. Stereoselective synthesis of the C1–C8 and C9–C16 fragments of revised structure of (−)-lyngbouilloside. *RSC Advances* **2014**, *4*, 3149–3152. (f) Sabitha, G.; Yadav, J. S.; Sirisha, K. Stereoselective synthesis of the C1–C8 and C9–C16 fragments of revised structure of (−)-lyngbouilloside. *RSC Advances* **2014**, *4*, 3149–3152. (g) Chegondi, R.; Hanson, P. R. Synthetic studies to lyngbouilloside: a phosphate tether-mediated synthesis of the macrolactone core. *Tetrahedron Lett.* **2015**, *56*, 3330–3333. (h) Fuwa, H.; Okuaki, Y.; Yamagata, N.; Sasaki, M. Total Synthesis, Stereochemical Reassignment, and Biological Evaluation of (−)-Lyngbyaloside B. *Angew. Chem.* **2015**, *127*, 882–887. (i) Fuwa, H., (−)-Lyngbyaloside B, a Marine Macrolide Glycoside: Total Synthesis and Stereochemical Revision. In *Strategies and Tactics in Organic Synthesis*, Elsevier 2016; Vol. 12, pp 143–168. (j) Ganguly, A.; Javed, S.; Bodugam, M.; Dissanayake, G. C.; Chegondi, R.; Hanson, P. R. Synthesis of the C1− C16 Polyol-containing Macrolactone of 13-desmethyl Lyngbouilloside, an Unnatural Analog of the Originally Assigned Structure of (−)-Lyngbouilloside. *Isr. J. Chem.* **2021**, *61*, 401–408.

[26] (a) Wright, A. E.; Botelho, J. C.; Guzmán, E.; Harmody, D.; Linley, P.; McCarthy, P. J.; Pitts, T. P.; Pomponi, S. A.; Reed, J. K. Neopeltolide, a macrolide from a lithistid sponge of the family Neopeltidae. *J. Nat. Prod.* **2007**, *70*, 412–416. (b) Youngsaye, W.; Lowe, J. T.; Pohlki, F.; Ralifo, P.; Panek, J. S. Total synthesis and stereochemical reassignment of (+)-neopeltolide. *Angew. Chem.* **2007**, *119*, 9371–9374. (c) Custar, D. W.; Zabawa, T. P.; Scheidt, K. A. Total synthesis and structural revision of the marine macrolide neopeltolide. *J. Am. Chem. Soc.* **2008**, *130*, 804–805. (d) Fuwa, H.; Naito, S.; Goto, T.; Sasaki, M. Total synthesis of (+)-neopeltolide. *Angew. Chem.* **2008**, *120*, 4815–4817. (e) Paterson, I.; Miller, N. A. Total synthesis of the marine macrolide (+)-neopeltolide. *Chem. Commun.* **2008**, 4708–4710. (f) Vintonyak, V. V.; Kunze, B.; Sasse, F.; Maier, M. E. Total synthesis and biological activity of neopeltolide and analogues. *Chem. Eur. J.* **2008**, *14*, 11132–11140. (g) Vintonyak, V. V.; Maier, M. E. Formal total synthesis of

neopeltolide. *Org. Lett.* **2008**, *10*, 1239–1242. (h) Fuwa, H.; Saito, A.; Sasaki, M. A concise total synthesis of (+)-neopeltolide. *Angew. Chem.* **2010**, *122*, 3105–3108. (i) Fuwa, H.; Saito, A.; Sasaki, M. A concise total synthesis of (+)-neopeltolide. *Angew. Chem.* **2010**, *122*, 3105–3108. (j) Hartmann, E.; Oestreich, M. Asymmetric Conjugate Silyl Transfer in Iterative Catalytic Sequences: Synthesis of the C7–C16 Fragment of (+)-Neopeltolide. *Angew. Chem. Int. Ed.* **2010**, *49*, 6195–6198. (k) Martinez-Solorio, D.; Jennings, M. P. Formal synthesis of (−)-neopeltolide featuring a highly stereoselective oxocarbenium formation/reduction sequence. *J. Org. Chem.* **2010**, *75*, 4095–4104. (l)Yang, Z.; Zhang, B.; Zhao, G.; Yang, J.; Xie, X.; She, X. Concise formal synthesis of (+)-neopeltolide. *Org. Lett.* **2011**, *13*, 5916–5919. (m) Athe, S.; Chandrasekhar, B.; Roy, S.; Pradhan, T. K.; Ghosh, S. Formal total synthesis of (+)-neopeltolide. *J. Org. Chem.* **2012**, *77*, 9840–9845. (n) Cui, Y.; Balachandran, R.; Day, B. W.; Floreancig, P. E. Synthesis and biological evaluation of neopeltolide and analogs. *J. Org. Chem.* **2012**, *77*, 2225–2235. (o) Raghavan, S.; Samanta, P. K. Stereoselective synthesis of the macrolactone core of (+)-neopeltolide. *Org. Lett.* **2012**, *14*, 2346–2349. (p) Fuwa, H.; Kawakami, M.; Noto, K.; Muto, T.; Suga, Y.; Konoki, K.; Yotsu-Yamashita, M.; Sasaki, M. Concise Synthesis and Biological Assessment of (+)-Neopeltolide and a 16-Member Stereoisomer Library of 8, 9-Dehydroneopeltolide: Identification of Pharmacophoric Elements. *Chem. Eur. J.* **2013**, *19*, 8100–8110. (q) Bai, Y.; Dai, M. Strategies and methods for the synthesis of anticancer natural product neopeltolide and its analogs. *Curr. Org. Chem.* **2015**, *19*, 871–885. (r) Meissner, A.; Tanaka, N.; Takamura, H.; Kadota, I. Stereocontrolled synthesis of the macrolactone core of neopeltolide. *Tetrahedron Lett.* **2019**, *60*, 432–434. (s) Xiong, M.-Q.; Chen, T.; Wang, Y.-X.; Zhu, X.-L.; Yang, G.-F. Design and synthesis of potent inhibitors of bc1 complex based on natural product neopeltolide. *Bioorg. Med. Chem. Lett.* **2020**, *30*, 127324–127329.

[27] (a) MacMillan, J. B.; Molinski, T. F. Caylobolide A, a Unique 36-Membered Macrolactone from a Bahamian Lyngbya m ajuscula. *Org. Lett.* **2002**, *4*, 1535–

1538. (b) Salvador, L. A.; Paul, V. J.; Luesch, H. Caylobolide B, a macrolactone from symplostatin 1-producing marine cyanobacteria Phormidium spp. from Florida. *J. Nat. Prod.* **2010**, *73*, 1606–1609. (c) De Joarder, D.; Jennings, M. P. Convergent enantioselective syntheses of two potential C25–C40 subunits of (−)-caylobolide A. *Tetrahedron Lett.* **2011**, *52*, 5124–5127. (d) De Joarder, D.; Jennings, M. P. Enantioselective synthesis of a potential 1, 5-syn-polyol C1–C24 subunit of (−)-caylobolide A. *Tetrahedron Lett.* **2013**, *54*, 5826–5829. (e) Yadav, J.; Swapnil, N.; Venkatesh, M.; Prasad, A. Studies directed toward the synthesis of caylobolide A: convergent synthesis of C21–C40 subunit. *Tetrahedron Lett.* **2014**, *55*, 1164–1167.

[28] (a) Bortolo, R.; Spera, S.; Guglielmetti, G.; Cassani, G. Ab023, novel polyene antibiotics II. Isolation and structure determination. *J. Antibiot.* **1993**, *46*, 255–264. (b) Cidaria, D.; Borgonovi, G.; Pirali, G. AB023, novel polyene antibiotics I. Taxonomy of the producing organism, fermentation and antifungal activity. *J. Antibiot.* **1993**, *46*, 251–254.

[29] (a) Fukuda, T.; Kim, Y.-P.; Iizima, K.; Tomoda, H.; Omura, S. Takanawaenes, Novel Antifungal Antibiotics Produced by Streptomyces sp. K99-5278 II. Structure Elucidation. *J. Antibiot* . **2003**, *56*, 454–458. (b) Kim, Y.-P.; Tomoda, H.; Iizima, K.; Fukuda, T.; Matsumoto, A.; Takahashi, Y.; Omura, S. Takanawaenes, Novel Antifungal Antibiotics Produced by Streptomyces sp. K99-5278 I. Taxonomy, Fermentation, Isolation and Biological Properties. *J. Antibiot* . **2003**, *56*, 448–453.

[30] Ghosh, A. K.; Liu, C. Total synthesis of antitumor depsipeptide (−)-doliculide. *Org. Lett.* **2001**, *3*, 635–638.

[31] (a) Kim, I. S.; Nagi, M. -Y.; Krische, M. J. Enantioselective Iridium Catalyzed Carbonyl Allylation from the Alcohol or Aldehyde Oxidation Level via Transfer Hydrogenative Coupling of Allyl Acetate: Departure from Chirally Modified Allyl Metal Reagents in Carbonyl Addition. *J. Am. Chem. Soc.* **2008**, *130*, 14891–14899. (b) Park, B. Y.; Nguyen, K. D.; Chaulagain, M. R.; Komanduri, V.; Krische, M. J. Alkynes as Allylmetal Equivalents in Redox-Triggered C-C Couplings to Primary

Alcohols: (Z)-Homoallylic Alcohols via Ruthenium Catalyzed Propargyl C-H Activation. *J. Am. Chem. Soc.* **2014**, *136*, 11902–11905.

[32] (a) Lee, S. J.; Gray, K. C.; Paek, J. S.; Burke, M. D. Simple, efficient, and modular syntheses of polyene natural products via iterative cross-coupling. *J. Am. Chem. Soc.* **2008**, *130*, 466–468. (b) Lee, S. J.; Anderson, T. M.; Burke, M. D. A Simple and General Platform for Generating Stereochemically Complex Polyene Frameworks by Iterative Cross-Coupling. *Angew. Chem. Int. Ed.* **2010**, *49*, 8860–8863.

[33] (a) Friedrich, R. M.; Bell, J. Q.; Garcia, A.; Shen, Z.; Friestad, G. K. Unified Strategy for 1,5,9- and 1,5,7-Triols via Configuration-Encoded 1,5-Polyol Synthesis: Preparation and Coupling of C15−C25 and C26−C40 Fragments of Tetrafibricin. *J. Org. Chem.* **2018**, *83*, 13650–13669.

[34] (a) Whitehead, A.; McReynolds, M. D.; Moore, J. D.; Hanson, P. R. Multivalent Activation in Phosphate Tethers: A New Tether for Small Molecule Synthesis. *Org. Lett.* **2005**, *7,* 3375–3378. (b) Venukadasula, P. K.; Chegondi, R.; Maitra, S.; Hanson, P. R. A concise, phosphate-mediated approach to the total synthesis of (−)-tetrahydrolipstatin. *Org. Lett.* **2010**, *12*, 1556–1559. (c) Hanson, P. R.; Chegondi, R.; Nguyen, J.; Thomas, C. D.; Waetzig, J. D.; Whitehead, A. Total synthesis of dolabelide C: A phosphate-mediated approach. *J. Org. Chem.* **2011**, *76*, 4358–4370. (d) Chegondi, R.; Tan, M. M.; Hanson, P. R. Phosphate Tether-Mediated Approach to the Formal Total Synthesis of (−)-Salicylihalamides A and B. *J. Org. Chem.* **2011**, *76*, 3909–3916. (e) Jayasinghe, S.; Venukadasula, P. K.; Hanson, P. R. An efficient, modular approach for the synthesis of (+)-strictifolione and a related natural product. *Org. Lett.* **2014**, *16*, 122–125. (f) Hanson, P. R.; Jayasinghe, S.; Maitra, S.; Ndi, C. N.; Chegondi, R. A Modular Phosphate Tether-Mediated Divergent Strategy to Complex Polyols. *Beilstein J. Org. Chem.* **2014**, *10*, 2332–2337. (g) Hanson, P. R.; Jayasinghe, S.; Maitra, S; Markley, J. L. (authors with equal contribution) Phosphate Tethers in Natural Product Synthesis. In Phosphorus Chemistry II: Synthetic Methods; Montchamp, J.-L., Ed.; Topics in Current

Chemistry 361; Springer-Verlag Berlin Heidelberg, **2015**; pp 253–271. (h) Chegondi, R.; Hanson, P. R. Synthetic Studies to Lyngbouilloside: A Phosphate Tether-Mediated Synthesis of the Macrolactone Core. *Tetrahedron Lett*. **2015**, 56, 3330–3333. (i) Maitra, S.; Bodugam, M.; Javed, S.; Hanson, P. R. Synthesis of the C9-C25 Subunit of Spirastrellolide B. *Org. Lett.* **2016**, *18*, 3094–3097. (j) Bodugam, M.; Javed, S.; Ganguly, A.; Torres, J.; Hanson, P. R. A Pot-Economical Approach to the Total Synthesis of Sch-725674. *Org. Lett.* **2016**, *18*, 516–519. (k) Javed, S.; Bodugam, M.; Torres, J.; Ganguly, A.; Hanson, P. R. Modular Synthesis of Novel Macrocycles Bearing α,b-Unsaturated Chemotypes through a Series of One-Pot, Sequential Protocols. *Chem. Eur. J.* **2016**, *22*, 6755–6758.

[35] (a) Markley, J. L.; Hanson, P. R. *P*-Stereogenic Bicyclo[4.3.1]Phosphite Boranes: Synthesis and Utility of Tunable *P*-Tether Systems for the Desymmetrization of C_2-Symmetric 1,3-*Anti*-Diols. *Org. Lett.* **2017**, *19*, 2552–2555. (b) Markley, J. L.; Hanson, P. R. A *P*-Tether-Mediated, Iterative S_N2'-Cuprate Alkylation Strategy to Skipped Polyol Stereotetrads: Utility of an Oxidative "Function Switch" with Phosphite-Borane Tethers. *Org. Lett.* **2017**, *19*, 2556–2559.

[36] (a) Waetzig, J. D.; Hanson, P. R. Temporary Phosphate Tethers: A Metathesis Strategy to Differentiated Polyol Subunits. *Org. Lett.* **2006**, *8*, 1673–1676. (b) Thomas, C. D.; McParland, J. P.; Hanson, P. R. Divalent and Multivalent Activation in Phosphate Triesters: A Versatile Method for the Synthesis of Advanced Polyol Synthons. *Eur. J. Org. Chem.* **2009**, *73*, 5487–5500. (c) Venukadasula, P. K. M.; Chegondi, R.; Suryn, G. M.; Hanson, P. R. A Phosphate Tether-Mediated, One-Pot, Sequential Ring-Closing Metathesis/Cross-Metathesis/Chemoselective Hydrogenation Protocol. *Org. Lett.* **2012**, *14*, 2634–2637.

[37] (a) Whitehead, A.; McParland, J. P.; Hanson, P. R. Divalent Activation in Temporary Phosphate Tethers: Highly Selective Cuprate Displacement Reactions. *Org. Lett.* **2006**, *8*, 5025–5028, and references cited therein. (b) Calaza, M. I.; Hupe, E.; Knochel, P., Highly anti-Selective S_N2' Substitutions of Chiral Cyclic 2-Iodo-

Allylic Alcohol Derivatives with Mixed Zinc−Copper Reagents. *Org. Lett.* **2003**, *5*, 1059–1061. For additional representative uses of allylic phosphates in synthesis, see (c) Kacprzynski, M. A.; Hoveyda, A. H. Cu-catalyzed asymmetric allylic alkylations of aromatic and aliphatic phosphates with alkylzinc reagents. An effective method for enantioselective synthesis of tertiary and quaternary carbons. *J. Am. Chem. Soc.* **2004**, *126*, 10676–10681. (d) Larsen, A. O.; Leu, W.; Oberhuber, C. N.; Campbell, J. E.; Hoveyda, A. H. Bidentate NHC-based chiral ligands for efficient Cu-catalyzed enantioselective allylic alkylations: structure and activity of an air-stable chiral Cu complex. *J. Am. Chem. Soc.* **2004**, *126*, 11130–11131. (e) Protti, S.; Fagnoni, M. Phosphate esters as "tunable" reagents in organic synthesis. *Chem. Commun.* **2008**, 3611–3621. (f) Shintani, R.; Takatsu, K.; Takeda, M.; Hayashi, T. Copper-Catalyzed Asymmetric Allylic Substitution of Allyl Phosphates with Aryl-and Alkenylboronates. *Angew. Chem. Int. Ed.* **2011**, *50*, 8656–8659. (g) Takeda, M.; Takatsu, K.; Shintani, R.; Hayashi, T. Synthesis of quaternary carbon stereocenters by copper-catalyzed asymmetric allylic substitution of allyl phosphates with arylboronates. *J. Org. Chem.* **2014**, *79*, 2354–2367. (h) Yasuda, Y.; Ohmiya, H.; Sawamura, M. Copper-Catalyzed Enantioselective Coupling between Allylboronates and Phosphates Using a Phenol–Carbene Chiral Ligand: Asymmetric Synthesis of Chiral Branched 1, 5-Dienes. *Synthesis* **2018**, *50*, 2235–2246.

[38] (a) Tanigawa, Y.; Nishimura, K.; Kawasa, A.; Murahashi, S-I. Palladium(0)-catalyzed Allylic Alkylation and Amination of Allylic Phosphates. *Tetrahedron Lett.* **1982**, *23*, 5549–5552. (b) Murahashi, S-I.; Taniguchi, Y.; Imada, Y.; Tanigawa, Y. Palladium(0)-catalyzed Azidation of Allyl Esters. Selective Synthesis of Allyl Azides, Primary Allylamines and related compounds. *J. Org. Chem.* **1989,** *54*, 3292–3303. (c) Murahashi, S-I.; Imada, Y.; Taniguchi, Y.; Higashiura, S. Palladium(0)-catalyzed Alkoxyarbonylation of Allyl Phosphates and Acetates. *J. Org. Chem.* **1993**, *58*, 1538–1545. (d) Trost, B. M.; Czabaniuk, L.C. Benzylic Phosphates as Electrophiles in the Palladium-Catalyzed Asymmetric

Benzylation of Azlactones *J. Am. Chem. Soc.* **2012**, *134*, 5778−5781. (e) Takeda, M.; Shintani, R.; Hayashi, T. Enantioselective Synthesis of α-Tri- and α-Tetrasubstituted Allylsilanes by Copper-Catalyzed Asymmetric Allylic Substitution of Allyl Phosphates with Silylboronates. *J. Org. Chem.* **2013**, *78*, 5007−5017.

[39] For reviews on Tsuji-Trost type allylic alkylation reactions, see: (a) Trost, B. M.; Van Vranken, D. L. Asymmetric transition metal-catalyzed allylic alkylations. *Chem. Rev.* **1996**, *96*, 395–422. (b) Trost, B. M.; Crawley, M. L. Asymmetric transition-metal-catalyzed allylic alkylations: applications in total synthesis. *Chem. Rev.* **2003**, *103*, 2921–2944. (c) Trost, B. M. Metal catalyzed allylic alkylation: its development in the trost laboratories. *Tetrahedron* **2015**, *71*, 5708–5733.

[40] For seminal tandem, metathesis/hydrogenation, see: (a) Louie, J.; Bielawski, C. W.; Grubbs, R. H. Tandem catalysis: The sequential mediation of olefin metathesis, hydrogenation, and hydrogen transfer with single-component Ru complexes. *J. Am. Chem. Soc.* **2001**, *123*, 11312–11313; For tandem RCM/CM and hydrogenation, see: (b) Virolleaud, M-. A.; Bressy, C.; Piva, O. A straightforward synthesis of (E)-δ-alkenyl-β, γ-unsaturated δ-lactones by a tandem ring-closing/cross-coupling metathesis process. *Tetrahedron Lett*. **2003**, *44*, 8081–8084. (c) Quinn, K. J.; Isaacs, A. K.; Arvary, R. A. Concise total synthesis of (−)-muricatacin by tandem ring-closing/cross metathesis. *Org. Lett.* **2004**, *6*, 4143–4145; (d) Virolleaud, M-. A.; Piva, O. Selective formation of dihydropyran derivatives by a tandem domino ring-closing metathesis/cross-metathesis. *Tetrahedron Lett*. **2007**, *48*, 1417–1420; (e) Quinn, K. L.; Curto, J. M.; McGrath, K. P.; Biddick, N. A. Facile synthesis of (−)-6-acetoxy-5-hexadecanolide by size-selective ring-closing/cross metathesis *Tetrahedron Lett.* **2009**, *50*, 7121–7123; For CM/hydrogenation/cyclization, see: (f) Cossy, J.; Bargiggia, F.; BouzBouz, S. Tandem cross-metathesis/hydrogenation/cyclization reactions by using compatible catalysts. *Org. Lett.* **2003**, *5*, 459–462; For tandem CM/amidation, see: (g) L. Ferrie, S. BouzBouz, J. Cossy, Acryloyl Chloride: An Excellent Substrate for Cross-Metathesis. A One-

Pot Sequence for the Synthesis of Substituted α, β-Unsaturated Carbonyl Derivatives. *Org. Lett.* **2009**, *11*, 5446–5448.

[41] Allyl benzyl ether **5** was synthesized by treating sodium allyl alkoxide with benzyl bromide in the presence of tetra n-butylammonium iodide as the additive.

[42] Garber, S. B.; Kingsbury, J. S.; Gray, B. L.; Hoveyda, A. H. Efficient and Recyclable Monomeric and Dendritic Ru-Based Metathesis Catalysts. *J. Am. Chem. Soc*. **2000**, *122,* 8168–8179.

[43] (a) Chatterjee, A. K.; Choi, T.-L.; Sanders, D. P.; Grubbs, R. H. A General Model for Selectivity in Olefin Cross Metathesis. *J. Am. Chem. Soc.* **2003**, *125*, 11360–11370. (b) Ogbaa, O. M.; Warnera, N. C.; O'Leary, D. J.; Grubbs, R. H. Recent advances in ruthenium-based olefin metathesis. *Chem. Soc. Rev*. **2018**, *47*, 4510–4544.

[44] (a) Myers, A. G.; Zheng, B.; Movassaghi, M., Preparation of the Reagent o-Nitrobenzenesulfonylhydrazide. *J. Org. Chem.* **1997**, *62*, 7507–7507. (b) Buszek, K. R.; Brown, N., Improved Method for the Diimide Reduction of Multiple Bonds on Solid-Supported Substrates. *J. Org. Chem.* **2007**, *72*, 3125–3128. (c) Haukaas, M. H.; O'Doherty, G. A., Enantioselective Synthesis of 2-Deoxy- and 2,3-Dideoxyhexoses. *Org. Lett.* **2002**, *4*, 1771–1774.

[45] (a) Corey, E. J.; Boaz, N. W. d-Orbital stereoelectronic control of the stereochemistry of S_N2' displacements by organocuprate reagents. *Tetrahedron Lett.* **1984**, *25*, 3063–3066. For reviews see: (b) Nakamura, E, Yoshikai, N. In The Chemistry of Organocopper Compounds; Rappoport, Z.; Marek, I., Eds.; Wiley: Chichester, 2009; Chapter 1, Part 1, pp 1–21.

[46] (a) Esumi, T.; Okamoto, N.; Hatakeyama, S. Versatile Enantiocontrolled Synthesis of (+)-Fostriecin. *Chem. Commun.* **2002**, 3042–3043. (b) Soltani, O.; De Brabander, J. A Concise Synthesis of (+)-SCH 351448. *Org. Lett*. **2005**, *7*, 2791–2793. (c) For selective esterification of a similar subunit, see reference 34d.

[47] For the synthesis and characterization of the Mono-TIPS and Mom-protected derivatives of tetrol **22**, see Supporting Information.

[48] Che, W.; Li, Y. Z.; Liu, J. C.; Zhu, S. F.; Xie, J. H.; Zhou, Q. L. Stereodiverse Iterative Synthesis of 1, 3-Polyol Arrays through Asymmetric Catalytic Hydrogenation. Formal Total Synthesis of (−)-Cyanolide A. *Org. Lett.* **2019,** *21,* 2369–2373.

Chapter 5

Supporting Information for Chapters 2–4:

Methods, Experimental Data, and NMR Spectra

5.1 Supporting Information for Chapter 2

Total Synthesis of Sanctolide A and Formal Synthesis of

(2S)-Sanctolide A

Table of Contents

Chapter 5, Section 1: Supporting Information for Chapter 2

Total Synthesis of Sanctolide A and Formal Synthesis of (2S)-Sanctolide A.

5.1.1 General Methods

General Experimental Section

All reactions were carried out in oven- or flame-dried glassware under argon atmosphere using standard gas-tight syringes, cannula, and septa. Stirring was achieved with oven-dried magnetic stir bars. Et_2O, THF and CH_2Cl_2 were purified by passage through a purification system (Pure Process Technology) employing activated Al_2O_3 (Pangborn, A. B.; Giardello, M. A.; Grubbs, R. H.; Rosen, R. K.; Timmers, F. J. Safe and Convenient Procedure for Solvent Purification *Organometallics* **1996**, *15*, 1518–1520). Et_3N was purified by passage over basic alumina and stored over KOH. Butyllithium was purchased from Aldrich and titrated prior to use. All olefin metathesis catalysts were acquired from Materia and used without further purification. Flash column chromatography was performed with Sorbent Technologies (30930M-25, Silica Gel 60 Å, 40-63 μm) and thin layer chromatography was performed on silica gel 60F254 plates (EM-5717, Merck). ^{1}H, ^{13}C, and ^{31}P NMR spectra were recorded on either a Bruker DRX-400 or Bruker DRX-500 MHz spectrometers operating at 400 MHz or 500 MHz for ^{1}H NMR, 101 MHz or 126 MHz for ^{13}C NMR, and 202 MHz for ^{31}P NMR using $CDCl_3$, acetone-d_6 and methanol-d_4 as solvents. The ^{1}H NMR data are reported as the chemical shift in parts per million, multiplicity (s, singlet; d, doublet; t, triplet; q, quartet; p, pentet; m, multiplet), coupling constant in hertz, and number of protons. High-resolution mass spectrometry (HRMS) was recorded on a LCT Premier Spectrometer (Micromass UK Limited) operating on ESI (MeOH). Observed rotations at 589 nm were measured using LAXCO POL301 model automatic polarimeter. IR was recorded on Thermo Scientific Nicolet iS5 FTIR instrument.

5.1.2 Experimental Section

(4*R*,6*R*)-2-((2-methylbut-3-en-1-yl)oxy)-4,6-divinyl-1,3,2-dioxaphosphinane 2-oxide ($C_{12}H_{19}O_4P$, 2.6.2)

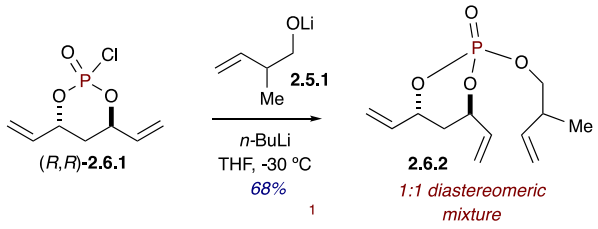

To a solution of 2-methyl-3-buten-1-ol **2.5.1** (0.853 mL, 12.5 mmol, 1.05 equiv.) in THF (25 mL), under argon at -30 ºC, was added *n*-butyllithium (5.0 mL, 2.5 M in hexanes, 12.5 mmol, 1.05 equiv.), dropwise. The reaction mixture was stirred at -30 ºC for 15 minutes, at which point a solution of monochlorophosphate[1] (2.5 g, 11.9 mmol, 1equiv.) in THF (54 mL) was added dropwise, slowly. The reaction continued to stir at -30 ºC for 30 minutes (complete by TLC), and the flask was removed from the cooling bath and quenched with saturated NH_4Cl (aqueous, ~40 mL). The mixture was stirred, vigorously, as the flask warmed to room temperature, and then the biphasic solution was separated. The aqueous layer was extracted with EtOAc (3 x 50 mL), and the organic layers were combined, washed with brine, dried over Na_2SO_4, and concentrated under reduced pressure. The crude mixture was purified via flash column chromatography (silica, 0%–60% EtOAc in hexanes) to provide triene **2.6.2** (2.2 g, 9.5 mmol, 80% yield) as a colorless liquid and a 1:1 mixture of inseparable diastereomers. TLC (EtOAc/Hexane, 1/1): R_f = 0.6.

[1]Whitehead, A.; McReynolds, M. D.; Moore, J. D.; Hanson, P. R. Multivalent Activation in Temporary Phosphate Tethers: A New Tether for Small Molecule Synthesis. *Org. Lett.* **2005**, *7*, 3375–3378.

FTIR (neat): 3083, 2966, 2928, 1642, 1425, 1281, 1118, 1014, 966, 928, 876, 759, 725 cm^{-1};

Optical Rotation: $[a]_D^{21}$ = -50.9 (c = 0.4, $CHCl_3$);

^{1}H NMR (500 MHz, $CDCl_3$) δ 6.03 (ddd, J = 16.9, 10.6, 6.0 Hz, 1H, CH_aH_b=C<u>H</u>CHO(P=O)CH_aH_b), 5.90 (dddd, J = 17.3, 10.7, 5.2, 1.7 Hz, 1H, CH_aH_bCHO(P=O)C<u>H</u>=CH_aH_b), 5.75 (ddd, J = 17.3, 10.4, 7.0 Hz, 1H, (P=O)OCH_2CH(Me)C<u>H</u>=CH_aH_b), 5.46 (d, J = 17.1 Hz, 1H, C<u>H</u>$_a$$H_b$=CHCHO(P=O)$CH_aH_b$), 5.37 (d, J = 17.4 Hz, 1H, CH_aH_bCHO(P=O)CH=C<u>H</u>$_a$$H_b$), 5.32–5.27 (m, 2H, CH_a<u>H</u>$_b$=CHCHO(P=O)CH_aH_b, CH_aH_bCHO(P=O)CH=CH_a<u>H</u>$_b$), 5.11 (d, J = 17.3 Hz, 1H, (P=O)OCH_2CH(Me)CH=C<u>H</u>$_a$$H_b$), 5.07 (dd, J = 10.4, 1.2 Hz, 1H, (P=O)OCH_2CH(Me)CH=CH_a<u>H</u>$_b$), 5.05–5.00 (m, 1H, CH_aH_b=CHC<u>H</u>O(P=O)CH_aH_b), 4.99–4.93 (m, 1H, CH_aH_bC<u>H</u>O(P=O)CH=CH_aH_b), 3.98 (td, J = 6.8, 3.3 Hz, 2H, (P=O)O<u>C</u>H_2CH(Me)CH=CH_aH_b), 2.56 (p, J = 6.8 Hz, 1H, (P=O)OCH_2C<u>H</u>(Me)CH=CH_aH_b), 2.16 (dddd, J = 12.9, 8.0, 4.8, 1.5 Hz, 1H, CH_aH_b=CHCHO(P=O)C<u>H</u>$_a$$H_b$), 2.04 (dddd, J = 14.4, 5.4, 3.6, 1.8 Hz, 1H, CH_aH_b=CHCHO(P=O)CH_a<u>H</u>$_b$), 1.06 (d, J = 6.8 Hz, 3H, (P=O)OCH_2CH(<u>Me</u>)CH=CH_aH_b);

^{13}C NMR (126 MHz, $CDCl_3$) δ 139.7 (<u>C</u>H=CH_2), 135.2 (2, <u>C</u>H=CH_2), 118.2 (CH=<u>C</u>H_2), 117.6 (CH=<u>C</u>H_2), 115.6 (CH=<u>C</u>H_2), 77.9 (d, J_{CP}= 6.6 Hz, <u>C</u>H), 76.2 (d, J_{CP}= 6.0 Hz, <u>C</u>H), 71.8 (d, J_{CP}= 6.2 Hz, <u>C</u>H_2), 38.3 (d, J_{CP}= 6.5 Hz, <u>C</u>H), 35.4 (<u>C</u>H_2), 16.1 (<u>C</u>H_3);

^{31}P NMR (202 MHz, $CDCl_3$) δ -7.62;

HRMS (ESI-TOF) m/z: $[M + Na]^+$ Calcd for $C_{12}H_{19}O_4PNa$ 281.0919; Found 281.0913.

(1*R*,4*S*,7*R*,9*R*,*Z*)-4-methyl-9-vinyl-2,10,11-trioxa-1-phosphabicyclo[5.3.1]undec-5-ene 1-oxide ($C_{10}H_{15}O_4P$, 2.6.3)

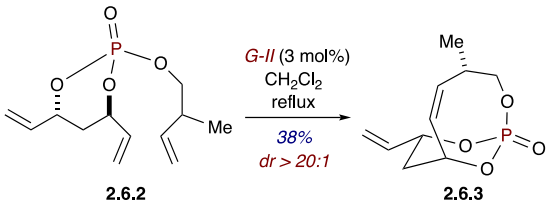

2.6.2 2.6.3

To a round bottom flask, equipped with a stir bar, reflux condenser, and argon inlet, was added triene **2.6.2** (2.0 g, 7.7 mmol, 1 equiv.), CH_2Cl_2 (1540 mL), and Grubbs second-generation catalyst [$(ImesH_2)(PCy_3)(Cl)_2Ru{=}CHPh$,[2] G-II] (98 mg, 0.115 mmol, 1.5 mol%). The reaction mixture was heated to reflux and stirred at reflux for 2 hours to ensure complete conversion of reactive starting material (~1:1 mix of starting material and product by TLC). The reaction mix was cooled to room temperature and concentrated under reduced pressure. Purification via flash column chromatography (silica, 0%–50% EtOAc in hexanes) provided bicyclic phosphate **2.6.3** (0.673 g, 2.9 mmol, 38% yield) as a white solid, along with unreacted starting material (0.722 g, 2.8 mmol). TLC (EtOAc/Hexane, 1/1): R_f = 0.5.

FTIR (neat): 3083, 2966, 2933, 2893,1643, 1424, 1282, 1118, 1014, 928, 875, 725 cm^{-1};

Optical Rotation: $[a]_D^{21}$ = -44.6 (c = 0.52, $CHCl_3$);

^{1}H NMR (500 MHz, $CDCl_3$) 5.84 (dddd, J = 17.1, 10.6, 5.4, 2.0 Hz, 1H, $CH_aH_b{=}C\underline{H}CHO(P{=}O)CH_aH_b$), 5.46–5.43 (m, 2H, $CH_aH_bCHO(P{=}O)C\underline{H}{=}C\underline{H}CH(Me)CH_aH_bO(P{=}O)$), 5.40 (dt, J = 17.1, 1.3 Hz, 1H, $C\underline{H}_aH_b{=}CHCHO(P{=}O)CH_aH_b$), 5.29–5.21 (m, 1H, $CH_aH_bC\underline{H}O(P{=}O)CH{=}CHCH(Me)CH_aH_bO(P{=}O)$), 5.25 (dt, J = 10.6, 1.3 Hz, 1H,

[2] Scholl, M.; Ding, S.; Lee, C. W.; Grubbs, R. H. Synthesis and Activity of a New Generation of Ruthenium-Based Olefin Metathesis Catalysts Coordinated with 1,3-Dimesityl-4,5-dihydroimidazol-2-ylidene Ligands. *Org. Lett.* **1999**, *1*, 953–956.

$CH_aH_bCHO(P=O)CH=CHCH(Me)CH_aH_bO(P=O)$), 5.07 (ddq, J = 11.8, 5.4, 1.5 Hz, 1H, $CH_2=CHCHO(P=O)CH_aH_b$), 4.32 (ddd, J = 10.8, 6.2, 2.2 Hz, 1H, $CH_aH_bCHO(P=O)CH=CHCH(Me)CH_aH_bO(P=O)$), 3.60–3.53 (m, 1H, $CH_aH_bCHO(P=O)CH=CHCH(Me)CH_aH_bO(P=O)$), 3.33 (ddd, J = 30.9, 12.6, 10.8 Hz, 1H, $CH_aH_bCHO(P=O)CH=CHCH(Me)CH_aH_bO(P=O)$), 2.19 (dddd, J = 14.6, 11.9, 6.0, 0.8 Hz, 1H, $CH_2=CHCHO(P=O)CH_aH_b$), 1.81 (ddd, J = 14.6, 2.0, 1.0 Hz, 1H, $CH_2=CHCHO(P=O)CH_aH_b$), 1.00 (d, J = 6.6 Hz, 3H, $CH_aH_bCHO(P=O)CH=CHCH(Me)CH_aH_bO(P=O)$);

^{13}C NMR (126 MHz, $CDCl_3$) δ 135.2 (d, J_{CP}= 10.0 Hz, $CH=CH_2$), 134.3 (2, $CH=CH$), 129.5 ($CH=CH_2$), 78.1 (d, J_{CP}= 7.2 Hz, CH), 77.3 (d, J_{CP}= 6.3 Hz, CH), 68.3 (d, J_{CP}= 5.4 Hz, CH_2), 36.4 (d, J_{CP}= 6.4 Hz, CH_2), 31.3 (CH), 16.7 (CH_3);

^{31}P NMR (162 MHz, $CDCl_3$) δ –8.02;

HRMS (ESI-TOF) m/z: $[M]^+$ Calcd for $C_{10}H_{15}O_4P$ 230.0708; Found 230.0699.

(2*S*,5*S*,7*S*)-2-methyldodecane-1,5,7-triol ($C_{13}H_{28}O_3$, (2*S*)-2.6.6)

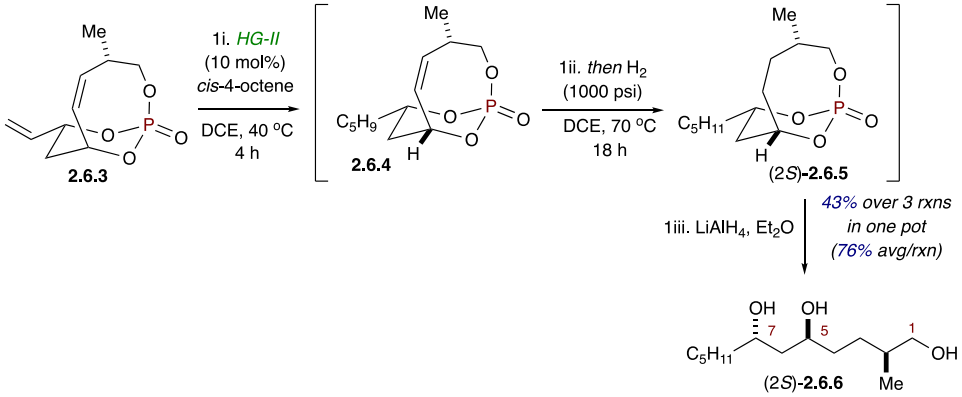

To a clean, dry round bottom flask equipped with a stir bar, reflux condenser, and argon inlet, was added **2.6.3** (600.0 mg, 2.6 mmol, 1 equiv.), 1,2-dichloroethane (1,2-DCE, 6.6 mL, 0.3 M), *cis*-4-octene (2.2 mL, 7.8 mmol, 3 equiv.), and Hoveyda-Grubbs second-generation catalyst (HG-II, 162.8 mg, 0.26 mmol, 10 mol%). The reaction was heated to 40 ºC and stirred at 40 ºC until **2.6.3** was consumed (4 h, monitored by TLC). The reaction was cooled to room temperature and cannulated into a Parr hydrogenation reaction vessel. The vessel was heated to 70 ºC, and H_2 pressure was applied (1000 psi). The reaction stirred at 70 ºC, under H_2 pressure, for 18 h (complete by TLC (EtOAc/Hexane, 3/1): $R_f = 0.4$)), at which point the reaction was cooled to room temperature and solvent removed under reduced pressure. The crude oil was dried under high vacuum (~8 h) to ensure complete removal of 1,2-DCE. The crude mix was taken up in diethyl ether (Et_2O, 26 mL, 0.1 M) and cooled to 0 ºC under argon. Solid lithium aluminum hydride ($LiAlH_4$, 0.4 g, 10.4 mmol, 4 equiv.) was added in three portions, and the reaction flask was removed from the cooling bath and allowed to warm to room temperature. The mixture stirred at room temperature for 4 hours (complete by TLC), and the reaction was cooled to 0 ºC and quenched with 10% Rochelle salt solution. The reaction was allowed to warm to room temperature and stir at room temperature for 2 hours. The crude mixture was filtered over Celite (washed

with CH_2Cl_2, EtOAc, and MeOH) and concentrated under reduced pressure. Purification via flash column chromatography (silica, 0%–100% EtOAc in hexanes) provided (2*S*)-**2.6.6** (259.5 mg, 0.118 mmol, 43% yield over 3 reactions in one pot, 76% average per reaction) as a white solid. TLC (EtOAc): R_f = 0.2.

FTIR (neat): 3338 (br), 2930, 2871, 2858, 1458, 1377, 1032, 937, 831 cm^{-1};

Optical Rotation: $[a]_D^{22}$ = -17.3 (c = 0.11, $CHCl_3$);

^{1}H NMR (500 MHz, $CDCl_3$) δ 3.98–3.89 (m, 2H, $CH_3(CH_2)_4C\underline{H}(OH)CH_2C\underline{H}(OH)CH_2$), 3.49 (dd, J = 6.1, 2.3 Hz, 2H, $CH(OH)CH_2CH_2CH(Me)C\underline{H}_2OH$), 1.69–1.64 (m, 1H, $CH(OH)C\underline{H}_aH_bCH(OH)CH_aH_b$), 1.65–1.53 (m, 3H, $CH(OH)CH_aH_bCH(OH)C\underline{H}_aH_bC\underline{H}_aH_b$, $C\underline{H}(Me)CH_2OH$), 1.55–1.47 (m, 3H, $C\underline{H}_aH_bCH(OH)CH_a\underline{H}_bCH(OH)CH_a\underline{H}_b$), 1.47–1.38 (m, 2H, $C\underline{H}_aH_bCH_a\underline{H}_bCH(OH)CH_aH_bCH(OH)$), 1.34–1.23 (m, 6H, $CH_3C\underline{H}_2C\underline{H}_2CH_a\underline{H}_bCH_aH_b$, $CH(OH)CH_aH_bCH(OH)CH_2CH_a\underline{H}_b$), 0.93 (d, J = 6.7 Hz, 3H, $CH(OH)CH_2CH_2CH(\underline{Me})CH_2OH$), 0.89 (t, J = 6.8 Hz, 3H, $C\underline{H}_3(CH_2)_4CH(OH)CH_2$);

^{13}C NMR (126 MHz, $CDCl_3$) δ 69.7 ($\underline{C}H$), 69.4 ($\underline{C}H$), 68.1 ($\underline{C}H_2$), 42.6 ($\underline{C}H_2$), 37.6 ($\underline{C}H_2$), 35.5 ($\underline{C}H$), 34.5 ($\underline{C}H_2$), 32.0 ($\underline{C}H_2$), 29.1 ($\underline{C}H_2$), 25.6 ($\underline{C}H_2$), 22.8 ($\underline{C}H_2$), 16.7 ($\underline{C}H_3$), 14.2 ($\underline{C}H_3$);

HRMS (ESI-TOF) m/z: $[M + Na]^+$ Calcd for $C_{13}H_{28}O_3Na$ 255.1936; Found 255.1939.

(3*S*,6*S*)-6-((*S*)-2-hydroxyheptyl)-3-methyltetrahydro-2*H*-pyran-2-one ($C_{13}H_{24}O_3$, (2*S*)-2.6.7)

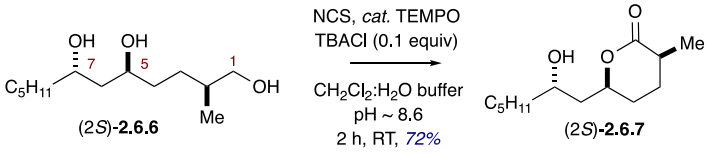

To a round bottom flask, equipped with a stir bar, was added (2*S*)-**2.6.6** (85 mg, 0.36 mmol, 1 equiv.), CH_2Cl_2 (7.2 mL, 0.05M), TEMPO (5.6 mg, 0.036 mmol, 10 mol%), tetrabutylammonium chloride (TBACl, 10.0 mg, 0.036 mmol, 10 mol%), and aqueous $NaHCO_3/K_2CO_3$ buffer (7.2 mL, 0.5 M $NaHCO_3$: 0.05 M K_2CO_3). To the stirring biphasic solution was added *N*-chlorosuccinimide (240 mg, 1.8 mmol, 5 equiv.) in one portion, and the reaction continued to vigorously stir at room temperature for 2 hours (complete by TLC). The biphasic solution was diluted with CH_2Cl_2 (0.5 mL) and water (0.5 mL), and the layers separated. The aqueous layer was extracted with CH_2Cl_2 (3 x 5 mL), and the organic layers were combined, dried over Na_2SO_4, filtered over Celite, and concentrated under reduced pressure. Purification via flash column chromatography (silica, 0%-70% EtOAc in hexanes) provided (2*S*)-**2.6.7** (59.1 mg, 0.026 mmol, 72% yield) as a colorless liquid. TLC (EtOAc/Hexane, 3/1): $R_f = 0.6$.

FTIR (neat): 3381 (br), 3067, 2976, 2932, 1722, 1641, 1540, 1435, 1353, 1047, 915, 750 cm^{-1};

Optical Rotation: $[a]_D^{22} = +22.8$ ($c = 0.4$, $CHCl_3$);

^{1}H NMR (500 MHz, $CDCl_3$) δ 4.63 (tt, $J = 10.5, 3.1$ Hz, 1H, $CH_3(CH_2)_4CH(OH)CH_aH_bC\underline{H}(OC{=}O)CH_aH_b$), 3.98–3.94 (m, 1H, $CH_3(CH_2)_4C\underline{H}(OH)CH_aH_bCH(OC{=}O)CH_aH_b$), 2.63 (dt, $J = 10.6, 7.2$ Hz, 1H, $CH(OC{=}O)CH_aH_bCH_aH_bC\underline{H}(Me)$), 2.11 (ddd, $J = 16.9, 11.6, 7.7$ Hz, 1H,

CH(OC=O)$CH_aH_bC\underline{H}_aH_bCH(Me)$), 1.91 (ddt, *J* = 13.3, 9.7, 3.9 Hz, 1H, $CH(OC=O)C\underline{H}_aH_bCH_aH_bCH(Me)$), 1.75 (ddd, *J* = 14.8, 9.8, 2.2 Hz, 1H, $CH_3(CH_2)_4CH(OH)C\underline{H}_aH_bCH(OC=O)$), 1.69–1.62 (m, 1H, $CH(OC=O)CH_a\underline{H}_bCH_aH_bCH(Me)$), 1.61–1.49 (m, 2H, $CH_3(CH_2)_4CH(OH)CH_a\underline{H}_bCH(OC=O)$, $CH(OC=O)CH_aH_bCH_a\underline{H}_bCH(Me)$), 1.46–1.42 (m, 3H, $CH_3(CH_2)_2C\underline{H}_2C\underline{H}_aH_bCH(OH)$), 1.35–1.15 (m, 5H, $CH_3(C\underline{H}_2)_2CH_2CH_a\underline{H}_bCH(OH)$), 1.22 (d, *J* = 6.7 Hz, 3H, $CH(OC=O)CH_aH_bCH_aH_bCH(\underline{Me})$), 0.89 (t, *J* = 6.7 Hz, 3H, $C\underline{H}_3(CH_2)_2CH_2CH_aH_bCH(OH)$);

^{13}C NMR (126 MHz, $CDCl_3$) δ 176.6 ($\underline{C}$=O), 75.0 ($\underline{C}$H), 67.7 ($\underline{C}$H), 42.9 ($\underline{C}H_2$), 38.2 ($\underline{C}H_2$), 33.3($\underline{C}$H), 31.9 ($\underline{C}H_2$), 27.4 ($\underline{C}H_2$), 25.8 ($\underline{C}H_2$), 25.3 ($\underline{C}H_2$) 22.7 ($\underline{C}H_2$), 16.2 ($\underline{C}H_3$), 14.2 ($\underline{C}H_3$);

HRMS (ESI-TOF) m/z: $[M + Na]^+$ Calcd for $C_{13}H_{24}O_3Na$ 251.1623; Found 251.1624.

(3*S*,6*S*)-6-((*S*)-2-methoxyheptyl)-3-methyltetrahydro-2*H*-pyran-2-one ($C_{14}H_{26}O_3$, (2*S*)-2.1.6)

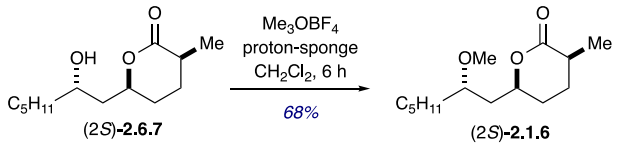

To a round bottom flask, equipped with a magnetic stir bar, was added (2*S*)-**2.6.7** (40 mg, 0.175 mmol, 1 equiv.) in CH_2Cl_2 (2 mL), proton sponge® (374 mg, 1.75 mmol, 10 equiv.), and trimethyloxonium tetrafluoroborte (258 mg, 1.75 mmol, 10 equiv.) and stirred the mixture for 6 hours (complete by TLC). The solution was diluted with CH_2Cl_2 (2 mL) and was added saturated $NaHCO_3$ (2 mL), and the layers separated. The aqueous layer was extracted with CH_2Cl_2 (3 x 3 mL), and the organic layers were combined, dried over Na_2SO_4, filtered, and concentrated under reduced pressure. Purification via flash column chromatography (silica, 0%-50% EtOAc in hexanes) provided (2*S*)-**2.1.6** (29 mg, 0.12 mmol, 68% yield) as a yellow liquid. TLC (EtOAc/Hexane, 1/1): R_f = 0.4.

FTIR (neat): 2930, 2871, 2858, 1733, 1460, 1377, 1238, 1172, 1091, 1012, 933, 747 cm $^{-1}$;

Optical Rotation: $[a]_D^{22}$ = +7.8 (*c* = 0.14 , $CHCl_3$);

^{1}H NMR (500 MHz, $CDCl_3$) δ 4.54 (tt, *J* = 11.5, 3.0 Hz, 1H, $CH_3(CH_2)_4CH(OMe)CH_aH_bC\underline{H}(OC{=}O)CH_aH_b$),

3.56–3.51 (m, 1H, $CH_3(CH_2)_4C\underline{H}(OMe)CH_aH_bCH(OC{=}O)CH_aH_b$), 3.34 (s, 3H, $CH_3(CH_2)_4CH(O\underline{Me})CH_aH_bCH(OC{=}O)CH_aH_b$) 2.64 (ddd, *J* = 10.3, 7.8, 6.5 Hz, 1H, $CH(OC{=}O)CH_aH_bCH_aH_bC\underline{H}(Me)$), 2.10 (m 1H, $CH(OC{=}O)CH_aH_bC\underline{H}_aH_bCH(Me)$), 1.89 (ddt, *J* = 13.6, 9.4, 3.8 Hz, 1H, $CH(OC{=}O)C\underline{H}_aH_bCH_aH_bCH(Me)$), 1.72 (ddd, *J* = 14.7, 9.8, 2.4 Hz 1H, $CH_3(CH_2)_4CH(OMe)C\underline{H}_aH_bCH(OC{=}O)$), 1.67–1.47 (m, 4H,

$CH_3(CH_2)_4CH(OMe)CH_a\underline{H}_bCH(OC{=}O)$, $CH(OC{=}O)CH_a\underline{H}_bCH_a\underline{H}_bCH(Me)$, $CH_3(CH_2)_3C\underline{H}_aH_bCH(OMe)$), 1.42 (dq, *J* = 13.6, 6.4 Hz 1H, $CH_3(CH_2)_3CH_a\underline{H}_bCH(OMe)$), 1.36–1.23 (m, 6H, $CH_3(C\underline{H}_2)_3CH_aH_bCH(OMe)$), 1.22 (d, *J* = 6.8 Hz, 3H, $CH(OC{=}O)CH_aH_bCH_aH_bCH(\underline{Me})$), 0.89 (t, *J* = 6.8 Hz, 3H, $C\underline{H}_3(CH_2)_2CH_2CH_aH_bCH(OMe)$);

^{13}C NMR (126 MHz, $CDCl_3$) δ 176.8 ($\underline{C}{=}O$), 76.6 ($\underline{C}H$), 74.9 ($\underline{C}H$), 57.2 ($\underline{C}H_3$), 41.0 ($\underline{C}H_2$), 33.5 ($\underline{C}H_2$), 33.3 ($\underline{C}H$), 32.2 ($\underline{C}H_2$), 27.5 ($\underline{C}H_2$), 25.8 ($\underline{C}H_2$), 24.4 ($\underline{C}H_2$) 22.8 ($\underline{C}H_2$), 16.2 ($\underline{C}H_3$), 14.2 ($\underline{C}H_3$);

HRMS (ESI-TOF) m/z: $[M + Na]^+$ Calcd for $C_{14}H_{26}O_3Na$ 265.1780; Found 265.1785.

(4*S*,6*S*)-nona-1,8-diene-4,6-diol ($C_9H_{16}O_2$, 2.7.3)

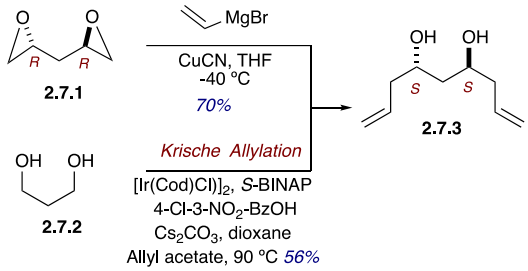

Method 1:

To a stirring solution of CuCN (360 mg, 4.0 mmol, 0.2 equiv.) in dry THF (10 mL) was added vinyl magnesium bromide (1 M in THF, 60 mL, 60.0 mmol, 3 equiv.) at -40 ºC and stirred for 15 minutes. To the reaction mixture then was cannulated the di-epoxide (2 g, 20.0 mmol) dissolved in THF (40 mL) and stirred vigorously for 6 h (complete by TLC). The solution was diluted with hexane and quenched with saturated ammonium chloride and layers separated. The aqueous layer was extracted with EtOAc (3 x 30 mL), and the organic layers were combined, dried over Na_2SO_4, filtered, and concentrated under reduced pressure. Purification via flash column chromatography (silica, 0%-60% EtOAc in hexanes) provided **2.7.3** (2.2 g, 14.1 mmol, 70% yield) as a colorless oil.

Method 2:

The decarbonylative allylation of 1,3-propanediol to deliver **2.7.3** was carried out according to the protocol developed by Krische and coworkers;[3] To an oven-dried sealed tube under argon gas charged with $[Ir(cod)Cl]_2$ (672 mg, 1.00 mmol, 5 mol%), (*S*)-BINAP (1.25 g, 2.00 mmol, 10 mol%), Cs_2CO_3 (2.61 g, 8.0 mmol, 0.4 equiv.) and 4-chloro-3-

[3] Perez, F.; Waldeck, A. R.; Krische, M. J. Total Synthesis of Cryptocaryol A by Enantioselective Iridium-Catalyzed Alcohol C− H Allylation. *Angew. Chem.* **2016**, *128*, 5133–5136.

nitrobenzoic acid (806 mg, 4 mmol, 0.2 equiv.) was added THF (50 mL) followed by allyl acetate (20 g, 200 mmol, 1.0 equiv.). The reaction mixture was stirred at 90 ºC for 30 minutes and cooled to room temperature. 1,3-propanediol (1.52 g, 20.0 mmol, 1.0 equiv.) in THF (50 mL, 0.2 M overall) was added and the reaction mixture was stirred at 100 ºC for 6 days. The reaction mixture was cooled to room temperature, filtered through Celite, and excess solvent was removed under reduced pressure. The crude material was dissolved in EtOAc (50 mL) and vigorously stirred. Et_2O (100 mL) was added slowly followed by hexanes (100 mL). The precipitate was filtered through Celite, and the solution was concentrated onto silica gel. Purification via flash column chromatography (silica, 0%-60% EtOAc in hexanes) provided **2.7.3** (1.7 g, 11.2 mmol, 56% yield) as a yellow oil.

The analytical data were in good agreement with the previously reported data.

(4*S*,6*S*)-4,6-diallyl-2-((2-methylallyl)oxy)-1,3,2-dioxaphosphinane 2-oxide ($C_{13}H_{21}O_4P$, 2.7.4)

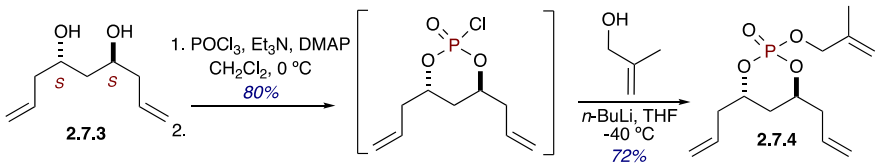

To a round bottom flask equipped with a stir bar and an argon inlet, was added the diol **2.7.3** (2.0 g, 12.8 mmol, 1.0 equiv.) in CH_2Cl_2 (64 mL, 0.2 M), Et_3N (5.3 mL, 38.4 mmol, 3 equiv.), DMAP (312 mg, 2.56 mmol, 0.2 equiv.) and stirred for 5 minutes at 0 ºC. To the reaction mixture at same temperature was added $POCl_3$ (1.3 mL, 14.1 mmol, 1.1 equiv.) dropwise, and stirred for 30 minutes (complete by TLC). Solvent was evaporated and filtered through a short silica column to obtain the monochlorophosphate (2.4 g, 10.24 mmol, 80%) as a yellow oil.

Next, to a solution of β-methallyl alcohol (0.433 mL, 10.7 mmol, 1.05 equiv.) in THF (26 mL, 0.4 M), under argon at -40 ºC, was added *n*-butyllithium (4.3 mL, 2.5 M in hexanes. 10.7 mmol, 1.05 equiv.), dropwise. The reaction mixture stirred at -30 ºC for 15 minutes, at which point a solution of monochlorophosphate (2.4 g, 10.2 mmol) in THF (50 mL) was cannulated dropwise, slowly. The reaction continued to stir at -40 ºC for 30 minutes (complete by TLC), and the flask was removed from the cooling bath and quenched with saturated NH_4Cl (aqueous, ~40 mL). The mixture was stirred, vigorously, as the flask warmed to room temperature, and then the biphasic solution was separated. The aqueous layer was extracted with EtOAc (3 x 50 mL), and the organic layers were combined, washed with brine, dried over Na_2SO_4, and concentrated under reduced pressure. The crude mixture was purified via flash column chromatography (silica, 0%–

60% EtOAc in hexanes) to provide triene **2.7.4** (2.1 g, 7.7 mmol, 72% yield) as a pale-yellow oil. TLC (EtOAc/Hexane, 1/1): R_f = 0.4.

FTIR (neat): 3087, 2978, 2928, 1643, 1433, 1287, 1096, 1009, 976, 732 cm^{-1};

Optical Rotation: $[\alpha]_D^{22}$ = -41.8 (c = 0.56 , $CHCl_3$);

^{1}H NMR (500 MHz, $CDCl_3$) δ 5.77 (ddt, J = 15.6, 8.7, 6.7 Hz, 2H, CH_2=C<u>H</u>$CH_aH_bCHO(P$=O)CH_aH_b, $CH_aH_bCHO(P$=O)CH_aH_bC<u>H</u>=CH_2), 5.20–5.09 (m, 4H, C<u>H</u>$_2$=$CHCH_aH_bCHO(P$=O) CH_aH_b, $CH_aH_bCHO(P$=O)CH_aH_bC<u>H</u>=CH_2), 5.04 (s, 1H, (P=O)$OCH_aH_bC(Me)$=C<u>H</u>$_aH_b$), 4.94 (s, 1H, (P=O)$OCH_aH_bC(Me)$=CH_a<u>H</u>$_b$), 4.62 (ddt, J = 20.2, 12.9, 5.9 Hz, 1H, CH_2=$CHCH_aH_bC$<u>H</u>O(P=O) CH_aH_b), 4.54–4.48 (m, 1H, CH_aH_bC<u>H</u>O(P=O)CH_aH_bCH=CH_2), 4.48 (s, 1H, (P=O)OC<u>H</u>$_aH_bC(Me)$=CH_a<u>H</u>$_b$), 4.46 (s, 1H, (P=O)OCH_a<u>H</u>$_bC(Me)$=CH_a<u>H</u>$_b$), 2.66 (dt, J = 13.9, 6.7 Hz, 1H, CH_2=$CHCH_aH_bCHO(P$=O)C<u>H</u>$_aH_b$), 2.55 (dt, J = 13.8, 6.6 Hz, 1H, CH_2=$CHCH_aH_bCHO(P$=O)CH_a<u>H</u>$_b$, CH_2=$CHCH_a$<u>H</u>$_bCHO(P$=O)CH_aH_b), 2.03 (ddd, J = 14.2, 8.6, 5.2 Hz, 1H, $CH_aH_bCHO(P$=O)C<u>H</u>$_aH_bCH$=CH_2), 1.88 (dt, J = 14.7, 4.2 Hz, 1H, $CH_aH_bCHO(P$=O)CH_a<u>H</u>$_bCH$=CH_2), 1.77 (s, 3H, (P=O)OCH_aH_bC(<u>Me</u>)=CH_aH_b);

^{13}C NMR (126 MHz, $CDCl_3$) δ 140.3 (d, J_{CP}= 7.26, <u>C</u>), 132.7 (<u>C</u>H=CH_2), 132.3 (<u>C</u>H=CH_2), 119.1 (CH=<u>C</u>H$_2$), 118.9 (CH=<u>C</u>H$_2$), 113.4 (CH=<u>C</u>H$_2$), 77.4 (d, J_{CP}= 4.6 Hz, <u>C</u>H), 75.7 (d, J_{CP}= 6.4 Hz, <u>C</u>H), 71.0 (d, J_{CP}= 5.46 Hz, <u>C</u>H$_2$), 40.1 (<u>C</u>H$_2$), 39.0 (d, J_{CP}= 2.9 Hz, <u>C</u>H$_2$), 33.3 (d, J_{CP}= 6.5 Hz, <u>C</u>H$_2$), 19.18 (<u>C</u>H$_3$);

^{31}P NMR (202 MHz, $CDCl_3$): δ -6.91

HRMS (ESI-TOF) m/z: $[M + Na]^+$ Calcd for $C_{13}H_{21}O_4PNa$ 295.1075; Found 295.1066.

(2*R*,5*S*,7*S*)-2-methyldodecane-1,5,7-triol ($C_{13}H_{28}O_3$, (2*R*)-2.6.6)

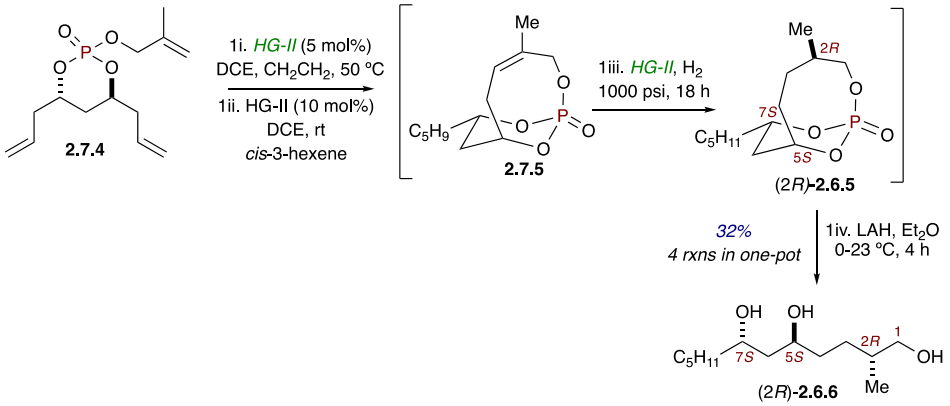

To a round bottom flask, equipped with a stir bar, reflux condenser, and argon inlet, was added triene **2.7.4** (2.0 g, 7.3 mmol, 1 equiv.), degassed 1,2-DCE (with Ar and then ethylene gas) (1450 mL), and Hoveyda-Grubbs second-generation catalyst (HG-II, 94 mg, 0.15 mmol, 2 mol%). The reaction mixture was heated to 50 ºC (with an ethylene gas filled balloon connected to a long needle submerged into the solvent) and stirred 2 hours to ensure complete conversion of reactive starting material. Next, the solvent was evaporated under vacuo and to the same reaction flask was added *cis*-3-hexene (2.7 mL, 21.9 mmol, 3 equiv.), freshly degassed 1,2-DCE (24 mL), and Hoveyda-Grubbs second-generation catalyst (HG-II, 365 mg, 0.58 mmol, 8 mol%). The reaction was stirred at room temperature for 2 hours until **2.7.4** was consumed (monitored by TLC). The reaction was cannulated into a Parr hydrogenation reaction vessel. The vessel was heated to 80 ºC, and H_2 pressure was applied (1000 psi). The reaction stirred at 80 ºC, under H_2 pressure, for 18 h (complete by TLC (EtOAc/Hexane, 3/1): R_f = 0.5), at which point the reaction was cooled to room temperature and solvent removed under reduced pressure. The crude oil was dried under high vacuum (~8 h) to ensure complete removal of 1,2-DCE. The crude mix was taken up in diethyl ether (Et_2O, 73 mL) and cooled to 0 ºC under argon. Solid lithium aluminum hydride ($LiAlH_4$, 1.1 g, 29.2 mmol, 4 equiv.) was added in one portion, and the

reaction flask was removed from the cooling bath and allowed to warm to room temperature. The mixture stirred at room temperature for 6 hours (complete by TLC), and the reaction was cooled to 0 ºC and quenched by 10% sodium potassium tartrate aqueous solution. The reaction was allowed to warm to room temperature and stir at room temperature for 2 hours. The crude mixture was filtered over Celite (washed with EtOAc) and concentrated under reduced pressure. Purification via flash column chromatography (silica, 0%–100% EtOAc in hexanes) provided (2*R*)-**2.6.6** (534 mg, 2.3 mmol, 32% yield over 4 reactions in one pot, 75% average per reaction) as a colorless liquid. TLC (EtOAc): $R_f = 0.3$.

FTIR (neat): 3339 (br), 2930, 2871, 2858, 1460, 1378, 1033, 831 cm^{-1};

Optical Rotation: $[\alpha]_D^{21} = +32.9$ ($c = 0.2$, $CHCl_3$);

^{1}H NMR (500 MHz, $CDCl_3$) δ 3.92 (q, *J* = 6.0, 5.5 Hz, 2H, $CH_3(CH_2)_4C\underline{H}(OH)CH_2C\underline{H}(OH)CH_2$), 3.48 (dd, *J* = 5.6, 4.9 Hz, 2H, $CH(OH)CH_2CH_2CH(Me)C\underline{H_2}OH$), 2.96 (s, 1H, R-OH), 2.63 (s, 1H, R-OH), 2.04 (s, 1H, R-OH), 1.65–1.56 (m, 4H, $CH(OH)C\underline{H_a}H_bCH(OH)C\underline{H_a}H_bC\underline{H_a}H_b$, $C\underline{H}(Me)CH_2OH$), 1.55–1.47 (m, 3H, $C\underline{H_a}H_bCH(OH)CH_a\underline{H_b}CH(OH)CH_a\underline{H_b}$), 1.46–1.38 (m, 2H, $C\underline{H_a}H_bCH_a\underline{H_b}CH(OH)CH_aH_bCH(OH)$), 1.34–1.24 (m, 5H, $CH_3C\underline{H_2}C\underline{H_2}CH_a\underline{H_b}CH_aH_b$), 1.14 (td, *J* = 10.8, 6.1 Hz, 1H, $CH(OH)CH_aH_bCH(OH)CH_2CH_a\underline{H_b}$), 0.92 (d, *J* = 6.6 Hz, 3H, $CH(OH)CH_2CH_2CH(\underline{Me})CH_2OH$), 0.89 (t, *J* = 6.5 Hz, 3H, $C\underline{H_3}(CH_2)_4CH(OH)CH_2$)

^{13}C NMR (126 MHz, $CDCl_3$) δ 69.9 ($\underline{C}H$), 69.6 ($\underline{C}H$), 68.0 ($\underline{C}H_2$), 42.5 ($\underline{C}H_2$), 37.6 ($\underline{C}H_2$), 35.9 ($\underline{C}H$), 34.9 ($\underline{C}H_2$), 32.0 ($\underline{C}H_2$), 29.3 ($\underline{C}H_2$), 25.6 ($\underline{C}H_2$), 22.8 ($\underline{C}H_2$), 16.9 ($\underline{C}H_3$), 14.2 ($\underline{C}H_3$);

HRMS (ESI-TOF) m/z: $[M + Na]^+$ Calcd for $C_{11}H_{24}O_3Na$ 227.1623; Found 227.1629.

(3*R*,6*S*)-6-((*S*)-2-hydroxyheptyl)-3-methyltetrahydro-2*H*-pyran-2-one ($C_{13}H_{24}O_3$, (2*R*)-2.6.6)

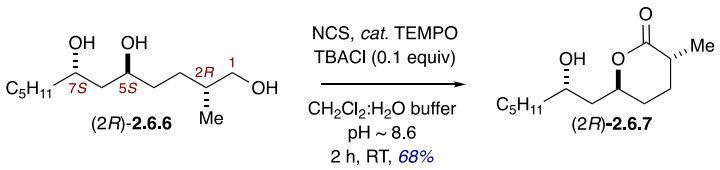

To a round bottom flask, equipped with a stir bar, was added (2*R*)-**2.6.6** (150 mg, 0.64 mmol, 1 equiv.), CH_2Cl_2 (16 mL, 0.04 M), TEMPO (10 mg, 0.064 mmol, 10 mol%), tetrabutylammonium chloride (TBACl, 109 mg, 0.064 mmol, 10 mol%), and aqueous $NaHCO_3/K_2CO_3$ buffer (16 mL, 0.5 M $NaHCO_3$: 0.05 M K_2CO_3). To the stirring biphasic solution was added *N*-chlorosuccinimide (434 mg, 3.3 mmol, 5 equiv.) in one portion, and the reaction continued to vigorously stir at room temperature for 2 hours (complete by TLC). The biphasic solution was diluted with CH_2Cl_2 (5 mL) and water (5 mL), and the layers separated. The aqueous layer was extracted with CH_2Cl_2 (3 x 10 mL), and the organic layers were combined, dried over Na_2SO_4, filtered over Celite, and concentrated under reduced pressure. Purification via flash column chromatography (silica, 0%-75% EtOAc in hexanes) provided (2*R*)-**2.6.7** (95 mg, 0.42 mmol, 68% yield) as a colorless oil. TLC (EtOAc/Hexane, 3/1): R_f = 0.65.

FTIR (neat): 3518 (br), 2957, 2930, 2860, 1733, 1715, 1466, 1378, 1261, 1182, 950 cm^{-1};

Optical Rotation: $[a]_D^{22}$ = -7.2 (*c* = 0.2, $CHCl_3$);

^{1}H NMR (500 MHz, $CDCl_3$) δ 4.60 (ddt, *J* = 11.1, 9.7, 3.0 Hz, 1H, $CH_3(CH_2)_4CH(OH)CH_aH_bC\underline{H}(OC{=}O)CH_aH_b$), 4.01–3.96 (m, 1H, $CH_3(CH_2)_4C\underline{H}(OH)CH_aH_bCH(OC{=}O)CH_aH_b$), 2.45 (dt, *J* = 11.3, 7.0, 4.4, 2.0 Hz, 1H, $CH(OC{=}O)CH_aH_bCH_aH_bC\underline{H}(Me)$), 2.05–2.00 (m, 1H, $CH(OC{=}O)CH_aH_bC\underline{H}_aH_bCH(Me)$), 1.94–1.90 (m, 1H, $CH(OC{=}O)C\underline{H}_aH_bCH_aH_bCH(Me)$,

1.77 (ddd, J = 14.5, 9.8, 2.4 Hz, 1H, $CH_3(CH_2)_4CH(OH)C\underline{H}_aH_bCH(OC{=}O)$), 1.64–1.55 (m, 3H, $CH_3(CH_2)_4CH(OH)CH_a\underline{H}_bCH(OC{=}O)$, $CH(OC{=}O)CH_a\underline{H}_bCH_a\underline{H}_bCH(Me)$), 1.47–1.39 (m, 3H, $CH_3(CH_2)_2C\underline{H}_2C\underline{H}_aH_bCH(OH)$, 1.30 (d J = 7.1Hz, 3H, $CH(OC{=}O)CH_aH_bCH_aH_bCH(\underline{Me})$, 1.28–1.22 (m, 5H, $CH_3(C\underline{H}_2)_2CH_2CH_a\underline{H}_bCH(OH)$), 0.89 (t, J = 6.9 Hz, 3H, $C\underline{H}_3(CH_2)_3CH_aH_bCH(OH)$);

^{13}C NMR (126 MHz, $CDCl_3$) δ 174.4 ($\underline{C}{=}O$), 78.8 ($\underline{C}H$), 67.6 ($\underline{C}H$), 43.9 ($\underline{C}H_2$), 38.1 ($\underline{C}H_2$), 36.3($\underline{C}H$), 31.9 ($\underline{C}H_2$), 30.0 ($\underline{C}H_2$), 28.8 ($\underline{C}H_2$), 25.4 ($\underline{C}H_2$) 22.8 ($\underline{C}H_2$), 17.6 ($\underline{C}H_3$), 14.2 ($\underline{C}H_3$);

HRMS (ESI-TOF) m/z: $[M + Na]^+$ Calcd for $C_{13}H_{24}O_3Na$ 251.1623; Found 251.1635.

(3*R*,6*S*)-6-((*S*)-2-methoxyheptyl)-3-methyltetrahydro-2*H*-pyran-2-one ($C_{14}H_{26}O_3$, (2*R*)-2.1.6)

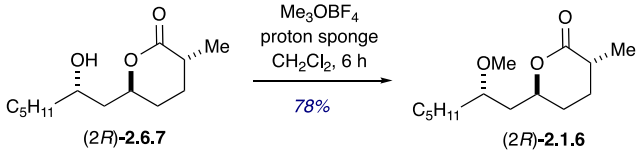

To a round bottom flask, equipped with a magnetic stir bar, was added (2*R*)-**2.6.7** (65 mg, 0.28 mmol, 1 equiv.) in CH_2Cl_2 (3 mL), proton sponge (600 mg, 2.8 mmol, 10 equiv.), and trimethyloxonium tetrafluoroborte (414 mg, 2.8 mmol, 10 equiv.) and stirred the mixture for 6 h (complete by TLC). The solution was diluted with CH_2Cl_2 5 mL and saturated $NaHCO_3$ (3 mL), and the layers separated. The aqueous layer was extracted with CH_2Cl_2 (3 x 5 mL), and the organic layers were combined, dried over Na_2SO_4, filtered, and concentrated under reduced pressure. Purification via flash column chromatography (silica, 0%-50% EtOAc in hexanes) provided (2*R*)-**2.1.6** (51 mg, 0.21 mmol, 78% yield) as a yellow oil. TLC (EtOAc/Hexane, 1/1): $R_f = 0.5$.

FTIR (neat): 2931, 2872, 2858, 1734, 1460, 1377, 1285, 1240, 1173, 1092, 1012, 933, 747 cm^{-1};

Optical Rotation: $[\alpha]_D^{23} = +21.0$ ($c = 0.1$, $CHCl_3$);

^{1}H NMR (500 MHz, $CDCl_3$) δ 4.51 (tq, $J = 9.7, 3.0$ Hz, 1H, $CH_3(CH_2)_4CH(OMe)CH_aH_bC\underline{H}(OC{=}O)CH_aH_b$), 3.56–3.51 (m, 1H, $CH_3(CH_2)_4C\underline{H}(OMe)CH_aH_bCH(OC{=}O)CH_aH_b$), 3.37 (s, 3H, $CH_3(CH_2)_4CH(O\underline{Me})CH_aH_bCH(OC{=}O)CH_aH_b$), 2.44 (dddd, $J = 11.3, 7.0, 4.4, 2.0$ Hz, 1H, $CH(OC{=}O)CH_aH_bCH_aH_bC\underline{H}(Me)$), 2.01 (m, 1H, $CH(OC{=}O)CH_aH_bC\underline{H}_aH_bCH(Me)$), 1.94–1.86 (m, 1H, $CH(OC{=}O)C\underline{H}_aH_bCH_aH_bCH(Me)$), 1.75–1.68 (m, 1H,

$CH_3(CH_2)_4CH(OMe)C\underline{H}_aH_bCH(OC{=}O)$), 1.63–1.55 (m, 3H, $CH_3(CH_2)_4CH(OMe)CH_a\underline{H}_bCH(OC{=}O)$, $CH(OC{=}O)CH_a\underline{H}_bCH_a\underline{H}_bCH(Me)$) 1.42 (dq, *J* = 1.55–1.47 (m, 1H, $CH_3(CH_2)_3C\underline{H}_aH_bCH(OMe)$), 1.46–1.37 (m, 1H, $CH_3(CH_2)_3C\underline{H}_aH_bCH(OMe)$), 1.46–1.37 (m, 1H, $CH_3(CH_2)_3CH_a\underline{H}_bCH(OMe)$), 1.31 (d, *J* = 7.1Hz, 3H, $CH(OC{=}O)CH_aH_bCH_aH_bCH(\underline{Me})$), 1.29–1.20 (m, 6H, $CH_3(C\underline{H}_2)_3CH_aH_bCH(OMe)$), 0.89 (td, *J* = 4.4, 3.6 Hz, 3H, $C\underline{H}_3(CH_2)_3CH_aH_bCH(OMe)$);

^{13}C NMR (126 MHz, $CDCl_3$) δ 174.5 ($\underline{C}{=}O$), 78.8 ($\underline{C}H$), 76.6 ($\underline{C}H$), 57.3 ($\underline{C}H_3$), 42.2 ($\underline{C}H_2$), 36.3 ($\underline{C}H$), 33.7 ($\underline{C}H_2$), 32.2 ($\underline{C}H_2$), 30.1 ($\underline{C}H_2$), 28.8 ($\underline{C}H_2$), 24.6 ($\underline{C}H_2$) 22.8 ($\underline{C}H_2$), 17.6 ($\underline{C}H_3$), 14.2 ($\underline{C}H_3$);

HRMS (ESI-TOF) m/z: $[M + Na]^+$ Calcd for $C_{14}H_{26}O_3Na$ 265.1780; Found 265.1786.

Data Table for ^{13}C ppm Values of Two Triols (2*S*)-2.6.6 and (2*R*)-2.6.6

Table 5.1

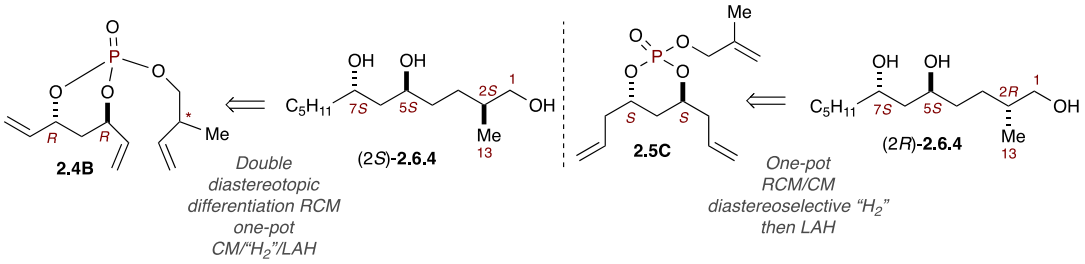

C#	(2*S*)-**2.6.6**	(2*R*)-**2.6.6**	Δδ ppm
1	67.9	68	0.1
2	34.3	36	1.7
3	29.2	29.3	0.1
4	25.5	25.6	0.1
5	69.5	69.9	0.4
6	37.4	37.5	0.1
7	69.2	69.6	0.4
13	16.6	16.9	0.3

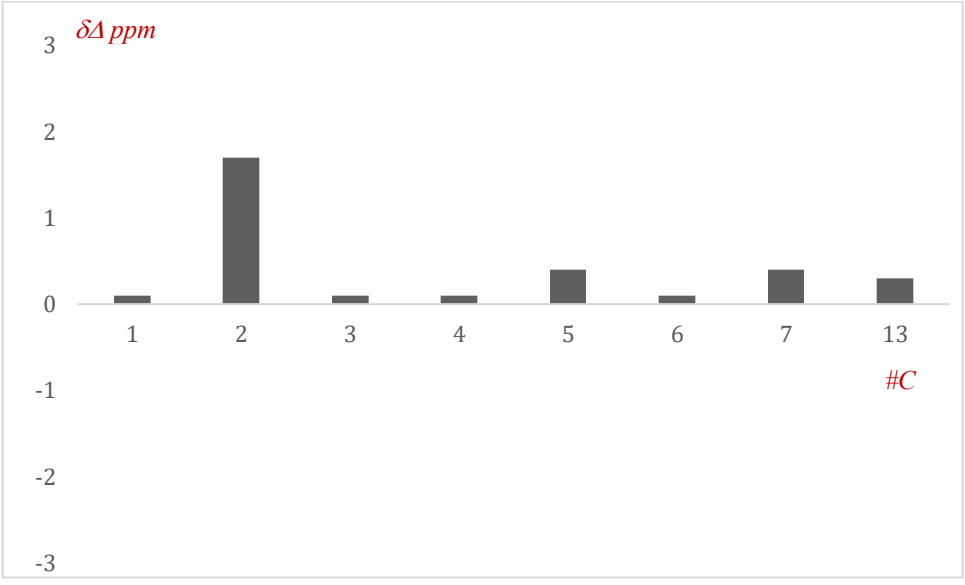

Figure 5.1 *^{13}C Δδ ppm values of two triols (2*S*)-**2.6.6** and (2*R*)-**2.6.6***

Data table for ^{13}C ppm values of two lactones (2*S*)-2.6.7 and (2*R*)-2.6.7

Table 5.2

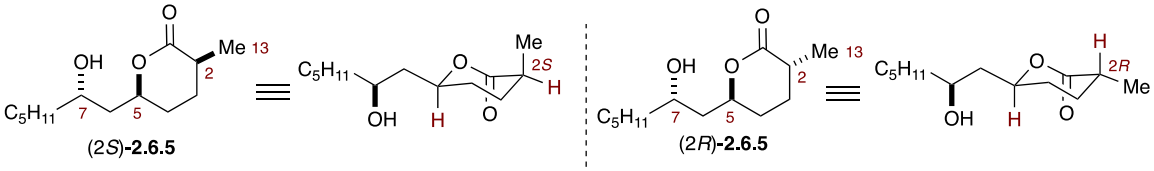

C#	(2*S*)-**2.6.7**	(2*R*)-**2.6.7**	Δδ ppm
1	176.6	174.4	-2.2
2	33.3	36.3	3
3	25.8	28.8	3
4	27.4	30	2.6
5	75	78.8	3.8
6	42.9	43.9	1
7	67.7	67.6	-0.1
13	16.2	17.6	1.4

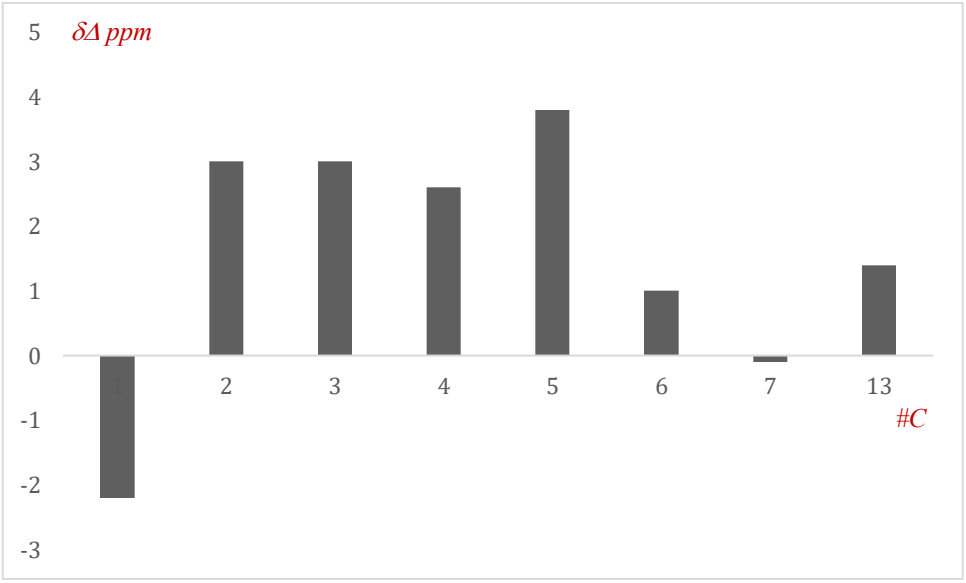

Figure 5.2 *^{13}C Δδ ppm values of two lactones (2*S*)-**2.6.7** and (2*R*)-**2.6.7***

Data table for ^{13}C ppm values of two lactone methyl ethers (2*S*)-2.1.6 from Brimble's synthesis and this synthesis

Table 5.3

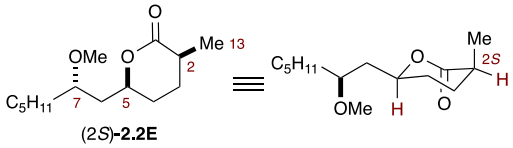

(2*S*)-**2.2E**

C#	Brimble NMR data[4] (2*S*)-**2.1.6**	this synthesis (2*S*)-**2.1.6**	Δδ ppm
1	176.5	176.8	0.3
2	33.1	33.3	0.2
3	25.7	25.8	0.1
4	27.3	27.5	0.2
5	74.8	74.9	0.1
6	40.9	41	0.1
7	76.5	76.6	0.1
13	16.1	16.2	0.1
OMe	57	57.2	0.2

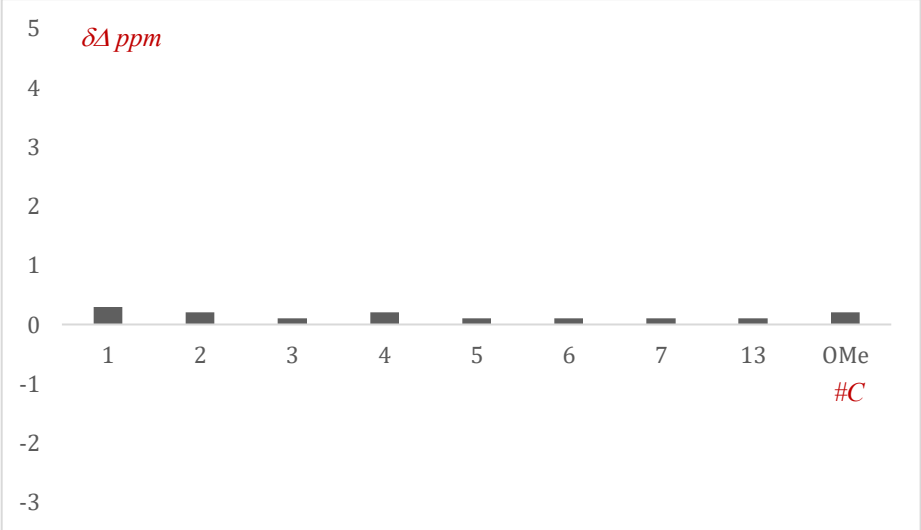

Figure 5.3 *^{13}C Δδ ppm values of two lactone methyl ethers (2*S*)-**2.1.6** from Brimble's synthesis and this synthesis*

[4] Wadsworth, A. D.; Furkert, D. P.; Brimble, M. A. Total Synthesis of the Macrocyclic *N*-Methyl Enamides Palmyrolide A and 2*S*-Sanctolide A. *J. Org. Chem.* **2014**, *79*, 11179–11193.

Data table for ^{13}C ppm values of two lactone methyl ethers (2*S*)-2.1.6 and (2*R*)-2.1.6

Table 5.3

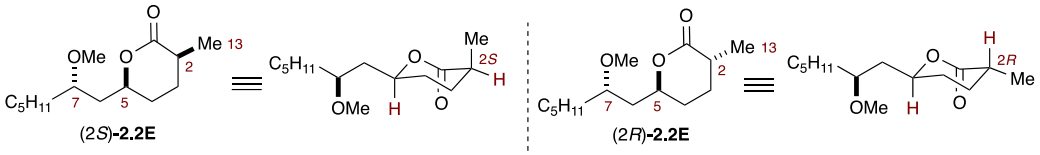

C#	(2*S*)-**2.1.6**	(2*R*)-**2.1.6**	Δδ ppm
1	176.8	174.5	-2
2	33.3	36.3	3.2
3	25.8	28.8	3.1
4	27.5	30.1	2.8
5	74.9	78.8	4
6	41	42	1.1
7	76.6	76.6	0.1
13	16.2	17.6	1.5
OMe	57.2	57.3	0.3

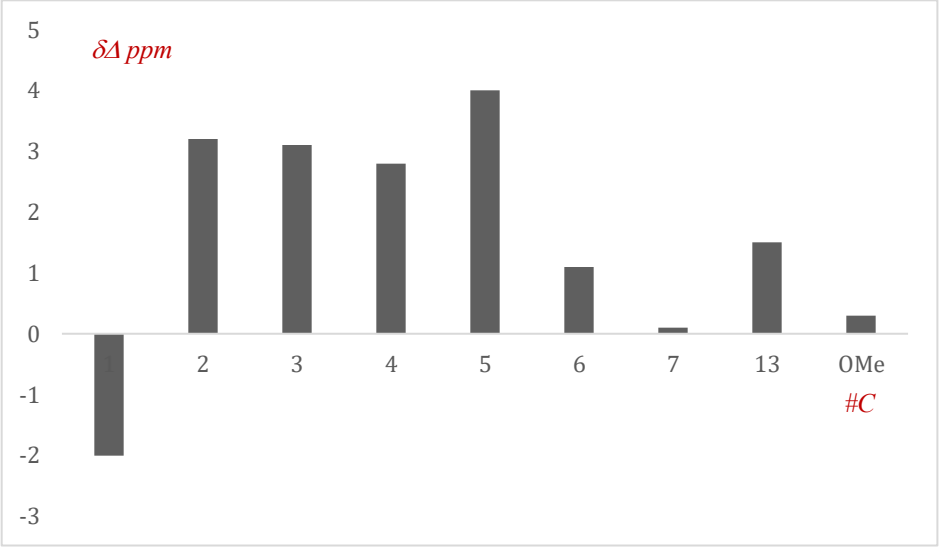

Figure 5.3 *^{13}C Δδ ppm values of two lactones (2*S*)-**2.1.6** and (2*R*)-**2.1.6***

Diastereomeric Rotamer Mixtures of (2*R*,5*S*,7*S*)-*N*-allyl-5-hydroxy-7-methoxy-*N*,2-dimethyldodecanamide ((2*R*)-2.2.2) and **(2*S*,5*S*,7*S*)-*N*-allyl-5-hydroxy-7-methoxy-*N*,2-dimethyldodecanamide ((2*S*)-2.2.2) ($C_{18}H_{35}NO_3$)**

Scheme 5.1

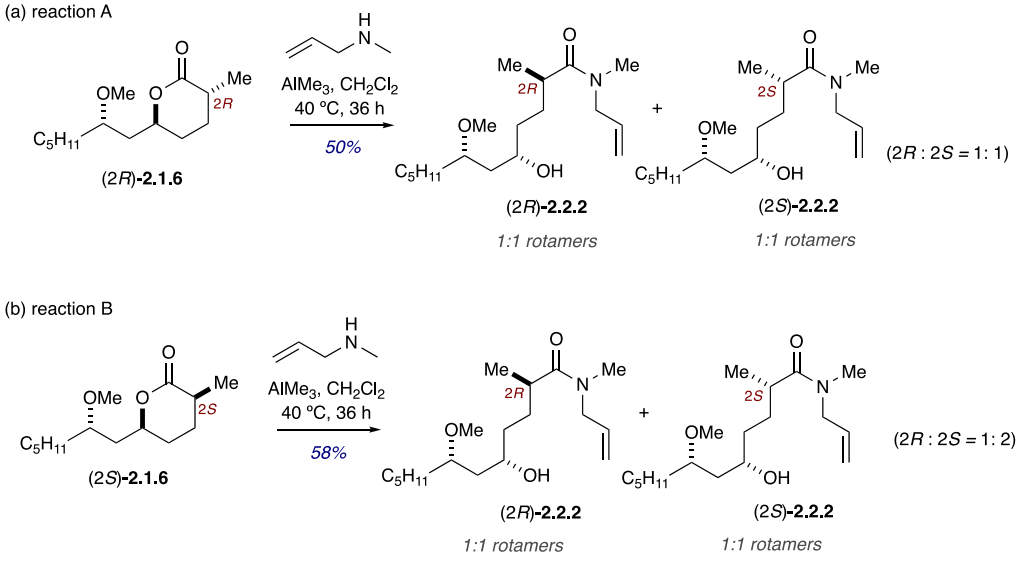

Reaction A

To a solution of *N*-allylmethylamine (40 µL, 0.4 mmol, 2 equiv.) in CH_2Cl_2 (2 mL, 0.2 M), was added trimethylaluminum (2 M in toluene, 0.175 mL, 0.35 mmol, 1.75 equiv.) at room temperature and stirred for 30 minutes. Then the mixture was cannulated under argon to a solution of lactone methyl ether (2*R*)-**2.1.6** (50 mg, 0.2 mmol, 1 equiv.) in CH_2Cl_2 (1 mL, 0.2 M) in a pressure vial and stirred at 40 ºC for 18 hours (TLC monitoring). Then the reaction mixture was cooled to room temperature and an additional 1.75 equivalence of *N*-allylmethylamine aluminum complex in CH_2Cl_2 was added and continued stirring for 12 more hours at 40 ºC (complete by TLC). Reaction mixture was diluted with CH_2Cl_2 (2 mL) and quenched carefully with 1 M HCl solution (1 mL) at 0 ºC. The aqueous layer was extracted with CH_2Cl_2 (3 x 2 mL), and the organic layers were combined, dried over Na_2SO_4, filtered, and concentrated under reduced pressure.

Purification via flash column chromatography (silica, 0%–100% EtOAc in hexanes) delivered the amide (2*R*)-**2.2.2** and (2*S*)-**2.2.2** (30 mg, 0.10 mmol, 50% yield) as a mixture of diastereomers (2*R*: 2*S*: 1: 1) and rotamers (1:1) as a colorless oil. TLC (EtOAc/Hexane, 2/3): R_f = 0.4.

FTIR (neat) 3429 (br), 3082, 2930, 2858, 1632, 1461, 1404, 1271, 1229, 1092, 990 cm^{-1};

Optical Rotation: $[a]_D^{22}$ = -10.1 (c = 0.32 , $CHCl_3$);

***Note: ^1H and ^{13}C NMR assignments for the mixture of 2*R* and 2*S*-diastereomers were made by comparing to the epimer (2*R*)-**2.2.2**.

^1H NMR (500 MHz, $CDCl_3$) δ 5.83–5.69 (m, 1H,(2*R*, 2*S*-isomer, two rotamers) C(O)N(Me)CH_2C<u>H</u>=CH_2), 5.24–5.09 (m, 2H,(2*R*, 2*S*-isomer, Two rotamers) C(O)N(Me)CH_2CH=C<u>H</u>$_2$), 4.07–3.92 (m, 2H,(2*R*, 2*S*-isomer, Two rotamers) C(O)N(Me)C<u>H</u>$_a$<u>H</u>$_b$CH=CH_2), 3.85 (t, J = 6.6 Hz, 0.5H,(2*R*-isomer, two rotamers) CH(OMe)$CH_a$$H_b$C<u>H</u>(OH)$CH_a$$H_b$), 3.79 (tt, J = 8.75, 4.01 Hz, 0.5H, (2*S*-isomer, two rotamers) CH(OMe)$CH_a$$H_b$C<u>H</u>(OH)$CH_a$$H_b$), 3.48–3.42 (m, 1H, (2*S*-, 2*R*-isomer, two rotamers), $CH_3(CH_2)_4$C<u>H</u>(OMe)$CH_a$$H_b$CH(OH)$CH_a$$H_b$), 3.35 (d, J = 8.75, 4.01 Hz, 3H,(2*R*, 2*S*-isomer, two rotamers) $CH_3(CH_2)_4$CH(O<u>Me</u>)$CH_a$$H_b$CH(OH)$CH_a$$H_b$), 2.96 (d, J = 32.6 Hz, 1.5H, (2*S*-isomer, two rotamers), C(O)N(<u>Me</u>)CH_2CH=CH_2), 2.95 (d, J = 30.0 Hz, 1.5H, (2*R*-isomer, two rotamers), C(O)N(<u>Me</u>)CH_2CH=CH_2), 2.76–2.57 (m, 1H, (2*S*-, 2*R*-isomer, two rotamers), CH(OH) CH_2CH_2C<u>H</u>(Me)C(O)N(Me)CH_2), 1.87–1.75 (m, 1H, CH(OH) CH_2C<u>H</u>$_a$<u>H</u>$_b$CH(Me)C(O)N(Me)CH_2), 1.69–1.60 (m, 2H, $CH_3(CH_2)_3$C<u>H</u>$_a$<u>H</u>$_b$CH(OMe)C<u>H</u>$_a$<u>H</u>$_b$CH(OH)), 1.57–1.49 (m, 1H, $CH_3(CH_2)_3CH_a$$H_b$CH(OMe)$CH_a$<u>H</u>$_b$CH(OH), 1.49–1.36 (m, 4H, $CH_3(CH_2)_3CH_a$<u>H</u>$_b$CH(OMe)$CH_a$$H_b$CH(OH),

CH(OH)C$\underline{H}_2$C$\underline{H}_a$H$_b$CH(Me)C(O)N(Me)CH$_2$), 1.32–1.23 (m, 6H, CH$_3$(C$\underline{H}_2$)$_3$CH$_a$H$_b$CH(OMe)), 1.12 (t, J = 6.7 Hz, 3H, (2*S*-, 2*R*-isomer, two rotamers) CH(OH)CH$_2$CH$_a$H$_b$CH($\underline{Me}$)C(O)N(Me)CH$_2$), 0.89 (t, J = 6.9 Hz, 3H, C$\underline{H}_3$(CH$_2$)$_3$CH$_a$H$_b$CH(OMe)CH$_a$H$_b$CH(OH));

^{13}C NMR (126 MHz, CDCl$_3$) δ 177.2 (C=O, amide)$_{2S}$, 177.0 (C=O, amide)$_{2R}$, 176.7 (C=O, amide)*$_{2S}$, 176.4 (C=O, amide)*$_{2R}$, 133.4 ($\underline{C}$H=CH$_2$)$_{2R}$, 133.3 ($\underline{C}$H=CH$_2$)$_{2S}$, 133.21 ($\underline{C}$H=CH$_2$)*$_{2R}$, 133.17 ($\underline{C}$H=CH$_2$)*$_{2S}$, 117.13 (CH=$\underline{C}$H$_2$)$_{2S}$, 117.09 (CH=$\underline{C}$H$_2$)$_{2R}$, 116.8 (CH=$\underline{C}$H$_2$)*$_{2S}$, 116.7 (CH=$\underline{C}$H$_2$)*$_{2R}$, 79.7 (2, $\underline{C}$H)$_{2R}$, 79.6 ($\underline{C}$H)$_{2S}$, 79.5 ($\underline{C}$H)*$_{2S}$, 68.8 (2, $\underline{C}$H)$_{2R}$, 68.3 ($\underline{C}$H)$_{2S}$, 68.1 ($\underline{C}$H)*$_{2S}$, 56.97 ($\underline{C}$H$_3$)$_{2S}$, 56.94 ($\underline{C}$H$_3$)*$_{2S}$, 56.9 (2, $\underline{C}$H$_3$)$_{2R}$, 52.20 ($\underline{C}$H$_2$)$_{2S}$, 52.16 ($\underline{C}$H$_2$)$_{2R}$, 50.4 ($\underline{C}$H$_2$)*$_{2S}$, 50.3 ($\underline{C}$H$_2$)*$_{2R}$, 39.6 ($\underline{C}$H$_2$)$_{2S}$, 39.4 ($\underline{C}$H$_2$)*$_{2S}$, 39.18 ($\underline{C}$H$_2$)$_{2R}$, 39.1 ($\underline{C}$H$_2$)*$_{2R}$, 36.2 ($\underline{C}$H)$_{2S}$, 35.93 ($\underline{C}$H)$_{2R}$, 35.90 ($\underline{C}$H)*$_{2S}$, 35.7 ($\underline{C}$H)*$_{2R}$, 36.1 ($\underline{C}$H$_2$)$_{2S}$, 36.0 ($\underline{C}$H$_2$)*$_{2S}$, 35.49 ($\underline{C}$H$_2$)$_{2R}$, 35.46 ($\underline{C}$H$_2$)*$_{2R}$, 34.9 ($\underline{C}$H$_3$)$_{2S}$, 34.8 ($\underline{C}$H$_3$)$_{2R}$, 34.0 ($\underline{C}$H$_3$)*$_{2S}$, 33.96 ($\underline{C}$H$_3$)*$_{2R}$, 33.2 ($\underline{C}$H$_2$)$_{2S}$, 33.1 ($\underline{C}$H$_2$)*$_{2S}$, 33.0 (2, $\underline{C}$H$_2$)$_{2R}$, 32.1 (4, CH$_2$)$_{2S,2R}$, 30.4 ($\underline{C}$H$_2$)$_{2S}$, 30.2 ($\underline{C}$H$_2$)$_{2R}$, 30.0 ($\underline{C}$H$_2$)*$_{2S}$, 29.9 ($\underline{C}$H$_2$)*$_{2R}$, 25.3 (4, $\underline{C}$H$_2$)$_{2S,2R}$, 22.8 (4, $\underline{C}$H$_2$)$_{2S,2R}$, 18.8 ($\underline{C}$H$_3$)$_{2S}$, 18.22 ($\underline{C}$H$_3$)*$_{2S}$, 18.2 ($\underline{C}$H$_3$)$_{2R}$, 17.6 ($\underline{C}$H$_3$)*$_{2R}$, 14.2 (4, $\underline{C}$H$_3$)$_{2S,2R}$;

* rotamer

HRMS (ESI-TOF) m/z: [M + Na]$^+$ Calcd for C$_{18}$H$_{35}$NO$_3$Na 336.2515; Found 336.2513.

Reaction B

To a solution of *N*-allylmethylamine (25 μL, 0.24 mmol, 2 equiv.) in CH_2Cl_2 (1 mL, 0.2 M), was added trimethylaluminum (2 M in toluene, 0.105 mL, 0.28 mmol, 1.75 equiv.) at room temperature and stirred for 30 minutes. Then the mixture was cannulated under argon to a solution of lactone methyl ether (2*S*)-**2.1.6** (30 mg, 0.12 mmol, 1 equiv.). in CH_2Cl_2 (0.5 mL, 0.2 M) in a pressure vial and stirred at 40 ºC for 18 hours (TLC monitoring). Then the reaction mixture was cooled to room temperature and an additional 1.75 equivalence of *N*-allylmethylamine aluminum complex in CH_2Cl_2 was added and continued stirring for 12 more hours at 40 ºC (complete by TLC). Reaction mixture was diluted with CH_2Cl_2 (2 mL) and quenched carefully with 1 M HCl solution (1 mL) at 0 ºC. The aqueous layer was extracted with CH_2Cl_2 (3 x 2 mL), and the organic layers were combined, dried over Na_2SO_4, filtered, and concentrated under reduced pressure. Purification via flash column chromatography (silica, 0%–100% EtOAc in hexanes) delivered the amide (2*R*)-**2.2.2** and (2*S*)-**2.2.2** (18 mg, 0.05 mmol, 48% yield) as a mixture of diastereomers (2*R*: 2*S*: 1: 2) and rotamers (1:1) as a colorless oil. TLC (EtOAc/Hexane, 2/3): $R_f = 0.4$.

FTIR (neat): 3429 (br), 3082, 2930, 2858, 1633, 1461, 1405, 1271, 1093, 990, 990, 802 cm^{-1};

Optical Rotation: $[a]_D^{22} = +19.0$ ($c = 0.1$, $CHCl_3$);

***Note: ^1H and ^{13}C NMR assignments for the mixture of 2*R* and 2*S*-diastereomers were made by comparing to the epimer (2*R*)-**2.2.2**.

^1H NMR (500 MHz, $CDCl_3$) δ 5.83–5.68 (m, 1H,(2*R*, 2*S*-isomer, two rotamers) C(O)N(Me)CH_2C<u>H</u>=CH_2), 5.25–5.09 (m, 2H,(2*R*, 2*S*-isomer, two rotamers)

C(O)N(Me)$CH_2CH=C\underline{H}_2$), 4.07–3.93 (m, 2H,(2*R*, 2*S*-isomer, two rotamers)

C(O)N(Me)$C\underline{H}_a\underline{H}_bCH=CH_2$), 3.88–3.82 (t, J = 6.6 Hz, 0.36H,(2*R*-isomer, two rotamers)

$CH(OMe)CH_aH_bC\underline{H}(OH)CH_aH_b$), 3.81–3.74 (tt, J = 8.75, 4.01 Hz, 0.69H, (2*S*-isomer, two rotamers) $CH(OMe)CH_aH_bC\underline{H}(OH)CH_aH_b$), 3.49–3.42 (m, 1H, (2*S*-, 2*R*-isomer, two rotamers),

$CH_3(CH_2)_4C\underline{H}(OMe)CH_aH_bCH(OH)CH_aH_b$), 3.35 (d, J = 8.75, 4.01 Hz, 3H,(2*R*, 2*S*-isomer, two rotamers) $CH_3(CH_2)_4CH(O\underline{Me})CH_aH_bCH(OH)CH_aH_b$), 2.96 (d, J = 32.6 Hz, 2H, (2*S*-isomer, two rotamers), C(O)N($\underline{Me}$)$CH_2CH=CH_2$), 2.95 (d, J = 30.0 Hz, 1H, (2*R*-isomer, two rotamer),

C(O)N($\underline{Me}$)$CH_2CH=CH_2$), 2.76–2.57 (m, 1H, (2*S*-, 2*R*-isomer, two rotamers), CH(OH)

$CH_2CH_2C\underline{H}$(Me)C(O)N(Me)CH_2), 1.87–1.74 (m, 1H, CH(OH)

$CH_2C\underline{H}_aH_bCH$(Me)C(O)N(Me)$CH_2$), 1.69–1.60 (m, 2H,

$CH_3(CH_2)_3C\underline{H}_aH_bCH(OMe)C\underline{H}_aH_bCH(OH)$), 1.57–1.49 (m, 1H,

$CH_3(CH_2)_3CH_aH_bCH(OMe)CH_a\underline{H}_bCH(OH)$, 1.49–1.36 (m, 4H,

$CH_3(CH_2)_3CH_a\underline{H}_bCH(OMe)CH_aH_bCH(OH)$,

$CH(OH)C\underline{H}_2C\underline{H}_aH_bCH$(Me)C(O)N(Me)$CH_2$), 1.32–1.23 (m, 6H,

$CH_3(C\underline{H}_2)_3CH_aH_bCH(OMe)$), 1.12 (t, J = 6.4 Hz, 3H, (2*S*-, 2*R*-isomer, two rotamers)

$CH(OH)CH_2CH_aH_bCH(\underline{Me})$C(O)N(Me)$CH_2$), 0.89 (t, J = 6.7 Hz, 3H,

$C\underline{H}_3(CH_2)_3CH_aH_bCH(OMe)CH_aH_bCH(OH)$);

^{13}C NMR (126 MHz, $CDCl_3$) δ 177.2 (C=O, amide)$_{2S}$, 177.0 (C=O, amide)$_{2R}$, 176.7 (C=O, amide)*$_{2S}$, 176.4 (C=O, amide)*$_{2R}$, 133.4 ($\underline{C}H=CH_2$)$_{2R}$, 133.3 ($\underline{C}H=CH_2$)$_{2S}$, 133.22 ($\underline{C}H=CH_2$)*$_{2R}$, 133.18 ($\underline{C}H=CH_2$)*$_{2S}$, 117.13 ($CH=\underline{C}H_2$)$_{2S}$, 117.09 ($CH=\underline{C}H_2$)$_{2R}$, 116.8 ($CH=\underline{C}H_2$)*$_{2S}$, 116.7 ($CH=\underline{C}H_2$)*$_{2R}$, 79.7 (2, $\underline{C}H$)$_{2R}$, 79.6 ($\underline{C}H$)$_{2S}$, 79.5 ($\underline{C}H$)*$_{2S}$, 68.8 (2, $\underline{C}H$)$_{2R}$, 68.3 ($\underline{C}H$)$_{2S}$, 68.1 ($\underline{C}H$)*$_{2S}$, 56.97 ($\underline{C}H_3$)$_{2S}$, 56.95 ($\underline{C}H_3$)*$_{2S}$, 56.9 (2, $\underline{C}H_3$)$_{2R}$, 52.20 ($\underline{C}H_2$)$_{2S}$, 52.16 ($\underline{C}H_2$)$_{2R}$, 50.4 ($\underline{C}H_2$)*$_{2S}$, 50.3 ($\underline{C}H_2$)*$_{2R}$, 39.6 ($\underline{C}H_2$)$_{2S}$, 39.4 ($\underline{C}H_2$)*$_{2S}$, 39.15

($\underline{C}H_2)_{2R}$, 39.1 ($\underline{C}H_2$)*$_{2R}$, 36.2 ($\underline{C}H)_{2S}$, 35.92 ($\underline{C}H)_{2R}$, 35.91 ($\underline{C}H$)*$_{2S}$, 35.7 ($\underline{C}H$)*$_{2R}$, 36.1 ($\underline{C}H_2)_{2S}$, 36.0 ($\underline{C}H_2$)*$_{2S}$, 35.48 ($\underline{C}H_2)_{2R}$, 35.46 ($\underline{C}H_2$)*$_{2R}$, 34.9 ($\underline{C}H_3)_{2S}$, 34.8 ($\underline{C}H_3)_{2R}$, 34.0 ($\underline{C}H_3$)*$_{2S}$, 33.96 ($\underline{C}H_3$)*$_{2R}$, 33.2 ($\underline{C}H_2)_{2S}$, 33.1 ($\underline{C}H_2$)*$_{2S}$, 33.0 (2, $\underline{C}H_2)_{2R}$, 32.1 (4, $CH_2)_{2S,2R}$, 30.4 ($\underline{C}H_2)_{2S}$, 30.2 ($\underline{C}H_2)_{2R}$, 30.0 ($\underline{C}H_2$)*$_{2S}$, 29.9 ($\underline{C}H_2$)*$_{2R}$, 25.3 (4, $\underline{C}H_2)_{2S,2R}$, 22.8 (4, $\underline{C}H_2)_{2S,2R}$, 18.8 ($\underline{C}H_3)_{2S}$, 18.23 ($\underline{C}H_3$)*$_{2S}$, 18.2 ($\underline{C}H_3)_{2R}$, 17.6 ($\underline{C}H_3$)*$_{2R}$, 14.2 (4, $\underline{C}H_3)_{2S,2R}$;

* rotamer

HRMS (ESI-TOF) m/z: $[M + Na]^+$ Calcd for $C_{18}H_{35}NO_3Na$ 336.2515; Found 336.2502.

^{13}C Comparison of the Epimeric Products of the Reactions A and B

2*R* and 2*S* epimers identified by comparing to 2*R* epimer (Table 5.5)

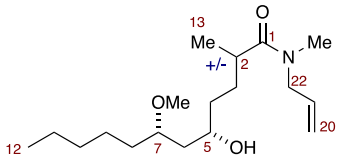

Table 5.4 ^{13}C data for products obtained from two reactions A and B (Scheme 5.1)

C #	Pdt of Reaction A ^{13}C (±0.1 ppm)	Pdt of Reaction B ^{13}C (±0.1 ppm)	δΔ ppm
C1(2*S*)	177.2	177.2	0.0
C1(2*R*)	177.0	177.0	0.0
C1(2*S*)*	176.7	176.7	0.0
C1(2*R*)*	176.4	176.4	0.0
C2(2*S*)	36.2	36.2	0.0
C2(2*R*)	35.9	35.9	0.0
C2(2*S*)*	35.9	35.9	0.0
C2(2*R*)*	35.7	35.7	0.0
C3(2*S*)	33.2	33.2	0.0
C3(2*R*)	33.1	33.1	0.0
C3(2*S*)*	33.0	33.0	0.0
C3(2*R*)*	33.0	33.0	0.0
C4(2S)	36.1	36.1	0.0
C4(2S)*	36.0	36.0	0.0
C4(2R)	35.5	35.5	0.0
C4(2R)*	35.5	35.5	0.0
C5(2*R*)	68.8	68.8	0.0
C5(2*R*)*	68.8	68.8	0.0
C5(2*S*)	68.3	68.3	0.0
C5(2*S*)*	68.1	68.1	0.0
C6(2*S*)	39.6	39.6	0.0
C6(2*S*)*	39.4	39.4	0.0
C6(2*R*)	39.2	39.1	0.1
C6(2*R*)*	39.1	39.1	0.0

Table 5.1 continued

C #	Pdt of Reaction A ^{13}C (±0.1 ppm)	Pdt of Reaction B ^{13}C (±0.1 ppm)	δΔ ppm
C7(2*R*)	79.7	79.7	0.0
C7(2*R*)*	79.7	79.7	0.0
C7(2*S*)	79.6	79.6	0.0
C7(2*S*)*	79.5	79.5	0.0
C8(2*S*)	30.4	30.4	0.0
C8(2*S*)*	30.2	30.2	0.0
C8(2*R*)	30.0	30.0	0.0
C8(2R)*	29.9	29.9	0.0
13(2*S*)	18.8	18.8	0.0
13(2*S*)*	18.2	18.2	0.0
13(2*R*)	18.2	18.2	0.0
13(2*R*)*	17.6	17.6	0.0
OMe(2*S*)	57.0	57.0	0.0
OMe 2*S*)*	56.9	56.9	0.0
OMe (2*R*)	56.9	56.9	0.0
OMe (2*R*)*	56.9	56.9	0.0
NMe(2*S*)	34.9	34.9	0.0
NMe (2*R*)	34.8	34.8	0.0
NMe (2*S*)*	34.0	34.0	0.0
NMe (2*R*)*	33.9	33.9	0.0
C20(2*S*)	117.1	117.1	0.0
C20(2*R*)	117.1	117.1	0.0
C20(2*S*)*	116.8	116.8	0.0
C20(2*R*)*	116.7	116.7	0.0
C21(2*R*)	133.4	133.4	0.0
C21(2*S*)	133.3	133.3	0.0
C21(2*R*)*	133.2	133.2	0.0
C21(2*S*)*	133.2	133.2	0.0
C22(2*S*)	52.2	52.2	0.0
C222*R*)	52.2	52.2	0.0
C22(2*S*)*	50.4	50.4	0.0
C22(2*R*)*	50.3	50.3	0.0

Note: For C9, C10, C11 and C12 single ^{13}C peaks were obtained at 32.1, 25.3, 22.8 and 14.2 ppm values respectively for both epimeric rotamers

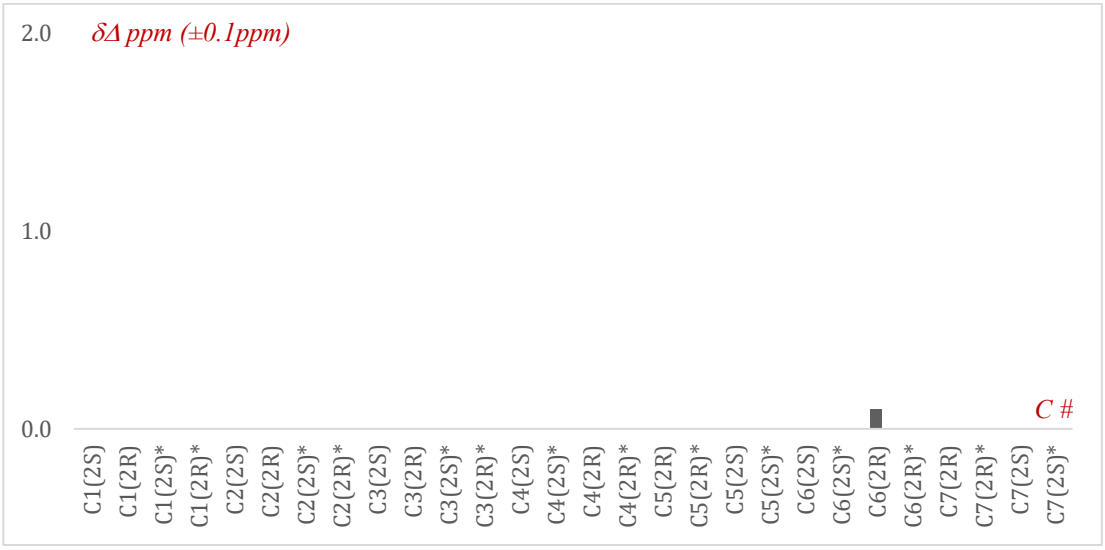

Figure 5.1(a) Graphical representation of δΔ ppm (±0.1 ppm) vs C number (C1–C7)

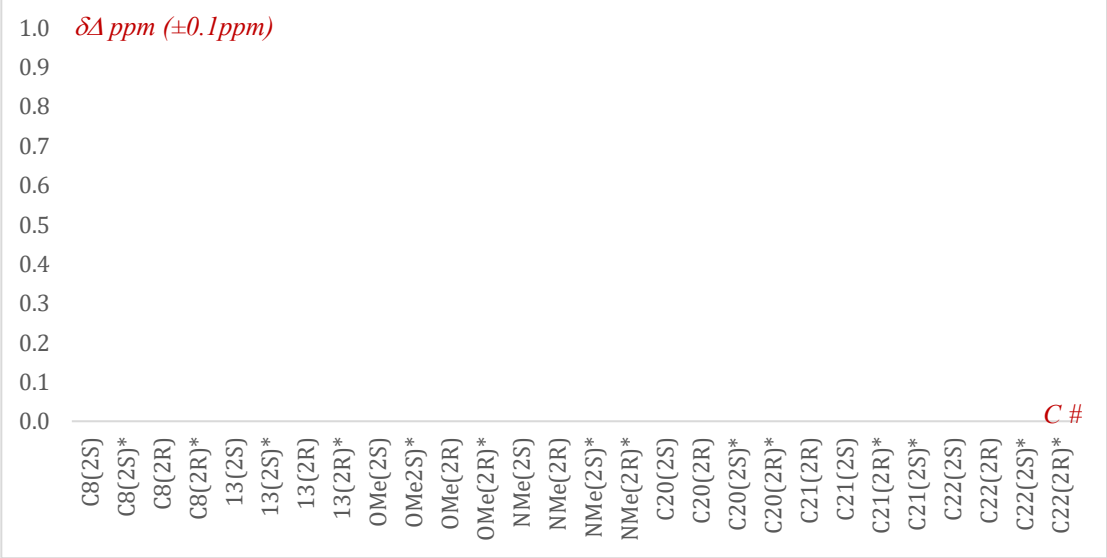

Figure 5.1(b) Graphical representation of δΔ ppm (±0.1 ppm) vs C number (C8–C18)

Epimeric mixture of (5*S*,7*S*)-1-(allyl(methyl)amino)-7-methoxy-2-methyl-1-oxododecan-5-yl (*S*)-2-(acryloyloxy)-3-methylbutanoate ($C_{26}H_{45}NO_6$, (2*R*)-, (2*S*)-2.2.4)

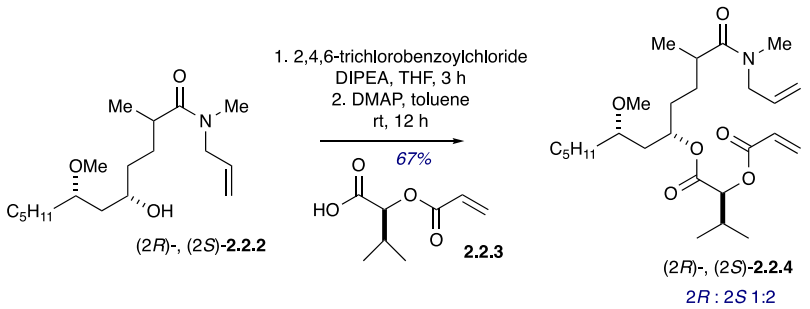

To a solution of (*S*)-2-(acryloyloxy)-3-methylbutanoic acid **2.2.3** (27.5 mg, 0.16 mmol, 2 equiv.) in dry THF (0.3 mL) was added freshly distilled *N*,*N*-diisopropylethylamine (22 µL, 0.14 mmol, 2.5 equiv.) followed by 2,4,6-trichlorobenzoyl chloride (TCBC) (27 µL, 0.25 mmol, 1.8 equiv.) and stirred at room temperature for 3 hours, and the resulted mixed anhydride was concentrated under reduced pressure. The crude mixture was then redissolved in dry toluene (0.3 mL) and cannulated to a stirring solution of amide (2*R*)-, (2*S*)-**2.2.2** (25 mg, 0.08 mmol, 1.0 equiv.) and DMAP (12 mg, 0.1 mmol, 1.2 equiv.) in toluene (0.3 mL) at 0 ºC. After stirring for 15 minutes at 0 ºC the reaction mixture was stirred for an additional 12 hours at room temperature (complete by TLC). Reaction mixture was diluted with CH_2Cl_2 (1 mL) and was added sat. $NaHCO_3$ (2 mL). The aqueous layer was extracted with CH_2Cl_2 (3 x 1.5 mL), and the organic layers were combined, dried over Na_2SO_4, filtered, and concentrated under reduced pressure. Purification via flash column chromatography (silica, 0%–50% EtOAc in hexanes) to obtain diene (2*R*)-, (2*S*)-**2.2.4** (23.5 mg, 0.05 mmol, 67% yield) in a mixture of diastereomeric rotamers (2*R*: 2*S* =1:2, 1:1 rotamers) as a colorless oil. TLC (EtOAc/Hexane, 1/1): R_f = 0.6.

FTIR (neat): 3202, 2955, 2924,2853, 1731, 1657, 1634, 1463, 1406, 1260, 1186, 804 cm^{-1};

Optical Rotation: $[a]_D^{22}$ = +2.3 (c = 0.4 , $CHCl_3$);

^{1}H NMR (500 MHz, $CDCl_3$) δ 6.46 (dd, J = 17.3 , 2.1 Hz, 1H, OC(O)CH(CH(CH_3)$_2$)OC(O)CH=CH_aH_b), 6.25–6.13 (m, 1H, OC(O)CH(CH(CH_3)$_2$)OC(O)CH=CH_aH_b), 5.89 (d, J = 10.5 Hz, 1H, OC(O)CH(CH(CH_3)$_2$)OC(O)CH=CH_aH_b), 5.80–5.68 (m, 1H, (2*R*, 2*S*-isomer, two rotamers) C(O)N(Me)CH_aH_bCH=CH_2), 5.21–5.10 (m, 3H, (2*R*, 2*S*-isomer, two rotamers) C(O)N(Me)CH_aH_bCH=CH_2, $CH_3(CH_2)_4$CH(OMe)CH_aH_bCH(OC(O))CH_aH_b), 4.88 (dd, J = 9.65, 4.2 Hz, 1H, OC(O)CH(CH(CH_3)$_2$)OC(O)CH=CH_aH_b), 4.00–3.88 (m, 1H, (2*R*, 2*S*-isomer, two rotamers) C(O)N(Me)CH_aH_bCH=CH_2), 3.29 (s, 3H, CH(OMe)CH_aH_bCH(OC(O))CH_aH_b), 3.10–3.03 (m, 1H, CH(OMe)CH_aH_bCH(OC(O))CH_aH_b), 2.95 (d, J = 33.8 Hz, 3H, (2*R*-isomer, two rotamers) C(O)N(Me)CH_aH_bCH=CH_2), 2.95 (d, J = 28.8 Hz, 3H, (2*S*-isomer, two rotamers) C(O)N(Me) CH_aH_bCH=CH_2), 2.77–2.58 (m, 1H, (2*R*, 2*S*-isomer, two rotamers) CH(OC(O))CH_2CH_2CH(Me)C(O)N(Me)CH_aH_b), 2.27 (pd, J = 7.0, 4.3 Hz, 1, OC(O)CH(CH(CH_3)$_2$)OC(O)CH=CH_aH_b), 1.77–1.68 (m, 1H, CH(OMe)CH_aH_bCH(OC(O))CH_2CH_aH_b), 1.73–1.62 (m, 6H, CH_2CH(OMe)CH_aH_bCH(OC(O))CH_2CH_aH_b), 1.45–1.35 (m, 1H, CH(OMe)CH_aH_bCH(OC(O))CH_2CH_aH_b), 1.34–1.21 (m, 6H, CH_3(CH_2)$_3$CH_aH_bCH(OMe), 1.11–1.06 (m, 3H, (2*R*, 2*S*-isomer, two rotamers) CH(Me)C(O)N(Me)CH_2), 1.03 (dd, J = 10.1, 6.8 Hz, 6H,

OC(O)CH(CH(C$\underline{H}_3$)$_2$)OC(O)CH=CH$_a$H$_b$), 0.89 (td, J = 7.0 Hz, 3H, C$\underline{H}_3$(CH$_2$)$_3$CH$_a$H$_b$CH(OMe);

^{13}C NMR (126 MHz, $CDCl_3$) δ 176.7 ($\underline{C}$=O, amide)$_{2S,2R}$, 176.0 ($\underline{C}$=O, amide)*$_{2R}$, 175.9 ($\underline{C}$=O, amide)*$_{2S}$, 169.6 ($\underline{C}$=O)$_{2R}$, 169.5 ($\underline{C}$=O)*$_{2R}$, 169.46 ($\underline{C}$=O)$_{2S}$, 169.44 ($\underline{C}$=O)*$_{2S}$,165.8 ($\underline{C}$=O) $_{2S,2R}$, 133.5 ($\underline{C}$H=CH$_2$)$_{2S}$, 133.4 ($\underline{C}$H=CH$_2$)$_{2R}$, 133.3 ($\underline{C}$H=CH$_2$)*$_{2S}$, 133.25 ($\underline{C}$H=CH$_2$)*$_{2R}$, 131.7 (CH=$\underline{C}$H$_2$) $_{2S,2R}$, 128.0 ($\underline{C}$H=CH$_2$) $_{2S,2R}$, 117.1 (CH=C$\underline{H}_2$)$_{2R}$, 116.97 (CH=C$\underline{H}_2$)$_{2S}$, 116.74 (CH=C$\underline{H}_2$)*$_{2R}$, 116.58 (CH=C$\underline{H}_2$)*$_{2S}$, 77.4 ($\underline{C}$H)$_{2S,2R}$, 77.3 ($\underline{C}$H) $_{2S,2R}$, 77.23 (CH)* $_{2S,2R}$, 73.0 ($\underline{C}$H) $_{2S}$, 72.9 ($\underline{C}$H)*$_{2S}$, 72.4 ($\underline{C}$H)$_{2R}$, 57.0 ($\underline{C}$H$_3$)$_{2S,2R}$, 52.18 ($\underline{C}$H$_2$)$_{2R}$, 52.15 ($\underline{C}$H$_2$)$_{2S}$, 50.27 ($\underline{C}$H$_2$)*$_{2S,2R}$, 39.4 ($\underline{C}$H$_2$)$_{2R}$, 39.36 ($\underline{C}$H$_2$)*$_{2R}$, 39.2 ($\underline{C}$H$_2$)$_{2S}$, 39.16 ($\underline{C}$H$_2$)*$_{2S}$, 35.6 ($\underline{C}$H)$_{2S}$, 35.5 ($\underline{C}$H)*$_{2S}$, 35.25 ($\underline{C}$H)$_{2R}$, 35.1 ($\underline{C}$H)*$_{2R}$, 34.8 ($\underline{C}$H$_3$)$_{2S,2R}$, 33.96 ($\underline{C}$H$_3$)*$_{2S}$, 33.93 ($\underline{C}$H$_3$)*$_{2R}$, 33.6 ($\underline{C}$H$_2$)$_{2S,2R}$, 32.3 ($\underline{C}$H$_2$)*$_{2S,2R}$, 32.7 ($\underline{C}$H$_2$)$_{2S}$, 32.6 ($\underline{C}$H$_2$)*$_{2S}$ 32.5 ($\underline{C}$H$_2$)$_{2R}$, 30.26 ($\underline{C}$H) $_{2S}$, 30.24 ($\underline{C}$H) $_{2R}$, 29.5 ($\underline{C}$H$_2$)$_{2S,2R}$, 29.2 ($\underline{C}$H$_2$)*$_{2S,2R}$, 29.1 ($\underline{C}$H$_2$)$_{2S,2R}$, 28.8 ($\underline{C}$H$_2$)*$_{2S,2R}$, 24.7($\underline{C}$H$_2$)$_{2S,2R}$, 22.8($\underline{C}$H$_2$)$_{2S,2R}$, 19.15 ($\underline{C}$H$_3$) $_{2R}$, 19.13 ($\underline{C}$H$_3$) $_{2S}$, 18.21 ($\underline{C}$H$_3$)$_{2R}$, 18.18 ($\underline{C}$H$_3$)$_{2S}$, 17.6 ($\underline{C}$H$_3$)*$_{2R}$, 17.5 ($\underline{C}$H$_3$)* $_{2S}$, 17.34 ($\underline{C}$H$_3$)$_{2S,2R}$, 14.2 ($\underline{C}$H$_3$) $_{2S,2R}$;

* rotamer

HRMS (ESI-TOF) m/z: $[M + Na]^+$ Calcd for $C_{26}H_{45}NO_6Na$ 490.3145; Found 490.3158.

Diastereomeric mixture of (3*S*,14*S*,*E*)-3-isopropyl-14-((*S*)-2-methoxyheptyl)-9,11-dimethyl-1,4-dioxa-9-azacyclotetradec-7-ene-2,5,10-trione ($C_{24}H_{41}NO_6$, (2*R*)-, (2*S*)-2.1-A)

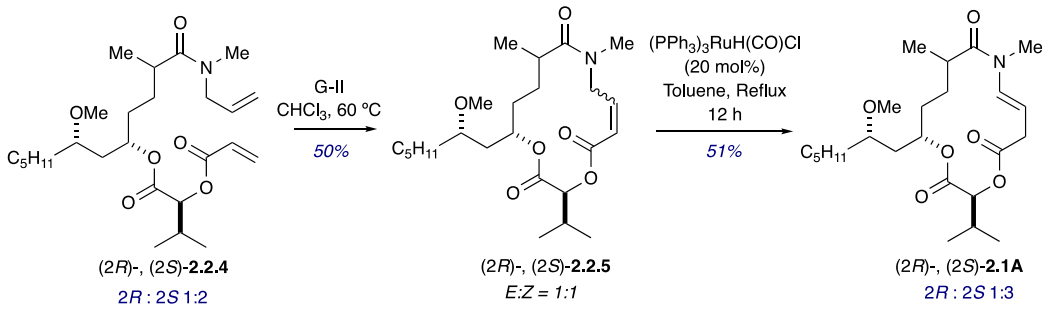

To a solution of diene (2*R*)-, (2*S*)-**2.2.4** (18 mg, 0.04 mmol) in degassed $CHCl_3$ (40 mL, 0.001 M) in a round-bottom flask was added G-II catalyst (6.5 mg, 0.008 mmol, 20 mol%) and stirred at 60 ºC for 18 hours (complete by TLC). The solvent was evaporated under reduced pressure. Flash column chromatography (silica, 0%–50% EtOAc in hexanes) was performed to obtain macrocycle (2*R*)-, (2*S*)-**2.2.5** (8.8 mg, 0.02 mmol, 50% yield) as a complex mixture of *E* and *Z* isomers. (TLC (EtOAc/Hexane, 3/1): R_f = 0.4) Product was confirmed via HRMS data and ^{1}H NMR.

HRMS (ESI-TOF) m/z: $[M + Na]^+$ Calcd for $C_{24}H_{41}NO_6Na$ 462.2832; Found 462.2859.

Next, to a solution of macrolactone (2*R*)-, (2*S*)-**2.2.5** (8.8 mg, 0.04 mmol, 1 equiv.) in degassed toluene (1 mL) was added $(PPh_3)_3RuH(CO)Cl$ catalyst under Ar and refluxed for 12 hours (complete by TLC). The solvent was evaporated under reduced pressure. Flash column chromatography (silica, 0%–50% EtOAc in hexanes) was performed to obtain enamide macrocycle (2*R*)-, (2*S*)-**2.1-A** (4.2 mg, 0.01 mmol, 51% yield) as a mixture of two diastereomers

(2*R*: 2*S* =1:3). TLC (EtOAc/Hexane, 1/1): R_f = 0.5.

Optical Rotation: $[a]_D^{22}$ = -18.7 (*c* = 0.16, $CHCl_3$);

^{1}H NMR (500 MHz, $CDCl_3$) δ 7.17 (d, *J* = 14.1 Hz, 1H, *2S* isomer C(O)N(Me)CH=C<u>H</u>CH$_a$H$_b$C(O)OCH(CH(CH$_3$)$_2$), 6.73 (d, *J* = 14.0 Hz, 0.3H, *2R* isomer C(O)N(Me)CH=C<u>H</u>CH$_a$H$_b$C(O)OCH(CH(CH$_3$)$_2$), 5.34–5.24 (m, 1H, CH(OMe)CH$_a$H$_b$C<u>H</u>(OC(O))CH$_a$H$_b$), 5.17–5.11 (m, 1H, *2S, 2R* isomers C(O)N(Me)C<u>H</u>=CHCH$_a$H$_b$C(O)OCH(CH(CH$_3$)$_2$), 5.03 (d, *J* = 4.7 Hz, 1H, C(O)N(Me)CH=CHCH$_a$H$_b$C(O)OC<u>H</u>(CH(CH$_3$)$_2$), 3.30 (s, 1H, minor *2R* isomer CH(O<u>Me</u>)CH$_a$H$_b$CH(OC(O))CH$_a$H$_b$), 3.29 (s, 3 H, major *2S* isomer CH(O<u>Me</u>)CH$_a$H$_b$CH(OC(O))CH$_a$H$_b$), 3.25–3.15 (m, 2H, major *2S* isomer C(O)N(Me)CH=CHC<u>H$_a$H$_b$</u>C(O)OCH(CH(CH$_3$)$_2$), 3.18–3.14 (m, 0.7H, minor *2R* isomer C(O)N(Me)CH=CHC<u>H$_a$H$_b$</u>C(O)OCH(CH(CH$_3$)$_2$), 3.14–3.11 (m, 1H, C<u>H</u>(OMe)CH$_a$H$_b$CH(OC(O))CH$_a$H$_b$), 3.09 (s, 3 H, major *2S* isomer C(O)N(<u>Me</u>)CH=CHCH$_a$H$_b$C(O)OCH), 3.08 (s, 1 H, minor *2R* isomer C(O)N(<u>Me</u>)CH=CHCH$_a$H$_b$C(O)OCH), 3.06–3.02 (m, 1H, major *2S* isomer CH(OC(O))CH$_2$CH$_2$C<u>H</u>(Me)C(O)N(Me), 2.63–2.53 (m, 0.3H, minor *2R* isomer CH(OC(O))CH$_2$CH$_2$C<u>H</u>(Me)C(O)N(Me), 2.41–2.34 (m, 1H, major *2S* isomer C(O)N(Me)CH=CHCH$_a$H$_b$C(O)OCH(C<u>H</u>(CH$_3$)$_2$), 2.32–2.25 (m, 0.3H, minor *2R* isomer C(O)N(Me)CH=CHCH$_a$H$_b$C(O)OCH(C<u>H</u>(CH$_3$)$_2$), 1.80–1.56 (m, 6H, CH$_3$(CH$_2$)$_3$CH$_a$H$_b$CH(OMe)C<u>H$_a$H$_b$</u>, CH(OC(O))C<u>H$_2$</u>C<u>H$_2$</u>CH(Me)C(O)N(Me)), 1.52–1.34 (m, 8H, CH$_3$(C<u>H$_2$</u>)$_3$C<u>H$_a$H$_b$</u>CH(OMe)CH$_a$H$_b$), 1.15 (d, *J* = 6.4 Hz, 1H, minor *2R* isomer CH(OC(O))CH$_2$CH$_2$CH(<u>Me</u>)C(O)N(Me)), 1.10 (d, *J* = 6.6 Hz, 3H, major *2S* isomer CH(OC(O))CH$_2$CH$_2$CH(<u>Me</u>)C(O)N(Me)), 1.03 (d, *J* = 6.6 Hz, 3H, major *2S* isomer C(O)N(Me)CH=CHCH$_a$H$_b$C(O)OCH(CH(C<u>H</u>$_3$)$_2$), 1.00 (d, *J* = 6.6 Hz, 3H, major *2S* isomer C(O)N(Me)CH=CHCH$_a$H$_b$C(O)OCH(CH(C<u>H</u>$_3$)$_2$), 0.97 (d, *J* = 6.8 Hz, 1H, minor *2R* isomer

C(O)N(Me)CH=CHCH$_a$H$_b$C(O)OCH(CH(C<u>H</u>$_3$)$_2$), 0.92 (d, *J* = 6.8 Hz, 1H, minor2*R* isomer C(O)N(Me)CH=CHCH$_a$H$_b$C(O)OCH(CH(C<u>H</u>$_3$)$_2$), 0.89 (t, *J* = 6.8 Hz, 3H, C<u>H</u>$_3$(CH$_2$)$_3$CH$_a$H$_b$CH(OMe)CH$_a$H$_b$);

^{13}C NMR (126 MHz, $CDCl_3$) δ 175.7 (C=O, amide), 170.5 (<u>C</u>=O),169.3 (<u>C</u>=O), 132.5 (C<u>H</u>=CH)$_{2R}$, 132.2 (C<u>H</u>=CH)$_{2S}$, 104.7 (C<u>H</u>=CH)$_{2S}$, 103.1 (C<u>H</u>=CH)$_{2R}$, 77.7 (<u>C</u>H)$_{2S,2R}$, 77.5 (<u>C</u>H)$_{2S,2R}$, 74.4 (<u>C</u>H)$_{2S}$, 74.4 (<u>C</u>H)$_{2R}$, 56.8 (<u>C</u>H$_3$)$_{2S,2R}$, 40.5 (<u>C</u>H$_2$)$_{2R}$, 38.6 (<u>C</u>H$_2$)$_{2S}$, 38.0 (<u>C</u>H)$_{2R}$, 36.3 (<u>C</u>H)$_{2S}$, 35.1 (<u>C</u>H$_2$)$_{2S}$, 34.3 (<u>C</u>H$_2$)$_{2R}$, 33.4 (<u>C</u>H$_2$)$_{2S}$, 33.37 (<u>C</u>H$_2$)$_{2R}$, 32.2 (<u>C</u>H$_2$)$_{2S}$, 33.1 (<u>C</u>H$_2$)$_{2R}$, 30.8 (<u>C</u>H$_3$)$_{2R}$, 30.7 (<u>C</u>H$_3$)$_{2S}$, 30.6 (<u>C</u>H$_2$)$_{2S,2R}$, 30.3 (<u>C</u>H)$_{2S}$, 29.6 (<u>C</u>H)$_{2R}$, 28.8 (<u>C</u>H$_2$)$_{2S,2R}$, 24.5 (<u>C</u>H$_2$)$_{2S,2R}$, 22.8 (<u>C</u>H$_2$)$_{2S,2R}$, 18.9 (<u>C</u>H$_3$)$_{2S}$, 18.7 (<u>C</u>H$_3$)$_{2R}$, 17.3 (<u>C</u>H$_3$)$_{2S}$, 17.3 (<u>C</u>H$_3$)$_{2R}$, 16.2 (<u>C</u>H$_3$)$_{2S}$, 14.9 (<u>C</u>H$_3$)$_{2R}$, 14.2 (<u>C</u>H$_3$)$_{2S,2R}$;

HRMS (ESI-TOF) m/z: $[M + Na]^+$ Calcd for $C_{24}H_{41}NO_6Na$ 462.2832; Found 462.2839.

(2*R*,5*S*,7*S*)-5-hydroxy-7-methoxy-*N*,2-dimethyldodecanamide ($C_{15}H_{31}NO_3$, 2.10.1)

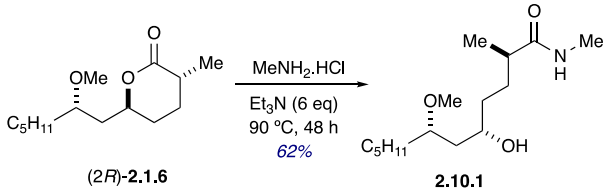

(2*R*)-**2.1.6** **2.10.1**

To a pressure vial equipped with a stir bar and the lactone methyl ether (2*R*)-**2.1.6** (20 mg, 0.08 mmol, 1 equiv.), was added triethylamine (Et_3N, 0.14 mL, 1 mmol, 12 equiv.), followed by hydrochloric salt of methyl amine ($MeNH_2$.HCl, 17 mg, 0.24 mmol, 3 equiv.). pressure vial was sealed and heated to 90 ºC, stirred for 48 hours (complete by TLC). Reaction mixture was diluted with CH_2Cl_2 (1 mL) and was added sat. NaCl (1 mL). The aqueous layer was extracted with CH_2Cl_2 (3 x 1.5 mL), and the organic layers were combined, dried over Na_2SO_4, filtered, and concentrated under reduced pressure. Purification via flash column chromatography (silica, 50%–100% EtOAc in hexanes then 5% MeOH in EtOAc) to obtain the amide **2.10.1** (12 mg, 0.05 mmol, 62% yield, yellow oil) as a single diastereomer (10:1 rotamers). TLC (EtOAc): R_f = 0.2.

FTIR (neat): 3331 (br), 2931, 2858, 2874, 2095, 1651, 1456, 1412, 1376, 1265, 1146 cm^{-1};

Optical Rotation: $[a]_D^{21}$ = +17.3 (c = 0.5 , $CHCl_3$);

^{1}H NMR (500 MHz, $CDCl_3$) δ 5.70–5.60 (m, 1H, C(O)N(Me)H), 3.86 (ddq, J = 9.3, 5.0, 2.4 Hz, 1H, CH(OMe)CH_aH_bCH(OH)CH_aH_b), 3.45 (qd, J = 6.5, 3.3 Hz, 1H, CH(OMe)CH_aH_bCH(OH)CH_aH_b), 3.35 (s, 3H, CH(OMe)CH_aH_bCH(OH)CH_aH_b), 2.79 (d, J = 4.8 Hz, 3H, C(O)N(Me)H), 1.08 (dt, J = 13.2, 1.8 Hz, 1H, $CH(OH)CH_2CH_2$CH(Me)C(O)N(Me)H), 1.80–1.72 (m, 1H, $CH(OH)CH_2CH_aH_b$CH(Me)C(O)N(Me)H), 1.69–1.57 (m, 2H,

C<u>H</u>$_a$H$_b$CH(OMe)C<u>H</u>$_a$H$_b$CH(OH), 1.56–1.50 (m, 1H, CH$_a$H$_b$CH(OMe)CH$_a$<u>H</u>$_b$CH(OH), 1.50–1.40 (m, 4H, CH$_a$<u>H</u>$_b$CH(OMe)CH$_a$H$_b$CH(OH), CH(OH)C<u>H</u>$_2$CH$_a$<u>H</u>$_b$CH(Me)C(O)N(Me)H), 1.32–1.25 (m, 6H, CH$_3$(C<u>H</u>$_2$)$_3$CH$_a$H$_b$CH(OMe), 1.14 (d, *J* = 6.9 Hz, 3H, CH(OH)CH$_2$CH$_a$H$_b$CH(<u>Me</u>)C(O)N(Me)H), 0.89 (t, *J* = 6.9 Hz, 3H, C<u>H</u>$_3$(CH$_2$)$_3$CH$_a$H$_b$CH(OMe);

^{13}C NMR (126 MHz, $CDCl_3$) δ 177.2 (C=O, amide) , 177.0 (C=O, amide)*, 79.7 (<u>C</u>H), 76.4 (<u>C</u>H)*, 68.7 (<u>C</u>H), 67.2 (<u>C</u>H)*, 56.9 (<u>C</u>H$_3$), 55.1 (<u>C</u>H$_3$)*, 42.6 (<u>C</u>H$_2$)*, 41.4 (<u>C</u>H), 39.0 (<u>C</u>H$_2$), 35.2 (<u>C</u>H$_2$), 35.0 (<u>C</u>H$_2$)*, 33.0 (<u>C</u>H$_2$), 32.7 (<u>C</u>H$_2$)*, 32.1 (<u>C</u>H$_2$), 31.7 (<u>C</u>H$_2$)*, 31.1 (<u>C</u>H$_2$)*, 30.19(<u>C</u>H), 30.0 (<u>C</u>H$_2$)*, 27.8 (<u>C</u>H$_2$)*, 26.3 (<u>C</u>H$_3$), 25.6 (<u>C</u>H$_2$)*, 25.3 (<u>C</u>H$_2$), 25.1 (<u>C</u>H$_3$)*, 22.7 (<u>C</u>H$_2$), 22.6 (<u>C</u>H$_2$)*, 18.1 (<u>C</u>H$_3$), 14.2 (<u>C</u>H$_3$);

* minor rotamer

HRMS (ESI-TOF) m/z: $[M + Na]^+$ Calcd for $C_{13}H_{27}NO_3Na$ 268.1889; Found 268.1891.

(2*R*,5*S*,7*S*)-5-((*tert*-butyldimethylsilyl)oxy)-7-methoxy-*N*,2-dimethyldodecanamide ($C_{21}H_{45}NO_3Si$, 2.10.2)

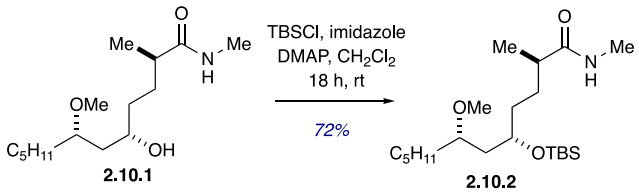

To a round bottom flask, equipped with a stir bar, and argon inlet, was added amide **2.10.1** (10 mg, 0.04 mmol, 1 equiv.) in CH_2Cl_2 (0.4 mL), TBSCl (18 mg, 0.12 mmol, 3 equiv.), imidazole (6.8 mg, 0.1 mmol, 2.5 equiv.), and DMAP (0.2 mg, 0.002 mmol, 0.04 equiv.). The reaction mixture was stirred at room temperature for 18 hours to ensure complete conversion of reactive starting material (complete by TLC). Reaction mixture was diluted with CH_2Cl_2 (1 mL) and was added sat. $NaHCO_3$ (1 mL). The aqueous layer was extracted with CH_2Cl_2 (3 x 1.5 mL), and the organic layers were combined, dried over Na_2SO_4, filtered, and concentrated under reduced pressure. Purification via flash column chromatography (silica, 0%–50% EtOAc in hexanes) to obtain the TBS protected amide alcohol **2.10.2** (12 mg, 0.03 mmol, 72% yield, colorless oil) as a single diastereomer. TLC (EtOAc/Hexane, 1:1): $R_f = 0.3$.

FTIR (neat): 2929, 2857, 1647, 1558, 1462, 1379, 1254, 1092, 938, 835, 773 cm^{-1};

Optical Rotation: $[a]_D^{22} = +23.2$ ($c = 0.26$, $CHCl_3$);

^{1}H NMR (500 MHz, $CDCl_3$) δ 5.44–5.37 (m, 1H, C(O)N(Me)H), 3.89–3.83 (m, 1H, CH(OMe)CH_aH_bCH(OTBS)CH_aH_b), 3.32–3.25 (m, 1H, CH(OMe)CH_aH_bCH(OTBS)CH_aH_b), 3.29 (s, 3H, CH(OMe)CH_aH_bCH(OTBS)CH_aH_b), 2.80 (d, $J = 4.8$ Hz, 3H, C(O)N(Me)H), 2.11 (p, $J = 6.6$ Hz, 1H, $CH(OH)CH_2CH_2$CH(Me)C(O)N(Me)H), 1.68–1.57 (m, 1H, $CH(OH)CH_2CH_aH_b$CH(Me)C(O)N(Me)H), 1.52–1.39 (m, 7H, CH_aH_bCH(OMe)CHaHb,

CH(OTBS)C<u>H</u>$_2$CH$_a$<u>H</u>$_b$CH(Me), 1.32–1.25 (m, 6H, CH$_3$(C<u>H</u>$_2$)$_3$CH$_a$H$_b$CH(OMe), 1.14 (d, *J* = 6.9 Hz, 3H, CH(OTBS)CH$_2$CH$_a$H$_b$CH(<u>Me</u>)C(O)N(Me)H), 0.92–0.89 (m, 3H, C<u>H</u>$_3$(CH$_2$)$_3$CH$_a$H$_b$CH(OMe), 0.88 (s, 9H, CH(OSi(Me)$_2$C(C<u>H</u>$_3$)$_3$), 0.05 (d, *J* = 3.5 Hz, 6H, CH(OSi(<u>Me</u>)$_2$C(CH$_3$)$_3$);

^{13}C NMR (126 MHz, CDCl$_3$) δ 177.2 (C=O, amide) , 77.4 (<u>C</u>H), 69.0 (<u>C</u>H), 55.9 (<u>C</u>H$_3$), 41.8 (<u>C</u>H$_2$), 41.7 (<u>C</u>H), 35.9 (<u>C</u>H$_2$), 33.1(<u>C</u>H$_2$), 29.7 (<u>C</u>H$_2$), 29.2 (<u>C</u>H$_2$), 26.3 (<u>C</u>H$_3$), 26.1 (3, Si(CH$_3$)$_2$C(<u>C</u>H$_3$)$_3$), 24.5 (<u>C</u>H$_2$), 22.8 (<u>C</u>H$_2$), 18.2 (Si(CH$_3$)$_2$<u>C</u>(CH$_3$)$_3$), 18.0 (<u>C</u>H$_3$), 14.2 (<u>C</u>H$_3$), -3.9 (Si(<u>C</u>H$_3$)$_2$C(CH$_3$)$_3$), -4.5 (Si(<u>C</u>H$_3$)$_2$C(CH$_3$)$_3$);

HRMS (ESI-TOF) m/z: [M + Na]$^+$ Calcd for C$_{19}$H$_{41}$NO$_3$SiNa 382.2753; Found 382.2764.

(2*R*,5*S*,7*S*)-*N*-allyl-5-((*tert*-butyldimethylsilyl)oxy)-7-methoxy-*N*,2-dimethyldodecanamide ($C_{24}H_{49}NO_3Si$, 2.10.3)

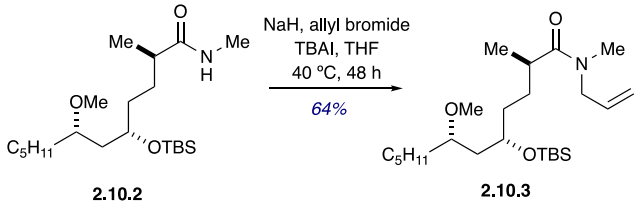

To a round bottom flask, equipped with a stir bar, argon inlet, and the amide alcohol **2.10.2** (10 mg, 0.04 mmol, 1 equiv.) in THF (0.4 mL) was added NaH (60% dispersion in mineral oil, 3 mg, 0.12 mmol, 3 equiv.) at 0 ºC and stirred for 15 minutes. Then was added tetrabutylammonium iodide (TBAI, 3 mg, 0.008 mmol, 0.2 equiv.) in one portion, followed by allyl bromide (17.3 µL, 0.2 mmol, 5 equiv.) in dropwise. The reaction mixture was stirred at 40 ºC for 48 hours to ensure complete conversion of reactive starting material (complete by TLC). Reaction mixture was diluted with EtOAc (2 mL) and was added sat. NH_4Cl (1 mL). The aqueous layer was extracted with EtOAc (3 x 1.5 mL), and the organic layers were combined, dried over Na_2SO_4, filtered, and concentrated under reduced pressure. Purification via flash column chromatography (silica, 0%–50% EtOAc in hexanes) to obtain the TBS protected amide alcohol **2.10.3**(10 mg, 0.03 mmol, 64% yield, colorless oil) as a single diastereomer (1:1 rotamers). TLC (EtOAc/Hexane, 1:1): R_f = 0.7.

FTIR (neat): 3434, 3080, 2933, 2860, 1634, 1468, 1408, 1091, 990 cm^{-1},

Optical Rotation: $[a]_D^{21}$ = +8.6 (c = 0.2, $CHCl_3$);

^{1}H NMR (500 MHz, $CDCl_3$) δ 5.94–5.68 (m, 1H, two rotamers C(O)N(Me)$CH_aH_bC\underline{H}$=CH_2), 5.24–5.08 (m, 2H, two rotamers C(O)N(Me)CCH_aH_bCH=$C\underline{H_2}$), 4.07–3.88 (m, 2H, two rotamers C(O)N(Me)$CC\underline{H_a}\underline{H_b}CH$=$CH_2$), 3.88–3.82 (m, 1H, CH(OMe)$CH_aH_bC\underline{H}$(OTBS)CH_aH_b), 3.32–3.28 (m, 1H, $C\underline{H}$(OMe)CH_aH_bCH(OTBS)CH_aH_b), 3.29 (s, 3H,

CH(O<u>Me</u>)CH_aH_bCH(OTBS)CH_aH_b), 2.94 (d, *J* = 26.6 Hz, 3H, two rotamers C(O)N(<u>Me</u>)CH_aH_bCH=CH_2), 2.64 (q, *J* = 6.5 Hz, 0.5H, rotamer CH(OH)CH_2CH_2C<u>H</u>(Me)C(O)N(Me)), 2.55–2.48 (m, 0.5H, rotamer CH(OH)CH_2CH_2C<u>H</u>(Me)C(O)N(Me)), 1.68–1.57 (m, 1H, CH(OH)CH_2C<u>H_a</u><u>H_b</u>CH(Me)C(O)N(Me)), 1.52–1.39 (m, 7H, C<u>H_a</u><u>H_b</u>CH(OMe)C<u>Ha</u><u>Hb</u>, CH(OTBS)C<u>H_2</u>CH_a<u>H_b</u>CH(Me)), 1.32–1.25 (m, 6H, CH_3(C<u>H_2</u>)$_3$$CH_aH_b$CH(OMe), 1.11 (t, *J* = 6.8 Hz, 3H, two rotamers CH(OTBS)$CH_2CH_aH_b$CH(<u>Me</u>)C(O)N(Me)), 0.92–0.89 (m, 3H, C<u>H_3</u>$(CH_2)_3CH_aH_b$CH(OMe)), 0.88 (s, 9H, CH(OSi(Me)$_2$C(C<u>H_3</u>)$_3$), 0.05 (t, *J* = 3.2 Hz, 6H, CH(OSi(<u>Me</u>)$_2$C$(CH_3)_3$);

^{13}C NMR (126 MHz, $CDCl_3$) δ 176.3 (C=O, amide) , 133.5 (<u>C</u>H=CH_2), 133.3 (<u>C</u>H=CH_2)*, 117.1 (CH=<u>C</u>H_2), 116.6 (CH=<u>C</u>H_2)*, 77.4 (<u>C</u>H), 77.37 (<u>C</u>H)*, 69.1 (<u>C</u>H), 69.0 (<u>C</u>H)*, 55.9 (<u>C</u>H_3), 52.2 (<u>C</u>H_2), 50.3 (<u>C</u>H_2)*, 41.72 (<u>C</u>H_2), 41.68 (<u>C</u>H_2)*, 36.1 (<u>C</u>H), 35.9 (<u>C</u>H_2), 35.8 (<u>C</u>H)*, 34.8 (<u>C</u>H_3), 34.0 (<u>C</u>H_3)*, 33.9 (<u>C</u>H_2), 29.1 (<u>C</u>H_2), 28.9 (<u>C</u>H_2)*, 27.1 (<u>C</u>H_2), 26.1 (3, Si$(CH_3)_2$C(<u>C</u>H_3)$_3$), 24.5 (<u>C</u>H_2), 23.1 (<u>C</u>H_2), 22.8 (<u>C</u>H_2)*, 18.2 (Si$(CH_3)_2$<u>C</u>$(CH_3)_3$), 18.0 (<u>C</u>H_3), 17.5 (<u>C</u>H_3)*, 14.2 (<u>C</u>H_3), -3.9 (Si(<u>C</u>H_3)$_2$C$(CH_3)_3$), -4.5 (Si(<u>C</u>H_3)$_2$C$(CH_3)_3$);

HRMS (ESI-TOF) m/z: $[M + Na]^+$ Calcd for $C_{24}H_{49}NO_3SiNa$ 450.3379; Found 450.3385.

(2*R*,5*S*,7*S*)-*N*-allyl-5-hydroxy-7-methoxy-*N*,2-dimethyldodecanamide ($C_{18}H_{35}NO_3$, (2*R*)-2.2.2)

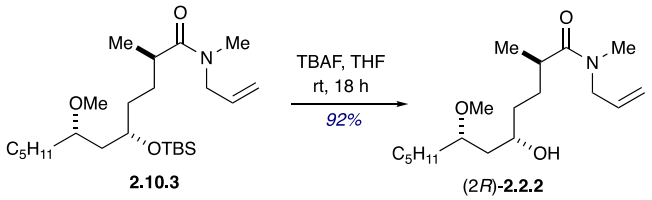

To a round bottom flask, equipped with a stir bar, argon inlet, and the TBS protected amide alcohol **2.10.3** (8 mg, 0.02 mmol, 1 equiv.) in THF (0.4 mL) was added TBAF (1 M in THF, 80 µL, 0.08 mmol, 4 equiv.) at room temperature and stirred for 18 hours (complete by TLC). Reaction mixture was diluted with EtOAc (2 mL) and was added sat. NH_4Cl (1 mL). The aqueous layer was extracted with EtOAc (3 x 1.5 mL), and the organic layers were combined, dried over Na_2SO_4, filtered, and concentrated under reduced pressure. Purification via flash column chromatography (silica, 0%–100% EtOAc in hexanes) to obtain the amide alcohol (2*R*)-**2.2.2** (6 mg, 0.018 mmol, 92% yield, colorless oil) as a single diastereomer (1:1 rotamers). TLC (EtOAc/Hexane, 2:1): $R_f = 0.6$.

FTIR (neat): 3420, 3034, 2928, 2848, 1634, 1560, 1456, 1091, 990 cm^{-1};

Optical Rotation: $[a]_D^{22} = +17.6$ ($c = 0.18$, $CHCl_3$);

^{1}H NMR (500 MHz, $CDCl_3$) δ 5.76 (dddd, $J = 24.3, 11.7, 10.1, 5.3$ Hz, 1H, two rotamers C(O)N(Me)$CH_aH_bC\underline{H}=CH_2$), 5.24–5.12 (m, 2H, two rotamers C(O)N(Me)$CCH_aH_bCH=C\underline{H}_2$), 4.09–3.92 (m, 2H, two rotamers C(O)N(Me)$CC\underline{H}_a\underline{H}_bCH=CH_2$), 3.90–3.81 (m, 1H, $CH(OMe)CH_aH_bC\underline{H}(OH)CH_aH_b$), 3.50–3.41 (m, 1H, $C\underline{H}(OMe)CH_aH_bCH(OH)CH_aH_b$), 3.36 (s, 3H, $CH(O\underline{Me})CH_aH_bCH(OH)CH_aH_b$), 2.95 (d, $J = 29.5$ Hz, 3H, two rotamers C(O)N($\underline{Me}$)$CH_aH_bCH=CH_2$), 2.78–2.70 (m, 0.5H, rotamer $CH(OH)CH_2CH_2C\underline{H}(Me)C(O)N(Me)$), 2.65–2.59 (m, 0.5H, rotamer $CH(OH)CH_2CH_2C\underline{H}(Me)C(O)N(Me)$), 2.38-2.29 (m, 1H,

CH(O<u>H</u>)CH_2CH_2C<u>H</u>(Me)C(O)N(Me)), 1.87–1.75 (m, 1H, CH(OH)CH_2C<u>H</u>$_a$H$_b$CH(Me)C(O)N(Me)), 1.66–1.49 (m, 7H, C<u>H</u>$_a$<u>H</u>$_b$CH(OMe)C<u>H</u>a<u>H</u>b, CH(OH)C<u>H</u>$_2$CH$_a$<u>H</u>$_b$CH(Me)), 1.44–1.35 (m, 6H, CH_3(C<u>H</u>$_2$)$_3$CH$_a$H$_b$CH(OMe), 1.12 (t, *J* = 6.7 Hz, 3H, two rotamers CH(OH)CH_2CH$_a$H$_b$CH(<u>Me</u>)C(O)N(Me)), 0.89 (m, 3H, C<u>H</u>$_3$(CH_2)$_3$CH$_a$H$_b$CH(OMe);

^{13}C NMR (126 MHz, $CDCl_3$) δ 177.0 (C=O, amide), 176.4 (C=O, amide)*, 133.4 (<u>C</u>H=CH_2), 133.2 (<u>C</u>H=CH_2)*, 117.1 (CH=<u>C</u>H_2), 116.7 (CH=<u>C</u>H_2)*, 79. 7 (<u>C</u>H), 68.8 (<u>C</u>H), 56.93 (<u>C</u>H_3), 52.17 (<u>C</u>H_2), 50.3 (<u>C</u>H_2)*, 39.13 (<u>C</u>H_2), 39.07 (<u>C</u>H_2)*, 35.9 (<u>C</u>H), 35.70 (<u>C</u>H)*, 35.48 (<u>C</u>H_2), 35.47 (<u>C</u>H_2)*, 34.8 (<u>C</u>H_3), 33.96 (<u>C</u>H_3)*, 33.0 (<u>C</u>H_2), 32.1 (<u>C</u>H_2), 30.18 (<u>C</u>H_2), 29.8 (<u>C</u>H_2)* ,25.3 (<u>C</u>H_2), 22.8 (<u>C</u>H_2), 18.2 (<u>C</u>H_3), 17.6 (<u>C</u>H_3)*, 14.2 (<u>C</u>H_3);

HRMS (ESI-TOF) m/z: $[M + Na]^+$ Calcd for $C_{18}H_{35}NO_3Na$ 336.2515; Found 336.2521.

Comparison of Diastereomeric Rotamer Mixture from $AlMe_3$-mediated Method and Diastereomerically pure (2*R*)-epimer form Alkylation Method

Table 5.5

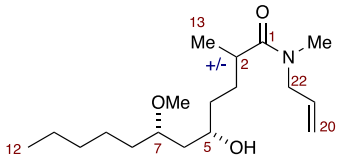

C #	Pdt of Reaction A ^{13}C (±0.1 ppm)	Pure epimer from alkylation ^{13}C (±0.1 ppm)	δΔ ppm
C1(2*S*)	177.2	-	-
C1(2*R*)	177.0	177.0	0.0
C1(2*S*)*	176.7	-	-
C1(2*R*)*	176.4	176.4	0.0
C2(2*S*)	36.2	-	-
C2(2*R*)	35.9	35.9	0.0
C2(2*S*)*	35.9	-	-
C2(2*R*)*	35.7	35.7	0.0
C3(2*S*)	33.2	-	-
C3(2*R*)	33.1	33.0	0.1
C3(2*S*)*	33.0	-	-
C3(2*R*)*	33.0	33.0	0.0
C4(2S)	36.1	-	-
C4(2S)*	36.0	-	-
C4(2R)	35.5	35.5	0.0
C4(2R)*	35.5	35.5	0.0
C5(2*R*)	68.8	68.8	0.0
C5(2*R*)*	68.8	68.8	0.0
C5(2*S*)	68.3	-	-
C5(2*S*)*	68.1	-	-
C6(2*S*)	39.6	-	-
C6(2*S*)*	39.4	-	-
C6(2*R*)	39.2	39.1	0.1
C6(2*R*)*	39.1	39.1	0.0

Table 5.5 continued

C #	Pdt of Reaction A ^{13}C (±0.1 ppm)	Pure epimer from alkylation ^{13}C (±0.1 ppm)	δΔ ppm
C7(2*R*)	79.7	79.7	0.0
C7(2*R*)*	79.7	79.7	0.0
C7(2*S*)	79.6	-	-
C7(2*S*)*	79.5	-	-
C8(2*S*)	30.4	-	-
C8(2*S*)*	30.2	-	-
C8(2*R*)	30.0	30.1	0.1
C8(2R)*	29.9	29.8	0.1
13(2*S*)	18.8	-	-
13(2*S*)*	18.2	-	-
13(2*R*)	18.2	18.2	0.00
13(2*R*)*	17.6	17.6	0.00
OMe(2*S*)	57.0	-	-
OMe 2*S*)*	56.9	-	-
OMe (2*R*)	56.9	56.9	0.0
OMe (2*R*)*	56.9	56.9	0.0
NMe(2*S*)	34.9	-	-
NMe (2*R*)	34.8	34.8	0.00
NMe (2*S*)*	34.0	-	-
NMe (2*R*)*	33.9	33.9	0.0
C20(2*S*)	117.1	-	-
C20(2*R*)	117.1	117.1	0.0
C20(2*S*)*	116.8	-	-
C20(2*R*)*	116.7	116.7	0.0
C21(2*R*)	133.4	133.4	0.0
C21(2*S*)	133.3	-	-
C21(2*R*)*	133.2	133.2	0.0
C21(2*S*)*	133.2	-	-
C22(2*S*)	52.2	-	-
C222*R*)	52.2	52.2	0.0
C22(2*S*)*	50.4	-	-
C22(2*R*)*	50.3	50.3	0.0

(2*R*,5*S*,7*S*)-1-(allyl(methyl)amino)-7-methoxy-2-methyl-1-oxododecan-5-yl (*S*)-2-(acryloyloxy)-3-methylbutanoate ($C_{26}H_{45}NO_6$, (2*R*)-2.2.4)

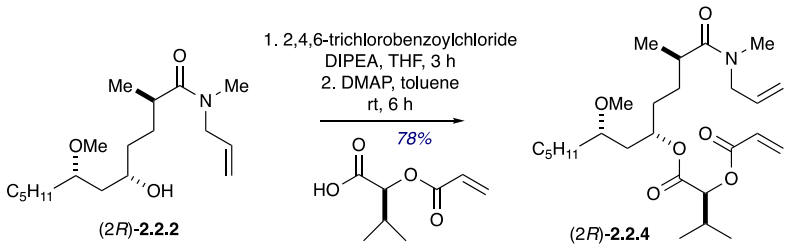

To a solution of (*S*)-2-(acryloyloxy)-3-methylbutanoic acid (7 mg, 0.04 mmol, 2 equiv.) in dry THF (0.3 mL) was added freshly distilled *N*,*N*-diisopropylethylamine (6 µL, 0.04 mmol, 2.5 equiv.) followed by 2,4,6-trichlorobenzoyl chloride (TCBC) (7 µL, 0.06 mmol, 1.8 equiv.) and stirred at room temperature for 3 hours, and the resulted mixed anhydride was concentrated under reduced pressure. The crude mixture was then redissolved in dry toluene (0.3 mL) and cannulated to a stirring solution of amide (2*R*)-**2.2.2** (6 mg, 0.02 mmol, 1.0 equiv.) and DMAP (3 mg, 0.025 mmol, 1.2 equiv.) in toluene (0.3 mL) at 0 ºC. After stirring for 15 minutes at 0 ºC the reaction mixture was stirred for an additional 12 hours at room temperature (complete by TLC). Reaction mixture was diluted with CH_2Cl_2 (1 mL) and was added sat. $NaHCO_3$ (2 mL). The aqueous layer was extracted with CH_2Cl_2 (3 x 1.5 mL), and the organic layers were combined, dried over Na_2SO_4, filtered, and concentrated under reduced pressure. Purification via flash column chromatography (silica, 0%–50% EtOAc in hexanes) to obtain diene (2*R*)-**2.2.4** (7 mg, 0.016 mmol, 78% yield, colorless oil) as a single diastereomer (1:1 rotamers). TLC (EtOAc/Hexane, 1/1): R_f = 0.6.

FTIR (neat): 3083, 2955, 2924,2852, 2728, 1731, 1660, 1463, 1406, 1260, 1187, 1094, 803, 721 cm^{-1};

Optical Rotation: $[a]_D^{23}$ = -7.6 (*c* = 0.18 , $CHCl_3$);

^{1}H NMR (500 MHz, $CDCl_3$) δ 6.46 (dd, *J* = 17.8 , 1.4 Hz, 1H, OC(O)CH(CH(CH_3)$_2$)OC(O)CH=CH_aH_b), 6.20 (dd, *J* = 17.3 , 10.5 Hz, 1H, OC(O)CH(CH(CH_3)$_2$)OC(O)CH= CH_aH_b), 5.90 (d, *J* = 10.0 Hz, 1H, OC(O)CH(CH(CH_3)$_2$)OC(O)CH=CH_aH_b), 5.83–5.67 (m, 1H, (two rotamers) C(O)N(Me)CH_aH_bCH=CH_2), 5.21–5.06 (m, 3H, (two rotamers) C(O)N(Me)CH_aH_bCH=CH_2, $CH_3(CH_2)_4$CH(OMe)CH_aH_bCH(OC(O))CH_aH_b), 4.89 (d, *J* = 4.3 Hz, 1H, OC(O)CH(CH(CH_3)$_2$)OC(O)CH=CH_aH_b), 4.01–3.89 (d, *J* = 5.7 Hz, 1H, (two rotamers) C(O)N(Me)CH_aH_bCH=CH_2), 3.96–3.87 (m, 1H, (two rotamers) C(O)N(Me)CH_2CH=CH_2), 3.29 (s, 3H, CH(OMe)CH_aH_bCH(OC(O))CH_aH_b), 3.10–3.01 (m, 1H, CH(OMe)CH_aH_bCH(OC(O))CH_aH_b), 2.95 (d, *J* = 33.5 Hz, 3H, (two rotamers) C(O)N(Me)CH_aH_bCH=CH_2), 2.75 (q, *J* = 2.8 Hz, 0.5H, (rotamer) CH(OC(O))CH_2CH_2CH(Me)C(O)N(Me)CH_2), 2.67–2.58 (m, 0.5H, (rotamer) CH(OC(O))CH_2CH_2CH(Me)C(O)N(Me)CH_2), 2.33–2.22 (m, 1H, OC(O)CH(CH(CH(CH_3)$_2$)OC(O)CH=CH_aH_b), 1.77–1.71 (m, 1H, CH(OMe)CH_aH_bCH(OC(O))CH_2CH_aH_b), 1.73–1.62 (m, 7H, CH_2CH(OMe)CH_aH_bCH(OC(O))CH_2CH_aH_b), 1.34–1.21 (m, 6H, CH_3(CH_2)$_3$CH_aH_bCH(OMe), 1.10 (t, 3H, (two rotamers) CH(Me)C(O)N(Me)CH_2), 1.03 (dd, *J* = 10.3, 7.5 Hz, 6H, OC(O)CH(CH(CH_3)$_2$)OC(O)CH=CH_aH_b), 0.89 (td, *J* = 7.0 Hz, 3H, CH_3(CH_2)$_3$CH_aH_bCH(OMe);

^{13}C NMR (126 MHz, $CDCl_3$) δ 176.7 (C=O, amide), , 176.0 (C=O, amide)*, 169.6 (C=O), 169.5 (C=O)*, 165.8 (C=O), 133.4 (CH=CH_2), 133.25 (CH=CH_2)*, 131.7 (CH=CH_2), 128.0 (CH=CH_2), 117.1 (CH=CH_2), 116.75 (CH=CH_2)*, 77.4 (CH), 77.3 (CH), 77.24 (CH)*, 72.4 (CH), 57.0 (CH_3), 52.18 (CH_2), 50.27 (CH_2)*, 39.4 (CH_2), 39.36 (CH_2)*, 35.25

(CH), 35.1 (CH)*, 34.8 (CH_3), 33.94 (CH_3)*, 33.6 (CH_2), 32.3 (CH_2)*, 32.5 (CH_2), 30.24 (CH), 29.5 (CH_2), 29.2 (CH_2)*, 29.1 (CH_2), 28.8 (CH_2)*, 24.7(CH_2), 22.8 (CH_2), 19.16 (CH_3), 18.22 (CH_3), 17.6 (CH_3)*, 17.37 (CH_3), 14.2 (CH_3);

* rotamer

HRMS (ESI-TOF) m/z: $[M + Na]^+$ Calcd for $C_{26}H_{45}NO_6Na$ 490.3145; Found 490.3144.

Sanctolide A [(3*S*,11*R*,14*S*,*E*)-3-isopropyl-14-((*S*)-2-methoxyheptyl)-9,11-dimethyl-1,4-dioxa-9-azacyclotetradec-7-ene-2,5,10-trione, ($C_{24}H_{41}NO_6$, (2*R*)-2.1-A]

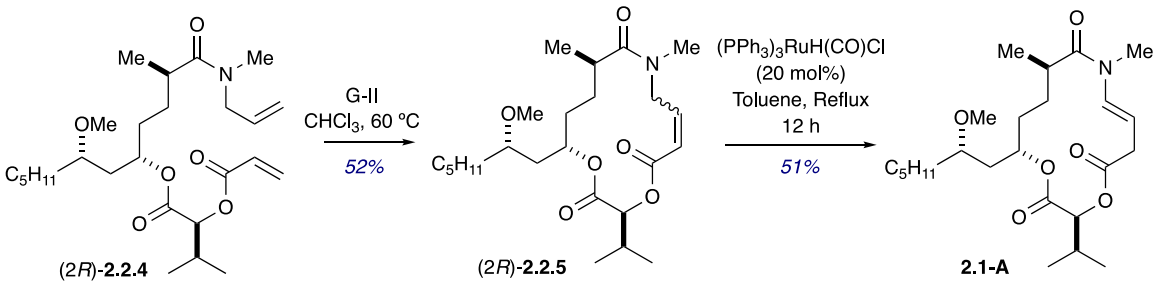

To a solution of diene (2*R*)-**2.2.4** (6 mg, 0.016 mmol) in degassed $CHCl_3$ (16 mL, 0.001 M) in a round-bottom flask was added G-II catalyst (2.5 mg, 0.003 mmol, 20 mol%) and stirred at 60 ºC for 18 hours (complete by TLC). The solvent was evaporated under reduced pressure. Flash column chromatography (silica, 0%–50% EtOAc in hexanes) was performed to obtain macrocycle (2*R*)-**2.2.5** (3.6 mg, 0.008 mmol, 52% yield) as a mixture of *E* and *Z* isomers. TLC (EtOAc/Hexane, 3/1): R_f= 0.4. Product was confirmed via HRMS data and ^{1}H NMR.

HRMS (ESI-TOF) m/z: $[M + Na]^+$ Calcd for $C_{24}H_{41}NO_6Na$ 462.2832; Found 462.2818.

Next, to a solution of macrolactone (2*R*)-**2.2.5** (3.6 mg, 0.008 mmol, 1 equiv.) in degassed toluene (0.3 mL) was added $(PPh_3)_3RuH(CO)Cl$ catalyst (1.5 mg, 20 mol%) under Ar and refluxed for 12 hours (complete by TLC). The solvent was evaporated under reduced pressure. Flash column chromatography (silica, 0%–50% EtOAc in hexanes) was performed to obtain enamide macrocycle **2.1-A** (1.6 mg, 0.01 mmol, 51% yield) as a single diastereomer. TLC (EtOAc/Hexane, 1/3): R_f= 0.4.

^{1}H NMR (400 MHz, $CDCl_3$) δ 6.73 (d, *J* = 14.5 Hz, 1H, C(O)N(Me)CH=C<u>H</u>CH$_a$H$_b$C(O)OCH(CH(CH$_3$)$_2$), 5.17–5.10 (m, 1H, C(O)N(Me)C<u>H</u>=CHCH$_a$H$_b$C(O)OCH(CH(CH$_3$)$_2$), 5.13 (d, *J* = 6.0 Hz, 1H, C(O)N(Me)CH=CHCH$_a$H$_b$C(O)OC<u>H</u>(CH(CH$_3$)$_2$), 5.05–4.99 (m, 1H,

CH(OMe)CH_aH_bC<u>H</u>(OC(O))CH_aH_b), 3.30 (s, 1H, CH(O<u>Me</u>)CH_aH_bCH(OC(O))CH_aH_b), 3.21 (d, *J* = 6.9 Hz, 1H, C(O)N(Me)CH=CHC<u>H</u>$_aH_b$C(O)OCH(CH(CH_3)$_2$), 3.17 (dd, *J* = 6.7 Hz, 1H, C(O)N(Me)CH=CHCH_a<u>H</u>$_b$C(O)OCH(CH(CH_3)$_2$), 3.15–3.21 (m, 1H, C<u>H</u>(OMe)CH_aH_bCH(OC(O))CH_aH_b), 3.09 (s, 3 H, C(O)N(<u>Me</u>)CH=CHCH_aH_bC(O)OCH), 2.63–2.55 (m, 1H, CH(OC(O))CH_2CH_2C<u>H</u>(Me)C(O)N(Me), 2.30–2.25 (m, 1H, C(O)N(Me)CH=CHCH_aH_bC(O)OCH(C<u>H</u>(CH_3)$_2$), 1.15 (d, *J* = 6.4 Hz, 1H, CH(OC(O))CH_2CH_2CH(<u>Me</u>)C(O)N(Me)), 0.97 (d, *J* = 6.9 Hz, 1H, C(O)N(Me)CH=CHCH_aH_bC(O)OCH(CH(C<u>H</u>$_3$)$_2$), 0.92 (d, *J* = 6.7 Hz, 1H, C(O)N(Me)CH=CHCH_aH_bC(O)OCH(CH(C<u>H</u>$_3$)$_2$), 0.89 (t, *J* = 6.8 Hz, 1H, C<u>H</u>$_3$(CH_2)$_3$CH_aH_bCH(OMe)CH_aH_b);

HRMS (ESI-TOF) m/z: $[M + Na]^+$ Calcd for $C_{24}H_{41}NO_6Na$ 462.2832; Found 462.2841.

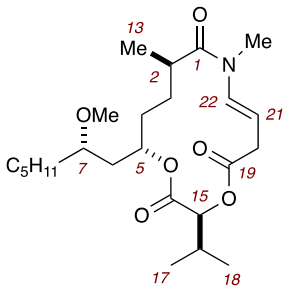

Table 5.6 *[1]H NMR chemical shifts comparison of original NMR (from isolation paper) and our final NMR (sanctolide numbering)*

C#	Original ^{1}H NMR sanctolide A in $CDCl_3$ ($CHCl_3$ reference of 7.24 ppm)	Final ^{1}H NMR of sanctolide A (2*R*)-**2.1-A** in $CDCl_3$ ($CHCl_3$ reference of 7.24 ppm)	δΔ ppm	Final ^{1}H NMR of sanctolide A (2*R*)-**2.1-A** in $CDCl_3$ ($CHCl_3$ reference of 7.26 ppm)
2	2.56	2.56	0.00	2.58
5	5.00	5.00	0.00	5.02
7	3.12	3.12	0.00	3.14
13	1.13	1.13	0.00	1.15
15	5.11	5.11	0.00	5.13
17	0.94	0.95	0.01	0.97
18	0.90	0.90	0.00	0.92
20a	3.15	3.15	0.00	3.17
20b	3.20	3.19	0.01	3.21
21	5.12	5.12	0.00	5.14
22	6.70	6.71	0.01	6.73
OMe	3.28	3.28	0.00	3.30
NMe	3.06	3.07	0.01	3.09

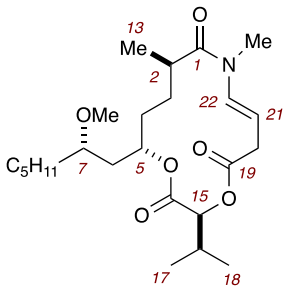

Table 5.7 *[1]H NMR chemical shifts comparison of Yadav NMR of sanctolide A, and the final NMR of the product from the RCM/isomerization of diene (2R)-**2.2.4** (sanctolide numbering).*

C#	Yadav ^{1}H NMR of sanctolide A in $CDCl_3$ ($CHCl_3$ reference of 7.24 ppm)	Final ^{1}H NMR of sanctolide A (2*R*)-**2.1-A** in $CDCl_3$ ($CHCl_3$ reference of 7.24 ppm)	δΔ ppm	Final ^{1}H NMR of sanctolide A (2*R*)-**2.1-A** in $CDCl_3$ ($CHCl_3$ reference of 7.26 ppm)
2	2.60–2.52	2.61–2.53	-	2.63–2.55
5	5.03–4.97	5.03–4.97	-	5.05–4.99
7	3.14–3.08	3.13–3.19	-	3.15–3.21
13	1.12	1.13	0.01	1.15
15	5.10	5.11	0.01	5.13
17	0.94	0.95	0.01	0.97
18	0.89	0.90	0.01	0.92
20a	3.15	3.15	0	3.17
20b	3.19	3.19	0	3.21
21	5.15–5.08	5.15–5.08	-	5.17–5.10
22	6.70	6.71	0.01	6.73
OMe	3.27	3.28	0.01	3.30
NMe	3.06	3.07	0.01	3.09

5.1.3 NMR Spectra

(4*R*,6*R*)-2-((2-methylbut-3-en-1-yl)oxy)-4,6-divinyl-1,3,2-dioxaphosphinane 2-oxide ($C_{12}H_{19}O_4P$, 2.6.2)

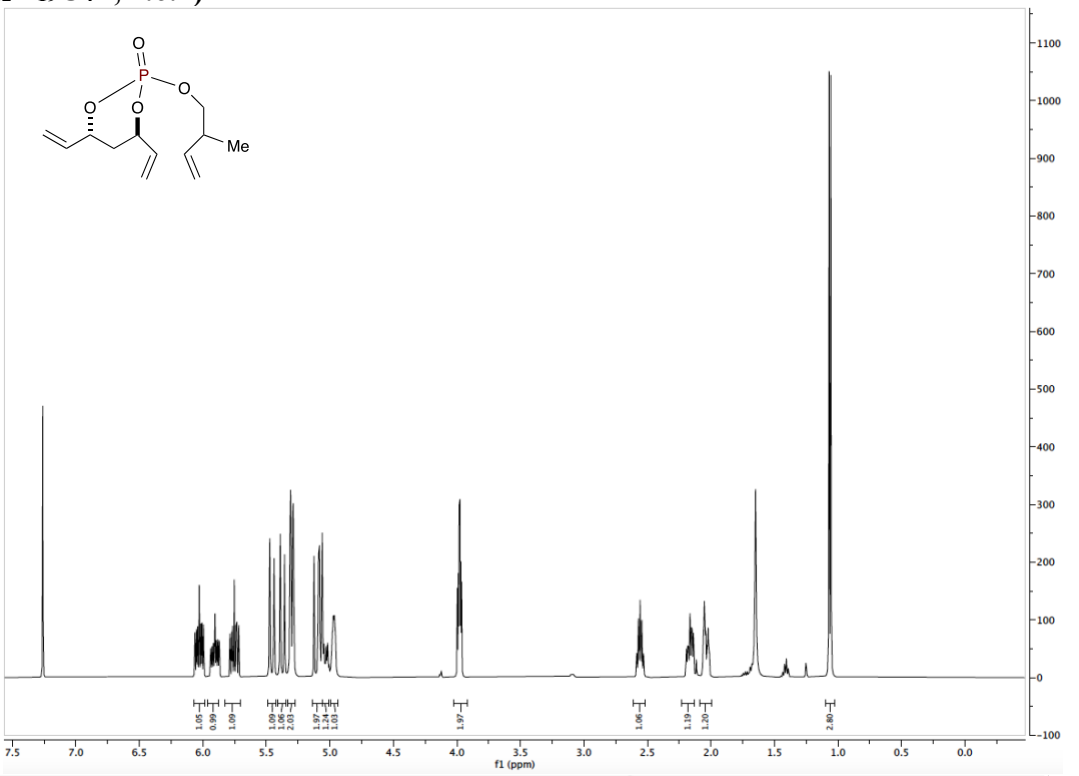

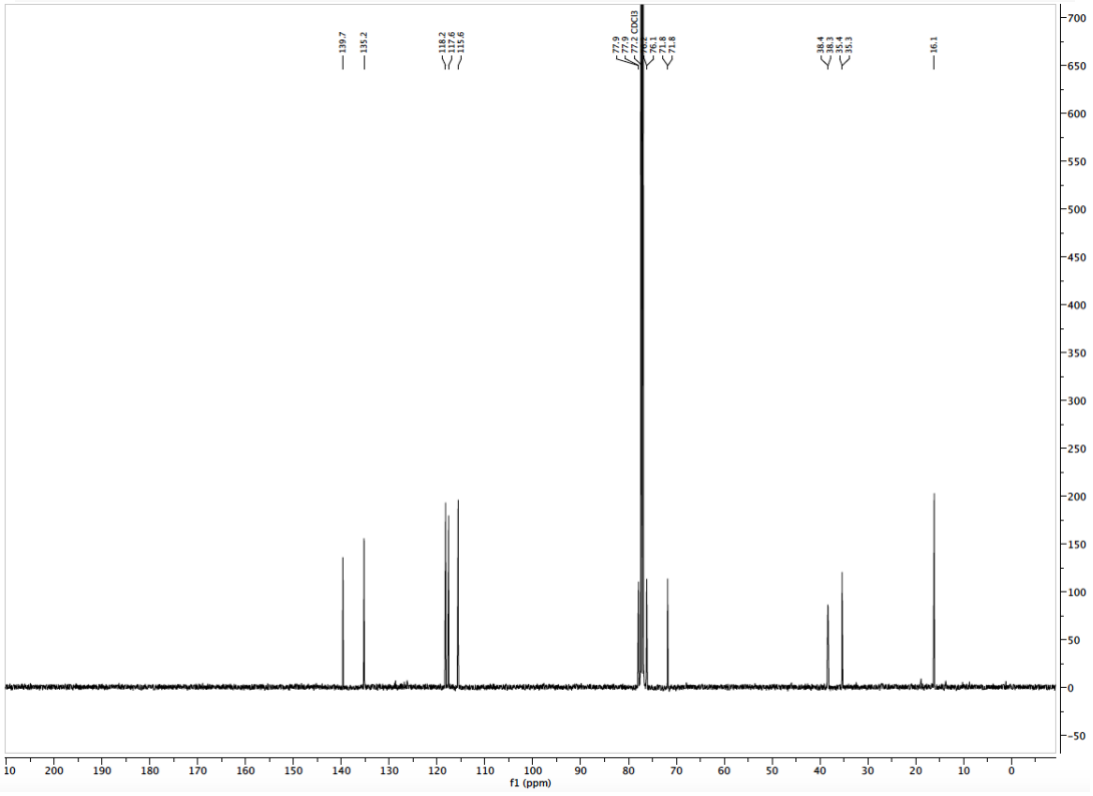

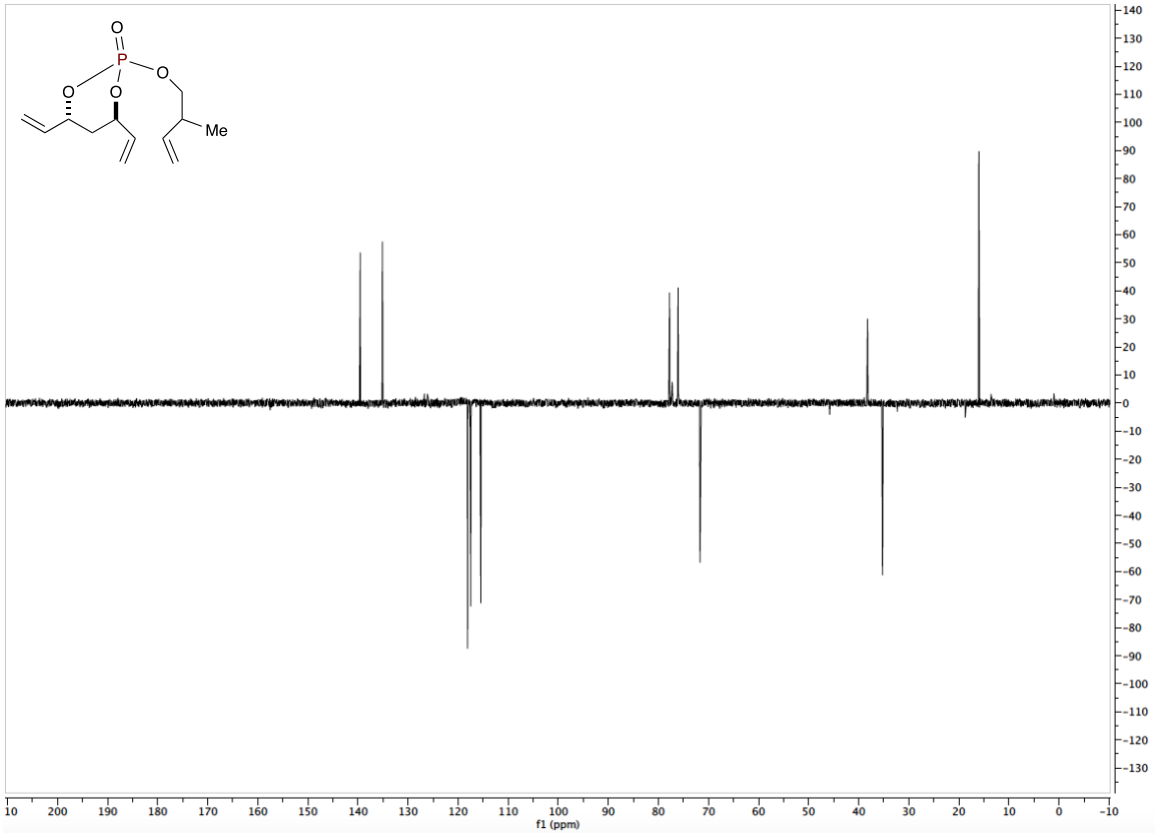
O
P
O
O
O
Me
f1 (ppm)

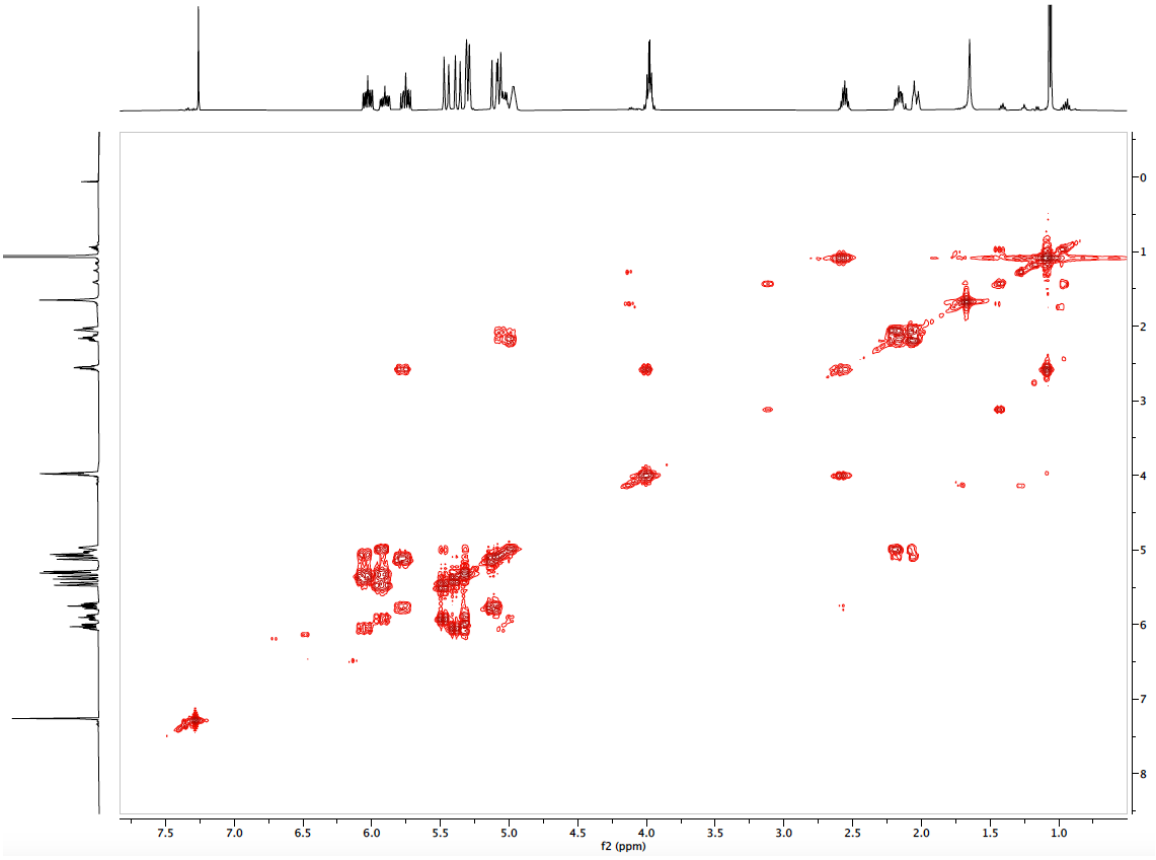
f2 (ppm)

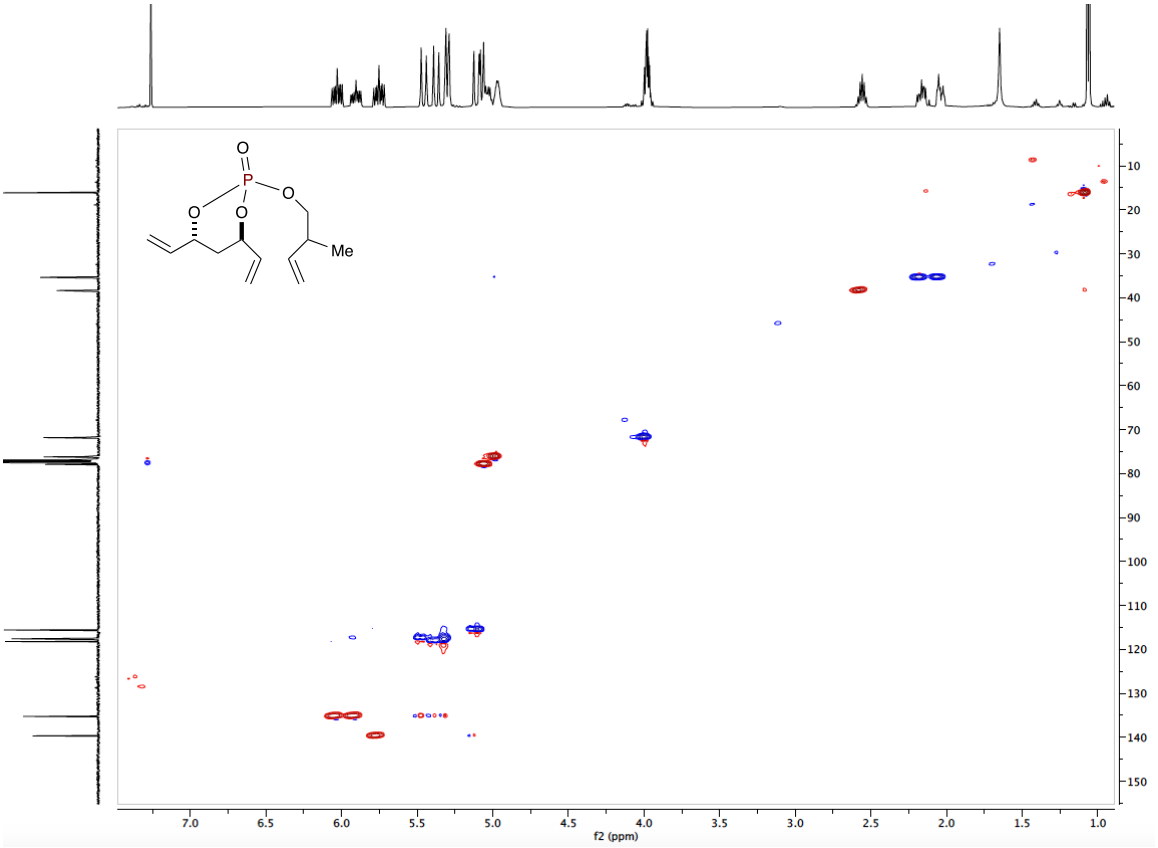
O
P
O
O
O
Me
7.0
6.5
6.0
5.5
5.0
4.5
4.0
3.5
3.0
2.5
2.0
1.5
1.0
f2 (ppm)

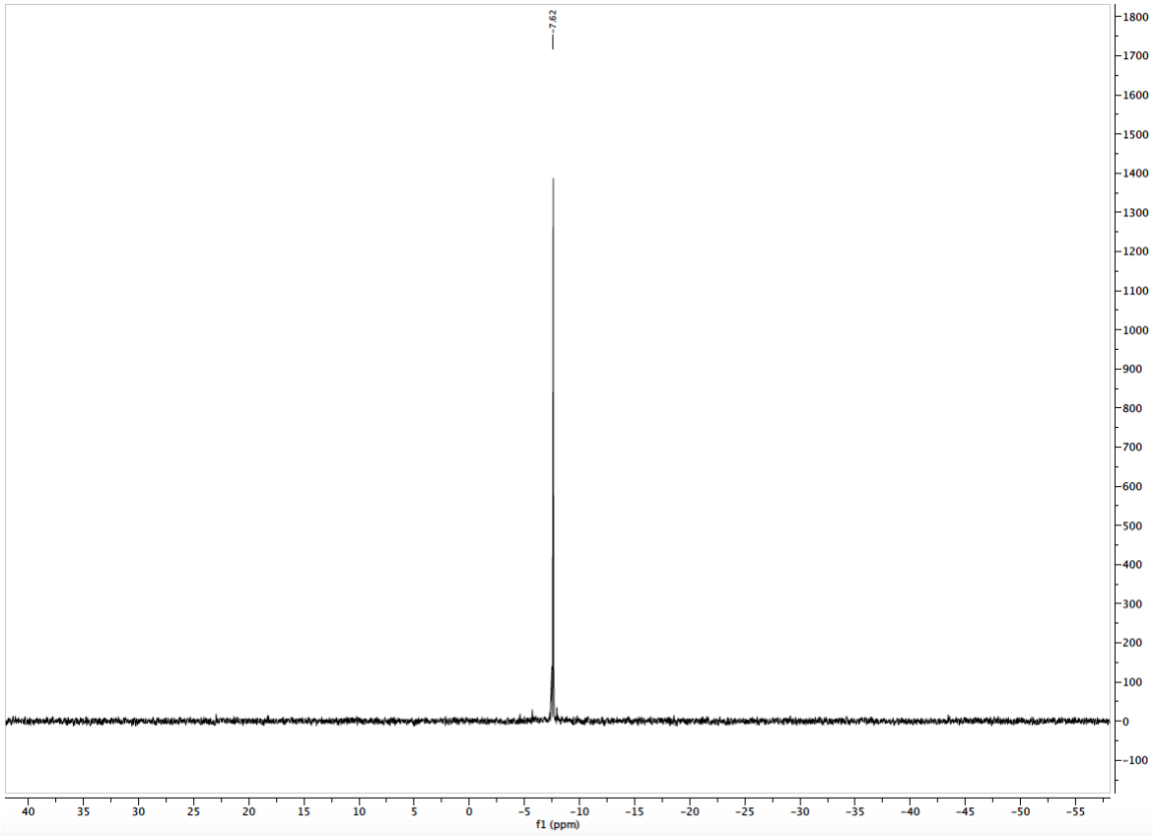
7.62
40
35
30
25
20
15
10
5
0
-5
-10
-15
-20
-25
-30
-35
-40
-45
-50
-55
f1 (ppm)

(1*R*,4*S*,7*R*,9*R*,*Z*)-4-methyl-9-vinyl-2,10,11-trioxa-1-phosphabicyclo[5.3.1]undec-5-ene 1-oxide ($C_{10}H_{15}O_4P$, 2.6.3)

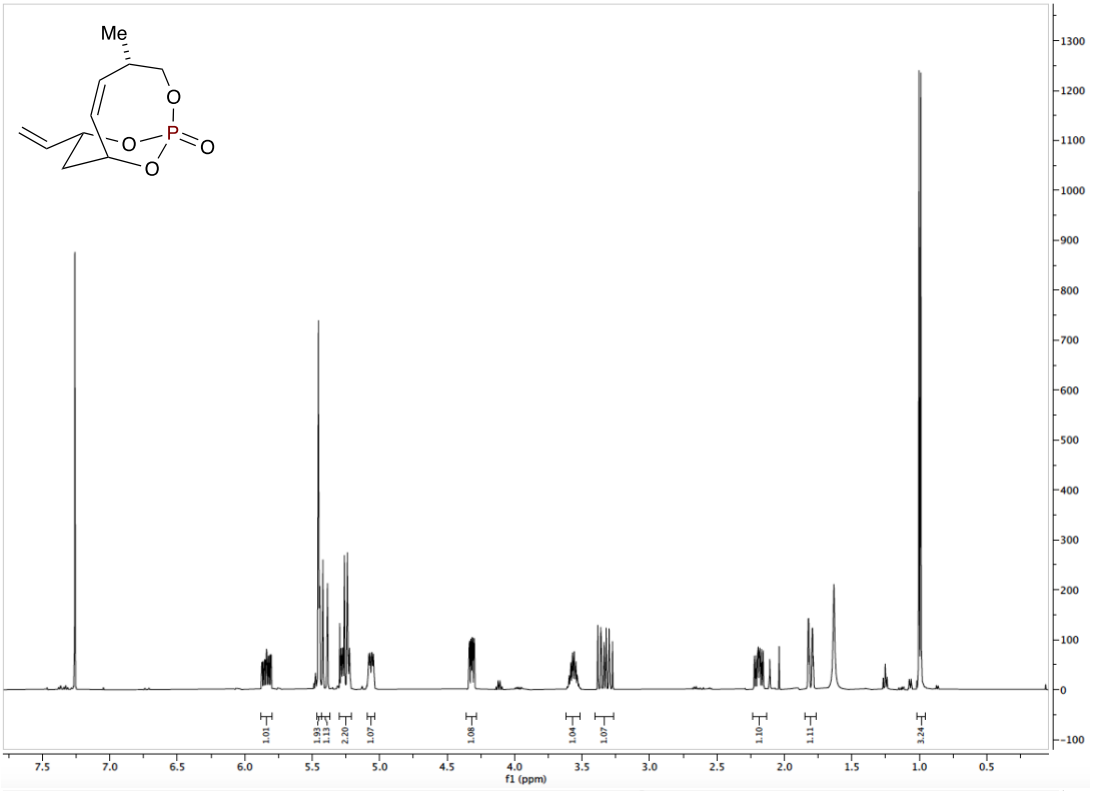

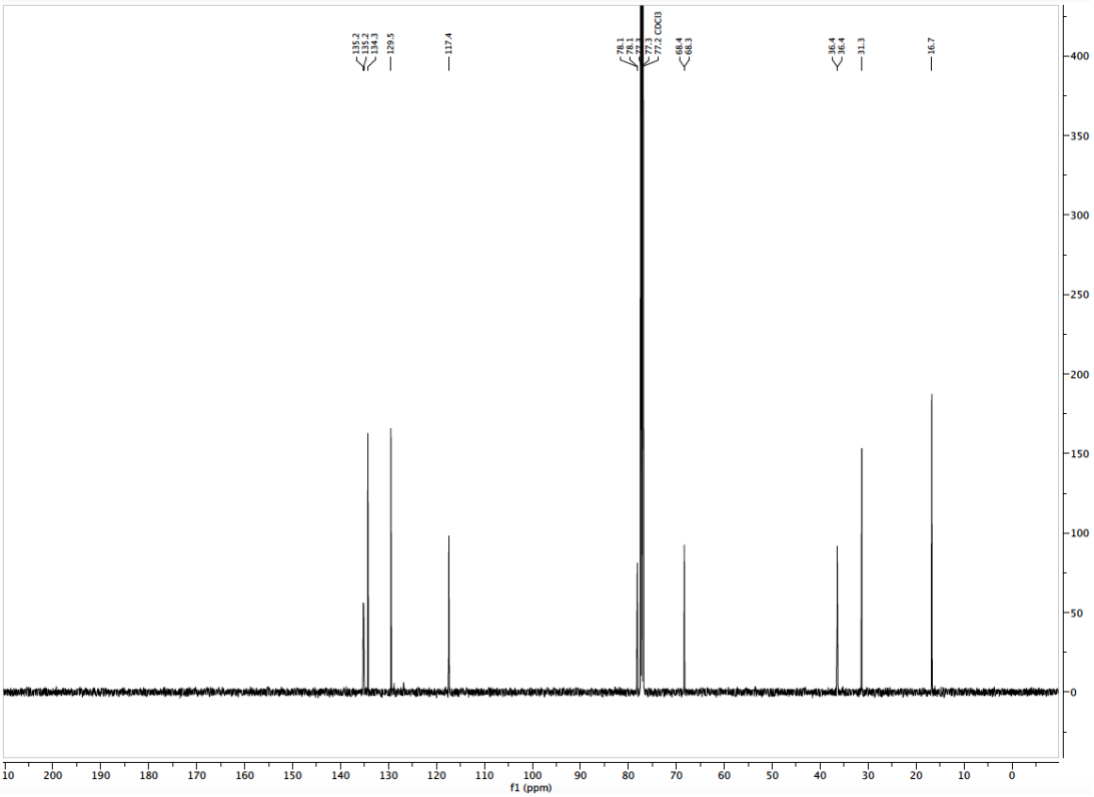

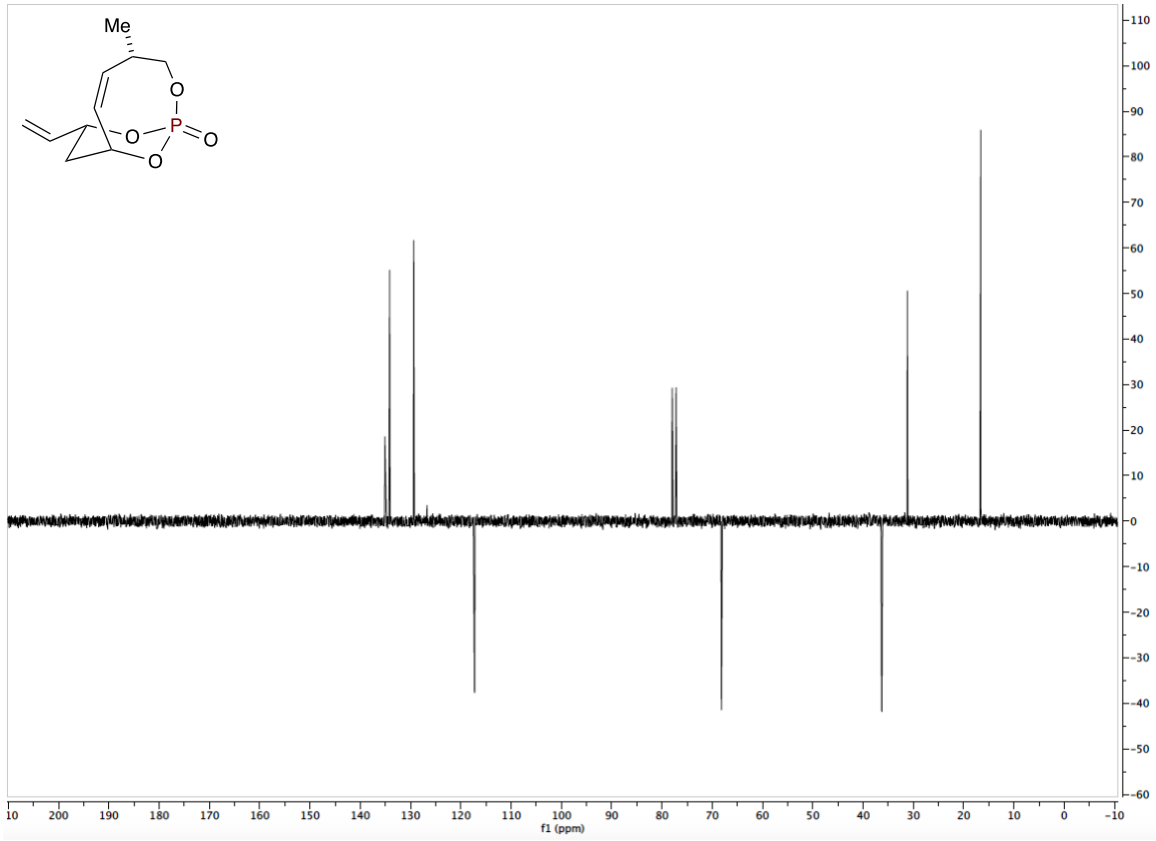
Me
O
O
P
O
O
f1 (ppm)

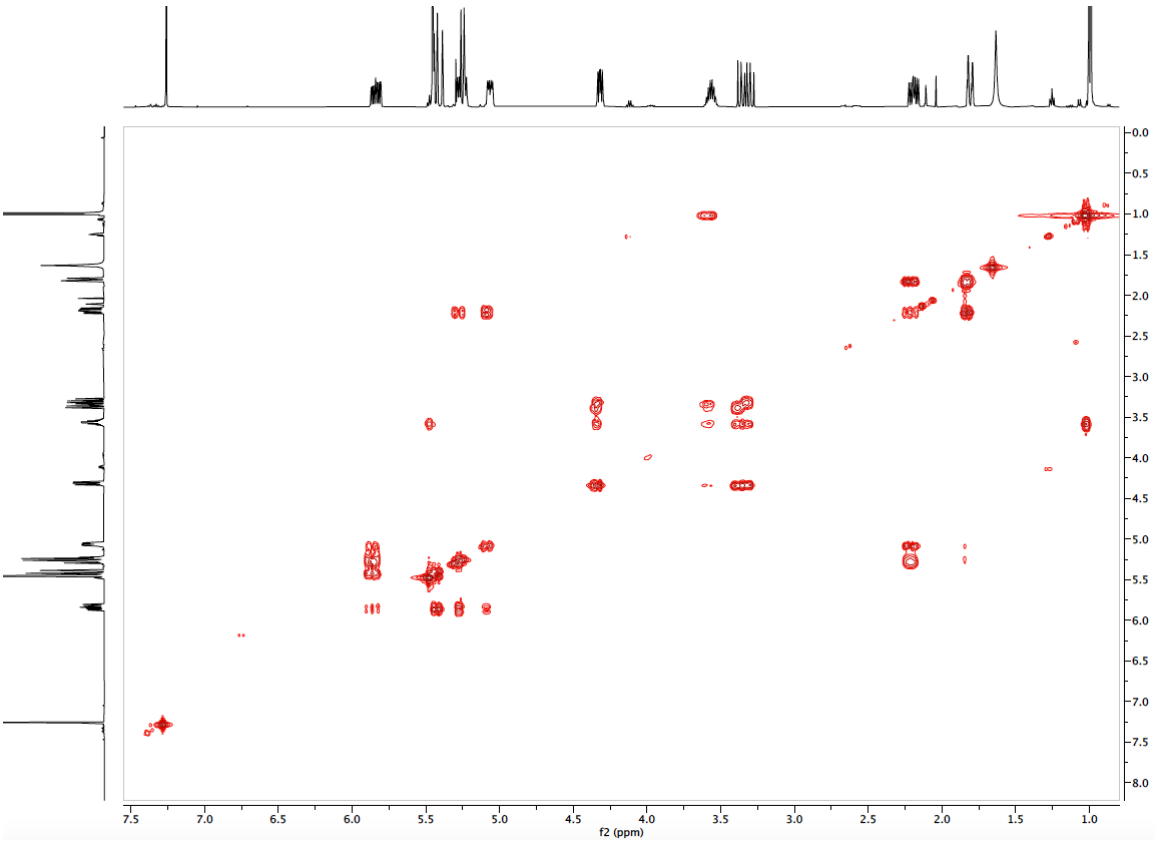
f2 (ppm)

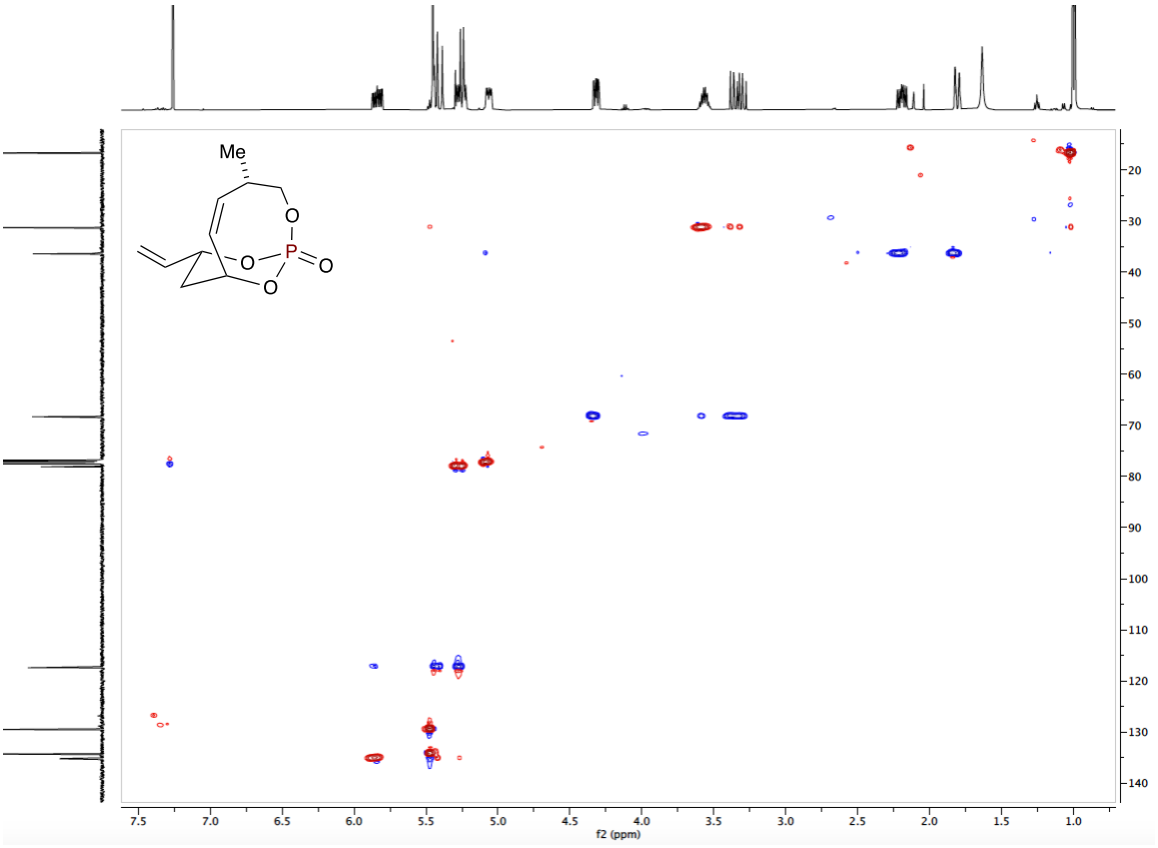
Me
O
O
P
O
O
7.5
7.0
6.5
6.0
5.5
5.0
4.5
4.0
3.5
3.0
2.5
2.0
1.5
1.0
f2 (ppm)
20
30
40
50
60
70
80
90
100
110
120
130
140

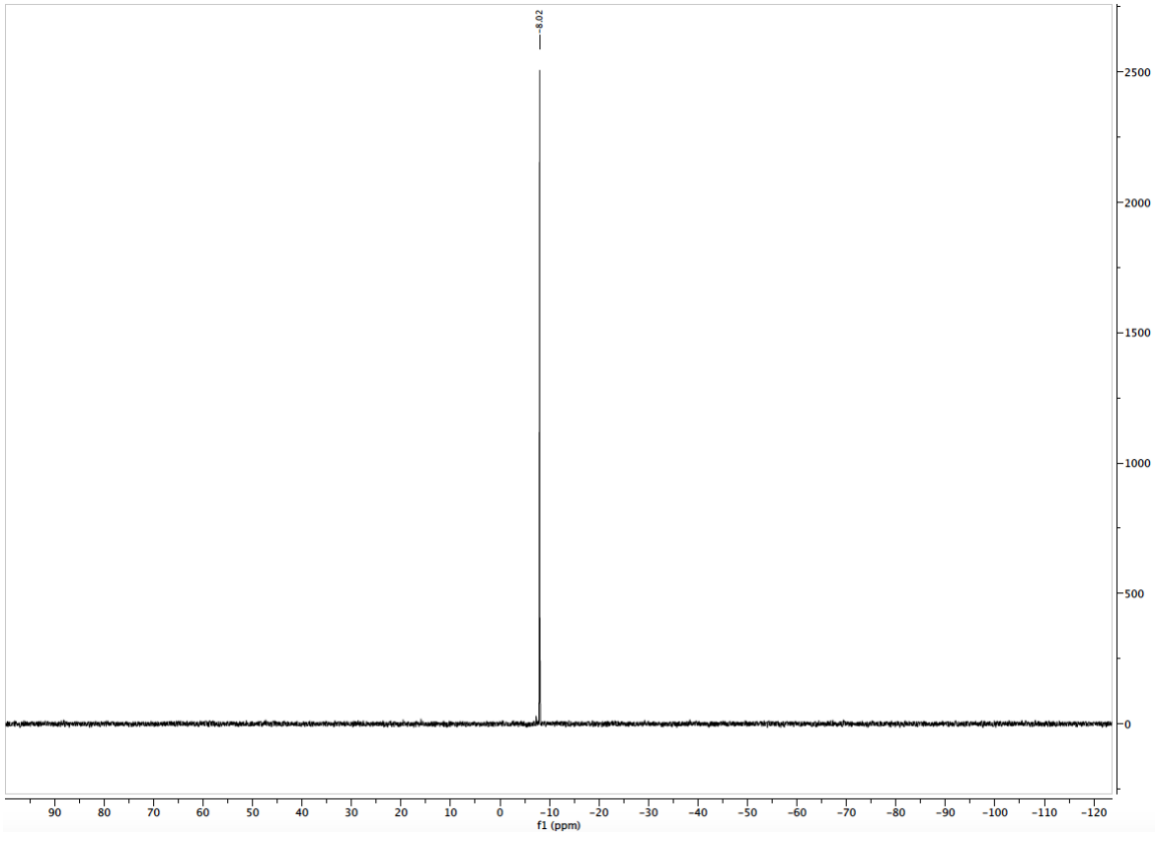
8.02
2500
2000
1500
1000
500
0
90
80
70
60
50
40
30
20
10
0
-10
-20
-30
-40
-50
-60
-70
-80
-90
-100
-110
-120
f1 (ppm)

(2*S*,5*S*,7*S*)-2-methyldodecane-1,5,7-triol ($C_{13}H_{28}O_3$, (2*S*)-2.6.6)

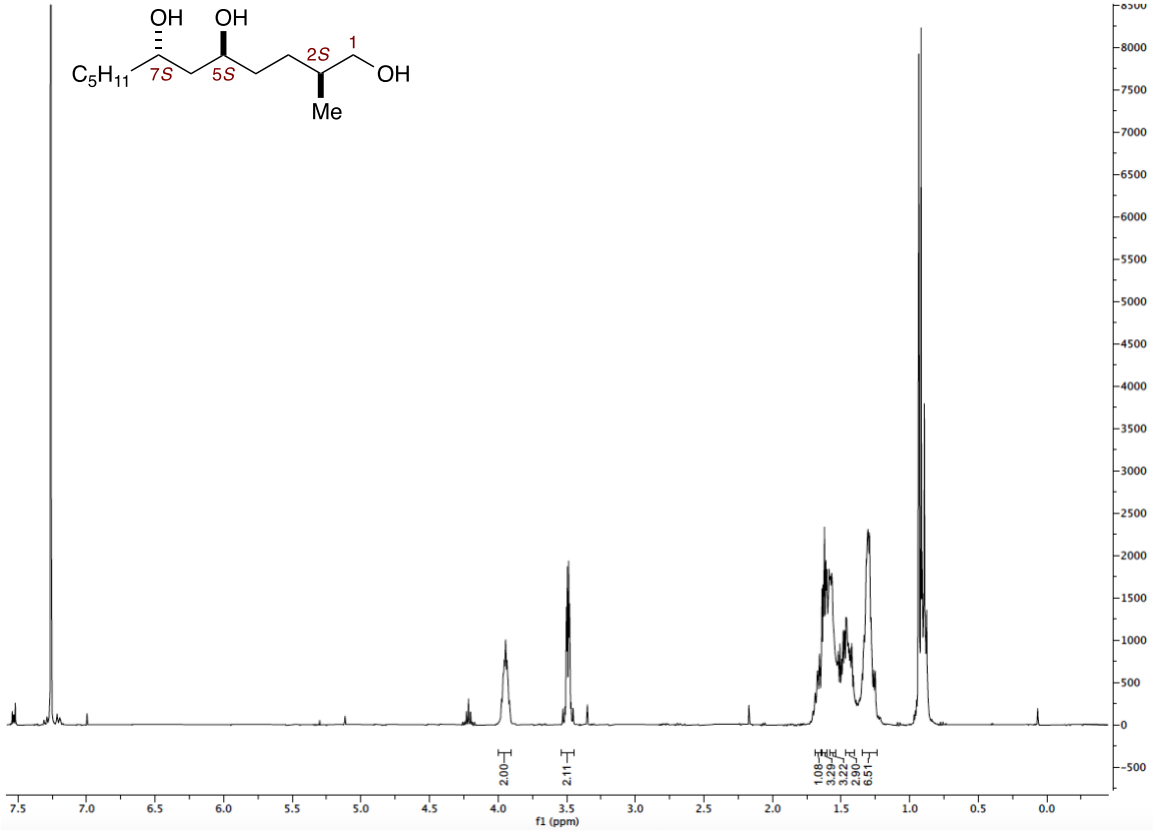

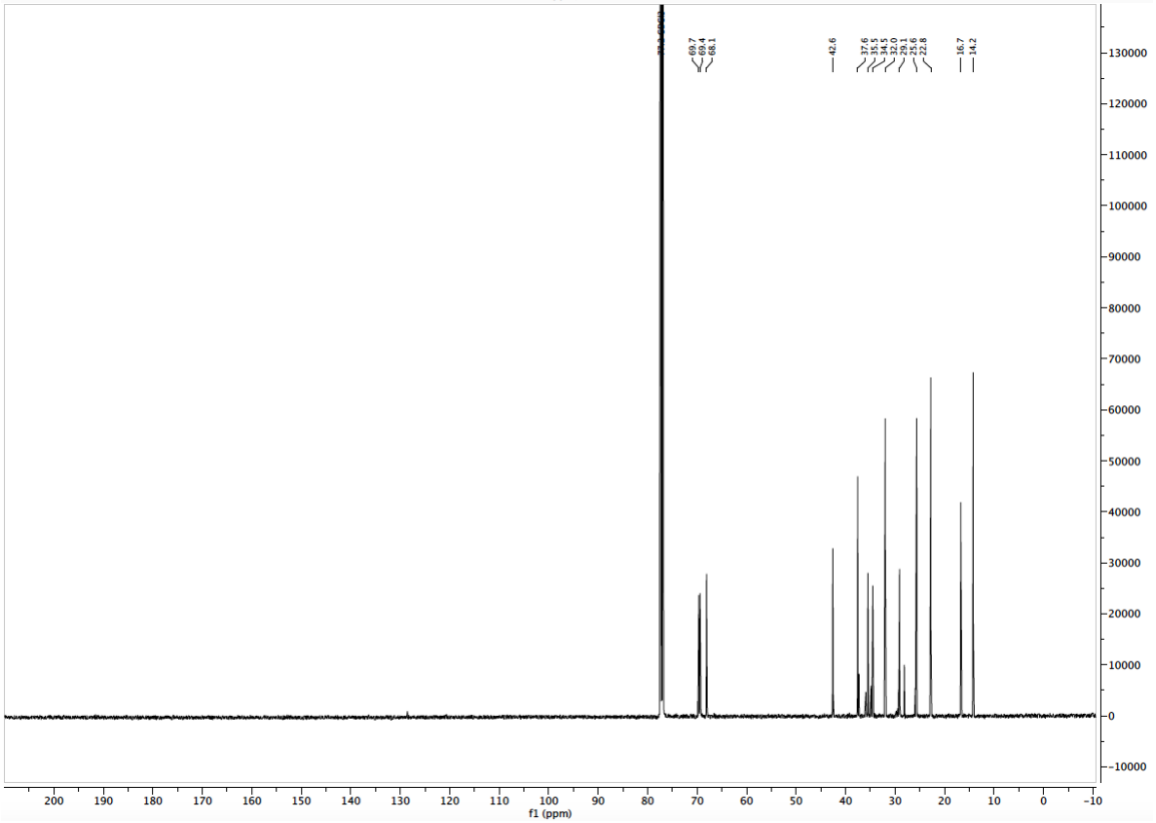

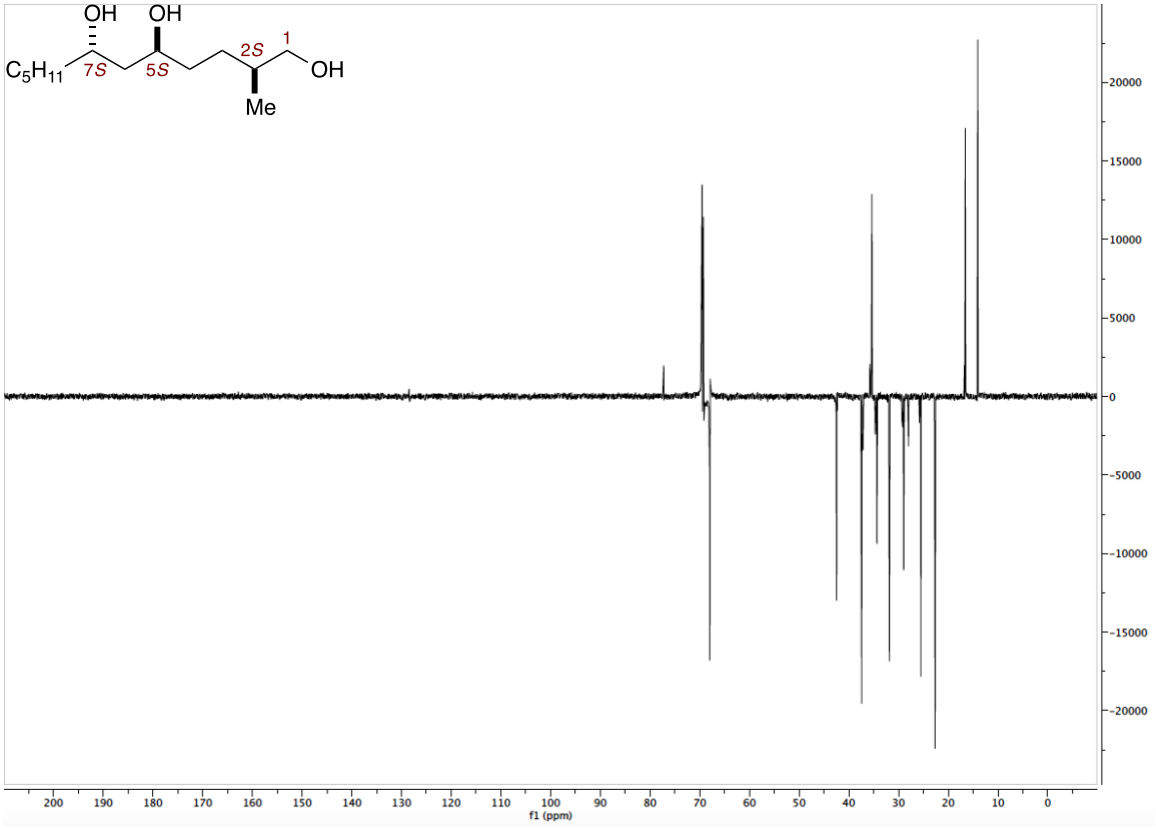
OH
OH
C_5H_{11}
7S
5S
2S
1
OH
Me
f1 (ppm)

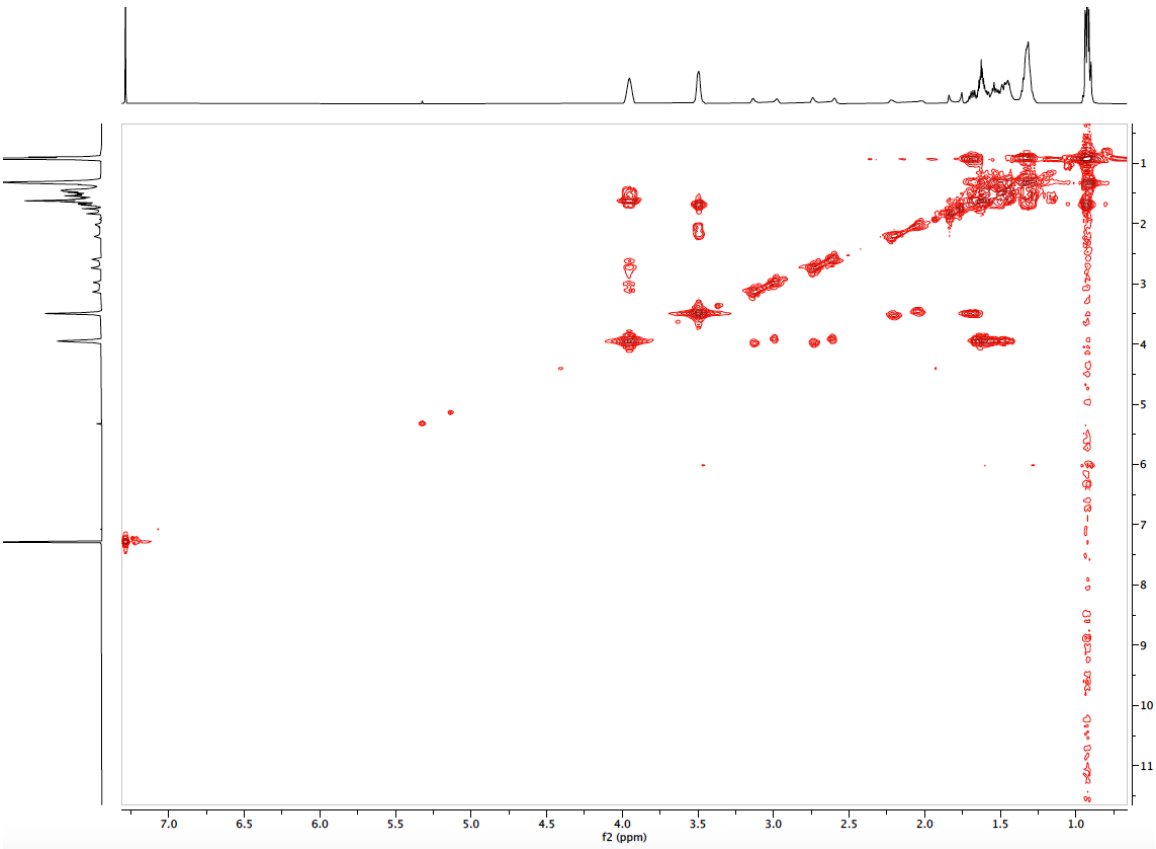
f2 (ppm)

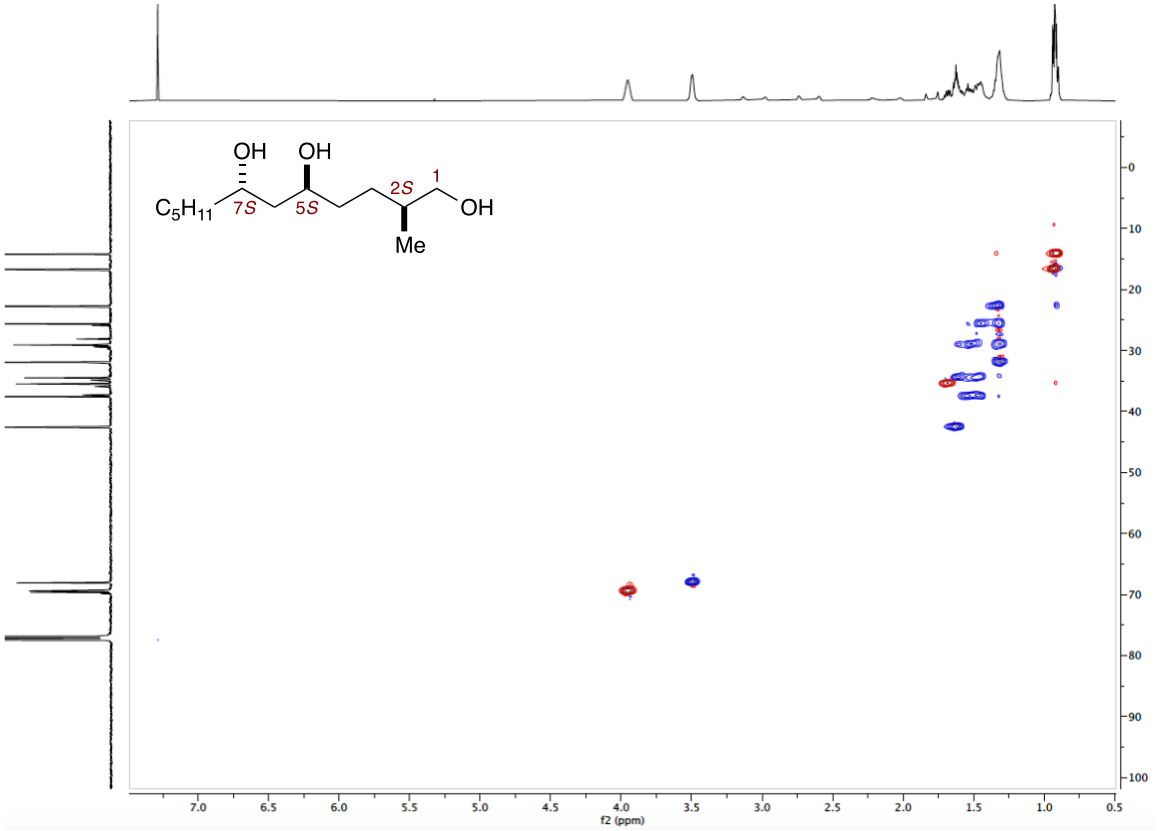
OH
OH
C_5H_{11}
7S
5S
2S
1
OH
Me
0
10
20
30
40
50
60
70
80
90
100
7.0
6.5
6.0
5.5
5.0
4.5
4.0
3.5
3.0
2.5
2.0
1.5
1.0
0.5
f2 (ppm)

(3*S*,6*S*)-6-((*S*)-2-hydroxyheptyl)-3-methyltetrahydro-2*H*-pyran-2-one ($C_{13}H_{24}O_3$, (2*S*)-2.6.7)

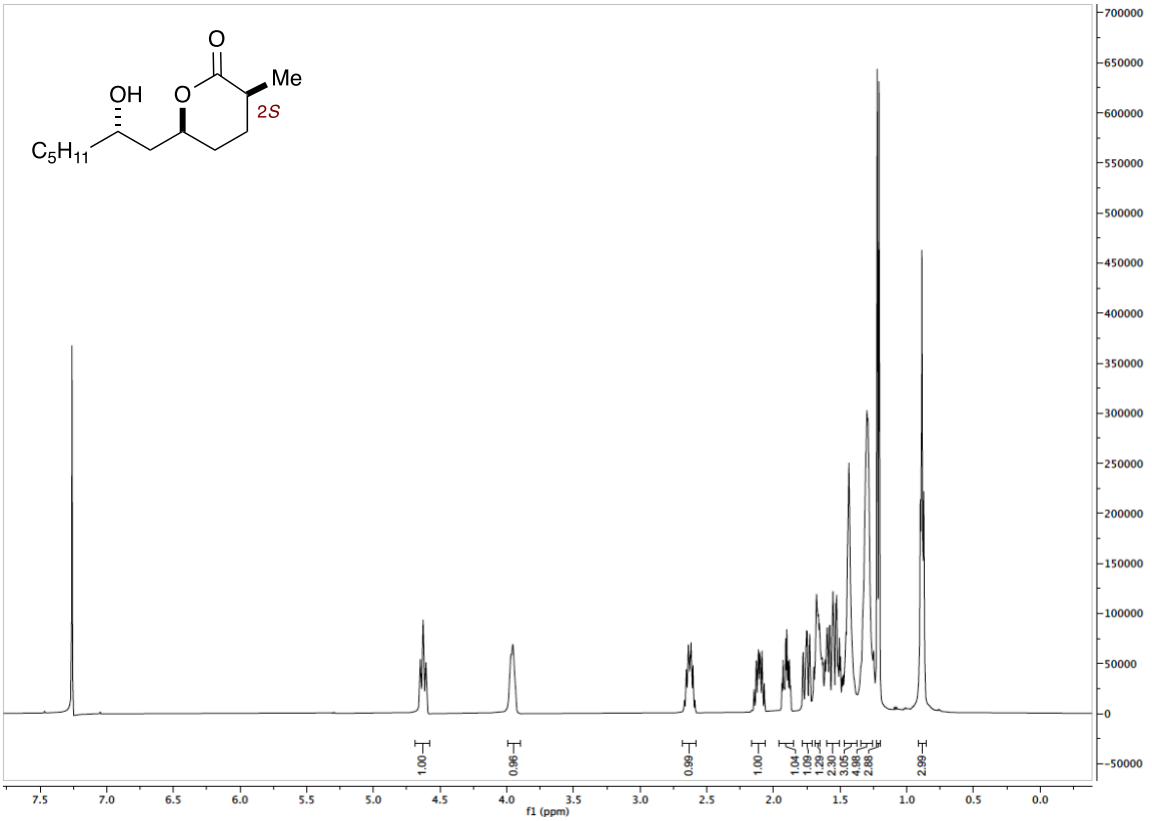

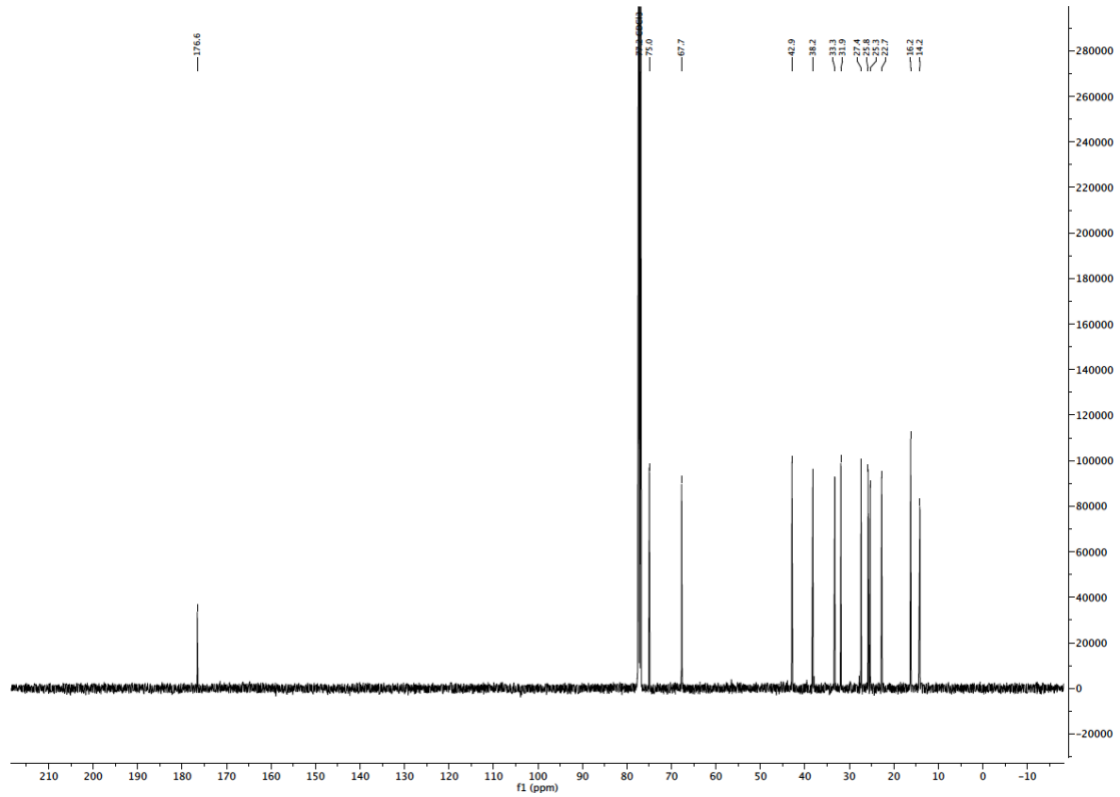

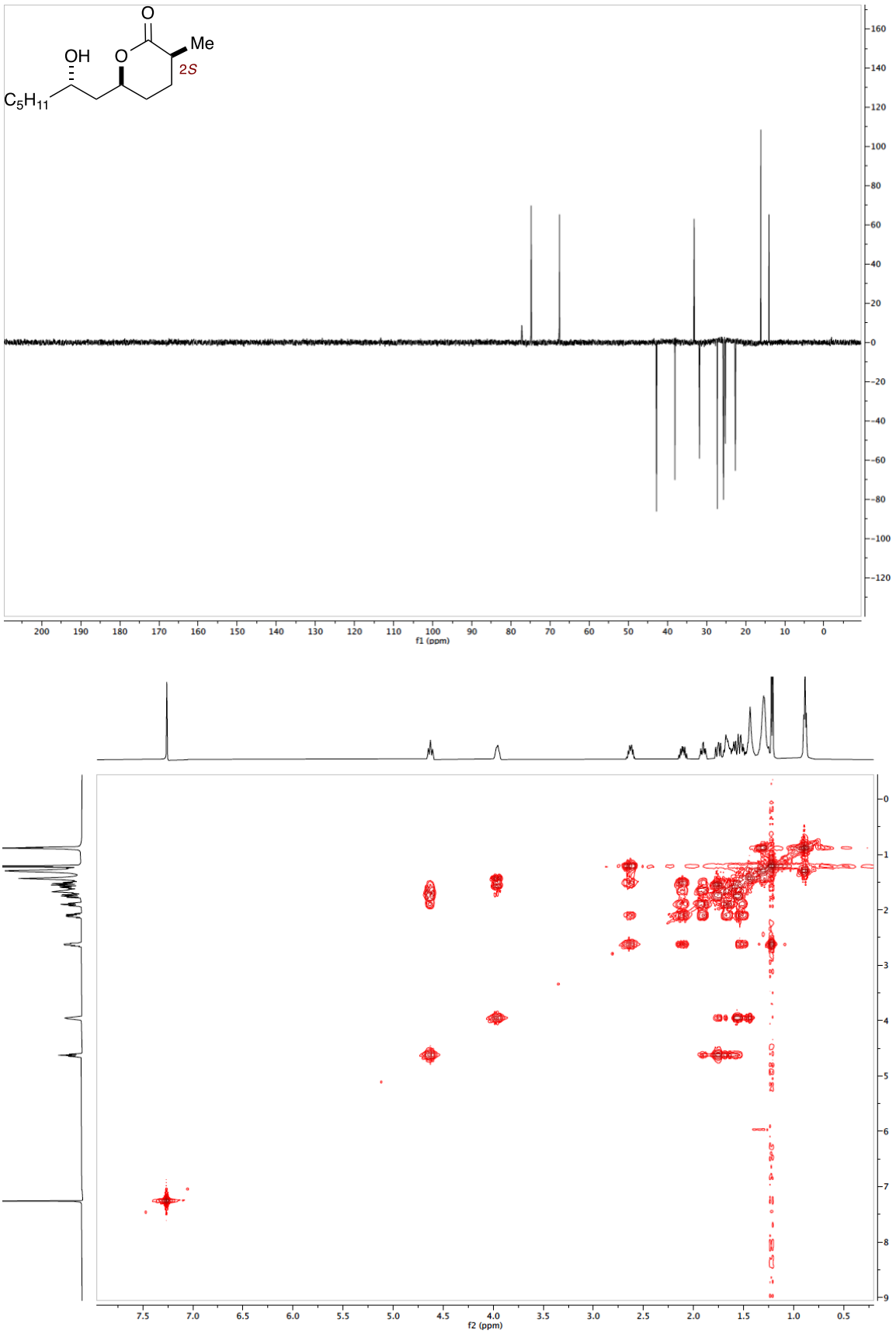
O
OH
O
Me
2S
C5H11
f1 (ppm)
f2 (ppm)

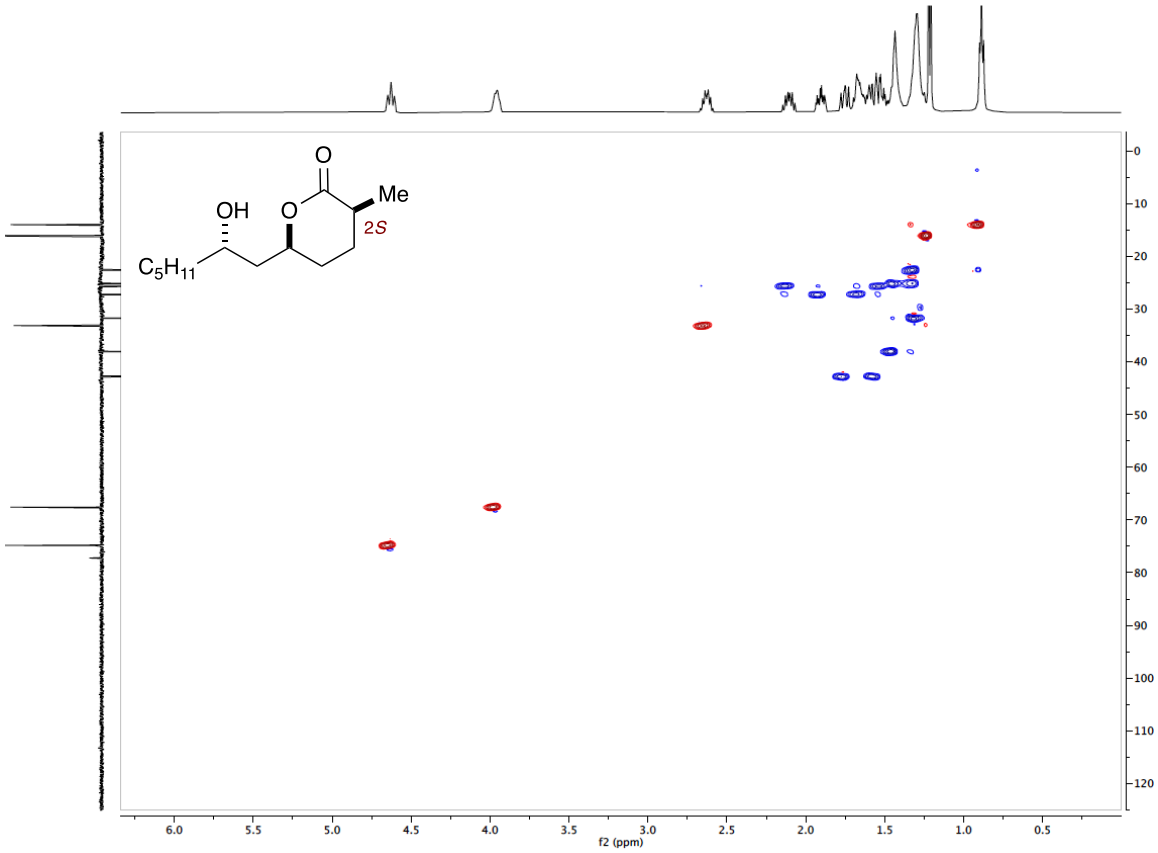
OH
O
O
Me
2S
C5H11
f2 (ppm)

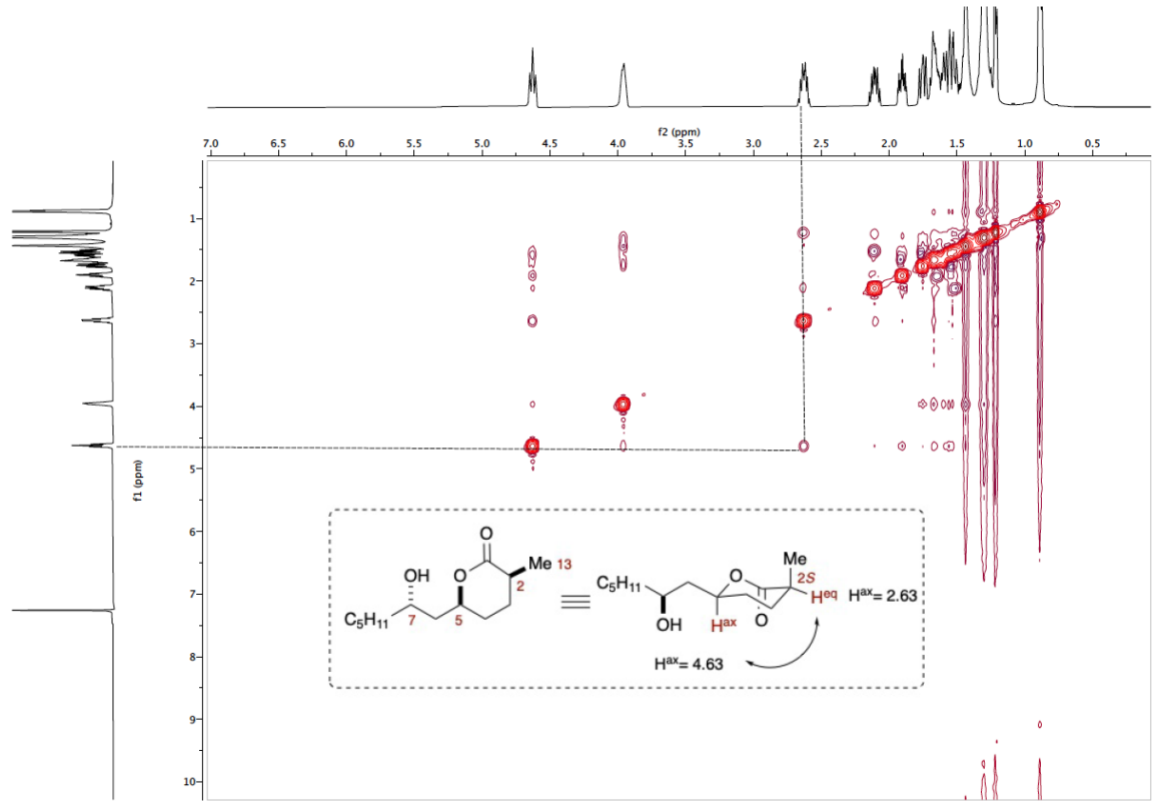
f2 (ppm)
f1 (ppm)
OH
O
O
Me 13
2
C5H11
7
5
Me
2S
Heq
Hax= 2.63
Hax= 4.63

(3*S*,6*S*)-6-((*S*)-2-methoxyheptyl)-3-methyltetrahydro-2*H*-pyran-2-one ($C_{14}H_{26}O_3$, (2*S*)-2.1.6)

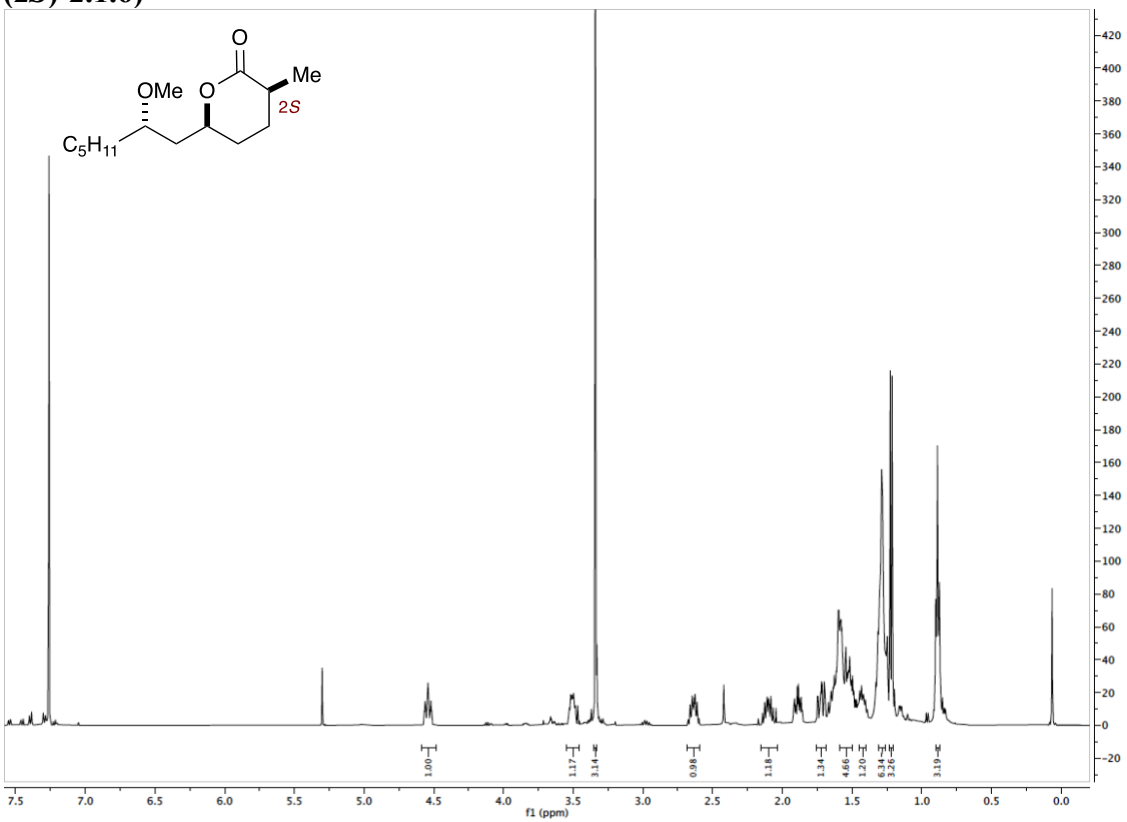

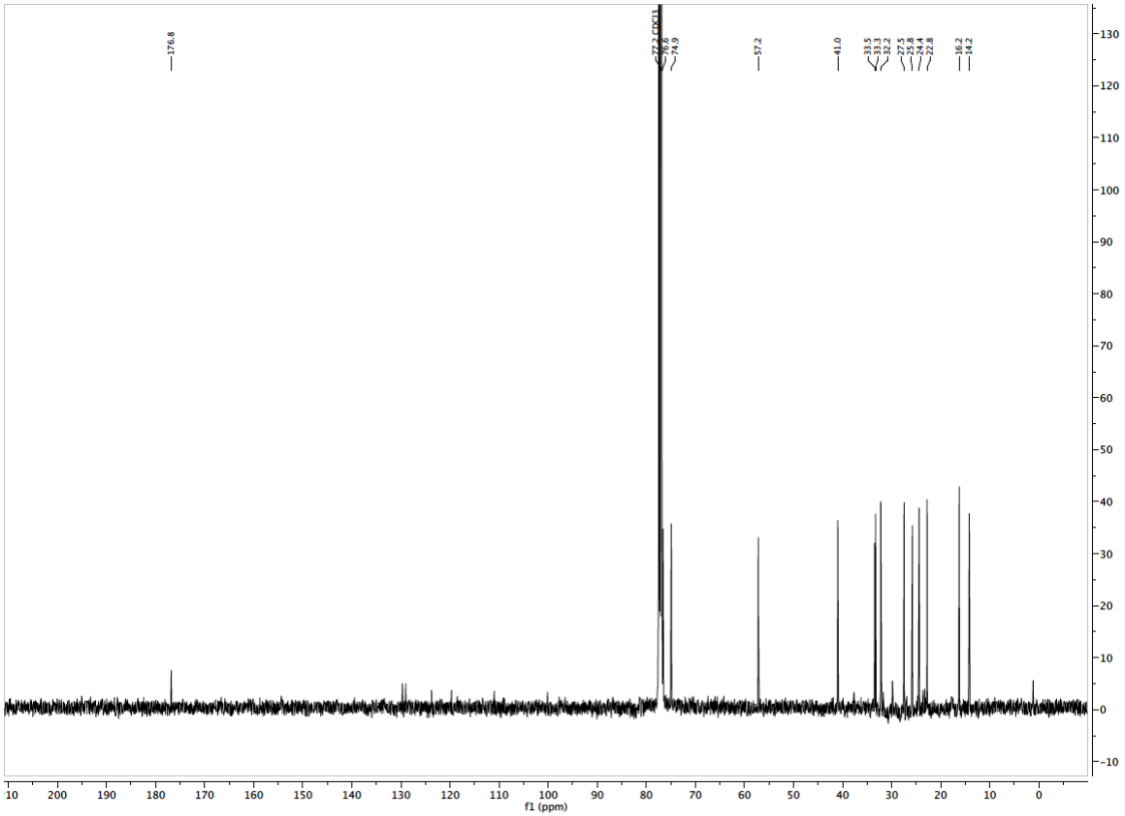

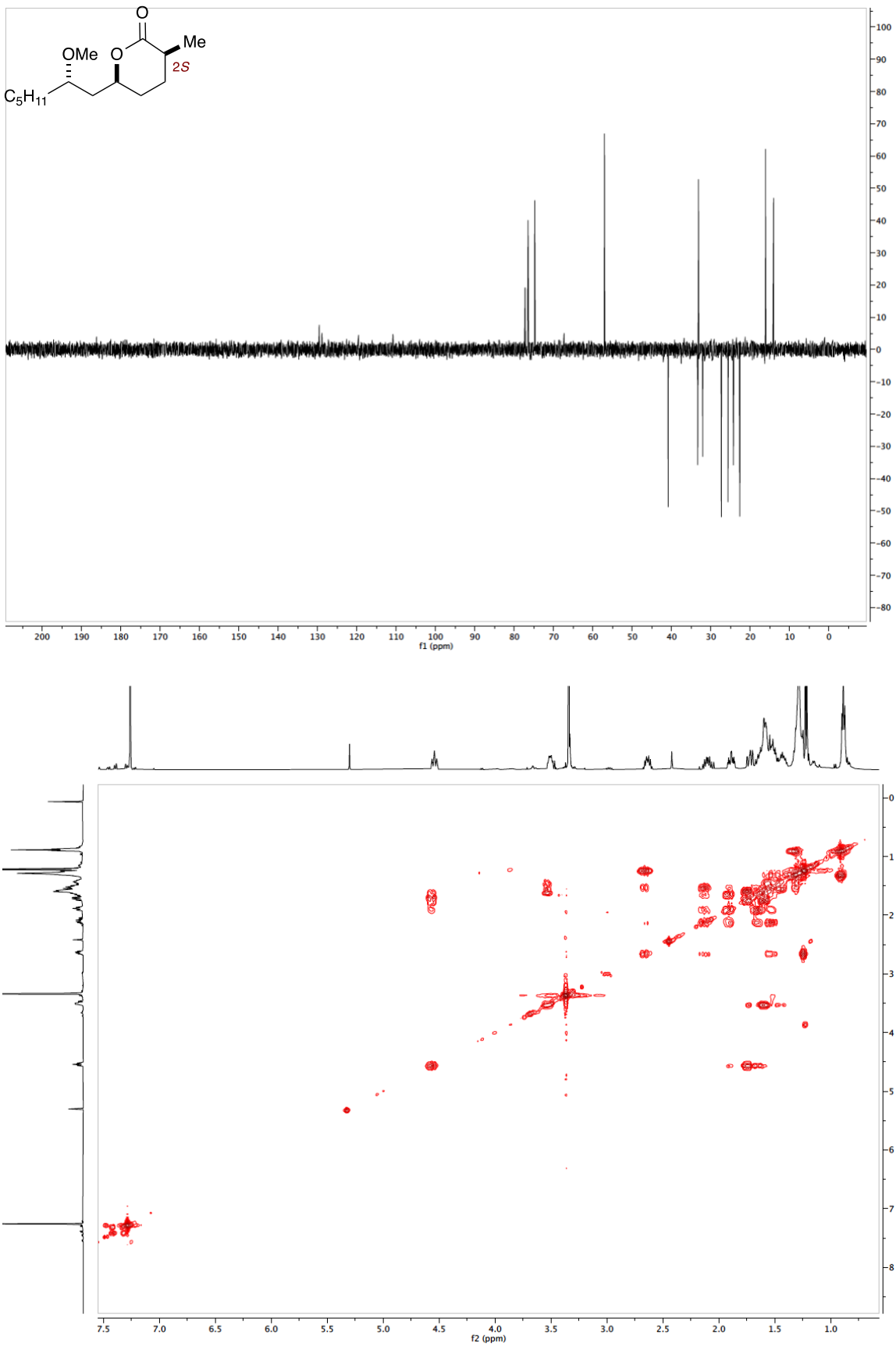
O
OMe
O
Me
2S
C5H11
f1 (ppm)
f2 (ppm)

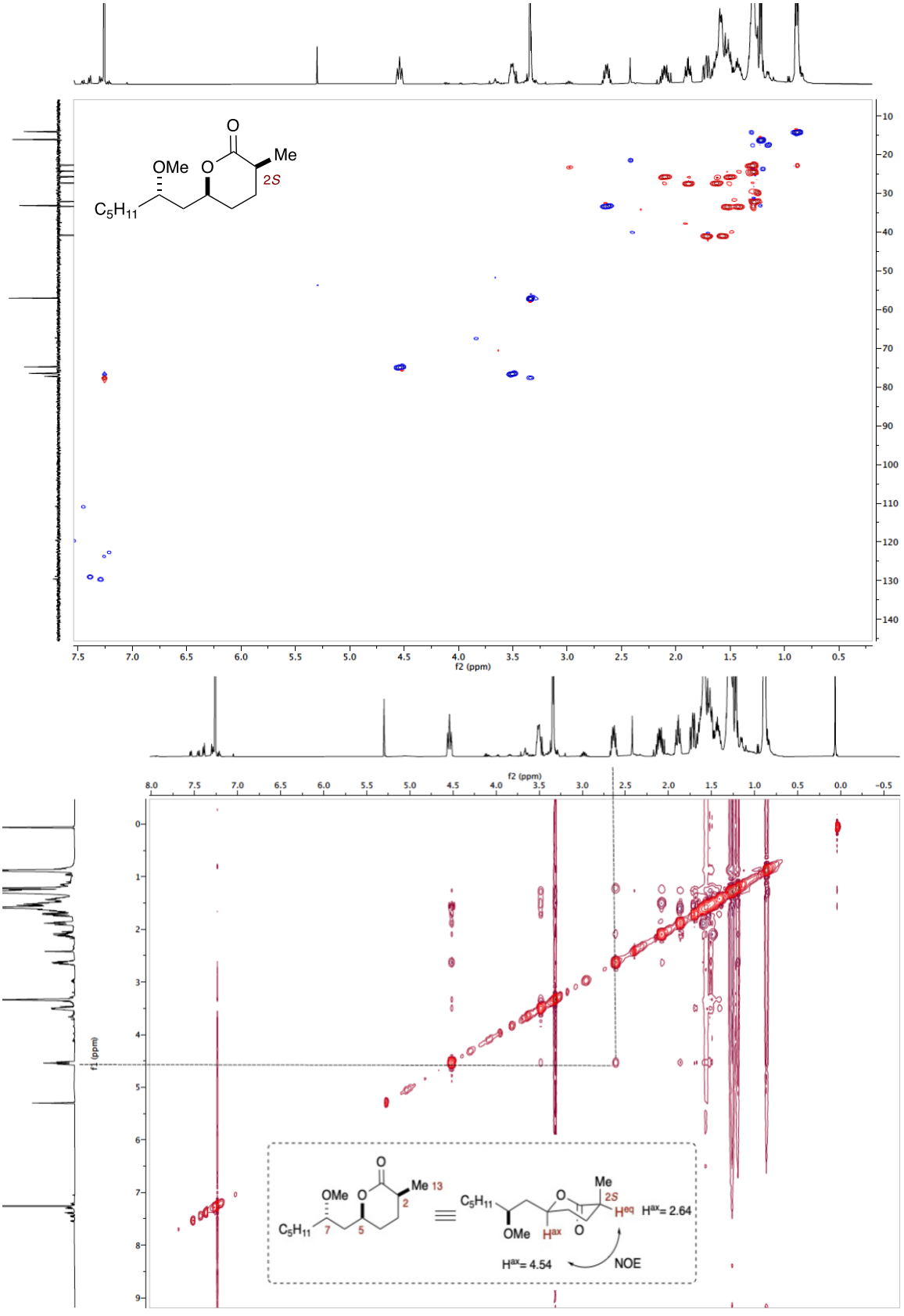
OMe
O
Me
2S
C5H11
f2 (ppm)
f1 (ppm)
Me 13
OMe
C5H11
7
5
2
Me
2S
Heq
Hax = 2.64
OMe
Hax
Hax = 4.54
NOE

(4*S*,6*S*)-4,6-diallyl-2-((2-methylallyl)oxy)-1,3,2-dioxaphosphinane 2-oxide ($C_{13}H_{21}O_4P$, 2.7.4)

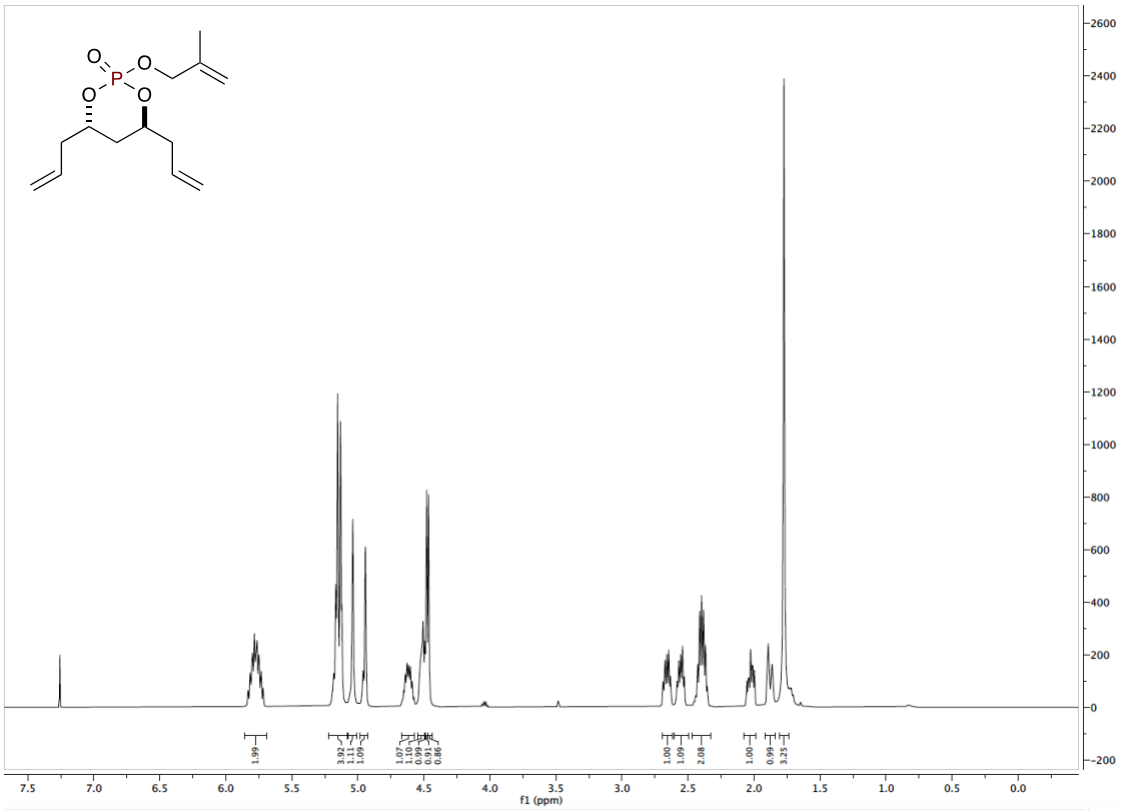

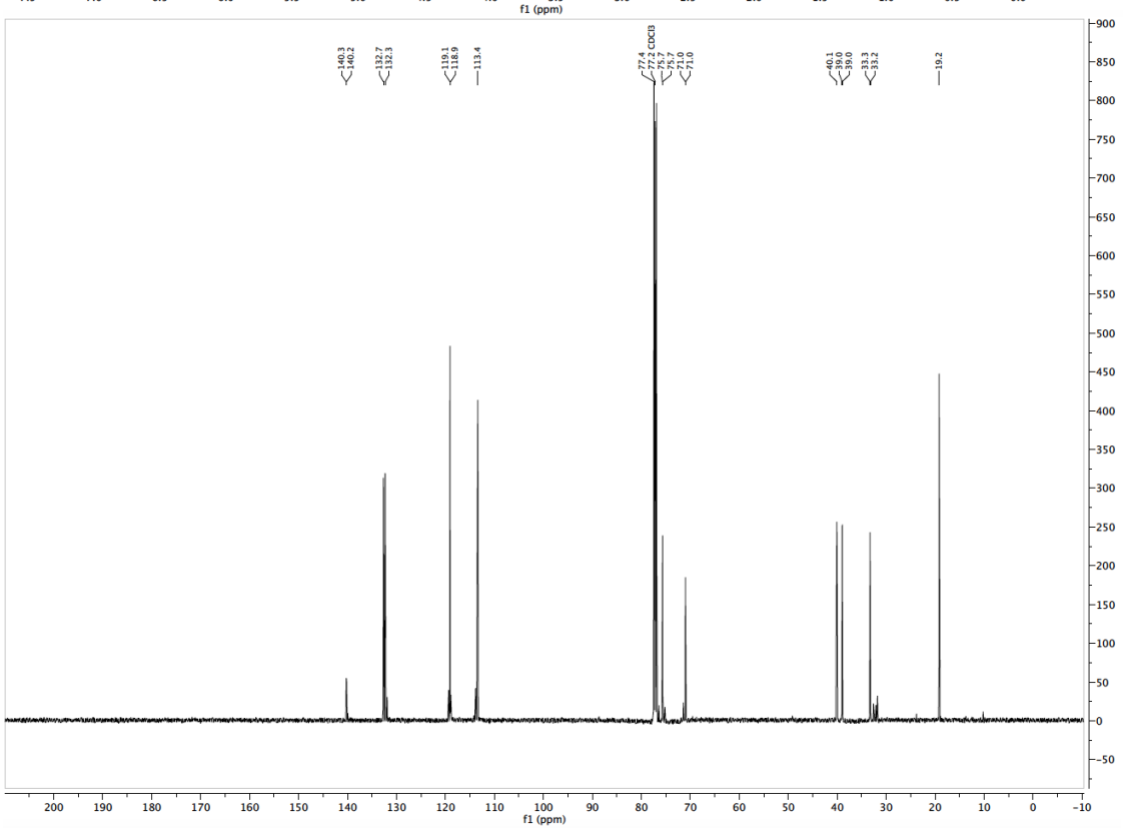

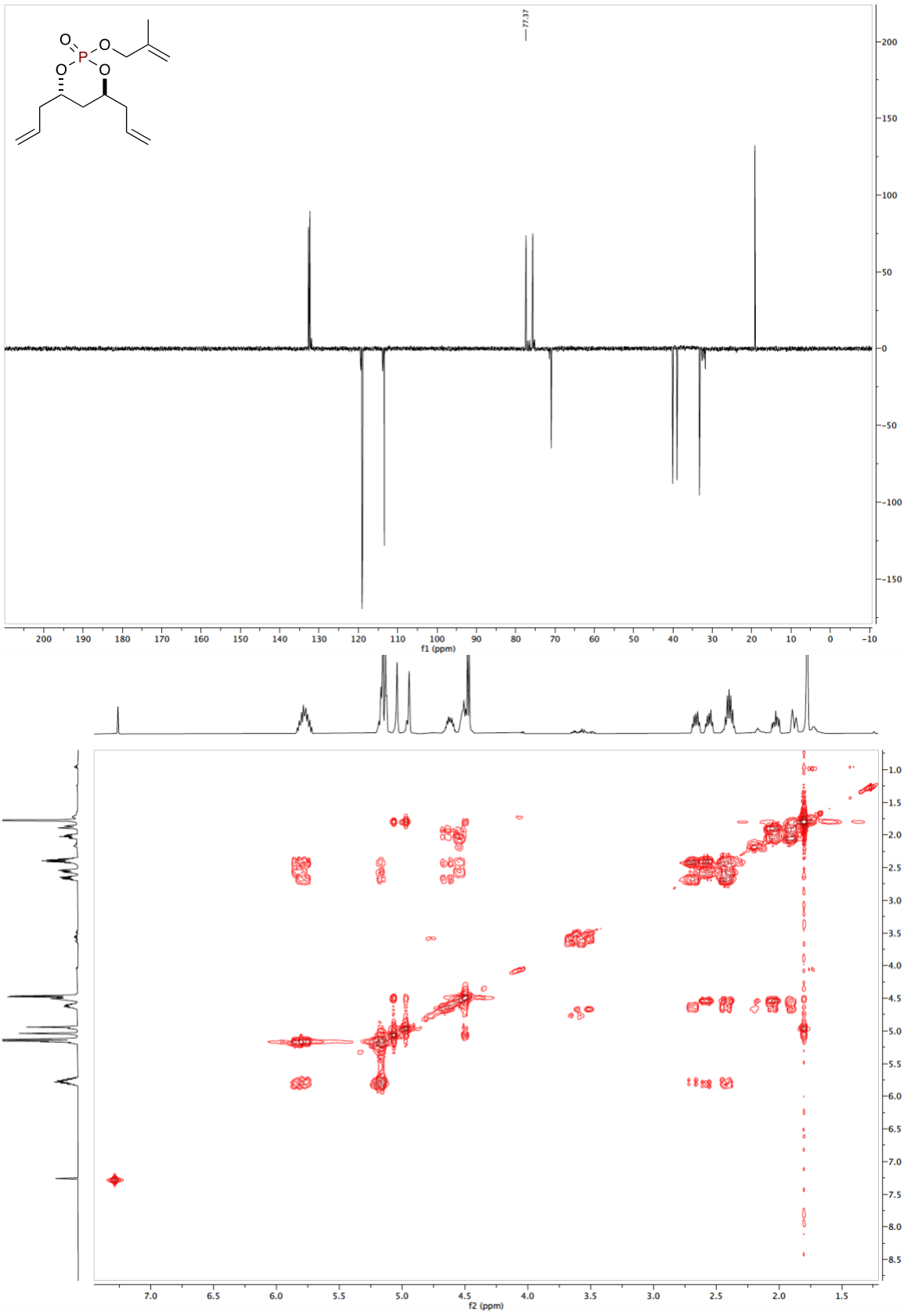
77.37
f1 (ppm)
f2 (ppm)

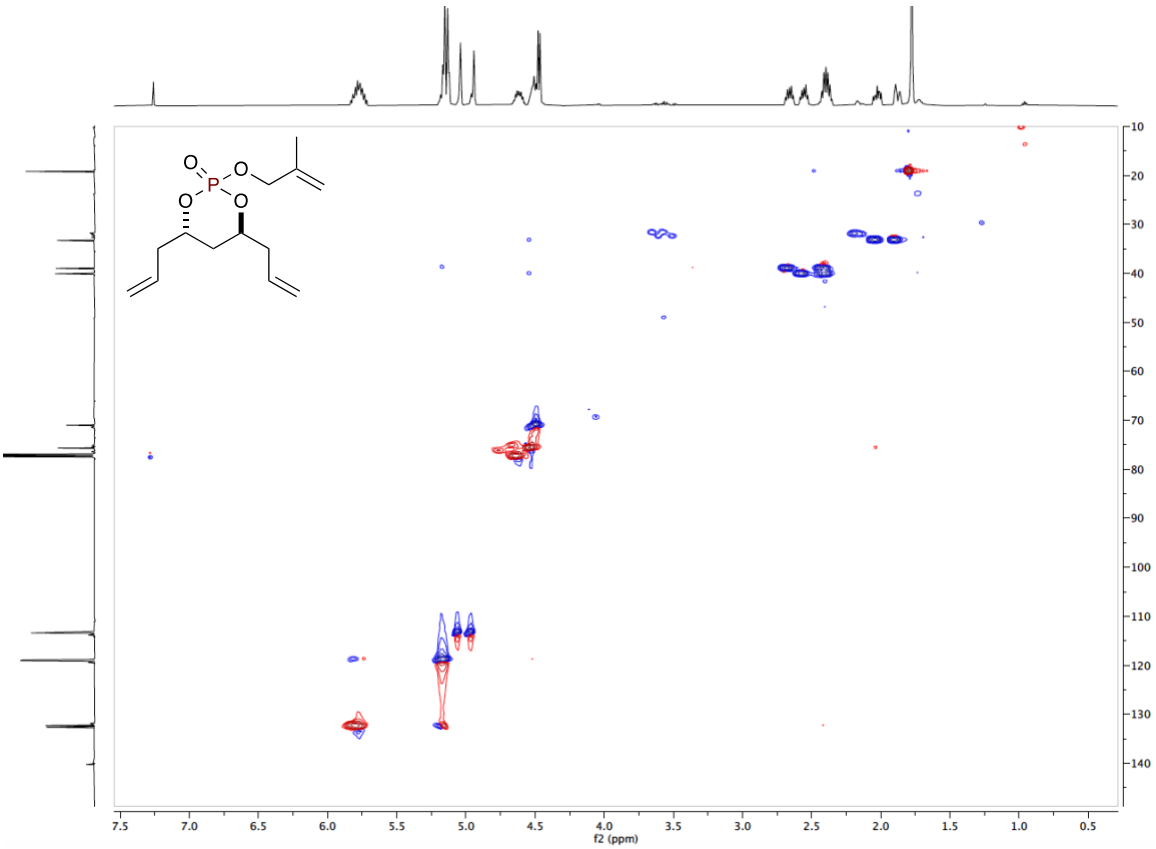
f2 (ppm)

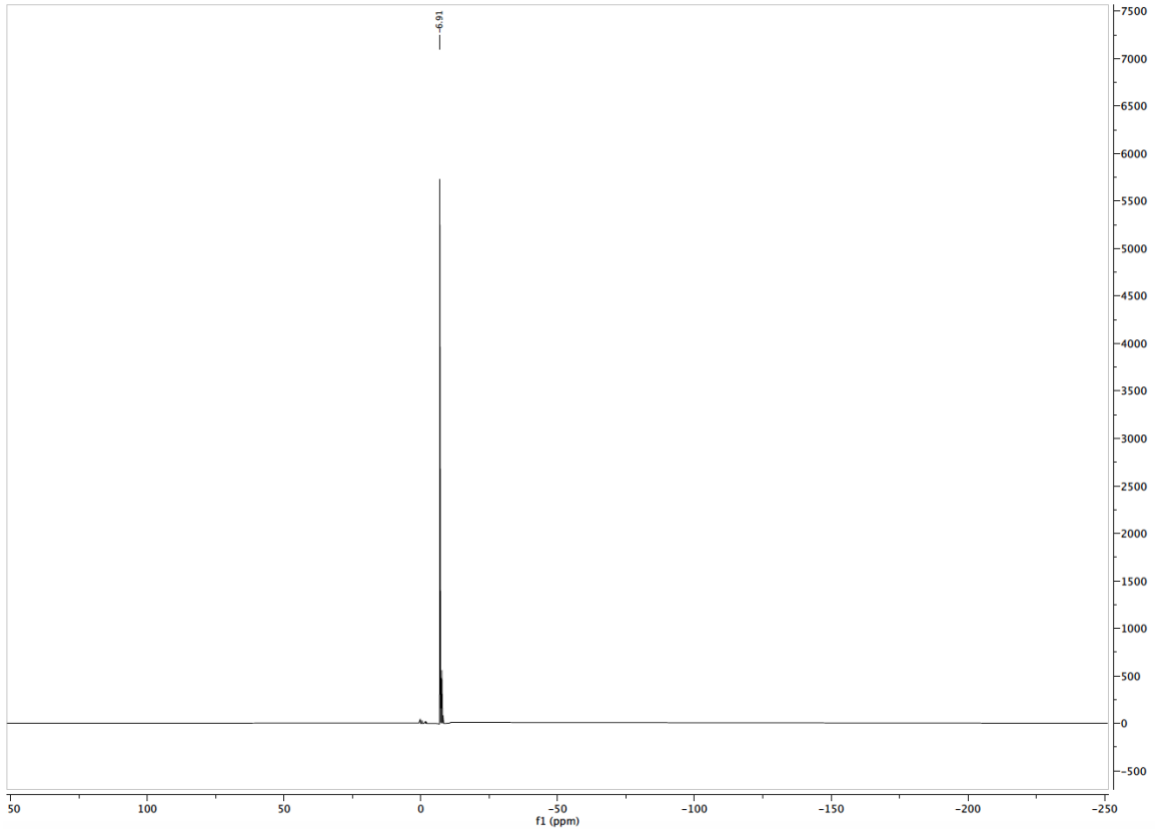
-6.91
f1 (ppm)

(2*R*,5*S*,7*S*)-2-methyldodecane-1,5,7-triol ($C_{13}H_{28}O_3$, (2*R*)-2.6.6)

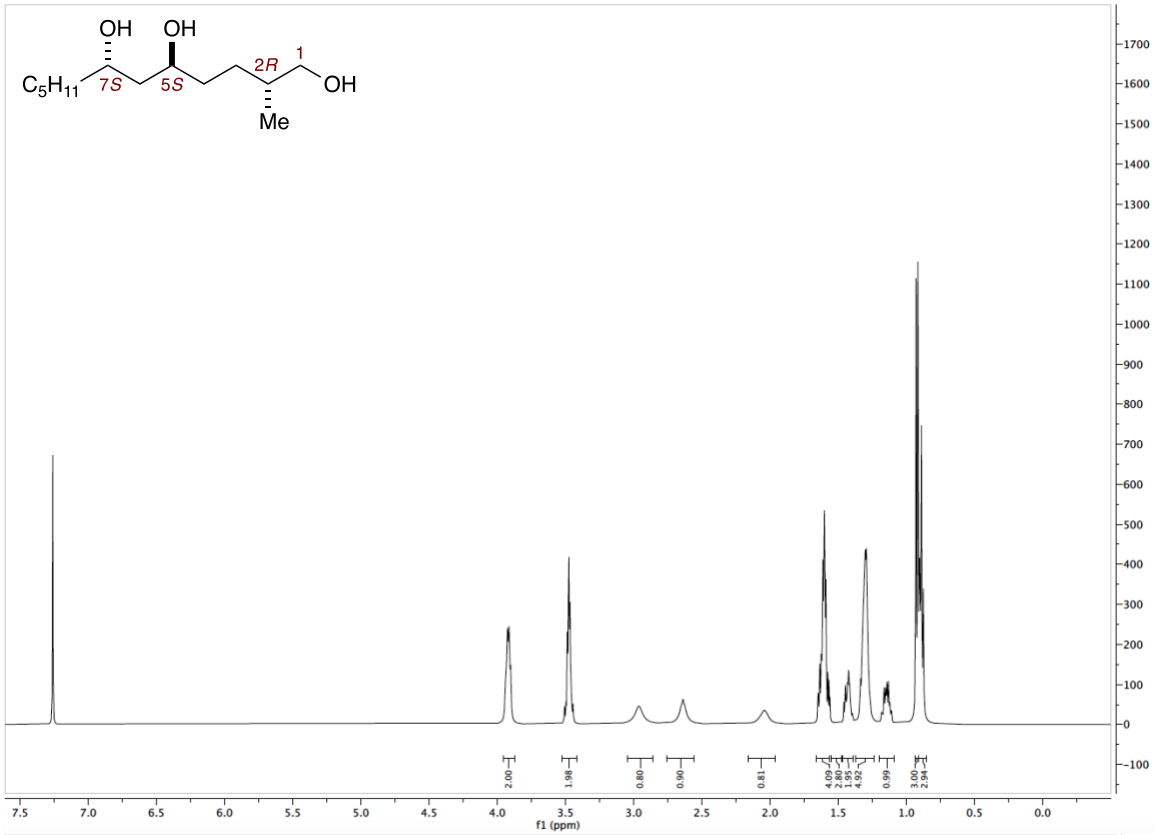

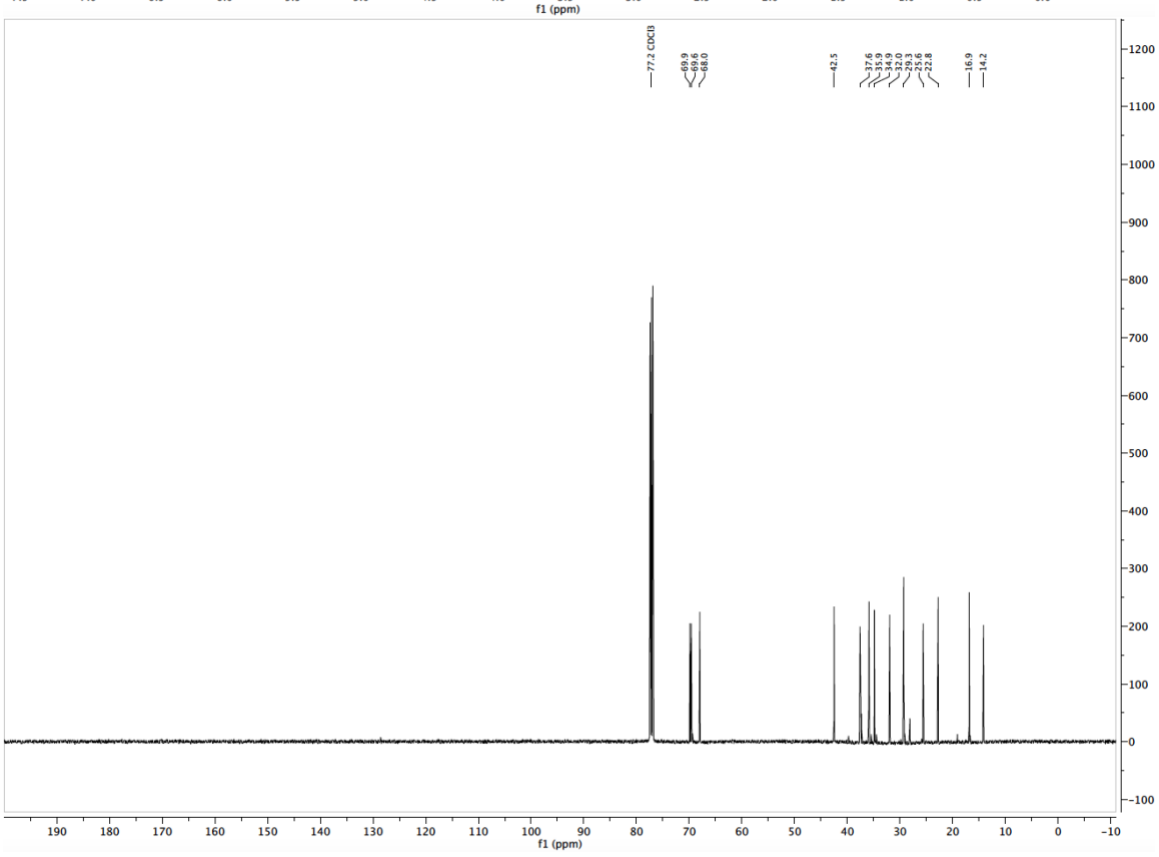

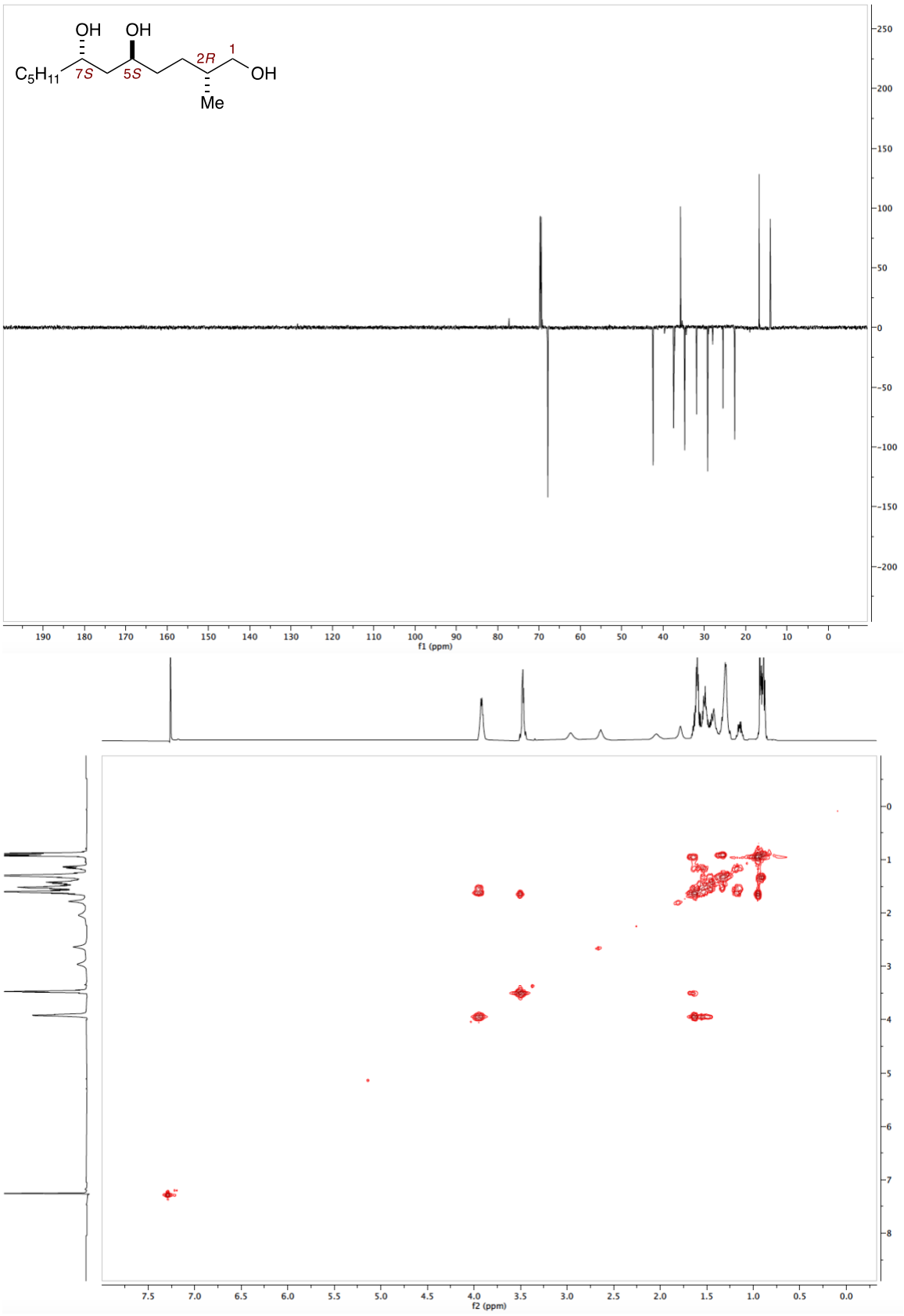
OH
OH
C_5H_{11}
7S
5S
2R
1
OH
Me
f1 (ppm)
f2 (ppm)

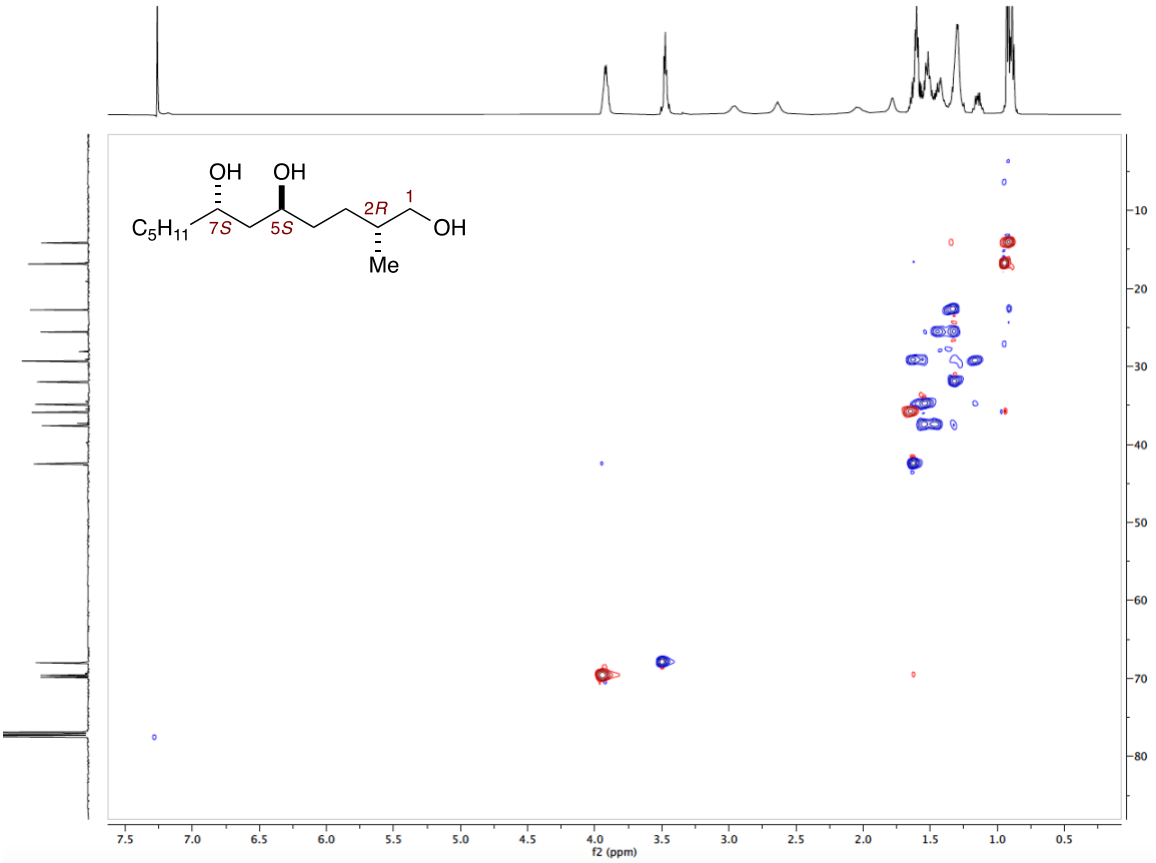
OH
OH
C5H11
7S
5S
2R
1
OH
Me
10
20
30
40
50
60
70
80
7.5
7.0
6.5
6.0
5.5
5.0
4.5
4.0
3.5
3.0
2.5
2.0
1.5
1.0
0.5
f2 (ppm)

(3*R*,6*S*)-6-((*S*)-2-hydroxyheptyl)-3-methyltetrahydro-2*H*-pyran-2-one ($C_{13}H_{24}O_3$, (2*R*)-2.6.7)

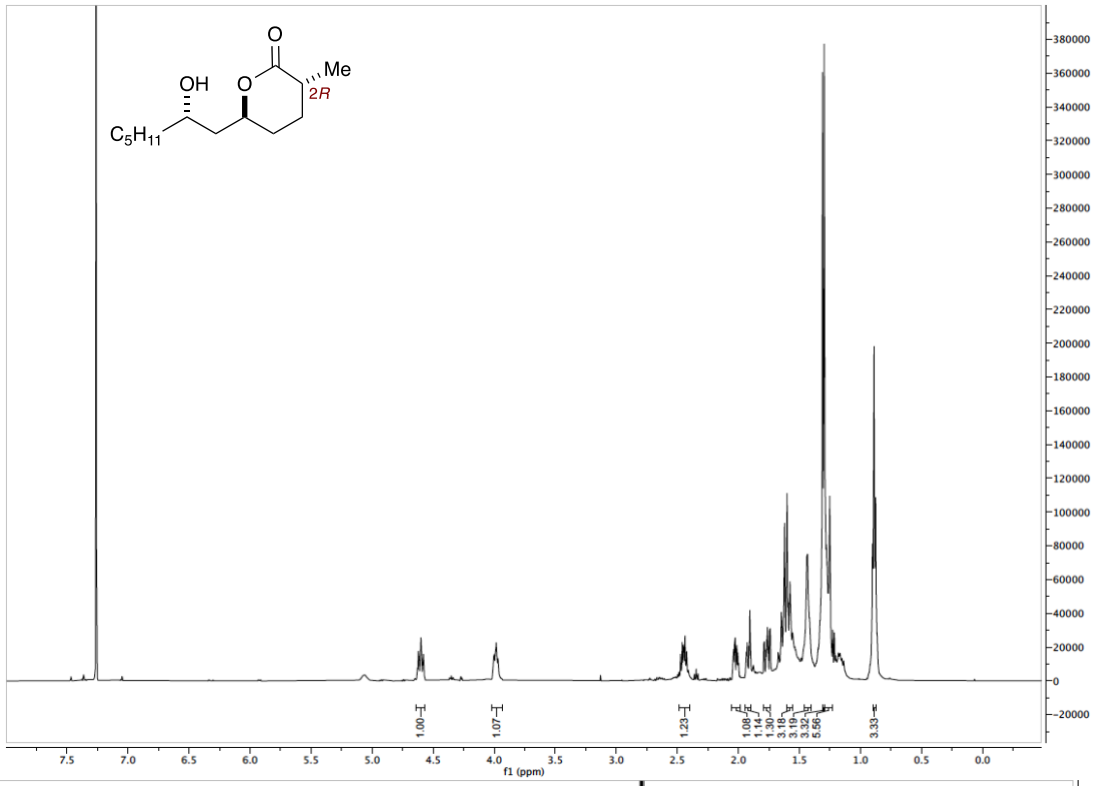

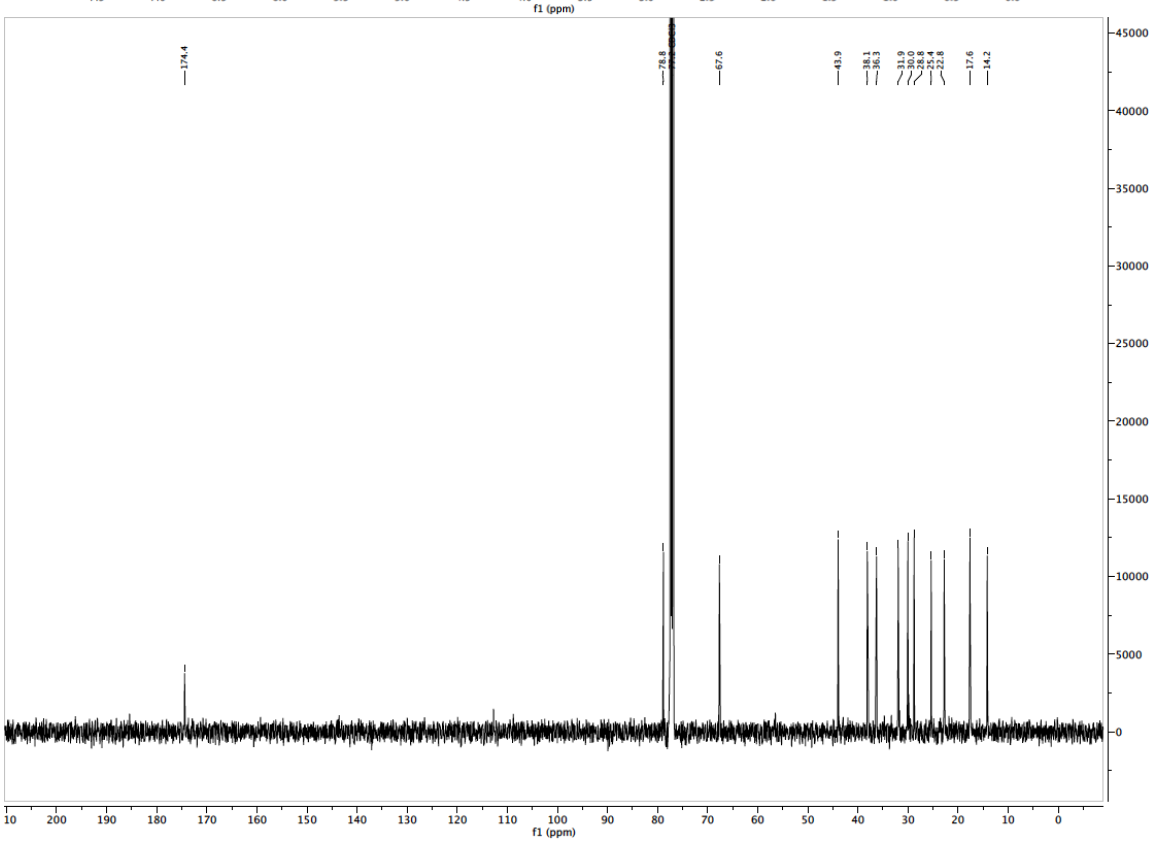

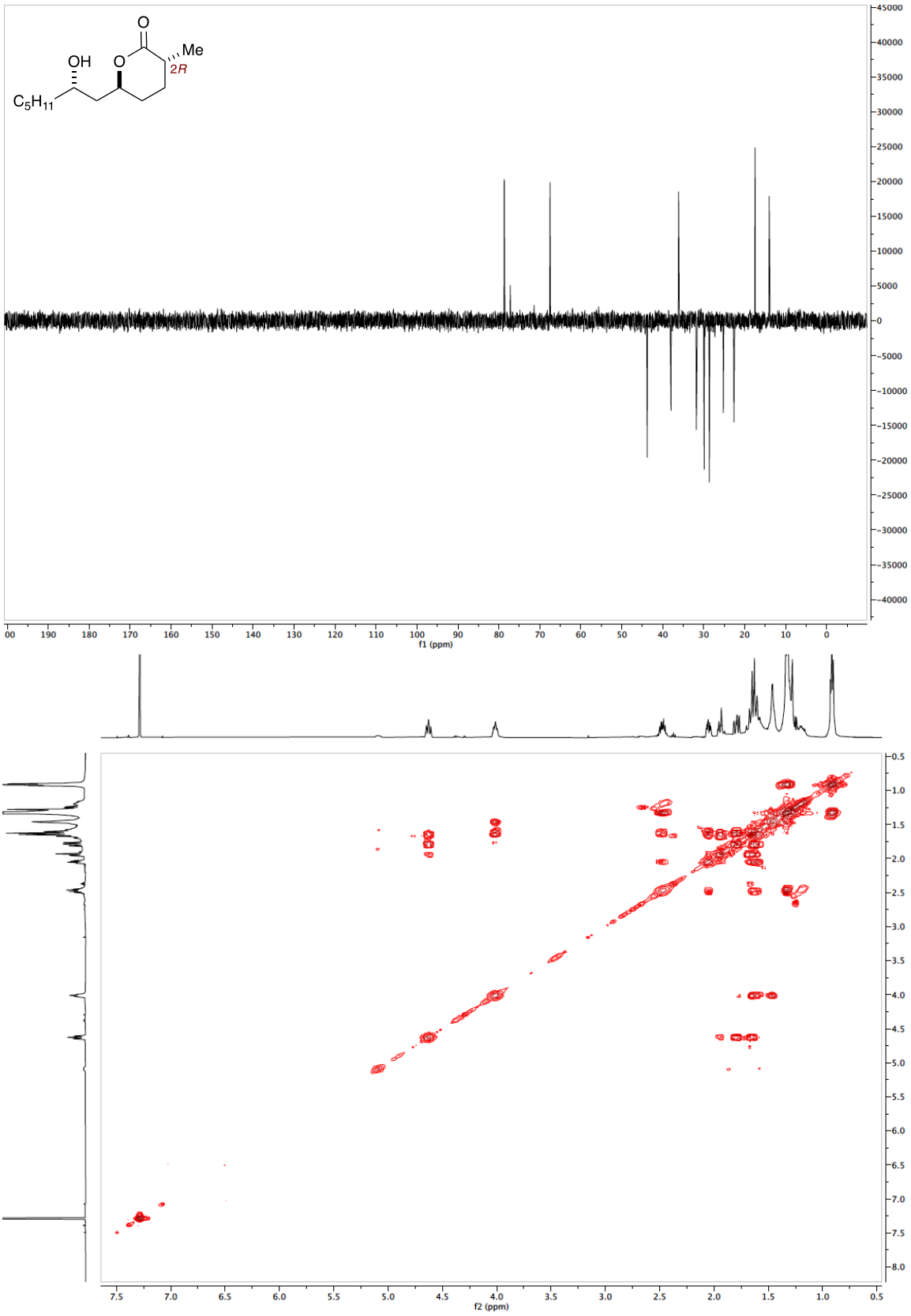
O
OH
O
Me
2R
C5H11
f1 (ppm)
f2 (ppm)

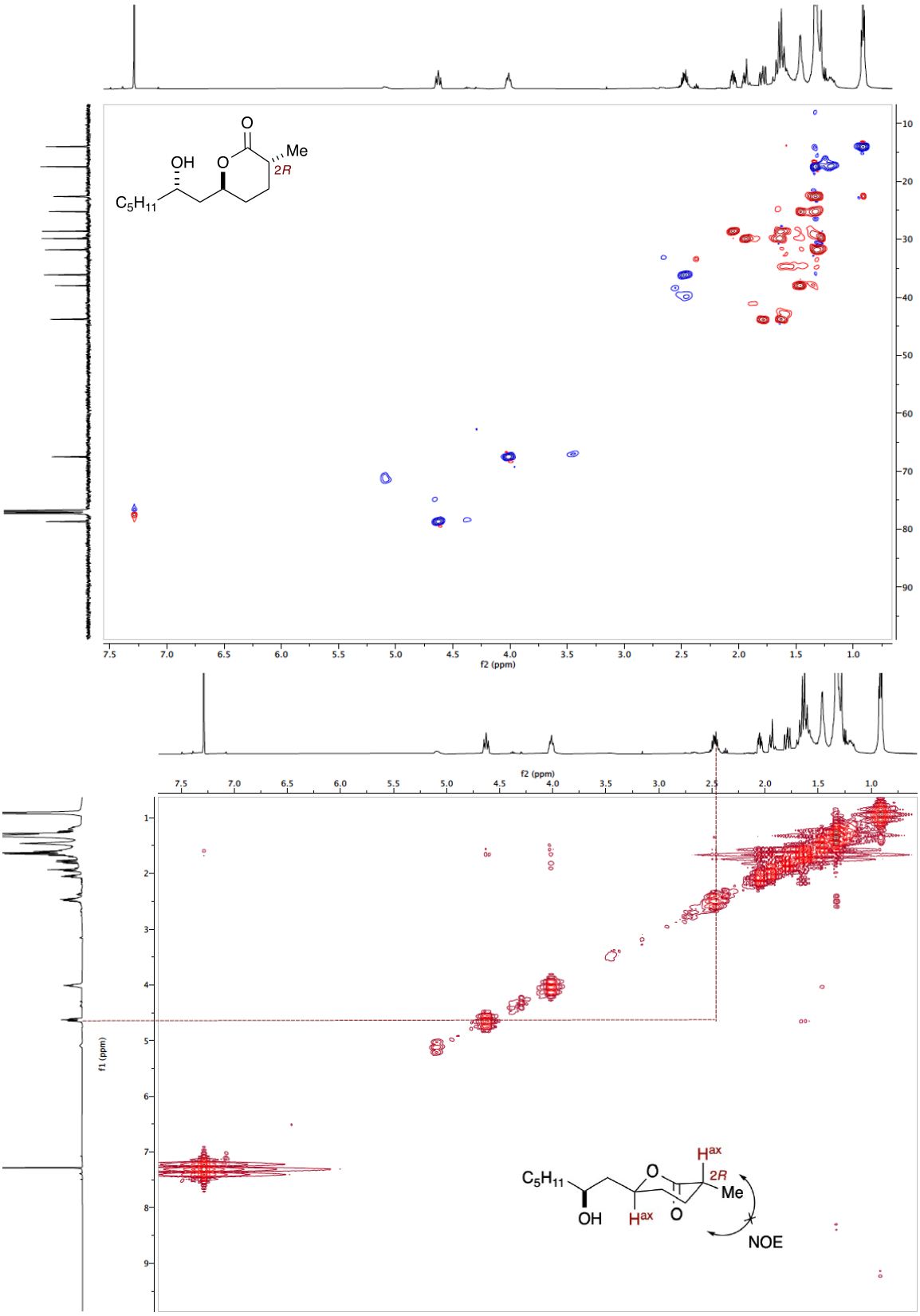
O
OH
O
Me
2R
C5H11
f2 (ppm)
f1 (ppm)
Hax
2R
Me
O
OH
Hax
O
NOE

(3*R*,6*S*)-6-((*S*)-2-methoxyheptyl)-3-methyltetrahydro-2*H*-pyran-2-one ($C_{14}H_{26}O_3$, (2*R*)-2.1.6)

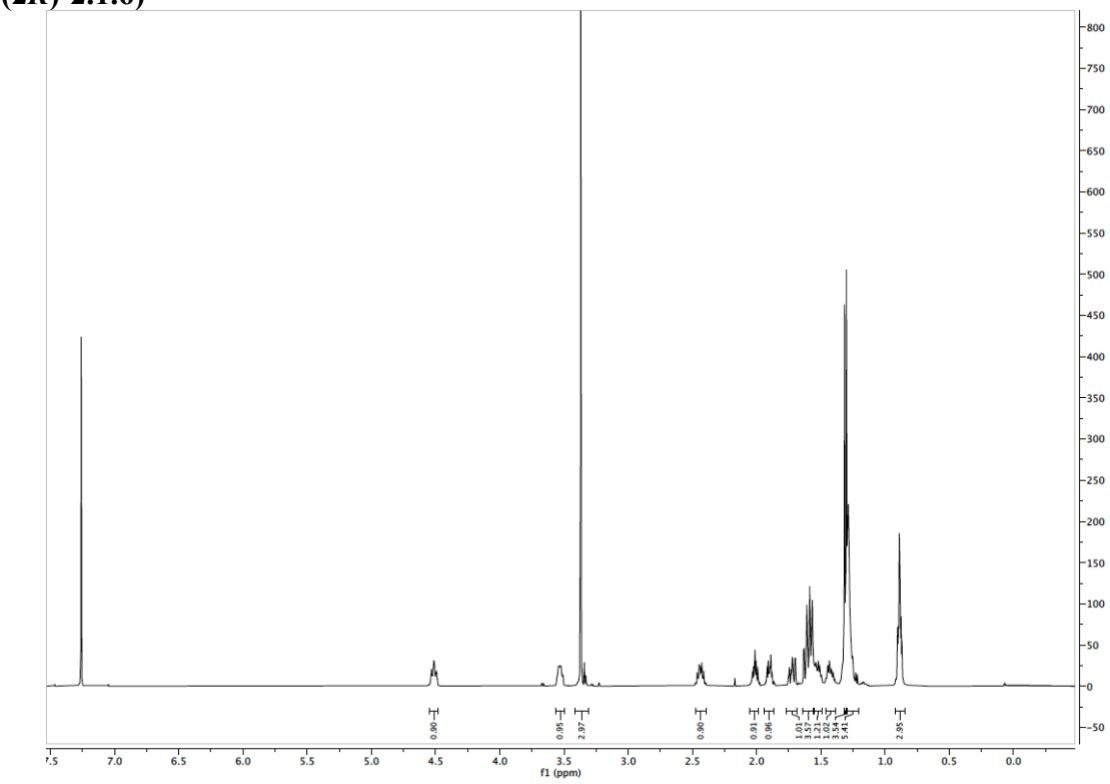

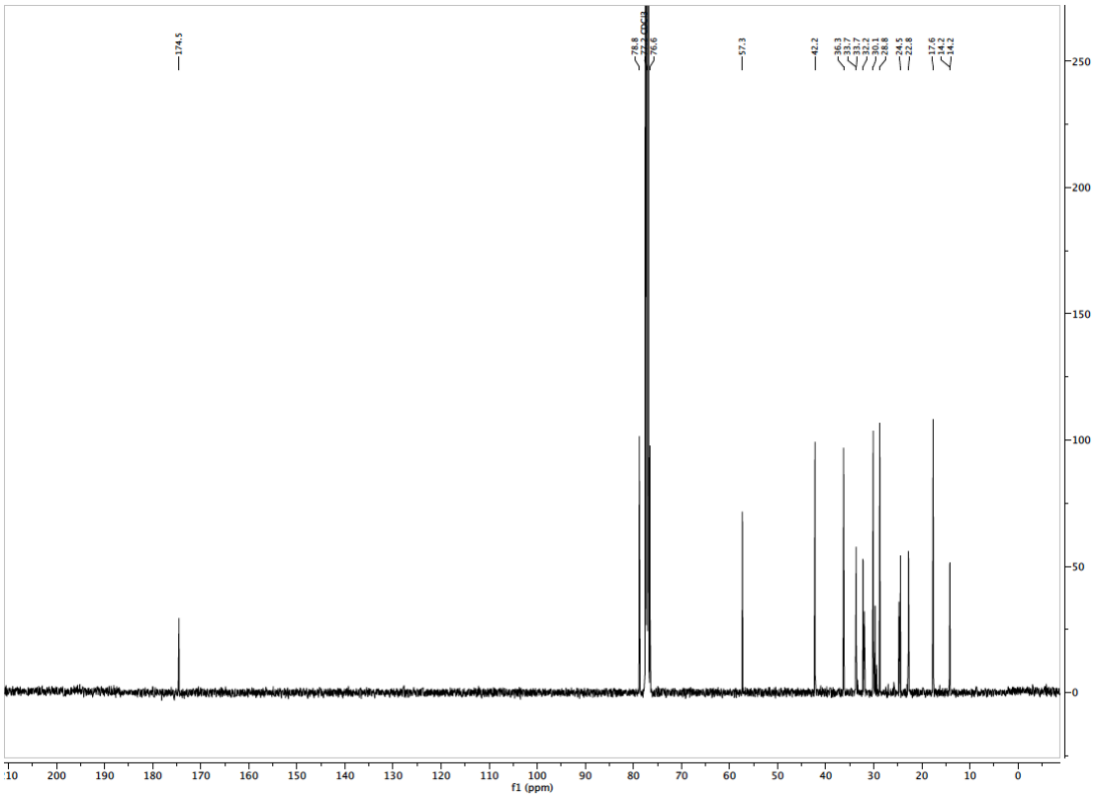

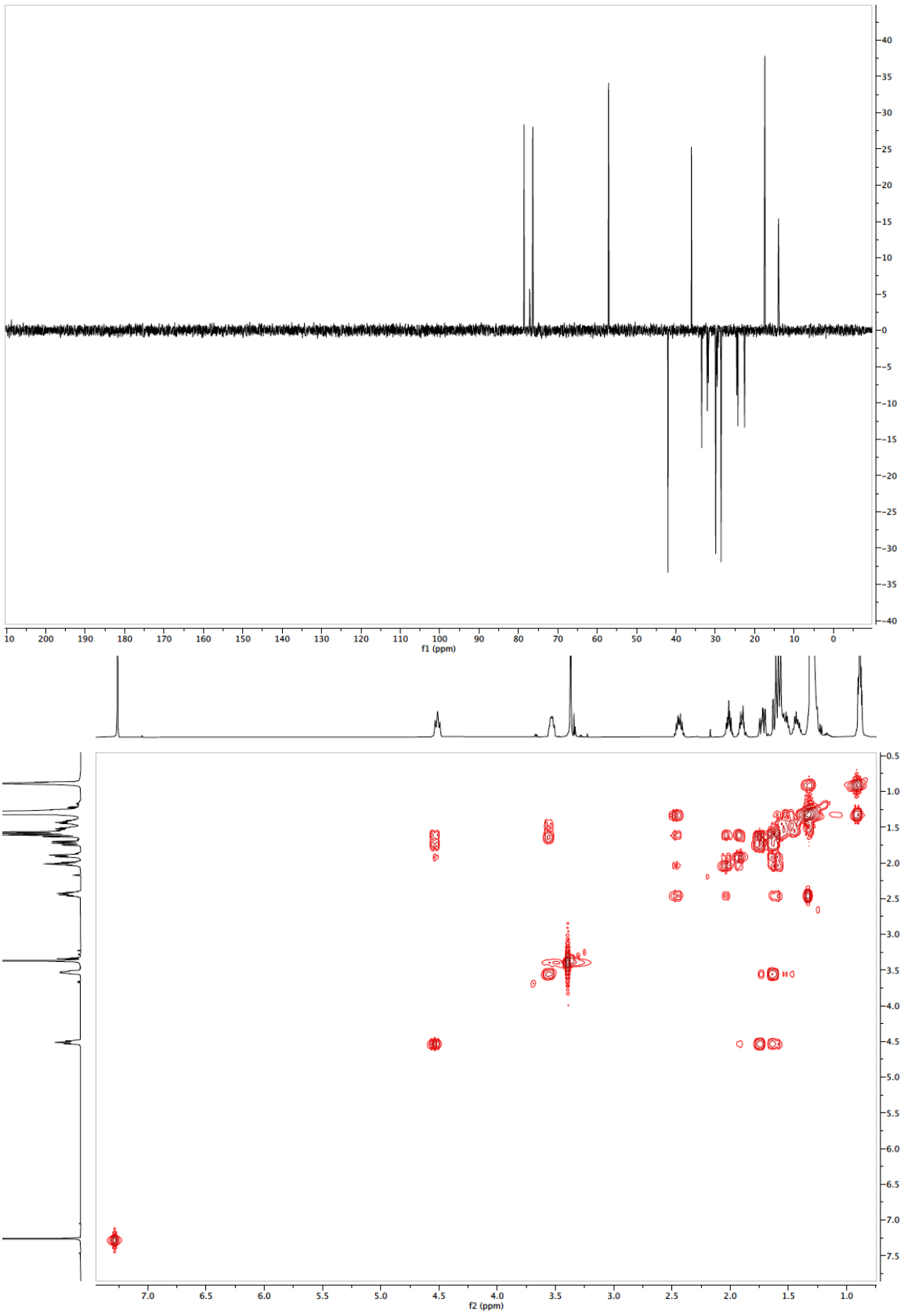
f1 (ppm)
f2 (ppm)

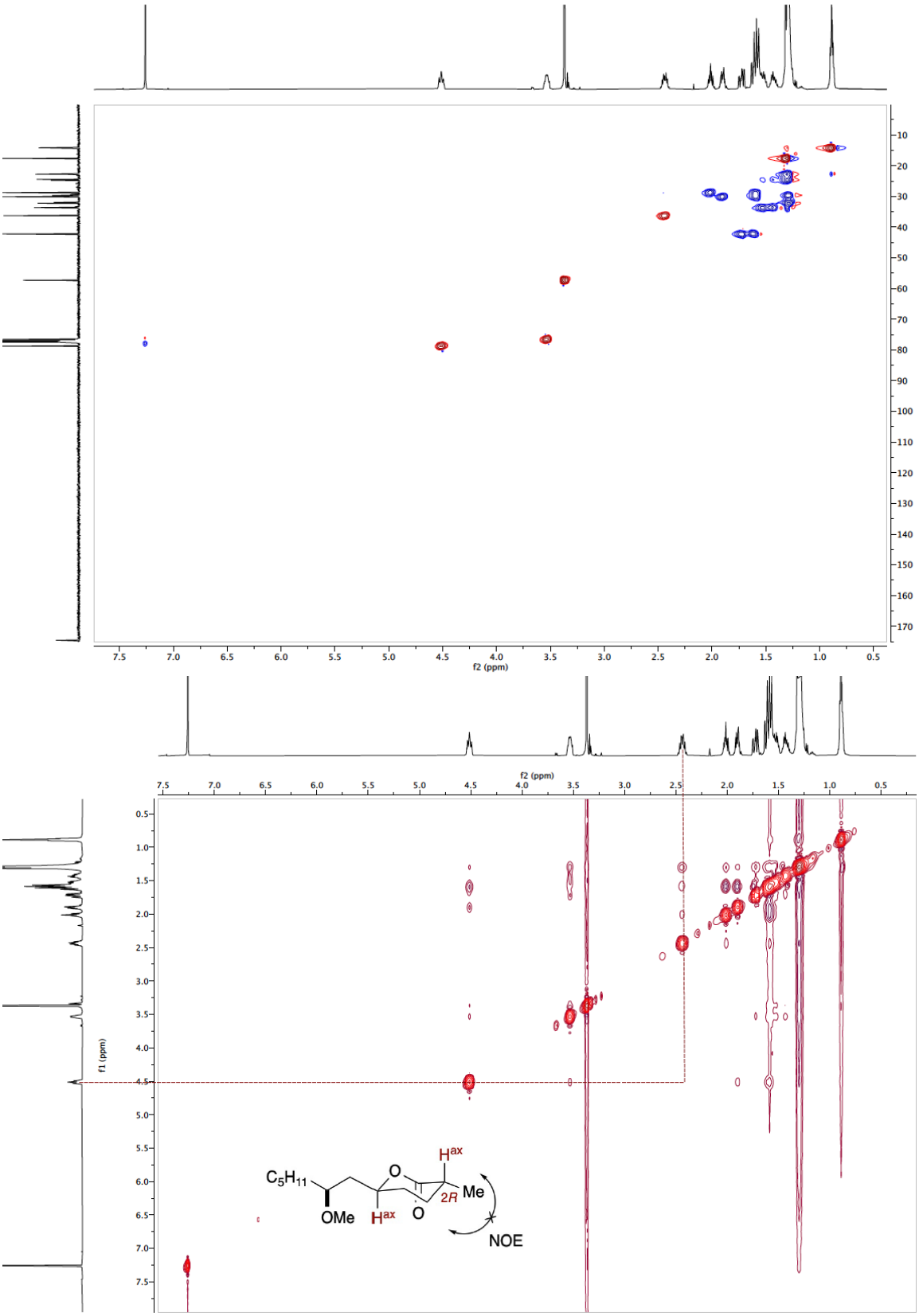
f2 (ppm)
f1 (ppm)
C_5H_{11}
OMe
H^{ax}
O
O
H^{ax}
2R
Me
NOE

Epimeric Rotamer Mixtures from **Reaction 1(Scheme 5.1)**
(2*R*,5*S*,7*S*)-*N*-allyl-5-hydroxy-7-methoxy-*N*,2-dimethyldodecanamide ((2*R*)-2.2.2),
(2*S*,5*S*,7*S*)-*N*-allyl-5-hydroxy-7-methoxy-*N*,2-dimethyldodecanamide ((2*S*)-2.2.2)

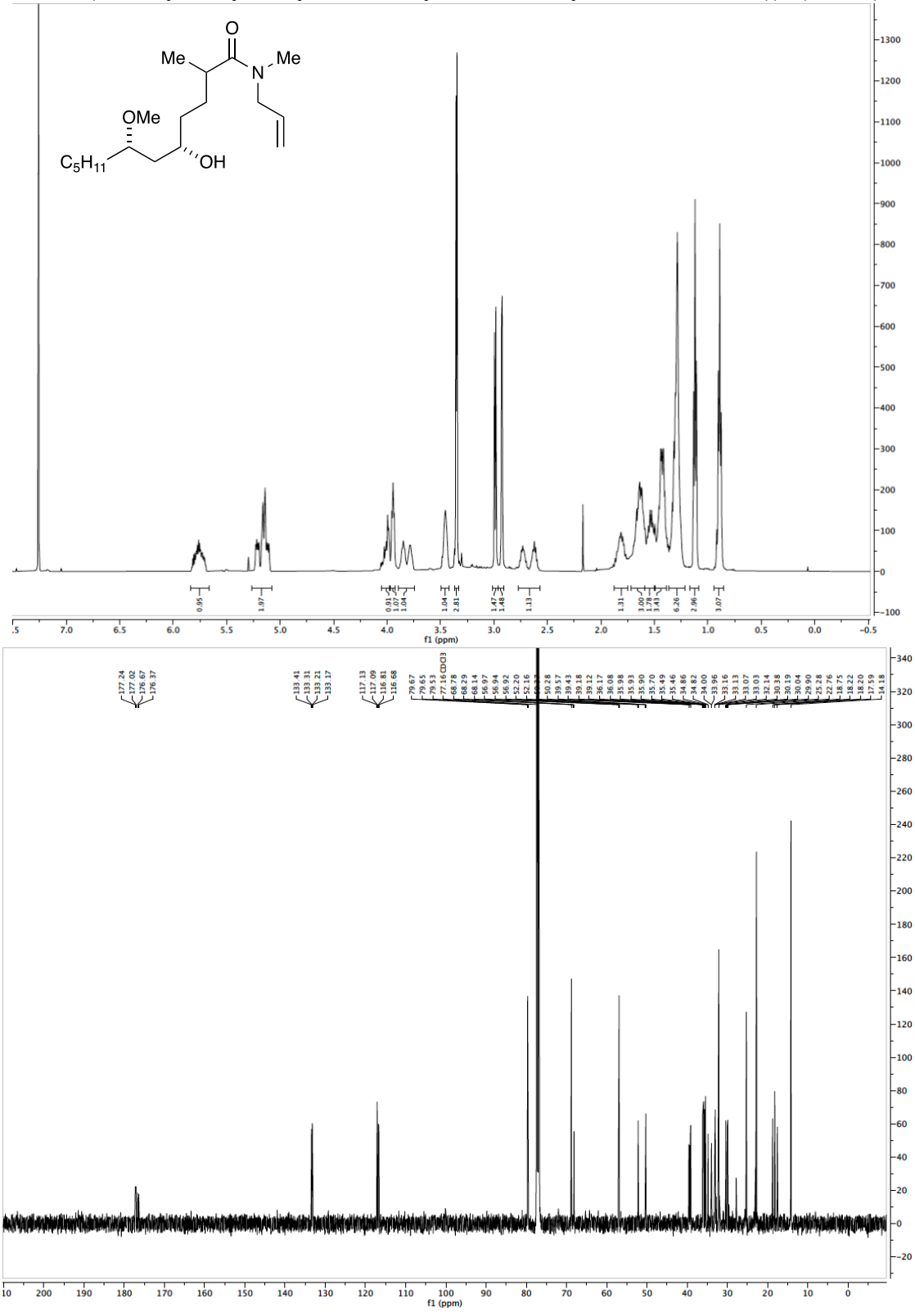

^{1}H and ^{13}C spectra with selected expansions to show diastereomeric rotamers

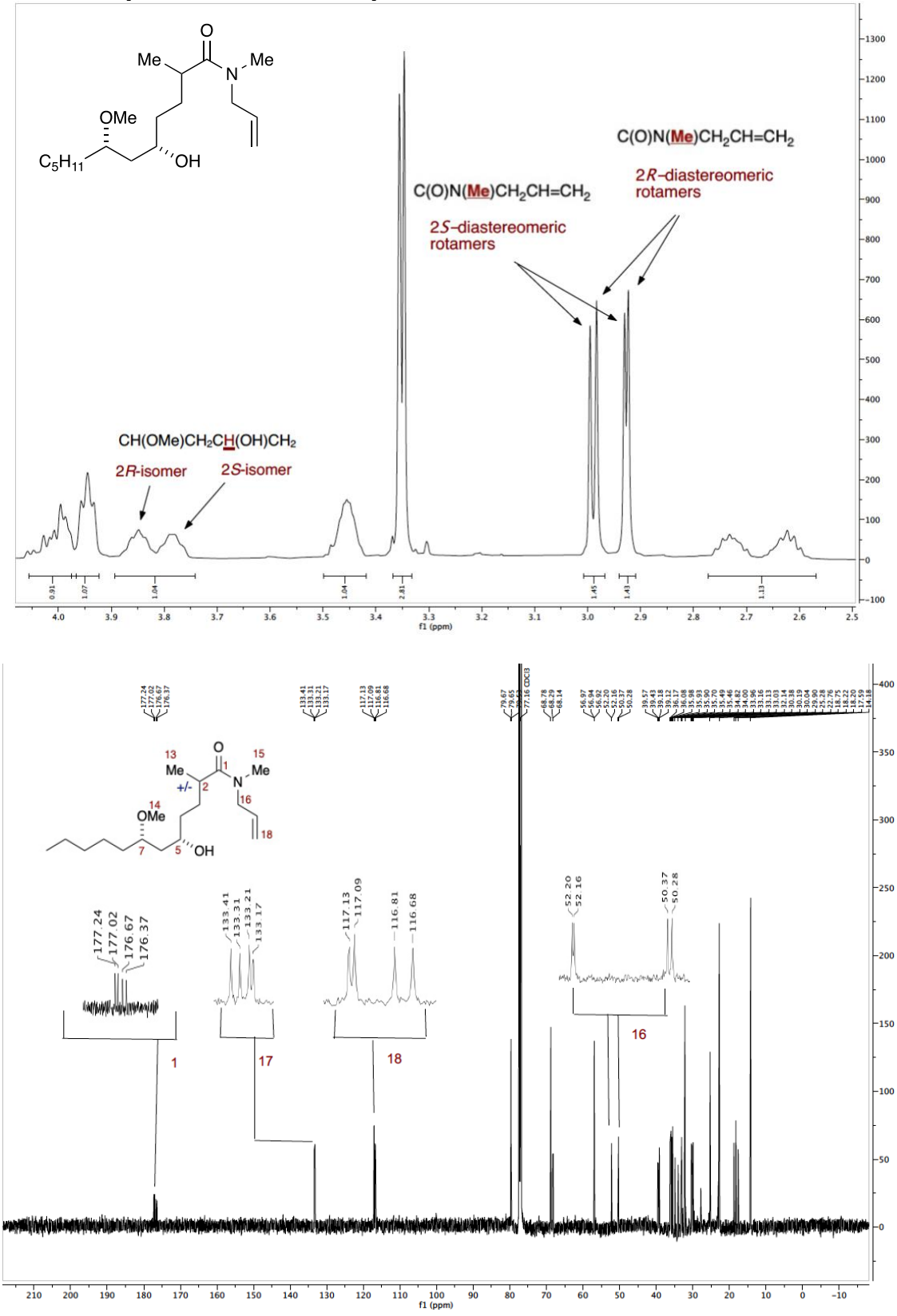

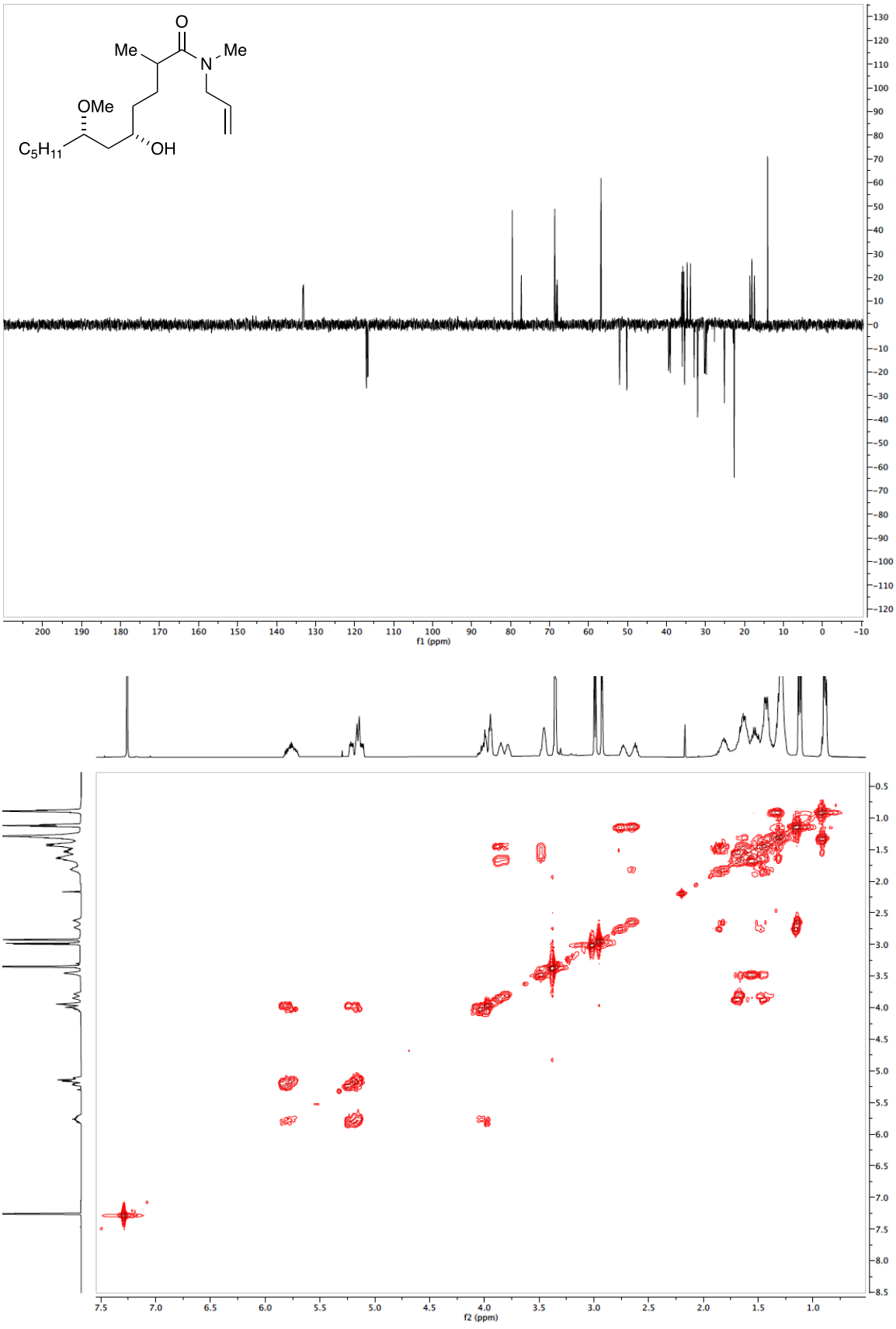
O
Me
N
Me
OMe
C_5H_{11}
OH
f1 (ppm)
f2 (ppm)

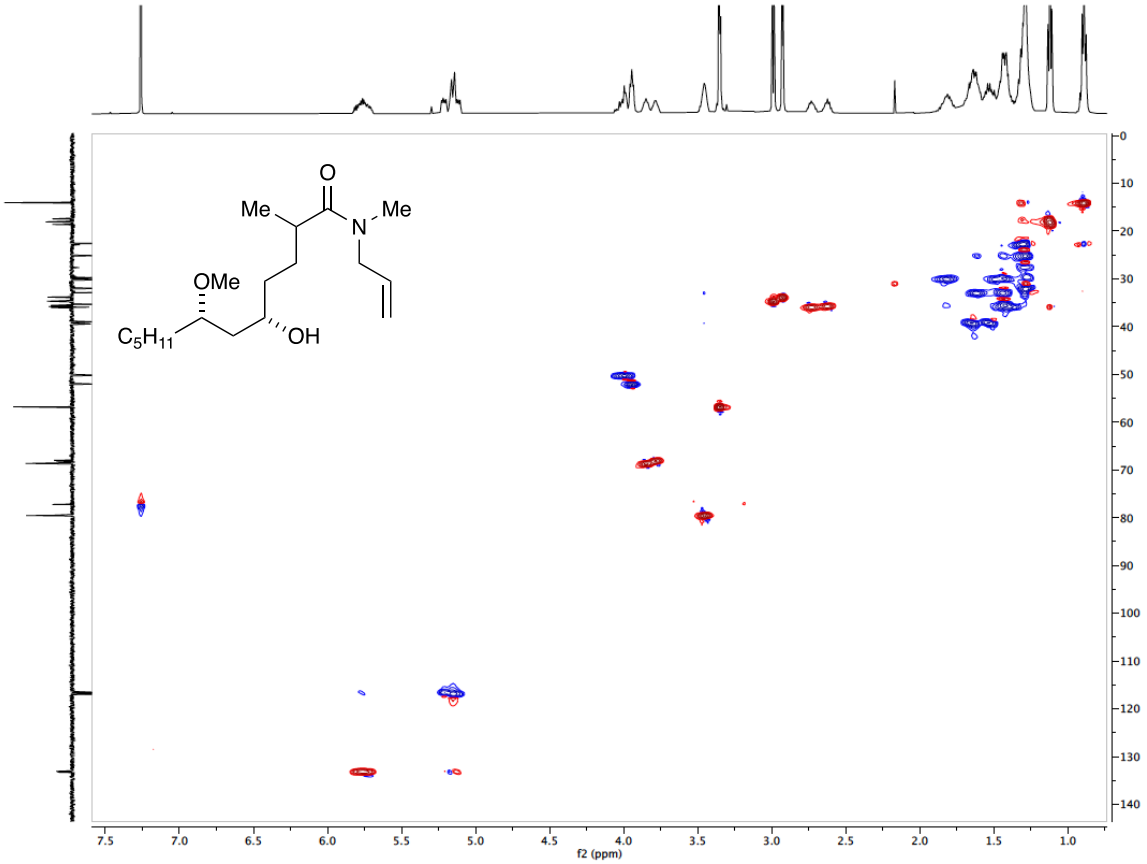
O
Me
N
Me
OMe
C5H11
OH
f2 (ppm)

Epimeric Rotamer Mixtures from Reaction 2 **(Scheme 5.1)**
(2*R*,5*S*,7*S*)-*N*-allyl-5-hydroxy-7-methoxy-*N*,2-dimethyldodecanamide ((2*R*)-2.2.2),
(2*S*,5*S*,7*S*)-*N*-allyl-5-hydroxy-7-methoxy-*N*,2-dimethyldodecanamide ((2*S*)-2.2.2)

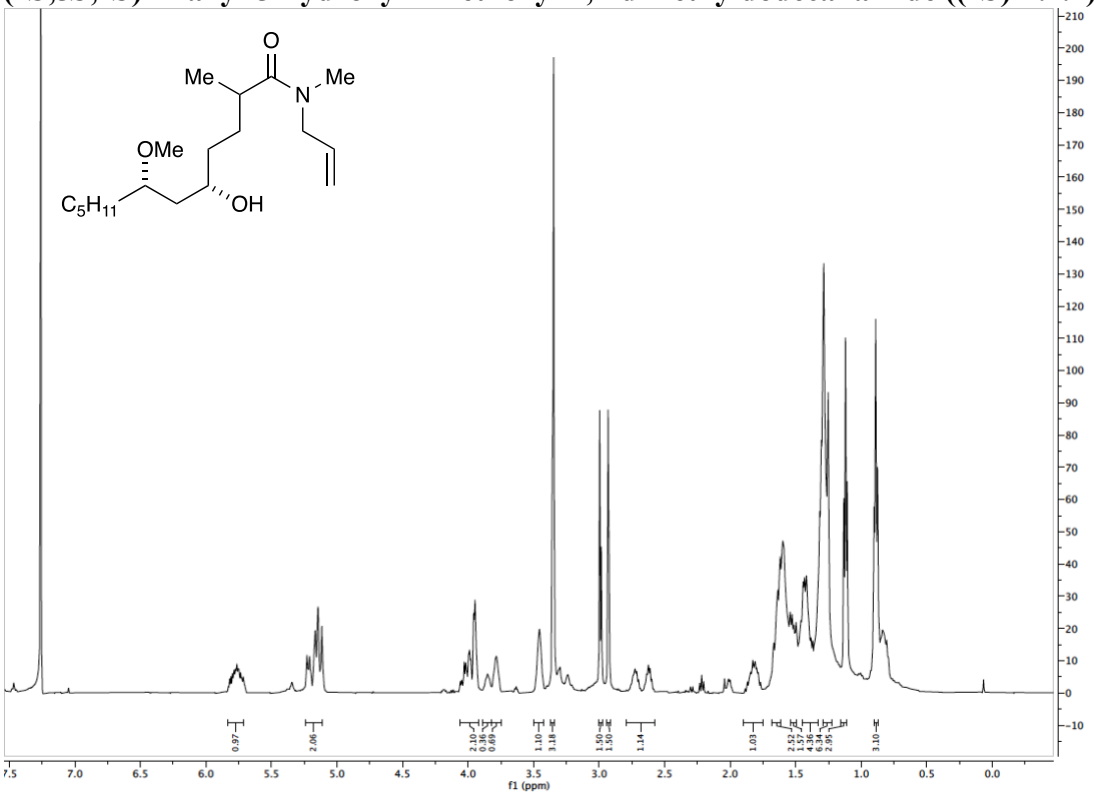

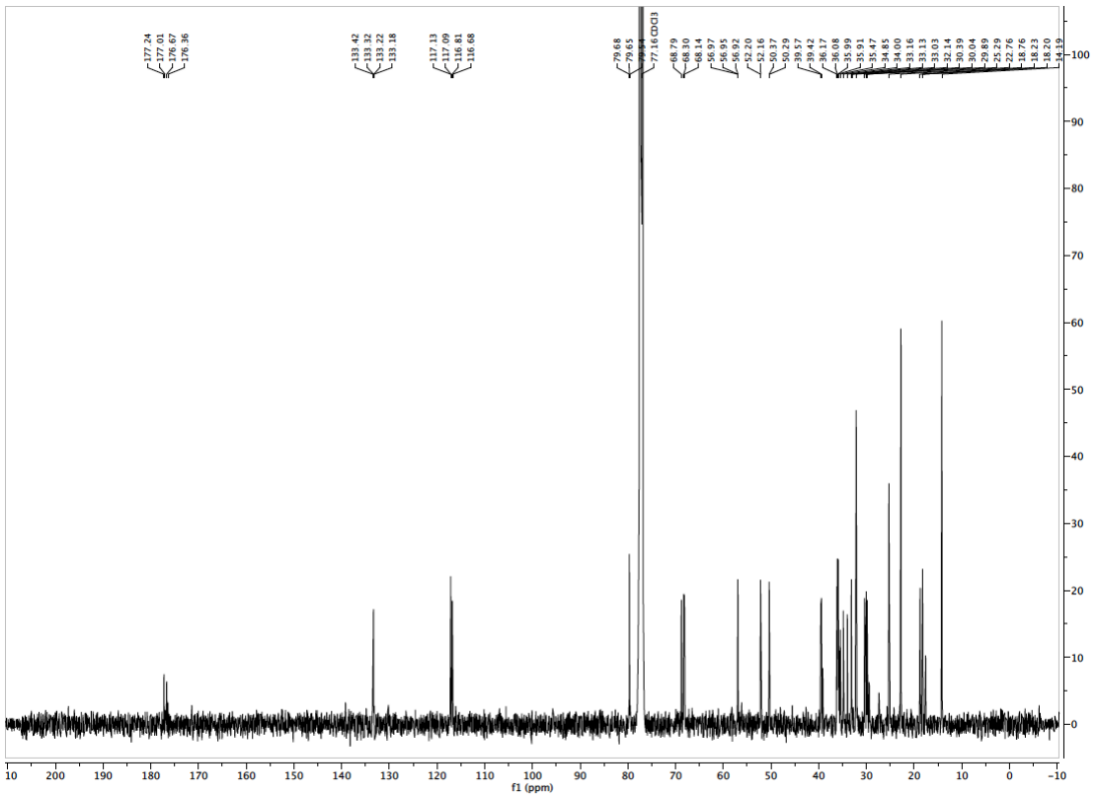

^{1}H and ^{13}C spectra with selected expansions to show diastereomeric rotamers

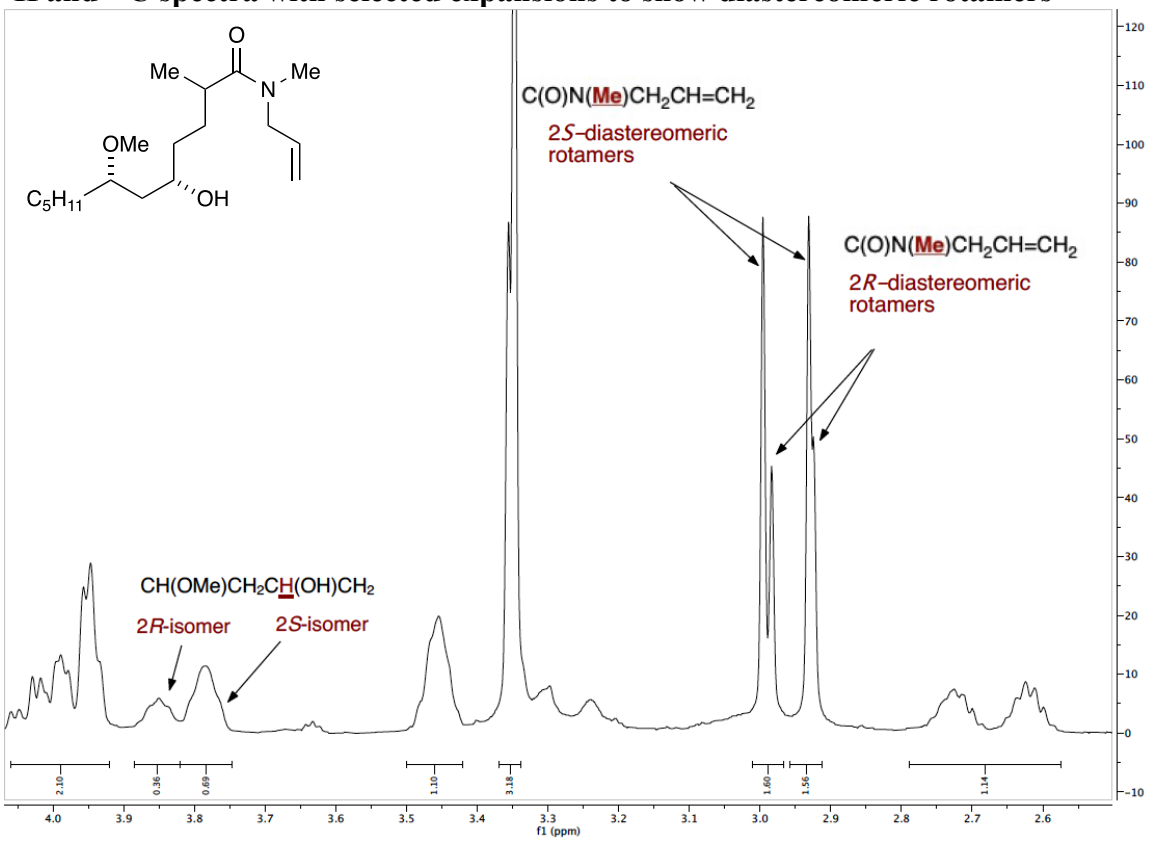

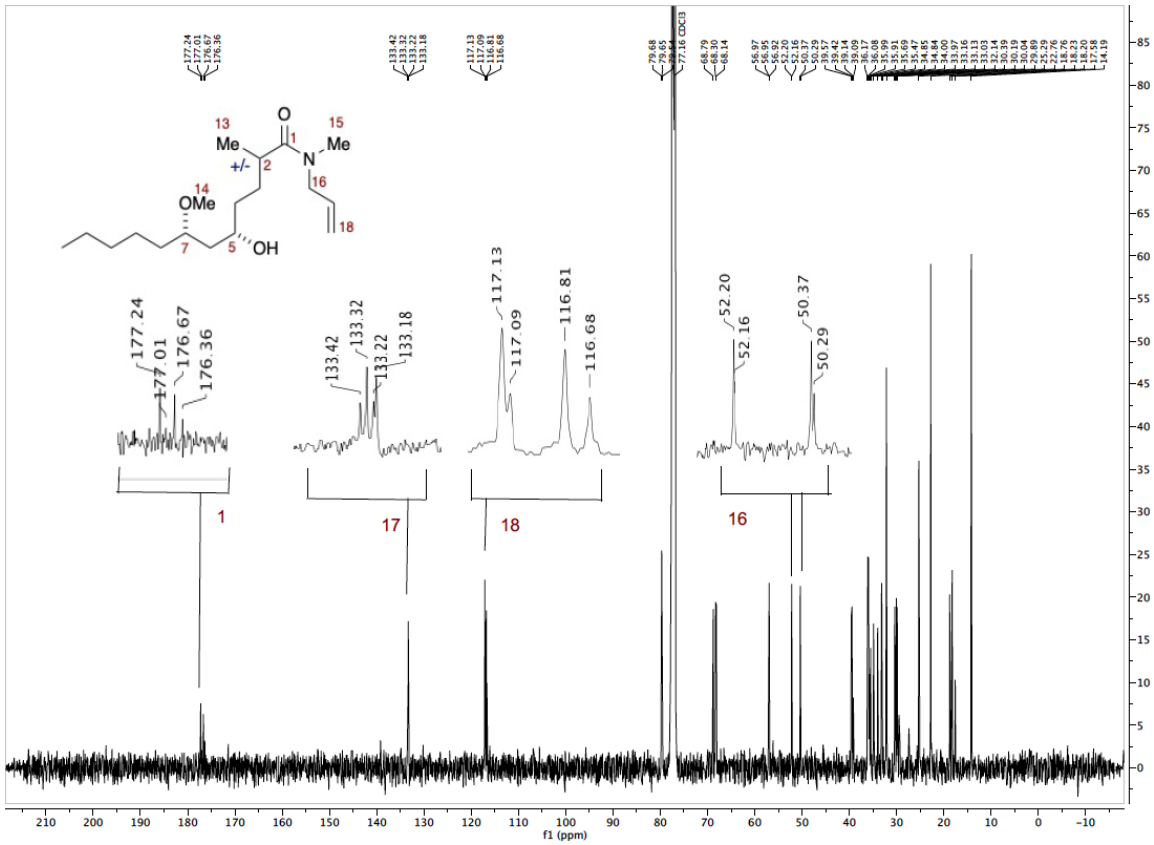

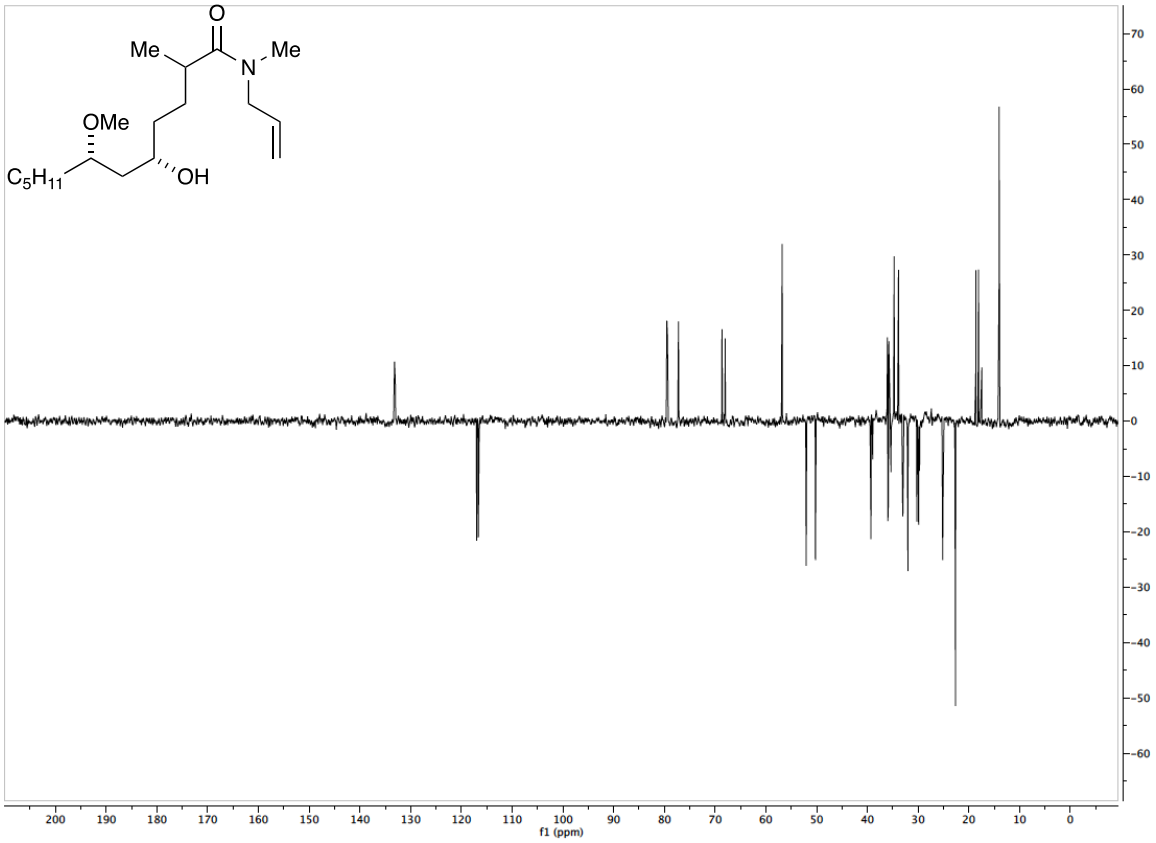
O
Me
N
Me
OMe
C_5H_{11}
OH
f1 (ppm)

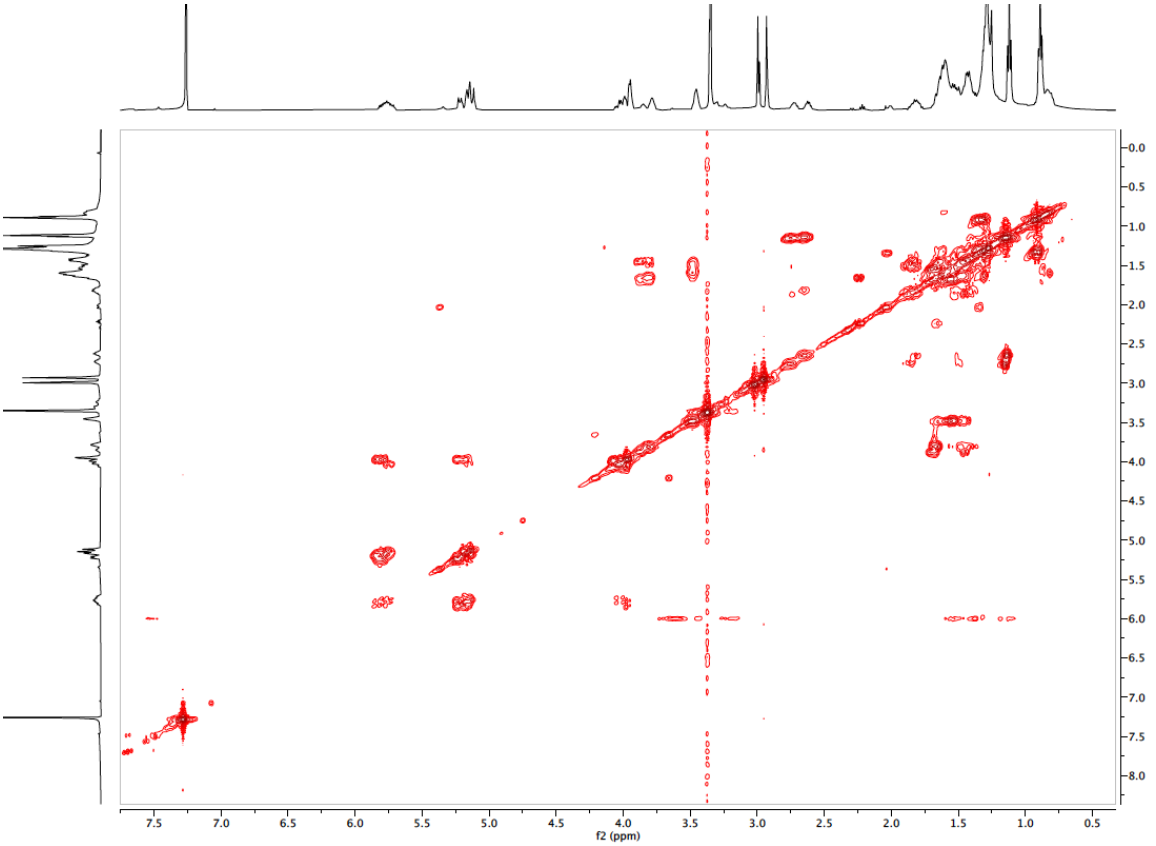
f2 (ppm)

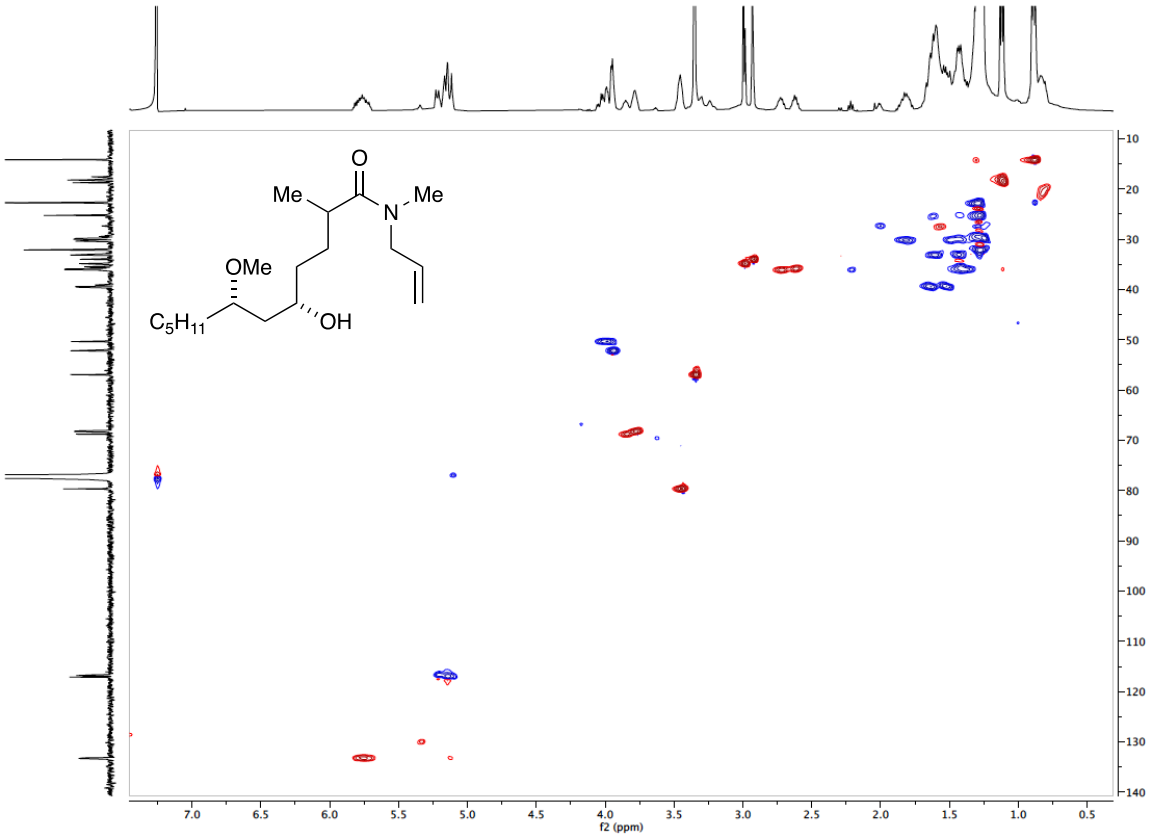
O
Me
N
Me
OMe
C5H11
OH
7.0
6.5
6.0
5.5
5.0
4.5
4.0
3.5
3.0
2.5
2.0
1.5
1.0
0.5
f2 (ppm)
10
20
30
40
50
60
70
80
90
100
110
120
130
140

Epimeric mixture of **(2*R*,5*S*,7*S*)-1-(allyl(methyl)amino)-7-methoxy-2-methyl-1-oxododecan-5-yl (*S*)-2-(acryloyloxy)-3-methylbutanoate ($C_{26}H_{45}NO_6$, 2.2.4)**

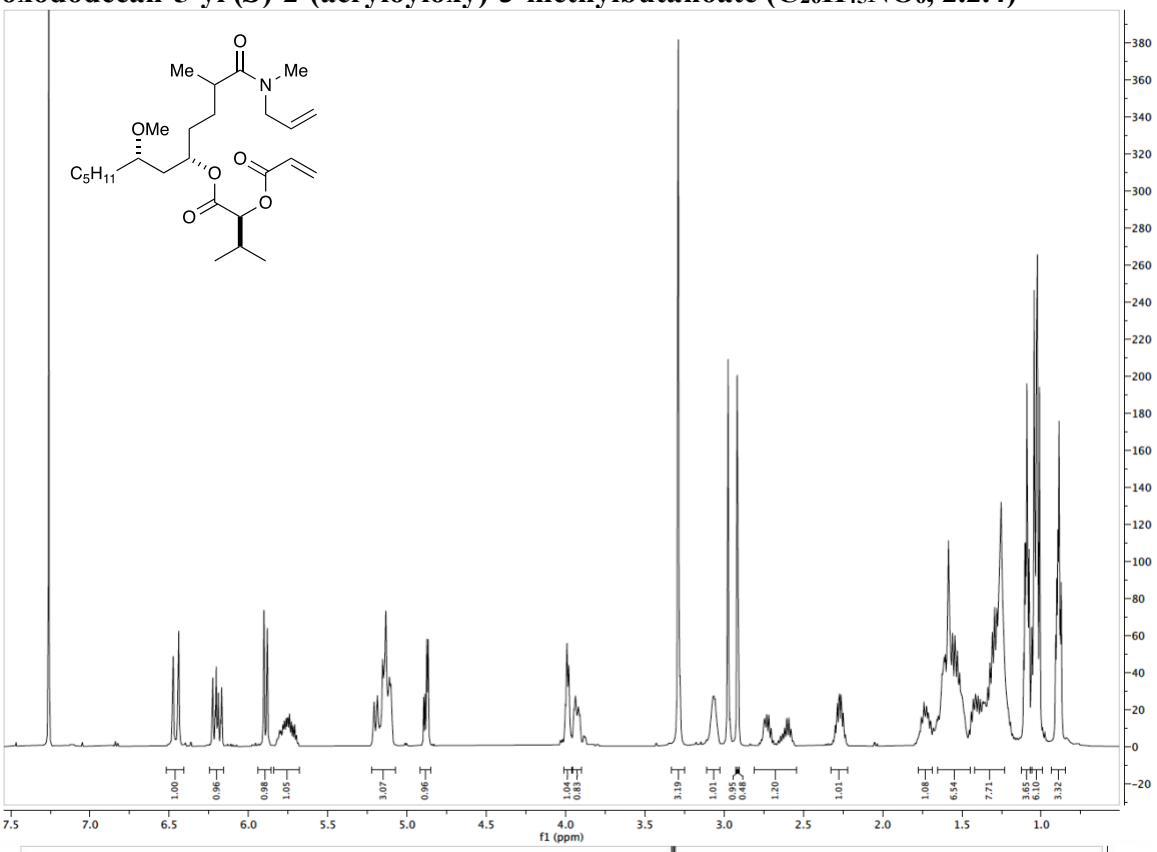

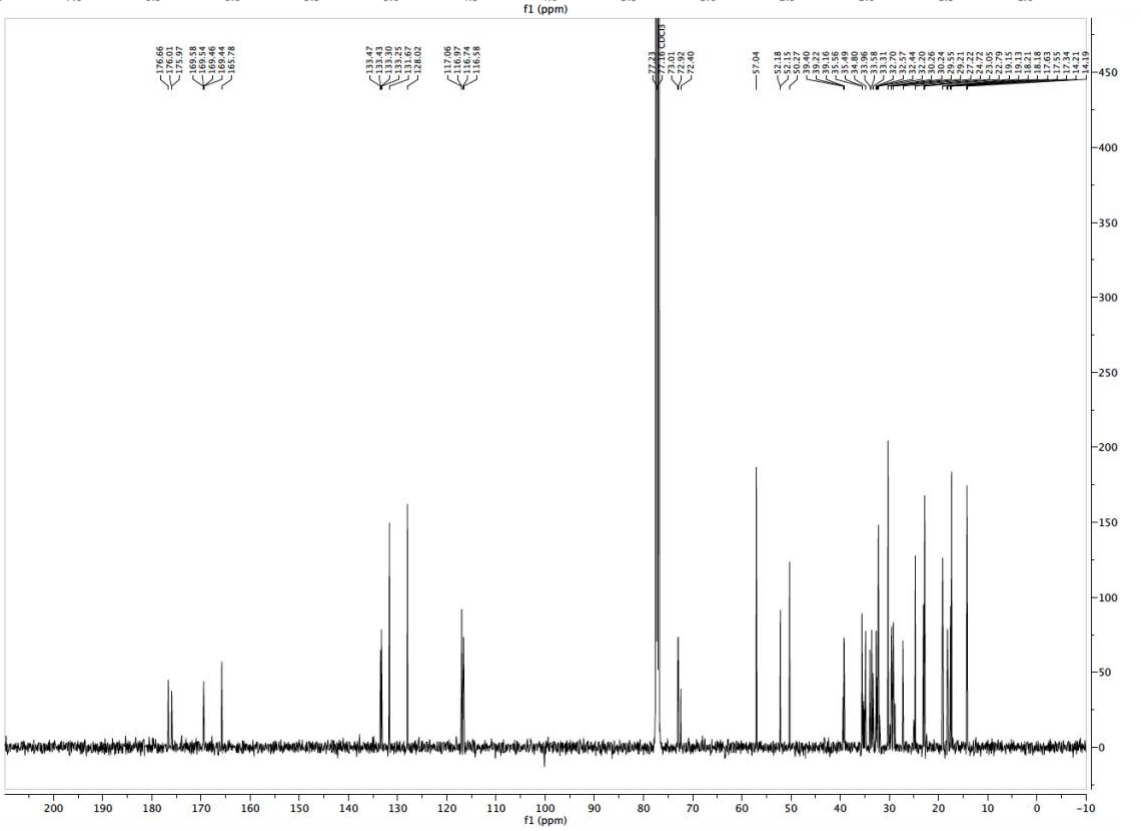

^{1}H and ^{13}C spectra with selected expansions to show diastereomeric rotamers

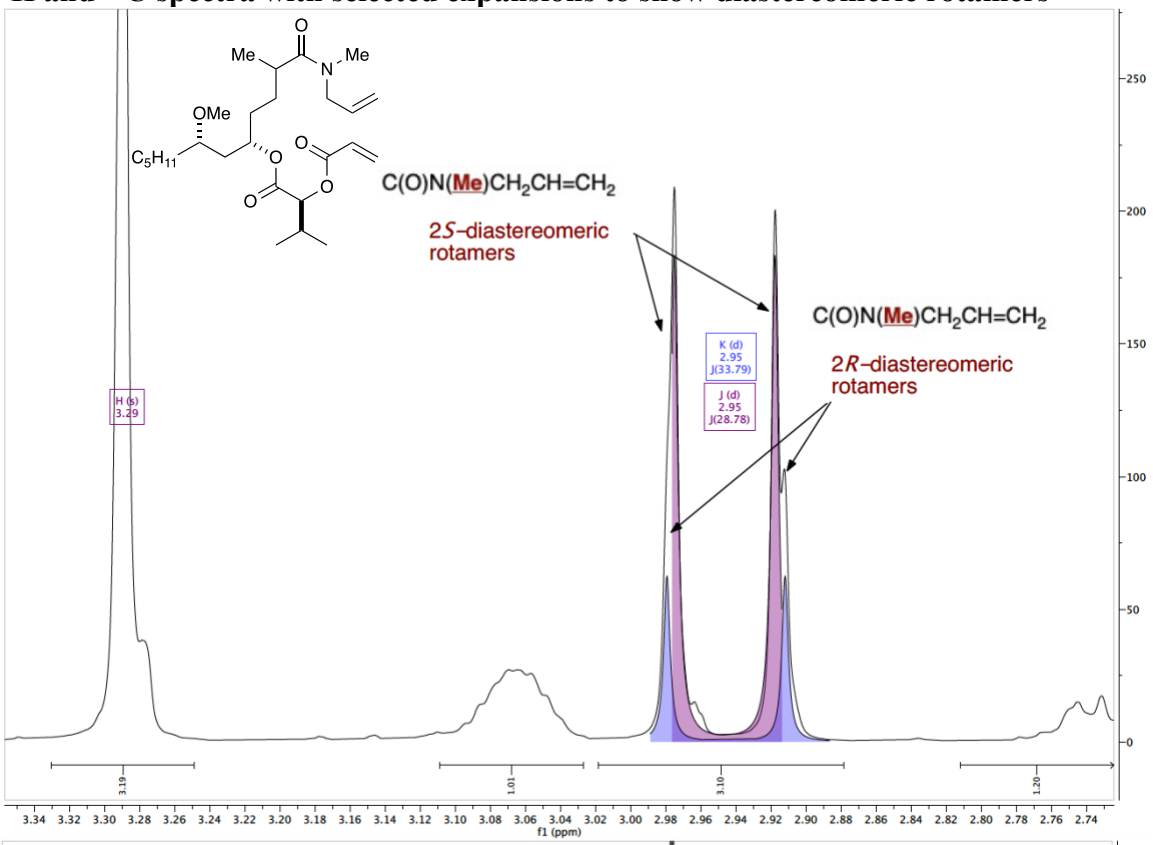

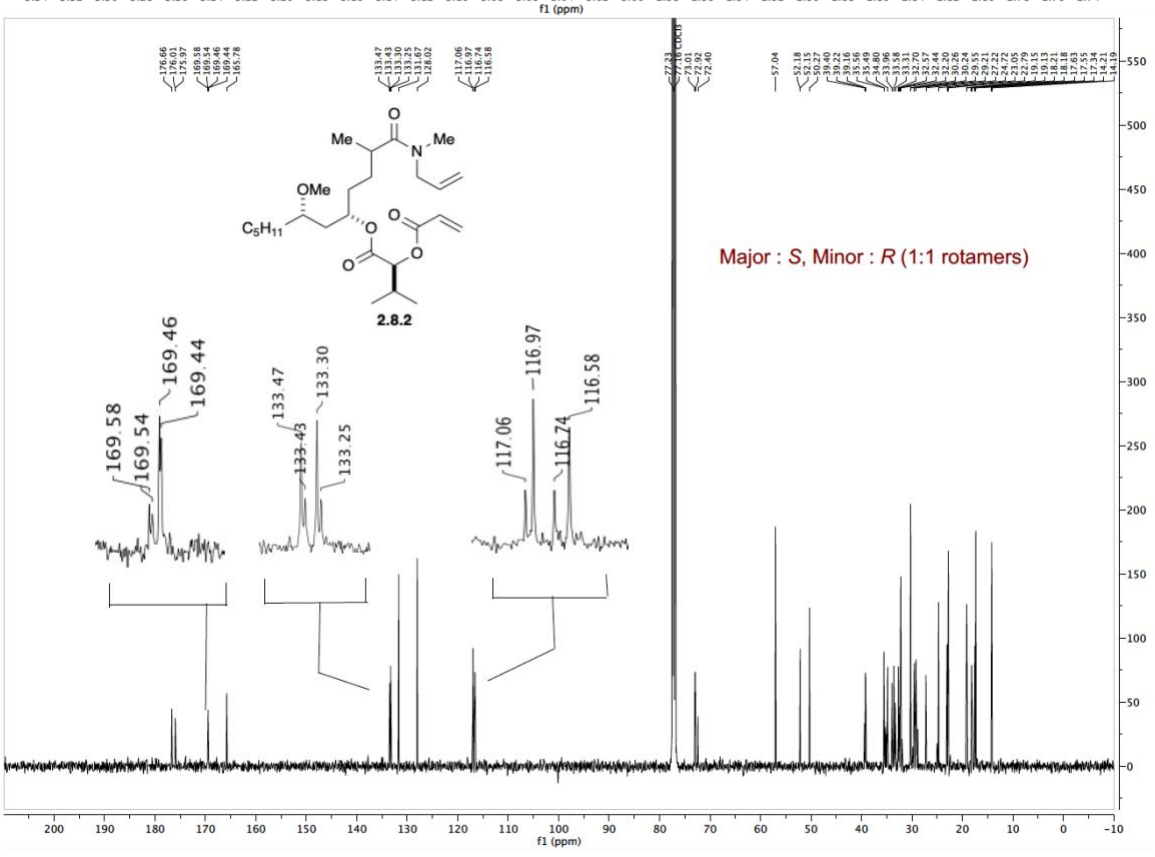

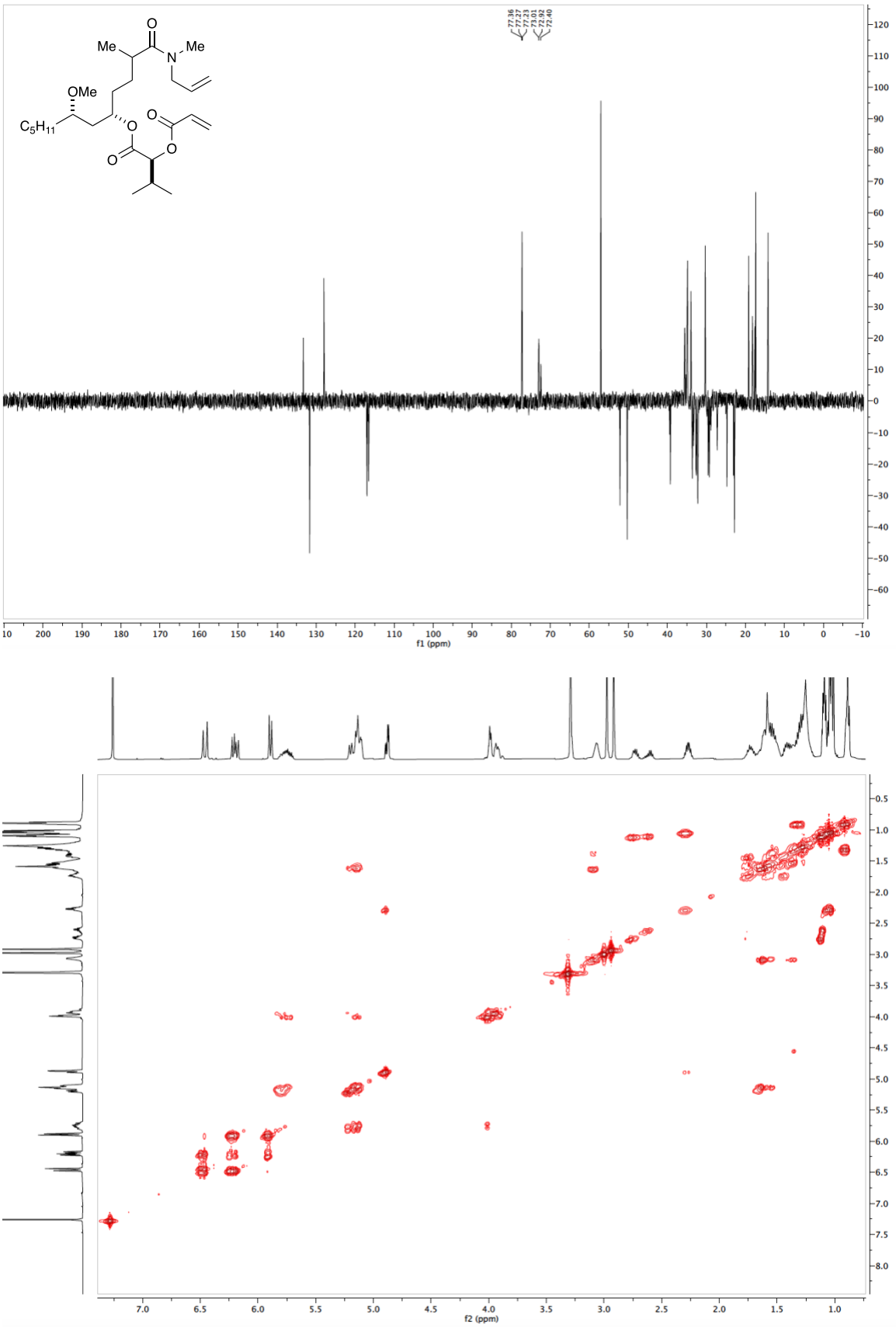
Me
O
N
Me
OMe
C_5H_{11}
O
O
O
O
77.36
77.17
77.23
73.01
72.92
72.40
f1 (ppm)
f2 (ppm)

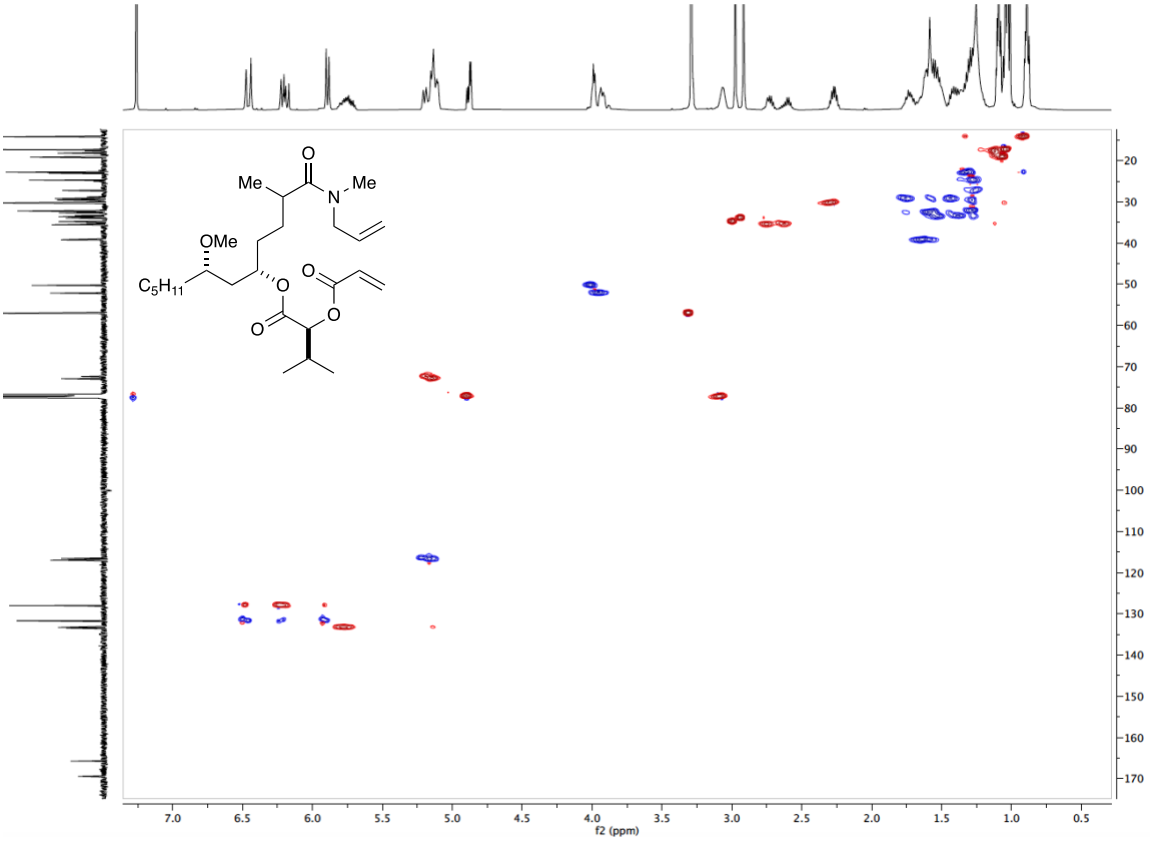
Me
O
N
Me
OMe
C_5H_{11}
O
O
O
O
20
30
40
50
60
70
80
90
100
110
120
130
140
150
160
170
7.0
6.5
6.0
5.5
5.0
4.5
4.0
3.5
3.0
2.5
2.0
1.5
1.0
0.5
f2 (ppm)

Epimeric mixture of **(3*S*,14*S*,*E*)-3-isopropyl-14-((*S*)-2-methoxyheptyl)-9,11-dimethyl-1,4-dioxa-9-azacyclotetradec-7-ene-2,5,10-trione ($C_{24}H_{41}NO_6$, (2*R*)-,(2*S*)-2.1-A)**

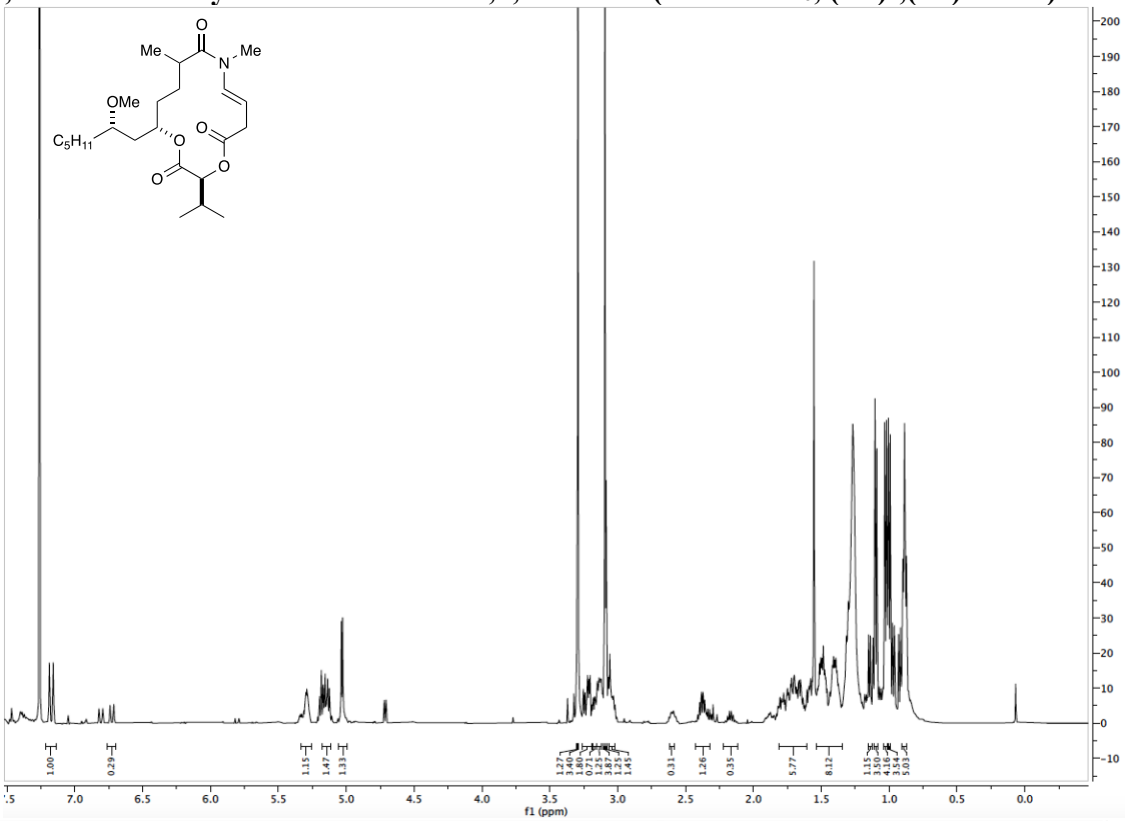

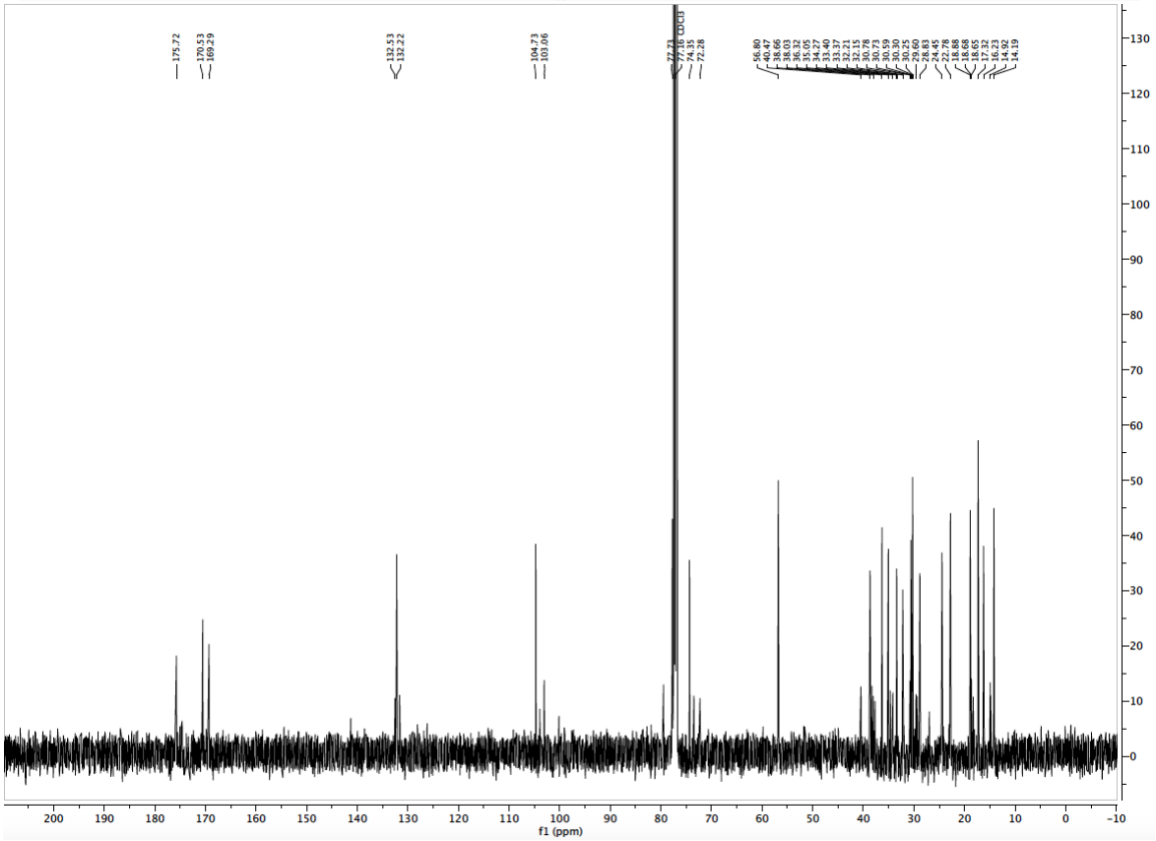

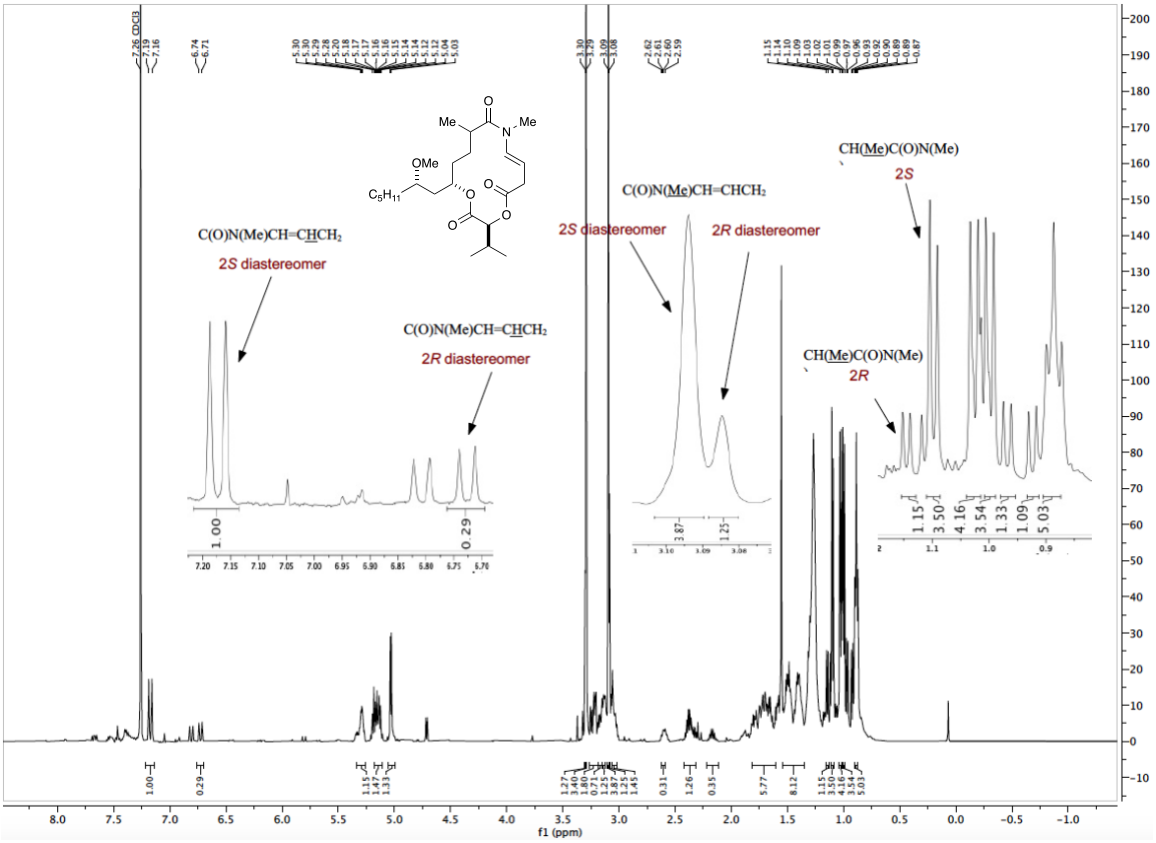
C(O)N(Me)CH=CHCH2
2S diastereomer
C(O)N(Me)CH=CHCH2
2R diastereomer
C(O)N(Me)CH=CHCH2
2S diastereomer
2R diastereomer
CH(Me)C(O)N(Me)
2S
CH(Me)C(O)N(Me)
2R
f1 (ppm)

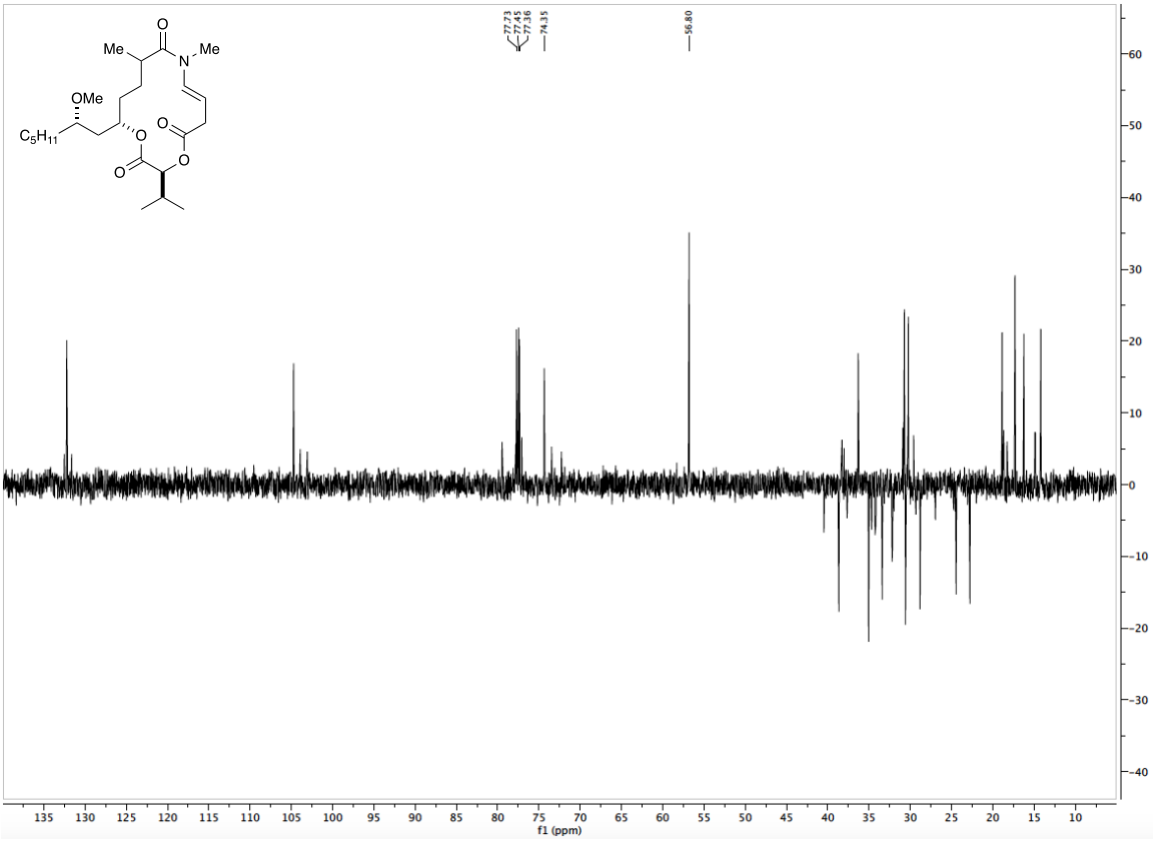
f1 (ppm)

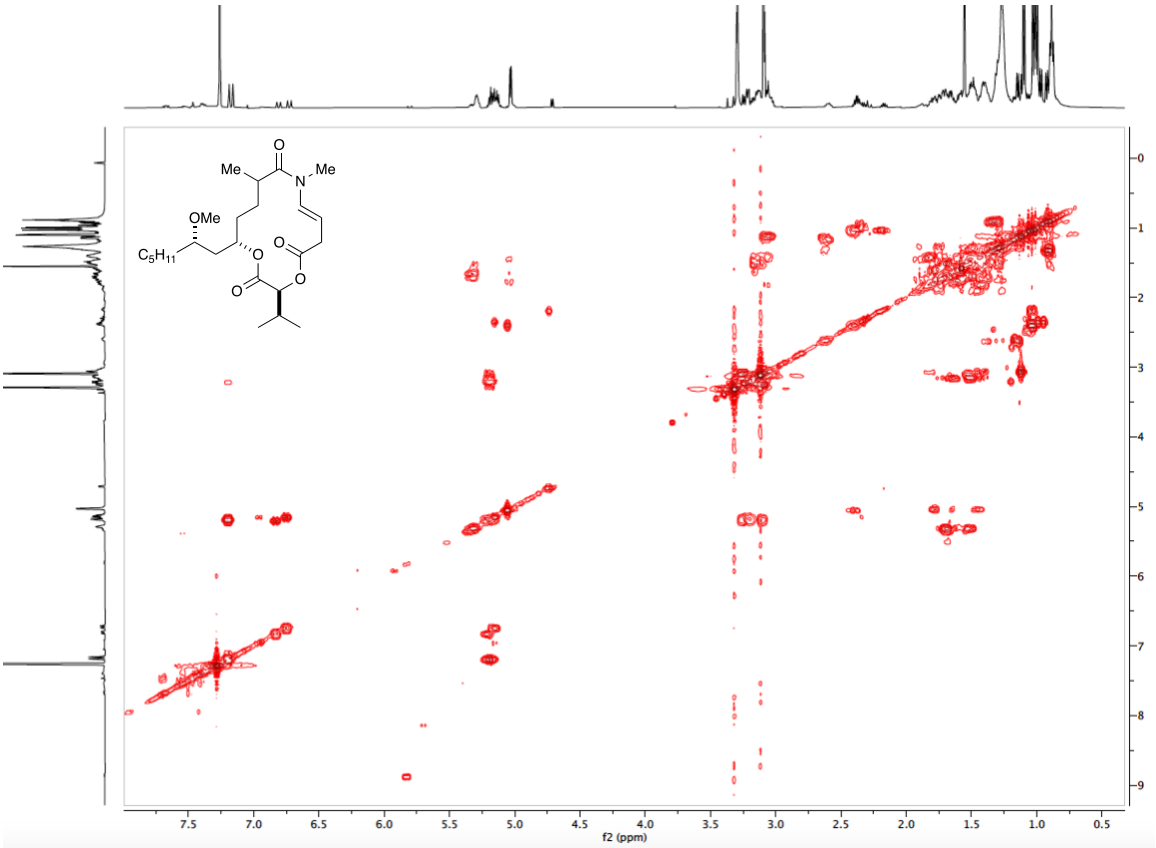
Me
N
Me
OMe
C_5H_{11}
O
O
O
O
O
7.5
7.0
6.5
6.0
5.5
5.0
4.5
4.0
3.5
3.0
2.5
2.0
1.5
1.0
0.5
f2 (ppm)

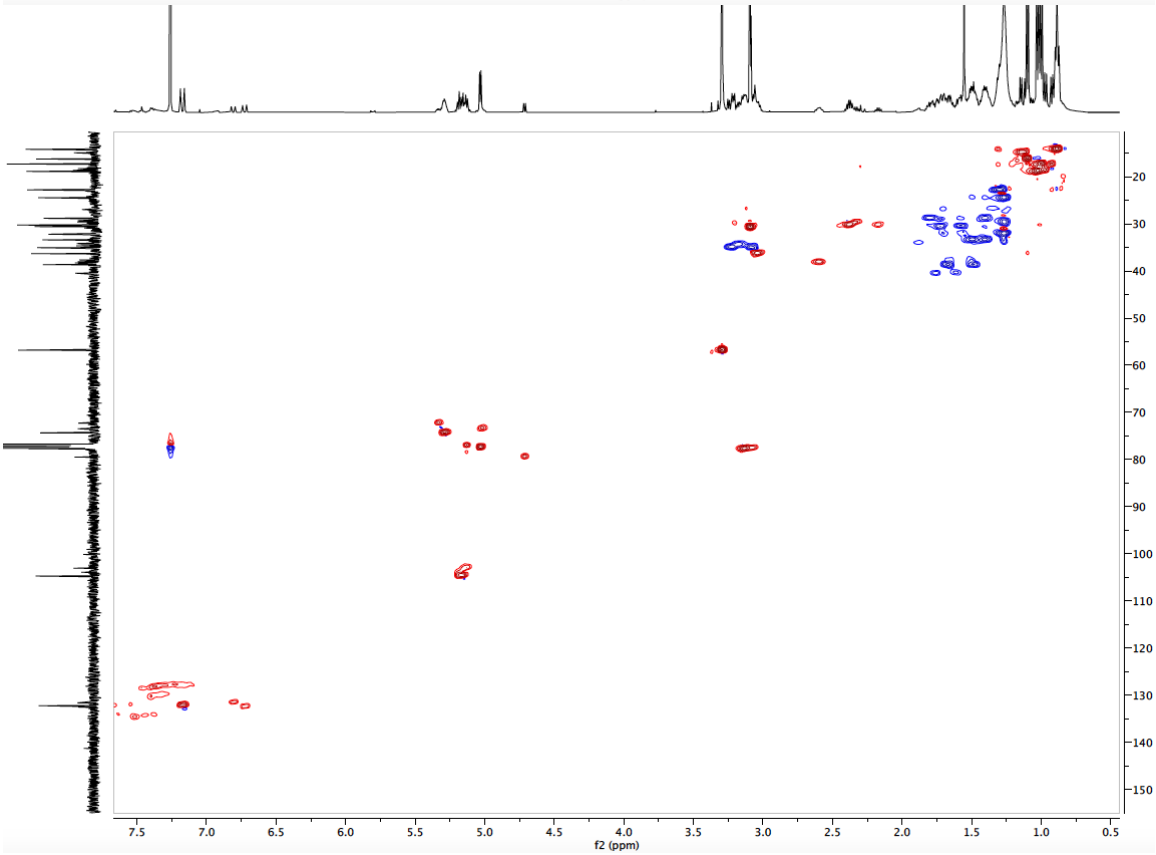
7.5
7.0
6.5
6.0
5.5
5.0
4.5
4.0
3.5
3.0
2.5
2.0
1.5
1.0
0.5
f2 (ppm)

(2*R*,5*S*,7*S*)-5-hydroxy-7-methoxy-*N*,2-dimethyldodecanamide ($C_{15}H_{31}NO_3$, 2.10.1)

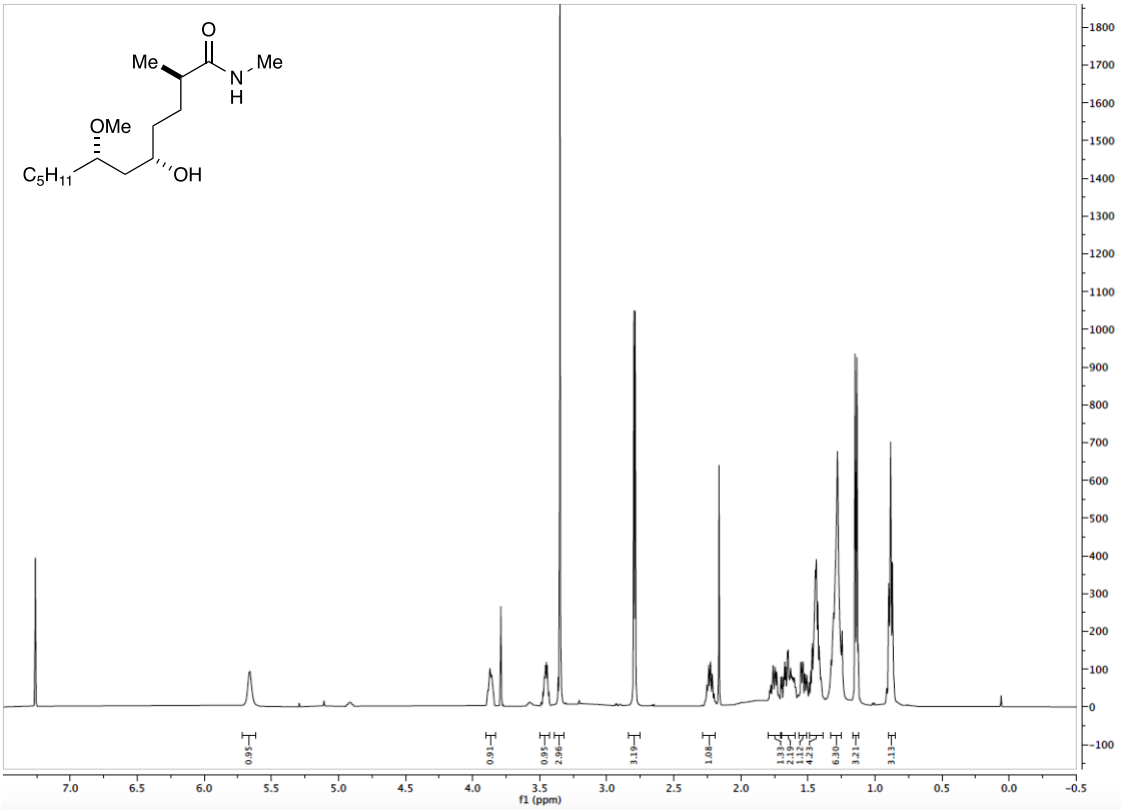

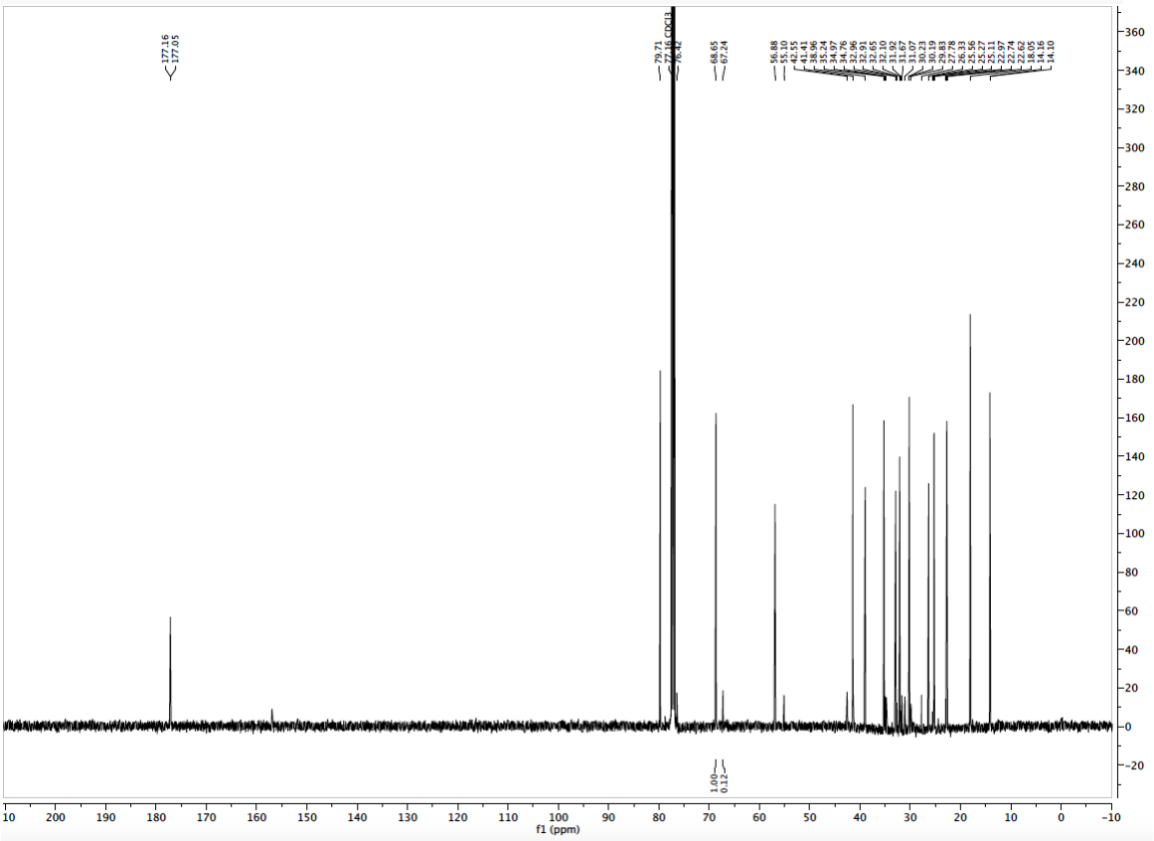

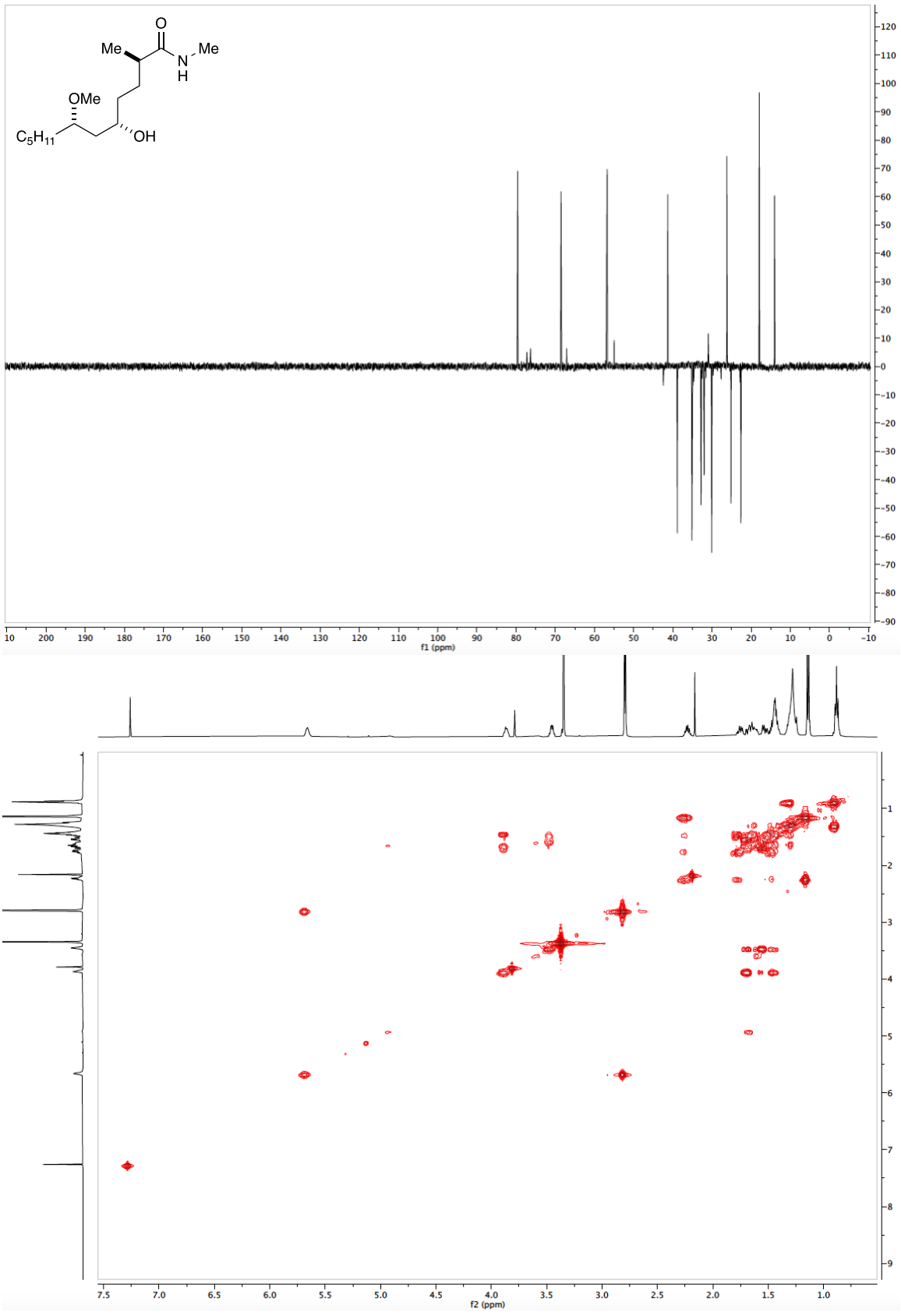
O
Me
N
H
Me
OMe
C_5H_{11}
OH
f1 (ppm)
f2 (ppm)

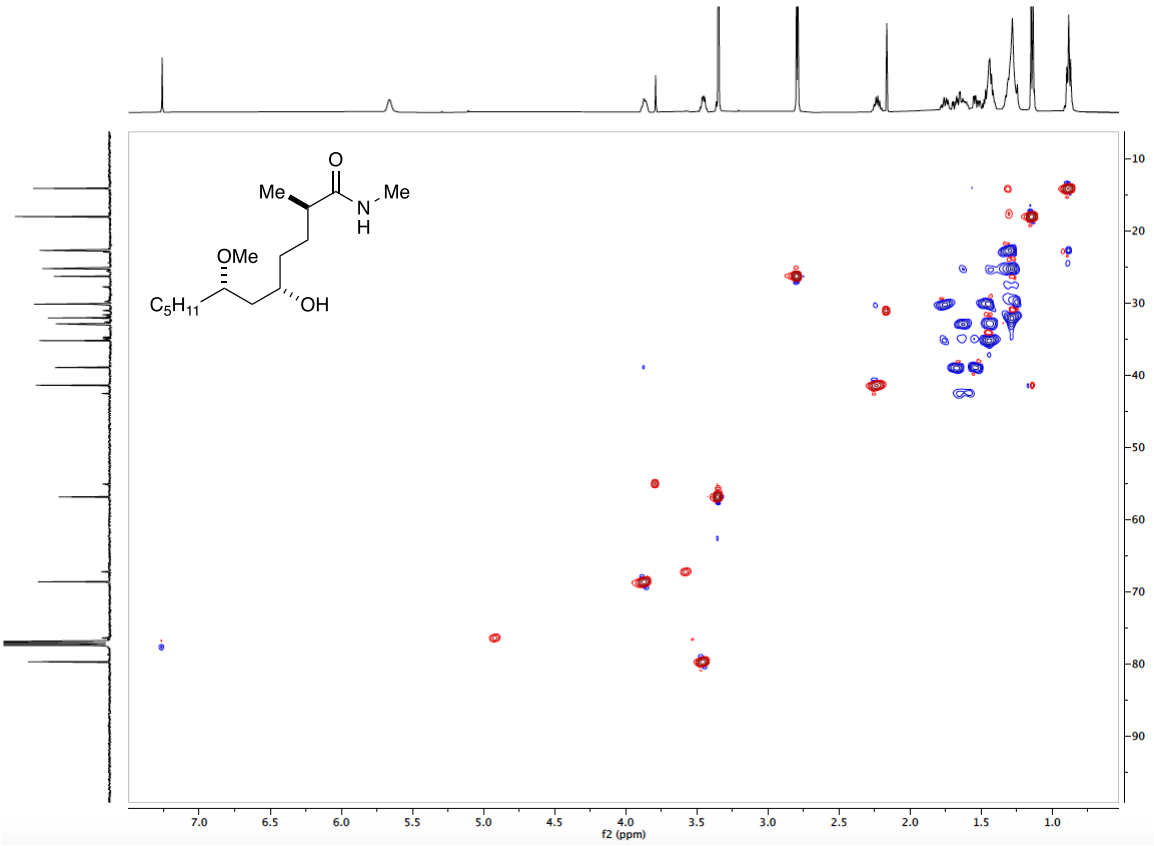
O
Me
N
H
Me
OMe
C_5H_{11}
OH
7.0
6.5
6.0
5.5
5.0
4.5
4.0
3.5
3.0
2.5
2.0
1.5
1.0
f2 (ppm)
10
20
30
40
50
60
70
80
90

(2*R*,5*S*,7*S*)-5-((*tert*-butyldimethylsilyl)oxy)-7-methoxy-*N*,2-dimethyldodecanamide ($C_{21}H_{45}NO_3Si$, 2.10.2)

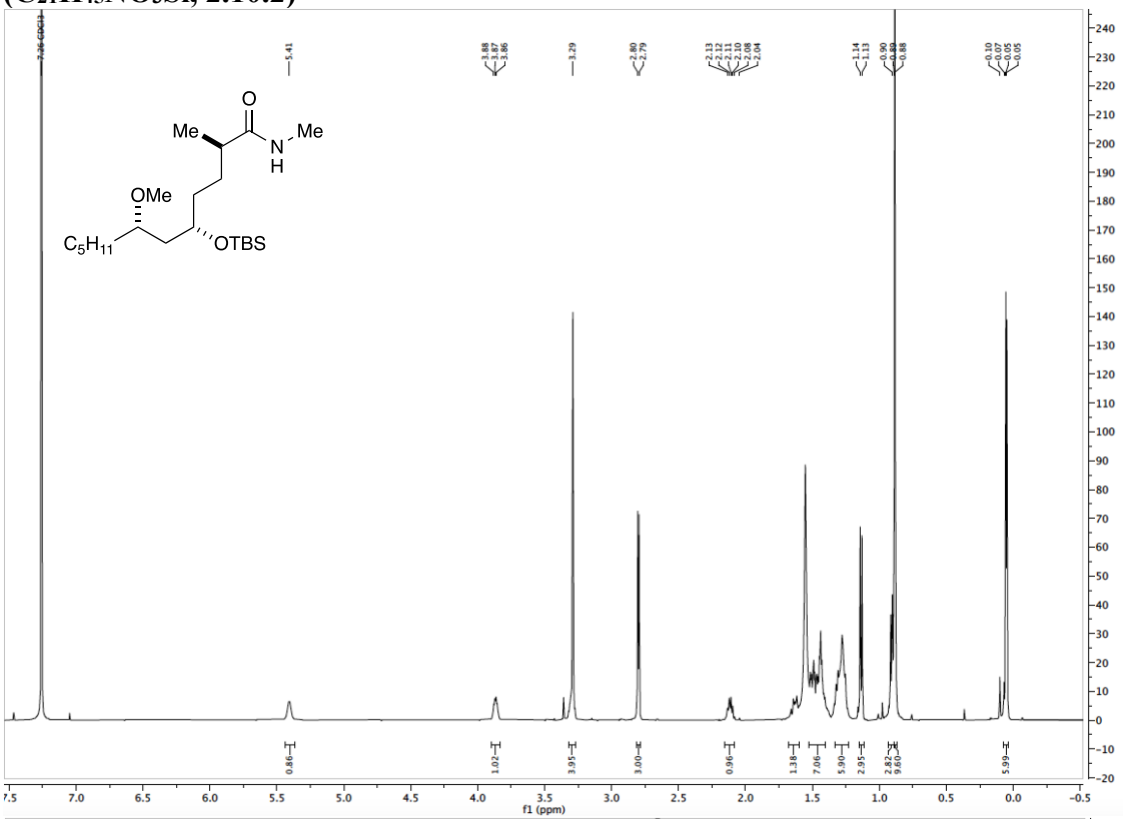

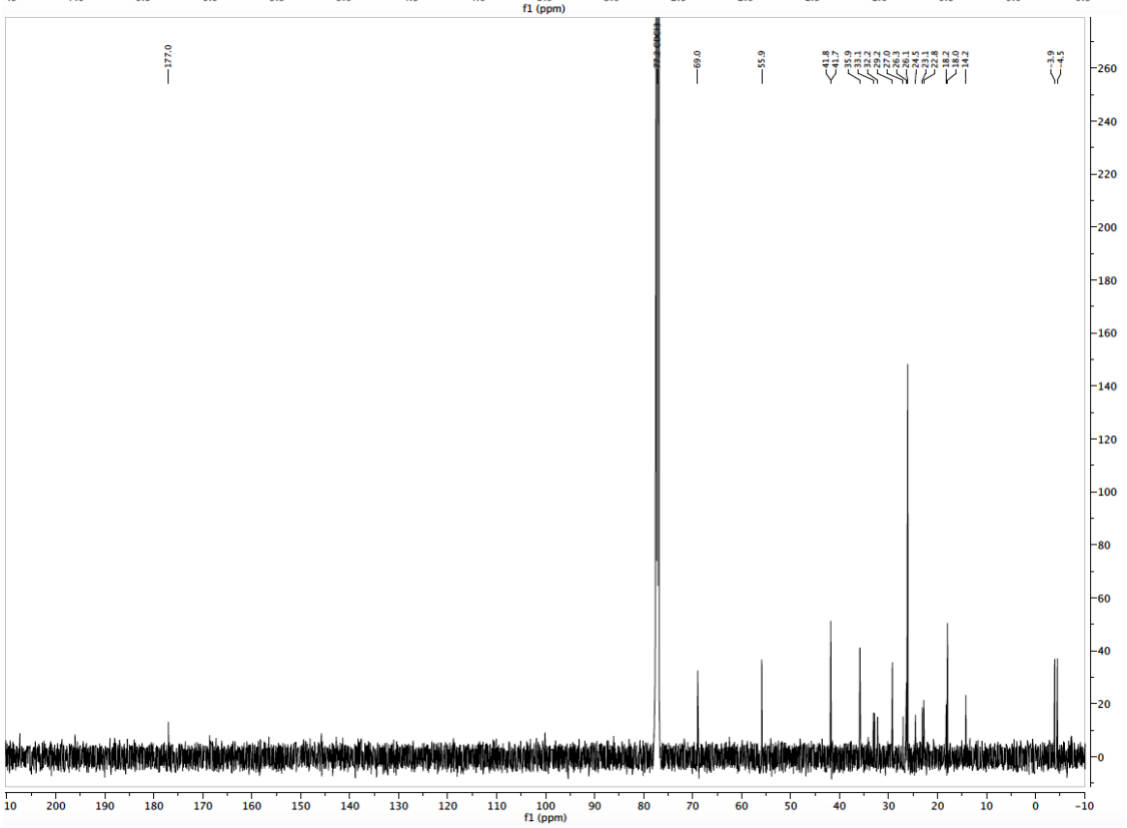

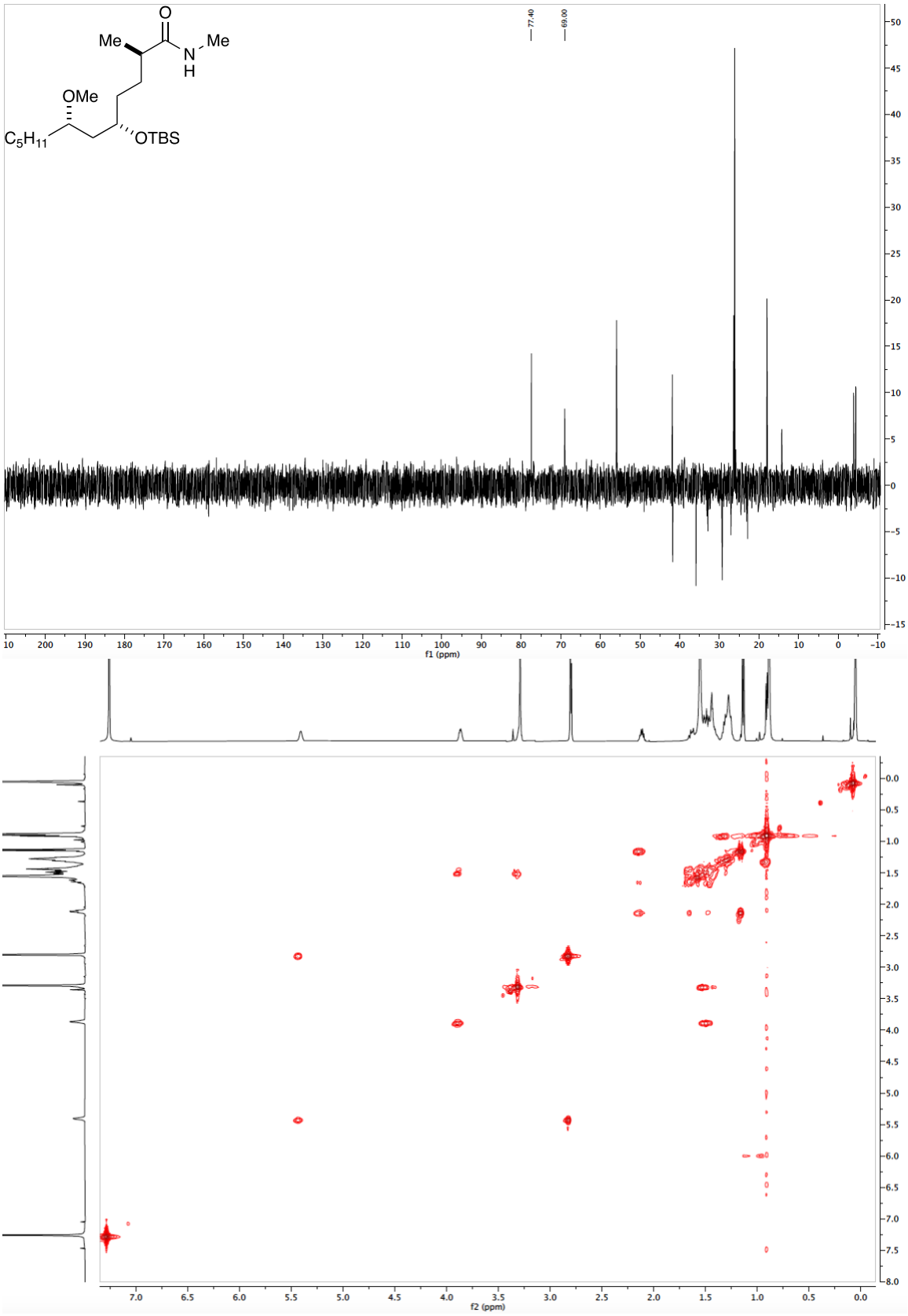
O
Me
N
H
Me
OMe
C5H11
OTBS
77.40
69.00
f1 (ppm)
f2 (ppm)

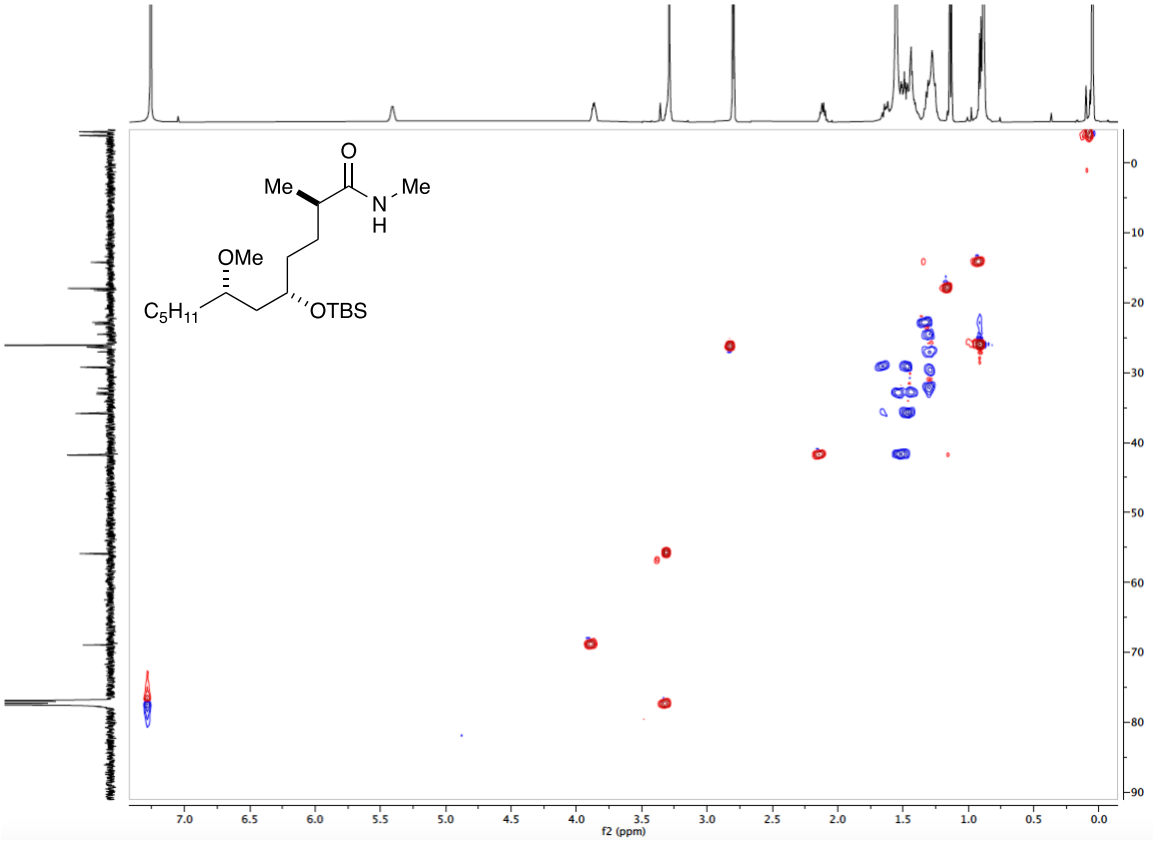
O
Me
N
H
Me
OMe
C5H11
OTBS
7.0
6.5
6.0
5.5
5.0
4.5
4.0
3.5
3.0
2.5
2.0
1.5
1.0
0.5
0.0
f2 (ppm)
0
10
20
30
40
50
60
70
80
90

(2*R*,5*S*,7*S*)-*N*-allyl-5-((*tert*-butyldimethylsilyl)oxy)-7-methoxy-*N*,2-dimethyldodecanamide ($C_{24}H_{49}NO_3Si$, 2.10.3)

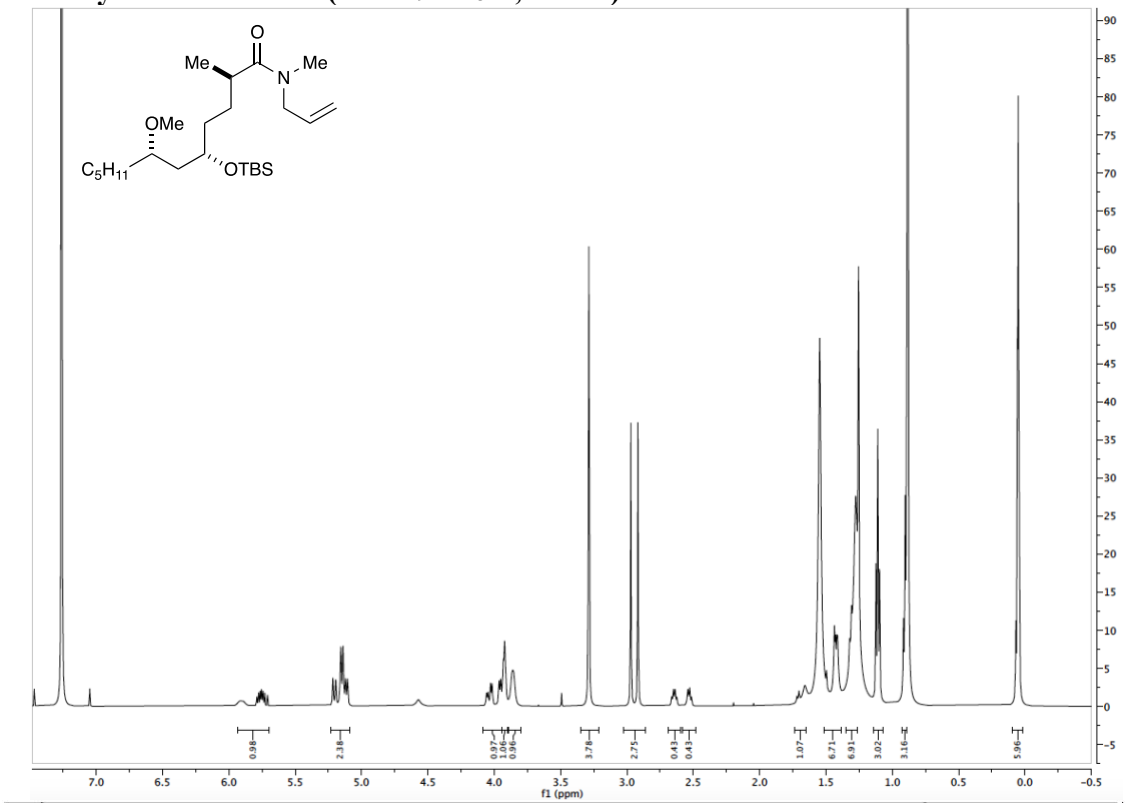

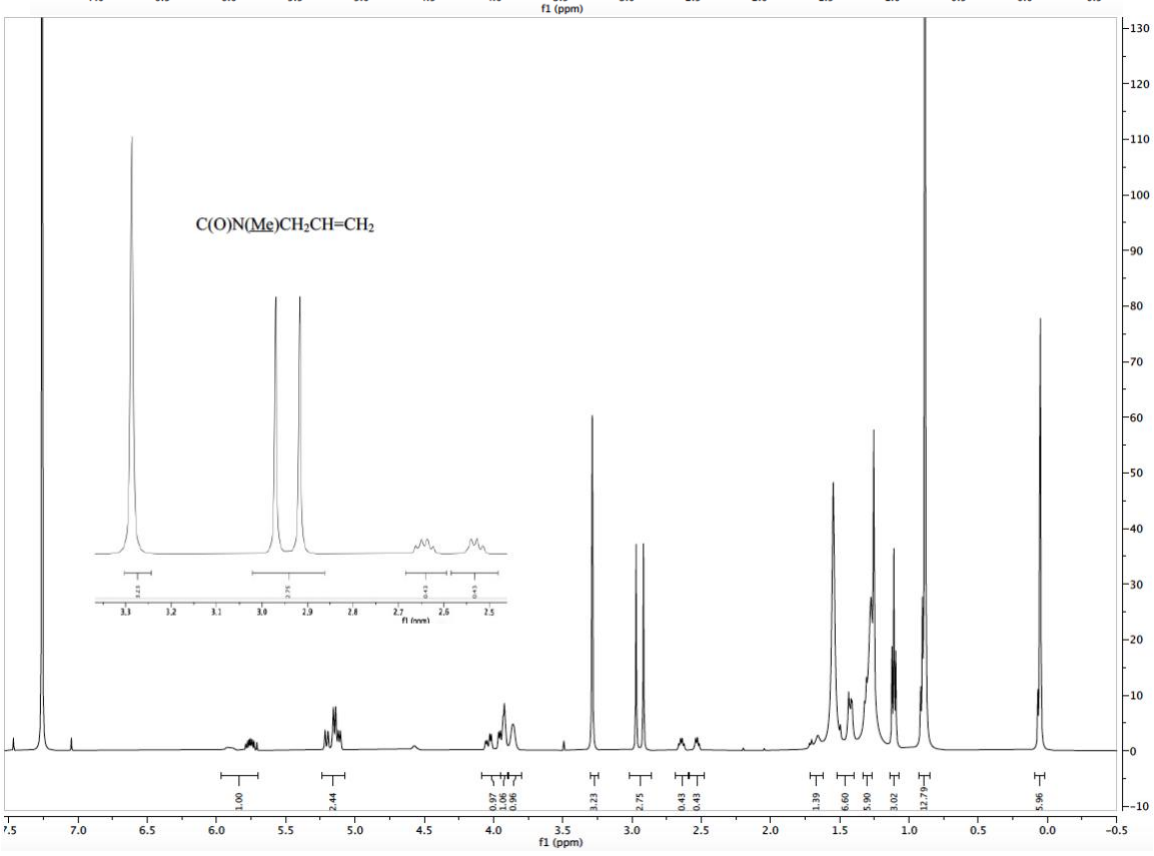

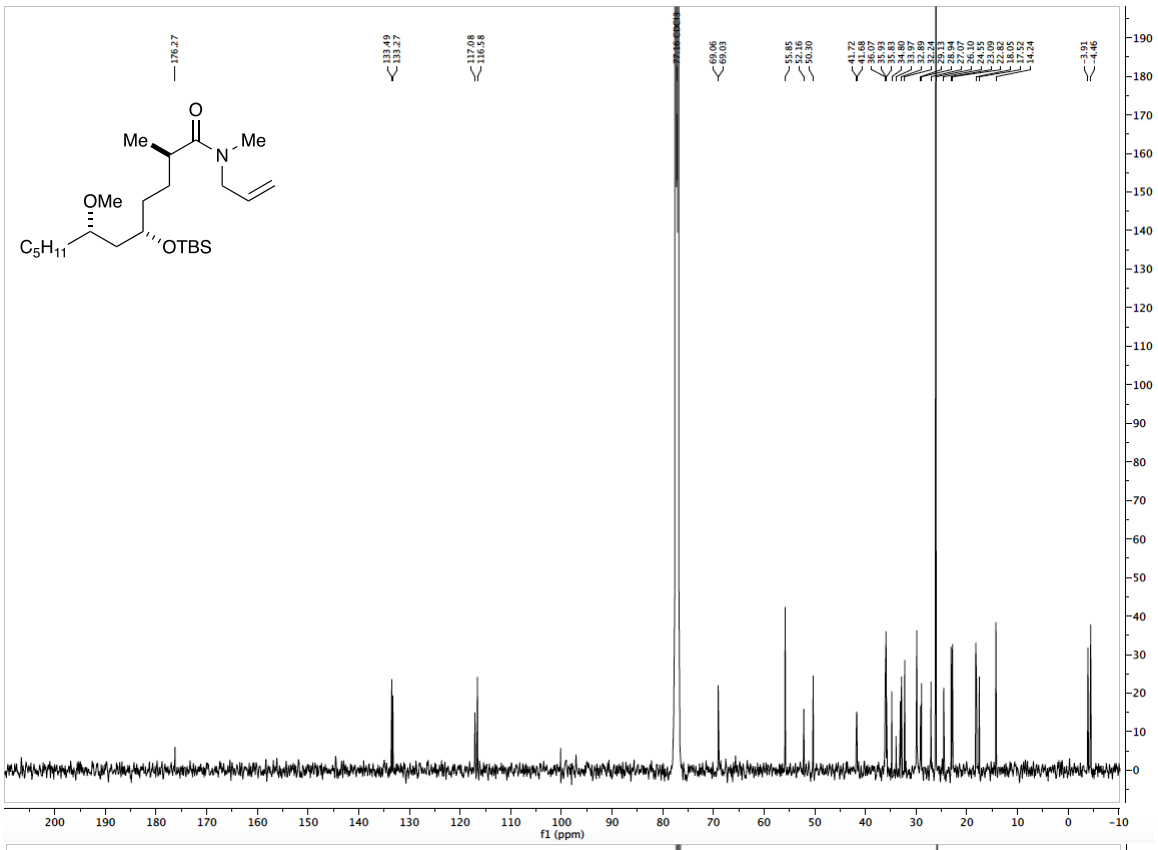
Me
O
N
Me
OMe
C_5H_{11}
OTBS
f1 (ppm)

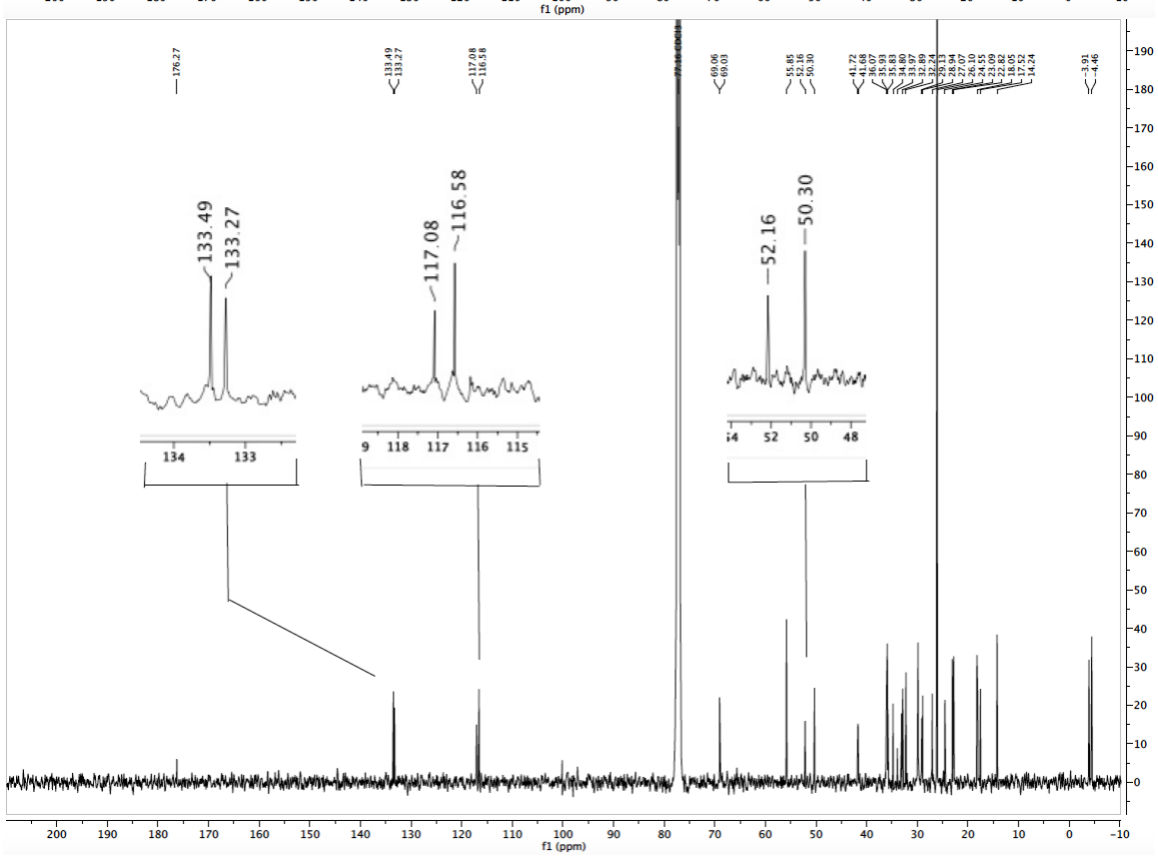
133.49
133.27
117.08
116.58
52.16
50.30
f1 (ppm)

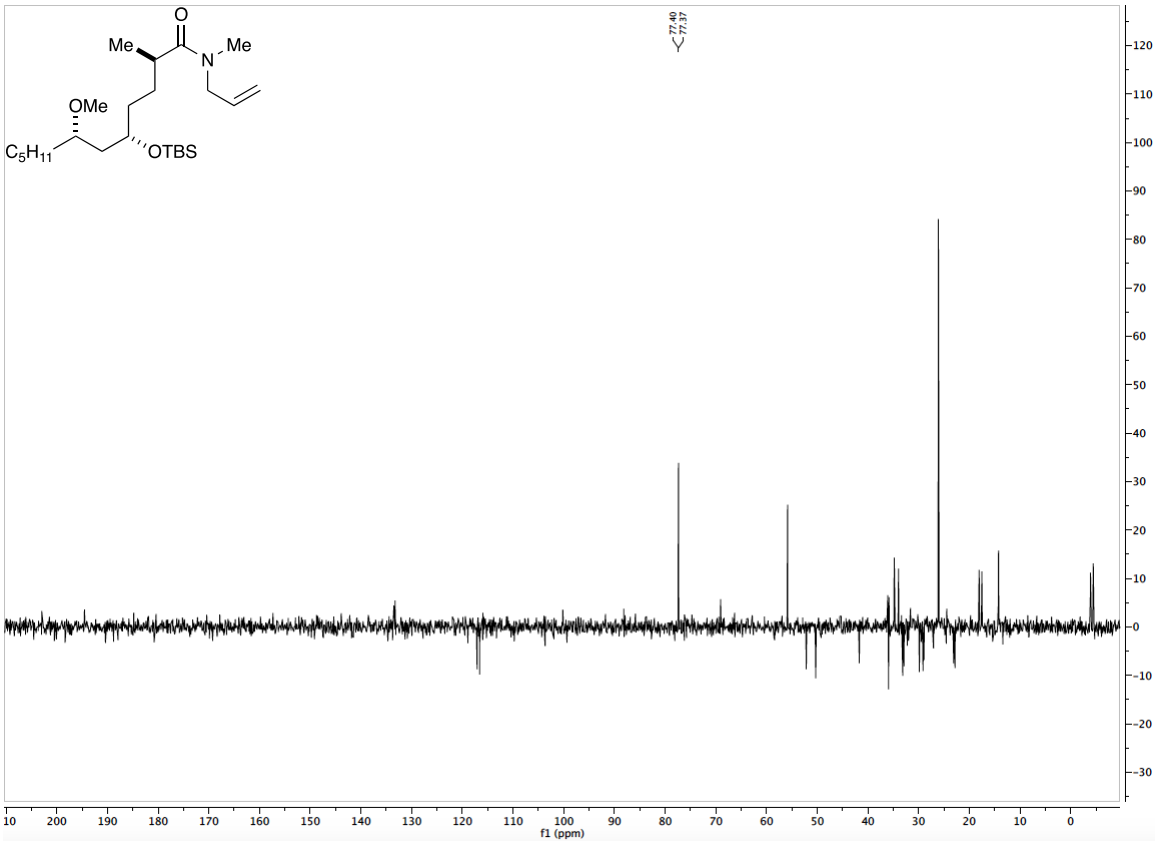
O
Me
N
Me
OMe
C5H11
OTBS
77.40
77.37
f1 (ppm)

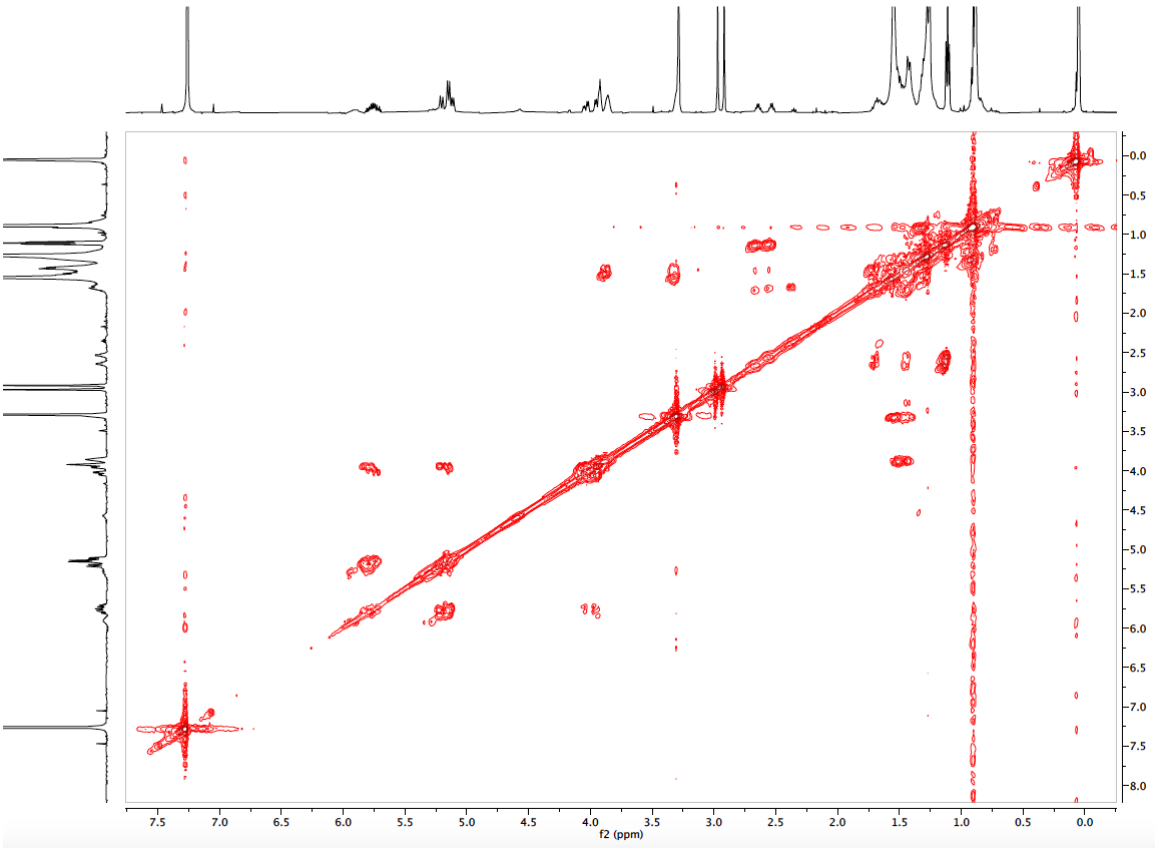
f2 (ppm)

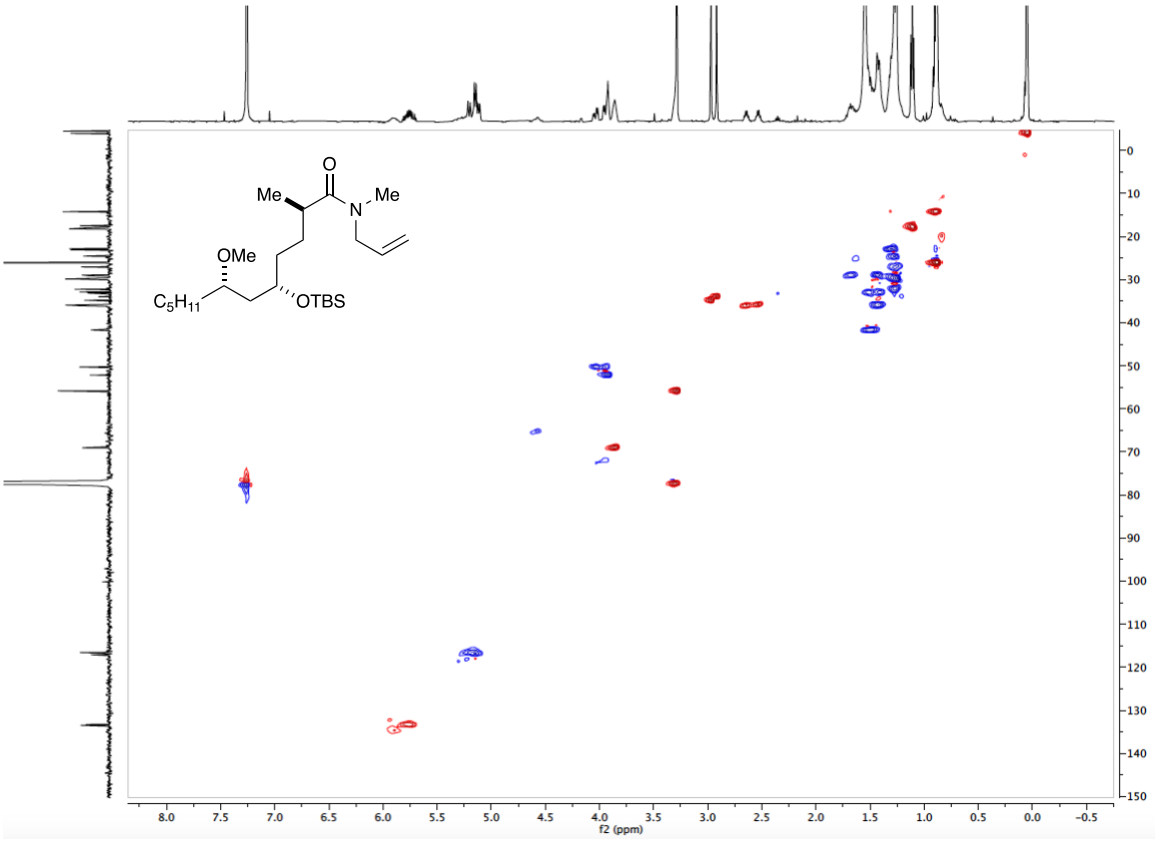
O
Me
N
Me
OMe
C5H11
OTBS
8.0
7.5
7.0
6.5
6.0
5.5
5.0
4.5
4.0
3.5
3.0
2.5
2.0
1.5
1.0
0.5
0.0
-0.5
f2 (ppm)
0
10
20
30
40
50
60
70
80
90
100
110
120
130
140
150

(2*R*,5*S*,7*S*)-*N*-allyl-5-hydroxy-7-methoxy-*N*,2-dimethyldodecanamide ($C_{18}H_{35}NO_3$, (2*R*)-2.2.2)

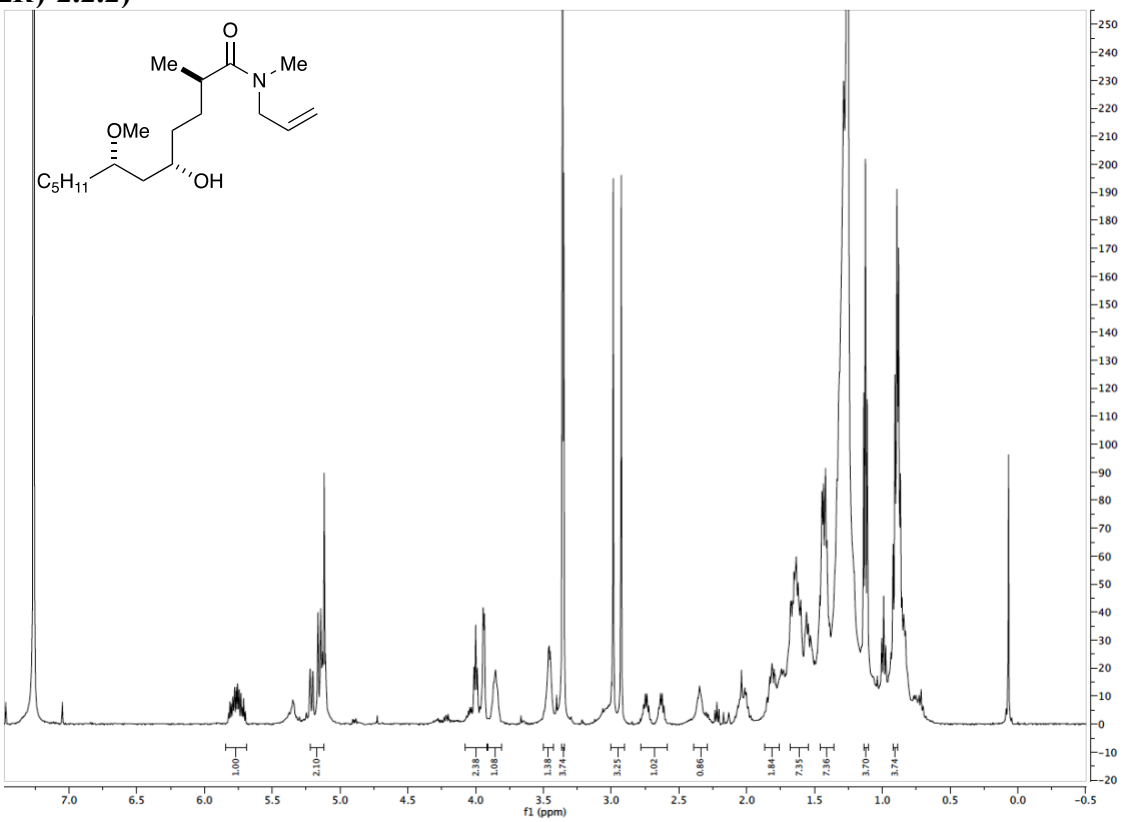

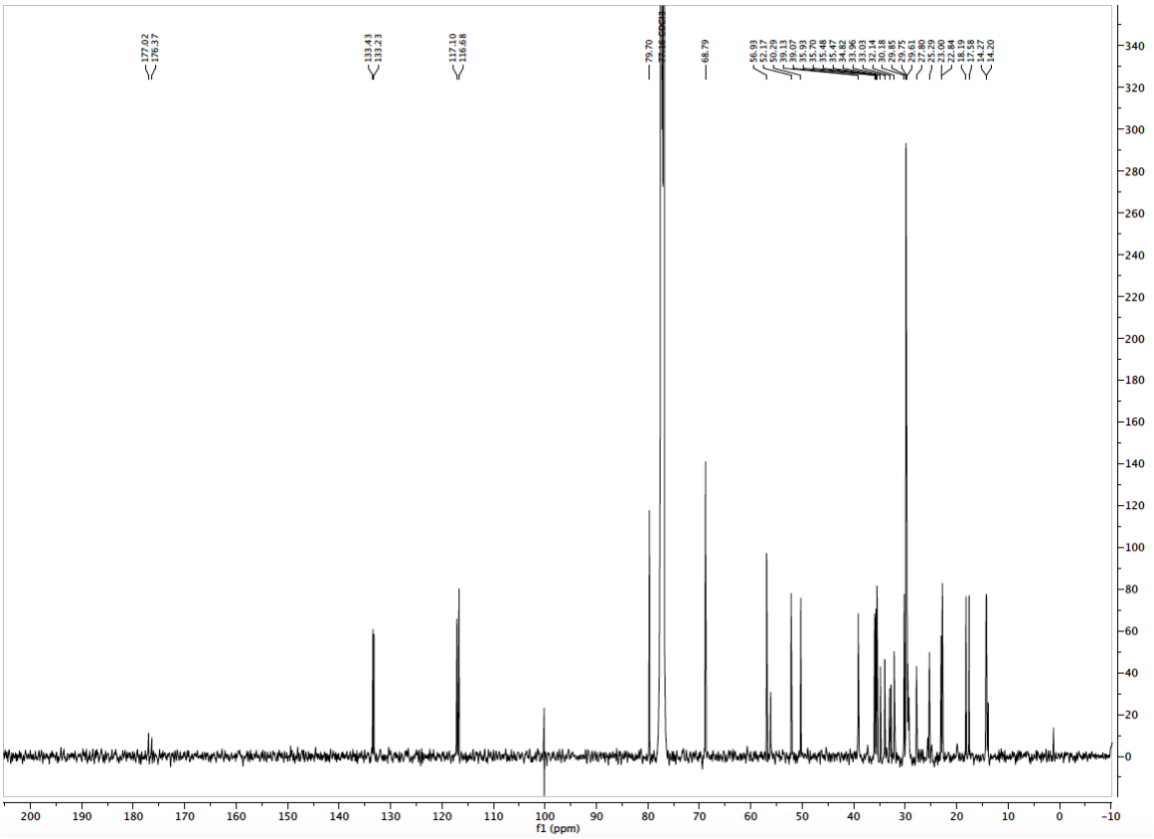

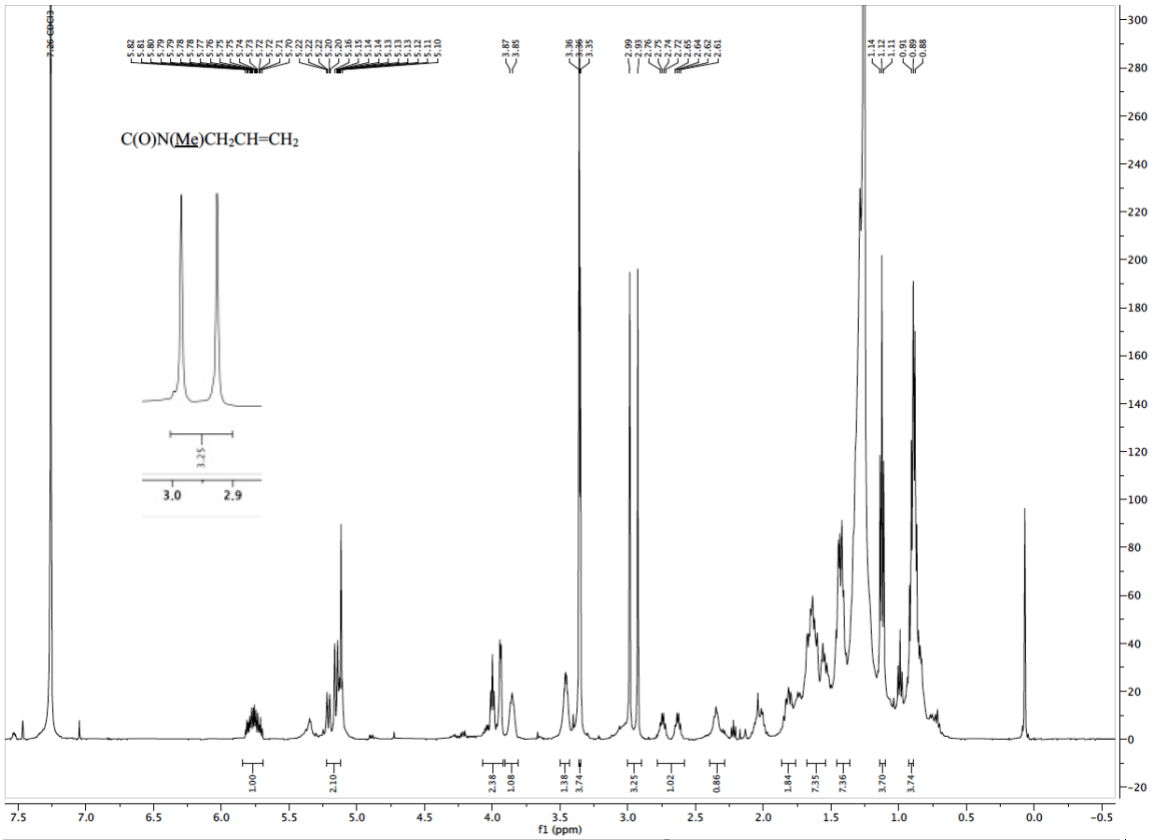
C(O)N(Me)CH2CH=CH2
f1 (ppm)

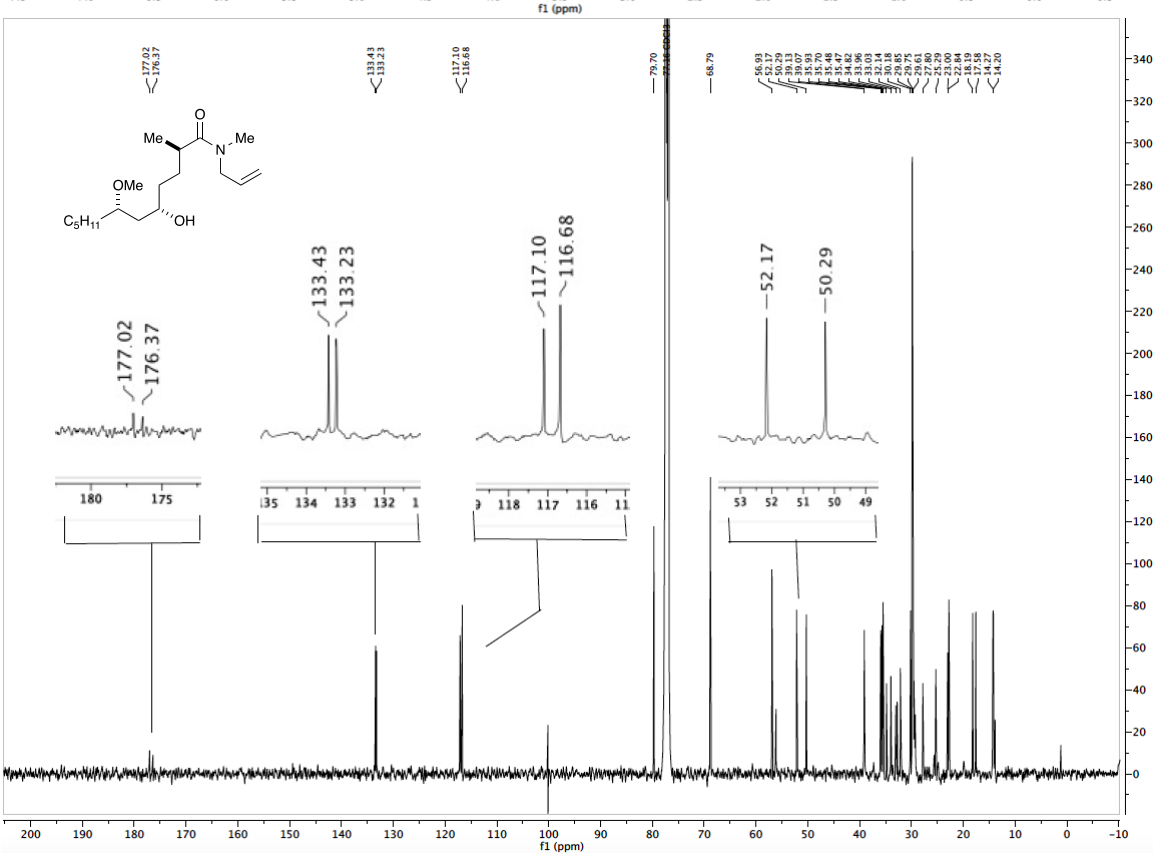
Me
N
Me
OMe
C5H11
OH
177.02
176.37
133.43
133.23
117.10
116.68
52.17
50.29
f1 (ppm)

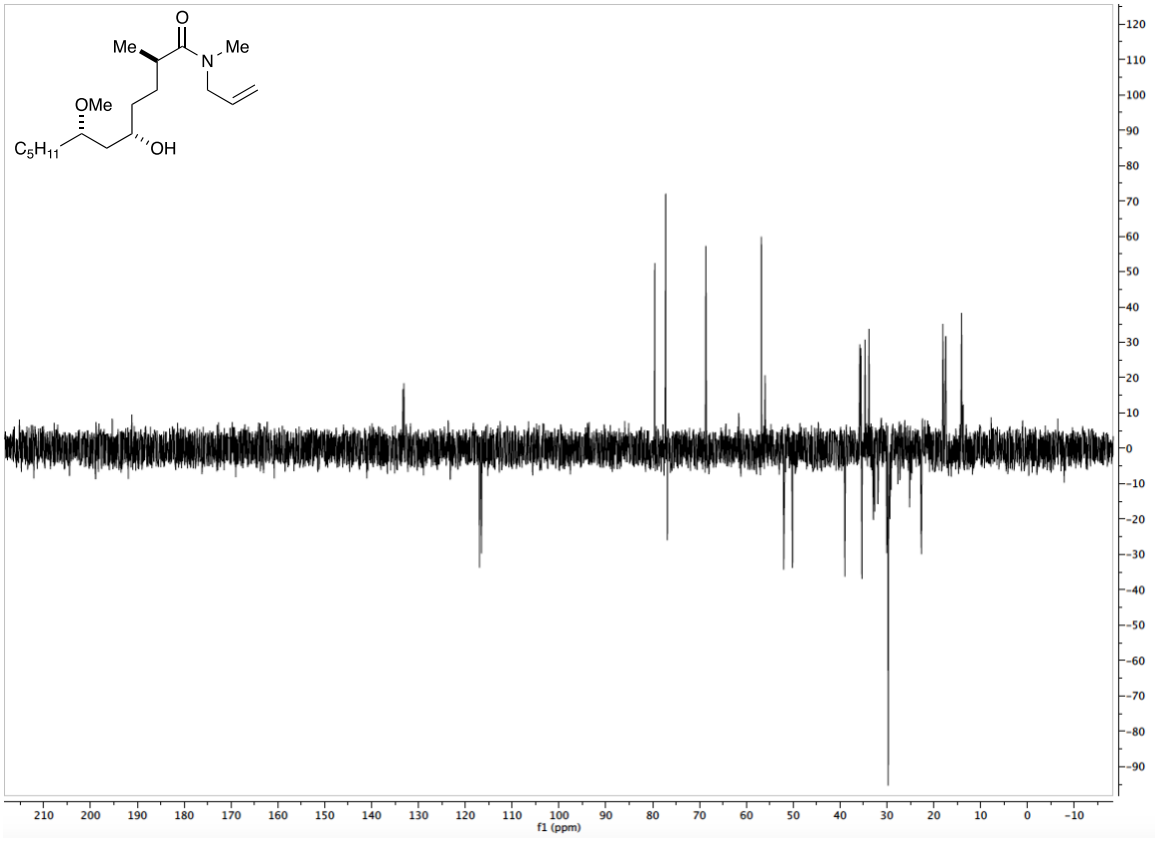
Me
O
N
Me
OMe
C_5H_{11}
OH
f1 (ppm)

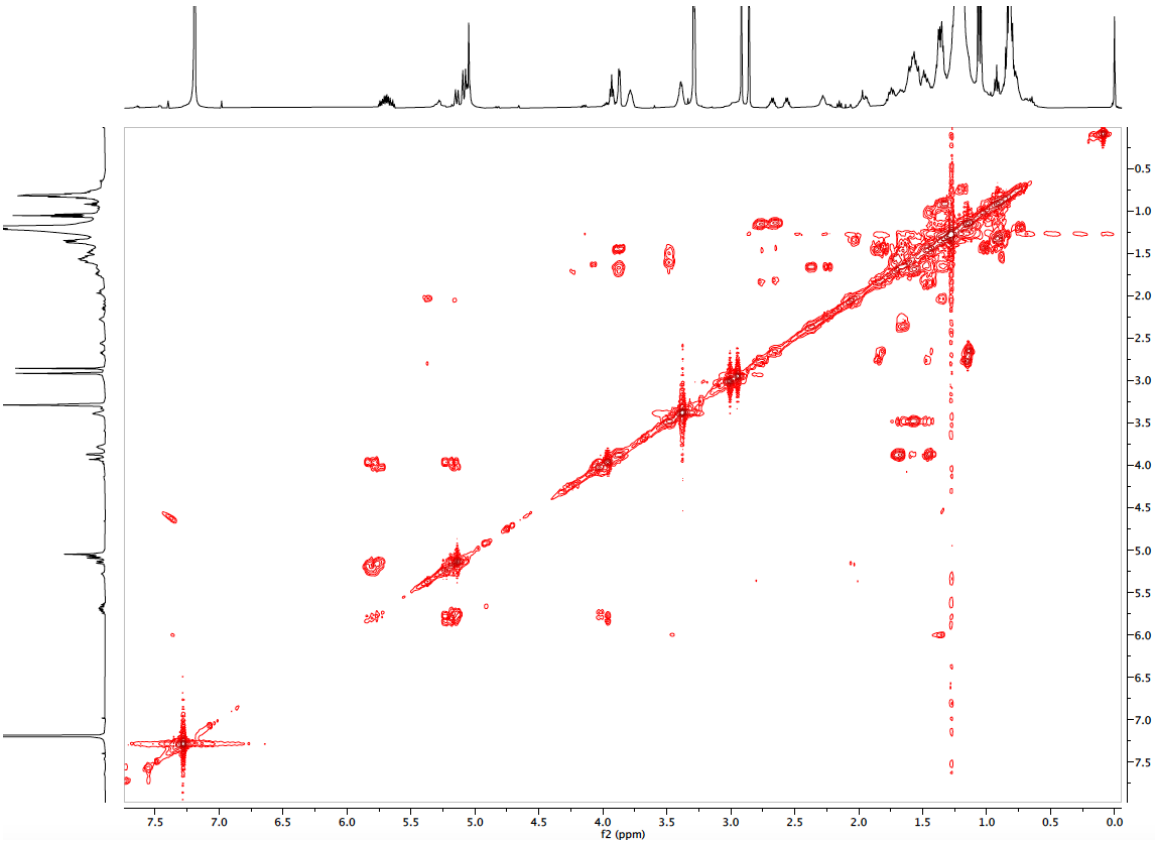
f2 (ppm)

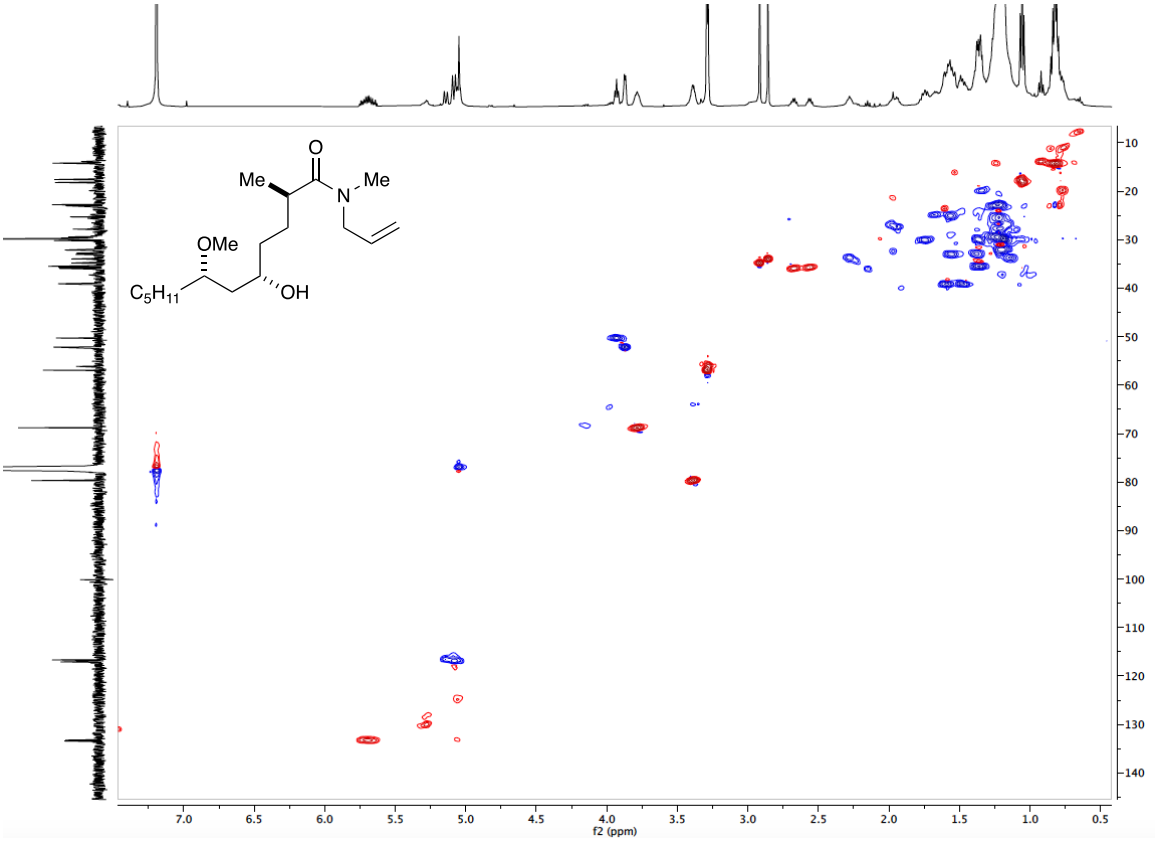
O
Me
N
Me
OMe
C5H11
OH
7.0
6.5
6.0
5.5
5.0
4.5
4.0
3.5
3.0
2.5
2.0
1.5
1.0
0.5
f2 (ppm)
10
20
30
40
50
60
70
80
90
100
110
120
130
140

(2*R*,5*S*,7*S*)-1-(allyl(methyl)amino)-7-methoxy-2-methyl-1-oxododecan-5-yl (*S*)-2-(acryloyloxy)-3-methylbutanoate ($C_{26}H_{45}NO_6$, (2*R*)-2.2.4)

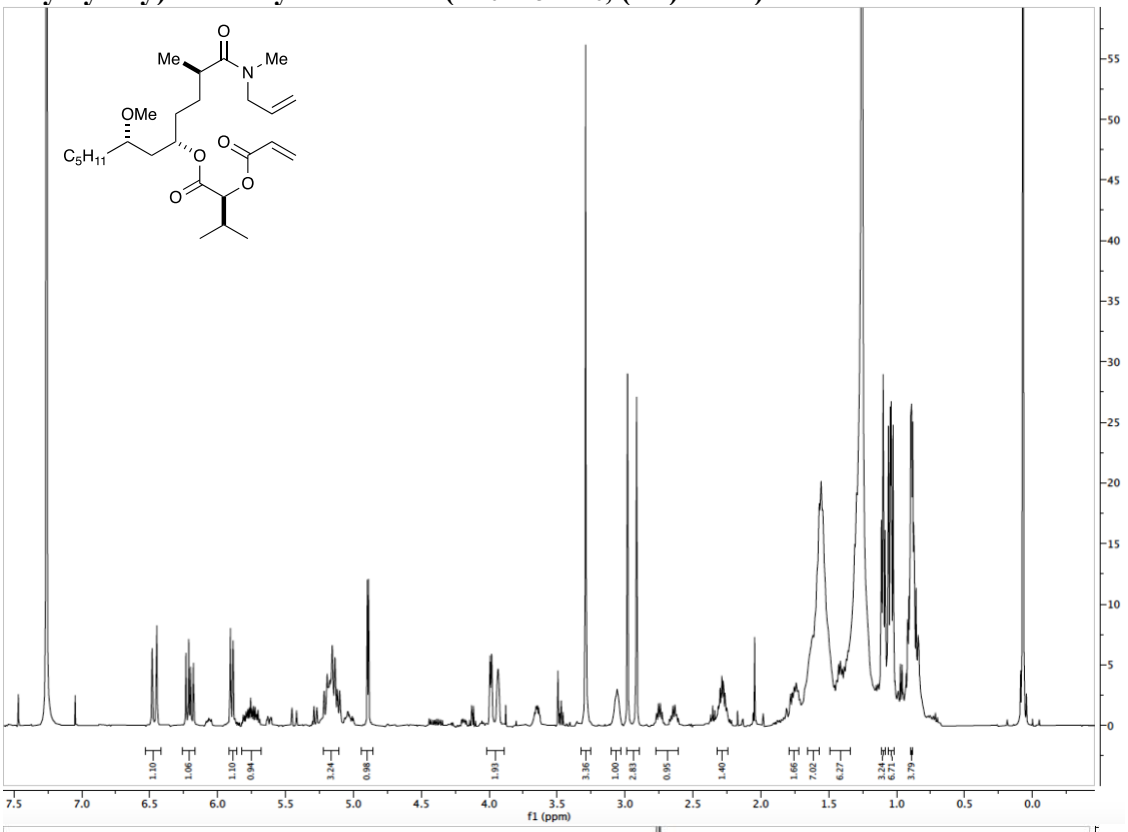

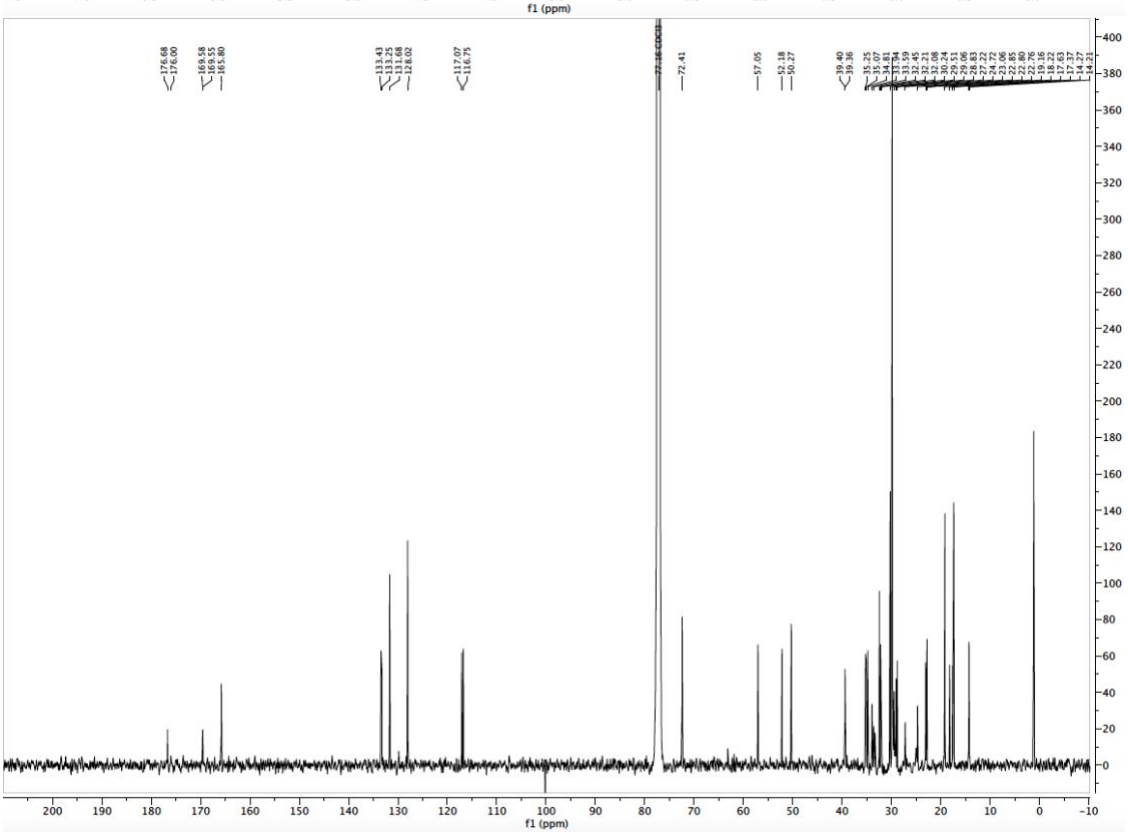

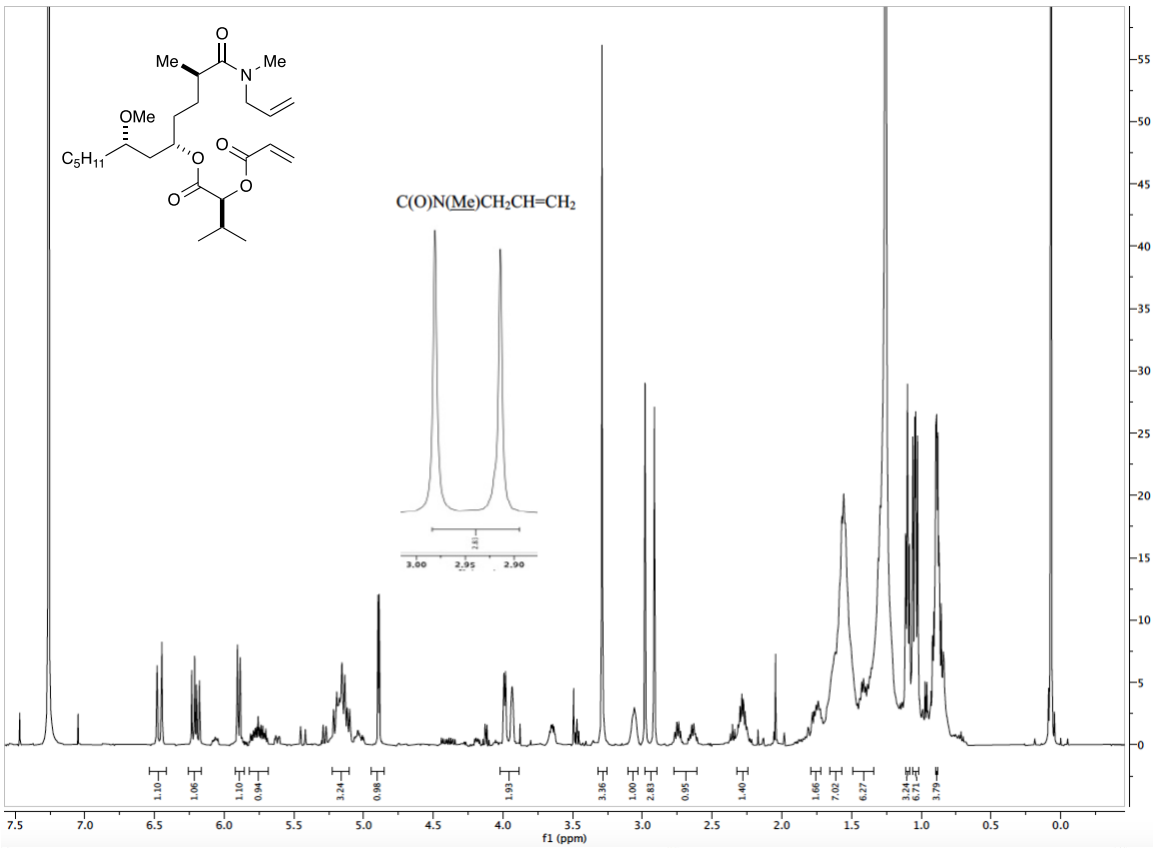
C(O)N(Me)CH2CH=CH2
f1 (ppm)

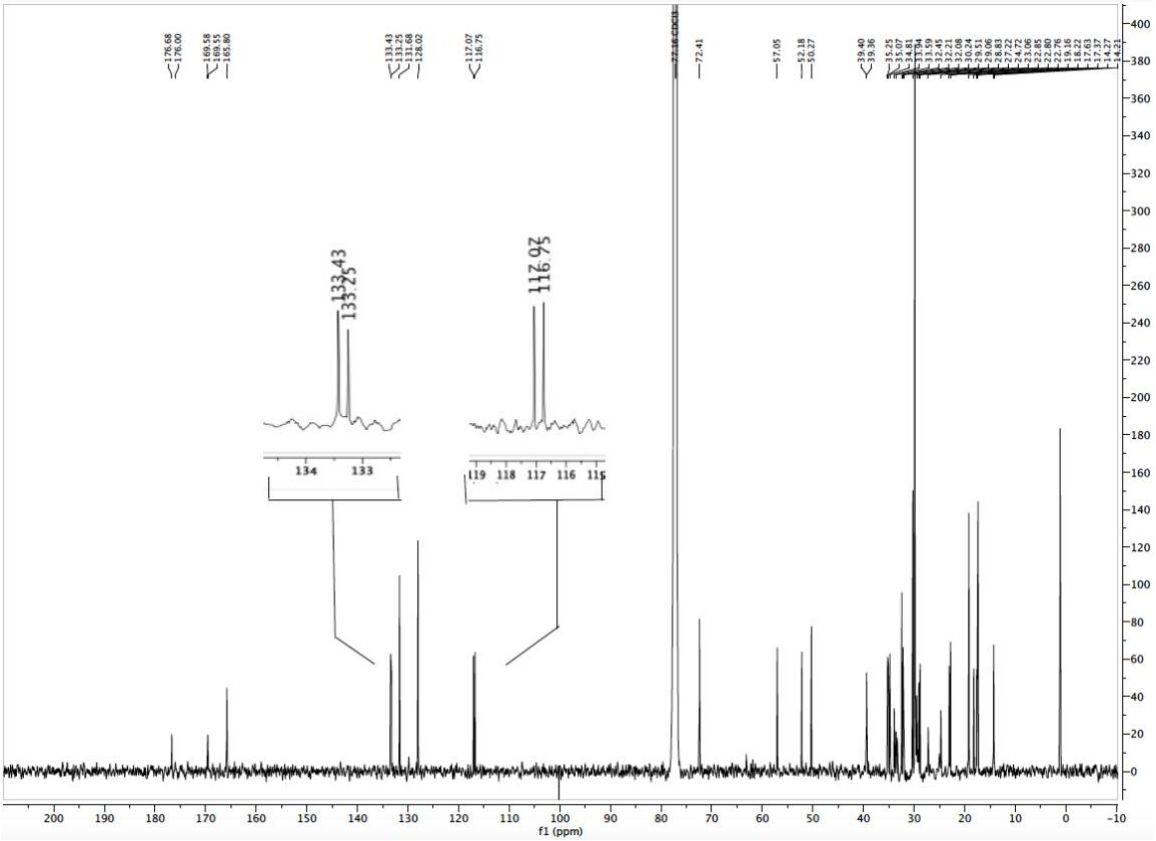
133.43
133.25
116.95
f1 (ppm)

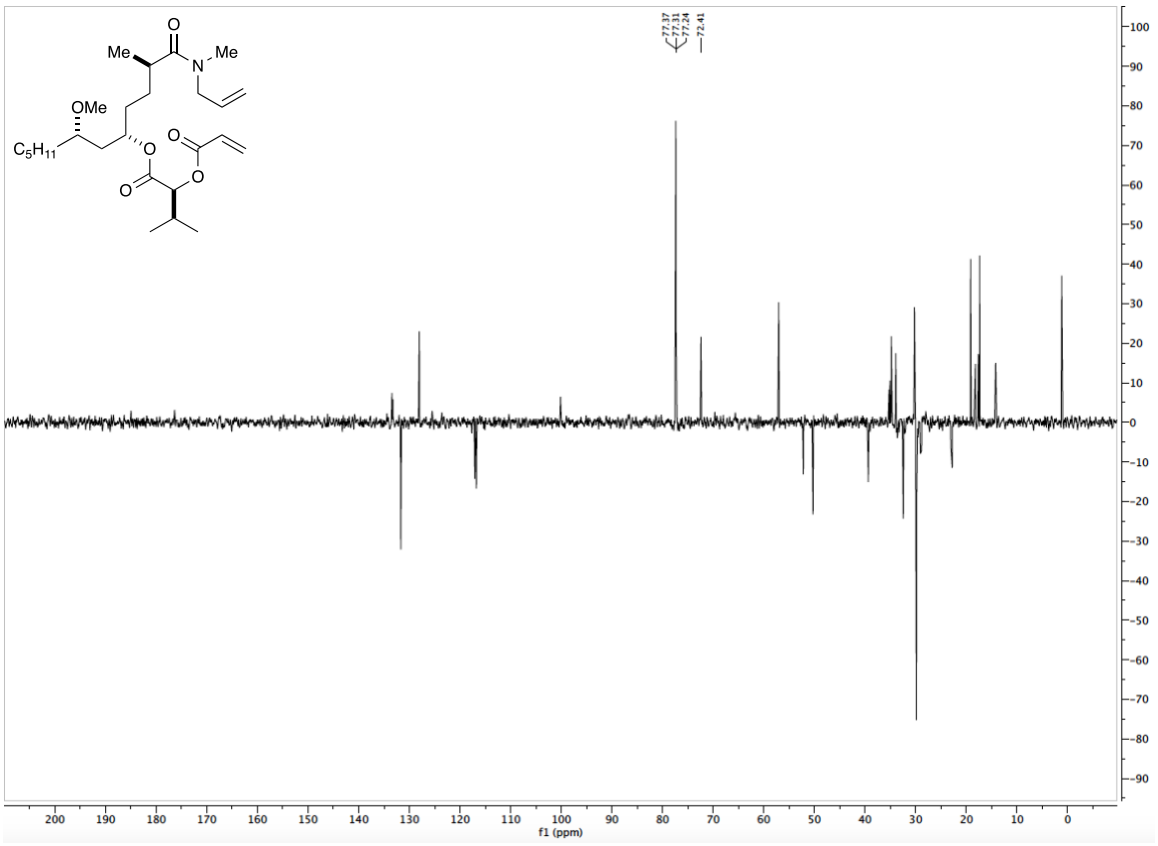
77.37
77.31
77.24
72.41
f1 (ppm)

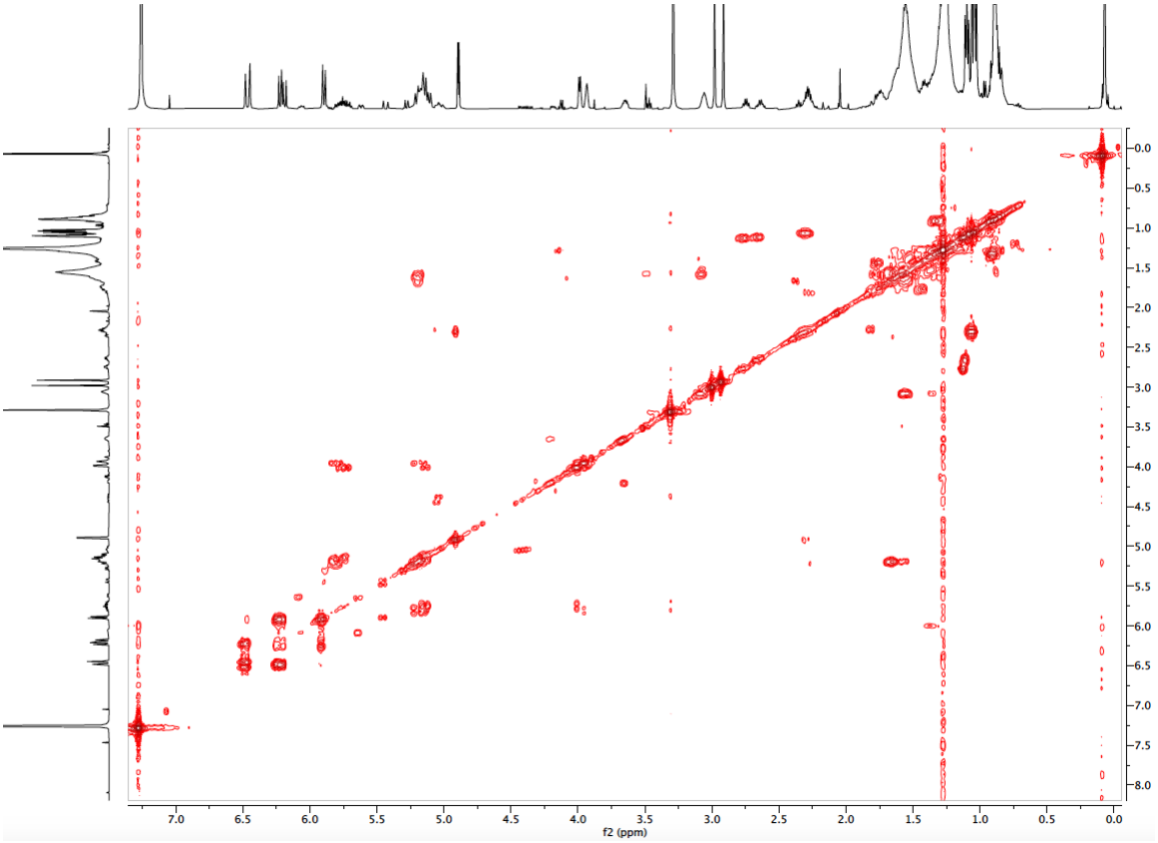
f2 (ppm)

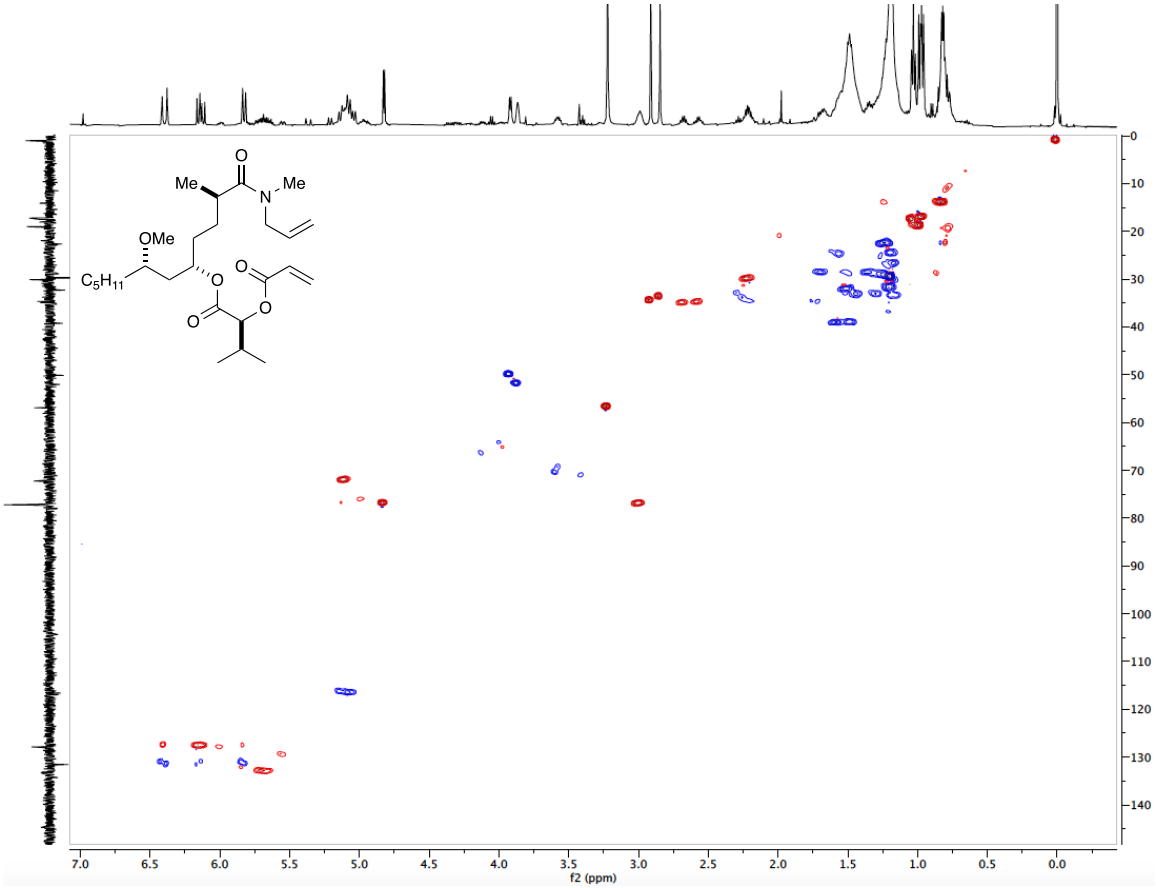
Me
O
N
Me
OMe
C5H11
O
O
O
O
0
10
20
30
40
50
60
70
80
90
100
110
120
130
140
7.0
6.5
6.0
5.5
5.0
4.5
4.0
3.5
3.0
2.5
2.0
1.5
1.0
0.5
0.0
f2 (ppm)

Sanctolide A [(3*S*,11*R*,14*S*,*E*)-3-isopropyl-14-((*S*)-2-methoxyheptyl)-9,11-dimethyl-1,4-dioxa-9-azacyclotetradec-7-ene-2,5,10-trione, ($C_{24}H_{41}NO_6$, (2*R*)-2.1-A]

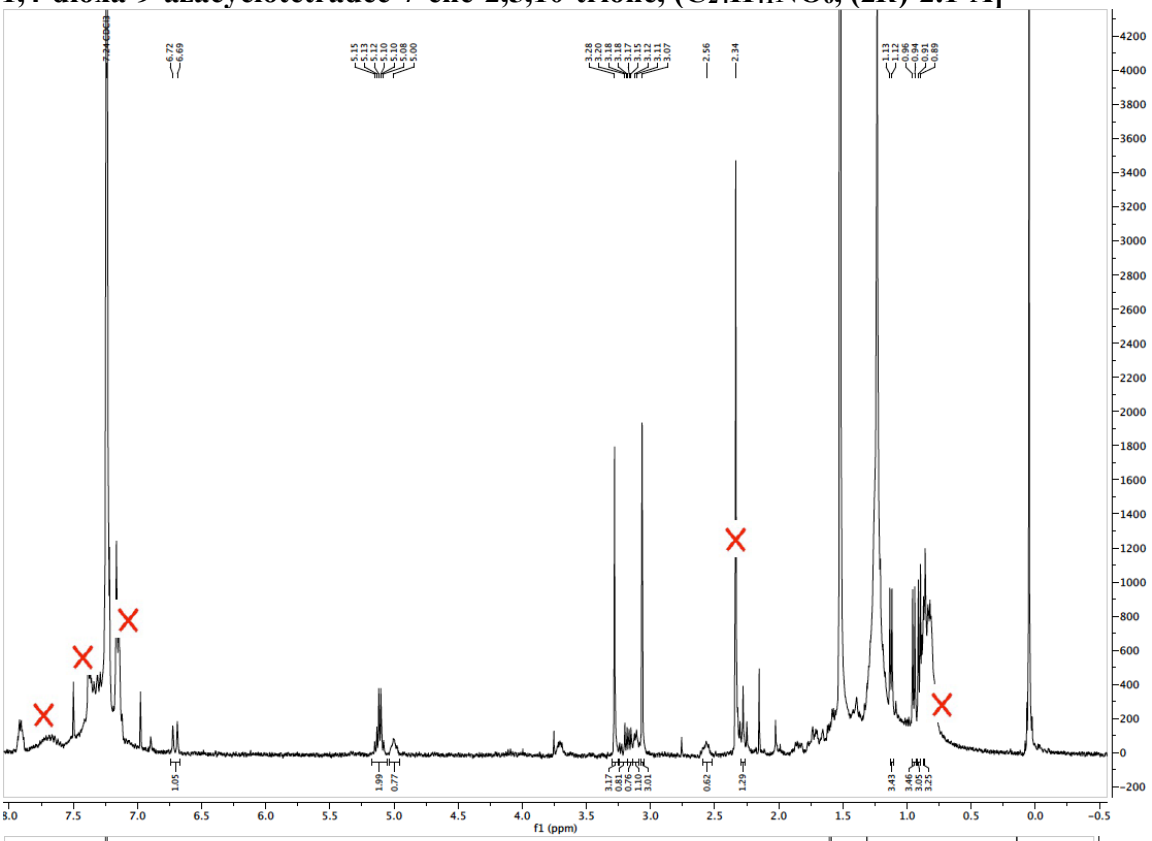

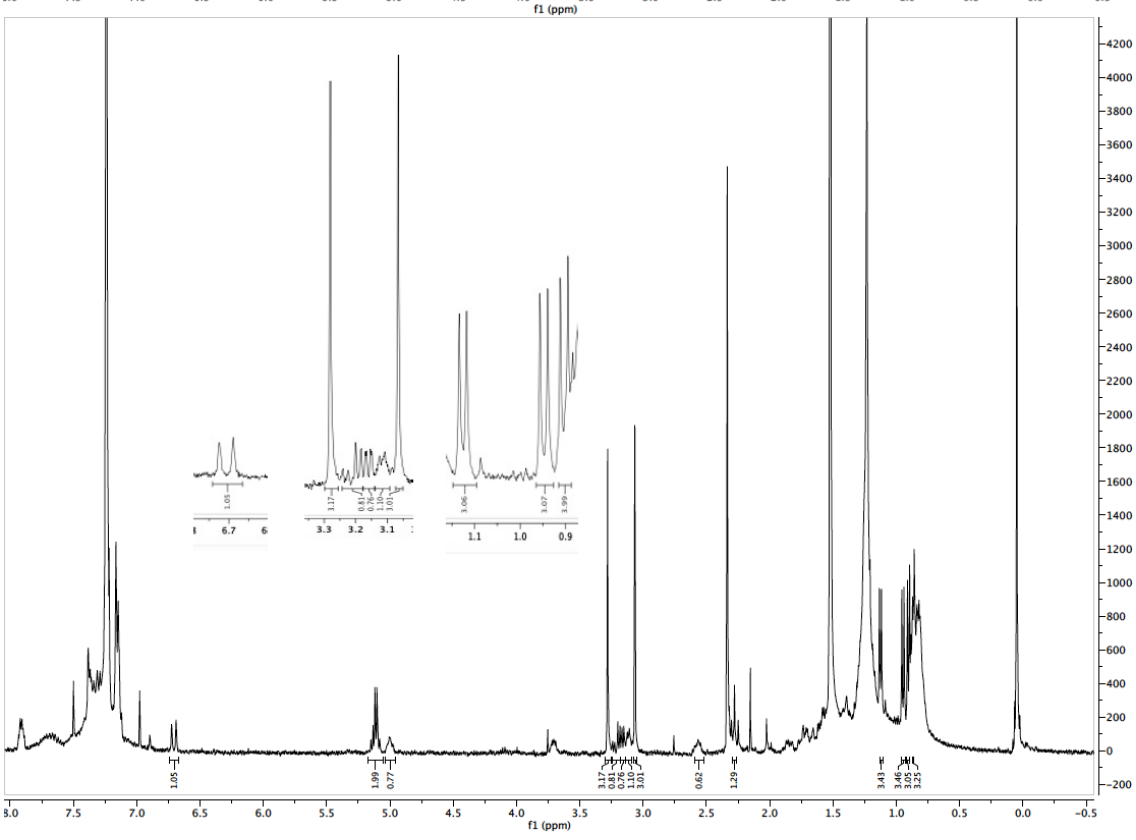

X-Ray Diffraction data

(1*R*,4*S*,7*R*,9*R*,*Z*)-4-methyl-9-vinyl-2,10,11-trioxa-1-phosphabicyclo[5.3.1]undec-5-ene 1-oxide ($C_{10}H_{15}O_4P$, 2.6.3)

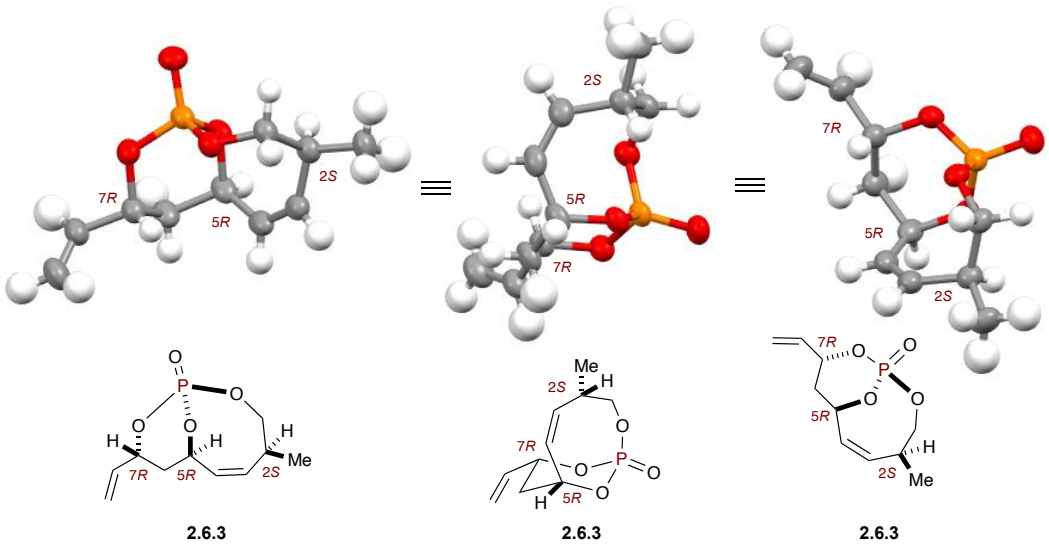

Atoms

Number	Label	Charge	SybylType	Xfrac + ESD	Yfrac + ESD	Zfrac + ESD	Symm. op.
1	P	0	P.3	0.237686	0.365577	0.243537	x,y,z
2	O1	0	O.3	0.195191	0.415368	0.136937	x,y,z
3	O2	0	O.3	0.186016	0.562651	0.295934	x,y,z
4	O3	0	O.3	0.50259	0.335579	0.260748	x,y,z
5	O4	0	O.2	0.102803	0.198643	0.269621	x,y,z
6	C1	0	C.2	0.337807	0.647081	-0.058787	x,y,z
7	H11	0	H	0.488871	0.636809	-0.037794	x,y,z
8	H12	0	H	0.284469	0.663593	-0.122289	x,y,z
9	C2	0	C.2	0.205132	0.621599	0.003984	x,y,z
10	H2	0	H	0.036999	0.614967	-0.018078	x,y,z
11	C3	0	C.3	0.285049	0.60471	0.105675	x,y,z
12	H3	0	H	0.450548	0.600345	0.114862	x,y,z
13	C4	0	C.3	0.195137	0.773923	0.160045	x,y,z
14	H41	0	H	0.026735	0.789624	0.151876	x,y,z
15	H42	0	H	0.246175	0.895954	0.141108	x,y,z
16	C5	0	C.3	0.265388	0.753934	0.264878	x,y,z
17	H5	0	H	0.180849	0.846669	0.298162	x,y,z

18	C6	0	C.2	0.513786	0.790123	0.295073	x,y,z
19	H6	0	H	0.566764	0.90504	0.26739	x,y,z
20	C7	0	C.2	0.662414	0.691654	0.357199	x,y,z
21	H7	0	H	0.821974	0.738944	0.368288	x,y,z
22	C8	0	C.3	0.621904	0.506781	0.412076	x,y,z
23	H8	0	H	0.471925	0.519455	0.430661	x,y,z
24	C9	0	C.3	0.629106	0.318421	0.353473	x,y,z
25	H91	0	H	0.782061	0.297591	0.341175	x,y,z
26	H92	0	H	0.574212	0.196482	0.386266	x,y,z
27	C10	0	C.3	0.799437	0.483928	0.497982	x,y,z
28	H101	0	H	0.779187	0.35332	0.530681	x,y,z
29	H102	0	H	0.793317	0.594416	0.538379	x,y,z
30	H103	0	H	0.931477	0.479849	0.478731	x,y,z

Bonds

Number	Atom1	Atom2	Type	Polymeric	Cyclicity	Length	Sybyl Type
1	P	O1	Unknown	no	cyclic	1.5696	1
1	O1	P	Unknown	no	cyclic	1.5696	1
2	P	O2	Unknown	no	cyclic	1.5758	1
2	O2	P	Unknown	no	cyclic	1.5758	1
3	P	O3	Unknown	no	cyclic	1.5691	1
3	O3	P	Unknown	no	cyclic	1.5691	1
4	P	O4	Unknown	no	acyclic	1.4564	un
4	O4	P	Unknown	no	acyclic	1.4564	un
5	O1	C3	Unknown	no	cyclic	1.4725	1
5	C3	O1	Unknown	no	cyclic	1.4725	1
6	O2	C5	Unknown	no	cyclic	1.4587	1
6	C5	O2	Unknown	no	cyclic	1.4587	1
7	O3	C9	Unknown	no	cyclic	1.4508	1
7	C9	O3	Unknown	no	cyclic	1.4508	1
8	C1	H11	Unknown	no	acyclic	0.9075	1
8	H11	C1	Unknown	no	acyclic	0.9075	1
9	C1	H12	Unknown	no	acyclic	0.9386	1
9	H12	C1	Unknown	no	acyclic	0.9386	1
10	C1	C2	Unknown	no	acyclic	1.2984	un
10	C2	C1	Unknown	no	acyclic	1.2984	un
11	C2	H2	Unknown	no	acyclic	1.0046	1
11	H2	C2	Unknown	no	acyclic	1.0046	1
12	C2	C3	Unknown	no	acyclic	1.4907	1
12	C3	C2	Unknown	no	acyclic	1.4907	1

13	C3	H3	Unknown	no	acyclic	0.9726	1
13	H3	C3	Unknown	no	acyclic	0.9726	1
14	C3	C4	Unknown	no	cyclic	1.5212	1
14	C4	C3	Unknown	no	cyclic	1.5212	1
15	C4	H41	Unknown	no	acyclic	0.995	1
15	H41	C4	Unknown	no	acyclic	0.995	1
16	C4	H42	Unknown	no	acyclic	0.927	1
16	H42	C4	Unknown	no	acyclic	0.927	1
17	C4	C5	Unknown	no	cyclic	1.5271	1
17	C5	C4	Unknown	no	cyclic	1.5271	1
18	C5	H5	Unknown	no	acyclic	0.9699	1
18	H5	C5	Unknown	no	acyclic	0.9699	1
19	C5	C6	Unknown	no	cyclic	1.4966	1
19	C6	C5	Unknown	no	cyclic	1.4966	1
20	C6	H6	Unknown	no	acyclic	0.943	1
20	H6	C6	Unknown	no	acyclic	0.943	1
21	C6	C7	Unknown	no	cyclic	1.3422	un
21	C7	C6	Unknown	no	cyclic	1.3422	un
22	C7	H7	Unknown	no	acyclic	0.9897	1
22	H7	C7	Unknown	no	acyclic	0.9897	1
23	C7	C8	Unknown	no	cyclic	1.5107	1
23	C8	C7	Unknown	no	cyclic	1.5107	1
24	C8	H8	Unknown	no	acyclic	0.9699	1
24	H8	C8	Unknown	no	acyclic	0.9699	1
25	C8	C9	Unknown	no	cyclic	1.5263	1
25	C9	C8	Unknown	no	cyclic	1.5263	1
26	C8	C10	Unknown	no	acyclic	1.5223	1
26	C10	C8	Unknown	no	acyclic	1.5223	1
27	C9	H91	Unknown	no	acyclic	0.96	1
27	H91	C9	Unknown	no	acyclic	0.96	1
28	C9	H92	Unknown	no	acyclic	1.0221	1
28	H92	C9	Unknown	no	acyclic	1.0221	1
29	C10	H101	Unknown	no	acyclic	1.0109	1
29	H101	C10	Unknown	no	acyclic	1.0109	1
30	C10	H102	Unknown	no	acyclic	0.9486	1
30	H102	C10	Unknown	no	acyclic	0.9486	1
31	C10	H103	Unknown	no	acyclic	0.8692	1
31	H103	C10	Unknown	no	acyclic	0.8692	1

Symmetry operations

Number	Symm. Op.	Description	Detailed Description	Order	Type
1	x,y,z	Identity	Identity	1	1
2	-x,1/2+y,-z	Screw axis (2-fold)	2-fold screw axis with direction [0, 1, 0] at 0, y, 0 with screw component [0, 1/2, 0]	2	2

All angles

Number	Atom1	Atom2	Atom3	Angle
1	O1	P	O2	106.5
2	O1	P	O3	101.6
3	O1	P	O4	113.77
4	O2	P	O3	106.84
5	O2	P	O4	111.43
6	O3	P	O4	115.81
7	P	O1	C3	118.24
8	P	O2	C5	119.52
9	P	O3	C9	122.17
10	H11	C1	H12	121.21
11	H11	C1	C2	115
12	H12	C1	C2	123.58
13	C1	C2	H2	117.11
14	C1	C2	C3	124.57
15	H2	C2	C3	118.32
16	O1	C3	C2	107.05
17	O1	C3	H3	109.56
18	O1	C3	C4	108.2
19	C2	C3	H3	108.11
20	C2	C3	C4	111.89
21	H3	C3	C4	111.91
22	C3	C4	H41	115.94
23	C3	C4	H42	110.44
24	C3	C4	C5	112.76
25	H41	C4	H42	103.68
26	H41	C4	C5	104.78
27	H42	C4	C5	108.61
28	O2	C5	C4	109.36
29	O2	C5	H5	101.27
30	O2	C5	C6	113.55
31	C4	C5	H5	110.75

32	C4	C5	C6	113.32
33	H5	C5	C6	107.93
34	C5	C6	H6	112.42
35	C5	C6	C7	130.02
36	H6	C6	C7	117.46
37	C6	C7	H7	118.3
38	C6	C7	C8	128.26
39	H7	C7	C8	113.39
40	C7	C8	H8	107.25
41	C7	C8	C9	111.34
42	C7	C8	C10	111.83
43	H8	C8	C9	109.12
44	H8	C8	C10	109.62
45	C9	C8	C10	107.66
46	O3	C9	C8	113.64
47	O3	C9	H91	102.5
48	O3	C9	H92	109.84
49	C8	C9	H91	109.05
50	C8	C9	H92	111.37
51	H91	C9	H92	110.08
52	C8	C10	H101	110.97
53	C8	C10	H102	110.25
54	C8	C10	H103	106.83
55	H101	C10	H102	111.51
56	H101	C10	H103	107.28
57	H102	C10	H103	109.85

All torsions

Number	Atom1	Atom2	Atom3	Atom4	Torsion
1	O2	P	O1	C3	44.46
2	O3	P	O1	C3	-67.21
3	O4	P	O1	C3	167.61
4	O1	P	O2	C5	-42.17
5	O3	P	O2	C5	65.81
6	O4	P	O2	C5	-166.77
7	O1	P	O3	C9	169.67
8	O2	P	O3	C9	58.26
9	O4	P	O3	C9	-66.53
10	P	O1	C3	C2	-175.48
11	P	O1	C3	H3	67.52

12	P	O1	C3	C4	-54.73
13	P	O2	C5	C4	50
14	P	O2	C5	H5	166.94
15	P	O2	C5	C6	-77.64
16	P	O3	C9	C8	-64.21
17	P	O3	C9	H91	178.27
18	P	O3	C9	H92	61.29
19	H11	C1	C2	H2	-172.61
20	H11	C1	C2	C3	8.32
21	H12	C1	C2	H2	2.11
22	H12	C1	C2	C3	-176.96
23	C1	C2	C3	O1	-124.52
24	C1	C2	C3	H3	-6.57
25	C1	C2	C3	C4	117.1
26	H2	C2	C3	O1	56.42
27	H2	C2	C3	H3	174.37
28	H2	C2	C3	C4	-61.96
29	O1	C3	C4	H41	-61.29
30	O1	C3	C4	H42	-178.79
31	O1	C3	C4	C5	59.49
32	C2	C3	C4	H41	56.41
33	C2	C3	C4	H42	-61.1
34	C2	C3	C4	C5	177.18
35	H3	C3	C4	H41	177.92
36	H3	C3	C4	H42	60.41
37	H3	C3	C4	C5	-61.31
38	C3	C4	C5	O2	-57.35
39	C3	C4	C5	H5	-168.13
40	C3	C4	C5	C6	70.42
41	H41	C4	C5	O2	69.61
42	H41	C4	C5	H5	-41.17
43	H41	C4	C5	C6	-162.62
44	H42	C4	C5	O2	179.91
45	H42	C4	C5	H5	69.13
46	H42	C4	C5	C6	-52.32
47	O2	C5	C6	H6	171.72
48	O2	C5	C6	C7	-12.07
49	C4	C5	C6	H6	46.16
50	C4	C5	C6	C7	-137.63
51	H5	C5	C6	H6	-76.87

52	H5	C5	C6	C7	99.34
53	C5	C6	C7	H7	-179.63
54	C5	C6	C7	C8	3.13
55	H6	C6	C7	H7	-3.58
56	H6	C6	C7	C8	179.18
57	C6	C7	C8	H8	-39.27
58	C6	C7	C8	C9	80.04
59	C6	C7	C8	C10	-159.47
60	H7	C7	C8	H8	143.38
61	H7	C7	C8	C9	-97.32
62	H7	C7	C8	C10	23.17
63	C7	C8	C9	O3	-45.22
64	C7	C8	C9	H91	68.43
65	C7	C8	C9	H92	-169.9
66	H8	C8	C9	O3	72.97
67	H8	C8	C9	H91	-173.38
68	H8	C8	C9	H92	-51.71
69	C10	C8	C9	O3	-168.14
70	C10	C8	C9	H91	-54.48
71	C10	C8	C9	H92	67.19
72	C7	C8	C10	H101	-174.67
73	C7	C8	C10	H102	61.28
74	C7	C8	C10	H103	-58.04
75	H8	C8	C10	H101	66.51
76	H8	C8	C10	H102	-57.54
77	H8	C8	C10	H103	-176.85
78	C9	C8	C10	H101	-52.06
79	C9	C8	C10	H102	-176.11
80	C9	C8	C10	H103	64.57

5.2 Supporting Information for Chapter 3

A Build-Couple-Couple-Pair (BCCP) Approach for the

Synthesis of 2-desmethyl Sanctolide A and Simplified Analogs

Table of Contents

Chapter 5, Section 2: Supporting Information for Chapter 3

A Build-Couple-Couple-Pair (BCCP) Approach for the Synthesis of 2-desmethyl Sanctolide A and Simplified Analogs

5.2.1 General Methods

General Experimental Section

All reactions were carried out in oven- or flame-dried glassware under argon atmosphere using standard gas-tight syringes, cannula, and septa. Stirring was achieved with oven-dried magnetic stir bars. Et_2O, THF and CH_2Cl_2 were purified by passage through a purification system (Pure Process Technology) employing activated Al_2O_3 (Pangborn, A. B.; Giardello, M. A.; Grubbs, R. H.; Rosen, R. K.; Timmers, F. J. Safe and Convenient Procedure for Solvent Purification *Organometallics* **1996**, *15*, 1518–1520). Et_3N was purified by passage over basic alumina and stored over KOH. Butyllithium was purchased from Aldrich and titrated prior to use. Flash column chromatography was performed with Sorbent Technologies (30930M-25, Silica Gel 60 Å, 40-63 μm) and thin layer chromatography was performed on silica gel 60F254 plates (EM-5717, Merck). ^1H, ^{13}C, and ^{31}P NMR spectra were recorded on either a Bruker DRX-400 or Bruker DRX-500 MHz spectrometers operating at 400 MHz or 500 MHz for ^1H NMR, 101 MHz or 126 MHz for ^{13}C NMR, and 202 MHz for ^{31}P NMR using $CDCl_3$, acetone-d_6 and methanol-d_4 as solvents. The ^1H NMR data are reported as the chemical shift in parts per million, multiplicity (s, singlet; d, doublet; t, triplet; q, quartet; p, pentet; m, multiplet), coupling constant in hertz, and number of protons. High-resolution mass spectrometry (HRMS) was recorded on a LCT Premier Spectrometer (Micromass UK Limited) operating on ESI (MeOH). Observed rotations at 589 nm were measured using LAXCO POL301 model automatic polarimeter. IR was recorded on Thermo Scientific Nicolet iS5 FTIR instrument.

5.2.2 Experimental Section

(4*S*,6*S*)-4,6-diallyl-2-(allyloxy)-1,3,2-dioxaphosphinane 2-oxide ($C_{12}H_{19}O_4P$, 3.6.2)

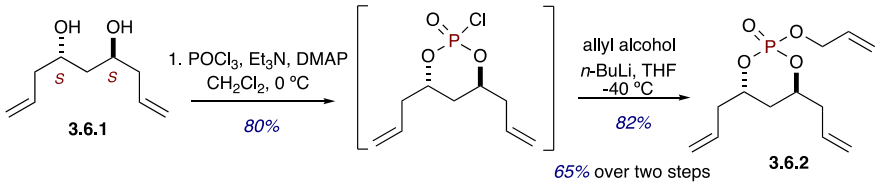

To a round-bottom flask equipped with a stir bar and an argon inlet was added the diol **3.6.1** (3.0 g, 19.2 mmol, 1.0 equiv.) in methylene chloride (100 mL, 0.2 M), Et_3N (8.3 mL, 57.6 mmol, 3 equiv.), and DMAP (470 mg, 3.8 mmol, 0.2 equiv.) and stirred for 5 minutes at 0 ºC. To the reaction mixture at the same temperature was added $POCl_3$ (1.9 mL, 21.1 mmol, 1.1 equiv.) dropwise and stirred for 30 minutes (complete by TLC). Solvent was evaporated and transferred to a short silica column to obtain the monochlorophosphate (3.59 g, 80% yield) as a yellow liquid.

Next, to a solution of allyl alcohol (1.1 mL, 15.9 mmol, 1.05 equiv.) in THF (40 mL, 0,4 M), under argon at -40 ºC, was added *n*-butyllithium (6.3 mL, 2.5 M in hexanes, 1.05 equiv.), dropwise. The reaction mixture was stirred at -30 ºC for 15 minutes, at which point a solution of the monochlorophosphate (3.59 g, 15.2 mmol) in THF (35 mL) was cannulated dropwise, to the reaction mixture. The reaction continued to stir at -30 ºC for 30 minutes (complete by TLC), and the flask was removed from the cooling bath and quenched with saturated NH_4Cl (aqueous, ~40 mL). The mixture was stirred, vigorously, as the flask warmed to room temperature, and then the biphasic solution was separated. The aqueous layer was extracted with EtOAc (3 x 50 mL), and the organic layers were combined, washed with brine, dried over Na_2SO_4, and concentrated under reduced pressure. The crude mixture was purified via flash column chromatography (silica, 0%–

60% EtOAc in hexanes) to provide triene **3.6.2** (3.24 g, 12.5 mmol, 65% yield over two steps) as a pale-yellow oil. TLC (EtOAc/hexane, 1/1): R_f = 0.4.

FTIR (neat): 3079, 2980, 2936, 1644, 1426, 1362, 1289, 1095, 1018 cm^{-1};

Optical Rotation: $[\alpha]_D^{21}$ = -48.6 (c = 2.1 , $CHCl_3$);

^{1}H NMR (500 MHz, $CDCl_3$) δ 5.95 (ddt, J = 16.5, 10.8, 5.7 Hz, 1H, (P=O)$OCH_2C\underline{H}$=CH_aH_b), 5.83–5.71 (m, 2H, CH_2=$C\underline{H}CH_aH_bCHO$(P=O)CH_aH_b, CH_aH_bCHO(P=O)$CH_aH_bC\underline{H}$=CH_2), 5.36 (d, 1H, (P=O)OCH_2CH=$C\underline{H}_aH_b$), 5.25 (d, 1H, (P=O)OCH_2CH=$CH_a\underline{H}_b$), 5.16–5.05 (m, 4H, $C\underline{H}_2$=$CHCH_aH_bCHO$(P=O)CH_aH_b, CH_aH_bCHO(P=O)CH_aH_bCH=$C\underline{H}_2$), 4.65–4.51 (m, 4H, CH_2=$CHCH_aH_bC\underline{H}O$(P=O)$CH_aH_bC\underline{H}O$(P=O), (P=O)$OC\underline{H}_2CH$=CH_aH_b), 2.66 (dt, J = 14.0, 6.8 Hz, 1H, CH_2=$CHCH_aH_bCHO$(P=O)$C\underline{H}_aH_b$), 2.55 (dt, J = 13.9, 6.6 Hz, 1H, CH_2=$CHC\underline{H}_aH_bCHO$(P=O)CH_aH_b), 2.45–2.33 (m, 2H, CH_2=$CHCH_a\underline{H}_bCHO$(P=O)$CH_a\underline{H}_b$), 2.02 (ddd, J = 14.2, 8.5, 5.1 Hz, 1H, CH_aH_bCHO(P=O)$C\underline{H}_aH_bCH$=CH_2), 1.87 (dt, J = 14.8, 4.5 Hz, 1H, CH_aH_bCHO(P=O)$CH_a\underline{H}_bCH$=CH_2);

^{13}C NMR (126 MHz, $CDCl_3$) δ 132.8 (d, J_{CP}= 7.2 Hz, $\underline{C}H$=CH_2), 132.7 ($\underline{C}H$=CH_2), 132.3 ($\underline{C}H$=CH_2), 119.1 (CH=$\underline{C}H_2$), 118.9 (CH=$\underline{C}H_2$), 118.4 (CH=$\underline{C}H_2$), 77.5 (d, J_{CP}= 6.9 Hz, $\underline{C}H$), 75.7 (d, J_{CP}= 6.5 Hz, $\underline{C}H$), 68.2 (d, J_{CP}= 5.4 Hz, $\underline{C}H_2$), 40.1 (d, J_{CP}= 7.8 Hz, $\underline{C}H_2$), 38.9 (d, J_{CP}= 3.3 Hz, $\underline{C}H_2$), 33.2 (d, J_{CP} = 7.1 Hz, $\underline{C}H_2$);

^{31}P NMR (202 MHz, $CDCl_3$): δ -6.88

HRMS (ESI-TOF) m/z: $[M + H]^+$ Calcd for $C_{11}H_{18}O_4P$ 245.0943; Found 245.0950.

(5*S*,7*S*)-dodecane-1,5,7-triol ($C_{12}H_{26}O_3$, 3.7.3)

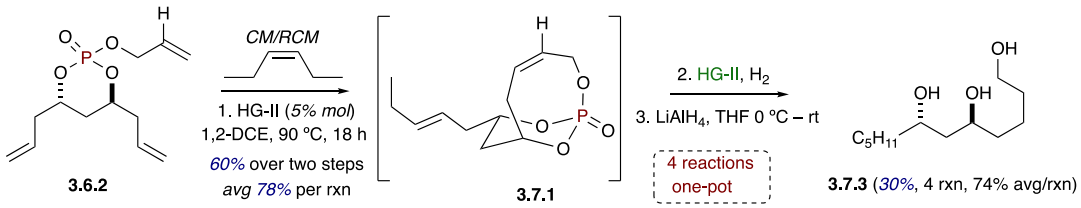

To a round-bottom flask, equipped with a stir bar, reflux condenser, and argon inlet, was added triene **3.6.2** (1.0 g, 3.8 mmol), degassed 1,2-dichloroethane (1,2-DCE) (40 mL, 0.1 M), Hoveyda-Grubbs second-generation catalyst (HG-II, 30.0 mg, 5 mol%), and *cis*-3-hexene (1.8 mL, 14.5 mmol, 2.5 equiv.). The reaction mixture was stirred at room temperature for 2 hours to ensure complete conversion of reactive starting material. Then, was added freshly degassed 1,2-DCE (760 mL, 0.005 M overall) and the temperature was elevated to 90 ºC and stirred for 18 hours (complete by TLC). The solvent was evaporated under vacuo and to the same reaction flask was added freshly degassed 1,2-DCE (20 mL, 0.2 M), and Hoveyda-Grubbs second-generation catalyst (HG-II, 4.2 mg, 0.5 mol%) and cannulated into a Parr hydrogenation reaction vessel under Ar. The vessel was heated to 80 ºC, and H_2 pressure was applied (1000 psi). The reaction stirred at 80 ºC, under H_2 pressure, for 16 h (complete by TLC), at which point the reaction was cooled to room temperature and solvent removed under reduced pressure. The crude oil was dried under high vacuum (~12 h) to ensure complete removal of 1,2-DCE. The crude mix was taken up in THF (38 mL, 0.1 M) and cooled to 0 ºC under argon. Lithium aluminum hydride (1 M in THF, 15.5 mL, 4 equiv.) was added slowly, and the reaction flask was removed from the cooling bath and allowed to warm to room temperature. The mixture stirred at room temperature for 4 hours (complete by TLC), and the reaction was cooled to 0 ºC and quenched with 10% sodium potassium tartrate aqueous solution. The reaction was allowed

to warm to room temperature and stir at room temperature 2 h. The crude mixture was filtered over celite (washed with EtOAc) and concentrated under reduced pressure. Purification via flash column chromatography (silica, 0%–100% EtOAc in hexanes) provided **3.7.3** (274.8 mg, 2.4 mmol, 30% yield over 4 reactions in one pot, 74% average per reaction) as a colorless oil. TLC (EtOAc): R_f = 0.3.

FTIR (neat): 3299, 2954, 2931, 2856, 1467, 1153, 1102, 1050 cm^{-1};

Optical Rotation: $[\alpha]_D^{21}$ = -2.5 (c = 0.24 , $CHCl_3$);

^{1}H NMR (500 MHz, $CDCl_3$) δ 3.94 (dt, J = 8.8, 3.7 Hz, 2H, $CH_3(CH_2)_4C\underline{H}(OH)CH_2C\underline{H}(OH)CH_2$), 3.66 (t, J = 6.24 Hz, 2H, $CH(OH)CH_2CH_2CH_2C\underline{H}_2OH$), 2.95–2.72 (m, 1H, R-OH), 2.63–2.39 (m, 1H, R-OH), 1.88–1.69 (m, 1H, R-OH), 1.64–1.55 (m, 4H, $CH(OH)CH_aH_bC\underline{H}_2C\underline{H}_2CH_2OH$), 1.55–1.49 (m, 3H, $CH_aH_bCH(OH)C\underline{H}_a\underline{H}_bCH(OH)C\underline{H}_aH_b$), 1.49–1.36 (m, 4H, $C\underline{H}_2C\underline{H}_aH_bCH(OH)CH_aH_bCH(OH)CH_a\underline{H}_b$), 1.34–1.24 (m, 5H, $CH_3C\underline{H}_2C\underline{H}_2CH_2CH_a\underline{H}_b$), 0.89 (t, J = 6.6 Hz, 3H, $C\underline{H}_3(CH_2)_4CH(OH)CH_2$);

^{13}C NMR (126 MHz, $CDCl_3$) δ 69.6 ($\underline{C}H$), 69.3 ($\underline{C}H$), 62.8 ($\underline{C}H_2$), 42.6 ($\underline{C}H_2$), 37.6 ($\underline{C}H_2$), 37.2 ($\underline{C}H_2$), 32.6 ($\underline{C}H_2$), 32.0 ($\underline{C}H_2$), 25.6 ($\underline{C}H_2$), 22.8 ($\underline{C}H_2$), 22.1 ($\underline{C}H_2$), 14.2 ($\underline{C}H_3$);

HRMS (ESI-TOF) m/z: $[M + Na]^+$ Calcd for $C_{12}H_{26}O_3Na$ 241.1780; Found 241.1770.

(5*S*,7*S*)-10-phenyldecane-1,5,7-triol ($C_{16}H_{26}O_3$, 3.7.4)

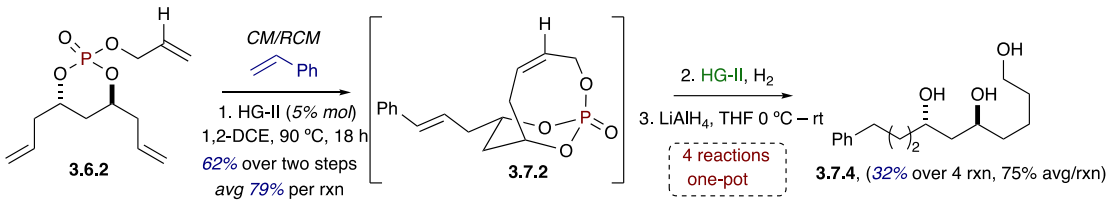

To a round-bottom flask, equipped with a stir bar, reflux condenser, and argon inlet, was added triene **3.6.2** (1.0 g, 3.8 mmol), degassed 1,2-DCE (40 mL, 0.1 M), Hoveyda-Grubbs second-generation catalyst (HG-II, 30.0 mg, 5 mol%), and styrene (1.1 mL, 9.6 mmol, 2.5 equiv.). The reaction mixture was stirred at room temperature for 2 hours to ensure complete conversion of reactive starting material. Then, was added freshly degassed 1,2-DCE (760 mL, 0.005 M overall) and the temperature was elevated to 90 ºC and stirred for 18 hours (complete by TLC). The solvent was evaporated under vacuo, and to the same reaction flask was added freshly degassed 1,2-DCE (20 mL, 0.2 M)), and Hoveyda-Grubbs second-generation catalyst (HG-II, 4.2 mg, 0.5 mol%) and cannulated into a Parr hydrogenation reaction vessel under Ar. The vessel was heated to 80 ºC, and H_2 pressure was applied (1000 psi). The reaction stirred at 80 ºC, under H_2 pressure, for 16 h (complete by TLC), at which point the reaction was cooled to room temperature and solvent removed under reduced pressure. The crude oil was dried under high vacuum (~12 h) to ensure complete removal of 1,2-DCE. The crude mix was dissolved in THF (38 mL, 0.1 M) and cooled to 0 ºC under argon. Lithium aluminum hydride (1 M in THF, 15.5 mL, 4 equiv.) was added slowly, and the reaction flask was removed from the cooling bath and allowed to warm to room temperature. The mixture stirred at room temperature for 4 hours (complete by TLC), and the reaction was cooled to 0 ºC and quenched with 10% sodium potassium tartrate aqueous solution. The reaction was allowed to warm to room

temperature and stir 2 h. The crude mixture was filtered over Celite (washed with EtOAc) and concentrated under reduced pressure. Purification via flash column chromatography (silica, 0%–100% EtOAc in hexanes) provided **3.7.4** (351 mg, 2.4 mmol, 32% yield over 4 reactions in one-pot, 75% average per reaction) as a colorless oil. TLC (EtOAc): $R_f = 0.25$.

FTIR (neat): 3341, 2935, 2859, 1602, 1495, 1453, 1057, cm^{-1};

Optical Rotation: $[\alpha]_D^{21}$ = -3.3 (c = 0.18 , $CHCl_3$);

^{1}H NMR (500 MHz, $CDCl_3$) δ 7.32–7.17 (m, 5H, $C_6\underline{H}_5(CH_2)_3C\underline{H}(OH)CH_2C\underline{H}(OH)CH_2$), 3.99–3.88 (m, 2H, $C_6H_5(CH_2)_3C\underline{H}(OH)CH_2C\underline{H}(OH)CH_2$), 3.65 (td, J = 6.3, 2.5 Hz, 2H, $CH(OH)CH_2CH_2CH_2C\underline{H}_2OH$), 2.64 (td, J = 7.5, 2.3 Hz, 2H, $C_6H_5C\underline{H}_2CH_aH_bCH_aH_bCH(OH)$), 2.31–2.11 (m, 3H, 3 X R-OH), 1.82–1.72 (m, 1H, $C_6H_5CH_2C\underline{H}_aH_bCH_aH_bCH(OH)$), 1.70–1.66 (m, 1H, $C_6H_5CH_2CH_a\underline{H}_bCH_aH_bCH(OH)$), 1.65–1.40 (m, 10H, $CH_aH_bCH(OH)C\underline{H}_a\underline{H}_bCH(OH)C\underline{H}_a\underline{H}_b$, $CH(OH)C\underline{H}_a\underline{H}_bC\underline{H}_2C\underline{H}_2CH_2OH$);

^{13}C NMR (126 MHz, $CDCl_3$) δ 142.4 (C_{Ar}), 128.5 (2, CH_{Ar}), 128.5 (2, CH_{Ar}), 125.9 (CH_{Ar}), 69.4 ($\underline{C}H$), 69.3 ($\underline{C}H$), 62.8 ($\underline{C}H_2$), 42.6 ($\underline{C}H_2$), 37.1 (2, $\underline{C}H_2$), 36.0 ($\underline{C}H_2$), 32.5 ($\underline{C}H_2$), 27.7 ($\underline{C}H_2$), 22.1 ($\underline{C}H_2$);

HRMS (ESI-TOF) m/z: $[M + Na]^+$ Calcd for $C_{16}H_{26}O_3Na$ 289.1780; Found 289.1768.

(*S*)-6-((*S*)-2-hydroxyheptyl)tetrahydro-2*H*-pyran-2-one ($C_{12}H_{22}O_3$, 3.7.5)

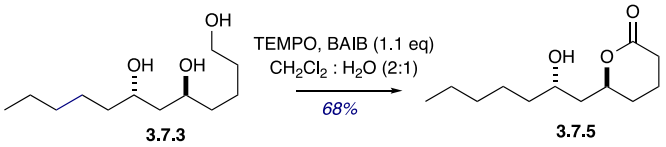

3.7.3 3.7.5

To solution of triol **3.7.3** (100 mg, 0.46 mmol, 1 equiv.) in methylene chloride and water (2:1, 5 mL) was added (diacetoxyiodo)benzene (163 mg, 0.42 mmol, 1.1 equiv.), TEMPO (7.2 mg, 0.046 mmol, 0.1 equiv.), and stirred for 2 hours (complete by TLC). Reaction was quenched with saturated sodium bicarbonate solution (2 mL) and extracted to methylene chloride (3 X 5 mL). Organic layers were combined, washed with brine, dried over Na_2SO_4, and concentrated under reduced pressure. The crude mixture was purified via flash column chromatography (silica, 0%–60% EtOAc in hexanes) to provide lactone **3.7.5** (67 mg, 0.27 mmol, 68% yield) as a colorless oil. TLC (EtOAc/hexane, 1/1): $R_f = 0.3$.

FTIR (neat): 3517, 2957, 2931, 2860, 1732, 1466, 1182, 1100 cm^{-1};

Optical Rotation: $[\alpha]_D^{21}$ = -11.1 (c = 0.27 , $CHCl_3$);

^{1}H NMR (500 MHz, $CDCl_3$) δ 4.60 (ddt, J = 11.0, 10.0, 2.5 Hz, 1H, $CH_3(CH_2)_4CH(OH)CH_aH_bC\underline{H}(OC{=}O)CH_aH_b$), 4.01–3.93 (m, 1H, $CH_3(CH_2)_4C\underline{H}(OH)CH_aH_bCH(OC{=}O)CH_aH_b$), 2.63–2.56 (m, 1H, $CH(OC{=}O)CH_aH_bCH_aH_bC\underline{H}_aH_b$), 2.49–2.41 (m, 1H, $CH(OC{=}O)CH_aH_bCH_aH_bCH_a\underline{H}_b$), 1.95–1.85 (m, 2H, $CH(OC{=}O)C\underline{H}_aH_bC\underline{H}_aH_bCH_aH_b$), 1.77 (ddd, J = 14.5, 9.8, 2.3 Hz, 1H, $CH_3(CH_2)_4CH(OH)C\underline{H}_aH_bCH(OC{=}O)$), 1.68–1.64 (m, 1H, $CH_3(CH_2)_4CH(O\underline{H})CH_aH_bCH(OC{=}O)$), 1.62–1.53 (m, 3H, $CH_a\underline{H}_bCH(OC{=}O)CH_a\underline{H}_bCH_a\underline{H}_bCH_aH_b$), 1.49–1.35 (m, 3H,

$CH_3(CH_2)_2C\underline{H}_a\underline{H}_bC\underline{H}_aH_bCH(OH)$), 1.35–1.25 (m, 5H, $CH_3(C\underline{H}_2)_2CH_aH_bCH_a\underline{H}_bCH(OH)$), 0.89 (t, J = 6.7 Hz, 3H, $C\underline{H}_3(CH_2)_3CH_aH_bCH(OH)$);

^{13}C NMR (126 MHz, $CDCl_3$) δ 172.0 ($\underline{C}$=O), 77.5 ($\underline{C}$H), 67.6 ($\underline{C}$H), 43.4 ($\underline{C}H_2$), 38.2 ($\underline{C}H_2$), 31.9 ($\underline{C}H_2$), 29.6 ($\underline{C}H_2$), 28.6 ($\underline{C}H_2$), 25.3 ($\underline{C}H_2$) 22.8 ($\underline{C}H_2$), 18.7 ($\underline{C}H_2$), 14.2 ($\underline{C}H_3$);

HRMS (ESI-TOF) m/z: $[M - H]^+$ Calcd for $C_{12}H_{21}O_3$ 213.1491; Found 213.1451.

(*S*)-6-((*S*)-2-hydroxy-5-phenylpentyl)tetrahydro-2*H*-pyran-2-one ($C_{16}H_{22}O_3$, 3.7.6)

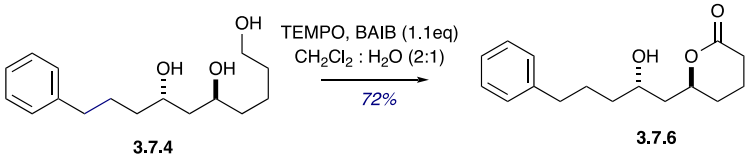

3.7.4 3.7.6

To solution of triol **3.7.4** (100 mg, 0.38 mmol, 1 equiv.) in CH_2Cl_2 and water (2:1, 4 mL) was added (diacetoxyiodo)benzene (134.5 mg, 0.42 mmol, 1.1 equiv.), TEMPO (6 mg, 0.038 mmol, 0.1 equiv.), and stirred for 2 hours (complete by TLC). Reaction was quenched with saturated $NaHCO_3$ solution (2 mL) and extracted to methylene chloride (3 X 5 mL). Organic layers were combined, washed with brine, dried over Na_2SO_4, and concentrated under reduced pressure. The crude mixture was purified via flash column chromatography (silica, 0%–60% EtOAc in hexanes) to provide lactone **3.7.6** (71.78 mg, 0.27 mmol, 72% yield) as a colorless oil. TLC (EtOAc/hexane, 1/1): R_f = 0.25.

FTIR (neat): 3383, 2924, 2853, 1737, 1588, 1093 cm^{-1};

Optical Rotation: $[a]_D^{21}$ = -6.6 (c = 0.15 , $CHCl_3$);

^{1}H NMR (500 MHz, $CDCl_3$) δ 7.29–7.14 (m, 5H, $C_6\underline{H}_5CH_2CH_2CH_aH_bCH(OH)$), 4.59 (tt, J = 10.7, 2.6 Hz, 1H, $C_6H_5(CH_2)_3CH(OH)CH_aH_bC\underline{H}(OC{=}O)CH_aH_b$), 4.01 (tdd, J = 10.0, 6.1, 2.3 Hz, 1H, $C_6H_5(CH_2)_3C\underline{H}(OH)CH_aH_bCH(OC{=}O)CH_aH_b$), 2.64 (t, J = 7.6 Hz, 2H, $C_6H_5C\underline{H}_2CH_2CH_aH_bCH(OH)$), 2.61–2.56 (m, 1H, $CH(OC{=}O)CH_aH_bCH_aH_bC\underline{H}_aH_b$), 2.49–2.41 (m, 1H, $CH(OC{=}O)CH_aH_bCH_aH_bCH_a\underline{H}_b$), 1.95–1.82 (m, 3H, $CH(OC{=}O)C\underline{H}_aH_bC\underline{H}_a\underline{H}_bCH_aH_b$), 1.81–1.72 (m, 2H, $C_6H_5CH_2CH_2C\underline{H}_aH_b(OH)C\underline{H}_aH_bCH(OC{=}O)$), 1.71–1.61 (m, 2H, $C_6H_5CH_2CH_2CH_a\underline{H}_b(OH)CH_a\underline{H}_bCH(OC{=}O)$), 1.55–1.44 (m, 3H, $C_6H_5CH_2C\underline{H}_2CH_aH_b(OH)$, $CH(OC{=}O)CH_a\underline{H}_bCH_aH_bCH_aH_b$)

^{13}C NMR (126 MHz, $CDCl_3$) δ 172.0 (<u>C</u>=O), 142.3 (C_{Ar}), 128.5 (2, CH_{Ar}), 128.5 (2, CH_{Ar}), 126.0 (CH_{Ar}), 77.3 (<u>C</u>H), 67.5 (<u>C</u>H), 43.4 (<u>C</u>H_2), 37.7 (<u>C</u>H_2), 35.9 (<u>C</u>H_2), 29.5 (<u>C</u>H_2), 28.5 (<u>C</u>H_2), 27.4 (<u>C</u>H_2), 18.7 (<u>C</u>H_2);

HRMS (ESI-TOF) m/z: $[M + Na]^+$ Calcd for $C_{16}H_{22}O_3Na$ 285.1467; Found 285.1475.

(*S*)-6-((*S*)-2-methoxyheptyl)tetrahydro-2*H*-pyran-2-one ($C_{13}H_{24}O_3$, 3.7.7)

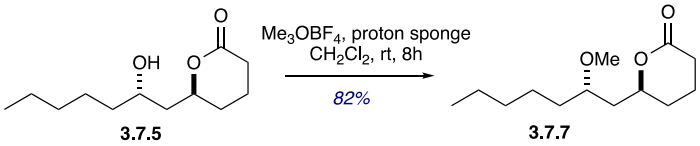

3.7.5 3.7.7

To a round-bottom flask, equipped with a magnetic stir bar, was added lactone **3.7.5** (75 mg, 0.35 mmol) in CH_2Cl_2 (4 mL, 0.1 M), proton sponge (750 mg, 3.5 mmol, 10 equiv.), and trimethyloxonium tetrafluoroborate (517.6 mg, 3.5 mmol, 10 equiv.) and stirred the mixture for 6 h (complete by TLC). The solution was diluted with CH_2Cl_2 (6 mL), was added saturated $NaHCO_3$ (0.5 mL), and the layers separated. The aqueous layer was extracted with CH_2Cl_2 (3 x 3 mL), and the organic layers were combined, dried over Na_2SO_4, filtered, and concentrated under reduced pressure. Purification via flash column chromatography (silica, 0%–50% EtOAc in hexanes) provided lactone methyl ether (**3.7.7**) (66.3 mg, 0.29 mmol, 83% yield) as a colorless oil. TLC (EtOAc/hexane, 1/1): R_f = 0.7.

FTIR (neat): 2928, 2856, 1734, 1461, 1156, 1092 cm^{-1};

Optical Rotation: $[a]_D^{21}$ = +6.1 (c = 0.10 , $CHCl_3$);

^{1}H NMR (500 MHz, $CDCl_3$) δ 4.52 (ddt, J = 10.3, 9.8, 2.5 Hz, 1H, $CH_3(CH_2)_4CH(OMe)CH_aH_bC\underline{H}(OC{=}O)CH_aH_b$), 3.57–3.47 (m, 1H, $CH_3(CH_2)_4C\underline{H}(OMe)CH_aH_bCH(OC{=}O)CH_aH_b$), 3.36 (s, 3H, $CH_3(CH_2)_4CH(O\underline{Me})CH_aH_bCH(OC{=}O)CH_aH_b$), 2.64–2.56 (m, 1H, $CH(OC{=}O)CH_aH_bCH_aH_bC\underline{H}_aH_b$), 2.50–2.39 (m, 1H, $CH(OC{=}O)CH_aH_bCH_aH_bCH_a\underline{H}_b$), 1.93–1.85 (m, 3H, $CH(OC{=}O)C\underline{H}_aH_bC\underline{H}_a\underline{H}_bCH_aH_b$), 1.76–1.70 (m, 1H, $CH_3(CH_2)_4CH(OMe)C\underline{H}_aH_bCH(OC{=}O)$), 1.65–1.57 (m, 1H, $CH_3(CH_2)_4CH(OMe)CH_a\underline{H}_bCH(OC{=}O)$), 1.56–1.48 (m, 2H, $CH(OC{=}O)CH_a\underline{H}_bCH_aH_bCH_aH_b$, $CH_3(CH_2)_3C\underline{H}_aH_bCH(OMe)$), 1.45–1.39 (m, 1H,

$CH_3(CH_2)_3CH_a\underline{H}_bCH(OMe)$), 1.33–1.26 (m, 6H, $CH_3(C\underline{H}_2)_3CH_aH_bCH(OMe)$), 0.88 (t, *J* = 6.6 Hz, 3H, $C\underline{H}_3(CH_2)_3CH_aH_bCH(OMe)$);

^{13}C NMR (126 MHz, $CDCl_3$) δ 172.3 (<u>C</u>=O), 77.4 (<u>C</u>H), 76.4 (<u>C</u>H), 57.3(<u>C</u>H_3), 41.6 (<u>C</u>H_2), 33.5 (<u>C</u>H_2), 32.2 (<u>C</u>H_2), 29.6 (<u>C</u>H_2), 28.6 (<u>C</u>H_2), 24.4 (<u>C</u>H_2) 22.8 (<u>C</u>H_2), 18.7 (<u>C</u>H_2), 14.2 (<u>C</u>H_3);

HRMS (ESI-TOF) m/z: $[M + Na]^+$ Calcd for $C_{13}H_{24}O_3Na$ 251.1623; Found 251.1627.

(*S*)-6-((*S*)-2-methoxy-5-phenylpentyl)tetrahydro-2*H*-pyran-2-one ($C_{17}H_{24}O_3$, 3.7.8)

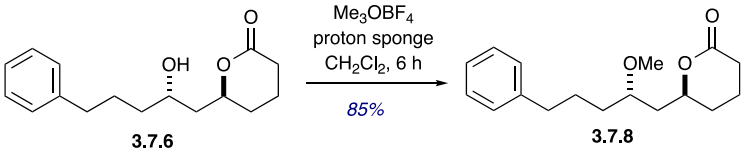

To a round-bottom flask, equipped with a magnetic stir bar, was added lactone **3.7.6** (75 mg, 0.28 mmol) in CH_2Cl_2 (3 mL, 0.1 M), proton sponge (600 mg, 2.8 mmol, 10 equiv.), and trimethyloxonium tetrafluoroborate (414 mg, 2.8 mmol, 10 equiv.) and stirred for 6 h (complete by TLC). The solution was diluted with CH_2Cl_2 (7 mL), was added saturated $NaHCO_3$ (0.5 mL), and the layers separated. The aqueous layer was extracted with CH_2Cl_2 (3 x 3 mL), and the organic layers were combined, dried over Na_2SO_4, filtered, and concentrated under reduced pressure. Purification via flash column chromatography (silica, 0%–50% EtOAc in hexanes) provided lactone methyl ether **3.7.8** (65.7 mg, 0.23 mmol, 85% yield) as a colorless oil. TLC (EtOAc/hexane, 1/1): R_f = 0.6.

FTIR (neat): 2925, 2851, 1732, 1602, 1453, 1158, 1092, 1040 cm^{-1};

Optical Rotation: $[a]_D^{21}$ = +6.6 (c = 0.15 , $CHCl_3$);

^{1}H NMR (500 MHz, $CDCl_3$) δ 7.31–7.14 (m, 5H, $C_6\underline{H}_5CH_2CH_2CH_aH_bCH(OMe)$), 4.50 (ddt, J = 12.0, 9.9. 3.0 Hz, 1H, $C_6H_5(CH_2)_3CH(OMe)CH_aH_bC\underline{H}(OC{=}O)CH_aH_b$), 3.55 (ddt, J = 10.6, 5.3, 2.7 Hz, 1H, $C_6H_5(CH_2)_3C\underline{H}(OMe)CH_aH_bCH(OC{=}O)CH_aH_b$), 3.34 (s, 3H, $C_6H_5CH_2CH_2CH_aH_bCH(O\underline{Me})$), 2.64 (td, J = 7.3, 2.5 Hz, 2H, $C_6H_5C\underline{H}_2CH_2CH_aH_bCH(OMe)$), 2.60–2.56 (m, 1H, $CH(OC{=}O)CH_aH_bCH_aH_bC\underline{H}_aH_b(C{=}O)$), 2.44 (dt, J = 17.6, 7.6 Hz, 1H, $CH(OC{=}O)CH_aH_bCH_aH_bCH_a\underline{H}_b(C{=}O)$), 1.82–1.74 (m, 3H, $CH(OC{=}O)C\underline{H}_aH_bC\underline{H}_a\underline{H}_bCH_aH_b(C{=}O)$), 1.81–1.60 (m, 4H,

$C_6H_5CH_2CH_2C\underline{H_a}\underline{H_b}CH(OMe)C\underline{H_a}\underline{H_b}CH(OC=O))$, 1.59–1.47 (m, 3H, $C_6H_5CH_2C\underline{H_2}CH_aH_bCH(OH)$, $CH(OC=O)CH_a\underline{H_b}CH_aH_bCH_aH_b(C=O))$;

^{13}C NMR (126 MHz, $CDCl_3$) δ 172.1 ($\underline{C}$=O), 142.4 (C_{Ar}), 128.5 (2, CH_{Ar}), 128.5 (2, CH_{Ar}), 126.0 (CH_{Ar}), 77.4 ($\underline{C}H$), 76.3 (CH_3), 57.4 ($\underline{C}H$), 41.6 ($\underline{C}H_2$), 36.2 ($\underline{C}H_2$), 33.2 ($\underline{C}H_2$), 29.6 ($\underline{C}H_2$), 28.6 ($\underline{C}H_2$), 26.5 ($\underline{C}H_2$), 18.7 ($\underline{C}H_2$);

HRMS (ESI-TOF) m/z: $[M + Na]^+$ Calcd for $C_{17}H_{24}O_3Na$ 299.1623; Found 299.1612.

(5*S*,7*S*)-*N*-allyl-5-hydroxy-7-methoxy-*N*-methyldodecanamide ($C_{17}H_{33}NO_3$, 3.8.1)

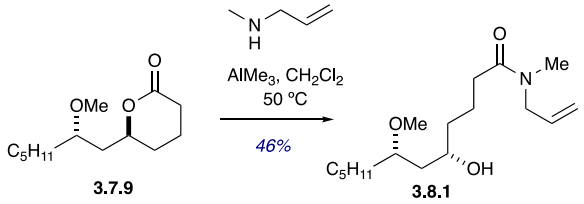

To a solution of *N*-allylmethylamine (42 µL, 0.44 mmol, 2 equiv.) in CH_2Cl_2 (1 mL), was added trimethylaluminum (2 M in toluene, 0.19 mL, 1.75 equiv.) at room temperature and stirred for 30 mins. Then the mixture was cannulated under argon to a solution of lactone methyl ether **3.7.9** (52 mg, 0.22 mmol, 1 equiv.) in CH_2Cl_2 (0.2 mL) in a pressure vial and stirred at 50 ºC for 18 hours (TLC monitoring). Then the reaction mixture was cooled to room temperature and an additional 1.75 equivalents of *N*-allylmethylamine aluminum complex was added and continued stirring for 12 more hours at 50 ºC (complete by TLC). The reaction mixture was diluted with CH_2Cl_2 (2 mL) and quenched carefully with 1 M HCl solution (1 mL) at 0 ºC. The aqueous layer was extracted with CH_2Cl_2 (3 x 2 mL), and the organic layers were combined, dried over Na_2SO_4, filtered, and concentrated under reduced pressure. Purification via flash column chromatography (silica, 0%–100% EtOAc in hexanes) amide **3.8.1** (30 mg, 0.10 mmol, 46% yield, 1:1 rotamers) as a colorless oil. TLC (EtOAc/hexane, 2/3): R_f = 0.4.

FTIR (neat): 3430, 3082, 2930, 2858, 1632, 1461, 1404, 1092, 990 cm^{-1},

Optical Rotation: $[\alpha]_D^{22}$ = +22 (*c* = 0.17 , $CHCl_3$);

^{1}H NMR (500 MHz, $CDCl_3$) δ 5.75 (ddt, *J* = 18.8, 9.5, 5.1 Hz, 1H, C(O)N(Me)CH_2C<u>H</u>=CH_2), 5.31–5.09 (m, 2H, C(O)N(Me)CH_2CH=C<u>H_2</u>), 4.05–3.93 (m, 2H, C(O)N(Me)C<u>H_2</u>CH=CH_2)$_{Major}$, 3.93–3.87 (m, 2H, C(O)N(Me)C<u>H_2</u>*CH=CH_2)$_{Minor}$, 3.88–3.79 (m, 1H, $CH_3(CH_2)_4$CH(OMe)CH_aH_bC<u>H</u>(OH)CH_aH_b), 3.47 (dddd, *J* = 6.7, 3.3

Hz, 1H, $CH_3(CH_2)_4C\underline{H}(OMe)CH_aH_bCH(OH)CH_aH_b$), 3.36 (s, 3H, $CH_3(CH_2)_4CH(O\underline{Me})CH_aH_bCH(OH))_{Major}$, 3.35 (s, 3H, $CH_3(CH_2)_4CH(O\underline{Me}^*)CH_aH_bCH(OH))_{Minor,}$ 2.94 (d, J = 3.0 Hz, 3H, $C(O)N(\underline{Me})CH_2CH=CH_2)_{Major}$, 2.92 (d, J = 3.0 Hz, 3H, $C(O)N(\underline{Me}^*)CH_2CH=CH_2)_{Minor}$, 2.38 (dd, J = 8.0, 3.1 Hz, 2H, CH(OH) $CH_2CH_2C\underline{H}_2C(O)N(Me)CH_2)_{Major}$, 2.34 (dd, J = 8.0, 3.1 Hz, 2H, CH(OH) $CH_2CH_2C\underline{H}_2^*C(O)N(Me)CH_2)_{Minor,}$ 1.83–1.70 (m, 2H, $CH(OH)CH_2C\underline{H}_2CH_2C(O)N(Me)CH_2$, $CH(OH)C\underline{H}_2^*CH_2CH_2C(O)N(Me)CH_2$), 1.69–1.60 (m, 2H, $CH_3(CH_2)_3C\underline{H}_aH_bCH(OMe)C\underline{H}_aH_bCH(OH)$), 1.56–1.41 (m, 4H, $CH_3(CH_2)_3CH_a\underline{H}_bCH(OMe)CH_a\underline{H}_bCH(OH)$, $CH(OH)C\underline{H}_2CH_2CH_2C(O)N(Me)CH_2$, $CH(OH)CH_2C\underline{H}_2^*CH_2C(O)N(Me)CH_2$), 1.32–1.23 (m, 6H, $CH_3(C\underline{H}_2)_3CH_aH_bCH(OMe)$), 0.88 (td, J = 6.9, 3.1 Hz, 3H, $C\underline{H}_3(CH_2)_3CH_aH_bCH(OMe)$);

^{13}C NMR (126 MHz, $CDCl_3$) δ 173.5 (amide $\underline{C}$=O), 173.1 (amide $\underline{C}$=O)*, 133.2 ($\underline{C}H=CH_2$), 132.6 ($\underline{C}H=CH_2$)*, 117.2 ($CH=\underline{C}H_2$), 116.7 ($CH=\underline{C}H_2$)*, 79.5 ($\underline{C}H$), 79.4 ($\underline{C}H$)*, 68.1 ($\underline{C}H$), 68.0 ($\underline{C}H$)*, 57.0 ($\underline{C}H_3$), 57.0 ($\underline{C}H_3$)*, 52.3 ($\underline{C}H_2$), 50.2 ($\underline{C}H_2$)*, 39.6 ($\underline{C}H_2$), 39.5 ($\underline{C}H_2$)*, 37.6 ($\underline{C}H_2$), 37.5 ($\underline{C}H_2$)*, 34.9 (N-$\underline{C}H_3$), 33.8 (N-$\underline{C}H_3$)*, 33.3 ($\underline{C}H_2$), 32.6 ($\underline{C}H_2$)*, 33.1 ($\underline{C}H_2$), 32.1 ($\underline{C}H_2$), 25.2 ($\underline{C}H_2$), 22.8 ($\underline{C}H_2$), 21.1 ($\underline{C}H_2$), 20.8 ($\underline{C}H_2$)*, 14.2 ($\underline{C}H_3$);

* rotamer

HRMS (ESI-TOF) m/z: $[M + Na]^+$ Calcd for $C_{17}H_{33}NO_3Na$ 322.2358; Found 322.2335.

(5*S*,7*S*)-*N*-allyl-5-hydroxy-7-methoxy-*N*-(4-(trifluoromethyl)benzyl)dodecanamide $C_{24}H_{36}F_3NO_3$, 3.8.7)

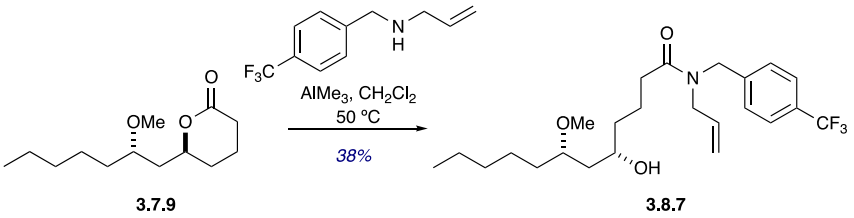

3.7.9 3.8.7

To a solution of *N*-(4-(trifluoromethyl)benzyl)prop-2-en-1-amine (56.0 mg, 0.26 mmol, 2 equiv.) in CH_2Cl_2 (1.3 mL), was added trimethylaluminum (2 M in toluene, 0.110 mL, 1.75 equiv.) at room temperature and stirred for 30 minutes. Then the mixture was cannulated under argon to a solution of lactone methyl ether **3.7.9** (30 mg, 0.13 mmol, 1 equiv.) in CH_2Cl_2 (0.2 mL) in a pressure vial and stirred at 50 ºC for 18 hours (TLC monitoring). Then the reaction mixture was cooled to room temperature and an additional 1.75 equivalents of amine-aluminum complex was added and continued stirring for 12 more hours at 50 ºC (complete by TLC). Reaction mixture was diluted with CH_2Cl_2 (1 mL) and quenched carefully with 1 M HCl solution (1 mL) at 0 ºC. The aqueous layer was extracted with CH_2Cl_2 (3 x 1.5 mL), and the organic layers were combined, dried over Na_2SO_4, filtered, and concentrated under reduced pressure. Purification via flash column chromatography (silica, 0%–80% EtOAc in hexanes) amide **3.8.7** (22.0 mg, 0.021 mmol, 38% yield, 2: 1 rotamers) as a colorless liquid. TLC (EtOAc/hexane, 2/3): $R_f = 0.6$.

FTIR (neat): 3437, 3071,2929, 2854, 1644, 1461, 1415, 1324 (CF_3), 1124 (CF_3), 1067, 990 cm^{-1};

Optical Rotation: $[a]_D^{22} = +11.3$ ($c = 0.16$, $CHCl_3$);

^{1}H NMR (500 MHz, $CDCl_3$) δ 7.62 (d, $J = 8.0$ Hz, 2H, $C(O)N(CH_2C_6\underline{H}_{2a}{*}H_{2b}CF_3)CH_2CH{=}CH_2)_{Minor}$, 7.56 (d, $J = 8.0$ Hz, 2H, $C(O)N(CH_2C_6\underline{H}_{2a}H_{2b}CF_3)CH_2CH{=}CH_2)_{Major}$, 7.34 (d, $J = 8.0$ Hz, 2H,

C(O)N(CH$_2$C$_6$H$_{2a}$H$_{2b}$CF$_3$)CH$_2$CH=CH$_2$)$_{Major}$, 7.29 (d, *J* = 8.3 Hz, 2H, C(O)N(CH$_2$C$_6$H$_{2a}$H$_{2b}$*CF$_3$)CH$_2$CH=CH$_2$)$_{Minor}$; 5.74 (ddt, *J* = 16.1, 10.2, 4.5 Hz, 1H, C(O)N(CH$_2$C$_6$H$_{2a}$H$_{2b}$CF$_3$)CH$_2$CH=CH$_2$), 5.29–5.05 (m, 2H, C(O)N(CH$_2$C$_6$H$_{2a}$H$_{2b}$CF$_3$)CH$_2$CH=CH$_2$), 4.63 (s, 2H, C(O)N(CH$_2$C$_6$H$_{2a}$H$_{2b}$CF$_3$)CH$_2$CH=CH$_2$)$_{Major}$, 4.57 (s, 2H, C(O)N(CH$_2$C$_6$H$_{2a}$H$_{2b}$CF$_3$)CH$_2$*CH=CH$_2$)$_{Minor}$, 4.02 (d, *J* = 6.01 Hz, 2H, C(O)N(CH$_2$C$_6$H$_{2a}$H$_{2b}$CF$_3$)CH$_2$*CH=CH$_2$)$_{Minor}$, 3.91–3.86 (m, 1H, CH(OMe)CH$_a$H$_b$CH(OH)CH$_a$H$_b$), 3.85 (d, *J* = 5.3 Hz, 2H, C(O)N(CH$_2$C$_6$H$_{2a}$H$_{2b}$CF$_3$)CH$_2$CH=CH$_2$), 3.51–3.42 (m, 1H, CH(OMe)CH$_a$H$_b$CH(OH)CH$_a$H$_b$), 3.36 (s, 3H, CH(OMe)CH$_a$H$_b$CH(OH)CH$_a$H$_b$)$_{Major}$, 3.35 (s, 3H, CH(OMe*)CH$_a$H$_b$CH(OH)CH$_a$H$_b$)$_{Minor}$, 2.44 (q, *J* = 6.8 Hz, 2H, CH(OH)CH$_2$CH$_2$CH$_2$C(O)N(Bn(4-CF$_3$))CH$_2$)$_{Major}$, 2.37 (dd, *J* = 6.5, 5.0 Hz, 2H, CH(OH)CH$_2$CH$_2$CH$_2$*C(O)N(Bn(4-CF$_3$))CH$_2$)$_{Minor}$, 1.80 (q, *J* = 7.8 Hz, 2H, CH(OH)CH$_2$CH$_2$CH$_2$C(O)N(Bn(4-CF$_3$))CH$_2$, $_{Major,}$ CH(OH)CH$_2^*$CH$_2$CH$_2$C(O)N(Bn(4-CF$_3$))CH$_2$)$_{Minor}$, 1.73–1.61 (m, 4H, CH$_3$(CH$_2$)$_3$CH$_a$H$_b$CH(OMe)CH$_a$H$_b$CH(OH), CH(OH)CH$_2$CH$_2$CH$_2$C(O)N(Bn(4-CF$_3$))CH$_2$, $_{Major,}$ CH(OH)CH$_2$CH$_2$*CH$_2$C(O)N(Bn(4-CF$_3$))CH$_2$ $_{Minor}$) 1.36–1.27 (m, 6H, CH$_3$(CH$_2$)$_3$CH$_a$H$_b$CH(OMe)CH$_a$H$_b$CH(OH), 0.89 (t, *J* = 6.6 Hz, 3H, CH$_3$(CH$_2$)$_3$CH$_a$H$_b$CH(OMe);

^{13}C NMR (126 MHz, CDCl3) δ 173.8 (amide C=O), 173.5 (amide C=O)*, 142.0 (C$_{Ar}$), 141.2(C$_{Ar}$)*, 132.9 (C$_{Ar}$), 132.5 (CH=CH$_2$), 131.9 (CH=CH$_2$)*, 128.4 (2, CH$_{Ar}$), 126.7 (2, CH$_{Ar}$)*, 126.1 (2, CH$_{Ar}$), 125.7 (2, CH$_{Ar}$)*, 118.0 (CH=CH$_2$)*, 117.3 (CH=CH$_2$), 79.6 (CH), 68.3 (CH), 56.9 (CH$_3$), 49.9 (CH$_2$)*, 49.6 (CH$_2$), 48.4 (CH$_2$)*, 48.2 (CH$_2$), 39.5

(CH_2), 37.5 (CH_2), 37.4 (CH_2)*, 33.1 (CH_2), 32.9 (CH_2)*, 32.1 (CH_2), 29.9 (CH_2), 25.2 (CH_2), 22.8 (CH_2), 21.2 (CH_2), 14.2 (CH_3);

* rotamer

Note: (^{13}C of CF_3 were not found; however, IR and 19F data confirmed the presence of CF_3 group)

^{19}F NMR (471 MHz, $CDCl_3$) δ -62.51_{Major}, -62.54^*_{Minor}.

HRMS (ESI-TOF) m/z: $[M + Na]^+$ Calcd for $C_{24}H_{36}F_3NO_3Na$ 466.2545; Found 466.2561.

2-(((5*S*,7*S*)-1-(allyl(methyl)amino)-7-methoxy-1-oxododecan-5-yl)oxy)-2-oxoethyl acrylate ($C_{22}H_{37}NO_6$, 3.8.4)

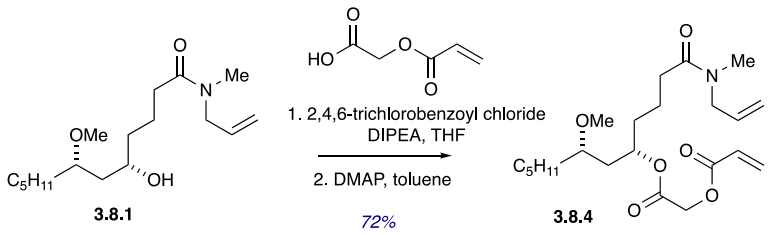

To a solution of 2-(acryloyloxy)acetic acid (13.0 mg, 0.1 mmol, 2 equiv.) in dry THF (0.3 mL) was added freshly distilled *N*,*N*-diisopropylethylamine (13.5 µL, 0.09 mmol, 2.5 equiv.) followed by 2,4,6-trichlorobenzoyl chloride (TCBC) (16.6 µL, 0.115 mmol, 1.8 equiv.) and stirred at room temperature for 3 hours, and the resulted mixed anhydride was concentrated under reduced pressure. The crude mixture was then redissolved in dry toluene (0.3 mL) and cannulated to a stirring solution of amide **3.8.1** (15 mg, 0.05 mmol, 1.0 equiv.) and DMAP (7.3 mg, 0.06 mmol, 1.2 equiv.) in toluene (0.3 mL) at 0 ºC. After stirring for 15 minutes at 0 ºC the reaction mixture was stirred for an additional 12 hours at room temperature (complete by TLC). The reaction mixture was diluted with CH_2Cl_2 (1 mL) and was added sat. $NaHCO_3$ (2 mL). The aqueous layer was extracted with CH_2Cl_2 (3 x 1.5 mL), and the organic layers were combined, dried over Na_2SO_4, filtered, and concentrated under reduced pressure. Purification via flash column chromatography (silica, 0%–50% EtOAc in hexanes) to obtain amide **3.8.4** (14.8 mg, 0.04 mmol, 72% yield) as a colorless liquid. TLC (EtOAc/hexane, 1/1): R_f = 0.4.

FTIR (neat): 3099, 3082, 2928, 2857, 1734, 1700, 1683, 1405, 1278, 1171, 984 cm^{-1};

Optical Rotation: $[\alpha]_D^{22}$ = +6.6 (c = 0.15 , $CHCl_3$);

^{1}H NMR (500 MHz, $CDCl_3$) δ 6.49 (d, J = 17.3 Hz, 1H, OC(O)CH_2OC(O)CH=C$\underline{H}_aH_b$), 6.21 (dd, J = 17.3, 10.4 Hz, 1H, OC(O)CH_2OC(O)C$\underline{H}$= CH_aH_b), 5.92 (d, J = 10.4 Hz,

1H, OC(O)CH_2OC(O)CH=CH_aH_b), 5.80–5.66 (m, 1H, C(O)N(Me)CH_aH_bCH=CH_2), 5.28–5.08 (m, 3H, C(O)N(Me) CH_aH_bCH=CH_2, $CH_3(CH_2)_4$CH(OMe)CH_aH_bCH(OC(O))CH_aH_b), 4.67 (s, 2H, OC(O)CH_2OC(O)CH=CH_aH_b), 3.98 (d, *J* = 6.0 Hz, 1H, C(O)N(Me) CH_aH_bCH=CH_2), 3.88 (d, *J* = 4.8 Hz, 1H, C(O)N(Me) CH_aH_bCH=CH_2), 3.29 (s, 3H, CH(OMe)CH_aH_bCH(OC(O))CH_aH_b), 3.12 (dd, *J* = 8.0, 6.9 Hz, 1H, CH(OMe)CH_aH_bCH(OC(O))CH_aH_b), 2.92 (s, 3H, C(O)N(Me)CH_2CH=CH_2), 2.42–2.27 (m, 2H, CH(OC(O))$CH_2CH_2CH_2$C(O)N(Me)CH_2), 1.70–1.59 (m, 6H, CH(OMe)CH_aH_bCH(OC(O))$CH_aH_bCH_2$), 1.54–1.48 (m, 1H, $CH_3(CH_2)_3CH_aH_b$CH(OMe)), 1.43–1.35 (m, 1H, $CH_3(CH_2)_3CH_aH_b$CH(OMe)), 1.34–1.23 (m, 6H, $CH_3(CH_2)_3CH_aH_b$CH(OMe)), 0.89 (t, *J* = 6.8 Hz, 3H, $CH_3(CH_2)_3CH_aH_b$CH(OMe));

^{13}C NMR (126 MHz, $CDCl_3$) δ 172.4 (C=O, amide)167.6 (C=O), 165.5 (C=O), 133.3 (CH=CH_2), 132.8 (CH=CH_2)*, 132.3 (CH=CH_2), 127.6 (CH=CH_2), 117.3 (CH=CH_2), 116.7 (CH=CH_2)*, 77.4 (CH), 72.8 (CH), 61.1 (CH_2), 57.1 (CH_3), 52.3 (CH_2), 50.2 (CH_2)*, 39.2 (CH_2), 34.8 (CH_3), 34.5 (CH_2), 33.8 (CH_3)*, 33.6 (CH_2), 33.0 (CH_2), 32.4 (CH_2)*, 32.2 (CH_2), 24.7 (CH_2), 22.8 (CH_2), 20.8 (CH_2), 20.5(CH_2)*, 14.2 (CH_3);

* rotamer

HRMS (ESI-TOF) m/z: $[M + Na]^+$ Calcd for $C_{22}H_{37}F_3NO_6Na$ 434.2519; Found 434.2528.

(5*S*,7*S*)-1-(allyl(methyl)amino)-7-methoxy-1-oxododecan-5-yl (*S*)-2-(acryloyloxy)-3-methylbutanoate ($C_{25}H_{43}NO_6$, 3.8.5)

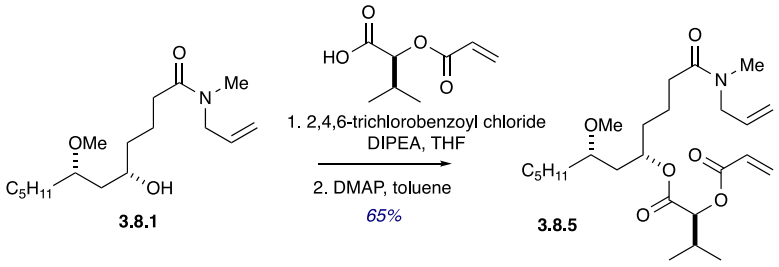

To a solution of (*S*)-2-(acryloyloxy)-3-methylbutanoic acid (17.2 mg, 0.1 mmol, 2 equiv.) in dry THF (0.3 mL) was added freshly distilled *N*,*N*-diisopropylethylamine (13.5 µL, 0.09 mmol, 2.5 equiv.) followed by 2,4,6-trichlorobenzoyl chloride (TCBC) (16.6 µL, 0.115 mmol, 1.8 equiv.) and stirred at room temperature for 3 hours, and the resulted mixed anhydride was concentrated under reduced pressure. The crude mixture was then redissolved in dry toluene (0.3 mL) and cannulated to a stirring solution of amide **3.8.1** (15 mg, 0.05 mmol, 1.0 equiv.) and DMAP (7.3 mg, 0.06 mmol, 1.2 equiv.) in toluene (0.3 mL) at 0 ºC. After stirring for 15 minutes at 0 ºC the reaction mixture was stirred for an additional 12 hours at room temperature (complete by TLC). Reaction mixture was diluted with CH_2Cl_2 (1 mL) and was added sat. $NaHCO_3$ (2 mL). The aqueous layer was extracted with CH_2Cl_2 (3 x 1.5 mL), and the organic layers were combined, dried over Na_2SO_4, filtered, and concentrated under reduced pressure. Purification via flash column chromatography (silica, 0%–50% EtOAc in hexanes) to obtain diene **3.8.5** (14.7 mg, 0.03 mmol, 65% yield) as a colorless liquid. TLC (EtOAc/hexane, 1/1): R_f = 0.5.

FTIR (neat): 3082, 2964, 2929,2874, 2856, 1730, 1648, 1405, 1260, 1186, 1065 cm^{-1};

Optical Rotation: $[a]_D^{22}$ = +6.1 (c = 0.10 , $CHCl_3$);

^{1}H NMR (500 MHz, $CDCl_3$) δ 6.46 (dd, J = 17.3 , 1.5 Hz, 1H, OC(O)CH(CH(CH_3)$_2$)OC(O)CH=C$\underline{H}_a$H$_b$), 6.20 (dd, J = 17.3, 10.4 Hz, 1H,

OC(O)CH(CH(CH_3)$_2$)OC(O)C<u>H</u>= CH_aH_b), 5.89 (dd, *J* = 10.4, 1.4 Hz, 1H, OC(O)CH(CH(CH_3)$_2$)OC(O)CH=CH_a<u>H_b</u>), 5.80–5.68 (m, 1H, C(O)N(Me)CH_2C<u>H</u>=CH_2), 5.24–5.05 (m, 3H, C(O)N(Me)CH_2CH=C<u>H_2</u>, $CH_3(CH_2)_4$CH(OMe)CH_aH_bC<u>H</u>(OC(O))CH_aH_b), 4.88 (d, *J* = 4.3 Hz, 1H, OC(O)C<u>H</u>(CH(CH_3)$_2$)OC(O)CH=CH_aH_b), 3.98 (d, *J* = 5.7 Hz, 1H, C(O)N(Me)C<u>H_2</u>CH=CH_2)$_{Major}$, 3.91–3.85 (m, 1H, C(O)N(Me)C<u>H_2</u>*CH=CH_2)$_{Minor}$, 3.29 (s, 3H, CH(O<u>Me</u>)CH_aH_bCH(OC(O))CH_aH_b), 3.12–3.05 (m, 1H, C<u>H</u>(OMe)CH_aH_bCH(OC(O))CH_aH_b), 2.92 (s, 3H, C(O)N(<u>Me</u>)CH_2CH=CH_2), 2.91 (s, 3H, C(O)N(<u>Me</u>)*CH_2CH=CH_2); 2.42–2.22 (m, 3H, OC(O)CH(C<u>H</u>(CH_3)$_2$)OC(O)CH=CH_aH_b, CH(OC(O))CH_2CH_2C<u>H_2</u>C(O)N(Me)CH_2), 1.73–1.62 (m, 6H, CH(OMe)C<u>H_aH_b</u>CH(OC(O))C<u>H_aH_b</u>C<u>H_2</u>), 1.55–1.47 (m, 1H, $CH_3(CH_2)_3$C<u>H_a</u>H_bCH(OMe)), 1.39–1.30 (m, 1H, $CH_3(CH_2)_3CH_a$<u>H_b</u>CH(OMe)), 1.30–1.20 (m, 6H, CH_3(C<u>H_2</u>)$_3CH_aH_b$CH(OMe)), 1.03 (dd, *J* = 8.3, 6.7 Hz, 6H, OC(O)CH(CH(C<u>H_3</u>)$_2$)OC(O)CH=CH_aH_b), 0.89 (td, *J* = 7.0 Hz, 3H, C<u>H_3</u>$(CH_2)_3CH_aH_b$CH(OMe));

^{13}C NMR (126 MHz, $CDCl_3$) δ 172.7 (<u>C</u>=O, amide), 169.5 (<u>C</u>=O), 165.8 (<u>C</u>=O), 133.5 (<u>C</u>H=CH_2), 133.0 (<u>C</u>H=CH_2)*, 131.4 (CH=C<u>H_2</u>), 128.2 (<u>C</u>H=CH_2), 117.1 (CH=C<u>H_2</u>), 116.7 (CH=C<u>H_2</u>)*, 77.5 (<u>C</u>H), 77.4 (<u>C</u>H), 72.8 (<u>C</u>H), 57.0 (<u>C</u>H_3), 52.4 (<u>C</u>H_2), 50.2 (<u>C</u>H_2)*, 39.4 (<u>C</u>H_2), 34.8 (<u>C</u>H_3), 34.6 (<u>C</u>H_2), 33.8 (<u>C</u>H_3)*, 33.8 (<u>C</u>H_2), 33.2 (<u>C</u>H_2), 32.6 (<u>C</u>H_2)*, 32.2 (CH_2), 30.3 (<u>C</u>H), 24.8 (<u>C</u>H_2), 22.8 (<u>C</u>H_2), 20.8 (<u>C</u>H_2), 20.5(<u>C</u>H_2)*, 19.9 (<u>C</u>H_3), 19.1 (<u>C</u>H_3), 14.1 (<u>C</u>H_3);

* rotamer

HRMS (ESI-TOF) m/z: $[M + Na]^+$ Calcd for $C_{25}H_{43}F_3NO_6Na$ 476.2988; Found 476.2987.

2-(((5*S*,7*S*)-1-(allyl(4-(trifluoromethyl)benzyl)amino)-7-methoxy-1-oxododecan-5-yl)oxy)-2-oxoethyl acrylate ($C_{29}H_{40}F_3NO_6$, 3.8.7)

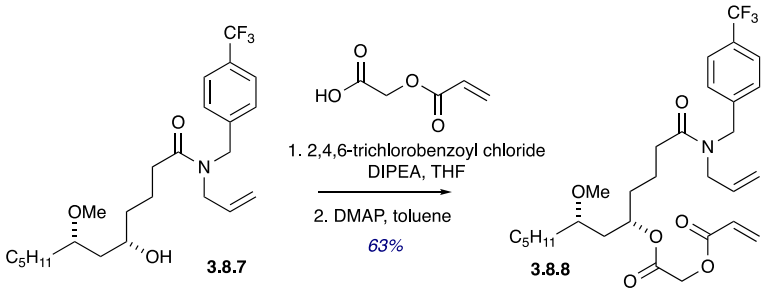

To a solution of 2-(acryloyloxy)acetic acid (7.8 mg, 0.06 mmol, 2 equiv.) in dry THF (0.3 mL) was added freshly distilled *N*,*N*-diisopropylethylamine (26 µL, 0.08 mmol, 2.5 equiv.) followed by 2,4,6-trichlorobenzoyl chloride (TCBC) (8 µL, 0.06 mmol, 1.8 equiv.) and stirred at room temperature for 3 hours, and the resulted mixed anhydride was concentrated under reduced pressure. Crude mixture was then redissolved in dry toluene (0.4 mL) and cannulated to a stirring solution of amide **3.8.7** (15.0 mg, 0.03 mmol, 1.0 equiv.) and DMAP (4.4 mg, 0.04 mmol, 1.2 equiv.) in toluene (0.4 mL) at 0 ºC. After stirring for 15 minutes at 0 ºC the reaction mixture was stirred for additional 12 hours at room temperature (complete by TLC). The reaction mixture was diluted with CH_2Cl_2 (1 mL) and was added sat. $NaHCO_3$ (1 mL). The aqueous layer was extracted with CH_2Cl_2 (3 x 1.5 mL), and the organic layers were combined, dried over Na_2SO_4, filtered, and concentrated under reduced pressure. Purification via flash column chromatography (silica, 0%–50% EtOAc in hexanes) to obtain amide **3.8.8** (10.5 mg, 0.04 mmol, 63% yield) as a colorless liquid. TLC (EtOAc/hexane, 1/1): R_f = 0.7.

FTIR (neat): 3079, 2930, 2859, 1735, 1649, 1619, 1580, 1325 (CF_3), 1209 (CF_3), 985 cm^{-1};

Optical Rotation: $[\alpha]_D^{22}$ = +13.2 (c = 0.14 , $CHCl_3$);

^{1}H NMR (500 MHz, $CDCl_3$) δ 7.62 (d, *J* = 8.0 Hz, 2H, $C(O)N(CH_2C_6\underline{H}_{2a}{*}H_{2b}CF_3)CH_2CH{=}CH_{2Minor}$), 7.57 (d, *J* = 8.0 Hz, 2H, $C(O)N(CH_2C_6\underline{H}_{2a}H_{2b}CF_3)CH_2CH{=}CH_{2Major}$), 7.34 (d, *J* = 8.0 Hz, 2H, $C(O)N(CH_2C_6H_{2a}\underline{H}_{2b}CF_3)CH_2CH{=}CH_{2Major}$), 7.28 (d, *J* = 8.7 Hz, 2H, $C(O)N(CH_2C_6H_{2a}\underline{H}_{2b}{*}CF_3)CH_2CH{=}CH_{2Minor}$), 6.48 (d, *J* = 17.3 Hz, 1H, $OC(O)CH_2OC(O)CH{=}C\underline{H}_aH_b$), 6.20 (dd, *J* = 17.3, 10.3 Hz, 1H, $OC(O)CH_2OC(O)C\underline{H}{=}CH_aH_b$), 5.91 (d, *J* = 10.4 Hz, 1H, $OC(O)CH_2OC(O)CH{=}CH_a\underline{H}_b$), 5.80–5.67 (m, 1H, $C(O)N(CH_2C_6H_{2a}H_{2b}CF_3)CH_2C\underline{H}{=}CH_2$), 5.30–5.05 (m, 3H, $C(O)N(CH_2C_6H_{2a}H_{2b}CF_3)CH_2CH{=}C\underline{H}_2$), $CH_3(CH_2)_4CH(OMe)CH_aH_bC\underline{H}(OC(O))CH_aH_b$), 4.68 (s, 2H, $OC(O)C\underline{H}_2OC(O)CH{=}CH_aH_b$), 4.65–4.53 (m, 2H, $C(O)N(C\underline{H}_2C_6H_{2a}H_{2b}CF_3)CH_2CH{=}CH_2$), 4.05–3.96 (m, 2H, $C(O)N(CH_2C_6H_{2a}H_{2b}CF_3)C\underline{H}_2{*}CH{=}CH_2)_{Minor}$, 3.89–3.79 (m, 2H, $C(O)N(CH_2C_6H_{2a}H_{2b}CF_3)C\underline{H}_2CH{=}CH_2)_{Major}$, 3.30 (s, 3H, $CH_3(CH_2)_4CH(O\underline{Me})CH_aH_b)_{Major}$, 3.27 (s, 3H, $CH_3(CH_2)_4CH(O\underline{Me}{*})CH_aH_b)_{Minor}$, 3.17–3.08 (m, 1H, $CH_3(CH_2)_4C\underline{H}(OMe{*})CH_aH_b$), 2.49–2.27 (m, 2H, $C\underline{H}_2C(O)N(CH_2C_6H_{2a}H_{2b}CF_3)CH_2$), 1.81–1.59 (m, 6H, $CH(OMe)C\underline{H}_a\underline{H}_bCH(OC(O))C\underline{H}_a\underline{H}_bC\underline{H}_2$), 1.57–1.48 (m, 1H, $CH_3(CH_2)_3C\underline{H}_aH_bCH(OMe)$), 1.45–1.35 (q, *J* = 6.6 Hz, 1H, $CH_3(CH_2)_3CH_a\underline{H}_bCH(OMe)$), 1.34–1.23 (m, 6H, $CH_3(C\underline{H}_2)_3CH_aH_bCH(OMe)$), 0.89 (t, *J* = 6.7 Hz, 3H, $C\underline{H}_3(CH_2)_3CH_aH_bCH(OMe)$);

^{13}C NMR (126 MHz, $CDCl_3$) δ 173.5 (C=O, amide), 173.2 (C=O, amide)*,167.7 ($\underline{C}$=O), 165.6 ($\underline{C}$=O), 141.8 (C_{Ar}), 136.2 (C_{Ar}), 132.8 ($\underline{C}H{=}CH_2$)*, 132.6 ($CH{=}\underline{C}H_2$)*, 132.4

(<u>C</u>H=CH_2), 132.3 (CH=<u>C</u>H_2), 128.2 (2, <u>C</u>H_{Ar}), 127.5 (<u>C</u>H=CH_2), 126.8 (2, <u>C</u>H_{Ar})*, 126.1 (2, <u>C</u>H_{Ar})*, 125.7 (2, <u>C</u>H_{Ar}), 118.1(CH=<u>C</u>H_2)*, 117.4 (CH=<u>C</u>H_2), 77.4 (<u>C</u>H), 72.6 (<u>C</u>H), 61.1 (<u>C</u>H_2), 57.1 (<u>C</u>H_3), 49.9 (<u>C</u>H_2)*, 49.7 (<u>C</u>H_2), 48.4 (<u>C</u>H_2)*, 48.3 (<u>C</u>H_2), 39.3 (<u>C</u>H_2), 34.5 (CH_2), 33.6 (CH_2), 32.8 (CH_2)*, 32.5(CH_2), 32.2(CH_2), 24.7 (CH_2), 22.8 (CH_2), 20.8 (CH_2), 14.2 (CH_3);

* rotamer

Note: (^{13}C of CF_3 was not found; however, IR and ^{19}F data confirmed the presence of CF_3 group)

^{19}F NMR (471 MHz, $CDCl_3$) δ -62.50$_{Major}$, -62.54*$_{Minor}$.

HRMS (ESI-TOF) m/z: $[M + Na]^+$ Calcd for $C_{29}H_{40}F_3NO_6Na$ 578.2705; Found 578.2706.

(5*S*,7*S*)-*N*-allyl-5-hydroxy-7-methoxy-*N*-methyl-10-phenyldecanamide ($C_{21}H_{33}NO_3$, 3.9.1)

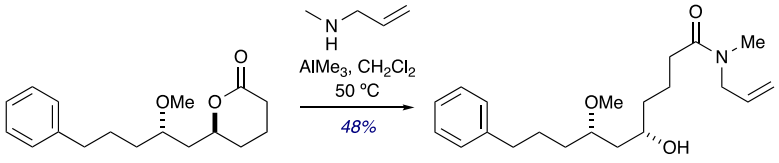

3.7.10 3.9.1

To a solution of *N*-allylmethylamine (38 µL, 0.4 mmol, 2 equiv.) in CH_2Cl_2 (1 mL), was added trimethylaluminum (2 M, toluene, 0.175 mL, 0.35 mmol, 1.75 equiv.) at room temperature and stirred for 30 minutes. Then the mixture was cannulated under argon to a solution of lactone methyl ether **3.7.10** (50 mg, 0.2 mmol, 1 equiv.) in CH_2Cl_2 (0.2 mL) in a pressure vial and stirred at 50 ºC for 18 hours (TLC monitoring). Then the reaction mixture was cooled to room temperature and an additional 1.75 equivalents of *N*-allylmethylamine aluminum complex was added and continued stirring for 12 more hours at 50 ºC (complete by TLC). Reaction mixture was diluted with CH_2Cl_2 (1 mL) and quenched carefully with 1 M HCl solution (1 mL) at 0 ºC. The aqueous layer was extracted with CH_2Cl_2 (3 x 1.5 mL), and the organic layers were combined, dried over Na_2SO_4, filtered, and concentrated under reduced pressure. Purification via flash column chromatography (silica, 0%–80% EtOAc in hexanes) amide **3.9.1** (33.4 mg, 0.096 mmol, 48% yield) as pale yellow oil. TLC (EtOAc/hexane, 3/2): R_f = 0.2.

FTIR (neat): 3418, 3029, 2928, 2845, 1634, 1558, 1456, 1086, 990 cm^{-1};

Optical Rotation: $[a]_D^{22}$ = +22.0 (c = 0.15 , $CHCl_3$);

^{1}H NMR (500 MHz, $CDCl_3$) δ 7.31–7.13 (m, 5H, $C_6\underline{H}_5CH_2CH_2CH_aH_bCH(OMe)$), 5.81–5.70 (m, 1H, $C(O)N(Me)CH_2C\underline{H}=CH_2$), 5.22–5.09 (m, 2H, $C(O)N(Me)CH_2CH=C\underline{H}_2$), 4.02–3.93 (m, 2H, $C(O)N(Me)C\underline{H}_2CH=CH_2)_{Major}$, 3.90–3.89 (m, 2H, $C(O)N(Me)C\underline{H}_2{*}CH=CH_2)_{Minor}$, 3.86–3.78 (m, 1H, $CH(OMe)CH_aH_bC\underline{H}(OH)CH_aH_b$),

3.51 (dtt, J = 15.9, 6.2, 3.0 Hz, 1H, C<u>H</u>(OMe)CH_aH_bCH(OH)CH_aH_b), 3.38 (s, 3H, CH(O<u>Me</u>)CH_aH_bCH(OH)CH_aH_b)$_{Major}$, 3.34 (s, 3H, CH(O<u>Me</u>*)CH_aH_bCH(OH))$_{Minor}$, 2.94 (s, 3H, C(O)N(<u>Me</u>)$CH_2CH{=}CH_2$)$_{Major}$, 2.92 (s, 3H, C(O)N(<u>Me</u>*)$CH_2CH{=}CH_2$)$_{Minor}$, 2.69–2.59 (m, 2H, $C_6H_5C\underline{H}_2CH_2CH_aH_b$CH(OMe)), 2.42–2.29 (m, 2H, $CH(OH)CH_2CH_2C\underline{H}_2$C(O)N(Me)$CH_2$, $CH(OH)CH_2CH_2C\underline{H}_2$*C(O)N(Me)$CH_2$), 1.80–1.70 (m, 3H, $CH(OH)CH_2C\underline{H}_2CH_2$C(O)N(Me)$CH_2$, $CH(OH)C\underline{H}_aH_bCH_2CH_2$C(O)N(Me)$CH_2$), 1.69–1.60 (m, 3H, $C\underline{H}_aH_bC\underline{H}_aH_b$CH(OMe)$C\underline{H}_aH_b$CH(OH), 1.54–1.36 (m, 4H, $CH_a\underline{H}_bCH_a\underline{H}_b$CH(OMe)$CH_a\underline{H}_b$CH(OH)$CH_a\underline{H}_b$);

^{13}C NMR (126 MHz, $CDCl_3$) δ 173.5 (amide <u>C</u>=O), 173.1 (amide <u>C</u>=O)*, 142.4 (C_{Ar}), 133.2 (<u>C</u>H=CH_2), 132.7 (<u>C</u>H=CH_2)*, 128.5 (2, CH_{Ar}), 128.4 (2, CH_{Ar}), 125.9 (CH_{Ar}), 117.2 (CH=<u>C</u>H_2), 116.7 (CH=<u>C</u>H_2)*, 79.2 (<u>C</u>H), 79.2 (<u>C</u>H)*, 68.1 (<u>C</u>H), 68.0 (<u>C</u>H)*, 57.1 (<u>C</u>H_3), 57.1 (<u>C</u>H_3)*, 52.3 (<u>C</u>H_2), 50.2 (<u>C</u>H_2)*, 39.9 (<u>C</u>H_2), 39.8 (<u>C</u>H_2)*, 37.6 (<u>C</u>H_2), 37.5 (<u>C</u>H_2)*, 36.1 (<u>C</u>H_2), 34.9 (N-<u>C</u>H_3), 33.8 (N-<u>C</u>H_3)*, 33.3 (<u>C</u>H_2), 32.7 (<u>C</u>H_2)*, 33.0 (<u>C</u>H_2), 27.3 (<u>C</u>H_2), 21.1 (<u>C</u>H_2), 20.8 (<u>C</u>H_2)*;

* rotamer

HRMS (ESI-TOF) m/z: $[M + Na]^+$ Calcd for $C_{21}H_{33}NO_3Na$ 370.2358; Found 370.2347.

2-(((5*S*,7*S*)-1-(allyl(methyl)amino)-7-methoxy-1-oxo-10-phenyldecan-5-yl)oxy)-2-oxoethyl acrylate ($C_{26}H_{37}NO_6$, 3.9.2)

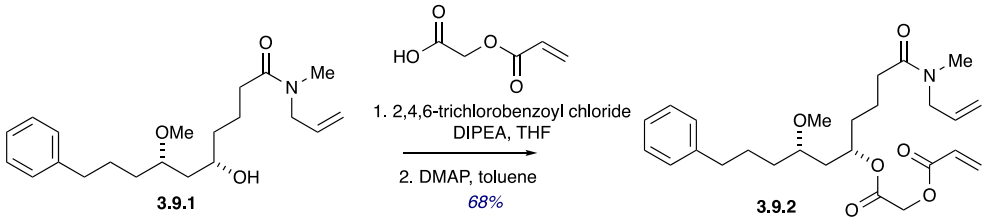

To a solution of 2-(acryloyloxy)acetic acid (15.6 mg, 0.12 mmol, 2 equiv.) in dry THF (1.2 mL) was added freshly distilled *N*,*N*-diisopropylethylamine (26 µL, 0.15 mmol, 2.5 equiv.) followed by 2,4,6-trichlorobenzoyl chloride (TCBC) (15.8 µL, 0.11 mmol, 1.8 equiv.) and stirred at room temperature for 3 hours and the resulted mixed anhydride was concentrated under reduced pressure. The crude mixture was then redissolved in dry toluene (0.6 mL) and cannulated to a stirring solution of amide **3.9.1** (20 mg, 0.06 mmol, 1.0 equiv.) and DMAP (8.8 mg, 0.07 mmol, 1.2 equiv.) in toluene (0.6 mL) at 0 ºC. After stirring for 15 minutes at 0 ºC the reaction mixture was stirred for an additional 12 hours at room temperature (complete by TLC). The reaction mixture was diluted with CH_2Cl_2 (2 mL) and was added sat. $NaHCO_3$ (2 mL). The aqueous layer was extracted with CH_2Cl_2 (3 x 1.5 mL), and the organic layers were combined, dried over Na_2SO_4, filtered, and concentrated under reduced pressure. Purification via flash column chromatography (silica, 0%–50% EtOAc in hexanes) to obtain amide **3.9.2** (18.4 mg, 0.04 mmol, 68% yield) as a yellow oil. TLC (EtOAc/hexane, 1/1): R_f = 0.65.

FTIR (neat): 3025, 2923, 2853, 1756, 1732, 1635, 1495, 1261, 1170, 981 cm^{-1};

Optical Rotation: $[\alpha]_D^{21}$ = +11.2 (c = 0.10 , $CHCl_3$);

^{1}H NMR (500 MHz, $CDCl_3$) δ 7.29–7.16 (m, 5H, $C_6\underline{H}_5CH_2(CH_2)_2CH(OMe)$, 6.48 (d, J = 17.4 Hz, 1H, $OC(O)CH_2OC(O)CH=C\underline{H}_aH_b$), 6.19 (dd, J = 17.4, 10.3 Hz, 1H,

OC(O)CH_2OC(O)C<u>H</u>= CH_aH_b), 5.92 (d, *J* = 10.5 Hz, 1H, OC(O)CH_2OC(O)CH=CH_a<u>H</u>$_b$), 5.80–5.66 (m, 1H, C(O)N(Me)CH_aH_bC<u>H</u>=CH_2), 5.27–5.20 (m, 1H, CH(OMe)CH_aH_bC<u>H</u>(OC(O))CH_aH_b), 5.16 (m, 2H, C(O)N(Me) CH_aH_bCH=C<u>H</u>$_2$), 4.65 (s, 2H, OC(O)C<u>H</u>$_2$OC(O)CH=CH_aH_b), 3.98 (d, *J* = 6.0 Hz, 1H, C(O)N(Me) C<u>H</u>$_a$$H_b$CH=$CH_2$), 3.88 (d, *J* = 4.7 Hz, 1H, C(O)N(Me) CH_a<u>H</u>$_b$CH=CH_2), 3.27 (s, 3H, CH(O<u>Me</u>)CH_aH_bCH(OC(O))CH_aH_b), 3.18–3.09 (m, 1H, C<u>H</u>(OMe)CH_aH_bCH(OC(O))CH_aH_b), 2.92 (s, 3H, C(O)N(<u>Me</u>)CH_2CH=CH_2)$_{Major}$, 2.91 (s, 3H, C(O)N(<u>Me</u>)*CH_2CH=CH_2)$_{Minor}$, 2.61 (t, *J* = 7.5 Hz, 2H, C_6H_5C<u>H</u>$_2$(CH_2)$_2$CH(OMe), 2.40–2.25 (m, 2H, CH(OC(O))CH_2CH_2C<u>H</u>$_2$C(O)N(Me)CH_2), 1.78–1.57 (m, 9H, CH(OMe)C<u>H</u>$_a$<u>H</u>$_b$CH(OC(O))C<u>H</u>$_a$<u>H</u>$_b$C<u>H</u>$_2$, $C_6H_5CH_2$C<u>H</u>$_2$C<u>H</u>$_a$$H_b$CH(OMe)), 1.46 (dt, *J* = 14.0, 6.8 Hz, 1H, $C_6H_5CH_2CH_2CH_a$<u>H</u>$_b$CH(OMe));

^{13}C NMR (126 MHz, $CDCl_3$) δ 172.8 (C=O, amide) 167.6 (<u>C</u>=O), 165.6 (<u>C</u>=O), 142.4 (C_{Ar}), 133.3 (<u>C</u>H=CH_2), 132.8 (<u>C</u>H=CH_2)*, 132.3 (CH=C<u>H</u>$_2$), 128.6 (2, CH_{Ar}), 128.5 (2, CH_{Ar}), 127.6 (<u>C</u>H=CH_2),125.9 (CH_{Ar}), 117.3 (CH=C<u>H</u>$_2$), 116.7 (CH=C<u>H</u>$_2$)*, 77.2 (<u>C</u>H), 72.7 (<u>C</u>H), 61.1 (<u>C</u>H_2), 57.2 (<u>C</u>H_3), 52.3 (<u>C</u>H_2), 50.1 (<u>C</u>H_2)*, 39.2 (<u>C</u>H_2), 36.2 (<u>C</u>H_2), 34.8 (CH_3), 34.5 (CH_2) , 33.8 (CH_3)*, 33.3 (CH_2), 33.0 (CH_2), 32.4 (CH_2)*, 26.9 (CH_2), 20.8 (CH_2), 20.5(CH_2)*.

* rotamer

HRMS (ESI-TOF) m/z: $[M + Na]^+$ Calcd for $C_{26}H_{37}NO_6Na$ 482.2519; Found 476.2549.

(5*S*,7*S*)-1-(allyl(methyl)amino)-7-methoxy-1-oxo-10-phenyldecan-5-yl (*S*)-2-(acryloyloxy)-3-methylbutanoate ($C_{29}H_{43}NO_6$, 3.9.3)

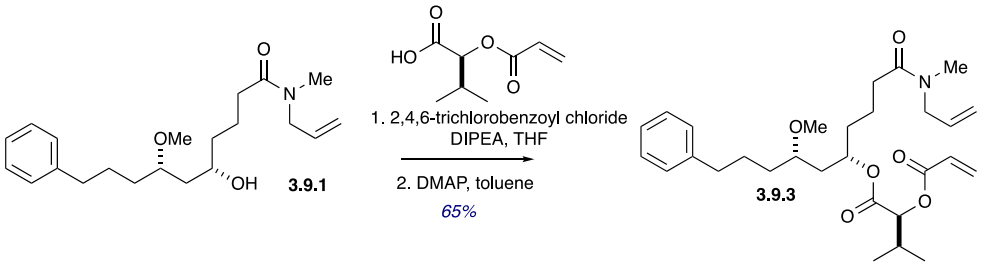

To a solution of (*S*)-2-(acryloyloxy)-3-methylbutanoic acid (20.6 mg,0.12 mmol, 2 equiv.) in dry THF (1.2 mL) was added freshly distilled *N*,*N*-diisopropylethylamine (26 µL, 0.15 mmol, 2.5 equiv.) followed by 2,4,6-trichlorobenzoyl chloride (TCBC) (15.8 µL, 0.11 mmol, 1.8 equiv.) and stirred at room temperature for 3 hours, and the resulted mixed anhydride was concentrated under reduced pressure. Crude mixture was then redissolved in dry toluene (0.6 mL) and cannulated to a stirring solution of amide **3.9.1** (20 mg, 0.06 mmol, 1.0 equiv.) and DMAP (8.8 mg, 0.07 mmol, 1.2 equiv.) in toluene (0.6 mL) at 0 ºC. After stirring for 15 minutes at 0 ºC the reaction mixture was stirred for an additional 12 hours at room temperature (complete by TLC). The reaction mixture was diluted with CH_2Cl_2 (2 mL) and was added sat. $NaHCO_3$ (2 mL). The aqueous layer was extracted with CH_2Cl_2 (3 x 1.5 mL), and the organic layers were combined, dried over Na_2SO_4, filtered, and concentrated under reduced pressure. Purification via flash column chromatography (silica, 0%–50% EtOAc in hexanes) to obtain amide **3.9.3** (19.5 mg, 0.04 mmol, 65% yield) as a yellow oil. TLC (EtOAc/hexane, 1/1): $R_f = 0.7$.

FTIR (neat): 3083, 3025, 2923, 2852, 1756, 1733, 1648, 1207, 1170, 1089, 1021 cm^{-1};

Optical Rotation: $[a]_D^{21}$ = +10.3 (c = 0.10 , $CHCl_3$);

^{1}H NMR (500 MHz, $CDCl_3$) δ 7.32–7.13 (m, 5H, $C_6\underline{H}_5CH_2(CH_2)_2CH(OMe)$), 6.42 (dd, J = 17.3, 1.4 Hz, 1H, $OC(O)CH(CH(Me)_2)OC(O)CH=C\underline{H}_aH_b$), 6.17 (dd, J = 17.3, 10.4 Hz, 1H, $OC(O)CH(CH(Me)_2)OC(O)C\underline{H}=CH_aH_b$), 5.84 (dd, J = 10.0, 1.4 Hz, 1H, $OC(O)CH(CH(Me)_2)OC(O)CH=CH_a\underline{H}_b$), 5.80–5.64 (m, 1H, $C(O)N(Me)CH_aH_bC\underline{H}=CH_2$), 5.23–5.10 (m, 3H, $CH(OMe)CH_aH_bC\underline{H}(OC(O))CH_aH_b$, $C(O)N(Me)CH_aH_bCH=C\underline{H}_2$), 4.86 (d, J = 4.2 Hz, 1H, $OC(O)C\underline{H}(CH(Me)_2)OC(O)CH=CH_aH_b$), 3.98 (dd, J = 6.0, 1.4 Hz, 1H, $C(O)N(Me)C\underline{H}_aH_bCH=CH_2$), 3.88 (dd, J = 4.9, 1.6 Hz, 1H, $C(O)N(Me)CH_a\underline{H}_bCH=CH_2$), 3.27 (s, 3H, $CH(O\underline{Me})CH_aH_bCH(OC(O))CH_aH_b)_{Major}$, 3.27 (s, 3H, $CH(O\underline{Me})*CH_aH_bCH(OC(O))CH_aH_b)_{Minor}$, 3.14–3.05 (m, 1H, $C\underline{H}(OMe)CH_aH_bCH(OC(O))CH_aH_b$), 2.92 (s, 3H, $C(O)N(\underline{Me})*CH_2CH=CH_2)_{Major}$, 2.90 (s, 3H, $C(O)N(\underline{Me})CH_2CH=CH_2)_{Minor}$, 2.60 (t, J = 7.4 Hz, 2H, $C_6H_5C\underline{H}_2(CH_2)_2CH(OMe)$), 2.40–2.19 (m, 3H, $CH(OC(O))CH_2CH_2C\underline{H}_2C(O)N(Me)CH_2$, $OC(O)CH(C\underline{H}(Me)_2)OC(O)CH=CH_aH_b$), 1.73–1.57 (m, 9H, $CH(OMe)C\underline{H}_a\underline{H}_bCH(OC(O))C\underline{H}_a\underline{H}_bC\underline{H}_2$, $C_6H_5CH_2C\underline{H}_2C\underline{H}_aH_bCH(OMe)$), 1.46–1.37 (m, 1H, $C_6H_5CH_2CH_2CH_a\underline{H}_bCH(OMe)$), 1.02 (ddd, J = 8.2, 6.9, 1.2 Hz, 6H, $OC(O)CH(CH(\underline{Me})_2)OC(O)CH=CH_aH_b$);

^{13}C NMR (126 MHz, $CDCl_3$) δ 172.9 (C=O, amide), 172.5 (C=O, amide)*,169.5 ($\underline{C}$=O), 165.8 ($\underline{C}$=O), 142.4 (C_{Ar}), 133.4 ($\underline{C}H=CH_2$), 132.8 ($\underline{C}H=CH_2$)*, 131.7 ($CH=C\underline{H}_2$), 128.5 (2, CH_{Ar}), 128.4 (2, CH_{Ar}), 127.9 ($\underline{C}H=CH_2$),125.9 (CH_{Ar}), 117.2 ($CH=C\underline{H}_2$), 116.7 ($CH=C\underline{H}_2$)*, 77.2 ($\underline{C}H$), 77.0 ($\underline{C}H$), 72.5 ($\underline{C}H$), 57.1 ($\underline{C}H_3$), 52.3 ($\underline{C}H_2$), 50.1 ($\underline{C}H_2$)*, 39.2

($\underline{C}H_2$), 36.2 ($\underline{C}H_2$), 34.8 ($\underline{C}H_3$), 34.4 ($\underline{C}H_2$) , 33.7 ($\underline{C}H_3$)*, 33.3 ($\underline{C}H_2$), 33.1 ($\underline{C}H_2$), 32.5 ($\underline{C}H_2$)*, 30.2 ($\underline{C}H$), 26.9 ($\underline{C}H_2$), 20.8 ($\underline{C}H_2$), 20.4($\underline{C}H_2$)*, 19.2 ($\underline{C}H_3$), 17.3 ($\underline{C}H_3$);

* rotamer

HRMS (ESI-TOF) m/z: $[M + Na]^+$ Calcd for $C_{29}H_{43}NO_6Na$ 524.2988; Found 524.2982.

(3*S*,14*S*,*Z*)-3-isopropyl-14-((*S*)-2-methoxyheptyl)-9-methyl-1,4-dioxa-9-azacyclotetradec-6-ene-2,5,10-trione ($C_{23}H_{39}NO_6$, 3.10.1)

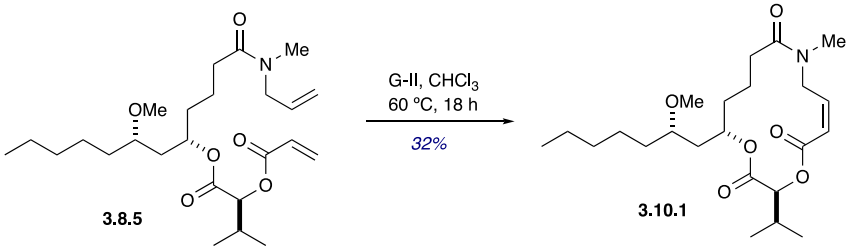

To a solution of diene **3.8.5** (10 mg, 0.02 mmol) in $CHCl_3$ (20 mL, 0.001 M) in a round-bottom flask was added G-II catalyst (3.4 mg, 0.004 mmol, 20 mol%) and stirred at 60 ºC for 18 hours (complete by TLC). The solvent was evaporated under reduced pressure. Flash column chromatography (silica, 0%–50% EtOAc in hexanes) was performed to obtain macrocycle (**3.10.1**) (3.1 mg, 0.021 mmol, 36% yield) as a thick brown oil. TLC (EtOAc/hexane, 3/1): R_f = 0.6.

FTIR (neat): 3060, 3025, 2928, 2854, 1729, 1634, 1266, 1187, 1045, 987 cm^{-1};

Optical Rotation: $[a]_D^{22}$ = -21.2 (c = 0.15, $CHCl_3$);

^{1}H NMR (500 MHz, $CDCl_3$) δ 6.25 (ddd, J = 11.7, 8.5, 5.9 Hz, 1H, C(O)N(Me)$CH_aH_bC\underline{H}$=CHC(O)OCH(CH(Me)$_2$), 6.00 (d, J = 17.8 Hz, 1H, C(O)N(Me)CH_aH_bCH=C$\underline{H}$C(O)OCH(CH(Me)$_2$), 5.27–5.21 (m, 1H, CH(OMe)$CH_aH_bC\underline{H}$(OC(O))CH_aH_b), 5.17 (d, J = 4.4 Hz, 1H, C(O)N(Me)CH_aH_bCH=CHC(O)OC$\underline{H}$(CH(Me)$_2$), 4.78 (dd, J = 16.7, 8.5 Hz, 1H, C(O)N(Me)C$\underline{H}_aH_b$CH=CHC(O)OCH(CH(Me)$_2$), 4.16 (dd, J = 16.6, 6.0 Hz, 1H, C(O)N(Me)$CH_a\underline{H}_b$CH=CHC(O)OCH(CH(Me)$_2$), 3.29 (s, 3H, CH(O$\underline{Me}$)CH_aH_bCH(OC(O))CH_aH_b), 3.12–3.07 (m, 1H, C$\underline{H}$(OMe)CH_aH_bCH(OC(O))CH_aH_b), 3.06 (s, 3H, C(O)N($\underline{Me}$)CH_aH_bCH=CHC(O)OCH(CH(Me)$_2$), 2.61–2.52 (m, 1H,

CH(OC(O))$CH_2CH_2C\underline{H}_aH_bC(O)N(Me)CH_aH_b$), 2.51–2.42 (m, 1H, $C(O)N(Me)CH_aH_bCH{=}CHC(O)OCH(C\underline{H}(Me)_2)$, 2.21–2-13 (m, 1H, $CH(OC(O))CH_2CH_2CH_a\underline{H}_bC(O)N(Me)CH_aH_b$), 1.75–1.57 (m, 7H, $CH(OMe)C\underline{H}_a\underline{H}_bCH(OC(O))C\underline{H}_a\underline{H}_bCH_2$, $CH_3CH_2CH_2C\underline{H}_aH_bC\underline{H}_a\underline{H}_bCH(OMe)$), 1.44–1.26 (m, 7H, $CH(OMe)CH_aH_bCH(OC(O))CH_aH_bC\underline{H}_2$, $CH_3C\underline{H}_2C\underline{H}_2CCH_a\underline{H}_bCH_aH_bCH(OMe)$), 1.04 (t, J = 6.4 Hz, 6H, $C(O)N(Me)CH_aH_bCH{=}CHC(O)OCH(CH(\underline{Me})_2)$, 0.89 (t, J = 6.4 Hz, 6H, $C\underline{H}_3CH_2CH_2CCH_aH_bCH_aH_bCH(OMe)$);

^{13}C NMR (126 MHz, $CDCl_3$) δ 172.9 (C=O, amide), 168.6 ($\underline{C}$=O),165.3 ($\underline{C}$=O), 140.2 ($C\underline{H}$=CH), 121.8 ($C\underline{H}$=CH), 77.7 ($\underline{C}$H), 77.4 ($\underline{C}$H), 73.9 ($\underline{C}$H), 56.9 ($\underline{C}H_3$), 48.2 ($\underline{C}H_2$), 37.6 ($\underline{C}H_2$), 34.2 ($\underline{C}H_2$), 34.1 ($\underline{C}H_3$), 33.4 ($\underline{C}H_2$) , 32.6 ($\underline{C}H_2$), 32.2 ($\underline{C}H_2$), 29.5 ($\underline{C}$H) 24.5 ($\underline{C}H_2$), 22.8 ($\underline{C}H_2$), 20.0 ($\underline{C}H_2$), 19.2 ($\underline{C}H_3$), 17.7 ($\underline{C}H_3$), 14.2 ($\underline{C}H_3$);

HRMS (ESI-TOF) m/z: $[M + Na]^+$ Calcd for $C_{23}H_{39}NO_6Na$ 448.2675; Found 448.2690.

(*S*,*Z*)-14-((*S*)-2-methoxyheptyl)-9-methyl-1,4-dioxa-9-azacyclotetradec-6-ene-2,5,10-trione ($C_{20}H_{33}NO_6$, 3.10.2)

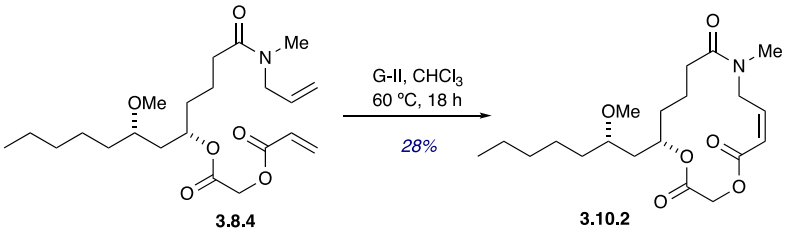

To a solution of diene **3.8.4** (12 mg, 0.03 mmol, 1 equiv.) in $CHCl_3$ (30 mL, 0.001 M) in a round-bottom flask added G-II catalyst (5.0 mg, 0.006 mmol, 20 mol%) and stirred at 60 ºC for 18 hours (complete by TLC). The solvent was evaporated under reduced pressure. Flash column chromatography (silica, 0%–50% EtOAc in hexanes) was performed to obtain macrocycle (**3.10.2**) (3.2 mg, 0.008 mmol, 28% yield) as a thick brown oil. TLC (EtOAc/hexane, 3/1): $R_f = 0.5$.

FTIR (neat): 3061, 3025, 2928, 2854, 1731, 1634, 1265, 1187, 1046, 986 cm^{-1};

Optical Rotation: $[\alpha]_D^{22}$ = -10.1 (c = 0.1 , $CHCl_3$);

^{1}H NMR (500 MHz, $CDCl_3$) δ 6.32 (td, J = 11.7, 3.8 Hz, 1H, C(O)N(Me)$CH_aH_bC\underline{H}$=CHC(O)OCH_aH_b), 6.02 (d, J = 11.5 Hz, 1H, C(O)N(Me)CH_aH_bCH=C$\underline{H}$C(O)OCH_aH_b), 5.50 (dd, J = 16.5, 10.8 Hz, 1H, C(O)N(Me)C$\underline{H}_aH_b$CH=CHC(O)OCH_aH_b), 5.36–5.31 (m, 1H, CH(OMe)$CH_aH_bC\underline{H}$(OC(O))CH_aH_b), 4.84 (d, J = 15.4 Hz, 1H, C(O)N(Me)CH_aH_bCH=CHC(O)OC$\underline{H}_aH_b$), 4.37 (d, J = 15.4 Hz, 1H, C(O)N(Me)CH_aH_bCH=CHC(O)O$CH_a\underline{H}_b$), 3.59–3.52 (m, 1H, C(O)N(Me)$CH_a\underline{H}_bCH$=CHC(O)OCH_aH_b), 3.21 (s, 3H, CH(O$\underline{Me}$)CH_aH_bCH(OC(O))CH_aH_b), 3.01–2.98 (m, 1H, C$\underline{H}$(OMe)CH_aH_bCH(OC(O))CH_aH_b), 2.98 (s, 3H,

C(O)N(Me)CH_aH_bCH=CHC(O)OCH_aH_b), 2.37–2.31 (m, 1H, CH(OC(O))$CH_2CH_2CH_aH_b$C(O)N(Me)CH_aH_b), 2.19–2.09 (m, 1H CH(OC(O))$CH_2CH_2CH_aH_b$C(O)N(Me)CH_aH_b), 1.66–1.55 (m, 6H, CH(OMe)CH_aH_bCH(OC(O))C$H_aH_b$$CH_2$, $CH_3CH_2CH_2CH_2CH_aH_b$CH(OMe)), 1.28–1.19 (m, 8H, CH(OMe)CH_aH_bCH(OC(O))CH_aH_bCH_2, $CH_3CH_2CH_2CH_2CH_aH_b$CH(OMe)), 0.89 (t, J = 6.5 Hz, 3H, $CH_3CH_2CH_2CH_2CH_aH_b$CH(OMe));

^{13}C NMR (126 MHz, $CDCl_3$) δ 173.7 (C=O, amide) 167.0 (C=O), 165.6 (C=O), 142.6 (CH=CH), 120.7 (CH=CH), 77.4 (CH), 72.6 (CH), 61.9 (CH_2), 57.1 (CH_3), 47.2 (CH_2), 36.6 (CH_2), 34.8 (CH_2), 33.7 (CH_3) , 33.2 (CH_2), 32.2 (CH_2), 29.9 (CH_2), 24.5 (CH_2), 22.8 (CH_2), 19.2 (CH_2), 14.2 (CH_3);

HRMS (ESI-TOF) m/z: $[M + Na]^+$ Calcd for $C_{20}H_{33}NO_6Na$ 406.2206; Found 406.2221.

(3*S*,14*S*,*Z*)-3-isopropyl-14-((*S*)-2-methoxy-5-phenylpentyl)-9-methyl-1,4-dioxa-9-azacyclotetradec-6-ene-2,5,10-trione ($C_{27}H_{39}NO_6$, 3.10.5)

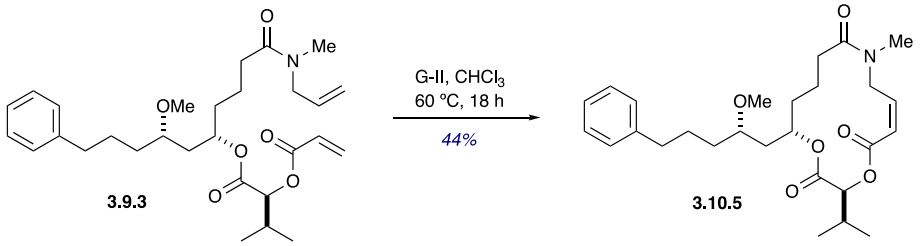

To a solution of diene **3.9.3** (12 mg, 0.02 mmol, 1 equiv.) in $CHCl_3$ (20 mL, 0.001 M) in a pressure vial was added G-II catalyst (4.1 mg, 0.004 mmol, 20 mol%) and stirred at 60 ºC for 18 hours (complete by TLC). The solvent was evaporated under reduced pressure. Flash column chromatography (silica, 0%–50% EtOAc in hexanes) was performed to obtain macrocycle **3.10.5** (4.2 mg, 0.008 mmol, 44% yield) as a thick brown oil. TLC (EtOAc/hexane, 3/1): R_f = 0.4.

FTIR (neat): 3024, 2923, 2852, 1737, 1646, 1454, 1260, 1167, 1098, 799 cm^{-1};

Optical Rotation: $[\alpha]_D^{22}$ = -12.4 (c = 0.15 , $CHCl_3$);

^{1}H NMR (500 MHz, $CDCl_3$) δ 7.29–7.14 (m, 5H, $C_6\underline{H}_5CH_2(CH_2)_2CH(OMe)$, 6.22 (ddd, J = 11.9, 8.5, 5.8 Hz, 1H, $C(O)N(Me)CH_aH_bC\underline{H}$=$CHC(O)OCH(CH(Me)_2)$, 5.94 (d, J = 17.8 Hz, 1H, $C(O)N(Me)CH_aH_bCH$=$C\underline{H}C(O)OCH(CH(Me)_2)$, 5.24 (dd, J = 8.6, 4.15 Hz, 1H, $CH(OMe)CH_aH_bC\underline{H}(OC(O))CH_aH_b$), 5.16 (d, J = 4.3 Hz, 1H, $C(O)N(Me)CH_aH_bCH$=$CHC(O)OC\underline{H}(CH(Me)_2)$, 4.78 (dd, J = 16.7, 8.6 Hz, 1H, $C(O)N(Me)C\underline{H}_aH_bCH$=$CHC(O)OCH(CH(Me)_2)$, 4.14 (dd, J = 16.0, 5.6 Hz, 1H, $C(O)N(Me)CH_a\underline{H}_bCH$=$CHC(O)OCH(CH(Me)_2)$, 3.27 (s, 3H, $CH(O\underline{Me})CH_aH_bCH(OC(O))CH_aH_b$), 3.15–3.08 (m, 1H, $C\underline{H}(OMe)CH_aH_bCH(OC(O))CH_aH_b$), 3.05 (s, 3H, $C(O)N(\underline{Me})CH_aH_bCH$=$CHC(O)OCH(CH(Me)_2)$, 2.61 (dd, J = 8.0, 4.7 Hz, 2H,

$C_6H_5C\underline{H}_2(CH_2)_2CH(OMe)$, 2.58–2.51 (m, 1H, $CH(OC(O))CH_2CH_2C\underline{H}_aH_bC(O)N(Me)CH_aH_b$), 2.50–2.43 (m, 1H, $C(O)N(Me)CH_aH_bCH{=}CHC(O)OCH(C\underline{H}(Me)_2)$, 2.15 (ddd, J = 15.6, 12.5, 4.7 Hz, 1H, $CH(OC(O))CH_2CH_2CH_a\underline{H}_bC(O)N(Me)CH_aH_b$), 1.78–1.57 (m, 10H, $CH(OMe)C\underline{H}_a\underline{H}_bCH(OC(O))C\underline{H}_a\underline{H}_bC\underline{H}_2$, $C_6H_5CH_2C\underline{H}_2C\underline{H}_a\underline{H}_bCH(OMe)$), 1.04 (t, J = 6.4 Hz, 6H, $C(O)N(Me)CH_aH_bCH{=}CHC(O)OCH(CH(\underline{Me})_2)$);

^{13}C NMR (126 MHz, $CDCl_3$) δ 173.5 (C=O, amide), 168.5 ($\underline{C}$=O),165.3 ($\underline{C}$=O), 142.4 ($\underline{C}_{Ar}$), 140.2 ($C\underline{H}$=CH), 128.6 (2, $\underline{C}H_{Ar}$), 128.4 (2, $\underline{C}H_{Ar}$), 125.9 ($\underline{C}H_{Ar}$), 121.7 ($C\underline{H}$=CH), 77.6 ($\underline{C}$H), 77.4 ($\underline{C}$H), 73.9 ($\underline{C}$H), 57.0 ($\underline{C}H_3$), 48.2 ($\underline{C}H_2$), 37.6 ($\underline{C}H_2$), 36.1 ($\underline{C}H_2$), 34.1 ($\underline{C}H_3$), 34.1 ($\underline{C}H_2$), 33.0 ($\underline{C}H_2$) , 32.5 ($\underline{C}H_2$), 29.8 ($\underline{C}$H) 26.6 ($\underline{C}H_2$), 19.9 ($\underline{C}H_2$), 19.2 ($\underline{C}H_3$), 17.7 ($\underline{C}H_3$);

HRMS (ESI-TOF) m/z: $[M + Na]^+$ Calcd for $C_{27}H_{39}NO_6Na$ 496.2675; Found 496.2667.

(*S*,*Z*)-14-((*S*)-2-methoxy-5-phenylpentyl)-9-methyl-1,4-dioxa-9-azacyclotetradec-6-ene-2,5,10-trione ($C_{24}H_{33}NO_6$, 3.10.4)

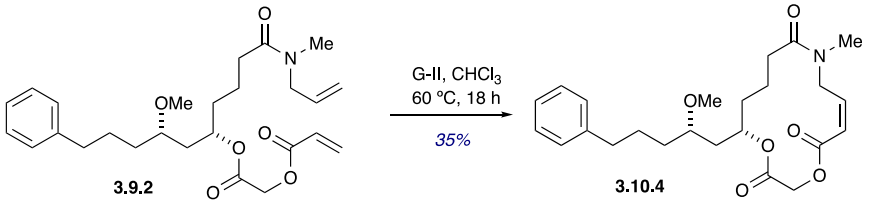

To a solution of diene **3.9.2** (8 mg, 0.02 mmol) in $CHCl_3$ (20 mL, 0.001 M) in a round-bottom flask, was added G-II catalyst (3.4 mg, 0.004 mmol, 20 mol%) and stirred at 60 ºC for 18 hours (complete by TLC). The solvent was evaporated under reduced pressure. Flash column chromatography (silica, 0%–50% EtOAc in hexanes) was performed to obtain macrocycle **3.10.4** (3.2 mg, 0.007 mmol, 35% yield) as a thick yellow oil. TLC (EtOAc/hexane, 3/1): R_f = 0.4.

FTIR (neat): 3024, 2923, 2852, 1736, 1645, 1454, 1426, 1283, 1028 cm^{-1};

Optical Rotation: $[a]_D^{21}$ = -7.1 (c = 0.14 , $CHCl_3$);

^{1}H NMR (500 MHz, $CDCl_3$) δ 7.30–7.14 (m, 5H, $C_6\underline{H}_5CH_2(CH_2)_2CH(OMe)$, 6.37 (td, J = 13.5, 11.4, 5.0 Hz, 1H, $C(O)N(Me)CH_aH_bC\underline{H}$=$CHC(O)OCH_aH_b$), 6.06 (d, J = 11.9 Hz, 1H, $C(O)N(Me)CH_aH_bCH$=$C\underline{H}C(O)OCH_aH_b$), 5.56 (dd, J = 16.7, 10.8 Hz, 1H, $C(O)N(Me)C\underline{H}_aH_bCH$=$CHC(O)OCH_aH_b$), 5.43–5.34 (m, 1H, $CH(OMe)CH_aH_bC\underline{H}(OC(O))CH_aH_b$), 4.89 (d, J = 15.4 Hz, 1H, $C(O)N(Me)CH_aH_bCH$=$CHC(O)OC\underline{H}_aH_b$), 4.40 (d, J = 15.5 Hz, 1H, $C(O)N(Me)CH_aH_bCH$=$CHC(O)OCH_a\underline{H}_b$), 3.66–3.57 (m, 1H, $C(O)N(Me)CH_a\underline{H}_bCH$=$CHC(O)OCH_aH_b$), 3.26 (s, 3H, $CH(O\underline{Me})CH_aH_bCH(OC(O))CH_aH_b$), 3.11–3.03 (m, 1H, $C\underline{H}(OMe)CH_aH_bCH(OC(O))CH_aH_b$), 3.04 (s, 3H,

C(O)N(Me)CH_aH_bCH=CHC(O)OCH_aH_b), 2.61 (t, *J* = 7.5 Hz, 2H, $C_6H_5CH_2(CH_2)_2$CH(OMe), 2.42–2.35 (m, 1H, CH(OC(O))$CH_2CH_2CH_aH_b$C(O)N(Me)CH_aH_b), 2.22–2.14 (m, 1H, CH(OC(O))$CH_2CH_2CH_aH_b$C(O)N(Me)CH_aH_b), 1.70–1.55 (m, 8H, CH(OMe)CH_aH_bCH(OC(O))$CH_aH_b$$CH_2$, $C_6H_5CH_2CH_2CH_aH_b$CH(OMe)), 1.31–1.25 (m, 2H, $C_6H_5CH_2CH_2CH_aH_b$CH(OMe));

^{13}C NMR (126 MHz, $CDCl_3$) δ 173.7 (C=O, amide) 167.0 (C=O), 165.6 (C=O), 142.6 (C_{Ar}), 142.6 (CH=CH), 128.6 (2, CH_{Ar}), 128.5 (2, CH_{Ar}), 125.9 (CH_{Ar}), 120.7 (CH=CH), 77.4 (CH), 72.5 (CH), 61.9 (CH_2), 57.1 (CH_3), 47.2 (CH_2), 36.6 (CH_2), 36.2 (CH_2), 34.7 (CH_2), 33.7 (CH_3) , 33.2 (CH_2), 29.8 (CH_2), 26.8 (CH_2), 19.2 (CH_2);

HRMS (ESI-TOF) m/z: $[M + Na]^+$ Calcd for $C_{24}H_{33}NO_6Na$ 454.2206; Found 454.2213.

(*S*,*Z*)-14-((*S*)-2-methoxyheptyl)-9-(4-(trifluoromethyl)benzyl)-1,4-dioxa-9-azacyclotetradec-6-ene-2,5,10-trione ($C_{27}H_{36}F_3NO_6$, 3.10.3)

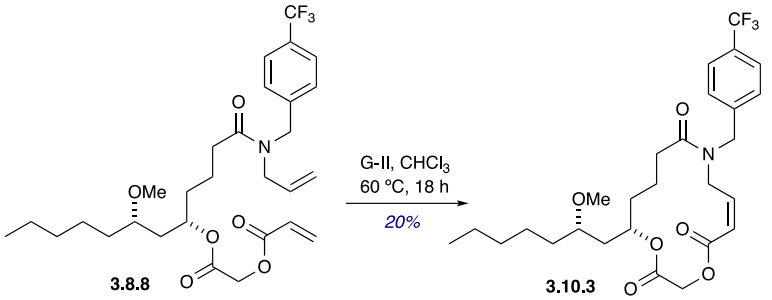

To a solution of diene **3.8.8** (8.5 mg, 0.015 mmol, 1 equiv.) in $CHCl_3$ (15 mL, 0.001 M) in a pressure vial was added G-II catalyst (2.5 mg, 0.003 mmol, 20 mol%) and stirred at 60 ºC for 18 hours (complete by TLC). The solvent was evaporated under reduced pressure. Flash column chromatography (silica, 0%–50% EtOAc in hexanes) was performed to obtain macrocycle **3.10.3** (1.6 mg, 0.003 mmol, 20% yield) as a thick brown oil. TLC (EtOAc/hexane, 1/1): R_f = 0.3.

FTIR (neat): 2924, 2853,1731, 1650, 1462, 1325, 1261, 1165, 1125 cm^{-1};

Optical Rotation: $[\alpha]_D^{20}$ = -10.0 (c = 0.04 , $CHCl_3$);

^{1}H NMR (500 MHz, $CDCl_3$) δ 7.60 (d, J = 8.0 Hz, 2H, C(O)N($CH_2C_6\underline{H}_{2a}H_{2b}CF_3$)$CH_2CH$=CH), 7.38 (d, J = 8.0 Hz, 2H, C(O)N($CH_2C_6H_{2a}\underline{H}_{2b}CF_3$)$CH_2CH$=CH), 6.16 (td, J = 11.0, 4.0 Hz, 1H, C(O)N($CH_2C_6H_{2a}H_{2b}CF_3$)$CH_aH_bC\underline{H}$=CHC(O)OCH_aH_b), 6.06 (d, J = 11.6 Hz, 1H, C(O)N($CH_2C_6H_{2a}H_{2b}CF_3$)CH_aH_bCH=C$\underline{H}$C(O)OCH_aH_b), 5.46–5.41 (m, 1H, CH(OMe)$CH_aH_bC\underline{H}$(OC(O))CH_aH_b), 5.41 (d, J = 10.2 Hz, 1H, C(O)N($CH_2C_6H_{2a}H_{2b}CF_3$)$C\underline{H}_aH_bCH$=CHC(O)OCH_aH_b), 5.05 (d, J = 15.2 Hz, 1H, C(O)N($C\underline{H}_aH_bC_6H_{2a}H_{2b}CF_3$)$CH_2CH$=CH), 4.92 (d, J = 15.5 Hz, 1H, C(O)N($CH_2C_6H_{2a}H_{2b}CF_3$)CH_aH_bCH=CHC(O)$OC\underline{H}_aH_b$), 4.46 (d, J = 15.5 Hz, 1H,

C(O)N($CH_2C_6H_{2a}H_{2b}CF_3$)CH_aH_bCH=CHC(O)O$CH_a\underline{H}_b$), 4.44 (d, *J* = 15.3 Hz, 1H, C(O)N($CH_a\underline{H}_bC_6H_{2a}H_{2b}CF_3$)$CH_2CH$=CH), 3.59–3.52 (m, 1H, C(O)N($CH_2C_6H_{2a}H_{2b}CF_3$)$CH_a\underline{H}_b$CH=CHC(O)OCH_aH_b), 3.29 (s, 3H, CH(O$\underline{Me}$)CH_aH_bCH(OC(O))CH_aH_b), 3.09 (dd, *J* = 9.4, 4.26 Hz, 1H, C$\underline{H}$(OMe)CH_aH_bCH(OC(O))CH_aH_b), 2.49–2.40 (m, 1H, C$\underline{H}_a$$H_b$C(O)N($CH_2C_6H_{2a}H_{2b}CF_3$)$CH_aH_b$), 2.32–2.26 (m, 1H, $CH_a\underline{H}_b$C(O)N($CH_2C_6H_{2a}H_{2b}CF_3$)CH_aH_b), 1.78–1.64 (m, 6H, CH(OMe)C$\underline{H}_a\underline{H}_b$CH(OC(O))C$\underline{H}_a\underline{H}_b$$CH_2$, $CH_3CH_2CH_2CH_2C\underline{H}_a\underline{H}_b$CH(OMe)), 1.34–1.28 (m, 8H, CH(OMe)CH_aH_bCH(OC(O))$CH_aH_bC\underline{H}_2$, $CH_3C\underline{H}_2C\underline{H}_2C\underline{H}_2CH_aH_b$CH(OMe)), 0.88–0.87 (m, 3H, C$\underline{H}_3CH_2CH_2CH_2CH_aH_b$CH(OMe));

^{13}C NMR (126 MHz, $CDCl_3$) δ 174.0 (C=O, amide) 167.0 (C=O), 165.4 (C=O), 142.4 (CH=CH), 141.6 (C_{Ar}), 128.4 (2, CH_{Ar}), 128.4 (C_{Ar}), 125.9 (2, CH_{Ar}), 121.4 (CH=CH), 77.7 (CH), 74.0 (CH), 61.7 (CH_2), 57.0 (CH_3), 49.0 (CH_2), 44.6 (CH_2), 36.5 (CH_2), 34.4 (CH_2), 33.5 (CH_2), 32.9 (CH_2), 32.2 (CH_2), 24.5 (CH_2), 22.8 (CH_2), 19.2 (CH_2), 14.2 (CH_3);

Note: (^{13}C of CF_3 was not found; however, IR and ^{19}F data confirmed the presence of CF_3 group)

^{19}F NMR (471 MHz, $CDCl_3$) δ -62.55;

HRMS (ESI-TOF) m/z: $[M + Na]^+$ Calcd for $C_{27}H_{36}F_3NO_6Na$ 550.2392; Found 550.2422.

(*S*,*E*)-14-((*S*)-2-methoxyheptyl)-9-methyl-1,4-dioxa-9-azacyclotetradec-7-ene-2,5,10-trione ($C_{20}H_{33}NO_6$, 3.11.1)

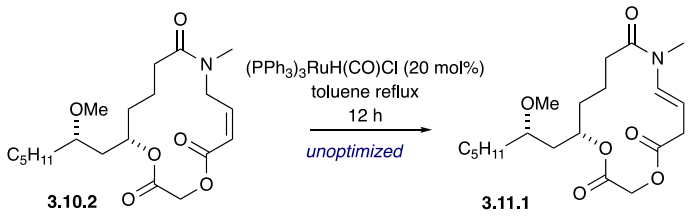

To a solution of diene **3.10.2** (3 mg, 0.007 mmol, 1 equiv.) in toluene (1 mL, ~0.1 M) in a pressure vial was added $(PPh_3)_3RuH(CO)Cl$ catalyst (1.5 mg, 0.0015 mmol, 20 mol%) and stirred at 80 ºC for 12 hours (complete by TLC). The solvent was evaporated under reduced pressure. Flash column chromatography (silica, 0%–50% EtOAc in hexanes) was performed to obtain macrocycle **3.11.1**. TLC (EtOAc/hexane, 1/1): R_f = 0.6. (rapid degradation was observed in standing conditions). The product was confirmed via NMR and Mass data of unpurified material.

^{1}H NMR (500 MHz, $CDCl_3$) δ 6.73 (d, *J* = 13.9 Hz, 1H, C(O)N(Me)CH=C<u>H</u>CH$_a$H$_b$C(O)OCH$_a$H$_b$), 5.16–5.05 (m, 2H, C(O)N(Me)C<u>H</u>=CHCH$_a$H$_b$C(O)OCH$_a$H$_b$, CH(OMe)CH$_a$H$_b$C<u>H</u>(OC(O))CH$_a$H$_b$), 4.57 (dd, *J* = 30.6, 16.7 Hz, 1H, C(O)N(Me)CH=CHCH$_a$H$_b$C(O)OC<u>H$_a$H$_b$</u>), 3.29–3.24 (m, 1H, C(O)N(Me)CH=CHC<u>H$_a$</u>H$_b$C(O)OCH$_a$H$_b$), 3.23 (s, 3H, CH(O<u>Me</u>)CH$_a$H$_b$CH(OC(O))CH$_a$H$_b$), 3.08 (d, *J* = 9.2 Hz, 1H, C(O)N(Me)CH=CHCH$_a$<u>H$_b$</u>C(O)OCH$_a$H$_b$), 3.05–3.02 (m, 1H, C<u>H</u>(OMe)CH$_a$H$_b$CH(OC(O))CH$_a$H$_b$), 3.00 (s, 3H, C(O)N(<u>Me</u>)CH=CHCH$_a$H$_b$C(O)OCH$_a$H$_b$), 2.61–2.55 (m, 1H, CH(OC(O))CH$_2$CH$_2$C<u>H$_a$</u>H$_b$C(O)N(Me), 2.40–2.49 (m, 1H,

$CH(OC(O))CH_2CH_2CH_a\underline{H}_bC(O)N(Me)$, Assignment of the protons from 2.00–0.00 ppm was difficult due to insufficient material and purification challenges ;

HRMS (ESI-TOF) m/z: $[M + Na]^+$ Calcd for $C_{20}H_{33}NO_6Na$ 406.2206; Found 406.2226.

5.2.3 NMR Spectra

(4*S*,6*S*)-4,6-diallyl-2-(allyloxy)-1,3,2-dioxaphosphinane 2-oxide ($C_{12}H_{19}O_4P$, 3.6.2)

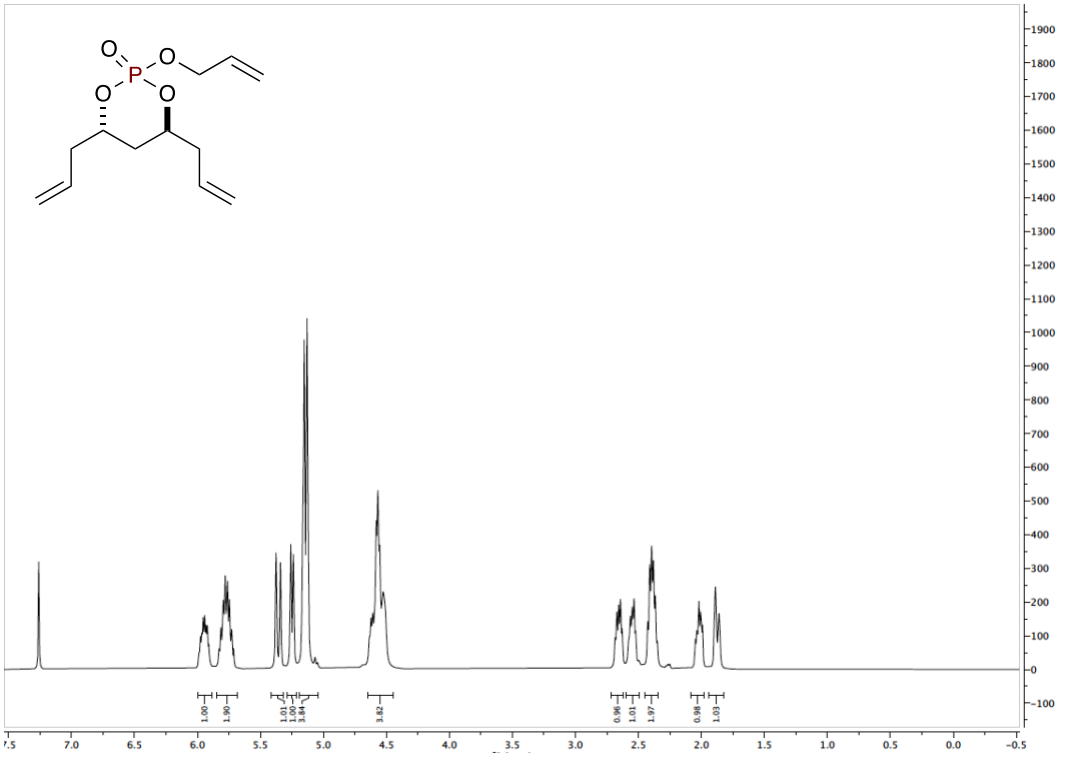

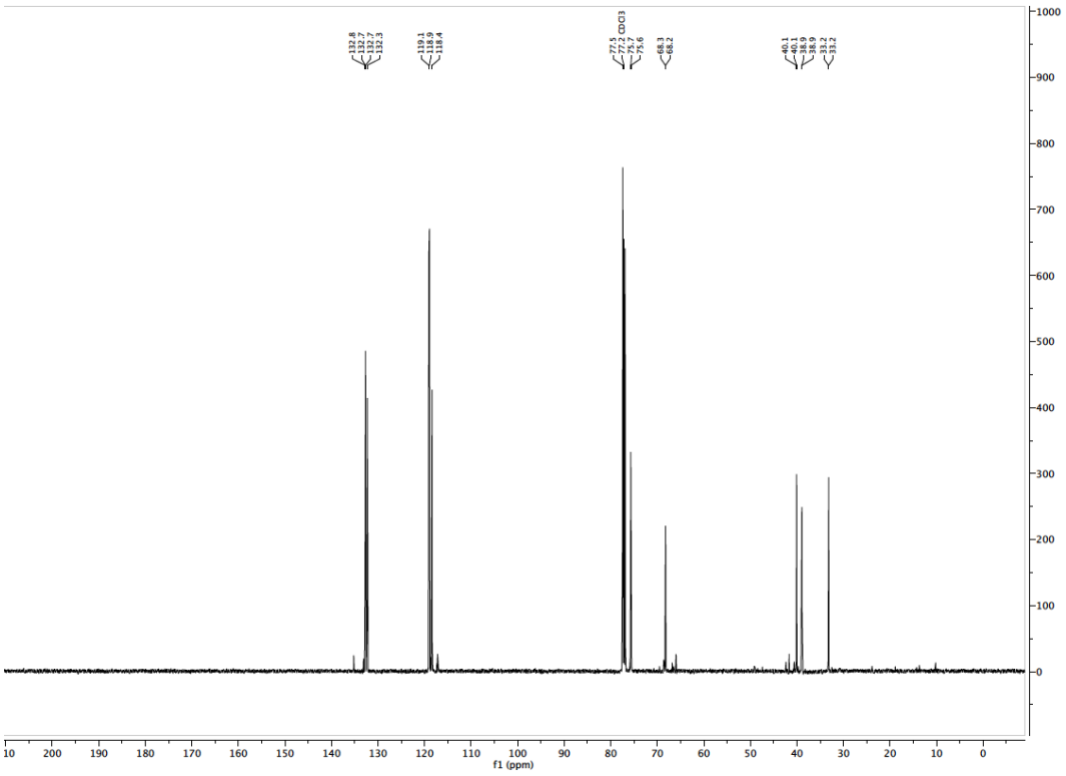

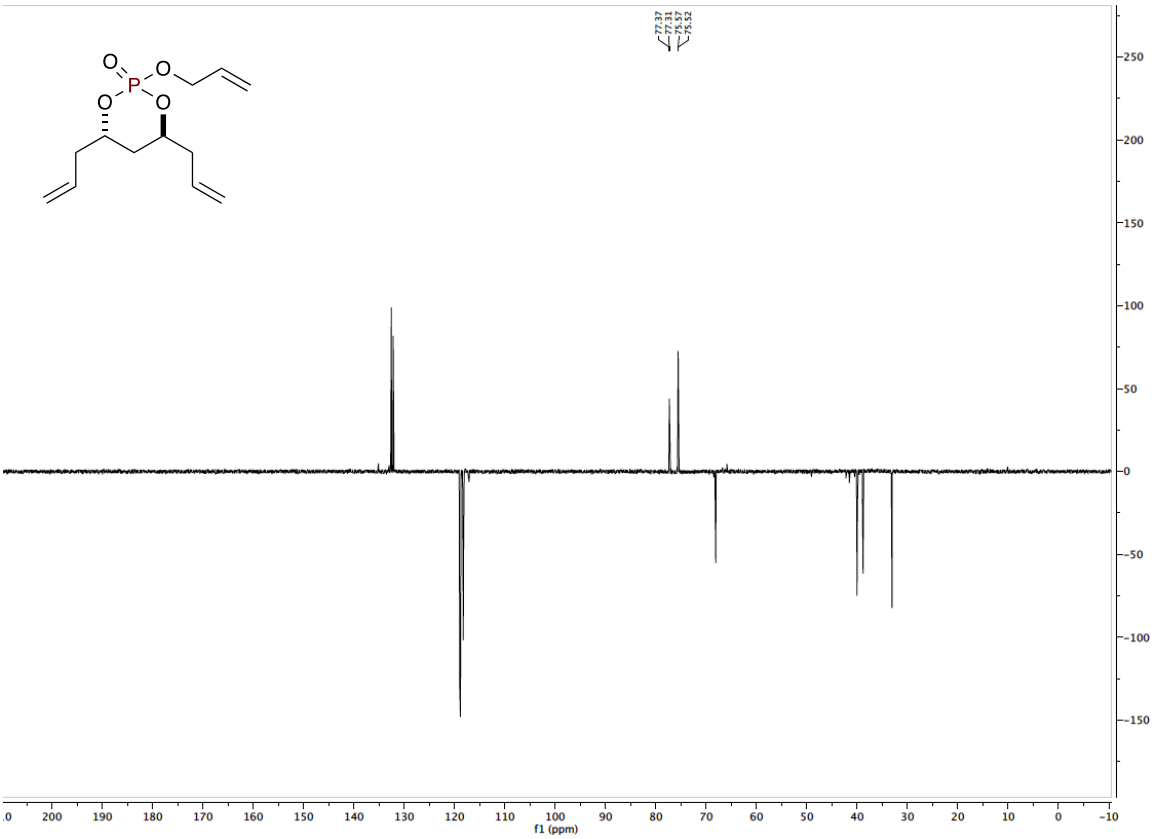
77.37
77.11
76.87
75.52
f1 (ppm)

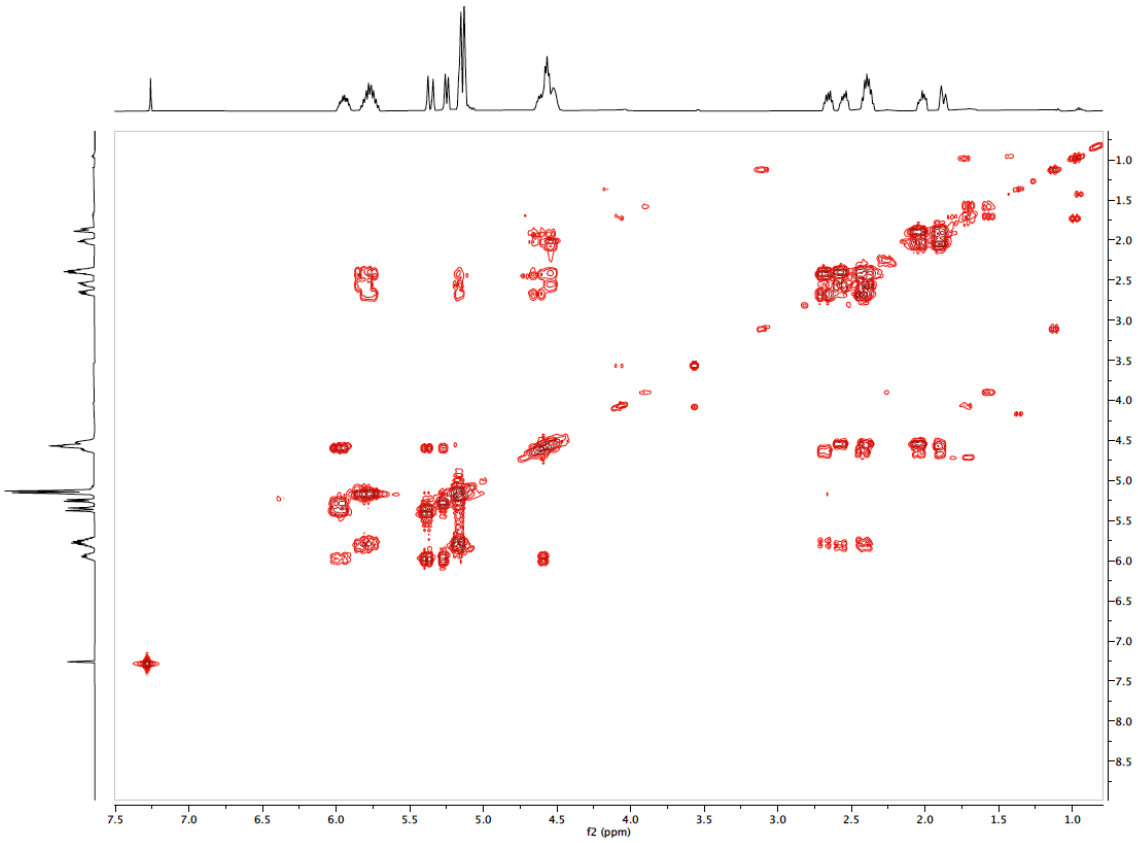
f2 (ppm)

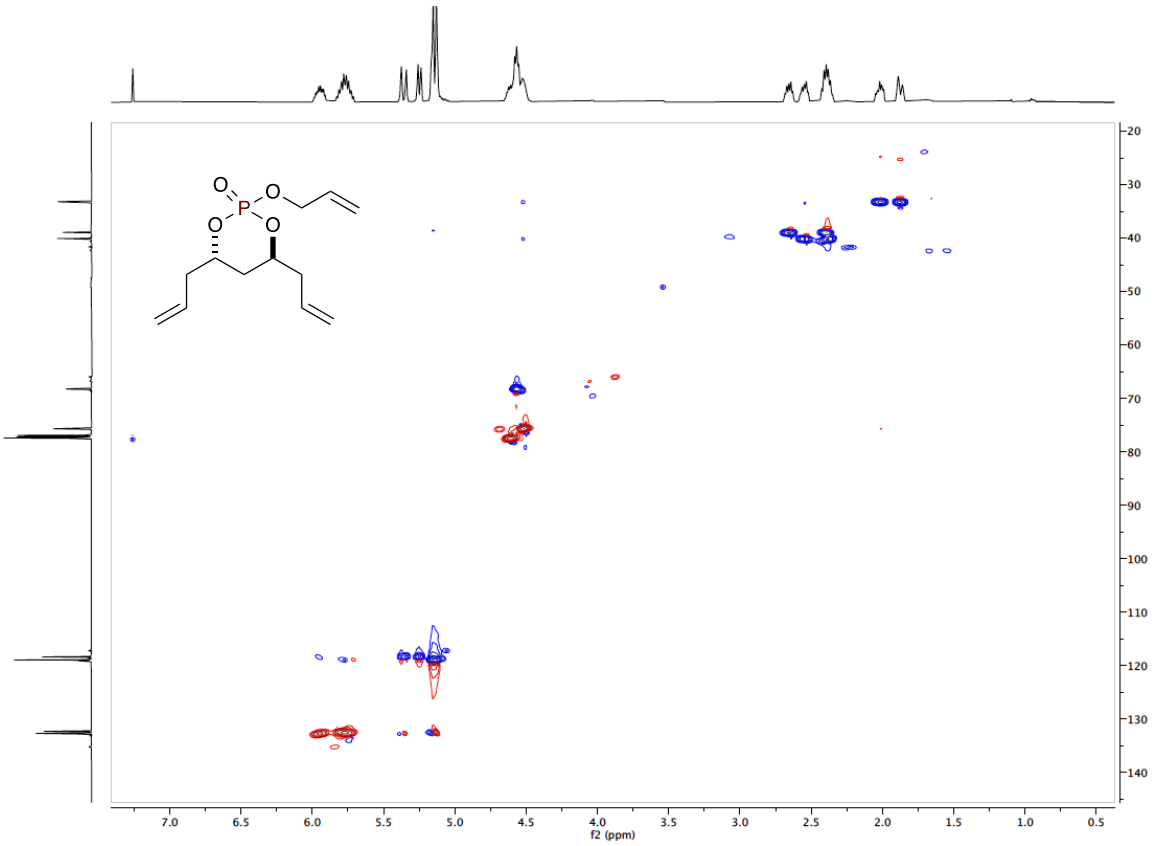
f2 (ppm)

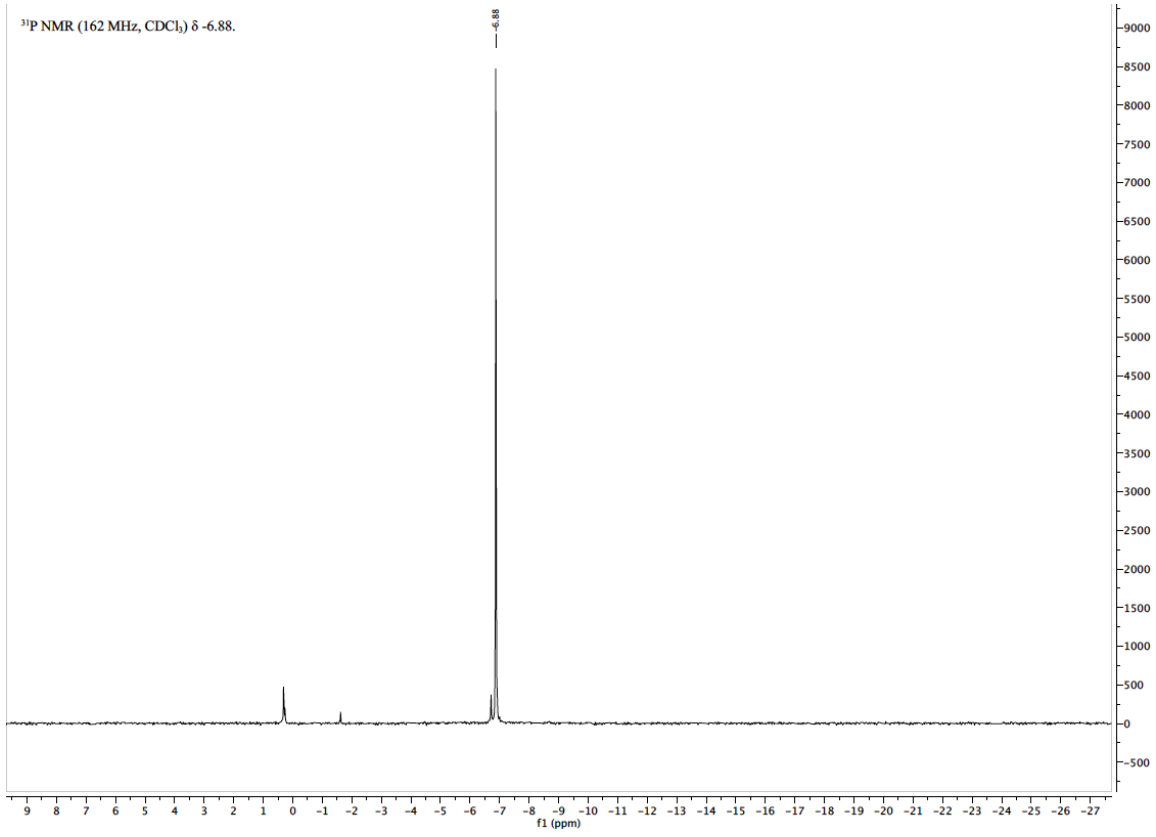
^{31}P NMR (162 MHz, $CDCl_3$) δ -6.88.
-6.88
f1 (ppm)

(5*S*,7*S*)-dodecane-1,5,7-triol ($C_{12}H_{26}O_3$, 3.7.3)

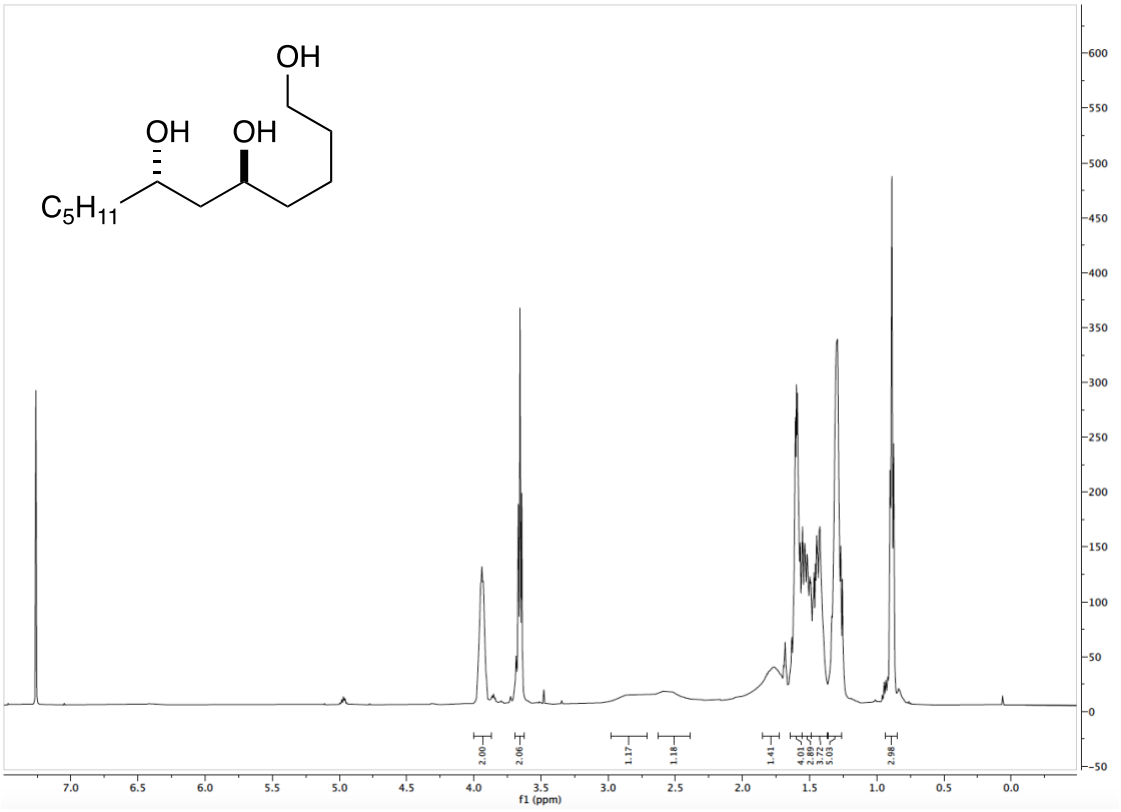

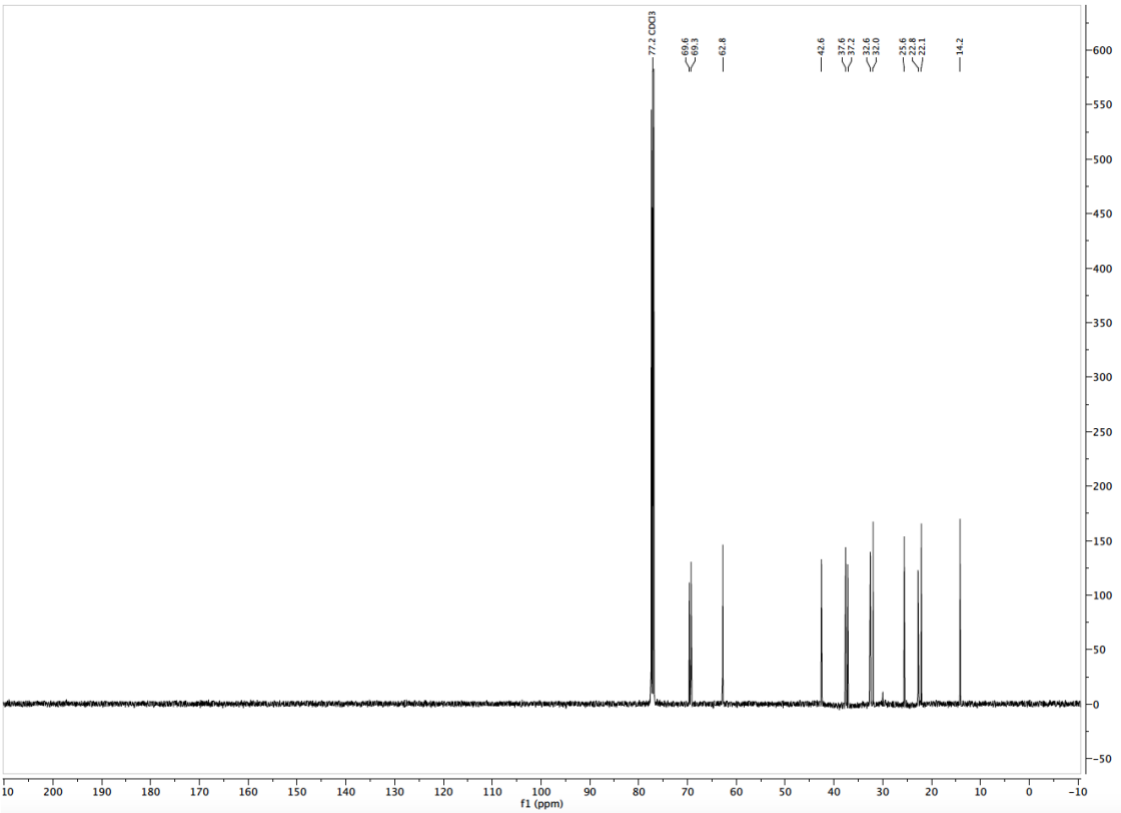

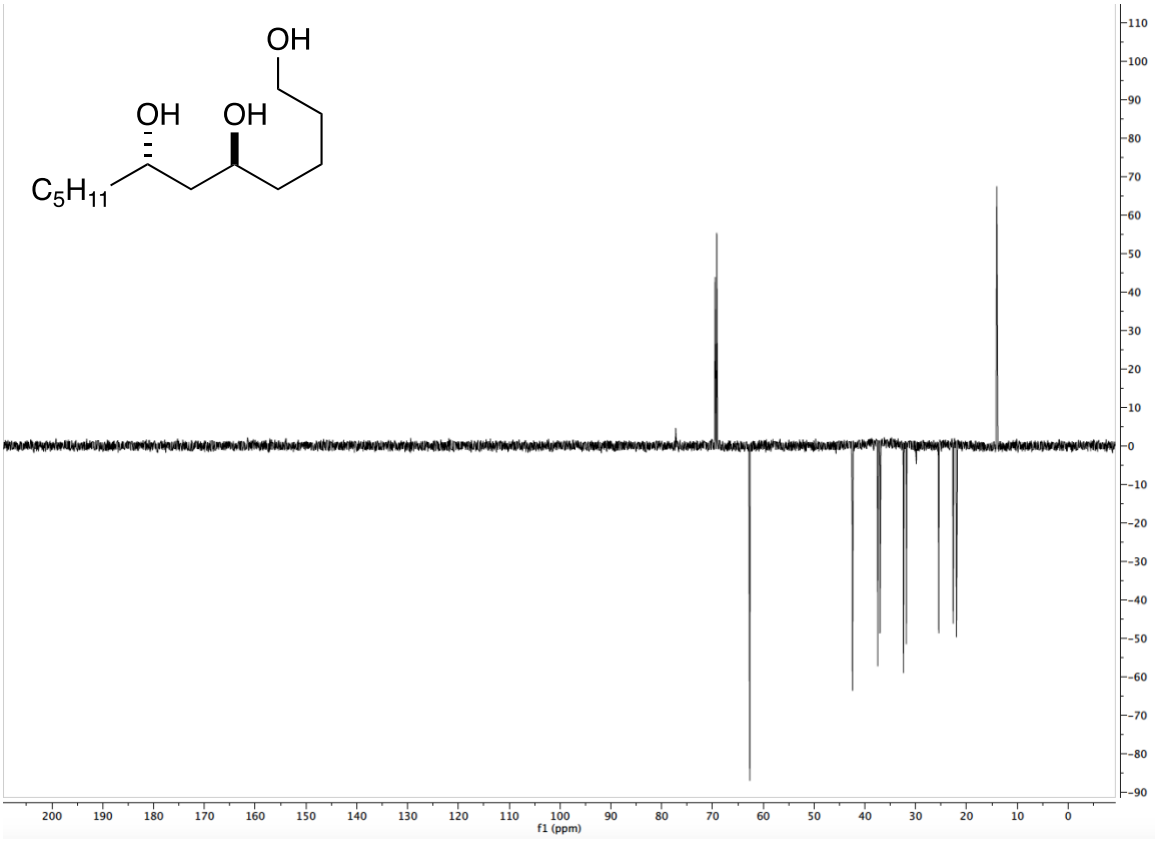
OH
OH
OH
C5H11
f1 (ppm)

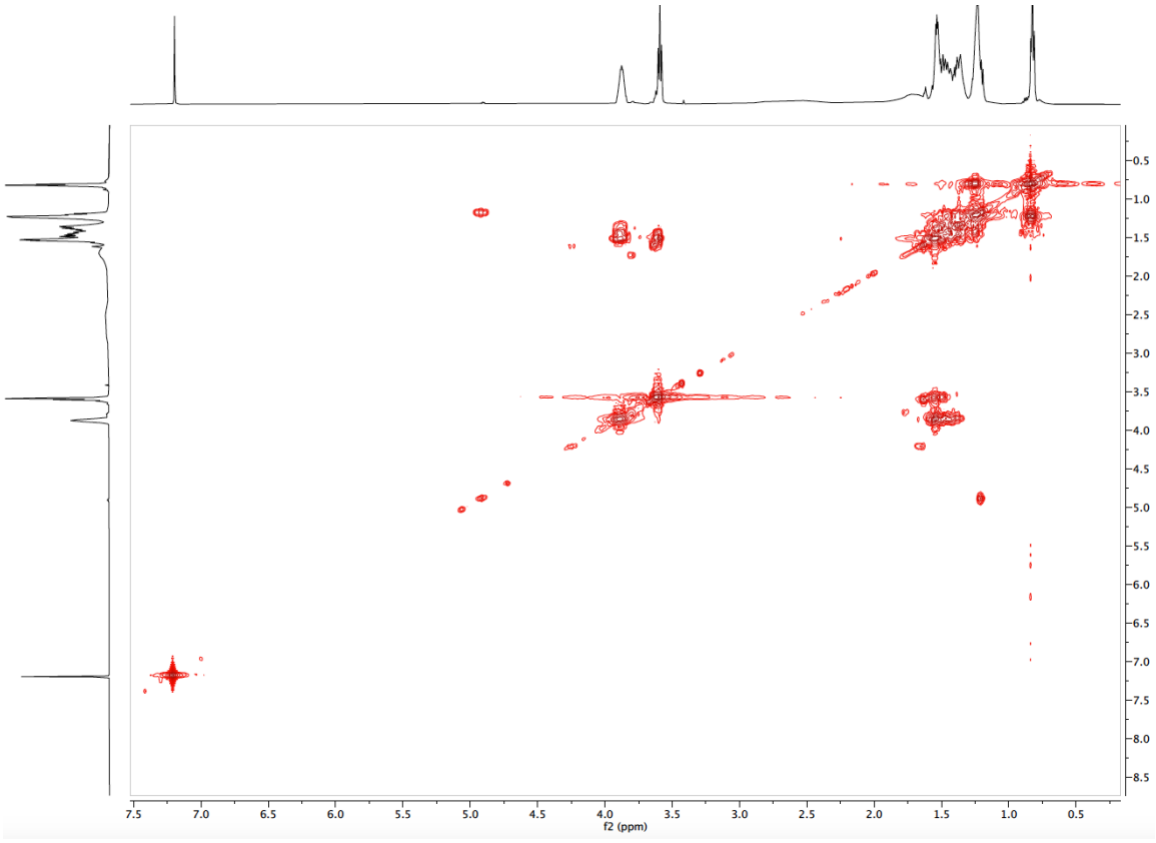
f2 (ppm)

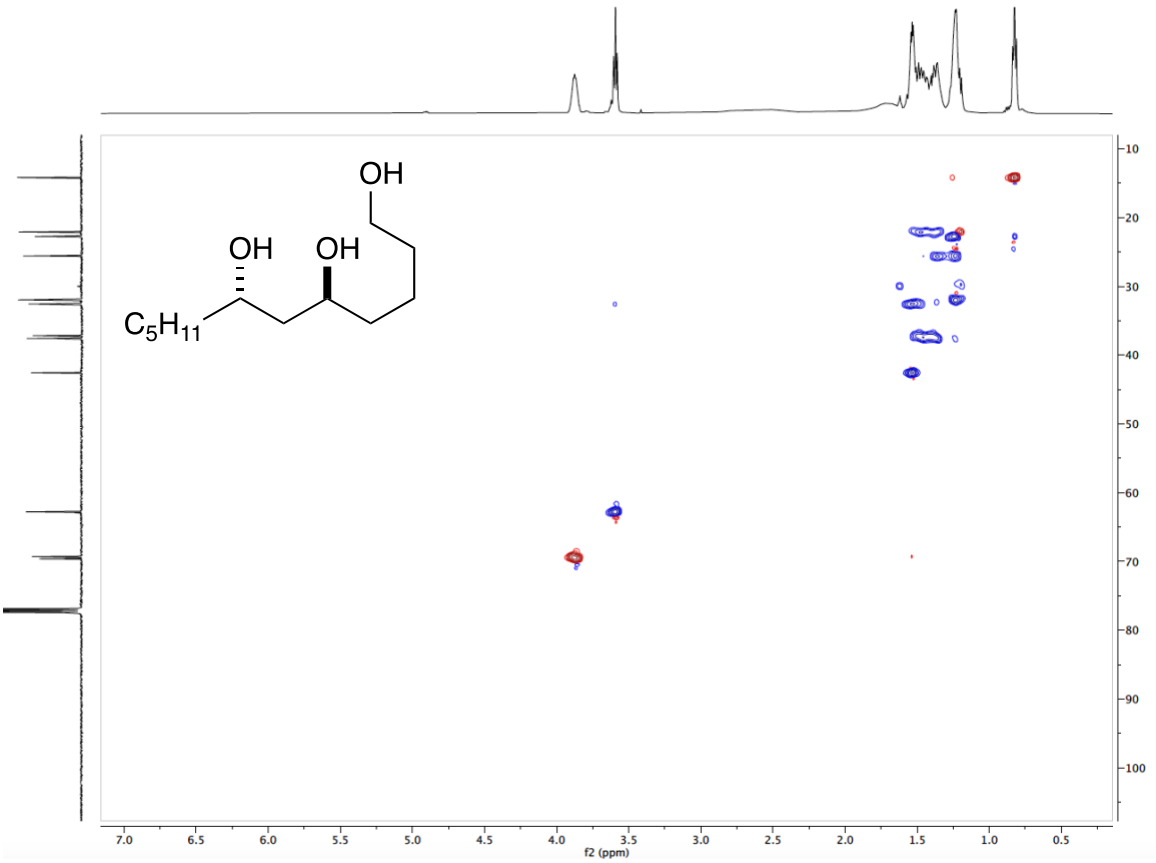
OH
OH
OH
C5H11
10
20
30
40
50
60
70
80
90
100
7.0
6.5
6.0
5.5
5.0
4.5
4.0
3.5
3.0
2.5
2.0
1.5
1.0
0.5
f2 (ppm)

(5*S*,7*S*)-10-phenyldecane-1,5,7-triol ($C_{16}H_{26}O_3$, 3.7.4)

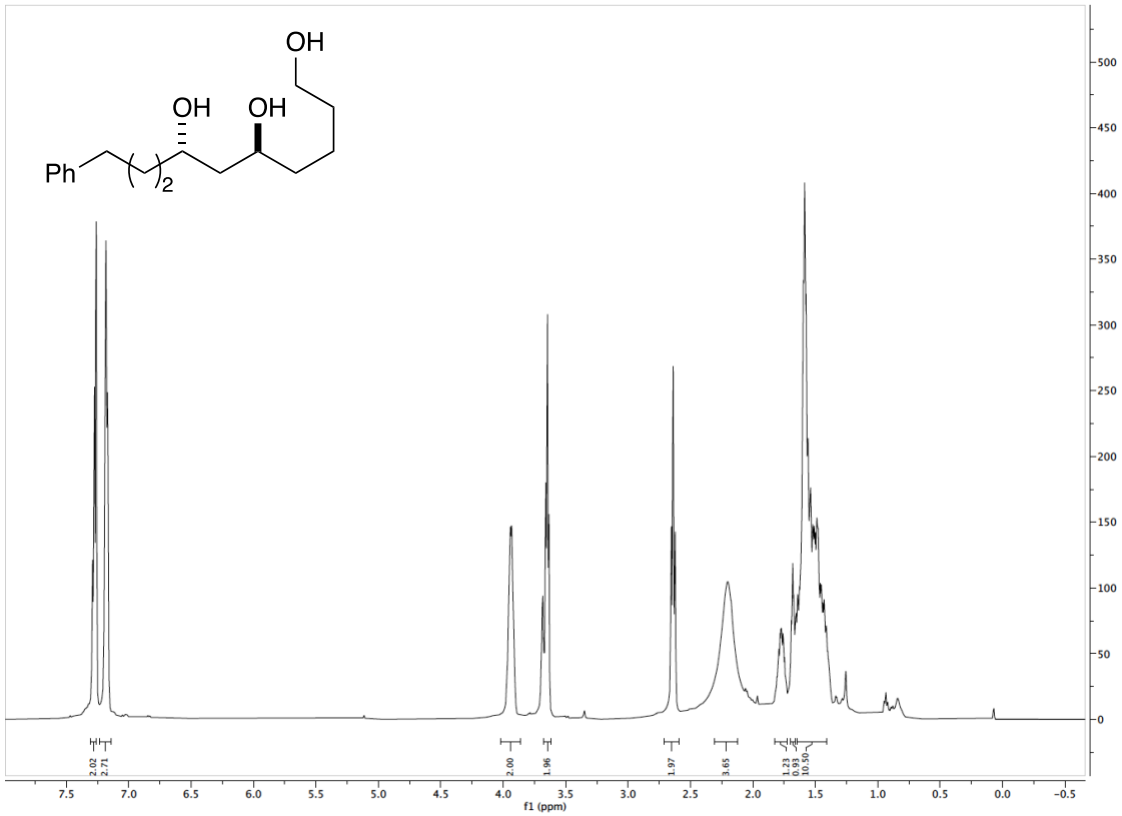

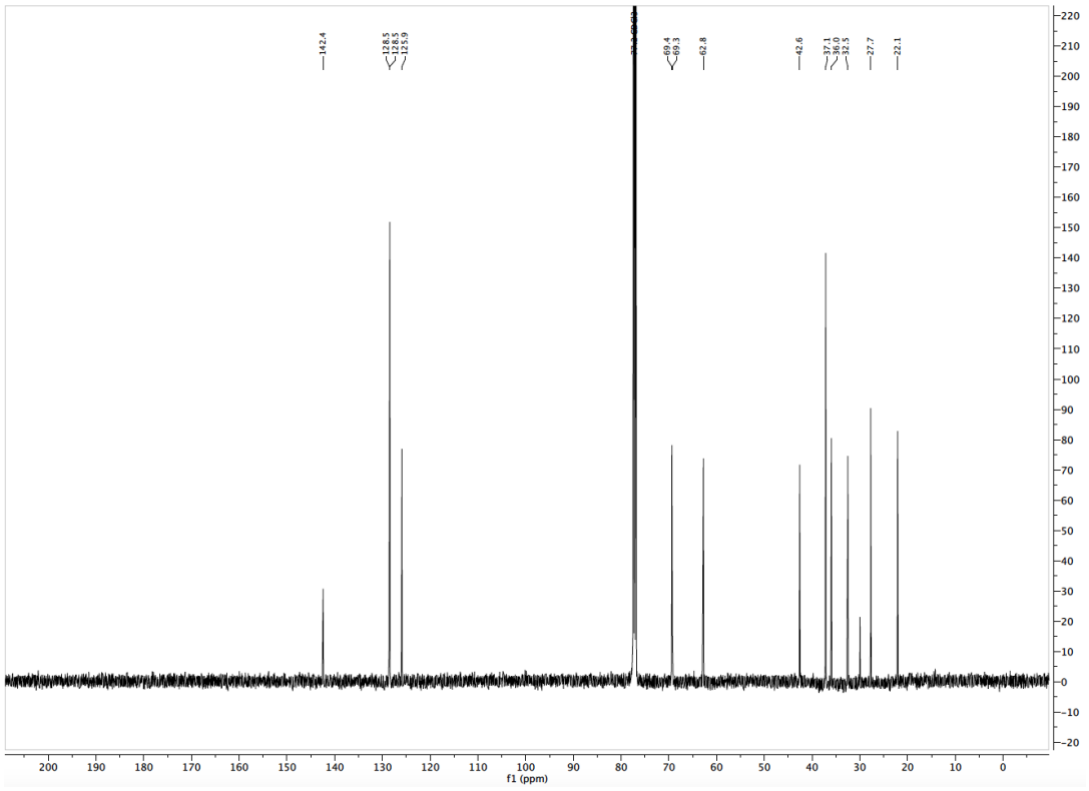

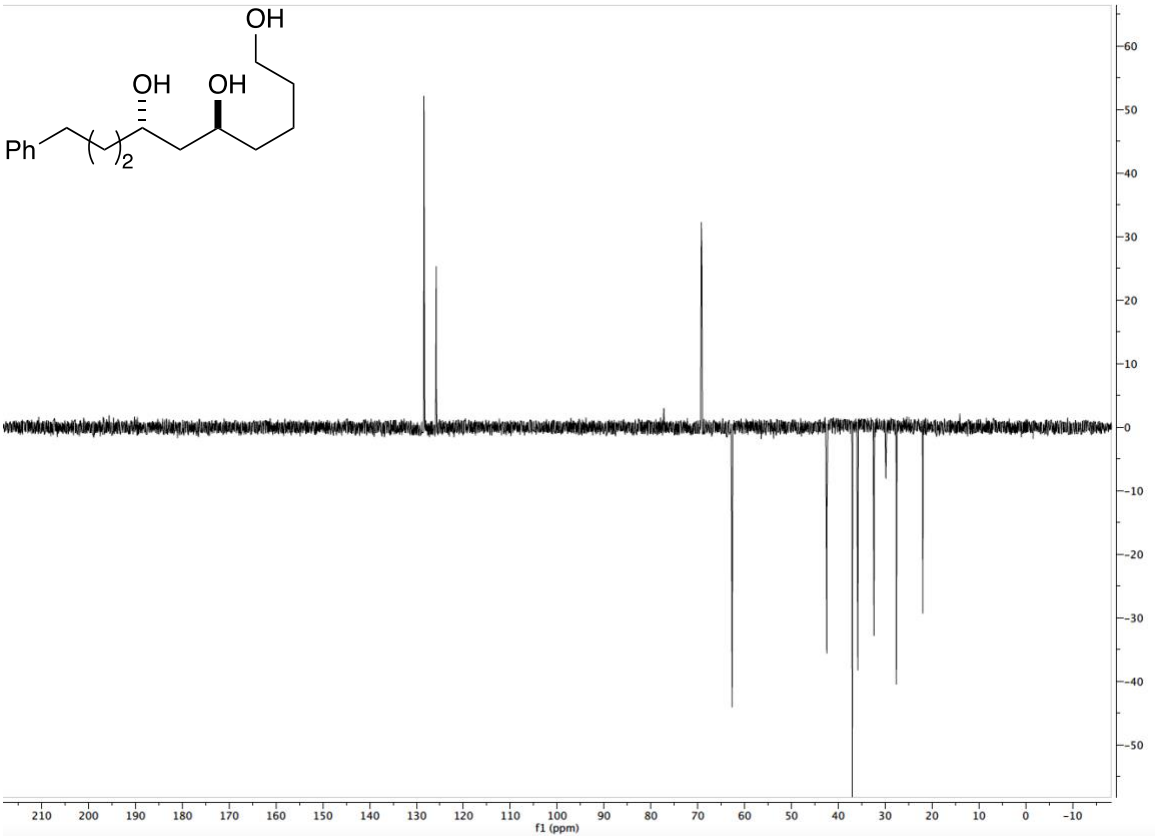
OH
OH
OH
Ph
2
f1 (ppm)

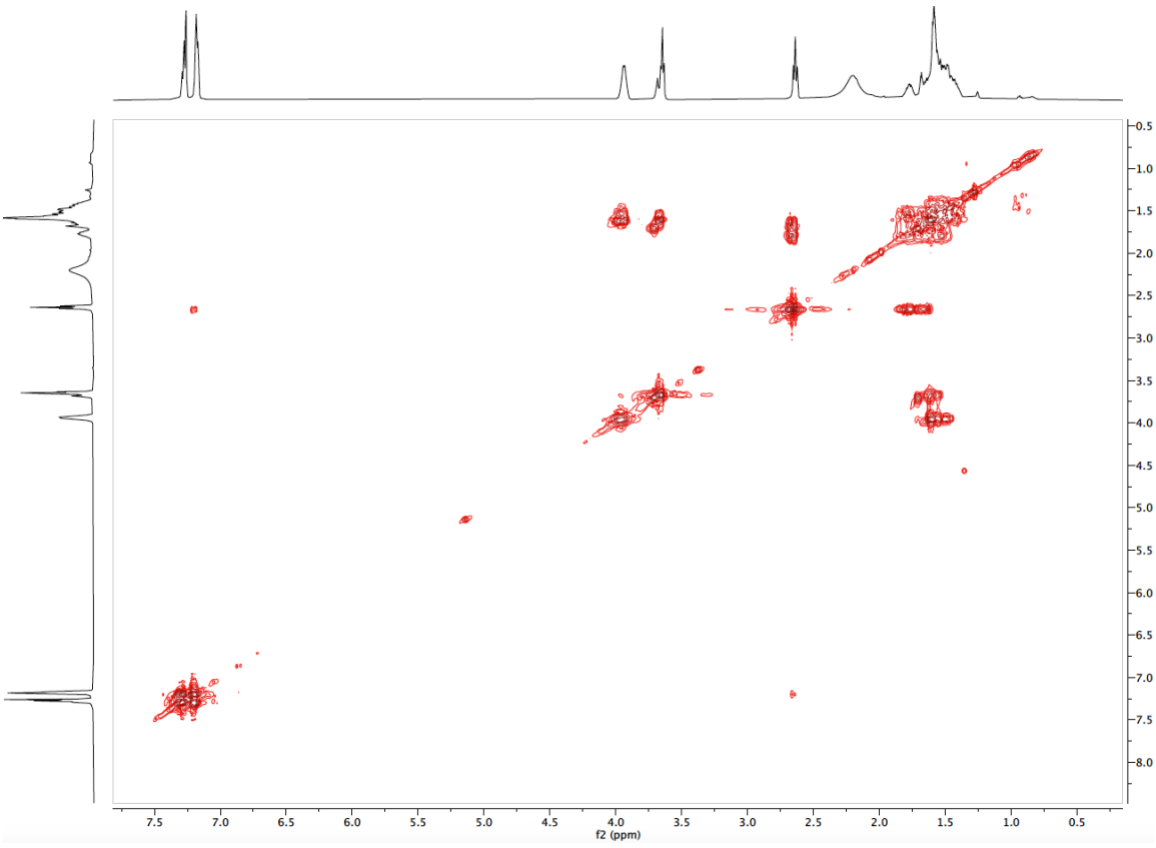
f2 (ppm)

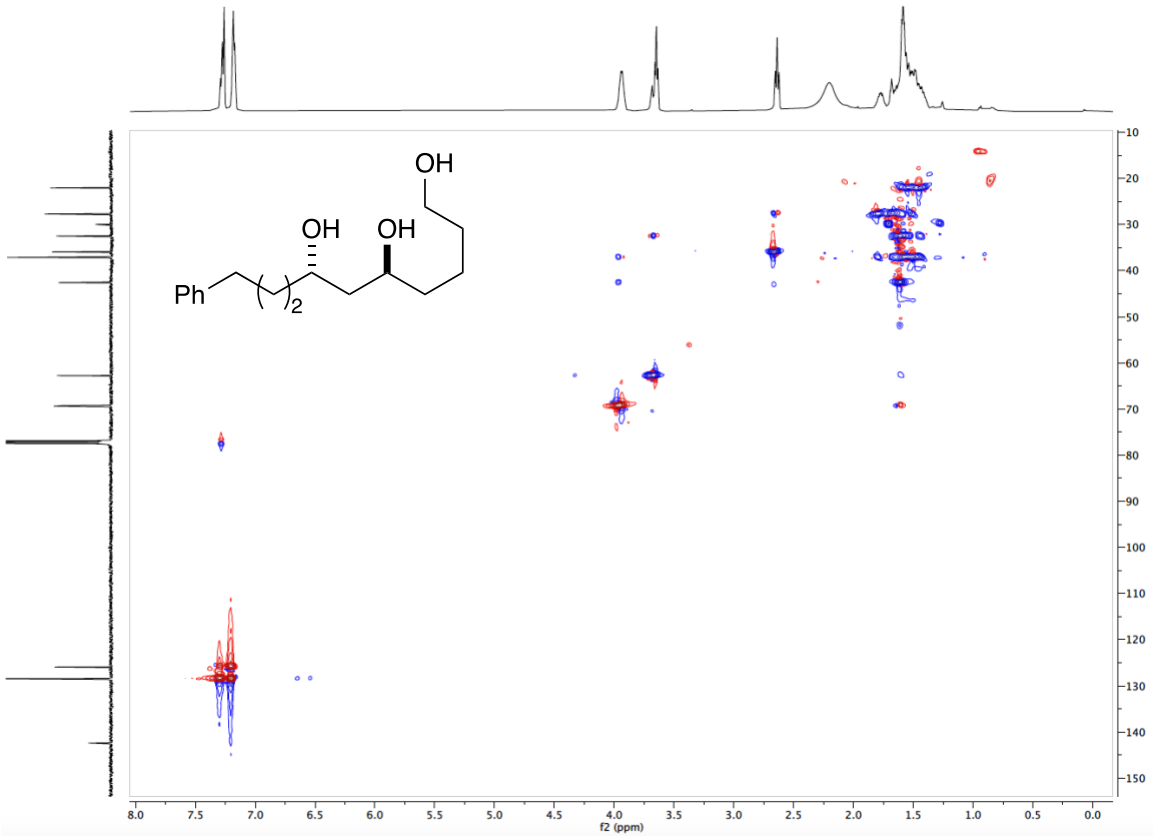
OH
OH
OH
Ph
2
8.0
7.5
7.0
6.5
6.0
5.5
5.0
4.5
4.0
3.5
3.0
2.5
2.0
1.5
1.0
0.5
0.0
f2 (ppm)
10
20
30
40
50
60
70
80
90
100
110
120
130
140
150

(*S*)-6-((*S*)-2-hydroxyheptyl)tetrahydro-2*H*-pyran-2-one ($C_{12}H_{22}O_3$, 3.7.5)

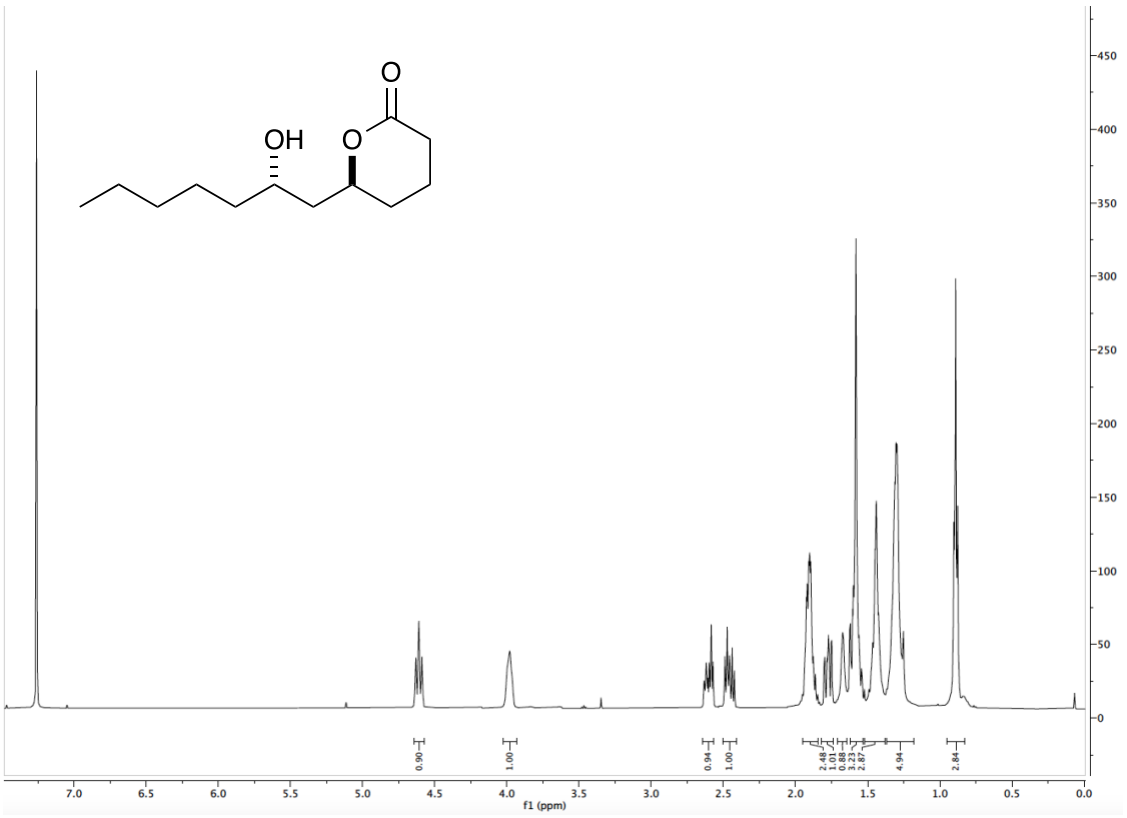

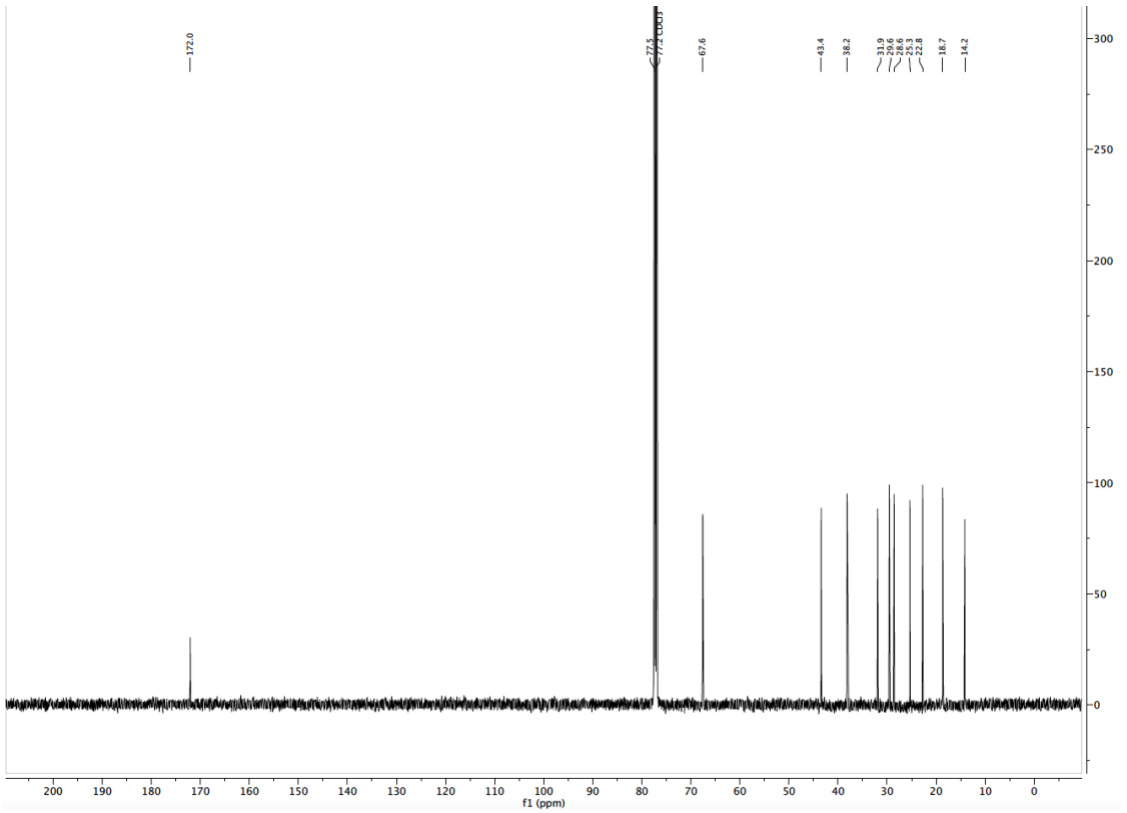

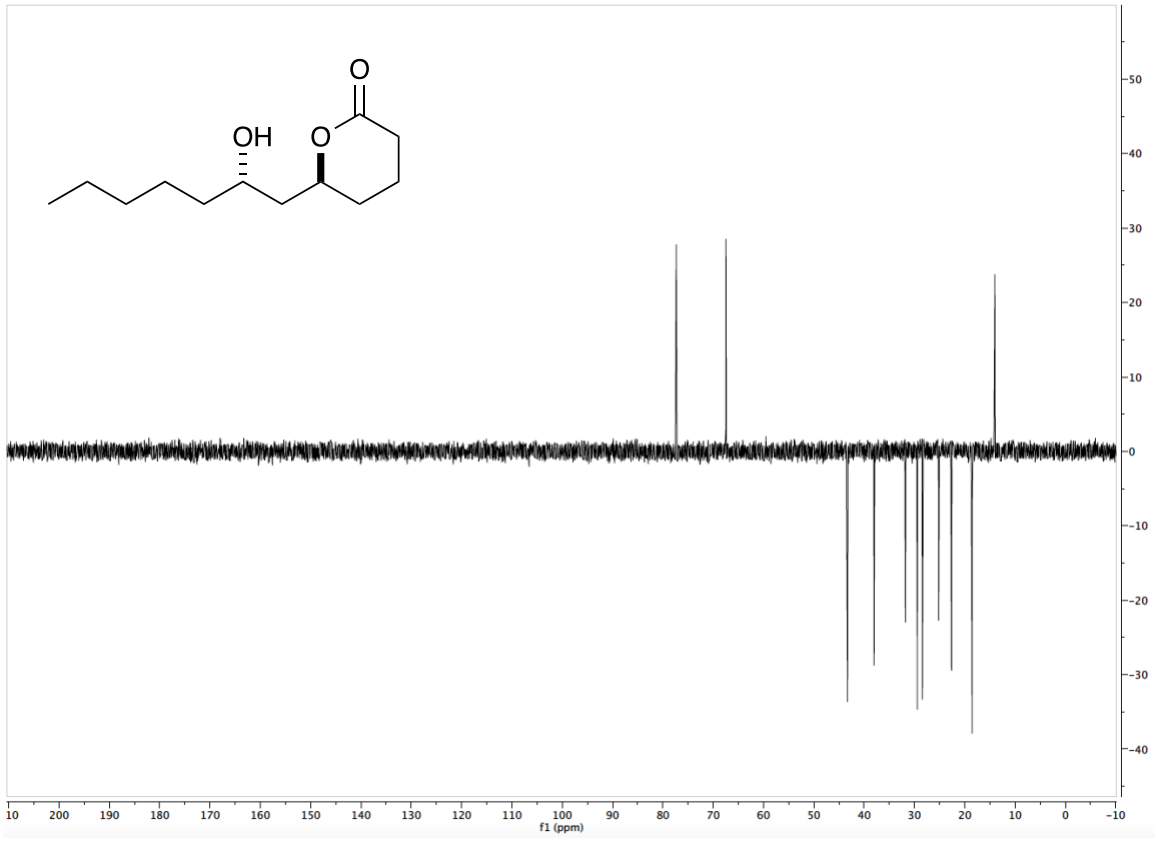
OH
O
O
f1 (ppm)

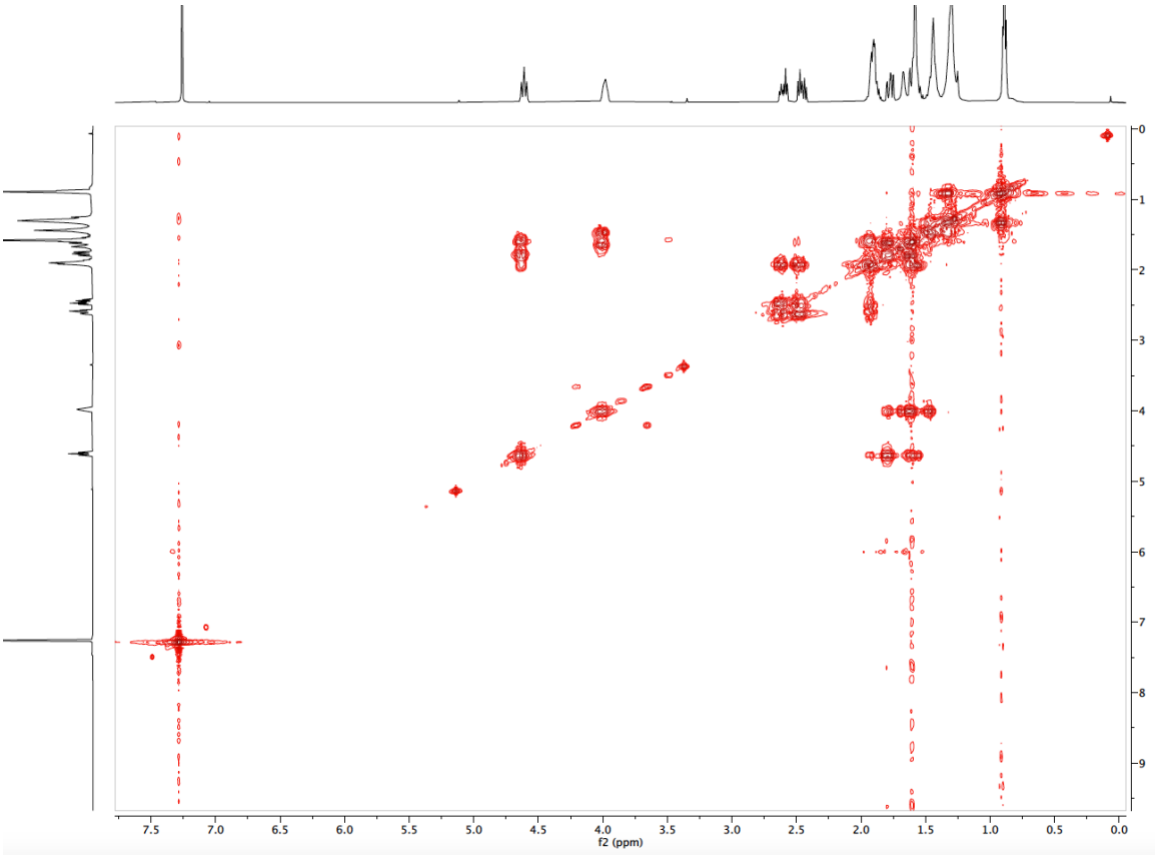
f2 (ppm)

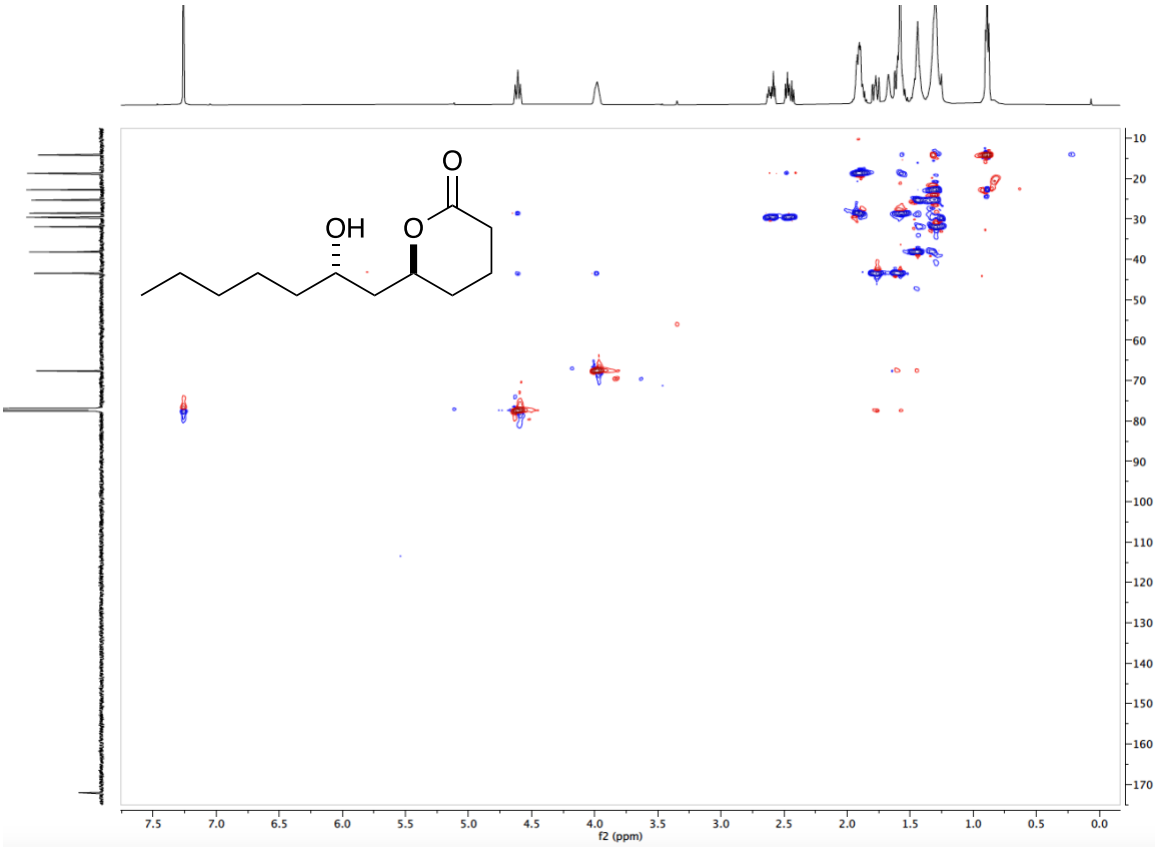
OH
O
O
7.5
7.0
6.5
6.0
5.5
5.0
4.5
4.0
3.5
3.0
2.5
2.0
1.5
1.0
0.5
0.0
f2 (ppm)
10
20
30
40
50
60
70
80
90
100
110
120
130
140
150
160
170

(*S*)-6-((*S*)-2-hydroxy-5-phenylpentyl)tetrahydro-2*H*-pyran-2-one ($C_{16}H_{22}O_3$, 3.7.6)

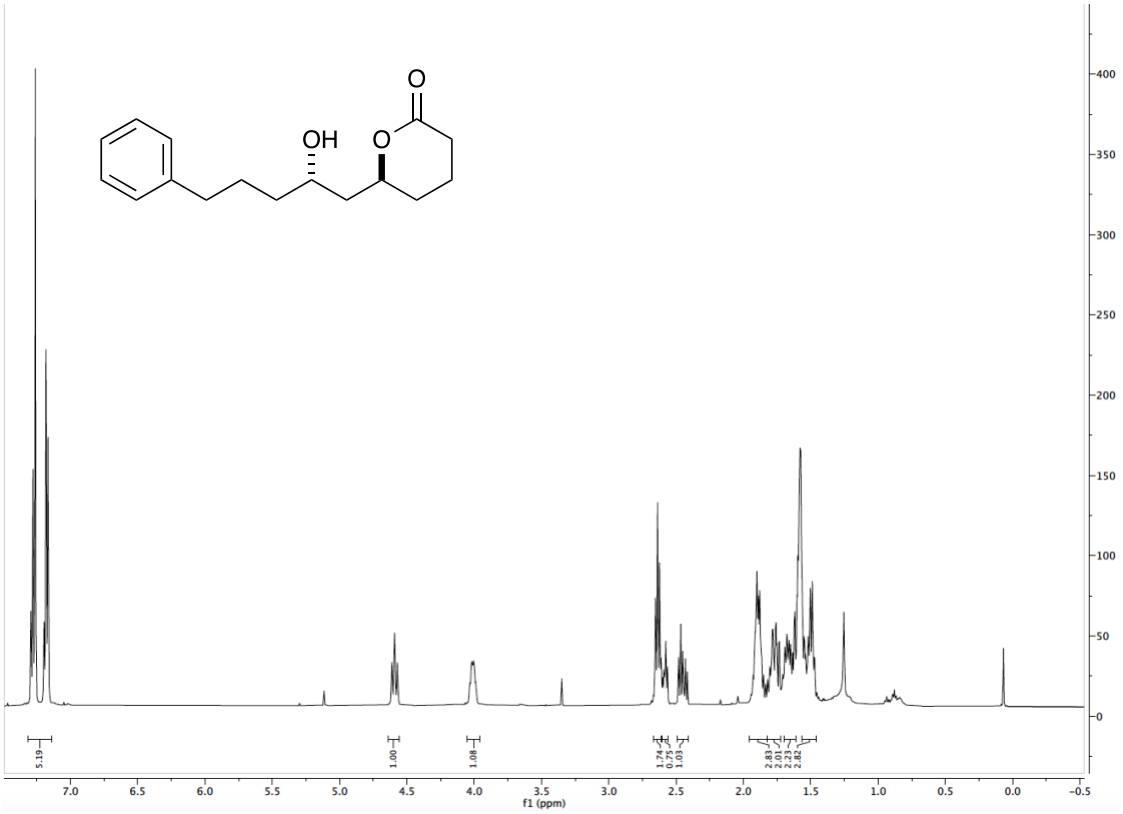

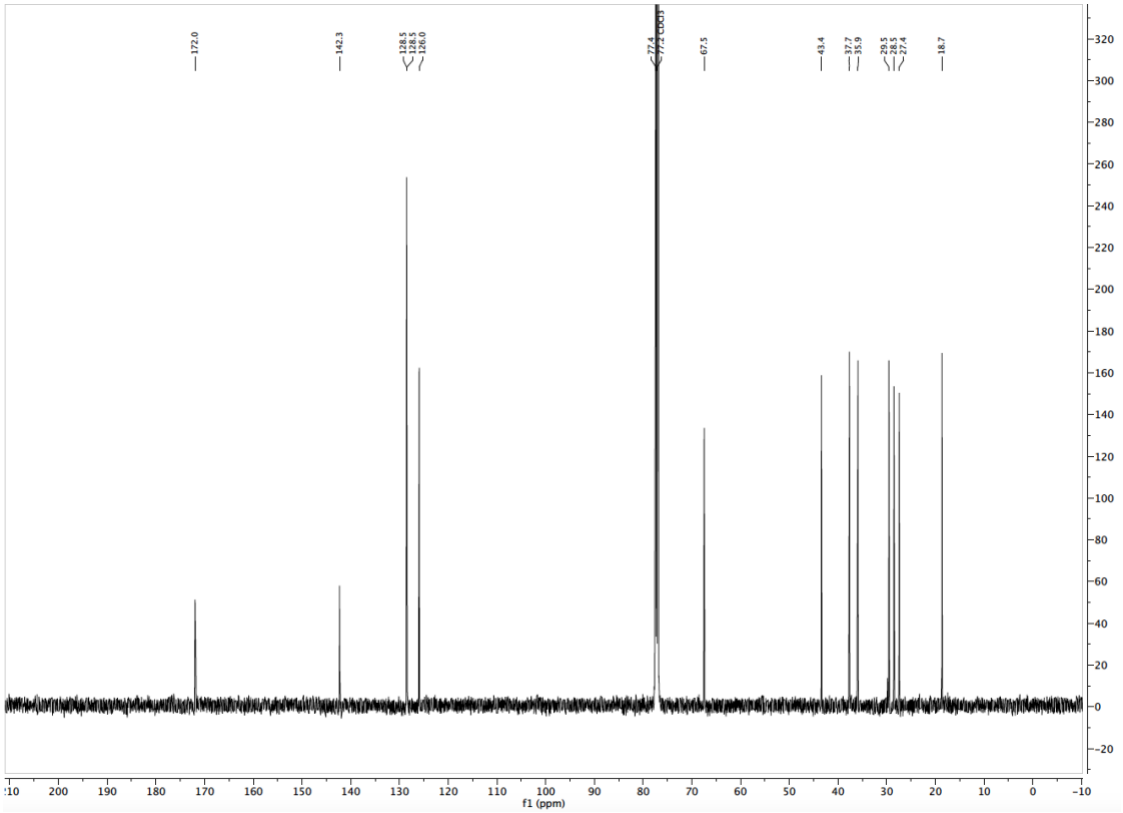

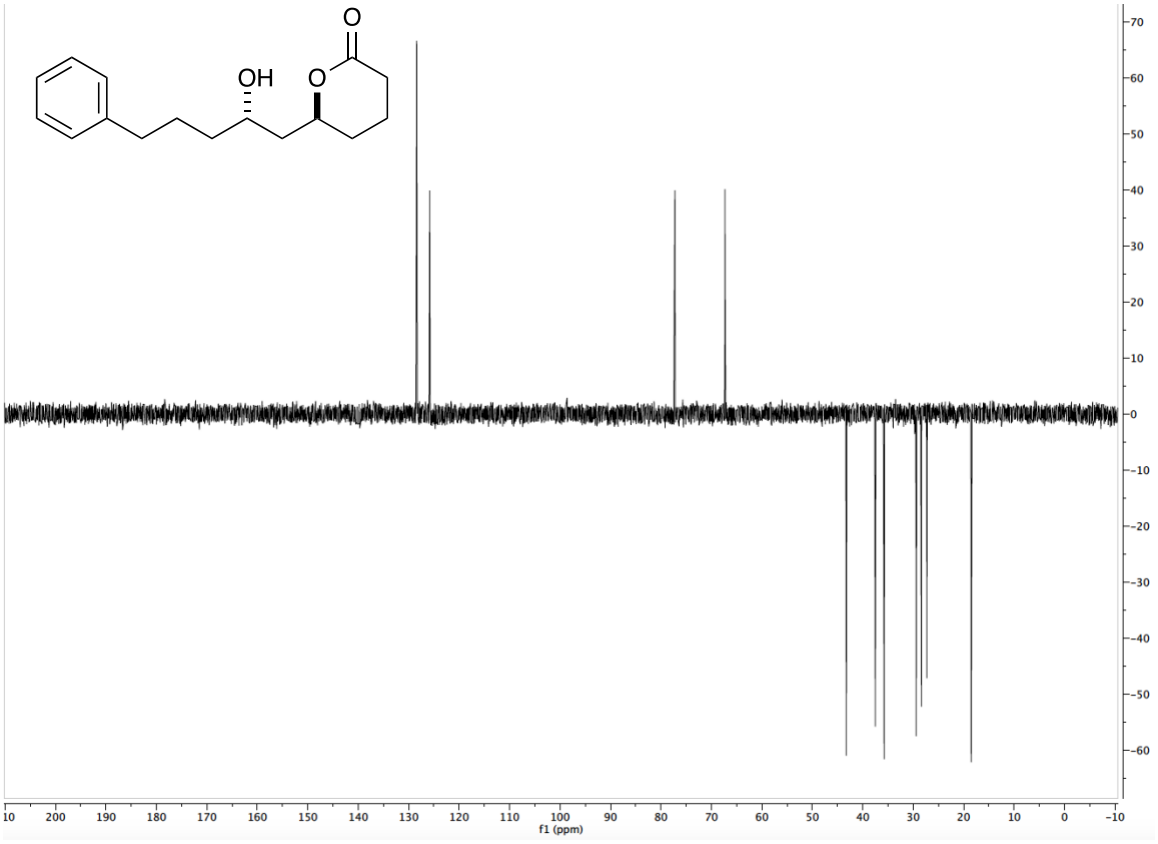
OH
O
O
f1 (ppm)

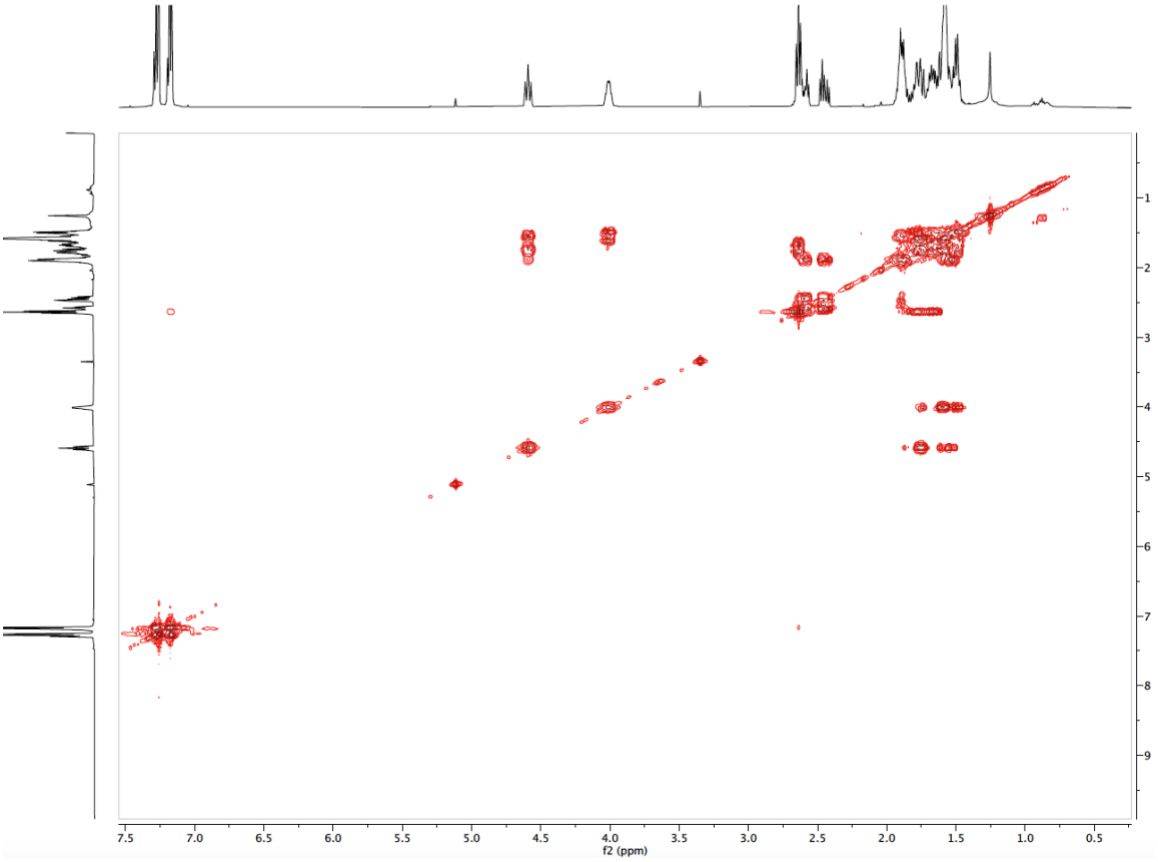
f2 (ppm)

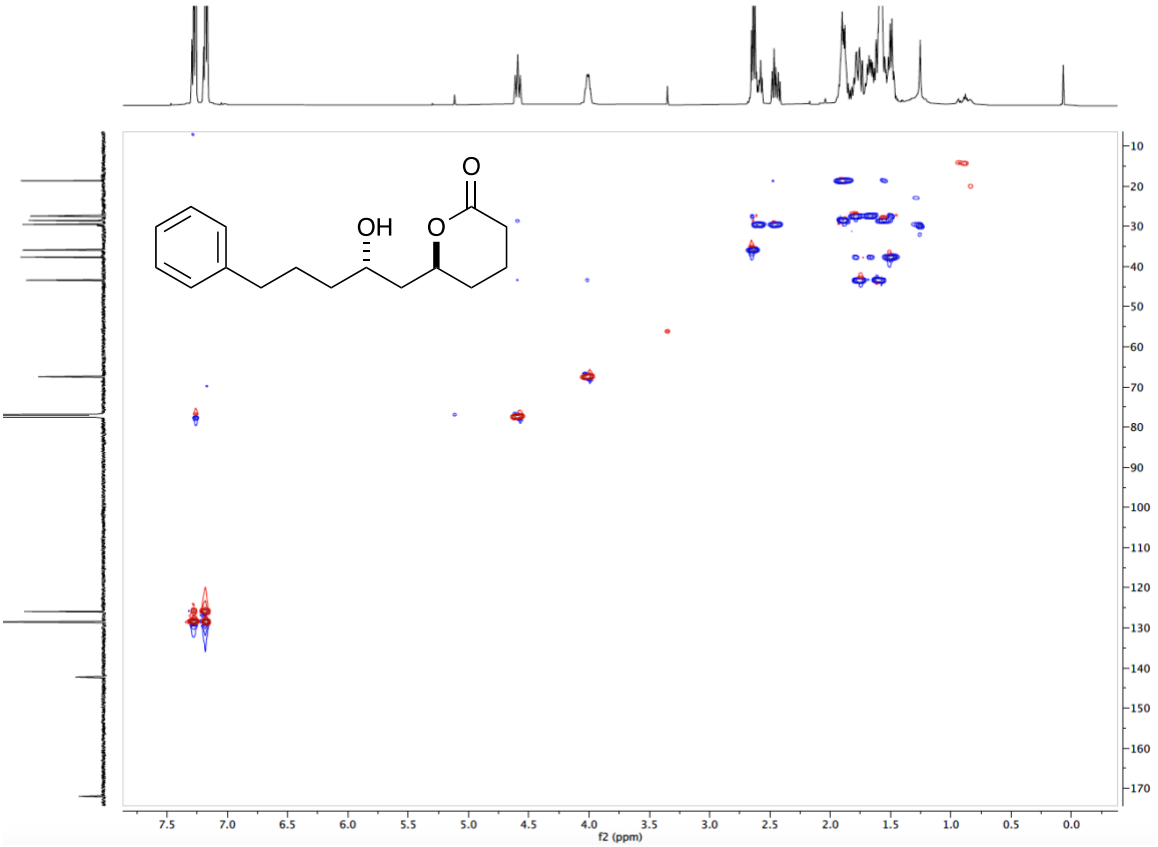
OH
O
O
7.5
7.0
6.5
6.0
5.5
5.0
4.5
4.0
3.5
3.0
2.5
2.0
1.5
1.0
0.5
0.0
f2 (ppm)
10
20
30
40
50
60
70
80
90
100
110
120
130
140
150
160
170

(*S*)-6-((*S*)-2-methoxyheptyl)tetrahydro-2*H*-pyran-2-one ($C_{13}H_{24}O_3$, 3.7.7)

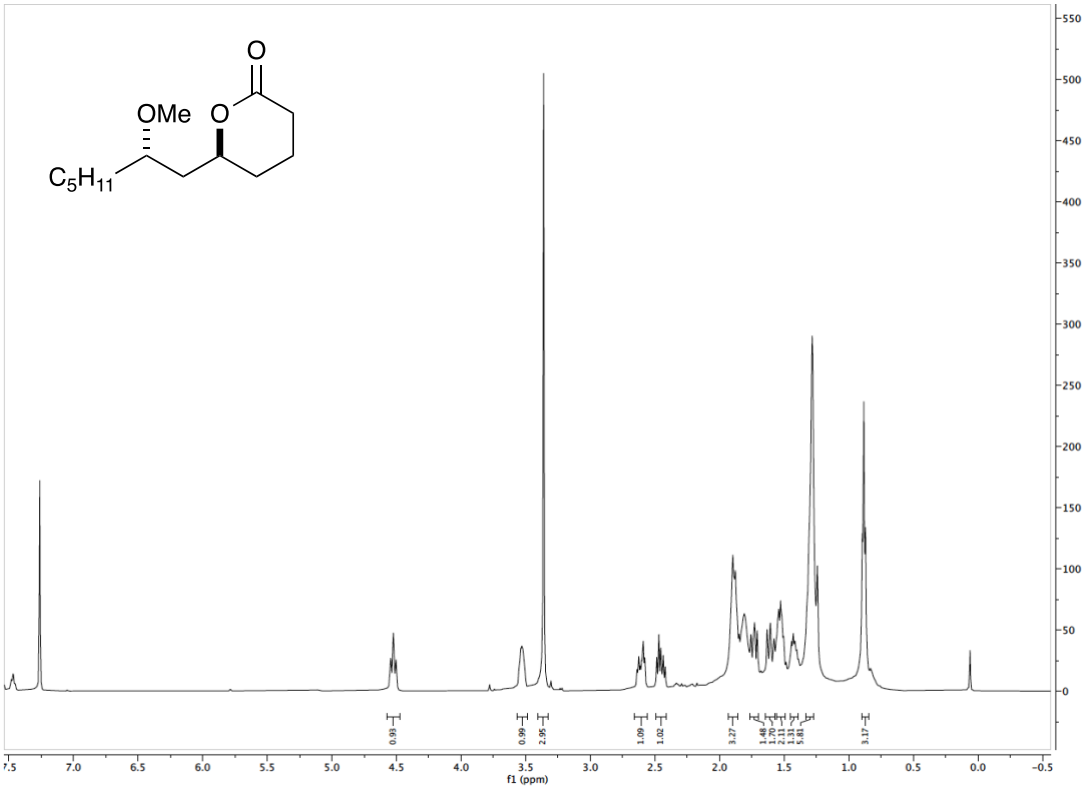

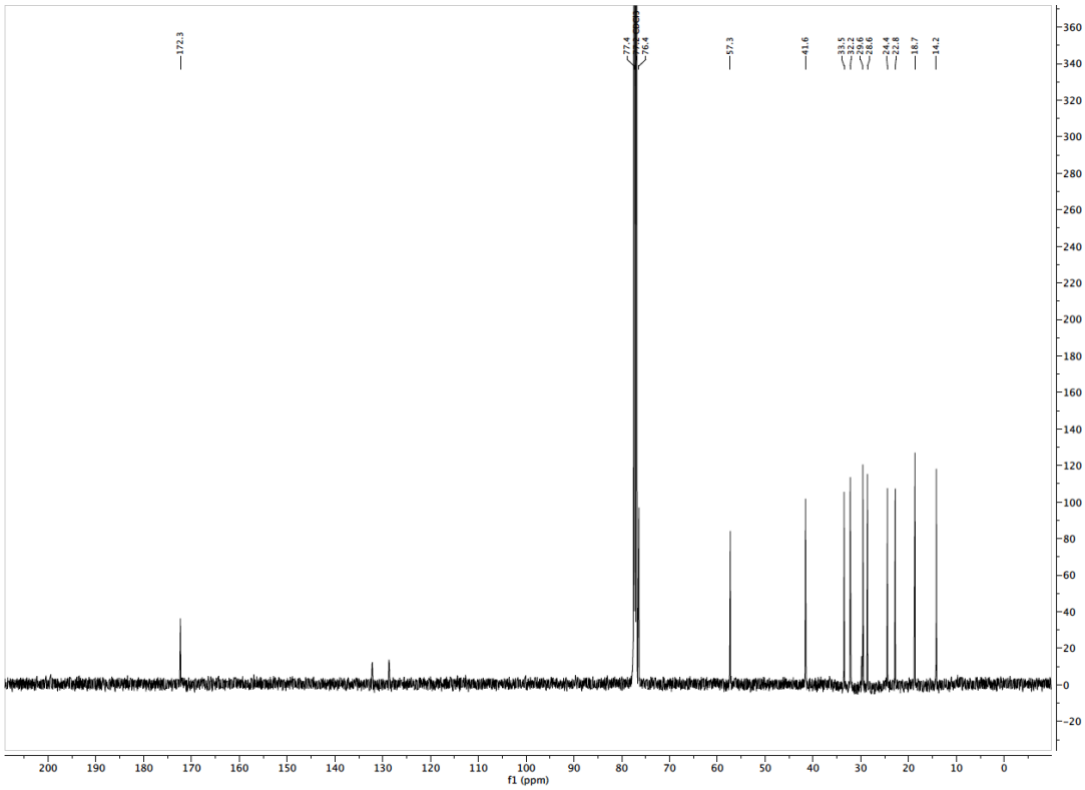

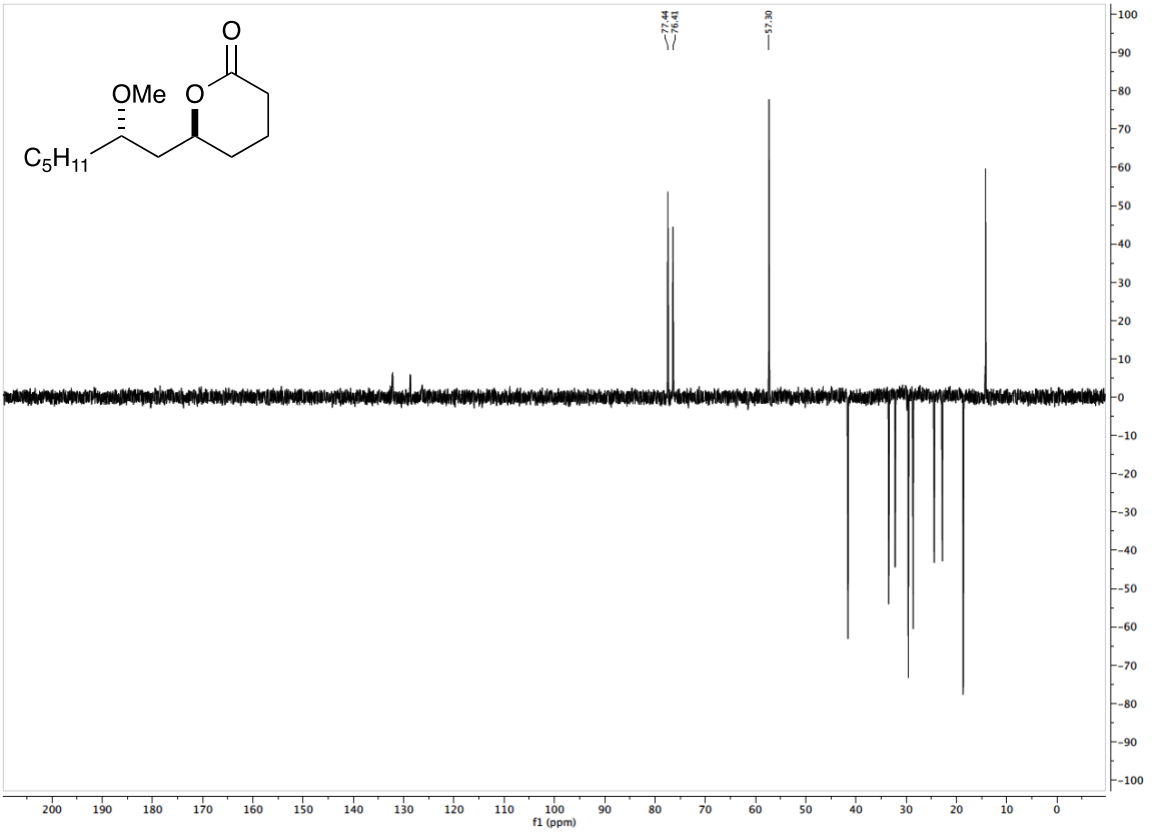
OMe
O
O
C_5H_{11}
77.44
76.41
57.30
f1 (ppm)

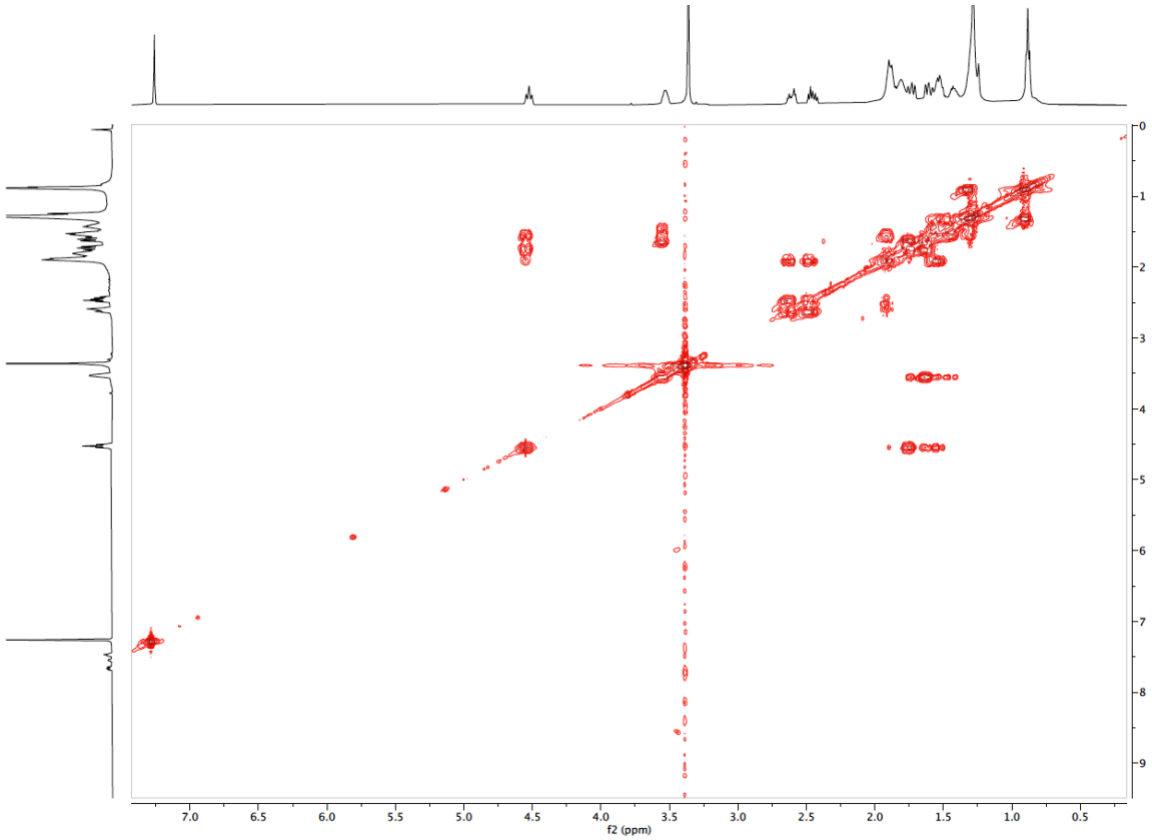
f2 (ppm)

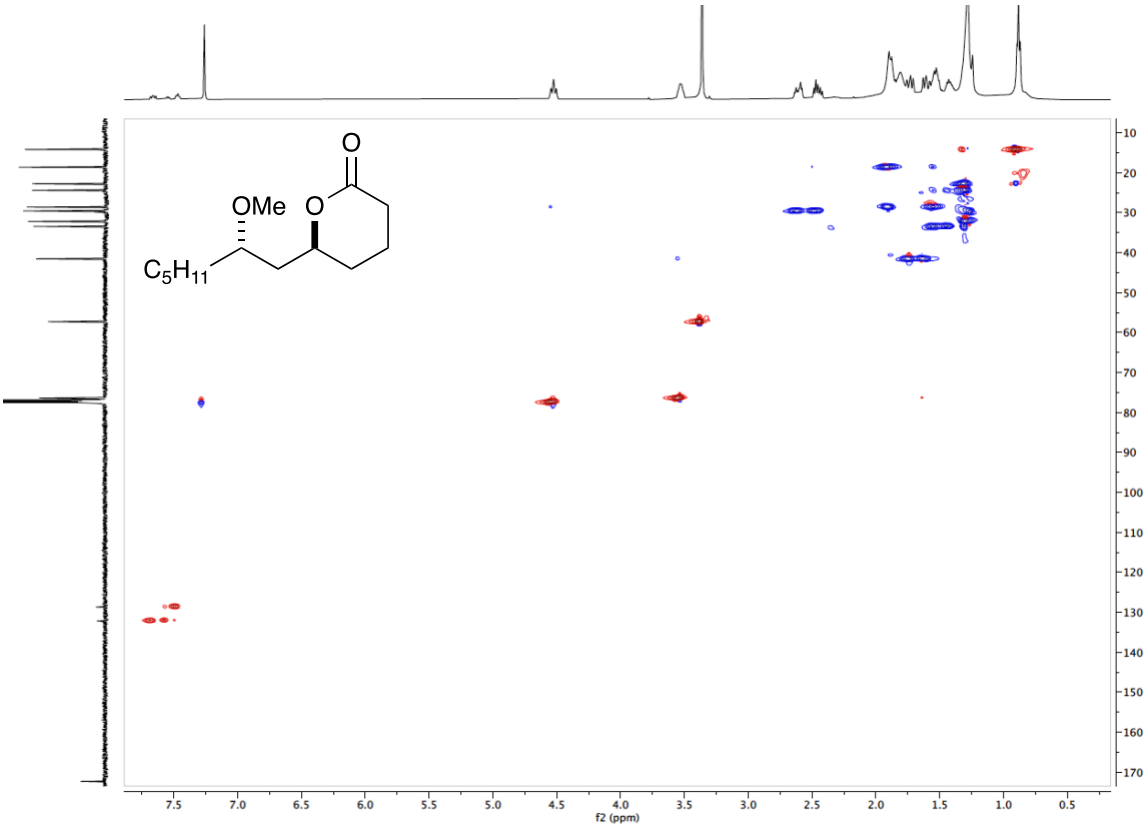
O
OMe
O
C5H11
7.5
7.0
6.5
6.0
5.5
5.0
4.5
4.0
3.5
3.0
2.5
2.0
1.5
1.0
0.5
f2 (ppm)
10
20
30
40
50
60
70
80
90
100
110
120
130
140
150
160
170

(*S*)-6-((*S*)-2-methoxy-5-phenylpentyl)tetrahydro-2*H*-pyran-2-one ($C_{17}H_{24}O_3$, 3.7.8)

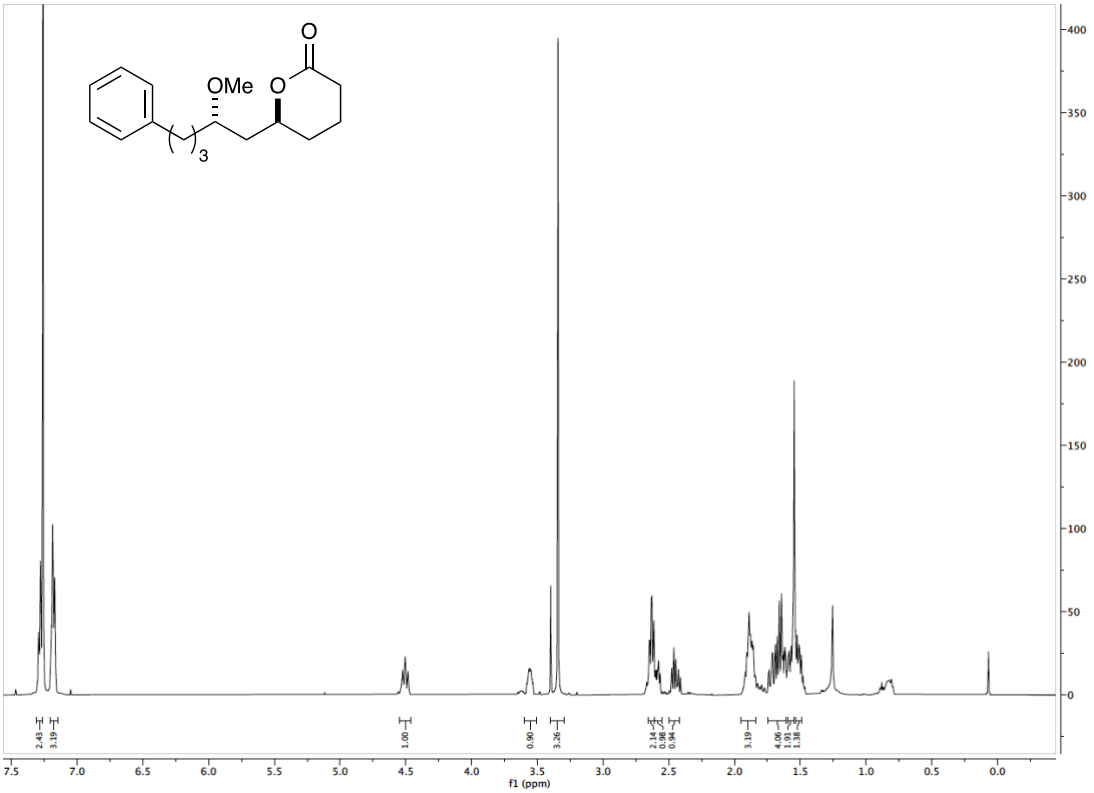

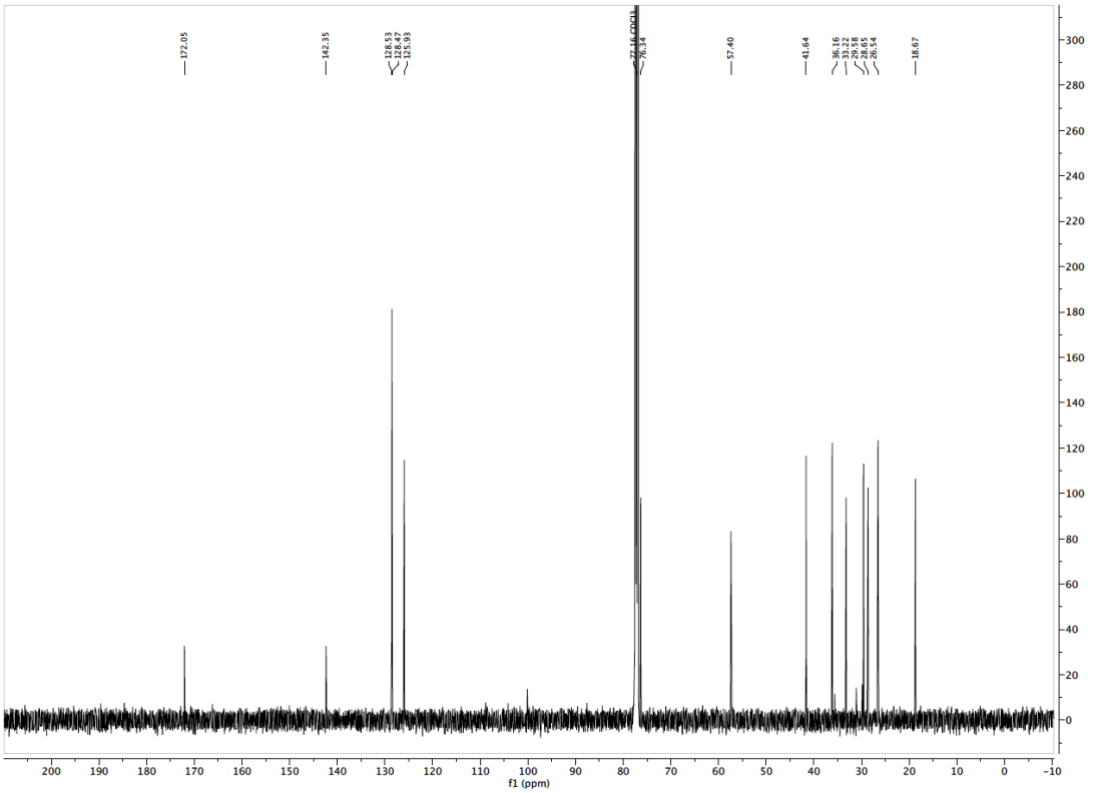

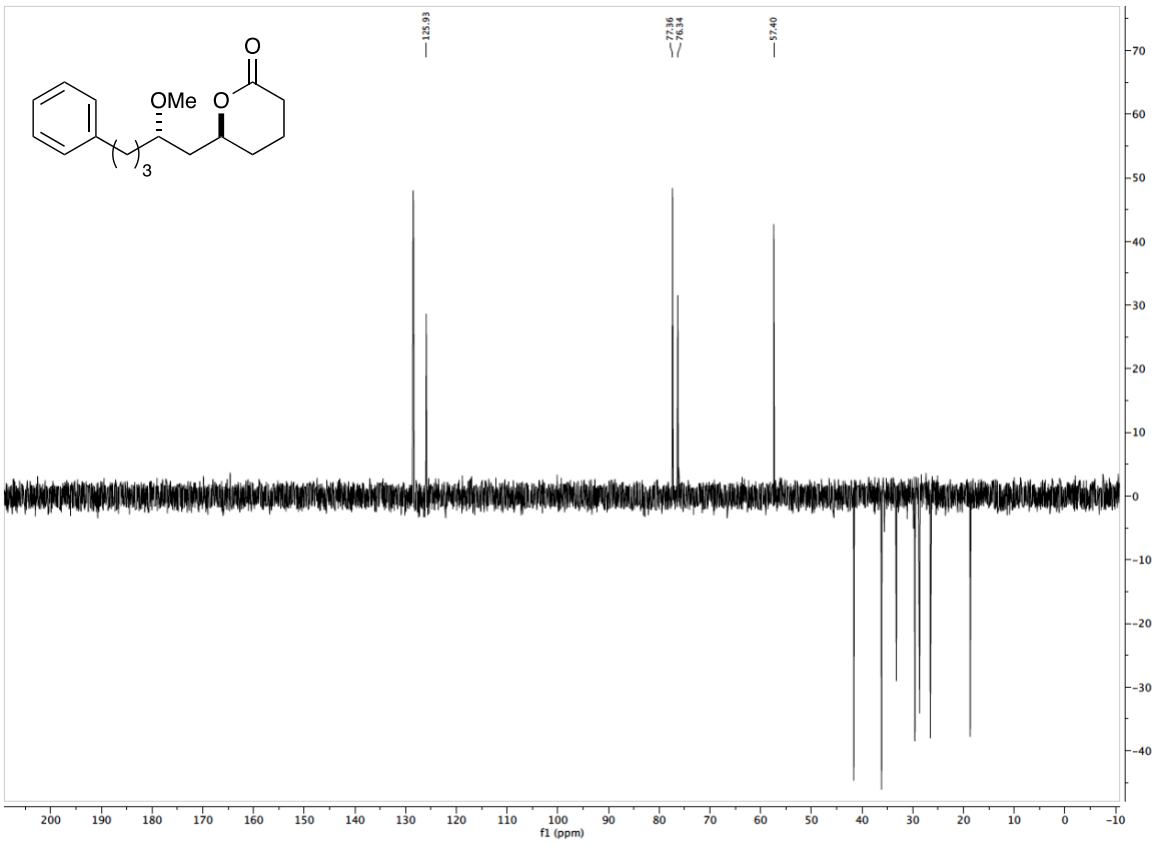
OMe
O
O
3
125.93
77.36
76.84
57.40
f1 (ppm)

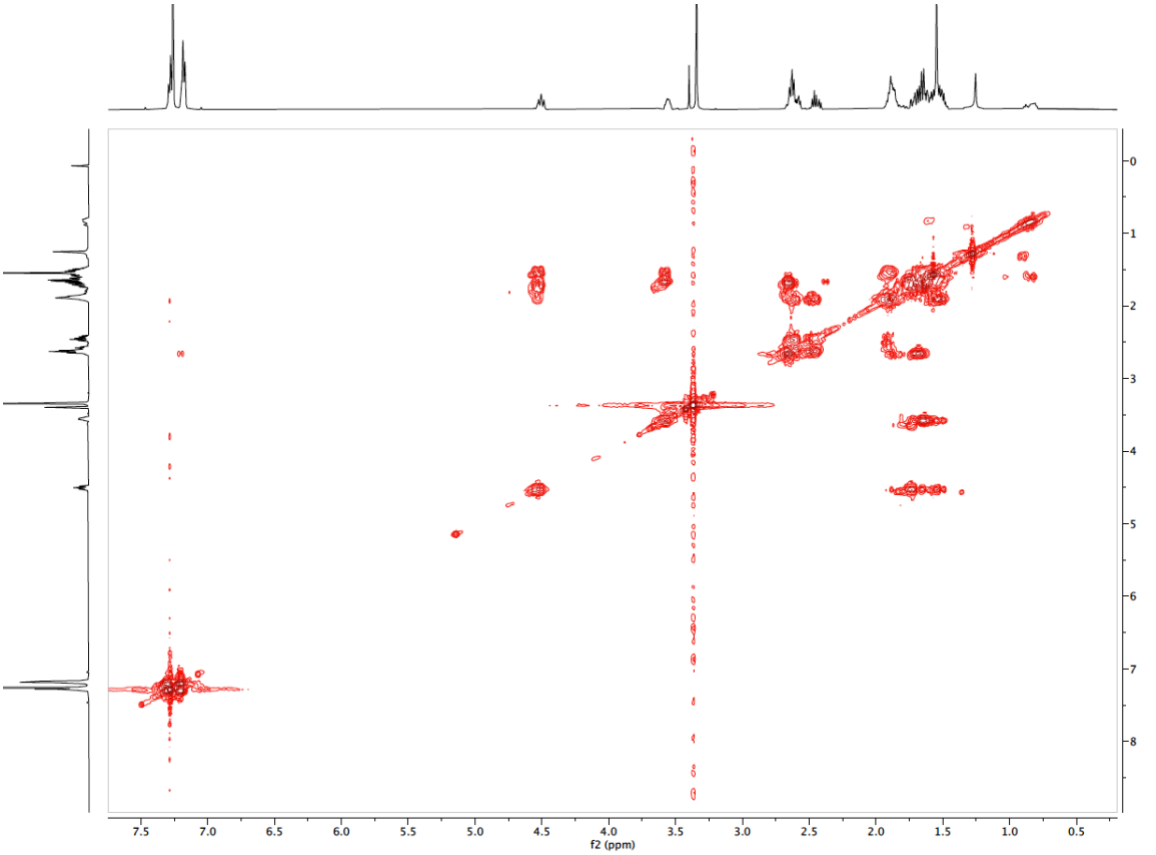
f2 (ppm)

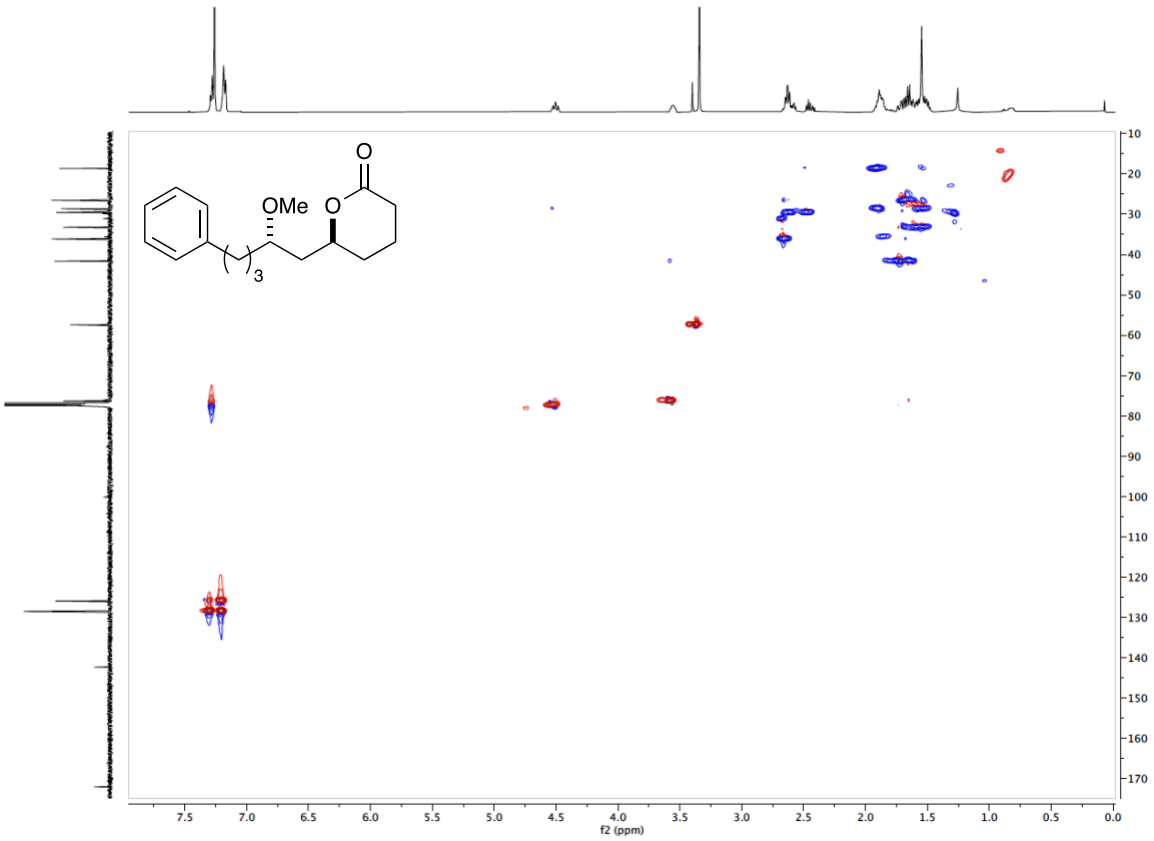
O
OMe
O
3
7.5
7.0
6.5
6.0
5.5
5.0
4.5
4.0
3.5
3.0
2.5
2.0
1.5
1.0
0.5
0.0
f2 (ppm)
10
20
30
40
50
60
70
80
90
100
110
120
130
140
150
160
170

(5*S*,7*S*)-*N*-allyl-5-hydroxy-7-methoxy-*N*-methyldodecanamide ($C_{17}H_{33}NO_3$, 3.8.1)

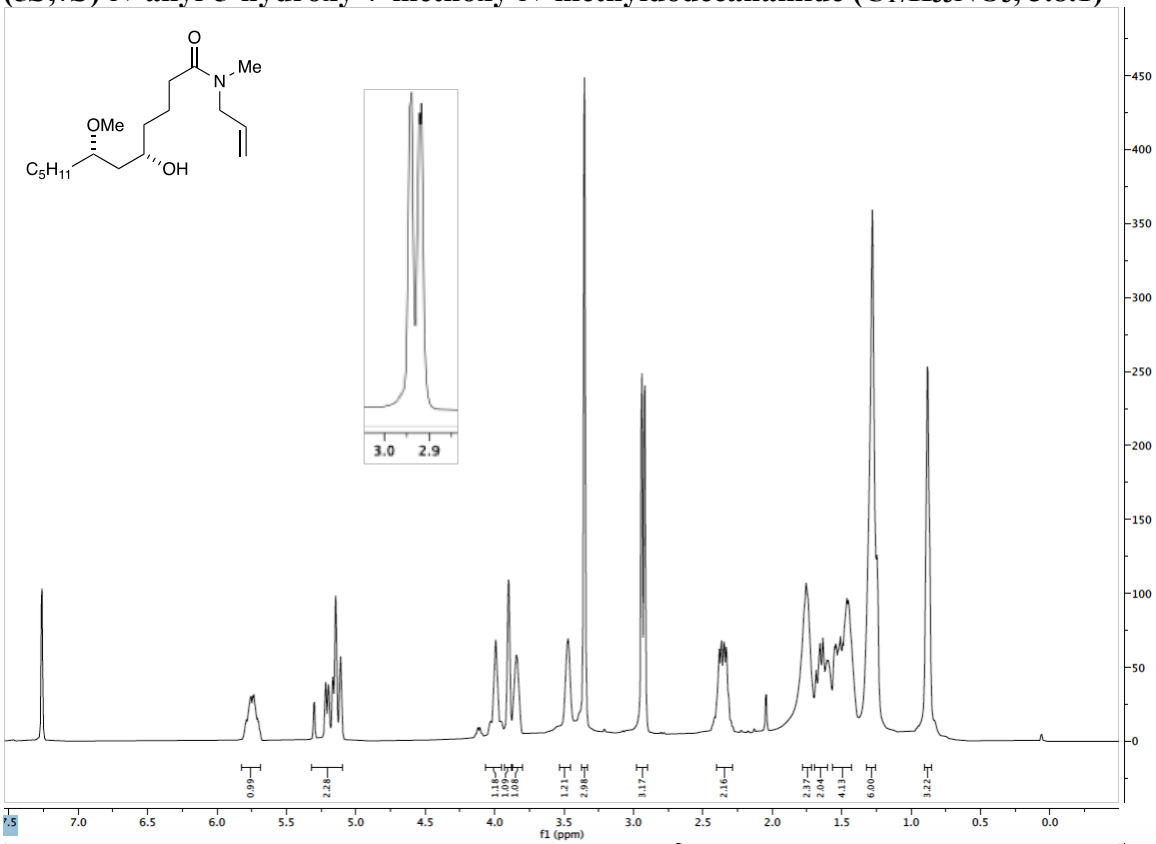

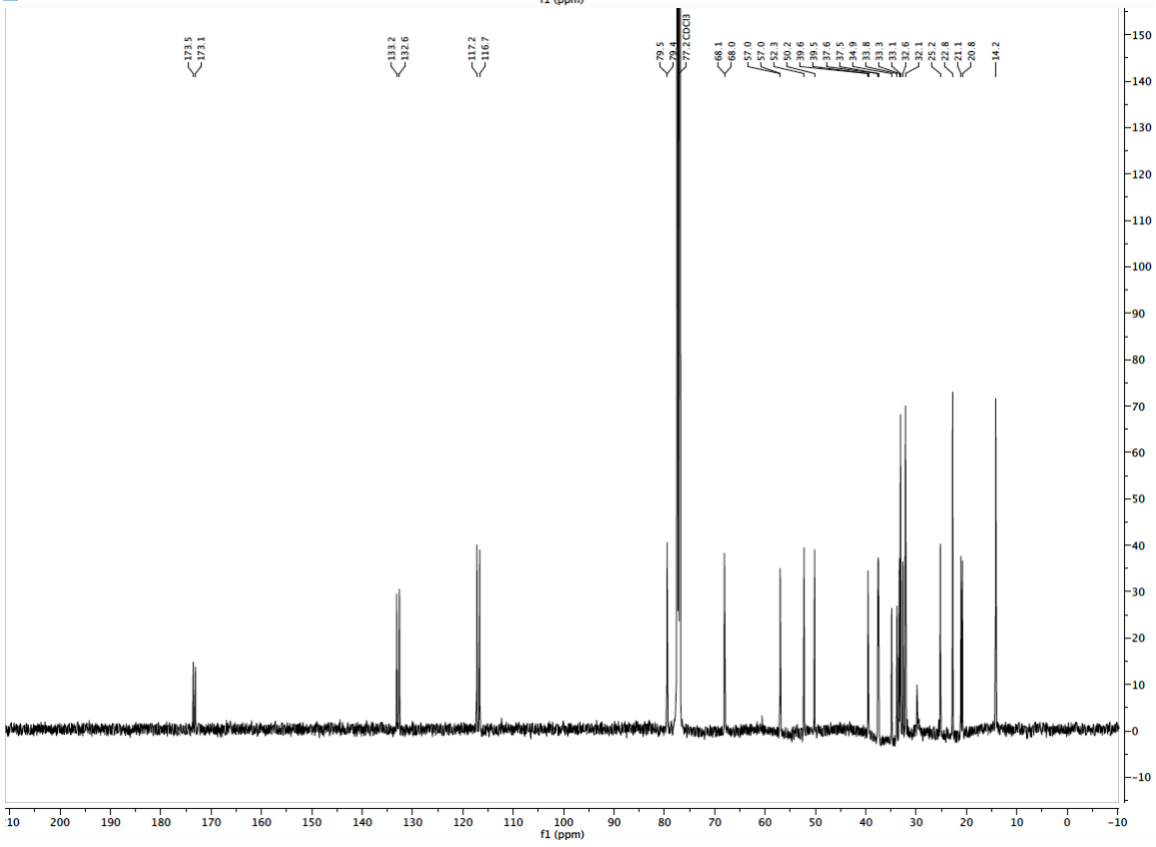

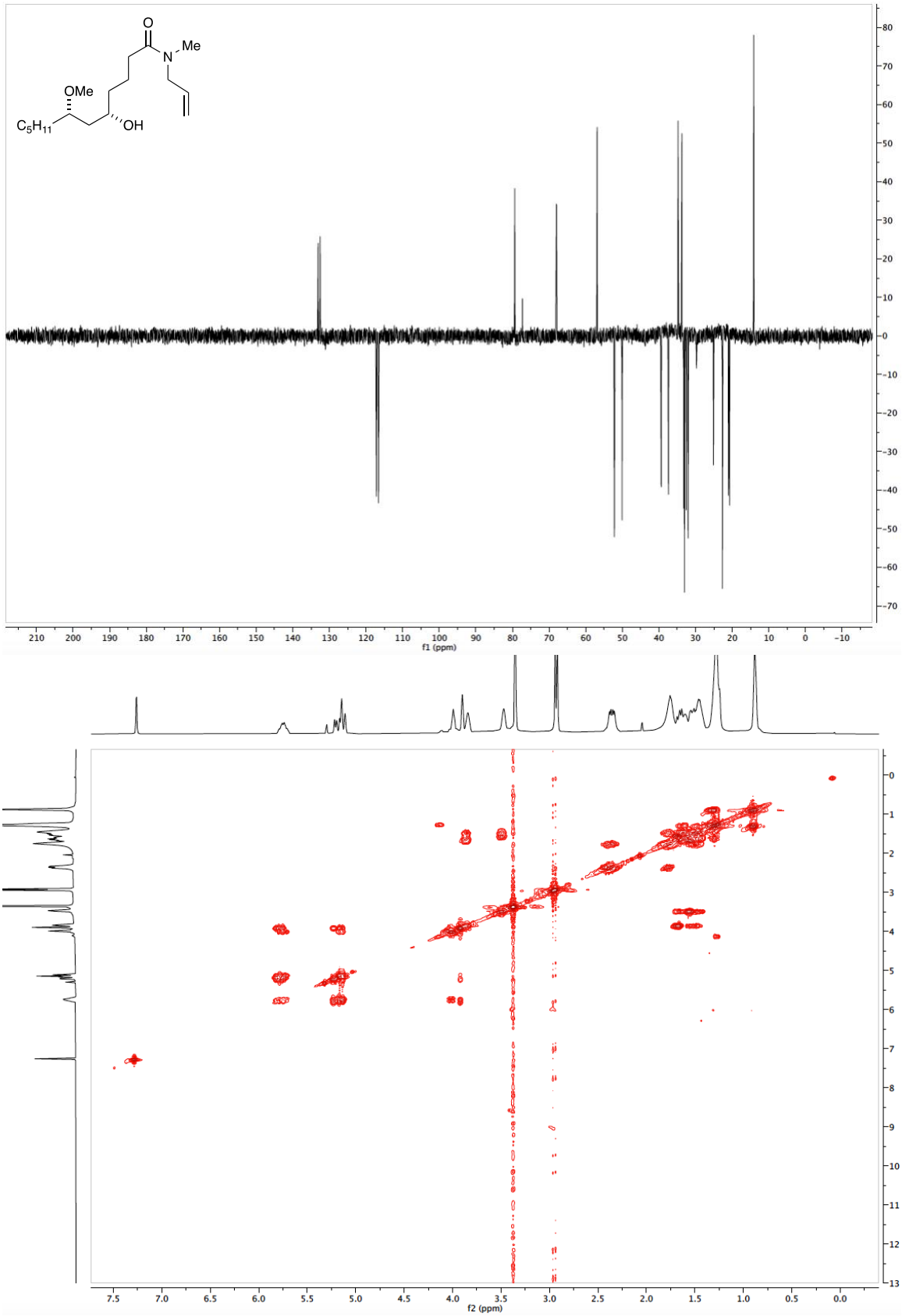
O
N
Me
OMe
C_5H_{11}
OH
f1 (ppm)
f2 (ppm)

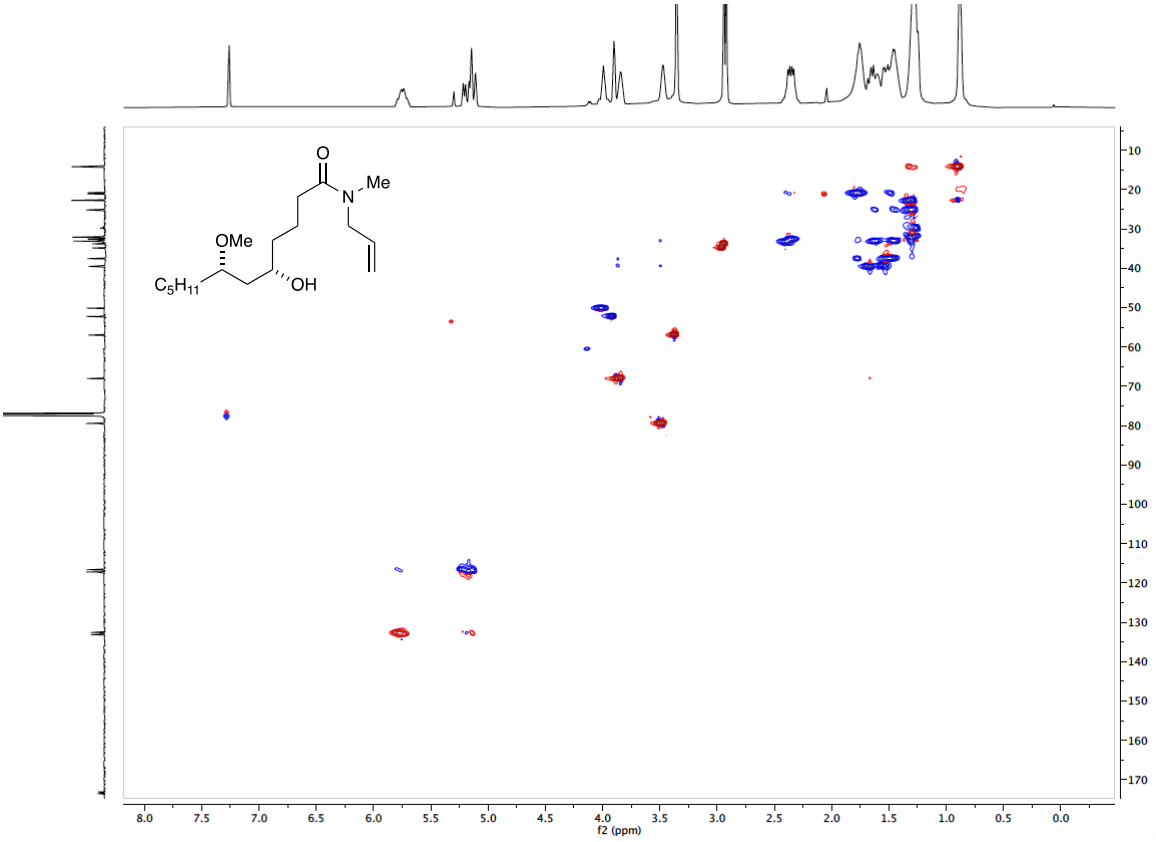
O
N
Me
OMe
C_5H_{11}
OH
8.0
7.5
7.0
6.5
6.0
5.5
5.0
4.5
4.0
3.5
3.0
2.5
2.0
1.5
1.0
0.5
0.0
f2 (ppm)
10
20
30
40
50
60
70
80
90
100
110
120
130
140
150
160
170

(5*S*,7*S*)-*N*-allyl-5-hydroxy-7-methoxy-*N*-(4-(trifluoromethyl)benzyl)dodecanamide $C_{24}H_{36}F_3NO_3$, 3.8.7)

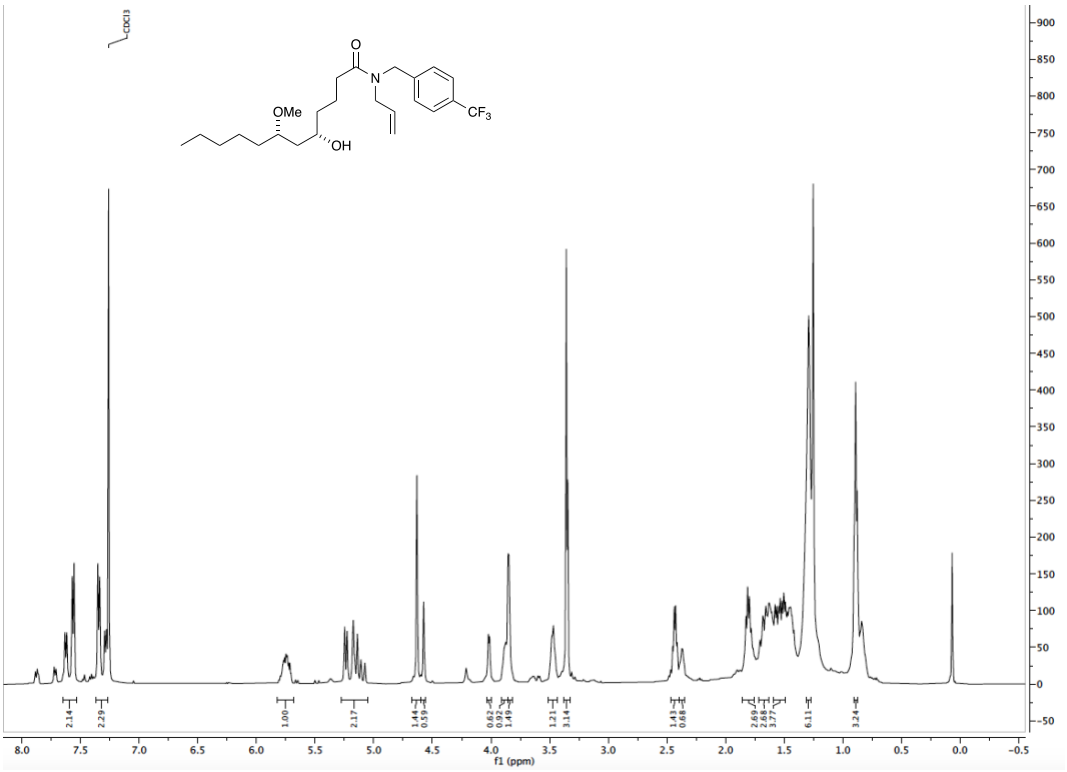

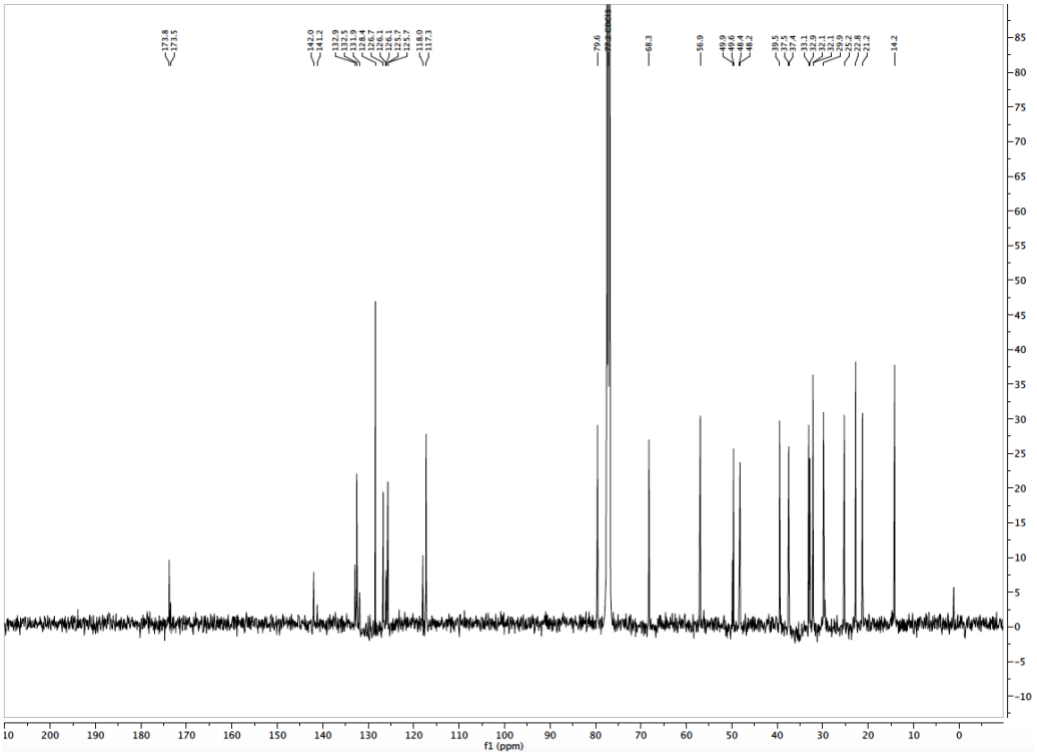

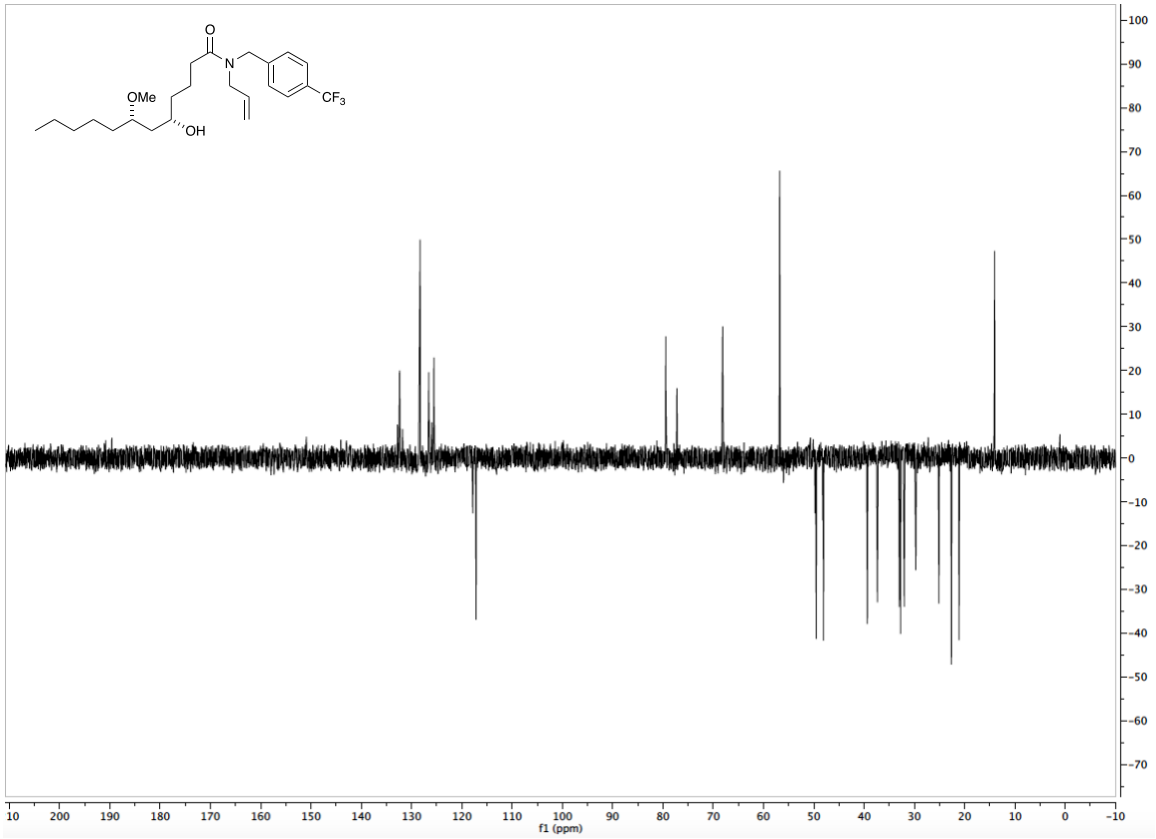
OMe
OH
N
O
CF3
f1 (ppm)

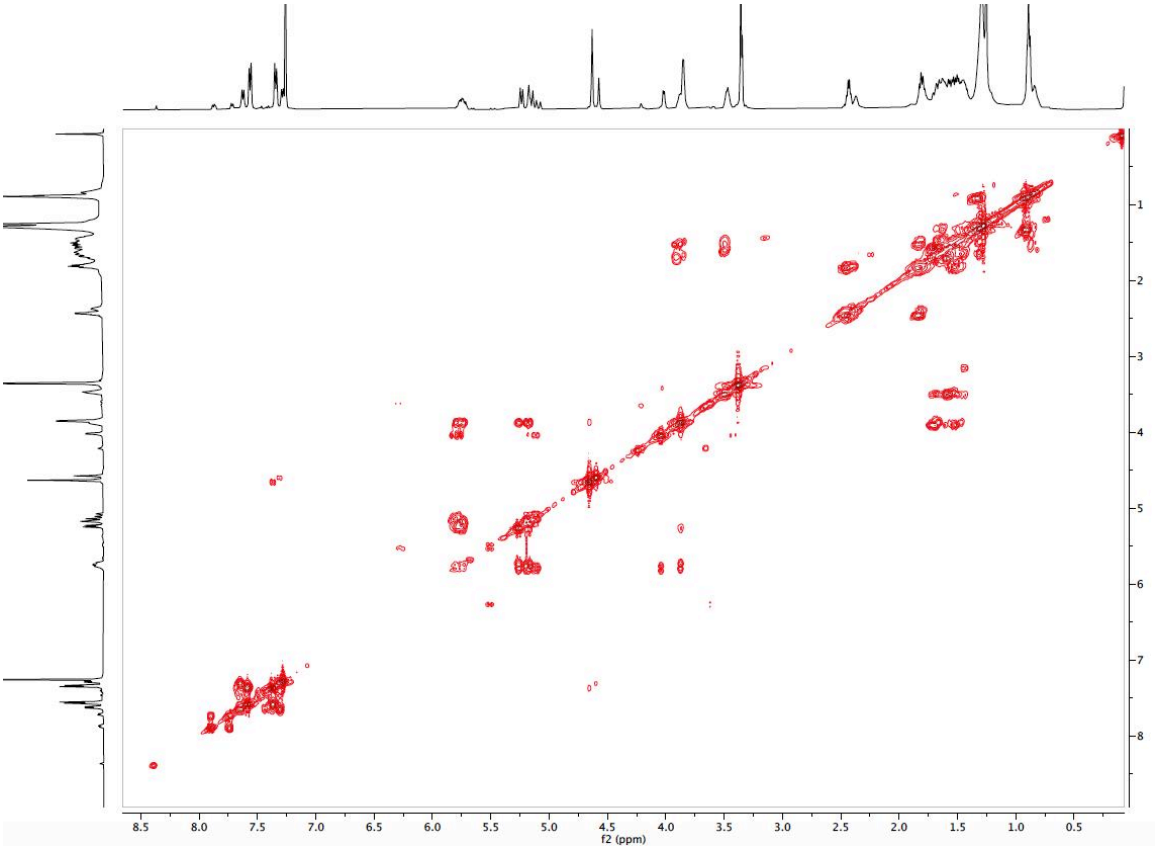
f2 (ppm)

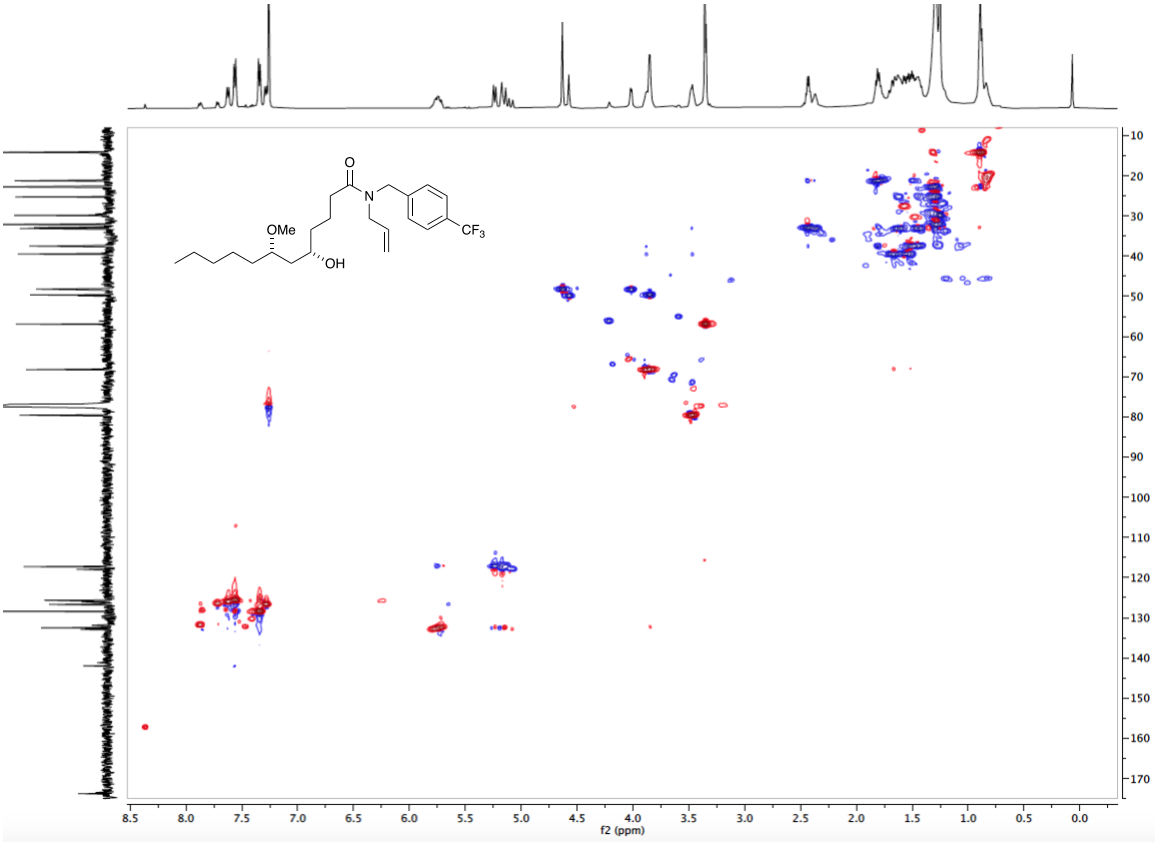
OMe
OH
O
N
CF3
f2 (ppm)

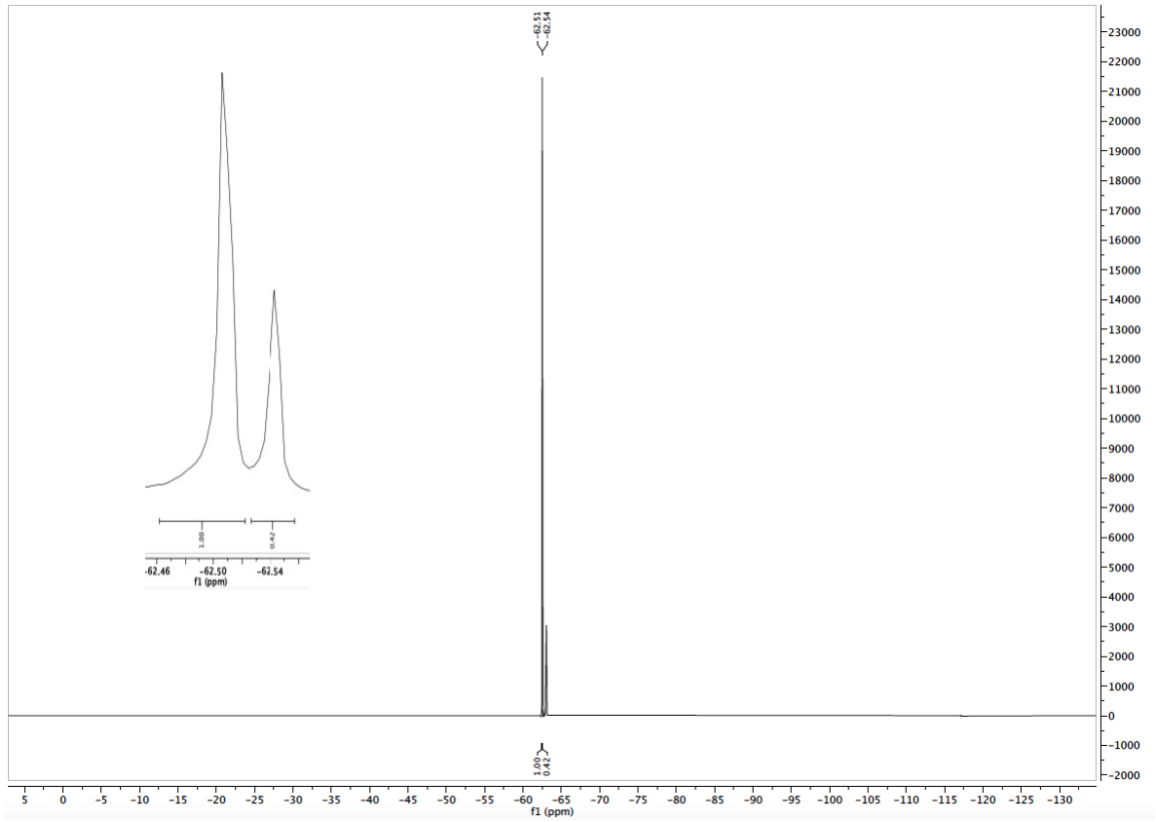
-62.51
-62.54
1.00
0.42
-62.46
-62.50
-62.54
f1 (ppm)

2-(((5*S*,7*S*)-1-(allyl(methyl)amino)-7-methoxy-1-oxododecan-5-yl)oxy)-2-oxoethyl acrylate ($C_{22}H_{37}NO_6$, 3.8.4)

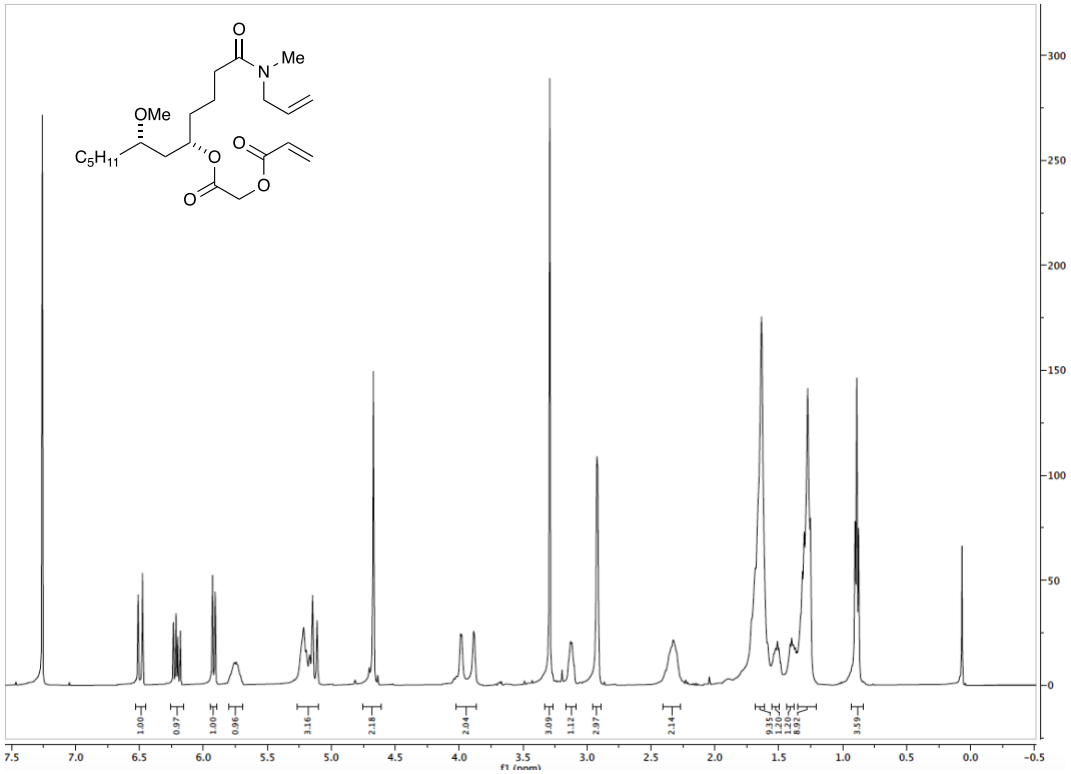

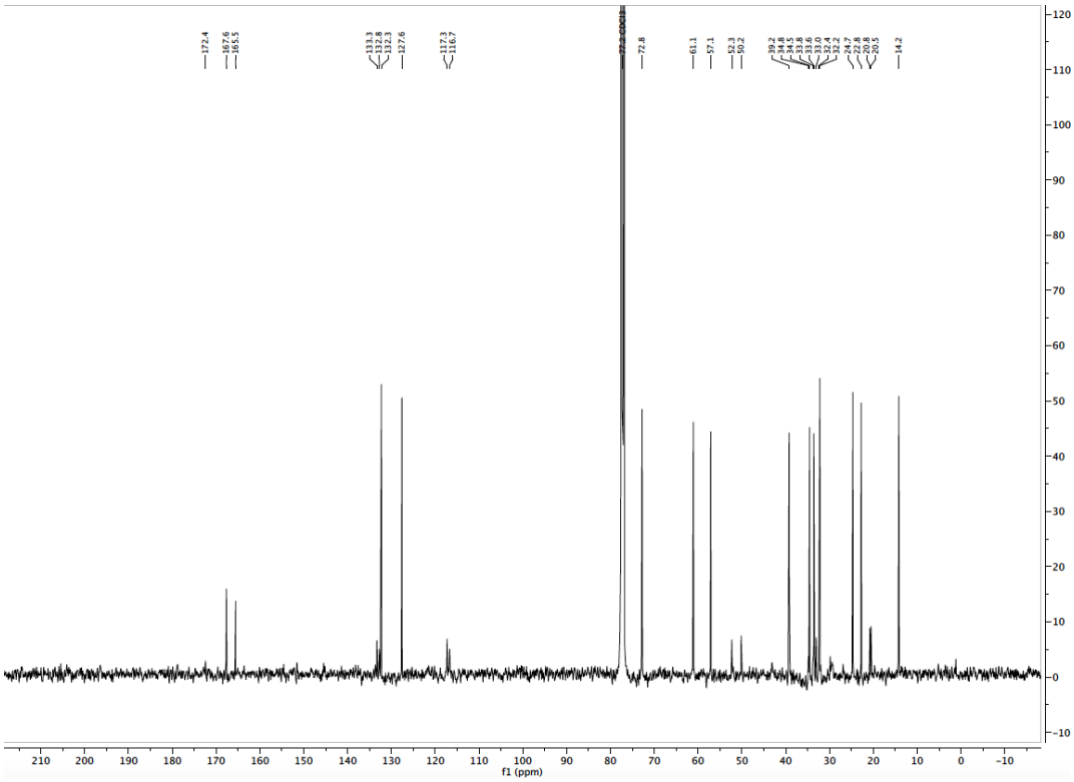

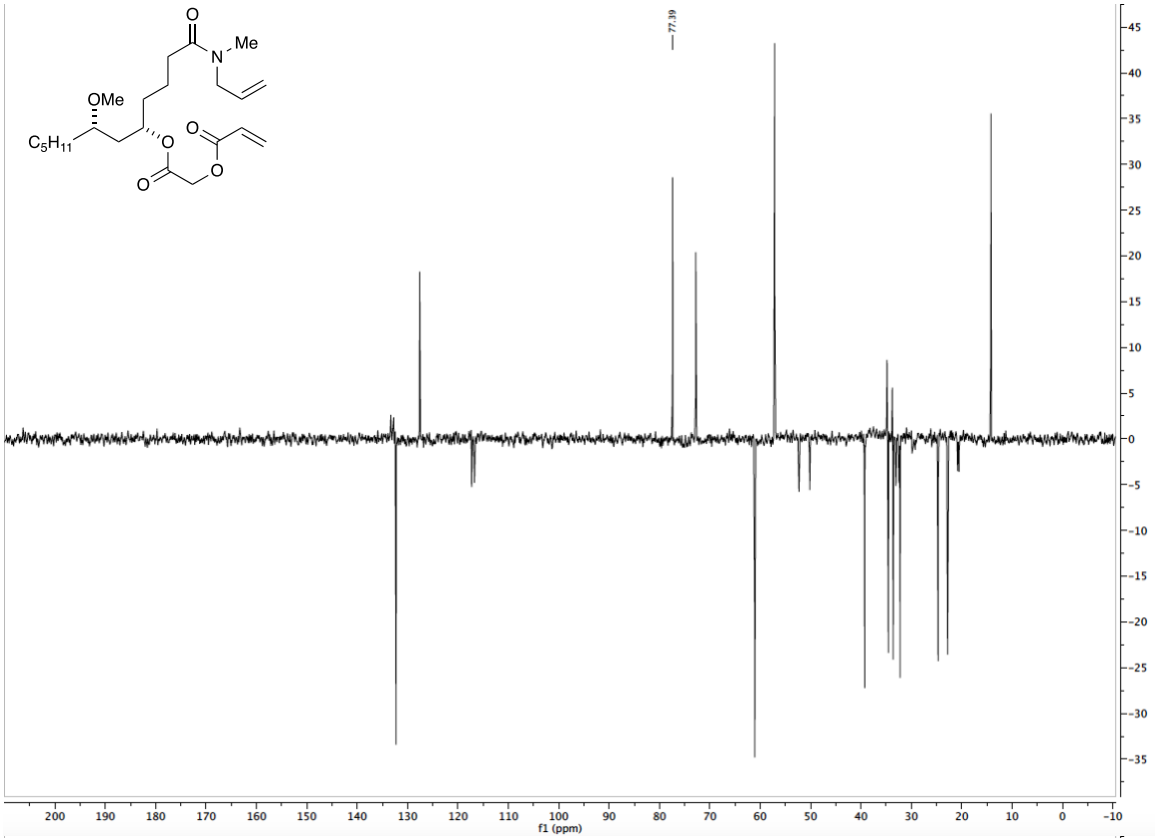
O
N
Me
OMe
C_5H_{11}
O
O
O
O
77.39
45
40
35
30
25
20
15
10
5
0
-5
-10
-15
-20
-25
-30
-35
200
190
180
170
160
150
140
130
120
110
100
90
80
70
60
50
40
30
20
10
0
-10
f1 (ppm)

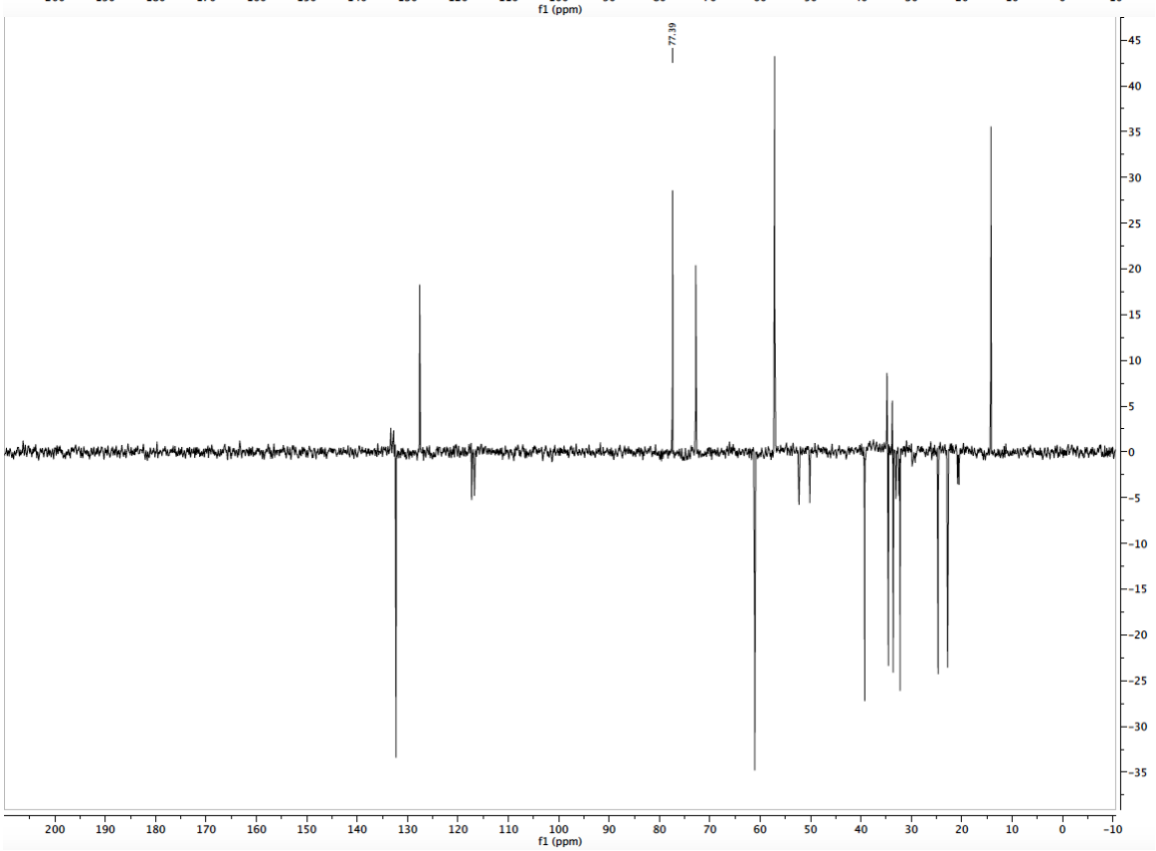
77.39
45
40
35
30
25
20
15
10
5
0
-5
-10
-15
-20
-25
-30
-35
200
190
180
170
160
150
140
130
120
110
100
90
80
70
60
50
40
30
20
10
0
-10
f1 (ppm)

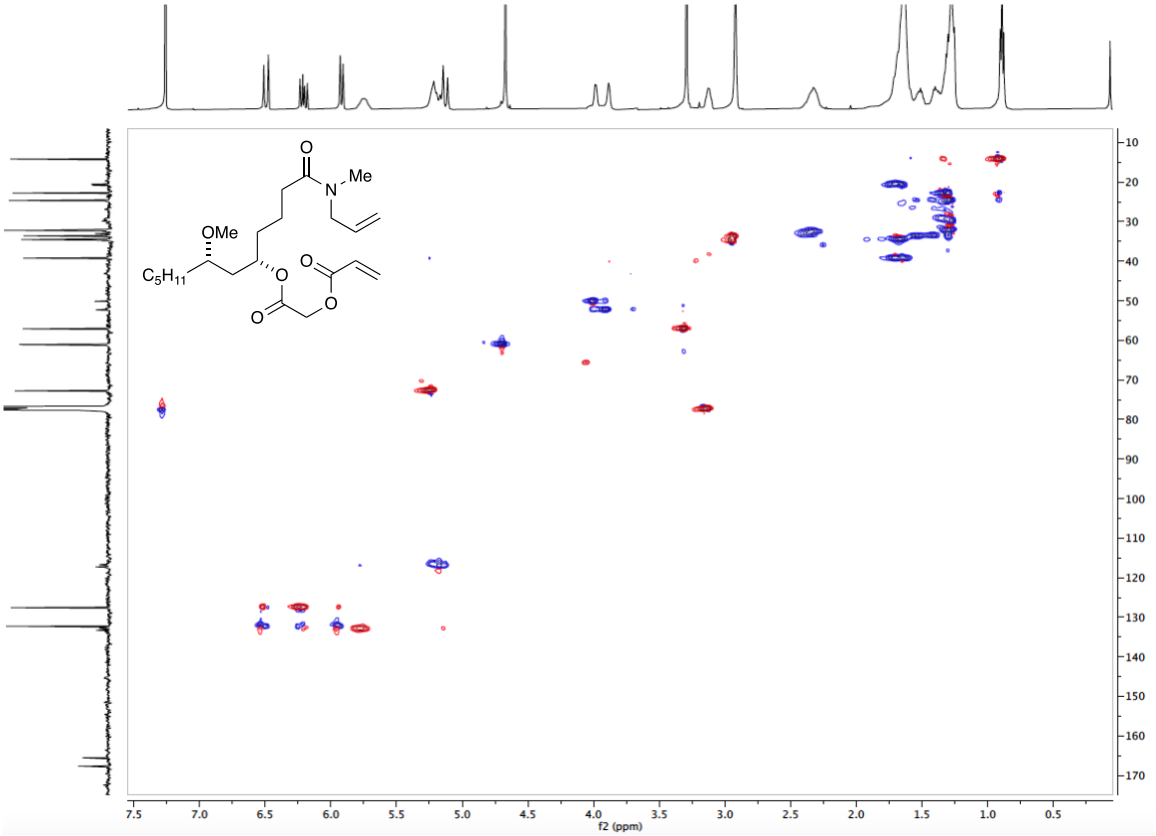
O
N
Me
OMe
C_5H_{11}
O
O
O
O
10
20
30
40
50
60
70
80
90
100
110
120
130
140
150
160
170
7.5
7.0
6.5
6.0
5.5
5.0
4.5
4.0
3.5
3.0
2.5
2.0
1.5
1.0
0.5
f2 (ppm)

(5*S*,7*S*)-1-(allyl(methyl)amino)-7-methoxy-1-oxododecan-5-yl (*S*)-2-(acryloyloxy)-3-methylbutanoate ($C_{25}H_{43}NO_6$, 3.8.5)

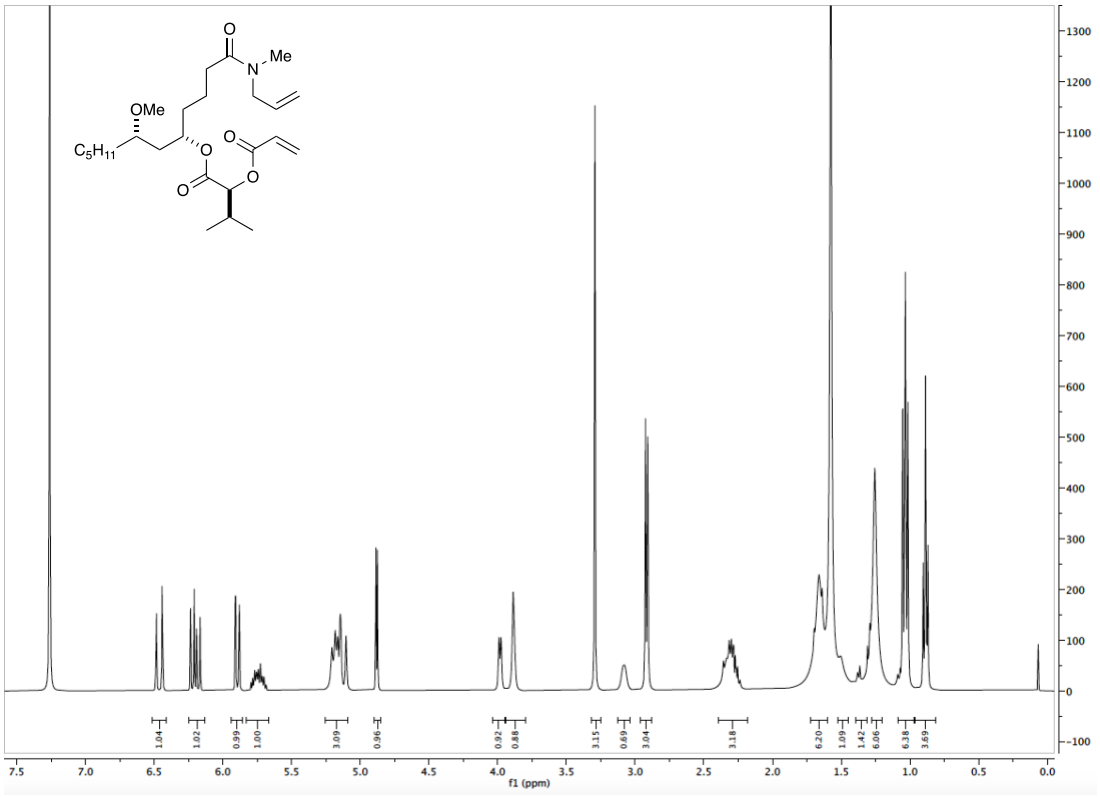

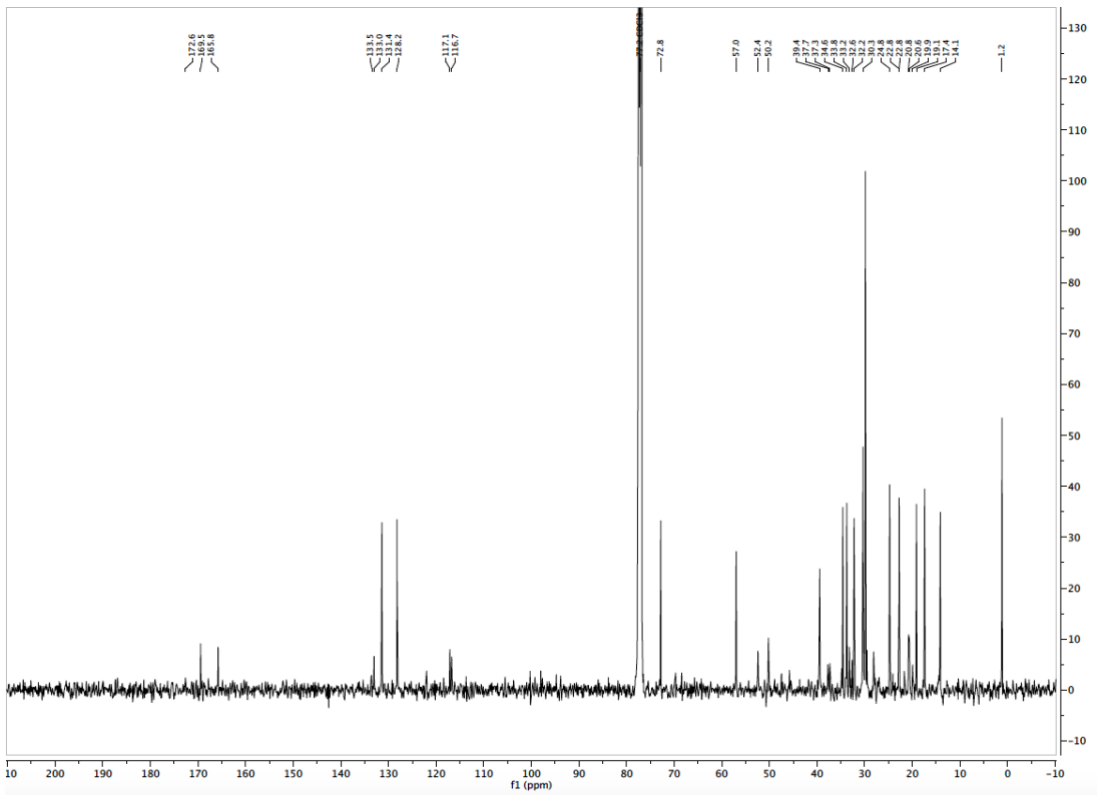

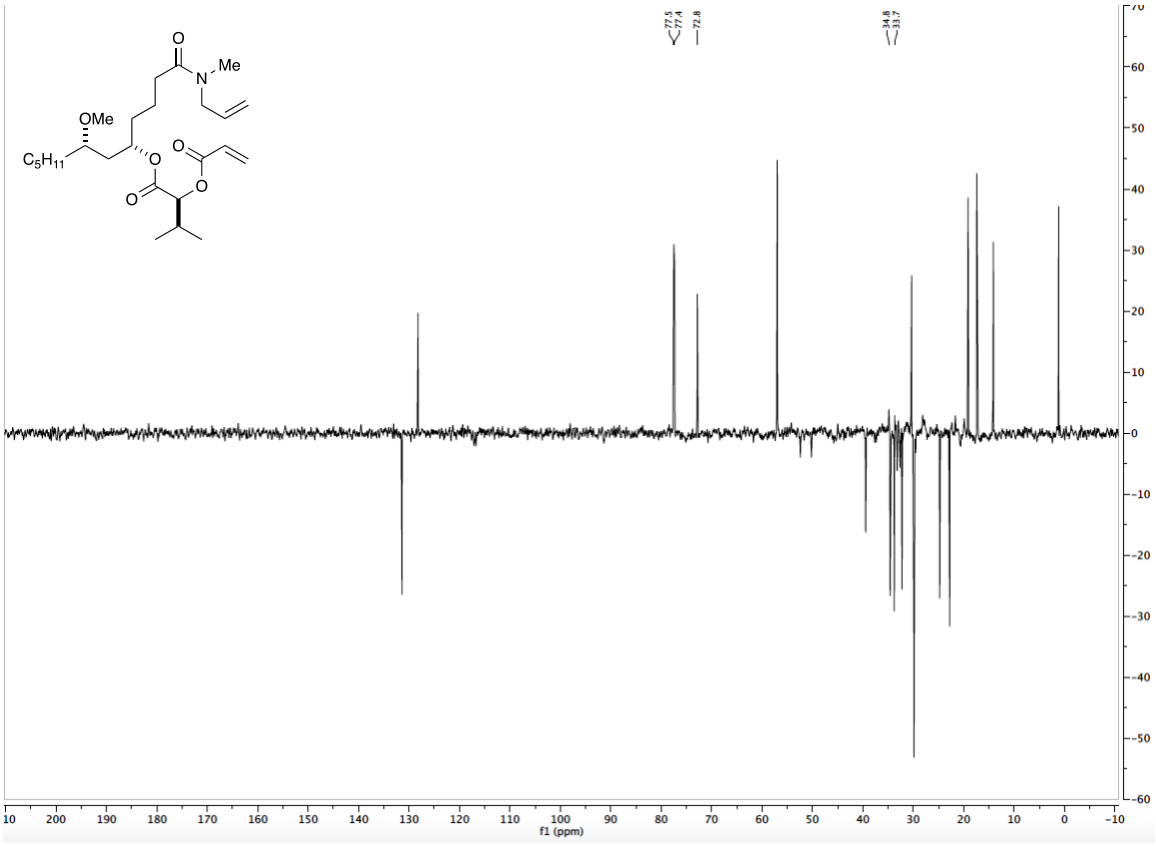
77.5
77.4
72.8
34.8
33.7
f1 (ppm)

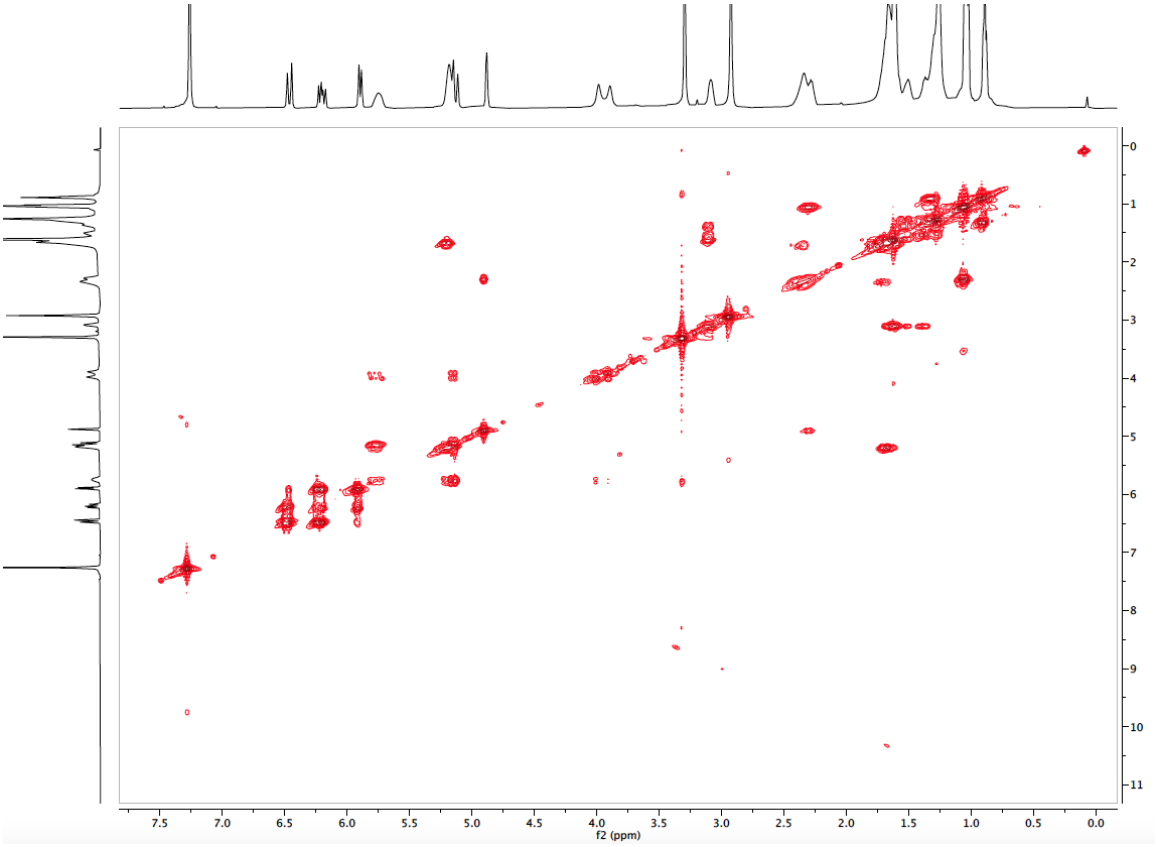
f2 (ppm)

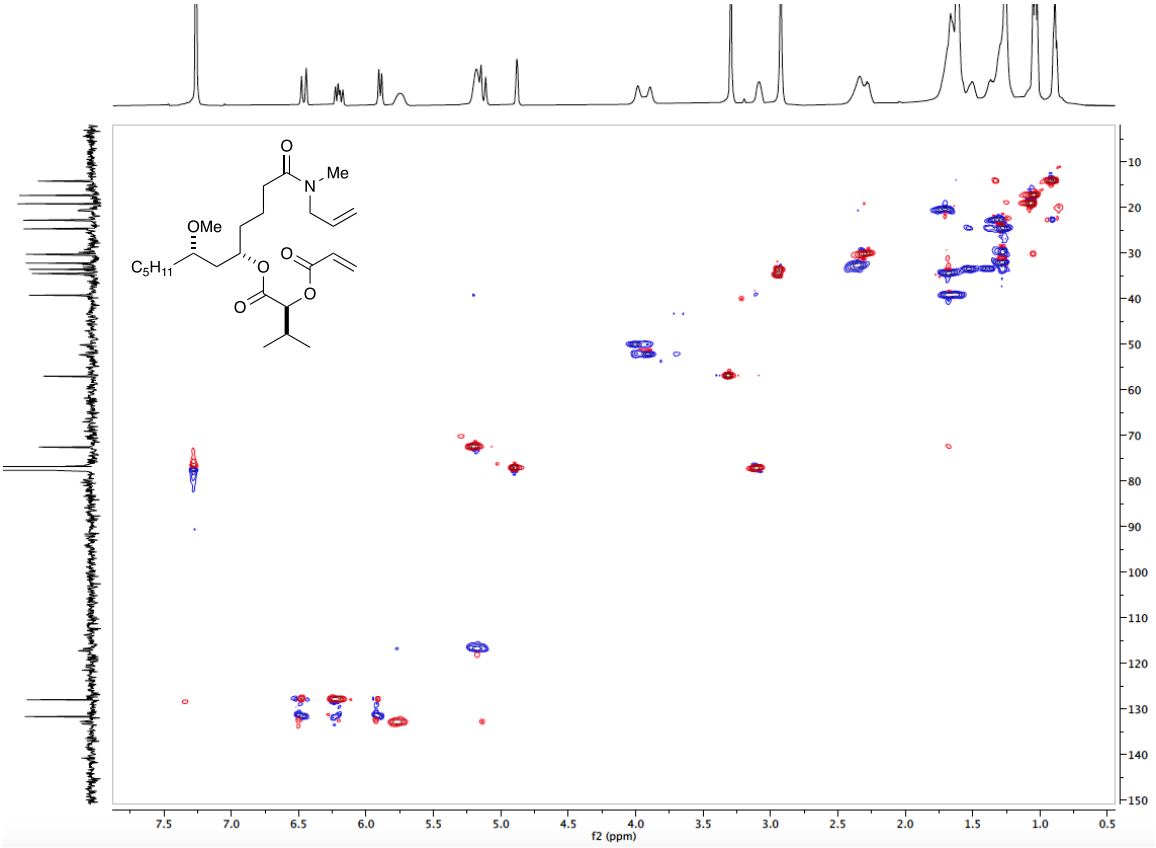
O
N
Me
OMe
C5H11
O
O
O
O
10
20
30
40
50
60
70
80
90
100
110
120
130
140
150
7.5
7.0
6.5
6.0
5.5
5.0
4.5
4.0
3.5
3.0
2.5
2.0
1.5
1.0
0.5
f2 (ppm)

2-(((5*S*,7*S*)-1-(allyl(4-(trifluoromethyl)benzyl)amino)-7-methoxy-1-oxododecan-5-yl)oxy)-2-oxoethyl acrylate ($C_{29}H_{40}F_3NO_6$, 3.8.8)

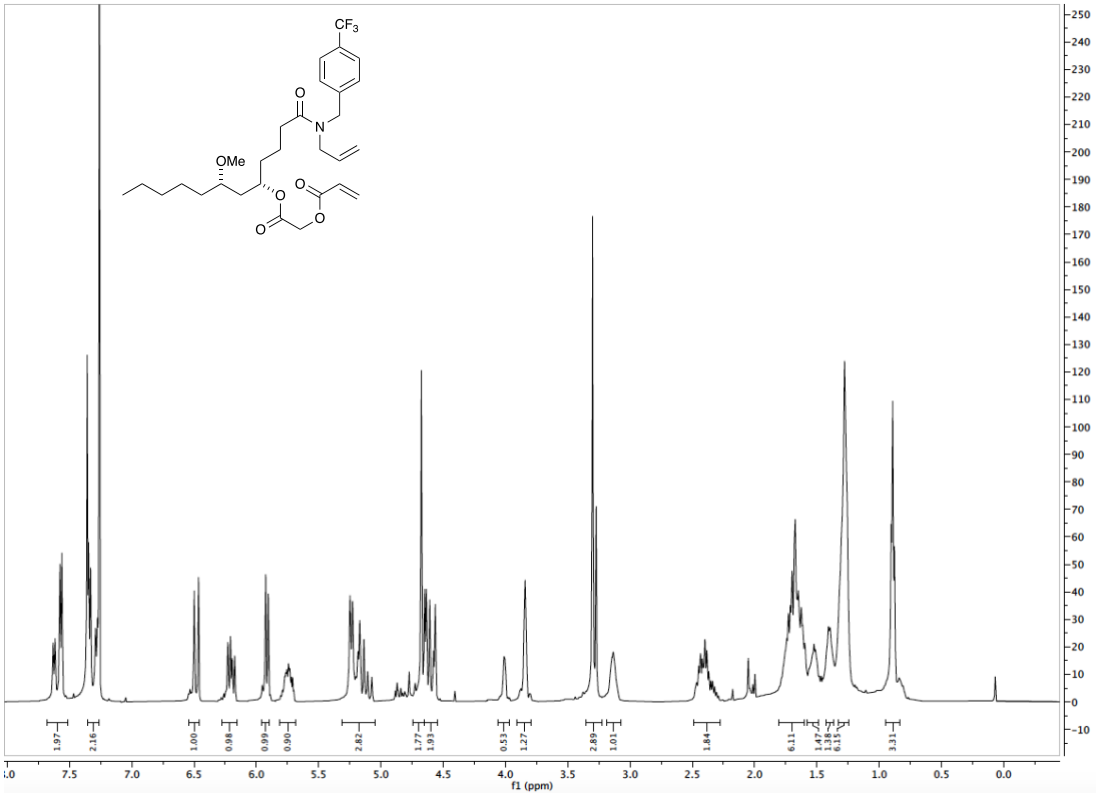

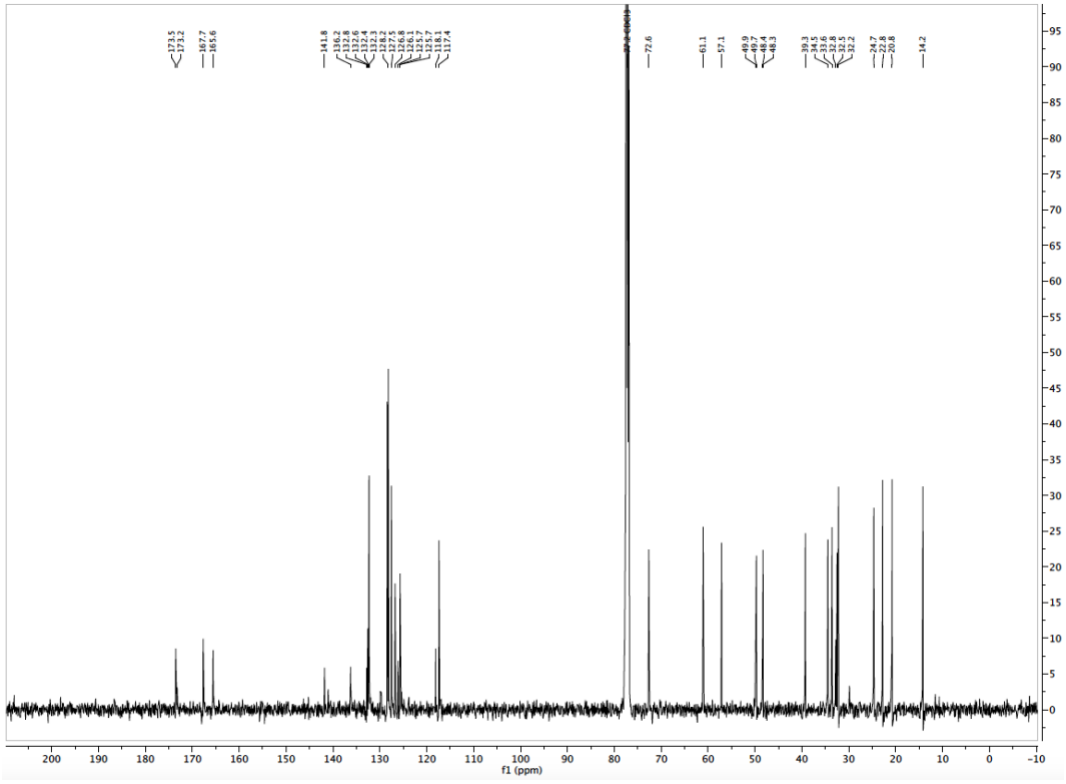

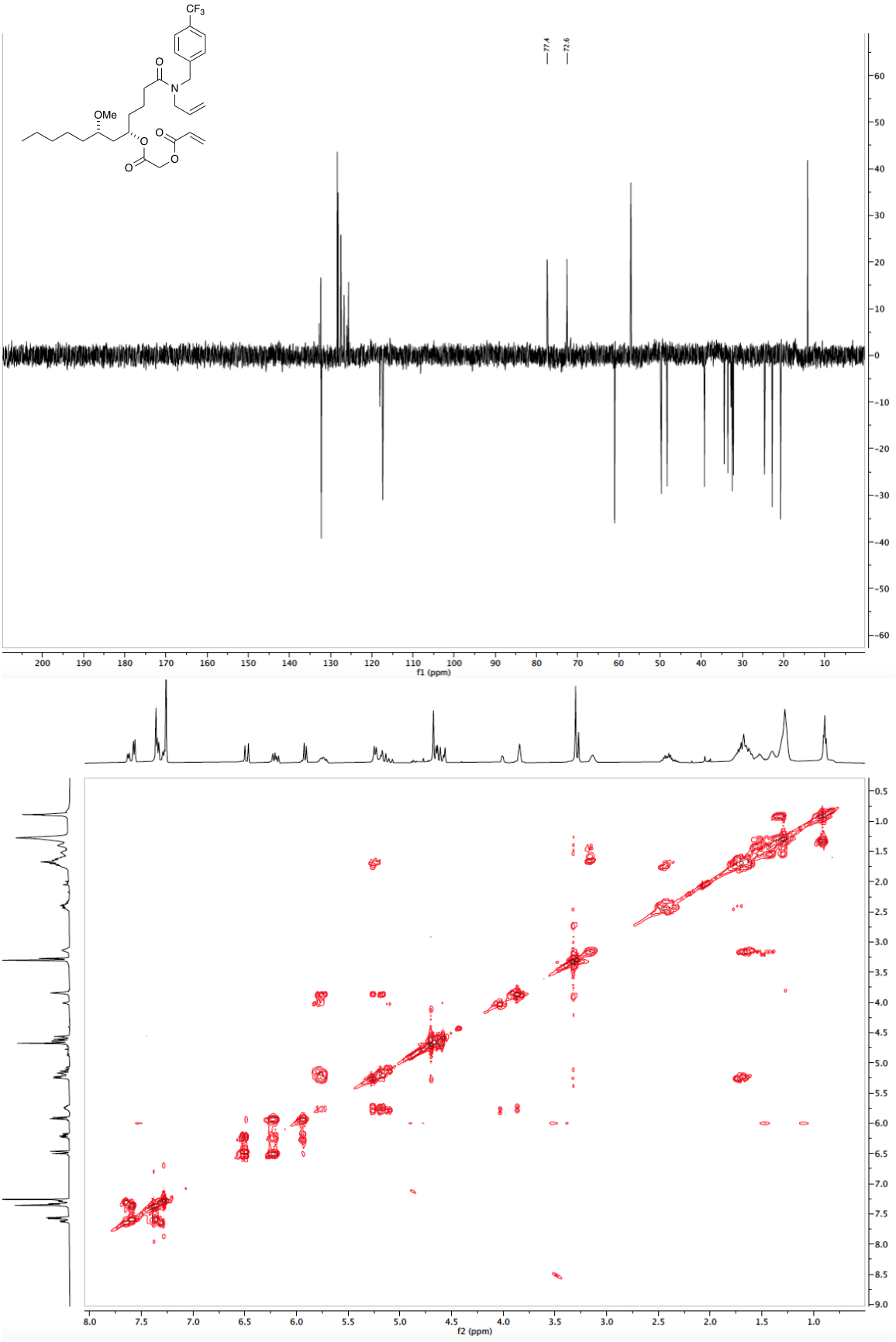
CF3
O
N
OMe
O
O
O
O
77.4
72.6
f1 (ppm)
f2 (ppm)

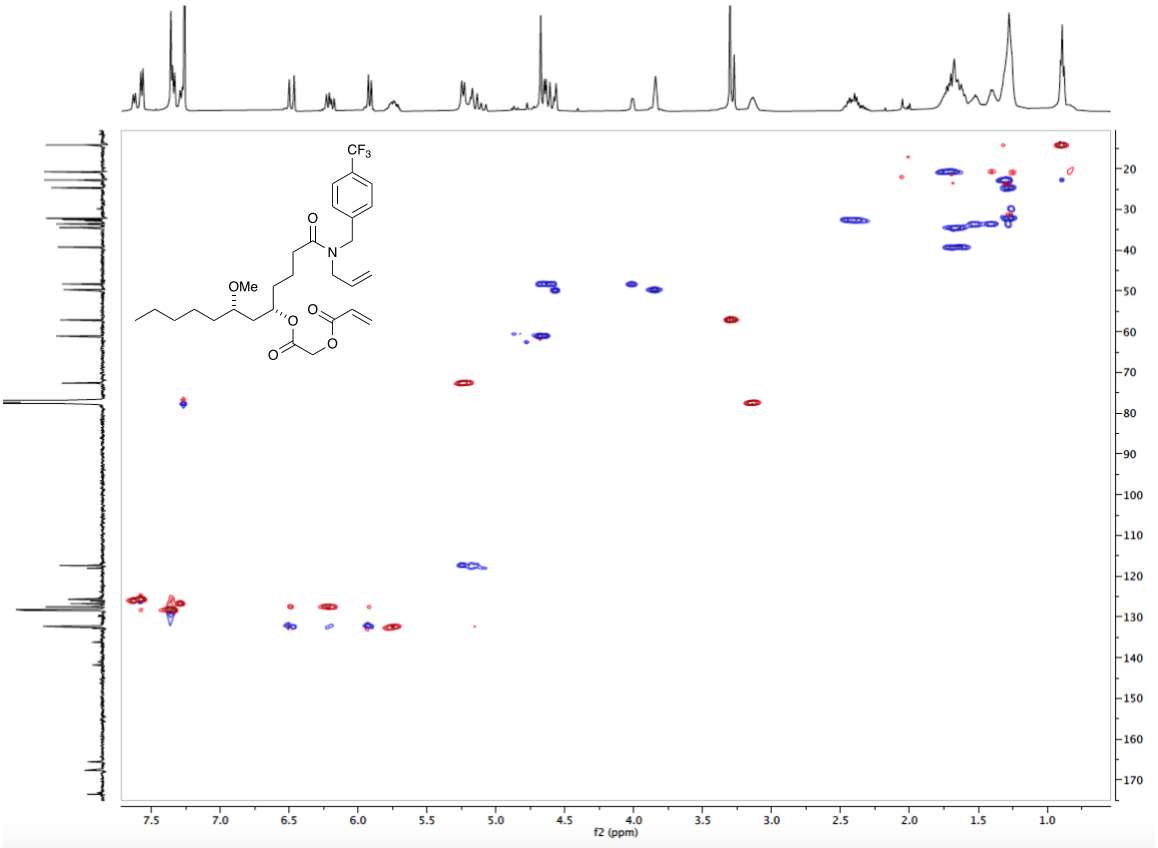
CF3
O
N
OMe
O
O
O
O
f2 (ppm)

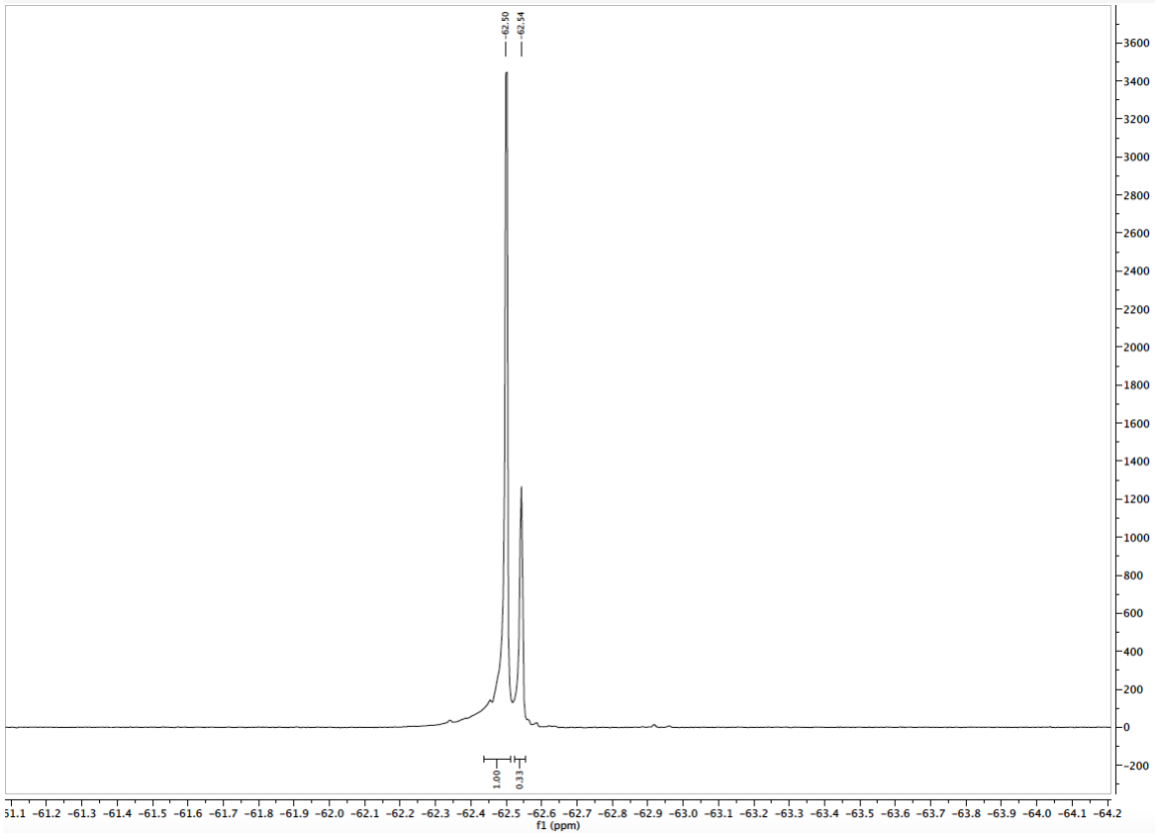
-62.50
-62.54
1.00
0.33
f1 (ppm)

(5*S*,7*S*)-*N*-allyl-5-hydroxy-7-methoxy-*N*-methyl-10-phenyldecanamide ($C_{21}H_{33}NO_3$, 3.9.1)

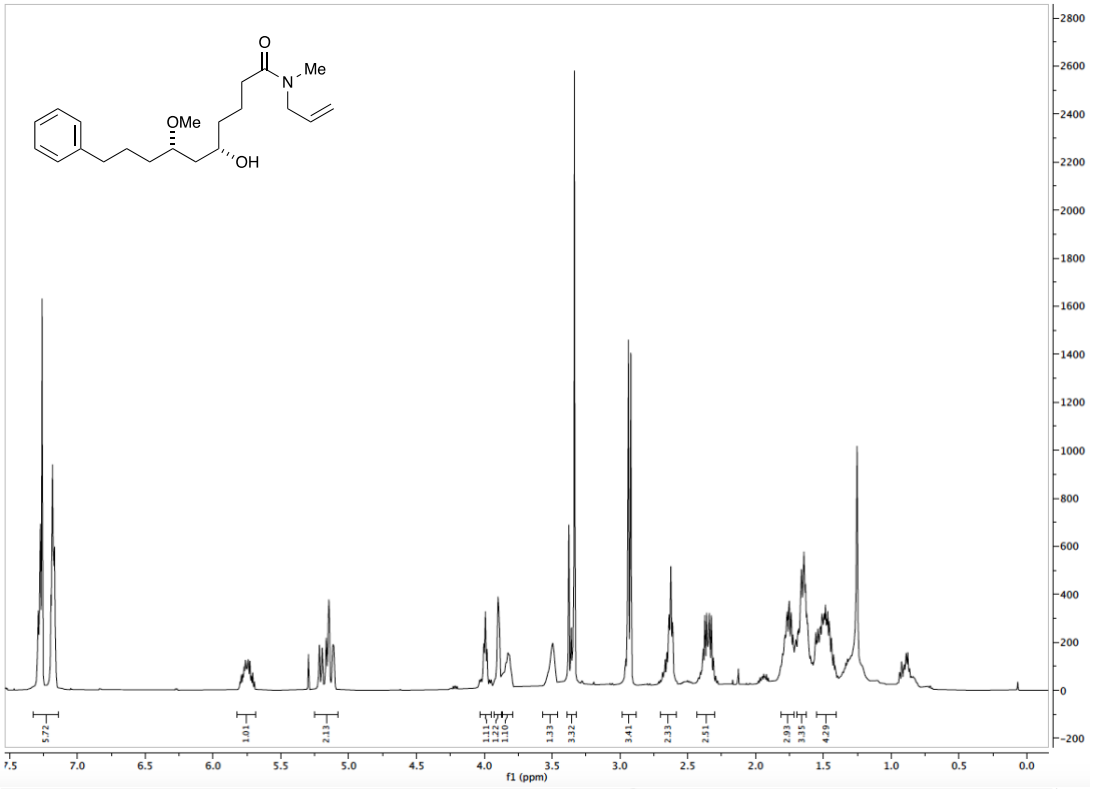

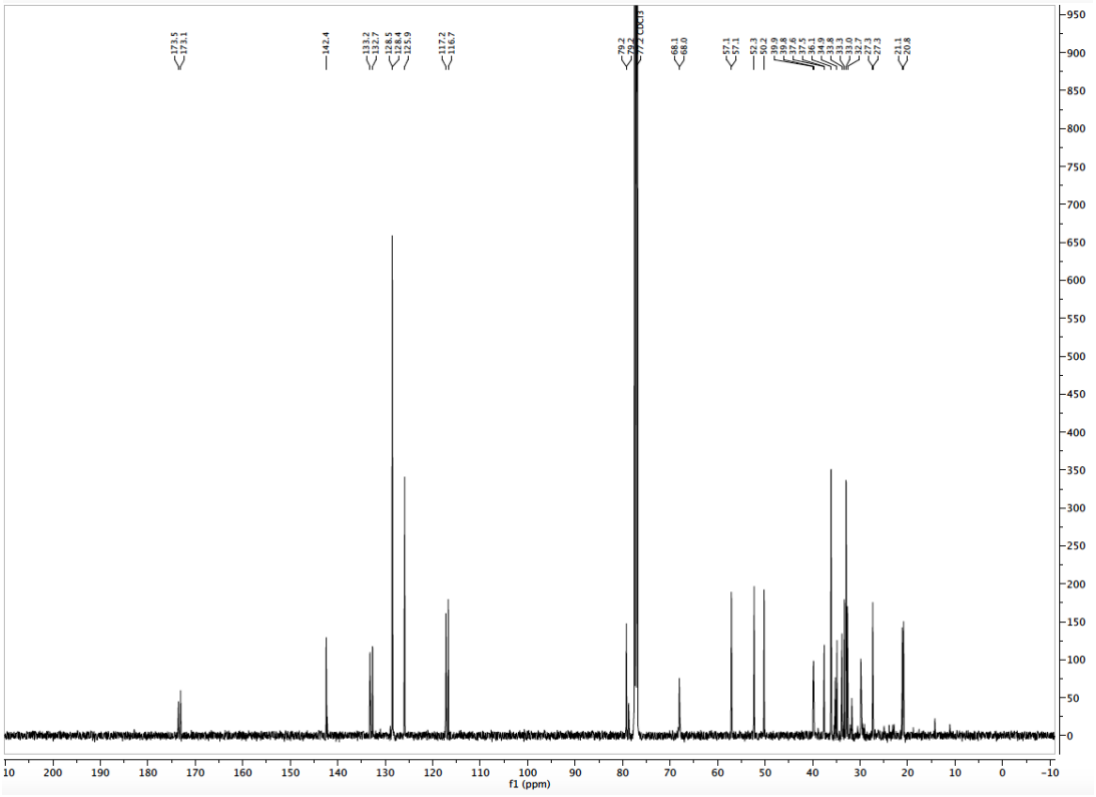

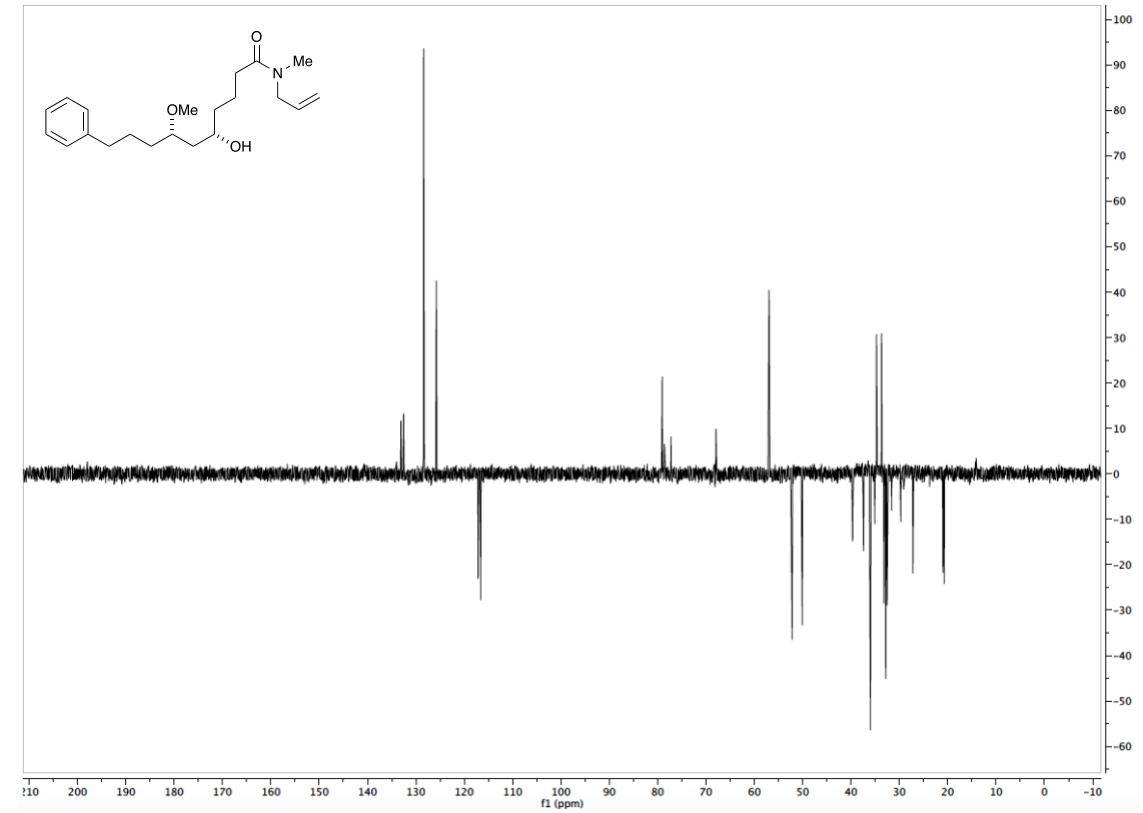
O
N
Me
OMe
OH
f1 (ppm)

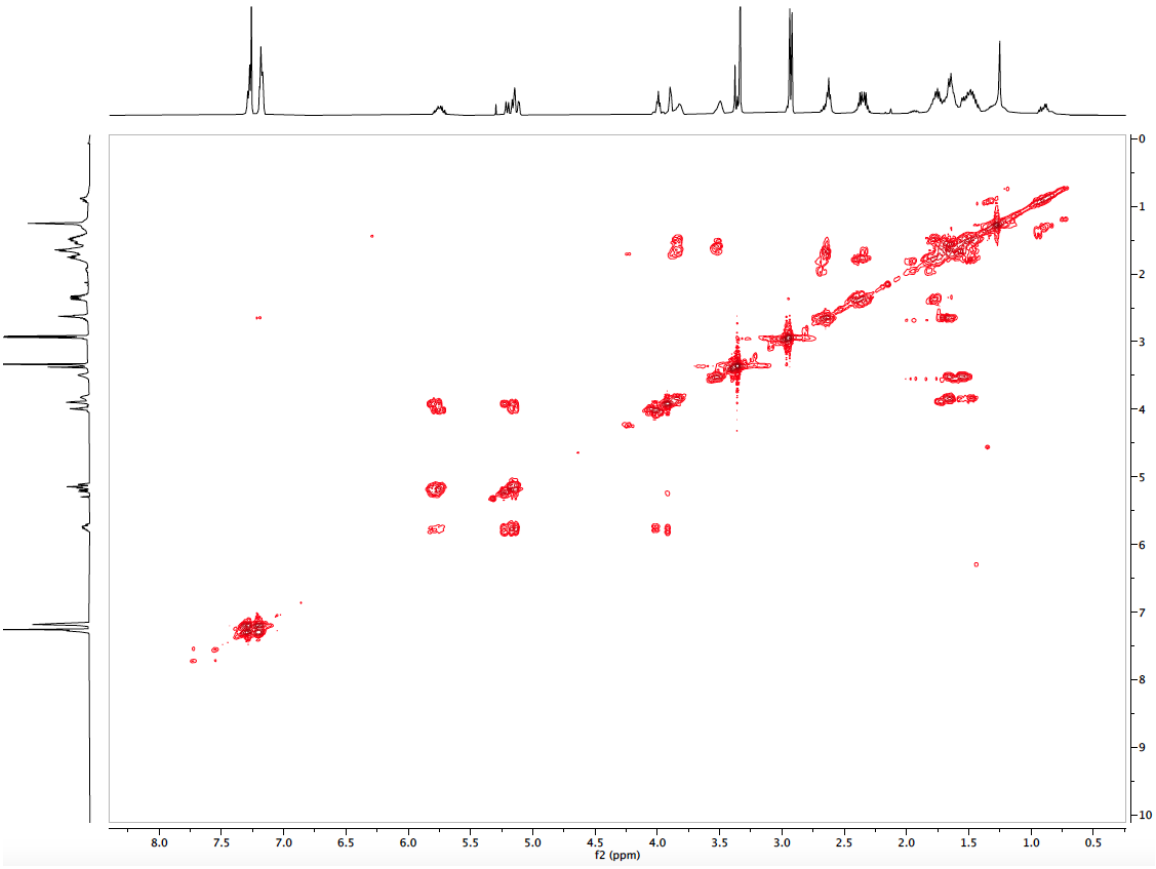
f2 (ppm)

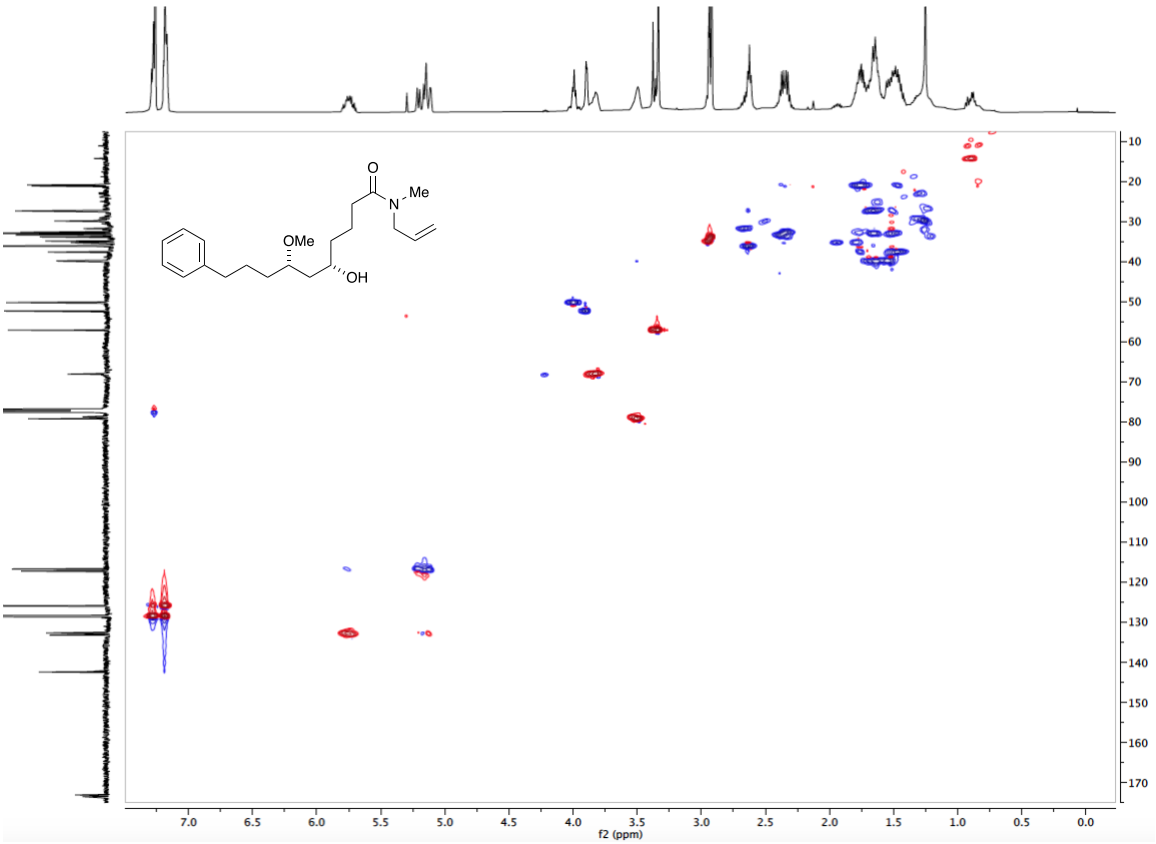
O
N
Me
OMe
OH
7.0
6.5
6.0
5.5
5.0
4.5
4.0
3.5
3.0
2.5
2.0
1.5
1.0
0.5
0.0
f2 (ppm)
10
20
30
40
50
60
70
80
90
100
110
120
130
140
150
160
170

2-(((5*S*,7*S*)-1-(allyl(methyl)amino)-7-methoxy-1-oxo-10-phenyldecan-5-yl)oxy)-2-oxoethyl acrylate ($C_{26}H_{37}NO_6$, 3.9.2)

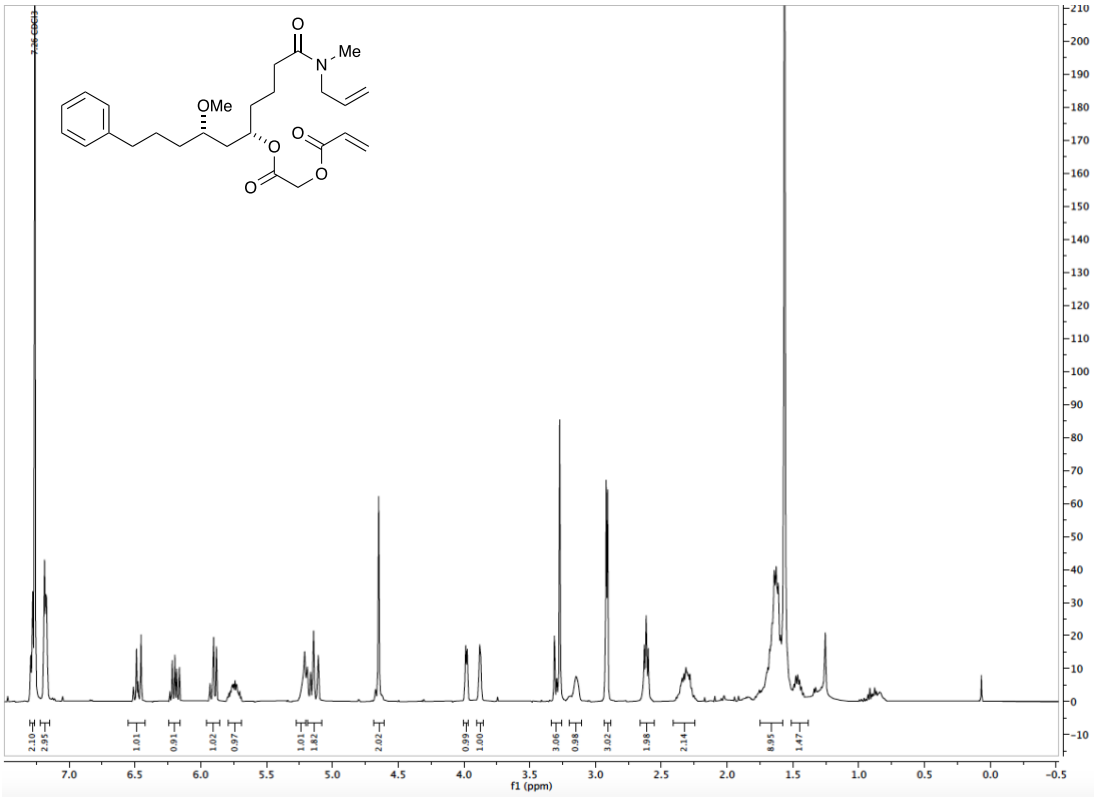

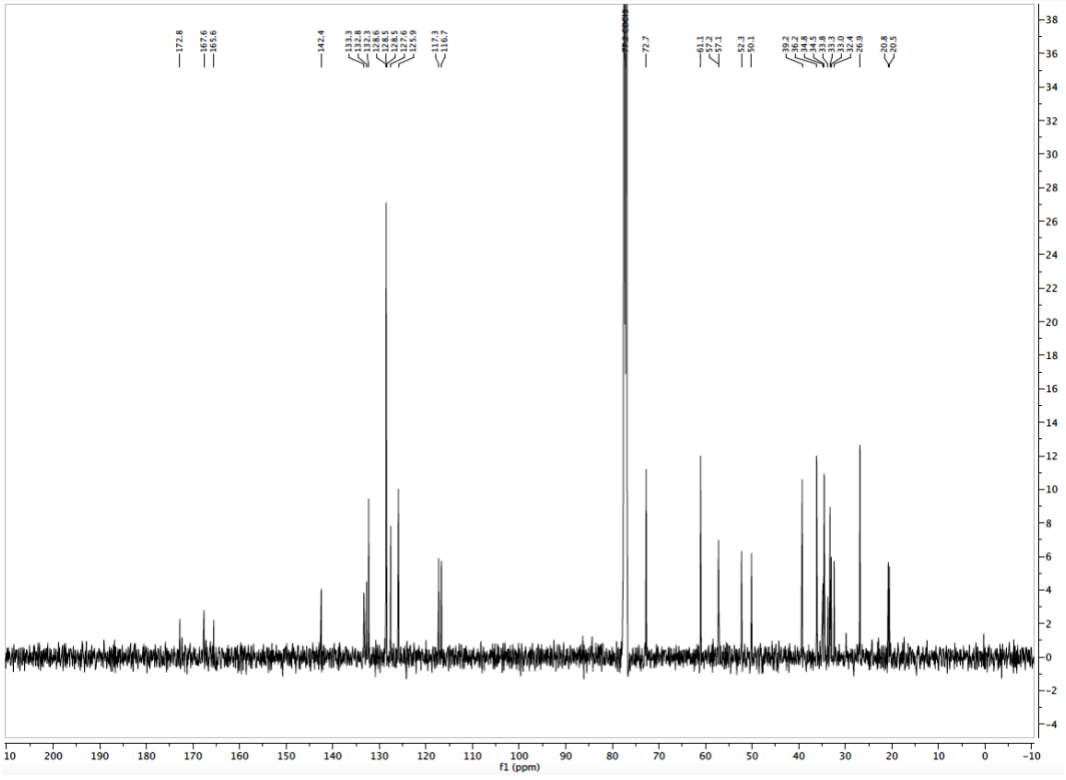

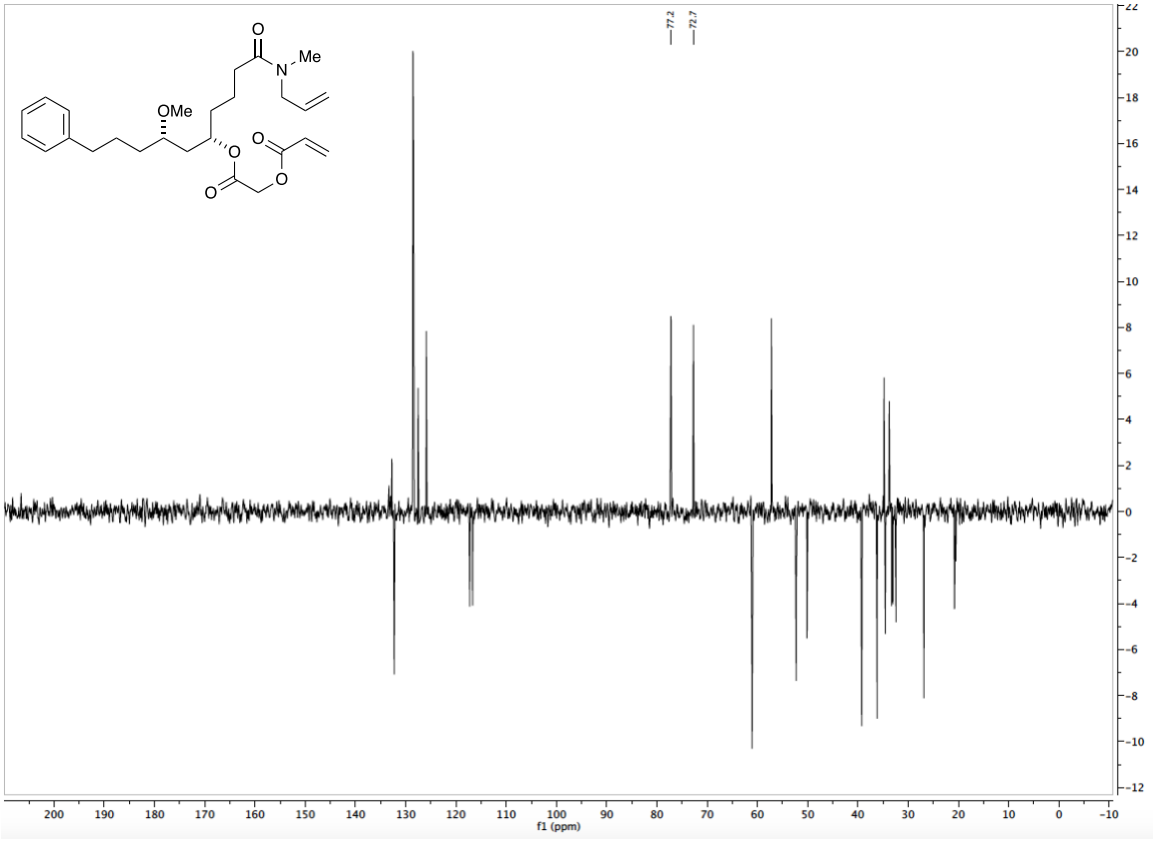
O
N
Me
OMe
O
O
O
O
77.2
72.7
f1 (ppm)

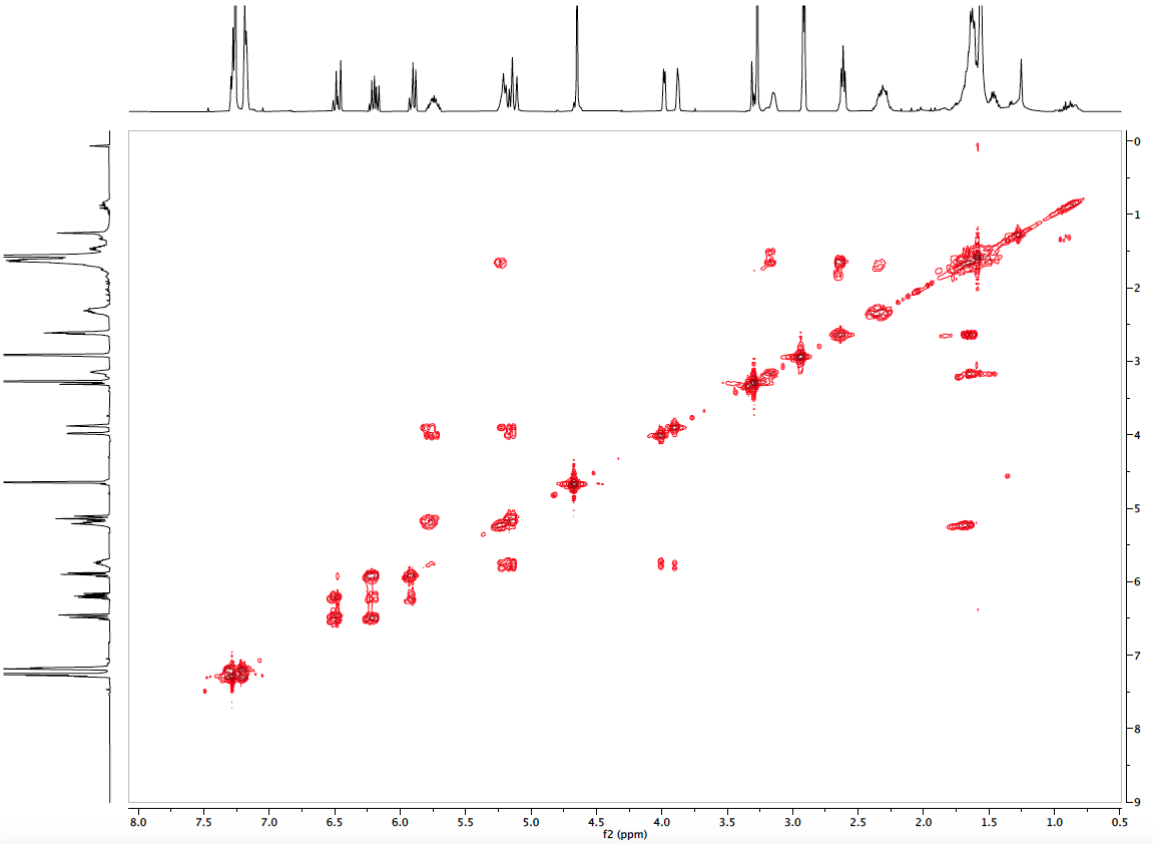
f2 (ppm)

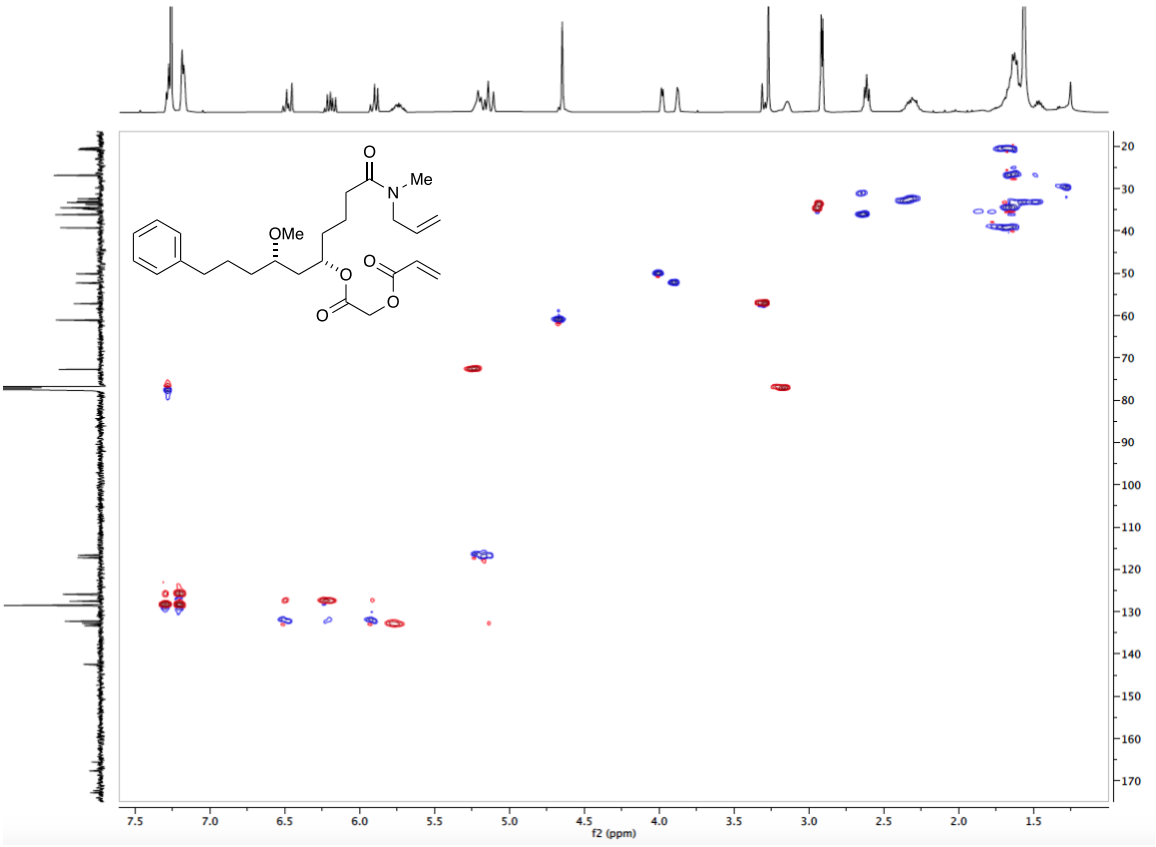
O
N
Me
OMe
O
O
O
O
20
30
40
50
60
70
80
90
100
110
120
130
140
150
160
170
7.5
7.0
6.5
6.0
5.5
5.0
4.5
4.0
3.5
3.0
2.5
2.0
1.5
f2 (ppm)

(5*S*,7*S*)-1-(allyl(methyl)amino)-7-methoxy-1-oxo-10-phenyldecan-5-yl (*S*)-2-(acryloyloxy)-3-methylbutanoate ($C_{29}H_{43}NO_6$, 3.9.3)

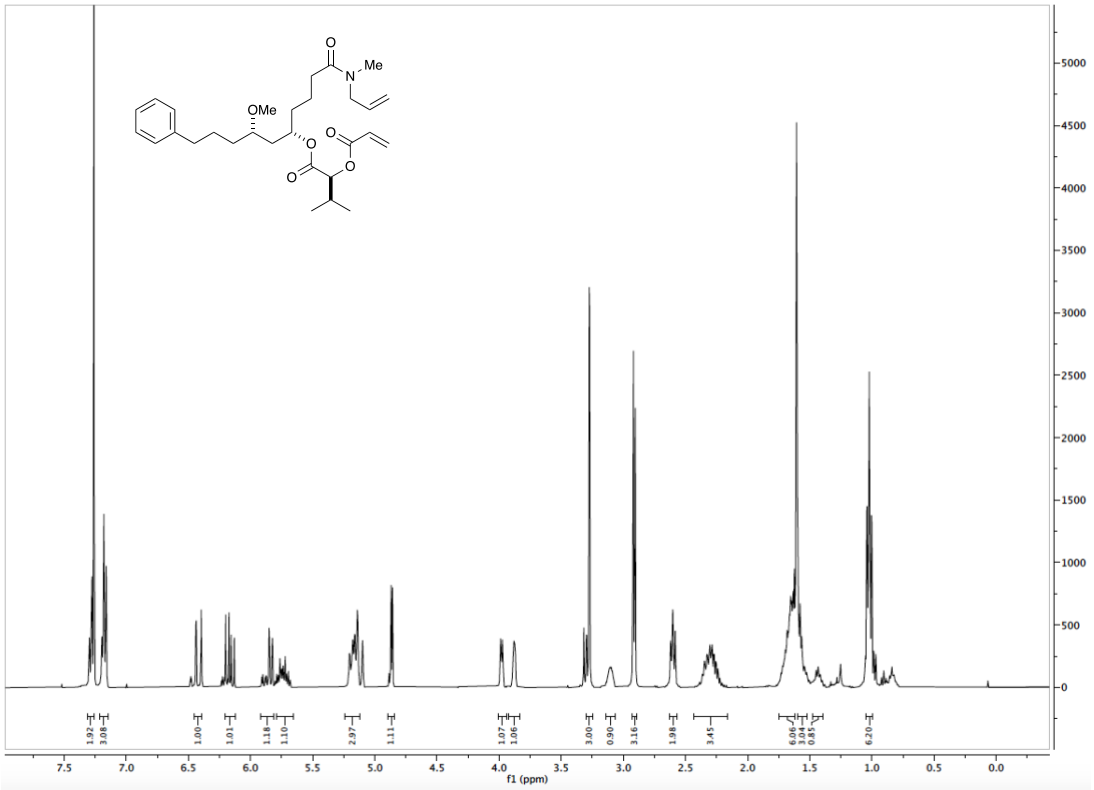

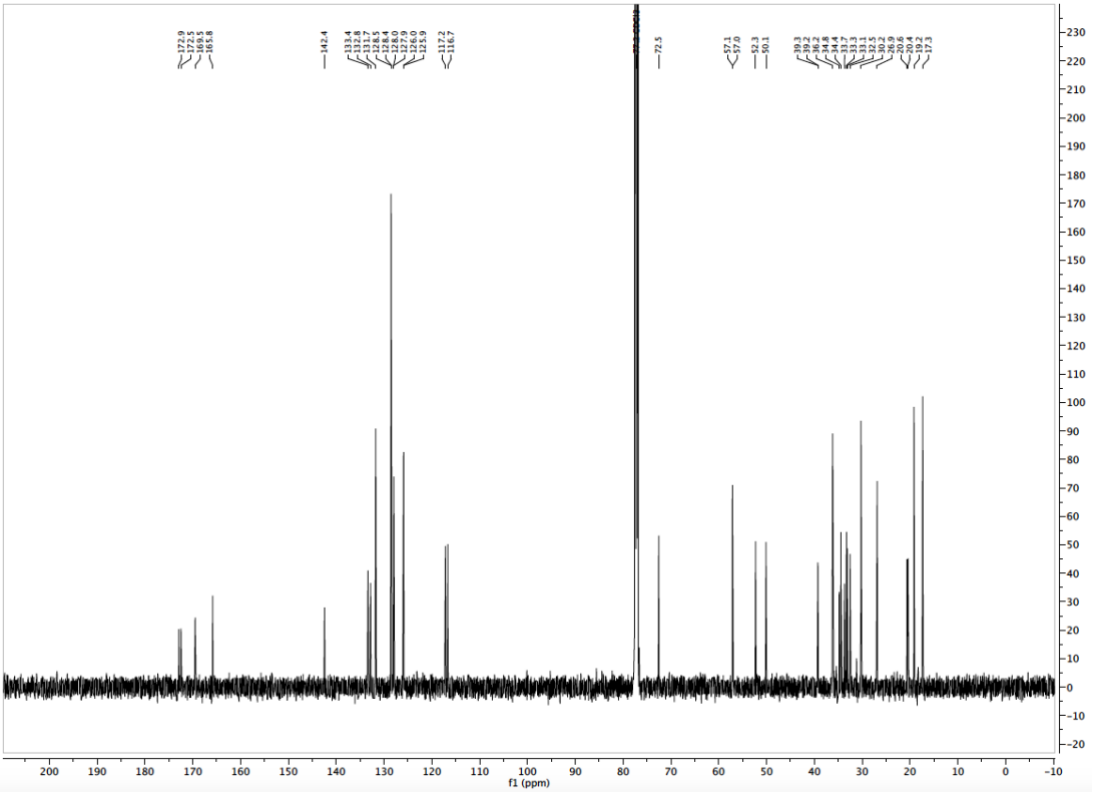

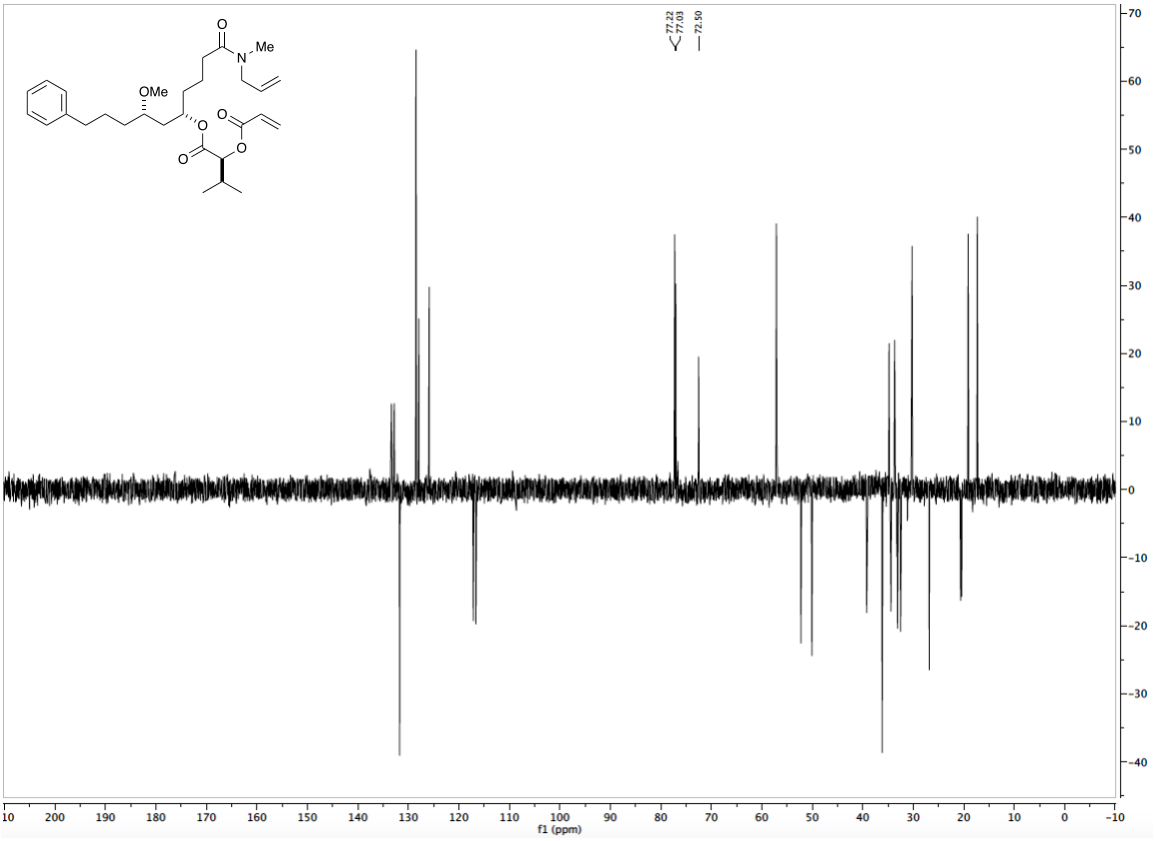
77.22
77.03
72.50
f1 (ppm)

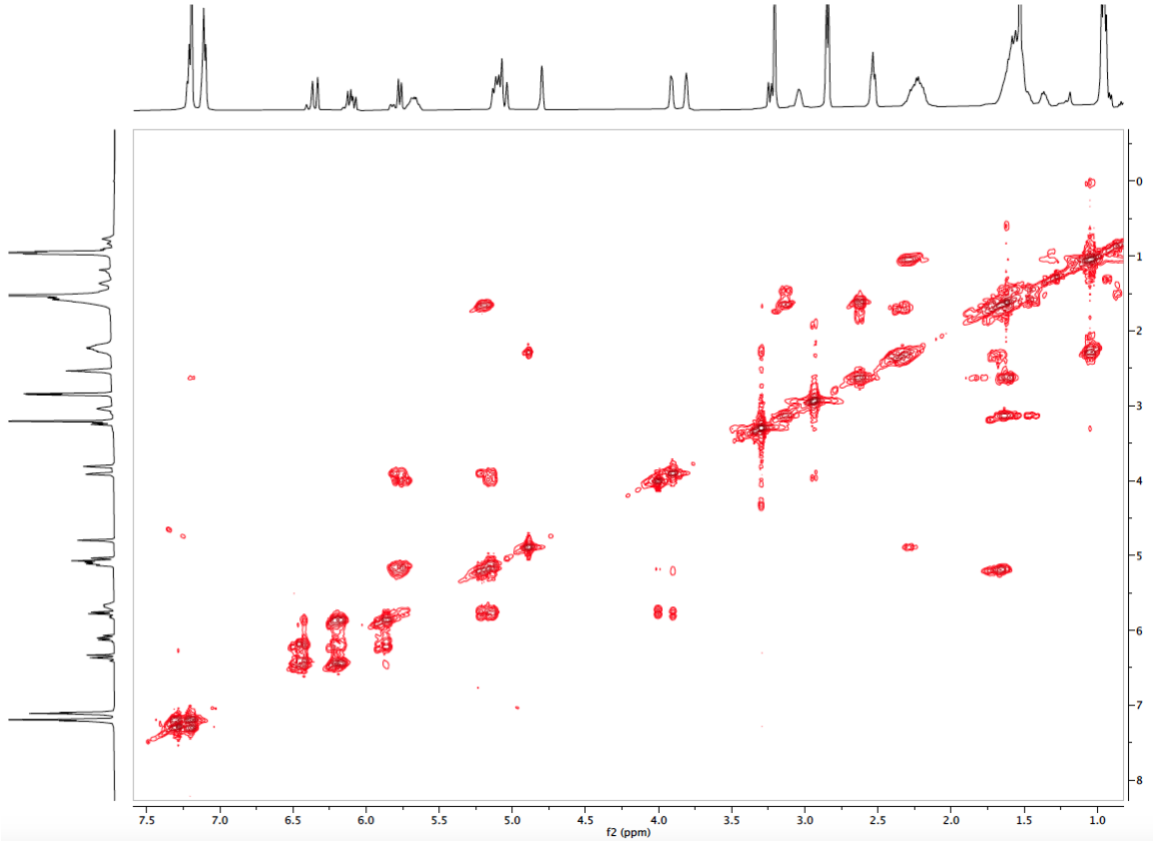
f2 (ppm)

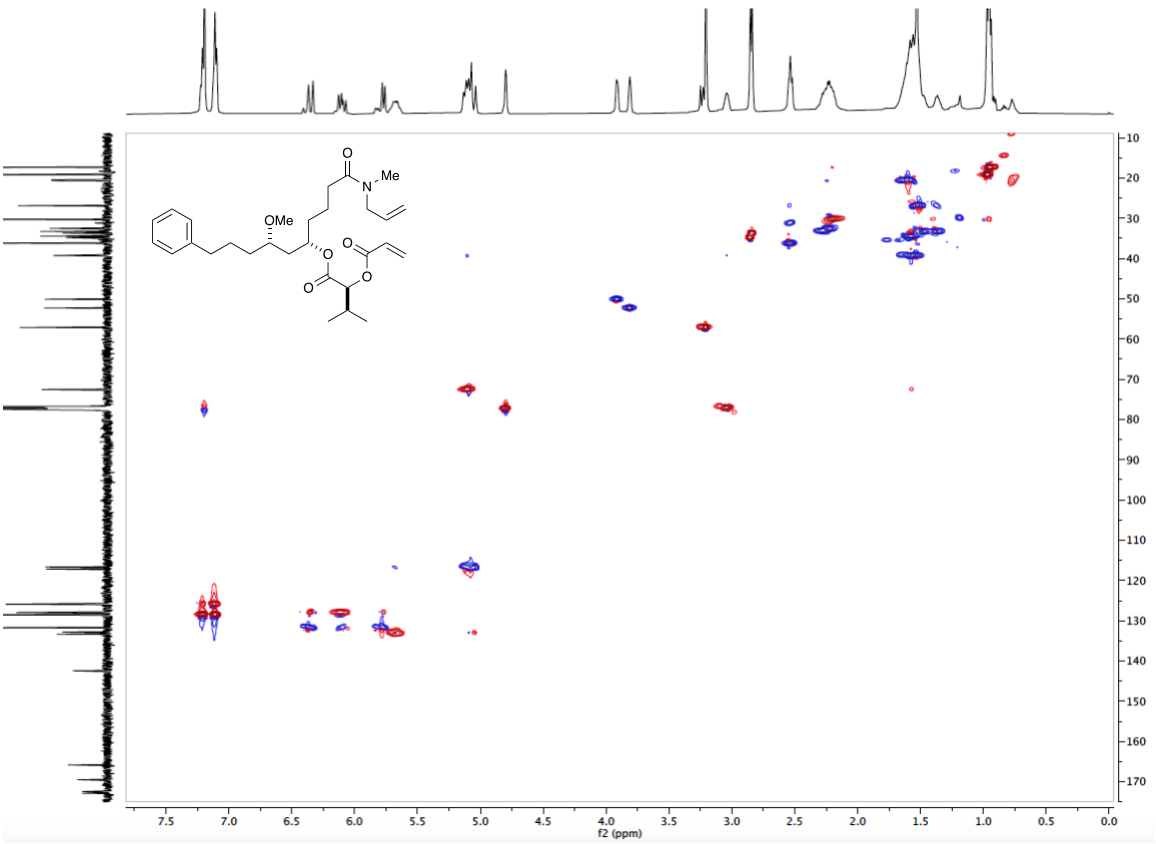
OMe
N
Me
O
O
O
O
O
10
20
30
40
50
60
70
80
90
100
110
120
130
140
150
160
170
7.5
7.0
6.5
6.0
5.5
5.0
4.5
4.0
3.5
3.0
2.5
2.0
1.5
1.0
0.5
0.0
f2 (ppm)

(3*S*,14*S*,*Z*)-3-isopropyl-14-((*S*)-2-methoxyheptyl)-9-methyl-1,4-dioxa-9-azacyclotetradec-6-ene-2,5,10-trione ($C_{23}H_{39}NO_6$, 3.10.1)

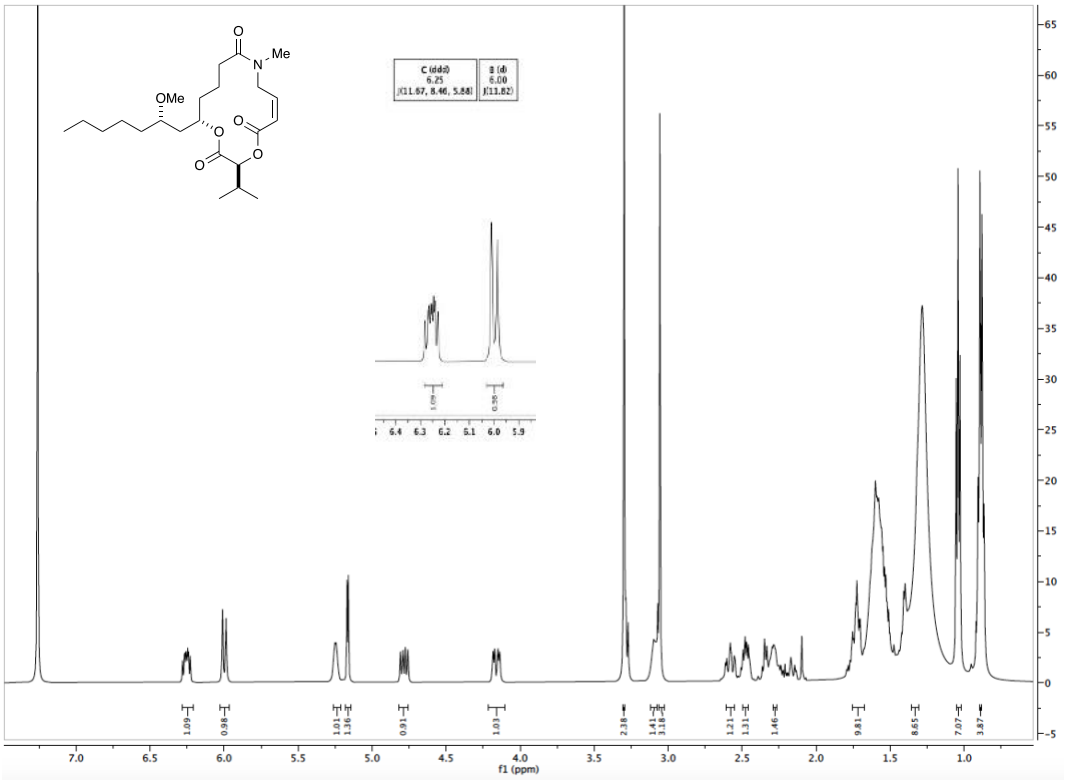

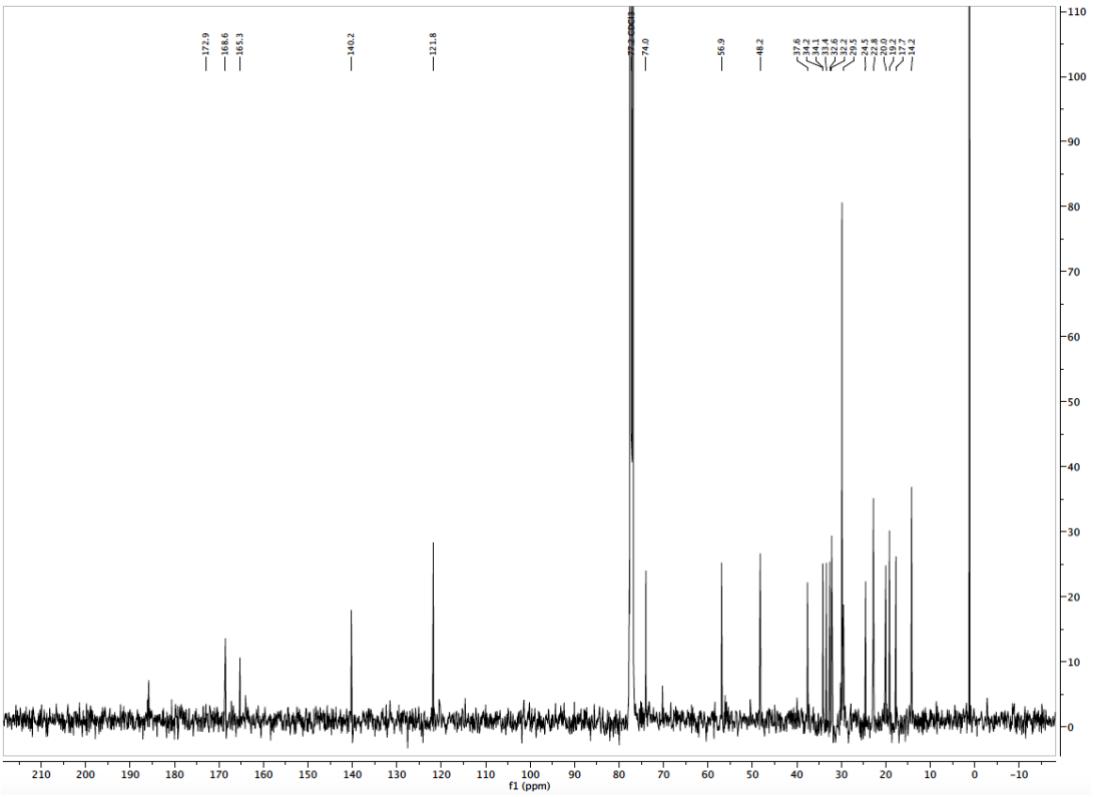

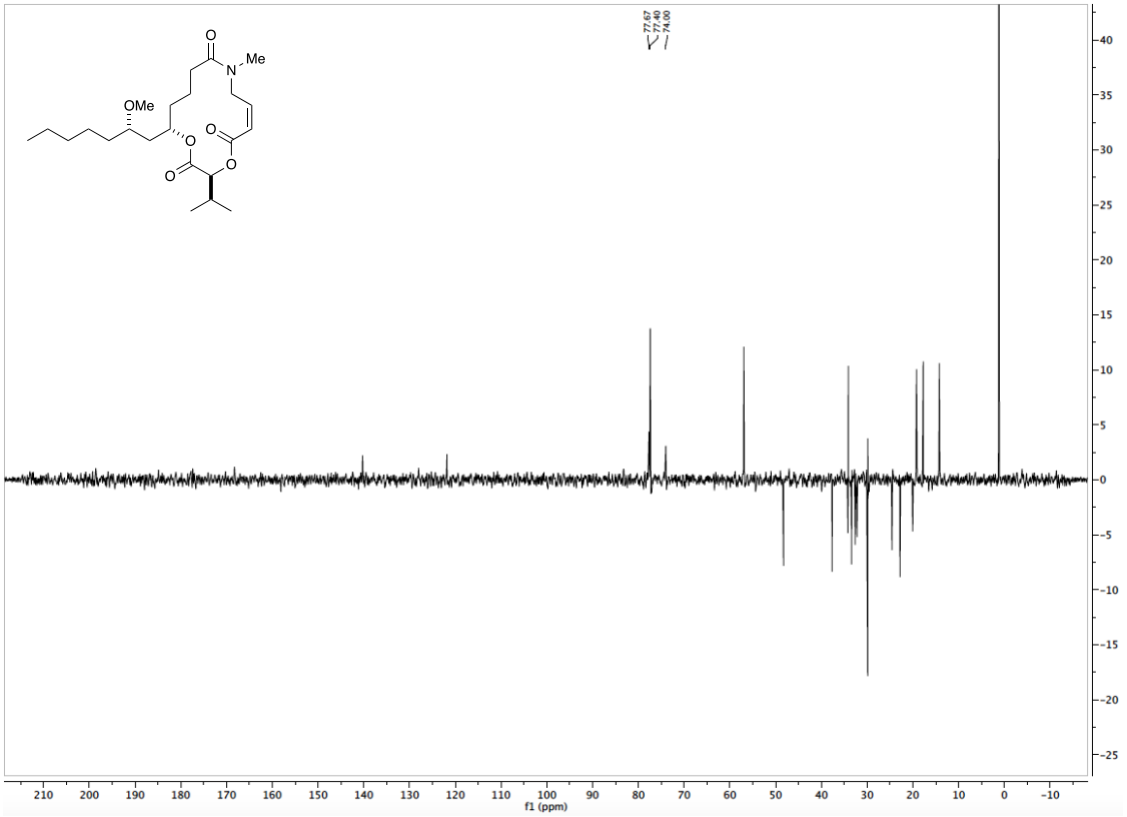
77.67
77.40
74.00
f1 (ppm)

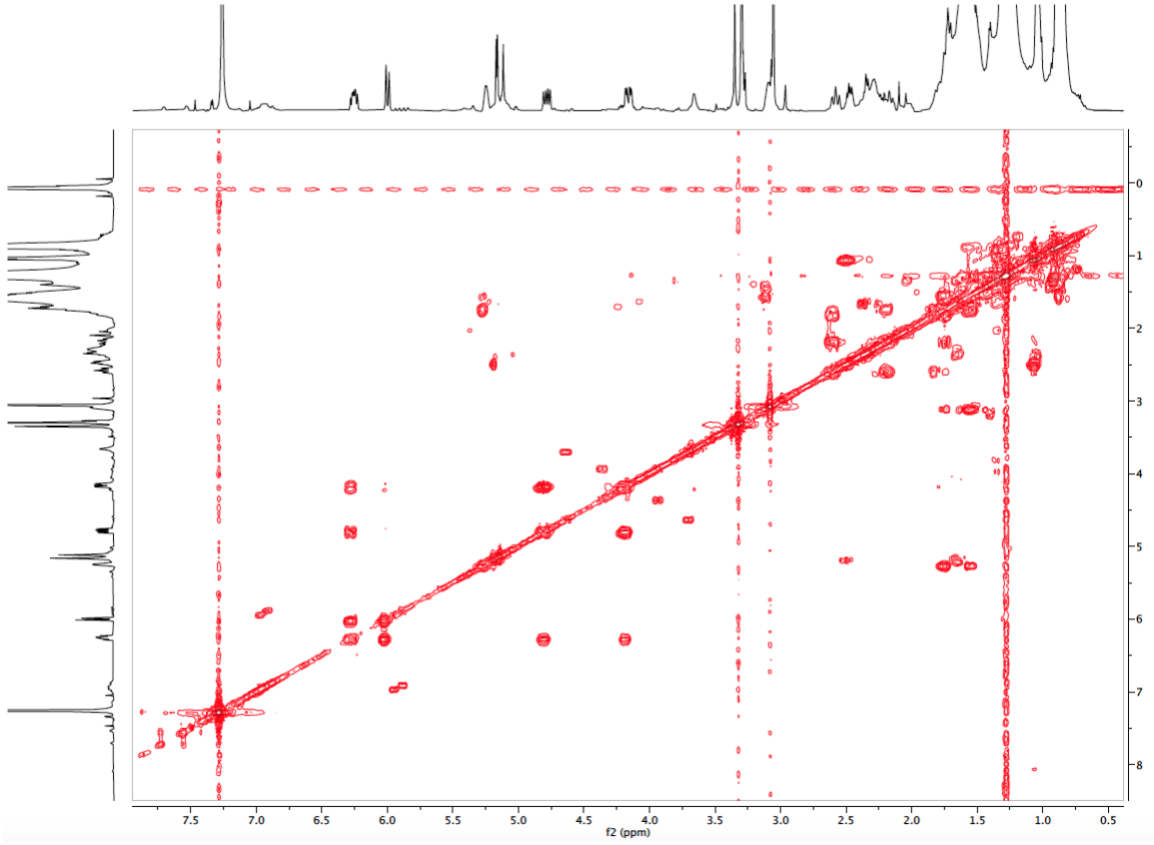
f2 (ppm)

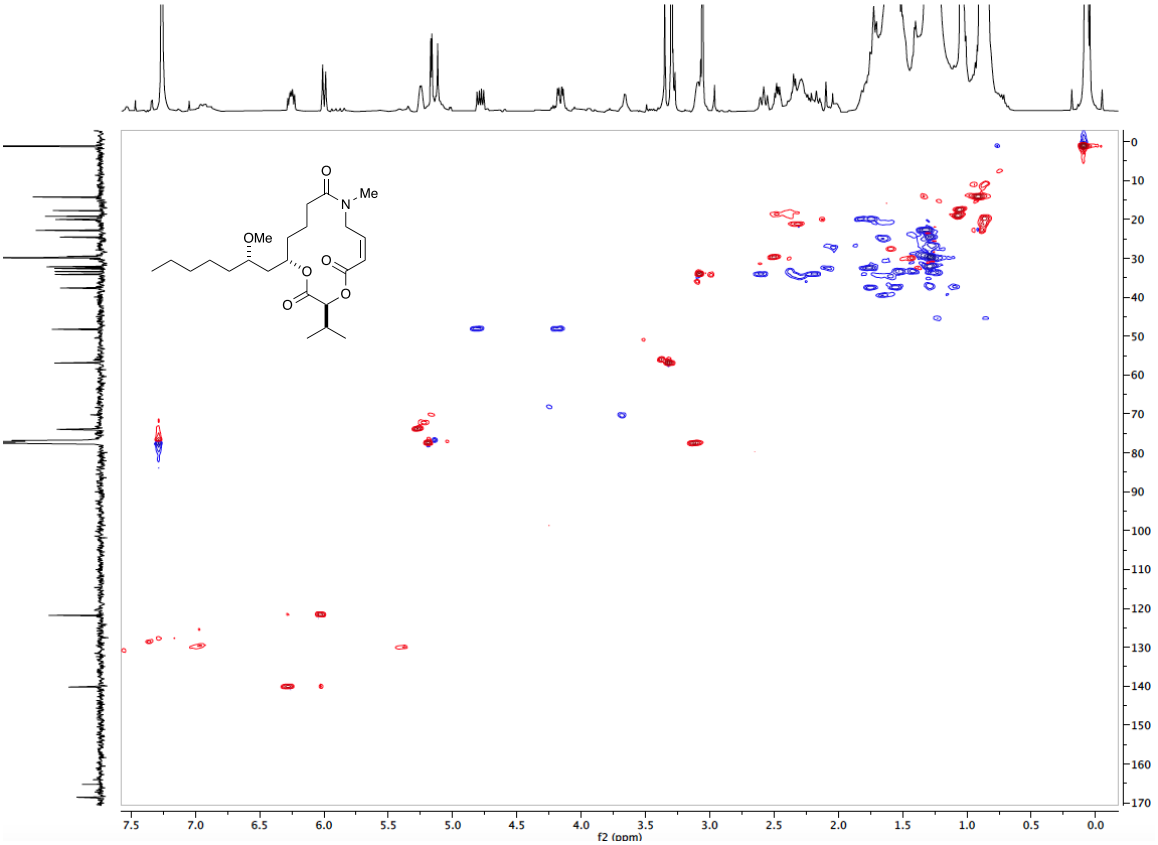
OMe
N
Me
O
O
O
O
O
7.5
7.0
6.5
6.0
5.5
5.0
4.5
4.0
3.5
3.0
2.5
2.0
1.5
1.0
0.5
0.0
f2 (ppm)
0
10
20
30
40
50
60
70
80
90
100
110
120
130
140
150
160
170

(*S*,*Z*)-14-((*S*)-2-methoxyheptyl)-9-methyl-1,4-dioxa-9-azacyclotetradec-6-ene-2,5,10-trione ($C_{20}H_{33}NO_6$, 3.10.2)

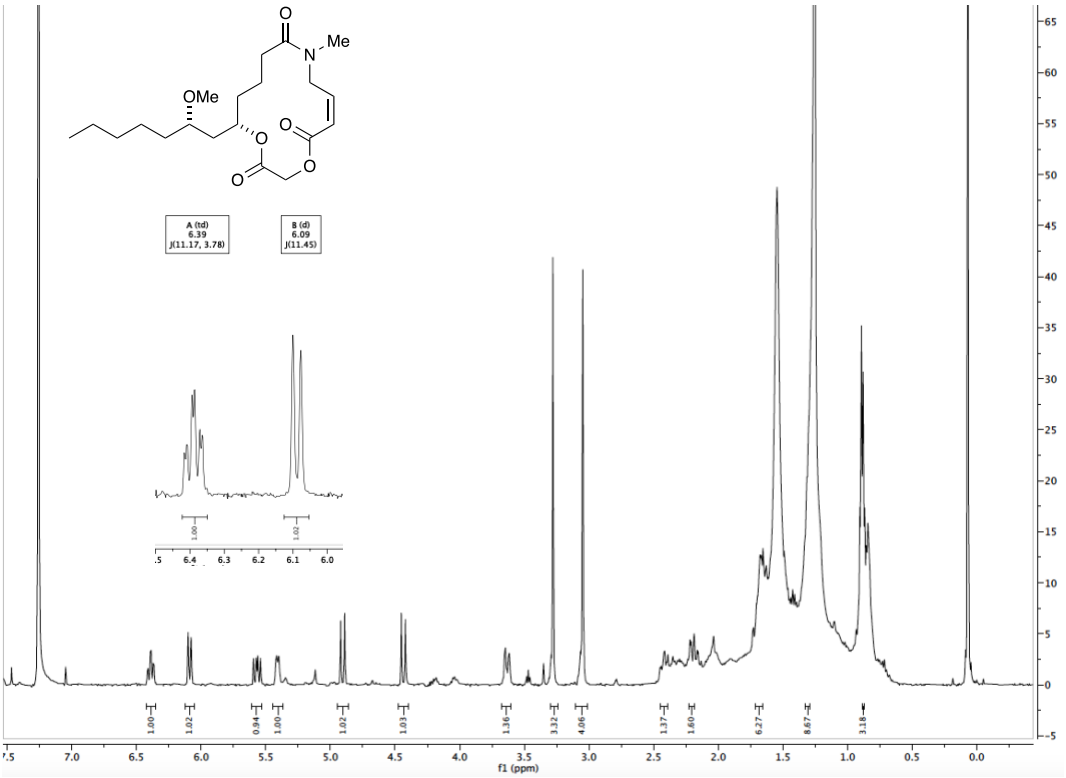

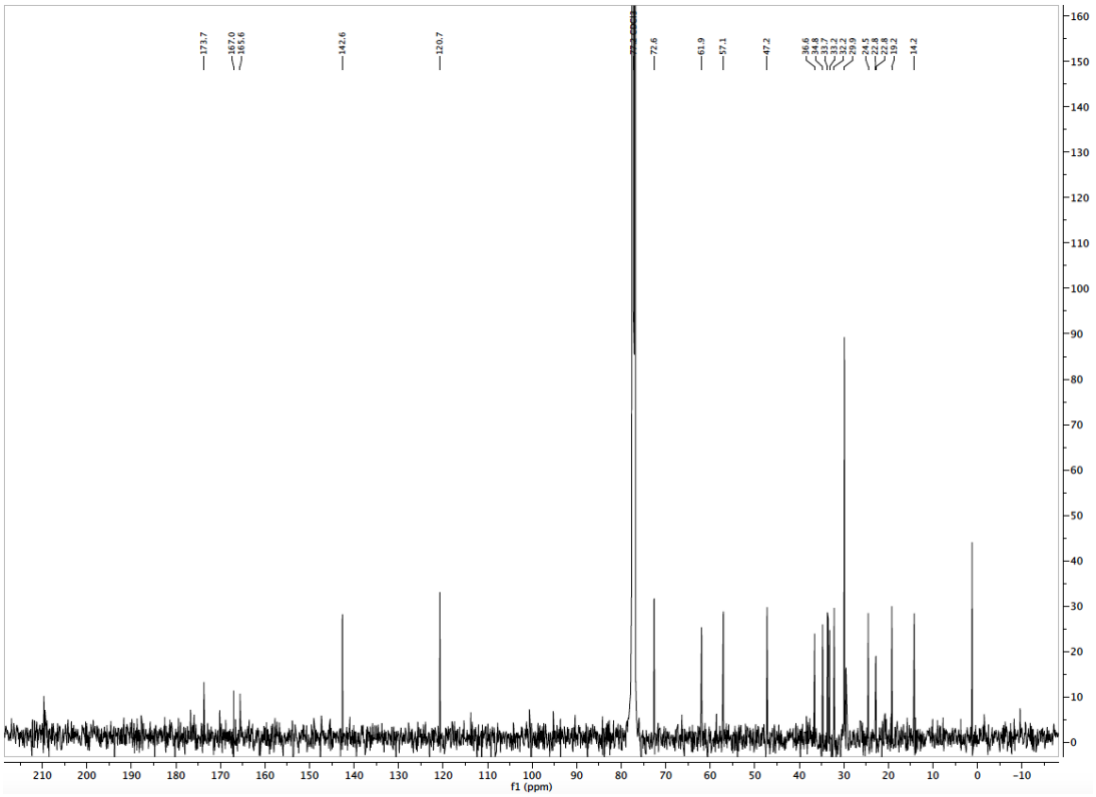

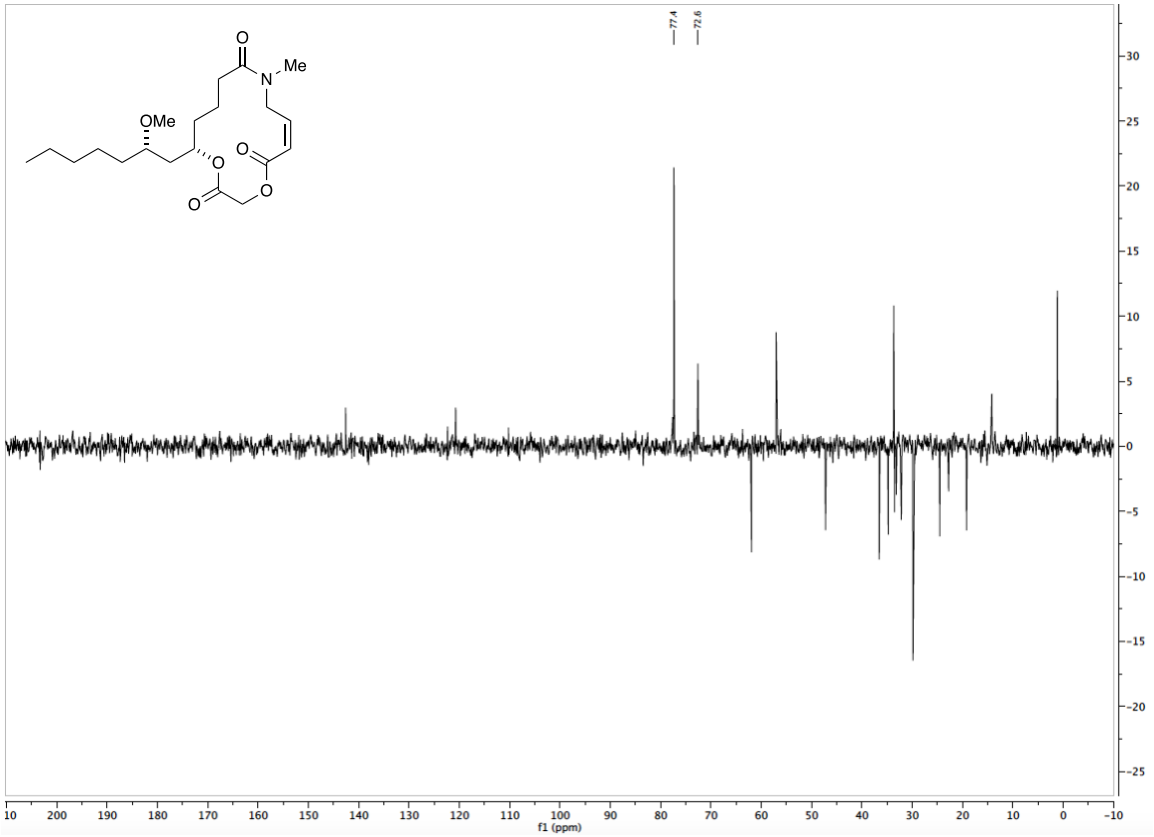
77.4
72.6
OMe
N
Me
O
f1 (ppm)

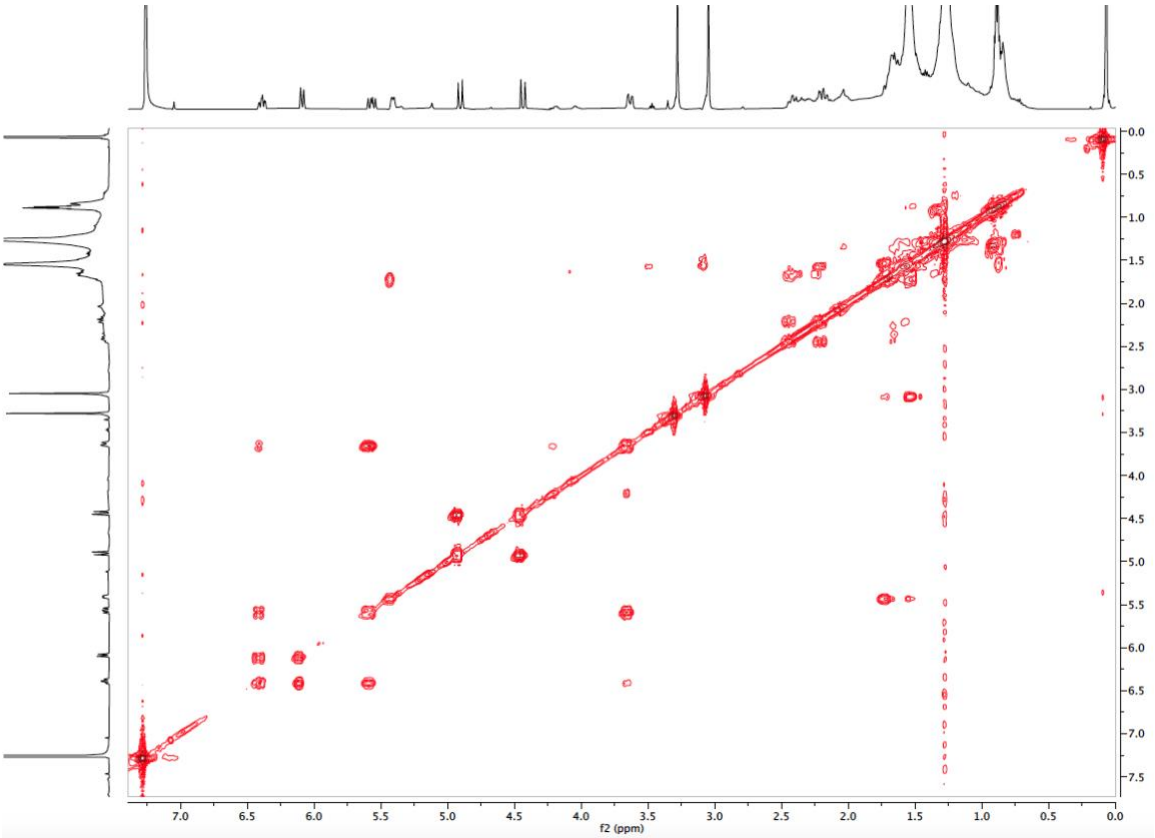
f2 (ppm)

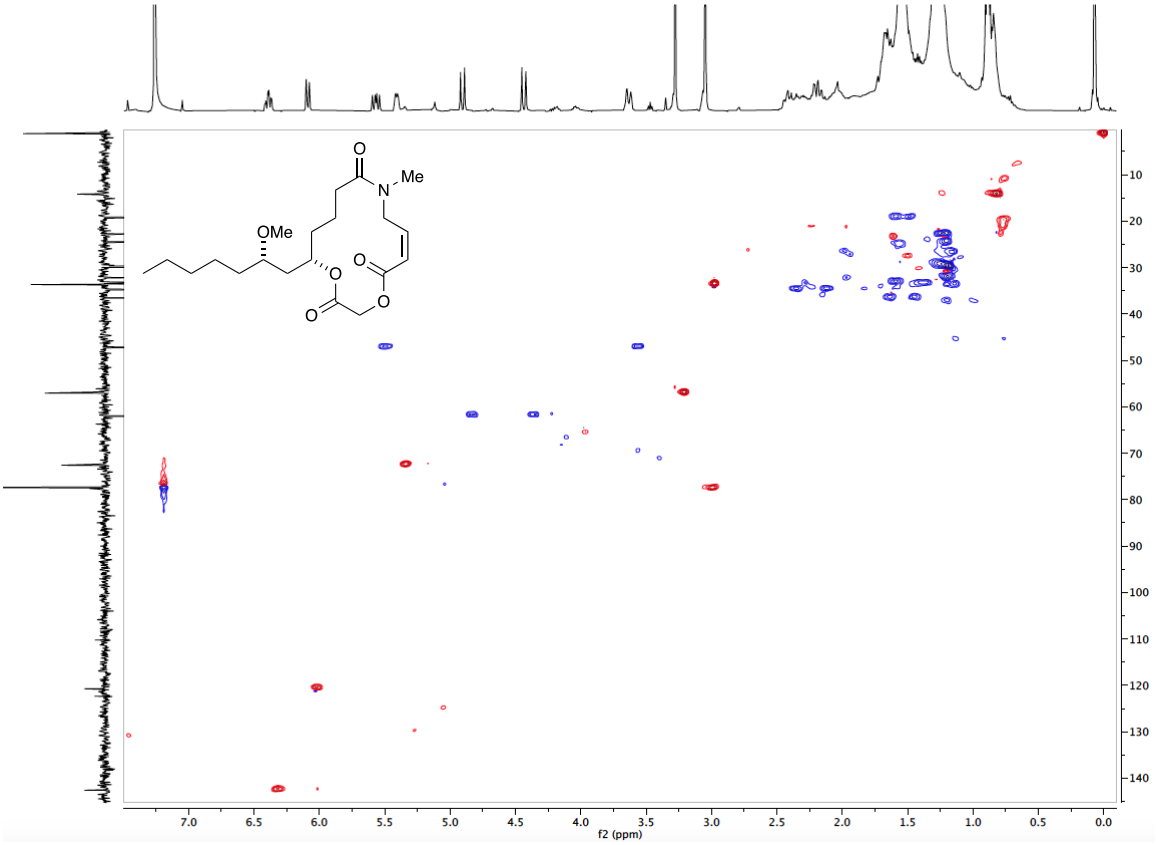
O
N
Me
OMe
O
O
O
O
10
20
30
40
50
60
70
80
90
100
110
120
130
140
7.0
6.5
6.0
5.5
5.0
4.5
4.0
3.5
3.0
2.5
2.0
1.5
1.0
0.5
0.0
f2 (ppm)

(3*S*,14*S*,*Z*)-3-isopropyl-14-((*S*)-2-methoxy-5-phenylpentyl)-9-methyl-1,4-dioxa-9-azacyclotetradec-6-ene-2,5,10-trione ($C_{27}H_{39}NO_6$, 3.10.5)

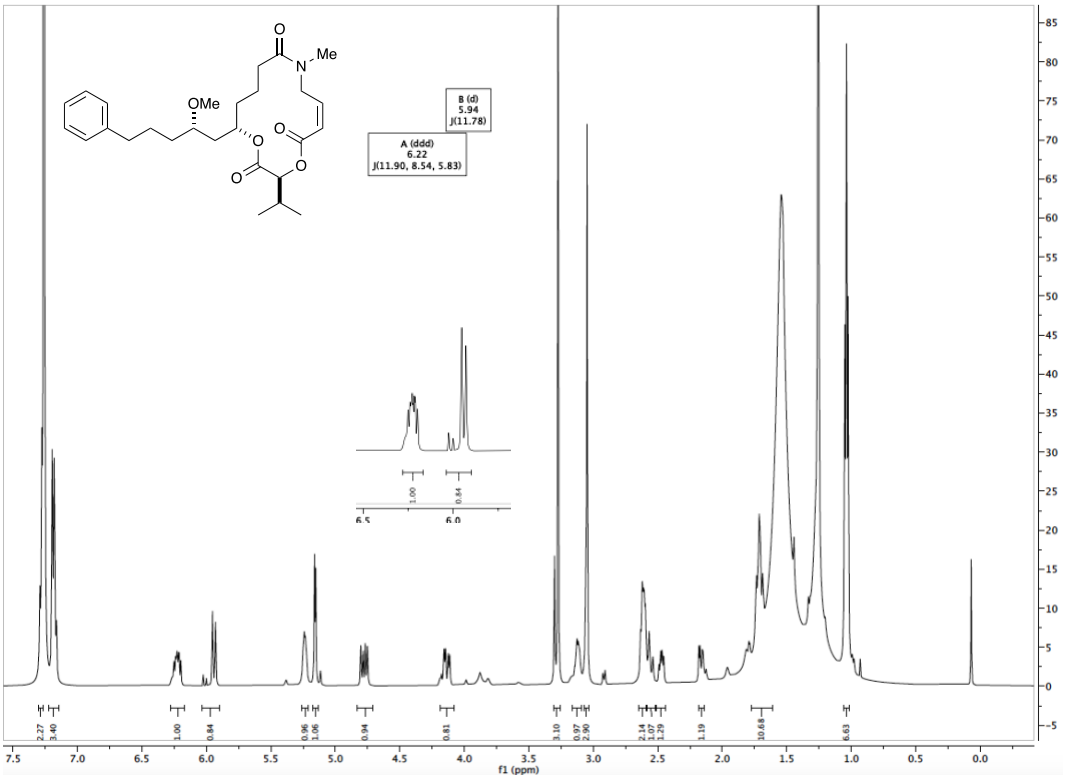

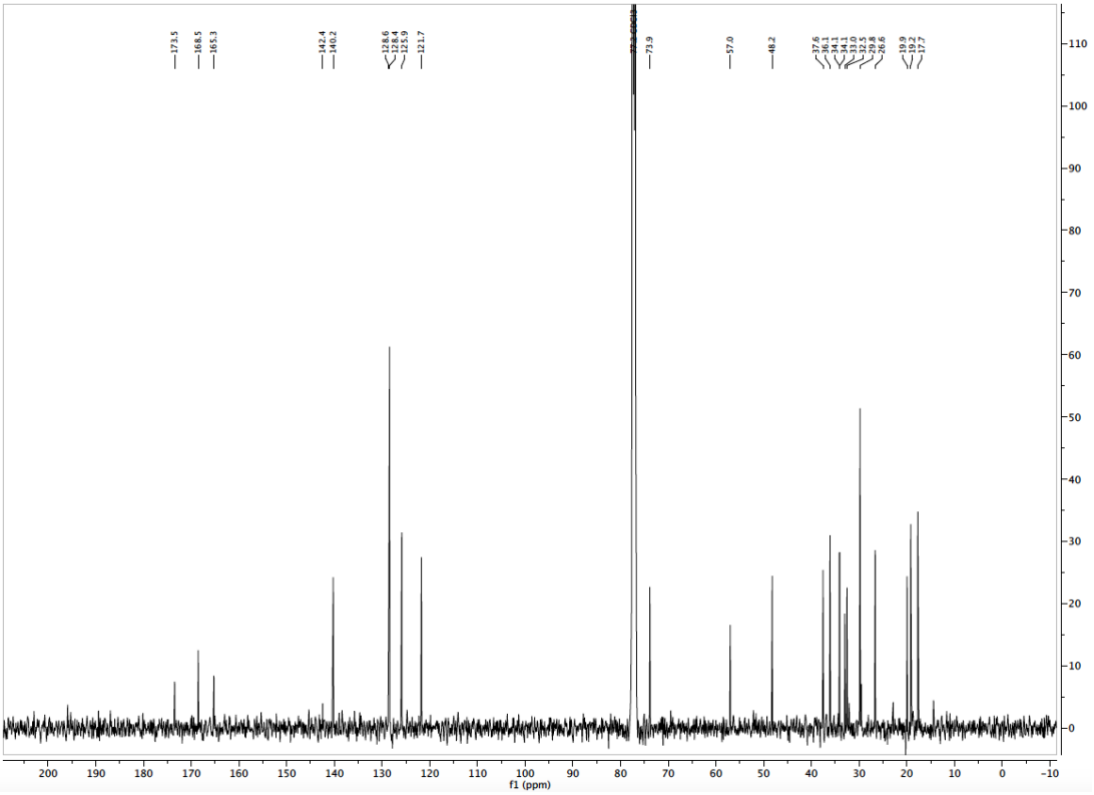

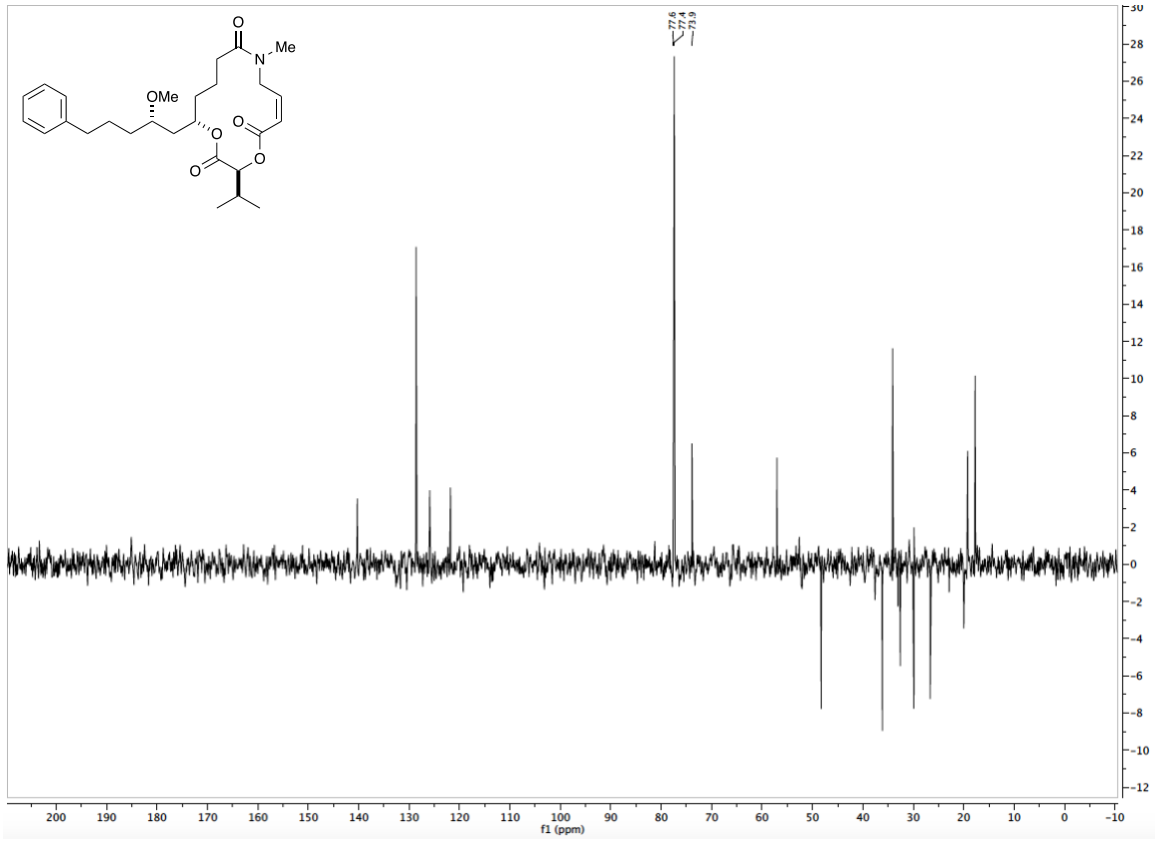
O
N
Me
OMe
O
O
O
O
77.6
77.4
77.0
f1 (ppm)

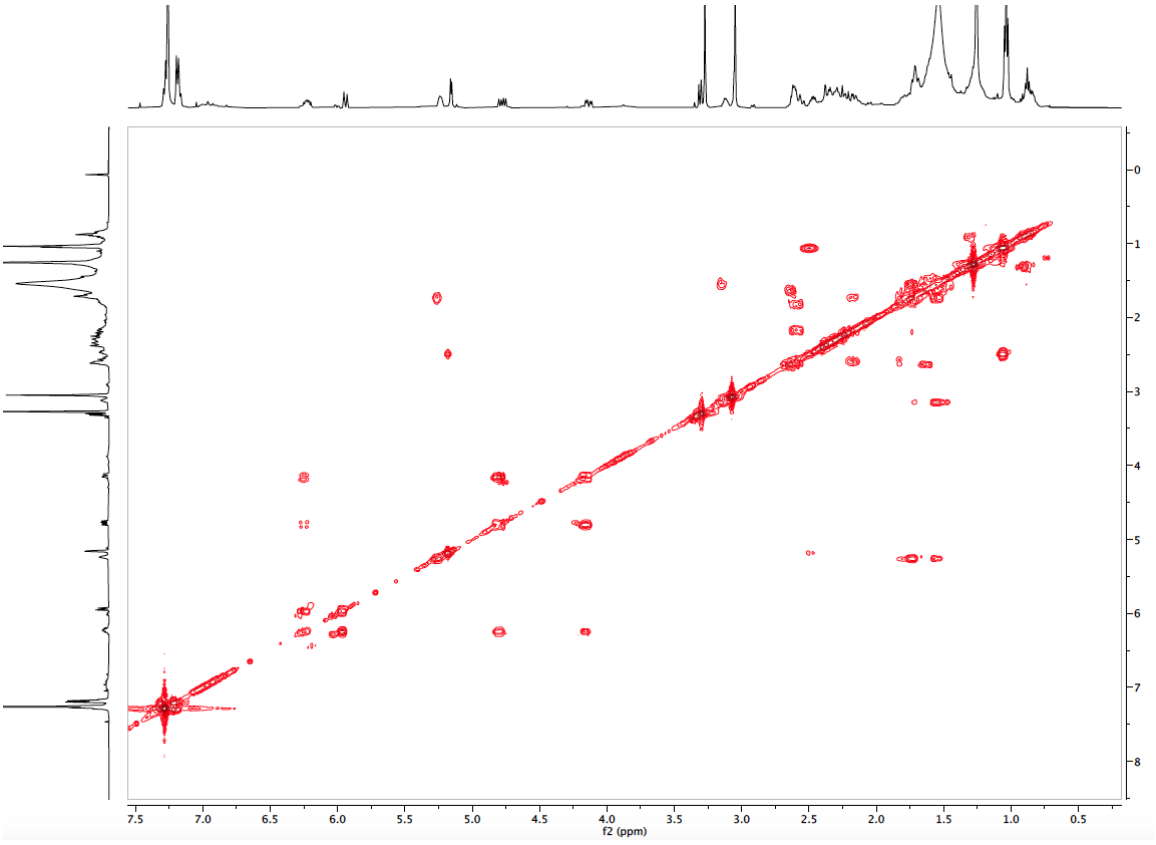
f2 (ppm)

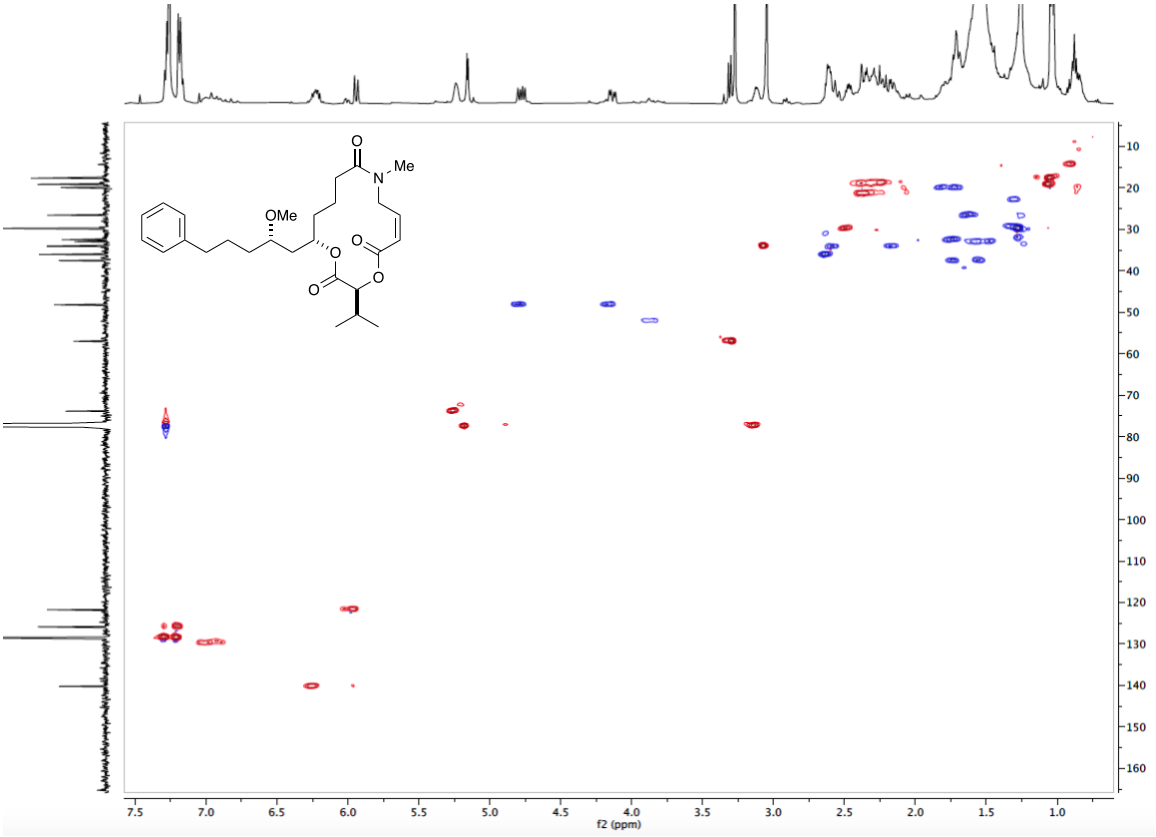
O
N
Me
OMe
O
O
O
O
7.5
7.0
6.5
6.0
5.5
5.0
4.5
4.0
3.5
3.0
2.5
2.0
1.5
1.0
f2 (ppm)
10
20
30
40
50
60
70
80
90
100
110
120
130
140
150
160

(*S*,*Z*)-14-((*S*)-2-methoxy-5-phenylpentyl)-9-methyl-1,4-dioxa-9-azacyclotetradec-6-ene-2,5,10-trione ($C_{24}H_{33}NO_6$, 3.10.4)

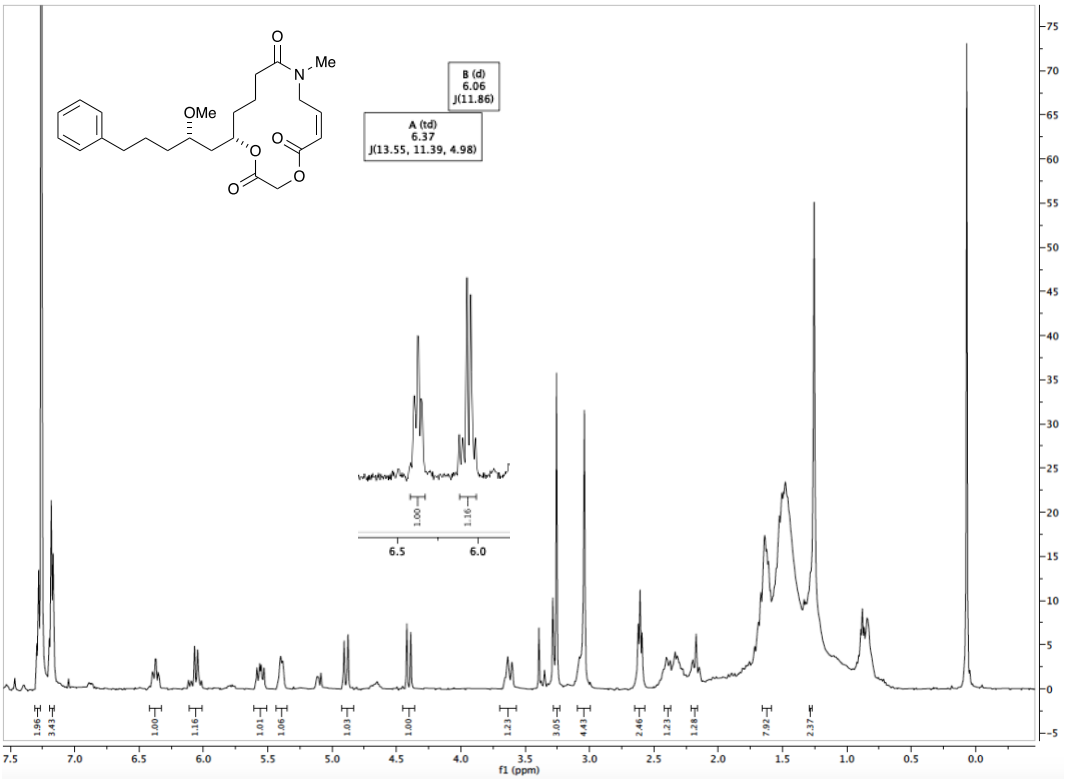

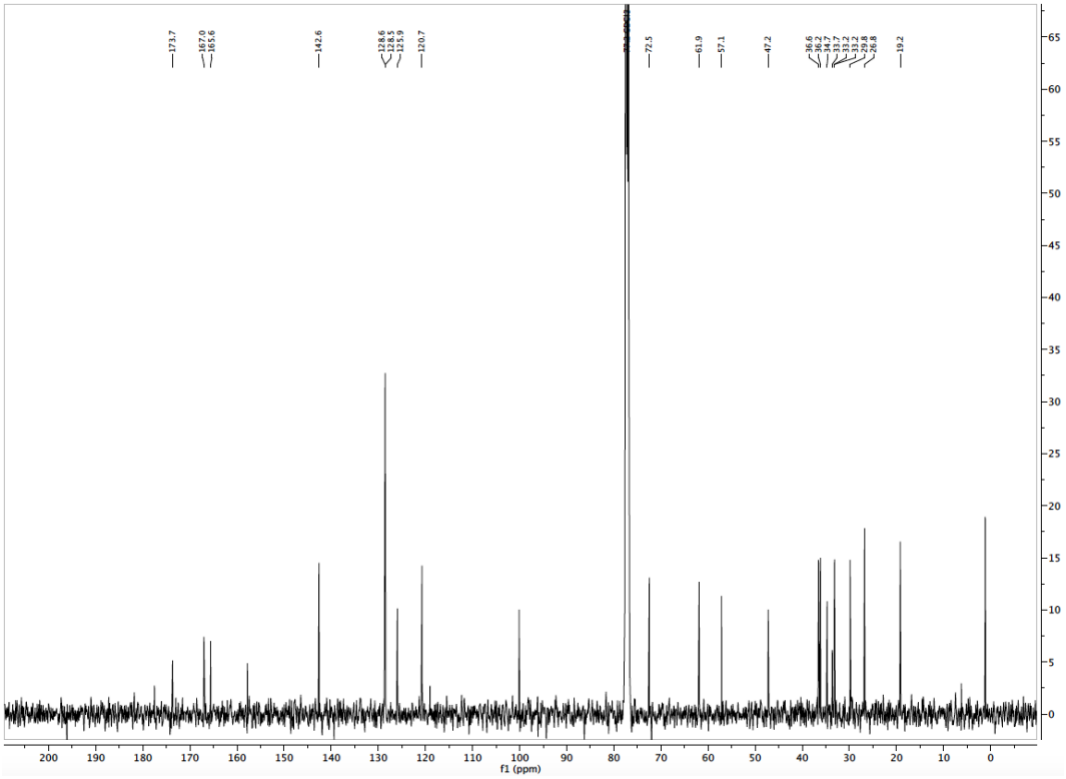

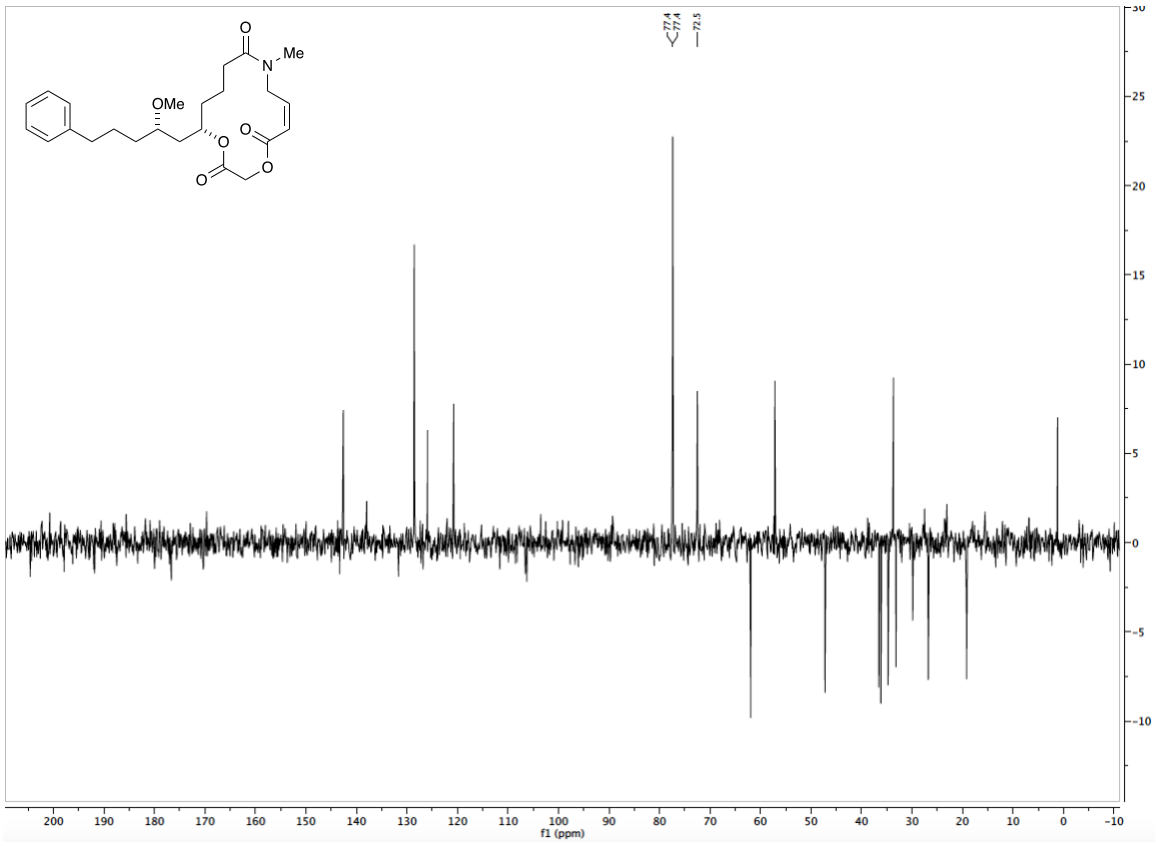
77.4
77.4
72.5
f1 (ppm)

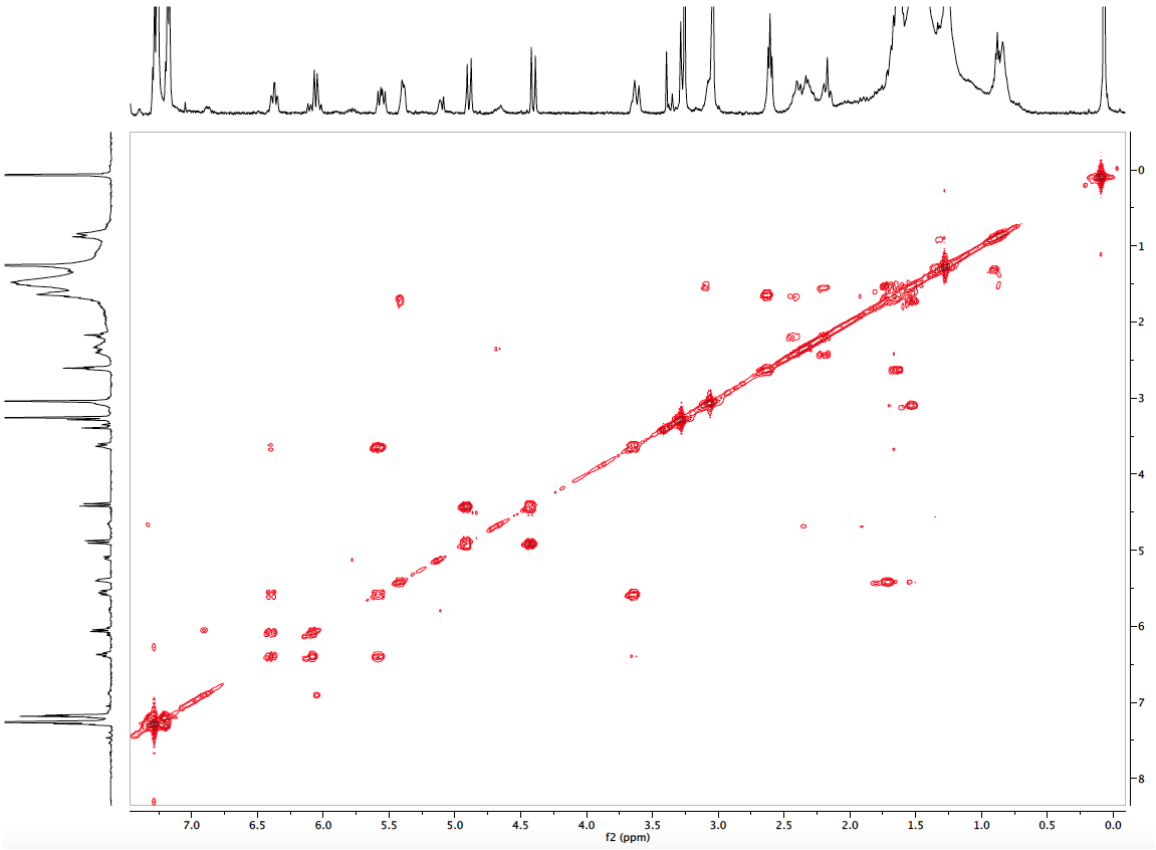
f2 (ppm)

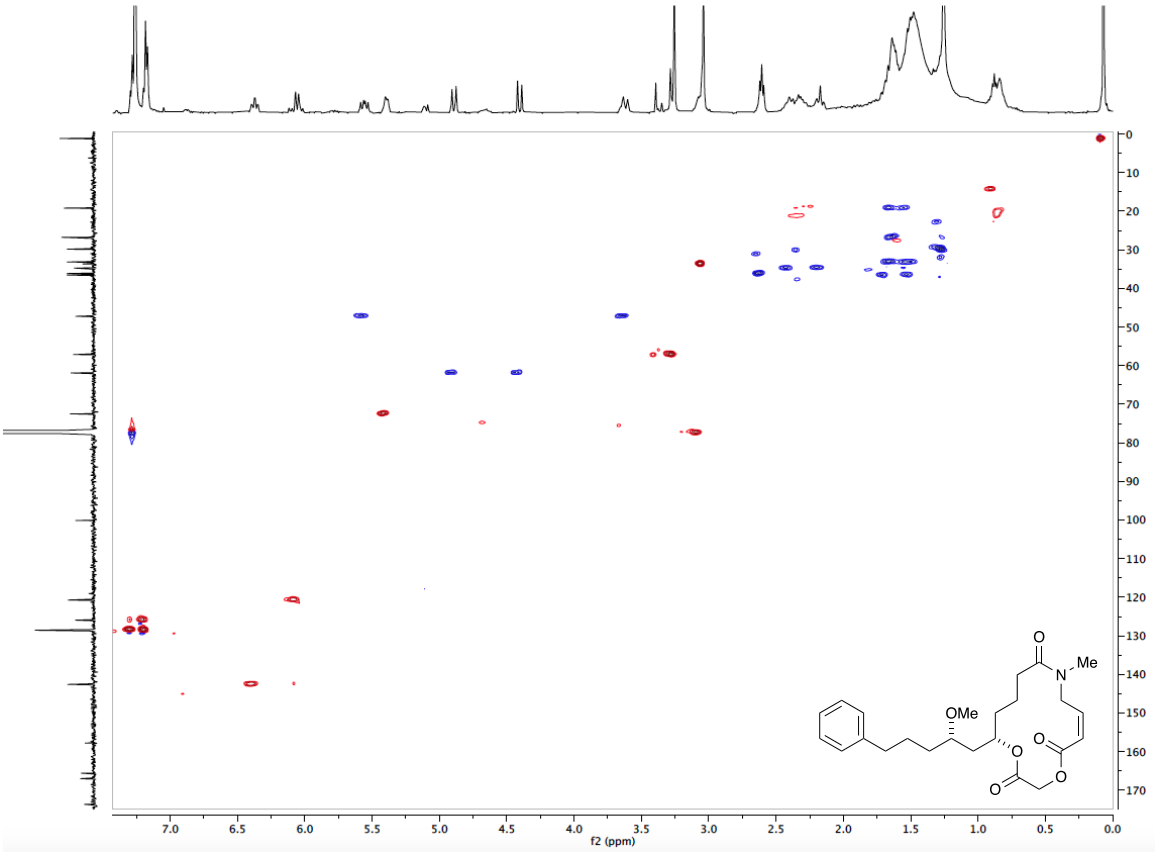
f2 (ppm)
OMe
N
Me
O

(*S*,*Z*)-14-((*S*)-2-methoxyheptyl)-9-(4-(trifluoromethyl)benzyl)-1,4-dioxa-9-azacyclotetradec-6-ene-2,5,10-trione ($C_{27}H_{36}F_3NO_6$, 3.10.3)

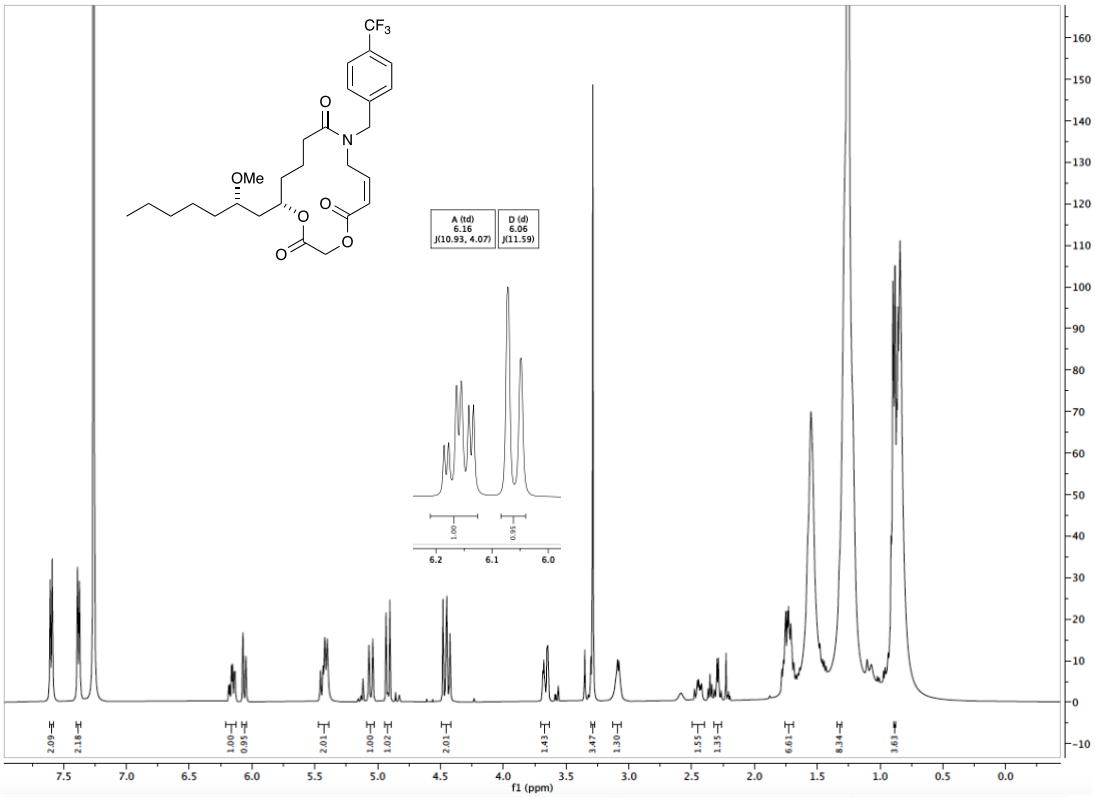

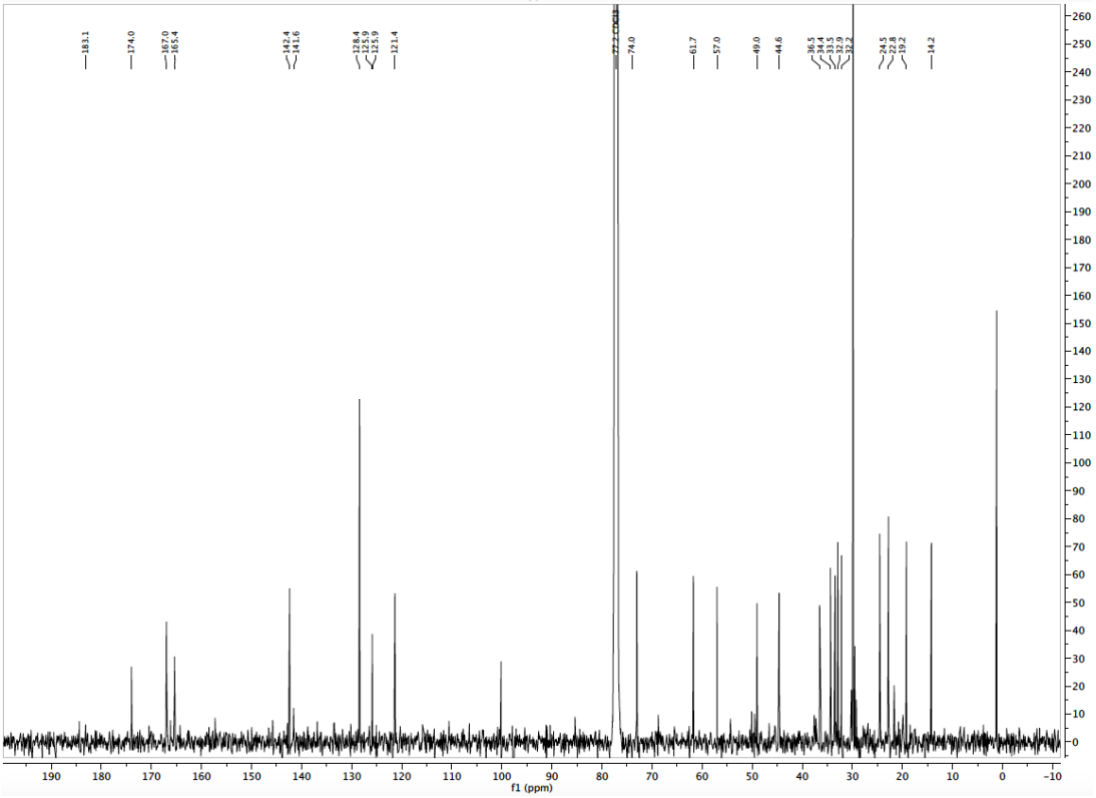

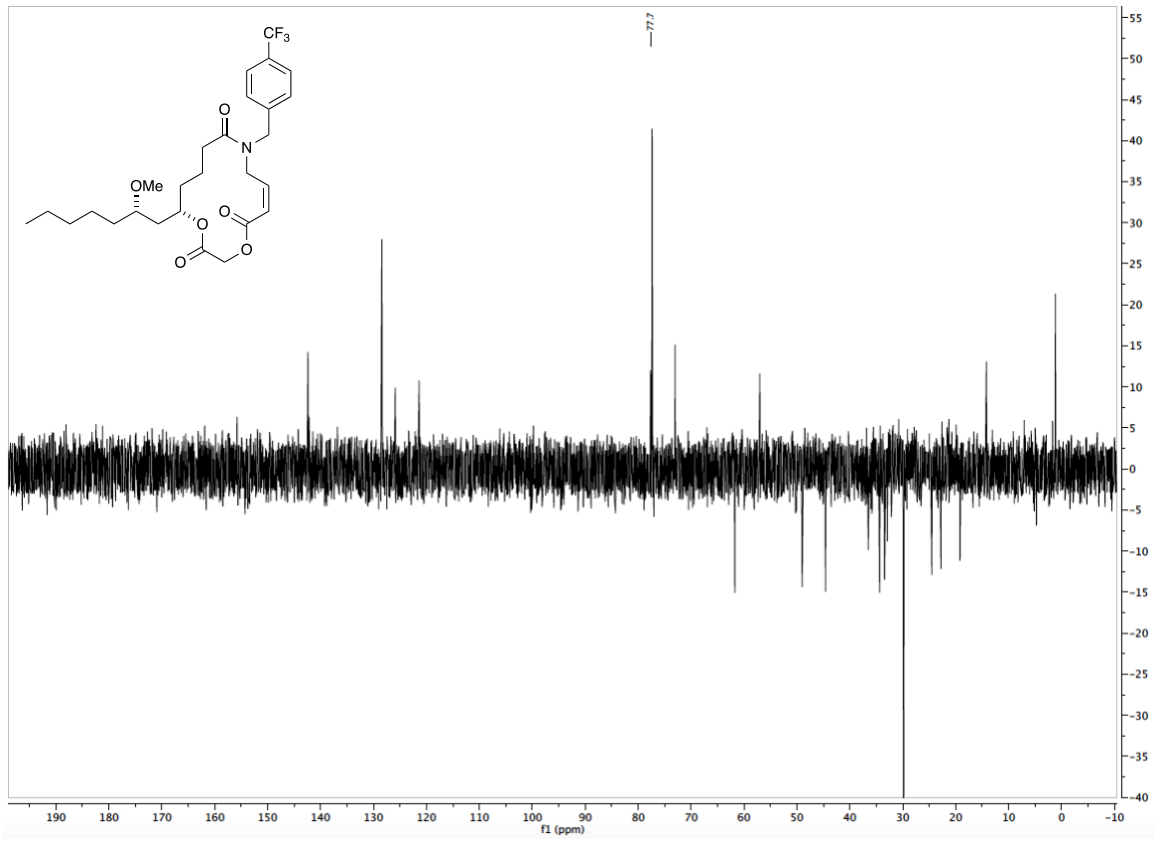
CF3
OMe
O
N
O
O
O
O
77.7
f1 (ppm)

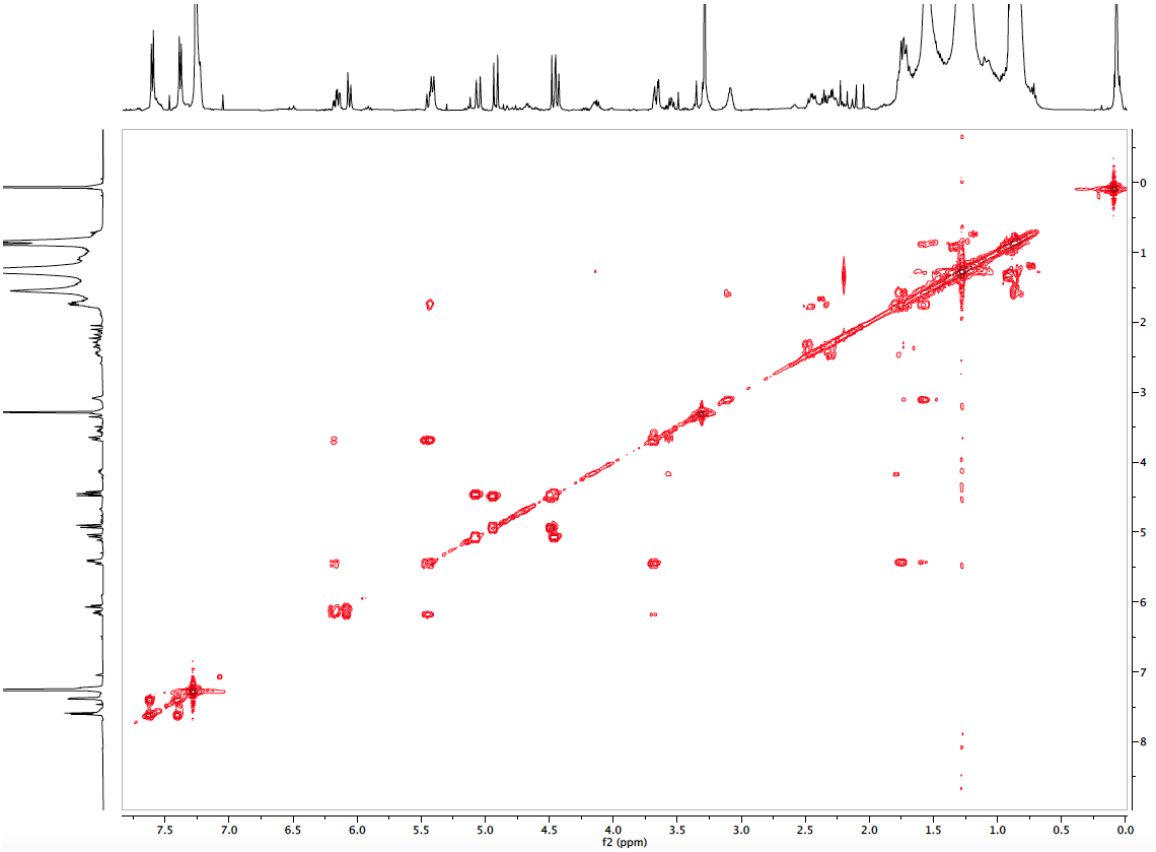
f2 (ppm)

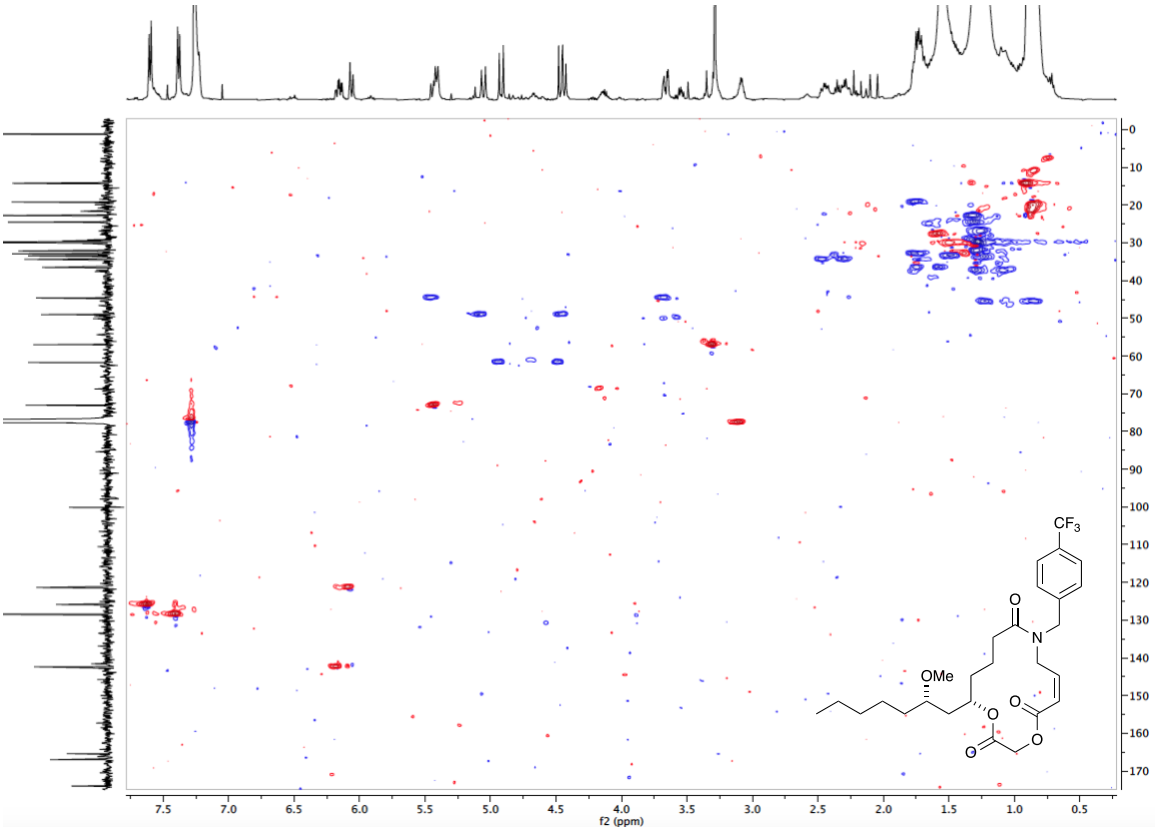
CF3
OMe
O
N
O
O
O
O
O
f2 (ppm)

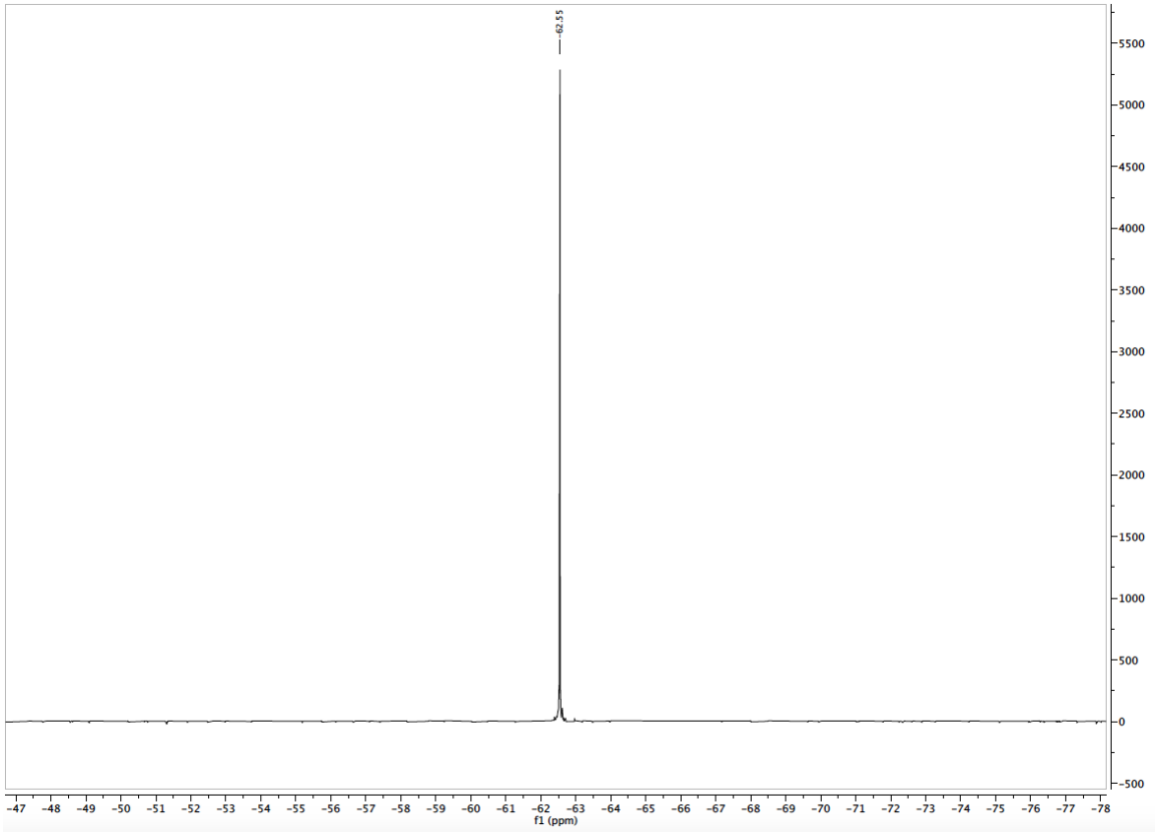
-62.55
f1 (ppm)

(*S*,*E*)-14-((*S*)-2-methoxyheptyl)-9-methyl-1,4-dioxa-9-azacyclotetradec-7-ene-2,5,10-trione ($C_{20}H_{33}NO_6$, 3.11.1)

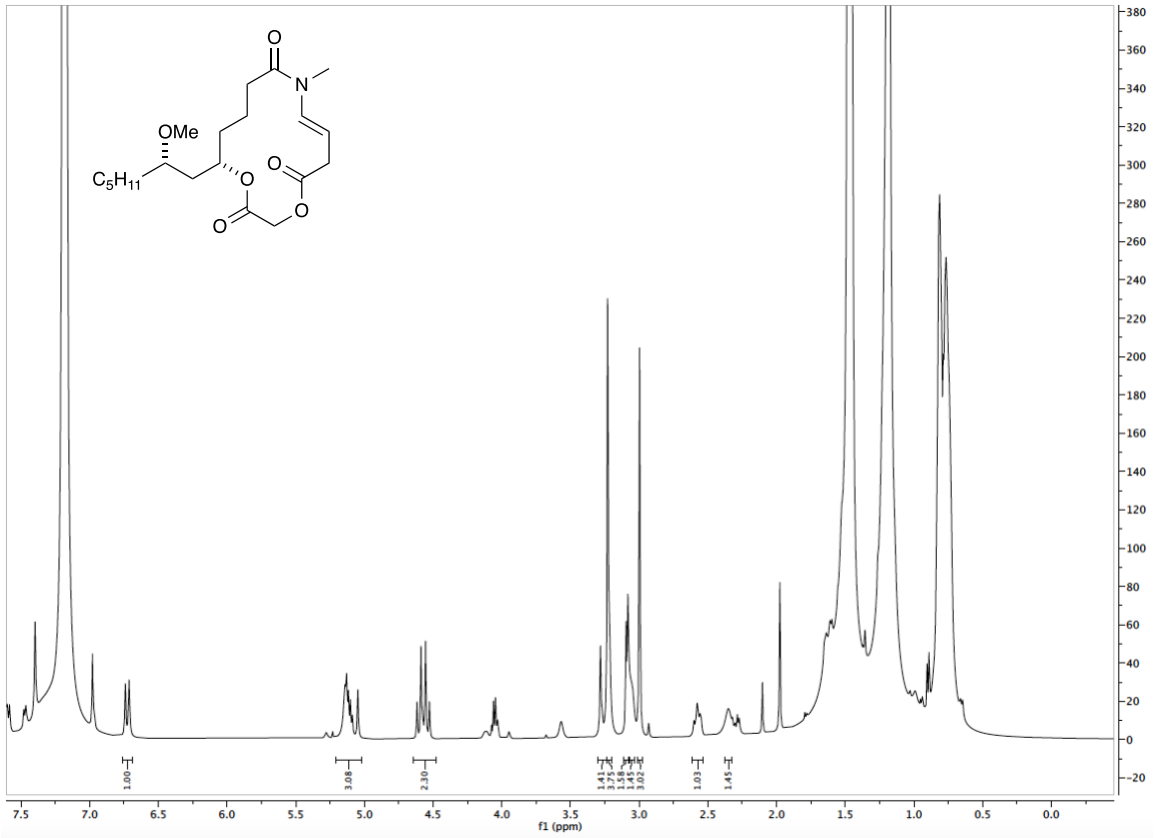

5.3 Supporting Information for Chapter 4

An Iterative Phosphate Tether-mediated Approach for the Synthesis of Complex Polyols Subunits

Table of Contents

Chapter 5, Section 3: Supporting Information for Chapter 4

An Iterative Phosphate Tether-mediated Approach for the Synthesis of Complex Polyols Subunits

5.3.1 General Methods

General Experimental Section

All reactions were carried out in oven- or flame-dried glassware under argon atmosphere using standard gas-tight syringes, cannula, and septa. Stirring was achieved with oven-dried magnetic stir bars. Et_2O, THF and CH_2Cl_2 were purified by passage through a purification system (Pure Process Technology) employing activated Al_2O_3 (Pangborn, A. B.; Giardello, M. A.; Grubbs, R. H.; Rosen, R. K.; Timmers, F. J. Safe and Convenient Procedure for Solvent Purification *Organometallics* **1996**, *15*, 1518–1520). Et_3N was purified by passage over basic alumina and stored over KOH. Butyllithium was purchased from Aldrich and titrated prior to use. All olefin metathesis catalysts were acquired from Materia and used without further purification. Flash column chromatography was performed with Sorbent Technologies (30930M-25, Silica Gel 60 Å, 40-63 μm) and thin layer chromatography was performed on silica gel 60F254 plates (EM-5717, Merck). ^1H, ^{13}C, and ^{31}P NMR spectra were recorded on either a Bruker DRX-400 or Bruker DRX-500 MHz spectrometers operating at 400 MHz or 500 MHz for ^1H NMR, 101 MHz or 126 MHz for ^{13}C NMR, and 162 or 202 MHz for ^{31}P NMR using $CDCl_3$, acetone-d_6 and methanol-d_4 as solvents. The ^1H NMR data are reported as the chemical shift in parts per million, multiplicity (s, singlet; d, doublet; t, triplet; q, quartet; p, pentet; m, multiplet), coupling constant in hertz, and number of protons. High-resolution mass spectrometry (HRMS) was recorded on a LCT Premier Spectrometer (Micromass UK Limited) operating on ESI (MeOH). Observed rotations at 589 nm were measured using LAXCO POL301 model automatic polarimeter. IR was recorded on Thermo Scientific Nicolet iS5 FTIR instrument.

5.3.2 Experimental Section

(1*S*,6*S*,8*R*)-8-(3-(benzyloxy)propyl)-2,9,10-trioxa-1-phosphabicyclo[4.3.1]dec-4-ene 1-oxide (4.2.2):

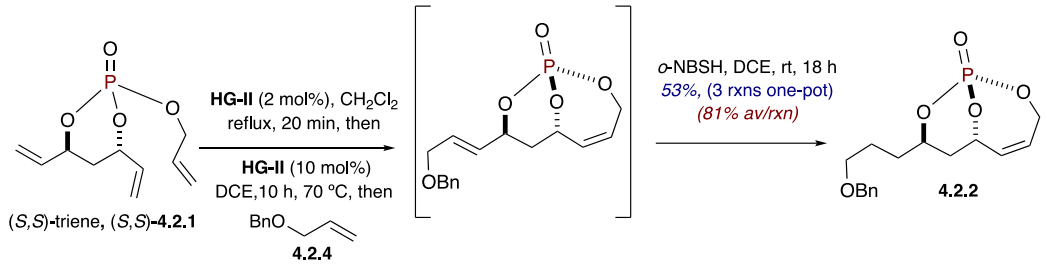

To a solution of (*S*,*S*)-triene (*S*,*S*)-**4.2.1** (200 mg, 0.85 mmol) in a degassed CH_2Cl_2 (347 mL, 0.005 M) was added **HG-II** (11 mg, 0.017 mmol, 2 mol%) the reaction mixture was refluxed in an oil bath for 20 minutes. After completion of the RCM reaction, CH_2Cl_2 was evaporated under reduced pressure. To the crude product was added freshly distilled, freeze-degas-thawed 1,2-dichloroethane (1,2-DCE) (9 mL, 0.1 M), the cross metathesis (CM) partner **4.2.4** (120 mg, 2.2 mmol) and HG-II (32 mg, 0.03 mmol, 6 mol%) under argon. The reaction mixture was stirred at 70 ºC in an oil bath for 5 h and a second portion of **HG-II** (21 mg, 0.034 mmol, 4 mol%) and CM partner (75 mg, 0.51 mmol) were added to the reaction mixture, and was stirred at 70 ºC for an additional 3 h (monitored by TLC). After completion of CM reaction, the reaction mixture was brought to room temperature and was added *o*-nitrobenzenesulfonyl hydrazine (*o*-NBSH) (1.8 g, 9 mmol) and Et_3N (3.7 mL, at 2 mL/g of *o*-NBSH), the reaction mixture was stirred for 12 h (Note: The reaction flask was wrapped with aluminum foil in order to avoid decomposition of *o*-NBSH due to light). A second portion of *o*-NBSH (1.8 g, 8.5 mmol) and Et_3N (3.6 mL, at 2 mL/g of o-NBSH) were added and the reaction mixture was stirred for an additional 8 h at room temperature. Reaction progress was monitored via crude NMR, which confirmed the complete reduction of the external double bond in the CM adduct. The reaction mixture

was diluted with EtOAc (150 mL) followed by addition of saturated aqueous solution of $NaHCO_3$ (100 mL). The organic layer was separated, and aqueous phase was extracted with EtOAc (3 x 100 mL). The combined organic layers were washed with brine (50 mL), dried (Na_2SO_4), concentrated under reduced pressure, and purified with flash chromatography (25% EtOAc/CH_2Cl_2), which furnished 182 mg of bicyclic phosphate **4.2.2** as a dark brown semi solid in 53% yield over three reactions in one-pot (81% av/rxn). TLC (EtOAc): R_f = 0.35.

FTIR (neat): 2929, 2852, 2356, 1470, 1298, 1009, 1506, 1068, 972, 885, 773 cm^{-1}.

Optical Rotation: $[\alpha]_D^{23}$= +45.5 (*c* 1.72, $CHCl_3$).

^{1}H NMR (500 MHz, Chloroform-*d*): δ 7.40–7.24 (m, 5H, Aromatic C‑H), 5.98 (dddd, *J* = 11.9, 6.8, 3.2, 2.1 Hz, 1H, CHO(P)CH=C<u>H</u>CH$_a$H$_b$), 5.53 (ddd, 11.8, 4.0, 2.5 Hz, 1H, CHO(P)C<u>H</u>=CHCH$_a$H$_b$), 5.16 (dddt, *J* = 24.5, 6.2, 4.0, 2.0 Hz, 1H, C<u>H</u>O(P)CH=CHCH$_a$H$_b$), 4.97 (ddd , *J* = 14.7, 5.6, 2.9 Hz, 1H, CHO(P)CH=CHC<u>H</u>$_a$H$_b$), 4.60 (dddd, *J* = 11.5, 7.6, 4.0, 2.0 Hz, 1H, C<u>H</u>O(P)CH$_a$H$_b$CHO(P)), 4.48 (s, 2H, PhC<u>H</u>$_2$OCH$_2$), 4.32 (ddd, *J* = 27.7, *J* = 14.8, 6.7 Hz, 1H, CHO(P)CH=CHCH$_a$<u>H</u>$_b$), 3.55–3.44 (m, 2H, BnOC<u>H</u>$_2$CH$_2$CH$_2$), 2.16 (ddd, *J* = 14.7, 11.8, 6.2 Hz, 1H, CHO(P)C<u>H</u>$_a$H$_b$CHO(P)), 1.86-1.67 (m, 5H, CHO(P)CH$_a$<u>H</u>$_b$CHO(P), BnOCH$_2$C<u>H</u>$_2$CH$_2$, BnOCH$_2$CH$_2$C<u>H</u>$_2$);

^{13}C NMR (126 MHz, $CDCl_3$): δ 138.5 (C_{Ar}), 130.0 (<u>C</u>H=CHCH$_2$), 128.5 (2, <u>C</u>H$_{Ar}$), 128.0 (<u>C</u>H$_{Ar}$), 127.8 (2, <u>C</u>H$_{Ar}$), 127.7 (CH=<u>C</u>H), 77.3 (CH J_{CP}= 6.5 Hz), 76.7 (CH J_{CP}= 7.0 Hz), 72.9 (CH_2), 69.6 (CH_2), 63.0 (CH_2 J_{CP}= 6.4 Hz), 34.9 (CH_2), 32.7 (CH_2), 24.9 (CH_2);

^{31}P NMR (202 MHz, $CDCl_3$): δ -3.54;

HRMS (ESI-TOF) m/z: $[M + Na]^+$ Calcd for $C_{16}H_{21}O_5PNa$ 347.1024; Found 347.1023.

(*S*)-((but-3-ene-1,2-diylbis(oxy))bis(methylene))dibenzene (4.2.5)

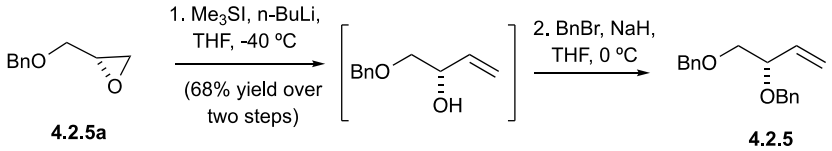

4.2.5a **4.2.5**

To a solution of flame-dried trimethylsulfonium iodide salt (13.7 g, 67.1 mmol) in dry THF (52 mL) was added n-butyl lithium solution (2.5 M in hexane, 24.4 mL, 61 mmol) under argon at -40 ºC. The reaction was stirred at the same temperature for 30 minutes and then was added a solution of (*S*)-benzyl glycidyl ether (5 g, 30.5 mmol) in THF (15 mL) and stirred for another 4 h. Upon completion, the reaction was quenched with sat. aq. solution of NH_4Cl (50 mL) and diluted with EtOAc (100 mL). The layers were separated, and the aqueous layer was extracted with EtOAc (3 x 50 mL). Combined organic layer was dried with Na_2SO_4 and concentrated under reduced pressure. The obtained crude was filtered through a small pad of silica and used for the next step. To the crude solution of (*S*)-1-(benzyloxy)but-3-en-2-ol, (5 g, 28.05 mmol) in THF (95 mL) under argon at 0 ºC, was added sodium hydride (60% dispersion in mineral oil) (1.6 g, 42.1 mmol), in small portions. The reaction mixture stirred at 0 ºC for 15 minutes, at which point a solution of freshly distilled benzyl bromide (3 mL, 25.25 mmol) in THF (50 mL) was added dropwise, slowly. The reaction continued to stir at rt for 12 hours (complete by TLC), and quenched with saturated NH_4Cl (aqueous, ~40 mL). The mixture was stirred vigorously, and then the biphasic solution was separated. The aqueous layer was extracted with EtOAc (3 x 50 mL), and the organic layers were combined, washed with brine, dried over Na_2SO_4, and concentrated under reduced pressure. The crude mixture was purified via flash column

chromatography to provide protected diol **4.2.5** (5.35 g, 19.95 mmol, 70% yield) as a colorless liquid. TLC (hexane/ EtOAc 10/1): $R_f = 0.5$.

FTIR (neat): 3087, 2859, 1951, 1605, 1496, 1404, 1388, 1363, 1329, 1096, 1072 735, 697 cm^{-1};

Optical Rotation: $[a]_D^{23} = +13.4$ (c 1.84, $CHCl_3$);

^{1}H NMR (500 MHz, $CDCl_3$): δ 7.41–7.31 (m, 10H, Aromatic C–H), 5.86 (ddd, J = 17.5, 10.5, 7.2 Hz, 1H, CH(OBn)C<u>H</u>=CH_2), 5.38 (dd, J = 17.3, 1.5 Hz, 1H, CH(OBn)CH=C<u>H</u>$_a$H$_b$), 5.34 (d, J = 10.4 Hz, 1H, CH(OBn)CH=CH$_a$<u>H</u>$_b$), 4.71 (d, J = 12.1 Hz, 1H, BnOCH$_2$CH(OC<u>H</u>$_a$H$_b$Ph)), 4.62 (ddd, J = 12.5, 11.0, 11.0 Hz, 2H, PhC<u>H</u>$_2$OCH$_2$CH(OBn)), 4.53 (d, J = 12.1 Hz, 1H, BnOCH$_2$CH(OCH$_a$<u>H</u>$_b$Ph)), 4.10 (td, J = 6.8, 4.7 Hz, 1H, C<u>H</u>(OBn)CH=CH_2), 3.65 (dd, J = 10.4, 6.5 Hz, 2H, BnOC<u>H</u>$_a$H$_b$CH(OCH$_2$Ph)), 3.59 (dd, J = 10.4, 4.4 Hz, 1H, BnOCH$_a$<u>H</u>$_b$CH(OCH$_2$Ph));

^{13}C NMR (126 MHz, $CDCl_3$): δ 138.7 (C_{Ar}), 138.5 (C_{Ar}), 136.0 (<u>C</u>H=CH_2), 128.4 (4, <u>C</u>H$_{Ar}$), 127.8 (2, <u>C</u>H$_{Ar}$), 127.7 (2, <u>C</u>H$_{Ar}$), 127.6 (2, <u>C</u>H$_{Ar}$), 118.5 (CH=<u>C</u>H$_2$), 79.5 (CH), 73.5 (CH_2), 73.2 (CH_2), 70.6 (CH_2);

HRMS (ESI-TOF) m/z: $[M + Na]^+$ Calcd for $C_{18}H_{20}O_2Na$ 291.1361; Found 291.1361.

6*S*,8*R*)-8-((*S*)-3,4-bis(benzyloxy)butyl)-2,9,10-trioxa-1-phosphabicyclo[4.3.1]dec-4-ene 1-oxide (4.2.3)

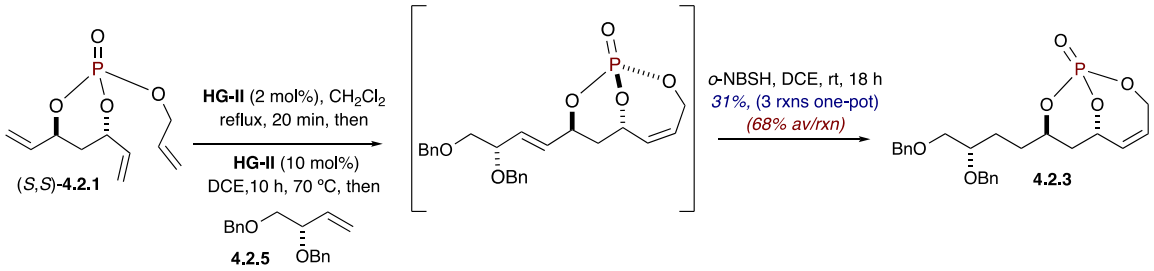

To a stirring solution of (*S*,*S*)-triene, (*S*,*S*)-**4.2.1** (2.0 g, 8.7 mmol) in degassed dichloromethane (1750 mL) under argon at 45 ºC, was added Grubbs second-generation catalyst [($ImesH_2$)(PCy_3)$(Cl)_2$Ru=CHPh] (G-II, 221.0 mg, 0.261 mmol) in one portion. The reaction mixture was stirred at 45 ºC in an oil bath for 30 minutes (complete by TLC). After completion of RCM reaction, CH_2Cl_2 was evaporated under reduced pressure. To the crude product was added freshly distilled, freeze-degas-thawed 1,2-DCE (29 mL) under argon was added the cross metathesis (CM) partner **4.2.5** (4.7 g, 17.4 mmol) and Hoveyda-Grubbs second-generation catalyst (HG-II, 327.0 mg, 0.522 mmol). Reaction mixture was stirred at 45 ºC in an oil bath for 12 hours (complete by TLC). After the complete consumption of starting material, the reaction mixture was brought to room temperature and to the crude mixture was added triethylamine (9 mL), *o*-nitrobenzenesulfonohydrazide (*o*-NBSH) (19 g, 87 mmol) and stirred for 12 hours. Since the reaction was not complete, was added triethylamine (4.5 mL) and *o*-NBSH (9.5 g, 43.5 mmol) and stirred for another 6 hours (complete by NMR) and quenched with saturated $NaHCO_3$ (aqueous, ~50 mL). The mixture was stirred vigorously, and then the biphasic solution was separated. The aqueous layer was extracted with CH_2Cl_2 (3 x 50 mL), and the organic layers were combined, washed with brine, dried over $MgSO_4$, and concentrated under reduced pressure.

The crude mixture was purified via flash column chromatography to provide **4.2.3** (1.2 g, 2.7 mmol, 31% yield over three steps) as a yellow color oil. TLC (EtOAc): R_f = 0.6.

FTIR (neat): 2985, 2906, 2818, 2367, 1470, 1298, 1110, 1082, 1068, 972, 814, 798 cm^{-1};

Optical Rotation: $[\alpha]_D^{23}$ = +27.6 (*c* 0.72, $CHCl_3$);

^{1}H NMR (500 MHz, $CDCl_3$): δ 7.36–7.29 (m, 10 H, Aromatic C‑H), 5.96 (ddt, *J* = 12.0, 6.0, 2.6 Hz, 1H, CHO(P)CH=C<u>H</u>CH_2), 5.50 (dt, *J* = 11.8, 3.3 Hz, 1H, CHO(P)C<u>H</u>=CHCH_aH_b), 5.14 (dq, *J* = 24.6, 3.5 Hz, 1H, C<u>H</u>O(P)CH=CHCH_aH_b), 4.96 (ddq, *J*= 14.5, 5.7, 2.9 Hz, 1H, CHO(P)CH=CHC<u>H</u>$_aH_b$), 4.69 (d, *J* = 11.8 Hz, 1H, $BnOCH_2CH(OC\underline{H}_aH_bPh)$), 4.57–4.53 (m, 1H, C<u>H</u>O(P)CH_aH_bCHO(P)), 4.54 (s, 2H, Ph$C\underline{H}_2OCH_2CH(OBn)$), 4.52 (d, *J* = 11.8 Hz, 1H, $BnOCH_2CH(OCH_a\underline{H}_bPh)$), 4.31 (ddd, *J* = 27.7, 14.7, 6.7 Hz, 1H, CHO(P)CH=CH$CH_a\underline{H}_b$), 3.62 (dt, *J* = 9.9, 4.9 Hz, 1H, $BnOCH_aH_bC\underline{H}(OBn)$), 3.54 (qd, *J* = 10.0, 4.7 Hz, 2H, $BnOC\underline{H}_a\underline{H}_bCH(OBn)$), 2.11 (ddd, *J* = 14.6, 11.8, 6.2 Hz, 1H, CHO(P)C<u>H</u>$_aH_b$CHO(P)), 1.82 (dtd, *J* = 13.1, 8.3, 4.9 Hz, 1H, $BnOCH_2CH(OBn)CH_2C\underline{H}_aH_b$), 1.72 (td, *J* = 10.8, 9.5, 5.9 Hz, 2H, $BnOCH_2CH(OBn)C\underline{H}_2CH_aH_b$), 1.67–1.64 (m, 1H, $BnOCH_2CH(OBn)CH_2CH_a\underline{H}_b$), 1.64–1.59 (m, 1H, CHO(P)CHa<u>H</u>bCHO(P));

^{13}C NMR (126 MHz, $CDCl_3$): *δ* 138.8 (C_{Ar}), 138.2 (C_{Ar}), 130.0 (H<u>C</u>=CH), 128.5 (2, <u>C</u>H_{Ar}), 128.4 (2, <u>C</u>H_{Ar}), 128.0 (<u>C</u>H_{Ar}), 127.9 (2, <u>C</u>H_{Ar}), 127.8 (2, <u>C</u>H_{Ar}), 127.8 (<u>C</u>H_{Ar}), 127.7 (CH=<u>C</u>H), 77.3 (CH J_{CP} = 6.7 Hz), 77.1 (CH), 76.4 (CH J_{CP} = 7.0 Hz), 73.5 (CH_2), 72.5 (CH_2), 71.8 (CH_2), 62.9 (CH_2 J_{CP} = 6.3 Hz), 34.8 (CH_2), 31.3 (CH_2), 26.6 (CH_2);

^{31}P NMR (202 MHz, $CDCl_3$): δ -3.74;

HRMS (ESI-TOF) m/z: $[M + Na]^+$ Calcd for $C_{24}H_{29}O_6PNa$ 467.1599; Found 467.1608.

(3*R*,4*S*,6*R*)-9-(benzyloxy)-3-methylnon-1-ene-4,6-diol (4.3.1):

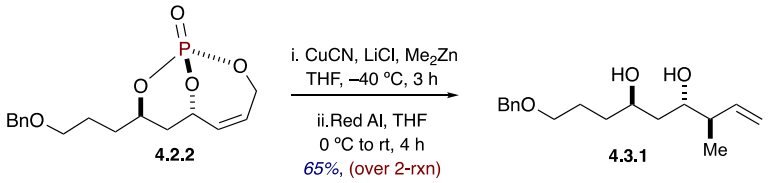

To a flame dried round bottom-flask was added CuCN (290 mg, 3.2 mmol) and LiCl (317 mg, 7.5 mmol) inside the glove box, followed by addition of dry THF (10 mL, 0.05 M) under argon and the reaction mixture was stirred at room temperature for 15 minutes. A pale green coloration was observed. The reaction mixture was cooled to -40 ºC followed by slow addition of a 1 M solution of Me_2Zn in THF (3.2 mL, 3.2 mmol). The reaction mixture was stirred for 40 minutes at -30 ºC and a solution of bicyclic phosphate **4.2.2** (350 mg, 1.08 mmol) in dry THF (10 mL, 0.05 M) was added dropwise via cannula to the reaction mixture. The reaction was slowly warmed to room temperature and allowed to stir for 3 h. Upon completion of reaction (monitored via TLC), the reaction mixture was quenched with saturated aqueous ammonium chloride (NH_4Cl, 2 mL), stirred for 15 minutes followed by the addition of anhydrous Na_2SO_4 (200 mg) stirred for another 30 minutes. The crude product was filtered through Celite pad and washed with excess EtOAc (3 x 50 mL), the filtrate was concentrated under reduce pressure, which afforded the crude acid as yellowish viscous oil, which was proceeded to the next reaction without further purification.

To a flask containing the crude acid was added THF (13.5 mL, 0.08 M). The reaction mixture was cooled to 0 ºC and was added 70% solution of Red-Al in toluene (1.5 mL, 5 mmol). The reaction mixture was brought to room temperature and stirred for 4 h. After completion of reaction (monitored by TLC), it was quenched with NH_4Cl (sat. aq.)

and was added (Na_2SO_4), stirred for 30 minutes, filtered through Celite pad. The residue was washed with EtOAc (3 x 50 mL). The organic layer was dried (Na_2SO_4) and the solvent was evaporated under reduced pressure. The crude product was purified via flash chromatography (30% EtOAc/Hexane), which afforded diol **4.3.1** (240 mg, with 65% yield over two reactions) as colorless viscous oil. TLC (hexane/EtOAc 3/1): R_f = 0.25.

FTIR (neat): 3458, 2943, 2866, 1718, 1699, 1456, 1390, 1097, 1027, 912, 842, 736, 697 cm^{-1};

Optical Rotation: $[\alpha]_D^{23}$ = 2.1 (*c* 0.8, $CHCl_3$).;

^{1}H NMR (500 MHz, Chloroform-*d*): δ 7.42–7.29 (m, 5H, Aromatic C–H), 5.78 (ddd, *J*= 17.9, 9.7, 7.9 Hz, 1H, $CH(CH_3)C\underline{H}=CH_2$), 5.16 (d, *J*= 0.97 Hz, 1H, $CH(CH_3)CH=C\underline{H}aHb$), 5.13 (ddd, *J* = 5.8, 1.9, 0.8 Hz, 1H, $CH(CH_3)CH=CHa\underline{H}b$), 4.55 (s, 2H, $PhC\underline{H}_2OCH_2$), 3.97 (ddd *J* = 8.1, 6.0, 4.2 Hz, 1H, $C\underline{H}(OH)CH_2CH(OH)CH(CH_3)$), 3.75 (tdd, *J* = 6.8, 5.3, 3.2 Hz, 1H, $CH(OH)CH_2C\underline{H}(OH)CH(CH_3)$), 3.57–3.54 (m, 2H, $BnOC\underline{H}_2CH_2CH_2CH(OH)$), 3.32 (d, *J* = 3.3 Hz, 1H, $CH(O\underline{H})CH_2CH(OH)CH(CH_3)$), 2.47 (d, *J* = 3.3 Hz, 1H, $CH(OH)CH_2CH(O\underline{H})CH(CH_3)$), 2.28 (ddq, *J* = 7.5, 7.0 Hz , 1H, $C\underline{H}(CH_3)CH=CH_2$), 1.84 (ddd, *J* = 9.5, 5.2, 2.3 Hz, 2H, $BnOCH_2C\underline{H}_2CH_2CH(OH)$), 1.66–1.65 (m, 1H, $BnOCH_2CH_2C\underline{H}_aH_b$), 1.64 (dd, *J* = 6.3, 5.5 Hz, 2H, $CH(OH)C\underline{H}_2CH(OH)CH(CH_3)$),1.62–1.59 (m, 1H, $BnOCH_2CH_2CH_a\underline{H}_b$), 1.04 (d, *J* = 6.8 Hz, 3H, $CH(C\underline{H}_3)CH=CH_2$);

^{13}C NMR (126 MHz, $CDCl_3$): δ 140.6 ($H\underline{C}=CH_2$), 138.1 (C_{Ar}), 128.4 (2, $\underline{C}H_{Ar}$), 127.8 (2, $\underline{C}H_{Ar}$), 127.7 ($\underline{C}H_{Ar}$), 116.4 ($HC=\underline{C}H_2$), 73.1(CH_2), 71.9 (CH), 70.6 (CH_2), 69.1 (CH), 44.4 (CH), 39.5 (CH_2), 34.9 (CH_2), 26.6 (CH_2), 16.1 (CH_3);

HRMS (ESI-TOF) m/z: $[M + Na]^+$ Calcd for $C_{17}H_{26}O_3Na$ 301.1780; Found 301.1781.

(3*R*,4*S*,6*R*)-9-(benzyloxy)-3-ethylnon-1-ene-4,6-diol (4.3.2)

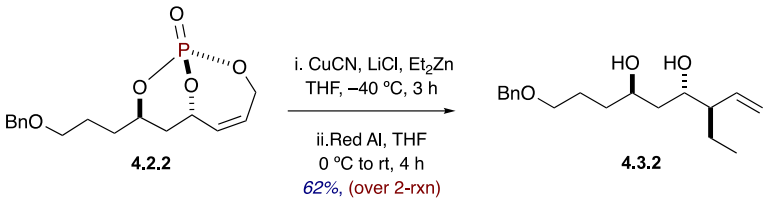

To a flame dried round bottom-flask was added CuCN (166 mg, 1.83 mmol) and LiCl (181 mg, 4.3 mmol) inside the glove box, followed by addition of dry THF (5.7 mL, 0.05 M) under argon and the reaction mixture was stirred at room temperature for 15 minutes. A pale green coloration was observed. The reaction mixture was cooled to -40 ºC followed by slow addition of a 1 M solution of Et_2Zn in THF (1.83 mL, 1.83 mmol). The reaction mixture was stirred for 40 minutes at -30 ºC and a solution of bicyclic phosphate **4.2.2** (200 mg, 0.57 mmol) in dry THF (5.7 mL, 0.05 M) was added dropwise via cannula to the reaction mixture. The reaction was slowly warmed to room temperature and allowed to stir for 3 h. Upon completion of reaction (monitored via TLC), the reaction mixture was quenched with saturated aqueous ammonium chloride (NH_4Cl, 1.5 mL), stirred for 15 minutes followed by the addition of anhydrous Na_2SO_4 (150 mg) stirred for another 30 minutes. The crude product was filtered through Celite pad and washed with excess EtOAc (3 x 50 mL), the filtrate was concentrated under reduce pressure, which afforded the crude acid as yellowish viscous oil, which was proceeded to the next reaction without further purification.

To a flask containing the crude acid was added THF (7.7 mL, 0.08 M). The reaction mixture was cooled to 0 ºC and was added 70% solution of Red-Al in toluene (0.85 mL, 5 mmol). The reaction mixture was brought to room temperature and stirred for 4 h. After

completion of reaction (monitored by TLC), it was quenched with NH_4Cl (sat. aq.) and was added (Na_2SO_4), stirred for 30 minutes, filtered through Celite pad. The residue was washed with EtOAc (3 x 50 mL). The organic layer was dried (Na_2SO_4) and the solvent was evaporated under reduced pressure. The crude product was purified via flash chromatography (30% EtOAc/Hexane), which afforded diol **4.3.2** (127 mg, with 62% yield over two reactions) as colorless viscous oil. TLC (hexane/EtOAc 3/1): R_f = 0.23.

FTIR (neat): 3395, 3067, 2930, 2871, 1638, 1453, 1362, 1204, 1098, 1028, 912, 735, 697, 612 cm^{-1};

Optical Rotation: $[a]_D^{23}$ = -13.76 (*c* 0.62, $CHCl_3$);

^{1}H NMR (500 MHz, Chloroform-*d*): δ 7.36–7.27 (m, 5H, Aromatic C‑H), 5.63 (dt, *J* = 17.2, 9.8 Hz, 1H, $CH(CH_2CH_3)C\underline{H}=CH_2$), 5.20 (dd, *J* = 10.2, 2.1 Hz, 1H, $CH(CH_2CH_3)CH=C\underline{H}_aH_b$), 5.11 (dd, *J* = 17.2, 2.1 Hz, 1H, $CH(CH_2CH_3)CH=CH_a\underline{H}_b$), 4.52 (s, 2H, $PhC\underline{H}_2OCH_2$), 3.93 (tt, *J* = 8.5, 3.7 Hz, 1H, $C\underline{H}(OH)CH_2CH(OH)CH(CH_2CH_3)$), 3.81 (ddd, *J* = 9.2, 6.1, 3.0 Hz, 1H, $CH(OH)CH_2C\underline{H}(OH)CH(CH_2CH_3)$), 3.52 (td, *J* = 6.1, 2.0 Hz, 2H, $BnOC\underline{H}_2CH_2CH_2$), 3.27 (s, 1H, $CH(O\underline{H})CH_2CH(OH)CH(CH_2CH_3)$), 2.38 (s, 1H, $CH(OH)CH_2CH(O\underline{H})CH(CH_2CH_3)$), 1.93 (tdd *J* = 9.9, 6.1, 4.1 Hz, 1H, $C\underline{H}(CH_2CH_3)CH=CH_2$), 1.75 (dq, *J* = 12.5, 6.5, 6.0 Hz, 2H, $BnOCH_2C\underline{H}_2CH_2$), 1.66–1.56 (m, 4H, $BnOCH_2CH_2C\underline{H}_2$, $CH(OH)C\underline{H}_2CH(OH)CH(CH_2CH_3)$), 1.56–1.49 (m, 1H, $CH(C\underline{H}_aH_bCH_3)CH=CH_2$), 1.32–1.25 (m, 1H, $CH(CH_a\underline{H}_bCH_3)CH=CH_2$), 0.87 (t, *J* = 7.4 Hz, 3H, $CH(CH_2C\underline{H}_3)CH=CH_2$);

^{13}C NMR (126 MHz, $CDCl_3$): δ 138.9 (<u>C</u>H=CH_2), 138.1 (C_{Ar}), 128.4 (2, <u>C</u>H_{Ar}), 127.8 (2, <u>C</u>H_{Ar}), 127.7 (<u>C</u>H_{Ar}), 118.2 (CH=<u>C</u>H_2), 73.1 (CH_2), 70.7 (CH), 70.6 (CH_2), 69.1 (CH), 52.6 (CH), 40.2 (CH_2), 34.8 (CH_2), 26.5 (CH_2), 23.4 (CH_2), 11.9 (CH_3);

HRMS (ESI-TOF) m/z: $[M + Na]^+$ Calcd for $C_{18}H_{28}O_3Na$ 315.1936; Found 315.1925;

(4*R*,6*S*,7*R*)-1-(benzyloxy)-7-vinyltridecane-4,6-diol (4.3.3)

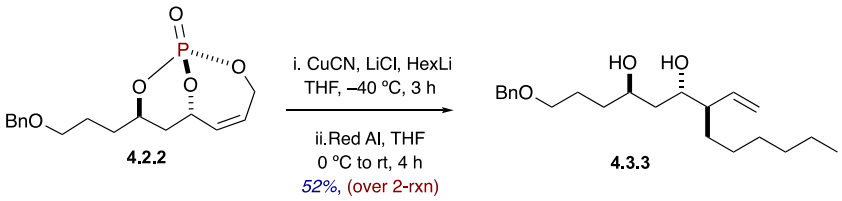

To a flame dried round bottom-flask was added CuCN (166 mg, 1.83 mmol) and LiCl (181 mg, 4.3 mmol) inside the glove box, followed by addition of dry THF (5.7 mL, 0.05 M) under argon and the reaction mixture was stirred at room temperature for 15 minutes. A pale green coloration was observed. The reaction mixture was cooled to -40 ºC followed by slow addition of a 1 M solution of Et_2Zn in THF (1.83 mL, 1.83 mmol). The reaction mixture was stirred for 40 minutes at -30 ºC and a solution of bicyclic phosphate **4.2.2** (200 mg, 0.57 mmol) in dry THF (5.7 mL, 0.05 M) was added dropwise via cannula to the reaction mixture. The reaction was slowly warmed to room temperature and allowed to stir for 4 h. Upon completion of reaction (monitored via TLC), the reaction mixture was quenched with saturated aqueous NH_4Cl (1.5 mL), stirred for 15 minutes followed by the addition of anhydrous Na_2SO_4 (150 mg) stirred for another 30 minutes. The crude product was filtered through Celite pad and washed with excess EtOAc (3 x 50 mL), the filtrate was concentrated under reduce pressure, which afforded the crude acid as a yellowish viscous oil, which was proceeded to the next reaction without further purification.

To a flask containing the crude acid was added THF (7.7 mL, 0.08 M). The reaction mixture was cooled to 0 ºC and was added 70% solution of Red-Al in toluene (0.85 mL, 5 mmol). The reaction mixture was brought to room temperature and stirred for 6 h. After

completion of reaction (monitored by TLC), it was quenched with NH_4Cl (sat. aq.) and was added (Na_2SO_4), stirred for 30 minutes, filtered through Celite pad. The residue was washed with EtOAc (3 x 50 mL). The organic layer was dried (Na_2SO_4) and the solvent was evaporated under reduced pressure. The crude product was purified via flash chromatography (30% EtOAc/Hexane), which afforded diol **4.3.3** (104 mg, with 52% yield over two reactions) as colorless viscous oil. TLC (hexane/EtOAc 3/1): R_f = 0.32.

FTIR (neat): 3458, 2943, 2866, 1718, 1699, 1456, 1390, 1097, 1027, 912, 842, 736, 697 cm^{-1};

Optical Rotation: $[a]_D^{23}$ = -6.92 (*c* 0.45, $CHCl_3$);

^{1}H NMR (500 MHz, Chloroform-*d*): δ 7.36–7.27 (m, 5H, Aromatic C–H), 5.63 (ddd *J* = 17.1, 10.2, 9.3 Hz, 1H, $CH(C_5H_{10}CH_3)C\underline{H}=CH_2$), 5.18 (dd, *J* = 10.3, 2.1 Hz, 1H, $CH(C_5H_{10}CH_3)CH=C\underline{H}_aH_b$), 5.10 (dd, *J* = 17.2, 2.1 Hz, 1H, $CH(C_5H_{10}CH_3)CH=CH_a\underline{H}_b$), 4.52 (s, 2H, $PhC\underline{H}_2OCH_2$), 3.92 (p, *J* = 6.0 Hz, 1H, $C\underline{H}(OH)CH_2CH(OH)CH(C_5H_{10}CH_3)$), 3.78–3.75 (m, 1H, $CH(OH)CH_2C\underline{H}(OH)CH(C_5H_{10}CH_3)$), 3.52 (td, *J* = 6.0, 1.5 Hz, 2H, $BnOC\underline{H}_2CH_2CH_2$), 3.23 (s, 1H, $CH(O\underline{H})CH_2CH(OH)CH(C_5H_{10}CH_3)$), 2.34 (s, 1H, $CH(OH)CH_2CH(O\underline{H})CH(C_5H_{10}CH_3)$), 2.02 (tdd *J* = 9.7, 5.8, 3.5 Hz, 1H, $C\underline{H}(C_5H_{10}CH_3)CH=CH_2$), 1.74 (ddt, *J* = 14.0, 12.6, 7.3 Hz, 2H, $BnOCH_2C\underline{H}_2CH_2$), 1.68–1.54 (m, 4H, $BnOCH_2CH_2C\underline{H}_2$, $CH(OH)C\underline{H}_2CH(OH)CH(C_5H_{10}CH_3)$), 1.44 (ddd, *J* = 16.0, 8.2, 4.0 Hz, 1H, $CH(C\underline{H}_aH_bC_4H_8CH_3)CH=CH_2$), 1.36–1.15 (m, 9H, $CH(CH_a\underline{H}_bC_4\underline{H}_8CH_3)CH=CH_2$), 0.87 (t, *J* = 7.0 Hz, 3H, $CH(C_5H_{10}C\underline{H}_3)CH=CH_2$);

^{13}C NMR (126 MHz, $CDCl_3$): δ 139.2 ($\underline{C}H=CH_2$), 138.1 (C_{Ar}), 128.4 (2, $\underline{C}H_{Ar}$), 127.8 ($\underline{C}H_{Ar}$) 127.7 (2, $\underline{C}H_{Ar}$), 118.0 ($CH=\underline{C}H_2$), 73.1 (CH_2), 70.9 (CH), 70.6 (CH_2), 69.1 (CH),

50.8 (CH), 40.1 (CH_2), 34.8 (CH_2), 31.8 (CH_2), 30.6 (CH_2), 29.3 (CH_2), 27.3 (CH_2), 26.5 (CH_2), 22.6 (CH_2), 14.1 (CH_3);

HRMS (ESI-TOF) m/z: $[M + Na]^+$ Calcd for $C_{22}H_{36}O_3Na$ 371.2562; Found 371.2569.

(4*R*,6*R*)-9-(benzyloxy)non-1-ene-4,6-diol (4.3.4)

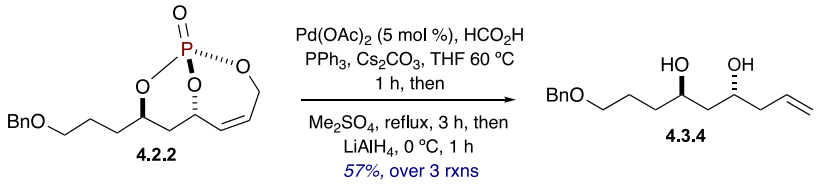

To a stirring solution of bicyclic phosphate **4.2.2** (250 mg, 0.77 mmol) in THF (2.6 mL, 0.3 M) under argon was added Cs_2CO_3 (1.25 gm, 3.85 mmol) and HCO_2H (78 μL, 1.92 mmol). Next, a solution of $Pd(OAc)_2$ (12.3 mg, 0.038 mmol, 5 mol%) and PPh_3 (19.2 mg, 0.077 mmol) in THF (1.9 mL) under argon was immediately transferred *via* cannula to the reaction mixture. The reaction mixture was stirred at 60 ºC in an oil bath for 1 h (monitored by TLC). After 1 h, all starting materials were consumed and the color of reaction mixture turned black. After the reaction was complete, Me_2SO_4 was added, and the reaction mixture was refluxed for 3 h (TLC showed that phosphoric acid was methylated completely). The reaction mixture was cooled to 0 ºC, then $LiAlH_4$ (85 mg, 2.3 mmol) was added portion-wise. Next, the reaction mixture was stirred at 0 ºC for 1 h. After the completion of reduction, it was quenched following the Fieser workup[5] *via* slow sequential addition of H_2O (1 mL/g of $LiAlH_4$), followed by 10% NaOH (1 mL/g of $LiAlH_4$) and finally H_2O (3 mL/g of $LiAlH_4$) and the ice bath was removed and the reaction mixture was stirred for 2 h. The reaction mixture was filtered, extracted with EtOAc (3 x 50 mL) and dried (Na_2SO_4). The resulting solution was filtered again, concentrated and purified using a short silica gel flash column chromatography (hexane/EtOAc 3:1), which afforded the diol **4.3.4** (114 mg,

[5]. L. F. Fieser, M. Fieser in *Reagents for Organic Synthesis*, *Vol. 1,* Wiley: New York, **1967**, pp. 581−595; b) V. M. Mićović, M. Mihailović, *J. Org. Chem.* **1953**, *18*, 1190–1200.

57% yield over 3 reactions, 81% av/rxn) as a colorless liquid. TLC (hexane/EtOAc 3/1): R_f = 0.22.

FTIR (neat): 3404, 3067, 2924, 2854, 1720, 1641, 1495, 1454, 1362, 1287, 1096, 1028, 995, 737 cm^{-1};

Optical Rotation: $[a]_D^{23}$ = -32.6 (*c* 2.1, $CHCl_3$);

^{1}H NMR (500 MHz, $CDCl_3$): δ 7.37–7.28 (m, 5H, Aromatic C–H), 5.82 (ddt, *J* = 16.4, 10.6, 7.1 Hz, 1H, $CH_2C\underline{H}=CH_2$), 5.14 (dt, *J* = 5.8, 1.8 Hz , 1H, $CH_2CH=C\underline{H}_aH_b$), 5.11 (t, *J* = 1.2 Hz, 1H, $CH_2CH=CH_a\underline{H}_b$), 4.52 (s, 2H, $PhC\underline{H}_2OCH_2$), 4.02–3.92 (m, 2H, $C\underline{H}(OH)CH_2C\underline{H}(OH)CH_2$), 3.52 (td, *J* = 5.8, 5.0, 3.7 Hz, 2H, $BnOC\underline{H}_2CH_2$), 3.33 (s, 1H, $CH(OH)CH_2CH(O\underline{H})CH_2$), 2.67 (s, 1H, $CH(O\underline{H})CH_2CH(OH)CH_2$), 2.27 (ddt, *J* = 7.6, 6.4, 1.3 Hz, 2H, $C\underline{H}_2CH=CH_2$), 1.75 (qd, *J* = 6.8, 5.0 Hz, 2H, $BnOCH_2C\underline{H}_2CH_2$), 1.65–1.59 (m, 2H, $CH(OH)C\underline{H}_2CH(OH)CH_2$), 1.59–1.55 (m, 2H, $BnOCH_2CH_2C\underline{H}_2$).

^{13}C NMR (126 MHz, $CDCl_3$): δ 138.0 (C_{Ar}), 134.9 ($\underline{C}H=CH_2$), 128.5 ($\underline{C}H_{Ar}$), 128.4 ($\underline{C}H_{Ar}$), 127.8 (2, $\underline{C}H_{Ar}$), 127.7 ($\underline{C}H_{Ar}$), 117.9 ($CH=\underline{C}H_2$), 73.2 (CH_2), 70.6 (CH_2), 69.2 (CH), 68.3 (CH), 42.0 (2, CH_2), 35.1 (CH_2), 26.6 (CH_2);

HRMS (ESI-TOF) m/z: $[M + Na]^+$ Calcd for $C_{16}H_{24}O_3Na$ 287.1623; Found 287.1631.

(3R,4S,6R,9S)-9,10-bis(benzyloxy)-3-methyldec-1-ene-4,6-diol (4.4.1)

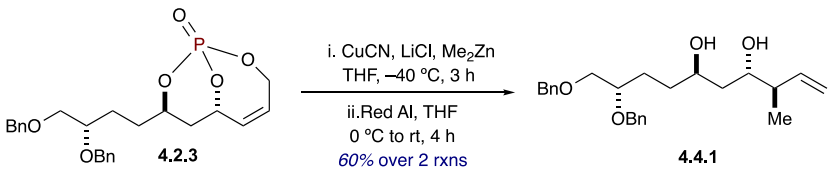

To a flame dried round bottom-flask was added CuCN (61 mg, 0.67 mmol) and LiCl (66 mg, 1.57 mmol) inside the glove box, followed by addition of dry THF (2.1 mL, 0.05 M) under argon and the reaction mixture was stirred at room temperature for 15 minutes. A pale green coloration was observed. The reaction mixture was cooled to -40 ºC followed by slow addition of a 1 M solution of Me_2Zn in THF (0.67 mL, 0.67 mmol). The reaction mixture was stirred for 40 minutes at -30 ºC and a solution of bicyclic phosphate **4.2.3** (100 mg, 0.22 mmol) in dry THF (2.1 mL, 0.05 M) was added dropwise via cannula to the reaction mixture. The reaction was slowly warmed to room temperature and allowed to stir for 3 h. Upon completion of reaction (monitored via TLC), the reaction mixture was quenched with saturated aqueous ammonium chloride (NH_4Cl, 0.8 mL), stirred for 15 minutes followed by the addition of anhydrous Na_2SO_4 (45 mg) stirred for another 30 minutes. The crude product was filtered through Celite pad and washed with excess EtOAc (3 x 50 mL), the filtrate was concentrated under reduce pressure, which afforded the crude acid as yellowish viscous oil, which was proceeded to the next reaction without further purification.

To a flask containing the crude acid was added THF (2.83 mL, 0.08 M). The reaction mixture was cooled to 0 ºC and was added 70% solution of Red-Al in toluene (0.31 mL, 5 mmol). The reaction mixture was brought to room temperature and stirred for 4 h. After completion of reaction (monitored by TLC), it was quenched with NH_4Cl (sat. aq.) and was added Na_2SO_4, stirred for 30 minutes, filtered through Celite pad. The residue

was washed with EtOAc (3 x 10 mL). The organic layer was dried (Na_2SO_4) and the solvent was evaporated under reduced pressure. The crude product was purified via flash chromatography (30% EtOAc/Hexane), which afforded diol **4.4.1** (51mg, with 60% yield over two reactions) as colorless viscous oil. TLC (hexane/EtOAc 3/1): R_f = 0.33.

FTIR (neat): 3406, 2926, 2360, 1601, 1451, 1315, 1276, 1135, 1070, 1026, 771, 665 cm^{-1};

Optical Rotation: $[a]_D^{23}$ = 12.3 (*c* 1.2, $CHCl_3$);

^{1}H NMR (500 MHz, $CDCl_3$): δ 7.36–7.27 (m, 10H, Aromatic C‑H), 5.74 (ddd, *J* = 16.4, 11.0, 8.3 Hz, 1H, $CH(CH_3)C\underline{H}{=}CH_aH_b$), 5.16–5.10 (m, 2H, $CH(CH_3)CH{=}C\underline{H}_a\underline{H}_b$), 4.71 (d, *J* = 11.7 Hz, 1H, $BnOCH_aH_bCH(OC\underline{H}_aH_bPh)$), 4.57 (d, *J* = 11.8 Hz, 1H, $BnOCH_aH_bCH(OCH_a\underline{H}_bPh)$), 4.55 (s, 2H, $PhC\underline{H}_2OCH_aH_bCH(OCH_aH_bPh)$), 3.88 (dq, *J* = 10.6, 4.3 Hz, 1H, $CH_aH_bC\underline{H}(OH)CH_aH_bCH(OH)CH(CH_3)$), 3.69 (ddd, *J* = 9.9, 7.3, 4.9 Hz, 1H, $CH(OH)CH_aH_bC\underline{H}(OH)CH(CH_3)$), 3.64 (dddd, *J* = 5.4 Hz, 1H, $BnOCH_2C\underline{H}(OBn)CH_2$), 3.59 (dd, *J* = 9.9, 5.4 Hz, 1H, $BnOC\underline{H}_a H_bC\underline{H}(OBn)CH_2$), 3.54 (dd, *J* = 9.8, 5.4 Hz, 1H, $BnOCH_a\underline{H}_bC\underline{H}(OBn)CH_2$), 2.95 (d, *J* = 4.3 Hz, 1H, $CH(OH)CH_aH_b(O\underline{H})CH(CH_3)$), 2.36 (d, *J* = 3.3 Hz, 1H, $CH(O\underline{H})CH_aH_b(OH)CH(CH_3)$), 2.23 (ddq, *J* = 8.7, 6.6 Hz, 1H, $CH(OH)C\underline{H}(CH_3)CH{=}CH_2$), 1.72–1.68 (m, 2H, $BnOCH_2CH(OBn)C\underline{H}_a\underline{H}_bCH_aH_b$), 1.65–1.61 (m, 1H, $BnOCH_2CH(OBn)CH_aH_bC\underline{H}_aH_b$), 1.60–1.58 (m, 2H, $CH(OH)C\underline{H}_a\underline{H}_bCH(OH)CH(CH_3)$), 1.56–1.51 (m, 1H, $BnOCH_2CH(OBn)CH_aH_bCH_a\underline{H}_b$), 1.00 (d , *J* = 6.9 Hz, 3H, $CH(OH)CH(C\underline{H}_3)CH{=}CH_2$).;

^{13}C NMR (126 MHz, $CDCl_3$): δ 140.7 ($\underline{C}H{=}CH_2$), 138.6 ($\underline{C}_{Ar}$), 138.4 ($\underline{C}_{Ar}$), 128.5 (2, $\underline{C}H_{Ar}$), 128.4 (2, $\underline{C}H_{Ar}$), 128.1 (2, $\underline{C}H_{Ar}$), 127.8 (2, $\underline{C}H_{Ar}$), 127.7 (2, $\underline{C}H_{Ar}$)), 116.6

(CH=CH_2), 78.1 (CH), 73.5 (CH_2OBn), 72.6 (CH_2), 72.1 (CH_2OBn), 72.0 (CH), 69.4 (CH_2), 44.5 (CH), 39.5 (CH_2), 33.2 (CH_2), 28.5 (CH_2), 16.2 (CH_3);

HRMS (ESI-TOF) m/z: $[M + Na]^+$ Calcd for $C_{25}H_{34}O_4Na$ 421.2355; Found 421.2339.

(4*R*,6*R*,9*S*)-9,10-bis(benzyloxy)dec-1-ene-4,6-diol (4.4.2)

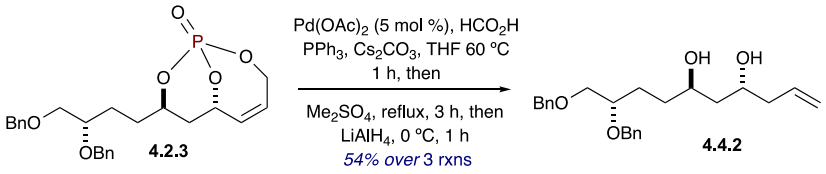

To a stirring solution of bicyclic phosphate **4.2.3** (100 mg, 0.22 mmol) in THF (0.75 mL, 0.3 M) under argon was added Cs_2CO_3 (470 mg, 1.1 mmol) and HCO_2H (23 μL, 0.56 mmol). Next, a solution of $Pd(OAc)_2$ (3.6 mg, 0.011 mmol, 5 mol%) and PPh_3 (5.6 mg, 0.022 mmol) in THF (1.6 mL) under argon was immediately transferred *via* cannula to the reaction mixture. The reaction mixture was stirred at 60 ºC in an oil bath for 1 h (monitored by TLC). After 1 h, all starting materials were consumed and the color of reaction mixture turned black. After the reaction was complete, Me_2SO_4 was added, and the reaction mixture was refluxed for 3 h (TLC showed that phosphoric acid was methylated completely). The reaction mixture was cooled to 0 ºC, then $LiAlH_4$ (25 mg, 0.68 mmol) was added portion-wise. Next, the reaction mixture was stirred at 0 ºC for 1 h. After the completion of reduction, it was quenched following the Fieser workup[6] *via* slow sequential addition of H_2O (1 mL/g of $LiAlH_4$), followed by 10% NaOH (1 mL/g of $LiAlH_4$) and finally H_2O (3 mL/g of $LiAlH_4$) and the ice bath was removed and the reaction mixture was stirred for 2 h. The reaction mixture was filtered, extracted with EtOAc (3 x 50 mL) and dried (Na_2SO_4). The resulting solution was filtered again, concentrated and purified using a short silica gel flash column chromatography (hexane/EtOAc 3:1), which afforded the TBS-protected diol **4.4.2** (43 mg, 54% yield over 3 reactions, 78% av/rxn) as a colorless liquid. TLC (hexane/EtOAc 3/1): $R_f = 0.41$.

[6]. L. F. Fieser, M. Fieser in *Reagents for Organic Synthesis*, *Vol. 1,* Wiley: New York, **1967**, pp. 581−595; b) V. M. Mićović, M. Mihailović, *J. Org. Chem.* **1953**, *18*, 1190–1200.

FTIR (neat): 3394, 3064, 2929, 2862, 1640, 1495,1453, 1364, 1027, 913, 736, 609 cm^{-1};

Optical Rotation: = $[a]_D^{23}$ = -25.6 (*c* 0.3, $CHCl_3$);

^{1}H NMR (500 MHz, $CDCl_3$): δ 7.37–7.28 (m, 10H, Aromatic C‑H), 5.81 (ddt, *J* = 18.7, 9.5, 7.1 Hz, 1H, $CH_2C\underline{H}=CH_2$), 5.17–5.09 (m, 2H, $CH_2CH=C\underline{H}_2$), 4.72 (d, *J* = 11.6 Hz, 1H, $BnOCH_2CH(OC\underline{H}_aH_bPh)$), 4.57 (d, *J* = 11.6 Hz, 1H, $BnOCH_2CH(OCH_a\underline{H}_bPh)$), 4.55 (s, 2H, $PhC\underline{H}_2OCH_2CH(OBn)$), 3.96 (q, *J* = 6.6, 4.3 Hz, 1H, $CH_2CH(OH)CH_2C\underline{H}(OH)CH_2$), 3.90 (dd, *J* = 8.3, 4.6, Hz, 1H, $C\underline{H}(OH)CH_2CH(OH)CH_2$), 3.65 (dt, *J* = 7.0, 4.7 Hz, 1H, $BnOCH_2C\underline{H}(OBn)CH_2$), 3.60 (dd, *J* = 9.9, 5.6 Hz, 1H, $BnOC\underline{H}_aH_bCH(OBn)CH_2$), 3.53 (dd, *J* = 9.9, 4.7 Hz, 1H, $BnOCH_a\underline{H}_bCH(OBn)CH_2$), 2.95 (s, 1H, $CH(OH)CH_2CH(O\underline{H})CH_2$), 2.36 (s, 1H, $CH(O\underline{H})CH_2CH(OH)CH_2$), 2.25 (t, *J* = 6.8 Hz, 2H, $CH(OH)C\underline{H}_2CH=CH_2$), 1.79–1.61 (m, 2H, $BnOCH_2CH(OBn)C\underline{H}_a\underline{H}_bCH_aH_b$), 1.61–1.58 (m, 2H, $CH(OH)C\underline{H}_a\underline{H}_bCH(OH)CH_2$), 1.58–1.49 (m, 2H, $BnOCH_2CH(OBn)CH_aH_bC\underline{H}_a\underline{H}_b$);

^{13}C NMR (126 MHz, $CDCl_3$): *δ* 138.5 ($\underline{C}_{Ar}$), 138.3 ($\underline{C}_{Ar}$), 134.9 ($\underline{C}H=CH_2$), 128.5 (2, $\underline{C}H_{Ar}$), 128.5 (2, $\underline{C}H_{Ar}$), 128.0 (2, $\underline{C}H_{Ar}$), 127.8 (2, $\underline{C}H_{Ar}$), 127.8 (2, $\underline{C}H_{Ar}$), 118.0 ($CH=\underline{C}H_2$), 78.2 (CH), 73.5 (CH_2), 72.6 (CH_2), 72.2 (CH_2), 69.2 (CH), 68.3 (CH), 42.4 (CH_2), 42.0 (CH_2), 33.4 (CH_2), 28.5 (CH_2);

HRMS (ESI-TOF) m/z: $[M + Na]^+$ Calcd for $C_{24}H_{32}O_4Na$ 407.2198; Found 407.2165.

(3*R*,4*S*,6*R*)-9-(benzyloxy)-3-methyl-6-((triisopropylsilyl)oxy)non-1-en-4-ol(4.5.1)

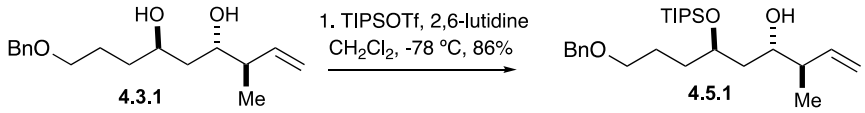

To a solution of **4.3.1** (300 mg, 1.07 mmol) in CH_2Cl_2 (1.07 mL, 0.1 M) was added 2,6 lutidine (313 µL, 2.6 mmol). The reaction mixture was cooled to -78 ºC and was added dropwise TIPSOTf (317 µL, 1.12 mmol). The reaction mixture was stirred for 30 minutes, and after completion of reaction (monitored via TLC), the reaction was quenched with aqueous $NaHCO_3$. The layers were separated, and the aqueous layer was extracted with CH_2Cl_2 (2 x 10 mL). The combined organic layers were washed with 10% aq. HCl solution, dried ($MgSO_4$), concentrated under reduced pressure. The crude product was purified using silica gel column chromatography (5% EtOAc/Hexanes), which furnished 397 mg of **4.5.1** in 86% yield as colorless viscous liquid. TLC (hexane/EtOAc 10/1): R_f = 0.2.

FTIR (neat): 3495, 3064, 2926, 2865, 1495, 1454, 1255, 1093, 997, 734, 696 cm^{-1};

Optical Rotation: $[a]_D^{23}$ = -2.8 (*c* 0.4, $CHCl_3$);

^{1}H NMR (500 MHz, Chloroform-*d*): δ 7.37–7.28 (m, 5H, Aromatic C‑H), 5.84 (ddd *J* = 20.0, 8.7, 7.8 Hz, 1H, $CH(CH_3)C\underline{H}=CH_2$), 5.07 (d, *J* = 1.0 Hz, 1H, $CH(CH_3)CH=C\underline{H}aHb$), 5.04 (ddd, *J* = 7.2, 2.0, 1.1 Hz, 1H, $CH(CH_3)CH=CHa\underline{H}b$), 4.50 (s, 2H, $PhC\underline{H}_2OCH_2$), 4.16 (dq, *J* = 8.7, 4.2 Hz, $C\underline{H}(OTIPS)CH_aH_bCH(OH)CH(CH_3)$), 3.88 (ddt, *J* = 10.8, 5.1, 1.8 Hz, 1H, $CH(OTIPS)CH_aH_bC\underline{H}(OH)CH(CH_3)$), 3.56 (d, *J* = 1.4 Hz, 1H, $CH(OTIPS)CH_aH_bCH(O\underline{H})CH(CH_3)$), 3.47 (td, *J* = 6.5, 3.6 Hz, 2H, $BnOC\underline{H}_2CH_2$), 2.20 (dqd, *J* = 7.9, 6.7, 4.9 Hz, 1H, $C\underline{H}(CH_3)CH=CH_2$), 1.81–1.77 (m, 1H, $BnOCH_2CH_2C\underline{H}_aH_bCH(OTIPS)$),1.76–1.72(m,1H, $CH(OTIPS)C\underline{H}_aH_bCH(OH)CH(CH_3)$), 1.71–1.67 (m, 1H, $CH(OTIPS)CH_a\underline{H}_bCH(OH)CH(CH_3)$), 1.57–1.56 (m, 1H,

BnOCH$_2$CH$_2$C$\underline{H}_a$H$_b$CH(OTIPS)), 1.60–1.52 (m, 2H, BnOCH$_2$C$\underline{H}_a\underline{H}_bCH_aH_b$CH(OTIPS)), 1.09–1.05 (m, 21H, OSi(C$\underline{H}$(C$\underline{H}_3$)$_2$)$_3$), 1.04 (d, *J* = 6.9 Hz, 3H, CH(OTIPS)CH$_2$CH(OH)CH(C$\underline{H}_3$));

^{13}C NMR (126 MHz, $CDCl_3$): δ 140.7 ($\underline{C}$H=CH$_2$), 138.5 (C$_{Ar}$), 128.4 (2, $\underline{C}$H$_{Ar}$), 127.6 (2, $\underline{C}$H$_{Ar}$), 127.5 ($\underline{C}$H$_{Ar}$), 116.1 (CH=$\underline{C}$H$_2$), 72.9 (CH$_2$), 72.0 (CH), 71.3 (CH), 70.3 (CH$_2$), 44.1 (CH), 37.0 (CH$_2$), 32.5 (CH$_2$), 26.0 (CH$_2$), 18.1 [6C, Si (CH ($\underline{C}$H$_3$)$_2$)$_3$], 15.6 (CH$_3$), 12.4 [3C, Si ($\underline{C}$H (CH$_3$)$_2$)$_3$];

HRMS (ESI-TOF) m/z: $[M + H]^+$ Calcd for $C_{26}H_{47}O_3Si$ 435.3294; Found 435.3338.

(5*S*,7*R*)-7-(3-(benzyloxy)propyl)-5-((*R*)-but-3-en-2-yl)-9,9-diisopropyl-10-methyl-2,4,8-trioxa-9-silaundecane (4.5.2):

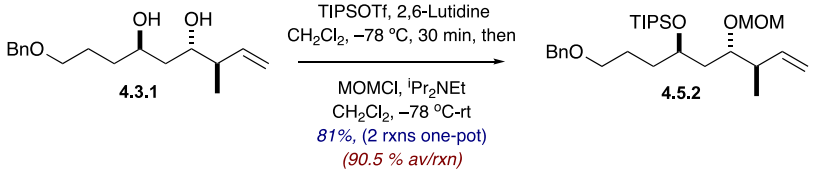

To a solution of **4.3.1** (240 mg, 0.86 mmol) in CH_2Cl_2 (8.6 mL, 0.1 M) was added 2,6 lutidine (251 µL, 2.1 mmol). The reaction mixture was cooled to -78 ºC and was added dropwise TIPSOTf (254 µL, 0.9 mmol). The reaction mixture was stirred for 30 minutes, after completion of reaction (monitored via TLC), it was added *N*,*N*-disopropylethylamine (600 µL, 3.44 mmol) followed by dropwise addition of chloro(methoxy)methane (130 µL, 1.72 mmol) and the reaction mixture was stirred for 12 h. After completion of reaction, it was quenched with saturated aqueous $NaHCO_3$, extracted with CH_2Cl_2, dried ($MgSO_4$), concentrated under reduced pressure. The crude product was purified using silica gel column chromatography (5% EtOAc/Hexanes), which furnished 348 mg of **13** in 81% yield over two reactions in one-pot (90.5% av/rxn) as colorless viscous liquid. TLC (hexane/EtOAc 20/1): R_f = 0.45.

FTIR (neat): 2943, 2866, 2352, 2329, 1693, 1556, 1454, 1348, 1151, 1099, 1041, 916, 883, 732 cm^{-1};

Optical Rotation: $[a]_D^{23}$ = -1.25 (*c* 1.43, $CHCl_3$);

^{1}H NMR (500 MHz, Chloroform-*d*): δ 7.40–7.29 (m, 5H, Aromatic C‑H), 5.78 (ddd, *J* = 17.3, 10.2, 6.9 Hz, 1H, $CH(CH_3)C\underline{H}=CH_2$), 5.05 (dt, *J* = 3.4, 1.8, 1.0 Hz, 1H, $CH(CH_3)CH=C\underline{H}_aH_b$), 5.02 (dt, *J* = 3.3, 1.5, 1.0 Hz, 1H, $CH(CH_3)CH=CH_a\underline{H}_b$), 4.67 (dd, *J* = 19.7, 6.4 Hz, 2H, $CH(OTIPS)CH_2CH(OC\underline{H}_2OCH_3)$), 4.50 (s, 2H, $PhC\underline{H}_2OCH_2$), 3.96 (tt, *J* = 6.2, 4.6 Hz, 1H, $C\underline{H}(OTIPS)CH_2CH(OMOM)CH(CH_3)$), 3.68 (dt *J* = 7.7, 3.8 Hz,

1H, CH(OTIPS)$CH_2C\underline{H}$(OMOM)$CH(CH_3)$), 3.47 (td, J = 6.5, 1.1 Hz, 2H, $BnOC\underline{H}_2CH_2$), 3.37 (s, 3H, CH(OTIPS)$CH_2CH(OCH_2OC\underline{H}_3)$), 2.53–2.49 (m, 1H, $C\underline{H}(CH_3)CH{=}CH_2$), 1.71–1.62 (m, 2H, $BnOCH_2C\underline{H}_a\underline{H}_bCH_2$), 1.61–1.59 (m, 1H, CH(OTIPS)$C\underline{H}_aCH_bCH(OCH_2OCH_3)$), 1.59–1.56 (m, 1H, $BnOCH_2CH_aH_bC\underline{H}_aH_b$), 1.56–1.53 (m, 1H, CH(OTIPS)$CH_aC\underline{H}_bCH(OCH_2OCH_3)$), 1.53–1.47 (m, 1H, $BnOCH_2CH_2CH_a\underline{H}_b$), 1.08–1.03 (m, 21H, $Si(C\underline{H}(C\underline{H}_3)_2)_3$), 1.03 (s, J = 6.9 Hz, 3H, $CH(C\underline{H}_3)CH{=}CH_2$);

^{13}C NMR (126 MHz, $CDCl_3$): δ 140.3 ($\underline{C}H{=}CH_2$), 138.8 (C_{Ar}), 128.5 (2, $\underline{C}H_{Ar}$), 127.7 (2, $\underline{C}H_{Ar}$), 127.6 ($\underline{C}H_{Ar}$), 115.1 ($CH{=}\underline{C}H_2$), 96.9 (CH_2), 79.9 (CH), 72.9 (CH_2), 70.8 (CH_2), 70.0 (CH), 55.9 (CH_3), 41.5 (CH), 38.6 (CH_2), 34.5 (CH_2), 25.0 (CH_2), 18.4 [6C, Si (CH ($\underline{C}H_3)_2)_3$], 14.4 (CH_3), 13.0 [3C, Si ($\underline{C}H$ $(CH_3)_2)_3$];

HRMS (ESI-TOF) m/z: $[M + Na]^+$ Calcd for $C_{28}H_{50}O_4SiNa$ 501.3376; Found 501.3375.

(5*R*,7*R*)-5-allyl-7-(3-(benzyloxy)propyl)-2,4,8,10-tetraoxaundecane (4.5.3)

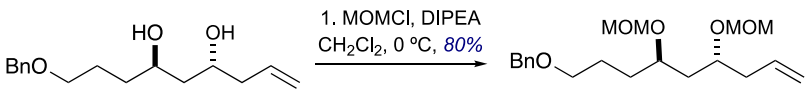

4.3.1 **4.5.3**

To a solution of **4.3.1** (200 mg, 0.76 mmol) in CH_2Cl_2 (7.6 mL, 0.1 M) was added *N*,*N*-disopropylethylamine (795 µL, 4.56 mmol) followed by dropwise addition of chloro(methoxy)methane (172 µL, 2.28 mmol) and the reaction mixture was stirred for 12 h. After completion of reaction, it was quenched with saturated aqueous $NaHCO_3$, extracted with CH_2Cl_2, dried ($MgSO_4$), concentrated under reduced pressure. The crude product was purified using silica gel column chromatography (5% EtOAc/Hexanes), which furnished 202 mg of **4.5.3** in 80% yield as colorless viscous liquid. TLC (hexane/EtOAc 5/1): R_f = 0.32.

FTIR (neat): 3065, 2947, 2359, 1640, 1495, 1453, 1363, 1219, 1101, 1040, 990, 917, 772, 737, 698 cm^{-1};

Optical Rotation: $[\alpha]_D^{23}$ = -28.62 (*c* 0.36, $CHCl_3$);

^{1}H NMR (500 MHz, Chloroform-*d*): δ 7.36–7.28 (m, 5H, Aromatic C‑H), 5.80 (dddd *J* = 17.3, 8.6, 6.3, 2.9 Hz, 1H, $CH_2C\underline{H}=CH_2$), 5.10–5.05 (m, 2H, $CH_2CH=C\underline{H_a}\underline{H_b}$), 4.82 (dq, *J* = 13.1, 6.8 Hz, 1H, $CH(OC\underline{H_a}H_bOCH_3)$), 4.85–4.77 (m, 1H, $CH(OCH_a\underline{H_b}OCH_3)$), 4.69–4.63 (m, 2H, $CH(OC\underline{H_a}\underline{H_b}OCH_3)$), 4.50 (s, 2H, $PhC\underline{H_2}OCH_2$), 3.81 (ddt, *J* = 14.1, 9.0, 5.1, 3.6 Hz, 1H, $C\underline{H}(OMOM)CH_2CH(OMOM)CH_2$), 3.73 (tdd, *J* = 14.0, 9.0, 5.2, 3.3 Hz, 1H, $CH(OMOM)CH_2C\underline{H}(OMOM)CH_2$), 3.47 (td, *J* = 6.3, 2.9 Hz, 2H, $BnOC\underline{H_2}CH_2$), 3.39–3.34 (m, 6H, 2 X $CH(OCH_2OC\underline{H_3})$), 2.33 (dddt, *J* = 7.0, 5.7, 3.0, 1.5 Hz, 2H, $CH(OH)C\underline{H_2}CH=CH_2$), 1.70–1.55 (m, 6H, $CH(OMOM)C\underline{H_2}CH(OMOM)CH_2$, BnOCH2C<u>H</u>2C<u>H</u>2);

^{13}C NMR (126 MHz, CDCl3): δ 138.7 (C_{Ar}), 134.6 (<u>C</u>H=CH_2), 128.6 (2, <u>C</u>H_{Ar}), 127.7 (2, <u>C</u>H_{Ar}), 127.6 (<u>C</u>H_{Ar}), 117.6 (CH=<u>C</u>H_2), 96.2 (CH_2), 93.3 (CH_2), 91.0 (CH_2), 75.1 (CH), 74.8 (CH), 73.0 (CH_2), 70.5 (CH_2), 55.8 (2, <u>C</u>H_3), 40.3 (CH_2), 39.9 (CH_2), 31.9 (CH_2), 25.3 (CH_2);

HRMS (ESI-TOF) m/z: $[M + Na]^+$ Calcd for $C_{20}H_{32}O_5Na$ 375.2147; Found 375.2157.

(1*R*,6*R*,8*S*)-8-((3*R*,4*S*,6*R*)-9-(benzyloxy)-4-hydroxy-3-methyl-6-((triisopropylsilyl) oxy)nonyl)-2,9,10-trioxa-1-phosphabicyclo[4.3.1]dec-4-ene 1-oxide (4.6.1)

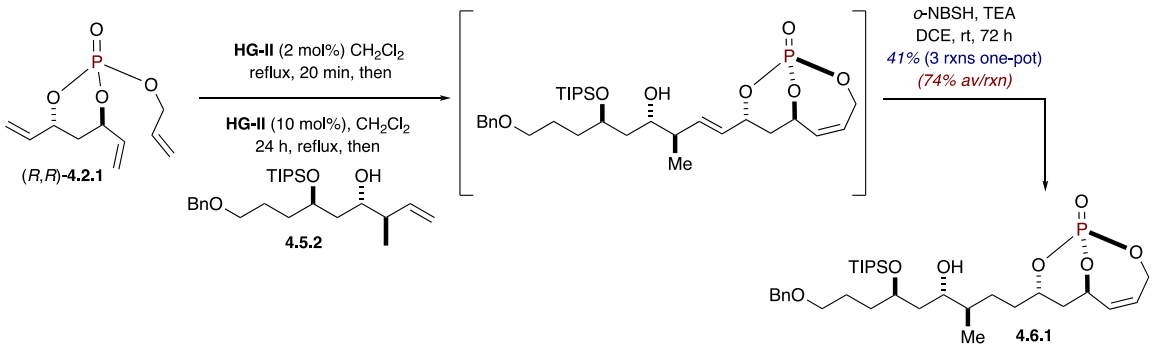

To a solution of (*R*,*R*)-triene **4.2.1** (100 mg, 0.43 mmol) in a degassed CH_2Cl_2 (100 mL, 0.005 M) was added **HG-II** (5.9 mg, 0.034 mmol, 2 mol%) the reaction mixture was refluxed in an oil bath for 20 minutes. After completion of RCM reaction, CH_2Cl_2 was evaporated under reduced pressure. To the crude product was added freshly distilled, freeze-degas-thawed 1,2-DCE (4.9 mL, 0.1 M), the CM partner **4.5.2** (282 mg, 0.59 mmol) and HG-II (18 mg, 0.03 mmol, 6 mol%) under inert atmosphere. The reaction mixture was stirred at 70 ºC in an oil bath for 12 h, a second portion of HG-II (6 mg, 0.01 mmol, 2 mol%) and CM partner (47 mg, 0.34 mmol) were added to the reaction mixture, was stirred at 70 ºC for 8 h and a third portion of HG-II (6 mg, 0.01 mmol, 2 mol%) and CM partner (47 mg, 0.34 mmol) were added and the reaction mixture was stirred for an additional 8 h. After completion of CM reaction, the crude product was subjected to chemoselective hydrogenation "H_2" reaction using *o*-NBSH and Et_3N (2 mL/1 g of *o*-NBSH) at room temperature. It should be noted that for the chemoselective hydrogenation of external olefin of the crude CM product, *o*-NBSH (0.54 g, 2.4 mmol) and Et_3N (1.04 mL, 2 mL/1 g of *o*-NBSH) were sequentially added after each 8–12 h and the reaction mixture was stirred for 72 h. Reaction progress was monitored via crude NMR, which confirmed the complete

reduction of external double bond in the CM adduct. The reaction mixture was diluted with EtOAc (30 mL) followed by addition of saturated aqueous solution of $NaHCO_3$ (15 mL). The organic layer was separated, and aqueous phase was extracted with EtOAc (3 x 30 mL). The combined organic layers were washed with brine (15 mL), dried (Na_2SO_4), concentrated under reduced pressure, and purified with flash chromatography (40% EtOAc/Hexane), which furnished 59 mg of bicyclic phosphate **4.6.1** as a colorless oil in 41% yield over three reactions in one-pot (75% av/rxn). TLC (EtOAc): $R_f = 0.55$.

FTIR (neat): 2945, 2864, 2351, 1556, 1305, 1245, 1101, 1039, 972, 773 cm^{-1};

Optical Rotation: $[a]_D^{23} = -21.7$ (c 0.17, $CHCl_3$);

^{1}H NMR (500 MHz, Chloroform-*d*): δ 7.35–7.27 (m, 5H, Aromatic C‑H), 6.04 (td, J = 12.0, 9.1, 8.1 Hz, 1H, CHO(P)CH=C<u>H</u>CH$_a$H$_b$), 5.58 (dd, J = 12.0, 2.4 Hz, 1H, CHO(P)C<u>H</u>=CHCH$_a$H$_b$), 5.17 (d, J = 24.8 Hz, 1H, C<u>H</u>O(P)CH=CHCH$_a$H$_b$), 5.08–4.93 (m, 1H, CHO(P)CH=CHC<u>H</u>$_a$H$_b$), 4.66–4.54 (m, 1H, C<u>H</u>O(P)CH$_a$H$_b$CHO(P)), 4.51 (s, 2H, PhC<u>H</u>$_2$OCH$_2$), 4.35 (ddd, J = 28.0, 14.8, 6.6 Hz, 1H, CHO(P)CH=CHCH$_a$<u>H</u>$_b$), 3.97 (tt, J = 8.1, 5.1 Hz, 1H, C<u>H</u>(OTIPS)CH$_2$CH(OH)), 3.52 (t, J = 7.3 Hz, 2H, PhCH$_2$OC<u>H</u>$_2$), 3.60–3.45 (m, 1H, CH(OTIPS)CH$_2$C<u>H</u>(OH)), 2.21–2.11 (m, 1H BnOCH$_2$C<u>H</u>$_a$H$_b$), 1.77–1.47 (m, 12H, BnOCH$_2$CH$_a$<u>H</u>$_b$C<u>H</u>$_2$CH(OTIPS)C<u>H</u>$_2$CH(OH)C<u>H</u>(Me)C<u>H</u>$_2$C<u>H</u>$_2$CH(OP)C<u>H</u>$_2$), 1.05 (d, J = 6.0 Hz, 21H, Si(CH(C<u>H</u>$_3$)$_2$)$_3$), 0.86 (d, J = 7.7 Hz, 3H, CH(C<u>H</u>$_3$)CH$_2$CH$_2$);

^{13}C NMR (126 MHz, $CDCl_3$): 138.7 (C_{Ar}), 130.1 (<u>C</u>H=CHCH$_2$), 128.5(2, CH_{Ar}), 128.1(CH_{Ar}), 127.8(2, <u>C</u>H$_{Ar}$), 127.7(<u>C</u>H=CHCH$_2$), 77. 3 (CH, J_{CP} = 4.5 Hz), 77.0 (CH, J_{CP} = 5.1 Hz), 75.7 (CH), 73.2 (CH_2), 71.6 (CH), 70.1 (CH_2), 63.1 (CH_2), 35.2 (CH_2),

35.0 (CH), 32.9 (CH_2), 32.0 (CH_2), 29.7 [6C, Si (CH ($\underline{C}H_3)_2)_3$], 28.9 (CH_2), 27.5 (CH_2), 26.0 (CH_2), 15.4 (CH_3), 14.3 [3C, Si ($\underline{C}H$ ($CH_3)_2)_3$];

^{31}P NMR (162 MHz, $CDCl_3$): δ -3.85;

HRMS (ESI-TOF) m/z: $[M + Na]^+$ Calcd for $C_{32}H_{55}O_7PSiNa$ 633.3352; Found 633.3368.

(4*S*,6*S*,9*R*,10*S*,12*R*)-15-(benzyloxy)-9-methylpentadec-1-ene-4,6,10,12-tetraol (4.6.2)

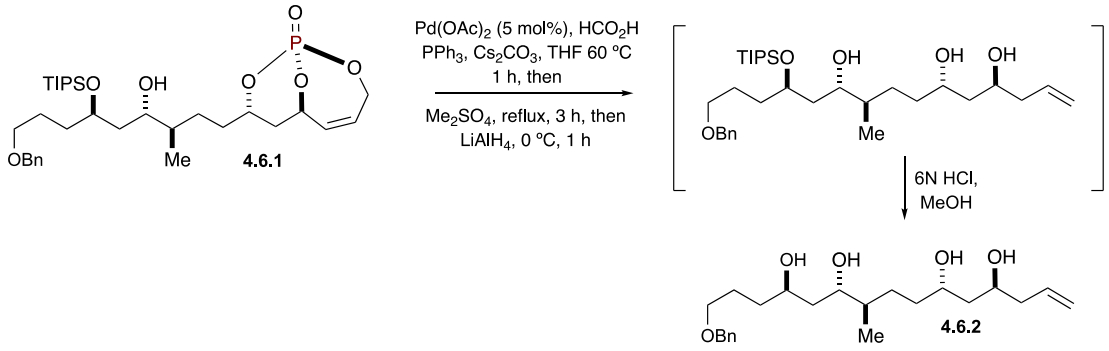

To a stirring solution of bicyclic phosphate **4.6.1** (40 mg, 0.061 mmol) in THF (0.2 mL, 0.3 M) under argon was added Cs_2CO_3 (101mg, 0.31 mmol) and HCO_2H (6.2 µL, 0.16 mmol). Next, a solution of $Pd(OAc)_2$ (1.1 mg, 0.003 mmol, 5 mol%) and PPh_3 (1.56 mg, 0.048 mmol) in THF (0.21 mL) under argon was immediately transferred *via* cannula to the reaction mixture. The reaction mixture was stirred at 60 ºC in an oil bath for 1 h (monitored by TLC). After 1 h, all starting materials were consumed and the color of reaction mixture turned black. After the reaction was complete, Me_2SO_4 was added, and the reaction mixture was refluxed for 3 h (TLC showed that phosphate acid was methylated completely). The reaction mixture was cooled to 0 ºC, then $LiAlH_4$ (53 mg, 1.44 mmol) was added portion-wise. Next, the reaction mixture was stirred at 0 ºC for 1 h. After the completion of reduction, it was quenched following the Fieser workup[7] *via* slow sequential addition of H_2O (1 mL/g of $LiAlH_4$), followed by 10% NaOH (1 mL/g of $LiAlH_4$) and finally H_2O (3 mL/g of $LiAlH_4$) and the ice bath was removed and the reaction mixture was stirred for 2 h. The reaction mixture was filtered, extracted with EtOAc (3 x 50 mL)

[7]. L. F. Fieser, M. Fieser in *Reagents for Organic Synthesis*, *Vol. 1,* Wiley: New York, **1967**, pp. 581−595; b) V. M. Mićović, M. Mihailović, *J. Org. Chem.* **1953**, *18*, 1190–1200.

and dried (Na_2SO_4). The resulting solution was filtered again, concentrated and the crude compound was utilized for the next step without further purification.

The crude compound from the previous step was dissolved in MeOH (0.2 mL) and treated with 6 N HCl (50 μL). The reaction was stirred for 4 h at room temperature. Upon completion (monitored by TLC), reaction was concentrated under reduced pressure and the residue was re-dissolved in EtOAc. The layers were separated, and the aqueous phase was extracted three times with EtOAc (3 x 10 mL). The organic layers were combined and dried with anhydrous Na_2SO_4. The resulting solution was filtered again, concentrated and the crude compound was purified using a short silica gel flash column chromatography (EtOAc/ MeOH 20:1), which afforded tetrol **4.6.2** (10.2 mg, 30% yield over 4 reactions). TLC (EtOAc/ MeOH 10:1): $R_f = 0.18$.

FTIR (neat): 3347, 2929, 1758,1454, 1241, 1099, 1026, 702, 698, 666 cm^{-1};

Optical Rotation: $[\alpha]_D^{23}$ = -4.3 (*c* 0.17, $CHCl_3$);

^{1}H NMR (500 MHz, $CDCl_3$): δ 7.36–7.27 (m, 5H, Aromatic C–H), 5.81 (ddt, *J* = 16.4, 10.6, 7.2 Hz, 1H, $CH_2C\underline{H}=CH_2$), 5.15–5.11 (m, 2H, $CH_2CH=C\underline{H}_2$), 4.52 (d, *J* = 1.5 Hz, 2H, $PhC\underline{H}_2OCH_2CH_2$), 3.98 (p, *J* = 6.1 Hz, 1H, $CH_2C\underline{H}(OH)CH_2CH=CH_2$), 3.95–3.87 (m, 2H, $BnOCH_2CH_2CH_2C\underline{H}(OH)$, $BnOCH_2CH_2CH_2CH(OH)CH_2C\underline{H}(OH)$), 3.72 (ddd, *J* = 9.0, 6.7, 2.9 Hz, 1H, $C\underline{H}(OH)CH_2CH(OH)CH_2CH=CH_2$), 3.52 (qt, *J* = 9.3, 5.9 Hz, 2H, $BnOC\underline{H}_2CH_2$), 2.26 (tt, *J* = 5.7, 1.4 Hz, 2H, $CH(OH)C\underline{H}_2CH=CH_2$), 1.76–1.70 (m, 2H, $BnOCH_2C\underline{H}_2CH_aH_b$), 1.70–1.65 (m, 1H, $BnOCH_2CH_2C\underline{H}_aH_b$), 1.62–1.52 (m, 7H, $CH(OH)C\underline{H}(CH_3)C\underline{H}_2C\underline{H}_2C\underline{H}_2CH(OH)CH_2CH=CH_2$), 1.50–1.40 (m, 2H, $C\underline{H}_2CH(OH)CH(CH_3)$), 1.20–1.12 (m, 1H, $BnOCH_2CH_2CH_a\underline{H}_b$), 0.87 (d, *J* = 6.8 Hz, 3H, $CH(C\underline{H}_3)CH_2$);

^{13}C NMR (126 MHz, $CDCl_3$): δ 138.0 (C_{Ar}), 134.9 (<u>C</u>H=CH_2), 128.6 (2, CH_{Ar}), 128.0 (2, CH_{Ar}), 127.9 (CH_{Ar}), 118.2 (CH=<u>C</u>H_2), 73.3 (CH_2), 73.0 (CH), 70.7 (CH), 69.8 (CH), 69.5 (CH), 68.4 (CH), 42.2 (CH_2), 42.0 (CH_2), 39.1 (CH_2), 39.0 (CH), 35.1 (CH_2), 35.0 (CH_2), 28.7 (CH_2), 26.8 (CH_2), 15.7 (CH_3);

HRMS (ESI-TOF) m/z: $[M + Na]^+$ Calcd for $C_{23}H_{38}O_5Na$ 417.2617; Found 417.2629.

(3*S*,4*R*,6*S*,9*R*,10*S*,12*R*)-15-(benzyloxy)-3,9-dimethylpentadec-1-ene-4,6,10,12-tetraol (4.6.3)

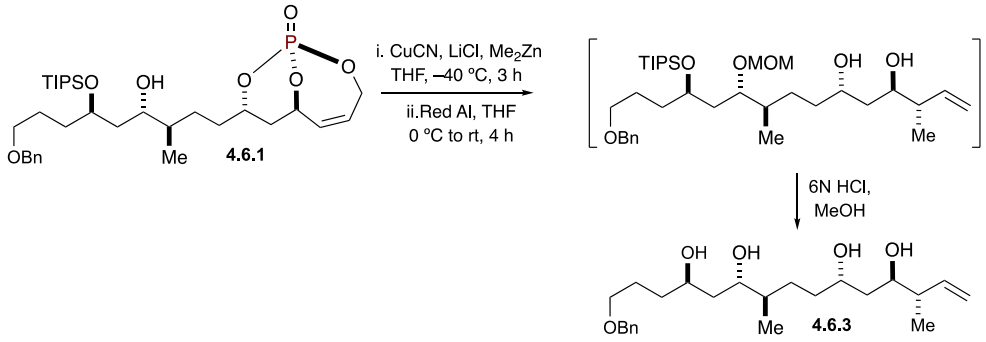

To a flame dried round bottom-flask was added CuCN (20.3mg, 0.22 mmol) and LiCl (22.2 mg, 0.52 mmol) inside the glove box, followed by addition of dry THF (0.7 mL, 0.05 M) under argon and the reaction mixture was stirred at room temperature for 15 minutes. A pale green coloration was observed. The reaction mixture was cooled to -40 ºC followed by slow addition of a 1 M solution of Me_2Zn in THF (0.22 mL, 0.22 mmol). The reaction mixture was stirred for 40 minutes at -30 ºC and a solution of bicyclic phosphate **4.6.1** (50 mg, 0.076 mmol) in dry THF (0.7 mL, 0.05 M) was added dropwise via cannula to the reaction mixture. The reaction was slowly warmed to room temperature and allowed to stir for 3 h. Upon completion of reaction (monitored via TLC), the reaction mixture was quenched with saturated aqueous ammonium chloride (NH_4Cl, 0.3 mL), stirred for 15 minutes followed by the addition of anhydrous Na_2SO_4 (14 mg) stirred for another 30 minutes. The crude product was filtered through Celite pad and washed with excess EtOAc (3 x 4 mL), the filtrate was concentrated under reduce pressure, which afforded the crude acid as yellowish viscous oil, which was proceeded to the next reaction without further purification.

To a flask containing the crude acid was added THF (0.95 mL, 0.08 M). The reaction mixture was cooled to 0 ºC and was added 70% solution of Red-Al in toluene (1.5

mL, 5 mmol). The reaction mixture was brought to room temperature and stirred for 4 h. After completion of reaction (monitored by TLC), it was quenched with NH_4Cl (sat. aq.) and was added (Na_2SO_4), stirred for 30 minutes, filtered through Celite pad. The residue was washed with EtOAc (3 x 4 mL). The organic layer was dried (Na_2SO_4) and the solvent was evaporated under reduced pressure. The resulting solution was filtered again, concentrated and the crude compound was utilized for the next step without further purification.

The crude compound from the previous step was dissolved in MeOH (0.2 mL) and treated with 6 N HCl (aq., 40 μL). The reaction was stirred for 4 h at room temperature. Upon completion (monitored by TLC), reaction was concentrated under reduced pressure and the residue was re-dissolved in EtOAc. The layers were separated, and the aqueous phase was extracted three times with EtOAc. The organic layers were combined and dried with anhydrous Na_2SO_4. The resulting solution was filtered again, concentrated and the crude compound was purified using a short silica gel flash column chromatography (hexane/EtOAc 3:1), which afforded tetrol **4.6.3** (12.2 mg, 28% yield over 4 reactions). TLC (EtOAc/ MeOH 10:1): $R_f = 0.1$.

FTIR (neat): 3353, 2930, 1758, 1454, 1364, 1241, 1099, 1026, 783, 698, 665 cm^{-1};

Optical Rotation: $[a]_D^{23}$ = -1.68 (*c* 0.16, $CHCl_3$);

^{1}H NMR (500 MHz, Chloroform-*d*): δ 7.37–7.28 (m, 5H, Aromatic C–H), 5.74 (dt, *J* = 19.1, 9.5, 8.6 Hz, 1H, $CH(CH_3)C\underline{H}=CH_2$), 5.15–5.10 (m, 2H, $CH(CH_3)CH=C\underline{H}_a\underline{H}_b$), 4.52 (d, *J* = 1.8 Hz, 2H, $PhC\underline{H}_2OCH_2CH_2$), 3.93–3.87 (m, 2H, $C\underline{H}(OH)CH_2CH(OH)CH(CH_3)CH_2$, $C\underline{H}(OH)CH_2CH(OH)CH(CH_3)$ $CH=CH_2$), 3.77–3.68 (m, 2H, $CH(OH)CH_2C\underline{H}(OH)CH(CH_3)CH_2$, $CH_2C\underline{H}(OH)CH(CH_3)CH=CH_2$), 3.53 (qt, *J*

= 9.3, 5.8 Hz, 2H, BnOC$\underline{H}_2CH_2$), 2.24 (dq, *J* = 15.0, 8.0, 6.5 Hz, 1H, CH(OH)C$\underline{H}$(CH_3)CH=CH_2), 1.74 (p, *J* = 6.5 Hz, 2H, BnOC$H_2C\underline{H}_2$), 1.66–1.53 (m, 8H, CH(OH)C$\underline{H}_2$CH(OH)CH(CH_3)C$\underline{H}_2$, C$\underline{H}_2$CH(OH)C$\underline{H}_2$CH(OH)CH(CH_3)CH=CH_2), 1.49 (tdd, *J* =8.0, 6.6, 3.8 Hz, 1H, BnOC$H_2CH_2C\underline{H}_aH_b$), 1.18 (dddd, *J* =13.2, 10.5, 8.2, 5.3 Hz, 1H, BnOC$H_2CH_2CH_a\underline{H}_b$), 1.02 (d, *J* = 6.8 Hz, 3H, CH(OH)CH(C$\underline{H}_3$)CH=CH_2), 0.88 (d, *J* = 6.8 Hz, 3H, CH(C$\underline{H}_3$)CH_2CH_2CH(OH));

^{13}C NMR (126 MHz, $CDCl_3$): δ 140.6 (C$\underline{H}$=CH_2), 138.0 (C_{Ar}), 128.6 (2, CH_{Ar}), 128.0 (2, CH_{Ar}), 127.9 (CH_{Ar}), 116.8 (CH=C$\underline{H}_2$), 73.3 (CH_2), 73.0 (CH), 72.1 (CH), 70.8 (CH_2), 69.8 (CH), 69.7 (CH), 44.6 (CH), 39.4 (CH_2), 39.1 (CH_2), 39.0 (CH_2), 35.2 (CH_2), 34.9 (CH_2), 28.7 (CH_2), 26.9 (CH_2), 16.2 (CH_3), 15.5 (CH_3);

HRMS (ESI-TOF) m/z: $[M + Na]^+$ Calcd for $C_{24}H_{40}O_5Na$ 431.2773; Found 431.2758.

.

(1*R*,6*R*,8*S*)-8-((3*R*,4*S*,6*R*)-9-(benzyloxy)-4-(methoxymethoxy)-3-methyl-6-((triiso-propylsilyl)oxy)nonyl)-2,9,10-trioxa-1-phosphabicyclo[4.3.1]dec-4-ene 1-oxide(4.7.1):

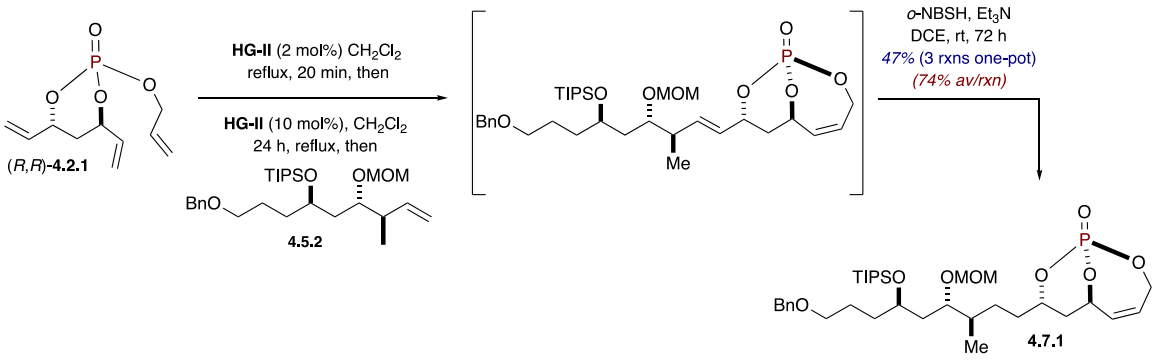

To a solution of (*R*,*R*)-triene (*R,R*)-**4.2.1** (394 mg, 1.7 mmol) in a degassed CH_2Cl_2 (347 mL, 0.005 M) was added **HG-II** (21.2 mg, 0.034 mmol, 2 mol%) the reaction mixture was refluxed in an oil bath for 20 minutes. After completion of RCM reaction, CH_2Cl_2 was evaporated under reduced pressure. To the crude product was added freshly distilled, freeze-degas-thawed 1,2-DCE (17 mL, 0.1 M), the CM partner **4.5.2** (975 mg, 2.04 mmol) and HG-II (63 mg, 0.102 mmol, 6 mol%) under inert atmosphere. The reaction mixture was stirred at 70 ºC in an oil bath for 12 h, a second portion of HG-II (21 mg, 0.034 mmol, 2 mol%) and CM partner (162 mg, 0.34 mmol) were added to the reaction mixture, was stirred at 70 ºC for 8 h and a third portion of HG-II (21 mg, 0.034 mmol, 2 mol%) and CM partner (162 mg, 0.34 mmol) were added and the reaction mixture was stirred for an additional 8 h. After completion of CM reaction, the crude product was subjected to chemoselective hydrogenation "H_2" reaction using *o*-NBSH and Et_3N (2 mL/1 g of *o*-NBSH) at room temperature. It should be noted that for the chemoselective hydrogenation of external olefin of the crude CM product, *o*-NBSH (1.8 g, 8.5 mmol) and Et_3N (3.6 mL, 2 mL/1 g of *o*-NBSH) were sequentially added after each 8–12 h and the reaction mixture was stirred for 72 h. Reaction progress was monitored via crude NMR, which confirmed

the complete reduction of external double bond in the CM adduct. The reaction mixture was diluted with EtOAc (100 mL) followed by addition of saturated aqueous solution of $NaHCO_3$ (50 mL). The organic layer was separated, and aqueous phase was extracted with EtOAc (3 x 100 mL). The combined organic layers were washed with brine (50 mL), dried (Na_2SO_4), concentrated under reduced pressure, and purified with flash chromatography (40% EtOAc/Hexane), which furnished 362 mg of bicyclic phosphate **4.7.1** as a dark brown semi solid in 47% yield over three reactions in one-pot (74% av/rxn). (hexane/EtOAc 1/1): $R_f = 0.12$.

FTIR (neat): 2945, 2864, 2351, 1556, 1305, 1245, 1101, 1039, 972, 773 cm^{-1}; **Optical Rotation**: $[\alpha]_D^{23}$ = -24.3 (*c* 0.63, $CHCl_3$);

^{1}H NMR (500 MHz, Chloroform-*d*): δ 7.35–7.27 (m, 5H, Aromatic C‑H), 6.02 (dddd, *J* = 11.9, 6.7, 3.2, 2.1 Hz, 1H, CHO(P)CH=C<u>H</u>-CH_aH_b), 5.57 (ddd, *J* = 12.0, 6.2, 2.4 Hz , 1H, CHO(P)C<u>H</u>=CHCH_aH_b), 5.17 (ddq, *J* = 24.4, 6.3, 2.0 Hz, 1H, C<u>H</u>O(P)CH=CHCH_aH_b), 5.00 (ddt, *J* = 14.7, 5.6, 2.8 Hz, 1H, CHO(P)CH=CHC<u>H</u>$_aH_b$), 4.64 (q, *J* = 6.9 Hz, 2H, CH_2CH(OC<u>H</u>$_2$$OCH_3$)CH(Me)), 4.57–4.51 (m, 1H, C<u>H</u>O(P)CH_aH_bCHO(P)), 4.50 (s, 2H, PhC<u>H</u>$_2$$OCH_2$), 4.35 (ddd, *J* = 27.7, 14.8, 6.7 Hz, 1H, CHO(P)CH=CHCH_a<u>H</u>$_b$), 3.97 (tt, *J* = 7.1, 3.3 Hz, 1H, C<u>H</u>(OTIPS)CH_2CH(OMOM)), 3.63 (dt, *J* = 8.9, 3.1 Hz, 1H, CH(OTIPS)CH_2C<u>H</u>(OMOM)), 3.47 (tq, *J* = 4.7, 2.9 Hz, 2H, PhCH_2OC<u>H</u>$_2$), 3.36–3.34 (m, 3H, CH_2CH(OCH_2OC<u>H</u>$_3$)CH(Me)), 2.19–2.11 (ddd, *J* = 20.4, 8.4, 3.2 Hz, 1H, CHO(P)C<u>H</u>$_a$$H_b$CHO(P)), 1.83–1.75 (m, 1H, CH(OMOM)C<u>H</u>(CH_3)CH_2CH_2), 1.72–1.49 (m, 9H, Ph$CH_2$$OCH_2$C<u>H</u>$_2$C<u>H</u>$_2$, CH(OTIPS)$CH_a$<u>H</u>$_b$CH(OMOM), CH($CH_3$)$CH_a$<u>H</u>$_b$C<u>H</u>$_2$, CHO(P)$CH_a$<u>H</u>$_b$CHO(P)), 1.41 (ddd, *J* = 14.2, 8.2, 2.8 Hz, 1H,

CH(OTIPS)C$\underline{H}_a$$H_b$CH(OMOM)), 1.19–1.11 (m, 1H, CH(OMOM)CH(CH_3)C$\underline{H}_a$$H_b$$CH_2$), 1.05 (d, J = 6.0 Hz, 21H, (Si(C$\underline{H}$($C\underline{H}_3$)$_2$)$_3$), 0.89 (d, J = 6.8 Hz, 3H, CH($C\underline{H}_3$)CH_2CH_2);

^{13}C NMR (126 MHz, $CDCl_3$)**:** δ 138.8 (C_{Ar}), 130.0 ($\underline{C}$H=$CHCH_2$), 128.5 (2, CH_{Ar}), 128.1 ($\underline{C}H_{Ar}$), 127.7 (2, $\underline{C}H_{Ar}$), 127.4 ($\underline{C}$H=$CHCH_2$), 97.0 (CH_2), 80.3 (CH), 76.9 (CH, J_{CP} = 4.7 Hz), 76.7 (CH), 76.4 (CH, J_{CP} = 4.7 Hz), 72.9 (CH_2), 70.1(CH), 63.0 (CH_2), 55.7 (CH_3), 37.9 (CH_2), 36.6 (CH), 34.8 (CH_2), 33.8 (CH_2), 27.7 (CH_2), 25.2 (CH_2), 18.4 [6C, Si (CH ($\underline{C}H_3$)$_2$)$_3$], 14.5 (CH_3), 13.1 [3C, Si ($\underline{C}$H (CH_3)$_2$)$_3$];

^{31}P NMR (202 MHz, $CDCl_3$): δ -3.84;

HRMS (ESI-TOF) m/z: $[M + Na]^+$ Calcd for $C_{34}H_{59}O_8PSiNa$ 677.3615; Found 677.3615;

(1*R*,6*R*,8*S*)-8-((4*R*,6*R*)-9-(benzyloxy)-4,6-bis(methoxymethoxy)nonyl)-2,9,10-trioxa-1-phosphabicyclo[4.3.1]dec-4-ene 1-oxide (4.7.2)

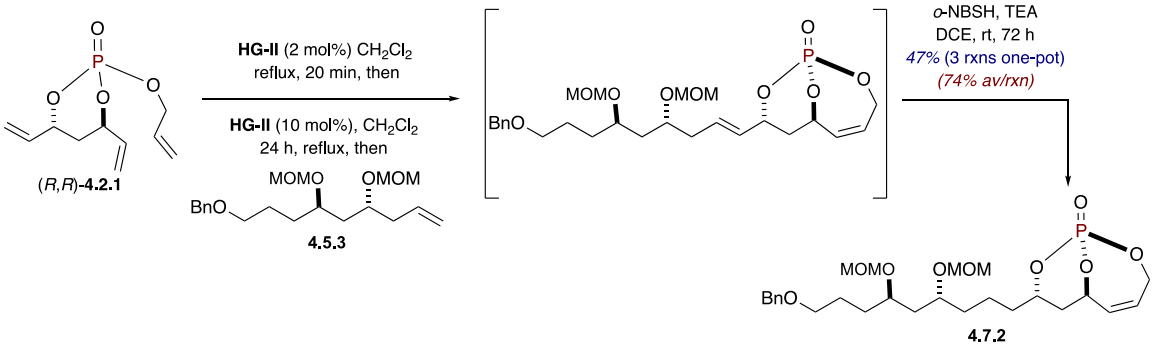

To a solution of (*R*,*R*)-triene (*R,R*)-**4.2.1** (80 mg, 0.34 mmol) in a degassed CH_2Cl_2 (79 mL, 0.005 M) was added **HG-II** (4.4 mg, 0.007 mmol, 2 mol%) the reaction mixture was refluxed in an oil bath for 20 minutes. After completion of RCM reaction, CH_2Cl_2 was evaporated under reduced pressure. To the crude product was added freshly distilled, freeze-degas-thawed 1,2-DCE (3.4 mL, 0.1 M), the cross metathesis (CM) partner **4.5.3** (152 mg, 0.44 mmol) and HG-II (13.2 mg, 0.02 mmol, 6 mol%) under argon. The reaction mixture was stirred at 70 ºC in an oil bath for 5 h and a second portion of **HG-II** (8.8 mg, 0.014 mmol, 4 mol%) and CM partner (76 mg, 0.22 mmol) were added to the reaction mixture, and was stirred at 70 ºC for an additional 3 h (monitored by TLC). After completion of CM reaction, the reaction mixture was brought to room temperature and was added *o*-nitrobenzenesulfonyl hydrazine (o-NBSH) (0.72 g, 3.4 mmol) and Et_3N (1.5 mL, at 2 mL/g of *o*-NBSH), the reaction mixture was stirred for 12 h (Note: The reaction flask was wrapped with aluminum foil in order to avoid decomposition of *o*-NBSH due to light). A second portion of *o*-NBSH (0.36 g, 1.7 mmol) and Et_3N (0.72 mL, at 2 mL/g of o-NBSH) were added and the reaction mixture was stirred for an additional 8 h at room temperature. Reaction progress was monitored via crude NMR, which confirmed the complete reduction

of the external double bond in the CM adduct. The reaction mixture was diluted with EtOAc (30 mL) followed by addition of saturated aqueous solution of $NaHCO_3$ (20 mL). The organic layer was separated, and aqueous phase was extracted with EtOAc (3 x 20 mL). The combined organic layers were washed with brine (10 mL), dried (Na_2SO_4), concentrated under reduced pressure, and purified with flash chromatography (25% EtOAc/CH_2Cl_2), which furnished 94 mg of bicyclic phosphate **4.7.2** as a colorless oil in 47% yield over three reactions in one-pot (81% av/rxn). TLC (EtOAc): $R_f = 0.42$.

FTIR (neat): 2929, 2852, 2356, 1470, 1298, 1009, 1506, 1068, 972, 885, 773 cm^{-1}; **Optical Rotation:** $[a]_D^{23}$ = - 39.5 (*c* 0.22, $CHCl_3$);

^{1}H NMR (500 MHz, Chloroform-*d*): δ 7.35–7.27 (m, 5H, Aromatic C‑H), 6.02 (ddd, *J* = 11.8, 6.1, 2.6 Hz, 1H, CHO(P)CH=C<u>H</u>CH$_a$H$_b$), 5.57 (dt, *J* = 12.1, 3.2 Hz, 1H, CHO(P)C<u>H</u>=CHCH$_a$H$_b$), 5.17 (dqd, *J* = 23.8, 3.4 Hz, 1H, C<u>H</u>O(P)CH=CHCH$_a$H$_b$), 5.00 (dt, *J* = 14.5, 6.0, 3.1 Hz, 1H, CHO(P)CH=CHC<u>H</u>$_a$H$_b$), 4.73–4.60 (m, 4H, 2 X CH(OC<u>H</u>$_2$OCH$_3$)), 4.59–4.53 (m, 1H, C<u>H</u>O(P)CH$_a$H$_b$CHO(P)), 4.50 (s, 2H, PhC<u>H</u>$_2$OCH$_2$), 4.35 (ddd, *J* = 27.7, 14.8, 6.3 Hz, 1H, CHO(P)CH=CHCH$_a$<u>H</u>$_b$)), 3.70 (dq, *J* = 8.0, 4.1 Hz, 2H, C<u>H</u>(OMOM)CH$_2$C<u>H</u>(OMOM)), 3.48 (t, *J* = 6.2 Hz, 2H, PhCH$_2$OC<u>H</u>$_2$), 3.37 (s, 6H, 2 X CH(OCH$_2$OC<u>H</u>$_3$)), 2.16 (ddd, *J* = 14.6, 11.8, 6.2 Hz, 1H, CHO(P)C<u>H</u>$_a$H$_b$CHO(P)), 1.80–1.50 (m, 13H, CH(OMOM)C<u>H</u>$_2$C<u>H</u>$_2$C<u>H</u>$_2$, PhCH$_2$OCH$_2$C<u>H</u>$_2$C<u>H</u>$_2$, CH(OMOM)C<u>H</u>$_a$<u>H</u>$_b$CH(OMOM), CHO(P)CH$_a$<u>H</u>$_b$CHO(P));

^{13}C NMR (126 MHz, $CDCl_3$): δ 138.6 (C_{Ar}), 129.9 (<u>C</u>H=CHCH$_2$), 128.4 (2, CH_{Ar}), 128.0 (<u>C</u>H=CHCH$_2$), 127.6 (2, <u>C</u>H$_{Ar}$), 127.5 (CH_{Ar}), 96.2 (CH_2), 96.0 (CH_2), 77.2 (CH, J_{CP} = 7.1 Hz), 76.5 (CH, J_{CP} = 6.6 Hz), 75.0 (CH), 75.1(CH), 72.9 (CH_2), 70.4 (CH_2), 62.9 (CH_2),

55.7 (2, CH_3), 40.3 (CH_2), 35.8 (CH_2), 34.8 (CH_2), 34.7 (CH_2), 31.7 (CH_2), 25.2 (CH_2), 20.0 (CH_2);

^{31}P NMR (202 MHz, $CDCl_3$): δ -3.76;

HRMS (ESI-TOF) m/z: $[M + Na]^+$ Calcd for $C_{26}H_{41}O_9PNa$ 551.2386; Found 551.2398;

(4*R*,6*S*,7*R*,10*S*,12*R*,13*S*)-6-(methoxymethoxy)-7-methyl-4-((triisopropylsilyl)oxy)-13-vinylnonadecane-1,10,12-triol (4.7.3)

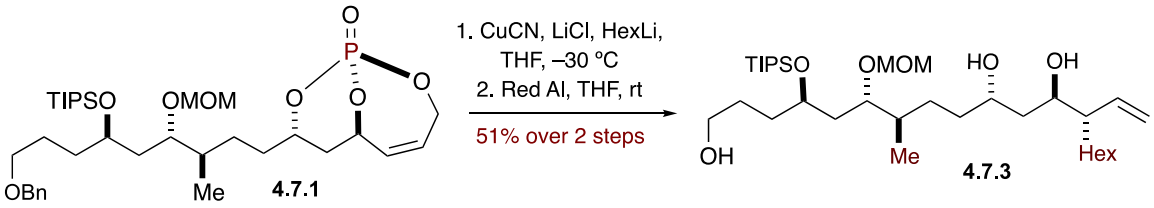

To a flame dried round bottom-flask was added CuCN (40 mg, 3.2 mmol) and LiCl (317 mg, 7.5 mmol) inside the glove box, followed by addition of dry THF (10 mL, 0.05 M) under argon and the reaction mixture was stirred at room temperature for 15 minutes. A pale green coloration was observed. The reaction mixture was cooled to -40 ºC followed by slow addition of a 1.2 M solution of HexLi in THF (3.2 mL, 3.2 mmol). The reaction mixture was stirred for 40 minutes at -30 ºC and a solution of bicyclic phosphate **4.7.1** (350 mg, 1.08 mmol) in dry THF (10 mL, 0.05 M) was added dropwise via cannula to the reaction mixture. The reaction was slowly warmed to room temperature and allowed to stir for 3 h. Upon completion of reaction (monitored via TLC), the reaction mixture was quenched with saturated aqueous ammonium chloride (NH_4Cl, 2 mL), stirred for 15 minutes followed by the addition of anhydrous Na_2SO_4 (200 mg) stirred for another 30 minutes. The crude product was filtered through Celite pad and washed with excess EtOAc (3 x 50 mL), the filtrate was concentrated under reduce pressure, which afforded the crude acid as yellowish viscous oil, which was proceeded to the next reaction without further purification.

To a flask containing the crude acid was added THF (13.5 mL, 0.08 M). The reaction mixture was cooled to 0 ºC and was added 70% solution of Red-Al in toluene (1.5 mL, 5 mmol). The reaction mixture was brought to room temperature and stirred for 12 h.

After completion of reaction (monitored by TLC), it was quenched with NH_4Cl (sat. aq.) and was added (Na_2SO_4), stirred for 30 minutes, filtered through Celite pad. The residue was washed with EtOAc (3 x 50 mL). The organic layer was dried (Na_2SO_4) and the solvent was evaporated under reduced pressure. The resulting solution was filtered again, concentrated and the crude compound was purified by flash chromatography to obtain 17 mg of triol **4.7.3** as a yellow oil in 51% yield over 2 steps. TLC (hexane/EtOAc 1:2): R_f = 0.37.

FTIR (neat): 3458, 2943, 2866, 1718, 1699, 1456, 1390, 1097, 1027, 912, 842, 736, 697 cm^{-1};

Optical Rotation: $[\alpha]_D^{23}$ = -8.24 (*c* 0.18, $CHCl_3$);

^{1}H NMR (500 MHz, Chloroform-*d*): δ 5.61 (ddt, *J* = 17.1, 10.3, 9.3 Hz, 1H, $CH(C_6H_{13})C\underline{H}=CH_2$), 5.23–5.08 (m, 2H, $CH(C_6H_{13})CH=C\underline{H}_2$), 4.65 (dq, *J* = 8.2, 7.0 Hz, 2H, $CH(OC\underline{H}_2OCH_3)$), 4.04–3.98 (m, 1H, $CH_2C\underline{H}(OTIPS)CH_2$), 3.91–3.85 (m, 1H, $C\underline{H}(OH)CH_2CH(OH)CH(C_6H_{13})$), 3.75 (ddd, *J* = 8.1, 6.6, 3.7 Hz, 1H, $CH(OH)CH_2C\underline{H}(OH)CH(C_6H_{13})$), 3.66–3.58 (m, 3H, $CH_2C\underline{H}(OTIPS)CH_2C\underline{H}(MOM)$, $HOC\underline{H}_2CH_2$), 3.37 (s, 3H, $CH(OCH_2OC\underline{H}_3)$), 2.06–1.98 (m, 1H, $C\underline{H}(C_6H_{13})CH=CH_2$), 1.83–1.76 (m, 1H, $CH(OMOM)C\underline{H}(CH_3)$), 1.70–1.43 (m, 11H, $HOCH_2C\underline{H}_2C\underline{H}_aH_bCH(OTIPS)C\underline{H}_2$, $CH(Me)C\underline{H}_2C\underline{H}_2CH(OH)C\underline{H}_2CH(OH)$), 1.36–1.20 (m, 10H, $CH(C_5\underline{H}_{10}CH_3)CH=C\underline{H}_2$), 1.15–1.06 (m, 1H, $HOCH_2CH_2CH_a\underline{H}_bCH(OTIPS)CH_2$), 1.08–1.05 (m, 21H, $CH(OSi(C\underline{H}(C\underline{H}_3)_2)_3$), 0.92 (d, *J*= 6.8 Hz, 3H, $CH(OMOM)CH(C\underline{H}_3)$), 0.88 (t, *J*= 6.9 Hz, 3H, $CH(C_5H_{10}C\underline{H}_3)CH=C\underline{H}_2$);

^{13}C NMR (126 MHz, $CDCl_3$): δ 139.1 ($\underline{C}H=CH_2$), 118.4 ($CH=\underline{C}H_2$), 96.6 (CH_2), 80.2 (CH), 70.8 (CH), 70.2 (CH), 69.6 (CH), 63.2 (CH_2), 55.7 (CH_3), 50.9(CH), 39.8 (CH_2),

37.1(CH_2), 36.7 (CH), 35.5 (CH_2), 34.2 (CH_2), 31.8 (CH_2), 30.5 (CH_2), 29.3 (CH_2), 28.8 (CH_2), 27.8 (CH_2), 27.2 (CH_2), 22.6 (CH_2), 18.3 [6C, Si (CH ($\underline{C}H_3)_2)_3$], 14.4 (CH_3), 14.1(CH_3), 12.9 [3C, Si ($\underline{C}H$ ($CH_3)_2)_3$];

HRMS (ESI-TOF) m/z: $[M + Na]^+$ Calcd for $C_{33}H_{66}O_7SiNa$ 625.4663; Found 625.4686.

(4*S*,6*S*,10*R*,12*R*)-15-(benzyloxy)-10,12-bis(methoxymethoxy)pentadec-1-ene-4,6-diol (4.7.4)

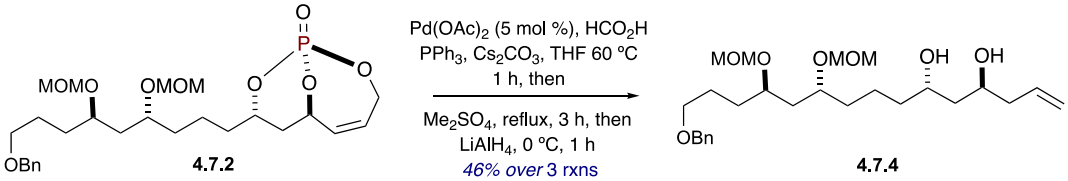

To a stirring solution of bicyclic phosphate **4.7.2** (25 mg, 0.05 mmol) in THF (1.6 mL, 0.3 M) under argon was added Cs_2CO_3 (80 mg, 0.26 mmol) and HCO_2H (0.05 µL, 1.2 mmol). Next, a solution of $Pd(OAc)_2$ (7.7 mg, 0.002 mmol, 5 mol%) and PPh_3 (12 mg, 0.048 mmol) in THF (1.6 mL) under argon was immediately transferred *via* cannula to the reaction mixture. The reaction mixture was stirred at 60 ºC in an oil bath for 1 h (monitored by TLC). After 1 h, all starting materials were consumed and the color of reaction mixture turned black. After the reaction was complete, Me_2SO_4 was added, and the reaction mixture was refluxed for 3 h (TLC showed that phosphate acid was methylated completely). The reaction mixture was cooled to 0 ºC, then $LiAlH_4$ (53 mg, 1.44 mmol) was added portion-wise. Next, the reaction mixture was stirred at 0 ºC for 1 h. After the completion of reduction, it was quenched following the Fieser workup[8] *via* slow sequential addition of H_2O (1 mL/g of $LiAlH_4$), followed by 10% NaOH (1 mL/g of $LiAlH_4$) and finally H_2O (3 mL/g of $LiAlH_4$) and the ice bath was removed and the reaction mixture was stirred for 2 h. The reaction mixture was filtered, extracted with EtOAc (3 x 50 mL) and dried (Na_2SO_4). The resulting solution was filtered again, concentrated and the crude compound was subjected to flash chromatography to obtain 8.2 mg of diol **4.7.4** in 46% yield over 3 steps. TLC (hexane/EtOAc 1:1): $R_f = 0.41$.

[8]. L. F. Fieser, M. Fieser in *Reagents for Organic Synthesis*, *Vol. 1,* Wiley: New York, **1967**, pp. 581−595; b) V. M. Mićović, M. Mihailović, *J. Org. Chem.* **1953**, *18*, 1190–1200.

FTIR (neat): 3473, 3066, 2932, 2822, 1639, 1495, 1453, 1377, 1313, 1275, 1147, 1098, 1042, 916, 752 cm^{-1};

Optical Rotation: $[a]_D^{23}$ = -8.6 (*c* 0.27, $CHCl_3$);

^{1}H NMR (500 MHz, $CDCl_3$): δ 7.36–7.28 (m, 5H, Aromatic C–H), 5.82 (ddt, *J* = 17.1, 9.5, 7.1 Hz, 1H, $CH_2C\underline{H}$= CH_aH_b), 5.18–5.14 (m, 1H, $CH(CH_3)CH=C\underline{H}_aH_b$), 5.16–5.13 (m, 1H, $CH(CH_3)CH=CH_a\underline{H}_b$), 4.66 (s, 4H, $CH(OC\underline{H}_2OCH_3)CH_2CH(OC\underline{H}_2OCH_3)$), 4.50 (s, 2H, $PhC\underline{H}_2OCH_2CH_2$), 3.96 (m, 2H, $BnOCH_2CH_2CH_2C\underline{H}$(OMOM), $CH_2C\underline{H}(OH)CH_2CH(OH)CH_2CH=CH_2$), 3.72 (m, 2H, $CH_2C\underline{H}(OH)CH_2CH=CH_2$, $CH_2C\underline{H}(OH)CH_2CH=CH_2$), 3.48 (t, *J* =6.2 Hz, 2H, $BnOC\underline{H}_2CH_2$), 3.37 (s, 6H, $CH(OCH_2OC\underline{H}_3)CH_2CH(OCH_2OC\underline{H}_3)$), 2.35 (t, *J* = 6.2 Hz, 1H, $CH(OH)C\underline{H}_a\underline{H}_bCH=CH_2$), 2.27 (q, *J* = 7.4, 6.4 Hz, 1H, $CH(OH)CH_a\underline{H}_bCH=CH_2$), 1.67–1.42 (m, 10H, $BnOCH_2C\underline{H}_2C\underline{H}_2CH$(OMOM), $C\underline{H}_2C\underline{H}_2CH(OH)C\underline{H}_2CH(OH)CH_2CH=CH_2$), 0.97–0.80 (m, 4H, $CH(OMOM)CH_2C\underline{H}_2C\underline{H}_2$);

^{13}C NMR (126 MHz, $CDCl_3$): δ 138.6 ($C\underline{H}=CH_2$), 134.6 (C_{Ar}), 128.5 (2, CH_{Ar}), 127.8 (2, CH_{Ar}), 127.7 (CH_{Ar}), 118.3 ($CH=\underline{C}H_2$), 96.3 (CH_2), 96.1 (CH_2), 75.5 (CH), 75.2 (CH), 73.0 (CH_2), 70.5 (CH2), 69.4 (CH), 68.3 (CH), 55.8 (CH_3), 55.8 (CH_3), 42.5 (CH_2), 42.2 (CH_2), 40.4 (CH_2), 39.8 (CH_2), 37.7 (CH_2), 35.1 (CH_2), 32.0 (CH_2), 29.8 (CH_2);

HRMS (ESI-TOF) m/z: $[M + Na]^+$ Calcd for $C_{26}H_{44}O_7Na$ 491.2985; Found 491.2984.

(5S,7R)-7-((S)-3,4-bis(benzyloxy)butyl)-5-((R)-but-3-en-2-yl)-9,9-diisopropyl-10-methyl-2,4,8-trioxa-9-silaundecane ($C_{36}H_{58}O_5Si$) (4.8.1)

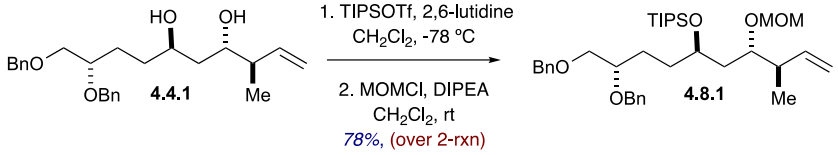

To a solution of diol **4.4.1** (120 mg, 0.3 mmol) in CH_2Cl_2 (3 mL, 0.1 M) was added 2,6 lutidine (88 µL, 0.73 mmol). The reaction mixture was cooled to -78 ºC and was added dropwise TIPSOTf (89 µL, 0.31 mmol). The reaction mixture was stirred for 30 min, after completion of reaction (monitored via TLC), it was added *N*,*N*-disopropylethylamine (210 µL, 1.20 mmol) followed by dropwise addition of chloro(methoxy)methane (45.5 µL, 0.60 mmol) and the reaction mixture was stirred for 12 h. After completion of reaction, it was quenched with saturated aqueous $NaHCO_3$, extracted with CH_2Cl_2, dried ($MgSO_4$), concentrated under reduced pressure. The crude product was purified using silica gel column chromatography (5% EtOAc/Hexanes), which furnished 143 mg of **4.8.1** in 78% yield over two reactions in one-pot (93% av/rxn) as colorless viscous liquid. TLC (hexane/EtOAc 20/1): $R_f = 0.6$.

FTIR (neat): 2942, 2865, 2359, 1451, 1276, 1097, 1039, 917, 882, 711 cm^{-1};

Optical Rotation: $[\alpha]_D^{23}$ = -1.2 (*c* 0.2, $CHCl_3$);

^{1}H NMR (500 MHz, $CDCl_3$): δ 7.35–7.27 (m, 10H, Aromatic C‑H), 5.77 (ddd, *J* = 17.3, 11.0, 7.1 Hz, 1H, $CH(CH_3)C\underline{H}{=}CH_aH_b$), 5.18 (ddt, *J* = 15.2, 3.5, 1.8 Hz, 2H, $CH(CH_3)CH{=}C\underline{H_a}\underline{H_b}$), 4.70 (d, *J* = 11.8 Hz, $BnOCH_aH_bCH(OC\underline{H_a}H_bPh)$), 4.65 (q, *J* = 6.0 Hz, 1H, $CH(OC\underline{H_2}OCH_3)CH(CH_3)$), 4.56 (d, *J* = 11.7 Hz, 1H, $BnOCH_aH_bCH(OCH_a\underline{H_b}Ph)$), 4.55 (s, 2H, $PhC\underline{H_2}OCH_aH_bCH(OCH_aH_bPh)$), 3.93 (tt, *J* = 7.0, 4.0 Hz, 1H, $BnOCH_aH_bC\underline{H}(OBn)CH_2$), 3.66 (dt, *J* = 7.8, 3.6 Hz, 1H,

CH_aH_bCH(OTIPS)CH_aH_b), 3.57 (dd, *J* = 9.9, 5.4 Hz, 2H, BnOCH_aH_bCH(OBn)CH_2 CH(OMOM)CH(CH_3)), 3.53 (dd, *J* = 9.8, 4.5 Hz , 1H, BnOCH_aH_bCH(OBn)CH_2), 3.36 (s, 3H, CH(OCH_2OCH_3)CH_aH_b), 2.51 (tdq, *J* = 7.1, 3.7, 1.8 Hz, 1H, CH(OMOM)CH(CH_3)$CH=CH_2$), 1.73 (tt, *J* = 12.0, 3.8 Hz, 1H, $BnOCH_2$CH(OBn)$CH_aH_bCH_aH_b$), 1.67–1.61 (m, 1H, $BnOCH_2$CH(OBn)$CH_aH_bCH_aH_b$), 1.57 (dq, *J* = 12.0, 4.0, 3.6 Hz, 2H, CH(OTIPS)CH_2CH(OMOM)), 1.49 (tdt *J* = 11.1, 7.7, 3.7 Hz , 2H, $BnOCH_2$CH(OBn)C$H_aH_b$$CH_aH_b$), 1.07–1.01 (m, 21H, (Si(CH(C$H3$)2)3), 1.01 (d, *J* = 7.0 Hz, 3H, CH(OMOM)CH(CH_3)$CH=CH_2$);

^{13}C NMR (126 MHz, $CDCl_3$): δ 140.4 (CH=CH_2), 139.0 (C_{Ar}), 138.5 (C_{Ar}), 128.5 (2, CH_{Ar}), 128.4 (2, CH_{Ar}), 127.9 (2, CH_{Ar}), 127.7(2, CH_{Ar}), 127.6 (CH_{Ar}), 127.5 (CH_{Ar}), 115.0 (CH=CH_2), 96.9 (CH_2), 79.9 (CH), 78.6 (CH), 73.5 (CH_2), 73.1(CH_2), 72.1(CH_2), 70.1 (CH), 55.8 (CH_3), 41.5 (CH), 38.5 (CH_2), 33.8 (CH_2), 27.1 (CH_2), 18.4 [6C, Si (CH (CH_3)$_2$)$_3$], 14.3 (CH_3), 13.0 [3C, Si (CH (CH_3)$_2$)$_3$];

HRMS (ESI-TOF) m/z: $[M + Na]^+$ Calcd for $C_{36}H_{58}O_5SiNa$ 621.3951; Found 621.3968;

(6R,8S)-8-((3R,4S,6R,9S)-9,10-bis(benzyloxy)-4-(methoxymethoxy)-3-methyl-6-((triisopropylsilyl)oxy)decyl)-2,9,10-trioxa-1-phosphabicyclo[4.3.1]dec-4-ene 1-oxide (4.8.2)

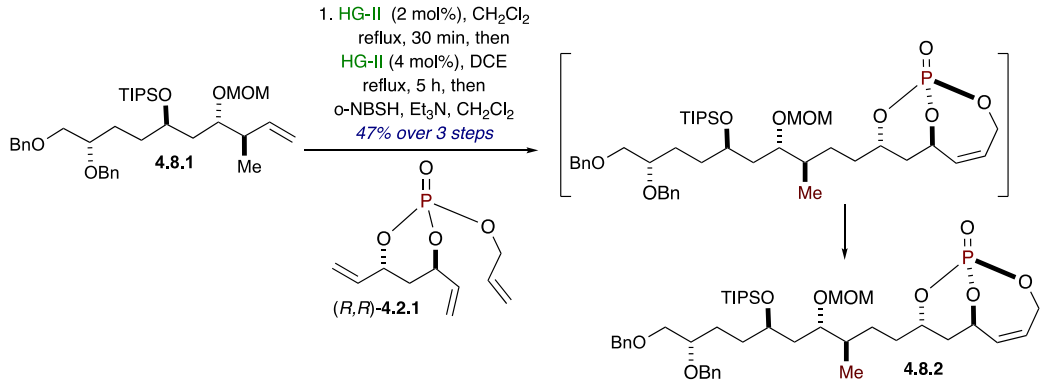

To a solution of (*R,R*)-triene (*R,R*)-**4.2.1** (394 mg, 1.7 mmol) in a degassed CH_2Cl_2 (347 mL, 0.005 M) was added **HG-II** (21.2 mg, 0.034 mmol, 2 mol%) the reaction mixture was refluxed in an oil bath for 20 minutes. After completion of RCM reaction, CH_2Cl_2 was evaporated under reduced pressure. To the crude product was added freshly distilled, freeze-degas-thawed 1,2-DCE (17 mL, 0.1 M), the CM partner **4.8.1** (975 mg, 2.04 mmol) and HG-II (63 mg, 0.102 mmol, 6 mol%) under inert atmosphere. The reaction mixture was stirred at 70 ºC in an oil bath for 12 h, a second portion of HG-II (21 mg, 0.034 mmol, 2 mol%) and CM partner (162 mg, 0.34 mmol) were added to the reaction mixture, was stirred at 70 ºC for 8 h and a third portion of HG-II (21 mg, 0.034 mmol, 2 mol%) and CM partner (162 mg, 0.34 mmol) were added and the reaction mixture was stirred for an additional 8 h. After completion of CM reaction, the crude product was subjected to chemoselective hydrogenation "H_2" reaction using *o*-NBSH and Et_3N (2 mL/1 g of *o*-NBSH) at room temperature. It should be noted that for the chemoselective hydrogenation of external olefin of the crude CM product, *o*-NBSH (1.8 g, 8.5 mmol) and Et_3N (3.6 mL, 2 mL/1 g of *o*-NBSH) were sequentially added after each 8–12 h and the reaction mixture was stirred for 72 h. Reaction progress was monitored via crude NMR, which confirmed

the complete reduction of external double bond in the CM adduct. The reaction mixture was diluted with EtOAc (100 mL) followed by addition of saturated aqueous solution of $NaHCO_3$ (50 mL). The organic layer was separated, and aqueous phase was extracted with EtOAc (3 x 100 mL). The combined organic layers were washed with brine (50 mL), dried (Na_2SO_4), concentrated under reduced pressure, and purified with flash chromatography (40% EtOAc/Hexane), which furnished 368 mg of bicyclic phosphate **4.8.2** as a colorless oil in 47% yield over three reactions in one-pot (74% av/rxn). TLC (EtOAc): R_f = 0.42.

FTIR (neat): 2931, 2847, 2356, 1472, 1298, 1056, 1068, 1009, 972, 885, 773 cm^{-1};

Optical Rotation: $[a]_D^{23}$ = -30.2 (*c* 0.2, $CHCl_3$);

^{1}H NMR (500 MHz, $CDCl_3$): δ 7.34–7.27 (m, 10H, Aromatic C‑H), 6.02 (ddt, *J* = 11.9, 6.6, 2.7 Hz, 1H, CHO(P)CH=C<u>H</u>CH$_a$H$_b$), 5.56 (ddd, *J* = 11.9, 4.0, 2.50 Hz, 1H, CHO(P)C<u>H</u>=CHCH$_a$H$_b$), 5.17 (dt, *J* = 24.6, 4.6 Hz, 1H, C<u>H</u>O(P)CH=CHCH$_a$H$_b$), 4.99 (ddq, *J* = 14.2, 5.6, 2.7 Hz, 1H, CHO(P)CH=CHC<u>H</u>$_a$H$_b$), 4.70 (d, *J* = 11.7 Hz, 1H, BnOCH$_2$CH(C<u>H</u>$_a$H$_b$Ph)), 4.63 (q, *J* = 6.8 Hz, 2H, CH$_2$CH(OC<u>H</u>$_2$OCH$_3$)CH(Me)), 4.55–4.53 (m, 3H, PhC<u>H</u>$_2$OCH$_2$CH(CH$_a$H$_b$Ph), C<u>H</u>O(P)CH$_a$H$_b$CHO(P)), 4.55 (d, *J* = 11.7 Hz, 1H, BnOCH$_2$CH(CH$_a$<u>H</u>$_b$Ph)), 4.35 (ddd, *J* = 27.7, 14.8, 6.8 Hz, 1H, CHO(P)CH=CHCH$_a$<u>H</u>$_b$), 3.94 (tt, *J* = 6.8, 3.3 Hz, 1H, C<u>H</u>(OTIPS)CH$_2$CH(OMOM)), 3.62 (dt, *J* = 9.2, 2.9 Hz, 1H, BnOCH$_2$C<u>H</u>(CH$_a$H$_b$Ph)), 3.58–3.53 (m, 2H, BnOC<u>H</u>$_2$CH(CH$_a$H$_b$Ph)), 3.54–3.50 (m, 1H, CH(OTIPS)CH$_2$C<u>H</u>(OMOM)), 3.34 (d, *J* = 8.5 Hz, 3H, CH$_2$CH(OCH$_2$OC<u>H</u>$_3$)CH(Me)), 2.15 (ddd, *J* = 11.6, 6.1, 2.4 Hz, 1H, CHO(P)C<u>H</u>$_a$H$_b$CHO(P)), 1.81–1.75 (m, 2H, CH(MOM)C<u>H</u>(CH$_3$)CH$_2$CH$_2$, CH(CH$_3$)CH$_a$H$_b$C<u>H</u>$_a$H$_b$), 1.71–1.66 (m, 3H, CHO(P)CH$_a$<u>H</u>$_b$CHO(P), BnOCH$_2$CH(OBn)C<u>H</u>$_a$<u>H</u>$_b$), 1.63–1.58 (m, 2H, BnOCH$_2$CH(OBn)CH$_a$H$_b$C<u>H</u>$_2$), 1.51–1.45

(m, 3H, CH(OTIPS)C$\underline{H}_a H_b$CH(OMOM), CH(CH_3)C$\underline{H}_a\underline{H}_b CH_a H_b$), 1.43–1.37 (m, 2H, CH(OTIPS)$CH_a\underline{H}_b$CH(OMOM), CH(CH_3)$CH_a H_b CH_a\underline{H}_b$), 1.04 (s, 21H, (Si(C$\underline{H}$($C\underline{H}_3$)$_2$)$_3$), 0.89 (d, J = 6.8 Hz, 3H, CH(C$\underline{H}_3$)CH_2CH_2);

^{13}C NMR (126 MHz, $CDCl_3$): δ 139.0 (C_{Ar}), 138.5(C_{Ar}), 130.0 ($\underline{C}$H=$CHCH_2$), 128.5 (2, CH_{Ar}), 128.4 (2, CH_{Ar}), 128.0 (CH_{Ar}), 127.9 (2, CH_{Ar}), 127.8 (2, CH_{Ar}), 127.7 ($\underline{C}$H=$CHCH_2$), 127.6 (CH_{Ar}), 97.0 (CH_2), 80.3 (CH_2), 78.6 (CH_2), 77.2 (CH, J_{CP} = 6.4 Hz), 77.0 (CH, J_{CP} = 7.1 Hz), 73.5 (CH_2), 73.1(CH_2), 72.2 (CH_2), 70.3 (CH), 63.1 (J_{CP} = 6.4 Hz), 55.8 (CH_3), 37.8 (CH_2), 36.7 (CH), 34.4 (CH_2), 33.9 (CH_2), 29.9 (CH_2), 27.7 (CH_2), 27.4 (CH_2), 18.5 [6C, Si (CH ($\underline{C}H_3$)$_2$)$_3$], 14.4, 13.1[3C, Si ($\underline{C}$H (CH_3)$_2$)$_3$];

^{31}P NMR (202 MHz, $CDCl_3$) δ -3.86;

HRMS (ESI-TOF) m/z: $[M + Na]^+$ Calcd for $C_{42}H_{67}O_9PSiNa$ 797.4190; Found 797.4199.

(3S,4R,6S,9R,10S,12R,15S)-15,16-bis(benzyloxy)-10-(methoxymethoxy)-3,9-dimethyl-12-((triisopropylsilyl)oxy)hexadec-1-ene-4,6-diol ($C_{43}H_{72}O_7Si$) (4.8.3)

To a flame dried round bottom-flask was added CuCN (290 mg, 3.2 mmol) and LiCl (317 mg, 7.5 mmol) inside the glove box, followed by addition of dry THF (10 mL, 0.05 M) under argon and the reaction mixture was stirred at room temperature for 15 minutes. A pale green coloration was observed. The reaction mixture was cooled to -40 ºC followed by slow addition of a 1 M solution of Me_2Zn in THF (3.2 mL, 3.2 mmol). The reaction mixture was stirred for 40 minutes at -30 ºC and a solution of bicyclic phosphate **4.8.2** (350 mg, 1.08 mmol) in dry THF (10 mL, 0.05 M) was added dropwise via cannula to the reaction mixture. The reaction was slowly warmed to room temperature and allowed to stir for 3 h. Upon completion of reaction (monitored via TLC), the reaction mixture was quenched with saturated aqueous ammonium chloride (NH_4Cl, 2 mL), stirred for 15 minutes followed by the addition of anhydrous Na_2SO_4 (200 mg) stirred for another 30 minutes. The crude product was filtered through Celite pad and washed with excess EtOAc (3 x 30 mL), the filtrate was concentrated under reduce pressure, which afforded the crude acid as yellowish viscous oil, which was proceeded to the next reaction without further purification.

To a flask containing the crude acid was added THF (13.5 mL, 0.08 M). The reaction mixture was cooled to 0 ºC and was added 70% solution of Red-Al in toluene (1.5 mL, 5 mmol). The reaction mixture was brought to room temperature and stirred for 4 h. After completion of reaction (monitored by TLC), it was quenched with NH_4Cl (sat. aq.)

and was added (Na_2SO_4), stirred for 30 minutes, filtered through Celite pad. The residue was washed with EtOAc (3 x 50 mL). The organic layer was dried (Na_2SO_4) and the solvent was evaporated under reduced pressure. The resulting solution was filtered again, concentrated and the crude compound was purified using a short silica gel flash column chromatography (hexane/EtOAc 1:1), which afforded tetrol **4.8.3** (120 mg, 56% yield over 2 reactions). TLC (hexane/EtOAc 1:2): R_f = 0.62.

FTIR (neat): 3422, 3065, 2926, 2865, 1665, 1640, 1462, 1379, 1095, 1040, 883, 844, 678, 664 cm^{-1};

Optical Rotation: $[a]_D^{23}$ = -1.2 (*c* 0.20, $CHCl_3$);

^{1}H NMR (500 MHz, $CDCl_3$): δ 7.34–7.27 (m, 10H, Aromatic C–H), 5.73 (dt, *J* = 19.1, 9.3, 8.4 Hz, 1H, $CH(CH_3)C\underline{H}=CH_2$), 5.17–5.10 (m, 2H, $CH(CH_3)CH=C\underline{H}_2$), 4.70 (d, *J* = 11.7 Hz, 1H, $BnOCH_2CH(OC\underline{H}_aH_bPh)$), 4.64 (q, *J* = 2.8 Hz, 2H, $CH_2CH(OC\underline{H}_2OCH_3)$), 4.55 (d, *J* = 11.7 Hz, 1H, $BnOCH_2CH(OCH_a\underline{H}_bPh)$), 4.55 (s, 2H, $PhC\underline{H}_2OCH_2CH(OBn)$), 3.95 (dd, *J* = 7.6, 3.7 Hz, 1H, $BnOCH_2CH(OBn)CH_2CH_2C\underline{H}(OTIPS)$), 3.90 (q, *J* = 6.04 Hz, 1H, $CH_2C\underline{H}(OH)CH_2CH(OH)CH(Me)$), 3.70–3.69 (m, 1H, $CH_2CH(OH)CH_2C\underline{H}(OH)CH(Me)$), 3.64 (dt, *J* = 9.2, 2.9 Hz, 1H, $CH(OTIPS)CH_2C\underline{H}(OMOM)$), 3.58–3.55 (m, 2H, $PhCH_2OC\underline{H}_a\underline{H}_bCH(OBn)$), 3.54–3.51 (m, 1H, $PhCH_2OCH_aH_bC\underline{H}(OBn)$), 3.34 (s, 3H, $CH_2CH(OCH_2OC\underline{H}_3)$), 2.43 (d, *J* = 4.7 Hz, 1H, $CH_2CH(O\underline{H})CH_2CH(OH)CH(Me)$), 2.24 (q, *J* = 7.2 Hz, 1H, $CH(OH)C\underline{H}(Me)CH=CH_2$), 2.18 (d, *J* = 3.1 Hz, 1H, $CH_2CH(OH)CH_2CH(O\underline{H})CH(Me)$), 1.84–1.74 (m, 2H, $CH(OTIPS)C\underline{H}_aH_bCH(OMOM)C\underline{H}(Me)$), 1.62 (dd, *J* = 6.3, 5.1 Hz, 3H, $CH_2CH(OH)C\underline{H}_2CH(OH)CH(Me)CH(OTIPS)CH_a\underline{H}_bCH(OMOM)C\underline{H}(Me)$), 1.55–1.46 (m, 6H, $BnOCH_2CH(OBn)C\underline{H}_2CH_2$, $CH(OMOM)CH(Me)C\underline{H}_2C\underline{H}_2$), 1.46–1.37 (m,

2H, $BnOCH_2CH(OBn)CH_2C\underline{H}_2CH(OTIPS)$), 1.04 (s, 21H, $CH(OSi(C\underline{H}(C\underline{H}_3)_2)_3$), 1.01 (d, J = 6.8 Hz, 3H, $CH(C\underline{H}_3)CH=CH_2$), 0.89 (d , J = 6.8 Hz, 3H, $CH(OMOM)CH(C\underline{H}_3)CH_2$);

^{13}C NMR (126 MHz, $CDCl_3$): δ 140.6 ($\underline{C}H=CH_2$), 139.0 (C_{Ar}), 138.5 (C_{Ar}), 128.5 (2, CH_{Ar}), 128.4 (2, CH_{Ar}), 127.9 (2, CH_{Ar}), 127.8 (2, CH_{Ar}), 127.7 (CH_{Ar}), 127.6 (CH_{Ar}), 117.0 ($CH=\underline{C}H_2$), 97.0 (CH_2), 80.5 (CH), 78.6 (CH), 73.5 (CH_2), 73.1 (CH_2), 72.2 (CH_2), 72.1 (CH), 70.3 (CH), 69.7 (CH), 55.8 (CH_3), 44.6 (CH), 39.3 (CH_2), 37.6 (CH_2), 37.0 (CH), 35.6 (CH_2), 34.3 (CH_2), 29.0 (CH_2), 27.3 (CH_2), 18.5 [6C, Si (CH ($\underline{C}H_3)_2)_3$], 16.3 (CH_3), 14.4 (CH_3), 13.1 [3C, $Si(\underline{C}H(CH_3)_2)_3$];

HRMS (ESI-TOF) m/z: $[M + Na]^+$ Calcd for $C_{43}H_{72}O_7SiNa$ 751. 4945; Found 751.4926.

(4*S*,6*S*,9*R*)-9-((4*S*,6*R*)-6-((*S*)-3,4-bis(benzyloxy)butyl)-1,3-dioxan-4-yl)dec-1-ene-4,6-diol (4.8.4)

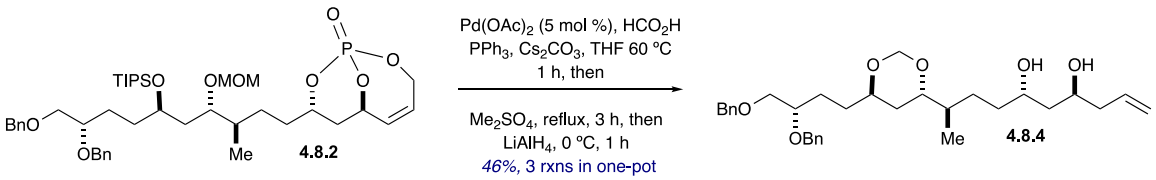

To a stirring solution of bicyclic phosphate **4.8.2** (38 mg, 0.032 mmol) in THF (1.6 mL, 0.3 M) under argon was added Cs_2CO_3 (780 mg, 0.16 mmol) and HCO_2H (48 μL, 0.08 mmol). Next, a solution of $Pd(OAc)_2$ (7.7 mg, 0.003 mmol, 5 mol%) and PPh_3 (12 mg, 0.006 mmol) in THF (1.6 mL) under argon was immediately transferred *via* cannula to the reaction mixture. The reaction mixture was stirred at 60 ºC in an oil bath for 1 h (monitored by TLC). After 1 h, all starting materials were consumed and the color of reaction mixture turned black. After the reaction was complete, Me_2SO_4 was added, and the reaction mixture was refluxed for 3 h (TLC showed that phosphate acid was methylated completely). The reaction mixture was cooled to 0 ºC, then $LiAlH_4$ (53 mg, 1.44 mmol) was added portion-wise. Next, the reaction mixture was stirred at 0 ºC for 1 h. After the completion of reduction, it was quenched following the Fieser workup[9] *via* slow sequential addition of H_2O (1 mL/g of $LiAlH_4$), followed by 10% NaOH (1 mL/g of $LiAlH_4$) and finally H_2O (3 mL/g of $LiAlH_4$) and the ice bath was removed and the reaction mixture was stirred for 2 h. The reaction mixture was filtered, extracted with EtOAc (3 x 50 mL) and dried (Na_2SO_4). The resulting solution was filtered again, concentrated and the crude compound was subjected to flash chromatography to obtain diol **4.8.4** in 46% yield over 3 steps. TLC (hexane/EtOAc 1:2): $R_f = 0.35$.

[9]. (a) L. F. Fieser, M. Fieser in *Reagents for Organic Synthesis*, *Vol. 1,* Wiley: New York, **1967**, pp. 581−595;
(b) V. M. Mićović, M. Mihailović, *J. Org. Chem.* **1953**, *18*, 1190–1200.

FTIR (neat): 3405, 2941, 2865, 1642, 1465, 1363, 1097, 1041, 997, 917, cm^{-1}.;

Optical Rotation: $[a]_D^{23}$ = -10.8 (*c* 0.22, $CHCl_3$);

^{1}H NMR (500 MHz, $CDCl_3$): δ 7.36–7.27 (m, 10H, Aromatic C–H), 5.81 (ddd, *J* = 24.3, 12.2, 7.2 Hz, 1H, $CH_aH_bC\underline{H}=CH_2$), 5.15 (dd, *J* = 10.7, 7.3 Hz, 2H, $CH_aH_bCH=C\underline{H}_2$), 4.85–4.75 (m, 2H, $CH_2CH(OC\underline{H}_2O)CH(Me)$), 4.70 (d, *J* = 11.8 Hz, 1H, $BnOCH_2CH(OC\underline{H}_aH_bPh)$), 4.56 (d, *J* = 11.8 Hz, 1H, $BnOCH_2CH(OCH_a\underline{H}_bPh)$), 4.58–4.54 (m, 2H, $PhC\underline{H}_2OCH_2CH(OBn)$), 4.02–3.89 (m, 1H, $C\underline{H}(OH)CH_aH_bCH=CH_2$), 3.88–3.80 (m, 1H, $CH_2C\underline{H}(OCH_2O)CH(Me)$), 3.67–3.59 (m, 2H, $C\underline{H}(OH)CH_2CH(OH)$, $CH_aH_bCH=CH_2C\underline{H}(OCH_2O)CH_2CH(OCH_2O)$), 3.49–3.43 (m, 2H, $PhCH_2OC\underline{H}_aH_bCH(OBn)$, $PhCH_2OCH_2C\underline{H}(OBn)$), 3.43–3.36 (m, 1H, $PhCH_2OCH_a\underline{H}_bCH(OBn)$), 2.34–2.20 (m, 1H, $C\underline{H}_aH_bCH=CH_2$), 1.99–1.90 (m, 1H, $CH_2CH(OCH_2O)C\underline{H}(Me)$), 1.83–1.73 (m, 1H, $BnOCH_2CH(OBn)CH_2C\underline{H}_aH_b$), 1.73–1.59 (m, 8H, $BnOCH_2CH(OBn)CH_2CH_a\underline{H}_b$ $C\underline{H}_aH_bC\underline{H}_2CH(OCH_2O)CH(Me)C\underline{H}_2C\underline{H}_2$, $CH_a\underline{H}_bCH=CH_2$), 1.52–1.40 (m, 3H, $BnOCH_2CH(OBn)CH_2CH_a\underline{H}_b$ $C\underline{H}_aH_bC\underline{H}_2CH(OH)$ $CH_aH_bCH=CH_2$), 0.85 (d, *J* = 6.5 Hz, 3H, $CH(C\underline{H}_3)CH_2CH_2$);

^{13}C NMR (126 MHz, $CDCl_3$): δ 138.8 (C_{Ar}), 138.3(C_{Ar}), 134.2 ($\underline{C}H=CH_2$), 128.7 (2, CH_{Ar}) , 128.6 (2, CH_{Ar}), 128.5 (2, CH_{Ar}), 128.5 (2, CH_{Ar}), 127.8 (CH_{Ar}), 127.7 (CH_{Ar}), 118.9 ($CH=\underline{C}H_2$), 87.4 (CH_2), 77.4 (CH), 77.2 (CH), 75.6 (CH), 72.7 (CH_2), 72.0 (CH_2), 71.5 (CH_2), 69.9 (CH), 68.3 (CH), 42.0 (CH_2), 35.3 (CH), 34.5 (CH_2), 32.1 (CH_2), 29.9 (CH_2), 28.5 (CH_2), 27.8 (CH_2), 27.5 (CH_2), 15.4 (CH_3);

HRMS (ESI-TOF) m/z: $[M + Na]^+$ Calcd for $C_{32}H_{46}O_6Na$ 549.3192; Found 549.3176.

5.3.3 NMR Spectra

(1*S*,6*S*,8*R*)-8-(3-(benzyloxy)propyl)-2,9,10-trioxa-1-phosphabicyclo[4.3.1]dec-4-ene 1-oxide (4.2.2):

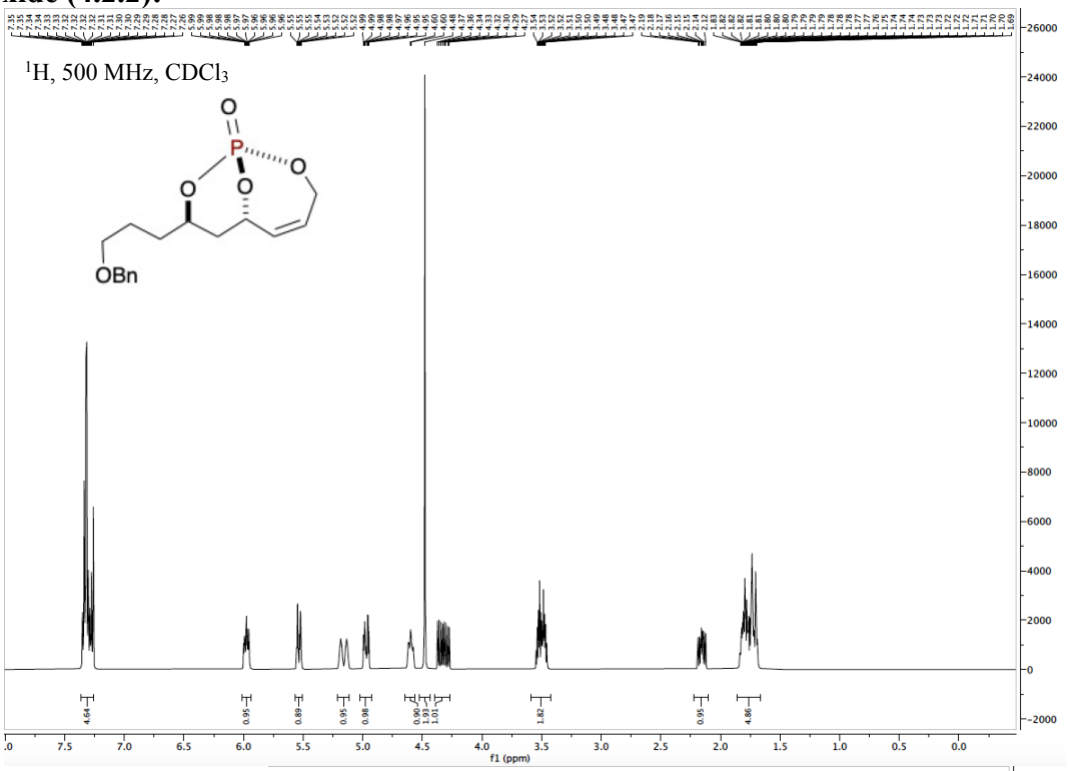

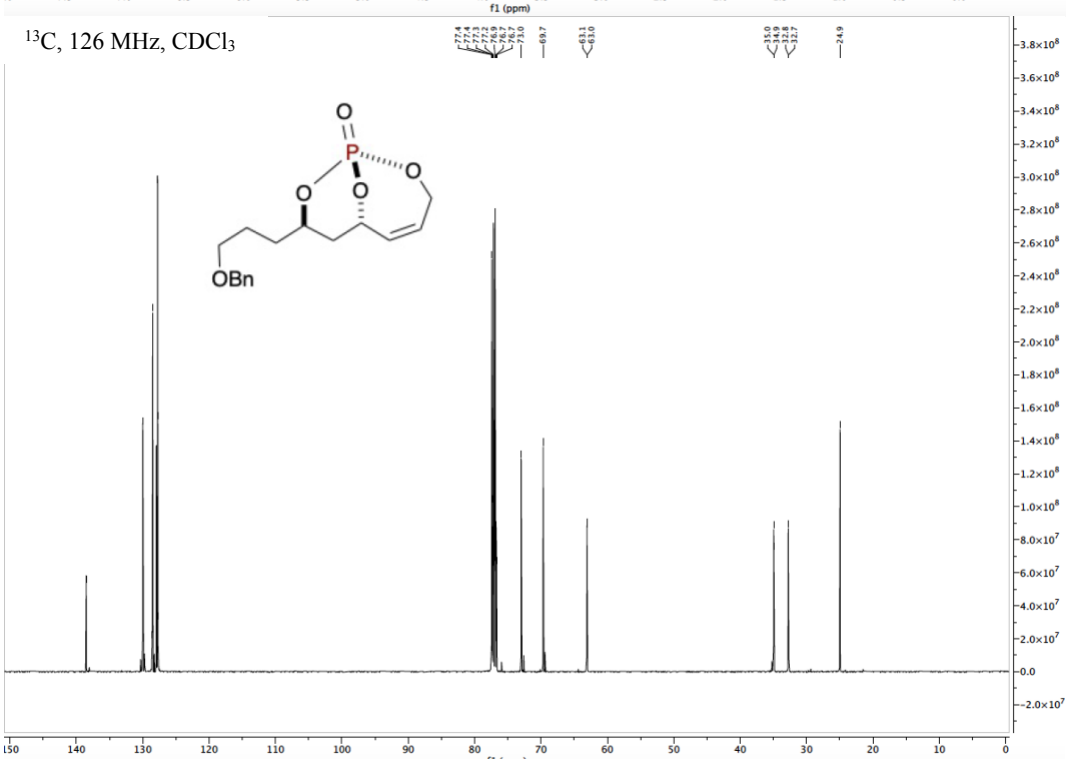

DEPT (135), 126 MHz, $CDCl_3$

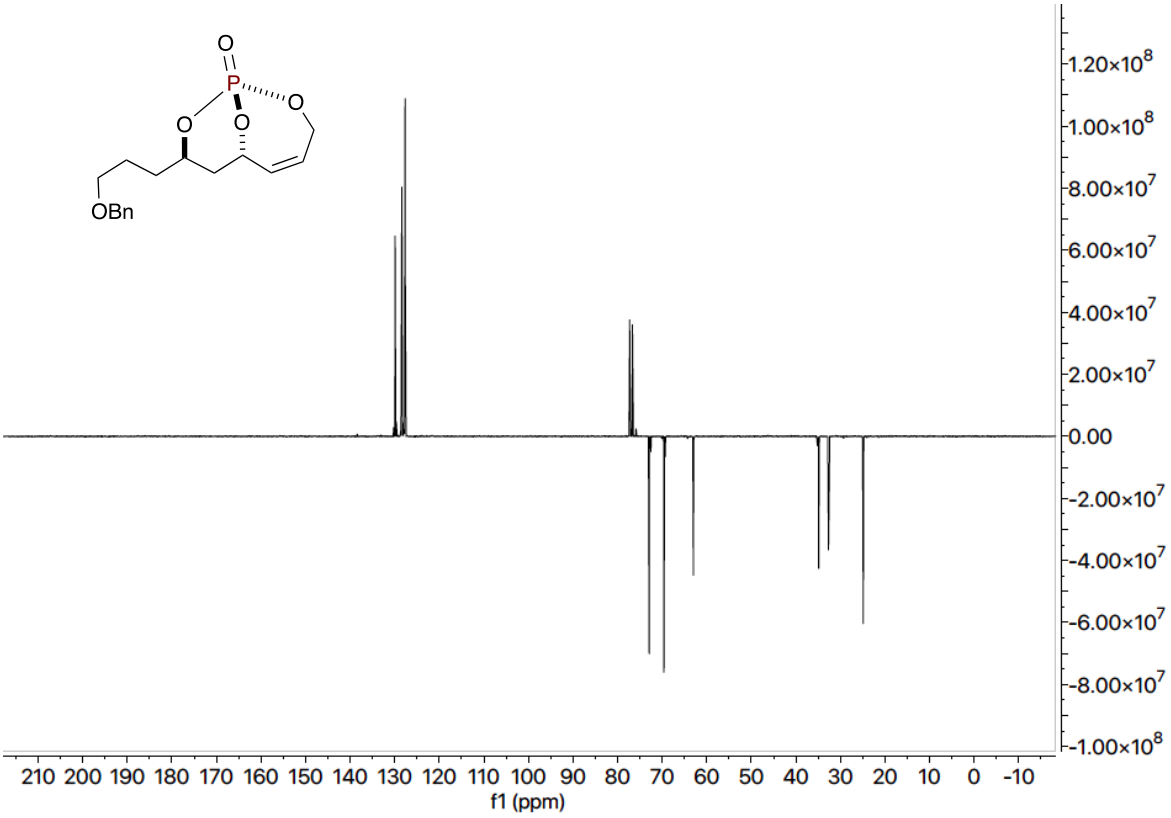

2D, $^{1}H^{1}H$, COSY, 500 MHz, $CDCl_3$

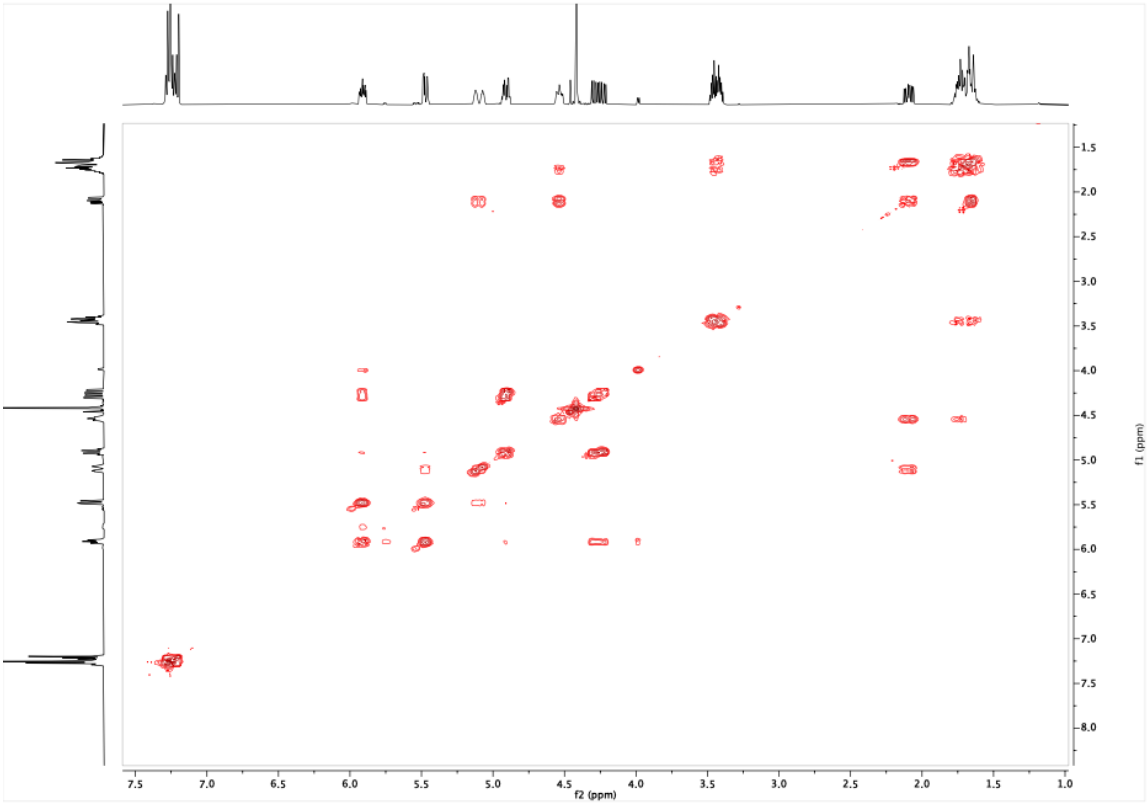

2D, $^{1}H^{13}C$, HSQC, 500 MHz, $CDCl_3$

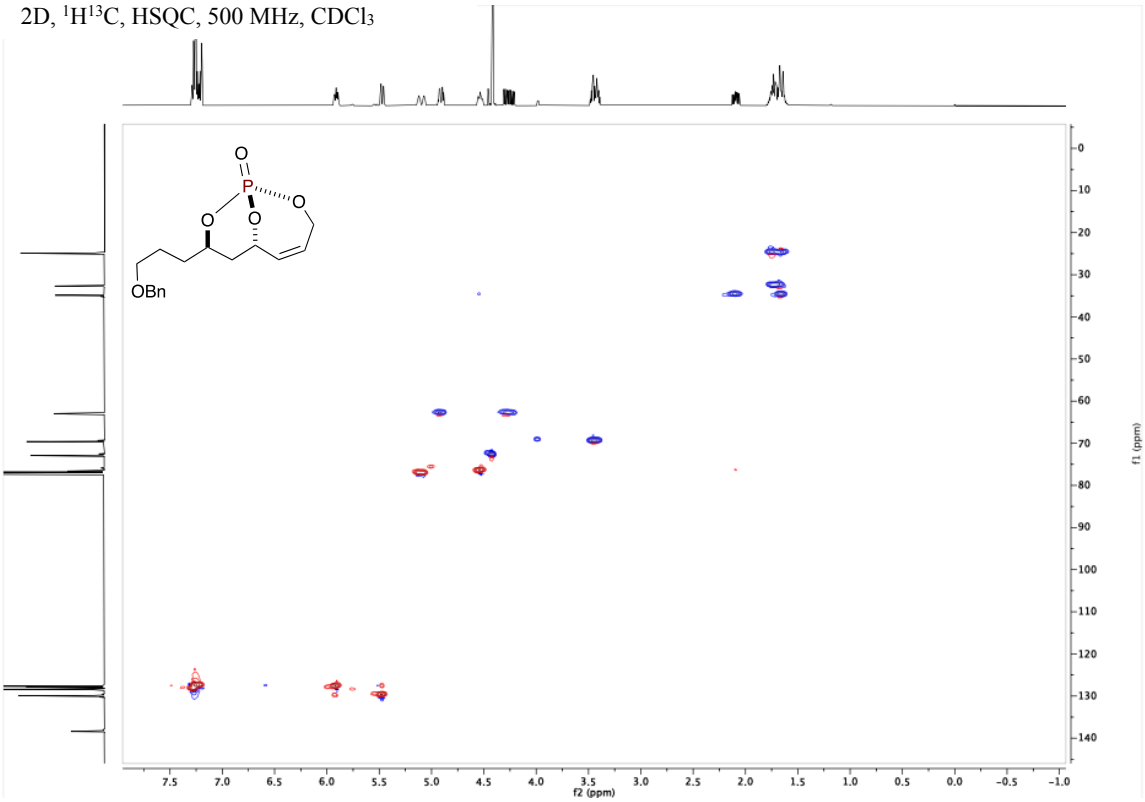

^{31}P, 202 MHz, $CDCl_3$

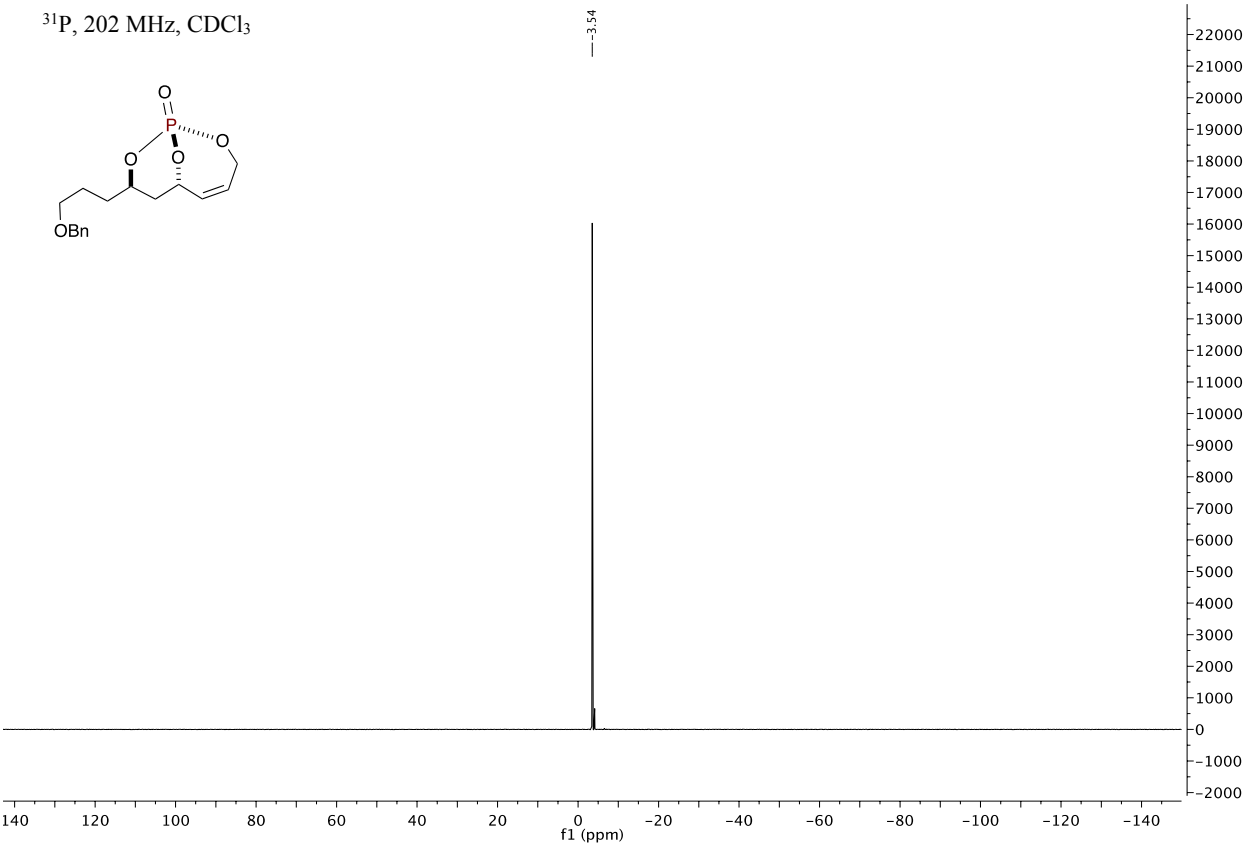

(*S*)-((but-3-ene-1,2-diylbis(oxy))bis(methylene))dibenzene (4.2.5)

^{1}H, 500 MHz, $CDCl_3$

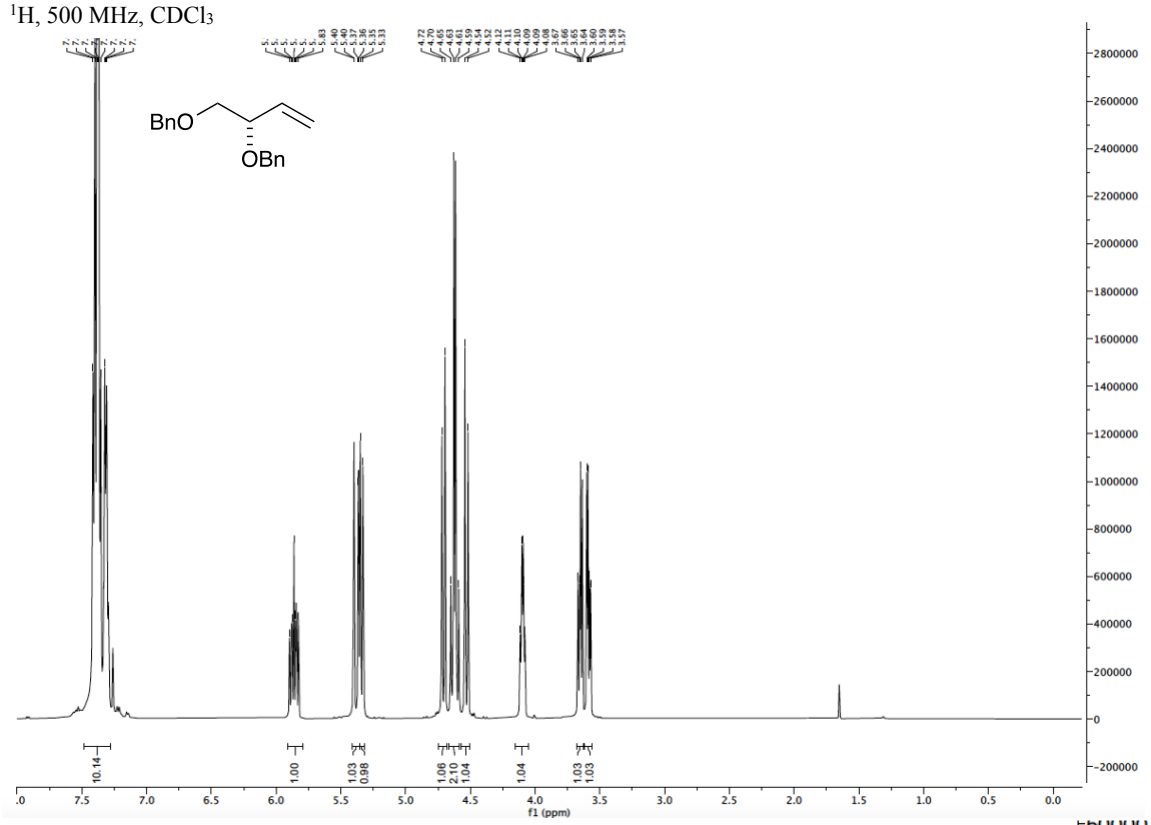

^{13}C, 126 MHz, $CDCl_3$

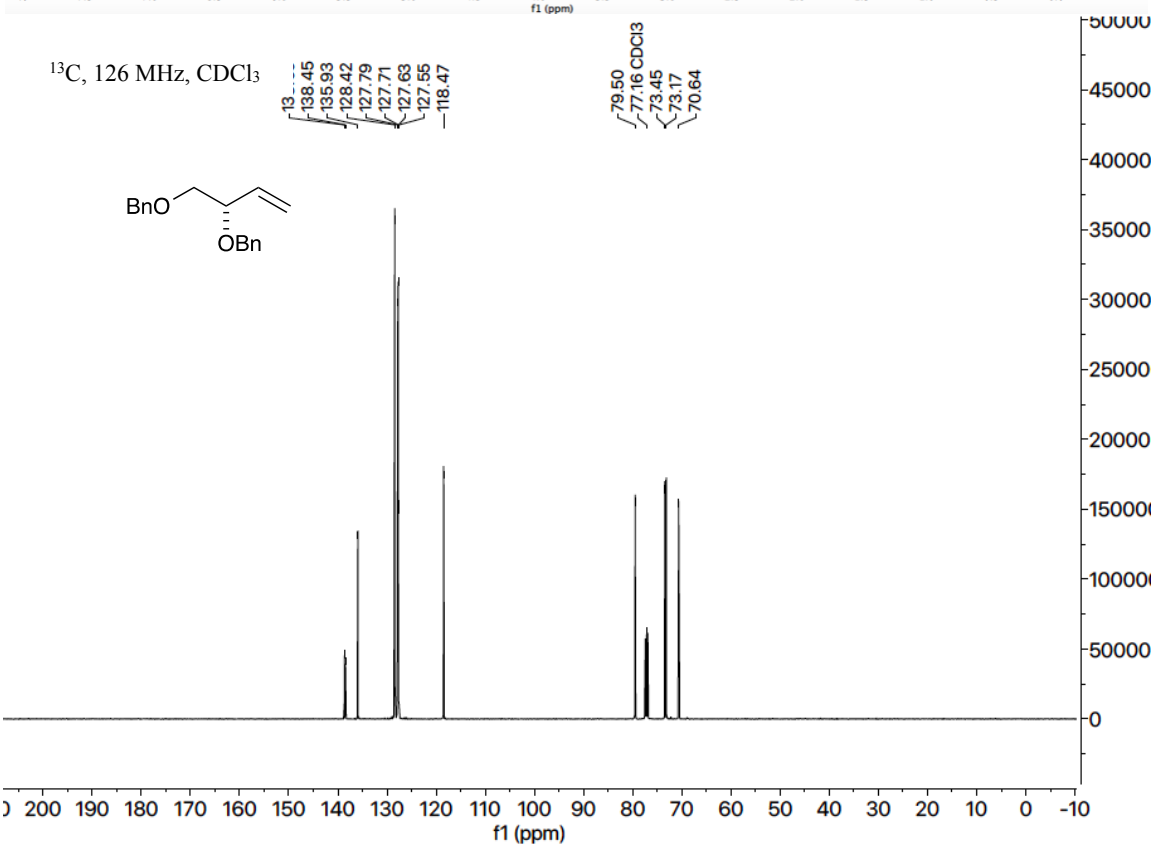

DEPT (135), 126 MHz, $CDCl_3$

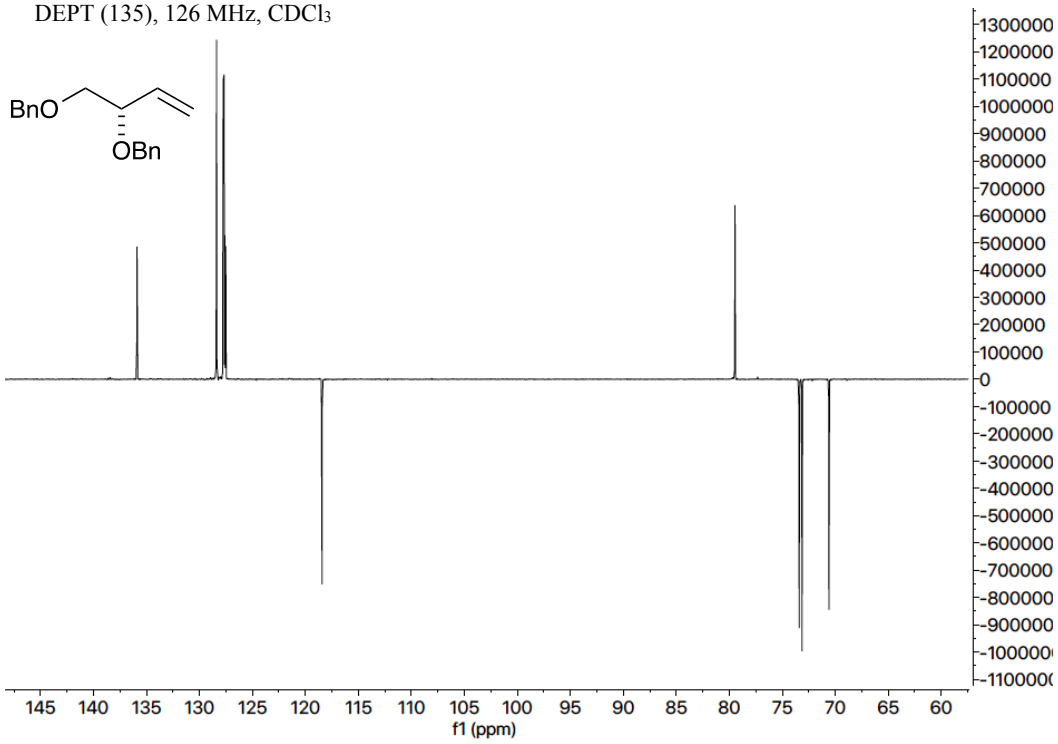

6*S*,8*R*)-8-((*S*)-3,4-bis(benzyloxy)butyl)-2,9,10-trioxa-1-phosphabicyclo[4.3.1]dec-4-ene 1-oxide (4.2.3)

^{1}H, 500 MHz, $CDCl_3$

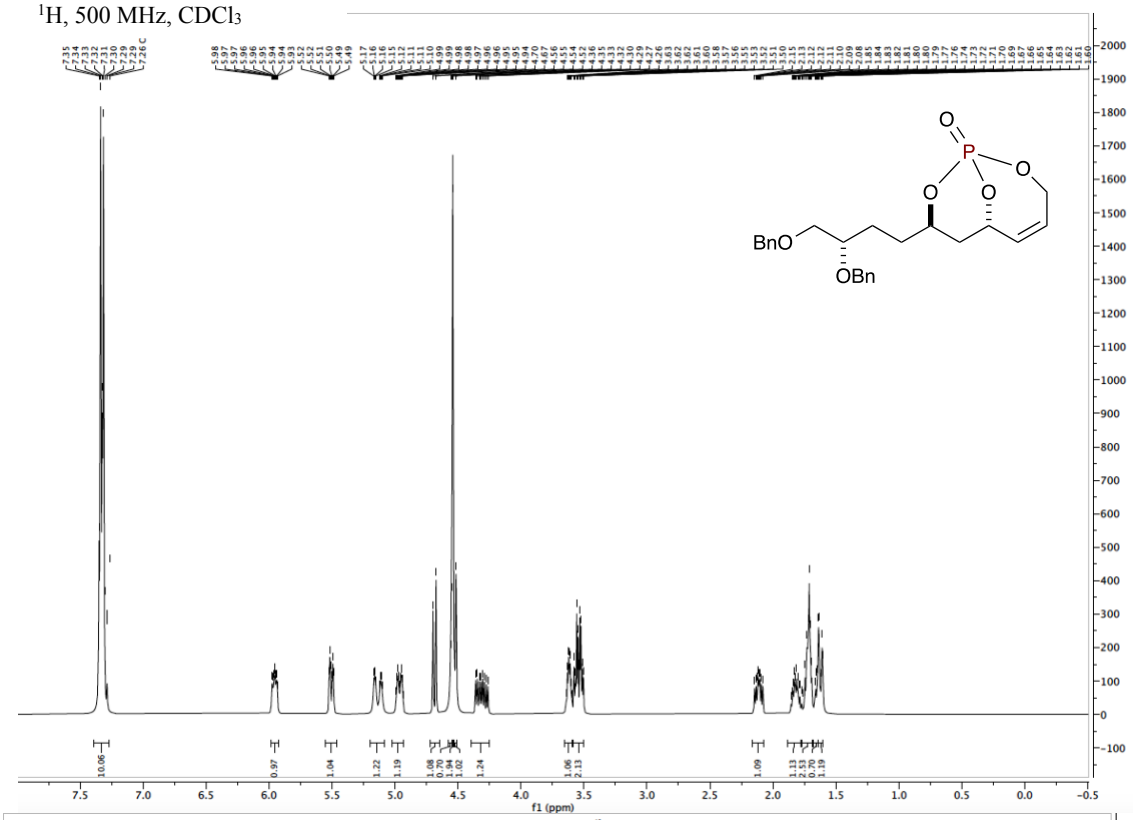

^{13}C,126 MHz, $CDCl_3$

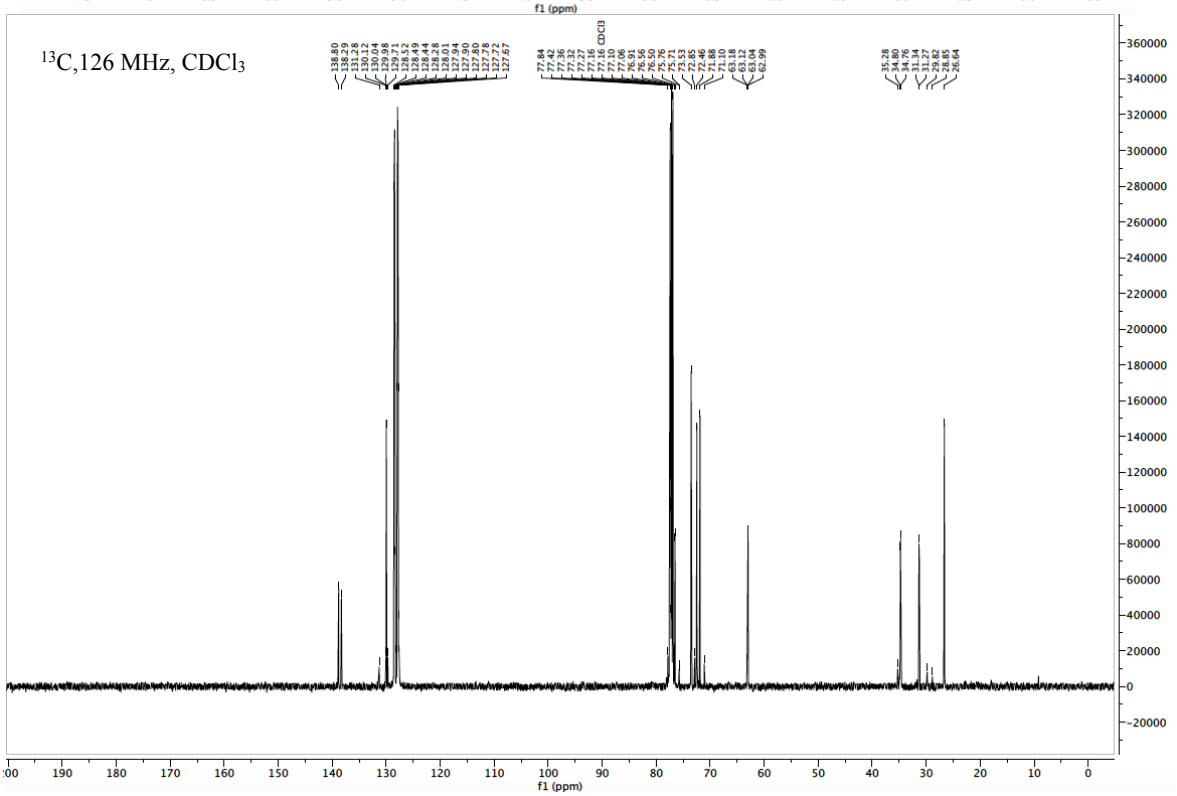

DEPT (135), 126 MHz, $CDCl_3$

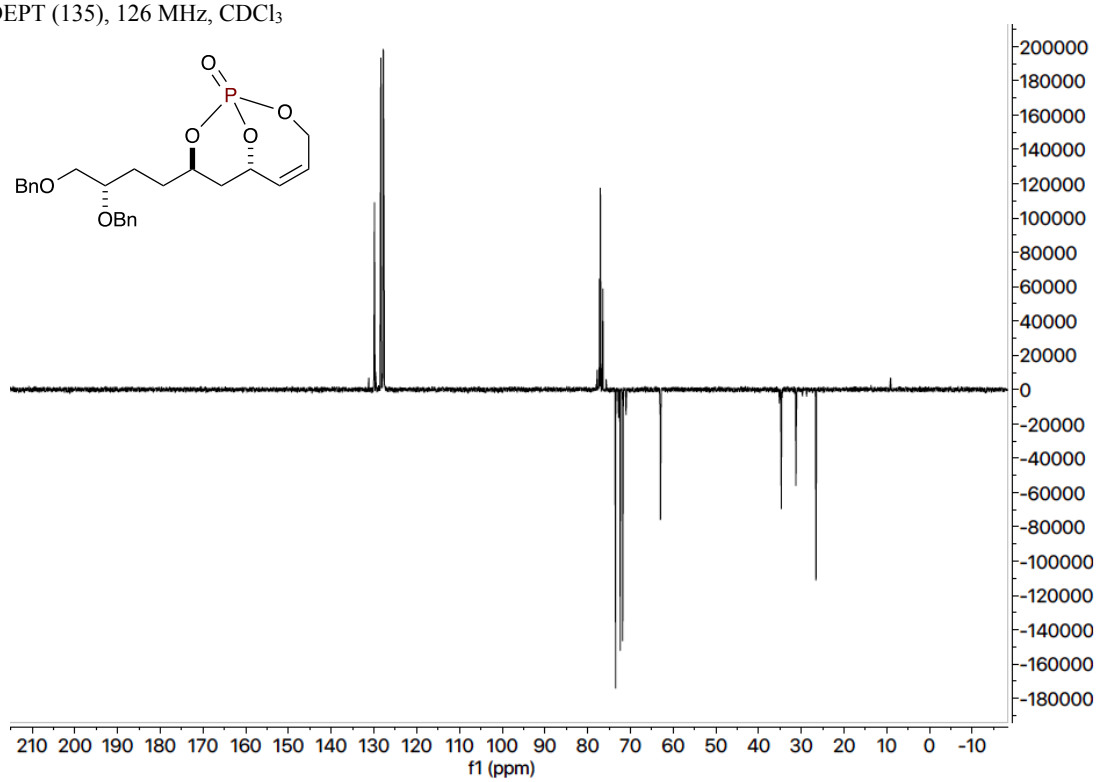

2D, $^{1}H^{1}H$, COSY, 500 MHz, $CDCl_3$

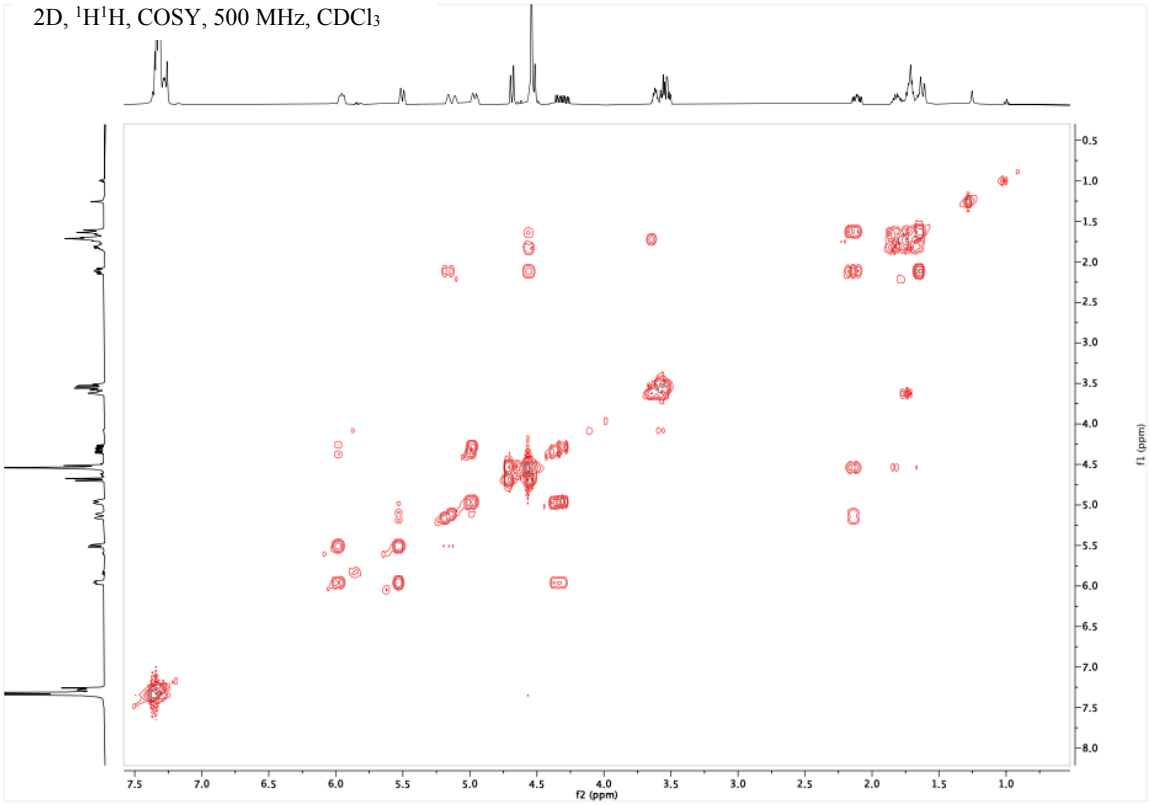

2D, $^{1}H^{13}C$, HSQC, 500 MHz, $CDCl_3$

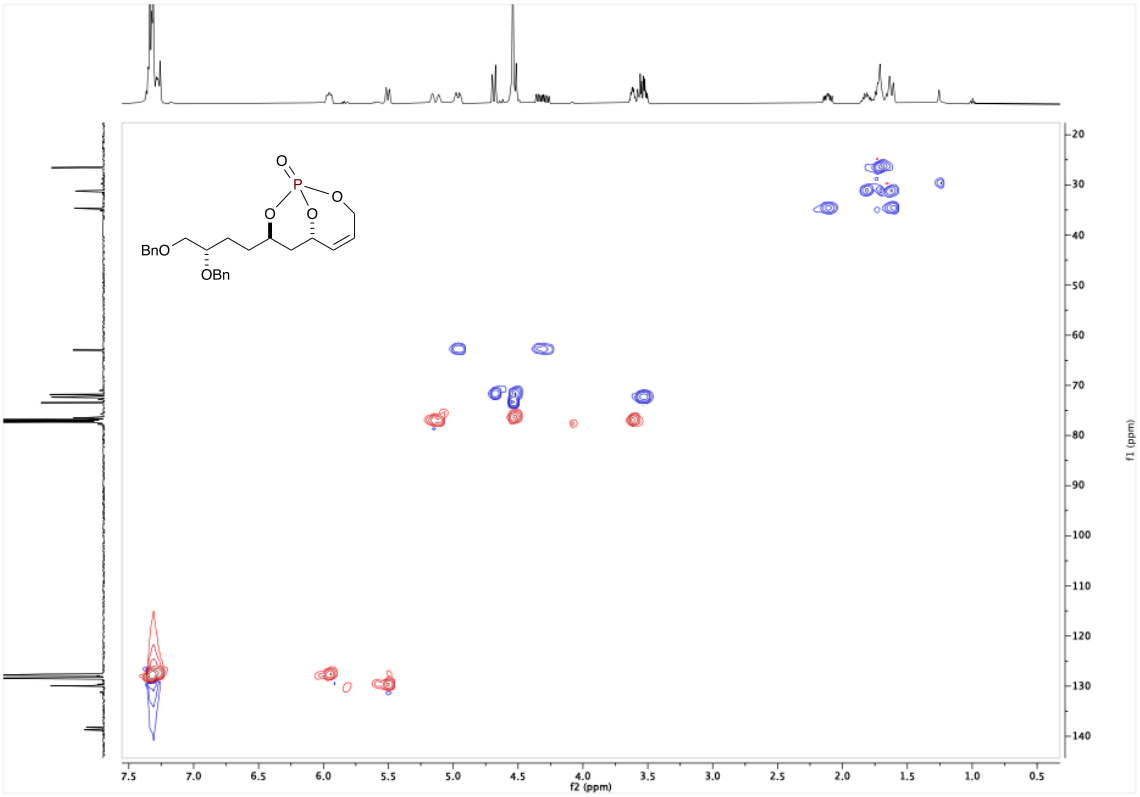

^{31}P, 202 MHz, $CDCl_3$

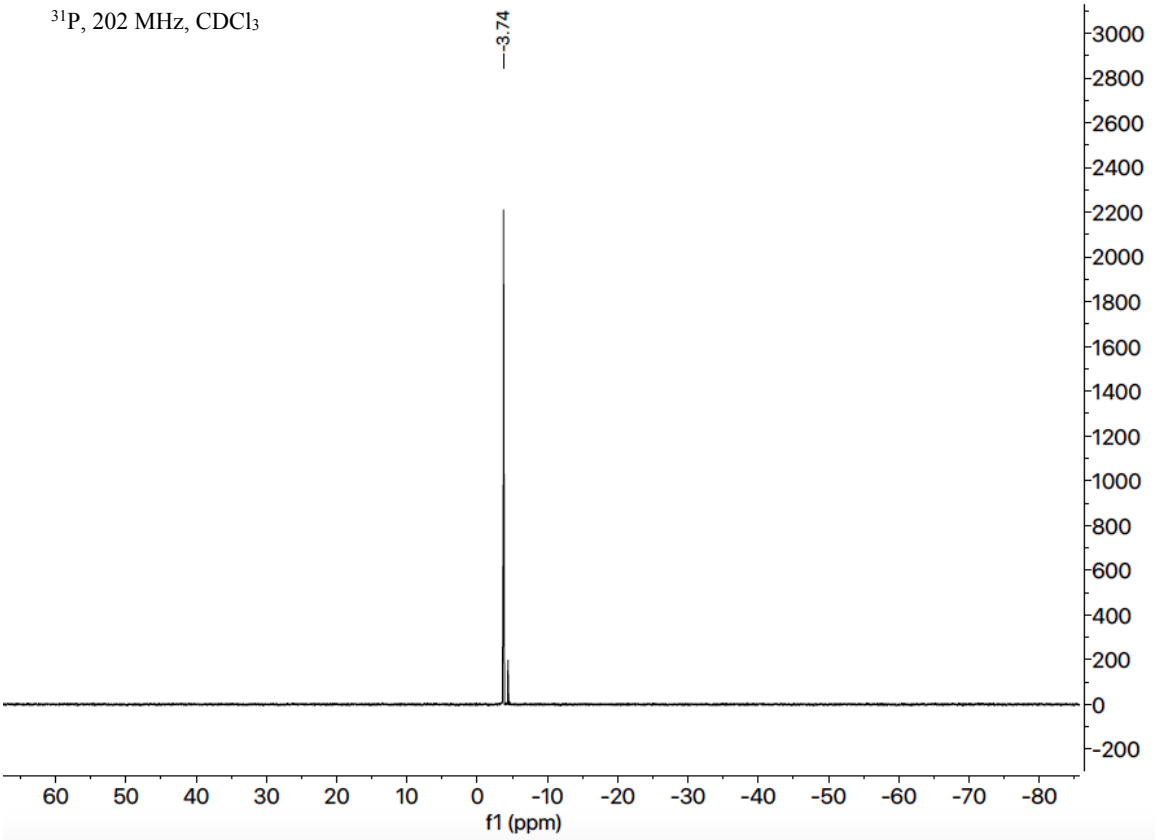

(3*R*,4*S*,6*R*)-9-(benzyloxy)-3-methylnon-1-ene-4,6-diol (4.3.1):

^{1}H, 500 MHz, $CDCl_3$

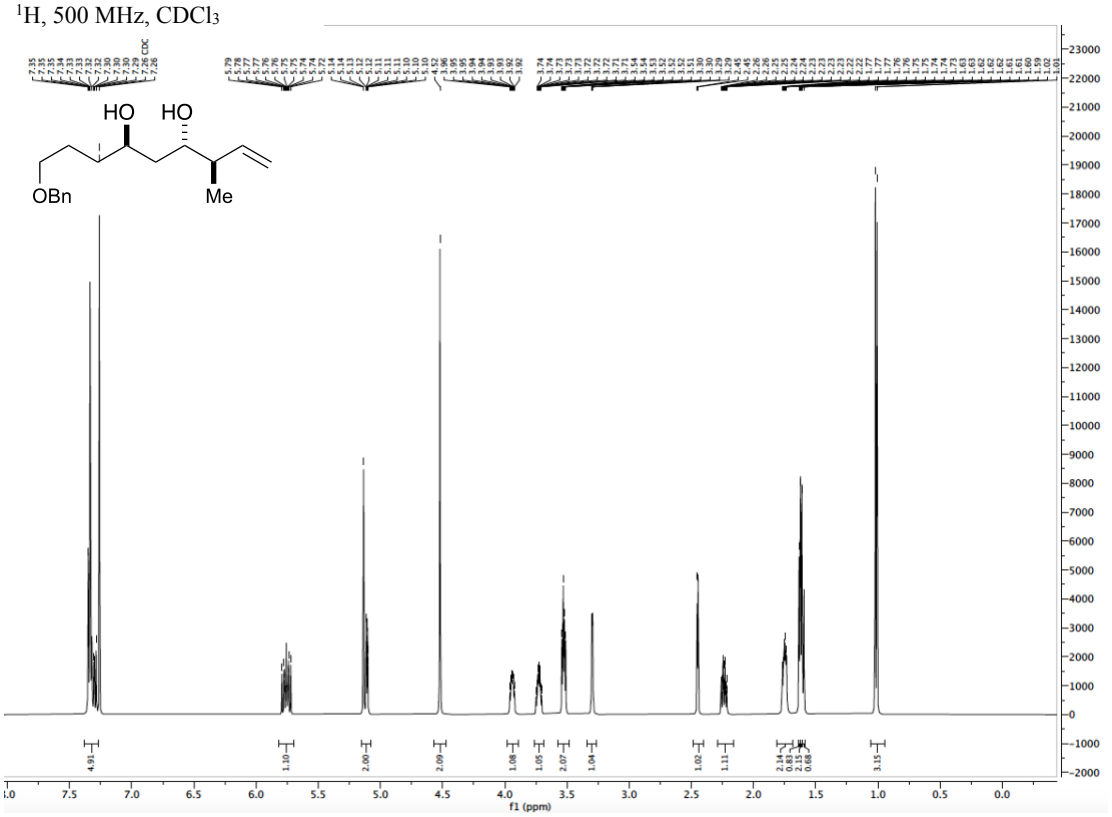

^{13}C,126 MHz, $CDCl_3$

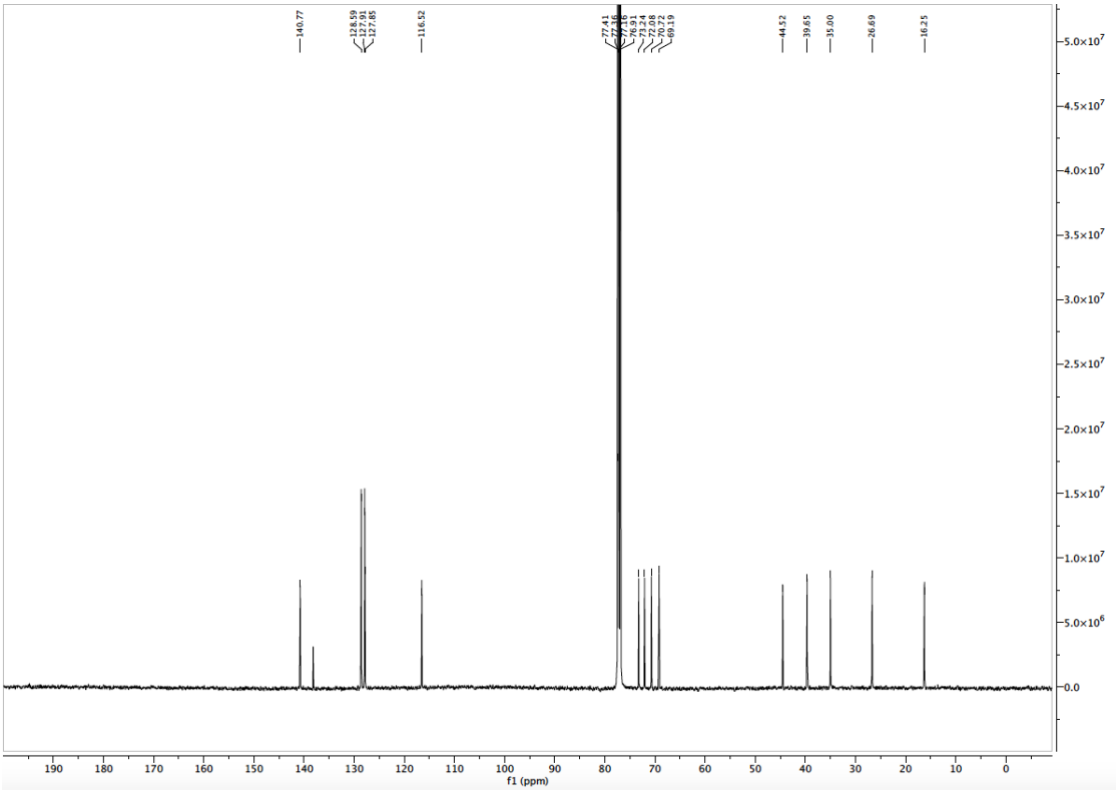

DEPT (135), 126 MHz, $CDCl_3$

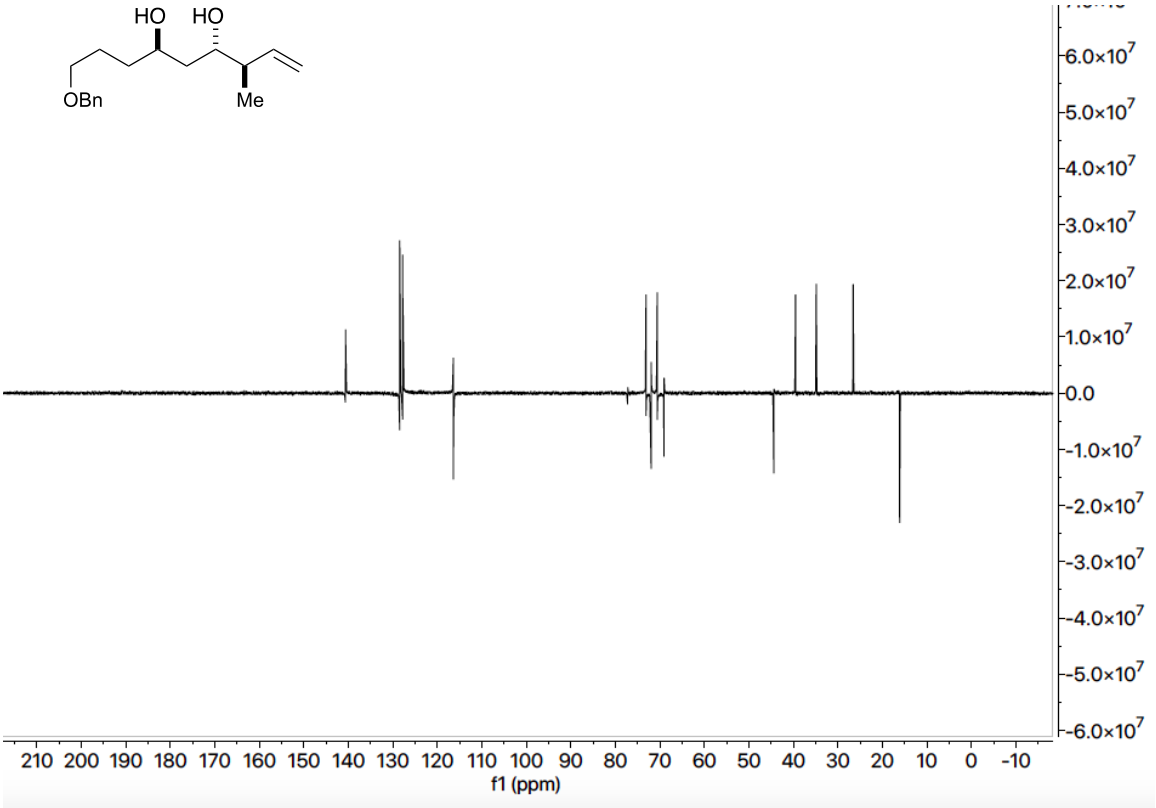

2D, $^1H^1H$, COSY, 500 MHz, $CDCl_3$

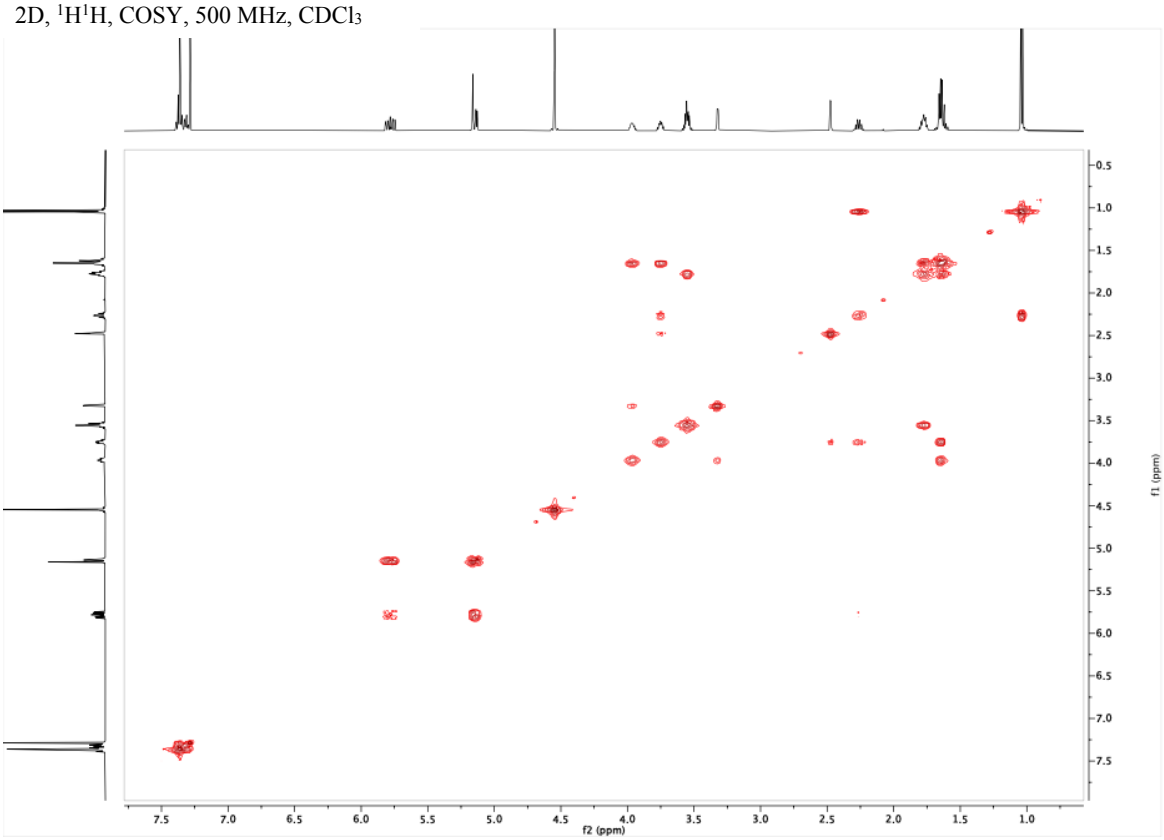

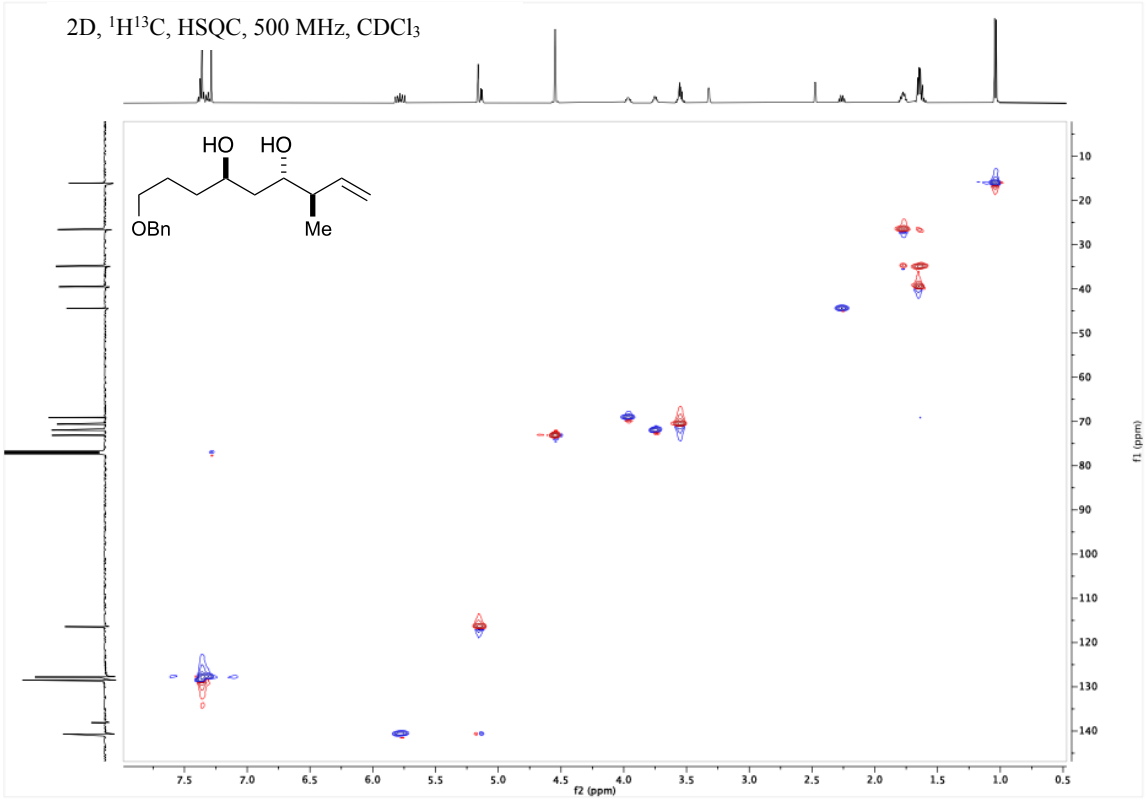
2D, $^{1}H^{13}C$, HSQC, 500 MHz, $CDCl_3$
HO
HO
OBn
Me
f2 (ppm)
f1 (ppm)

3*R*,4*S*,6*R*)-9-(benzyloxy)-3-ethylnon-1-ene-4,6-diol (4.3.2)

^{1}H, 500 MHz, $CDCl_3$

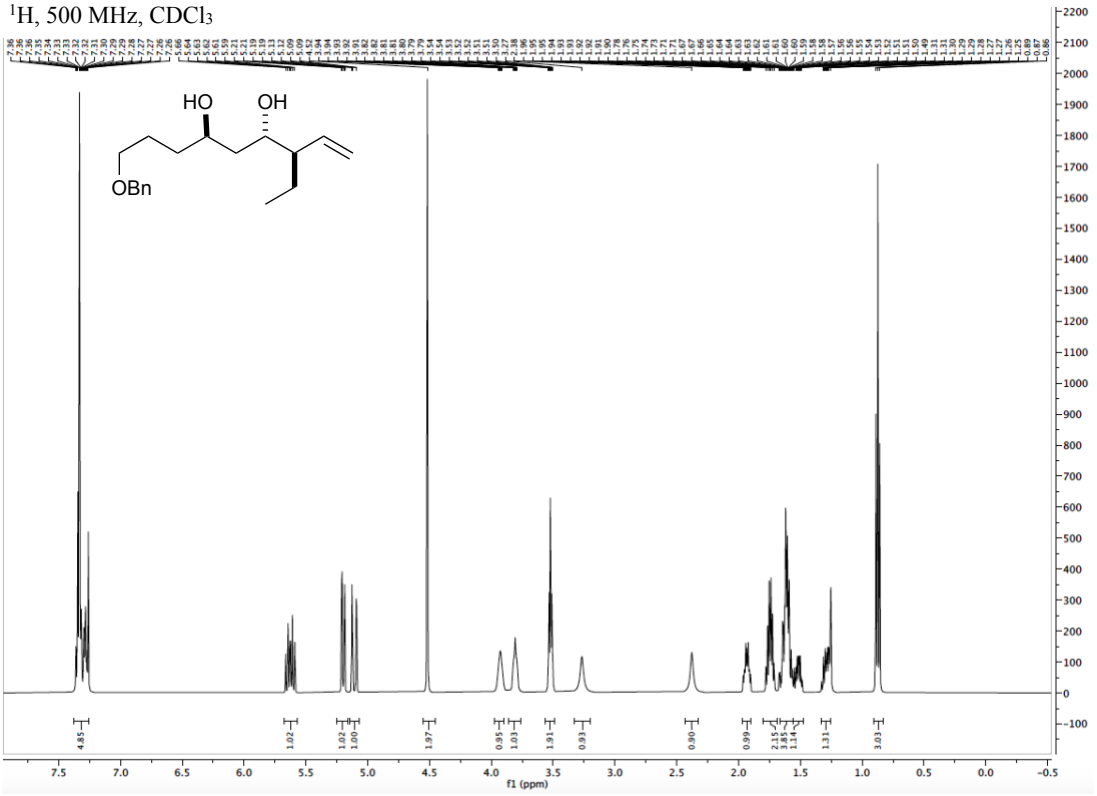

^{13}C, 126 MHz, $CDCl_3$

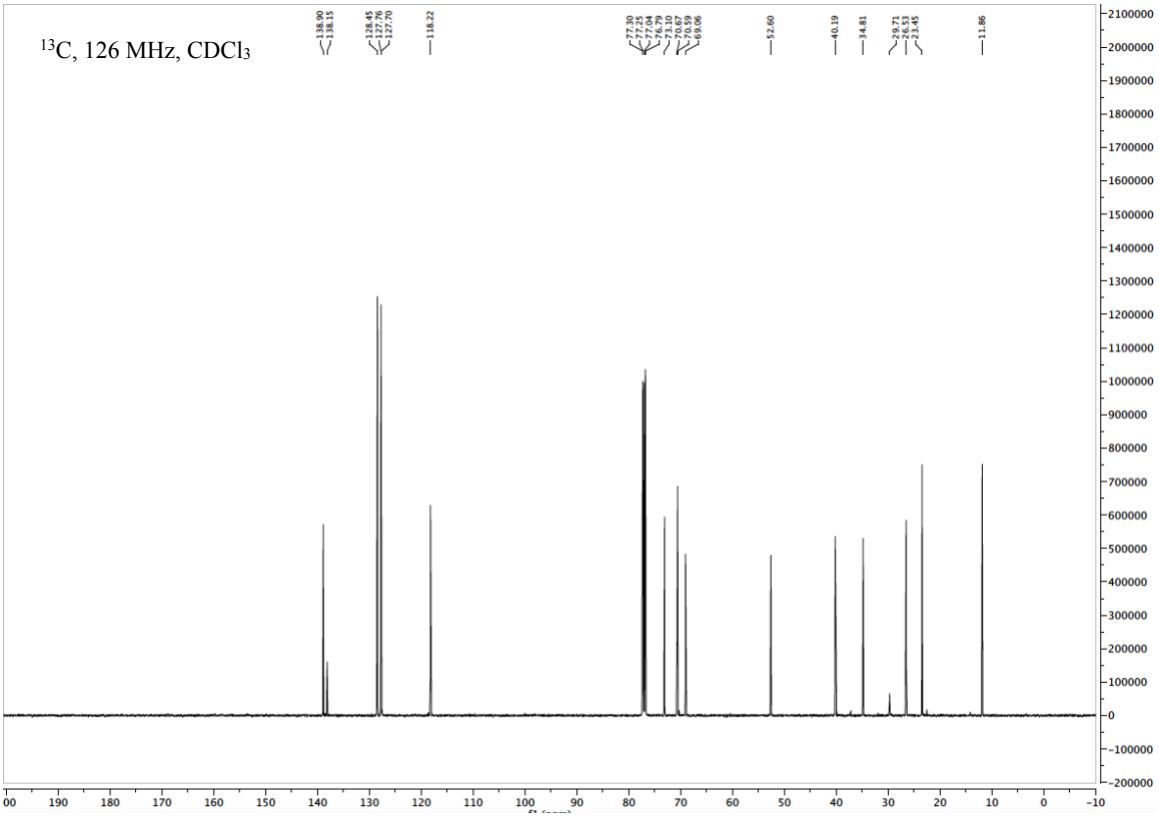

DEPT (135), 126 MHz, $CDCl_3$

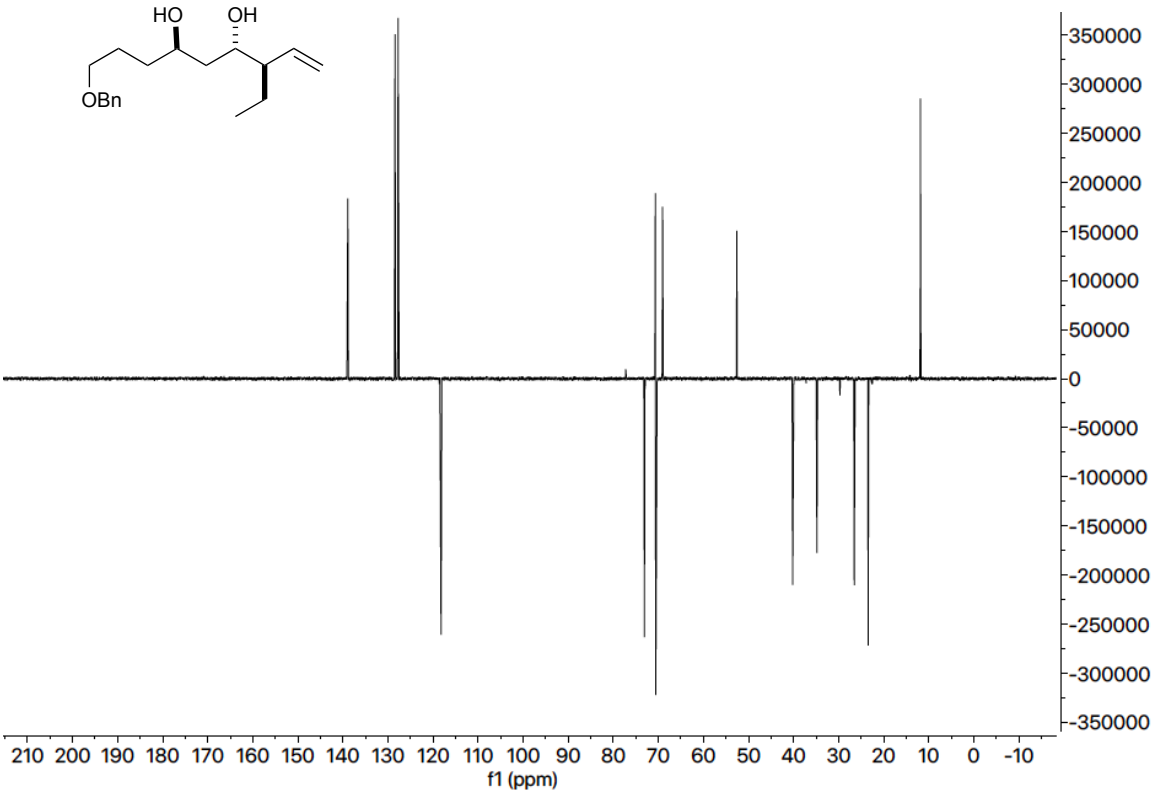

2D, $^{1}H^{1}H$, COSY, 500 MHz, $CDCl_3$

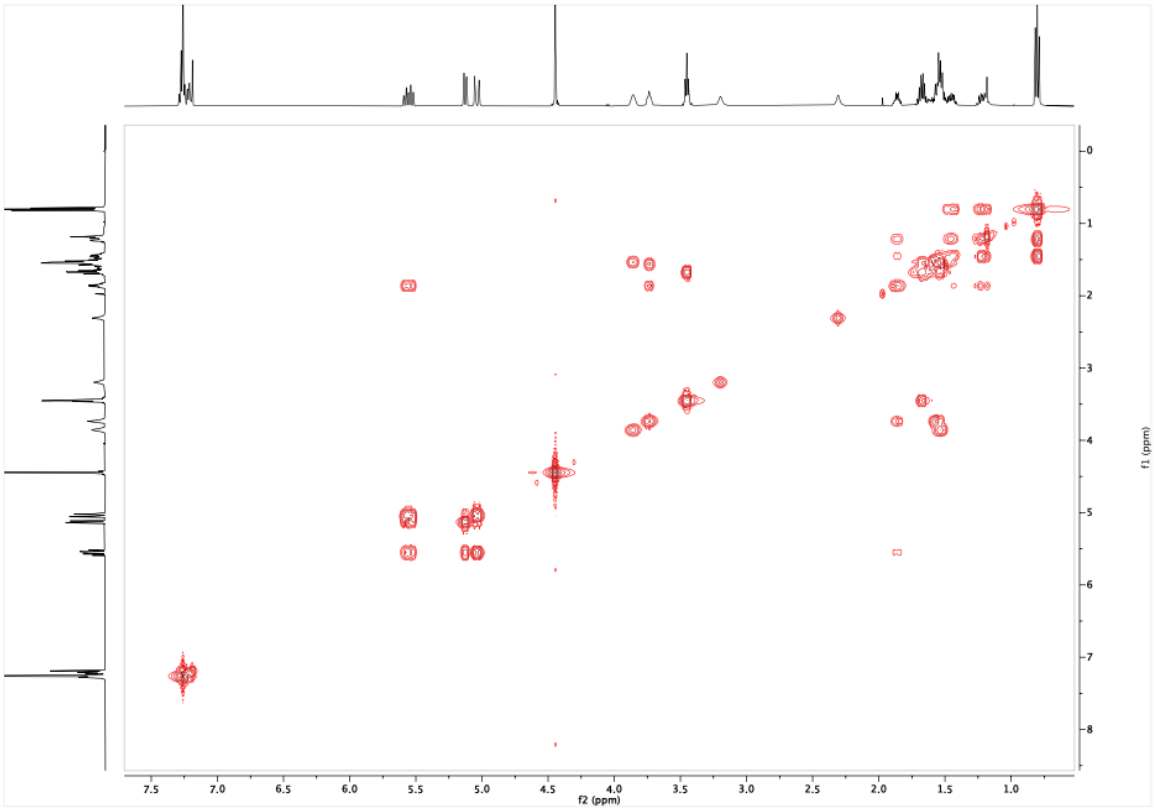

2D, $^{1}H^{13}C$, HSQC, 500 MHz, $CDCl_3$

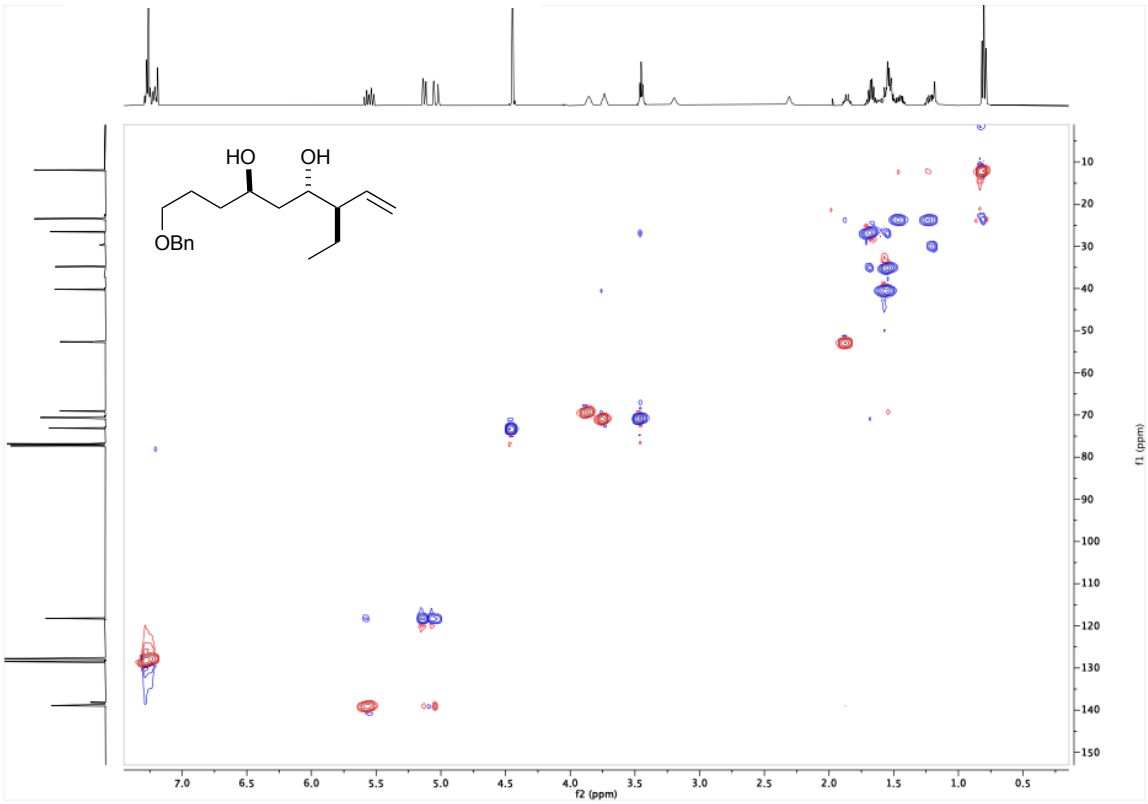

(4*R*,6*S*,7*R*)-1-(benzyloxy)-7-vinyltridecane-4,6-diol (4.3.3)

^{1}H, 500 MHz, $CDCl_3$

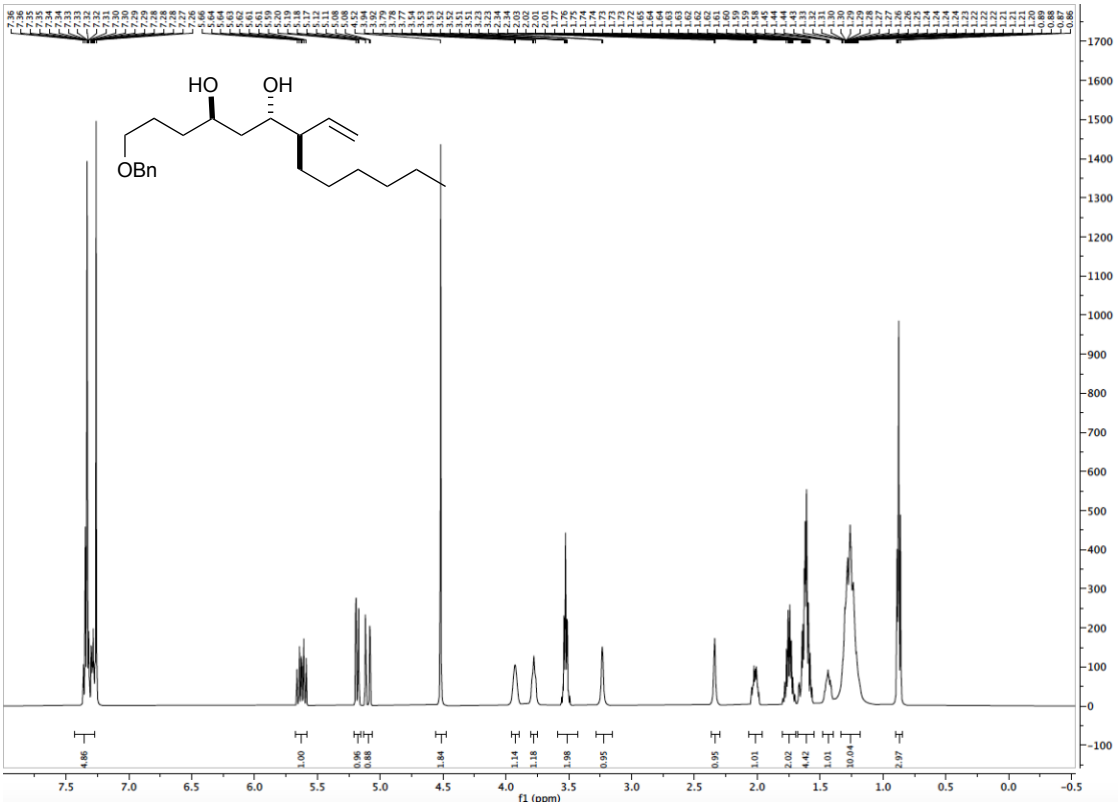

^{13}C, 126 MHz, $CDCl_3$

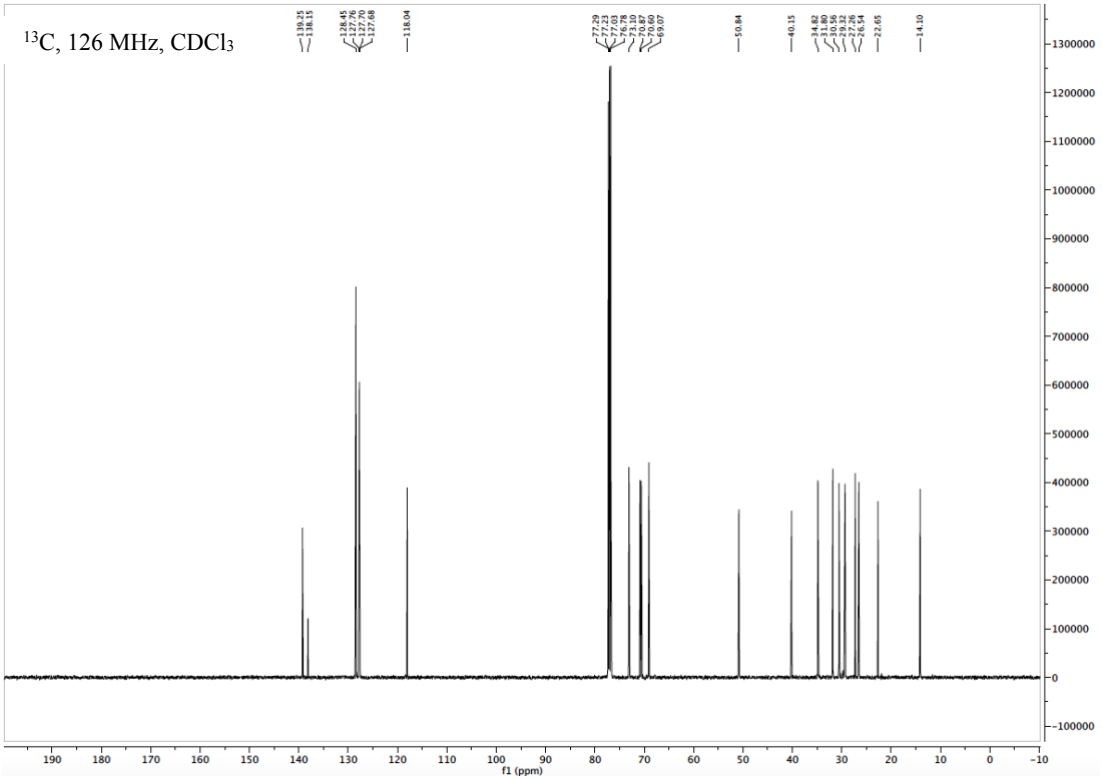

DEPT (135), 126 MHz, $CDCl_3$

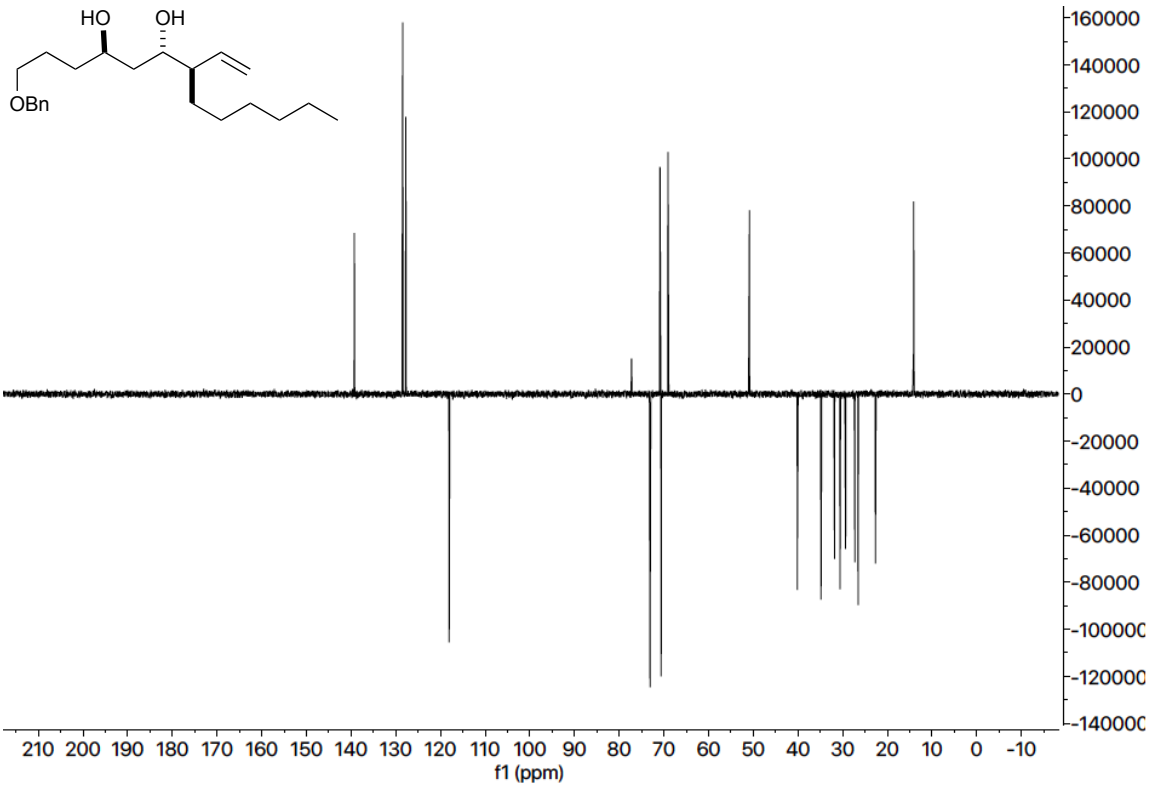

2D, $^{1}H^{1}H$, COSY, 500 MHz, $CDCl_3$

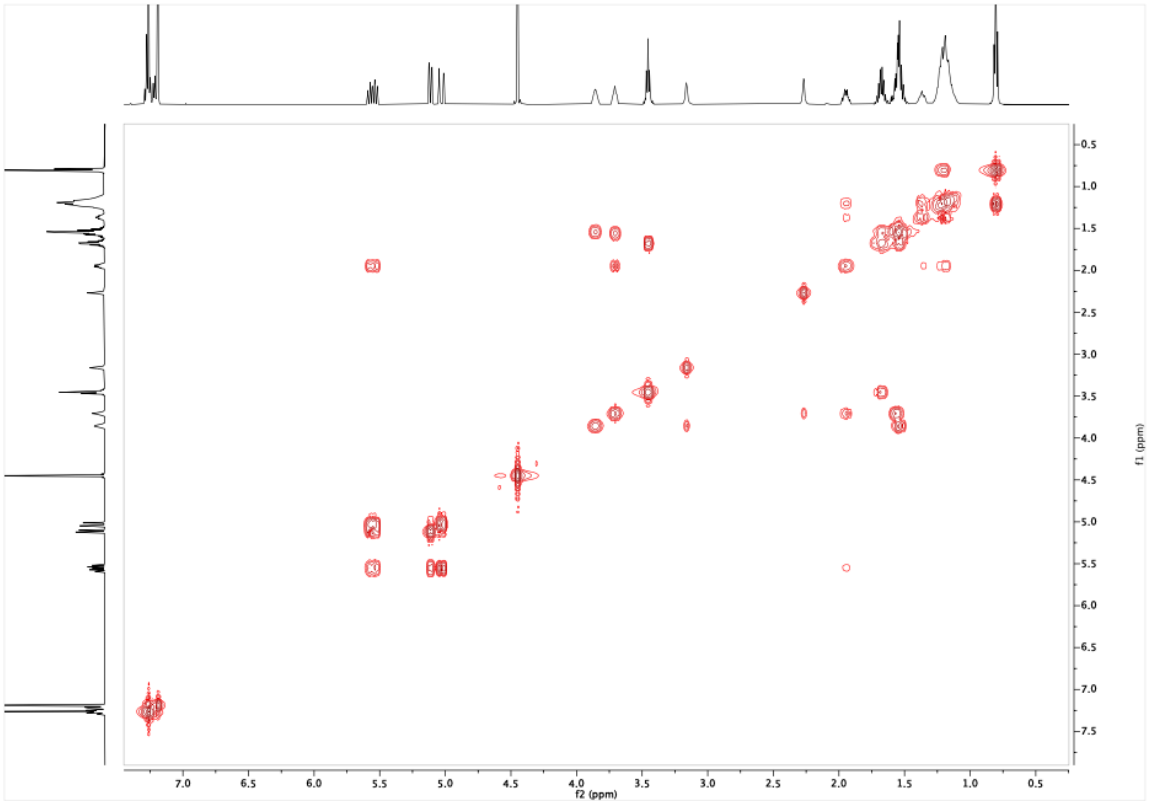

2D, $^{1}H^{13}C$, HSQC, 500 MHz, $CDCl_3$

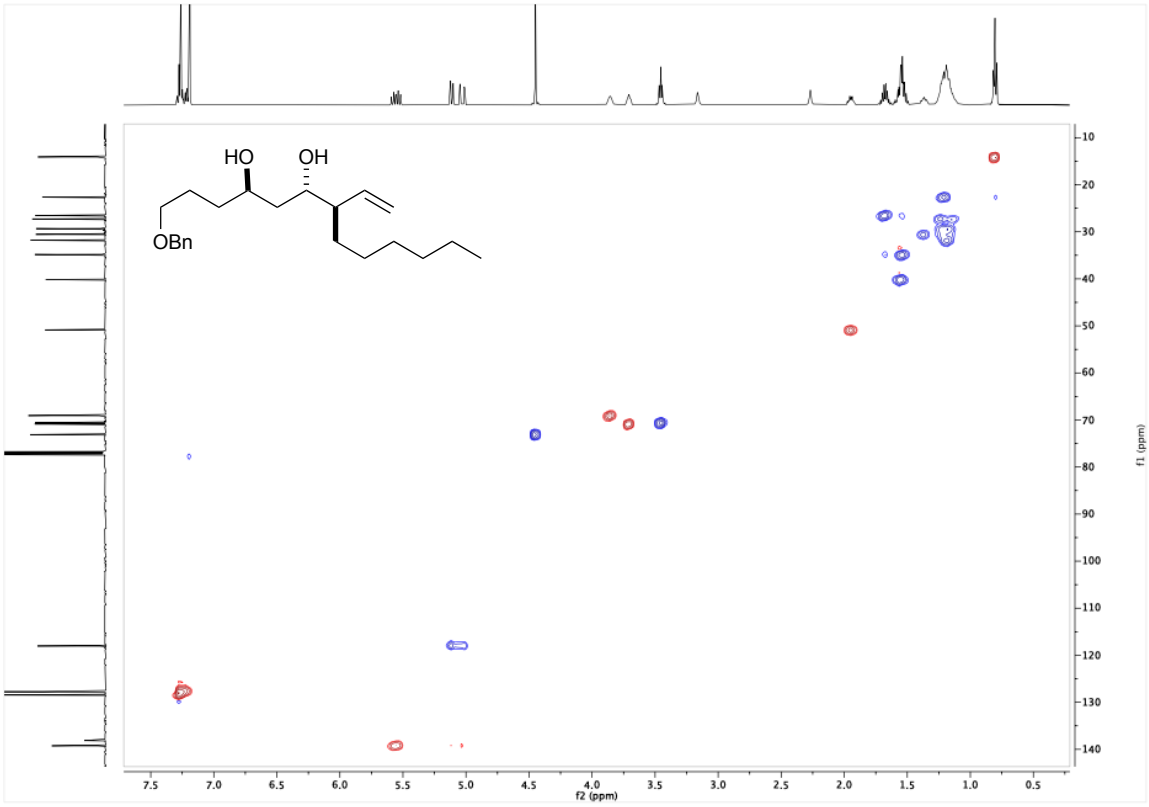

(4*R*,6*R*)-9-(benzyloxy)non-1-ene-4,6-diol (4.3.4):

^{1}H, 500 MHz, $CDCl_3$

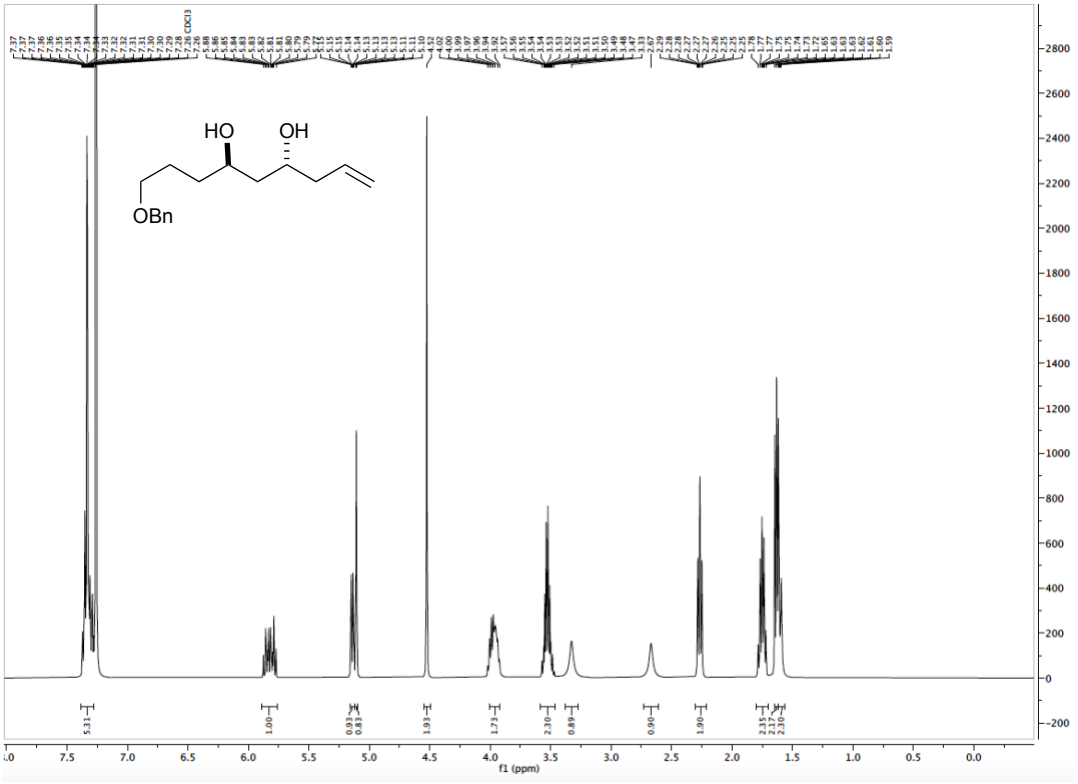

^{13}C, 126 MHz, $CDCl_3$

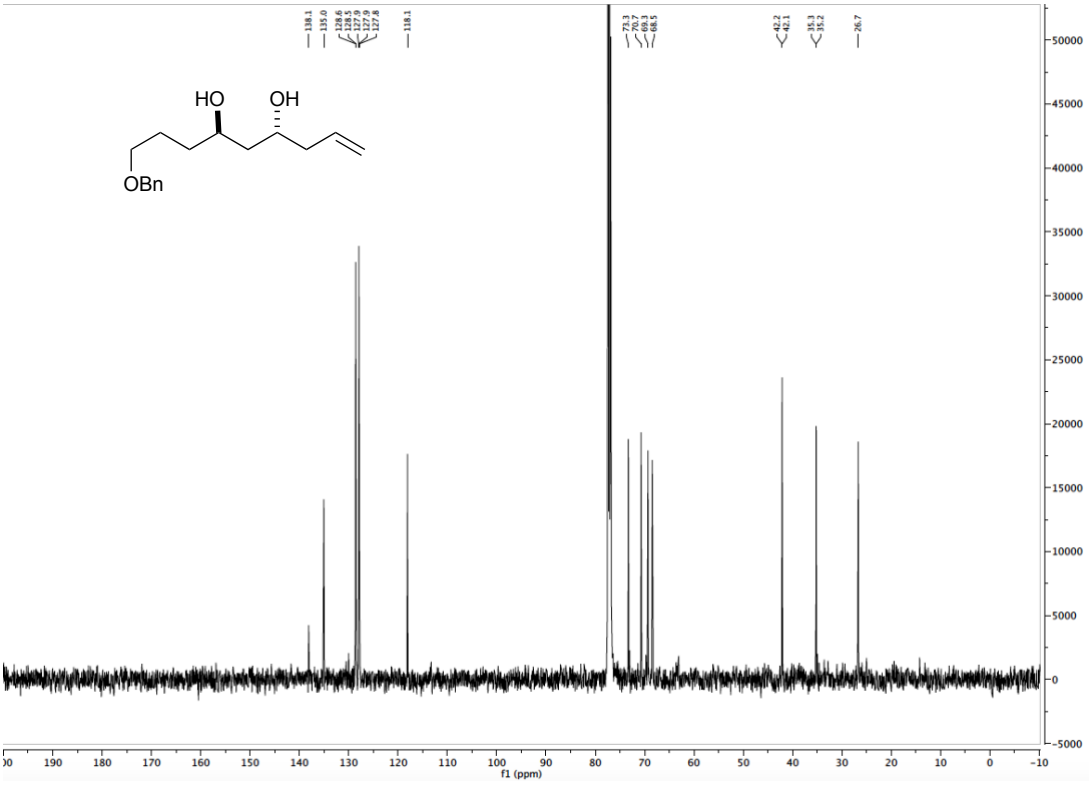

DEPT (135), 126 MHz, $CDCl_3$

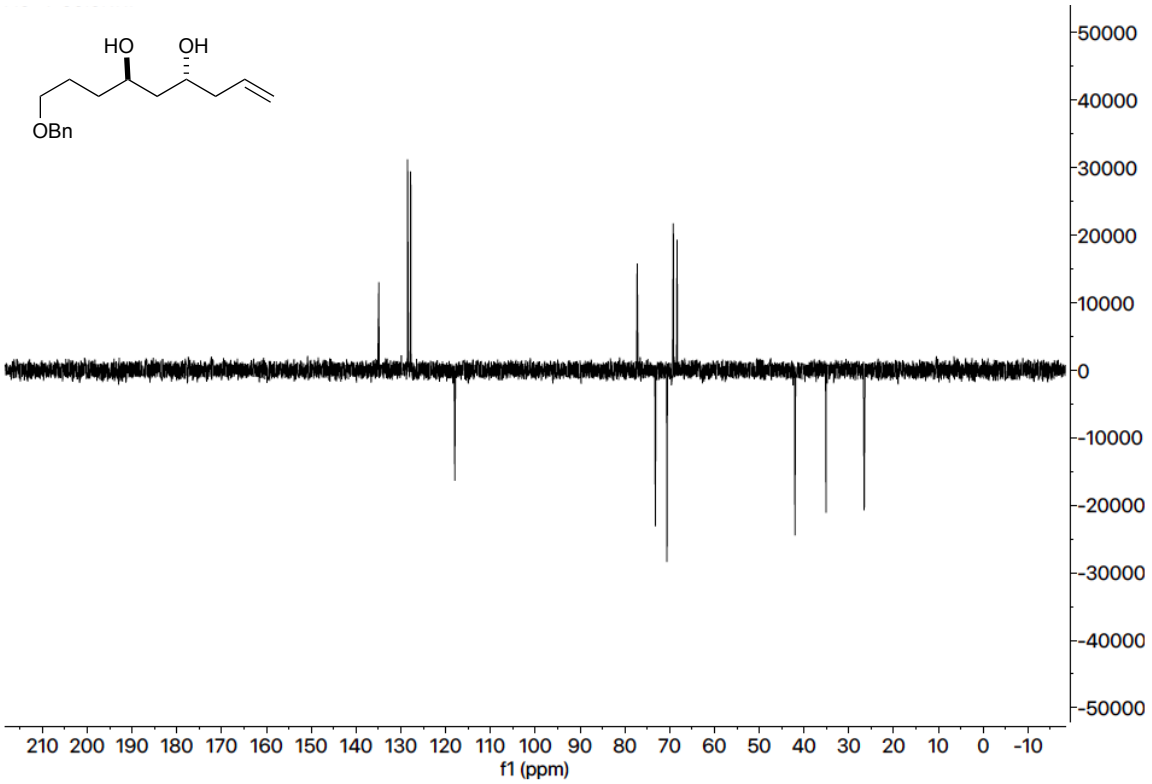

2D, $^{1}H^{1}H$, COSY, 500 MHz, $CDCl_3$

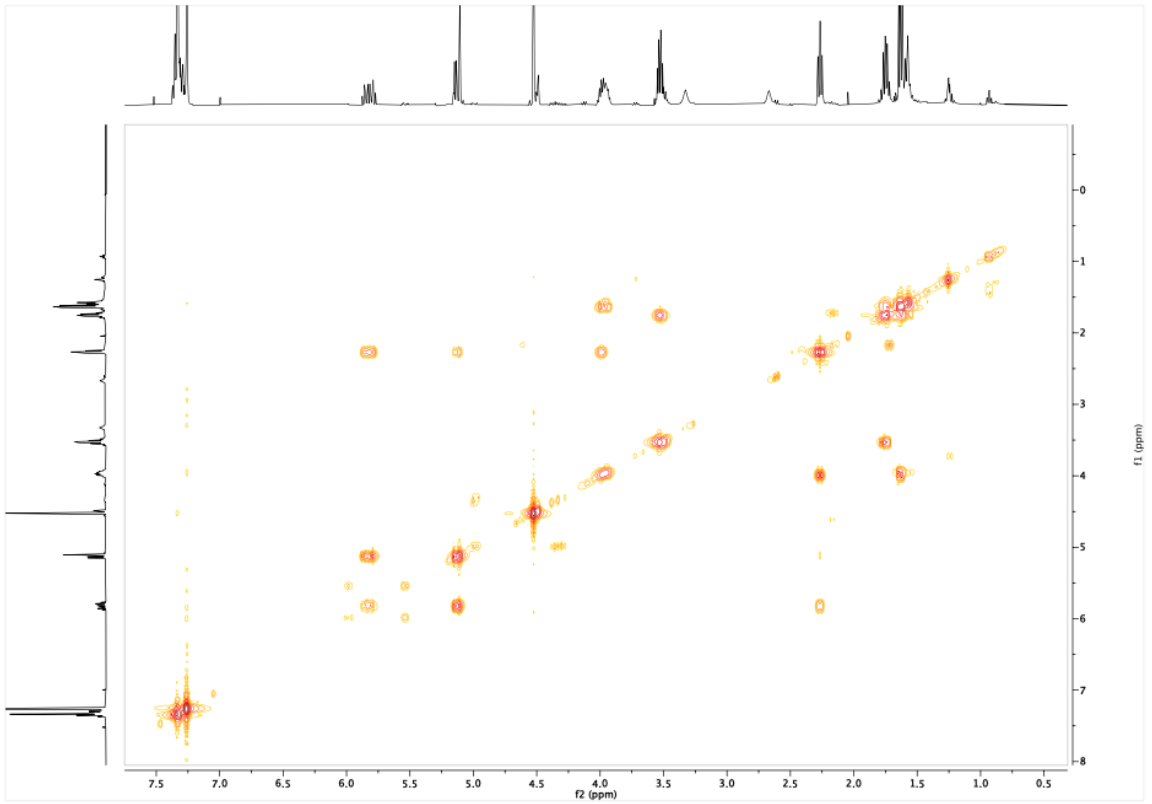

2D, $^{1}H^{13}C$, HSQC, 500 MHz, $CDCl_3$

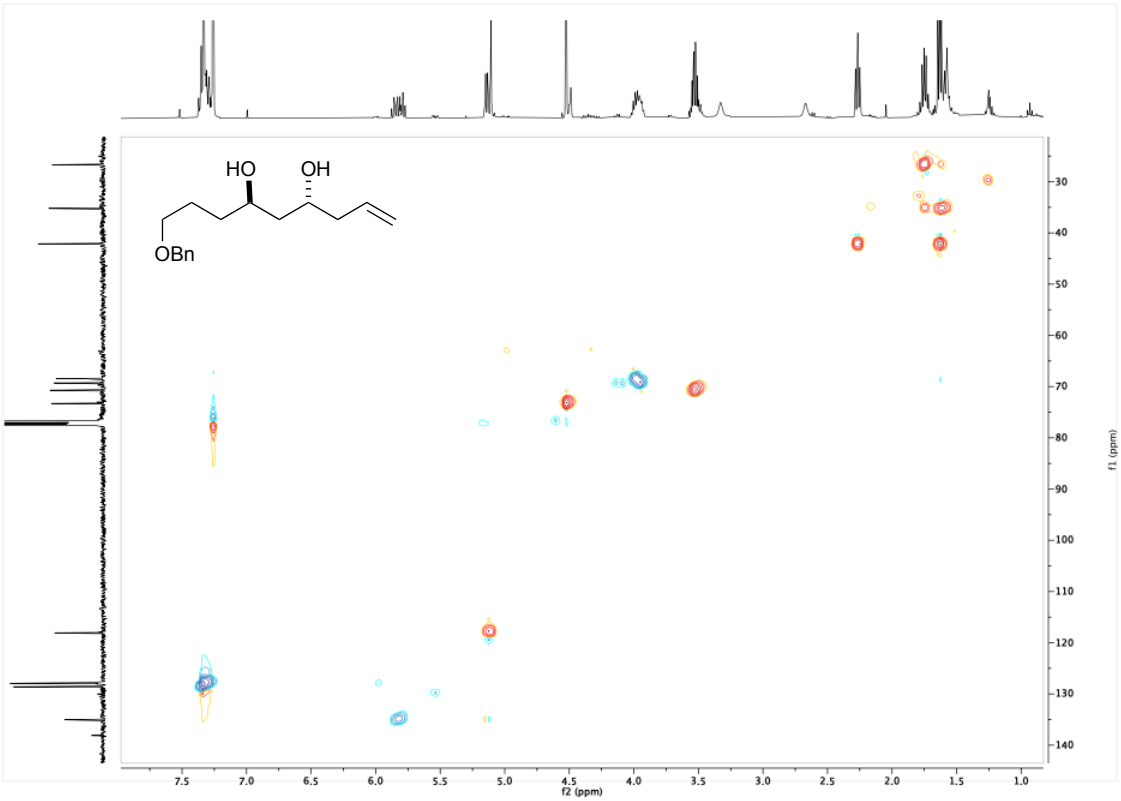

(3R,4S,6R,9S)-9,10-bis(benzyloxy)-3-methyldec-1-ene-4,6-diol (4.4.1)

^{1}H, 500 MHz, $CDCl_3$

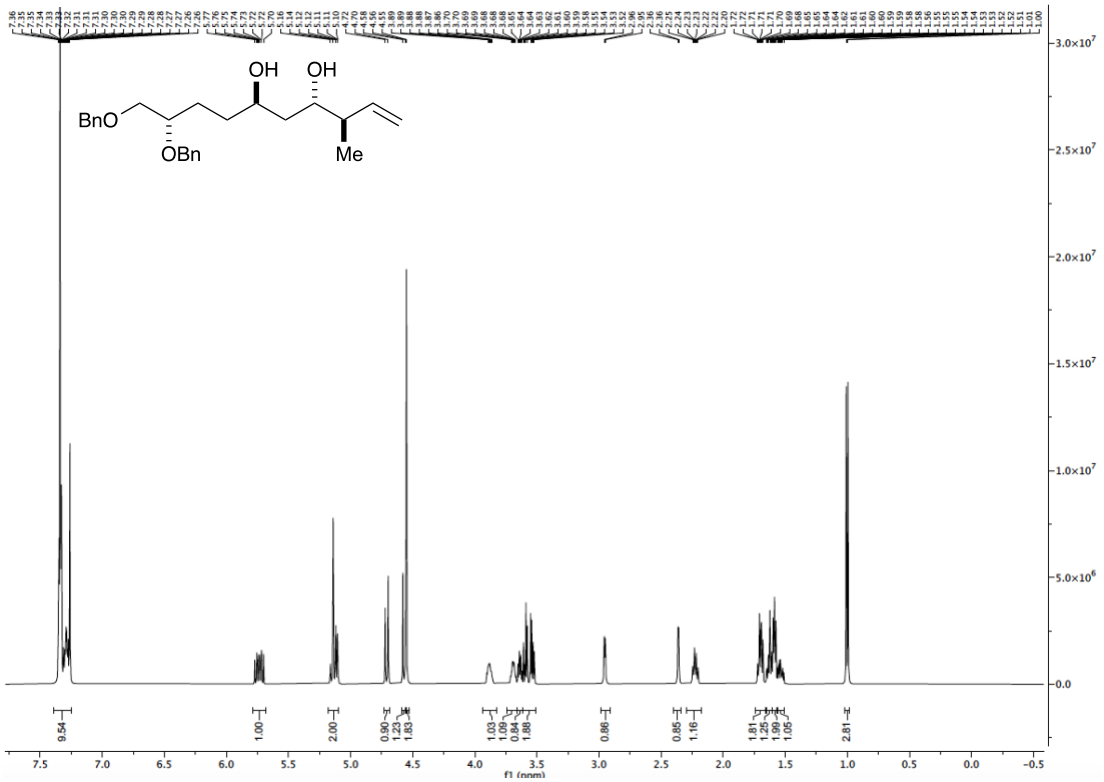

^{13}C, 126 MHz, $CDCl_3$

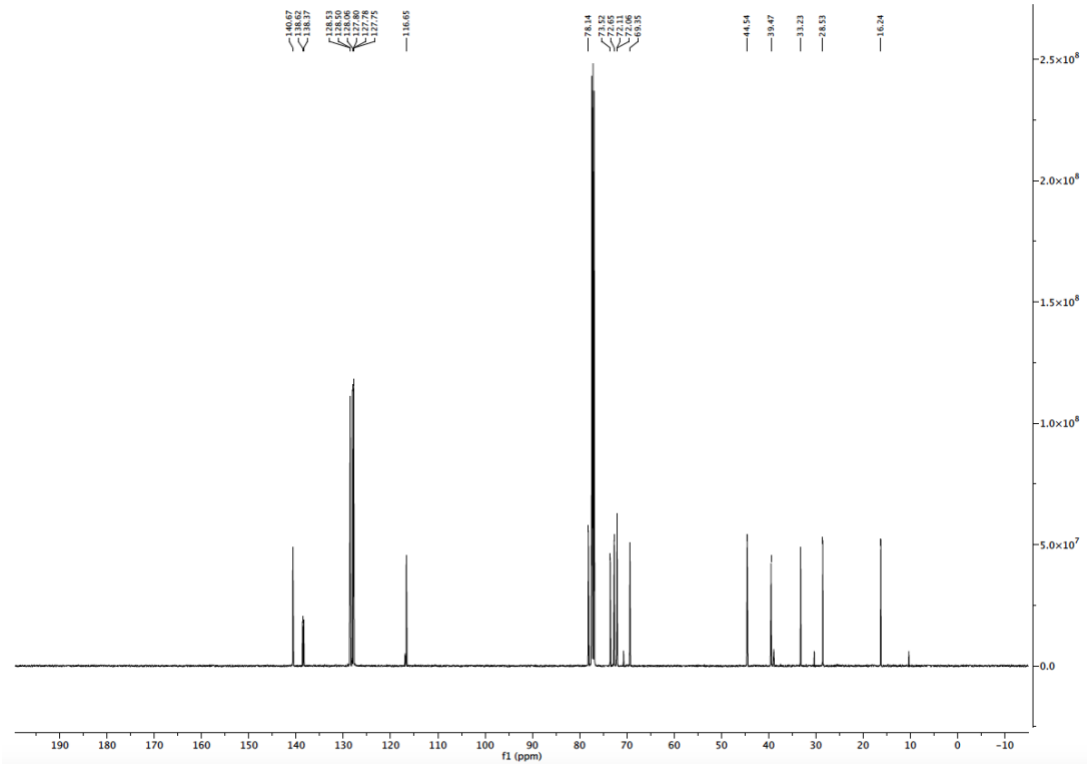

DEPT (135), 126 MHz, $CDCl_3$

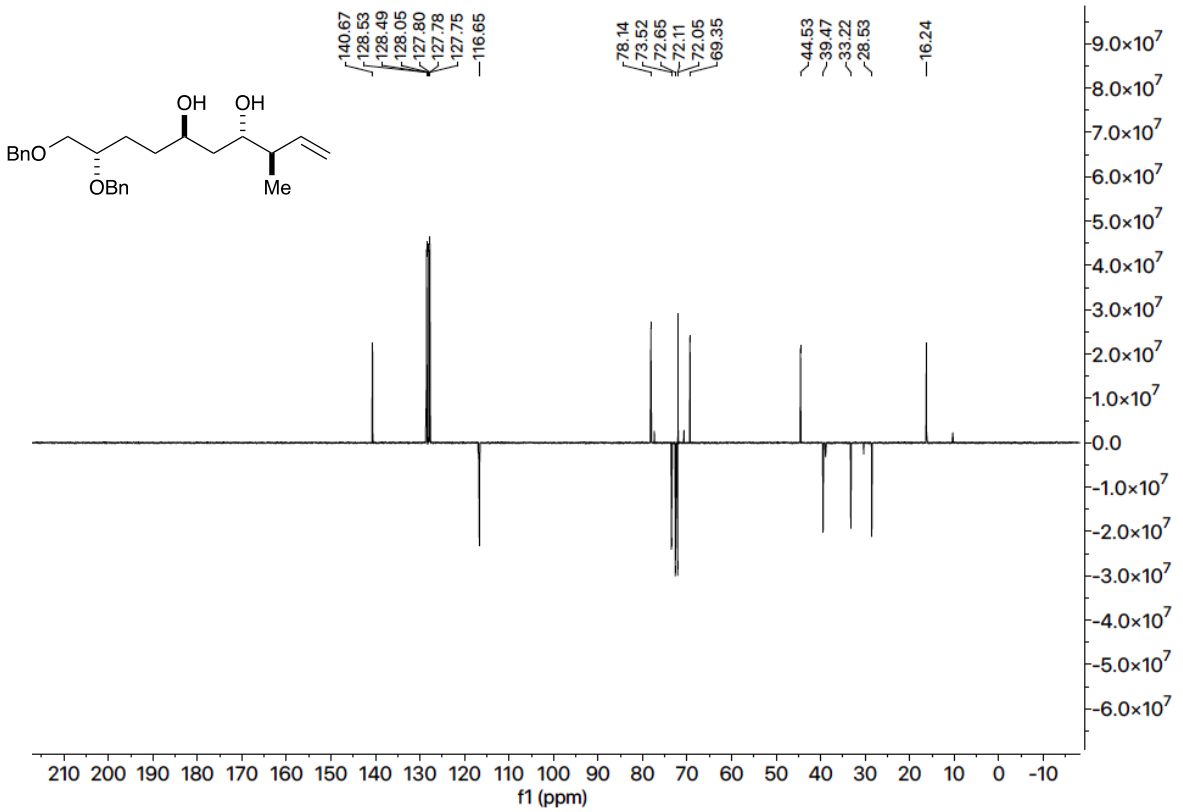

2D, $^{1}H^{1}H$, COSY, 500 MHz, $CDCl_3$

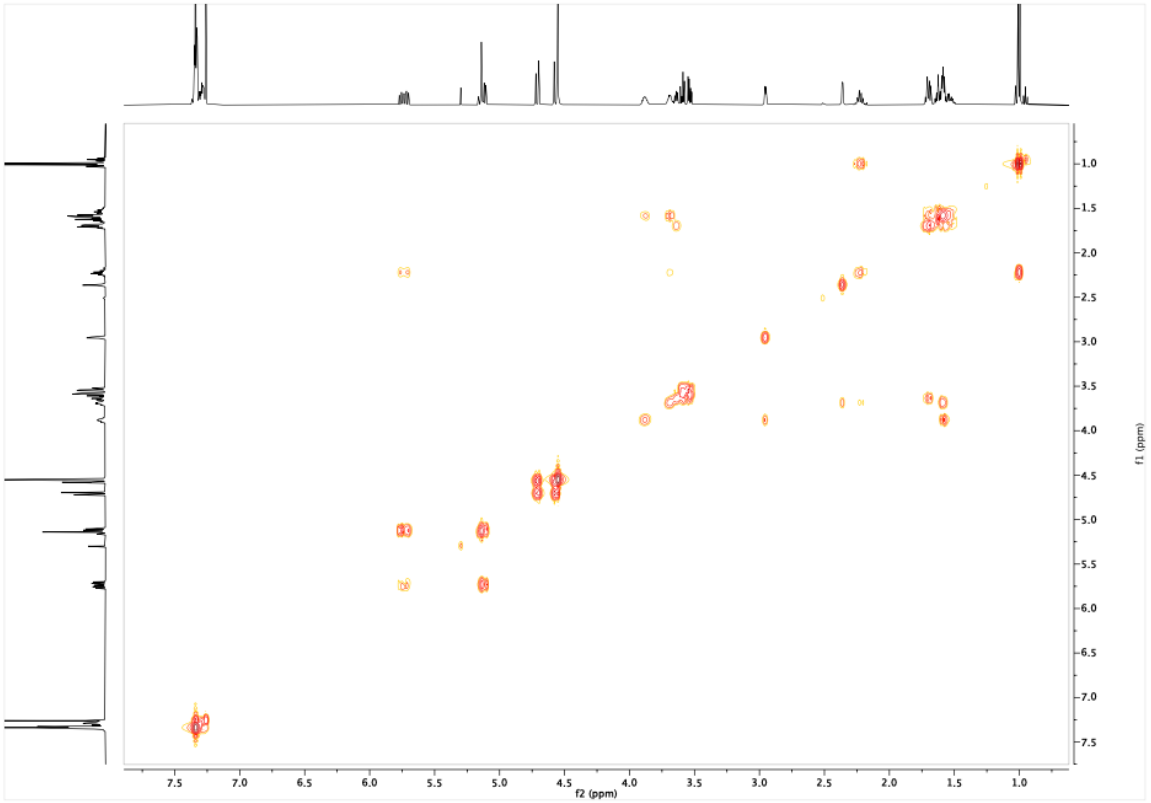

2D, $^{1}H^{13}C$, HSQC, 500 MHz, $CDCl_3$

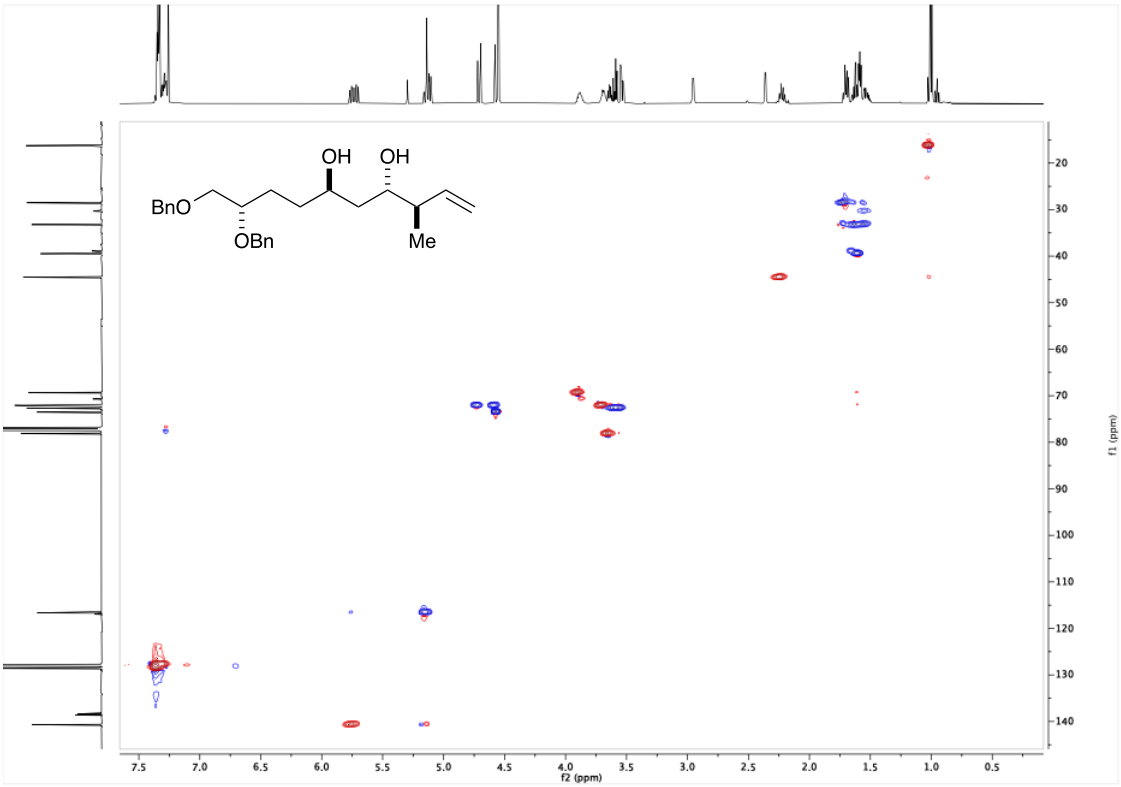

(4*R*,6*R*,9*S*)-9,10-bis(benzyloxy)dec-1-ene-4,6-diol (4.4.2)

^{1}H, 500 MHz, $CDCl_3$

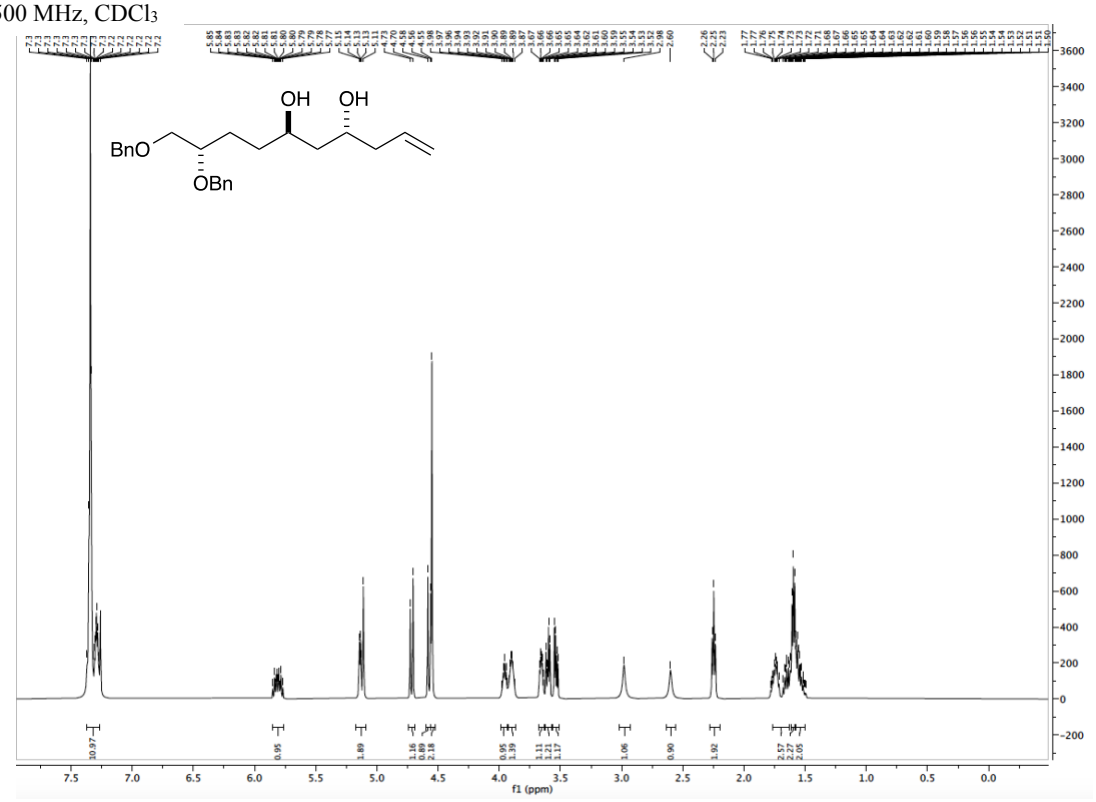

^{13}C, 126 MHz, $CDCl_3$

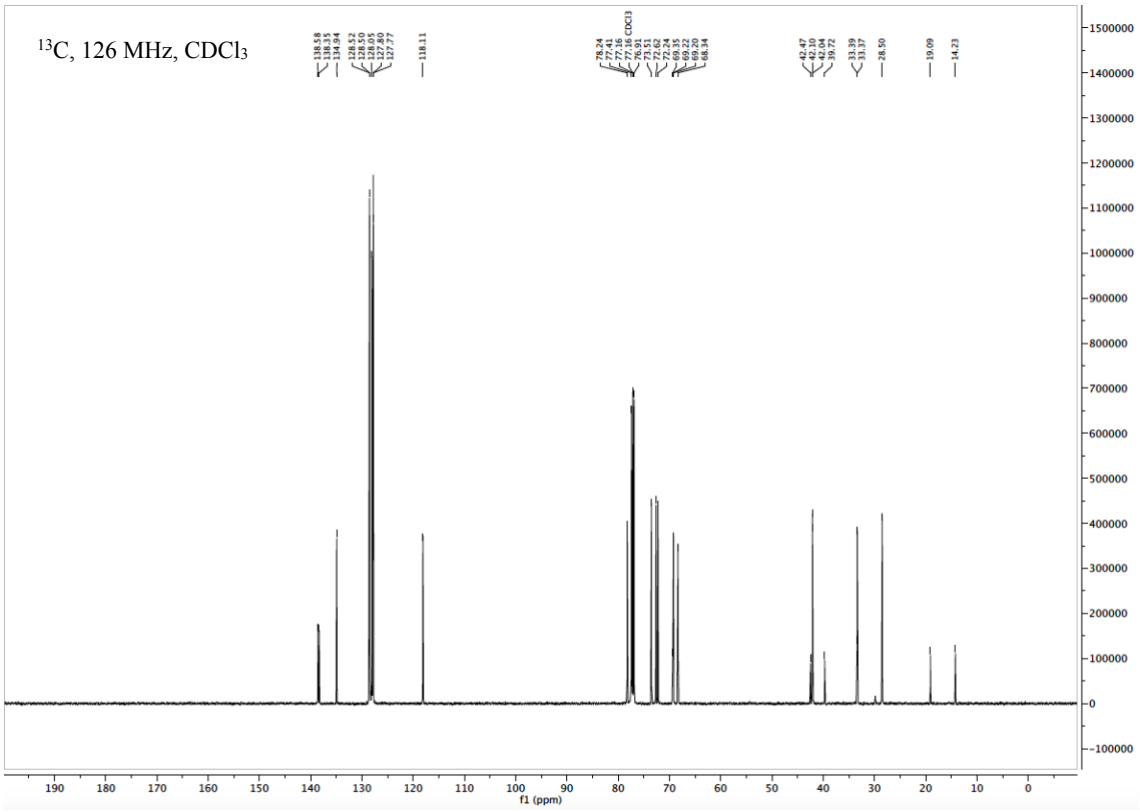

DEPT (135), 126 MHz, $CDCl_3$

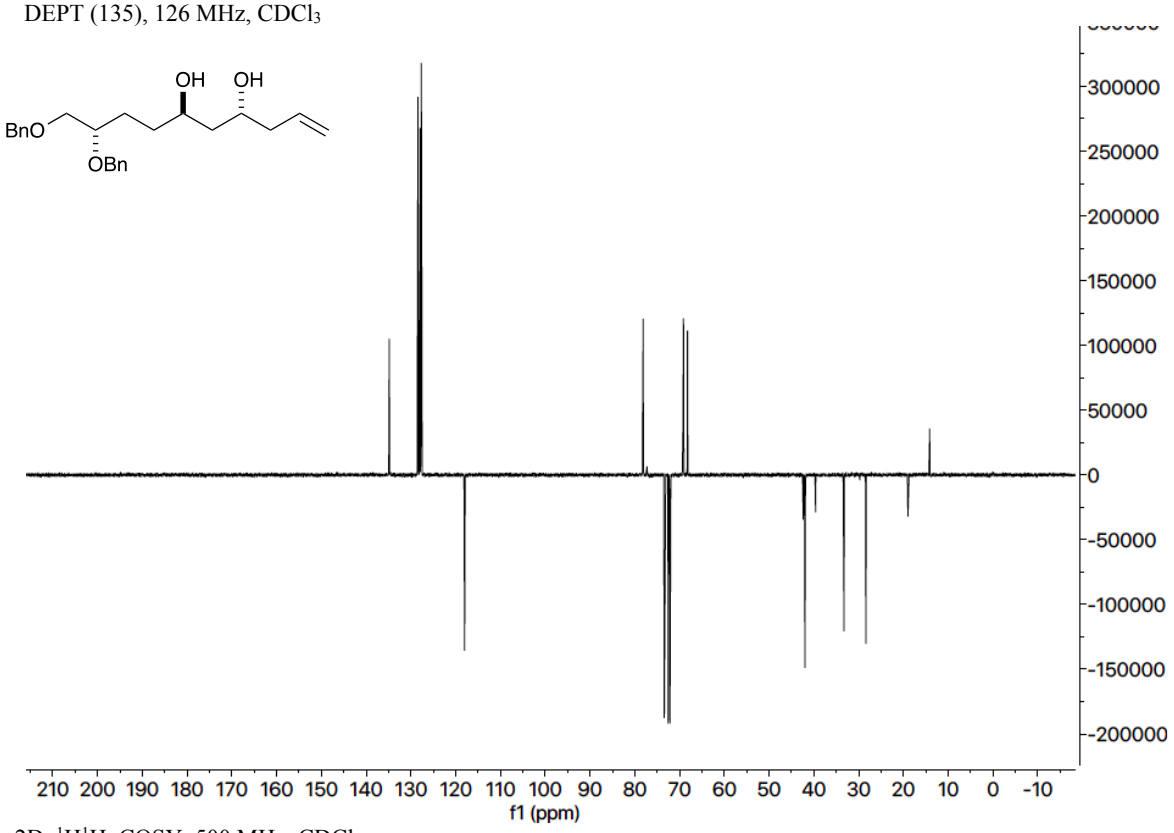

2D, $^1H^1H$, COSY, 500 MHz, $CDCl_3$

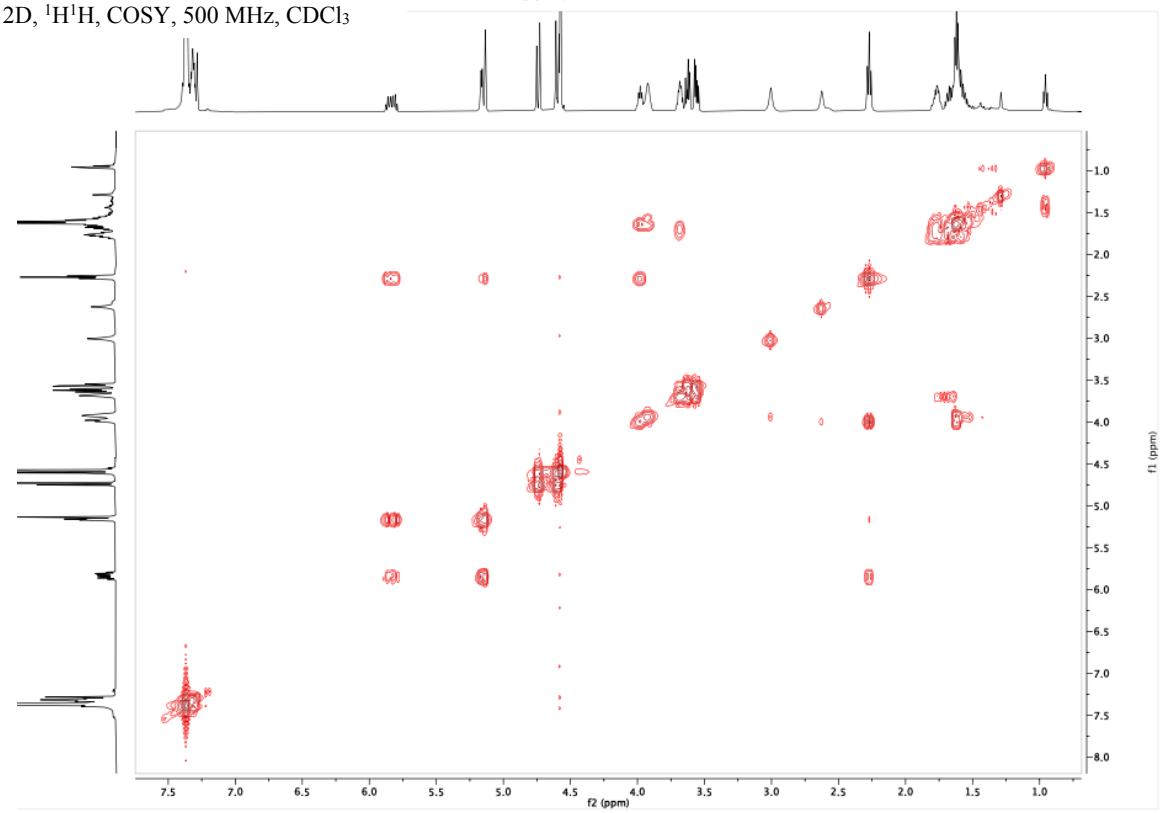

2D, $^{1}H^{13}C$, HSQC, 500 MHz, $CDCl_3$

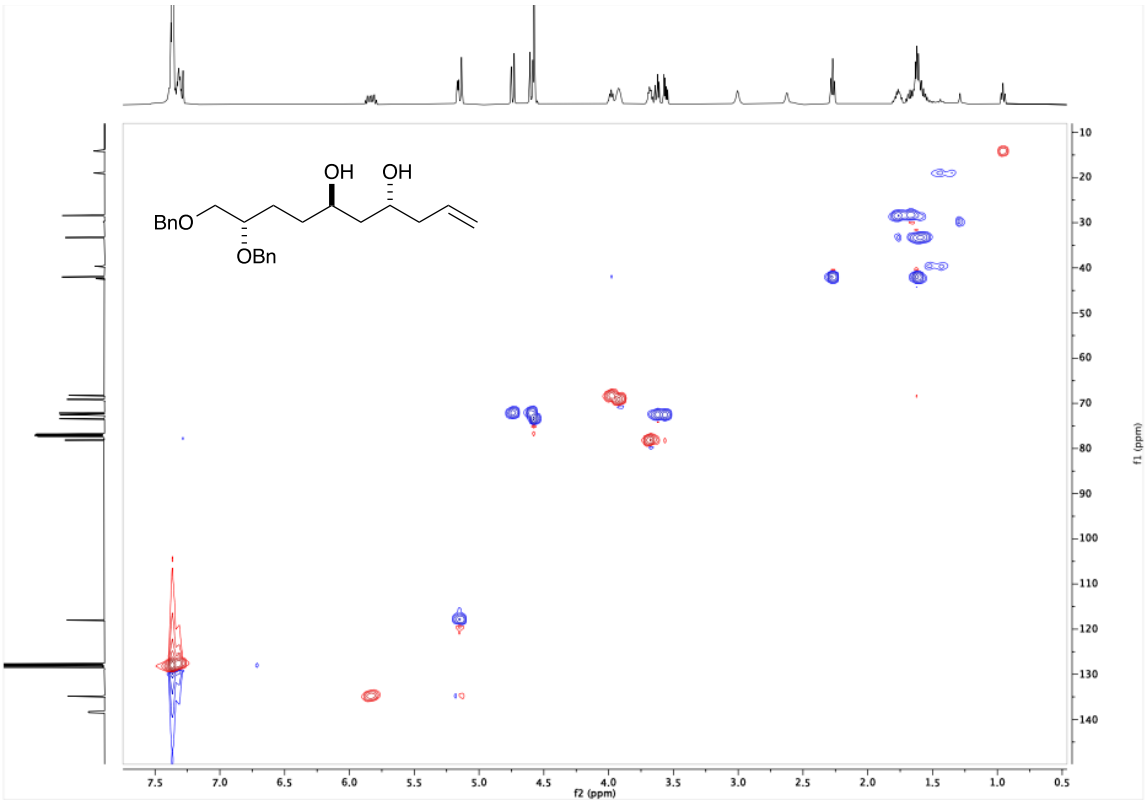

(3*R*,4*S*,6*R*)-9-(benzyloxy)-3-methyl-6-((triisopropylsilyl)oxy)non-1-en-4-ol (4.5.1)

^{1}H, 500 MHz, $CDCl_3$

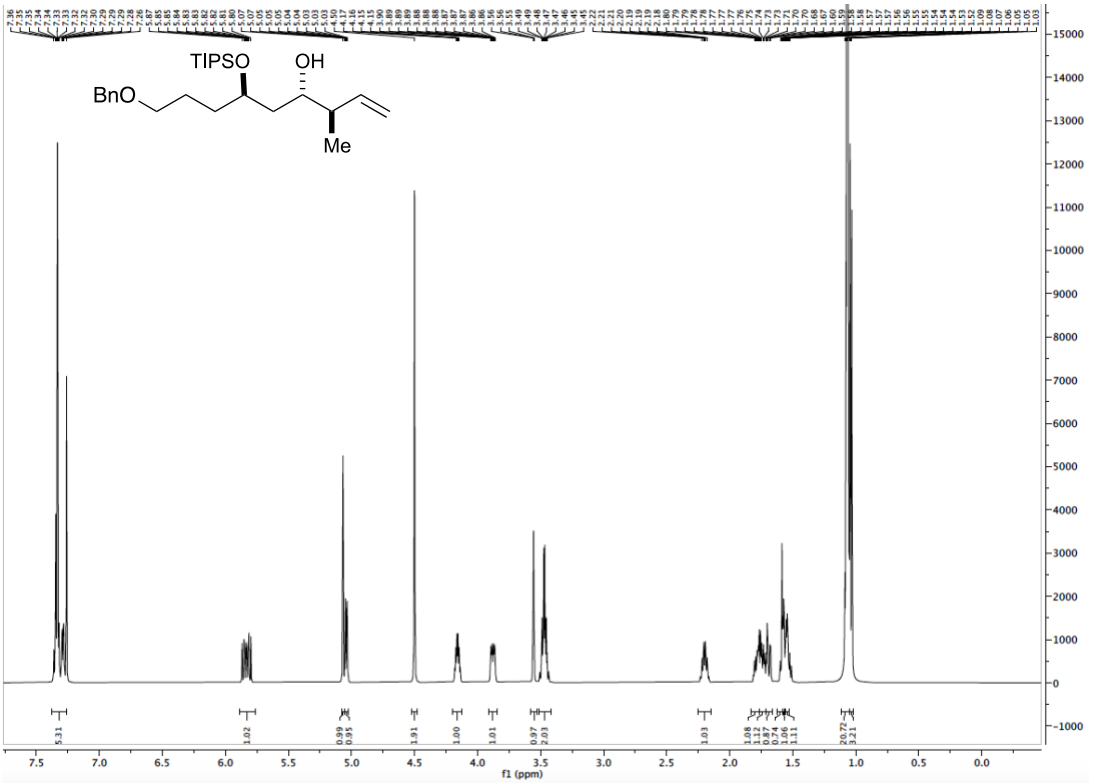

^{13}C, 126 MHz, $CDCl_3$

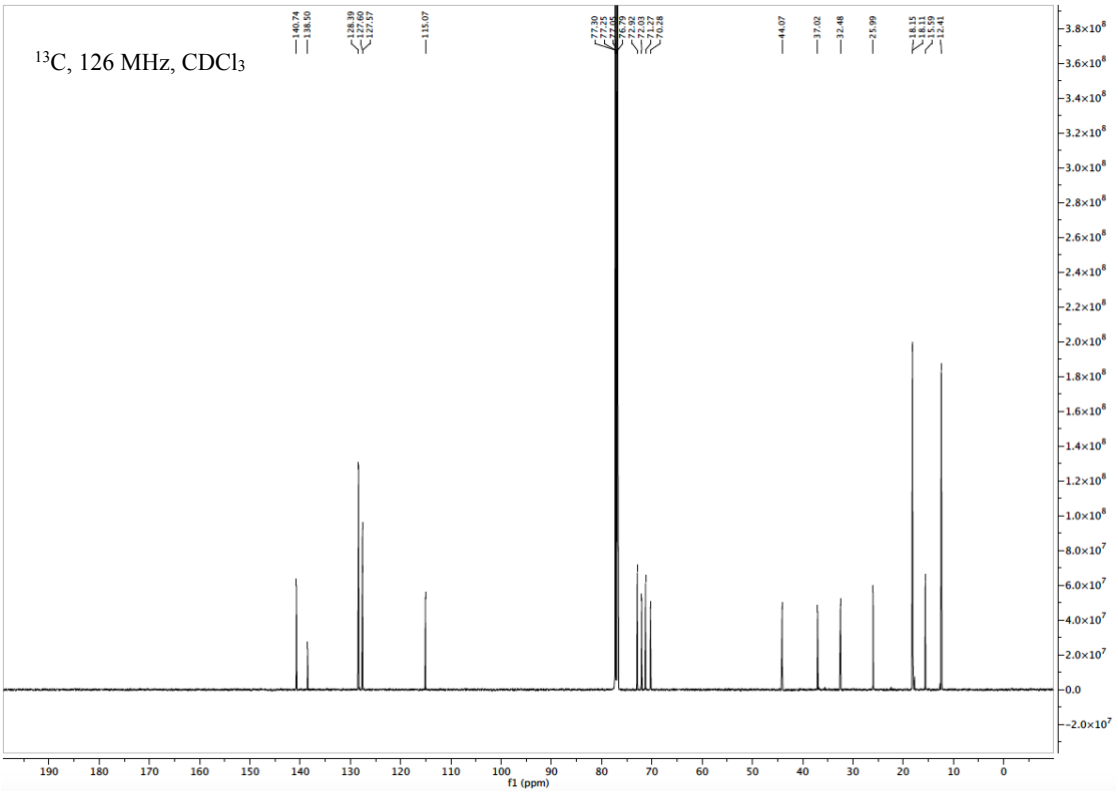

DEPT (135), 126 MHz, $CDCl_3$

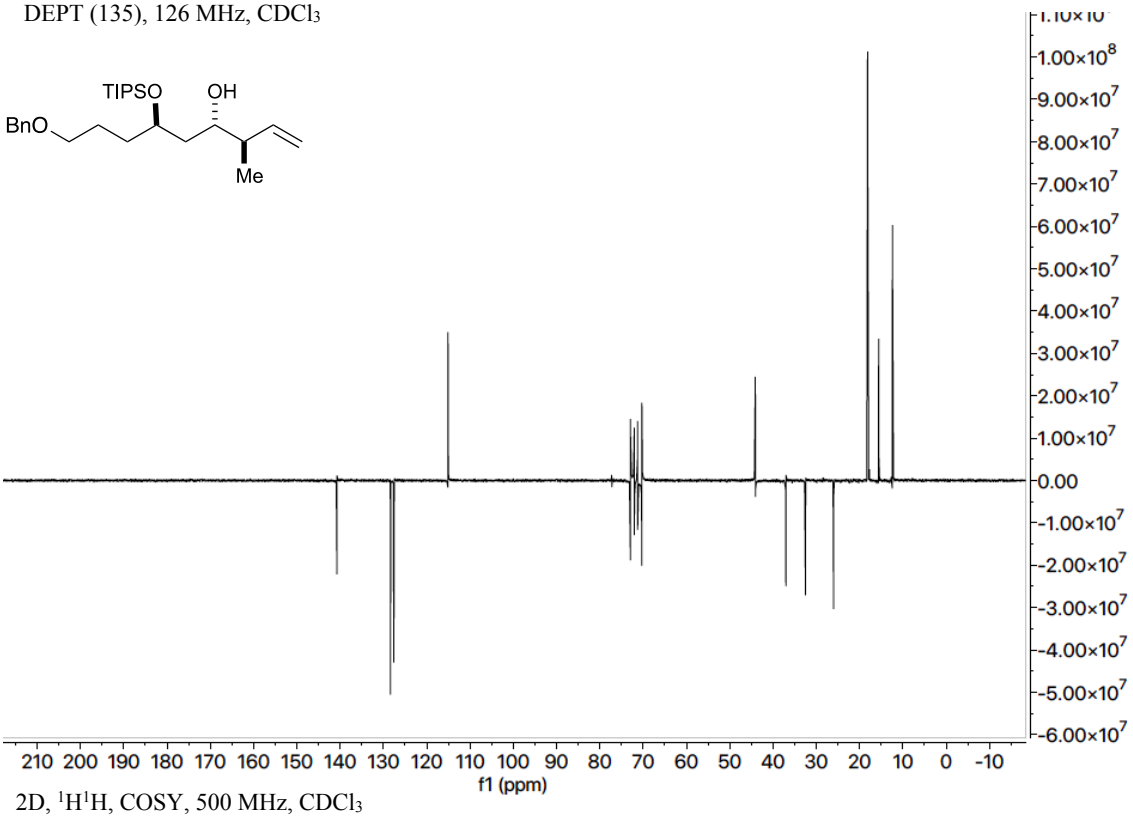

2D, $^1H^1H$, COSY, 500 MHz, $CDCl_3$

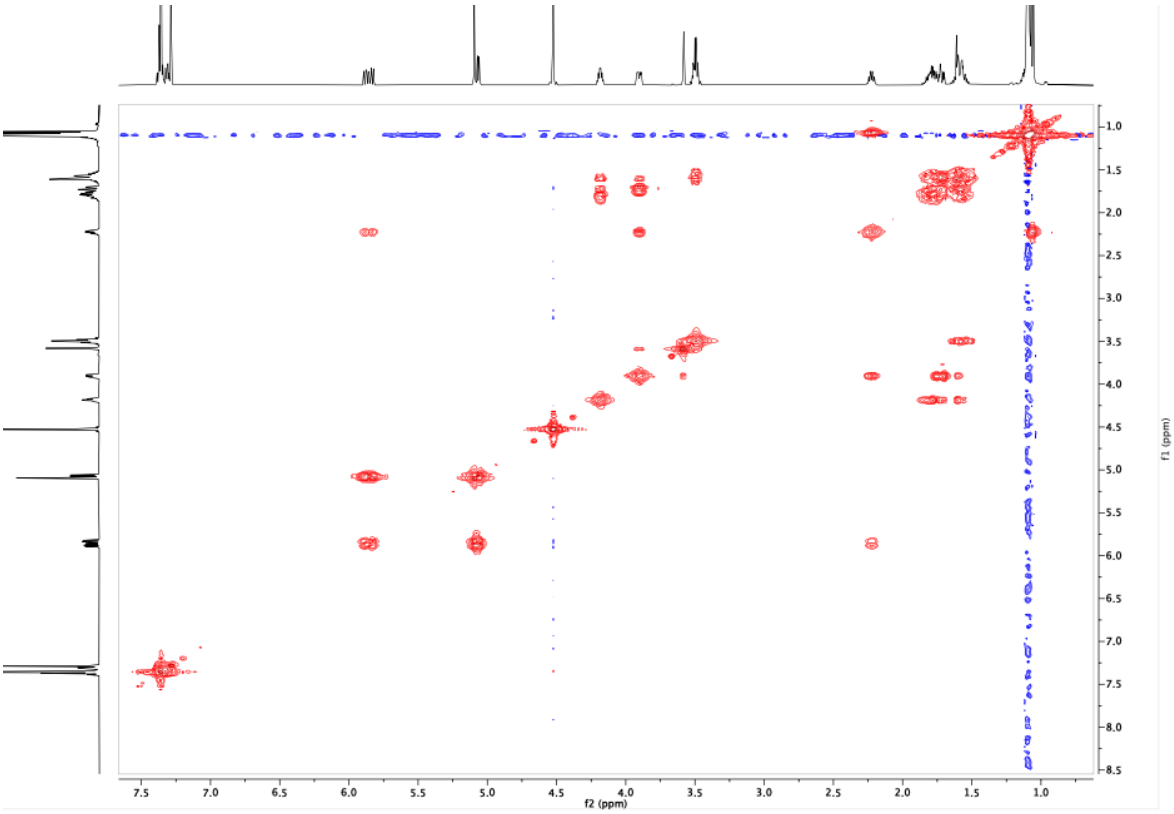

2D, $^{1}H^{13}C$, HSQC, 500 MHz, $CDCl_3$

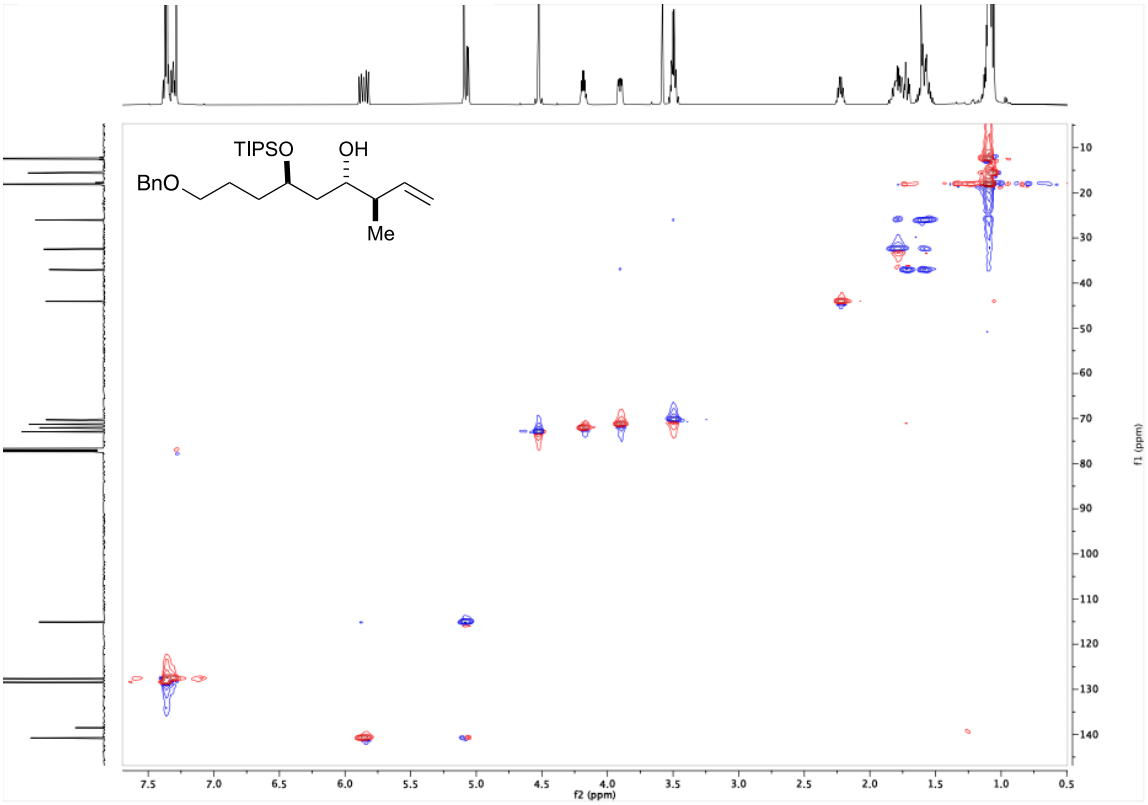

(5*S*,7*R*)-7-(3-(benzyloxy)propyl)-5-((*R*)-but-3-en-2-yl)-9,9-diisopropyl-10-methyl-2,4,8-trioxa-9-silaundecane (4.5.2):

^{1}H, 500 MHz, $CDCl_3$

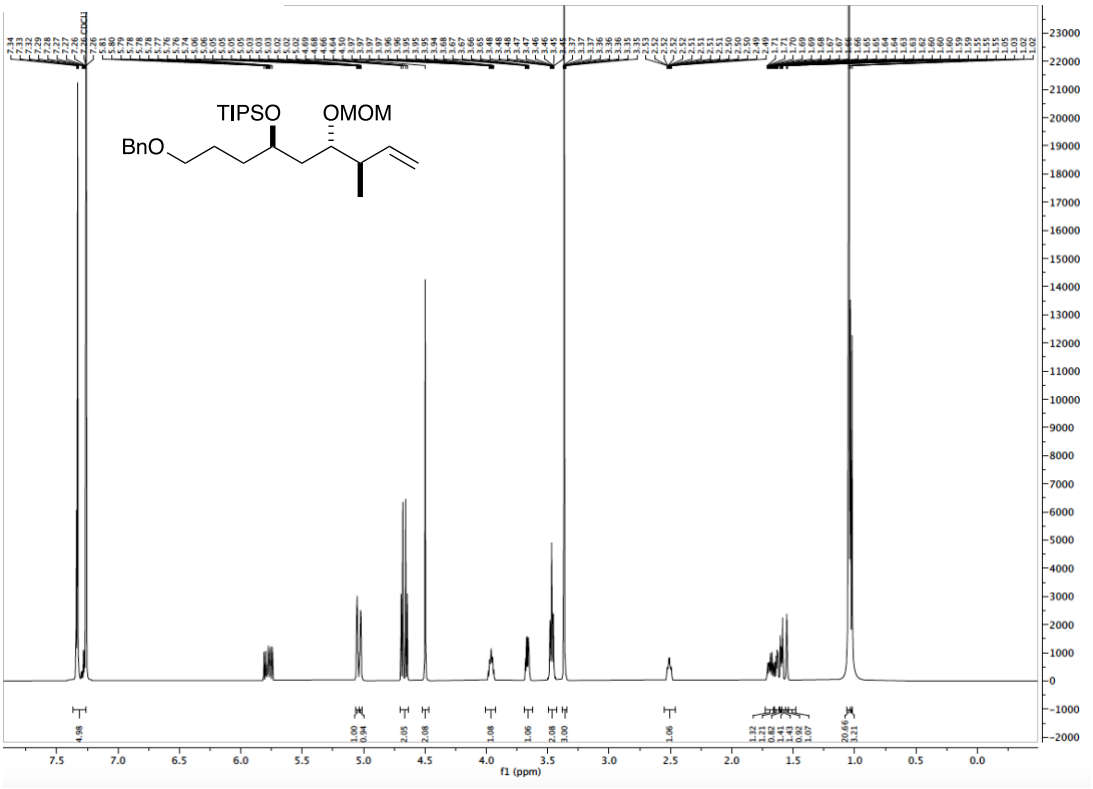

^{13}C, 126 MHz, $CDCl_3$

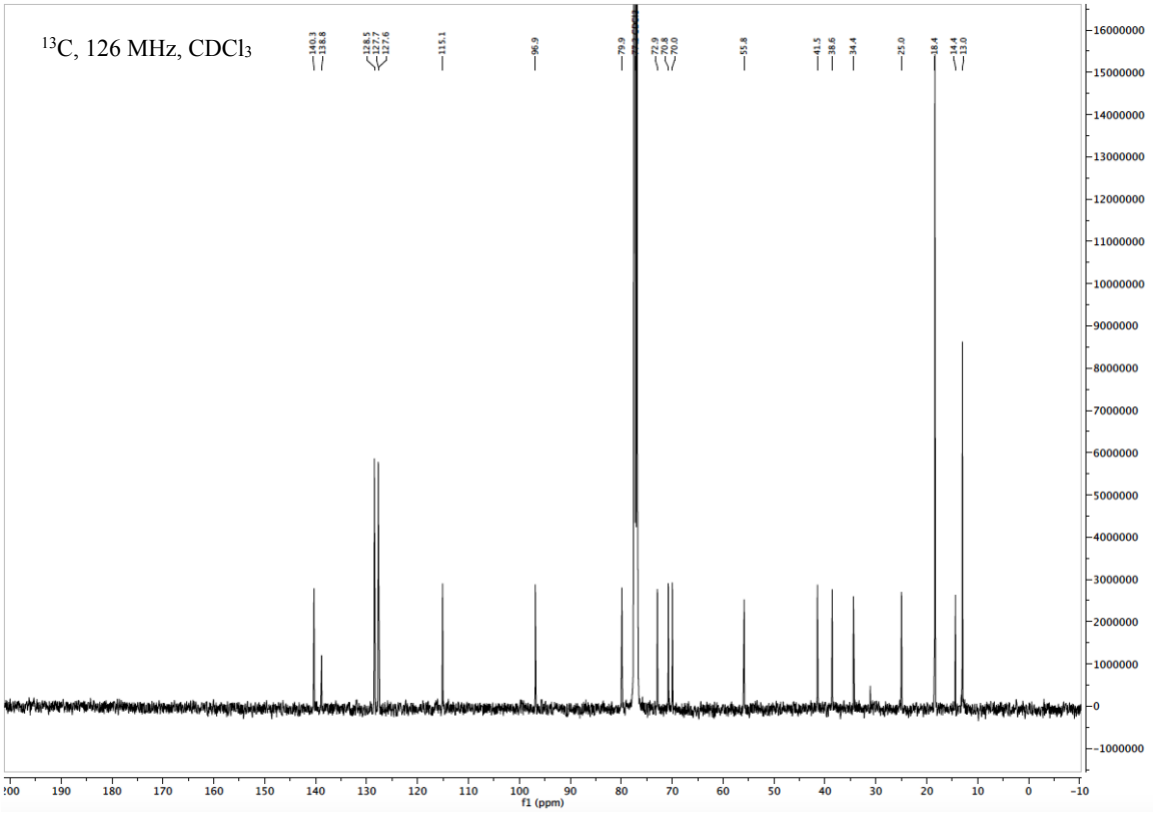

DEPT (135), 126 MHz, $CDCl_3$

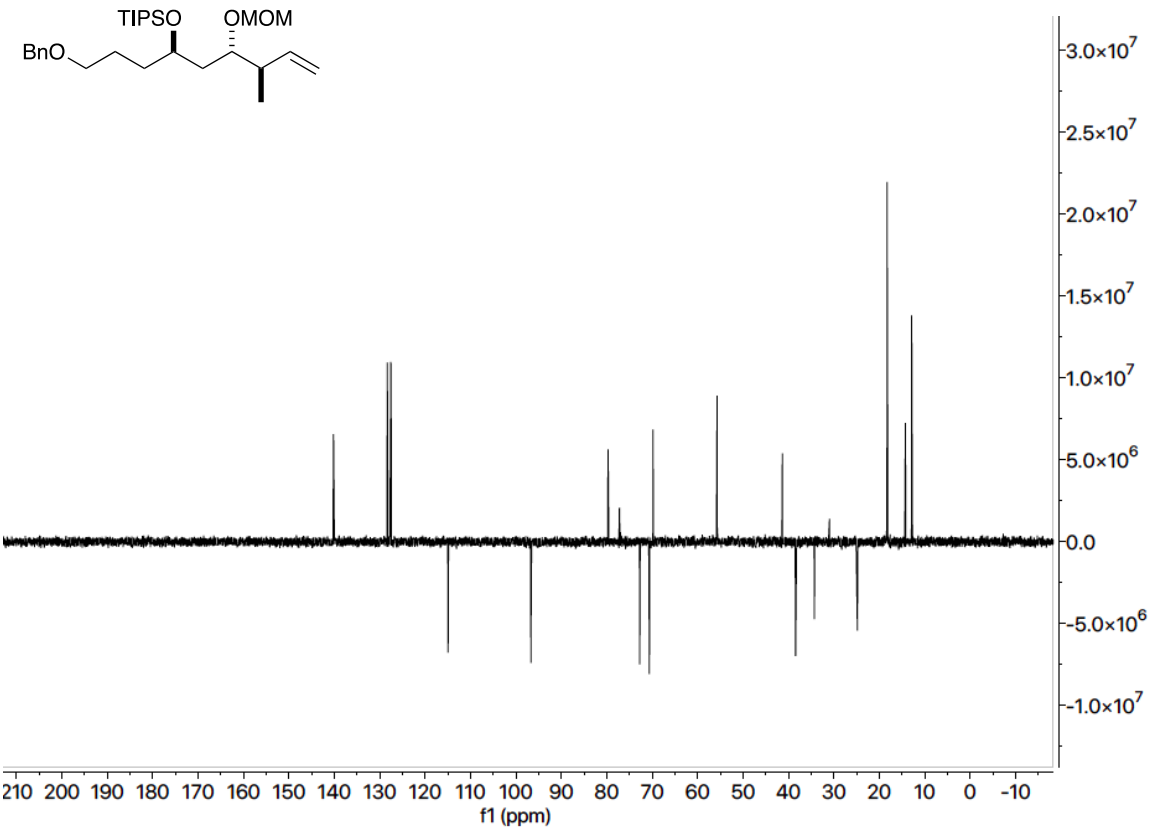

2D, $^1H^1H$, COSY, 500 MHz, $CDCl_3$

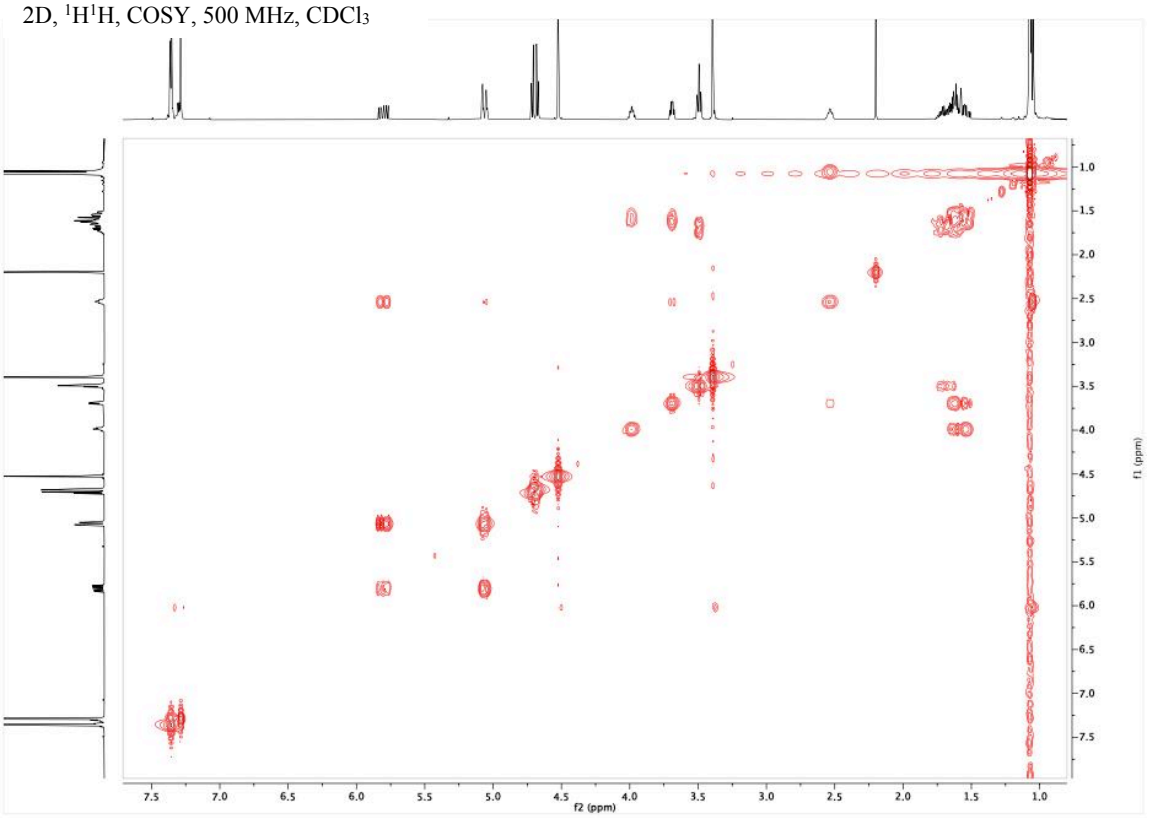

2D, $^{1}H^{13}C$, HSQC, 500 MHz, $CDCl_3$

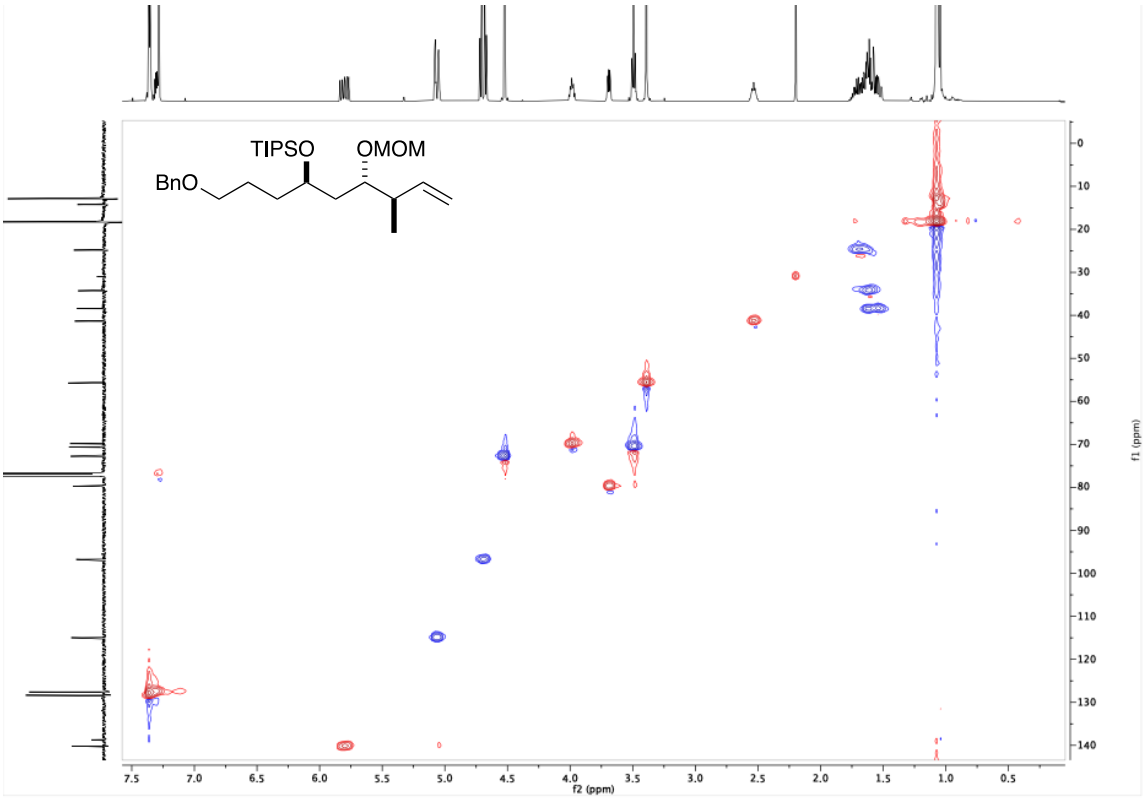

(5*R*,7*R*)-5-allyl-7-(3-(benzyloxy)propyl)-2,4,8,10-tetraoxaundecane (4.5.3)

^{1}H, 500 MHz, $CDCl_3$

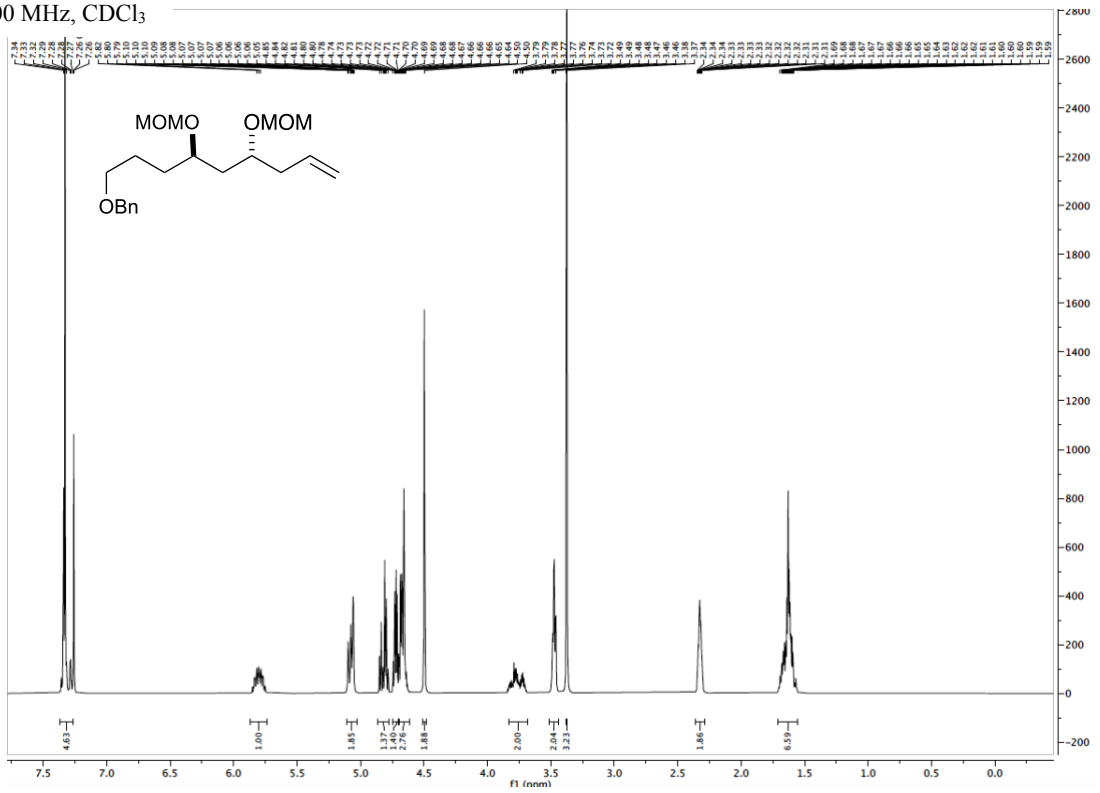

^{13}C, 126 MHz, $CDCl_3$

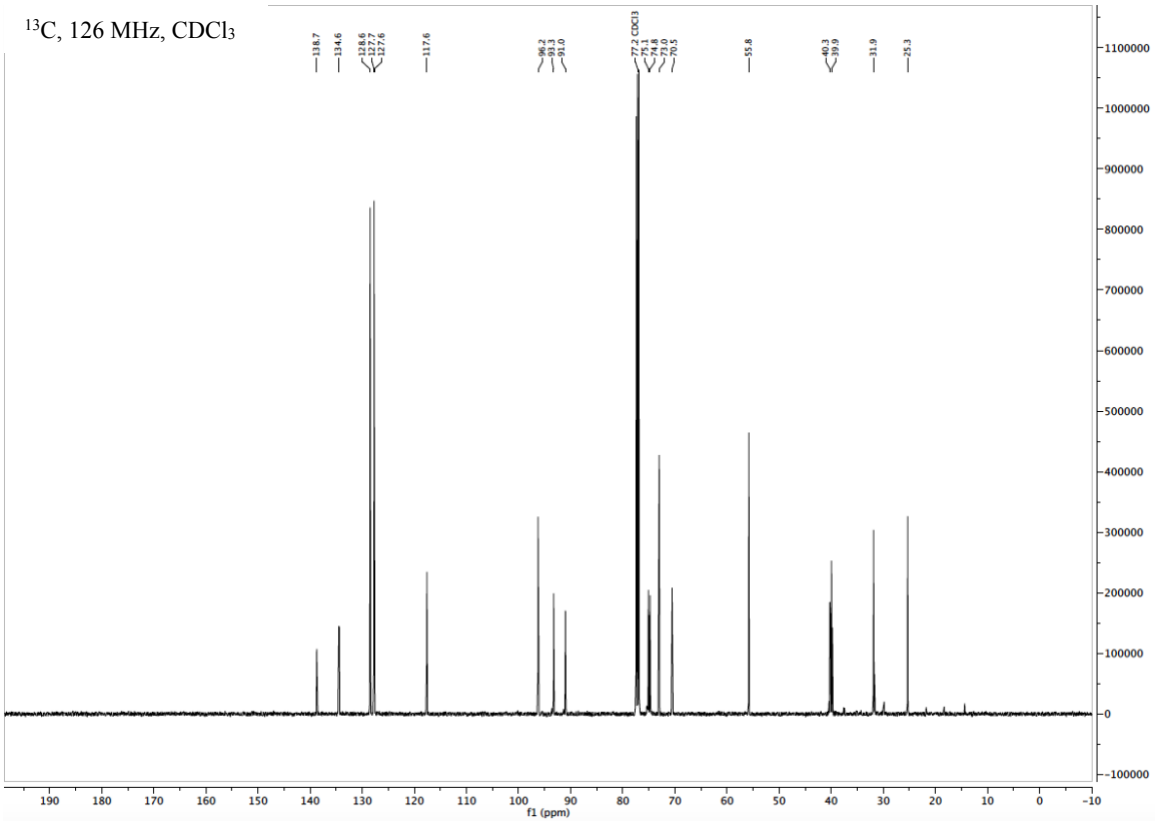

DEPT (135), 126 MHz, $CDCl_3$

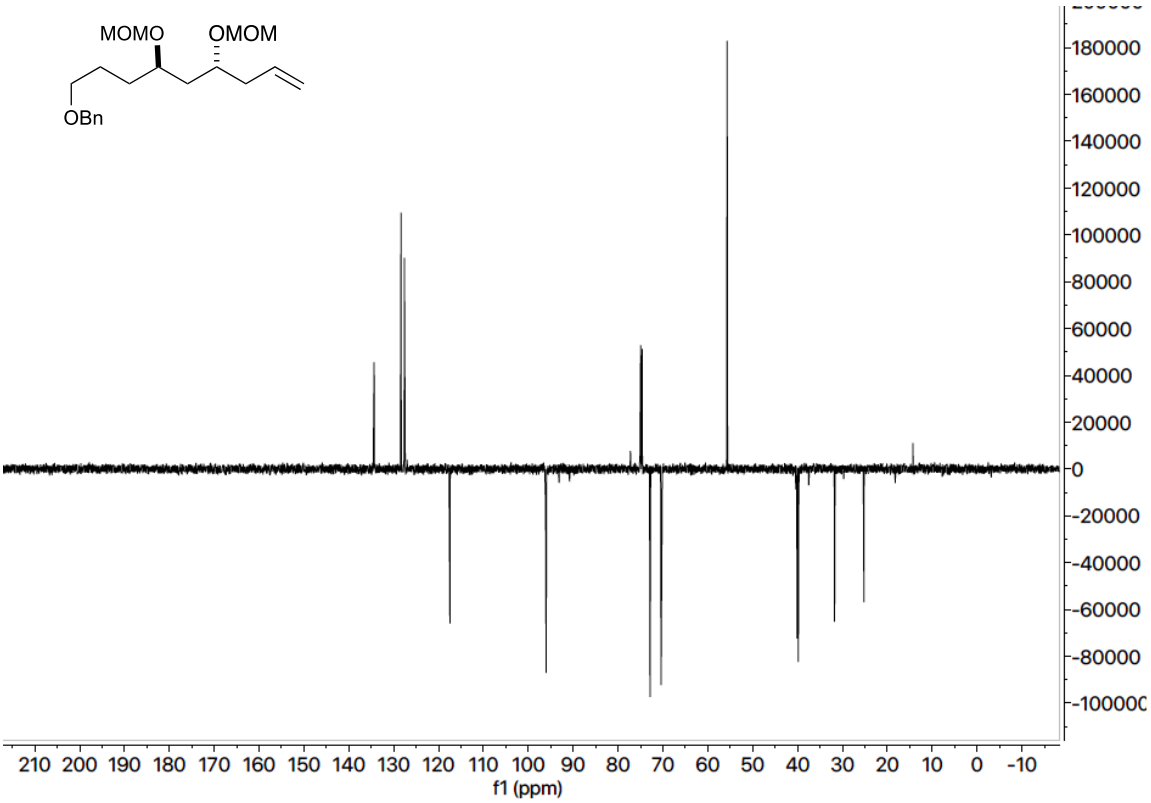

2D, $^{1}H^{1}H$, COSY, 500 MHz, $CDCl_3$

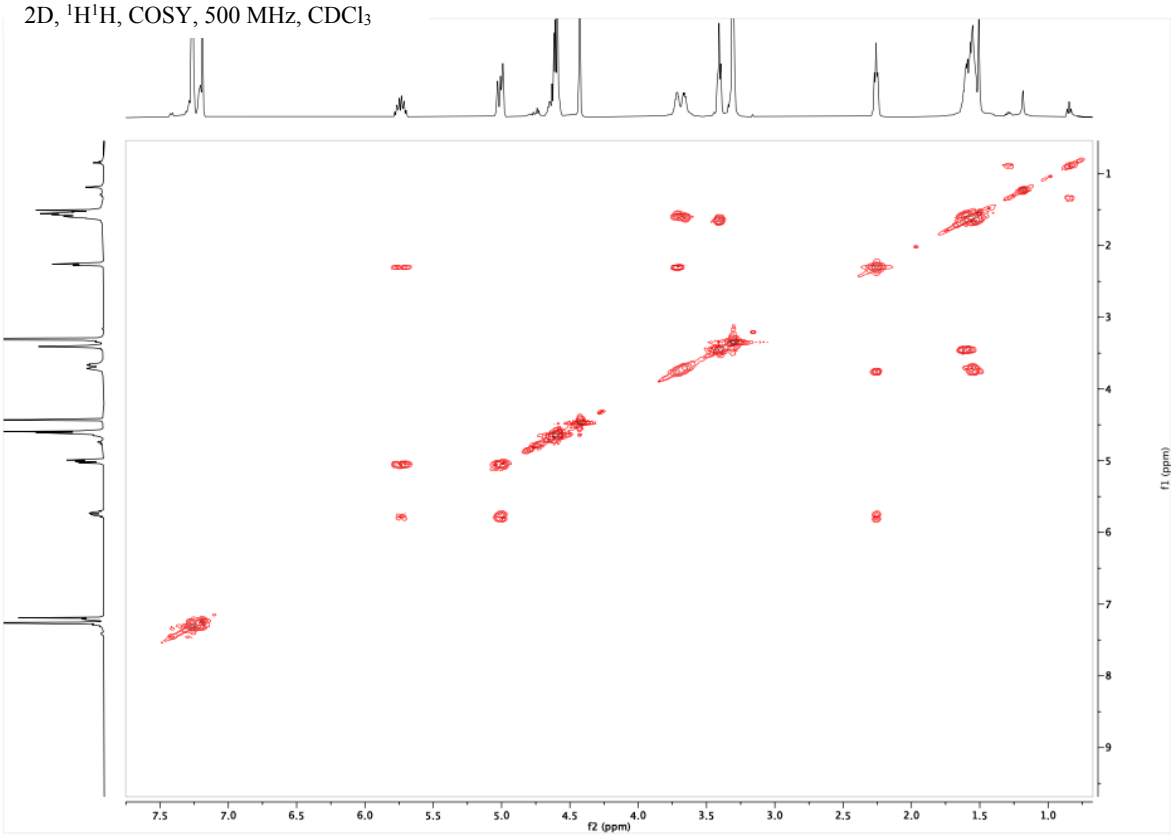

2D, $^{1}H^{13}C$, HSQC, 500 MHz, $CDCl_3$

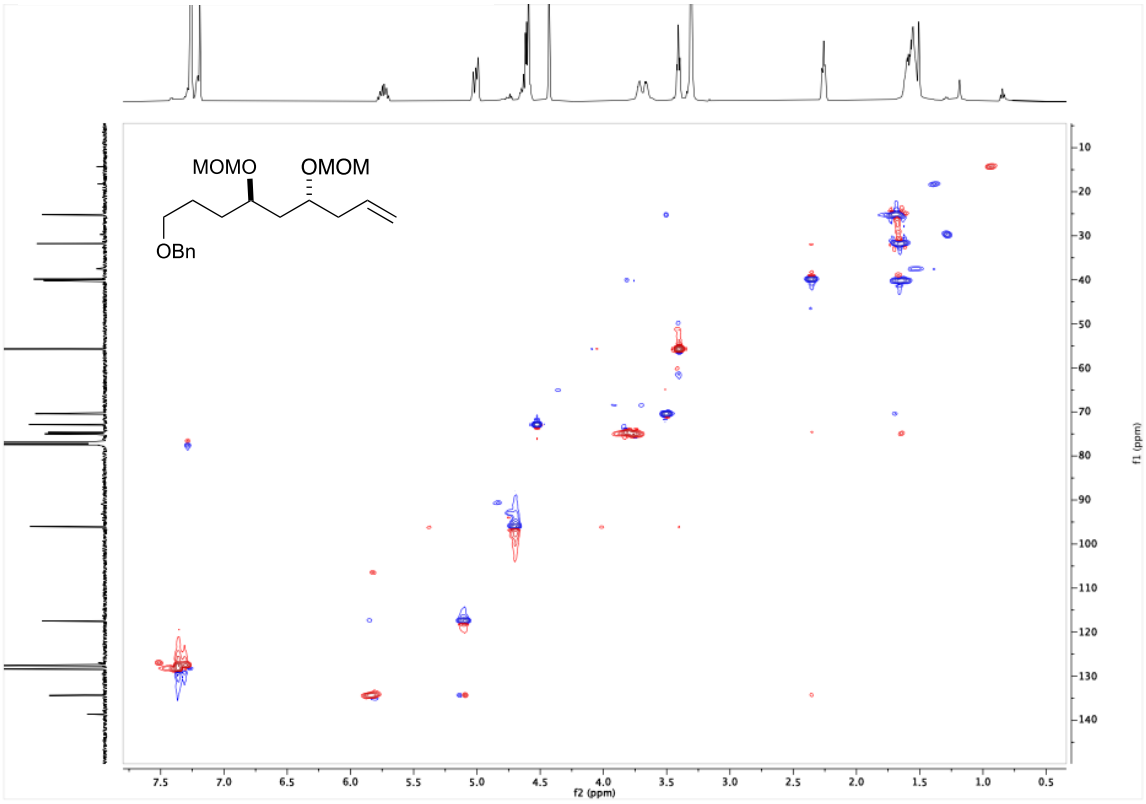

(1*R*,6*R*,8*S*)-8-((3*R*,4*S*,6*R*)-9-(benzyloxy)-4-hydroxy-3-methyl-6-((triisopropylsilyl)oxy)nonyl)-2,9,10-trioxa-1-phosphabicyclo[4.3.1]dec-4-ene 1-oxide (4.6.1)

^{1}H, 500 MHz, $CDCl_3$

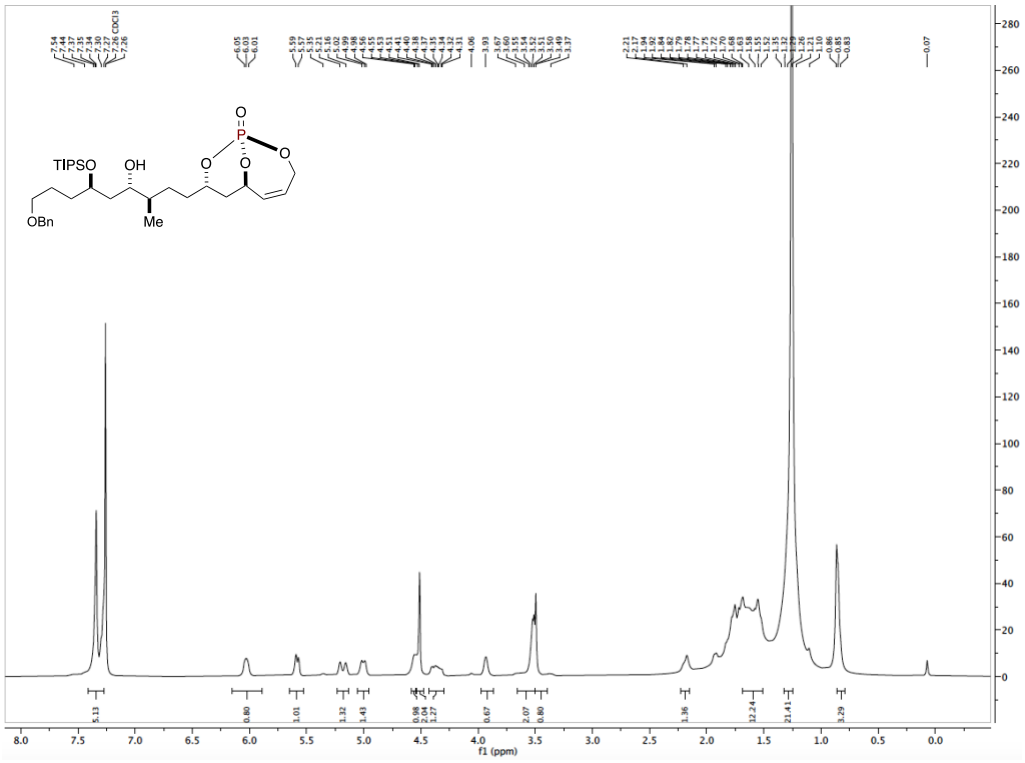

^{13}C, 126 MHz, $CDCl_3$

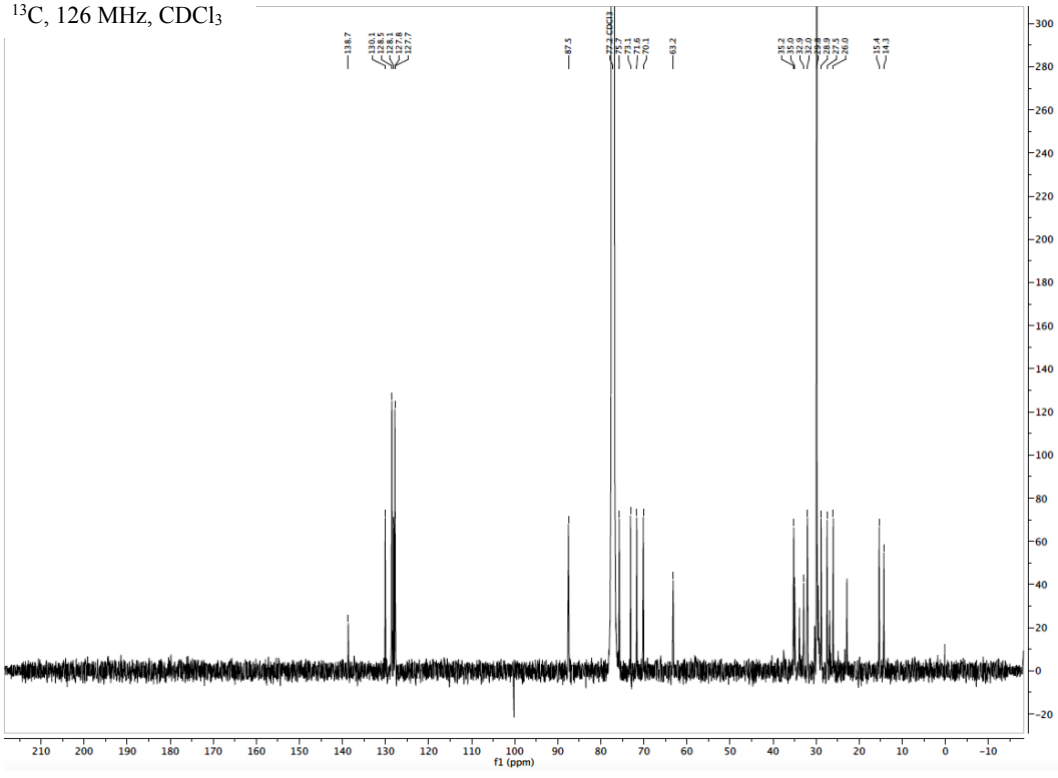

DEPT (135), 126 MHz, $CDCl_3$

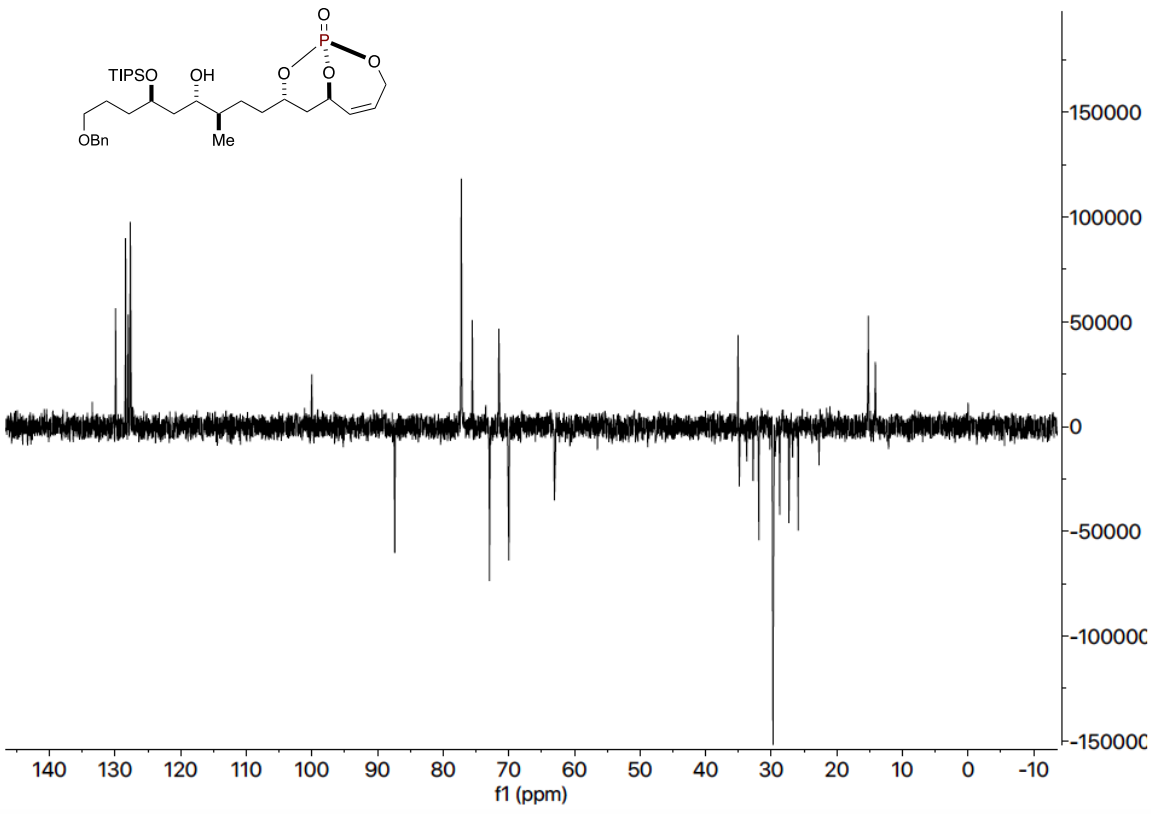

2D, $^{1}H^{1}H$, COSY, 500 MHz, $CDCl_3$

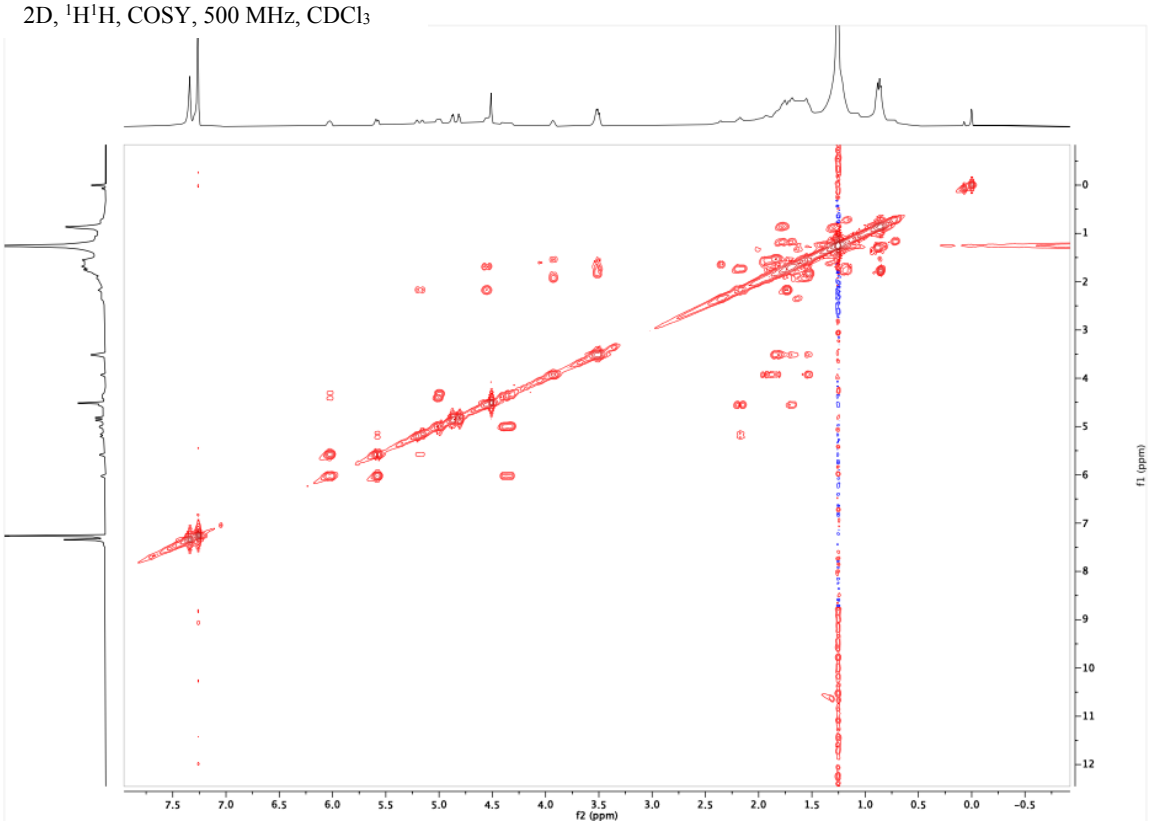

2D, $^{1}H^{13}C$, HSQC, 500 MHz, $CDCl_3$

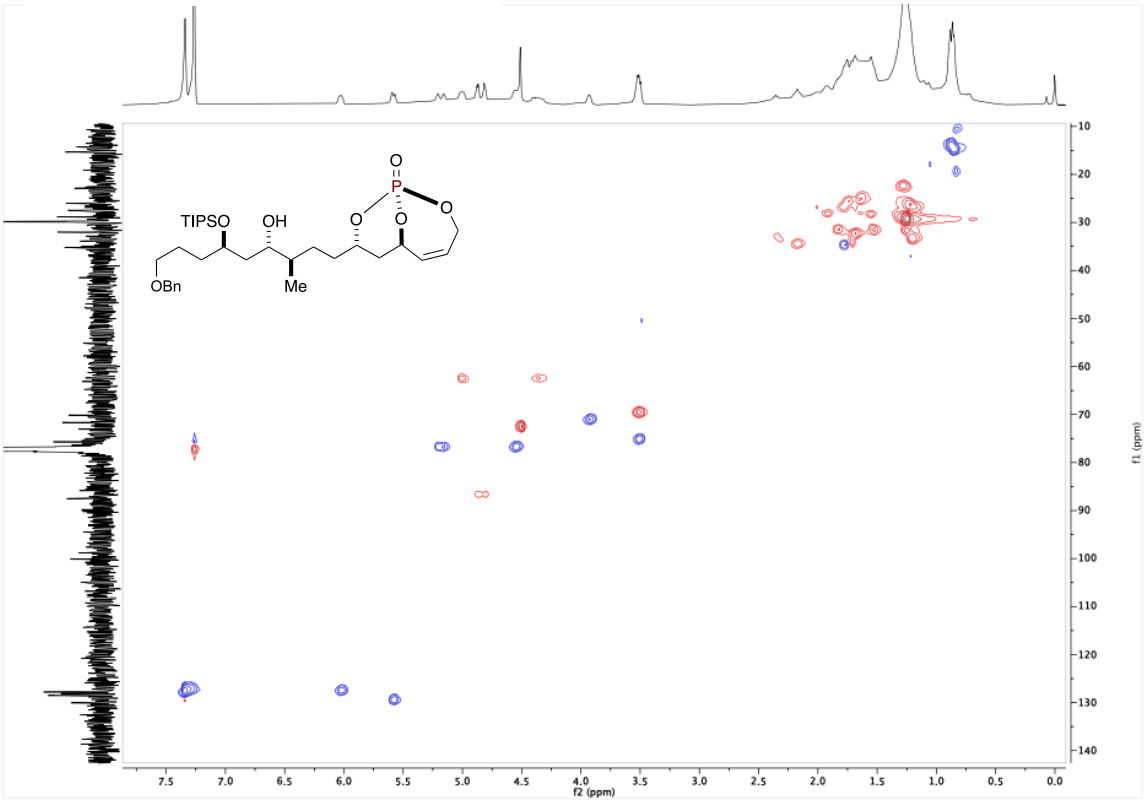

^{31}P, 162 MHz, $CDCl_3$

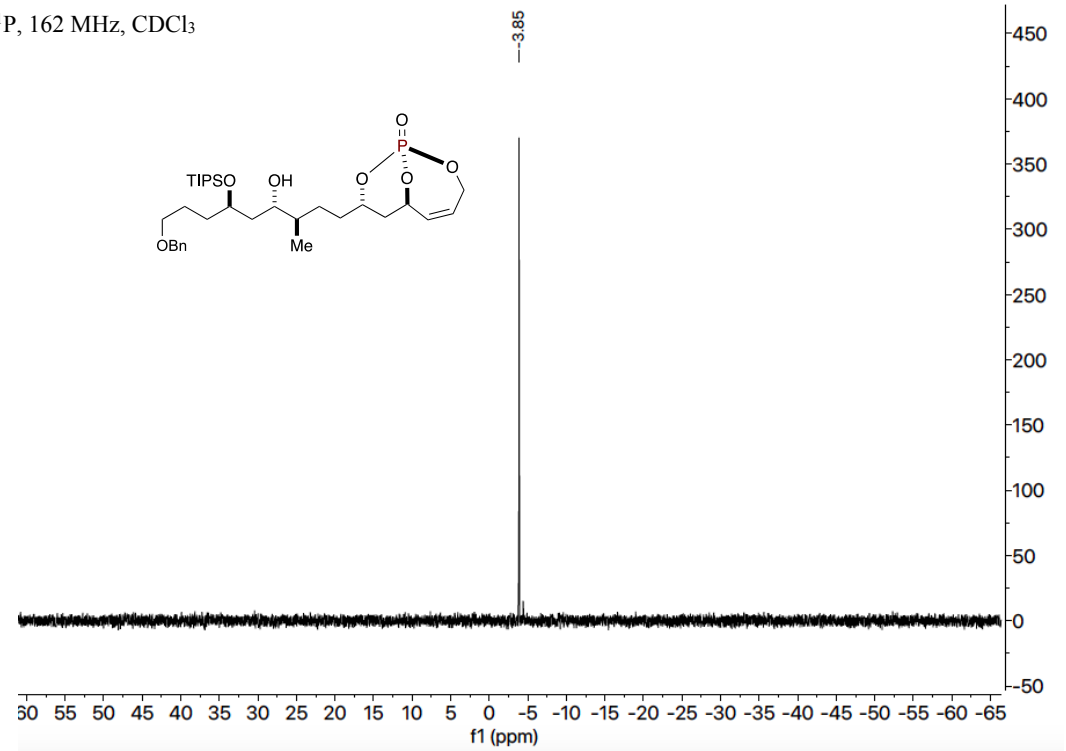

(4*S*,6*S*,9*R*,10*S*,12*R*)-15-(benzyloxy)-9-methylpentadec-1-ene-4,6,10,12-tetraol (4.6.2)

^{1}H, 500 MHz, $CDCl_3$

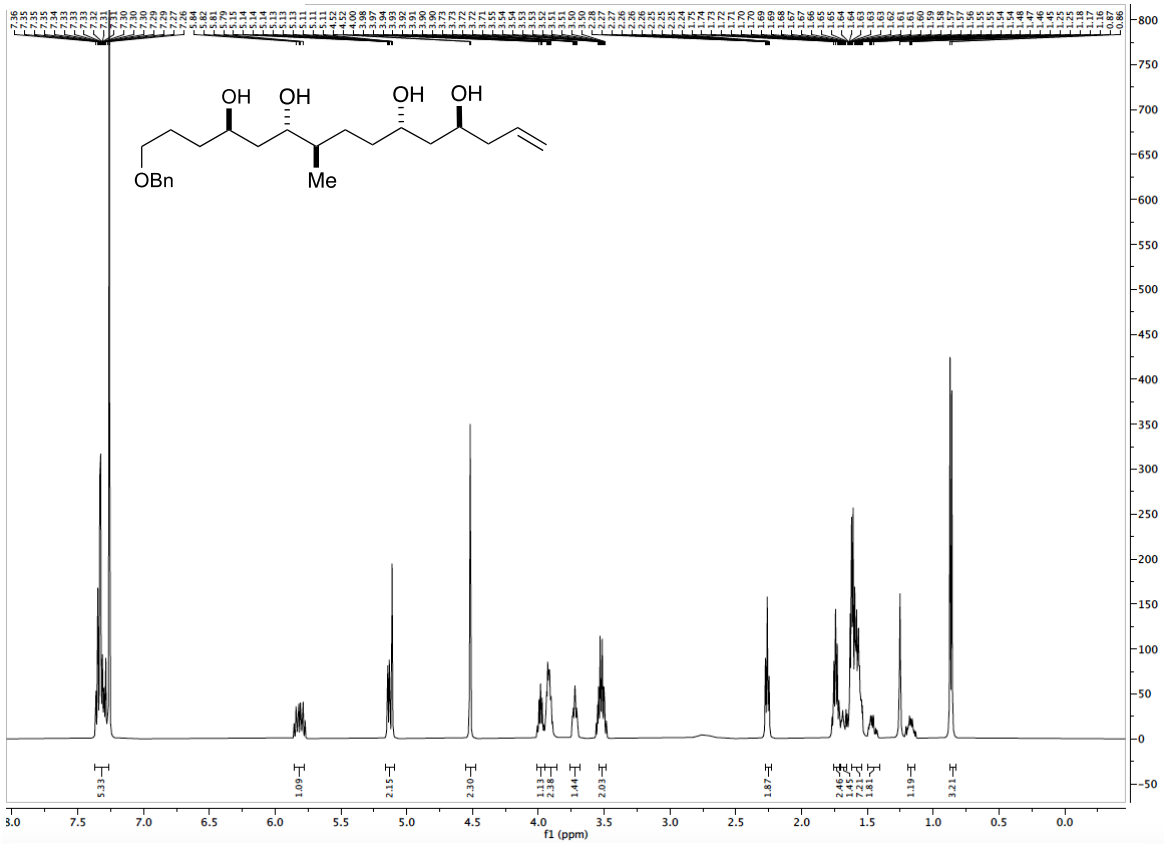

^{13}C, 126 MHz, $CDCl_3$

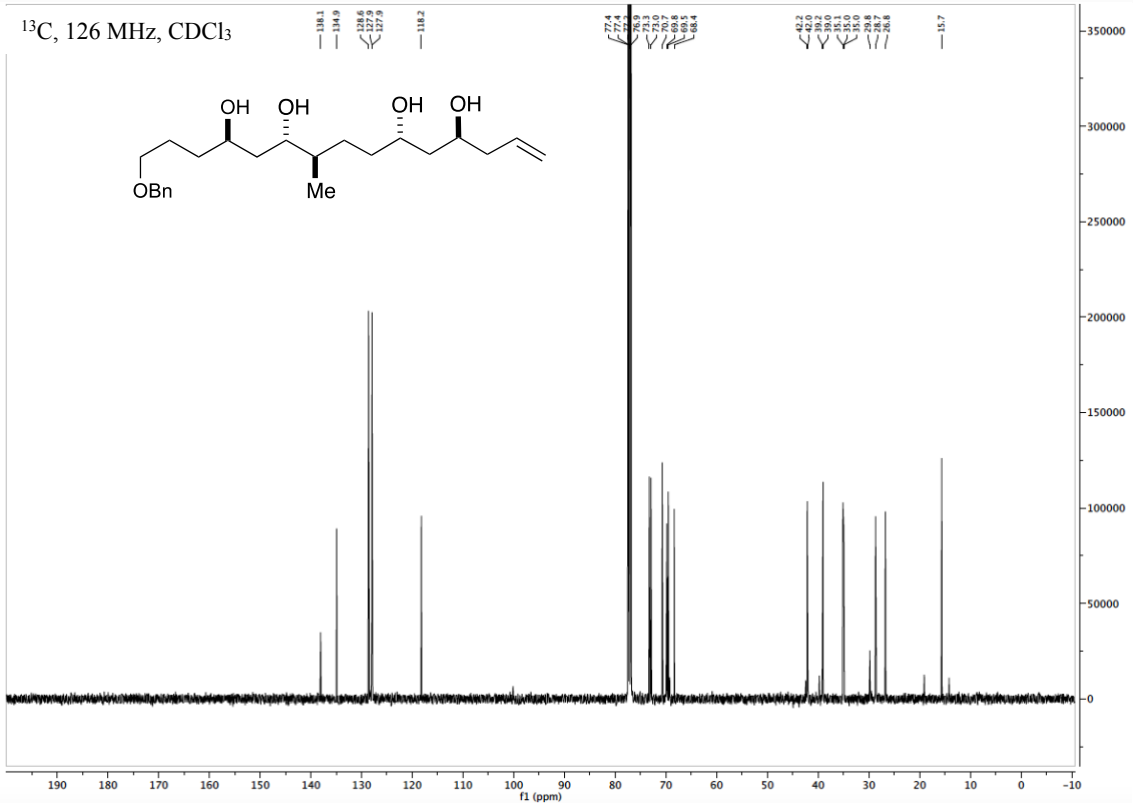

DEPT (135), 126 MHz, $CDCl_3$

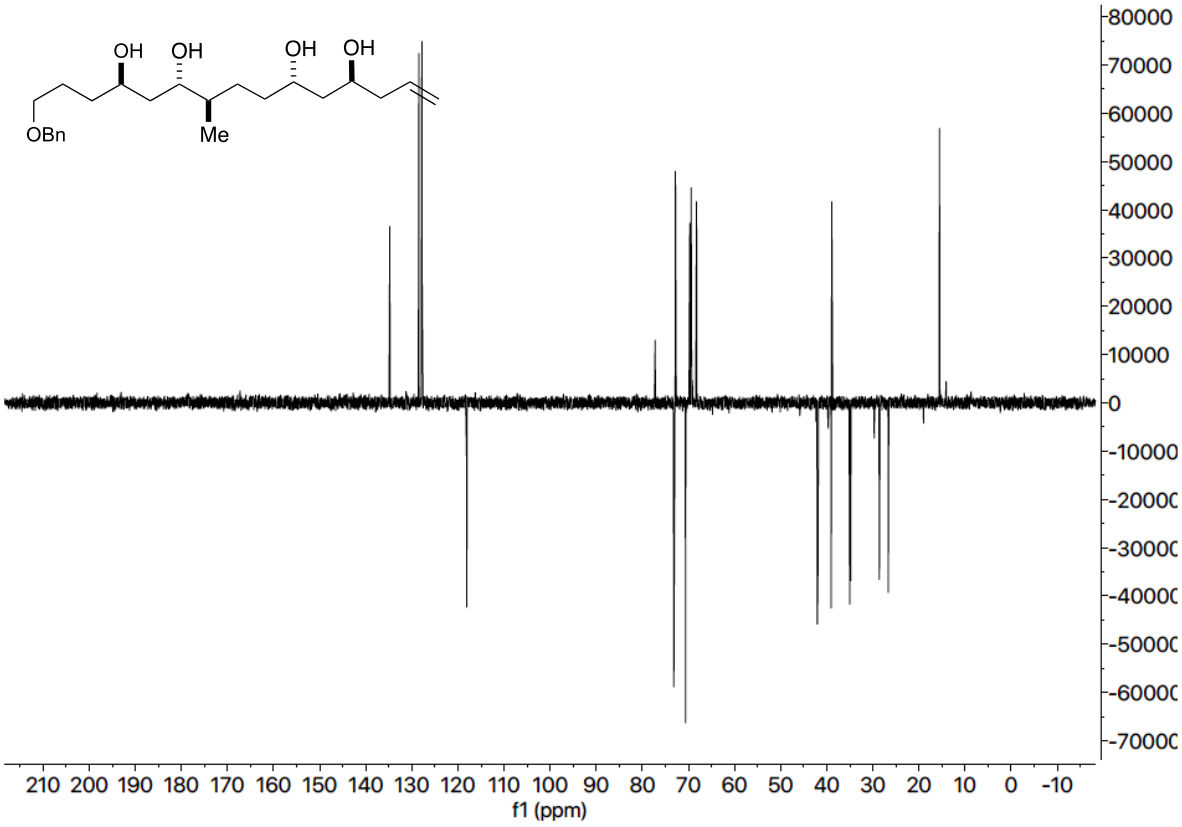

2D, $^1H^1H$, COSY, 500 MHz, $CDCl_3$

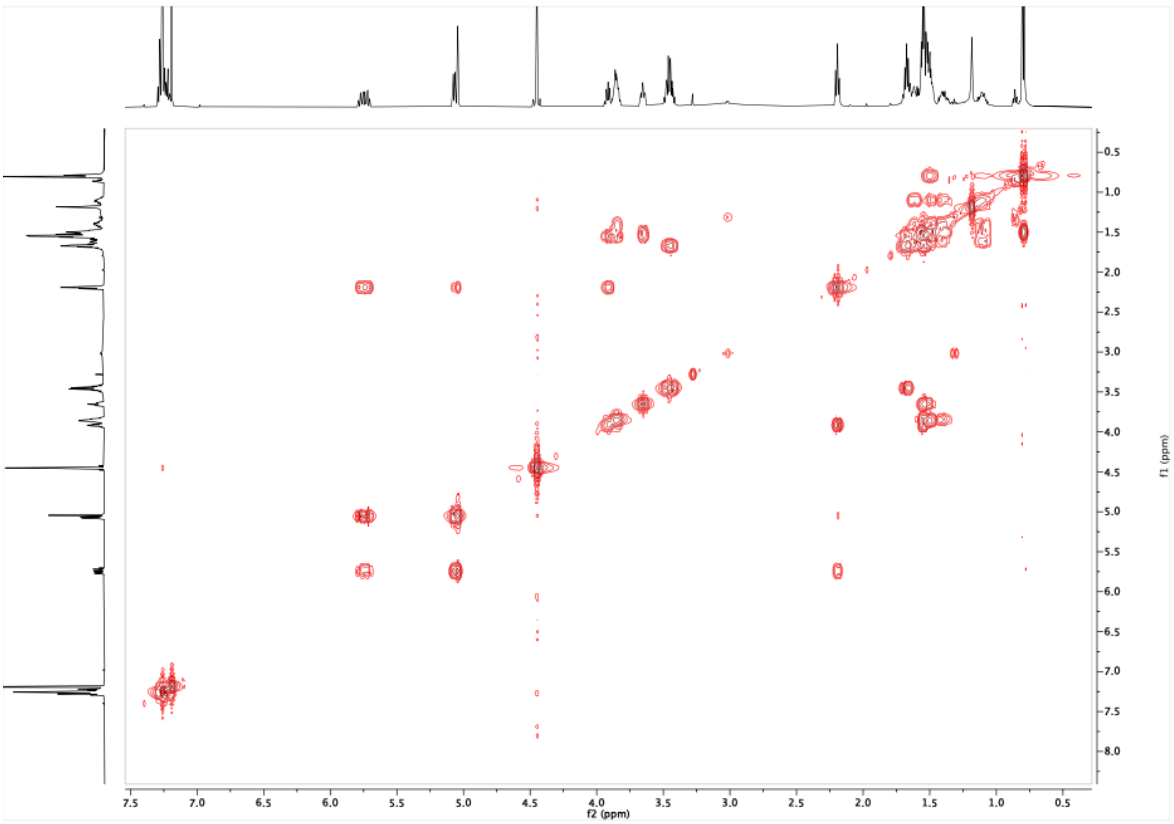

2D, $^{1}H^{13}C$, HSQC, 500 MHz, $CDCl_3$

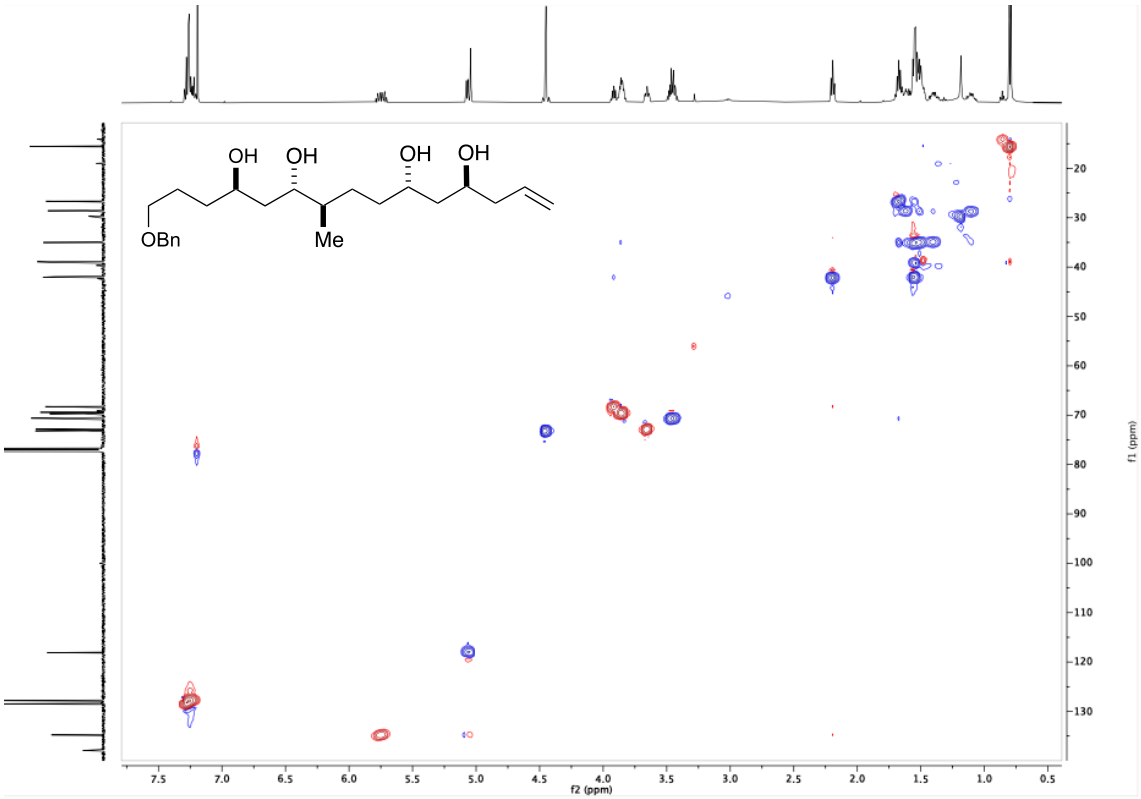

(3*S*,4*R*,6*S*,9*R*,10*S*,12*R*)-15-(benzyloxy)-3,9-dimethylpentadec-1-ene-4,6,10,12-tetraol (4.6.3)

^{1}H, 500 MHz, $CDCl_3$

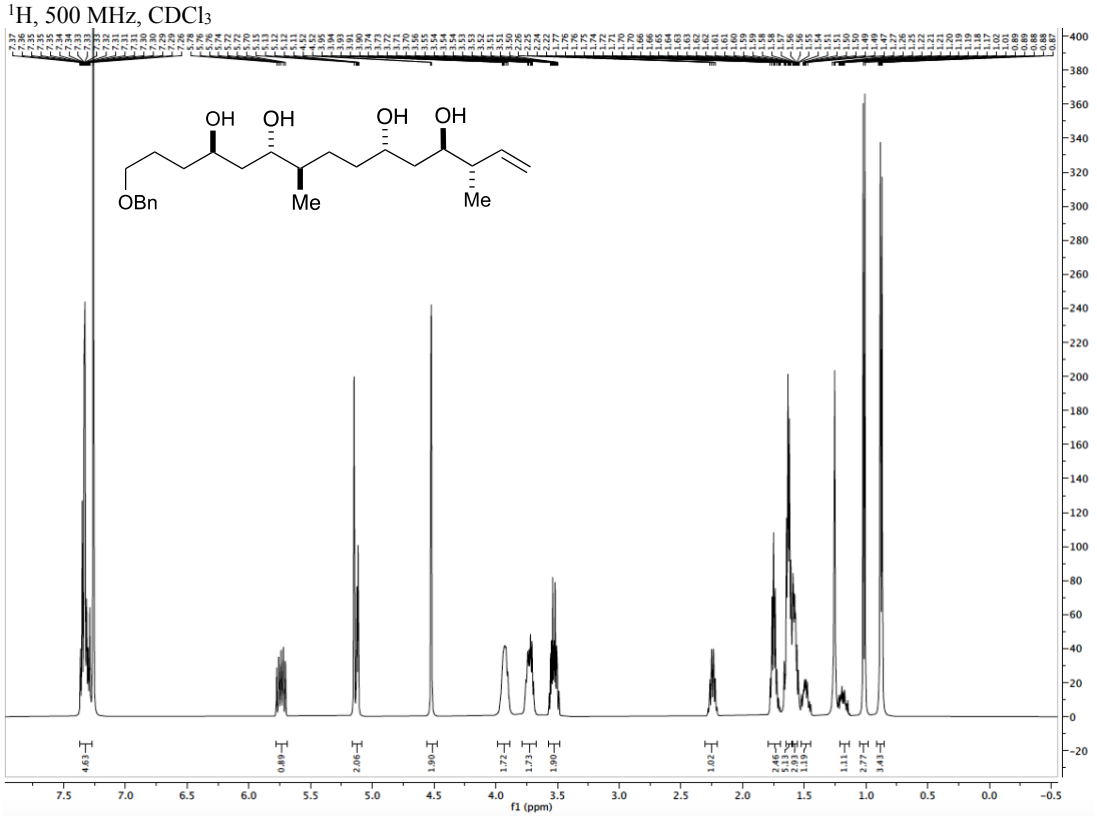

^{13}C, 126 MHz, $CDCl_3$

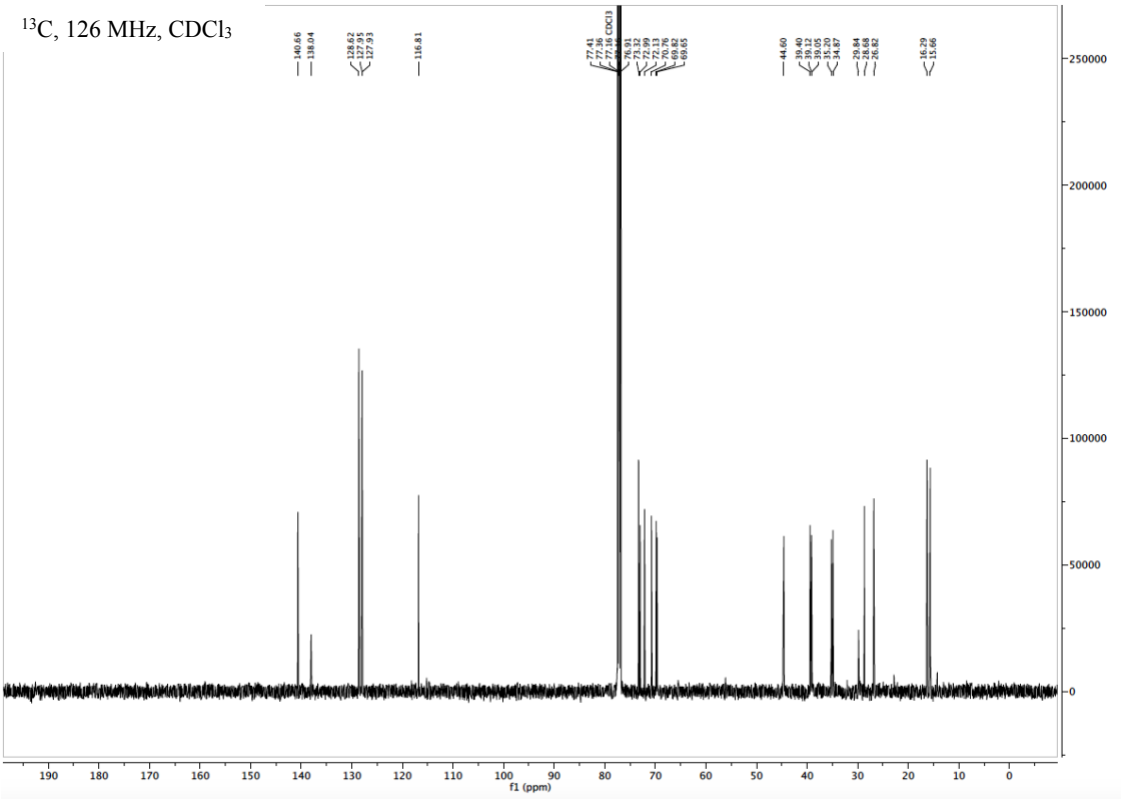

DEPT (135), 126 MHz, $CDCl_3$

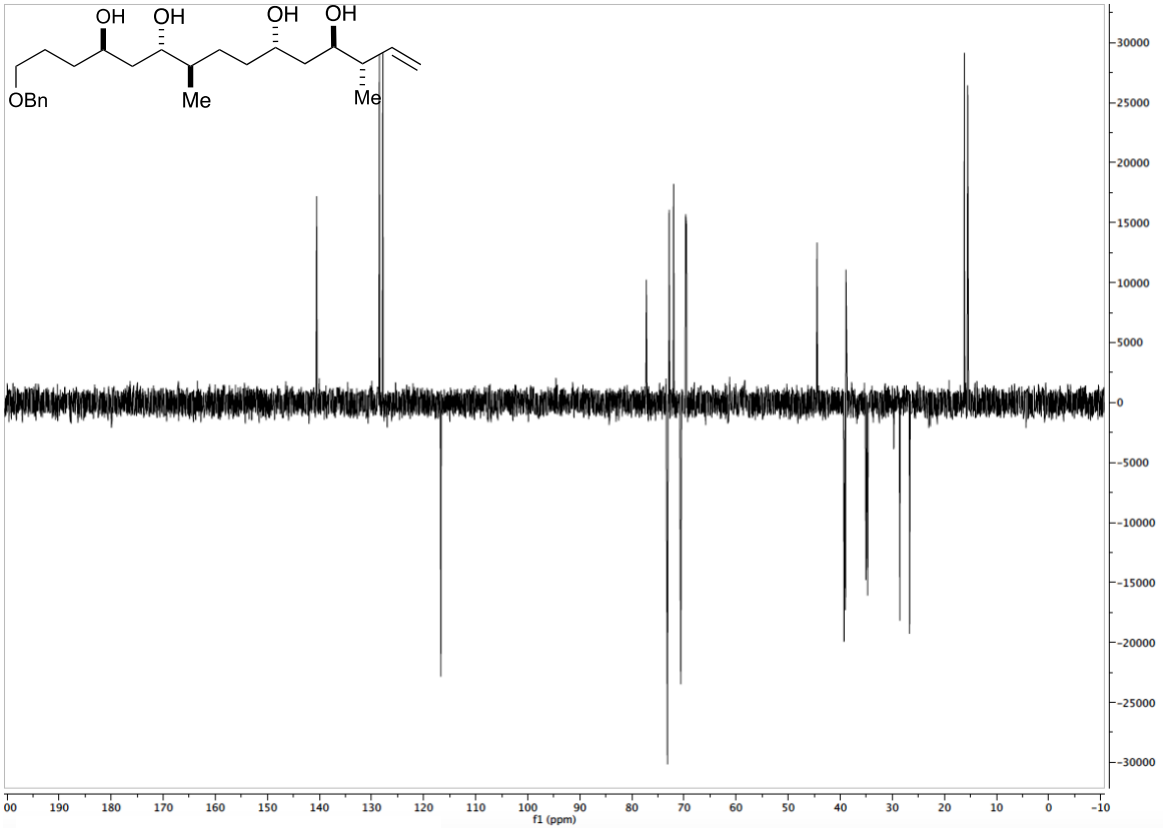

2D, $^{1}H^{1}H$, COSY, 500 MHz, $CDCl_3$

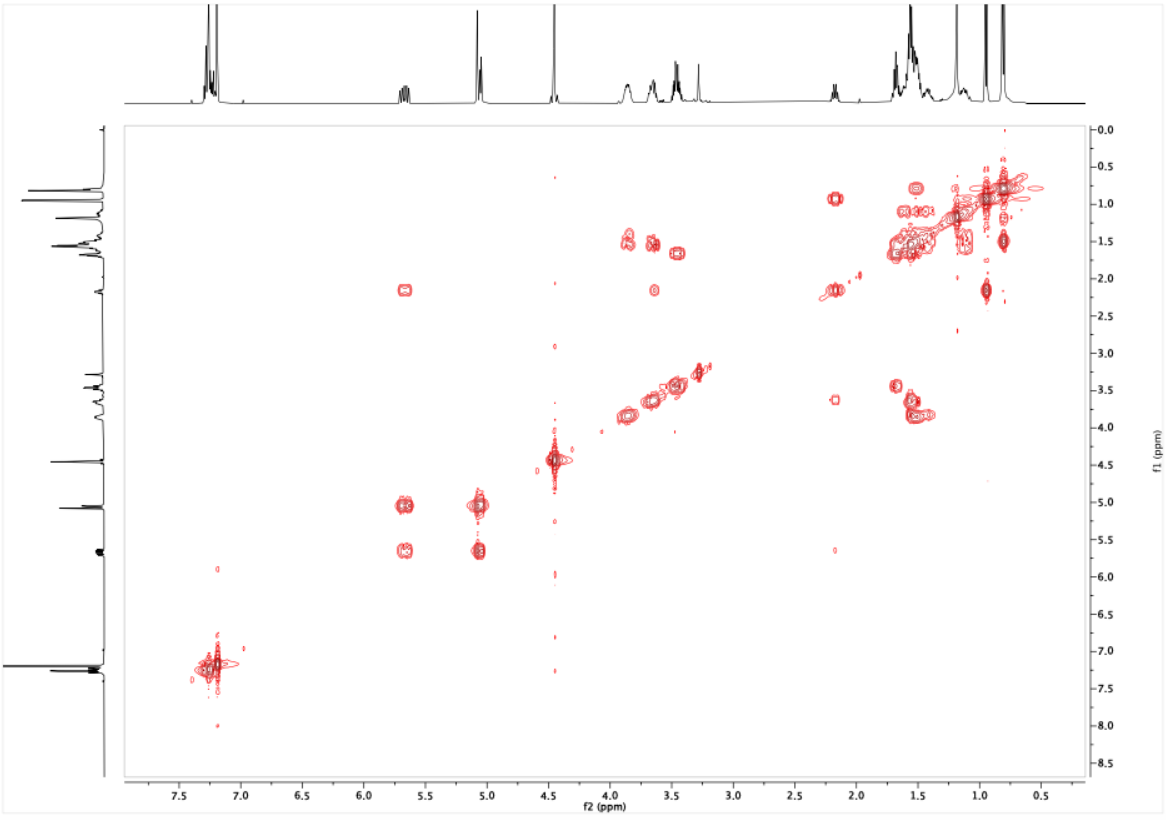

2D, $^{1}H^{13}C$, HSQC, 500 MHz, $CDCl_3$

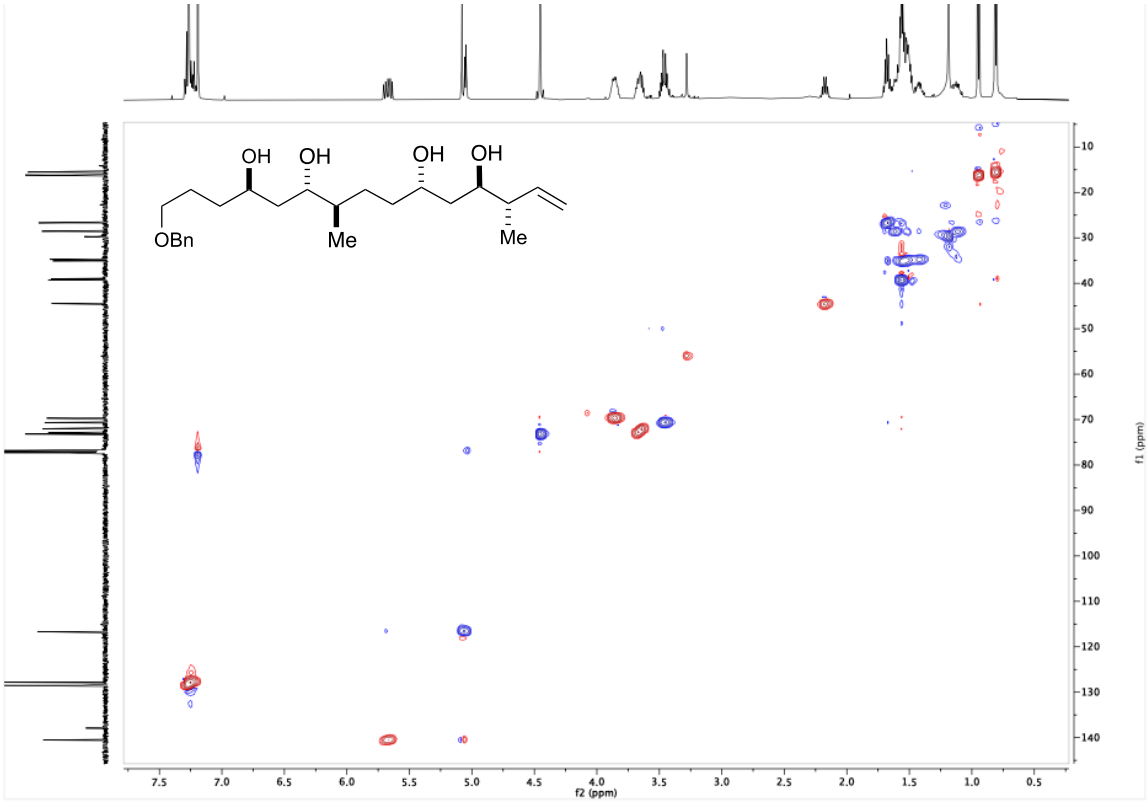

(1*R*,6*R*,8*S*)-8-((3*R*,4*S*,6*R*)-9-(benzyloxy)-4-(methoxymethoxy)-3-methyl-6-((triiso-propylsilyl)oxy)nonyl)-2,9,10-trioxa-1-phosphabicyclo[4.3.1]dec-4-ene 1-oxide (4.7.1): ^{1}H, 500 MHz, $CDCl_3$

^{13}C, 126 MHz, $CDCl_3$

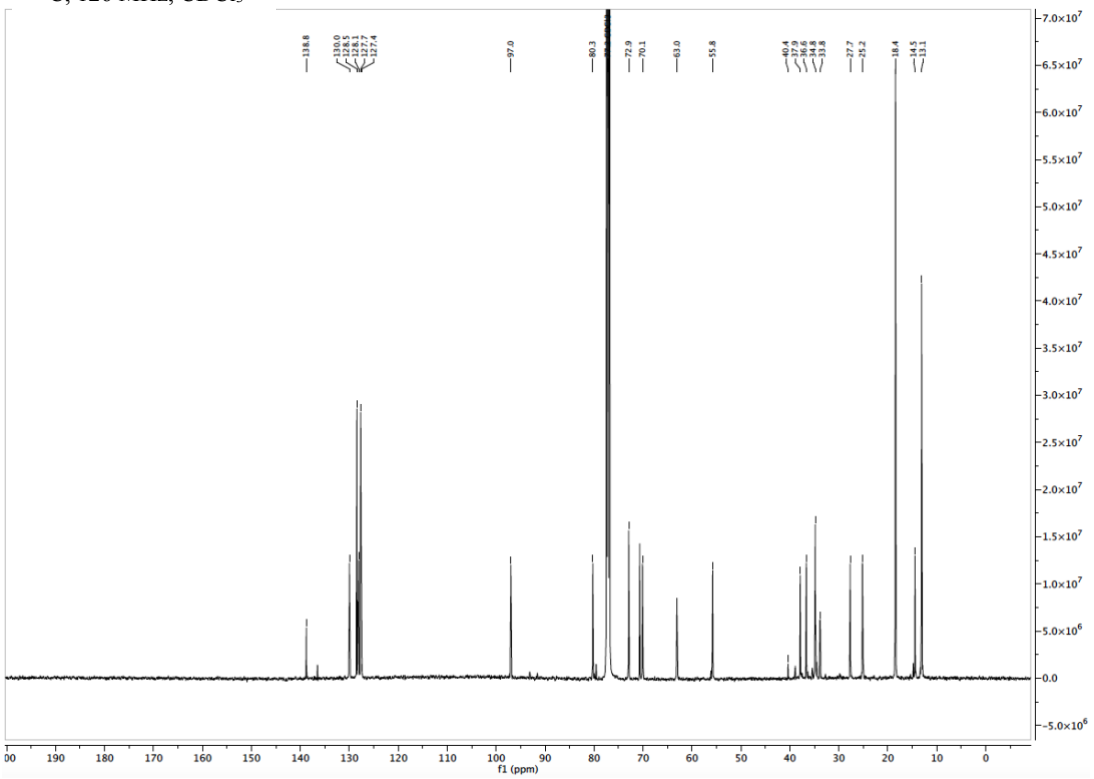

DEPT (135), 126 MHz, $CDCl_3$

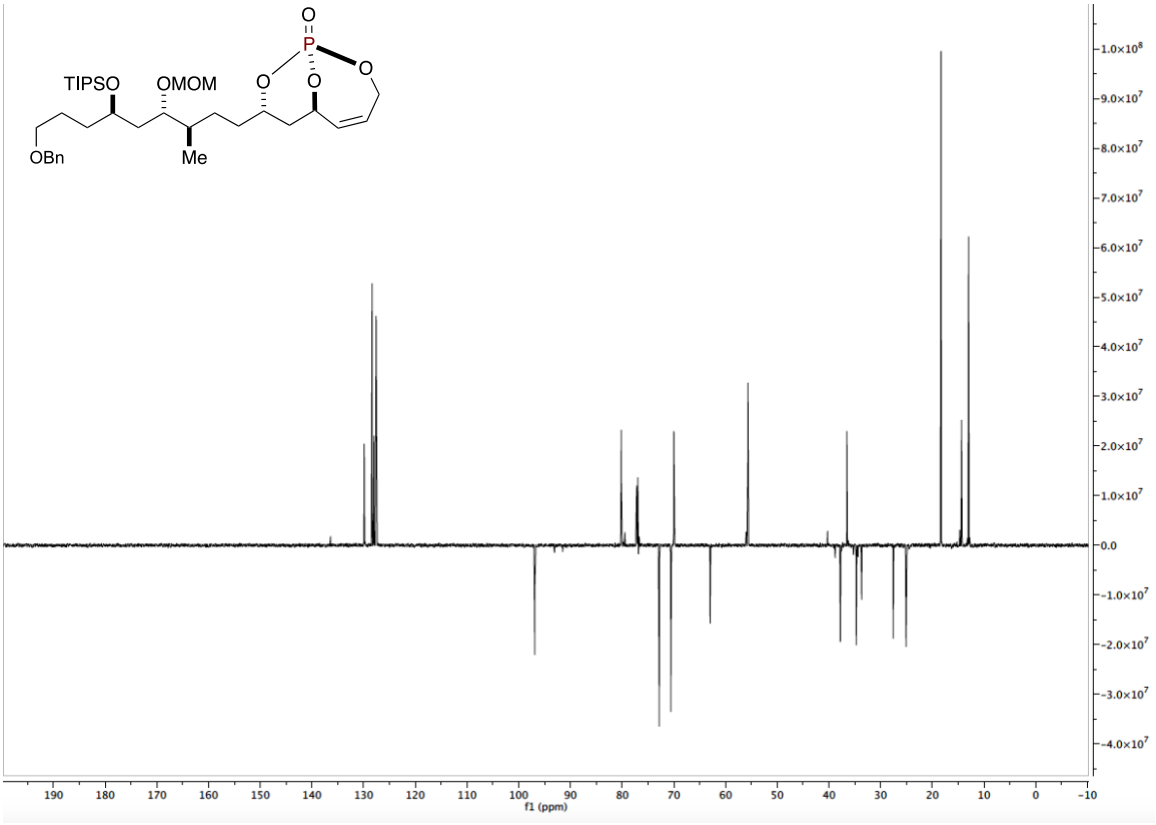

2D, $^1H^1H$, COSY, 500 MHz, $CDCl_3$

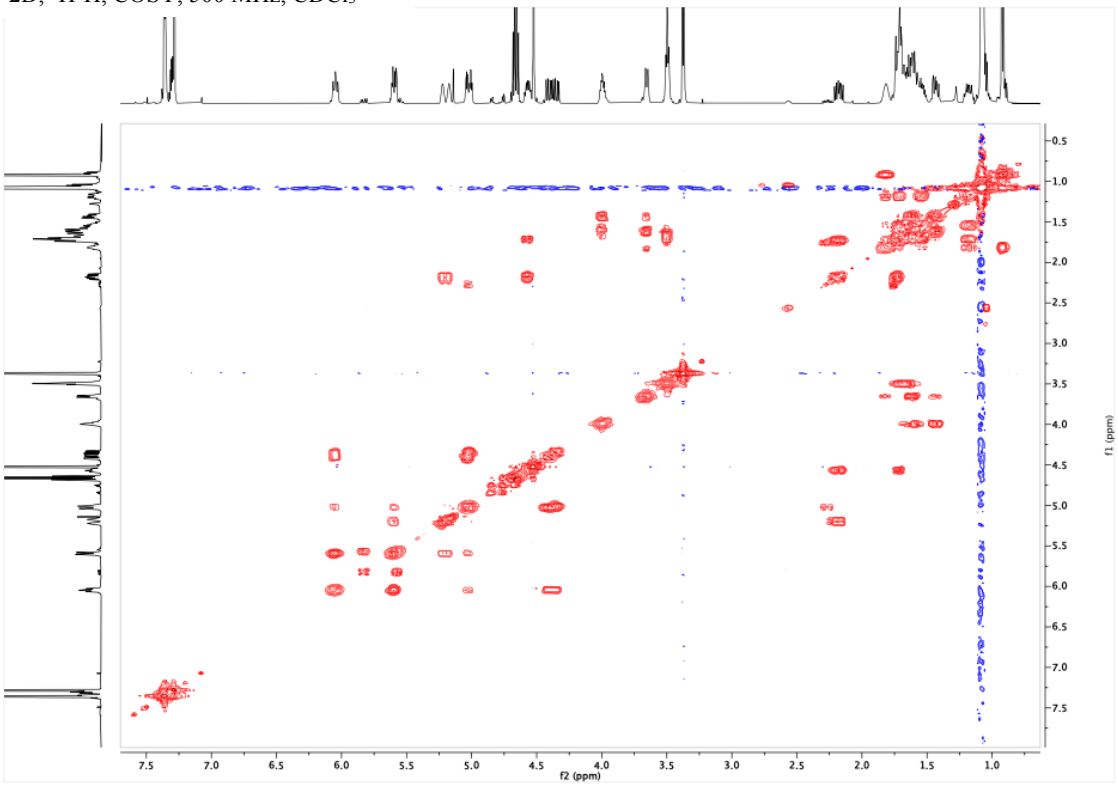

2D, $^{1}H^{13}C$, HSQC, 500 MHz, $CDCl_3$

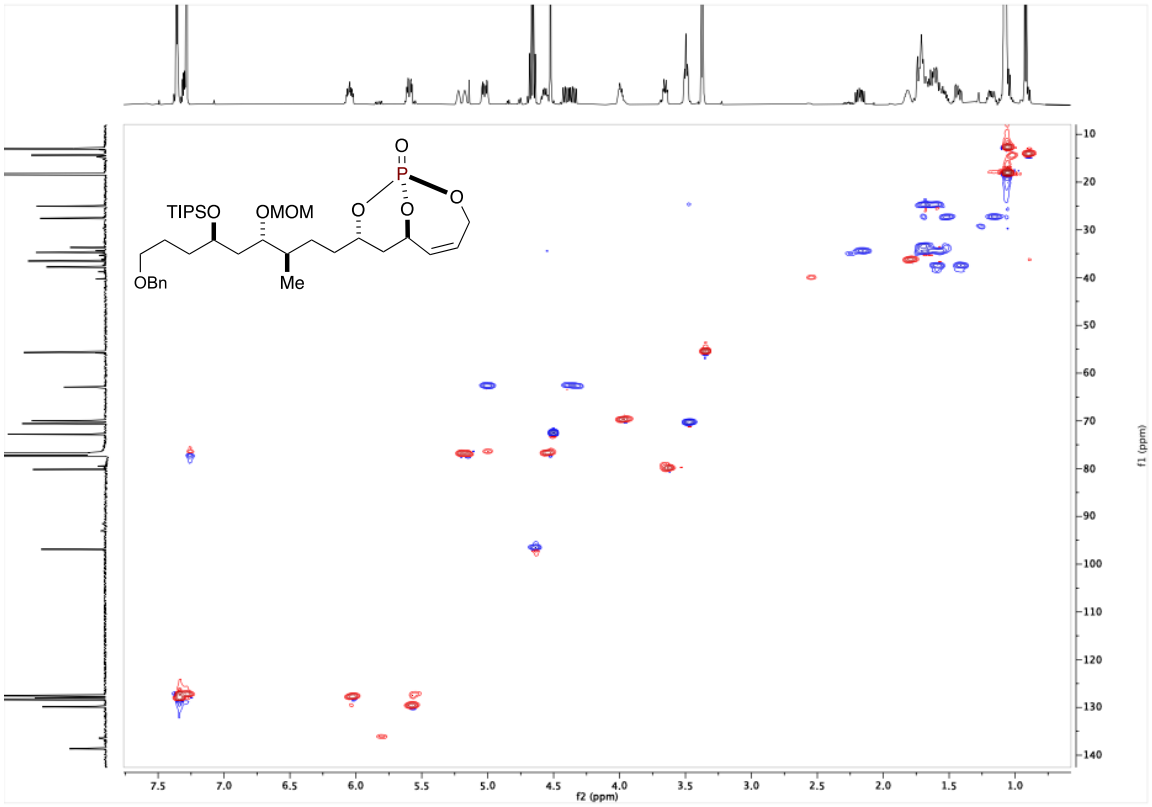

^{31}P, 202 MHz, $CDCl_3$

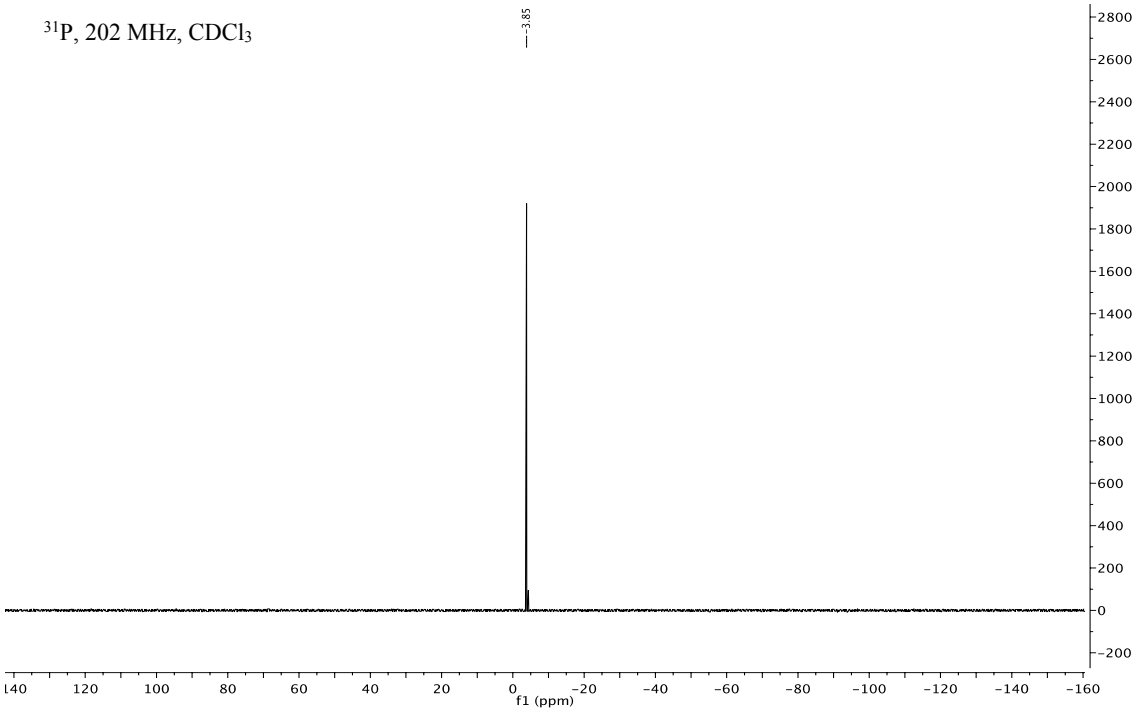

(1*R*,6*R*,8*S*)-8-((4*R*,6*R*)-9-(benzyloxy)-4,6-bis(methoxymethoxy)nonyl)-2,9,10-trioxa-1-phosphabicyclo[4.3.1]dec-4-ene 1-oxide (4.7.2)

^{1}H, 500 MHz, $CDCl_3$

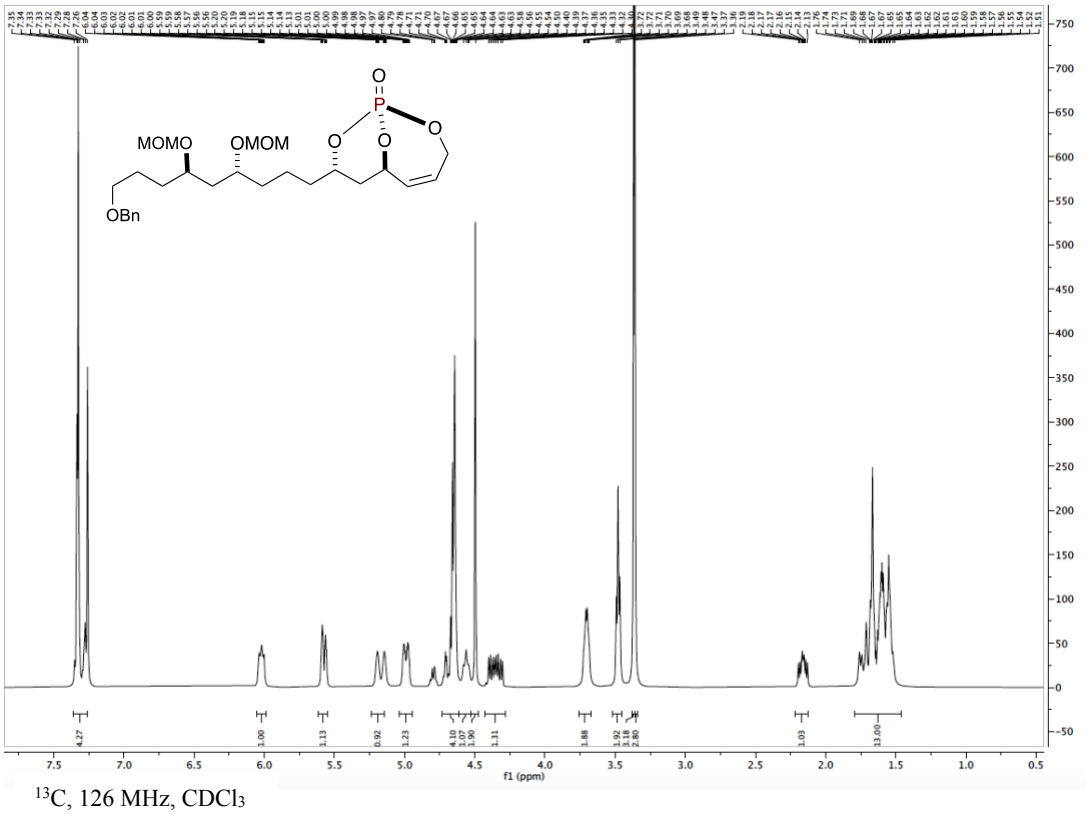

^{13}C, 126 MHz, $CDCl_3$

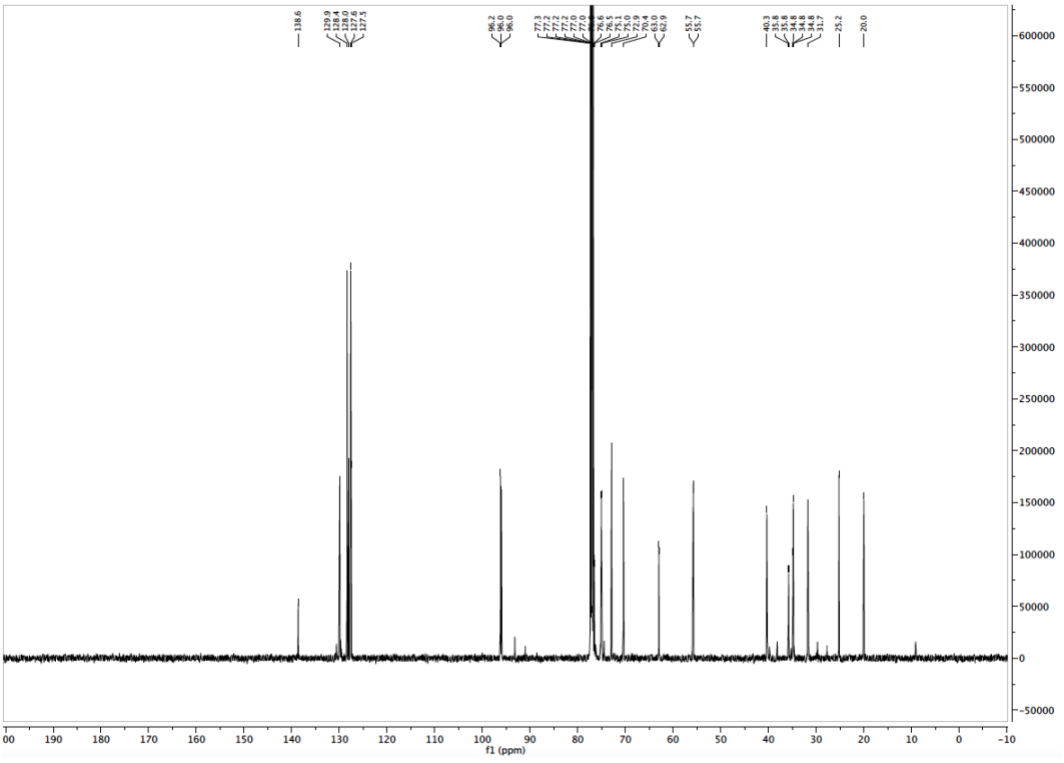

DEPT (135), 126 MHz, $CDCl_3$

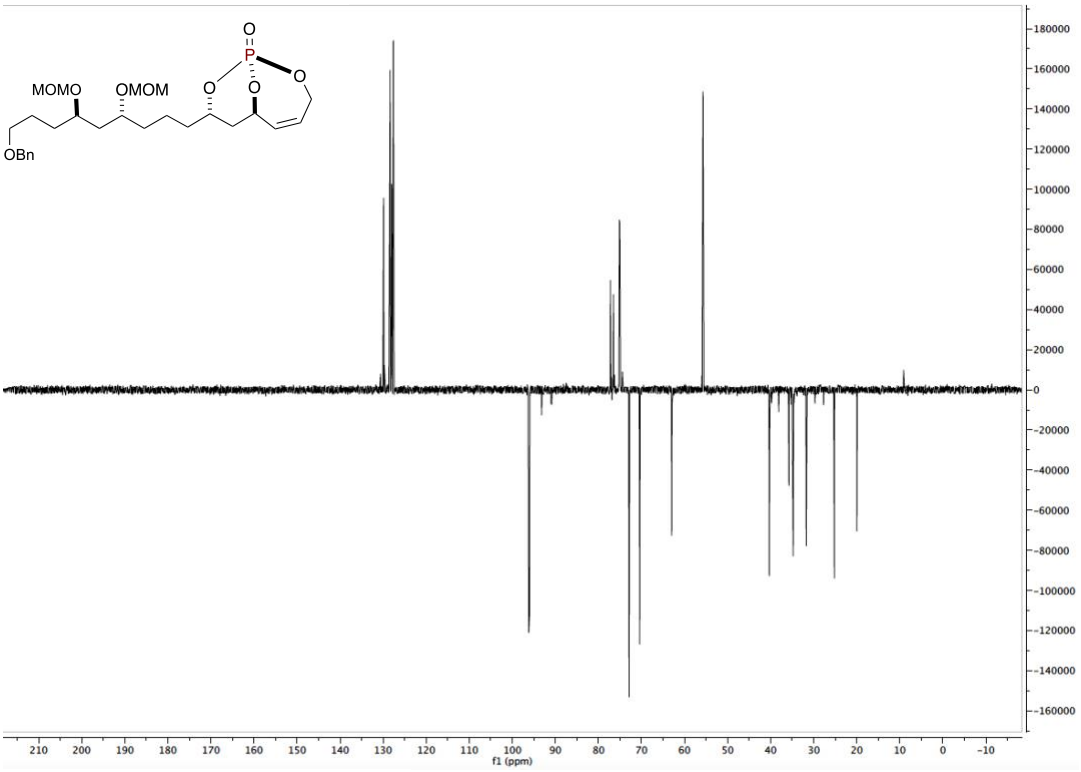

2D, $^1H^1H$, COSY, 500 MHz, $CDCl_3$

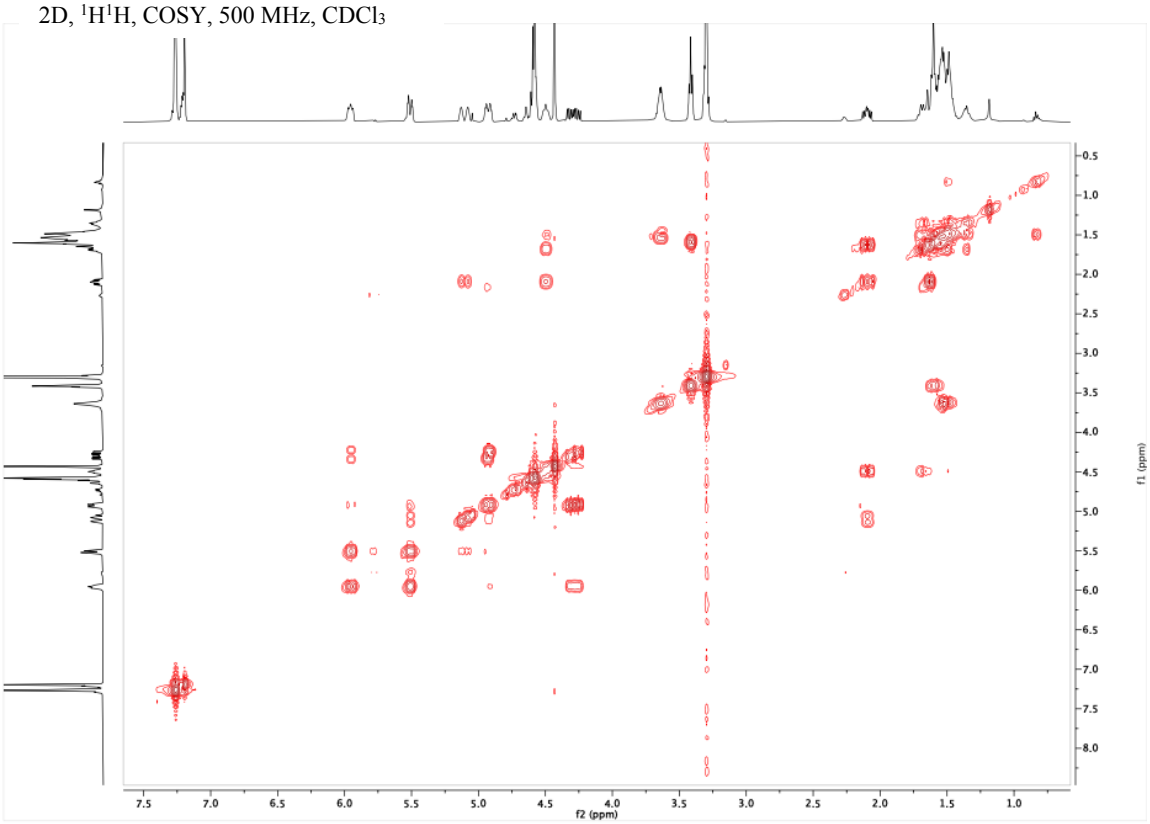

2D, $^{1}H^{13}C$, HSQC, 500 MHz, $CDCl_3$

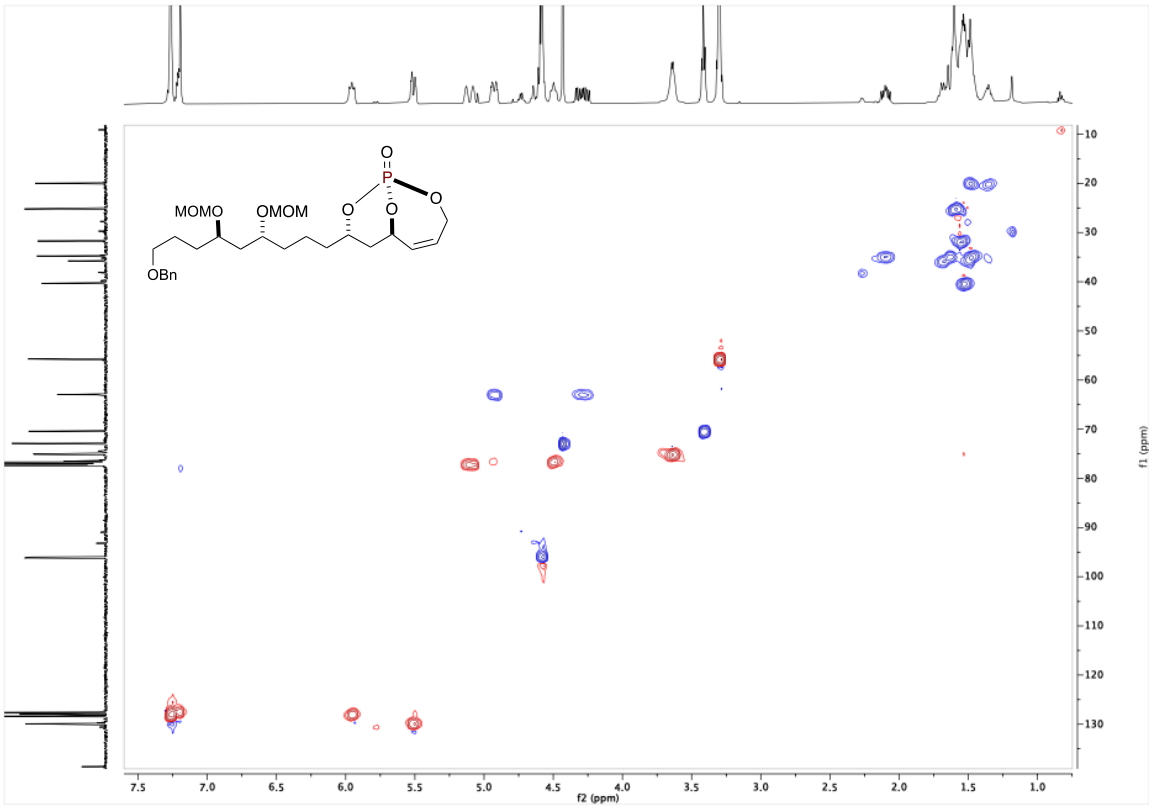

^{31}P, 202 MHz, $CDCl_3$

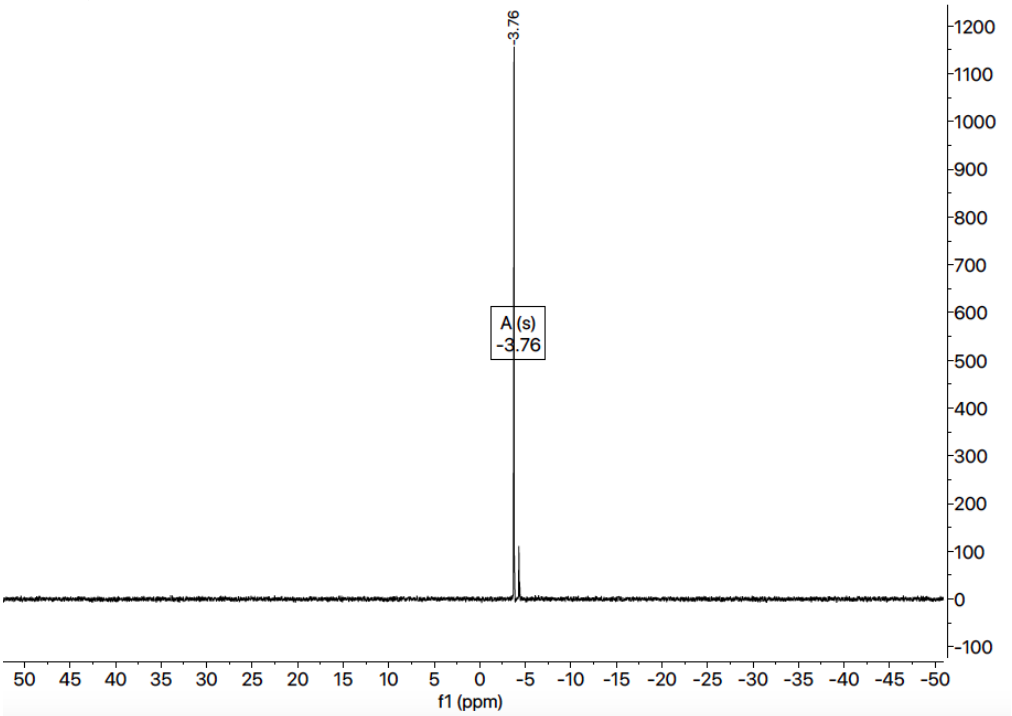

(4*R*,6*S*,7*R*,10*S*,12*R*,13*S*)-6-(methoxymethoxy)-7-methyl-4-((triisopropylsilyl)oxy)-13-vinylnonadecane-1,10,12-triol (4.7.3)

^{1}H, 500 MHz, $CDCl_3$

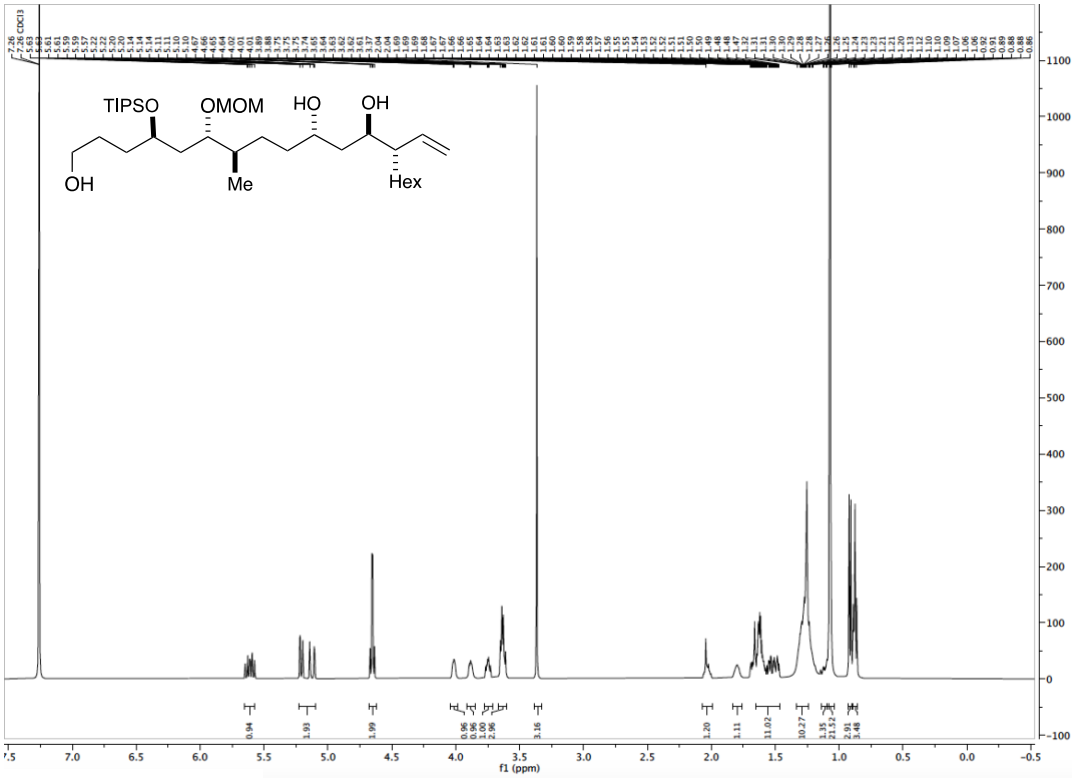

^{13}C, 126 MHz, $CDCl_3$

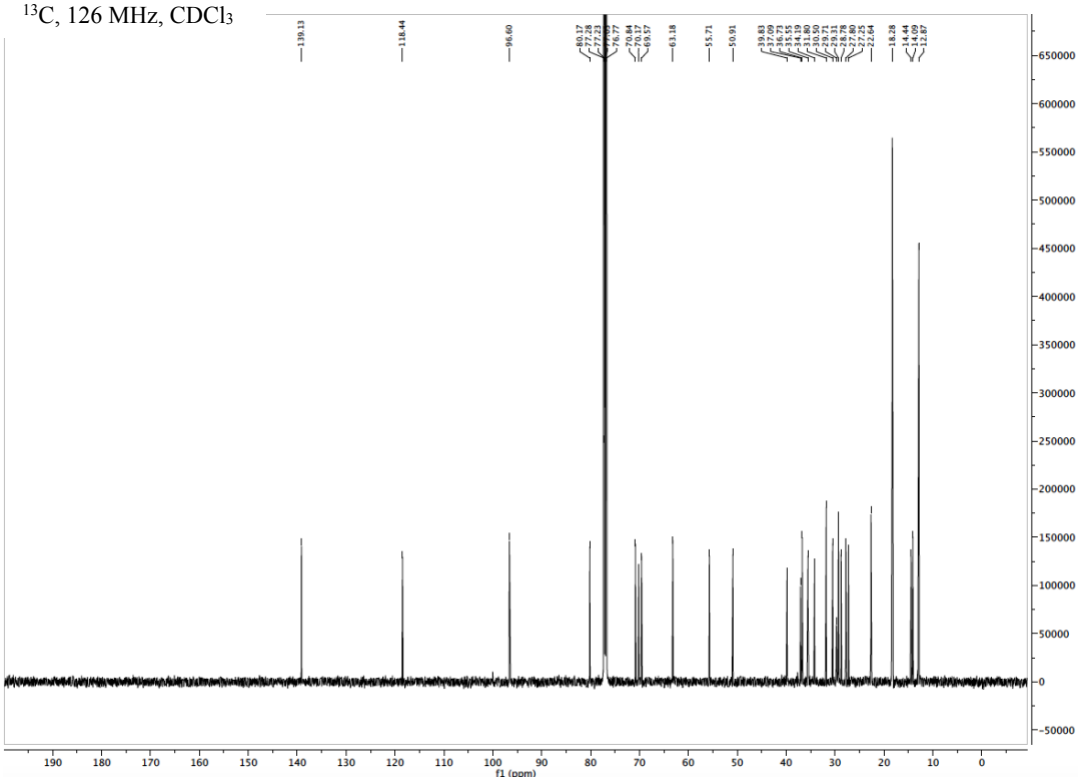

DEPT (135), 126 MHz, $CDCl_3$

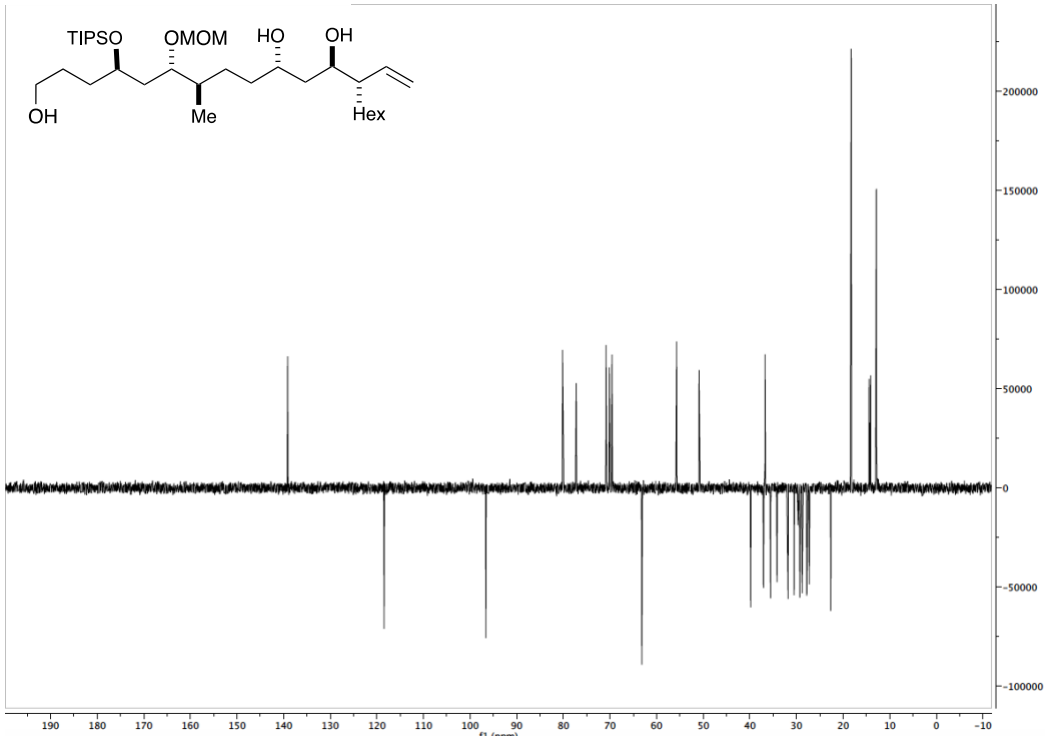

2D, $^1H^1H$, COSY, 500 MHz, $CDCl_3$

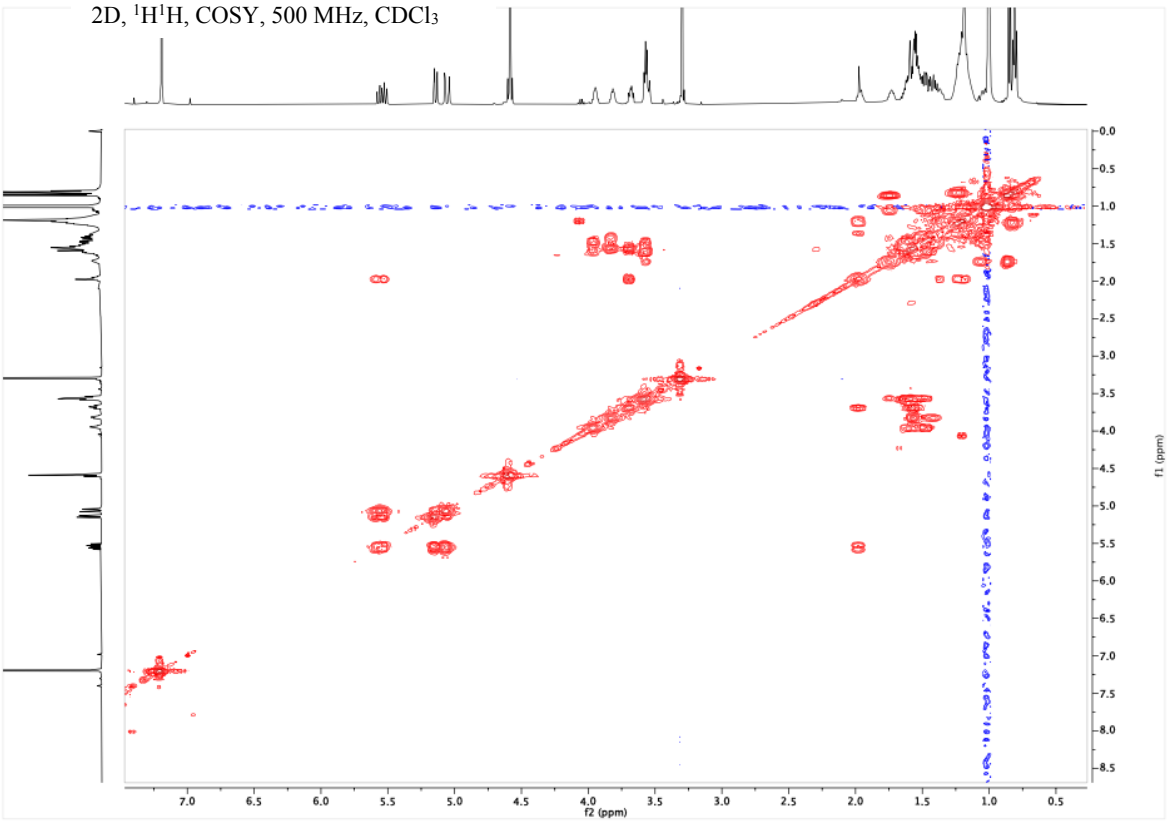

2D, $^{1}H^{13}C$, HSQC, 500 MHz, $CDCl_3$

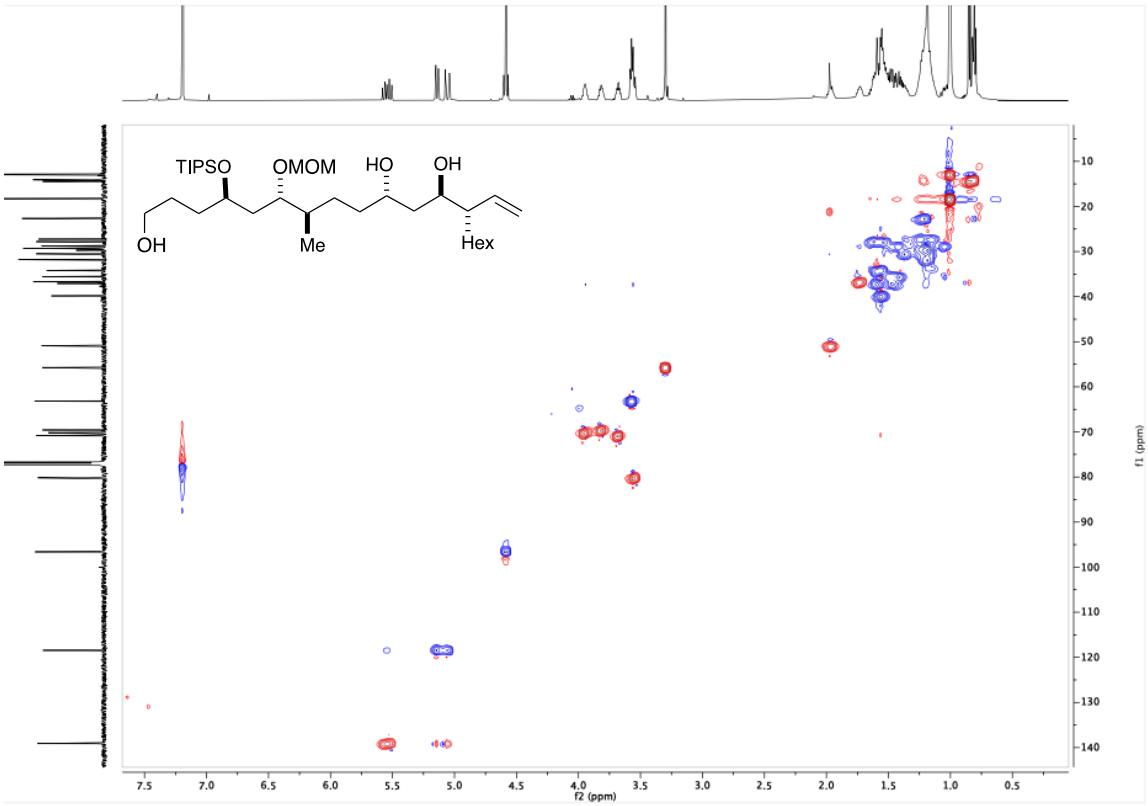

(4*S*,6*S*,10*R*,12*R*)-15-(benzyloxy)-10,12-bis(methoxymethoxy)pentadec-1-ene-4,6-diol (4.7.4)

^{1}H, 500 MHz, $CDCl_3$

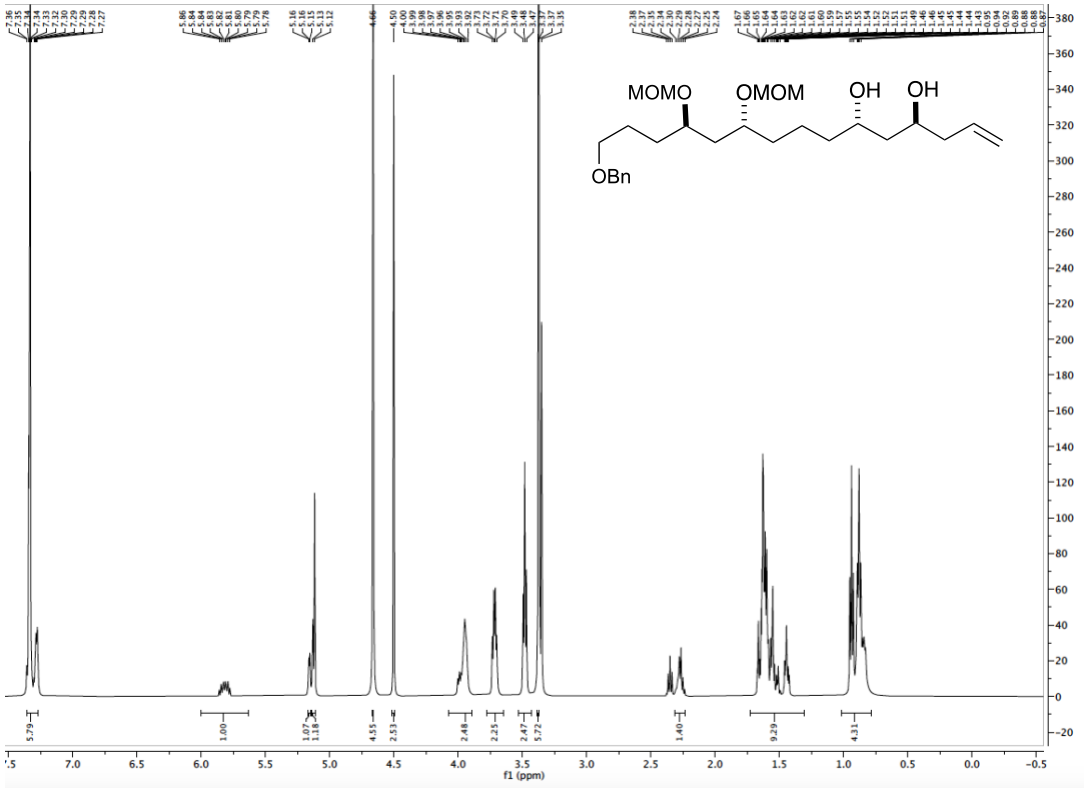

^{13}C, 126 MHz, $CDCl_3$

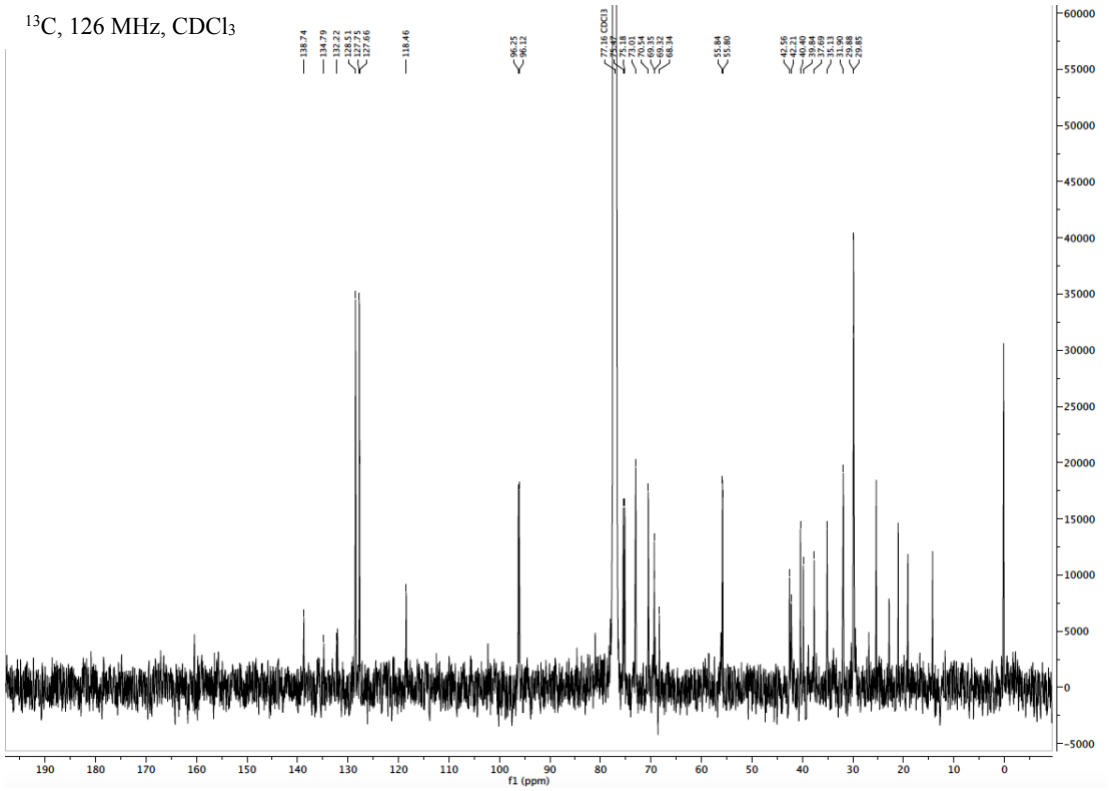

(5S,7R)-7-((S)-3,4-bis(benzyloxy)butyl)-5-((R)-but-3-en-2-yl)-9,9-diisopropyl-10-methyl-2,4,8-trioxa-9-silaundecane (4.8.1)

^{1}H, 500 MHz, $CDCl_3$

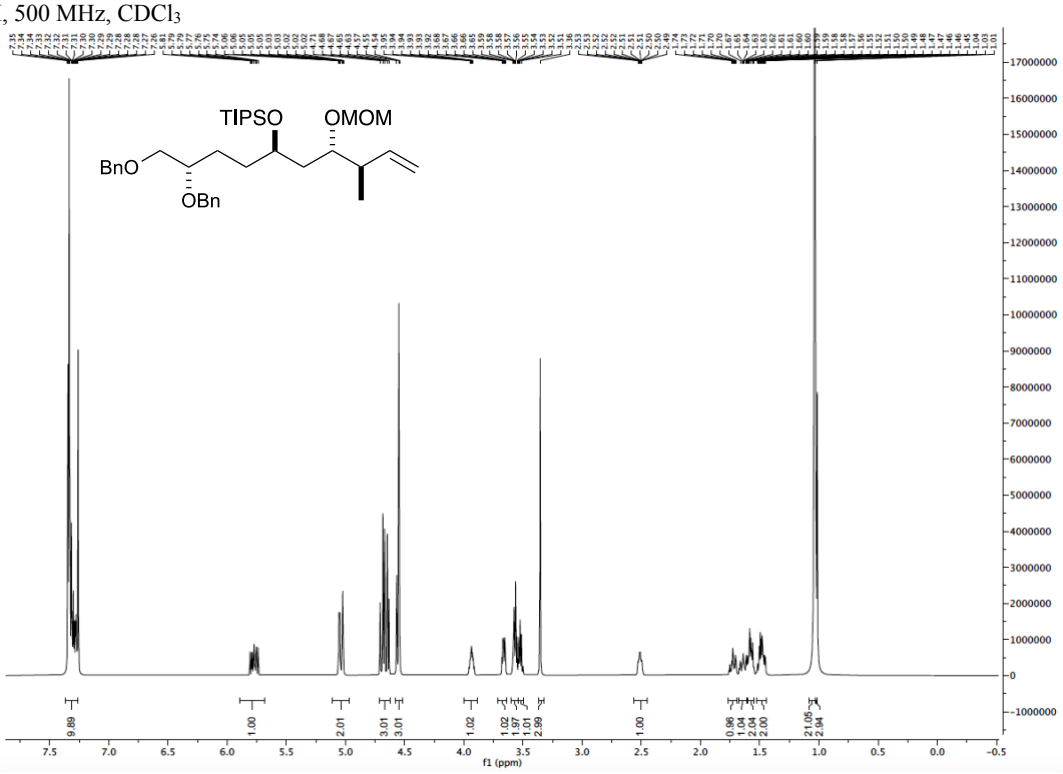

^{13}C, 126 MHz, $CDCl_3$

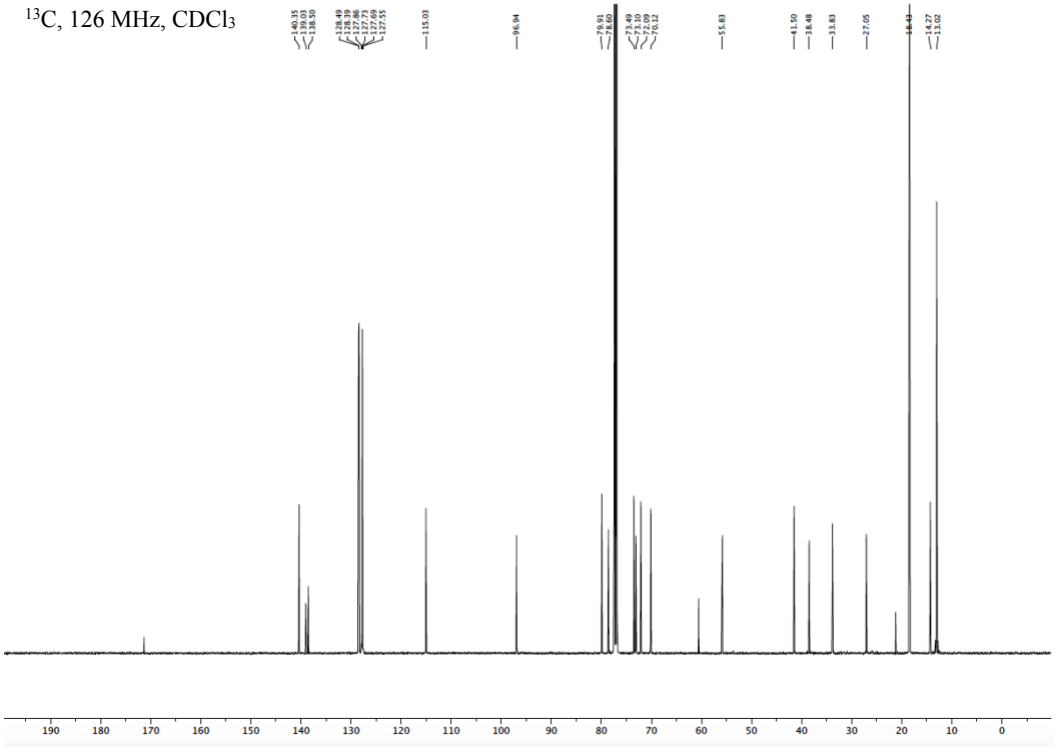

DEPT (135), 126 MHz, $CDCl_3$

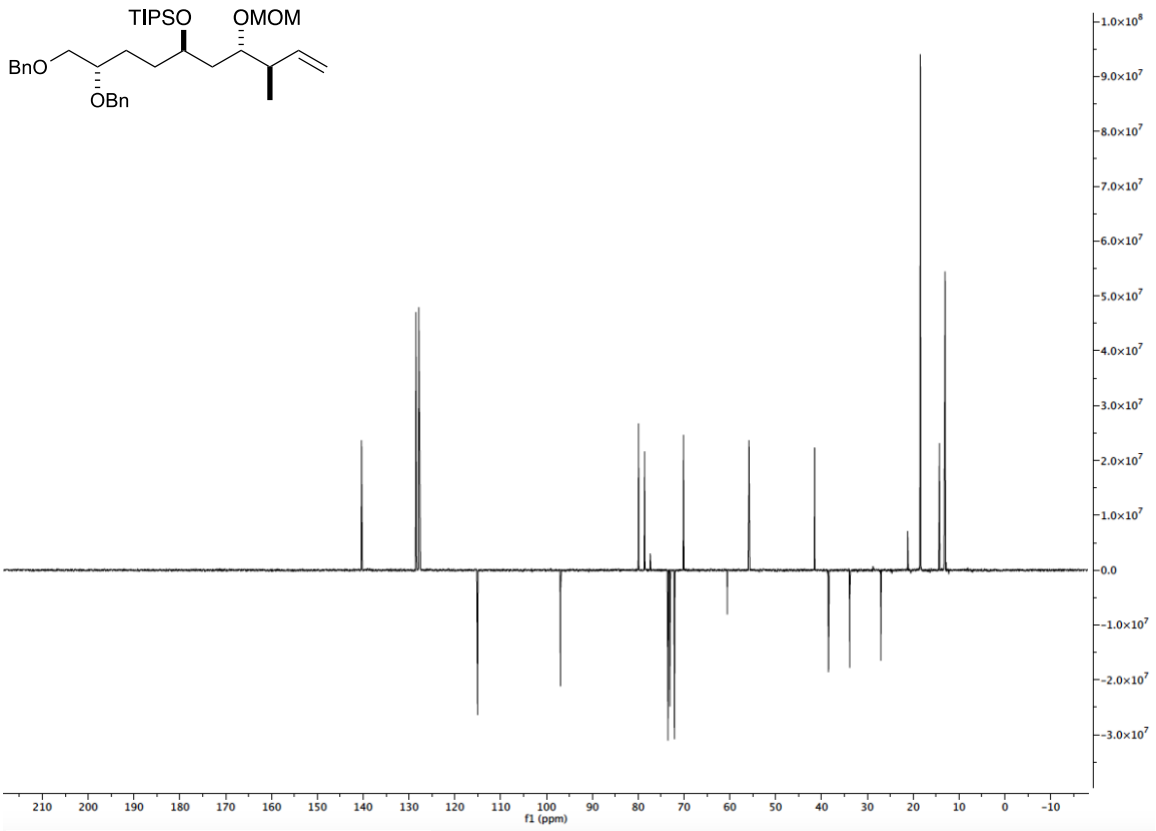

2D, $^1H^1H$, COSY, 500 MHz, $CDCl_3$

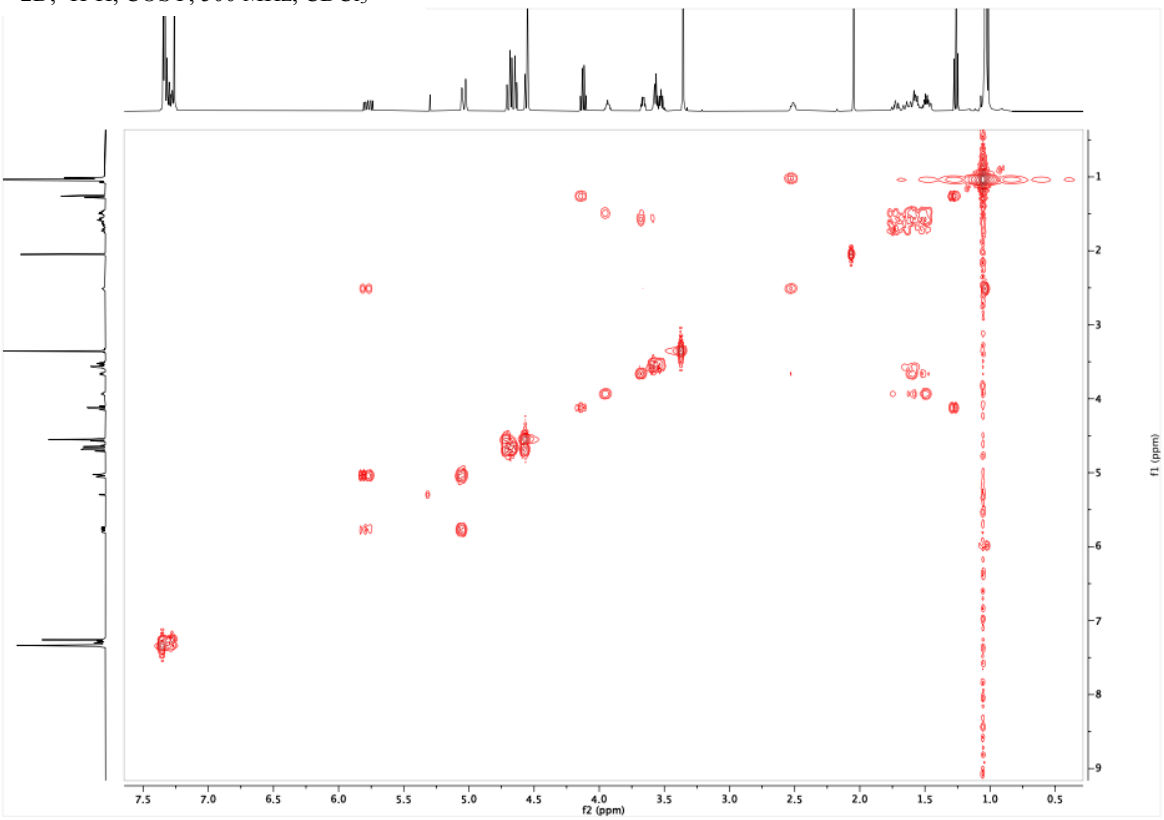

2D, $^{1}H^{13}C$, HSQC, 500 MHz, $CDCl_3$

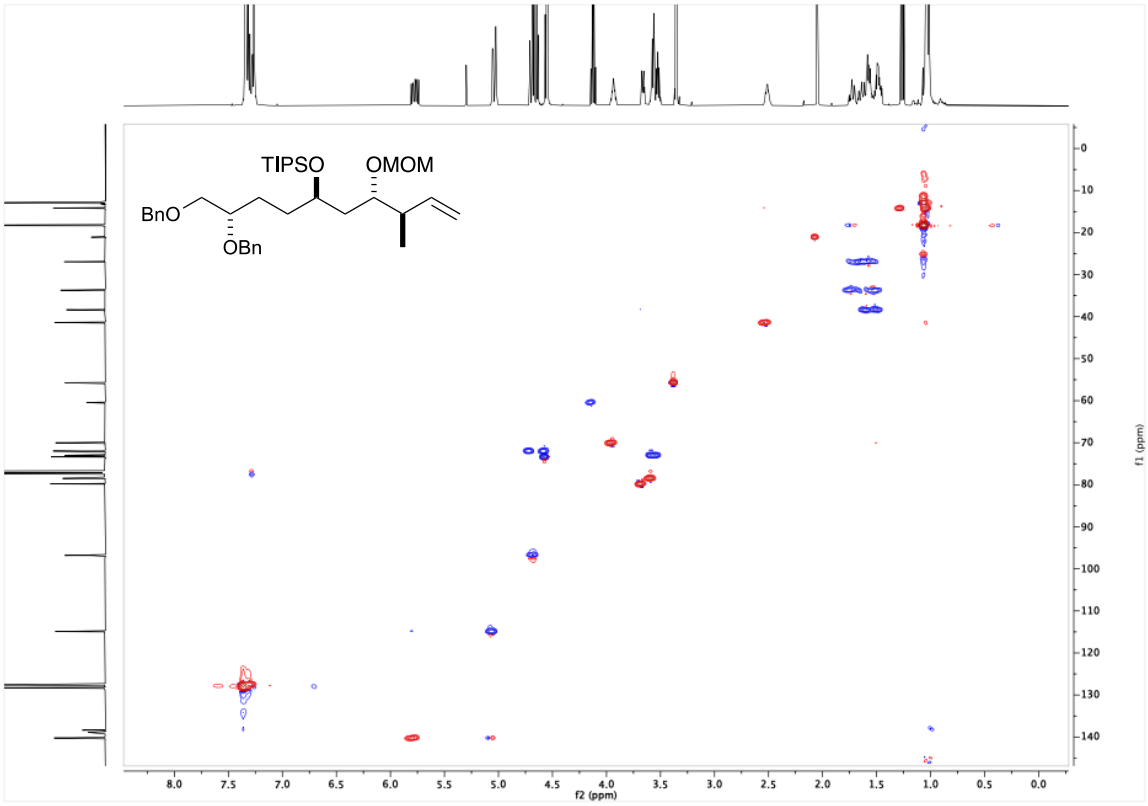

(6R,8S)-8-((3R,4S,6R,9S)-9,10-bis(benzyloxy)-4-(methoxymethoxy)-3-methyl-6-((triisopropylsilyl)oxy)decyl)-2,9,10-trioxa-1-phosphabicyclo[4.3.1]dec-4-ene 1-oxide (4.8.2)

^{1}H, 500 MHz, $CDCl_3$

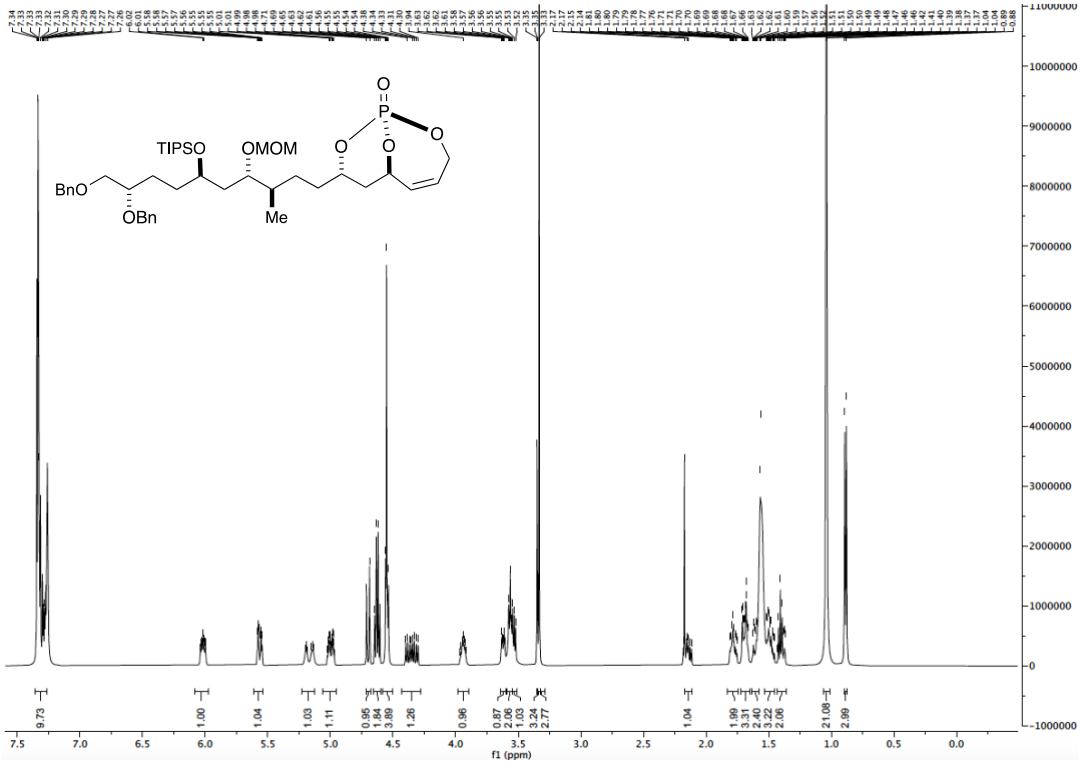

^{13}C, 126 MHz, $CDCl_3$

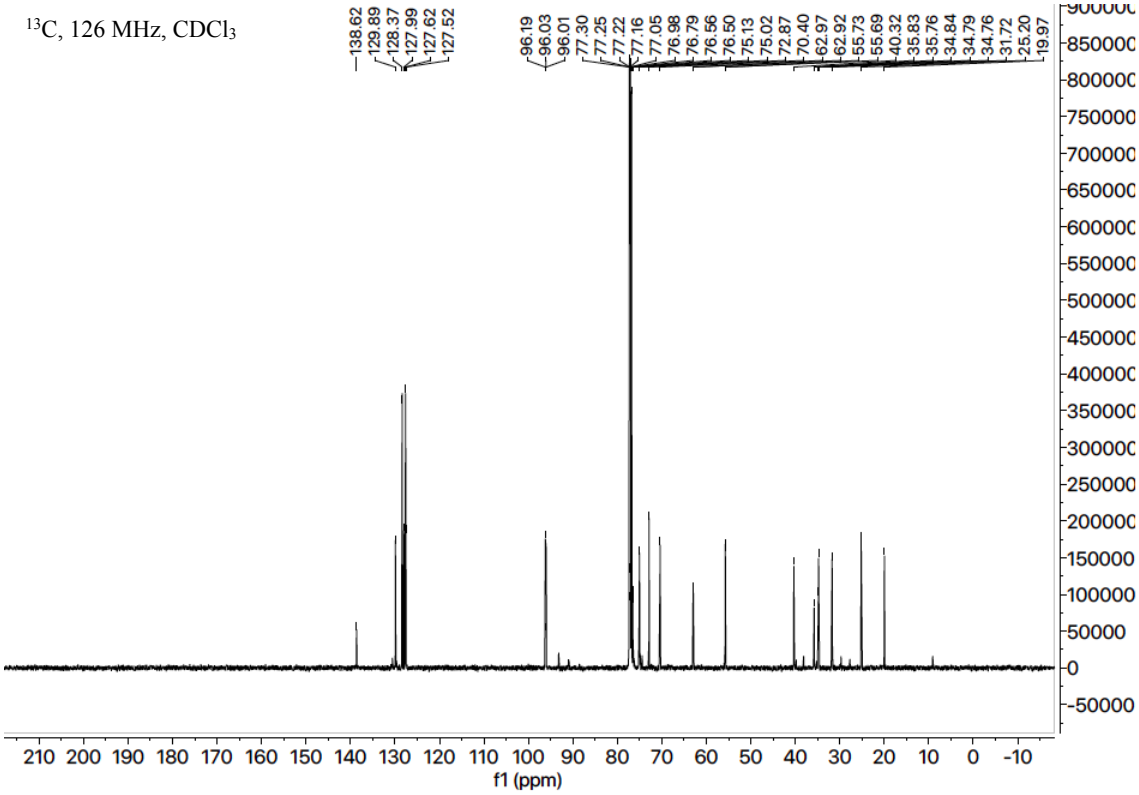

DEPT (135), 126 MHz, $CDCl_3$

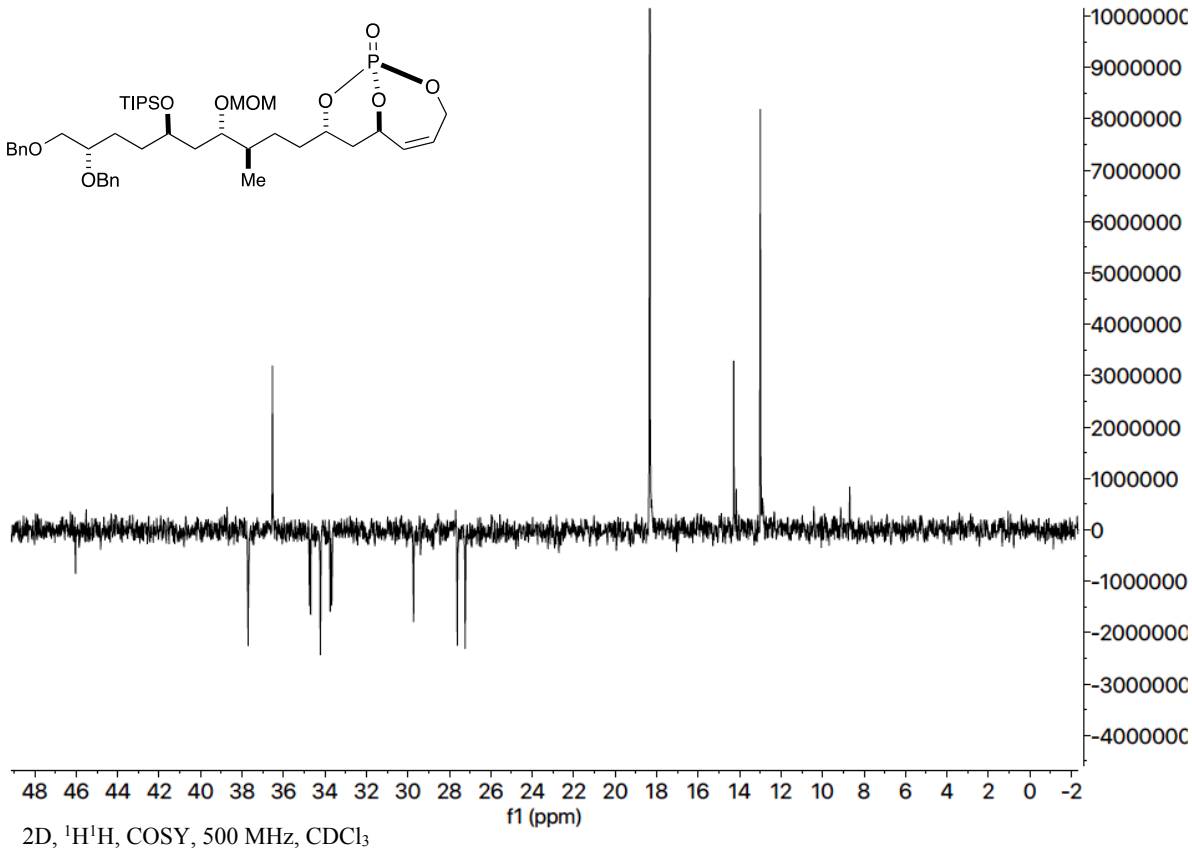

2D, $^1H^1H$, COSY, 500 MHz, $CDCl_3$

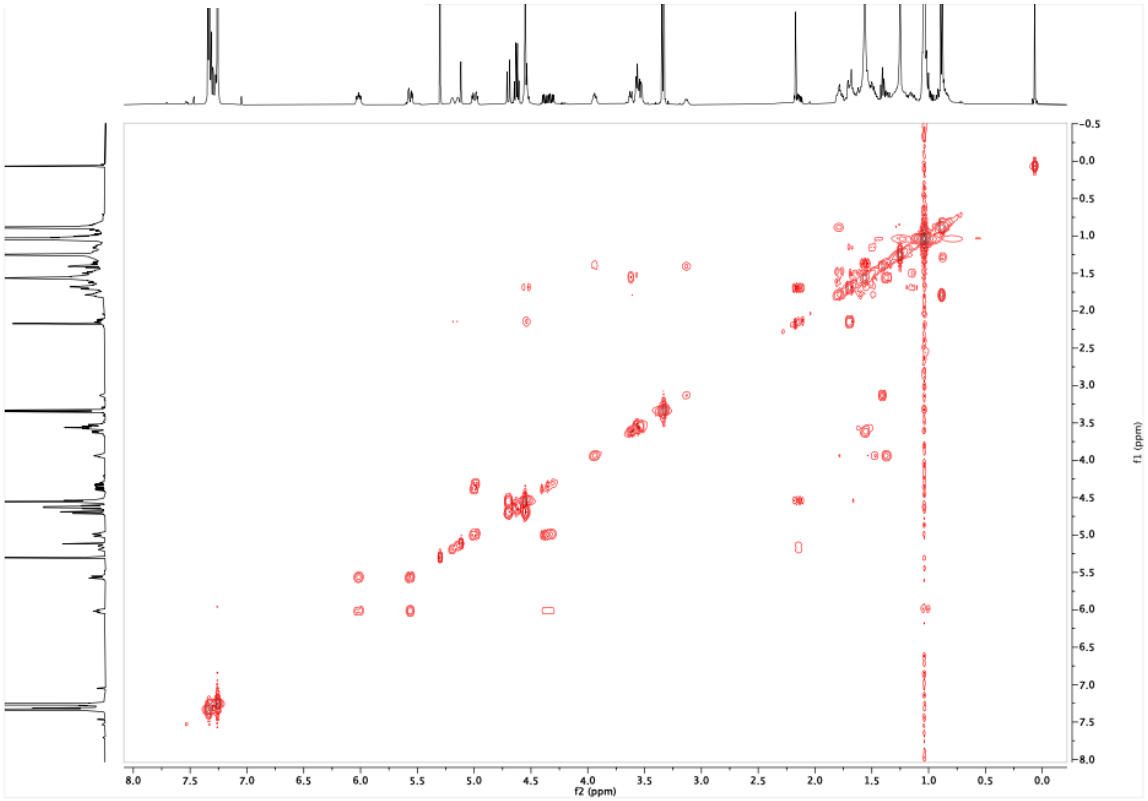

2D, $^{1}H^{13}C$, HSQC, 500 MHz, $CDCl_3$

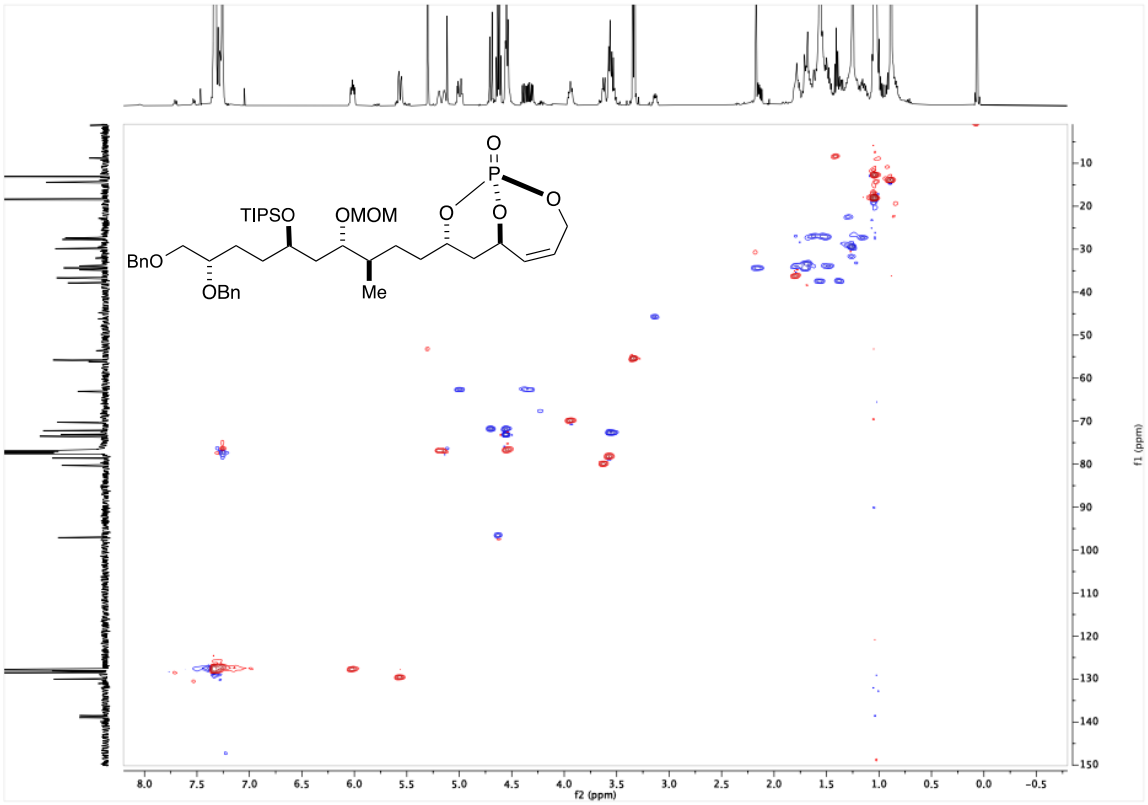

^{31}P, 202 MHz, $CDCl_3$

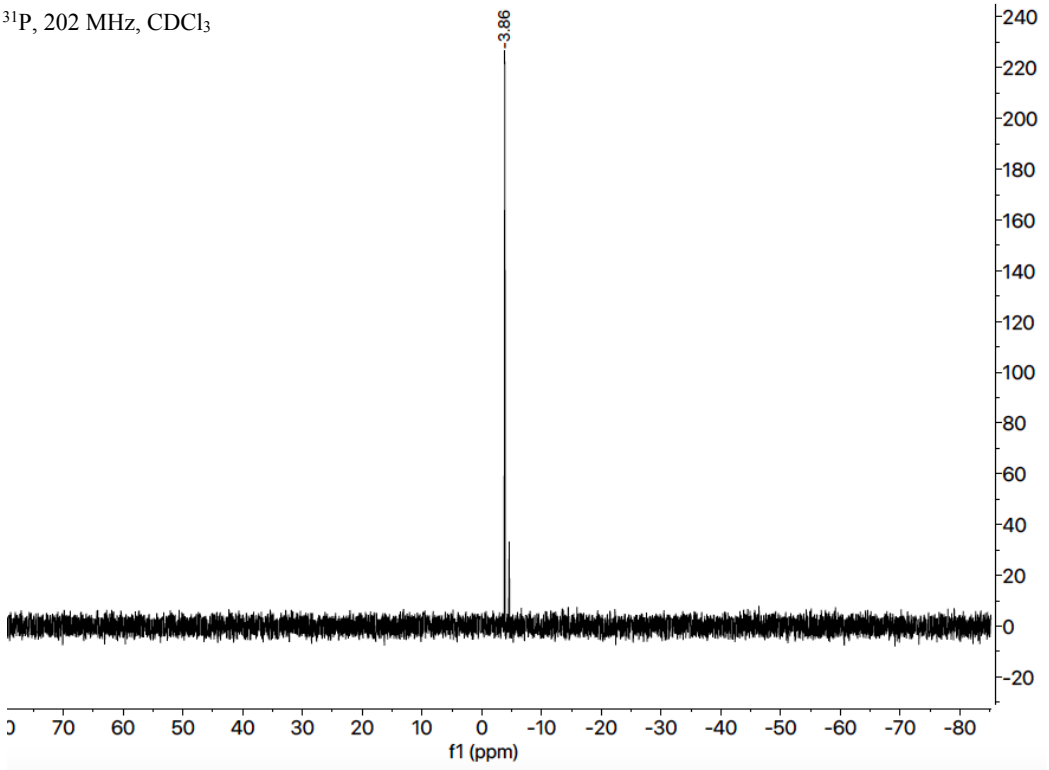

(3S,4R,6S,9R,10S,12R,15S)-15,16-bis(benzyloxy)-10-(methoxymethoxy)-3,9-dimethyl-12-((triisopropylsilyl)oxy)hexadec-1-ene-4,6-diol (4.8.3)

^{1}H, 500 MHz, $CDCl_3$

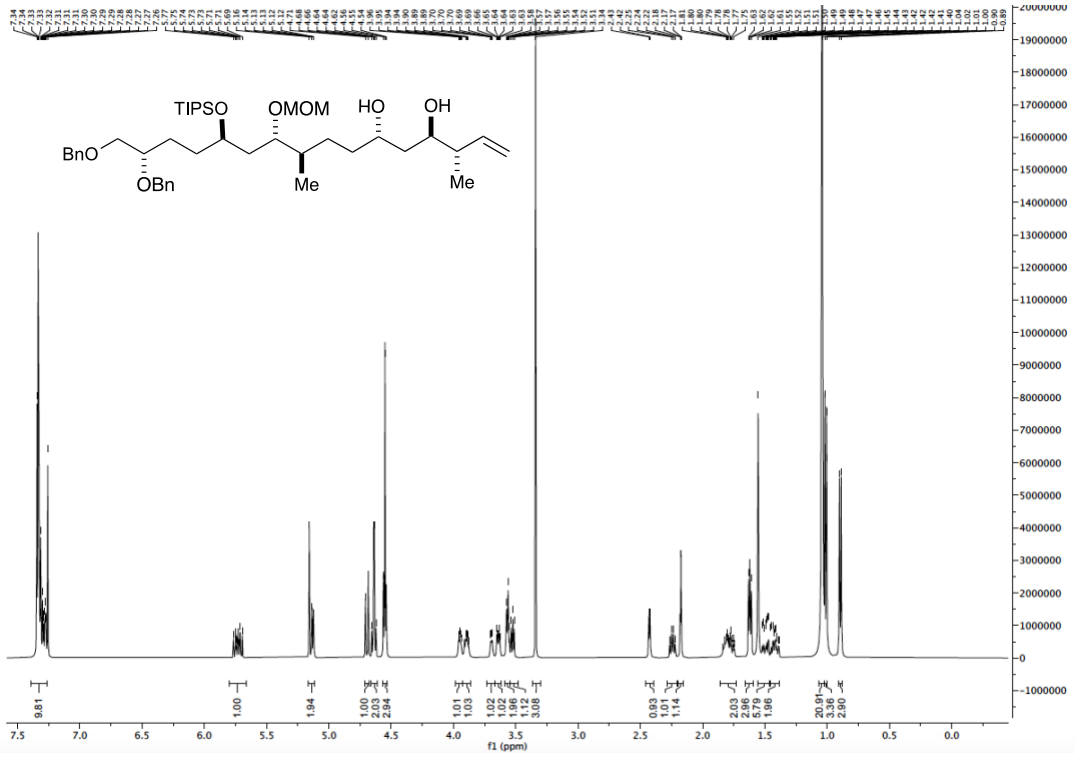

^{13}C, 126 MHz, $CDCl_3$

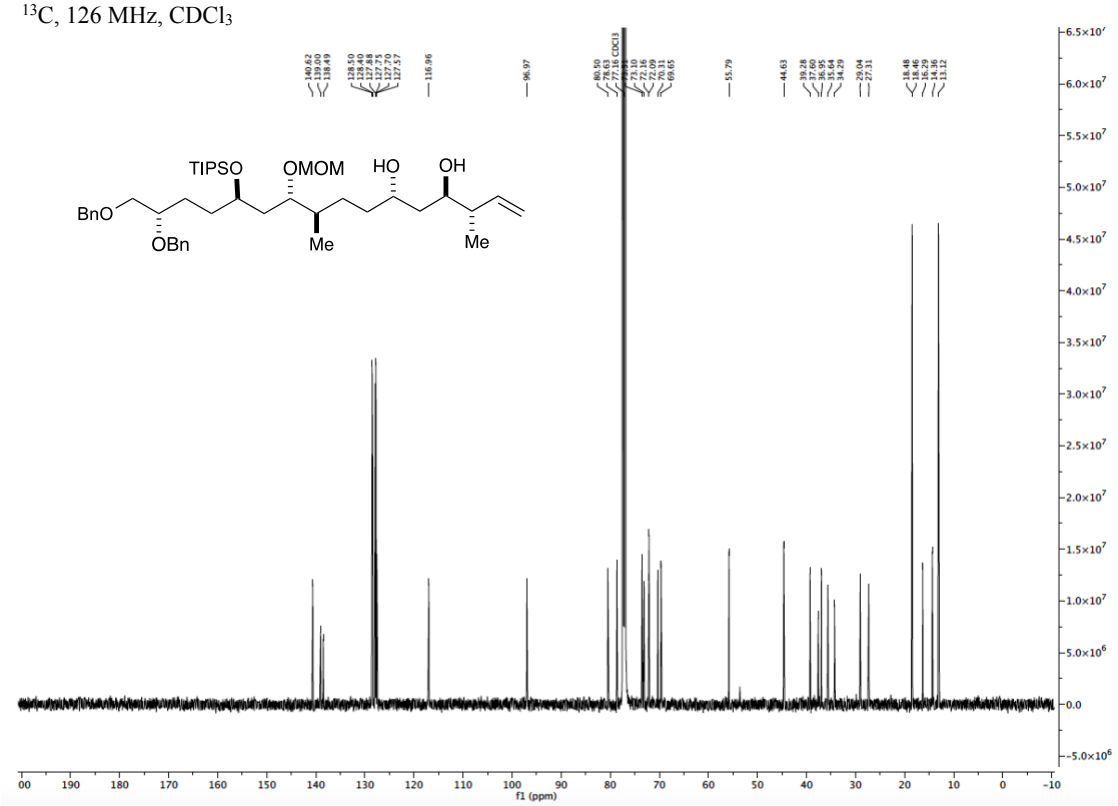

DEPT (135), 126 MHz, $CDCl_3$

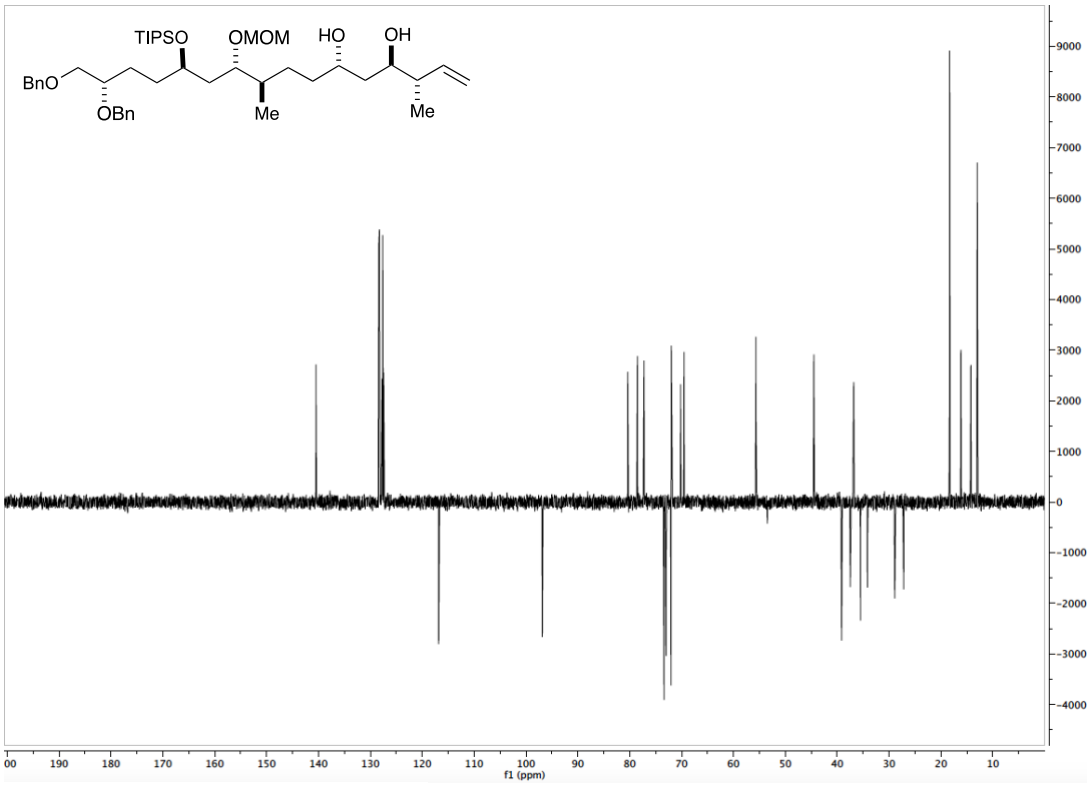

2D, $^1H^1H$, COSY, 500 MHz, $CDCl_3$

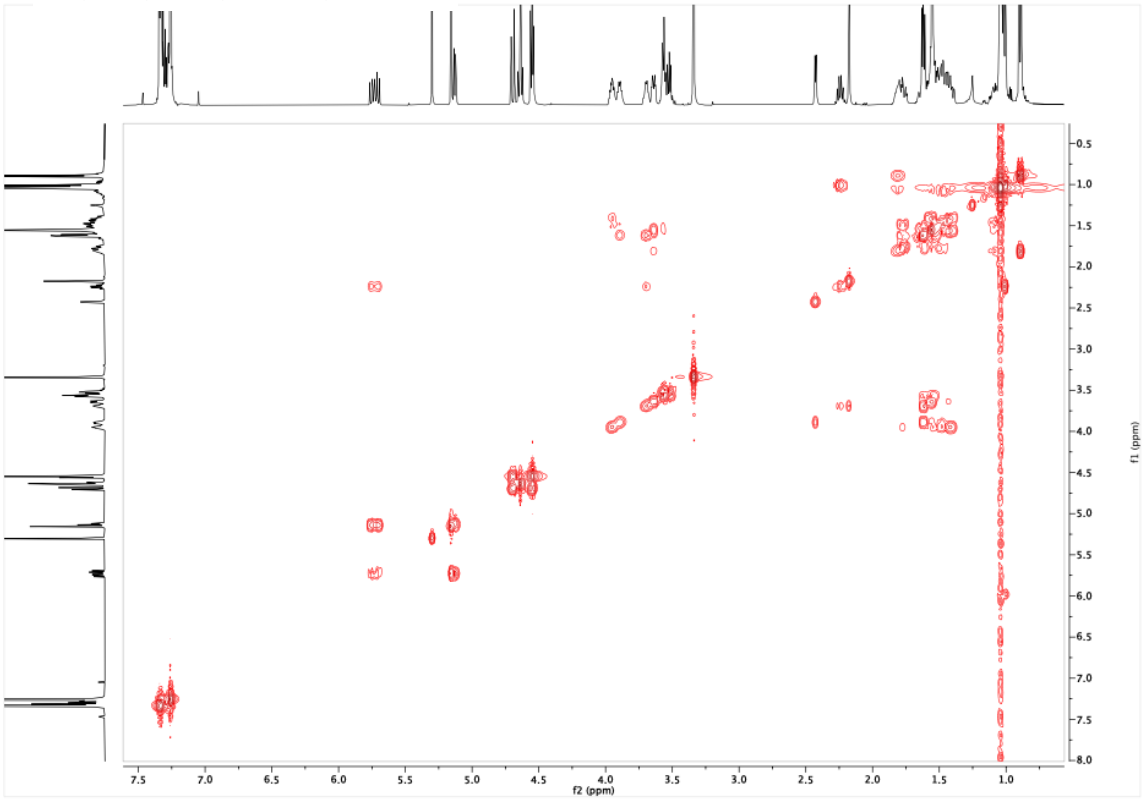

2D, $^{1}H^{13}C$, HSQC, 500 MHz, $CDCl_3$

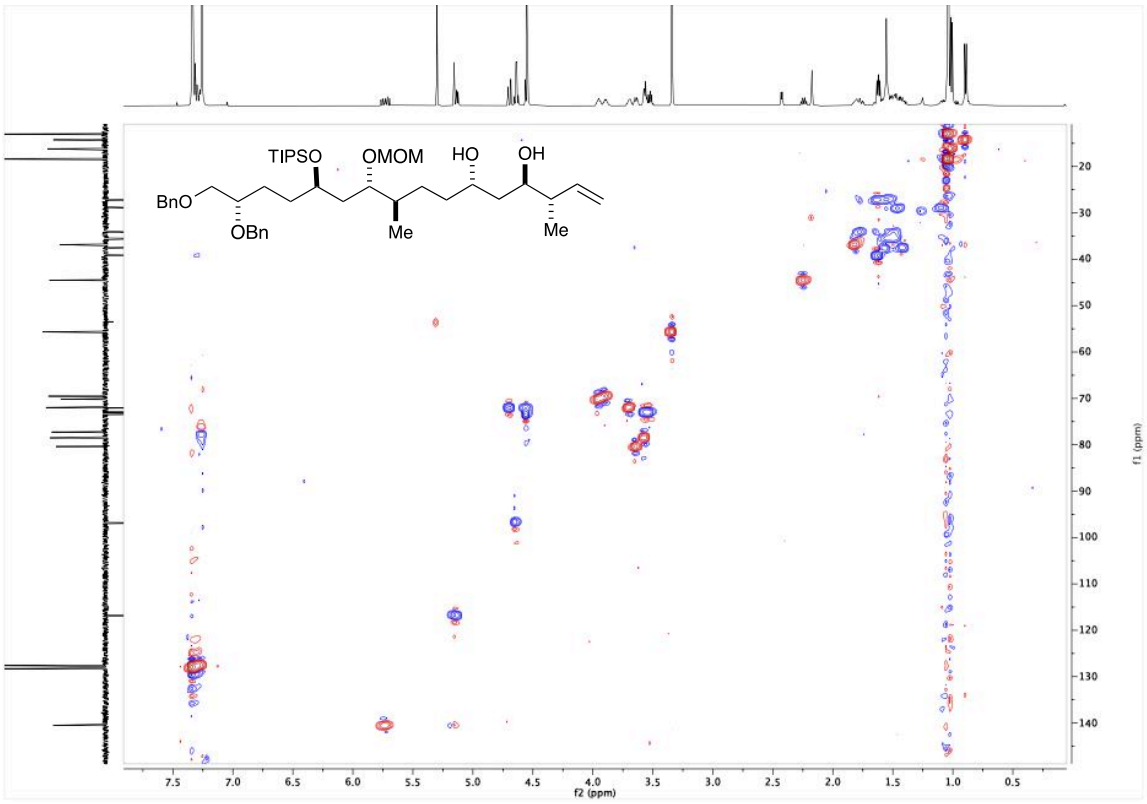

(4*S*,6*S*,9*R*)-9-((4*S*,6*R*)-6-((*S*)-3,4-bis(benzyloxy)butyl)-1,3-dioxan-4-yl)dec-1-ene-4,6-diol (4.8.4): ^{1}H, 500 MHz, $CDCl_3$

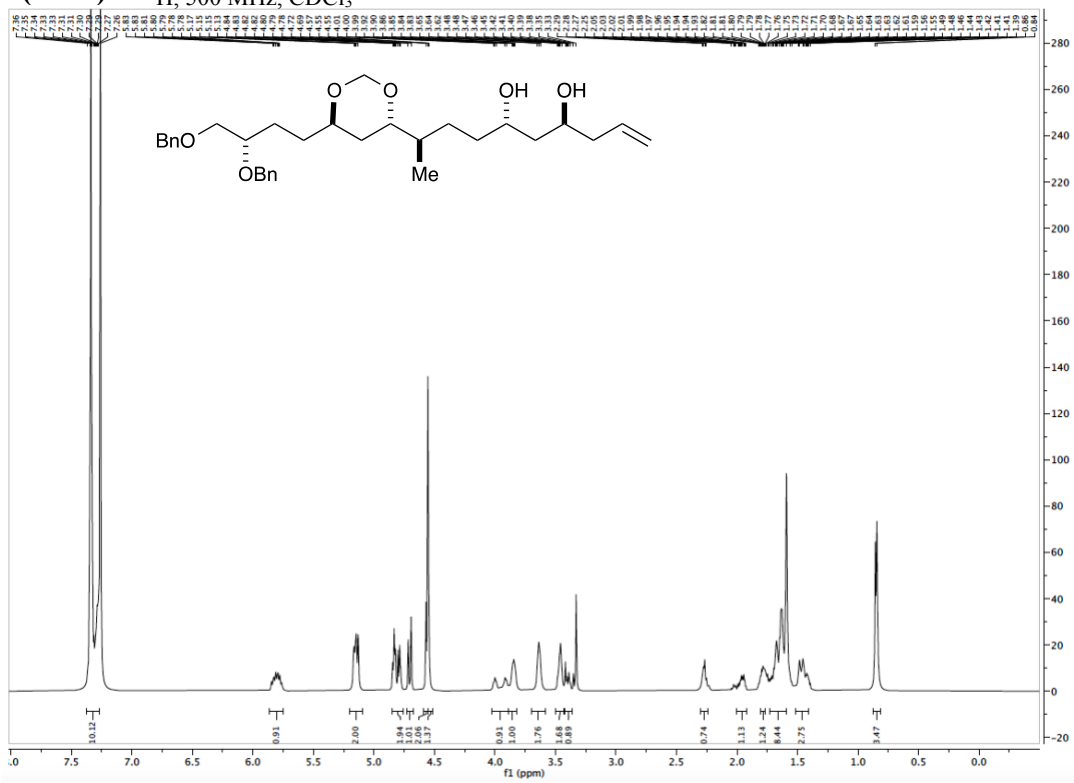

^{13}C, 126 MHz, $CDCl_3$

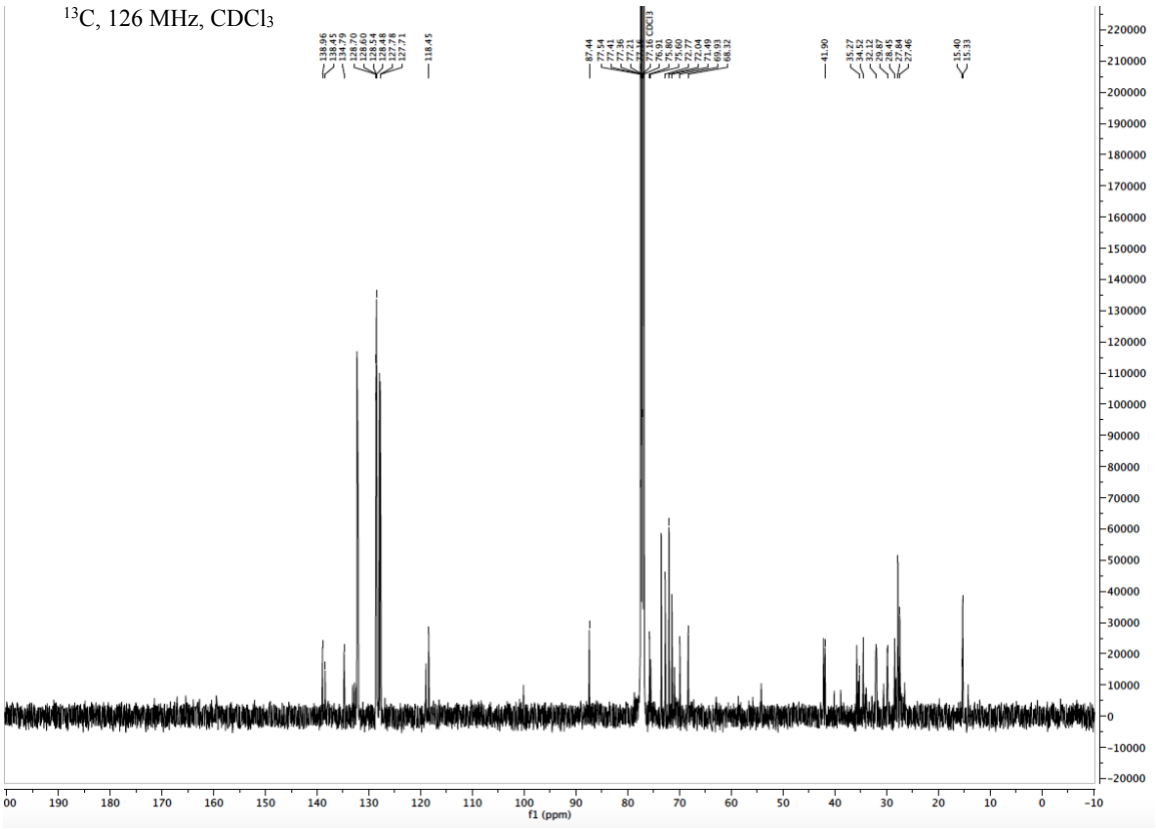

DEPT (135), 126 MHz, $CDCl_3$

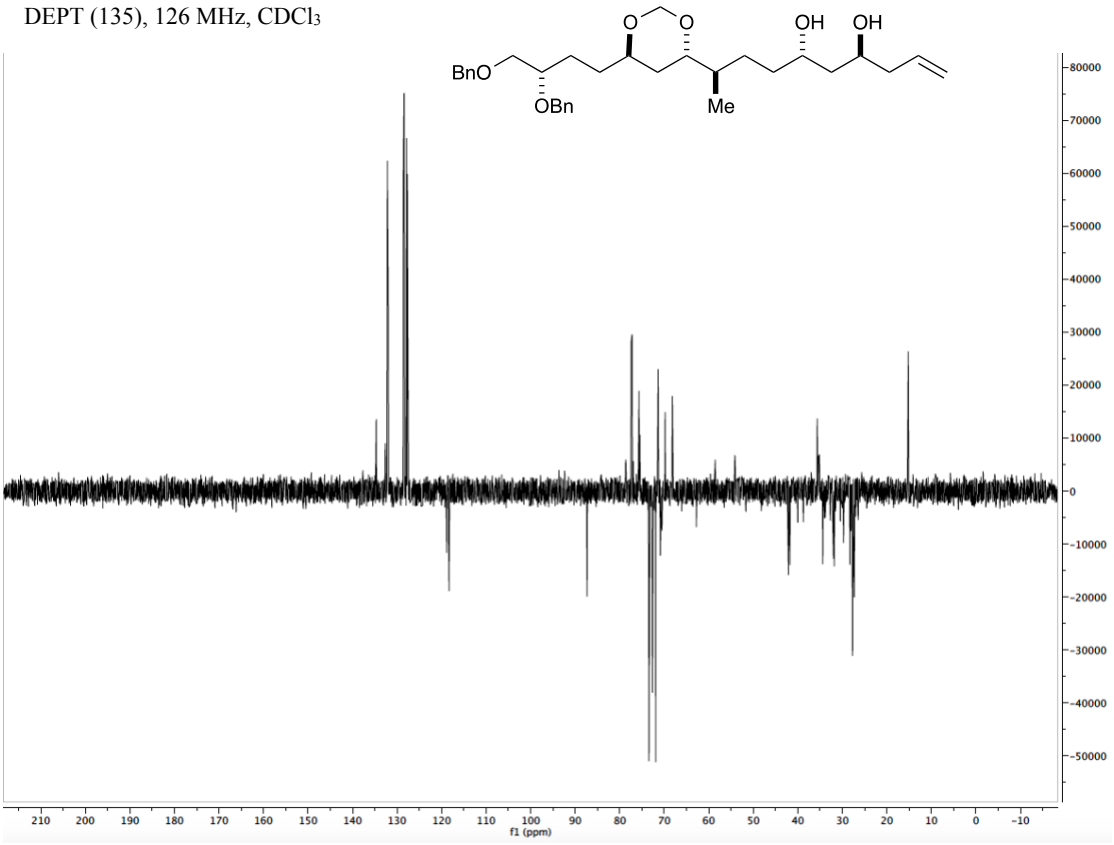

2D, $^1H^1H$, COSY, 500 MHz, $CDCl_3$

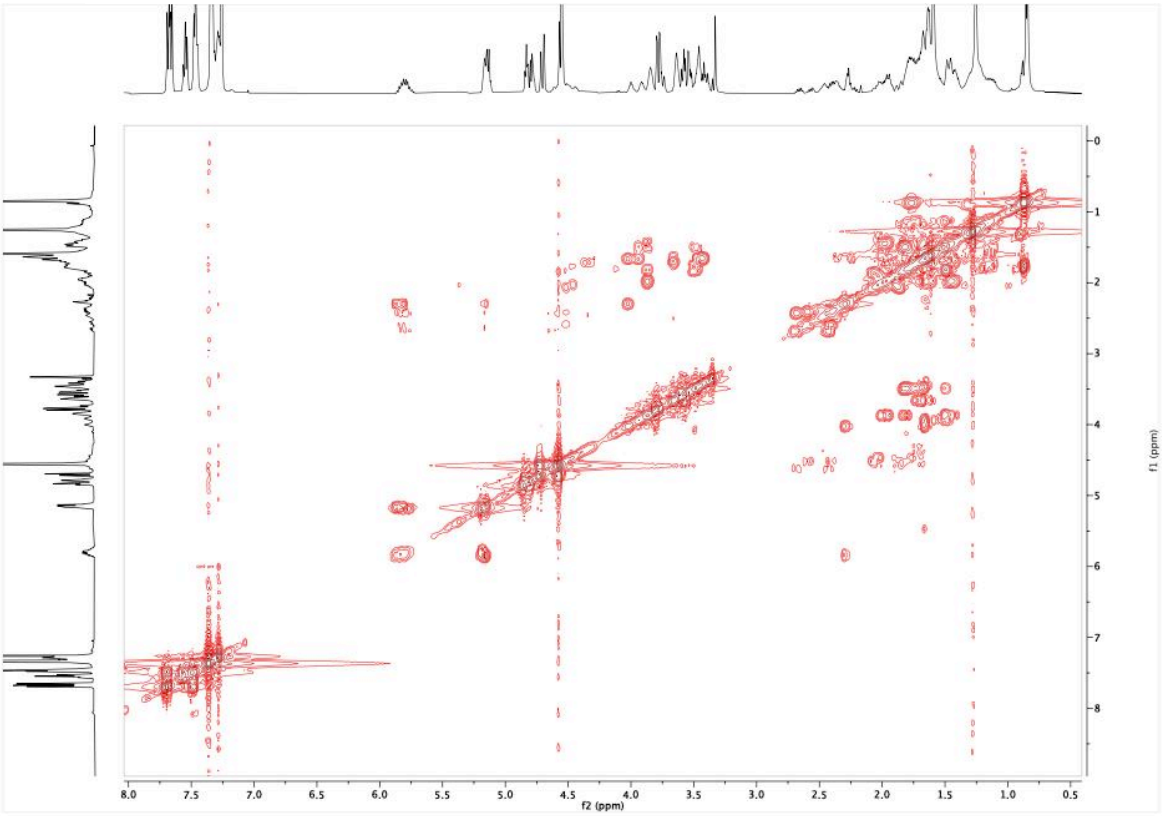

2D, $^{1}H^{13}C$, HSQC, 500 MHz, $CDCl_3$